(12) INTERNATIONAL APPLICATION PUBLISHED UNDER THE PATENT COOPERATION TREATY (PCT)

(19) World Intellectual Property Organization
International Bureau

(43) International Publication Date
11 April 2019 (11.04.2019)

WIPO | PCT

(10) International Publication Number
WO 2019/070755 A1

(51) International Patent Classification:
G06F 19/22 (2011.01) *C12Q 1/68* (2018.01)
G16H 50/20 (2018.01)

(21) International Application Number:
PCT/US2018/054020

(22) International Filing Date:
02 October 2018 (02.10.2018)

(25) Filing Language: English

(26) Publication Language: English

(30) Priority Data:

62/567,153	02 October 2017 (02.10.2017)	US
62/573,117	16 October 2017 (16.10.2017)	US
62/588,025	17 November 2017 (17.11.2017)	US
62/595,327	06 December 2017 (06.12.2017)	US
62/630,158	13 February 2018 (13.02.2018)	US
62/680,545	04 June 2018 (04.06.2018)	US

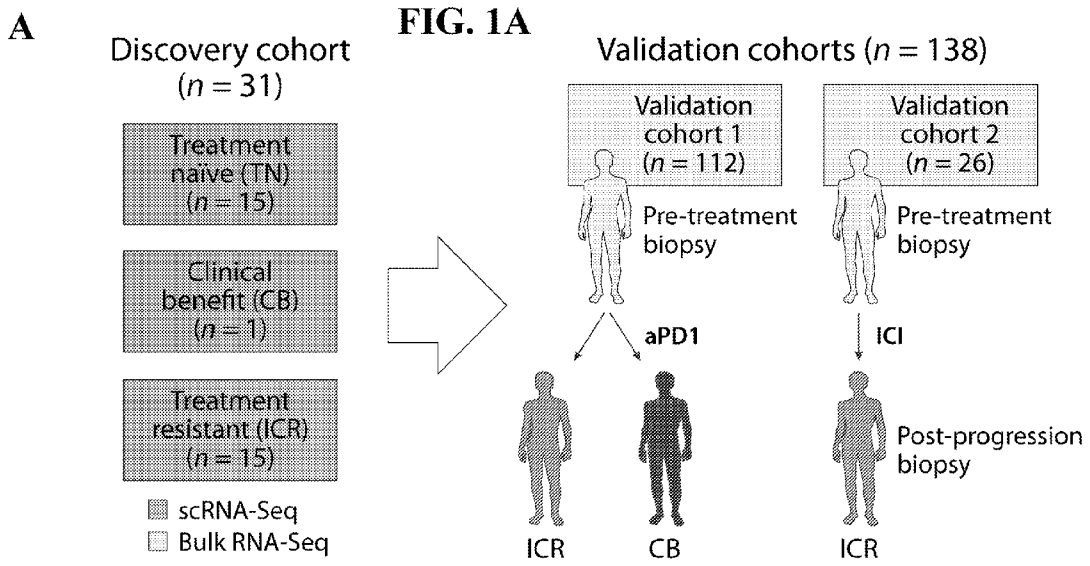
(71) Applicants: **THE BROAD INSTITUTE, INC.** [US/US]; 415 Main Street, Cambridge, Massachusetts 02142 (US). **MASSACHUSETTS INSTITUTE OF TECHNOLOGY** [US/US]; 77 Massachusetts Avenue, Cambridge, Massachusetts 02139 (US). **DANA-FARBER CANCER INSTITUTE, INC.** [US/US]; 450 Brookline Avenue, Boston, Massachusetts 02215 (US).

(72) Inventor; and
(71) Applicant: **JERBY, Livnat** [US/US]; c/o 415 Main Street, Cambridge, Massachusetts 02142 (US).

(72) Inventors: **REGEV, Aviv**; c/o 415 Main Street, Cambridge, Massachusetts 02142 (US). **ROZENBLATT-ROSEN, Orit**; c/o 415 Main Street, Cambridge, Massachusetts 02142 (US). **IZAR, Benjamin**; c/o 450 Brookline Avenue, Boston, Massachusetts 02215 (US).

(54) Title: METHODS AND COMPOSITIONS FOR DETECTING AND MODULATING AN IMMUNOTHERAPY RESISTANCE GENE SIGNATURE IN CANCER

FIG. 1A



(57) Abstract: The subject matter disclosed herein is generally directed to detecting and modulating novel gene signatures for the treatment and prognosis of cancer. The novel gene signatures predict overall survival in cancer and can be targeted therapeutically. Specifically, disclosed is a resistance program identified by a comprehensive single-cell profiling study in melanoma patients, which was validated in two large validation cohorts. Using a large-scale in silico prediction, CDK4/6 inhibitors were identified as a class of drugs that may reverse this resistance program. These predictions were validated in melanoma cell lines, patient-derived co-culture models, and melanoma in vivo models, which show that the combination of abemaciclib and immune checkpoint blockade (ICB) overcome intrinsic drug resistance. The present invention provides for detecting an immunotherapy resistance signature and modulating the signature with CDK4/6 inhibition. Also provided is a novel phased immunotherapy and CDK4/6 inhibitor combination therapy

WO 2019/070755 A1

[Continued on next page]

ROTEM, Asaf; c/o 450 Brookline Avenue, Boston, Massachusetts 02215 (US).

(74) **Agent: SCHER, Michael B.** et al.; Johnson, Marcou & Isaacs, LLC, P.O. Box 691, Hoschton, Georgia 30548 (US).

(81) **Designated States** *(unless otherwise indicated, for every kind of national protection available)*: AE, AG, AL, AM, AO, AT, AU, AZ, BA, BB, BG, BH, BN, BR, BW, BY, BZ, CA, CH, CL, CN, CO, CR, CU, CZ, DE, DJ, DK, DM, DO, DZ, EC, EE, EG, ES, FI, GB, GD, GE, GH, GM, GT, HN, HR, HU, ID, IL, IN, IR, IS, JO, JP, KE, KG, KH, KN, KP, KR, KW, KZ, LA, LC, LK, LR, LS, LU, LY, MA, MD, ME, MG, MK, MN, MW, MX, MY, MZ, NA, NG, NI, NO, NZ, OM, PA, PE, PG, PH, PL, PT, QA, RO, RS, RU, RW, SA, SC, SD, SE, SG, SK, SL, SM, ST, SV, SY, TH, TJ, TM, TN, TR, TT, TZ, UA, UG, US, UZ, VC, VN, ZA, ZM, ZW.

(84) **Designated States** *(unless otherwise indicated, for every kind of regional protection available)*: ARIPO (BW, GH, GM, KE, LR, LS, MW, MZ, NA, RW, SD, SL, ST, SZ, TZ, UG, ZM, ZW), Eurasian (AM, AZ, BY, KG, KZ, RU, TJ, TM), European (AL, AT, BE, BG, CH, CY, CZ, DE, DK, EE, ES, FI, FR, GB, GR, HR, HU, IE, IS, IT, LT, LU, LV, MC, MK, MT, NL, NO, PL, PT, RO, RS, SE, SI, SK, SM, TR), OAPI (BF, BJ, CF, CG, CI, CM, GA, GN, GQ, GW, KM, ML, MR, NE, SN, TD, TG).

Published:

— *with international search report (Art. 21(3))*
— *with sequence listing part of description (Rule 5.2(a))*

METHODS AND COMPOSITIONS FOR DETECTING AND MODULATING AN IMMUNOTHERAPY RESISTANCE GENE SIGNATURE IN CANCER

CROSS-REFERENCE TO RELATED APPLICATIONS

[0001] This application claims the benefit of U.S. Provisional Application Nos. 62/567,153, filed October 2, 2017, 62/573,117, filed October 16, 2017, 62/588,025, filed November 17, 2017, 62/595,327, filed December 6, 2017, 62/630,158, filed February 13, 2018, and 62/680,545, filed June 4, 2018. The entire contents of the above-identified applications are hereby fully incorporated herein by reference.

STATEMENT REGARDING FEDERALLY SPONSORED RESEARCH

[0002] This invention was made with government support under grant Nos. CA222663, CA180922, CA202820 and CA14051 awarded by the National Institutes of Health. The government has certain rights in the invention.

REFERENCE TO AN ELECTRONIC SEQUENCE LISTING

[0003] The contents of the electronic sequence listing (BROD_2630WP_ST25.txt"; Size is 4 Kilobytes and it was created on September 28, 2018) is herein incorporated by reference in its entirety.

TECHNICAL FIELD

[0004] The subject matter disclosed herein is generally directed to detecting and modulating novel gene signatures for the treatment and prognosis of cancer.

BACKGROUND

[0005] One reason that cancer cells thrive is because they are able to hide from the immune system. Certain cancer cells avoid the immune system better than others and could be a factor in determining survival. Immunotherapies have been developed to enhance immune responses against cancer and lead to prolonged survival. Immune checkpoint inhibitors (ICI) have transformed the therapeutic landscape of several cancer types (Sharma and Allison, 2015). In particular, immune checkpoint inhibitors (ICI) lead to durable responses in ~35% of patients with metastatic melanoma by unleashing T cells from oncogenic suppression (Sharma, et al., 2015; and Hodi, et al., 2016). Nonetheless, many patients manifest ICI resistance (ICR), which is often intrinsic (Sharma et al., 2017). ICR is

often unpredictable and poorly understood (Sharma, et al., 2017), hampering appropriate selection of patients for therapies, rational enrollment to clinical trials and the development of new therapeutic strategies that could overcome ICR (Sharma, et al., 2015).

[0006] Because ICI targets cell-cell interactions, resistance can stem from different cells and their interactions in the tumor ecosystem. Recent studies illuminated ICI resistance with Whole Exome Sequencing (WES) and transcriptional profiles of bulk tumors (Hugo et al., 2016; Riaz et al., 2017; Van Allen et al., 2015), but had limited ability to dissect the cancer-immune interplay and generate reliable response biomarkers. These studies demonstrated that tumors with a high mutational load (Van Allen et al., 2015) or high immune cell infiltration (Tumeh et al., 2014; and Riaz et al., 2017) are more likely to respond, and linked ICR in patients to functional immune evasion phenotypes, including defects in the JAK/STAT pathway (Zaretsky et al., 2016) and interferon gamma (IFN-γ) response (Zaretsky et al., 2016; and Gao et al., 2016), impaired antigen presentation (Hugo et al., 2016; and Zaretsky et al., 2016), PTEN loss Peng et al., 2016, and increased WNT-ß-catenin signaling (Spranger, et al., 2015). However, thus far, the predictive power of these and other (Gibney, et al., 2016) approaches has been limited, either because they report on only some facets of the causes of resistance (WES) and/or because they are highly confounded by tumor composition (RNA and copy-number variations). Indeed, because ICI targets the interactions between different cells in the tumor, its impact depends on multicellular circuits of malignant and non-malignant cells (Tirosh et al., 2016), which are challenging to study in bulk tumor specimens. Single-cell RNA-seq (scRNA-seq) of patient tumors (Tirosh et al., 2016) can alleviate this limitation. Single-cell genomics, especially single cell RNA-Seq (scRNA-Seq), provides a unique tool to comprehensively map the tumor ecosystem (Tirosh et al., 2016a; Patel et al., 2014; Tirosh et al., 2016b; Venteicher et al., 2017; and Li et al., 2017), but has thus far not been used to study ICR.

[0007] Infiltration of the tumor with T cells has been associated with patient survival and improved immunotherapy responses (Fridman et al., 2012), but the determinants that dictate if a tumor will have high (“hot”) or low (“cold”) levels of T cell infiltration are only partially understood. Among multiple factors, malignant cells may play an important role in determining this phenotype. However, while current methods use bulk genomics to deconvolve the tumor’s composition (Newman et al., 2015), they cannot recover the salient

intracellular programs of malignant cells. Hence linking malignant cell states to T cell infiltration levels has been challenging.

[0008] Thus, there is a need to better understand tumor immunity and resistance to immunotherapy.

[0009] Citation or identification of any document in this application is not an admission that such document is available as prior art to the present invention.

SUMMARY

[0010] Immune checkpoint inhibitors (ICI) produce durable responses in some melanoma patients, but many patients derive no clinical benefit, and the molecular underpinnings of such resistance remain elusive.

[0011] It is an objective of the present invention to identify molecular signatures for diagnosis, prognosis and treatment of subjects suffering from cancer. It is a further objective to understand tumor immunity and to leverage this knowledge for treating subjects suffering from cancer. It is another objective for identifying gene signatures for predicting response to checkpoint blockade therapy. It is another objective, for modulating the molecular signatures in order to increase efficacy of immunotherapy (e.g., checkpoint blockade therapy).

[0012] Here, Applicants leveraged single-cell RNA-seq (scRNA-seq) from 33 melanoma tumors and computational analyses to interrogate malignant cell states that promote immune evasion. Applicants identified a resistance program expressed by malignant cells that is associated with T cell exclusion and immune evasion. The program is expressed prior to immunotherapy, characterizes cold niches *in situ*, and predicts clinical responses to anti-PD-1 therapy in an independent cohort of 112 melanoma patients. CDK4/6-inhibition represses this program in individual malignant cells, induces senescence (Senescence Associated Secretory Phenotype (SASP)), and reduces melanoma tumor outgrowth in mouse models *in vivo* when given in combination with immunotherapy. The disclosed study provides a high-resolution landscape of ICI resistant cell states, identifies clinically predictive signatures, and suggests new therapeutic strategies to overcome immunotherapy resistance. Applicants additionally applied single-nuclei RNA-seq (sNuc-seq) to characterize thousands of cells from estrogen-receptor–positive metastatic breast cancer (MBC). ER+ MBC is currently treated with CDK4/6-inhibitors (see, e.g., Vasan et al., State-of-the-Art Update: CDK4/6 Inhibitors in ER+ Metastatic Breast Cancer, AJHO. 2017;13(4):16-22). Finally, Applicants applied single-cell RNA-seq (scRNA-seq) to characterize thousands of cells from colon cancer.

[0013] In one aspect, the present invention provides for a method of treating a cancer in a subject in need thereof comprising detecting the expression or activity of an ICR and/or exclusion signature according to any embodiment herein in a tumor obtained from the subject and administering a treatment, wherein if an ICR and/or exclusion signature is detected the treatment comprises administering a checkpoint inhibitor and a CDK4/6 inhibitor.

[0014] In another aspect, the present invention provides for a method of treating a cancer in a subject in need thereof comprising administering a checkpoint inhibitor and a CDK4/6 inhibitor.

[0015] In certain embodiments, the CDK4/6 inhibitor comprises abemaciclib. In certain embodiments, the immunotherapy comprises a check point inhibitor. The checkpoint inhibitor may comprise anti-CTLA4, anti-PD-L1, anti-PD1, anti-TIM3, anti-TIGIT, anti-LAG3 or a combination thereof. In certain embodiments, the cancer is melanoma or breast cancer.

[0016] In another aspect, the present invention provides for a method of detecting an immune checkpoint inhibitor resistance (ICR) gene signature in a tumor comprising, detecting in tumor cells obtained from a subject in need thereof the expression or activity of a malignant cell gene signature comprising: one or more genes or polypeptides selected from the group consisting of PPIA, RPL31, RPL37A, RPL41, RPS21, RPS27A, SAE1, UBA52, C19orf48, CHCHD2, FARSA, NONO, RPL27, RPL36, RPS13, RPS14, RPS15, RPS28, ARMC6, BOLA2, BOLA2B, CDC123, CKS1B, CMSS1, DDX39A, DNAJC9, FAM60A, HN1, MRPL47, NDUFA13, PET100, PFDN4, PSMA7, RNASEH2A, ROMO1, RPL35A, SLIRP, SLMO2, SNRPF, SNRPG, TPRKB, TXNDC17, UBL5, USMG5, AHNAK, APOD, ATP1A1, B2M, CD44, CD63, CTSB, CTSD, FOS, GRN, HLA-A, HLA-B, HLA-C, HLA-E, HLA-H, LAMP2, LGALS3, LGALS3BP, NPC2, PSAP, SERPINE2, TAPBP, TIMP2, CTSO, KLF4, LEF1-AS1, STOM, TAPBPL, VAT1, ACTA2, C6orf226, CCR10, CITED1, CORO1A, CXCR4, DDX17, FLJ39051, FMN1, FRZB, FSTL3, FTH1, HLA-DRB5, IDI2-AS1, JMJD7, LCP1, LINC00518, LOC100506714, LOC100507463, LY96, NMRK1, P2RX4, PIK3IP1, PYGB, RAB27A, RBP7, RNF213, RTP4, SDCBP, SLC22A18, SLC7A5P1, SP100, SPESP1, SPINT1, ST3GAL6-AS1, ST6GALNAC2, TFAP2A, TRIM22, TTLL1 and UCN2; or one or more genes or polypeptides selected from the group consisting of BZW2, CCT3, CDK4, GPATCH4, ISYNA1, MDH2, PPIA, RPL31, RPL37A, RPL41, RPS21, RPS27A, RUVBL2, SAE1, UBA52, AHCY, C17orf76-AS1, C19orf48, C1QBP, CCT6A, CHCHD2, CTPS1, EEF1G, EIF2S3, EIF3K, EIF4A1, FARSA, FBL, FKBP4,

GAS5, GNB2L1, GPI, HNRNPA1, HNRNPC, IDH2, ILF2, NACA, NCL, NME1, NOLC1, NONO, PABPC1, PAICS, PFN1, POLD2, PPA1, PTMA, PUF60, RPL10A, RPL11, RPL12, RPL13, RPL13A, RPL13AP5, RPL17, RPL18, RPL18A, RPL21, RPL26, RPL27, RPL28, RPL29, RPL3, RPL36, RPL36A, RPL37, RPL4, RPL5, RPL6, RPL8, RPLP0, RPLP1, RPS10, RPS11, RPS13, RPS14, RPS15, RPS15A, RPS16, RPS17, RPS17L, RPS18, RPS19, RPS23, RPS24, RPS27, RPS28, RPS3, RPS4X, RPS5, RPS6, RPS7, RPS8, RPS9, RPSA, RRS1, SERPINF1, SET, SHMT2, SLC19A1, SLC25A13, SNHG6, SNRPE, SOX4, SSR2, TIMM50, TOP1MT, TUBB, UQCRFS1, UQCRH, VDAC2, ACTB, AEN, ANP32E, APP, ARMC6, ATP5A1, ATP5D, ATP5G2, ATP5G3, BOLA2, BOLA2B, BOP1, BTF3, C20orf112, C6orf48, CA14, CACYBP, CBX5, CCT2, CCT4, CCT7, CDC123, CDCA7, CFL1, CKS1B, CMSS1, CNRIP1, CS, DARS, DCAF13, DCT, DCTPP1, DDX21, DDX39A, DDX39B, DLL3, DNAJC9, EEF1B2, EEF1D, EEF2, EIF3E, EIF3F, EIF3G, EIF3M, EIF4EBP2, ENO1, EXOSC5, FAM174B, FAM60A, FAM92A1, FBLN1, FOXRED2, FTL, FUS, GABARAP, GGH, GNL3, GRWD1, H3F3A, H3F3AP4, HMGA1, HMGB1, HN1, HNRNPA1P10, HNRNPH1, HNRNPM, HSP90AB1, HSPA8, HSPD1, IFRD2, ILF3, IMPDH2, ITM2C, KIAA0101, LDHB, LSM4, LSM7, LYPLA1, MAGEA4, MAGEC1, MCM7, METAP2, MID1, MIR4461, MKI67IP, MLLT11, MPZL1, MRPL15, MRPL37, MRPL4, MRPL47, MRPS12, MRPS21, NDUFA11, NDUFA13, NDUFS2, NME2, NOP16, NPM1, NREP, PA2G4, PAFAH1B3, PET100, PFDN2, PFDN4, PGAM1, PIH1D1, PLEKHJ1, POLR1D, POLR2E, PPP2R1A, PRMT1, PSMA7, PSMD4, RAN, RBM34, RNASEH2A, RNF2, ROMO1, RPAIN, RPL10, RPL14, RPL15, RPL19, RPL22, RPL27A, RPL30, RPL32, RPL35, RPL35A, RPL39, RPL7, RPL7A, RPL9, RPLP2, RPS12, RPS2, RPS20, RPS25, RPS3A, RQCD1, RSL1D1, RTKN, SCD, SCNM1, SERBP1, SF3B4, SKP2, SLC25A3, SLC25A6, SLIRP, SLMO2, SMARCA4, SMIM15, SMS, SNAI2, SNHG15, SNRPB, SNRPC, SNRPD1, SNRPD2, SNRPF, SNRPG, SRM, SRP14, SSB, TIMM13, TIMM44, TMC6, TP53, TPI1, TPRKB, TRAP1, TRIM28, TRPM1, TSR1, TUBA1B, TULP4, TXNDC17, TYMS, UBL5, UCK2, UHRF1, USMG5, USP22, VCY1B, VPS72, XIST, YWHAE, ZFAS1, ZNF286A, AHNAK, APOD, ATP1A1, B2M, CD44, CD63, CTSB, CTSD, FOS, GRN, HLA-A, HLA-B, HLA-C, HLA-E, HLA-H, LAMP2, LGALS3, LGALS3BP, NPC2, PSAP, SERPINE2, TAPBP, TIMP2, A2M, ACSL3, AEBP1, AGA, APOC2, APOE, ATP1B1, CD151, CD47, CD58, CD59, CDH19, CSPG4, CST3, CTSA, CTSL1, CTSO, CYP27A1, DAG1, DDR1, EEA1, EMP1, EVA1A, FBXO32, FGFR1, GAA, GPNMB, GSN, HLA-F, HSPA1A, IRF4, ITGA3, KCNN4, KLF4, LEF1-AS1, LRPAP1,

MFGE8, MIA, MT2A, NEAT1, NPC1, NSG1, PROS1, S100A6, S100B, SAT1, SCARB2, SDC3, SEC11C, SERPINA3, SGK1, SLC26A2, SLC5A3, STOM, STX7, TAPBPL, TIMP1, TIMP3, TM4SF1, TMED10, TPP1, TSC22D3, TYR, UBC, VAT1, WBP2, XAGE1D, ACSL4, ACTA2, ADM, ANGPTL4, ANXA1, ANXA2, APLP2, APOL1, ARL6IP5, ARSA, ATF3, ATP1B3, ATP6V0C, BACE2, BBX, BCL6, C4A, C6orf226, CALU, CARD16, CASP1, CAST, CAV1, CAV2, CCND3, CCR10, CD9, CDH1, CHI3L1, CITED1, CLIC4, CORO1A, CRELD1, CRYAB, CSGALNACT1, CXCR4, CYP4V2, DCBLD2, DDX17, DDX5, DPYSL2, DUSP4, DUSP6, ECM1, EGR1, EPHX2, ERBB3, EZH1, FAM3C, FCGR2C, FCRLA, FLJ39051, FLJ43663, FLNA, FMN1, FRZB, FSTL3, FTH1, GADD45B, GATSL3, GEM, GJB1, GOLGB1, GPR155, GPR56, HLA-DRB5, HLA-G, HPCAL1, HTATIP2, IDI2-AS1, IFI27, IFI27L2, IFI35, IFI6, IGF1R, IGFBP7, IGSF8, IL1RAP, IL6ST, ITGA6, ITGA7, ITGB1, ITGB3, ITM2B, JMJD7, JUN, KLF6, LAMB2, LCP1, LEPROT, LGALS1, LGMN, LINC00518, LOC100126784, LOC100506190, LOC100506714, LOC100507463, LPL, LY6E, LY96, LYRM9, MAGEC2, MALAT1, MATN2, MCAM, MFI2, MMP14, MPZ, MT1E, MT1M, MT1X, MTRNR2L1, MTRNR2L10, MTRNR2L2, MTRNR2L3, MTRNR2L4, MTRNR2L5, MTRNR2L6, MTRNR2L7, MTRNR2L8, MYO1D, NAV2, NFE2L1, NFKBIA, NFKBIZ, NMRK1, NNMT, NR4A1, P2RX4, PAGE5, PDE4DIP, PDK4, PERP, PIK3IP1, PLP2, PRKCDBP, PRNP, PRSS23, PSMB9, PTRF, PYGB, QPCT, RAB27A, RBP7, RDH5, RNF145, RNF213, RPS4Y1, RTP4, S100A1, S100A13, SCCPDH, SDCBP, SEL1L, SEMA3B, SERINC1, SERPINA1, SGCE, SHC4, SLC20A1, SLC22A18, SLC39A14, SLC7A5P1, SLC7A8, SNX9, SOD1, SORT1, SP100, SPESP1, SPINT1, SPON2, SPP1, SPRY2, SQSTM1, SRPX, ST3GAL6-AS1, ST6GALNAC2, STRIP2, SYNE2, SYNGR2, SYPL1, TF, TFAP2A, TGOLN2, THBD, TMBIM6, TMED9, TMEM255A, TMEM66, TMX4, TNC, TNFSF4, TRIM22, TRIML2, TSPYL2, TTLL1, TXNIP, UCN2, UPP1, WDFY1, ZBTB20 and ZBTB38; or one or more genes or polypeptides selected from Table 27B.1.

[0017] In certain embodiments, the ICR signature comprises a ICR-down signature, said signature comprising one or more genes selected from the group consisting of: AHNAK, APOD, ATP1A1, B2M, CD44, CD63, CTSB, CTSD, FOS, GRN, HLA-A, HLA-B, HLA-C, HLA-E, HLA-H, LAMP2, LGALS3, LGALS3BP, NPC2, PSAP, SERPINE2, TAPBP, TIMP2, CTSO, KLF4, LEF1-AS1, STOM, TAPBPL, VAT1, ACTA2, C6orf226, CCR10, CITED1, CORO1A, CXCR4, DDX17, FLJ39051, FMN1, FRZB, FSTL3, FTH1, HLA-DRB5, IDI2-AS1, JMJD7, LCP1, LINC00518, LOC100506714, LOC100507463, LY96,

NMRK1, P2RX4, PIK3IP1, PYGB, RAB27A, RBP7, RNF213, RTP4, SDCBP, SLC22A18, SLC7A5P1, SP100, SPESP1, SPINT1, ST3GAL6-AS1, ST6GALNAC2, TFAP2A, TRIM22, TTLL1 and UCN2; or AHNAK, APOD, ATP1A1, B2M, CD44, CD63, CTSB, CTSD, FOS, GRN, HLA-A, HLA-B, HLA-C, HLA-E, HLA-H, LAMP2, LGALS3, LGALS3BP, NPC2, PSAP, SERPINE2, TAPBP, TIMP2, A2M, ACSL3, AEBP1, AGA, APOC2, APOE, ATP1B1, CD151, CD47, CD58, CD59, CDH19, CSPG4, CST3, CTSA, CTSL1, CTSO, CYP27A1, DAG1, DDR1, EEA1, EMP1, EVA1A, FBXO32, FGFR1, GAA, GPNMB, GSN, HLA-F, HSPA1A, IRF4, ITGA3, KCNN4, KLF4, LEF1-AS1, LRPAP1, MFGE8, MIA, MT2A, NEAT1, NPC1, NSG1, PROS1, S100A6, S100B, SAT1, SCARB2, SDC3, SEC11C, SERPINA3, SGK1, SLC26A2, SLC5A3, STOM, STX7, TAPBPL, TIMP1, TIMP3, TM4SF1, TMED10, TPP1, TSC22D3, TYR, UBC, VAT1, WBP2, XAGE1D, ACSL4, ACTA2, ADM, ANGPTL4, ANXA1, ANXA2, APLP2, APOL1, ARL6IP5, ARSA, ATF3, ATP1B3, ATP6V0C, BACE2, BBX, BCL6, C4A, C6orf226, CALU, CARD16, CASP1, CAST, CAV1, CAV2, CCND3, CCR10, CD9, CDH1, CHI3L1, CITED1, CLIC4, CORO1A, CRELD1, CRYAB, CSGALNACT1, CXCR4, CYP4V2, DCBLD2, DDX17, DDX5, DPYSL2, DUSP4, DUSP6, ECM1, EGR1, EPHX2, ERBB3, EZH1, FAM3C, FCGR2C, FCRLA, FLJ39051, FLJ43663, FLNA, FMN1, FRZB, FSTL3, FTH1, GADD45B, GATSL3, GEM, GJB1, GOLGB1, GPR155, GPR56, HLA-DRB5, HLA-G, HPCAL1, HTATIP2, IDI2-AS1, IFI27, IFI27L2, IFI35, IFI6, IGF1R, IGFBP7, IGSF8, IL1RAP, IL6ST, ITGA6, ITGA7, ITGB1, ITGB3, ITM2B, JMJD7, JUN, KLF6, LAMB2, LCP1, LEPROT, LGALS1, LGMN, LINC00518, LOC100126784, LOC100506190, LOC100506714, LOC100507463, LPL, LY6E, LY96, LYRM9, MAGEC2, MALAT1, MATN2, MCAM, MFI2, MMP14, MPZ, MT1E, MT1M, MT1X, MTRNR2L1, MTRNR2L10, MTRNR2L2, MTRNR2L3, MTRNR2L4, MTRNR2L5, MTRNR2L6, MTRNR2L7, MTRNR2L8, MYO1D, NAV2, NFE2L1, NFKBIA, NFKBIZ, NMRK1, NNMT, NR4A1, P2RX4, PAGE5, PDE4DIP, PDK4, PERP, PIK3IP1, PLP2, PRKCDBP, PRNP, PRSS23, PSMB9, PTRF, PYGB, QPCT, RAB27A, RBP7, RDH5, RNF145, RNF213, RPS4Y1, RTP4, S100A1, S100A13, SCCPDH, SDCBP, SEL1L, SEMA3B, SERINC1, SERPINA1, SGCE, SHC4, SLC20A1, SLC22A18, SLC39A14, SLC7A5P1, SLC7A8, SNX9, SOD1, SORT1, SP100, SPESP1, SPINT1, SPON2, SPP1, SPRY2, SQSTM1, SRPX, ST3GAL6-AS1, ST6GALNAC2, STRIP2, SYNE2, SYNGR2, SYPL1, TF, TFAP2A, TGOLN2, THBD, TMBIM6, TMED9, TMEM255A, TMEM66, TMX4, TNC, TNFSF4, TRIM22, TRIML2, TSPYL2, TTLL1, TXNIP, UCN2, UPP1, WDFY1, ZBTB20 and ZBTB38, wherein said ICR-down signature is

downregulated in a tumor with a high ICR score and upregulated in a tumor with a low ICR score.

[0018] In certain embodiments, the ICR signature comprises a ICR-up signature, said signature comprising one or more genes selected from the group consisting of: PPIA, RPL31, RPL37A, RPL41, RPS21, RPS27A, SAE1, UBA52, C19orf48, CHCHD2, FARSA, NONO, RPL27, RPL36, RPS13, RPS14, RPS15, RPS28, ARMC6, BOLA2, BOLA2B, CDC123, CKS1B, CMSS1, DDX39A, DNAJC9, FAM60A, HN1, MRPL47, NDUFA13, PET100, PFDN4, PSMA7, RNASEH2A, ROMO1, RPL35A, SLIRP, SLMO2, SNRPF, SNRPG, TPRKB, TXNDC17, UBL5 and USMG5; or BZW2, CCT3, CDK4, GPATCH4, ISYNA1, MDH2, PPIA, RPL31, RPL37A, RPL41, RPS21, RPS27A, RUVBL2, SAE1, UBA52, AHCY, C17orf76-AS1, C19orf48, C1QBP, CCT6A, CHCHD2, CTPS1, EEF1G, EIF2S3, EIF3K, EIF4A1, FARSA, FBL, FKBP4, GAS5, GNB2L1, GPI, HNRNPA1, HNRNPC, IDH2, ILF2, NACA, NCL, NME1, NOLC1, NONO, PABPC1, PAICS, PFN1, POLD2, PPA1, PTMA, PUF60, RPL10A, RPL11, RPL12, RPL13, RPL13A, RPL13AP5, RPL17, RPL18, RPL18A, RPL21, RPL26, RPL27, RPL28, RPL29, RPL3, RPL36, RPL36A, RPL37, RPL4, RPL5, RPL6, RPL8, RPLP0, RPLP1, RPS10, RPS11, RPS13, RPS14, RPS15, RPS15A, RPS16, RPS17, RPS17L, RPS18, RPS19, RPS23, RPS24, RPS27, RPS28, RPS3, RPS4X, RPS5, RPS6, RPS7, RPS8, RPS9, RPSA, RRS1, SERPINF1, SET, SHMT2, SLC19A1, SLC25A13, SNHG6, SNRPE, SOX4, SSR2, TIMM50, TOP1MT, TUBB, UQCRFS1, UQCRH, VDAC2, ACTB, AEN, ANP32E, APP, ARMC6, ATP5A1, ATP5D, ATP5G2, ATP5G3, BOLA2, BOLA2B, BOP1, BTF3, C20orf112, C6orf48, CA14, CACYBP, CBX5, CCT2, CCT4, CCT7, CDC123, CDCA7, CFL1, CKS1B, CMSS1, CNRIP1, CS, DARS, DCAF13, DCT, DCTPP1, DDX21, DDX39A, DDX39B, DLL3, DNAJC9, EEF1B2, EEF1D, EEF2, EIF3E, EIF3F, EIF3G, EIF3M, EIF4EBP2, ENO1, EXOSC5, FAM174B, FAM60A, FAM92A1, FBLN1, FOXRED2, FTL, FUS, GABARAP, GGH, GNL3, GRWD1, H3F3A, H3F3AP4, HMGA1, HMGB1, HN1, HNRNPA1P10, HNRNPH1, HNRNPM, HSP90AB1, HSPA8, HSPD1, IFRD2, ILF3, IMPDH2, ITM2C, KIAA0101, LDHB, LSM4, LSM7, LYPLA1, MAGEA4, MAGEC1, MCM7, METAP2, MID1, MIR4461, MKI67IP, MLLT11, MPZL1, MRPL15, MRPL37, MRPL4, MRPL47, MRPS12, MRPS21, NDUFA11, NDUFA13, NDUFS2, NME2, NOP16, NPM1, NREP, PA2G4, PAFAH1B3, PET100, PFDN2, PFDN4, PGAM1, PIH1D1, PLEKHJ1, POLR1D, POLR2E, PPP2R1A, PRMT1, PSMA7, PSMD4, RAN, RBM34, RNASEH2A, RNF2, ROMO1, RPAIN, RPL10, RPL14, RPL15, RPL19, RPL22, RPL27A, RPL30, RPL32,

RPL35, RPL35A, RPL39, RPL7, RPL7A, RPL9, RPLP2, RPS12, RPS2, RPS20, RPS25, RPS3A, RQCD1, RSL1D1, RTKN, SCD, SCNM1, SERBP1, SF3B4, SKP2, SLC25A3, SLC25A6, SLIRP, SLMO2, SMARCA4, SMIM15, SMS, SNAI2, SNHG15, SNRPB, SNRPC, SNRPD1, SNRPD2, SNRPF, SNRPG, SRM, SRP14, SSB, TIMM13, TIMM44, TMC6, TP53, TPI1, TPRKB, TRAP1, TRIM28, TRPM1, TSR1, TUBA1B, TULP4, TXNDC17, TYMS, UBL5, UCK2, UHRF1, USMG5, USP22, VCY1B, VPS72, XIST, YWHAE, ZFAS1 and ZNF286A, wherein said ICR-up signature is upregulated in a tumor with a high ICR score and downregulated in a tumor with a low ICR score.

[0019] In another aspect, the present invention provides for a method of detecting an immune checkpoint inhibitor resistance (ICR) gene signature in a tumor comprising, detecting in tumor cells obtained from a subject in need thereof the expression or activity of a malignant cell gene signature comprising one or more genes or polypeptides selected from the group consisting of BZW2, CCT3, CDK4, GPATCH4, ISYNA1, MDH2, PPIA, RPL31, RPL37A, RPL41, RPS21, RPS27A, RUVBL2, SAE1, UBA52, C17orf76-AS1, C1QBP, CTPS1, EEF1G, EIF2S3, EIF3K, EIF4A1, FBL, GAS5, GNB2L1, GPI, HNRNPA1, HNRNPC, IDH2, ILF2, NACA, NCL, NOLC1, NONO, PABPC1, PFN1, PPA1, PTMA, RPL10A, RPL11, RPL12, RPL13, RPL13A, RPL13AP5, RPL17, RPL18, RPL18A, RPL21, RPL26, RPL28, RPL29, RPL3, RPL36A, RPL37, RPL4, RPL5, RPL6, RPL8, RPLP0, RPLP1, RPS10, RPS11, RPS15A, RPS16, RPS17, RPS17L, RPS18, RPS19, RPS23, RPS24, RPS27, RPS3, RPS4X, RPS5, RPS6, RPS7, RPS8, RPS9, RPSA, SERPINF1, SET, SHMT2, SNHG6, SNRPE, SOX4, SSR2, TIMM50, TUBB, UQCRFS1, UQCRH, VDAC2, ACTB, AEN, ANP32E, ATP5A1, ATP5G2, C20orf112, CA14, CBX5, CCT2, CFL1, CNRIP1, CS, DCAF13, DCT, DDX39B, DLL3, EIF4EBP2, FAM174B, FBLN1, FOXRED2, FTL, FUS, GABARAP, GRWD1, H3F3A, H3F3AP4, HMGA1, HNRNPA1P10, HSPA8, ITM2C, KIAA0101, MAGEA4, METAP2, MID1, MIR4461, MLLT11, MPZL1, MRPS21, NDUFS2, PA2G4, PAFAH1B3, PFDN2, PGAM1, PIH1D1, PPP2R1A, PSMD4, RAN, RBM34, RNF2, RPAIN, RPS12, SCD, SCNM1, SF3B4, SKP2, SLC25A3, SMS, SNAI2, SRP14, TMC6, TP53, TRPM1, TSR1, TUBA1B, TULP4, USP22, VCY1B, VPS72, YWHAE, ZNF286A, AHNAK, APOD, ATP1A1, B2M, CD44, CD63, CTSB, CTSD, FOS, GRN, HLA-A, HLA-B, HLA-C, HLA-E, HLA-H, LAMP2, LGALS3, LGALS3BP, NPC2, PSAP, SERPINE2, TAPBP, TIMP2, A2M, ACSL3, AEBP1, AGA, APOE, ATP1B1, CD151, CD47, CD58, CD59, CDH19, CSPG4, CST3, CTSA, CTSL1, DAG1, DDR1, EEA1, EMP1, EVA1A, FBXO32, FGFR1, GAA, GPNMB, GSN, HLA-F, HSPA1A, ITGA3, KCNN4, KLF4,

LRPAP1, MFGE8, MIA, MT2A, NEAT1, NPC1, NSG1, PROS1, S100A6, S100B, SAT1, SCARB2, SDC3, SERPINA3, SGK1, SLC26A2, SLC5A3, STOM, TAPBPL, TIMP1, TIMP3, TM4SF1, TMED10, TPP1, TSC22D3, TYR, UBC, ACSL4, ADM, ANGPTL4, ANXA1, ANXA2, APLP2, ARL6IP5, ATF3, ATP1B3, BACE2, BBX, BCL6, CALU, CASP1, CAST, CAV1, CCND3, CD9, CHI3L1, CLIC4, CRELD1, CRYAB, CSGALNACT1, DCBLD2, DDX5, DPYSL2, DUSP4, DUSP6, ECM1, EGR1, EPHX2, ERBB3, EZH1, FAM3C, FCGR2C, FCRLA, FLJ43663, GADD45B, GEM, GOLGB1, HPCAL1, HTATIP2, IFI35, IGF1R, IL1RAP, IL6ST, ITGA6, ITGB1, ITGB3, ITM2B, JUN, KLF6, LEPROT, LGALS1, LPL, MAGEC2, MFI2, MT1E, MT1M, MT1X, NFKBIA, NFKBIZ, NNMT, NR4A1, PDK4, PLP2, PRKCDBP, PRNP, PRSS23, PSMB9, PTRF, RNF145, RPS4Y1, SCCPDH, SEL1L, SEMA3B, SGCE, SLC20A1, SLC39A14, SOD1, SPRY2, SQSTM1, SRPX, SYNGR2, SYPL1, TF, TGOLN2, TMED9, TMEM66, TMX4, TNC, UPP1, ZBTB20 and ZBTB38.

[0020] In certain embodiments, the ICR signature comprises an ICR-down signature, said signature comprising one or more genes selected from the group consisting of: AHNAK, APOD, ATP1A1, B2M, CD44, CD63, CTSB, CTSD, FOS, GRN, HLA-A, HLA-B, HLA-C, HLA-E, HLA-H, LAMP2, LGALS3, LGALS3BP, NPC2, PSAP, SERPINE2, TAPBP, TIMP2, A2M, ACSL3, AEBP1, AGA, APOE, ATP1B1, CD151, CD47, CD58, CD59, CDH19, CSPG4, CST3, CTSA, CTSL1, DAG1, DDR1, EEA1, EMP1, EVA1A, FBXO32, FGFR1, GAA, GPNMB, GSN, HLA-F, HSPA1A, ITGA3, KCNN4, KLF4, LRPAP1, MFGE8, MIA, MT2A, NEAT1, NPC1, NSG1, PROS1, S100A6, S100B, SAT1, SCARB2, SDC3, SERPINA3, SGK1, SLC26A2, SLC5A3, STOM, TAPBPL, TIMP1, TIMP3, TM4SF1, TMED10, TPP1, TSC22D3, TYR, UBC, ACSL4, ADM, ANGPTL4, ANXA1, ANXA2, APLP2, ARL6IP5, ATF3, ATP1B3, BACE2, BBX, BCL6, CALU, CASP1, CAST, CAV1, CCND3, CD9, CHI3L1, CLIC4, CRELD1, CRYAB, CSGALNACT1, DCBLD2, DDX5, DPYSL2, DUSP4, DUSP6, ECM1, EGR1, EPHX2, ERBB3, EZH1, FAM3C, FCGR2C, FCRLA, FLJ43663, GADD45B, GEM, GOLGB1, HPCAL1, HTATIP2, IFI35, IGF1R, IL1RAP, IL6ST, ITGA6, ITGB1, ITGB3, ITM2B, JUN, KLF6, LEPROT, LGALS1, LPL, MAGEC2, MFI2, MT1E, MT1M, MT1X, NFKBIA, NFKBIZ, NNMT, NR4A1, PDK4, PLP2, PRKCDBP, PRNP, PRSS23, PSMB9, PTRF, RNF145, RPS4Y1, SCCPDH, SEL1L, SEMA3B, SGCE, SLC20A1, SLC39A14, SOD1, SPRY2, SQSTM1, SRPX, SYNGR2, SYPL1, TF, TGOLN2, TMED9, TMEM66, TMX4, TNC, UPP1, ZBTB20 and ZBTB38, wherein said ICR-down signature is downregulated in a tumor with a high ICR score and

upregulated in a tumor with a low ICR score.

[0021] In certain embodiments, the ICR signature comprises an ICR-up signature, said signature comprising one or more genes selected from the group consisting of: BZW2, CCT3, CDK4, GPATCH4, ISYNA1, MDH2, PPIA, RPL31, RPL37A, RPL41, RPS21, RPS27A, RUVBL2, SAE1, UBA52, C17orf76-AS1, C1QBP, CTPS1, EEF1G, EIF2S3, EIF3K, EIF4A1, FBL, GAS5, GNB2L1, GPI, HNRNPA1, HNRNPC, IDH2, ILF2, NACA, NCL, NOLC1, NONO, PABPC1, PFN1, PPA1, PTMA, RPL10A, RPL11, RPL12, RPL13, RPL13A, RPL13AP5, RPL17, RPL18, RPL18A, RPL21, RPL26, RPL28, RPL29, RPL3, RPL36A, RPL37, RPL4, RPL5, RPL6, RPL8, RPLP0, RPLP1, RPS10, RPS11, RPS15A, RPS16, RPS17, RPS17L, RPS18, RPS19, RPS23, RPS24, RPS27, RPS3, RPS4X, RPS5, RPS6, RPS7, RPS8, RPS9, RPSA, SERPINF1, SET, SHMT2, SNHG6, SNRPE, SOX4, SSR2, TIMM50, TUBB, UQCRFS1, UQCRH, VDAC2, ACTB, AEN, ANP32E, ATP5A1, ATP5G2, C20orf112, CA14, CBX5, CCT2, CFL1, CNRIP1, CS, DCAF13, DCT, DDX39B, DLL3, EIF4EBP2, FAM174B, FBLN1, FOXRED2, FTL, FUS, GABARAP, GRWD1, H3F3A, H3F3AP4, HMGA1, HNRNPA1P10, HSPA8, ITM2C, KIAA0101, MAGEA4, METAP2, MID1, MIR4461, MLLT11, MPZL1, MRPS21, NDUFS2, PA2G4, PAFAH1B3, PFDN2, PGAM1, PIH1D1, PPP2R1A, PSMD4, RAN, RBM34, RNF2, RPAIN, RPS12, SCD, SCNM1, SF3B4, SKP2, SLC25A3, SMS, SNAI2, SRP14, TMC6, TP53, TRPM1, TSR1, TUBA1B, TULP4, USP22, VCY1B, VPS72, YWHAE and ZNF286A, wherein said ICR-up signature is upregulated in a tumor with a high ICR score and downregulated in a tumor with a low ICR score.

[0022] In certain embodiments, the ICR signature according to any embodiment herein is detected in cycling cells and/or expanded cells.

[0023] In another aspect, the present invention provides for a method of detecting an immune cell exclusion gene signature in a tumor comprising, detecting in tumor cells obtained from a subject in need thereof the expression or activity of a malignant cell gene signature comprising: one or more genes or polypeptides selected from the group consisting of BZW2, CCT3, CDK4, GPATCH4, ISYNA1, MDH2, RUVBL2, AHCY, CCT6A, FKBP4, NME1, PAICS, POLD2, PUF60, RRS1, SLC19A1, SLC25A13, TOP1MT, HSP90AB1, RTKN, APOC2, CYP27A1, IRF4, SEC11C, STX7, WBP2, XAGE1D, PAGE5 and WDFY1; or one or more genes or polypeptides selected from the group consisting of BZW2, CCT3, CDK4, GPATCH4, ISYNA1, MDH2, PPIA, RPL31, RPL37A, RPL41, RPS21, RPS27A, RUVBL2, SAE1, UBA52, AHCY, C17orf76-AS1, C19orf48, C1QBP, CCT6A, CHCHD2,

CTPS1, EEF1G, EIF2S3, EIF3K, EIF4A1, FARSA, FBL, FKBP4, GAS5, GNB2L1, GPI, HNRNPA1, HNRNPC, IDH2, ILF2, NACA, NCL, NME1, NOLC1, PABPC1, PAICS, PFN1, POLD2, PPA1, PTMA, PUF60, RPL10A, RPL11, RPL12, RPL13, RPL13A, RPL13AP5, RPL17, RPL18, RPL18A, RPL21, RPL26, RPL27, RPL28, RPL29, RPL3, RPL36, RPL36A, RPL37, RPL4, RPL5, RPL6, RPL8, RPLP0, RPLP1, RPS10, RPS11, RPS13, RPS14, RPS15, RPS15A, RPS16, RPS17, RPS17L, RPS18, RPS19, RPS23, RPS24, RPS27, RPS28, RPS3, RPS4X, RPS5, RPS6, RPS7, RPS8, RPS9, RPSA, RRS1, SERPINF1, SET, SHMT2, SLC19A1, SLC25A13, SNHG6, SNRPE, SOX4, SSR2, TIMM50, TOP1MT, TUBB, UQCRFS1, UQCRH, VDAC2, APP, ATP5D, ATP5G3, BOP1, BTF3, C6orf48, CACYBP, CCT4, CCT7, CDCA7, DARS, DCTPP1, DDX21, EEF1B2, EEF1D, EEF2, EIF3E, EIF3F, EIF3G, EIF3M, ENO1, EXOSC5, FAM92A1, GGH, GNL3, HMGB1, HNRNPH1, HNRNPM, HSPD1, IFRD2, ILF3, IMPDH2, LDHB, LSM4, LSM7, LYPLA1, MAGEC1, MCM7, MKI67IP, MRPL15, MRPL37, MRPL4, MRPS12, NDUFA11, NME2, NOP16, NPM1, NREP, PLEKHJ1, POLR1D, POLR2E, PRMT1, RPL10, RPL14, RPL15, RPL19, RPL22, RPL27A, RPL30, RPL32, RPL35, RPL39, RPL7, RPL7A, RPL9, RPLP2, RPS2, RPS20, RPS25, RPS3A, RQCD1, RSL1D1, SERBP1, SLC25A6, SMARCA4, SMIM15, SNHG15, SNRPB, SNRPC, SNRPD1, SNRPD2, SRM, SSB, TIMM13, TIMM44, TPI1, TRAP1, TRIM28, TYMS, UCK2, UHRF1, XIST, ZFAS1, AHNAK, APOD, ATP1A1, B2M, CD44, CD63, CTSB, CTSD, FOS, GRN, HLA-A, HLA-B, HLA-C, HLA-E, HLA-H, LAMP2, LGALS3, LGALS3BP, NPC2, PSAP, SERPINE2, TAPBP, TIMP2, A2M, ACSL3, AEBP1, AGA, APOC2, APOE, ATP1B1, CD151, CD47, CD58, CD59, CDH19, CSPG4, CST3, CTSA, CTSL1, CTSO, CYP27A1, DAG1, DDR1, EEA1, EMP1, EVA1A, FBXO32, FGFR1, GAA, GPNMB, GSN, HLA-F, HSPA1A, IRF4, ITGA3, KCNN4, LEF1-AS1, LRPAP1, MFGE8, MIA, MT2A, NEAT1, NPC1, NSG1, PROS1, S100A6, S100B, SAT1, SCARB2, SDC3, SEC11C, SERPINA3, SGK1, SLC26A2, SLC5A3, STX7, TIMP1, TIMP3, TM4SF1, TMED10, TPP1, TSC22D3, TYR, UBC, VAT1, WBP2, XAGE1D, APOL1, ARSA, ATP6V0C, C4A, CARD16, CAV2, CDH1, CYP4V2, FLNA, GATSL3, GJB1, GPR155, GPR56, HLA-G, IFI27, IFI27L2, IFI6, IGFBP7, IGSF8, ITGA7, LAMB2, LGMN, LOC100126784, LOC100506190, LY6E, LYRM9, MALAT1, MATN2, MCAM, MMP14, MPZ, MTRNR2L1, MTRNR2L10, MTRNR2L2, MTRNR2L3, MTRNR2L4, MTRNR2L5, MTRNR2L6, MTRNR2L7, MTRNR2L8, MYO1D, NAV2, NFE2L1, PDE4DIP, PERP, QPCT, RDH5, S100A1, S100A13, SERINC1, SERPINA1, SHC4, SLC7A8, SNX9, SORT1, SPON2, SPP1, STRIP2, SYNE2, THBD, TMBIM6, TMEM255A, TNFSF4, TRIML2,

TSPYL2 and TXNIP.

[0024] In certain embodiments, the exclusion signature comprises an exclusion-down signature, said signature comprising one or more genes selected from the group consisting of: APOC2, CYP27A1, IRF4, SEC11C, STX7, WBP2, XAGE1D, PAGE5 and WDFY1; or AHNAK, APOD, ATP1A1, B2M, CD44, CD63, CTSB, CTSD, FOS, GRN, HLA-A, HLA-B, HLA-C, HLA-E, HLA-H, LAMP2, LGALS3, LGALS3BP, NPC2, PSAP, SERPINE2, TAPBP, TIMP2, A2M, ACSL3, AEBP1, AGA, APOC2, APOE, ATP1B1, CD151, CD47, CD58, CD59, CDH19, CSPG4, CST3, CTSA, CTSL1, CTSO, CYP27A1, DAG1, DDR1, EEA1, EMP1, EVA1A, FBXO32, FGFR1, GAA, GPNMB, GSN, HLA-F, HSPA1A, IRF4, ITGA3, KCNN4, LEF1-AS1, LRPAP1, MFGE8, MIA, MT2A, NEAT1, NPC1, NSG1, PROS1, S100A6, S100B, SAT1, SCARB2, SDC3, SEC11C, SERPINA3, SGK1, SLC26A2, SLC5A3, STX7, TIMP1, TIMP3, TM4SF1, TMED10, TPP1, TSC22D3, TYR, UBC, VAT1, WBP2, XAGE1D, APOL1, ARSA, ATP6V0C, C4A, CARD16, CAV2, CDH1, CYP4V2, FLNA, GATSL3, GJB1, GPR155, GPR56, HLA-G, IFI27, IFI27L2, IFI6, IGFBP7, IGSF8, ITGA7, LAMB2, LGMN, LOC100126784, LOC100506190, LY6E, LYRM9, MALAT1, MATN2, MCAM, MMP14, MPZ, MTRNR2L1, MTRNR2L10, MTRNR2L2, MTRNR2L3, MTRNR2L4, MTRNR2L5, MTRNR2L6, MTRNR2L7, MTRNR2L8, MYO1D, NAV2, NFE2L1, PDE4DIP, PERP, QPCT, RDH5, S100A1, S100A13, SERINC1, SERPINA1, SHC4, SLC7A8, SNX9, SORT1, SPON2, SPP1, STRIP2, SYNE2, THBD, TMBIM6, TMEM255A, TNFSF4, TRIML2, TSPYL2 and TXNIP, wherein said exclusion-down signature is downregulated in a tumor with T cell exclusion and is upregulated in a tumor with T cell infiltration.

[0025] In certain embodiments, the exclusion signature comprises an exclusion-up signature, said signature comprising one or more genes selected from the group consisting of: BZW2, CCT3, CDK4, GPATCH4, ISYNA1, MDH2, RUVBL2, AHCY, CCT6A, FKBP4, NME1, PAICS, POLD2, PUF60, RRS1, SLC19A1, SLC25A13, TOP1MT, HSP90AB1 and RTKN; or BZW2, CCT3, CDK4, GPATCH4, ISYNA1, MDH2, PPIA, RPL31, RPL37A, RPL41, RPS21, RPS27A, RUVBL2, SAE1, UBA52, AHCY, C17orf76-AS1, C19orf48, C1QBP, CCT6A, CHCHD2, CTPS1, EEF1G, EIF2S3, EIF3K, EIF4A1, FARSA, FBL, FKBP4, GAS5, GNB2L1, GPI, HNRNPA1, HNRNPC, IDH2, ILF2, NACA, NCL, NME1, NOLC1, PABPC1, PAICS, PFN1, POLD2, PPA1, PTMA, PUF60, RPL10A, RPL11, RPL12, RPL13, RPL13A, RPL13AP5, RPL17, RPL18, RPL18A, RPL21, RPL26, RPL27, RPL28, RPL29, RPL3, RPL36, RPL36A, RPL37, RPL4, RPL5, RPL6, RPL8, RPLP0,

RPLP1, RPS10, RPS11, RPS13, RPS14, RPS15, RPS15A, RPS16, RPS17, RPS17L, RPS18, RPS19, RPS23, RPS24, RPS27, RPS28, RPS3, RPS4X, RPS5, RPS6, RPS7, RPS8, RPS9, RPSA, RRS1, SERPINF1, SET, SHMT2, SLC19A1, SLC25A13, SNHG6, SNRPE, SOX4, SSR2, TIMM50, TOP1MT, TUBB, UQCRFS1, UQCRH, VDAC2, APP, ATP5D, ATP5G3, BOP1, BTF3, C6orf48, CACYBP, CCT4, CCT7, CDCA7, DARS, DCTPP1, DDX21, EEF1B2, EEF1D, EEF2, EIF3E, EIF3F, EIF3G, EIF3M, ENO1, EXOSC5, FAM92A1, GGH, GNL3, HMGB1, HNRNPH1, HNRNPM, HSPD1, IFRD2, ILF3, IMPDH2, LDHB, LSM4, LSM7, LYPLA1, MAGEC1, MCM7, MKI67IP, MRPL15, MRPL37, MRPL4, MRPS12, NDUFA11, NME2, NOP16, NPM1, NREP, PLEKHJ1, POLR1D, POLR2E, PRMT1, RPL10, RPL14, RPL15, RPL19, RPL22, RPL27A, RPL30, RPL32, RPL35, RPL39, RPL7, RPL7A, RPL9, RPLP2, RPS2, RPS20, RPS25, RPS3A, RQCD1, RSL1D1, SERBP1, SLC25A6, SMARCA4, SMIM15, SNHG15, SNRPB, SNRPC, SNRPD1, SNRPD2, SRM, SSB, TIMM13, TIMM44, TPI1, TRAP1, TRIM28, TYMS, UCK2, UHRF1, XIST and ZFAS1, wherein said exclusion-up signature is upregulated in a tumor with T cell exclusion and is downregulated in a tumor with T cell infiltration.

[0026] In certain embodiments, the method according to any embodiment herein further comprises detecting the abundance of tumor infiltrating lymphocytes (TIL). In certain embodiments, the gene signature is detected in a bulk tumor sample, whereby the gene signature is detected by deconvolution of bulk expression data such that gene expression is assigned to malignant cells and non-malignant cells in said tumor sample. In certain embodiments, detecting the gene signature comprises detecting downregulation of the down signature and/or upregulation of the up signature, and wherein not detecting the gene signature comprises detecting upregulation of the down signature and/or downregulation of the up signature. In certain embodiments, detecting the signature and/or TILs indicates lower progression free survival and/or resistance to checkpoint blockade therapy, and wherein not detecting the signature and/or TILs indicates higher progression free survival and/or sensitivity to checkpoint blockade therapy. In certain embodiments, detecting the gene signature indicates a 10-year survival rate less than 40% and wherein not detecting the signature indicates a 10-year survival rate greater than 60%.

[0027] In certain embodiments, detecting an ICR signature in a tumor further comprises detecting in tumor infiltrating lymphocytes (TIL) obtained from the subject in need thereof the expression or activity of a CD8 T cell gene signature, said signature comprising one or more genes or polypeptides selected from Table 27B.2.

[0028] In certain embodiments, detecting an ICR signature in a tumor further comprises detecting in macrophages obtained from the subject in need thereof the expression or activity of a macrophage gene signature, said signature comprising one or more genes or polypeptides selected from Table 27C.

[0029] In another aspect, the present invention provides for a method of stratifying cancer patients into a high survival group and a low survival group comprising detecting the expression or activity of an ICR and/or exclusion signature in a tumor according to any embodiment herein, wherein if the signature is detected the patient is in the low survival group and if the signature is not detected the patient is in the high survival group. In certain embodiments, patients in the high survival group are immunotherapy responders and patients in the low survival group are immunotherapy non-responders.

[0030] In another aspect, the present invention provides for a method of treating a cancer in a subject in need thereof comprising detecting the expression or activity of an ICR and/or exclusion signature according to any embodiment herein in a tumor obtained from the subject and administering a treatment, wherein if an ICR and/or exclusion signature is detected the treatment comprises administering a treatment regimen comprising an immunotherapy followed by a CDK4/6 inhibitor and an immunotherapy.

[0031] In another aspect, the present invention provides for a method of treating a cancer in a subject in need thereof comprising administering a treatment regimen comprising an immunotherapy followed by a CDK4/6 inhibitor and an immunotherapy.

[0032] In certain embodiments, the CDK4/6 inhibitor comprises abemaciclib. In certain embodiments, the CDK4/6 inhibitor inhibits the expression or activity of one or more CDK7 targets selected from the group consisting of GPATCH4, RPL31, RPL41, C19orf48, EIF4A1, NME1, PABPC1, PTMA, RPL10A, RPL13, RPL28, RPL29, RPL3, RPL36, RPL5, RPLP0, RPLP1, RPS11, RPS15, RPS15A, RPS27, RPS28, RPS3, RPS5, RPS6, RPS7, RPS8, RPS9, SNRPE, SOX4, ACTB, ANP32E, C6orf48, CCT4, DDX39B, EIF3G, FTL, HNRNPH1, HSP90AB1, HSPA8, IMPDH2, LSM7, MRPL15, MRPL47, NDUFS2, NPM1, RPL10, RPL7A, RPS12, RPS2, RPS20, RPS3A, RSL1D1, SCNM1, SNRPC, TPI1, TRIM28, TUBA1B and YWHAE. In certain embodiments, the immunotherapy comprises a check point inhibitor. In certain embodiments, the checkpoint inhibitor comprises anti-CTLA4, anti-PD-L1, anti-PD1, anti-TIM3, anti-TIGIT, anti-LAG3 or a combination thereof. In certain embodiments, the cancer is melanoma or breast cancer. In certain embodiments, the checkpoint inhibitors are administered and the CDK4/6 inhibitor and checkpoint inhibitor are

administered between 14 days and 6 months after the first checkpoint inhibitors are administered.

[0033] In another aspect, the present invention provides for a method of treating a cancer in a subject in need thereof comprising administering a combination treatment regimen comprising an immunotherapy and one or more drugs selected from Table 16.

[0034] In another aspect, the present invention provides for a method of detecting an immune checkpoint inhibitor resistance (ICR) gene signature in a tumor comprising, detecting in tumor cells obtained from a subject in need thereof the expression or activity of a malignant cell gene signature comprising: one or more genes or polypeptides selected from the group consisting of C1QBP, CCT2, CCT6A, DCAF13, EIF4A1, ILF2, MAGEA4, NONO, PA2G4, PGAM1, PPA1, PPIA, RPL18A, RPL26, RPL31, RPS11, RPS15, RPS21, RPS5, RUVBL2, SAE1, SNRPE, UBA52, UQCRH, VDAC2, AEBP1, AHNAK, APOC2, APOD, APOE, B2M, C10orf54, CD63, CTSD, EEA1, EMP1, FBXO32, FYB, GATSL3, HCP5, HLA-A, HLA-B, HLA-C, HLA-E, HLA-F, HLA-H, ITGA3, LAMP2, LYRM9, MFGE8, MIA, NPC2, NSG1, PROS1, RDH5, SERPINA1, TAPBP, TIMP2, TNFSF4 and TRIML2 (refined uICR, see table 5); or one or more genes or polypeptides selected from the group consisting of ACAT1, ACP5, ACTB, ACTG1, ADSL, AEN, AK2, ANP32E, APP, ASAP1, ATP5A1, ATP5D, ATP5G2, BANCR, BCAN, BZW2, C17orf76-AS1, C1QBP, C20orf112, C6orf48, CA14, CBX5, CCT2, CCT3, CCT6A, CDK4, CEP170, CFL1, CHP1, CNRIP1, CRABP2, CS, CTPS1, CYC1, DAP3, DCAF13, DCT, DDX21, DDX39B, DLL3, EDNRB, EEF1D, EEF1G, EEF2, EIF1AX, EIF2S3, EIF3E, EIF3K, EIF3L, EIF4A1, EIF4EBP2, ESRP1, FAM174B, FAM178B, FAM92A1, FBL, FBLN1, FOXRED2, FTL, FUS, GABARAP, GAS5, GNB2L1, GPATCH4, GPI, GRWD1, GSTO1, H3F3A, H3F3AP4, HMGA1, HNRNPA1, HNRNPA1P10, HNRNPC, HSPA8, IDH2, IFI16, ILF2, IMPDH2, ISYNA1, ITM2C, KIAA0101, LHFPL3-AS1, LOC100190986, LYPLA1, MAGEA4, MARCKS, MDH2, METAP2, MID1, MIR4461, MLLT11, MPZL1, MRPL37, MRPS12, MRPS21, MYC, NACA, NCL, NDUFS2, NF2, NID1, NOLC1, NONO, NPM1, NUCKS1, OAT, PA2G4, PABPC1, PAFAH1B3, PAICS, PFDN2, PFN1, PGAM1, PIH1D1, PLTP, PPA1, PPIA, PPP2R1A, PSAT1, PSMD4, PTMA, PYCARD, RAN, RASA3, RBM34, RNF2, RPAIN, RPL10, RPL10A, RPL11, RPL12, RPL13, RPL13A, RPL13AP5, RPL14, RPL17, RPL18, RPL18A, RPL21, RPL26, RPL28, RPL29, RPL3, RPL30, RPL31, RPL35, RPL36A, RPL37, RPL37A, RPL39, RPL4, RPL41, RPL5, RPL6, RPL7, RPL7A, RPL8, RPLP0, RPLP1, RPS10, RPS11, RPS12, RPS15, RPS15A, RPS16, RPS17, RPS17L, RPS18,

RPS19, RPS2, RPS21, RPS23, RPS24, RPS26, RPS27, RPS27A, RPS3, RPS3A, RPS4X, RPS5, RPS6, RPS7, RPS8, RPS9, RPSA, RSL1D1, RUVBL2, SAE1, SCD, SCNM1, SERBP1, SERPINF1, SET, SF3B4, SHMT2, SKP2, SLC19A1, SLC25A3, SLC25A5, SLC25A6, SMS, SNAI2, SNHG16, SNHG6, SNRPE, SORD, SOX4, SRP14, SSR2, TIMM13, TIMM50, TMC6, TOP1MT, TP53, TRAP1, TRPM1, TSR1, TUBA1B, TUBB, TUBB4A, TULP4, TXLNA, TYRP1, UBA52, UCK2, UQCRFS1, UQCRH, USP22, VCY1B, VDAC2, VPS72, YWHAE, ZFAS1, ZNF286A, A2M, ACSL3, ACSL4, ADM, AEBP1, AGA, AHNAK, ANGPTL4, ANXA1, ANXA2, APLP2, APOC2, APOD, APOE, ARF5, ARL6IP5, ATF3, ATP1A1, ATP1B1, ATP1B3, ATRAID, B2M, BACE2, BBX, BCL6, C10orf54, C4A, CALU, CASP1, CAST, CAV1, CBLB, CCND3, CD151, CD44, CD47, CD58, CD59, CD63, CD9, CDH19, CHI3L1, CHN1, CLIC4, CLU, CPVL, CRELD1, CRYAB, CSGALNACT1, CSPG4, CST3, CTSA, CTSB, CTSD, CTSL1, DAG1, DCBLD2, DDR1, DDX5, DPYSL2, DSCR8, DUSP4, DUSP6, DYNLRB1, ECM1, EEA1, EGR1, EMP1, EPHX2, ERBB3, EVA1A, EZH1, EZR, FAM3C, FBXO32, FCGR2C, FCRLA, FGFR1, FLJ43663, FOS, FYB, GAA, GADD45B, GATSL3, GEM, GOLGB1, GPNMB, GRN, GSN, HCP5, HLA-A, HLA-B, HLA-C, HLA-E, HLA-F, HLA-H, HPCAL1, HSPA1A, HSPA1B, HTATIP2, ID2, IFI27L2, IFI35, IGF1R, IL1RAP, IL6ST, ISCU, ITGA3, ITGA6, ITGA7, ITGB1, ITGB3, ITM2B, JUN, KCNN4, KLF4, KLF6, KRT10, LAMP2, LEPROT, LGALS1, LGALS3, LGALS3BP, LOC100506190, LPL, LRPAP1, LTBP3, LYRM9, MAEL, MAGEC2, MAP1B, MATN2, MFGE8, MFI2, MIA, MRPS6, MT1E, MT1M, MT1X, MT2A, NDRG1, NEAT1, NFKBIA, NFKBIZ, NNMT, NPC1, NPC2, NR4A1, NSG1, OCIAD2, PAGE5, PDK4, PERP, PKM, PLP2, PRKCDBP, PRNP, PROS1, PRSS23, PSAP, PSMB9, PTRF, RDH5, RNF145, RPS4Y1, S100A13, S100A6, S100B, SAT1, SCARB2, SCCPDH, SDC3, SEL1L, SEMA3B, SERPINA1, SERPINA3, SERPINE2, SGCE, SGK1, SLC20A1, SLC26A2, SLC39A14, SLC5A3, SNX9, SOD1, SPON2, SPRY2, SQSTM1, SRPX, STOM, SYNGR2, SYPL1, TAPBP, TAPBPL, TF, TGOLN2, THBD, TIMP1, TIMP2, TIMP3, TIPARP, TM4SF1, TMBIM6, TMED10, TMED9, TMEM66, TMX4, TNC, TNFSF4, TPP1, TRIML2, TSC22D3, TSPYL2, TXNIP, TYR, UBC, UPP1, XAGE1A, XAGE1B, XAGE1C, XAGE1D, XAGE1E, ZBTB20 and ZBTB38 (uICR, see table 5); or one or more genes or polypeptides selected from the group consisting of ANP32E, CTPS1, DDX39B, EIF4A1, ESRP1, FBL, FUS, HNRNPA1, ILF2, KIAA0101, NUCKS1, PTMA, RPL21, RUVBL2, SET, SLC25A5, TP53, TUBA1B, UCK2, YWHAE, APLP2, ARL6IP5, CD63, CLU, CRELD1, CTSD, CTSL1, FOS, GAA, GRN,

HLA-F, ITM2B, LAMP2, MAP1B, NPC2, PSAP, SCARB2, SDC3, SEL1L, TMED10 and TSC22D3 (uICR, see Fig. 3C); or one or more genes or polypeptides selected from the group consisting of MT1E, MT1M, MT1X and MT2A.

[0035] In certain embodiments, the ICR signature may comprises a ICR-down signature, said signature comprising one or more genes selected from the group consisting of: AEBP1, AHNAK, APOC2, APOD, APOE, B2M, C10orf54, CD63, CTSD, EEA1, EMP1, FBXO32, FYB, GATSL3, HCP5, HLA-A, HLA-B, HLA-C, HLA-E, HLA-F, HLA-H, ITGA3, LAMP2, LYRM9, MFGE8, MIA, NPC2, NSG1, PROS1, RDH5, SERPINA1, TAPBP, TIMP2, TNFSF4 and TRIML2 (refined uICR-down, see table 5); or A2M, ACSL3, ACSL4, ADM, AEBP1, AGA, AHNAK, ANGPTL4, ANXA1, ANXA2, APLP2, APOC2, APOD, APOE, ARF5, ARL6IP5, ATF3, ATP1A1, ATP1B1, ATP1B3, ATRAID, B2M, BACE2, BBX, BCL6, C10orf54, C4A, CALU, CASP1, CAST, CAV1, CBLB, CCND3, CD151, CD44, CD47, CD58, CD59, CD63, CD9, CDH19, CHI3L1, CHN1, CLIC4, CLU, CPVL, CRELD1, CRYAB, CSGALNACT1, CSPG4, CST3, CTSA, CTSB, CTSD, CTSL1, DAG1, DCBLD2, DDR1, DDX5, DPYSL2, DSCR8, DUSP4, DUSP6, DYNLRB1, ECM1, EEA1, EGR1, EMP1, EPHX2, ERBB3, EVA1A, EZH1, EZR, FAM3C, FBXO32, FCGR2C, FCRLA, FGFR1, FLJ43663, FOS, FYB, GAA, GADD45B, GATSL3, GEM, GOLGB1, GPNMB, GRN, GSN, HCP5, HLA-A, HLA-B, HLA-C, HLA-E, HLA-F, HLA-H, HPCAL1, HSPA1A, HSPA1B, HTATIP2, ID2, IFI27L2, IFI35, IGF1R, IL1RAP, IL6ST, ISCU, ITGA3, ITGA6, ITGA7, ITGB1, ITGB3, ITM2B, JUN, KCNN4, KLF4, KLF6, KRT10, LAMP2, LEPROT, LGALS1, LGALS3, LGALS3BP, LOC100506190, LPL, LRPAP1, LTBP3, LYRM9, MAEL, MAGEC2, MAP1B, MATN2, MFGE8, MFI2, MIA, MRPS6, MT1E, MT1M, MT1X, MT2A, NDRG1, NEAT1, NFKBIA, NFKBIZ, NNMT, NPC1, NPC2, NR4A1, NSG1, OCIAD2, PAGE5, PDK4, PERP, PKM, PLP2, PRKCDBP, PRNP, PROS1, PRSS23, PSAP, PSMB9, PTRF, RDH5, RNF145, RPS4Y1, S100A13, S100A6, S100B, SAT1, SCARB2, SCCPDH, SDC3, SEL1L, SEMA3B, SERPINA1, SERPINA3, SERPINE2, SGCE, SGK1, SLC20A1, SLC26A2, SLC39A14, SLC5A3, SNX9, SOD1, SPON2, SPRY2, SQSTM1, SRPX, STOM, SYNGR2, SYPL1, TAPBP, TAPBPL, TF, TGOLN2, THBD, TIMP1, TIMP2, TIMP3, TIPARP, TM4SF1, TMBIM6, TMED10, TMED9, TMEM66, TMX4, TNC, TNFSF4, TPP1, TRIML2, TSC22D3, TSPYL2, TXNIP, TYR, UBC, UPP1, XAGE1A, XAGE1B, XAGE1C, XAGE1D, XAGE1E, ZBTB20 and ZBTB38 (uICR-down, see table 5); or APLP2, ARL6IP5, CD63, CLU, CRELD1, CTSD, CTSL1, FOS, GAA, GRN, HLA-F, ITM2B, LAMP2, MAP1B, NPC2, PSAP, SCARB2,

SDC3, SEL1L, TMED10 and TSC22D3 (uICR-down, see Fig. 3C), wherein said ICR-down signature is downregulated in a tumor with a high ICR score and upregulated in a tumor with a low ICR score.

[0036] In certain embodiments, the ICR signature comprises a ICR-up signature, said signature comprising one or more genes selected from the group consisting of: C1QBP, CCT2, CCT6A, DCAF13, EIF4A1, ILF2, MAGEA4, NONO, PA2G4, PGAM1, PPA1, PPIA, RPL18A, RPL26, RPL31, RPS11, RPS15, RPS21, RPS5, RUVBL2, SAE1, SNRPE, UBA52, UQCRH and VDAC2 (refined uICR-up, see table 5); or ACAT1, ACP5, ACTB, ACTG1, ADSL, AEN, AK2, ANP32E, APP, ASAP1, ATP5A1, ATP5D, ATP5G2, BANCR, BCAN, BZW2, C17orf76-AS1, C1QBP, C20orf112, C6orf48, CA14, CBX5, CCT2, CCT3, CCT6A, CDK4, CEP170, CFL1, CHP1, CNRIP1, CRABP2, CS, CTPS1, CYC1, DAP3, DCAF13, DCT, DDX21, DDX39B, DLL3, EDNRB, EEF1D, EEF1G, EEF2, EIF1AX, EIF2S3, EIF3E, EIF3K, EIF3L, EIF4A1, EIF4EBP2, ESRP1, FAM174B, FAM178B, FAM92A1, FBL, FBLN1, FOXRED2, FTL, FUS, GABARAP, GAS5, GNB2L1, GPATCH4, GPI, GRWD1, GSTO1, H3F3A, H3F3AP4, HMGA1, HNRNPA1, HNRNPA1P10, HNRNPC, HSPA8, IDH2, IFI16, ILF2, IMPDH2, ISYNA1, ITM2C, KIAA0101, LHFPL3-AS1, LOC100190986, LYPLA1, MAGEA4, MARCKS, MDH2, METAP2, MID1, MIR4461, MLLT11, MPZL1, MRPL37, MRPS12, MRPS21, MYC, NACA, NCL, NDUFS2, NF2, NID1, NOLC1, NONO, NPM1, NUCKS1, OAT, PA2G4, PABPC1, PAFAH1B3, PAICS, PFDN2, PFN1, PGAM1, PIH1D1, PLTP, PPA1, PPIA, PPP2R1A, PSAT1, PSMD4, PTMA, PYCARD, RAN, RASA3, RBM34, RNF2, RPAIN, RPL10, RPL10A, RPL11, RPL12, RPL13, RPL13A, RPL13AP5, RPL14, RPL17, RPL18, RPL18A, RPL21, RPL26, RPL28, RPL29, RPL3, RPL30, RPL31, RPL35, RPL36A, RPL37, RPL37A, RPL39, RPL4, RPL41, RPL5, RPL6, RPL7, RPL7A, RPL8, RPLP0, RPLP1, RPS10, RPS11, RPS12, RPS15, RPS15A, RPS16, RPS17, RPS17L, RPS18, RPS19, RPS2, RPS21, RPS23, RPS24, RPS26, RPS27, RPS27A, RPS3, RPS3A, RPS4X, RPS5, RPS6, RPS7, RPS8, RPS9, RPSA, RSL1D1, RUVBL2, SAE1, SCD, SCNM1, SERBP1, SERPINF1, SET, SF3B4, SHMT2, SKP2, SLC19A1, SLC25A3, SLC25A5, SLC25A6, SMS, SNAI2, SNHG16, SNHG6, SNRPE, SORD, SOX4, SRP14, SSR2, TIMM13, TIMM50, TMC6, TOP1MT, TP53, TRAP1, TRPM1, TSR1, TUBA1B, TUBB, TUBB4A, TULP4, TXLNA, TYRP1, UBA52, UCK2, UQCRFS1, UQCRH, USP22, VCY1B, VDAC2, VPS72, YWHAE, ZFAS1 and ZNF286A (uICR-up, see table 5); or ANP32E, CTPS1, DDX39B, EIF4A1, ESRP1, FBL, FUS, HNRNPA1, ILF2, KIAA0101, NUCKS1, PTMA,

RPL21, RUVBL2, SET, SLC25A5, TP53, TUBA1B, UCK2 and YWHAE (uICR-up, see Fig. 3C), wherein said ICR-up signature is upregulated in a tumor with a high ICR score and downregulated in a tumor with a low ICR score.

[0037] In another aspect, the present invention provides for a method of detecting an immune checkpoint inhibitor resistance (ICR) gene signature in a tumor comprising, detecting in tumor cells obtained from a subject in need thereof the expression or activity of a malignant cell gene signature comprising: one or more genes or polypeptides selected from the group consisting of ACTB, AEN, ANP32E, ATP5A1, ATP5G2, BZW2, C17orf76-AS1, C1QBP, C20orf112, CA14, CBX5, CCT2, CCT3, CDK4, CFL1, CNRIP1, CRABP2, CS, CTPS1, DCAF13, DCT, DDX39B, DLL3, EEF1G, EIF2S3, EIF3K, EIF4A1, EIF4EBP2, FAM174B, FBL, FBLN1, FOXRED2, FTL, FUS, GABARAP, GAS5, GNB2L1, GPATCH4, GPI, GRWD1, H3F3A, H3F3AP4, HMGA1, HNRNPA1, HNRNPA1P10, HNRNPC, HSPA8, IDH2, ILF2, ISYNA1, ITM2C, KIAA0101, MAGEA4, MDH2, METAP2, MID1, MIR4461, MLLT11, MPZL1, MRPS21, NACA, NCL, NDUFS2, NOLC1, NONO, PA2G4, PABPC1, PAFAH1B3, PFDN2, PFN1, PGAM1, PIH1D1, PPA1, PPIA, PPP2R1A, PSMD4, PTMA, RAN, RBM34, RNF2, RPAIN, RPL10A, RPL11, RPL12, RPL13, RPL13A, RPL13AP5, RPL17, RPL18, RPL18A, RPL21, RPL26, RPL28, RPL29, RPL3, RPL31, RPL36A, RPL37, RPL37A, RPL39, RPL4, RPL41, RPL5, RPL6, RPL8, RPLP0, RPLP1, RPS10, RPS11, RPS12, RPS15A, RPS16, RPS17, RPS17L, RPS18, RPS19, RPS21, RPS23, RPS24, RPS26, RPS27, RPS27A, RPS3, RPS4X, RPS5, RPS6, RPS7, RPS8, RPS9, RPSA, RUVBL2, SAE1, SCD, SCNM1, SERPINF1, SET, SF3B4, SHMT2, SKP2, SLC25A3, SMS, SNAI2, SNHG6, SNRPE, SOX4, SRP14, SSR2, TIMM50, TMC6, TP53, TRPM1, TSR1, TUBA1B, TUBB, TULP4, UBA52, UQCRFS1, UQCRH, USP22, VCY1B, VDAC2, VPS72, YWHAE, ZNF286A, A2M, ACSL3, ACSL4, ADM, AEBP1, AGA, AHNAK, ANGPTL4, ANXA1, ANXA2, APLP2, APOD, APOE, ARL6IP5, ATF3, ATP1A1, ATP1B1, ATP1B3, B2M, BACE2, BBX, BCL6, CALU, CASP1, CAST, CAV1, CCND3, CD151, CD44, CD47, CD58, CD59, CD63, CD9, CDH19, CHI3L1, CLIC4, CRELD1, CRYAB, CSGALNACT1, CSPG4, CST3, CTSA, CTSB, CTSD, CTSL1, DAG1, DCBLD2, DDR1, DDX5, DPYSL2, DUSP4, DUSP6, ECM1, EEA1, EGR1, EMP1, EPHX2, ERBB3, EVA1A, EZH1, FAM3C, FBXO32, FCGR2C, FCRLA, FGFR1, FLJ43663, FOS, GAA, GADD45B, GEM, GOLGB1, GPNMB, GRN, GSN, HLA-A, HLA-B, HLA-C, HLA-E, HLA-F, HLA-H, HPCAL1, HSPA1A, HTATIP2, IFI35, IGF1R, IL1RAP, IL6ST, ITGA3, ITGA6, ITGB1, ITGB3, ITM2B, JUN, KCNN4, KLF4, KLF6, LAMP2, LEPROT, LGALS1,

LGALS3, LGALS3BP, LPL, LRPAP1, MAGEC2, MFGE8, MFI2, MIA, MT1E, MT1M, MT1X, MT2A, NEAT1, NFKBIA, NFKBIZ, NNMT, NPC1, NPC2, NR4A1, NSG1, PDK4, PLP2, PRKCDBP, PRNP, PROS1, PRSS23, PSAP, PSMB9, PTRF, RNF145, RPS4Y1, S100A6, S100B, SAT1, SCARB2, SCCPDH, SDC3, SEL1L, SEMA3B, SERPINA3, SERPINE2, SGCE, SGK1, SLC20A1, SLC26A2, SLC39A14, SLC5A3, SOD1, SPRY2, SQSTM1, SRPX, STOM, SYNGR2, SYPL1, TAPBP, TAPBPL, TF, TGOLN2, TIMP1, TIMP2, TIMP3, TIPARP, TM4SF1, TMED10, TMED9, TMEM66, TMX4, TNC, TPP1, TSC22D3, TYR, UBC, UPP1, ZBTB20 and ZBTB38 (oncogenic ICR, see table 5); or one or more genes or polypeptides selected from the group consisting of AEN, ATP5A1, C20orf112, CCT2, DCAF13, DDX39B, ISYNA1, NDUFS2, NOLC1, PA2G4, PPP2R1A, RBM34, RNF2, RPL6, RPL21, SERPINF1, SF3B4, SMS, TMC6, VPS72, ANXA1, ATF3, BCL6, CD58, CD9, CTSB, DCBLD2, EMP1, HLA-F, HTATIP2, IL1RAP, ITGA6, KCNN4, KLF4, MT1E, MT1M, MT1X, MT2A, NNMT, PRKCDBP, S100A6 and TSC22D3 (oncogenic ICR, see Fig. 2B); or one or more genes or polypeptides selected from the group consisting of ACTB, ANP32E, CBX5, FUS, HNRNPA1, IDH2, KIAA0101, NCL, PFN1, PPIA, PTMA, RAN, RPLP0, TUBA1B, TUBB, VCY1B, A2M, APOD, BCL6, CD44, CD59, CD63, CDH19, CHI3L1, CTSA, CTSB, CTSD, FOS, GPNMB, GRN, HLA-A, HLA-B, HLA-H, ITM2B, LGALS3BP, NEAT1, PDK4, PSAP, SCARB2, SERPINA3, SLC26A2, TAPBPL, TMEM66 and TYR (oncogenic ICR, see Fig. 10B); or one or more genes or polypeptides selected from the group consisting of MT1E, MT1M, MT1X and MT2A.

[0038] In certain embodiments, the ICR signature comprises an ICR-down signature, said signature comprising one or more genes selected from the group consisting of: A2M, ACSL3, ACSL4, ADM, AEBP1, AGA, AHNAK, ANGPTL4, ANXA1, ANXA2, APLP2, APOD, APOE, ARL6IP5, ATF3, ATP1A1, ATP1B1, ATP1B3, B2M, BACE2, BBX, BCL6, CALU, CASP1, CAST, CAV1, CCND3, CD151, CD44, CD47, CD58, CD59, CD63, CD9, CDH19, CHI3L1, CLIC4, CRELD1, CRYAB, CSGALNACT1, CSPG4, CST3, CTSA, CTSB, CTSD, CTSL1, DAG1, DCBLD2, DDR1, DDX5, DPYSL2, DUSP4, DUSP6, ECM1, EEA1, EGR1, EMP1, EPHX2, ERBB3, EVA1A, EZH1, FAM3C, FBXO32, FCGR2C, FCRLA, FGFR1, FLJ43663, FOS, GAA, GADD45B, GEM, GOLGB1, GPNMB, GRN, GSN, HLA-A, HLA-B, HLA-C, HLA-E, HLA-F, HLA-H, HPCAL1, HSPA1A, HTATIP2, IFI35, IGF1R, IL1RAP, IL6ST, ITGA3, ITGA6, ITGB1, ITGB3, ITM2B, JUN, KCNN4, KLF4, KLF6, LAMP2, LEPROT, LGALS1, LGALS3, LGALS3BP, LPL, LRPAP1, MAGEC2, MFGE8, MFI2, MIA, MT1E, MT1M, MT1X, MT2A, NEAT1, NFKBIA,

NFKBIZ, NNMT, NPC1, NPC2, NR4A1, NSG1, PDK4, PLP2, PRKCDBP, PRNP, PROS1, PRSS23, PSAP, PSMB9, PTRF, RNF145, RPS4Y1, S100A6, S100B, SAT1, SCARB2, SCCPDH, SDC3, SEL1L, SEMA3B, SERPINA3, SERPINE2, SGCE, SGK1, SLC20A1, SLC26A2, SLC39A14, SLC5A3, SOD1, SPRY2, SQSTM1, SRPX, STOM, SYNGR2, SYPL1, TAPBP, TAPBPL, TF, TGOLN2, TIMP1, TIMP2, TIMP3, TIPARP, TM4SF1, TMED10, TMED9, TMEM66, TMX4, TNC, TPP1, TSC22D3, TYR, UBC, UPP1, ZBTB20 and ZBTB38 (oncogenic ICR down, see table 5); or ANXA1, ATF3, BCL6, CD58, CD9, CTSB, DCBLD2, EMP1, HLA-F, HTATIP2, IL1RAP, ITGA6, KCNN4, KLF4, MT1E, MT1M, MT1X, MT2A, NNMT, PRKCDBP, S100A6 and TSC22D3 (oncogenic ICR down, see Fig. 2B); or A2M, APOD, BCL6, CD44, CD59, CD63, CDH19, CHI3L1, CTSA, CTSB, CTSD, FOS, GPNMB, GRN, HLA-A, HLA-B, HLA-H, ITM2B, LGALS3BP, NEAT1, PDK4, PSAP, SCARB2, SERPINA3, SLC26A2, TAPBPL, TMEM66 and TYR (oncogenic ICR down, see Fig. 10B), wherein said ICR-down signature is downregulated in a tumor with a high ICR score and upregulated in a tumor with a low ICR score.

[0039] In certain embodiments, the ICR signature comprises an ICR-up signature, said signature comprising one or more genes selected from the group consisting of: ACTB, AEN, ANP32E, ATP5A1, ATP5G2, BZW2, C17orf76-AS1, C1QBP, C20orf112, CA14, CBX5, CCT2, CCT3, CDK4, CFL1, CNRIP1, CRABP2, CS, CTPS1, DCAF13, DCT, DDX39B, DLL3, EEF1G, EIF2S3, EIF3K, EIF4A1, EIF4EBP2, FAM174B, FBL, FBLN1, FOXRED2, FTL, FUS, GABARAP, GAS5, GNB2L1, GPATCH4, GPI, GRWD1, H3F3A, H3F3AP4, HMGA1, HNRNPA1, HNRNPA1P10, HNRNPC, HSPA8, IDH2, ILF2, ISYNA1, ITM2C, KIAA0101, MAGEA4, MDH2, METAP2, MID1, MIR4461, MLLT11, MPZL1, MRPS21, NACA, NCL, NDUFS2, NOLC1, NONO, PA2G4, PABPC1, PAFAH1B3, PFDN2, PFN1, PGAM1, PIH1D1, PPA1, PPIA, PPP2R1A, PSMD4, PTMA, RAN, RBM34, RNF2, RPAIN, RPL10A, RPL11, RPL12, RPL13, RPL13A, RPL13AP5, RPL17, RPL18, RPL18A, RPL21, RPL26, RPL28, RPL29, RPL3, RPL31, RPL36A, RPL37, RPL37A, RPL39, RPL4, RPL41, RPL5, RPL6, RPL8, RPLP0, RPLP1, RPS10, RPS11, RPS12, RPS15A, RPS16, RPS17, RPS17L, RPS18, RPS19, RPS21, RPS23, RPS24, RPS26, RPS27, RPS27A, RPS3, RPS4X, RPS5, RPS6, RPS7, RPS8, RPS9, RPSA, RUVBL2, SAE1, SCD, SCNM1, SERPINF1, SET, SF3B4, SHMT2, SKP2, SLC25A3, SMS, SNAI2, SNHG6, SNRPE, SOX4, SRP14, SSR2, TIMM50, TMC6, TP53, TRPM1, TSR1, TUBA1B, TUBB, TULP4, UBA52, UQCRFS1, UQCRH, USP22, VCY1B, VDAC2, VPS72, YWHAE and ZNF286A (oncogenic ICR up, see table 5); or AEN, ATP5A1, C20orf112, CCT2, DCAF13, DDX39B, ISYNA1, NDUFS2,

NOLC1, PA2G4, PPP2R1A, RBM34, RNF2, RPL6, RPL21, SERPINF1, SF3B4, SMS, TMC6, VPS72 (oncogenic ICR up, see Fig. 2B); or ACTB, ANP32E, CBX5, FUS, HNRNPA1, IDH2, KIAA0101, NCL, PFN1, PPIA, PTMA, RAN, RPLP0, TUBA1B, TUBB and VCY1B (oncogenic ICR up, see Fig. 10B), wherein said ICR-up signature is upregulated in a tumor with a high ICR score and downregulated in a tumor with a low ICR score. In certain embodiments, the ICR signature is detected in cycling cells.

[0040] In another aspect, the present invention provides for a method of detecting an immune cell exclusion gene signature in a tumor comprising, detecting in tumor cells obtained from a subject in need thereof the expression or activity of a malignant cell gene signature comprising: one or more genes or polypeptides selected from the group consisting of ACAT1, ACP5, ACTG1, ADSL, AK2, APP, ASAP1, ATP5D, BANCR, BCAN, BZW2, C17orf76-AS1, C1QBP, C6orf48, CA14, CCT3, CCT6A, CEP170, CHP1, CTPS1, CYC1, DAP3, DCT, DDX21, EDNRB, EEF1D, EEF1G, EEF2, EIF1AX, EIF2S3, EIF3E, EIF3K, EIF3L, EIF4A1, ESRP1, FAM178B, FAM92A1, FTL, GAS5, GNB2L1, GPI, GSTO1, IFI16, ILF2, IMPDH2, LHFPL3-AS1, LOC100190986, LYPLA1, MARCKS, MDH2, MRPL37, MRPS12, MYC, NCL, NF2, NID1, NOLC1, NPM1, NUCKS1, OAT, PABPC1, PAICS, PLTP, PSAT1, PYCARD, RASA3, RPL10, RPL10A, RPL11, RPL12, RPL13, RPL13A, RPL13AP5, RPL14, RPL17, RPL18, RPL18A, RPL28, RPL29, RPL3, RPL30, RPL35, RPL37A, RPL39, RPL4, RPL5, RPL6, RPL7, RPL7A, RPL8, RPLP0, RPLP1, RPS10, RPS11, RPS15, RPS15A, RPS16, RPS17, RPS17L, RPS18, RPS19, RPS2, RPS24, RPS27, RPS3, RPS3A, RPS4X, RPS5, RPS7, RPS8, RPS9, RPSA, RSL1D1, SCD, SERBP1, SERPINF1, SLC19A1, SLC25A5, SLC25A6, SNAI2, SNHG16, SNHG6, SORD, SOX4, TIMM13, TIMM50, TOP1MT, TRAP1, TUBB4A, TXLNA, TYRP1, UCK2, UQCRFS1, ZFAS1, A2M, AGA, AHNAK, ANXA1, APLP2, APOC2, ARF5, ATP1A1, ATP1B1, ATRAID, B2M, C10orf54, C4A, CBLB, CCND3, CD151, CD47, CD58, CD59, CDH19, CHN1, CLU, CPVL, CST3, CTSB, CTSD, CTSL1, DDR1, DPYSL2, DSCR8, DUSP6, DYNLRB1, EMP1, EZR, FAM3C, FGFR1, FYB, GAA, GATSL3, GRN, GSN, HCP5, HLA-B, HLA-C, HLA-F, HLA-H, HSPA1A, HSPA1B, ID2, IFI27L2, ISCU, ITGA3, ITGA7, ITGB3, KCNN4, KRT10, LOC100506190, LTBP3, LYRM9, MAEL, MAP1B, MATN2, MFGE8, MFI2, MIA, MRPS6, MT2A, NDRG1, NFKBIA, NPC1, OCIAD2, PAGE5, PERP, PKM, RDH5, S100A13, S100A6, SERPINA1, SERPINA3, SERPINE2, SGCE, SLC26A2, SLC5A3, SNX9, SPON2, THBD, TIMP1, TM4SF1, TMBIM6, TNFSF4, TPP1, TRIML2, TSC22D3, TSPYL2, TXNIP, UBC, XAGE1A, XAGE1B, XAGE1C,

XAGE1D and XAGE1E (exclusion, see table 5); or one or more genes or polypeptides selected from the group consisting of ACTG1, ADSL, C17orf76-AS1, C1QBP, CTPS1, EIF2S3, EIF3E, ILF2, NCL, NF2, NOLC1, PABPC1, PAICS, RPL10A, RPL18, RPL6, RPS24, RSL1D1, SERPINF1, SOX4, AHNAK, ANXA1, CCND3, CD151, CD47, CD58, CST3, CTSB, CTSD, EMP1, FGFR1, HLA-C, HLA-F, ITGB3, KCNN4, MIA, MT2A, S100A6, SLC5A3, TIMP1 and TSC22D3 (exclusion, see fig. 2H); or one or more genes or polypeptides selected from the group consisting of C17orf76-AS1, C1QBP, CTPS1, EIF2S3, ILF2, NCL, NOLC1, PABPC1, RPL10A, RPL18, RPL6, RPS24, SERPINF1, SOX4, AHNAK, ANXA1, CCND3, CD151, CD47, CD58, CST3, CTSB, CTSD, EMP1, FGFR1, HLA-C, HLA-F, ITGB3, KCNN4, MIA, MT2A, S100A6, SLC5A3, TIMP1 and TSC22D3 (exclusion, see fig. 2H).

[0041] In certain embodiments, the exclusion signature comprises an exclusion-down signature, said signature comprising one or more genes selected from the group consisting of: A2M, AGA, AHNAK, ANXA1, APLP2, APOC2, ARF5, ATP1A1, ATP1B1, ATRAID, B2M, C10orf54, C4A, CBLB, CCND3, CD151, CD47, CD58, CD59, CDH19, CHN1, CLU, CPVL, CST3, CTSB, CTSD, CTSL1, DDR1, DPYSL2, DSCR8, DUSP6, DYNLRB1, EMP1, EZR, FAM3C, FGFR1, FYB, GAA, GATSL3, GRN, GSN, HCP5, HLA-B, HLA-C, HLA-F, HLA-H, HSPA1A, HSPA1B, ID2, IFI27L2, ISCU, ITGA3, ITGA7, ITGB3, KCNN4, KRT10, LOC100506190, LTBP3, LYRM9, MAEL, MAP1B, MATN2, MFGE8, MFI2, MIA, MRPS6, MT2A, NDRG1, NFKBIA, NPC1, OCIAD2, PAGE5, PERP, PKM, RDH5, S100A13, S100A6, SERPINA1, SERPINA3, SERPINE2, SGCE, SLC26A2, SLC5A3, SNX9, SPON2, THBD, TIMP1, TM4SF1, TMBIM6, TNFSF4, TPP1, TRIML2, TSC22D3, TSPYL2, TXNIP, UBC, XAGE1A, XAGE1B, XAGE1C, XAGE1D and XAGE1E (exclusion-down, see table 5); or AHNAK, ANXA1, CCND3, CD151, CD47, CD58, CST3, CTSB, CTSD, EMP1, FGFR1, HLA-C, HLA-F, ITGB3, KCNN4, MIA, MT2A, S100A6, SLC5A3, TIMP1 and TSC22D3 (exclusion-down, see fig. 2H), wherein said exclusion-down signature is downregulated in a tumor with T cell exclusion and is upregulated in a tumor with T cell infiltration.

[0042] In certain embodiments, the exclusion signature comprises an exclusion-up signature, said signature comprising one or more genes selected from the group consisting of: ACAT1, ACP5, ACTG1, ADSL, AK2, APP, ASAP1, ATP5D, BANCR, BCAN, BZW2, C17orf76-AS1, C1QBP, C6orf48, CA14, CCT3, CCT6A, CEP170, CHP1, CTPS1, CYC1, DAP3, DCT, DDX21, EDNRB, EEF1D, EEF1G, EEF2, EIF1AX, EIF2S3, EIF3E, EIF3K,

EIF3L, EIF4A1, ESRP1, FAM178B, FAM92A1, FTL, GAS5, GNB2L1, GPI, GSTO1, IFI16, ILF2, IMPDH2, LHFPL3-AS1, LOC100190986, LYPLA1, MARCKS, MDH2, MRPL37, MRPS12, MYC, NCL, NF2, NID1, NOLC1, NPM1, NUCKS1, OAT, PABPC1, PAICS, PLTP, PSAT1, PYCARD, RASA3, RPL10, RPL10A, RPL11, RPL12, RPL13, RPL13A, RPL13AP5, RPL14, RPL17, RPL18, RPL18A, RPL28, RPL29, RPL3, RPL30, RPL35, RPL37A, RPL39, RPL4, RPL5, RPL6, RPL7, RPL7A, RPL8, RPLP0, RPLP1, RPS10, RPS11, RPS15, RPS15A, RPS16, RPS17, RPS17L, RPS18, RPS19, RPS2, RPS24, RPS27, RPS3, RPS3A, RPS4X, RPS5, RPS7, RPS8, RPS9, RPSA, RSL1D1, SCD, SERBP1, SERPINF1, SLC19A1, SLC25A5, SLC25A6, SNAI2, SNHG16, SNHG6, SORD, SOX4, TIMM13, TIMM50, TOP1MT, TRAP1, TUBB4A, TXLNA, TYRP1, UCK2, UQCRFS1 and ZFAS1 (exclusion-up, see table 5); or ACTG1, ADSL, C17orf76-AS1, C1QBP, CTPS1, EIF2S3, EIF3E, ILF2, NCL, NF2, NOLC1, PABPC1, PAICS, RPL10A, RPL18, RPL6, RPS24, RSL1D1, SERPINF1 and SOX4 (exclusion-up, see fig. 2H); or C17orf76-AS1, C1QBP, CTPS1, EIF2S3, ILF2, NCL, NOLC1, PABPC1, RPL10A, RPL18, RPL6, RPS24, SERPINF1 and SOX4 (exclusion-up, see fig. 2H), wherein said exclusion-up signature is upregulated in a tumor with T cell exclusion and is downregulated in a tumor with T cell infiltration.

[0043] In certain embodiments, the method according to any embodiment herein further comprises detecting tumor infiltrating lymphocytes (TIL). Not being bound by a theory, detecting tumor infiltration of immune cells is an independent indicator of immunotherapy resistance and progression free survival and combining detection of TILs with any of the above signatures may increase the prognostic value.

[0044] In certain embodiments, the gene signature according to any embodiment herein is detected in a bulk tumor sample, whereby the gene signature is detected by deconvolution of bulk expression data such that gene expression is assigned to malignant cells and non-malignant cells in said tumor sample.

[0045] In certain embodiments, detecting the gene signature comprises detecting downregulation of the down signature and/or upregulation of the up signature. In certain embodiments, not detecting the gene signature comprises detecting upregulation of the down signature and/or downregulation of the up signature. In certain embodiments, detecting the signature and/or TILs indicates lower progression free survival and/or resistance to checkpoint blockade therapy. In certain embodiments, not detecting the signature and/or TILs indicates higher progression free survival and/or sensitivity to checkpoint blockade therapy.

In certain embodiments, detecting the gene signature indicates a 10-year survival rate less than 40% and wherein not detecting the signature indicates a 10-year survival rate greater than 60%.

[0046] In certain embodiments, detecting an ICR signature in a tumor further comprises detecting in tumor infiltrating lymphocytes (TIL) obtained from the subject in need thereof the expression or activity of a CD8 T cell gene signature, said signature comprising one or more genes or polypeptides selected from the group consisting of CEP19, EXO5, FAM153C, FCRL6, GBP2, GBP5, HSPA1B, IER2, IRF1, KLRK1, LDHA, LOC100506083, MBOAT1, SEMA4D, SIRT3, SPDYE2, SPDYE2L, STAT1, STOM, UBE2Q2P3, ACP5, AKNA, BTN3A2, CCDC141, CD27, CDC42SE1, DDIT4, FAU, FKBP5, GPR56, HAVCR2, HLA-B, HLA-C, HLA-F, IL6ST, ITGA4, KIAA1551, KLF12, MIR155HG, MTA2, MTRNR2L1, MTRNR2L3, PIK3IP1, RPL26, RPL27, RPL27A, RPL35A, RPS11, RPS16, RPS20, RPS26, SPOCK2, SYTL3, TOB1, TPT1, TTN, TXNIP, WNK1 and ZFP36L2. In certain embodiments, detecting an ICR signature in a tumor further comprises detecting in macrophages obtained from the subject in need thereof the expression or activity of a macrophage gene signature, said signature comprising one or more genes or polypeptides selected from the group consisting of APOL1, CD274, CSTB, DCN, HLA-DPB2, HLA-DQA1, HLA-G, HSPA8, HSPB1, IL18BP, TMEM176A, UBD, A2M, ADAP2, ADORA3, ARL4C, ASPH, BCAT1, C11orf31, C3, C3AR1, C6orf62, CAPN2, CD200R1, CD28, CD9, CD99, COMT, CREM, CRTAP, CYFIP1, DDOST, DHRS3, EGFL7, EIF1AY, ETS2, FCGR2A, FOLR2, GATM, GBP3, GNG2, GSTT1, GYPC, HIST1H1E, HPGDS, IFI44L, IGFBP4, ITGA4, KCTD12, LGMN, LOC441081, LTC4S, LYVE1, MERTK, METTL7B, MS4A4A, MS4A7, MTSS1, NLRP3, OLFML3, PLA2G15, PLXDC2, PMP22, POR, PRDX2, PTGS1, RNASE1, ROCK1, RPS4Y1, S100A9, SCAMP2, SEPP1, SESN1, SLC18B1, SLC39A1, SLC40A1, SLC7A8, SORL1, SPP1, STAB1, TMEM106C, TMEM86A, TMEM9, TNFRSF1B, TNFRSF21, TPD52L2, ULK3 and ZFP36L2.

[0047] In another aspect, the present invention provides for a method of stratifying cancer patients into a high survival group and a low survival group comprising detecting the expression or activity of an ICR and/or exclusion signature in a tumor according to any embodiment herein, wherein if the signature is detected the patient is in the low survival group and if the signature is not detected the patient is in the high survival group. The patients in the high survival group may be immunotherapy responders and patients in the low survival group may be immunotherapy non-responders.

[0048] In another aspect, the present invention provides for a method of treating a cancer in a subject in need thereof comprising detecting the expression or activity of an ICR and/or exclusion signature according to any embodiment herein in a tumor obtained from the subject and administering a treatment, wherein if an ICR and/or exclusion signature is detected the treatment comprises administering an agent capable of reducing expression or activity of said signature, and wherein if an ICR and/or exclusion signature is not detected the treatment comprises administering an immunotherapy. The agent capable of reducing expression or activity of said signature may comprise a CDK4/6 inhibitor, a drug selected from Table 16, a cell cycle inhibitor, a PKC activator, an inhibitor of the NFκB pathway, an IGF1R inhibitor, or Reserpine. The agent capable of reducing expression or activity of said signature may comprise an agent capable of modulating expression or activity of a gene selected from the group consisting of MAZ, NFKBIZ, MYC, ANXA1, SOX4, MT2A, PTP4A3, CD59, DLL3, SERPINE2, SERPINF1, PERP, EGR1, SERPINA3, SEMA3B, SMARCA4, IFNGR2, B2M, and PDL1. The agent capable of reducing expression or activity of said signature may comprise an agent capable of targeting or binding to one or more up-regulated secreted or cell surface exposed ICR and/or exclusion signature genes or polypeptides. The method may further comprise detecting the expression or activity of an ICR and/or exclusion signature according to any embodiment herein in a tumor obtained from the subject after the treatment and administering an immunotherapy if said signature is reduced or below a reference level. The agent capable of reducing expression or activity of said signature may be a CDK4/6 inhibitor. The method may further comprise detecting the expression or activity of an ICR and/or exclusion signature according to any embodiment herein in a tumor obtained from the subject before the treatment and administering an immunotherapy if said signature is not detected or below a reference level.

[0049] In certain embodiments, the method further comprises administering an immunotherapy to the subject administered an agent capable of reducing the expression or activity of said signature. The immunotherapy may comprise a check point inhibitor or adoptive cell transfer (ACT). The adoptive cell transfer may comprise a CAR T cell or activated autologous T cells. The checkpoint inhibitor may comprise anti-CTLA4, anti-PD-L1 and/or anti-PD1 therapy.

[0050] In another aspect, the present invention provides for a method of treating a cancer in a subject in need thereof comprising detecting the expression or activity of an ICR and/or exclusion signature according to any embodiment herein in a tumor obtained from the

subject, wherein if an ICR and/or exclusion signature is detected the treatment comprises administering an agent capable of modulating expression or activity of one or more genes or polypeptides in a network of genes disrupted by perturbation of a gene selected from the group consisting of MAZ, NFKBIZ, MYC, ANXA1, SOX4, MT2A, PTP4A3, CD59, DLL3, SERPINE2, SERPINF1, PERP, EGR1, SERPINA3, SEMA3B, SMARCA4, IFNGR2, B2M, and PDL1.

[0051] In another aspect, the present invention provides for a method of treating a cancer in a subject in need thereof comprising administering to the subject a therapeutically effective amount of an agent: capable of modulating the expression or activity of one or more ICR and/or exclusion signature genes or polypeptides according to any embodiment herein; or capable of targeting or binding to one or more cell surface exposed ICR and/or exclusion signature genes or polypeptides, wherein the gene or polypeptide is up-regulated in the ICR and/or exclusion signature; or capable of targeting or binding to one or more receptors or ligands specific for a cell surface exposed ICR and/or exclusion signature gene or polypeptide, wherein the gene or polypeptide is up-regulated in the ICR and/or exclusion signature; or comprising a secreted ICR and/or exclusion signature gene or polypeptide, wherein the gene or polypeptide is down-regulated in the ICR and/or exclusion signature; or capable of targeting or binding to one or more secreted ICR and/or exclusion signature genes or polypeptides, wherein the genes or polypeptides are up-regulated in the ICR and/or exclusion signature; or capable of targeting or binding to one or more receptors specific for a secreted ICR and/or exclusion signature gene or polypeptide, wherein the secreted gene or polypeptide is up-regulated in the ICR and/or exclusion signature; or comprising a CDK4/6 inhibitor, a drug selected from Table 16, a cell cycle inhibitor, a PKC activator, an inhibitor of the NFκB pathway, an IGF1R inhibitor, or Reserpine.

[0052] In certain embodiments, the agent comprises a therapeutic antibody, antibody fragment, antibody-like protein scaffold, aptamer, protein, CRISPR system or small molecule.

[0053] In certain embodiments, the agent capable of targeting or binding to one or more cell surface exposed ICR and/or exclusion signature polypeptides or one or more receptors specific for a secreted ICR and/or exclusion signature gene or polypeptide comprises a CAR T cell capable of targeting or binding to one or more cell surface exposed ICR and/or exclusion signature genes or polypeptides or one or more receptors specific for a secreted ICR and/or exclusion signature gene or polypeptide.

[0054] In certain embodiments, the agent capable of modulating the expression or activity of one or more ICR and/or exclusion signature genes or polypeptides comprises a CDK4/6 inhibitor. The CDK4/6 inhibitor may comprise Abemaciclib.

[0055] In certain embodiments, the method further comprises administering an immunotherapy to the subject. The immunotherapy may comprise a check point inhibitor. The checkpoint inhibitor may comprise anti-CTLA4, anti-PD-L1 and/or anti-PD1 therapy.

[0056] In another aspect, the present invention provides for a method of monitoring a cancer in a subject in need thereof comprising detecting the expression or activity of an ICR and/or exclusion gene signature according to any embodiment herein in tumor samples obtained from the subject for at least two time points. The at least one sample may be obtained before treatment. The at least one sample may be obtained after treatment.

[0057] In certain embodiments, the cancer according to any embodiment herein is melanoma.

[0058] In certain embodiments, the ICR and/or exclusion signature is expressed in response to administration of an immunotherapy.

[0059] In another aspect, the present invention provides for a method of detecting an ICR signature in a tumor comprising, detecting in tumor cells obtained from a subject in need thereof who has been treated with an immunotherapy the expression or activity of a malignant cell gene signature comprising: a) one or more down regulated genes selected from the group consisting of genes associated with coagulation, apoptosis, TNF-α signaling via NFκb, Antigen processing and presentation, metallothionein and IFNGR2; and/or b) one or more up regulated genes selected from the group consisting of genes associated with negative regulation of angiogenesis and MYC targets.

[0060] In another aspect, the present invention provides for a kit comprising reagents to detect at least one ICR and/or exclusion signature gene or polypeptide according to any embodiment herein. The kit may comprise at least one antibody, antibody fragment, or aptamer. The kit may comprise primers and/or probes for quantitative RT-PCR or fluorescently bar-coded oligonucleotide probes for hybridization to RNA.

[0061] In another aspect, the present invention provides for a CD8 T cell specific cycling signature (see Table 7). In certain embodiments, modulating target genes in this signature can allow boosting T cell proliferation without activating tumor growth. Not being bound by a theory proliferating CD8 T cells express features that are not present in proliferating malignant cells. In certain embodiments, induction of oxidative phosphorylation and/or

repression of hematopoietic lineage genes (e.g., CD37, IL11RA, and IL7R) may increase CD8 T cell proliferation without affecting tumor proliferation.

[0062] In another aspect, the present invention provides for a method of detecting an immunotherapy resistance (ITR) gene signature in a tumor comprising, detecting in tumor cells obtained from a subject in need thereof the expression or activity of a malignant cell gene signature comprising:

a) one or more genes or polypeptides selected from the group consisting of ACOT7, ACSL3, ACTN1, ADAM15, ADI1, AEBP1, AGPAT1, AGRN, AHCY, AIF1L, AKAP12, AKT3, ANXA5, APOA1BP, APOD, APOE, ARL2, ARNT2, ARPC1A, ASPH, ATP1A1, ATP1B1, ATP6V0A1, B3GNT1, BACE2, BAIAP2, BCAN, BIRC7, BTBD3, C11orf24, C17orf89, C1orf198, C1orf21, C1orf85, CALD1, CALU, CAPN3, CAV1, CBR1, CCND1, CCT3, CD151, CD276, CD59, CD63, CD9, CDC42BPA, CDC42EP4, CDH19, CDK2, CDK2AP1, CECR7, CELSR2, CERCAM, CERS2, CHCHD6, CHL1, CHPF, CLDN12, CLIC4, CNIH4, CNN3, CNP, CNPY2, COA3, COL16A1, COMT, CRIP2, CRNDE, CRTAP, CRYAB, CSAG1, CSAG3, CSPG4, CSRP1, CTDSPL, CTHRC1, CTNNAL1, CTNNB1, CTSF, CTSK, CTTN, CYB5R1, CYP27A1, CYSTM1, CYTH3, DAAM2, DCBLD2, DCT, DDR1, DDR2, DIP2C, DLC1, DNAH14, DOCK7, DST, DSTN, DUSP6, ECM1, EDNRB, EFNA5, EIF4EBP1, EMP1, ENTPD6, EPS8, ERBB3, ETV4, ETV5, EVA1A, EXOSC4, FAM127A, FAM127B, FAM167B, FARP1, FARP2, FASN, FKBP10, FKBP4, FKBP9, FN1, FNBP1L, FRMD6, FSTL1, FXYD3, G6PC3, GALE, GCSH, GDF15, GJB1, GLI3, GNG12, GOLM1, GPM6B, GPR143, GPRC5B, GSTA4, GSTP1, GULP1, GYG2, H1F0, HIBADH, HMCN1, HMG20B, HOXB7, HOXC10, HSBP1, HSP90AB1, HSPB1, HSPD1, HSPG2, IFI27, IGF1R, IGFBP7, IGSF11, IGSF3, IGSF8, IMPDH2, ISYNA1, ITFG3, ITGA3, ITGB3, KIRREL, LAMB1, LAMB2, LAMC1, LAPTM4A, LAPTM4B, LDLRAD3, LGALS1, LGALS3BP, LINC00473, LINC00673, LMNA, LOC100126784, LOC100130370, LOC645166, LOXL4, LRP6, MAGEA12, MAGEA2B, MAGEA3, MAGEA6, MAGED1, MAGED2, MAP1B, MARCKSL1, MDK, MFAP2, MFGE8, MFI2, MGST3, MIA, MIF, MITF, MLANA, MLPH, MMP14, MORF4L2, MORN2, MPZL1, MRPL24, MT2A, MTUS1, MXI1, MYH10, MYO10, MYO1D, NAV2, NCKAP1, NDST1, NENF, NES, NGFRAP1, NGRN, NHSL1, NID1, NME1, NME2, NME4, NRP2, NRSN2, NSG1, OSBPL1A, P4HA2, PACSIN2, PAX3, PCDHGC3, PEG10, PFDN2, PFKM, PFN2, PGRMC1, PHB, PHLDB1, PIR, PKNOX2, PLEKHB1, PLK2, PLOD1, PLOD3, PLP1, PLS3, PLXNA1, PLXNB3, PMEL, PMP22,

POLR2F, POLR2L, PON2, PPT2, PRAME, PRDX4, PRDX6, PRKCDBP, PROS1, PRSS23, PSMB5, PTGFRN, PTGR1, PTK2, PTPLAD1, PTPRM, PTPRS, PTRH2, PTTG1IP, PYCR1, PYGB, PYGL, QDPR, QPCT, RAB13, RAB17, RAB34, RAB38, RAI14, RBFOX2, RCAN1, RCN1, RCN2, RDX, RGS20, RND3, ROBO1, ROPN1, ROPN1B, RTKN, S100A1, S100A13, S100A16, S100B, SCARB1, SCCPDH, SCD, SDC3, SDC4, SDCBP, SELENBP1, SEMA3B, SEMA3C, SEMA6A, SEPT10, SERPINA3, SERPINE2, SERPINH1, SGCD, SGCE, SHC1, SHC4, SLC19A2, SLC24A5, SLC25A13, SLC25A4, SLC35B2, SLC39A1, SLC39A6, SLC45A2, SLC6A15, SLC7A8, SMARCA1, SNAI2, SNCA, SNHG16, SNRPE, SORT1, SOX10, SOX13, SOX4, SPARC, SPR, SPRY4, SPTBN1, SRPX, SSFA2, ST3GAL4, ST5, ST6GALNAC2, STK32A, STMN1, STXBP1, SYNGR1, TANC1, TBC1D16, TBC1D7, TCEAL4, TEAD1, TENC1, TEX2, TFAP2A, TIMP2, TIMP3, TJP1, TMEM147, TMEM14C, TMEM9, TMEM98, TNFRSF19, TOM1L1, TRIM2, TRIM63, TSC22D1, TSPAN3, TSPAN4, TSPAN6, TTLL4, TUBB2A, TUBB2B, TUBB3, TYR, UBL3, VAT1, VIM, VKORC1, WASL, WBP5, WIPI1, WLS, XAGE1A, XAGE1B, XAGE1C, XAGE1D, XAGE1E, XYLB, YWHAE and ZNF462; or

b) one or more genes or polypeptides selected from Figure 3C; or

c) one or more genes or polypeptides selected from the group consisting of ABHD2, ACSL4, AHNAK, AHR, AIM2, ANGPTL4, ANXA1, ANXA2, APOD, ATF3, ATP1A1, ATP1B3, BBX, BCL6, BIRC3, BSG, C16orf45, C8orf40, CALU, CARD16, CAV1, CBFB, CCDC109B, CCND3, CD151, CD200, CD44, CD46, CD47, CD58, CD59, CD9, CD97, CDH19, CERS5, CFB, CHI3L2, CLEC2B, CLIC4, COL16A1, COL5A2, CREG1, CRELD1, CRYAB, CSPG4, CST3, CTNNAL1, CTSA, CTSB, CTSD, DCBLD2, DCTN6, EGR1, EMP1, EPDR1, FAM114A1, FAM46A, FCRLA, FN1, FNDC3B, FXYD3, G6PD, GAA, GADD45B, GALNS, GBP2, GEM, GRAMD3, GSTM2, HLA-A, HLA-C, HLA-E, HLA-F, HPCAL1, HSP90B1, HTATIP2, IFI27L2, IFI44, IFI6, IFITM3, IGF1R, IGFBP3, IGFBP7, IL1RAP, ITGA6, ITGB3, ITM2B, JUNB, KCNN4, KIAA1551, KLF4, KLF6, LAMB1, LAMP2, LGALS1, LGALS3BP, LINC00116, LOC100127888, LOXL2, LOXL3, LPL, LXN, MAGEC2, MFI2, MIA, MT1E, MT1F, MT1G, MT1M, MT1X, MT2A, NFE2L1, NFKBIZ, NNMT, NOTCH2, NR4A1, OS9, P4HA2, PDE4B, PELI1, PIGT, PMAIP1, PNPLA8, PPAPDC1B, PRKCDBP, PRNP, PROS1, PRSS23, PSMB9, PSME1, PTPMT1, PTRF, RAMP1, RND3, RNH1, RPN2, S100A10, S100A6, SCCPDH, SERINC1, SERPINA3, SERPINE1, SERPINE2, SLC20A1, SLC35A5, SLC39A14, SLC5A3, SMIM3, SPARC, SPRY2, SQRDL, STAT1, SUMF1, TAP1, TAPBP, TEKT4P2, TF, TFAP2C,

TMEM43, TMX4, TNC, TNFRSF10B, TNFRSF12A, TSC22D3, TSPAN31, UBA7, UBC, UBE2L6, XPO7, ZBTB20, ZDHHC5, ZMYM6NB, ACAA2, ADSL, AEN, AHCY, ALDH1B1, ARHGEF1, ARPC5, ATXN10, ATXN2L, B4GALT3, BCCIP, BGN, C10orf32, C16orf88, C17orf76-AS1, C20orf112, CDCA7, CECR5, CPSF1, CS, CTCFL, CTPS1, DLL3, DTD2, ECHDC1, ECHS1, EIF4A1, EIF4EBP2, EIF6, EML4, ENY2, ESRG, FAM174B, FAM213A, FBL, FBLN1, FDXR, FOXRED2, FXN, GALT, GEMIN8, GLOD4, GPATCH4, HDAC2, HMGN3, HSD17B14, IDH2, ILF2, ISYNA1, KIAA0020, KLHDC8B, LMCD1, LOC100505876, LYPLA1, LZTS2, MAZ, METAP2, MID1, MIR4461, MPDU1, MPZL1, MRPS16, MSTO1, MTG1, MYADM, MYBBP1A, MYL6B, NARS2, NCBP1, NDUFAF6, NDUFS2, NF2, NHEJ1, NME6, NNT, NOLC1, NTHL1, OAZ2, OXA1L, PABPC1, PAICS, PAK1IP1, PFN1, POLR2A, PPA1, PRAME, PRDX3, PSTPIP2, PTGDS, PTP4A3, RBM34, RBM4, RPL10A, RPL17, RPP30, RPS3, RPS7, RPSA, RUVBL2, SAMM50, SBNO1, SERPINF1, SKP2, SLC45A2, SMC3, SMG7, SMS, SNAI2, SORD, SOX4, SRCAP, SRSF7, STARD10, TBXA2R, THOC5, TIMM22, TIMM23, TMC6, TOMM22, TPM1, TSNAX, TSR1, TSTA3, TULP4, UBAP2L, UCHL5, UROS, VPS72, WDR6, XPNPEP1, XRCC5, YDJC, ZFP36L1, and ZNF286A; or

d) one or more genes or polypeptides selected from the group consisting of AHNAK, AHR, ANXA1, ATP1B3, BBX, BCL6, BIN3, C16orf45, CARD16, CAST, CAV1, CAV2, CD59, CD9, CDH19, CLEC2B, CRYAB, CYSTM1, FAM114A1, FAM46A, FCRLA, FXYD3, G6PD, GBP2, HLA-A, HLA-E, HLA-F, IGF1R, IL1RAP, IL6ST, ITGB1, ITM2B, KCNN4, KLF4, KLF6, LAMP2, LEPROT, LGALS1, LOC100127888, MT1X, MT2A, MVP, NFAT5, NFE2L1, NFKBIZ, PLP2, PROS1, PRSS23, RNF145, S100A10, SEL1L, SERINC1, SERPINA3, SERPINE2, SPRY2, SQRDL, SQSTM1, TAPBP, TF, TMBIM1, TNFRSF10B, TNFRSF12A, UBE2B, and ZBTB20; or

e) one or more genes or polypeptides selected from the group consisting of TM4SF1, ANXA1, MT2A, SERPINA3, EMP1, MIA, ITGA3, CDH19, CTSB, SERPINE2, MFI2, APOC2, ITGB8, S100A6, NNMT, SLC5A3, SEMA3B, TSC22D3, ITGB3, MATN2, CRYAB, PERP, CSPG4, SGCE, CD9, A2M, FGFR1, CST3, DDR1, CD59, DPYSL2, KCNN4, SLC26A2, CD151, SLC39A14, AHNAK, ATP1A1, PROS1, TIMP1, TRIML2, EGR1, TNC, DCBLD2, DUSP4, DUSP6, CD58, FAM3C, ATP1B1, MT1E, TNFRSF12A, FXYD3, SCCPDH, GAA, TIMP3, LEF1-AS1, CAV1, MFGE8, NR4A1, LGALS3, CCND3, CALU, RDH5, APOD, LINC00116, IL1RAP, SERPINA1, NFKBIZ, HSPA1A, PRSS23, MAP1B, ITGA7, PLP2, IGFBP7, GSN, LOXL3, PTRF, LGALS1, IGF1R, SERPINE1,

MT1X, ATP1B3, SDC3, ZBTB38, NSG1, FCGR2A, KLF4, EGR3, DAG1, CTSD, CPVL, EEA1, SLC20A1, CLU, GBP2, SPON2, TNFSF4, NPC1, PRKCDBP, HTATIP2, C16orf45, SERPINF1, DCT, SNAI2, PTP4A3, RPS19, BCAN, FOXRED2, FAM174B, TRPM1, ESRP1, PABPC1, CA14, TMC6, C17orf76-AS1, RPL13AP5, TP53, BANCR, RPL28, IDH2, LOC100133445, TYRP1, DLL3, LHFPL3-AS1, SCIN, EIF4EBP2, TIMM50, CD68, GPI, MIR4461, RPS27, C1QBP, EGFL8, RPL21, FAM178B, RPS24, SAE1, KLHDC8B, KCNAB2, RPLP0, SCD, TULP4, IL6R, LINC00439, TSTD1, NF2, TUBB4A, SOX4, RPS3, NAPRT1, RPS6, LIMD2, CDKN2A, PTGDS, ISYNA1, ARHGDIB, CNRIP1, H3F3A, TBXA2R, PSTPIP2, SERPINB9, TMEM204, SORD, RPS5, CDH3, RPL18A, RPL8, VPS53, RBM34, FES, ESRG, RPS7, HSD17B14, TTC39A, FBLN1, SLC45A2, AEN, ACP5, BCL11A, CHP1, XIST, MAZ, FAM92A1, CTPS1, ASAP1, RPL6, MARCKS, MAGEA4, NPL, RPS16, NENF, SLC19A1, FTL, RNF2, MYBBP1A, PPAP2C, GRWD1, SKP2, WDR81, DCUN1D2, LAMP2 and MPZL1; or

f) one or more genes or polypeptides selected from the group consisting of TM4SF1, MT2A, SERPINA3, CDH19, SERPINE2, CRYAB, SGCE, A2M, DDR1, CD59, DPYSL2, DUSP6, MFGE8, NFKBIZ, and PRSS23; or

g) one or more genes or polypeptides selected from the group consisting of SERPINA3, MT2A, SERPINF1, SERPINE2, SOX4, DDR1, CD59, DUSP6, PERP, SEMA3B, PTP4A3, BANCR, DLL3, and LAMP2; or

h) one or more genes or polypeptides selected from the group consisting of MT2A, MT1E, MT1X, MT1M, MT1F, MT1G, MTX1 and MTG1.

[0063] In one embodiment, the ITR signature further comprises one or more genes or polypeptides selected from the group consisting of IFNGR2, B2M, and PDL1.

[0064] In one embodiment, said ITR signature comprises a post-immunotherapy signature-down (PIT-down) module, said module comprising one or more genes selected from the group consisting of: ABHD2, ACSL4, AHNAK, AHR, AIM2, ANGPTL4, ANXA1, ANXA2, APOD, ATF3, ATP1A1, ATP1B3, BBX, BCL6, BIRC3, BSG, C16orf45, C8orf40, CALU, CARD16, CAV1, CBFB, CCDC109B, CCND3, CD151, CD200, CD44, CD46, CD47, CD58, CD59, CD9, CD97, CDH19, CERS5, CFB, CHI3L2, CLEC2B, CLIC4, COL16A1, COL5A2, CREG1, CRELD1, CRYAB, CSPG4, CST3, CTNNAL1, CTSA, CTSB, CTSD, DCBLD2, DCTN6, EGR1, EMP1, EPDR1, FAM114A1, FAM46A, FCRLA, FN1, FNDC3B, FXYD3, G6PD, GAA, GADD45B, GALNS, GBP2, GEM, GRAMD3, GSTM2, HLA-A, HLA-C, HLA-E, HLA-F, HPCAL1, HSP90B1, HTATIP2, IFI27L2, IFI44,

IFI6, IFITM3, IGF1R, IGFBP3, IGFBP7, IL1RAP, ITGA6, ITGB3, ITM2B, JUNB, KCNN4, KIAA1551, KLF4, KLF6, LAMB1, LAMP2, LGALS1, LGALS3BP, LINC00116, LOC100127888, LOXL2, LOXL3, LPL, LXN, MAGEC2, MFI2, MIA, MT1E, MT1F, MT1G, MT1M, MT1X, MT2A, NFE2L1, NFKBIZ, NNMT, NOTCH2, NR4A1, OS9, P4HA2, PDE4B, PELI1, PIGT, PMAIP1, PNPLA8, PPAPDC1B, PRKCDBP, PRNP, PROS1, PRSS23, PSMB9, PSME1, PTPMT1, PTRF, RAMP1, RND3, RNH1, RPN2, S100A10, S100A6, SCCPDH, SERINC1, SERPINA3, SERPINE1, SERPINE2, SLC20A1, SLC35A5, SLC39A14, SLC5A3, SMIM3, SPARC, SPRY2, SQRDL, STAT1, SUMF1, TAP1, TAPBP, TEKT4P2, TF, TFAP2C, TMEM43, TMX4, TNC, TNFRSF10B, TNFRSF12A, TSC22D3, TSPAN31, UBA7, UBC, UBE2L6, XPO7, ZBTB20, ZDHHC5 and ZMYM6NB; or TM4SF1, ANXA1, MT2A, SERPINA3, EMP1, MIA, ITGA3, CDH19, CTSB, SERPINE2, MFI2, APOC2, ITGB8, S100A6, NNMT, SLC5A3, SEMA3B, TSC22D3, ITGB3, MATN2, CRYAB, PERP, CSPG4, SGCE, CD9, A2M, FGFR1, CST3, DDR1, CD59, DPYSL2, KCNN4, SLC26A2, CD151, SLC39A14, AHNAK, ATP1A1, PROS1, TIMP1, TRIML2, EGR1, TNC, DCBLD2, DUSP4, DUSP6, CD58, FAM3C, ATP1B1, MT1E, TNFRSF12A, FXYD3, SCCPDH, GAA, TIMP3, LEF1-AS1, CAV1, MFGE8, NR4A1, LGALS3, CCND3, CALU, RDH5, APOD, LINC00116, IL1RAP, SERPINA1, NFKBIZ, HSPA1A, PRSS23, MAP1B, ITGA7, PLP2, IGFBP7, GSN, LOXL3, PTRF, LGALS1, IGF1R, SERPINE1, MT1X, ATP1B3, SDC3, ZBTB38, NSG1, FCGR2A, KLF4, EGR3, DAG1, CTSD, CPVL, EEA1, SLC20A1, CLU, GBP2, SPON2, TNFSF4, NPC1, PRKCDBP, HTATIP2, and C16orf45; or an mICR down gene in Figure 3C, wherein said PIT-down module is downregulated in a tumor resistant to immunotherapy and upregulated in a tumor sensitive to immunotherapy as compared to a reference level.

[0065] In one embodiment, said ITR signature comprises a post-immunotherapy signature-up (PIT-up) module, said module comprising one or more genes selected from the group consisting of: ACAA2, ADSL, AEN, AHCY, ALDH1B1, ARHGEF1, ARPC5, ATXN10, ATXN2L, B4GALT3, BCCIP, BGN, C10orf32, C16orf88, C17orf76-AS1, C20orf112, CDCA7, CECR5, CPSF1, CS, CTCFL, CTPS1, DLL3, DTD2, ECHDC1, ECHS1, EIF4A1, EIF4EBP2, EIF6, EML4, ENY2, ESRG, FAM174B, FAM213A, FBL, FBLN1, FDXR, FOXRED2, FXN, GALT, GEMIN8, GLOD4, GPATCH4, HDAC2, HMGN3, HSD17B14, IDH2, ILF2, ISYNA1, KIAA0020, KLHDC8B, LMCD1, LOC100505876, LYPLA1, LZTS2, MAZ, METAP2, MID1, MIR4461, MPDU1, MPZL1, MRPS16, MSTO1, MTG1, MYADM, MYBBP1A, MYL6B, NARS2, NCBP1, NDUFAF6,

NDUFS2, NF2, NHEJ1, NME6, NNT, NOLC1, NTHL1, OAZ2, OXA1L, PABPC1, PAICS, PAK1IP1, PFN1, POLR2A, PPA1, PRAME, PRDX3, PSTPIP2, PTGDS, PTP4A3, RBM34, RBM4, RPL10A, RPL17, RPP30, RPS3, RPS7, RPSA, RUVBL2, SAMM50, SBNO1, SERPINF1, SKP2, SLC45A2, SMC3, SMG7, SMS, SNAI2, SORD, SOX4, SRCAP, SRSF7, STARD10, TBXA2R, THOC5, TIMM22, TIMM23, TMC6, TOMM22, TPM1, TSNAX, TSR1, TSTA3, TULP4, UBAP2L, UCHL5, UROS, VPS72, WDR6, XPNPEP1, XRCC5, YDJC, ZFP36L1 and ZNF286A; or SERPINF1, DCT, SNAI2, PTP4A3, RPS19, BCAN, FOXRED2, FAM174B, TRPM1, ESRP1, PABPC1, CA14, TMC6, C17orf76-AS1, RPL13AP5, TP53, BANCR, RPL28, IDH2, LOC100133445, TYRP1, DLL3, LHFPL3-AS1, SCIN, EIF4EBP2, TIMM50, CD68, GPI, MIR4461, RPS27, C1QBP, EGFL8, RPL21, FAM178B, RPS24, SAE1, KLHDC8B, KCNAB2, RPLP0, SCD, TULP4, IL6R, LINC00439, TSTD1, NF2, TUBB4A, SOX4, RPS3, NAPRT1, RPS6, LIMD2, CDKN2A, PTGDS, ISYNA1, ARHGDIB, CNRIP1, H3F3A, TBXA2R, PSTPIP2, SERPINB9, TMEM204, SORD, RPS5, CDH3, RPL18A, RPL8, VPS53, RBM34, FES, ESRG, RPS7, HSD17B14, TTC39A, FBLN1, SLC45A2, AEN, ACP5, BCL11A, CHP1, XIST, MAZ, FAM92A1, CTPS1, ASAP1, RPL6, MARCKS, MAGEA4, NPL, RPS16, NENF, SLC19A1, FTL, RNF2, MYBBP1A, PPAP2C, GRWD1, SKP2, WDR81, DCUN1D2, and MPZL1; or an mICR up gene in Figure 3C, wherein said PIT-up module is upregulated in a tumor resistant to immunotherapy and downregulated in a tumor sensitive to immunotherapy as compared to a reference level.

[0066] Detecting an immunotherapy resistance gene signature in a tumor may further comprise detecting in tumor infiltrating lymphocytes (TIL) obtained from the subject in need thereof the expression or activity of a CD8 T cell gene signature, said signature comprising one or more genes or polypeptides selected from the group consisting of APOBEC3G, CBLB, CCL4, CCL4L1, CCL4L2, CCL5, CD27, CD8A, CD8B, CST7, CTSW, CXCL13, CXCR6, DTHD1, DUSP2, EOMES, FASLG, FCRL3, GBP5, GZMA, GZMB, GZMH, GZMK, HCST, HLA-A, HLA-B, HLA-H, ID2, IFNG, IL2RB, KLRC3, KLRC4, KLRC4-KLRK1, KLRD1, KLRK1, LAG3, LSP1, LYST, NKG7, PDCD1, PRF1, PSTPIP1, PYHIN1, RARRES3, SH2D1A, SH2D2A, TARP, TIGIT, TNFRSF9 and TOX.

[0067] Detecting an immunotherapy resistance gene signature in a tumor may further comprise detecting in tumor infiltrating lymphocytes (TIL) obtained from the subject in need thereof the expression or activity of a CD4 T cell gene signature, said signature comprising one or more genes or polypeptides selected from the group consisting of AIM1, ANK3,

AQP3, CAMK4, CCR4, CCR8, CD28, CD40LG, DGKA, EML4, FAAH2, FBLN7, FKBP5, FLT3LG, FOXP3, FXYD5, IL6R, IL7R, ITGB2-AS1, JUNB, KLRB1, LEPROTL1, LOC100128420, MAL, OXNAD1, PBXIP1, PIK3IP1, PIM2, PRKCQ-AS1, RORA, RPL35A, RPL4, RPL6, RPS15A, RPS27, RPS28, 6-Sep, SLAMF1, SORL1, SPOCK2, SUSD3, TCF7, TMEM66, TNFRSF18, TNFRSF25, TNFRSF4, TNFSF8, TRABD2A, TSC22D3 and TXK.

[0068] Detecting an immunotherapy resistance gene signature in a tumor may further comprise detecting in macrophages obtained from the subject in need thereof the expression or activity of a macrophage gene signature, said signature comprising one or more genes or polypeptides selected from the group consisting of AIF1, ALDH2, ANPEP, C15orf48, C1orf162, C1QA, C1QB, C1QC, C3AR1, CCR1, CD14, CD163, CD300A, CD300C, CD300LF, CD33, CD86, CFP, CLEC10A, CLEC12A, CLEC4A, CLEC5A, CMKLR1, CSF1R, CSF2RB, CSF3R, CSTA, CXCL9, CXCR2P1, DSC2, FAM26F, FBP1, FCER1G, FCGR1A, FCGR1B, FCGR1C, FCGR3A, FCGR3B, FCN1, FOLR2, FPR1, FPR2, FPR3, GGTA1P, GNA15, GPR84, HCK, HK3, IGSF6, IL1B, IL1RN, IL4I1, ITGAM, KYNU, LGALS2, LILRA1, LILRA2, LILRA3, LILRA4, LILRB2, LILRB4, LILRB5, LST1, MAFB, MARCO, MNDA, MRC1, MS4A4A, MS4A6A, MSR1, NCF2, OLR1, P2RY13, PILRA, PLAU, PLBD1, PLXDC2, PRAM1, RAB20, RAB31, RASSF4, RBM47, RGS18, S100A8, S100A9, SECTM1, SIGLEC1, SIGLEC7, SIGLEC9, SLAMF8, SLC31A2, SLC43A2, SLC7A7, SLC8A1, SLCO2B1, SPI1, STAB1, TBXAS1, TFEC, TGFBI, TLR2, TLR4, TLR8, TMEM176A, TMEM176B, TNFSF13, TNFSF13B, TREM2, TYROBP, VSIG4 and ZNF385A.

[0069] Detecting an immunotherapy resistance gene signature in a tumor may further comprise detecting in B cells obtained from the subject in need thereof the expression or activity of a B cell gene signature, said signature comprising one or more genes or polypeptides selected from the group consisting of ADAM19, AKAP2, BACH2, BANK1, BCL11A, BLK, CD19, CD1C, CD22, CD79A, CD79B, CLEC17A, CNR2, COL19A1, COL4A3, CPNE5, CR2, CXCR5, EBF1, ELK2AP, FAM129C, FAM177B, FCER2, FCRL1, FCRL2, FCRL5, FCRLA, HLA-DOB, IGJ, IGLL1, IGLL3P, IGLL5, KIAA0125, KIAA0226L, LOC283663, MS4A1, P2RX5, PAX5, PNOC, POU2AF1, POU2F2, RASGRP3, SEL1L3, SNX29P1, ST6GAL1, STAP1, SWAP70, TCL1A, TMEM154 and VPREB3.

[0070] The gene signature may be detected in a bulk tumor sample, whereby the gene signature is detected by deconvolution of bulk expression data such that gene expression is assigned to malignant cells and non-malignant cells in said tumor sample.

[0071] Detecting the ITR gene signature may comprise detecting downregulation of the PIT-down module and/or upregulation of the PIT-up module. Not detecting the ITR gene signature may comprise detecting upregulation of the PIT-down module and/or downregulation of the PIT-up module. The detecting an ITR gene signature may indicates a 10-year survival rate less than 40% and wherein not detecting said signature may indicate a 10-year survival rate greater than 60%. The detecting an ITR gene signature may indicate exclusion of T cells from a tumor and wherein not detecting said signature may indicate infiltration of T cells in a tumor.

[0072] In another aspect, the present invention provides for a method of stratifying cancer patients into a high survival group and a low survival group comprising detecting the expression or activity of an immunotherapy resistance gene signature in a tumor, wherein if an immunotherapy resistance gene signature is detected the patient is in the low survival group and if an immunotherapy resistance gene signature is not detected the patient is in the high survival group. The patients in the high survival group may be immunotherapy responders and patients in the low survival group may be immunotherapy non-responders.

[0073] In another aspect, the present invention provides for a method of treating a cancer in a subject in need thereof comprising detecting the expression or activity of an immunotherapy resistance gene signature according to any of claims 1 to 10 in a tumor obtained from the subject and administering a treatment, wherein if an immunotherapy resistance signature is detected the treatment comprises administering an agent capable of reducing expression or activity of said signature, and wherein if an immunotherapy resistance signature is not detected the treatment comprises administering an immunotherapy. The agent capable of reducing expression or activity of said signature may comprise a drug selected from Table 16, a PKC activator, an inhibitor of the NFκB pathway, an IGF1R inhibitor, or Reserpine. The agent capable of reducing expression or activity of said signature may comprise an agent capable of modulating expression or activity of a gene selected from the group consisting of MAZ, NFKBIZ, MYC, ANXA1, SOX4, MT2A, PTP4A3, CD59, DLL3, SERPINE2, SERPINF1, PERP, EGR1, SERPINA3, SEMA3B, SMARCA4, IFNGR2, B2M, and PDL1. The agent capable of reducing expression or activity of said signature may comprise an agent capable of targeting or binding to one or more up-regulated secreted or

cell surface exposed immunotherapy resistance signature genes or polypeptides. The method may further comprise detecting the expression or activity of an immunotherapy resistance gene signature in a tumor obtained from the subject after the treatment and administering an immunotherapy if said signature is not detected. The method may further comprise administering an immunotherapy to the subject administered an agent capable of reducing the expression or activity of said signature. The immunotherapy may comprise a check point inhibitor or adoptive cell transfer (ACT). The adoptive cell transfer may comprise a CAR T cell or activated autologous T cells. The checkpoint inhibitor may comprise anti-CTLA4, anti-PD-L1 and/or anti-PD1 therapy.

[0074] In another aspect, the present invention provides for a method of treating a cancer in a subject in need thereof comprising detecting the expression or activity of an immunotherapy resistance gene signature according to any embodiment herein in a tumor obtained from the subject, wherein if an immunotherapy resistance signature is detected the treatment comprises administering an agent capable of modulating expression or activity of one or more genes or polypeptides in a network of genes disrupted by perturbation of a gene selected from the group consisting of MAZ, NFKBIZ, MYC, ANXA1, SOX4, MT2A, PTP4A3, CD59, DLL3, SERPINE2, SERPINF1, PERP, EGR1, SERPINA3, SEMA3B, SMARCA4, IFNGR2, B2M, and PDL1.

[0075] In another aspect, the present invention provides for a method of treating a cancer in a subject in need thereof comprising administering to the subject a therapeutically effective amount of an agent: capable of modulating the expression or activity of one or more immunotherapy resistance signature genes or polypeptides; or capable of targeting or binding to one or more cell surface exposed immunotherapy resistance signature genes or polypeptides, wherein the gene or polypeptide is up-regulated in the ITR signature; or capable of targeting or binding to one or more receptors or ligands specific for a cell surface exposed immunotherapy resistance signature gene or polypeptide, wherein the gene or polypeptide is up-regulated in the ITR signature; or comprising a secreted immunotherapy resistance signature gene or polypeptide, wherein the gene or polypeptide is down-regulated in the ITR signature; or capable of targeting or binding to one or more secreted immunotherapy resistance signature genes or polypeptides, wherein the genes or polypeptides are up-regulated in the ITR signature; or capable of targeting or binding to one or more receptors specific for a secreted immunotherapy resistance signature gene or polypeptide, wherein the secreted gene or polypeptide is up-regulated in the ITR signature; or

comprising a drug selected from Table 16, a PKC activator, an inhibitor of the NFκB pathway, an IGF1R inhibitor, or Reserpine. The agent capable of modulating the expression or activity of one or more immunotherapy resistance signature genes or polypeptides may comprise a CDK4/6 inhibitor. The CDK4/6 inhibitor may comprise Abemaciclib. The method may further comprise administering an immunotherapy to the subject. The immunotherapy may comprise a check point inhibitor. The checkpoint inhibitor may comprise anti-CTLA4, anti-PD-L1 and/or anti-PD1 therapy. Not being bound by a theory, the CDK4/6 inhibitor may sensitize a subject to checkpoint blockade therapy. The agent may comprise a therapeutic antibody, antibody fragment, antibody-like protein scaffold, aptamer, protein, CRISPR system or small molecule. The agent capable of targeting or binding to one or more cell surface exposed immunotherapy resistance signature polypeptides or one or more receptors specific for a secreted immunotherapy resistance signature gene or polypeptide may comprise a CAR T cell capable of targeting or binding to one or more cell surface exposed immunotherapy resistance signature genes or polypeptides or one or more receptors specific for a secreted immunotherapy resistance signature gene or polypeptide.

[0076] In another aspect, the present invention provides for a method of monitoring a cancer in a subject in need thereof comprising detecting the expression or activity of an immunotherapy resistance gene signature according to any embodiment herein in tumor samples obtained from the subject for at least two time points. The at least one sample may be obtained before treatment. The at least one sample may be obtained after treatment.

[0077] The cancer according to any embodiment may be melanoma. The ITR gene signature may be expressed in response to administration of an immunotherapy.

[0078] In another aspect, the present invention provides for a method of detecting T cell infiltration of a tumor comprising detection in malignant cells expression or activity of one or more genes selected from the group consisting of: HLA-C, FGFR1, ITGB3, CD47, AHNAK, CTSD, TIMP1, SLC5A3, CST3, CD151, CCND3, MIA, CD58, CTSB, S100A6, EMP1, HLA-F, TSC22D3, ANXA1, KCNN4 and MT2A; or A2M, AEBP1, AHNAK, ANXA1, APOC2, APOD, APOE, ATP1A1, ATP1B1, C4A, CAPN3, CAV1, CD151, CD59, CD63, CDH19, CRYAB, CSPG4, CSRP1, CST3, CTSB, CTSD, DAG1, DDR1, DUSP6, ETV5, EVA1A, FBXO32, FCGR2A, FGFR1, GAA, GATSL3, GJB1, GRN, GSN, HLA-B, HLA-C, HLA-F, HLA-H, IFI35, IGFBP7, IGSF8, ITGA3, ITGA7, ITGB3, LAMP2, LGALS3, LOXL4, LRPAP1, LY6E, LYRM9, MATN2, MFGE8, MIA, MPZ, MT2A, MTRNR2L3, MTRNR2L6, NPC1, NPC2, NSG1, PERP, PKM, PLEKHB1, PROS1, PRSS23, PYGB,

RDH5, ROPN1, S100A1, S100A13, S100A6, S100B, SCARB2, SCCPDH, SDC3, SEMA3B, SERPINA1, SERPINA3, SERPINE2, SGCE, SGK1, SLC26A2, SLC5A3, SPON2, SPP1, TIMP1, TIMP2, TIMP3, TM4SF1, TMEM255A, TMX4, TNFSF4, TPP1, TRIML2, TSC22D3, TXNIP, TYR, UBC and WBP2; or HLA-A, HLA-B, HLA-C, B2M, TAPBP, IFI27, IFI35, IRF4, IRF9 and STAT2; or B2M, CTSB, CTSL1, HLA-B/C/F, HSPA1A, HSPA1B, NFKBIA and CD58, wherein detection indicates sensitivity to immunotherapy.

[0079] In another aspect, the present invention provides for a method of detecting T cell exclusion of a tumor comprising detection in malignant cells expression or activity of one or more genes selected from the group consisting of: SERPINF1, RPL6, NOLC1, RSL1D1, ILF2, SOX4, ACTG1, C17orf76-AS1, PABPC1, RPS24, ADSL, C1QBP, PAICS, CTPS1, NF2, EIF2S3, RPL18 and RPL10A; or AHCY, BZW2, CCNB1IP1, CCT6A, EEF2, EIF3B, GGCT, ILF3, IMPDH2, MDH2, MYBBP1A, NT5DC2, PAICS, PFKM, POLD2, PTK7, SLC19A1, SMARCA4, STRAP, TIMM13, TOP1MT, TRAP1 and USP22; or MYC, STRAP and SMARCA4; or MYC, SNAI2 and SOX4, wherein detection indicates resistance to immunotherapy.

[0080] In another aspect, the present invention provides for a method of detecting an immunotherapy resistance gene signature in a tumor comprising, detecting in tumor cells obtained from a subject in need thereof who has been treated with an immunotherapy the expression or activity of a malignant cell gene signature comprising: one or more down regulated genes selected from the group consisting of genes associated with coagulation, apoptosis, TNF-α signaling via NFκb, Antigen processing and presentation, metallothionein and IFNGR2; and/or one or more up regulated genes selected from the group consisting of genes associated with negative regulation of angiogenesis and MYC targets.

[0081] In another aspect, the present invention provides for a kit comprising reagents to detect at least one immunotherapy resistance signature gene or polypeptide according to the present invention. The kit may comprise at least one antibody, antibody fragment, or aptamer. The kit may comprise primers and/or probes for quantitative RT-PCR or fluorescently bar-coded oligonucleotide probes for hybridization to RNA.

[0082] It is noted that in this disclosure and particularly in the claims and/or paragraphs, terms such as "comprises", "comprised", "comprising" and the like can have the meaning attributed to it in U.S. Patent law; e.g., they can mean "includes", "included", "including", and the like; and that terms such as "consisting essentially of" and "consists essentially of"

have the meaning ascribed to them in U.S. Patent law, e.g., they allow for elements not explicitly recited, but exclude elements that are found in the prior art or that affect a basic or novel characteristic of the invention.

[0083] These and other aspects, objects, features, and advantages of the example embodiments will become apparent to those having ordinary skill in the art upon consideration of the following detailed description of illustrated example embodiments.

BRIEF DESCRIPTION OF THE DRAWINGS

[0084] The following detailed description, given by way of example, but not intended to limit the invention solely to the specific embodiments described, may best be understood in conjunction with the accompanying drawings.

[0085] **FIG. 1 – Study design and T cell analysis of ICR. (A)** Overview. 31 samples from patients with metastatic melanoma (discovery cohort) were profiled by scRNA-sequencing (left), of which 15 were TN, 15 had ICI resistance (ICR) and one had clinical benefit (CB). Signatures were tested in two validation cohorts collected independently (right), with bulk RNA-seq of melanoma tumors from 112 patients who underwent biopsies prior to receiving pembrolizumab (anti-PD-1; cohort 1) and from 26 patients, 12 with matched pre-treatment and post-progression (ICR) biopsies (cohort 2). **(B-C)** Distinct profiles of malignant and non-malignant cells. Shown are tSNE plots of single cell profiles (dots) from malignant (B) or non-malignant (C) cells, shaded by *post-hoc* annotation (**materials and methods**) or by patient. **(D)** Variation in T cells ICR. Shown is a tSNE plot of CD8 T cells that Applicants generated based on the genes of the tICR signatures, with cells shaded by treatment category (right), overall expression (OE) of the tICR signature (middle), and clonality (right). Larger dots: cells from large (> 20 cells) clones. **(E)** Similar relationship between exhaustion and cytotoxicity signatures in TN and ICR CD8 T cells. For each cell (dot), the exhaustion (y axis) and cytotoxicity (x axis) scores are shown (**materials and methods**).: TN;: ICR;: CB. Cells from the CB patient have lower than expected exhaustion scores. **(F)** CD8 T cell clones. Shown is the distribution of clone sizes. Tumors with large (>20 cells) clones are marked. **(G)** Expanded clones have higher tICR expression. Box plots show the distribution of tICR OE scores (y axis) in CD8 T-cells from patients stratified by clinical context and by overall clonality level. Left: only CD8 T-cells with reconstructed TCRs are shown; Right: only CD8 T-cells that were not from the three ICR patients with major clonal expansion are shown (right). Box-plots: the middle line represents

the median; box edges are the 25th and 75th percentiles, and whiskers represent the most extreme points that do not exceed ±IQR*1.5; points beyond the distance are plotted as single points. **(H)** CD8 T cell specific cell-cycle program. Shown are the distribution of OE scores for the CD8 specific cell cycle program in malignant cells (left) and CD8 T cells (right). The p-values were computed by comparing the cycling and non-cycling cells in each cell type with a one-sided t-test.

[0086] FIG. 2 – Malignant cell ICR programs. (A) Robust classification by the oncogenic-ICR signature. Left: Box-plot shows the distribution of OE scores for the oncogenic-ICR signature in malignant cells from ICR and TN patients, when obtained in a cross-validation (CV) procedure and tested on withheld data. Middle line: median; box edges: 25th and 75th percentiles, whiskers: most extreme points that do not exceed ±IQR*1.5; further outliers are marked individually. Right: Receiver Operating Characteristic (ROC) curve of the performances of different signatures in classifying cells as ICR or TN; the CV oncogenic-ICR signature was obtained by leave-one (patient) out CV; the first and second Area under the curve (AUC) values are for classification of cells and samples, respectively. **(B)** Genes in the oncogenic-ICR program. Heatmap shows the (centered and scaled) expression of the top 40 oncogenic-ICR-up and oncogenic-ICR-down genes (columns) across the malignant cells (rows), sorted by TN or ICR tumors (shaded bar, left) and clustered within each class. Leftmost bar: cycling and non-cycling cells within each group. Right: The OE of the oncogenic-ICR signature for each cell. **(C)** Differentially expressed gene sets in ICR *vs.* TN malignant cells. Box-plots (formatted as in (A)) show the distribution of OE scores for each signature in malignant cells from ICR vs. TN tumors. **(D-E)** Inverse relationship of the oncogenic-ICR-down and -up programs. Shown are the OE scores of the oncogenic-ICR-down (y-axis) and oncogenic-ICR-up (x-axis) programs in (D) the single cell profiles from TN and ICR tumors, and in (E) lesions of cutaneous and uveal melanoma. The Pearson correlation coefficient (r) and p-value are marked. **(F)** Workflow for identification of the exclusion signatures. **(G-H)** Congruence between the oncogenic-ICR and exclusion programs. (G) Violin plots of the distribution of OE scores of exclusion signatures across malignant cells from ICR and TN patients. (H) Left: Heat map of the (centered and scaled) expression of the 40 most differentially expressed exclusion-up and exclusion-down (black) genes (columns) in the malignant cells (rows), sorted by ICR and TN tumors (left shaded bar) and clustered within class. Leftmost shaded bar labels cycling and non-cycling (black) cells

within each group. Gene names in the oncogenic-ICR-up or oncogenic-ICR-down signatures (**table 5**) are marked by shading, respectively. Right: OE scores of the exclusion signature in each cell.

[0087] FIG. 3 – The uICR program has immune evasion properties, and can be reversed by CDK4/6 inhibition. (A-C) Reversal of resistance programs by a CDK4/6 inhibitor, abemaciclib. **(A)** Significance (y axis, $-\log_{10}$(p-value), Wilcoxon rank sum test) of induction (dark green) or repression (light green) of each signatures in tumors from abemaciclib treated mice compared to vehicle (*31*). **(B)** Distribution of uICR OE scores in breast cancer cell lines (M361, MCF and M453) treated with abemaciclib ("abe") or with DMSO vehicle ("con"). Box-plots: the middle line represents the median; box edges are the 25th and 75th percentiles, and whiskers represent the most extreme points that do not exceed $\pm$IQR*1.5; points beyond the distance are plotted as single points. **(C)** The relative expression of the 40 most differentially expressed uICR genes (rows) in abemaciclib-treated and control (purple) breast cancer cells lines (columns). Expression values are normalized according to the cell-line specific expression in the control state or denote over- or under-expression, respectively. Bottom: OE scores of the uICR signature for each cell line. **(D)** Higher uICR scores in uveal melanoma. Shown are the distributions of OE scores of the uICR program in cutaneous (black) *vs.* uveal melanoma tumors from TCGA, scored after filtering TME contributions (**materials and methods**). *P*-value: t-test. **(E)** Suppression of cell-cell interactions in ICR. Bar plots show for each malignant signature (x-axis) the number of genes (y-axis, top) in the signature that can engage in a physical interaction with other cell types and the corresponding statistical enrichment (y-axis, $-\log_{10}$(P-value), hypergeometric test, bottom). Values above the dashed line are statistically significant.

[0088] FIG. 4 – The resistance signatures in malignant cells are prognostic and predictive in validation cohorts. (A) Resistance signatures predict melanoma patient survival based in bulk RNA-seq from TCGA (*37*). Kaplan-Meier (KM) plots are stratified by high (top 25%), low (bottom 25%), or intermediate (neither high nor low) expression of the respective signature. *Pc* p-values test if the signature further enhances the predictive power of models with T-cell infiltration levels as a covariate. See **fig. 11** for additional signatures. **(B, C)** Resistance signatures distinguish clinical benefit (CB) and non-CB in mouse models and melanoma patients. Box plots show the distribution of the OE score of the uICR in bulk RNA-Seq from a lung cancer mouse model treated with anti-CTLA-4 therapy (*35*) (B) or

from biopsies of melanoma patients prior to treatment with pembrolizumab (*5*). Middle line: median; box edges: 25th and 75th percentiles, whiskers: most extreme points that do not exceed ±IQR*1.5; further outliers are marked individually. *P*-value: one-sided t-test. **(D-F)** Resistance signatures predict melanoma patient outcomes following pembrolizumab treatment from pre-treatment RNA-Seq in an independent cohort of 112 patients. **(D)** KM plots of progression-free survival (PFS) for the 104 patients in the cohort with available PFS data, when the patients are stratified by high (top 25%), low (bottom 25%), or intermediate (neither high nor low) expression of the respective signature. Prediction is enhanced when controlling for cell cycle as a confounder (two right plots, **materials and methods**). See **figs. 12 to 13**. **(E)** Bar plot shows predictive value for PFS for the 104 patients as in (D) with a COX regression model that accounts for inferred T-cell infiltration levels ($-\log_{10}$(p-value), x axis). Light bars: enhances PFS; grey bars: reduces PFS. Bars with black border denote the new signatures identified in this study for malignant resistance. Dashed line: $p < 0.05$. Resistance signatures are significantly more predictive compared to others ($P = 3.37*10^{-6}$, Wilcoxon-ranksum test)). **(F)** Distribution of OE scores (y axis) of each signature in the pre-treatment bulk RNA-Seq profiles, showing patients with either intrinsic resistance (Non-CB, n=49) or with clinical benefit (CB, n=39), with the latter also further stratified based on duration of response (CB < 6mo, n=5; 6mo < CB < 1 year, n=9; CB > 1 year, n=25). Twenty-four patients with unknown response or stable disease are not shown here (see **fig. 14**). Distinctions are enhanced when accounting for inferred T-cell infiltration levels (right). *P1* and *P2* are the one-sided t-test p-value obtained when comparing the non-CB patients to the CB or CB > 1yr patients, respectively. The AUC at the top was obtained when predicting long-term CB (CB > 1yr) in all patients with a recorder response (n =101). Box plots formatted as in (B). **(G)** Box-plots show the distribution of OE scores (y axis) of each signature in the pre-treatment bulk RNA-Seq profiles, for patients with complete response (CR, n=14), partial response (PR, n=25), or progressive disease (PD, n=49). *P* is the one-sided t-test p-value obtained when comparing the CR patients to the PR and PD patients. The AUC at the top was obtained when predicting CR in all patients with a recorder response (n =101). **(H)** Bar plot shows predictive value for predicting complete response with the different signatures ($-\log_{10}$(t-test p-value), x-axis) in 101 patients with a recorded response. Light bars: positive impact; grey bars: negative impact. Bars with black border denote the new signatures identified in this study for malignant resistance. Dashed line: $p = 0.05$. Resistance signatures are significantly more predictive compared to other signatures (P =

1.64*10-8, Wilcoxon ranksum test). AUC values are marked next to the bar for each significant association. (I) Model for ICR based on this study.

[0089] FIG. 5 – Classification of malignant and non-malignant cells. (**A**) Inferred large-scale CNVs distinguish malignant (right) from nonmalignant (left) cells. Shown are the inferred CNVs (amplification, deletion) along the chromosomes (x axis) for cells (y axis) in two representative tumors. (**B-E**) Congruence between different assignment methods. (**B**) Each plot shows the relation between two different scorings, by showing for CD45$^-$cells the distribution of scores (y axis) by one scheme, stratified to two categories by another scheme. CNV: inference of malignant and non-malignant CD45$^-$ cells as in (A, **materials and methods**); signature based: assignment of CD45$^-$ cells as malignant or stroma by scoring the corresponding expression signatures (**materials and methods**); differential similarity to melanoma: assignment of CD45$^-$cells as malignant or non-malignant by similarity to bulk melanoma tumors compared to normal tissue. Middle line: median; box edges: 25th and 75th percentiles; whiskers: most extreme points that do not exceed ±IQR*1.5; points beyond the distance: single points. **(C)** Distribution of CNV-R-score for cells identified as malignant and non-malignant. The CNV-R-score of a cell is defined as the Spearman correlation coefficient (r) between the cell's CNV profile and its tumor's inferred CNV profile (**materials and methods**). **(D)** The distribution of CNV-R-scores across each identified cell type. **(E)** The CNV-R-score (y axis) at each overall CNV signal (**materials and methods**) for malignant and non-malignant cells; Non-malignant cells with values that exceed the dashed lines were considered unresolved and were omitted from further analyses.

[0090] FIG. 6 – Non-malignant cells. Shown are tSNE plots of all non-malignant cells (dots), shaded by **(A)** OE scores (bar) of well-established cell type markers (**table 26C**), or **(B)** detection of *CD4* or *CD8* (*CD8A* or *CD8B*).

[0091] FIG. 7 – Cell type specific ICR signatures. Left panels: Box-plots show the distribution of OE scores for the ICR signature in each cell type in ICR and TN patients. Middle line: median; box edges: 25th and 75th percentiles; whiskers: most extreme points that do not exceed ±IQR*1.5; points beyond the distance: single points. Middle and right panels: Receiver Operating Characteristic (ROC) curves of the performances of different signatures in classifying cells (middle) or samples (left) as ICR or TN. **(A)** Malignant cells, **(B)** CD4 T cells, **(C)** CD8 T cells, **(D)** B cells, **(E)** macrophages.

[0092] FIG. 8 – Shift in the balance of cytotoxicity and exhaustion states in CD8 T-cells in the patient with CB. (A) The distribution of expression levels of each of five

key checkpoint genes in CD8 T cells from ICR, TN, and CB tumors. **(B)** Distinct relationship between exhaustion and cytotoxicity signatures in CD8 T cells from a CB patient. For each cell (dot) shown are the cytotoxicity (x-axis) and exhaustion (y-axis) scores (**materials and methods**), using different exhaustion signatures from (*1*) and (*17*). TN; ICR; CB. Cells from the CB patient have lower than expected exhaustion scores (p-values, hypergeometric test **materials and methods**).

[0093] FIG. 9 – Clonal expansion of CD8 T cells. (A) TCR reconstruction. Shown is the fraction (*y*-axis) of T-cells with one (α or β), both or no TCR chain reconstructed at full length (**materials and methods**). **(B)** Variation in CD8 T cell expansion across tumors. Violin plots show the distribution of estimated proportions of CD8 T cell clones in each tumor. Tumors are shaded by treatment group. The tumors of ICR patients have higher T-cell clonal expansion ($P = 3.2*10^{-2}$, one-sided Wilcoxon ranksum test). **(C,D)** Persistence of clones over time in one patient (Mel75). Shown are the number (C) and relative proportions (D) of cells in each clone for two post-ICI lesions collected, a year apart, from patient Mel75.

[0094] FIG. 10 – The relationship between the malignant ICR program and cell cycle. (A, B) Higher ICR in cycling cells. **(A)** Box plots of the distribution of OE scores of the oncogenic-ICR signatures (y-axis) in cycling and non-cycling cells from ICR and TN tumors (x-axis). The middle line represents the median; box edges are the 25^{th} and 75^{th} percentiles, and whiskers represent the most extreme points that do not exceed ±IQR*1.5; points beyond the distance are plotted as single points. **(B)** Heatmap of the expression of ICR-up (bar) and down (black bar) genes (rows) that are also induced (repressed) in cycling vs. non-cycling malignant cells. Cells (columns) are sorted by TN and ICR tumors and clustered within each set (bar on top); the cells' cycling status in each category is marked by the bar on top. Bottom: Oncogenic ICR signature score (y axis) in each cell (x axis). **(C)** Abemaciclib represses the uICR program in breast cancer cell lines. Heatmap of the relative expression of all the uICR genes (rows) in Abemaciclib-treated and control breast cancer cells lines (columns), based on the data in (24). Gene expression is relative to the basal expression level in each cell line. Bottom: OE scores (y axis) of the uICR signature for each cell line (x axis).

[0095] FIG. 11 – The resistance signatures score in TCGA tumors predict survival of melanoma patients. Kaplan-Meier (KM) plots stratified by high, intermediate

or low OE of the respective signature in bulk RNA-Seq of TCGA tumors. *Pc* p-values test if the signature further enhances the predictive power of models with inferred T-cell infiltration levels as a covariate.

[0096] FIG. 12 – The resistance signature scores in pre-treatment biopsies predict response to anti-PD-1 therapy in an independent cohort. KM plots of progression-free survival (PFS) for the 104 of 112 patients in validation cohort 1 with PFS data, with patients stratified by high, intermediate and low OE score of the respective signature. *Pc* p-values test if the signature further enhances the predictive power of models with inferred T cell infiltration levels as a covariate.

[0097] FIG. 13 – The predictive performance of resistance signatures is enhanced when controlling for the cell cycle. KM plots of progression-free survival (PFS) for the 104 of 112 patients in validation cohort 1 with PFS data, with patients stratified by high, intermediate and low OE score of the respective, after controlling for cell cycle as a confounding factor (**materials and methods**).

[0098] FIG. 14 – The expression of the resistance signatures in 101 melanoma patients, stratified according to their clinical response to pembrolizumab. Distribution of OE scores (y axis) of each signature in the pre-treatment bulk RNA-Seq profiles, showing overall 101patients with complete response (CR, n = 14), partial response or stable disease (PR/SD, n = 38), or progressive disease (PD, n = 49). P is the one-sided t-test p-value obtained when comparing the CR patients to the PR, SD and PD patients. AUC is also marked on top. Middle line: median; box edges: 25^{th} and 75^{th} percentiles; whiskers: most extreme points that do not exceed ±IQR*1.5.

[0099] FIG. 15 – Pan-cancer analysis of the resistance signatures. Box-plots of the distribution of OE scores (x-axis) of the uICR signature in bulk RNA-seq profiles of 9,559 tumors across 33 cancer types (y-axis) from TCGA either scored **(A)** "as-is" or **(B)** with a regression-based process to control for TME-related signals (**materials and methods**). Middle line: median; box edges: 25th and 75th percentiles; whiskers: most extreme points that do not exceed ±IQR*1.5; points beyond the distance: single points.

[0100] FIG. 16 – An unbiased analysis reveals a malignant cell state linked to ICR.

[0101] FIG. 17 – An overview of the patients analyzed.

[0102] FIG. 18 – Separation of immunotherapy treated and untreated tumors by Principle Component (PC) analysis.

[0103] **FIG. 19** – Correlation between the resistance signature and patients that are naïve or resistant to immunotherapy.

[0104] **FIG. 20** – A leave-one-out cross validation analysis.

[0105] **FIG. 21** – Mutual exclusive expression of the ITR up and down genes across malignant cells, and their anti-correlation in TCGA.

[0106] **FIG. 22** – Correlation between the resistance signature and MHC-I expression.

[0107] **FIG. 23** – Association of metallothionein expression and treated and untreated subjects.

[0108] **FIG. 24** – Association of the resistance signature with prognosis.

[0109] **FIG. 25** – The resistance signature compared to other single-cell based signatures.

[0110] **FIG. 26** – The ITR signature is predictive of eventual outcome in both mouse and human data.

[0111] **FIG. 27** – Association of complete responders and non-complete responders to genes up-regulated post-treatment with immunotherapy.

[0112] **FIG. 28** – Association of complete responders and non-complete responders to genes down-regulated post-treatment with immunotherapy.

[0113] **FIG. 29** – Malignant cells ITR signatures have higher exclusion signatures and treatment naive malignant cells have higher infiltration signatures.

[0114] **FIG. 30** – Analysis of CD8 T cells.

[0115] **FIG. 31** – Analysis of CD8 T cells.

[0116] **FIG. 32** Analysis of CD8 T cells.

[0117] **FIG. 33** – The CD8 ITR signature is strongly associated with clonal expansion.

[0118] **FIG. 34** – An interaction map of genes in the ITR signature and immune and stromal genes.

[0119] **FIG. 35** – The number of interactions between differentially expressed malignant genes and immune and stromal genes.

[0120] **FIG. 36** – ITR versus T cell scores in different cancers.

[0121] **FIG. 37** – ITR scores in two melanomas.

[0122] **FIG. 38** – tSNE analysis of ER+ metastatic breast cancer using single nuclei RNA-seq (snRNA-seq) on fresh and frozen tissue samples.

[0123] **FIG. 39** – tSNE analysis of 22 colon cancer samples using scRNA-seq.

[0124] **FIG. 40** – The expanded T cell state is highly correlated with the overall T cell infiltration level of tumors in an independent lung cancer cohort (**Table 10**).

[0125] **FIG. 41** – CDK4/6 inhibitors sensitize melanoma cells.

[0126] **FIG. 42** – CDK4/6 inhibitors induce markers of differentiation, senescence and immunogenicity in melanoma.

[0127] **FIG. 43** – CDK4/6 inhibitors eliminate a resistant subpopulation of melanoma cells.

[0128] **FIG. 44 – Identification of a T cell exclusion program in malignant cells. (A)** Study overview. 31 tumors from melanoma patients (discovery cohort) were profiled by scRNA-seq (left, tan) and integrated analytically with bulk RNA-Seq data from TCGA (473 melanoma tumors). The discovered program was tested in two validation cohorts of bulk RNA-Seq collected independently (right). **(B)** Analysis approach to discover malignant cell programs associated with immune cell infiltration or exclusion. **(C-D)** Distinct profiles of malignant and nonmalignant cells. tSNE plots of single cell profiles (dots) from malignant **(C)** or nonmalignant **(D)** cells, shaded by *post-hoc* annotation (**Methods**, D left) or by tumor **(C, D right)**. **(E)** Exclusion program. Expression (centered and scaled; bar) of the top genes (columns) in the exclusion program across the malignant cells (rows), sorted by untreated or post-treatment tumors (bar, left) and clustered within each class. Leftmost bar: cycling and non-cycling cells within each group. Right: The overall expression (**Methods**) of the exclusion program in each cell. See also **FIG. 51** and **Tables 1,2 and 26C.**

[0129] **FIG. 45 – Exclusion and resistance programs characterizing individual malignant cells from patients who failed immunotherapy. (A)** Post-treatment program in malignant cells. Left: The Overall expression (**Methods**) of the post-treatment program in malignant cells from post-treatment and untreated patients, when obtained in a cross-validation (CV) procedure and tested on withheld data. Middle line: median; box edges: 25^{th} and 75^{th} percentiles, whiskers: most extreme points that do not exceed $\pm$IQR*1.5; further outliers are marked individually. Right: Receiver Operating Characteristic (ROC) curve of the performances of different programs in classifying cells as post-treatment or untreated; the CV post-treatment signature was obtained by leave-one (patient) out CV; the first and second Area Under the Curve (AUC) values are for classification of cells and samples, respectively. **(B)** Significant overlap between the exclusion and post-treatment programs. Venn diagram of the number of genes in each program and in their overlap. P-value: hypergeometric test. **(C)** Program genes. Expression (centered and scaled, bar) of the top genes (columns) in the post-treatment program across the malignant cells (rows), sorted by untreated or post-treatment

tumors (bar, left) and clustered within each class. Leftmost bar: cycling and non-cycling cells within each group. Right: overall expression of the post-treatment program in each cell. **(D)** Repressed and induced processes. The distribution of overall expression scores of differentially expressed gene sets in malignant cells from post-treatment and untreated (gray) tumors (formatted as in (A)). **(E)** The exclusion program is higher in post-treatment malignant cells. The distribution of overall expression scores of the exclusion program in malignant cells from post-treatment and untreated (gray) tumors. See also **Tables 5 and 8.**

[0130] FIG. 46 – The resistance program is a coherently regulated module that represses cell-cell interactions. (A) The immune resistance program is higher in uveal vs. cutaneous melanoma. The distribution of overall expression scores of the immune resistance program in cutaneous *vs.* uveal melanoma tumors from TCGA, scored after filtering tumor microenvironment contributions (**Methods**). **(B)** Cell-cell interaction genes are repressed in the immune resistance program. The number of genes (y axis, top) in each part of the program encoding proteins that engage in a physical interaction with other cell types and the significance of the corresponding enrichment (y axis, $-\log_{10}$(P-value), hypergeometric test, bottom). Values above the dashed line are statistically significant. **(C-D)** Co-regulation of the immune resistance program. **(C)** The overall expression of the induced (*x* axis) and repressed (*y* axis) parts of the immune resistance programs in each malignant cell (top, scRNA-seq data) and in cutaneous melanoma tumors (bottom, TCGA RNA-Seq data, after filtering tumor microenvironment signals). The Pearson correlation coefficient (*r*) and p-value are marked. **(D)** Gene-gene Pearson correlation coefficients (bar) between the genes in the resistance program, across individual malignant cells from the same tumor (top, average coefficient) or across cutaneous melanoma tumors from TCGA skin (bottom, after filtering tumor microenvironment effects). See also **FIG. 52**.

[0131] FIG. 47 – The resistance program is associated with the cold niche *in situ*. (A-B) Multiplex imaging relates resistance program genes to hot or cold niches. Malignant cells expressing high or low/moderate protein levels of HLA-A **(A)** and c-Jun **(B)** and their proximity to $CD3^+$ T cells or $CD3^+CD8^+$ T cells in three representative tumors. **(C)** Congruence of multiplex protein and scRNA-seq profiles. Left and middle: tSNE plots of co-embedding of cells from the scRNA-seq data and the images of a specific tumor (Mel112; others shown in **FIG. 53**), with cells shaded by clusters (top left), data source (bottom left), and source and cell type (right). Right: Log-odds ratio (bar, **Methods**) assessing for each

pair of cell types (rows, columns) if they are assigned to the same cluster significantly more (>0) or less (<0) than expected by chance. See also **FIG. 53.**

[0132] FIG. 48 – The resistance program is prognostic and predictive in validation cohorts. (A) The program predicts melanoma patient survival based on bulk RNA-Seq from TCGA (Akbani et al., 2015). Kaplan-Meier (KM) plots stratified by high (top 25%), low (bottom 25%), or intermediate (remainder) expression of the respective program subset. *P*: COX regression p-value; *Pc:* COX regression p-value that tests if the program further enhances the predictive power of a model with inferred T cell infiltration levels as a covariate. **(B, C)** Resistance signatures distinguish responders and non-responders in mouse models and melanoma patients. The distribution of overall expression of the resistance program in bulk RNA-Seq from **(B)** a lung cancer mouse model treated with anti-CTLA-4 therapy (Lesterhuis et al., 2015) or **(C)** biopsies of melanoma patients collected prior to treatment with pembrolizumab (Hugo et al., 2016). Middle line: median; box edges: 25^{th} and 75^{th} percentiles, whiskers: most extreme points that do not exceed $\pm$IQR*1.5; further outliers are marked individually. **(D-F)** The program predicts melanoma patient outcomes following pembrolizumab treatment from pre-treatment RNA-Seq in an independent cohort of 112 patients. **(D)** KM plots of progression-free survival (PFS) for the 104 patients in the cohort with available PFS data, stratified by high (top 25%), low (bottom 25%), or intermediate (remainder) expression of the respective program subset. **(E)** Predictive value for PFS ($-\log_{10}$(p-value), x axis, COX regression model that accounts for inferred T cell infiltration levels) for the 104 patients in (D). Bars: positive/negative correlation between expression and PFS. Black border: subsets of the resistance program. Dashed line: p = 0.05. **(F)** Overall expression of the resistance program (y axis) in the pre-treatment bulk RNA-Seq profiles of patients with intrinsic resistance (Non-CB, n=49) or clinical benefit (CB, n=39), latter further stratified by response duration (CB < 6mo, n=5; 6mo < CB < 1 year, n=9; CB > 1 year, n=25). Twenty four patients with unknown response or stable disease are not shown here. *P1* and *P2*: one-tailed t-test p-value when comparing the non-CB patients to the CB or to CB > 1yr patients, respectively. AUC for predicting CB > 1yr in all patients with a recorded response (n = 101) is denoted. Box plots formatted as in (B). **(G)** Overall expression values of the resistance program (y axis) in the pre-treatment bulk RNA-Seq profiles of patients with complete response (CR, n = 14), partial response (PR, n = 25), or progressive disease (PD, n = 49). *P*: one-tailed t-test p-value comparing CR patients to PR and PD patients. AUC for

predicting CR in all patients with a recorded response (n = 101). **(H)** Predictive value of different signatures for complete response (-$\log_{10}$(t-test p-value), x axis) in 101 patients with a recorded response. Bars: expression associated with CR/non-CR, respectively. Black border: subsets of the resistance program. Dashed line: p = 0.05. AUC values are marked next to the bar for each significant association. See also **FIG. 54, 55, 57** and **Table 10**.

[0133] FIG. 49 – The resistance program can be reversed by CDK4/6 inhibition. (A-C) Impact on breast cancer tumors and cell lines. **(A)** Significance (y axis, -$\log_{10}$(p-value), Wilcoxon rank sum test) of induction (dark green) or repression (light green) of the program subsets in breast cancer tumors from abemaciclib treated mice compared to vehicle (Goel et al., 2017). **(B)** Overall expression of the program in breast cancer cell lines (M361, MCF and M453) treated with abemaciclib ("abe") or with DMSO vehicle ("con"). Middle line: median; box edges: 25th and 75th percentiles, whiskers: most extreme points that do not exceed ±IQR*1.5; further outliers are marked individually. *P*-value: paired t-test. **(C)** Expression of 40 program genes (columns; shaded bar) that were most differentially expressed in abemaciclib-treated vs. control breast cancer cells lines (rows). Expression is normalized to each cell line's control. Right: overall expression values of the program for each cell line. **(D-G)** CDK4/6 inhibition reverses the program in melanoma cell lines and induces the SASP. (D,E) tSNE plots of 4,024 IGR137 **(D)** and 7,340 UACC257 **(E)** melanoma cells, shaded by (left to right): treatment, clusters, or the expression of a cell cycle signature, resistance program, MITF signature, SASP signature and *DNMT1*. **(F)** Concentration (pg/ml, y axis) of secreted chemokines in the supernatant of melanoma cells treated for 7 days with abemaciclib (500 nM) or with DMSO control. **P<0.01, ***P<0.001 *t*-test. **(G)** Senescence associated alpha-galactosidase activity and morphological alterations in melanoma cells treated for 10 days with abemaciclib (500 nM, right) vs. DMSO control (left). See also **FIG. 56** and **Table 23.**

[0134] FIG. 50 – Immune resistance model. Malignant cells that evade the immune system have a unique transcriptional state, which distinguishes between responders and non-responders to immunotherapy. This state is tightly linked to the exclusion of T cells from the tumor, the repression of SASP and cell-cell communication routes, and the inhibition of cytokine secretion. CDK4/6 inhibition can reverse this state in malignant cells.

[0135] FIG. 51 – Assignment of cells into cell types by scRNA-seq; related to FIG. 44. (A) Inferred large-scale CNVs distinguish malignant from nonmalignant cells.

Shown are the inferred CNVs (amplification, deletion) along the chromosomes (x axis) for cells (y axis) in two representative tumors partitioned as malignant (left) or nonmalignant (right) by CD45 sorting and transcriptional features. **(B-E)** Congruence between different assignment methods. **(B)** Each plot shows the relation between two different scorings, by showing for $CD45^-$ cells the distribution of scores (y axis) by one scheme, stratified to two categories by another scheme. CNV: inference of malignant and nonmalignant $CD45^-$ cells (as in A, **Methods**); signature based: assignment of $CD45^-$ cells as malignant or stroma by scoring the corresponding expression signatures (**Methods**); differential similarity to melanoma: assignment of $CD45^-$ cells as malignant or nonmalignant by similarity to bulk melanoma tumors compared to normal tissue. Middle line: median; box edges: 25^{th} and 75^{th} percentiles, whiskers: most extreme points that do not exceed $\pm$IQR*1.5; further outliers are marked individually. **(C)** Distribution of CNV-R-scores for cells called as malignant or nonmalignant. The CNV-R-score of a cell is the Spearman correlation coefficient (*r*) between the cell's CNV profile and its tumor's inferred CNV profile (**Methods**). **(D)** The distribution of CNV-R-scores across each identified cell subset. Box plots as in (B). **(E)** The CNV-R-score (y axis) *vs.* the overall CNV signal (x axis, **Methods**) for malignant and nonmalignant cells; Nonmalignant cells with values that exceed the dashed lines were considered unresolved and were omitted from further analyses. **(F-G)** tSNE plots of all nonmalignant cells (dots), shaded by **(F)** overall expression (bar) of well-established cell type markers (**Table 26C**), or **(G)** detection of *CD4* or *CD8* (*CD8A* or *CD8B*).

[0136] FIG. 52 – Co-variation of the resistance signature genes across single cells within each tumor; related to FIG. 46. Gene-gene Pearson correlation coefficients (bar) between the genes in the resistance program, across individual malignant cells from each specific tumor (as labeled). Genes are sorted in the same order in all heatmaps (and in FIG. 46D). The consistent intra-tumor correlation suggests shared regulation.

[0137] FIG. 53 – Integrative analysis of scRNA-seq and spatial multiplex protein IHC data; related to FIG. 47. (A-D) Integrative analysis of scRNA-seq and CyCIF multiplex protein data from each of four tumors: **(A)** Mel79, **(B)** Mel80, **(C)** Mel74, and **(D)** Mel89. Left: tSNE plots of co-embedding of cells from scRNA-seq and images of each tumors, with cells shaded by (from left): clusters, data source, or source and cell type. Right: Log-odds ratio (bar, **Methods**) assessing for each pair of cell types (rows, columns) if they are assigned to the same cluster significantly more (>0) or less (<0) than expected by chance.

[0138] FIG. 54 – The immune resistance program predicts survival of TCGA melanoma patients; related to FIG. 48. Kaplan-Meier (KM) plots stratified by high, intermediate or low Over expression of the respective signature in bulk RNA-Seq of TCGA tumors. P: COX regression p-value; *Pc:* COX regression p-value that tests if the program further enhances the predictive power of a model with inferred T cell infiltration levels as a covariate.

[0139] FIG. 55 – The immune resistance program predicts response to anti-PD-1 therapy in an independent cohort; related to FIG. 48. (A-E) KM plots of progression-free survival (PFS) for the 104 of 112 patients in validation cohort 2 with PFS data, with patients stratified by high, intermediate and low over expression values of the respective signature, after controlling for cell cycle as a confounding factor (**Methods**). *Pc* p-values test if the signature further enhances the predictive power of models with inferred T cell infiltration levels as a covariate. **(F)** Distribution of overall expression values (y axis) of each signature in the pre-treatment bulk RNA-Seq profiles, showing overall 101 patients with either complete response (CR, n = 14), partial response/stable disease (PR/SD, n = 38), or progressive disease (PD, n = 49). P is the one-sided t-test p-value obtained when comparing CR patients vs. PR, SD and PD patients. AUC is also marked on top. Middle line: median; box edges: 25^{th} and 75^{th} percentiles, whiskers: most extreme points that do not exceed ±IQR*1.5; further outliers are marked individually.

[0140] FIG. 56 – Relationship between the resistance program and cell cycle; related to FIG. 48. (A, B) Higher expression of the resistance program in cycling cells. **(A)** Distribution of overall expression values of the resistance program (y axis) in cycling and non-cycling cells from either post-treatment or untreated tumors (x axis). Solid line: mean of the respective distribution; dashed line: mean across *all* malignant cells. **(B)** Expression of genes from the resistance program (rows) that are also differentially expressed in cycling *vs.* non-cycling malignant cells. Cells (columns) are sorted by untreated and post-treatment tumors and clustered within each set (bar on top); the cells' cycling status in each category is marked by the bar on top. **(C)** Abemaciclib represses the resistance program in breast cancer cell lines. The relative expression of all genes in the resistance program (rows) in abemaciclib-treated and control breast cancer cells lines (columns), based on the data in (Goel et al., 2017). Expression levels are relative to the basal expression level in each cell line. Bottom: overall expression (y axis)

of the resistance program in each cell line (x axis).

[0141] FIG. 57 – Pan-cancer analysis of the resistance program; related to FIG. 48. (A-B) Overall expression of the resistance program (x axis) in 9,559 tumors from 33 cancer types (y axis) from TCGA. In (**B**) a regression-based approach controls for tumor microenvironment-related signals (**Methods**). Middle line: median; box edges: 25th and 75th percentiles, whiskers: most extreme points that do not exceed ±IQR*1.5; further outliers are marked individually.

[0142] FIG. 58 – B16 Study design. Mouse study using checkpoint inhibitors and CDK4/6 inhibitors.

[0143] FIG. 59 – Growth curves. B16 implanted mice were treated as indicated and tumor growth was measured.

[0144] FIG. 60 – Survival curves. B16 implanted mice were treated as indicated and survival was measured.

[0145] FIG. 61 – Growth curves. (A-C) Additional growth curves at day 4 (B) and day 7 (C). CD8 depletion shows dependence on CD8 T cells.

[0146] FIG. 62 – Identification of a T cell exclusion program in malignant cells. (A) Study overview. **(B)** Method to discover malignant cell programs associated with immune cell infiltration or exclusion. **(C,D)** Distinct profiles of malignant and non-malignant cells. tSNE of single cell profiles (dots) from malignant **(C)** or non-malignant **(D)** cells, shaded by *post-hoc* annotation (D left) or by tumor (C, D right). In (C) only tumors with at least 50 malignant cells are shown. **(E)** Exclusion program. Expression (centered and scaled; bar) of the top genes (columns) in the exclusion program across malignant cells (rows), sorted by untreated or post-treatment tumors (bar, left). Leftmost bar: cycling and non-cycling (black) cells. Right: Overall Expression (OE) (**Methods**) of the exclusion program. See also **Figures 69-70** and **Tables 24-27**.

[0147] FIG. 63 – Exclusion and resistance programs characterizing individual malignant cells from patients with resistance to ICI. (A) Post-treatment program in malignant cells. Left: OE of the post-treatment program in malignant cells from post-treatment and untreated patients, tested on withheld data (**Methods**). Middle line: median; box edges: 25th and 75th percentiles, whiskers: most extreme points that do not exceed ±IQR*1.5; further outliers are marked individually. Right: The performances of different programs in classifying cells as post-treatment or untreated; the first and second Area Under

the Curve (AUC) values are for classifying cells and samples, respectively. **(B)** Significant overlap between the exclusion and post-treatment programs. **(C)** Expression (centered and scaled, bar) of the top genes (columns) in the post-treatment program across malignant cells (rows), sorted by untreated or post-treatment tumors (bar, left). Leftmost bar: cycling and non-cycling cells. Right: OE of the post-treatment program. **(D)** Distribution of OE scores (as in (A)) of differentially expressed gene sets in malignant cells from post-treatment and untreated tumors. **(E)** Distribution of OE scores (as in (A)) of the exclusion program in malignant cells from post-treatment and untreated tumors. See also **Figure 70** and **Tables 27-28**.

[0148] FIG. 64 – The resistance program is a coherently regulated module that represses cell-cell interactions. (A) Distribution of program OE scores in cutaneous *vs.* uveal melanoma from TCGA, after filtering microenvironment contributions (**Methods**). **(B)** Right: Number of genes in each part of the program that mediate physical interactions with other cell types, and the significance of the corresponding enrichment. Dashed line: statistical significance. **(C-D)** Co-regulation of the program. **(C)** OE of the induced and repressed parts of the immune resistance programs in malignant cells (left, scRNA-seq data) and cutaneous melanoma tumors (right, TCGA RNA-Seq data, after filtering microenvironment signals). Pearson correlation coefficient (*r*) and p-value are marked. **(D)** Pearson correlation coefficients (bar) between the program's genes, across malignant cells from the same tumor (left, average coefficient) or across cutaneous melanoma from TCGA (right, after filtering microenvironment effects). See also **Figure 71**.

[0149] FIG. 65 – The resistance program is associated with the cold niche *in situ*. (A,B) Congruence of *in situ* multiplex protein and scRNA-seq profiles. **(A)** Co-embedding of profiles from scRNA-seq and multiplex imaging of the Mel112 tumor (others in **Figure 72**), with cells shaded by clusters (top left), data source (bottom left), or source and cell type (right). **(B)** Log-odds ratio (bar, **Methods**) assessing for each pair of cell types (rows, columns) if they are assigned to the same cluster significantly more (>0) or less (<0) than expected by chance. **(C-D)** Multiplex imaging relates program genes to hot or cold niches. Malignant cells expressing high or low/moderate levels of the MHC Class I **(C)** and c-Jun **(D)** proteins and their proximity to $CD3^+$ T cells or $CD3^+CD8^+$ T cells in three representative tumors. See also **Figure 72**.

[0150] FIG. 66 – The resistance program is prognostic and predictive in validation cohorts. (A) The program predicts melanoma patient survival in bulk RNA-Seq from TCGA.

Kaplan-Meier (KM) curves stratified by high (top 25%), low (bottom 25%), or intermediate (remainder) OE of the respective program. Number of subjects at risk indicated at the bottom of the KM curves for five time points. *P*: COX regression p-value; *Pc:* COX regression p-value that tests if the program enhances the predictive power of a model with inferred T cell infiltration levels as a covariate. **(B, C)** Distribution of OE of the resistance program in bulk tumors from **(B)** a lung cancer mouse model treated with anti-CTLA-4 therapy (Lesterhuis et al., 2015) or **(C)** melanoma patients prior to pembrolizumab treatment (Hugo et al., 2016). Middle line: median; box edges: 25th and 75th percentiles, whiskers: most extreme points that do not exceed ▒IQR*1.5; outliers are marked individually. **(D-F)** The program predicts ICI responses in Validation cohort 2. **(D)** KM plots for PFS for the 104 patients in the cohort with available PFS data, stratified by high (top 25%), low (bottom 25%), or intermediate (remainder) OE of the respective program (**Methods**). **(E)** OE of the resistance program (y axis) in the pre-treatment profiles of patients with intrinsic resistance (PD, n = 49) or objective response (OR, n = 39), the latter further stratified by response duration. Patients with unknown response or stable disease are not shown. *P1* and *P2*: one-tailed t-test p-value when comparing the PD patients to all the OR patients or to OR > 1yr patients, respectively. AUC for predicting OR > 1yr in all patients with a recorded response (n = 101) is denoted. Formatted as in (B). **(F)** OE scores of the resistance program (y axis) in the pre-treatment bulk RNA-Seq profiles of patients with complete response (CR, n = 14), partial response (PR, n = 25), or progressive disease (PD, n = 49). *P*: one-tailed t-test p-value comparing CR patients to PR and PD patients. AUC for predicting CR in all patients with a recorded response (n = 101). **(G,H)** Predictive value (y axis) compared to alternative signature-based predictors. Blue/grey bars: signatures positively/negatively associated with response. Black outline of bars: subsets of the resistance program denoted with numbered legends at the bottom. Dashed line: p = 0.05. **(G)** Predictive value for PFS (P^c as in (D), **STAR Methods**). **(H)** Predictive value for complete response. See also **Figures 73-74** and **Table 29**.

[0151] FIG. 67 – The resistance program can be reversed by CDK4/6 inhibition. (A) OE of the resistance program across cancer cell lines which are resistant or sensitive to both abemaciclib and palbociclib. **(B-D)** Impact of CDK4/6i on breast cancer tumors and cell line profiles. **(B)** Significance (y axis, -log^{10}(p-value), Wilcoxon rank sum test) of induction (dark) or repression (light) of the program subsets in tumors from abemaciclib treated mice compared to vehicle (Goel et al., 2017). **(C)** OE of the program in cell lines (M361, M453, and MCF) treated with abemaciclib ("abe") or with DMSO vehicle ("con"). Middle line:

median; box edges: 25th and 75th percentiles, whiskers: most extreme points that do not exceed ▒IQR*1.5; outliers are marked individually. *P*-value: paired t-test. **(D)** Expression of 40 program genes (columns) that were most differentially expressed in abemaciclib-treated vs. control (purple) cells lines (rows) (**Methods**). Expression is normalized in each cell line. Right: OE scores for each cell line. **(E-H)** CDK4/6i reverses the program in RB1-sufficient melanoma cell lines and induces the SASP. (**E,F**) tSNE of 4,024 IGR137 **(E)** and 7,340 UACC257 **(F)** melanoma cells, shaded by (1) treatment, (2) clusters, or the expression of (3) cell cycle signature, (4) resistance program, (5) MITF signature, (6) SASP signature and (7) *DNMT1*. **(G)** Concentration (pg/ml, y axis) of secreted chemokines in the supernatant of melanoma cells treated for 7 days with abemaciclib (500 nM) or with DMSO control. $^{**}P<0.01$, $^{***}P<0.001$ *t*-test (**Table 30B**). **(G)** Senescence-associated β -galactosidase activity and morphological alterations in melanoma cells treated for 10 days with abemaciclib (500 nM, right) *vs.* DMSO control (left). See also **Figure 75** and **Table 30**.

[0152] FIG. 68 – CDK4/6 inhibition combined with immunotherapy improves response and survival i*n vivo*. **(A)** Study design. n=9-19 per treatment group. **(B)** Rate of tumor outgrowth (ratio for every graph) is reduced in animals treated with phased combination (ICI followed by ICI plus abemaciclib) and (**C**) results in higher survival rates compared to other treatments. **(D)** Immune resistance model. See also **Figure 75**.

[0153] FIG. 69 – Cell type assignments; related to Figure 62. (A) Inferred large-scale CNVs distinguish malignant from nonmalignant cells. The inferred CNVs (amplification; deletion) of two representative tumors (Mel79 and Mel102) are shown along the chromosomes (x axis) for cells (y axis) that were classified as malignant (left) or non-malignant (right) according CD45 sorting and transcriptional features. **(B-E)** Congruence between different assignment methods (**Methods**). **(B)** Each plot shows the distribution of scores (y axis) by one scheme, when assigning the $CD45^-$ cells to malignant and nonmalignant cells according to anther scheme. Each scheme evaluates the likelihood that a given cell is malignant in a different way: CNV inference (as in A); the overall expression of melanoma and stroma cell signatures; differential similarity to bulk melanoma tumors compared to normal tissue. Middle line: median; box edges: 25th and 75th percentiles, whiskers: most extreme points that do not exceed ▒IQR*1.5; further outliers are marked individually. **(C)** Distribution of CNV-R-scores for cells classified as malignant or non-malignant. The CNV-R-score of a cell is the Spearman correlation coefficient (r^s) between

the cell's CNV profile and its tumor's inferred CNV profile (**Methods**). **(D)** The distribution of CNV-R-scores across each identified cell subset. Box plots as in (B). **(E)** The CNV-R-score (y axis) *vs.* the overall CNV signal (x axis, **Methods**) for malignant and non-malignant cells; Nonmalignant cells with values that exceed the dashed lines were considered unresolved and were omitted from further analyses. **(F-G)** tSNE plots of all non-malignant cells (dots), shaded by **(F)** overall expression (bar) of *de novo* cell type signatures (**Table 26B**), and **(G)** detection of T cell markers *CD4* or *CD8* (*CD8A* or *CD8B*), and B cell markers (*CD19* and *CD22*).

[0154] FIG. 70 – The immune resistance program is robust to varying definitions of T cell infiltration and can be decoupled from cell cycle; related to Figures 62-63. (A-C) Congruence between the transcriptional programs in malignant that are associated with the exclusion of different T cell subsets. **(A)** The inferred abundance of different T cell subsets is highly correlated across TCGA melanoma tumors. Pearson correlation coefficient (bar) between the inferred proportions of T cells of different subsets. **(B,C)** Overlap (B, Jaccard similarity coefficient) and correlation in expression across melanoma cells (C, left) or bulk tumors (C, middle and right) between malignant cell programs associated with the exclusion of different T cell subsets (rows, columns). **(D)** Congruence between exclusion programs derived with and without controlling for the cell cycle. Venn diagrams show the number of genes shared in upregulated (left) and downregulated (right) portions of indicated programs when they are derived with (top) and without (bottom) regressing out cell cycle from the scRNA-seq and bulk RNA-Seq data. **(E)** Resistance program is stronger in cycling cells even when filtering cell cycle effects. The distribution of Overall Expression scores of the resistance program (y axis) derived with (right) and without (left) filtering out cell cycle effects (**Methods**). Solid line: mean of the respective distribution; dashed line: mean across *all* malignant cells. **(F-G)** Regression of cell cycle effects masks differences between cycling and non-cycling cells, but preserves differences in the resistance program. **(F)** Expression of cell cycle genes (columns) across the malignant cells (rows), with (left) and without (right) regressing out cell cycle. Cells are sorted as cycling or non-cycling (red/black, respectively; leftmost bar). **(G)** Expression of genes in the exclusion (right) and post-treatment (left) programs (columns), after regressing out cell cycle from the data. Cells (rows) are sorted by untreated and post-treatment tumors (right bar) and clustered within each set; rightmost bar: cycling status.

[0155] FIG. 71 – Co-variation of the immune resistance program genes across single cells within each tumor; related to Figure 64. Gene-gene Pearson correlation coefficients (bar) between the genes in the resistance program, across individual malignant cells from each specific tumor (as labeled). Genes are sorted in the same order in all heatmaps (and in **Figure 64D**). The consistent intra-tumor correlation suggests shared regulation.

[0156] FIG. 72 – Integrative analysis of scRNA-seq and *in situ* immunofluorescence data; related to Figure 65. (A-D) Integrative analysis of scRNA-seq and CyCIF multiplex protein data (**Methods**) from each of four representative tumors: **(A)** Mel79, **(B)** Mel80, **(C)** Mel74, and **(D)** Mel89. Left: tSNE plots of co-embedding of cells from scRNA-seq and images of each tumors, with cells shaded by (from left): clusters, data source, or combined source and cell type. Right: Log-odds ratio (bar, **STAR Methods**) assessing for each pair of cell types (rows, columns) if they are assigned to the same cluster significantly more (>0) or less (<0) than expected by chance.

[0157] FIG. 73 – The immune resistance program predicts survival of TCGA melanoma patients; related to Figure 66. (A-D) Kaplan-Meier (KM) plots stratified by high, intermediate or low Overall Expression of the respective signature in bulk RNA-Seq of TCGA tumors. P: COX regression p-value; *Pc:* COX regression p-value that tests if the program further enhances the predictive power of a model with inferred $CD8^+$ T cell infiltration levels as a covariate compared to its prognostic value alone **(E)**. The number of subjects at risk are indicated for each group at the bottom of the KM curves for five different time points.

[0158] FIG. 74 – The immune resistance program predicts response to anti-PD-1 therapy in an independent cohort; related to Figure 66. (A-E) KM plots of progression-free survival (PFS) for the 104 of 112 patients in validation cohort 2 with PFS data, with patients stratified by high, intermediate and low Overall Expression values of the respective signature (labeled on top, see **Tables 24C**), after controlling for cell cycle as a confounding factor (**Methods**). *Pc* p-values test if the signature further enhances the predictive power of models with inferred $CD8^+$ T cell infiltration levels as a covariate. The number of subjects at risk are indicated for each group at the bottom of the KM curves for six different time points.

[0159] FIG. 75 – The immune resistance program in cell cultures, mouse cell lines, and various tumor types; related to Figures 67-68. (A) The distribution of the immune resistance scores across three human melanoma cell lines, in control conditions and following abemaciclib treatment. (B) The transcriptional state of patient-derived melanoma cells grown

in monoculture or in co-culture with autologous *ex vivo* expanded TILs, with and without abemaciclib; right: tSNE plots; left: the fraction of immune resistant and sensitive cells in each condition. **(C,D)** Differences in expression of the resistance program are aligned with the different level of resistance of mouse cell line models to ICI. **(C)** Distribution of Overall Expression of the resistance program (x axis) across single cells of three mouse cell lines (B16, CT26 and MC38) grown in *in vitro* monocultures. **(D)** Heatmap (bottom) shows genes (rows) from the immune resistance program that are differentially expressed between MC38 (bar), CT26 (green bar) and B16 (red bar) cells (columns) by the comparisons indicated on the left bar and legend; cells are first sorted by model and then by Overall Expression of the resistance program (top); the corresponding cell cycle score are shown in the middle panel. **(E,F)** To test the effect of CD8+ T cell depletion on response to phased combination of CDK4/6i and immunotherapy. B16 cells were implanted in C7BL/6 mice and treated with either vehicle control (n=5), phased combination of ICI and abemaciclib (n=10) or phased combination following CD8+ T cell depletion (n=9, STAR Methods). **(E)** The reduction in tumor outgrowth rate seen with phased therapy is lost in animals without CD8+ T cells. **(F)** KM survival curves of animals in (E). **(G,H)** The resistance program across tumor types. Distribution of Overall Expression scores of the resistance program (*x* axis) in 9,559 tumors from 33 cancer types (y axis) from TCGA, either scored as-is **(G)** or with a regression-based approach that controls for tumor microenvironment-related signals (**H**, **Methods**). Middle line: median; box edges: 25th and 75th percentiles, whiskers: most extreme points that do not exceed ▒IQR*1.5; further outliers are marked individually.

[0160] **FIG. 76 – In vivo perturbation of tumor cells.** tSNE analysis of B16 cells implanted subcutaneously into B6 animals followed by treatment with either vehicle, abemaciclib alone, immune checkpoint inhibitors (ICI) alone or ICI plus abema.

[0161] **FIG. 77 – Ex vivo perturb-seq.** Ex vivo melanoma cells obtained from a human patient were perturbed with a CRISPR system including barcoded guide sequences targeting the indicated genes. The barcodes from this experiment were isolated and sequenced. The graph indicates the barcode detection.

DETAILED DESCRIPTION OF THE EXAMPLE EMBODIMENTS

General Definitions

[0162] Unless defined otherwise, technical and scientific terms used herein have the same meaning as commonly understood by one of ordinary skill in the art to which this disclosure

pertains. Definitions of common terms and techniques in molecular biology may be found in Molecular Cloning: A Laboratory Manual, 2nd edition (1989) (Sambrook, Fritsch, and Maniatis); Molecular Cloning: A Laboratory Manual, 4th edition (2012) (Green and Sambrook); Current Protocols in Molecular Biology (1987) (F.M. Ausubel et al. eds.); the series Methods in Enzymology (Academic Press, Inc.): PCR 2: A Practical Approach (1995) (M.J. MacPherson, B.D. Hames, and G.R. Taylor eds.): Antibodies, A Laboraotry Manual (1988) (Harlow and Lane, eds.): Antibodies A Laboraotry Manual, 2nd edition 2013 (E.A. Greenfield ed.); Animal Cell Culture (1987) (R.I. Freshney, ed.); Benjamin Lewin, Genes IX, published by Jones and Bartlet, 2008 (ISBN 0763752223); Kendrew *et al.* (eds.), The Encyclopedia of Molecular Biology, published by Blackwell Science Ltd., 1994 (ISBN 0632021829); Robert A. Meyers (ed.), Molecular Biology and Biotechnology: a Comprehensive Desk Reference, published by VCH Publishers, Inc., 1995 (ISBN 9780471185710); Singleton *et al.*, Dictionary of Microbiology and Molecular Biology 2nd ed., J. Wiley & Sons (New York, N.Y. 1994), March, Advanced Organic Chemistry Reactions, Mechanisms and Structure 4th ed., John Wiley & Sons (New York, N.Y. 1992); and Marten H. Hofker and Jan van Deursen, Transgenic Mouse Methods and Protocols, 2nd edition (2011) .

[0163] As used herein, the singular forms "a", "an", and "the" include both singular and plural referents unless the context clearly dictates otherwise.

[0164] The term "optional" or "optionally" means that the subsequent described event, circumstance or substituent may or may not occur, and that the description includes instances where the event or circumstance occurs and instances where it does not.

[0165] The recitation of numerical ranges by endpoints includes all numbers and fractions subsumed within the respective ranges, as well as the recited endpoints.

[0166] The terms "about" or "approximately" as used herein when referring to a measurable value such as a parameter, an amount, a temporal duration, and the like, are meant to encompass variations of and from the specified value, such as variations of +/-10% or less, +/-5% or less, +/-1% or less, and +/-0.1% or less of and from the specified value, insofar such variations are appropriate to perform in the disclosed invention. It is to be understood that the value to which the modifier "about" or "approximately" refers is itself also specifically, and preferably, disclosed.

[0167] Reference throughout this specification to "one embodiment", "an embodiment," "an example embodiment," means that a particular feature, structure or characteristic

described in connection with the embodiment is included in at least one embodiment of the present invention. Thus, appearances of the phrases "in one embodiment," "in an embodiment," or "an example embodiment" in various places throughout this specification are not necessarily all referring to the same embodiment, but may. Furthermore, the particular features, structures or characteristics may be combined in any suitable manner, as would be apparent to a person skilled in the art from this disclosure, in one or more embodiments. Furthermore, while some embodiments described herein include some but not other features included in other embodiments, combinations of features of different embodiments are meant to be within the scope of the invention. For example, in the appended claims, any of the claimed embodiments can be used in any combination.

[0168] Reference is made to international patent application serial number PCT/US18/25507, filed March 30, 2018.

[0169] All publications, published patent documents, and patent applications cited in this application are indicative of the level of skill in the art(s) to which the application pertains. All publications, published patent documents, and patent applications cited herein are hereby incorporated by reference to the same extent as though each individual publication, published patent document, or patent application was specifically and individually indicated as being incorporated by reference.

Overview

[0170] Embodiments disclosed herein provide methods and compositions for detecting and modulating an immunotherapy resistance gene signature in cancer. Embodiments disclosed herein also provide for diagnosing, prognosing, monitoring and treating tumors based on detection of an immunotherapy resistance gene signature.

[0171] As used herein, the immunotherapy resistance signature is referred to as "ITR", "immunotherapy resistance signature", "ICR", "immune checkpoint inhibitor resistance", "mICR", "malignant immune checkpoint inhibitor resistance", "PIT", "post-immunotherapy", oncogenic-ICR", "unified-ICR", "uICR", "uICR-up", "uICR-down", "refined uICR", "immune resistant", "refined immune resistant", "functional immune resistance", "post treatment", "exclusion-up", or "exclusion-down". All of these terms may be used in reference to a gene signature in malignant cells from a subject that is resistant to immune checkpoint inhibitors (ICI). In regards to the exclusion signatures, these signatures refer to signatures in malignant cells that correlate to immune cell exclusion. In other words, exclusion-up refers to genes that are upregulated in malignant cells and that are correlated

with exclusion, while exclusion-down refer to genes downregulated in malignant cells that are correlated with exclusion. In certain embodiments, exclusion-down refers to genes upregulated when there is immune cell infiltration and thus can be referred to as the infiltration signature. In regards to "oncogenic ICR", "mICR", "malignant immune checkpoint inhibitor resistance", "Post-treatment", "PIT", or "post-immunotherapy", these terms all refer to genes differentially expressed in malignant cells after immunotherapy. All of "unified-ICR", "uICR", "uICR-up", "uICR-down", "refined uICR", "refined immune resistant", "functional immune resistance" refer to an immunotherapy resistant signature that includes genes from the post immunotherapy and exclusion signatures. "Immune resistance, "unified-ICR" or "uICR" refers to all genes in the exclusion signature and post treatment signature. The "functional immune resistance", "refined uICR" and "refined immune resistant" signatures are shortened lists from the immune resistance signature that include the best performing genes from the exclusion and post treatment signatures for predicting immunotherapy sensitivity. In regards to CD8 T cells "tICR" refers to T cell immune checkpoint inhibitor resistance signature.

[0172] As used herein the term "cancer-specific survival" refers to the percentage of patients with a specific type and stage of cancer who have not died from their cancer during a certain period of time after diagnosis. The period of time may be 1 year, 2 years, 5 years, etc., with 5 years being the time period most often used. Cancer-specific survival is also called disease-specific survival. In most cases, cancer-specific survival is based on causes of death listed in medical records.

[0173] As used herein the term "relative survival" refers to a method used to estimate cancer-specific survival that does not use information about the cause of death. It is the percentage of cancer patients who have survived for a certain period of time after diagnosis compared to people who do not have cancer.

[0174] As used herein the term "overall survival" refers to the percentage of people with a specific type and stage of cancer who have not died from any cause during a certain period of time after diagnosis.

[0175] As used herein the term "disease-free survival" refers to the percentage of patients who have no signs of cancer during a certain period of time after treatment. Other names for this statistic are recurrence-free or progression-free survival.

[0176] As used herein a "signature" may encompass any gene or genes, protein or proteins, or epigenetic element(s) whose expression profile or whose occurrence is associated

with a specific cell type, subtype, or cell state of a specific cell type or subtype within a population of cells (e.g., immune evading tumor cells, immunotherapy resistant tumor cells, tumor infiltrating lymphocytes, macrophages). In certain embodiments, the expression of the immunotherapy resistant, T cell signature and/or macrophage signature is dependent on epigenetic modification of the genes or regulatory elements associated with the genes. Thus, in certain embodiments, use of signature genes includes epigenetic modifications that may be detected or modulated. For ease of discussion, when discussing gene expression, any of gene or genes, protein or proteins, or epigenetic element(s) may be substituted. As used herein, the terms "signature", "expression profile", or "expression program" may be used interchangeably. It is to be understood that also when referring to proteins (e.g. differentially expressed proteins), such may fall within the definition of "gene" signature. Levels of expression or activity may be compared between different cells in order to characterize or identify for instance signatures specific for cell (sub)populations. Increased or decreased expression or activity or prevalence of signature genes may be compared between different cells in order to characterize or identify for instance specific cell (sub)populations. The detection of a signature in single cells may be used to identify and quantitate for instance specific cell (sub)populations. A signature may include a gene or genes, protein or proteins, or epigenetic element(s) whose expression or occurrence is specific to a cell (sub)population, such that expression or occurrence is exclusive to the cell (sub)population. A gene signature as used herein, may thus refer to any set of up- and/or down-regulated genes that are representative of a cell type or subtype. A gene signature as used herein, may also refer to any set of up- and/or down-regulated genes between different cells or cell (sub)populations derived from a gene-expression profile. For example, a gene signature may comprise a list of genes differentially expressed in a distinction of interest.

[0177] The signature as defined herein (being it a gene signature, protein signature or other genetic or epigenetic signature) can be used to indicate the presence of a cell type, a subtype of the cell type, the state of the microenvironment of a population of cells, a particular cell type population or subpopulation, and/or the overall status of the entire cell (sub)population. Furthermore, the signature may be indicative of cells within a population of cells *in vivo*. The signature may also be used to suggest for instance particular therapies, or to follow up treatment, or to suggest ways to modulate immune systems. The signatures of the present invention may be discovered by analysis of expression profiles of single-cells within a population of cells from isolated samples (e.g. tumor samples), thus allowing the discovery

of novel cell subtypes or cell states that were previously invisible or unrecognized. The presence of subtypes or cell states may be determined by subtype specific or cell state specific signatures. The presence of these specific cell (sub)types or cell states may be determined by applying the signature genes to bulk sequencing data in a sample. Not being bound by a theory the signatures of the present invention may be microenvironment specific, such as their expression in a particular spatio-temporal context. Not being bound by a theory, signatures as discussed herein are specific to a particular pathological context. Not being bound by a theory, a combination of cell subtypes having a particular signature may indicate an outcome. Not being bound by a theory, the signatures can be used to deconvolute the network of cells present in a particular pathological condition. Not being bound by a theory the presence of specific cells and cell subtypes are indicative of a particular response to treatment, such as including increased or decreased susceptibility to treatment. The signature may indicate the presence of one particular cell type. In one embodiment, the novel signatures are used to detect multiple cell states or hierarchies that occur in subpopulations of cells that are linked to particular pathological condition, or linked to a particular outcome or progression of the disease, or linked to a particular response to treatment of the disease (e.g. resistance to immunotherapy).

[0178] The signature according to certain embodiments of the present invention may comprise or consist of one or more genes, proteins and/or epigenetic elements, such as for instance 1, 2, 3, 4, 5, 6, 7, 8, 9, 10 or more. In certain embodiments, the signature may comprise or consist of two or more genes, proteins and/or epigenetic elements, such as for instance 2, 3, 4, 5, 6, 7, 8, 9, 10 or more. In certain embodiments, the signature may comprise or consist of three or more genes, proteins and/or epigenetic elements, such as for instance 3, 4, 5, 6, 7, 8, 9, 10 or more. In certain embodiments, the signature may comprise or consist of four or more genes, proteins and/or epigenetic elements, such as for instance 4, 5, 6, 7, 8, 9, 10 or more. In certain embodiments, the signature may comprise or consist of five or more genes, proteins and/or epigenetic elements, such as for instance 5, 6, 7, 8, 9, 10 or more. In certain embodiments, the signature may comprise or consist of six or more genes, proteins and/or epigenetic elements, such as for instance 6, 7, 8, 9, 10 or more. In certain embodiments, the signature may comprise or consist of seven or more genes, proteins and/or epigenetic elements, such as for instance 7, 8, 9, 10 or more. In certain embodiments, the signature may comprise or consist of eight or more genes, proteins and/or epigenetic elements, such as for instance 8, 9, 10 or more. In certain embodiments, the signature may

comprise or consist of nine or more genes, proteins and/or epigenetic elements, such as for instance 9, 10 or more. In certain embodiments, the signature may comprise or consist of ten or more genes, proteins and/or epigenetic elements, such as for instance 10, 11, 12, 13, 14, 15, or more. It is to be understood that a signature according to the invention may for instance also include genes or proteins as well as epigenetic elements combined.

[0179] In certain embodiments, a signature is characterized as being specific for a particular cell or cell (sub)population if it is upregulated or only present, detected or detectable in that particular cell or cell (sub)population, or alternatively is downregulated or only absent, or undetectable in that particular cell or cell (sub)population. In this context, a signature consists of one or more differentially expressed genes/proteins or differential epigenetic elements when comparing different cells or cell (sub)populations, including comparing different immune cells or immune cell (sub)populations (e.g., T cells), as well as comparing immune cells or immune cell (sub)populations with other immune cells or immune cell (sub)populations. It is to be understood that "differentially expressed" genes/proteins include genes/proteins which are up- or down-regulated as well as genes/proteins which are turned on or off. When referring to up-or down-regulation, in certain embodiments, such up- or down-regulation is preferably at least two-fold, such as two-fold, three-fold, four-fold, five-fold, or more, such as for instance at least ten-fold, at least 20-fold, at least 30-fold, at least 40-fold, at least 50-fold, or more. Alternatively, or in addition, differential expression may be determined based on common statistical tests, as is known in the art.

[0180] As discussed herein, differentially expressed genes/proteins, or differential epigenetic elements may be differentially expressed on a single cell level, or may be differentially expressed on a cell population level. Preferably, the differentially expressed genes/ proteins or epigenetic elements as discussed herein, such as constituting the gene signatures as discussed herein, when as to the cell population level, refer to genes that are differentially expressed in all or substantially all cells of the population (such as at least 80%, preferably at least 90%, such as at least 95% of the individual cells). This allows one to define a particular subpopulation of cells. As referred to herein, a "subpopulation" of cells preferably refers to a particular subset of cells of a particular cell type (e.g., resistant) which can be distinguished or are uniquely identifiable and set apart from other cells of this cell type. The cell subpopulation may be phenotypically characterized, and is preferably characterized by the signature as discussed herein. A cell (sub)population as referred to

herein may constitute of a (sub)population of cells of a particular cell type characterized by a specific cell state.

[0181] When referring to induction, or alternatively reducing or suppression of a particular signature, preferable is meant induction or alternatively reduction or suppression (or upregulation or downregulation) of at least one gene/protein and/or epigenetic element of the signature, such as for instance at least two, at least three, at least four, at least five, at least six, or all genes/proteins and/or epigenetic elements of the signature.

[0182] Various aspects and embodiments of the invention may involve analyzing gene signatures, protein signature, and/or other genetic or epigenetic signature based on single cell analyses (e.g. single cell RNA sequencing) or alternatively based on cell population analyses, as is defined herein elsewhere.

[0183] The invention further relates to various uses of the gene signatures, protein signature, and/or other genetic or epigenetic signature as defined herein, as well as various uses of the immune cells or immune cell (sub)populations as defined herein. Particular advantageous uses include methods for identifying agents capable of inducing or suppressing particular immune cell (sub)populations based on the gene signatures, protein signature, and/or other genetic or epigenetic signature as defined herein. The invention further relates to agents capable of inducing or suppressing particular immune cell (sub)populations based on the gene signatures, protein signature, and/or other genetic or epigenetic signature as defined herein, as well as their use for modulating, such as inducing or repressing, a particular gene signature, protein signature, and/or other genetic or epigenetic signature. In one embodiment, genes in one population of cells may be activated or suppressed in order to affect the cells of another population. In related aspects, modulating, such as inducing or repressing, a particular gene signature, protein signature, and/or other genetic or epigenetic signature may modify overall immune composition, such as immune cell composition, such as immune cell subpopulation composition or distribution, or functionality.

[0184] The signature genes of the present invention were discovered by analysis of expression profiles of single-cells within a population of tumor cells, thus allowing the discovery of novel cell subtypes that were previously invisible in a population of cells within a tumor. The presence of subtypes may be determined by subtype specific signature genes. The presence of these specific cell types may be determined by applying the signature genes to bulk sequencing data in a patient. Not being bound by a theory, many cells that make up a microenvironment, whereby the cells communicate and affect each other in specific ways. As

such, specific cell types within this microenvironment may express signature genes specific for this microenvironment. Not being bound by a theory the signature genes of the present invention may be microenvironment specific, such as their expression in a tumor. The signature genes may indicate the presence of one particular cell type. In one embodiment, the expression may indicate the presence of immunotherapy resistant cell types. Not being bound by a theory, a combination of cell subtypes in a subject may indicate an outcome (e.g., resistant cells, cytotoxic T cells, Tregs).

[0185] In certain embodiments, the present invention provides for gene signature screening. The concept of signature screening was introduced by Stegmaier et al. (Gene expression-based high-throughput screening (GE-HTS) and application to leukemia differentiation. Nature Genet. 36, 257–263 (2004)), who realized that if a gene-expression signature was the proxy for a phenotype of interest, it could be used to find small molecules that effect that phenotype without knowledge of a validated drug target. The signature of the present may be used to screen for drugs that reduce the signature in cancer cells or cell lines having a resistant signature as described herein. The signature may be used for GE-HTS. In certain embodiments, pharmacological screens may be used to identify drugs that are selectively toxic to cancer cells having an immunotherapy resistant signature. In certain embodiments, drugs selectively toxic to cancer cells having an immunotherapy resistant signature are used for treatment of a cancer patient. In certain embodiments, cells having an immunotherapy resistant signature as described herein are treated with a plurality of drug candidates not toxic to non-tumor cells and toxicity is assayed.

[0186] The Connectivity Map (cmap) is a collection of genome-wide transcriptional expression data from cultured human cells treated with bioactive small molecules and simple pattern-matching algorithms that together enable the discovery of functional connections between drugs, genes and diseases through the transitory feature of common gene-expression changes (see, Lamb et al., The Connectivity Map: Using Gene-Expression Signatures to Connect Small Molecules, Genes, and Disease. Science 29 Sep 2006: Vol. 313, Issue 5795, pp. 1929-1935, DOI: 10.1126/science.1132939; and Lamb, J., The Connectivity Map: a new tool for biomedical research. Nature Reviews Cancer January 2007: Vol. 7, pp. 54-60). Cmap can be used to screen for a signature in silico.

[0187] In one embodiment, the signature genes may be detected by immunofluorescence, immunohistochemistry, fluorescence activated cell sorting (FACS), mass cytometry (CyTOF), Drop-seq, RNA-seq, scRNA-seq, InDrop, single cell qPCR, MERFISH (multiplex

(in situ) RNA FISH) and/or by in situ hybridization. Other methods including absorbance assays and colorimetric assays are known in the art and may be used herein.

[0188] All gene name symbols refer to the gene as commonly known in the art. The examples described herein refer to the human gene names and it is to be understood that the present invention also encompasses genes from other organisms (e.g., mouse genes). Gene symbols may be those referred to by the HUGO Gene Nomenclature Committee (HGNC) or National Center for Biotechnology Information (NCBI). Any reference to the gene symbol is a reference made to the entire gene or variants of the gene. The signature as described herein may encompass any of the genes described herein. In certain embodiments, the gene signature includes surface expressed and secreted proteins. Not being bound by a theory, surface proteins may be targeted for detection and isolation of cell types, or may be targeted therapeutically to modulate an immune response.

[0189] As used herein, "modulating" or "to modulate" generally means either reducing or inhibiting the expression or activity of, or alternatively increasing the expression or activity of a target gene. In particular, "modulating" or "to modulate" can mean either reducing or inhibiting the activity of, or alternatively increasing a (relevant or intended) biological activity of, a target or antigen as measured using a suitable *in vitro*, cellular or *in vivo* assay (which will usually depend on the target involved), by at least 5%, at least 10%, at least 25%, at least 50%, at least 60%, at least 70%, at least 80%, at least 90%, or more, compared to activity of the target in the same assay under the same conditions but without the presence of an agent. An "increase" or "decrease" refers to a statistically significant increase or decrease respectively. For the avoidance of doubt, an increase or decrease will be at least 10% relative to a reference, such as at least 10%, at least 20%, at least 30%, at least 40%, at least 50%,a t least 60%, at least 70%, at least 80%, at least 90%, at least 95%, at least 97%, at least 98%, or more, up to and including at least 100% or more, in the case of an increase, for example, at least 2-fold, at least 3-fold, at least 4-fold, at least 5-fold, at least 6-fold, at least 7-fold, at least 8-fold, at least 9-fold,at least 10-fold, at least 50-fold, at least 100-fold, or more. "Modulating" can also involve effecting a change (which can either be an increase or a decrease) in affinity, avidity, specificity and/or selectivity of a target or antigen, such as a receptor and ligand. "Modulating" can also mean effecting a change with respect to one or more biological or physiological mechanisms, effects, responses, functions, pathways or activities in which the target or antigen (or in which its substrate(s), ligand(s) or pathway(s) are involved, such as its signaling pathway or metabolic pathway and their associated

biological or physiological effects) is involved. Again, as will be clear to the skilled person, such an action as an agonist or an antagonist can be determined in any suitable manner and/or using any suitable assay known or described herein (e.g., *in vitro* or cellular assay), depending on the target or antigen involved.

[0190] Modulating can, for example, also involve allosteric modulation of the target and/or reducing or inhibiting the binding of the target to one of its substrates or ligands and/or competing with a natural ligand, substrate for binding to the target. Modulating can also involve activating the target or the mechanism or pathway in which it is involved. Modulating can for example also involve effecting a change in respect of the folding or confirmation of the target, or in respect of the ability of the target to fold, to change its conformation (for example, upon binding of a ligand), to associate with other (sub)units, or to disassociate. Modulating can for example also involve effecting a change in the ability of the target to signal, phosphorylate, dephosphorylate, and the like.

Modulating Agents

[0191] As used herein, an "agent" can refer to a protein-binding agent that permits modulation of activity of proteins or disrupts interactions of proteins and other biomolecules, such as but not limited to disrupting protein-protein interaction, ligand-receptor interaction, or protein-nucleic acid interaction. Agents can also refer to DNA targeting or RNA targeting agents. Agents may include a fragment, derivative and analog of an active agent. The terms “fragment,” “derivative” and “analog” when referring to polypeptides as used herein refers to polypeptides which either retain substantially the same biological function or activity as such polypeptides. An analog includes a proprotein which can be activated by cleavage of the proprotein portion to produce an active mature polypeptide. Such agents include, but are not limited to, antibodies ("antibodies" includes antigen-binding portions of antibodies such as epitope- or antigen-binding peptides, paratopes, functional CDRs; recombinant antibodies; chimeric antibodies; humanized antibodies; nanobodies; tribodies; midibodies; or antigen-binding derivatives, analogs, variants, portions, or fragments thereof), protein-binding agents, nucleic acid molecules, small molecules, recombinant protein, peptides, aptamers, avimers and protein-binding derivatives, portions or fragments thereof. An “agent” as used herein, may also refer to an agent that inhibits expression of a gene, such as but not limited to a DNA targeting agent (e.g., CRISPR system, TALE, Zinc finger protein) or RNA targeting agent (e.g., inhibitory nucleic acid molecules such as RNAi, miRNA, ribozyme).

[0192] The agents of the present invention may be modified, such that they acquire advantageous properties for therapeutic use (e.g., stability and specificity), but maintain their biological activity.

[0193] It is well known that the properties of certain proteins can be modulated by attachment of polyethylene glycol (PEG) polymers, which increases the hydrodynamic volume of the protein and thereby slows its clearance by kidney filtration. (See, e.g., Clark et al., J. Biol. Chem. 271: 21969-21977 (1996)). Therefore, it is envisioned that certain agents can be PEGylated (e.g., on peptide residues) to provide enhanced therapeutic benefits such as, for example, increased efficacy by extending half-life *in vivo*. In certain embodiments, PEGylation of the agents may be used to extend the serum half-life of the agents and allow for particular agents to be capable of crossing the blood-brain barrier.

[0194] In regards to peptide PEGylation methods, reference is made to Lu et al., Int. J. Pept. Protein Res.43: 127-38 (1994); Lu et al., Pept. Res. 6: 140-6 (1993); Felix et al., Int. J. Pept. Protein Res. 46: 253-64 (1995); Gaertner et al., Bioconjug. Chem. 7: 38-44 (1996); Tsutsumi et al., Thromb. Haemost. 77: 168-73 (1997); Francis et al., hit. J. Hematol. 68: 1-18 (1998); Roberts et al., J. Pharm. Sci. 87: 1440-45 (1998); and Tan et al., Protein Expr. Purif. 12: 45-52 (1998). Polyethylene glycol or PEG is meant to encompass any of the forms of PEG that have been used to derivatize other proteins, including, but not limited to, mono-(C1-10) alkoxy or aryloxy-polyethylene glycol. Suitable PEG moieties include, for example, 40 kDa methoxy poly(ethylene glycol) propionaldehyde (Dow, Midland, Mich.); 60 kDa methoxy poly(ethylene glycol) propionaldehyde (Dow, Midland, Mich.); 40 kDa methoxy poly(ethylene glycol) maleimido-propionamide (Dow, Midland, Mich.); 31 kDa alpha-methyl-w-(3-oxopropoxy), polyoxyethylene (NOF Corporation, Tokyo); mPEG2-NHS-40k (Nektar); mPEG2-MAL-40k (Nektar), SUNBRIGHT GL2-400MA ((PEG)240kDa) (NOF Corporation, Tokyo), SUNBRIGHT ME-200MA (PEG20kDa) (NOF Corporation, Tokyo). The PEG groups are generally attached to the peptide (e.g., neuromedin U receptor agonists or antagonists) via acylation or alkylation through a reactive group on the PEG moiety (for example, a maleimide, an aldehyde, amino, thiol, or ester group) to a reactive group on the peptide (for example, an aldehyde, amino, thiol, a maleimide, or ester group).

[0195] The PEG molecule(s) may be covalently attached to any Lys, Cys, or K(CO(CH2)2SH) residues at any position in a peptide. In certain embodiments, the neuromedin U receptor agonists described herein can be PEGylated directly to any amino acid at the N-terminus by way of the N-terminal amino group. A “linker arm” may be added

to a peptide to facilitate PEGylation. PEGylation at the thiol side-chain of cysteine has been widely reported (see, e.g., Caliceti & Veronese, Adv. Drug Deliv. Rev. 55: 1261-77 (2003)). If there is no cysteine residue in the peptide, a cysteine residue can be introduced through substitution or by adding a cysteine to the N-terminal amino acid.

[0196] Substitutions of amino acids may be used to modify an agent of the present invention. The phrase "substitution of amino acids" as used herein encompasses substitution of amino acids that are the result of both conservative and non-conservative substitutions. Conservative substitutions are the replacement of an amino acid residue by another similar residue in a polypeptide. Typical but not limiting conservative substitutions are the replacements, for one another, among the aliphatic amino acids Ala, Val, Leu and Ile; interchange of Ser and Thr containing hydroxy residues, interchange of the acidic residues Asp and Glu, interchange between the amide-containing residues Asn and Gln, interchange of the basic residues Lys and Arg, interchange of the aromatic residues Phe and Tyr, and interchange of the small-sized amino acids Ala, Ser, Thr, Met, and Gly. Non-conservative substitutions are the replacement, in a polypeptide, of an amino acid residue by another residue which is not biologically similar. For example, the replacement of an amino acid residue with another residue that has a substantially different charge, a substantially different hydrophobicity, or a substantially different spatial configuration.

[0197] The term "antibody" is used interchangeably with the term "immunoglobulin" herein, and includes intact antibodies, fragments of antibodies, e.g., Fab, F(ab')2 fragments, and intact antibodies and fragments that have been mutated either in their constant and/or variable region (e.g., mutations to produce chimeric, partially humanized, or fully humanized antibodies, as well as to produce antibodies with a desired trait, e.g., enhanced binding and/or reduced FcR binding). The term "fragment" refers to a part or portion of an antibody or antibody chain comprising fewer amino acid residues than an intact or complete antibody or antibody chain. Fragments can be obtained via chemical or enzymatic treatment of an intact or complete antibody or antibody chain. Fragments can also be obtained by recombinant means. Exemplary fragments include Fab, Fab', F(ab')2, Fabc, Fd, dAb, V_{HH} and scFv and/or Fv fragments.

[0198] As used herein, a preparation of antibody protein having less than about 50% of non-antibody protein (also referred to herein as a "contaminating protein"), or of chemical precursors, is considered to be "substantially free." 40%, 30%, 20%, 10% and more preferably 5% (by dry weight), of non-antibody protein, or of chemical precursors is

considered to be substantially free. When the antibody protein or biologically active portion thereof is recombinantly produced, it is also preferably substantially free of culture medium, i.e., culture medium represents less than about 30%, preferably less than about 20%, more preferably less than about 10%, and most preferably less than about 5% of the volume or mass of the protein preparation.

[0199] The term "antigen-binding fragment" refers to a polypeptide fragment of an immunoglobulin or antibody that binds antigen or competes with intact antibody (i.e., with the intact antibody from which they were derived) for antigen binding (i.e., specific binding). As such these antibodies or fragments thereof are included in the scope of the invention, provided that the antibody or fragment binds specifically to a target molecule.

[0200] It is intended that the term "antibody" encompass any Ig class or any Ig subclass (e.g. the IgG1, IgG2, IgG3, and IgG4 subclassess of IgG) obtained from any source (e.g., humans and non-human primates, and in rodents, lagomorphs, caprines, bovines, equines, ovines, etc.).

[0201] The term "Ig class" or "immunoglobulin class", as used herein, refers to the five classes of immunoglobulin that have been identified in humans and higher mammals, IgG, IgM, IgA, IgD, and IgE. The term "Ig subclass" refers to the two subclasses of IgM (H and L), three subclasses of IgA (IgA1, IgA2, and secretory IgA), and four subclasses of IgG (IgG1, IgG2, IgG3, and IgG4) that have been identified in humans and higher mammals. The antibodies can exist in monomeric or polymeric form; for example, lgM antibodies exist in pentameric form, and IgA antibodies exist in monomeric, dimeric or multimeric form.

[0202] The term "IgG subclass" refers to the four subclasses of immunoglobulin class IgG - IgG1, IgG2, IgG3, and IgG4 that have been identified in humans and higher mammals by the heavy chains of the immunoglobulins, V1 - γ4, respectively. The term "single-chain immunoglobulin" or "single-chain antibody" (used interchangeably herein) refers to a protein having a two-polypeptide chain structure consisting of a heavy and a light chain, said chains being stabilized, for example, by interchain peptide linkers, which has the ability to specifically bind antigen. The term "domain" refers to a globular region of a heavy or light chain polypeptide comprising peptide loops (e.g., comprising 3 to 4 peptide loops) stabilized, for example, by β pleated sheet and/or intrachain disulfide bond. Domains are further referred to herein as "constant" or "variable", based on the relative lack of sequence variation within the domains of various class members in the case of a "constant" domain, or the significant variation within the domains of various class members in the case of a "variable" domain.

Antibody or polypeptide "domains" are often referred to interchangeably in the art as antibody or polypeptide "regions". The "constant" domains of an antibody light chain are referred to interchangeably as "light chain constant regions", "light chain constant domains", "CL" regions or "CL" domains. The "constant" domains of an antibody heavy chain are referred to interchangeably as "heavy chain constant regions", "heavy chain constant domains", "CH" regions or "CH" domains). The "variable" domains of an antibody light chain are referred to interchangeably as "light chain variable regions", "light chain variable domains", "VL" regions or "VL" domains). The "variable" domains of an antibody heavy chain are referred to interchangeably as "heavy chain constant regions", "heavy chain constant domains", "VH" regions or "VH" domains).

[0203] The term "region" can also refer to a part or portion of an antibody chain or antibody chain domain (e.g., a part or portion of a heavy or light chain or a part or portion of a constant or variable domain, as defined herein), as well as more discrete parts or portions of said chains or domains. For example, light and heavy chains or light and heavy chain variable domains include "complementarity determining regions" or "CDRs" interspersed among "framework regions" or "FRs", as defined herein.

[0204] The term "conformation" refers to the tertiary structure of a protein or polypeptide (e.g., an antibody, antibody chain, domain or region thereof). For example, the phrase "light (or heavy) chain conformation" refers to the tertiary structure of a light (or heavy) chain variable region, and the phrase "antibody conformation" or "antibody fragment conformation" refers to the tertiary structure of an antibody or fragment thereof.

[0205] The term “antibody-like protein scaffolds” or “engineered protein scaffolds” broadly encompasses proteinaceous non-immunoglobulin specific-binding agents, typically obtained by combinatorial engineering (such as site-directed random mutagenesis in combination with phage display or other molecular selection techniques). Usually, such scaffolds are derived from robust and small soluble monomeric proteins (such as Kunitz inhibitors or lipocalins) or from a stably folded extra-membrane domain of a cell surface receptor (such as protein A, fibronectin or the ankyrin repeat).

[0206] Such scaffolds have been extensively reviewed in Binz et al. (Engineering novel binding proteins from nonimmunoglobulin domains. Nat Biotechnol 2005, 23:1257-1268), Gebauer and Skerra (Engineered protein scaffolds as next-generation antibody therapeutics. Curr Opin Chem Biol. 2009, 13:245-55), Gill and Damle (Biopharmaceutical drug discovery using novel protein scaffolds. Curr Opin Biotechnol 2006, 17:653-658), Skerra (Engineered

protein scaffolds for molecular recognition. J Mol Recognit 2000, 13:167-187), and Skerra (Alternative non-antibody scaffolds for molecular recognition. Curr Opin Biotechnol 2007, 18:295-304), and include without limitation affibodies, based on the Z-domain of staphylococcal protein A, a three-helix bundle of 58 residues providing an interface on two of its alpha-helices (Nygren, Alternative binding proteins: Affibody binding proteins developed from a small three-helix bundle scaffold. FEBS J 2008, 275:2668-2676); engineered Kunitz domains based on a small (ca. 58 residues) and robust, disulphide-crosslinked serine protease inhibitor, typically of human origin (e.g. LACI-D1), which can be engineered for different protease specificities (Nixon and Wood, Engineered protein inhibitors of proteases. Curr Opin Drug Discov Dev 2006, 9:261-268); monobodies or adnectins based on the 10th extracellular domain of human fibronectin III (10Fn3), which adopts an Ig-like beta-sandwich fold (94 residues) with 2–3 exposed loops, but lacks the central disulphide bridge (Koide and Koide, Monobodies: antibody mimics based on the scaffold of the fibronectin type III domain. Methods Mol Biol 2007, 352:95-109); anticalins derived from the lipocalins, a diverse family of eight-stranded beta-barrel proteins (ca. 180 residues) that naturally form binding sites for small ligands by means of four structurally variable loops at the open end, which are abundant in humans, insects, and many other organisms (Skerra, Alternative binding proteins: Anticalins—harnessing the structural plasticity of the lipocalin ligand pocket to engineer novel binding activities. FEBS J 2008, 275:2677-2683); DARPins, designed ankyrin repeat domains (166 residues), which provide a rigid interface arising from typically three repeated beta-turns (Stumpp et al., DARPins: a new generation of protein therapeutics. Drug Discov Today 2008, 13:695-701); avimers (multimerized LDLR-A module) (Silverman et al., Multivalent avimer proteins evolved by exon shuffling of a family of human receptor domains. Nat Biotechnol 2005, 23:1556-1561); and cysteine-rich knottin peptides (Kolmar, Alternative binding proteins: biological activity and therapeutic potential of cystine-knot miniproteins. FEBS J 2008, 275:2684-2690).

[0207] "Specific binding" of an antibody means that the antibody exhibits appreciable affinity for a particular antigen or epitope and, generally, does not exhibit significant cross reactivity. "Appreciable" binding includes binding with an affinity of at least 25 μM. Antibodies with affinities greater than 1 x 10^7 M^{-1} (or a dissociation coefficient of 1μM or less or a dissociation coefficient of 1nm or less) typically bind with correspondingly greater specificity. Values intermediate of those set forth herein are also intended to be within the scope of the present invention and antibodies of the invention bind with a range of affinities,

for example, 100nM or less, 75nM or less, 50nM or less, 25nM or less, for example 10nM or less, 5nM or less, 1nM or less, or in embodiments 500pM or less, 100pM or less, 50pM or less or 25pM or less. An antibody that "does not exhibit significant crossreactivity" is one that will not appreciably bind to an entity other than its target (e.g., a different epitope or a different molecule). For example, an antibody that specifically binds to a target molecule will appreciably bind the target molecule but will not significantly react with non-target molecules or peptides. An antibody specific for a particular epitope will, for example, not significantly crossreact with remote epitopes on the same protein or peptide. Specific binding can be determined according to any art-recognized means for determining such binding. Preferably, specific binding is determined according to Scatchard analysis and/or competitive binding assays.

[0208] As used herein, the term "affinity" refers to the strength of the binding of a single antigen-combining site with an antigenic determinant. Affinity depends on the closeness of stereochemical fit between antibody combining sites and antigen determinants, on the size of the area of contact between them, on the distribution of charged and hydrophobic groups, etc. Antibody affinity can be measured by equilibrium dialysis or by the kinetic BIACORE™ method. The dissociation constant, Kd, and the association constant, Ka, are quantitative measures of affinity.

[0209] As used herein, the term "monoclonal antibody" refers to an antibody derived from a clonal population of antibody-producing cells (e.g., B lymphocytes or B cells) which is homogeneous in structure and antigen specificity. The term "polyclonal antibody" refers to a plurality of antibodies originating from different clonal populations of antibody-producing cells which are heterogeneous in their structure and epitope specificity but which recognize a common antigen. Monoclonal and polyclonal antibodies may exist within bodily fluids, as crude preparations, or may be purified, as described herein.

[0210] The term "binding portion" of an antibody (or "antibody portion") includes one or more complete domains, e.g., a pair of complete domains, as well as fragments of an antibody that retain the ability to specifically bind to a target molecule. It has been shown that the binding function of an antibody can be performed by fragments of a full-length antibody. Binding fragments are produced by recombinant DNA techniques, or by enzymatic or chemical cleavage of intact immunoglobulins. Binding fragments include Fab, Fab', F(ab')2, Fabc, Fd, dAb, Fv, single chains, single-chain antibodies, e.g., scFv, and single domain antibodies.

[0211] "Humanized" forms of non-human (e.g., murine) antibodies are chimeric antibodies that contain minimal sequence derived from non-human immunoglobulin. For the most part, humanized antibodies are human immunoglobulins (recipient antibody) in which residues from a hypervariable region of the recipient are replaced by residues from a hypervariable region of a non-human species (donor antibody) such as mouse, rat, rabbit or nonhuman primate having the desired specificity, affinity, and capacity. In some instances, FR residues of the human immunoglobulin are replaced by corresponding non-human residues. Furthermore, humanized antibodies may comprise residues that are not found in the recipient antibody or in the donor antibody. These modifications are made to further refine antibody performance. In general, the humanized antibody will comprise substantially all of at least one, and typically two, variable domains, in which all or substantially all of the hypervariable regions correspond to those of a non-human immunoglobulin and all or substantially all of the FR regions are those of a human immunoglobulin sequence. The humanized antibody optionally also will comprise at least a portion of an immunoglobulin constant region (Fc), typically that of a human immunoglobulin.

[0212] Examples of portions of antibodies or epitope-binding proteins encompassed by the present definition include: (i) the Fab fragment, having V_L, C_L, V_H and C_H1 domains; (ii) the Fab' fragment, which is a Fab fragment having one or more cysteine residues at the C-terminus of the C_H1 domain; (iii) the Fd fragment having V_H and C_H1 domains; (iv) the Fd' fragment having V_H and C_H1 domains and one or more cysteine residues at the C-terminus of the CHI domain; (v) the Fv fragment having the V_L and V_H domains of a single arm of an antibody; (vi) the dAb fragment (Ward et al., 341 Nature 544 (1989)) which consists of a V_H domain or a V_L domain that binds antigen; (vii) isolated CDR regions or isolated CDR regions presented in a functional framework; (viii) $F(ab')_2$ fragments which are bivalent fragments including two Fab' fragments linked by a disulphide bridge at the hinge region; (ix) single chain antibody molecules (e.g., single chain Fv; scFv) (Bird et al., 242 Science 423 (1988); and Huston et al., 85 PNAS 5879 (1988)); (x) "diabodies" with two antigen binding sites, comprising a heavy chain variable domain (V_H) connected to a light chain variable domain (V_L) in the same polypeptide chain (see, e.g., EP 404,097; WO 93/11161; Hollinger et al., 90 PNAS 6444 (1993)); (xi) "linear antibodies" comprising a pair of tandem Fd segments (V_H-C_h1-V_H-C_h1) which, together with complementary light chain polypeptides, form a pair of antigen binding regions (Zapata et al., Protein Eng. 8(10):1057-62 (1995); and U.S. Patent No. 5,641,870).

[0213] As used herein, a "blocking" antibody or an antibody "antagonist" is one which inhibits or reduces biological activity of the antigen(s) it binds. In certain embodiments, the blocking antibodies or antagonist antibodies or portions thereof described herein completely inhibit the biological activity of the antigen(s).

[0214] Antibodies may act as agonists or antagonists of the recognized polypeptides. For example, the present invention includes antibodies which disrupt receptor/ligand interactions either partially or fully. The invention features both receptor-specific antibodies and ligand-specific antibodies. The invention also features receptor-specific antibodies which do not prevent ligand binding but prevent receptor activation. Receptor activation (i.e., signaling) may be determined by techniques described herein or otherwise known in the art. For example, receptor activation can be determined by detecting the phosphorylation (e.g., tyrosine or serine/threonine) of the receptor or of one of its down-stream substrates by immunoprecipitation followed by western blot analysis. In specific embodiments, antibodies are provided that inhibit ligand activity or receptor activity by at least 95%, at least 90%, at least 85%, at least 80%, at least 75%, at least 70%, at least 60%, or at least 50% of the activity in absence of the antibody.

[0215] The invention also features receptor-specific antibodies which both prevent ligand binding and receptor activation as well as antibodies that recognize the receptor-ligand complex. Likewise, encompassed by the invention are neutralizing antibodies which bind the ligand and prevent binding of the ligand to the receptor, as well as antibodies which bind the ligand, thereby preventing receptor activation, but do not prevent the ligand from binding the receptor. Further included in the invention are antibodies which activate the receptor. These antibodies may act as receptor agonists, i.e., potentiate or activate either all or a subset of the biological activities of the ligand-mediated receptor activation, for example, by inducing dimerization of the receptor. The antibodies may be specified as agonists, antagonists or inverse agonists for biological activities comprising the specific biological activities of the peptides disclosed herein. The antibody agonists and antagonists can be made using methods known in the art. See, e.g., PCT publication WO 96/40281; U.S. Pat. No. 5,811,097; Deng et al., Blood 92(6):1981-1988 (1998); Chen et al., Cancer Res. 58(16):3668-3678 (1998); Harrop et al., J. Immunol. 161(4):1786-1794 (1998); Zhu et al., Cancer Res. 58(15):3209-3214 (1998); Yoon et al., J. Immunol. 160(7):3170-3179 (1998); Prat et al., J. Cell. Sci. III (Pt2):237-247 (1998); Pitard et al., J. Immunol. Methods 205(2):177-190 (1997); Liautard et al., Cytokine 9(4):233-241 (1997); Carlson et al., J. Biol. Chem. 272(17):11295-11301

(1997); Taryman et al., Neuron 14(4):755-762 (1995); Muller et al., Structure 6(9):1153-1167 (1998); Bartunek et al., Cytokine 8(1):14-20 (1996).

[0216] The antibodies as defined for the present invention include derivatives that are modified, i.e., by the covalent attachment of any type of molecule to the antibody such that covalent attachment does not prevent the antibody from generating an anti-idiotypic response. For example, but not by way of limitation, the antibody derivatives include antibodies that have been modified, e.g., by glycosylation, acetylation, pegylation, phosphylation, amidation, derivatization by known protecting/blocking groups, proteolytic cleavage, linkage to a cellular ligand or other protein, etc. Any of numerous chemical modifications may be carried out by known techniques, including, but not limited to specific chemical cleavage, acetylation, formylation, metabolic synthesis of tunicamycin, etc. Additionally, the derivative may contain one or more non-classical amino acids.

[0217] Simple binding assays can be used to screen for or detect agents that bind to a target protein, or disrupt the interaction between proteins (e.g., a receptor and a ligand). Because certain targets of the present invention are transmembrane proteins, assays that use the soluble forms of these proteins rather than full-length protein can be used, in some embodiments. Soluble forms include, for example, those lacking the transmembrane domain and/or those comprising the IgV domain or fragments thereof which retain their ability to bind their cognate binding partners. Further, agents that inhibit or enhance protein interactions for use in the compositions and methods described herein, can include recombinant peptido-mimetics.

[0218] Detection methods useful in screening assays include antibody-based methods, detection of a reporter moiety, detection of cytokines as described herein, and detection of a gene signature as described herein.

[0219] Another variation of assays to determine binding of a receptor protein to a ligand protein is through the use of affinity biosensor methods. Such methods may be based on the piezoelectric effect, electrochemistry, or optical methods, such as ellipsometry, optical wave guidance, and surface plasmon resonance (SPR).

[0220] The disclosure also encompasses nucleic acid molecules, in particular those that inhibit a signature gene. Exemplary nucleic acid molecules include aptamers, siRNA, artificial microRNA, interfering RNA or RNAi, dsRNA, ribozymes, antisense oligonucleotides, and DNA expression cassettes encoding said nucleic acid molecules. Preferably, the nucleic acid molecule is an antisense oligonucleotide. Antisense

oligonucleotides (ASO) generally inhibit their target by binding target mRNA and sterically blocking expression by obstructing the ribosome. ASOs can also inhibit their target by binding target mRNA thus forming a DNA-RNA hybrid that can be a substance for RNase H. Preferred ASOs include Locked Nucleic Acid (LNA), Peptide Nucleic Acid (PNA), and morpholinos Preferably, the nucleic acid molecule is an RNAi molecule, i.e., RNA interference molecule. Preferred RNAi molecules include siRNA, shRNA, and artificial miRNA. The design and production of siRNA molecules is well known to one of skill in the art (e.g., Hajeri PB, Singh SK. Drug Discov Today. 2009 14(17-18):851-8). The nucleic acid molecule inhibitors may be chemically synthesized and provided directly to cells of interest. The nucleic acid compound may be provided to a cell as part of a gene delivery vehicle. Such a vehicle is preferably a liposome or a viral gene delivery vehicle.

[0221] In certain embodiments, the one or more agents is a small molecule. The term "small molecule" refers to compounds, preferably organic compounds, with a size comparable to those organic molecules generally used in pharmaceuticals. The term excludes biological macromolecules (e.g., proteins, peptides, nucleic acids, etc.). Preferred small organic molecules range in size up to about 5000 Da, e.g., up to about 4000, preferably up to 3000 Da, more preferably up to 2000 Da, even more preferably up to about 1000 Da, e.g., up to about 900, 800, 700, 600 or up to about 500 Da. In certain embodiments, the small molecule may act as an antagonist or agonist (e.g., blocking an enzyme active site or activating a receptor by binding to a ligand binding site).

[0222] One type of small molecule applicable to the present invention is a degrader molecule. Proteolysis Targeting Chimera (PROTAC) technology is a rapidly emerging alternative therapeutic strategy with the potential to address many of the challenges currently faced in modern drug development programs. PROTAC technology employs small molecules that recruit target proteins for ubiquitination and removal by the proteasome (see, e.g., Bondeson and Crews, Targeted Protein Degradation by Small Molecules, Annu Rev Pharmacol Toxicol. 2017 Jan 6; 57: 107–123; and Lai et al., Modular PROTAC Design for the Degradation of Oncogenic BCR-ABL Angew Chem Int Ed Engl. 2016 Jan 11; 55(2): 807–810).

Adoptive Cell Therapy

[0223] As used herein, "ACT", "adoptive cell therapy" and "adoptive cell transfer" may be used interchangeably. In certain embodiments, Adoptive cell therapy (ACT) can refer to the transfer of cells to a patient with the goal of transferring the functionality and

characteristics into the new host by engraftment of the cells (see, e.g., Mettananda et al., Editing an α-globin enhancer in primary human hematopoietic stem cells as a treatment for β-thalassemia, Nat Commun. 2017 Sep 4;8(1):424). As used herein, the term "engraft" or "engraftment" refers to the process of cell incorporation into a tissue of interest *in vivo* through contact with existing cells of the tissue. Adoptive cell therapy (ACT) can refer to the transfer of cells, most commonly immune-derived cells, back into the same patient or into a new recipient host with the goal of transferring the immunologic functionality and characteristics into the new host. If possible, use of autologous cells helps the recipient by minimizing GVHD issues. The adoptive transfer of autologous tumor infiltrating lymphocytes (TIL) (Besser et al., (2010) Clin. Cancer Res 16 (9) 2646–55; Dudley et al., (2002) Science 298 (5594): 850–4; and Dudley et al., (2005) Journal of Clinical Oncology 23 (10): 2346–57.) or genetically re-directed peripheral blood mononuclear cells (Johnson et al., (2009) Blood 114 (3): 535–46; and Morgan et al., (2006) Science 314(5796) 126-9) has been used to successfully treat patients with advanced solid tumors, including melanoma and colorectal carcinoma, as well as patients with CD19-expressing hematologic malignancies (Kalos et al., (2011) Science Translational Medicine 3 (95): 95ra73). In certain embodiments, allogenic cells immune cells are transferred (see, e.g., Ren et al., (2017) Clin Cancer Res 23 (9) 2255-2266). As described further herein, allogenic cells can be edited to reduce alloreactivity and prevent graft-versus-host disease. Thus, use of allogenic cells allows for cells to be obtained from healthy donors and prepared for use in patients as opposed to preparing autologous cells from a patient after diagnosis.

[0224] Aspects of the invention involve the adoptive transfer of immune system cells, such as T cells, specific for selected antigens, such as tumor associated antigens or tumor specific neoantigens (see, e.g., Maus et al., 2014, Adoptive Immunotherapy for Cancer or Viruses, Annual Review of Immunology, Vol. 32: 189-225; Rosenberg and Restifo, 2015, Adoptive cell transfer as personalized immunotherapy for human cancer, Science Vol. 348 no. 6230 pp. 62-68; Restifo et al., 2015, Adoptive immunotherapy for cancer: harnessing the T cell response. Nat. Rev. Immunol. 12(4): 269-281; and Jenson and Riddell, 2014, Design and implementation of adoptive therapy with chimeric antigen receptor-modified T cells. Immunol Rev. 257(1): 127–144; and Rajasagi et al., 2014, Systematic identification of personal tumor-specific neoantigens in chronic lymphocytic leukemia. Blood. 2014 Jul 17;124(3):453-62).

[0225] In certain embodiments, an antigen (such as a tumor antigen) to be targeted in adoptive cell therapy (such as particularly CAR or TCR T-cell therapy) of a disease (such as particularly of tumor or cancer) may be selected from a group consisting of: B cell maturation antigen (BCMA) (see, e.g., Friedman et al., Effective Targeting of Multiple BCMA-Expressing Hematological Malignancies by Anti-BCMA CAR T Cells, Hum Gene Ther. 2018 Mar 8; Berdeja JG, et al. Durable clinical responses in heavily pretreated patients with relapsed/refractory multiple myeloma: updated results from a multicenter study of bb2121 anti-Bcma CAR T cell therapy. Blood. 2017;130:740; and Mouhieddine and Ghobrial, Immunotherapy in Multiple Myeloma: The Era of CAR T Cell Therapy, Hematologist, May-June 2018, Volume 15, issue 3); PSA (prostate-specific antigen); prostate-specific membrane antigen (PSMA); PSCA (Prostate stem cell antigen); Tyrosine-protein kinase transmembrane receptor ROR1; fibroblast activation protein (FAP); Tumor-associated glycoprotein 72 (TAG72); Carcinoembryonic antigen (CEA); Epithelial cell adhesion molecule (EPCAM); Mesothelin; Human Epidermal growth factor Receptor 2 (ERBB2 (Her2/neu)); Prostase; Prostatic acid phosphatase (PAP); elongation factor 2 mutant (ELF2M); Insulin-like growth factor 1 receptor (IGF-1R); gplOO; BCR-ABL (breakpoint cluster region-Abelson); tyrosinase; New York esophageal squamous cell carcinoma 1 (NY-ESO-1); κ-light chain, LAGE (L antigen); MAGE (melanoma antigen); Melanoma-associated antigen 1 (MAGE-A1); MAGE A3; MAGE A6; legumain; Human papillomavirus (HPV) E6; HPV E7; prostein; survivin; PCTA1 (Galectin 8); Melan-A/MART-1; Ras mutant; TRP-1 (tyrosinase related protein 1, or gp75); Tyrosinase-related Protein 2 (TRP2); TRP-2/INT2 (TRP-2/intron 2); RAGE (renal antigen); receptor for advanced glycation end products 1 (RAGE1); Renal ubiquitous 1, 2 (RU1, RU2); intestinal carboxyl esterase (iCE); Heat shock protein 70-2 (HSP70-2) mutant; thyroid stimulating hormone receptor (TSHR); CD123; CD171; CD19; CD20; CD22; CD26; CD30; CD33; CD44v7/8 (cluster of differentiation 44, exons 7/8); CD53; CD92; CD100; CD148; CD150; CD200; CD261; CD262; CD362; CS-1 (CD2 subset 1, CRACC, SLAMF7, CD319, and 19A24); C-type lectin-like molecule-1 (CLL-1); ganglioside GD3 (aNeu5Ac(2-8)aNeu5Ac(2-3)bDGalp(1-4)bDGlcp(1-1)Cer); Tn antigen (Tn Ag); Fms-Like Tyrosine Kinase 3 (FLT3); CD38; CD138; CD44v6; B7H3 (CD276); KIT (CD117); Interleukin-13 receptor subunit alpha-2 (IL-13Ra2); Interleukin 11 receptor alpha (IL-11Ra); prostate stem cell antigen (PSCA); Protease Serine 21 (PRSS21); vascular endothelial growth factor receptor 2 (VEGFR2); Lewis(Y) antigen; CD24; Platelet-derived growth factor receptor beta (PDGFR-beta); stage-specific embryonic antigen-4

(SSEA-4); Mucin 1, cell surface associated (MUC1); mucin 16 (MUC16); epidermal growth factor receptor (EGFR); epidermal growth factor receptor variant III (EGFRvIII); neural cell adhesion molecule (NCAM); carbonic anhydrase IX (CAIX); Proteasome (Prosome, Macropain) Subunit, Beta Type, 9 (LMP2); ephrin type-A receptor 2 (EphA2); Ephrin B2; Fucosyl GM1; sialyl Lewis adhesion molecule (sLe); ganglioside GM3 (aNeu5Ac(2-3)bDGalp(1-4)bDGlcp(1-1)Cer); TGS5; high molecular weight-melanoma-associated antigen (HMWMAA); o-acetyl-GD2 ganglioside (OAcGD2); Folate receptor alpha; Folate receptor beta; tumor endothelial marker 1 (TEM1/CD248); tumor endothelial marker 7-related (TEM7R); claudin 6 (CLDN6); G protein-coupled receptor class C group 5, member D (GPRC5D); chromosome X open reading frame 61 (CXORF61); CD97; CD179a; anaplastic lymphoma kinase (ALK); Polysialic acid; placenta-specific 1 (PLAC1); hexasaccharide portion of globoH glycoceramide (GloboH); mammary gland differentiation antigen (NY-BR-1); uroplakin 2 (UPK2); Hepatitis A virus cellular receptor 1 (HAVCR1); adrenoceptor beta 3 (ADRB3); pannexin 3 (PANX3); G protein-coupled receptor 20 (GPR20); lymphocyte antigen 6 complex, locus K 9 (LY6K); Olfactory receptor 51E2 (OR51E2); TCR Gamma Alternate Reading Frame Protein (TARP); Wilms tumor protein (WT1); ETS translocation-variant gene 6, located on chromosome 12p (ETV6-AML); sperm protein 17 (SPA17); X Antigen Family, Member 1A (XAGE1); angiopoietin-binding cell surface receptor 2 (Tie 2); CT (cancer/testis (antigen)); melanoma cancer testis antigen-1 (MAD-CT-1); melanoma cancer testis antigen-2 (MAD-CT-2); Fos-related antigen 1; p53; p53 mutant; human Telomerase reverse transcriptase (hTERT); sarcoma translocation breakpoints; melanoma inhibitor of apoptosis (ML-IAP); ERG (transmembrane protease, serine 2 (TMPRSS2) ETS fusion gene); N-Acetyl glucosaminyl-transferase V (NA17); paired box protein Pax-3 (PAX3); Androgen receptor; Cyclin B1; Cyclin D1; v-myc avian myelocytomatosis viral oncogene neuroblastoma derived homolog (MYCN); Ras Homolog Family Member C (RhoC); Cytochrome P450 1B1 (CYP1B1); CCCTC-Binding Factor (Zinc Finger Protein)-Like (BORIS); Squamous Cell Carcinoma Antigen Recognized By T Cells-1 or 3 (SART1, SART3); Paired box protein Pax-5 (PAX5); proacrosin binding protein sp32 (OY-TES1); lymphocyte-specific protein tyrosine kinase (LCK); A kinase anchor protein 4 (AKAP-4); synovial sarcoma, X breakpoint-1, -2, -3 or -4 (SSX1, SSX2, SSX3, SSX4); CD79a; CD79b; CD72; Leukocyte-associated immunoglobulin-like receptor 1 (LAIR1); Fc fragment of IgA receptor (FCAR); Leukocyte immunoglobulin-like receptor subfamily A member 2 (LILRA2); CD300 molecule-like family member f (CD300LF); C-type lectin domain family

12 member A (CLEC12A); bone marrow stromal cell antigen 2 (BST2); EGF-like module-containing mucin-like hormone receptor-like 2 (EMR2); lymphocyte antigen 75 (LY75); Glypican-3 (GPC3); Fc receptor-like 5 (FCRL5); mouse double minute 2 homolog (MDM2); livin; alphafetoprotein (AFP); transmembrane activator and CAML Interactor (TACI); B-cell activating factor receptor (BAFF-R); V-Ki-ras2 Kirsten rat sarcoma viral oncogene homolog (KRAS); immunoglobulin lambda-like polypeptide 1 (IGLL1); 707-AP (707 alanine proline); ART-4 (adenocarcinoma antigen recognized by T4 cells); BAGE (B antigen; b-catenin/m, b-catenin/mutated); CAMEL (CTL-recognized antigen on melanoma); CAP1 (carcinoembryonic antigen peptide 1); CASP-8 (caspase-8); CDC27m (cell-division cycle 27 mutated); CDK4/m (cycline-dependent kinase 4 mutated); Cyp-B (cyclophilin B); DAM (differentiation antigen melanoma); EGP-2 (epithelial glycoprotein 2); EGP-40 (epithelial glycoprotein 40); Erbb2, 3, 4 (erythroblastic leukemia viral oncogene homolog-2, -3, 4); FBP (folate binding protein); , fAchR (Fetal acetylcholine receptor); G250 (glycoprotein 250); GAGE (G antigen); GnT-V (N-acetylglucosaminyltransferase V); HAGE (helicose antigen); ULA-A (human leukocyte antigen-A); HST2 (human signet ring tumor 2); KIAA0205; KDR (kinase insert domain receptor); LDLR/FUT (low density lipid receptor/GDP L-fucose: b-D-galactosidase 2-a-L fucosyltransferase); L1CAM (L1 cell adhesion molecule); MC1R (melanocortin 1 receptor); Myosin/m (myosin mutated); MUM-1, -2, -3 (melanoma ubiquitous mutated 1, 2, 3); NA88-A (NA cDNA clone of patient M88); KG2D (Natural killer group 2, member D) ligands; oncofetal antigen (h5T4); p190 minor bcr-abl (protein of 190KD bcr-abl); Pml/RARa (promyelocytic leukaemia/retinoic acid receptor a); PRAME (preferentially expressed antigen of melanoma); SAGE (sarcoma antigen); TEL/AML1 (translocation Ets-family leukemia/acute myeloid leukemia 1); TPI/m (triosephosphate isomerase mutated); CD70; and any combination thereof.

[0226] In certain embodiments, an antigen to be targeted in adoptive cell therapy (such as particularly CAR or TCR T-cell therapy) of a disease (such as particularly of tumor or cancer) is a tumor-specific antigen (TSA).

[0227] In certain embodiments, an antigen to be targeted in adoptive cell therapy (such as particularly CAR or TCR T-cell therapy) of a disease (such as particularly of tumor or cancer) is a neoantigen.

[0228] In certain embodiments, an antigen to be targeted in adoptive cell therapy (such as particularly CAR or TCR T-cell therapy) of a disease (such as particularly of tumor or cancer) is a tumor-associated antigen (TAA).

[0229] In certain embodiments, an antigen to be targeted in adoptive cell therapy (such as particularly CAR or TCR T-cell therapy) of a disease (such as particularly of tumor or cancer) is a universal tumor antigen. In certain preferred embodiments, the universal tumor antigen is selected from the group consisting of: a human telomerase reverse transcriptase (hTERT), survivin, mouse double minute 2 homolog (MDM2), cytochrome P450 1B 1 (CYP1B), HER2/neu, Wilms' tumor gene 1 (WT1), livin, alphafetoprotein (AFP), carcinoembryonic antigen (CEA), mucin 16 (MUC16), MUC1, prostate-specific membrane antigen (PSMA), p53, cyclin (Dl), and any combinations thereof.

[0230] In certain embodiments, an antigen (such as a tumor antigen) to be targeted in adoptive cell therapy (such as particularly CAR or TCR T-cell therapy) of a disease (such as particularly of tumor or cancer) may be selected from a group consisting of: CD19, BCMA, CD70, CLL-1, MAGE A3, MAGE A6, HPV E6, HPV E7, WT1, CD22, CD171, ROR1, MUC16, and SSX2. In certain preferred embodiments, the antigen may be CD19. For example, CD19 may be targeted in hematologic malignancies, such as in lymphomas, more particularly in B-cell lymphomas, such as without limitation in diffuse large B-cell lymphoma, primary mediastinal b-cell lymphoma, transformed follicular lymphoma, marginal zone lymphoma, mantle cell lymphoma, acute lymphoblastic leukemia including adult and pediatric ALL, non-Hodgkin lymphoma, indolent non-Hodgkin lymphoma, or chronic lymphocytic leukemia. For example, BCMA may be targeted in multiple myeloma or plasma cell leukemia (see, e.g., 2018 American Association for Cancer Research (AACR) Annual meeting Poster: Allogeneic Chimeric Antigen Receptor T Cells Targeting B Cell Maturation Antigen). For example, CLL1 may be targeted in acute myeloid leukemia. For example, MAGE A3, MAGE A6, SSX2, and/or KRAS may be targeted in solid tumors. For example, HPV E6 and/or HPV E7 may be targeted in cervical cancer or head and neck cancer. For example, WT1 may be targeted in acute myeloid leukemia (AML), myelodysplastic syndromes (MDS), chronic myeloid leukemia (CML), non-small cell lung cancer, breast, pancreatic, ovarian or colorectal cancers, or mesothelioma. For example, CD22 may be targeted in B cell malignancies, including non-Hodgkin lymphoma, diffuse large B-cell lymphoma, or acute lymphoblastic leukemia. For example, CD171 may be targeted in neuroblastoma, glioblastoma, or lung, pancreatic, or ovarian cancers. For example, ROR1 may be targeted in ROR1+ malignancies, including non-small cell lung cancer, triple negative breast cancer, pancreatic cancer, prostate cancer, ALL, chronic lymphocytic leukemia, or mantle cell lymphoma. For example, MUC16 may be targeted in

MUC16ecto+ epithelial ovarian, fallopian tube or primary peritoneal cancer. For example, CD70 may be targeted in both hematologic malignancies as well as in solid cancers such as renal cell carcinoma (RCC), gliomas (e.g., GBM), and head and neck cancers (HNSCC). CD70 is expressed in both hematologic malignancies as well as in solid cancers, while its expression in normal tissues is restricted to a subset of lymphoid cell types (see, e.g., 2018 American Association for Cancer Research (AACR) Annual meeting Poster: Allogeneic CRISPR Engineered Anti-CD70 CAR-T Cells Demonstrate Potent Preclinical Activity Against Both Solid and Hematological Cancer Cells).

[0231] Various strategies may for example be employed to genetically modify T cells by altering the specificity of the T cell receptor (TCR) for example by introducing new TCR α and β chains with selected peptide specificity (see U.S. Patent No. 8,697,854; PCT Patent Publications: WO2003020763, WO2004033685, WO2004044004, WO2005114215, WO2006000830, WO2008038002, WO2008039818, WO2004074322, WO2005113595, WO2006125962, WO2013166321, WO2013039889, WO2014018863, WO2014083173; U.S. Patent No. 8,088,379).

[0232] As an alternative to, or addition to, TCR modifications, chimeric antigen receptors (CARs) may be used in order to generate immunoresponsive cells, such as T cells, specific for selected targets, such as malignant cells, with a wide variety of receptor chimera constructs having been described (see U.S. Patent Nos. 5,843,728; 5,851,828; 5,912,170; 6,004,811; 6,284,240; 6,392,013; 6,410,014; 6,753,162; 8,211,422; and, PCT Publication WO9215322).

[0233] In general, CARs are comprised of an extracellular domain, a transmembrane domain, and an intracellular domain, wherein the extracellular domain comprises an antigen-binding domain that is specific for a predetermined target. While the antigen-binding domain of a CAR is often an antibody or antibody fragment (e.g., a single chain variable fragment, scFv), the binding domain is not particularly limited so long as it results in specific recognition of a target. For example, in some embodiments, the antigen-binding domain may comprise a receptor, such that the CAR is capable of binding to the ligand of the receptor. Alternatively, the antigen-binding domain may comprise a ligand, such that the CAR is capable of binding the endogenous receptor of that ligand.

[0234] The antigen-binding domain of a CAR is generally separated from the transmembrane domain by a hinge or spacer. The spacer is also not particularly limited, and it is designed to provide the CAR with flexibility. For example, a spacer domain may

comprise a portion of a human Fc domain, including a portion of the CH3 domain, or the hinge region of any immunoglobulin, such as IgA, IgD, IgE, IgG, or IgM, or variants thereof. Furthermore, the hinge region may be modified so as to prevent off-target binding by FcRs or other potential interfering objects. For example, the hinge may comprise an IgG4 Fc domain with or without a S228P, L235E, and/or N297Q mutation (according to Kabat numbering) in order to decrease binding to FcRs. Additional spacers/hinges include, but are not limited to, CD4, CD8, and CD28 hinge regions.

[0235] The transmembrane domain of a CAR may be derived either from a natural or from a synthetic source. Where the source is natural, the domain may be derived from any membrane bound or transmembrane protein. Transmembrane regions of particular use in this disclosure may be derived from CD8, CD28, CD3, CD45, CD4, CD5, CDS, CD9, CD 16, CD22, CD33, CD37, CD64, CD80, CD86, CD 134, CD137, CD 154, TCR. Alternatively, the transmembrane domain may be synthetic, in which case it will comprise predominantly hydrophobic residues such as leucine and valine. Preferably a triplet of phenylalanine, tryptophan and valine will be found at each end of a synthetic transmembrane domain. Optionally, a short oligo- or polypeptide linker, preferably between 2 and 10 amino acids in length may form the linkage between the transmembrane domain and the cytoplasmic signaling domain of the CAR. A glycine-serine doublet provides a particularly suitable linker.

[0236] Alternative CAR constructs may be characterized as belonging to successive generations. First-generation CARs typically consist of a single-chain variable fragment of an antibody specific for an antigen, for example comprising a VL linked to a VH of a specific antibody, linked by a flexible linker, for example by a CD8α hinge domain and a CD8α transmembrane domain, to the transmembrane and intracellular signaling domains of either CD3ζ or FcRγ (scFv-CD3ζ or scFv-FcRγ; see U.S. Patent No. 7,741,465; U.S. Patent No. 5,912,172; U.S. Patent No. 5,906,936). Second-generation CARs incorporate the intracellular domains of one or more costimulatory molecules, such as CD28, OX40 (CD134), or 4-1BB (CD137) within the endodomain (for example scFv-CD28/OX40/4-1BB-CD3ζ; see U.S. Patent Nos. 8,911,993; 8,916,381; 8,975,071; 9,101,584; 9,102,760; 9,102,761). Third-generation CARs include a combination of costimulatory endodomains, such a CD3ζ-chain, CD97, GDI la-CD18, CD2, ICOS, CD27, CD154, CDS, OX40, 4-1BB, CD2, CD7, LIGHT, LFA-1, NKG2C, B7-H3, CD30, CD40, PD-1, or CD28 signaling domains (for example scFv-CD28-4-1BB-CD3ζ or scFv-CD28-OX40-CD3ζ; see U.S. Patent No. 8,906,682; U.S. Patent

No. 8,399,645; U.S. Pat. No. 5,686,281; PCT Publication No. WO2014134165; PCT Publication No. WO2012079000). In certain embodiments, the primary signaling domain comprises a functional signaling domain of a protein selected from the group consisting of CD3 zeta, CD3 gamma, CD3 delta, CD3 epsilon, common FcR gamma (FCERIG), FcR beta (Fc Epsilon R1b), CD79a, CD79b, Fc gamma RIIa, DAP10, and DAP12. In certain preferred embodiments, the primary signaling domain comprises a functional signaling domain of CD3ζ or FcRγ. In certain embodiments, the one or more costimulatory signaling domains comprise a functional signaling domain of a protein selected, each independently, from the group consisting of: CD27, CD28, 4-1BB (CD137), OX40, CD30, CD40, PD-1, ICOS, lymphocyte function-associated antigen-1 (LFA-1), CD2, CD7, LIGHT, NKG2C, B7-H3, a ligand that specifically binds with CD83, CDS, ICAM-1, GITR, BAFFR, HVEM (LIGHTR), SLAMF7, NKp80 (KLRF1), CD160, CD19, CD4, CD8 alpha, CD8 beta, IL2R beta, IL2R gamma, IL7R alpha, ITGA4, VLA1, CD49a, ITGA4, IA4, CD49D, ITGA6, VLA-6, CD49f, ITGAD, CD11d, ITGAE, CD103, ITGAL, CD11a, LFA-1, ITGAM, CD11b, ITGAX, CD11c, ITGB1, CD29, ITGB2, CD18, ITGB7, TNFR2, TRANCE/RANKL, DNAM1 (CD226), SLAMF4 (CD244, 2B4), CD84, CD96 (Tactile), CEACAM1, CRTAM, Ly9 (CD229), CD160 (BY55), PSGL1, CD100 (SEMA4D), CD69, SLAMF6 (NTB-A, Lyl08), SLAM (SLAMF1, CD150, IPO-3), BLAME (SLAMF8), SELPLG (CD162), LTBR, LAT, GADS, SLP-76, PAG/Cbp, NKp44, NKp30, NKp46, and NKG2D. In certain embodiments, the one or more costimulatory signaling domains comprise a functional signaling domain of a protein selected, each independently, from the group consisting of: 4-1BB, CD27, and CD28. In certain embodiments, a chimeric antigen receptor may have the design as described in U.S. Patent No. 7,446,190, comprising an intracellular domain of CD3ζ chain (such as amino acid residues 52-163 of the human CD3 zeta chain, as shown in SEQ ID NO: 14 of US 7,446,190), a signaling region from CD28 and an antigen-binding element (or portion or domain; such as scFv). The CD28 portion, when between the zeta chain portion and the antigen-binding element, may suitably include the transmembrane and signaling domains of CD28 (such as amino acid residues 114-220 of SEQ ID NO: 10, full sequence shown in SEQ ID NO: 6 of US 7,446,190; these can include the following portion of CD28 as set forth in Genbank identifier NM_006139 (sequence version 1, 2 or 3): IEVMYPPPYLDNEKSNGTIIHVKGKHLCPSPLFPGPSKPFWVLVVVGGVLACYSLLVT VAFIIFWVRSKRSRLLHSDYMNMTPRRPGPTRKHYQPYAPPRDFAAYRS) (SEQ ID NO: 1). Alternatively, when the zeta sequence lies between the CD28 sequence and the

antigen-binding element, intracellular domain of CD28 can be used alone (such as amino sequence set forth in SEQ ID NO: 9 of US 7,446,190). Hence, certain embodiments employ a CAR comprising (a) a zeta chain portion comprising the intracellular domain of human CD3ζ chain, (b) a costimulatory signaling region, and (c) an antigen-binding element (or portion or domain), wherein the costimulatory signaling region comprises the amino acid sequence encoded by SEQ ID NO: 6 of US 7,446,190.

[0237] Alternatively, costimulation may be orchestrated by expressing CARs in antigen-specific T cells, chosen so as to be activated and expanded following engagement of their native αβTCR, for example by antigen on professional antigen-presenting cells, with attendant costimulation. In addition, additional engineered receptors may be provided on the immunoresponsive cells, for example to improve targeting of a T-cell attack and/or minimize side effects

[0238] By means of an example and without limitation, Kochenderfer et al., (2009) J Immunother. 32 (7): 689-702 described anti-CD19 chimeric antigen receptors (CAR). FMC63-28Z CAR contained a single chain variable region moiety (scFv) recognizing CD19 derived from the FMC63 mouse hybridoma (described in Nicholson et al., (1997) Molecular Immunology 34: 1157–1165), a portion of the human CD28 molecule, and the intracellular component of the human TCR-ζ molecule. FMC63-CD828BBZ CAR contained the FMC63 scFv, the hinge and transmembrane regions of the CD8 molecule, the cytoplasmic portions of CD28 and 4-1BB, and the cytoplasmic component of the TCR-ζ molecule. The exact sequence of the CD28 molecule included in the FMC63-28Z CAR corresponded to Genbank identifier NM_006139; the sequence included all amino acids starting with the amino acid sequence IEVMYPPPY and continuing all the way to the carboxy-terminus of the protein. To encode the anti-CD19 scFv component of the vector, the authors designed a DNA sequence which was based on a portion of a previously published CAR (Cooper et al., (2003) Blood 101: 1637–1644). This sequence encoded the following components in frame from the 5' end to the 3' end: an XhoI site, the human granulocyte-macrophage colony-stimulating factor (GM-CSF) receptor α-chain signal sequence, the FMC63 light chain variable region (as in Nicholson et al., *supra*), a linker peptide (as in Cooper et al., *supra*), the FMC63 heavy chain variable region (as in Nicholson et al., *supra*), and a NotI site. A plasmid encoding this sequence was digested with XhoI and NotI. To form the MSGV-FMC63-28Z retroviral vector, the XhoI and NotI-digested fragment encoding the FMC63 scFv was ligated into a second XhoI and NotI-digested fragment that encoded the MSGV retroviral backbone (as in

Hughes et al., (2005) Human Gene Therapy 16: 457–472) as well as part of the extracellular portion of human CD28, the entire transmembrane and cytoplasmic portion of human CD28, and the cytoplasmic portion of the human TCR-ζ molecule (as in Maher et al., 2002) Nature Biotechnology 20: 70–75). The FMC63-28Z CAR is included in the KTE-C19 (axicabtagene ciloleucel) anti-CD19 CAR-T therapy product in development by Kite Pharma, Inc. for the treatment of *inter alia* patients with relapsed/refractory aggressive B-cell non-Hodgkin lymphoma (NHL). Accordingly, in certain embodiments, cells intended for adoptive cell therapies, more particularly immunoresponsive cells such as T cells, may express the FMC63-28Z CAR as described by Kochenderfer et al. (*supra*). Hence, in certain embodiments, cells intended for adoptive cell therapies, more particularly immunoresponsive cells such as T cells, may comprise a CAR comprising an extracellular antigen-binding element (or portion or domain; such as scFv) that specifically binds to an antigen, an intracellular signaling domain comprising an intracellular domain of a CD3ζ chain, and a costimulatory signaling region comprising a signaling domain of CD28. Preferably, the CD28 amino acid sequence is as set forth in Genbank identifier NM_006139 (sequence version 1, 2 or 3) starting with the amino acid sequence IEVMYPPPY and continuing all the way to the carboxy-terminus of the protein. The sequence is reproduced herein: IEVMYPPPYLDNEKSNGTIIHVKGKHLCPSPLFPGPSKPFWVLVVVGGVLACYSLLVT VAFIIFWVRSKRSRLLHSDYMNMTPRRPGPTRKHYQPYAPPRDFAAYRS. Preferably, the antigen is CD19, more preferably the antigen-binding element is an anti-CD19 scFv, even more preferably the anti-CD19 scFv as described by Kochenderfer et al. (*supra*).

[0239] Additional anti-CD19 CARs are further described in WO2015187528. More particularly Example 1 and Table 1 of WO2015187528, incorporated by reference herein, demonstrate the generation of anti-CD19 CARs based on a fully human anti-CD19 monoclonal antibody (47G4, as described in US20100104509) and murine anti-CD19 monoclonal antibody (as described in Nicholson et al. and explained above). Various combinations of a signal sequence (human CD8-alpha or GM-CSF receptor), extracellular and transmembrane regions (human CD8-alpha) and intracellular T-cell signalling domains (CD28-CD3ζ; 4-1BB-CD3ζ; CD27-CD3ζ; CD28-CD27-CD3ζ, 4-1BB-CD27-CD3ζ; CD27-4-1BB-CD3ζ; CD28-CD27-FcεRI gamma chain; or CD28-FcεRI gamma chain) were disclosed. Hence, in certain embodiments, cells intended for adoptive cell therapies, more particularly immunoresponsive cells such as T cells, may comprise a CAR comprising an

extracellular antigen-binding element that specifically binds to an antigen, an extracellular and transmembrane region as set forth in Table 1 of WO2015187528 and an intracellular T-cell signalling domain as set forth in Table 1 of WO2015187528. Preferably, the antigen is CD19, more preferably the antigen-binding element is an anti-CD19 scFv, even more preferably the mouse or human anti-CD19 scFv as described in Example 1 of WO2015187528. In certain embodiments, the CAR comprises, consists essentially of or consists of an amino acid sequence of SEQ ID NO: 1, SEQ ID NO: 2, SEQ ID NO: 3, SEQ ID NO: 4, SEQ ID NO: 5, SEQ ID NO: 6, SEQ ID NO: 7, SEQ ID NO: 8, SEQ ID NO: 9, SEQ ID NO: 10, SEQ ID NO: 11, SEQ ID NO: 12, or SEQ ID NO: 13 as set forth in Table 1 of WO2015187528.

[0240] By means of an example and without limitation, chimeric antigen receptor that recognizes the CD70 antigen is described in WO2012058460A2 (see also, Park et al., CD70 as a target for chimeric antigen receptor T cells in head and neck squamous cell carcinoma, Oral Oncol. 2018 Mar;78:145-150; and Jin et al., CD70, a novel target of CAR T-cell therapy for gliomas, Neuro Oncol. 2018 Jan 10;20(1):55-65). CD70 is expressed by diffuse large B-cell and follicular lymphoma and also by the malignant cells of Hodgkins lymphoma, Waldenstrom's macroglobulinemia and multiple myeloma, and by HTLV-1- and EBV-associated malignancies. (Agathanggelou et al. Am.J.Pathol. 1995;147: 1152-1160; Hunter et al., Blood 2004; 104:4881. 26; Lens et al., J Immunol. 2005;174:6212-6219; Baba et al., J Virol. 2008;82:3843-3852.) In addition, CD70 is expressed by non-hematological malignancies such as renal cell carcinoma and glioblastoma. (Junker et al., J Urol. 2005;173:2150-2153; Chahlavi et al., Cancer Res 2005;65:5428-5438) Physiologically, CD70 expression is transient and restricted to a subset of highly activated T, B, and dendritic cells.

[0241] By means of an example and without limitation, chimeric antigen receptor that recognizes BCMA has been described (see, e.g., US20160046724A1; WO2016014789A2; WO2017211900A1; WO2015158671A1; US20180085444A1; WO2018028647A1; US20170283504A1; and WO2013154760A1).

[0242] In certain embodiments, the immune cell may, in addition to a CAR or exogenous TCR as described herein, further comprise a chimeric inhibitory receptor (inhibitory CAR) that specifically binds to a second target antigen and is capable of inducing an inhibitory or immunosuppressive or repressive signal to the cell upon recognition of the second target antigen. In certain embodiments, the chimeric inhibitory receptor comprises an extracellular

antigen-binding element (or portion or domain) configured to specifically bind to a target antigen, a transmembrane domain, and an intracellular immunosuppressive or repressive signaling domain. In certain embodiments, the second target antigen is an antigen that is not expressed on the surface of a cancer cell or infected cell or the expression of which is downregulated on a cancer cell or an infected cell. In certain embodiments, the second target antigen is an MHC-class I molecule. In certain embodiments, the intracellular signaling domain comprises a functional signaling portion of an immune checkpoint molecule, such as for example PD-1 or CTLA4. Advantageously, the inclusion of such inhibitory CAR reduces the chance of the engineered immune cells attacking non-target (e.g., non-cancer) tissues.

[0243] Alternatively, T-cells expressing CARs may be further modified to reduce or eliminate expression of endogenous TCRs in order to reduce off-target effects. Reduction or elimination of endogenous TCRs can reduce off-target effects and increase the effectiveness of the T cells (U.S. 9,181,527). T cells stably lacking expression of a functional TCR may be produced using a variety of approaches. T cells internalize, sort, and degrade the entire T cell receptor as a complex, with a half-life of about 10 hours in resting T cells and 3 hours in stimulated T cells (von Essen, M. et al. 2004. J. Immunol. 173:384-393). Proper functioning of the TCR complex requires the proper stoichiometric ratio of the proteins that compose the TCR complex. TCR function also requires two functioning TCR zeta proteins with ITAM motifs. The activation of the TCR upon engagement of its MHC-peptide ligand requires the engagement of several TCRs on the same T cell, which all must signal properly. Thus, if a TCR complex is destabilized with proteins that do not associate properly or cannot signal optimally, the T cell will not become activated sufficiently to begin a cellular response.

[0244] Accordingly, in some embodiments, TCR expression may eliminated using RNA interference (e.g., shRNA, siRNA, miRNA, etc.), CRISPR, or other methods that target the nucleic acids encoding specific TCRs (e.g., TCR-α and TCR-β) and/or CD3 chains in primary T cells. By blocking expression of one or more of these proteins, the T cell will no longer produce one or more of the key components of the TCR complex, thereby destabilizing the TCR complex and preventing cell surface expression of a functional TCR.

[0245] In some instances, CAR may also comprise a switch mechanism for controlling expression and/or activation of the CAR. For example, a CAR may comprise an extracellular, transmembrane, and intracellular domain, in which the extracellular domain comprises a target-specific binding element that comprises a label, binding domain, or tag that is specific for a molecule other than the target antigen that is expressed on or by a target cell. In such

embodiments, the specificity of the CAR is provided by a second construct that comprises a target antigen binding domain (e.g., an scFv or a bispecific antibody that is specific for both the target antigen and the label or tag on the CAR) and a domain that is recognized by or binds to the label, binding domain, or tag on the CAR. See, e.g., WO 2013/044225, WO 2016/000304, WO 2015/057834, WO 2015/057852, WO 2016/070061, US 9,233,125, US 2016/0129109. In this way, a T-cell that expresses the CAR can be administered to a subject, but the CAR cannot bind its target antigen until the second composition comprising an antigen-specific binding domain is administered.

[0246] Alternative switch mechanisms include CARs that require multimerization in order to activate their signaling function (see, e.g., US 2015/0368342, US 2016/0175359, US 2015/0368360) and/or an exogenous signal, such as a small molecule drug (US 2016/0166613, Yung et al., Science, 2015), in order to elicit a T-cell response. Some CARs may also comprise a "suicide switch" to induce cell death of the CAR T-cells following treatment (Buddee et al., PLoS One, 2013) or to downregulate expression of the CAR following binding to the target antigen (WO 2016/011210).

[0247] Alternative techniques may be used to transform target immunoresponsive cells, such as protoplast fusion, lipofection, transfection or electroporation. A wide variety of vectors may be used, such as retroviral vectors, lentiviral vectors, adenoviral vectors, adeno-associated viral vectors, plasmids or transposons, such as a Sleeping Beauty transposon (see U.S. Patent Nos. 6,489,458; 7,148,203; 7,160,682; 7,985,739; 8,227,432), may be used to introduce CARs, for example using 2nd generation antigen-specific CARs signaling through CD3ζ and either CD28 or CD137. Viral vectors may for example include vectors based on HIV, SV40, EBV, HSV or BPV.

[0248] Cells that are targeted for transformation may for example include T cells, Natural Killer (NK) cells, cytotoxic T lymphocytes (CTL), regulatory T cells, human embryonic stem cells, tumor-infiltrating lymphocytes (TIL) or a pluripotent stem cell from which lymphoid cells may be differentiated. T cells expressing a desired CAR may for example be selected through co-culture with γ-irradiated activating and propagating cells (AaPC), which co-express the cancer antigen and co-stimulatory molecules. The engineered CAR T-cells may be expanded, for example by co-culture on AaPC in presence of soluble factors, such as IL-2 and IL-21. This expansion may for example be carried out so as to provide memory CAR+ T cells (which may for example be assayed by non-enzymatic digital array and/or multi-panel flow cytometry). In this way, CAR T cells may be provided that have specific cytotoxic

activity against antigen-bearing tumors (optionally in conjunction with production of desired chemokines such as interferon-γ). CAR T cells of this kind may for example be used in animal models, for example to treat tumor xenografts.

[0249] In certain embodiments, ACT includes co-transferring CD4+ Th1 cells and CD8+ CTLs to induce a synergistic antitumour response (see, e.g., Li et al., Adoptive cell therapy with CD4+ T helper 1 cells and CD8+ cytotoxic T cells enhances complete rejection of an established tumour, leading to generation of endogenous memory responses to non-targeted tumour epitopes. Clin Transl Immunology. 2017 Oct; 6(10): e160).

[0250] In certain embodiments, Th17 cells are transferred to a subject in need thereof. Th17 cells have been reported to directly eradicate melanoma tumors in mice to a greater extent than Th1 cells (Muranski P, et al., Tumor-specific Th17-polarized cells eradicate large established melanoma. Blood. 2008 Jul 15; 112(2):362-73; and Martin-Orozco N, et al., T helper 17 cells promote cytotoxic T cell activation in tumor immunity. Immunity. 2009 Nov 20; 31(5):787-98). Those studies involved an adoptive T cell transfer (ACT) therapy approach, which takes advantage of $CD4^+$ T cells that express a TCR recognizing tyrosinase tumor antigen. Exploitation of the TCR leads to rapid expansion of Th17 populations to large numbers *ex vivo* for reinfusion into the autologous tumor-bearing hosts.

[0251] In certain embodiments, ACT may include autologous iPSC-based vaccines, such as irradiated iPSCs in autologous anti-tumor vaccines (see e.g., Kooreman, Nigel G. et al., Autologous iPSC-Based Vaccines Elicit Anti-tumor Responses In Vivo, Cell Stem Cell 22, 1–13, 2018, doi.org/10.1016/j.stem.2018.01.016).

[0252] Unlike T-cell receptors (TCRs) that are MHC restricted, CARs can potentially bind any cell surface-expressed antigen and can thus be more universally used to treat patients (see Irving et al., Engineering Chimeric Antigen Receptor T-Cells for Racing in Solid Tumors: Don't Forget the Fuel, Front. Immunol., 03 April 2017, doi.org/10.3389/fimmu.2017.00267). In certain embodiments, in the absence of endogenous T-cell infiltrate (e.g., due to aberrant antigen processing and presentation), which precludes the use of TIL therapy and immune checkpoint blockade, the transfer of CAR T-cells may be used to treat patients (see, e.g., Hinrichs CS, Rosenberg SA. Exploiting the curative potential of adoptive T-cell therapy for cancer. Immunol Rev (2014) 257(1):56–71. doi:10.1111/imr.12132).

[0253] Approaches such as the foregoing may be adapted to provide methods of treating and/or increasing survival of a subject having a disease, such as a neoplasia, for example by

administering an effective amount of an immunoresponsive cell comprising an antigen recognizing receptor that binds a selected antigen, wherein the binding activates the immunoresponsive cell, thereby treating or preventing the disease (such as a neoplasia, a pathogen infection, an autoimmune disorder, or an allogeneic transplant reaction).

[0254] In certain embodiments, the treatment can be administered after lymphodepleting pretreatment in the form of chemotherapy (typically a combination of cyclophosphamide and fludarabine) or radiation therapy. Initial studies in ACT had short lived responses and the transferred cells did not persist in vivo for very long (Houot et al., T-cell-based immunotherapy: adoptive cell transfer and checkpoint inhibition. Cancer Immunol Res (2015) 3(10):1115–22; and Kamta et al., Advancing Cancer Therapy with Present and Emerging Immuno-Oncology Approaches. Front. Oncol. (2017) 7:64). Immune suppressor cells like Tregs and MDSCs may attenuate the activity of transferred cells by outcompeting them for the necessary cytokines. Not being bound by a theory lymphodepleting pretreatment may eliminate the suppressor cells allowing the TILs to persist.

[0255] In one embodiment, the treatment can be administrated into patients undergoing an immunosuppressive treatment (e.g., glucocorticoid treatment). The cells or population of cells, may be made resistant to at least one immunosuppressive agent due to the inactivation of a gene encoding a receptor for such immunosuppressive agent. In certain embodiments, the immunosuppressive treatment provides for the selection and expansion of the immunoresponsive T cells within the patient.

[0256] In certain embodiments, the treatment can be administered before primary treatment (e.g., surgery or radiation therapy) to shrink a tumor before the primary treatment. In another embodiment, the treatment can be administered after primary treatment to remove any remaining cancer cells.

[0257] In certain embodiments, immunometabolic barriers can be targeted therapeutically prior to and/or during ACT to enhance responses to ACT or CAR T-cell therapy and to support endogenous immunity (see, e.g., Irving et al., Engineering Chimeric Antigen Receptor T-Cells for Racing in Solid Tumors: Don't Forget the Fuel, Front. Immunol., 03 April 2017, doi.org/10.3389/fimmu.2017.00267).

[0258] The administration of cells or population of cells, such as immune system cells or cell populations, such as more particularly immunoresponsive cells or cell populations, as disclosed herein may be carried out in any convenient manner, including by aerosol inhalation, injection, ingestion, transfusion, implantation or transplantation. The cells or

population of cells may be administered to a patient subcutaneously, intradermally, intratumorally, intranodally, intramedullary, intramuscularly, intrathecally, by intravenous or intralymphatic injection, or intraperitoneally. In some embodiments, the disclosed CARs may be delivered or administered into a cavity formed by the resection of tumor tissue (i.e. intracavity delivery) or directly into a tumor prior to resection (i.e. intratumoral delivery). In one embodiment, the cell compositions of the present invention are preferably administered by intravenous injection.

[0259] The administration of the cells or population of cells can consist of the administration of 10^4- 10^9 cells per kg body weight, preferably 10^5 to 10^6 cells/kg body weight including all integer values of cell numbers within those ranges. Dosing in CAR T cell therapies may for example involve administration of from 10^6 to 10^9 cells/kg, with or without a course of lymphodepletion, for example with cyclophosphamide. The cells or population of cells can be administrated in one or more doses. In another embodiment, the effective amount of cells are administrated as a single dose. In another embodiment, the effective amount of cells are administrated as more than one dose over a period time. Timing of administration is within the judgment of managing physician and depends on the clinical condition of the patient. The cells or population of cells may be obtained from any source, such as a blood bank or a donor. While individual needs vary, determination of optimal ranges of effective amounts of a given cell type for a particular disease or conditions are within the skill of one in the art. An effective amount means an amount which provides a therapeutic or prophylactic benefit. The dosage administrated will be dependent upon the age, health and weight of the recipient, kind of concurrent treatment, if any, frequency of treatment and the nature of the effect desired.

[0260] In another embodiment, the effective amount of cells or composition comprising those cells are administrated parenterally. The administration can be an intravenous administration. The administration can be directly done by injection within a tumor.

[0261] To guard against possible adverse reactions, engineered immunoresponsive cells may be equipped with a transgenic safety switch, in the form of a transgene that renders the cells vulnerable to exposure to a specific signal. For example, the herpes simplex viral thymidine kinase (TK) gene may be used in this way, for example by introduction into allogeneic T lymphocytes used as donor lymphocyte infusions following stem cell transplantation (Greco, et al., Improving the safety of cell therapy with the TK-suicide gene. Front. Pharmacol. 2015; 6: 95). In such cells, administration of a nucleoside prodrug such as

ganciclovir or acyclovir causes cell death. Alternative safety switch constructs include inducible caspase 9, for example triggered by administration of a small-molecule dimerizer that brings together two nonfunctional icasp9 molecules to form the active enzyme. A wide variety of alternative approaches to implementing cellular proliferation controls have been described (see U.S. Patent Publication No. 20130071414; PCT Patent Publication WO2011146862; PCT Patent Publication WO2014011987; PCT Patent Publication WO2013040371; Zhou et al. BLOOD, 2014, 123/25:3895 – 3905; Di Stasi et al., The New England Journal of Medicine 2011; 365:1673-1683; Sadelain M, The New England Journal of Medicine 2011; 365:1735-173; Ramos et al., Stem Cells 28(6):1107-15 (2010)).

[0262] In a further refinement of adoptive therapies, genome editing may be used to tailor immunoresponsive cells to alternative implementations, for example providing edited CAR T cells (see Poirot et al., 2015, Multiplex genome edited T-cell manufacturing platform for "off-the-shelf" adoptive T-cell immunotherapies, Cancer Res 75 (18): 3853; Ren et al., 2017, Multiplex genome editing to generate universal CAR T cells resistant to PD1 inhibition, Clin Cancer Res. 2017 May 1;23(9):2255-2266. doi: 10.1158/1078-0432.CCR-16-1300. Epub 2016 Nov 4; Qasim et al., 2017, Molecular remission of infant B-ALL after infusion of universal TALEN gene-edited CAR T cells, Sci Transl Med. 2017 Jan 25;9(374); Legut, et al., 2018, CRISPR-mediated TCR replacement generates superior anticancer transgenic T cells. Blood, 131(3), 311-322; and Georgiadis et al., Long Terminal Repeat CRISPR-CAR-Coupled “Universal” T Cells Mediate Potent Anti-leukemic Effects, Molecular Therapy, In Press, Corrected Proof, Available online 6 March 2018). Cells may be edited using any CRISPR system and method of use thereof as described herein. CRISPR systems may be delivered to an immune cell by any method described herein. In preferred embodiments, cells are edited ex vivo and transferred to a subject in need thereof. Immunoresponsive cells, CAR T cells or any cells used for adoptive cell transfer may be edited. Editing may be performed for example to insert or knock-in an exogenous gene, such as an exogenous gene encoding a CAR or a TCR, at a preselected locus in a cell (e.g. TRAC locus); to eliminate potential alloreactive T-cell receptors (TCR) or to prevent inappropriate pairing between endogenous and exogenous TCR chains, such as to knock-out or knock-down expression of an endogenous TCR in a cell; to disrupt the target of a chemotherapeutic agent in a cell; to block an immune checkpoint, such as to knock-out or knock-down expression of an immune checkpoint protein or receptor in a cell; to knock-out or knock-down expression of other gene or genes in a cell, the reduced expression or lack of expression of which can enhance the

efficacy of adoptive therapies using the cell; to knock-out or knock-down expression of an endogenous gene in a cell, said endogenous gene encoding an antigen targeted by an exogenous CAR or TCR; to knock-out or knock-down expression of one or more MHC constituent proteins in a cell; to activate a T cell; to modulate cells such that the cells are resistant to exhaustion or dysfunction; and/or increase the differentiation and/or proliferation of functionally exhausted or dysfunctional CD8+ T-cells (see PCT Patent Publications: WO2013176915, WO2014059173, WO2014172606, WO2014184744, and WO2014191128).

[0263] In certain embodiments, editing may result in inactivation of a gene. By inactivating a gene, it is intended that the gene of interest is not expressed in a functional protein form. In a particular embodiment, the CRISPR system specifically catalyzes cleavage in one targeted gene thereby inactivating said targeted gene. The nucleic acid strand breaks caused are commonly repaired through the distinct mechanisms of homologous recombination or non-homologous end joining (NHEJ). However, NHEJ is an imperfect repair process that often results in changes to the DNA sequence at the site of the cleavage. Repair via non-homologous end joining (NHEJ) often results in small insertions or deletions (Indel) and can be used for the creation of specific gene knockouts. Cells in which a cleavage induced mutagenesis event has occurred can be identified and/or selected by well-known methods in the art. In certain embodiments, homology directed repair (HDR) is used to concurrently inactivate a gene (e.g., TRAC) and insert an endogenous TCR or CAR into the inactivated locus.

[0264] Hence, in certain embodiments, editing of cells (such as by CRISPR/Cas), particularly cells intended for adoptive cell therapies, more particularly immunoresponsive cells such as T cells, may be performed to insert or knock-in an exogenous gene, such as an exogenous gene encoding a CAR or a TCR, at a preselected locus in a cell. Conventionally, nucleic acid molecules encoding CARs or TCRs are transfected or transduced to cells using randomly integrating vectors, which, depending on the site of integration, may lead to clonal expansion, oncogenic transformation, variegated transgene expression and/or transcriptional silencing of the transgene. Directing of transgene(s) to a specific locus in a cell can minimize or avoid such risks and advantageously provide for uniform expression of the transgene(s) by the cells. Without limitation, suitable 'safe harbor' loci for directed transgene integration include CCR5 or AAVS1. Homology-directed repair (HDR) strategies are known and

described elsewhere in this specification allowing to insert transgenes into desired loci (e.g., TRAC locus).

[0265] Further suitable loci for insertion of transgenes, in particular CAR or exogenous TCR transgenes, include without limitation loci comprising genes coding for constituents of endogenous T-cell receptor, such as T-cell receptor alpha locus (TRA) or T-cell receptor beta locus (TRB), for example T-cell receptor alpha constant (TRAC) locus, T-cell receptor beta constant 1 (TRBC1) locus or T-cell receptor beta constant 2 (TRBC1) locus. Advantageously, insertion of a transgene into such locus can simultaneously achieve expression of the transgene, potentially controlled by the endogenous promoter, and knock-out expression of the endogenous TCR. This approach has been exemplified in Eyquem et al., (2017) Nature 543: 113-117, wherein the authors used CRISPR/Cas9 gene editing to knock-in a DNA molecule encoding a CD19-specific CAR into the TRAC locus downstream of the endogenous promoter; the CAR-T cells obtained by CRISPR were significantly superior in terms of reduced tonic CAR signaling and exhaustion.

[0266] T cell receptors (TCR) are cell surface receptors that participate in the activation of T cells in response to the presentation of antigen. The TCR is generally made from two chains, α and β, which assemble to form a heterodimer and associates with the CD3-transducing subunits to form the T cell receptor complex present on the cell surface. Each α and β chain of the TCR consists of an immunoglobulin-like N-terminal variable (V) and constant (C) region, a hydrophobic transmembrane domain, and a short cytoplasmic region. As for immunoglobulin molecules, the variable region of the α and β chains are generated by V(D)J recombination, creating a large diversity of antigen specificities within the population of T cells. However, in contrast to immunoglobulins that recognize intact antigen, T cells are activated by processed peptide fragments in association with an MHC molecule, introducing an extra dimension to antigen recognition by T cells, known as MHC restriction. Recognition of MHC disparities between the donor and recipient through the T cell receptor leads to T cell proliferation and the potential development of graft versus host disease (GVHD). The inactivation of TCRα or TCRβ can result in the elimination of the TCR from the surface of T cells preventing recognition of alloantigen and thus GVHD. However, TCR disruption generally results in the elimination of the CD3 signaling component and alters the means of further T cell expansion.

[0267] Hence, in certain embodiments, editing of cells (such as by CRISPR/Cas), particularly cells intended for adoptive cell therapies, more particularly immunoresponsive

cells such as T cells, may be performed to knock-out or knock-down expression of an endogenous TCR in a cell. For example, NHEJ-based or HDR-based gene editing approaches can be employed to disrupt the endogenous TCR alpha and/or beta chain genes. For example, gene editing system or systems, such as CRISPR/Cas system or systems, can be designed to target a sequence found within the TCR beta chain conserved between the beta 1 and beta 2 constant region genes (TRBC1 and TRBC2) and/or to target the constant region of the TCR alpha chain (TRAC) gene.

[0268] Allogeneic cells are rapidly rejected by the host immune system. It has been demonstrated that, allogeneic leukocytes present in non-irradiated blood products will persist for no more than 5 to 6 days (Boni, Muranski et al. 2008 Blood 1;112(12):4746-54). Thus, to prevent rejection of allogeneic cells, the host's immune system usually has to be suppressed to some extent. However, in the case of adoptive cell transfer the use of immunosuppressive drugs also have a detrimental effect on the introduced therapeutic T cells. Therefore, to effectively use an adoptive immunotherapy approach in these conditions, the introduced cells would need to be resistant to the immunosuppressive treatment. Thus, in a particular embodiment, the present invention further comprises a step of modifying T cells to make them resistant to an immunosuppressive agent, preferably by inactivating at least one gene encoding a target for an immunosuppressive agent. An immunosuppressive agent is an agent that suppresses immune function by one of several mechanisms of action. An immunosuppressive agent can be, but is not limited to a calcineurin inhibitor, a target of rapamycin, an interleukin-2 receptor α-chain blocker, an inhibitor of inosine monophosphate dehydrogenase, an inhibitor of dihydrofolic acid reductase, a corticosteroid or an immunosuppressive antimetabolite. The present invention allows conferring immunosuppressive resistance to T cells for immunotherapy by inactivating the target of the immunosuppressive agent in T cells. As non-limiting examples, targets for an immunosuppressive agent can be a receptor for an immunosuppressive agent such as: CD52, glucocorticoid receptor (GR), a FKBP family gene member and a cyclophilin family gene member.

[0269] In certain embodiments, editing of cells (such as by CRISPR/Cas), particularly cells intended for adoptive cell therapies, more particularly immunoresponsive cells such as T cells, may be performed to block an immune checkpoint, such as to knock-out or knock-down expression of an immune checkpoint protein or receptor in a cell. Immune checkpoints are inhibitory pathways that slow down or stop immune reactions and prevent excessive

tissue damage from uncontrolled activity of immune cells. In certain embodiments, the immune checkpoint targeted is the programmed death-1 (PD-1 or CD279) gene (PDCD1). In other embodiments, the immune checkpoint targeted is cytotoxic T-lymphocyte-associated antigen (CTLA-4). In additional embodiments, the immune checkpoint targeted is another member of the CD28 and CTLA4 Ig superfamily such as BTLA, LAG3, ICOS, PDL1 or KIR. In further additional embodiments, the immune checkpoint targeted is a member of the TNFR superfamily such as CD40, OX40, CD137, GITR, CD27 or TIM-3.

[0270] Additional immune checkpoints include Src homology 2 domain-containing protein tyrosine phosphatase 1 (SHP-1) (Watson HA, et al., SHP-1: the next checkpoint target for cancer immunotherapy? Biochem Soc Trans. 2016 Apr 15;44(2):356-62). SHP-1 is a widely expressed inhibitory protein tyrosine phosphatase (PTP). In T-cells, it is a negative regulator of antigen-dependent activation and proliferation. It is a cytosolic protein, and therefore not amenable to antibody-mediated therapies, but its role in activation and proliferation makes it an attractive target for genetic manipulation in adoptive transfer strategies, such as chimeric antigen receptor (CAR) T cells. Immune checkpoints may also include T cell immunoreceptor with Ig and ITIM domains (TIGIT/Vstm3/WUCAM/VSIG9) and VISTA (Le Mercier I, et al., (2015) Beyond CTLA-4 and PD-1, the generation Z of negative checkpoint regulators. Front. Immunol. 6:418).

[0271] WO2014172606 relates to the use of MT1 and/or MT2 inhibitors to increase proliferation and/or activity of exhausted CD8+ T-cells and to decrease CD8+ T-cell exhaustion (e.g., decrease functionally exhausted or unresponsive CD8+ immune cells). In certain embodiments, metallothioneins are targeted by gene editing in adoptively transferred T cells.

[0272] In certain embodiments, targets of gene editing may be at least one targeted locus involved in the expression of an immune checkpoint protein. Such targets may include, but are not limited to CTLA4, PPP2CA, PPP2CB, PTPN6, PTPN22, PDCD1, ICOS (CD278), PDL1, KIR, LAG3, HAVCR2, BTLA, CD160, TIGIT, CD96, CRTAM, LAIR1, SIGLEC7, SIGLEC9, CD244 (2B4), TNFRSF10B, TNFRSF10A, CASP8, CASP10, CASP3, CASP6, CASP7, FADD, FAS, TGFBRII, TGFRBRI, SMAD2, SMAD3, SMAD4, SMAD10, SKI, SKIL, TGIF1, IL10RA, IL10RB, HMOX2, IL6R, IL6ST, EIF2AK4, CSK, PAG1, SIT1, FOXP3, PRDM1, BATF, VISTA, GUCY1A2, GUCY1A3, GUCY1B2, GUCY1B3, MT1, MT2, CD40, OX40, CD137, GITR, CD27, SHP-1, TIM-3, CEACAM-1, CEACAM-3, or CEACAM-5. In preferred embodiments, the gene locus involved in the expression of PD-1 or

CTLA-4 genes is targeted. In other preferred embodiments, combinations of genes are targeted, such as but not limited to PD-1 and TIGIT.

[0273] By means of an example and without limitation, WO2016196388 concerns an engineered T cell comprising (a) a genetically engineered antigen receptor that specifically binds to an antigen, which receptor may be a CAR; and (b) a disrupted gene encoding a PD-L1, an agent for disruption of a gene encoding a PD- L1, and/or disruption of a gene encoding PD-L1, wherein the disruption of the gene may be mediated by a gene editing nuclease, a zinc finger nuclease (ZFN), CRISPR/Cas9 and/or TALEN. WO2015142675 relates to immune effector cells comprising a CAR in combination with an agent (such as CRISPR, TALEN or ZFN) that increases the efficacy of the immune effector cells in the treatment of cancer, wherein the agent may inhibit an immune inhibitory molecule, such as PD1, PD-L1, CTLA-4, TIM-3, LAG-3, VISTA, BTLA, TIGIT, LAIR1, CD160, 2B4, TGFR beta, CEACAM-1, CEACAM-3, or CEACAM-5. Ren et al., (2017) Clin Cancer Res 23 (9) 2255-2266 performed lentiviral delivery of CAR and electro-transfer of Cas9 mRNA and gRNAs targeting endogenous TCR, β-2 microglobulin (B2M) and PD1 simultaneously, to generate gene-disrupted allogeneic CAR T cells deficient of TCR, HLA class I molecule and PD1.

[0274] In certain embodiments, cells may be engineered to express a CAR, wherein expression and/or function of methylcytosine dioxygenase genes (TET1, TET2 and/or TET3) in the cells has been reduced or eliminated, such as by CRISPR, ZNF or TALEN (for example, as described in WO201704916).

[0275] In certain embodiments, editing of cells (such as by CRISPR/Cas), particularly cells intended for adoptive cell therapies, more particularly immunoresponsive cells such as T cells, may be performed to knock-out or knock-down expression of an endogenous gene in a cell, said endogenous gene encoding an antigen targeted by an exogenous CAR or TCR, thereby reducing the likelihood of targeting of the engineered cells. In certain embodiments, the targeted antigen may be one or more antigen selected from the group consisting of CD38, CD138, CS-1, CD33, CD26, CD30, CD53, CD92, CD100, CD148, CD150, CD200, CD261, CD262, CD362, human telomerase reverse transcriptase (hTERT), survivin, mouse double minute 2 homolog (MDM2), cytochrome P450 1B1 (CYP1B), HER2/neu, Wilms' tumor gene 1 (WT1), livin, alphafetoprotein (AFP), carcinoembryonic antigen (CEA), mucin 16 (MUC16), MUC1, prostate-specific membrane antigen (PSMA), p53, cyclin (D1), B cell maturation antigen (BCMA), transmembrane activator and CAML Interactor (TACI), and B-

cell activating factor receptor (BAFF-R) (for example, as described in WO2016011210 and WO2017011804).

[0276] In certain embodiments, editing of cells (such as by CRISPR/Cas), particularly cells intended for adoptive cell therapies, more particularly immunoresponsive cells such as T cells, may be performed to knock-out or knock-down expression of one or more MHC constituent proteins, such as one or more HLA proteins and/or beta-2 microglobulin (B2M), in a cell, whereby rejection of non-autologous (e.g., allogeneic) cells by the recipient's immune system can be reduced or avoided. In preferred embodiments, one or more HLA class I proteins, such as HLA-A, B and/or C, and/or B2M may be knocked-out or knocked-down. Preferably, B2M may be knocked-out or knocked-down. By means of an example, Ren et al., (2017) Clin Cancer Res 23 (9) 2255-2266 performed lentiviral delivery of CAR and electro-transfer of Cas9 mRNA and gRNAs targeting endogenous TCR, β-2 microglobulin (B2M) and PD1 simultaneously, to generate gene-disrupted allogeneic CAR T cells deficient of TCR, HLA class I molecule and PD1.

[0277] In other embodiments, at least two genes are edited. Pairs of genes may include, but are not limited to PD1 and TCRα, PD1 and TCRβ, CTLA-4 and TCRα, CTLA-4 and TCRβ, LAG3 and TCRα, LAG3 and TCRβ, Tim3 and TCRα, Tim3 and TCRβ, BTLA and TCRα, BTLA and TCRβ, BY55 and TCRα, BY55 and TCRβ, TIGIT and TCRα, TIGIT and TCRβ, B7H5 and TCRα, B7H5 and TCRβ, LAIR1 and TCRα, LAIR1 and TCRβ, SIGLEC10 and TCRα, SIGLEC10 and TCRβ, 2B4 and TCRα, 2B4 and TCRβ, B2M and TCRα, B2M and TCRβ.

[0278] In certain embodiments, a cell may be multiply edited (multiplex genome editing) as taught herein to (1) knock-out or knock-down expression of an endogenous TCR (for example, TRBC1, TRBC2 and/or TRAC), (2) knock-out or knock-down expression of an immune checkpoint protein or receptor (for example PD1, PD-L1 and/or CTLA4); and (3) knock-out or knock-down expression of one or more MHC constituent proteins (for example, HLA-A, B and/or C, and/or B2M, preferably B2M).

[0279] Whether prior to or after genetic modification of the T cells, the T cells can be activated and expanded generally using methods as described, for example, in U.S. Patents 6,352,694; 6,534,055; 6,905,680; 5,858,358; 6,887,466; 6,905,681; 7,144,575; 7,232,566; 7,175,843; 5,883,223; 6,905,874; 6,797,514; 6,867,041; and 7,572,631. T cells can be expanded in vitro or in vivo.

[0280] Immune cells may be obtained using any method known in the art. In one embodiment, allogenic T cells may be obtained from healthy subjects. In one embodiment T cells that have infiltrated a tumor are isolated. T cells may be removed during surgery. T cells may be isolated after removal of tumor tissue by biopsy. T cells may be isolated by any means known in the art. In one embodiment, T cells are obtained by apheresis. In one embodiment, the method may comprise obtaining a bulk population of T cells from a tumor sample by any suitable method known in the art. For example, a bulk population of T cells can be obtained from a tumor sample by dissociating the tumor sample into a cell suspension from which specific cell populations can be selected. Suitable methods of obtaining a bulk population of T cells may include, but are not limited to, any one or more of mechanically dissociating (e.g., mincing) the tumor, enzymatically dissociating (e.g., digesting) the tumor, and aspiration (e.g., as with a needle).

[0281] The bulk population of T cells obtained from a tumor sample may comprise any suitable type of T cell. Preferably, the bulk population of T cells obtained from a tumor sample comprises tumor infiltrating lymphocytes (TILs).

[0282] The tumor sample may be obtained from any mammal. Unless stated otherwise, as used herein, the term "mammal" refers to any mammal including, but not limited to, mammals of the order Logomorpha, such as rabbits; the order Carnivora, including Felines (cats) and Canines (dogs); the order Artiodactyla, including Bovines (cows) and Swines (pigs); or of the order Perssodactyla, including Equines (horses). The mammals may be non-human primates, e.g., of the order Primates, Ceboids, or Simoids (monkeys) or of the order Anthropoids (humans and apes). In some embodiments, the mammal may be a mammal of the order Rodentia, such as mice and hamsters. Preferably, the mammal is a non-human primate or a human. An especially preferred mammal is the human.

[0283] T cells can be obtained from a number of sources, including peripheral blood mononuclear cells, bone marrow, lymph node tissue, spleen tissue, and tumors. In certain embodiments of the present invention, T cells can be obtained from a unit of blood collected from a subject using any number of techniques known to the skilled artisan, such as Ficoll separation. In one preferred embodiment, cells from the circulating blood of an individual are obtained by apheresis or leukapheresis. The apheresis product typically contains lymphocytes, including T cells, monocytes, granulocytes, B cells, other nucleated white blood cells, red blood cells, and platelets. In one embodiment, the cells collected by apheresis may be washed to remove the plasma fraction and to place the cells in an appropriate buffer

or media for subsequent processing steps. In one embodiment of the invention, the cells are washed with phosphate buffered saline (PBS). In an alternative embodiment, the wash solution lacks calcium and may lack magnesium or may lack many if not all divalent cations. Initial activation steps in the absence of calcium lead to magnified activation. As those of ordinary skill in the art would readily appreciate a washing step may be accomplished by methods known to those in the art, such as by using a semi-automated "flow-through" centrifuge (for example, the Cobe 2991 cell processor) according to the manufacturer's instructions. After washing, the cells may be resuspended in a variety of biocompatible buffers, such as, for example, Ca-free, Mg-free PBS. Alternatively, the undesirable components of the apheresis sample may be removed and the cells directly resuspended in culture media.

[0284] In another embodiment, T cells are isolated from peripheral blood lymphocytes by lysing the red blood cells and depleting the monocytes, for example, by centrifugation through a PERCOLL™ gradient. A specific subpopulation of T cells, such as CD28+, CD4+, CDC, CD45RA+, and CD45RO+ T cells, can be further isolated by positive or negative selection techniques. For example, in one preferred embodiment, T cells are isolated by incubation with anti-CD3/anti-CD28 (i.e., 3×28)-conjugated beads, such as DYNABEADS® M-450 CD3/CD28 T, or XCYTE DYNABEADS™ for a time period sufficient for positive selection of the desired T cells. In one embodiment, the time period is about 30 minutes. In a further embodiment, the time period ranges from 30 minutes to 36 hours or longer and all integer values there between. In a further embodiment, the time period is at least 1, 2, 3, 4, 5, or 6 hours. In yet another preferred embodiment, the time period is 10 to 24 hours. In one preferred embodiment, the incubation time period is 24 hours. For isolation of T cells from patients with leukemia, use of longer incubation times, such as 24 hours, can increase cell yield. Longer incubation times may be used to isolate T cells in any situation where there are few T cells as compared to other cell types, such in isolating tumor infiltrating lymphocytes (TIL) from tumor tissue or from immunocompromised individuals. Further, use of longer incubation times can increase the efficiency of capture of CD8+ T cells.

[0285] Enrichment of a T cell population by negative selection can be accomplished with a combination of antibodies directed to surface markers unique to the negatively selected cells. A preferred method is cell sorting and/or selection via negative magnetic immunoadherence or flow cytometry that uses a cocktail of monoclonal antibodies directed to cell surface markers present on the cells negatively selected. For example, to enrich for

CD4+ cells by negative selection, a monoclonal antibody cocktail typically includes antibodies to CD14, CD20, CD11b, CD16, HLA-DR, and CD8.

[0286] Further, monocyte populations (i.e., CD14+ cells) may be depleted from blood preparations by a variety of methodologies, including anti-CD14 coated beads or columns, or utilization of the phagocytotic activity of these cells to facilitate removal. Accordingly, in one embodiment, the invention uses paramagnetic particles of a size sufficient to be engulfed by phagocytotic monocytes. In certain embodiments, the paramagnetic particles are commercially available beads, for example, those produced by Life Technologies under the trade name Dynabeads™. In one embodiment, other non-specific cells are removed by coating the paramagnetic particles with "irrelevant" proteins (e.g., serum proteins or antibodies). Irrelevant proteins and antibodies include those proteins and antibodies or fragments thereof that do not specifically target the T cells to be isolated. In certain embodiments, the irrelevant beads include beads coated with sheep anti-mouse antibodies, goat anti-mouse antibodies, and human serum albumin.

[0287] In brief, such depletion of monocytes is performed by preincubating T cells isolated from whole blood, apheresed peripheral blood, or tumors with one or more varieties of irrelevant or non-antibody coupled paramagnetic particles at any amount that allows for removal of monocytes (approximately a 20:1 bead:cell ratio) for about 30 minutes to 2 hours at 22 to 37 degrees C., followed by magnetic removal of cells which have attached to or engulfed the paramagnetic particles. Such separation can be performed using standard methods available in the art. For example, any magnetic separation methodology may be used including a variety of which are commercially available, (e.g., DYNAL® Magnetic Particle Concentrator (DYNAL MPC®)). Assurance of requisite depletion can be monitored by a variety of methodologies known to those of ordinary skill in the art, including flow cytometric analysis of CD14 positive cells, before and after depletion.

[0288] For isolation of a desired population of cells by positive or negative selection, the concentration of cells and surface (e.g., particles such as beads) can be varied. In certain embodiments, it may be desirable to significantly decrease the volume in which beads and cells are mixed together (i.e., increase the concentration of cells), to ensure maximum contact of cells and beads. For example, in one embodiment, a concentration of 2 billion cells/ml is used. In one embodiment, a concentration of 1 billion cells/ml is used. In a further embodiment, greater than 100 million cells/ml is used. In a further embodiment, a concentration of cells of 10, 15, 20, 25, 30, 35, 40, 45, or 50 million cells/ml is used. In yet

another embodiment, a concentration of cells from 75, 80, 85, 90, 95, or 100 million cells/ml is used. In further embodiments, concentrations of 125 or 150 million cells/ml can be used. Using high concentrations can result in increased cell yield, cell activation, and cell expansion. Further, use of high cell concentrations allows more efficient capture of cells that may weakly express target antigens of interest, such as CD28-negative T cells, or from samples where there are many tumor cells present (i.e., leukemic blood, tumor tissue, etc). Such populations of cells may have therapeutic value and would be desirable to obtain. For example, using high concentration of cells allows more efficient selection of CD8+ T cells that normally have weaker CD28 expression.

[0289] In a related embodiment, it may be desirable to use lower concentrations of cells. By significantly diluting the mixture of T cells and surface (e.g., particles such as beads), interactions between the particles and cells is minimized. This selects for cells that express high amounts of desired antigens to be bound to the particles. For example, CD4+ T cells express higher levels of CD28 and are more efficiently captured than CD8+ T cells in dilute concentrations. In one embodiment, the concentration of cells used is 5×10^6/ml. In other embodiments, the concentration used can be from about 1×10^5/ml to 1×10^6/ml, and any integer value in between.

[0290] T cells can also be frozen. Wishing not to be bound by theory, the freeze and subsequent thaw step provides a more uniform product by removing granulocytes and to some extent monocytes in the cell population. After a washing step to remove plasma and platelets, the cells may be suspended in a freezing solution. While many freezing solutions and parameters are known in the art and will be useful in this context, one method involves using PBS containing 20% DMSO and 8% human serum albumin, or other suitable cell freezing media, the cells then are frozen to −80° C at a rate of 1° per minute and stored in the vapor phase of a liquid nitrogen storage tank. Other methods of controlled freezing may be used as well as uncontrolled freezing immediately at −20° C. or in liquid nitrogen.

[0291] T cells for use in the present invention may also be antigen-specific T cells. For example, tumor-specific T cells can be used. In certain embodiments, antigen-specific T cells can be isolated from a patient of interest, such as a patient afflicted with a cancer or an infectious disease. In one embodiment, neoepitopes are determined for a subject and T cells specific to these antigens are isolated. Antigen-specific cells for use in expansion may also be generated in vitro using any number of methods known in the art, for example, as described in U.S. Patent Publication No. US 20040224402 entitled, Generation and Isolation of

Antigen-Specific T Cells, or in U.S. Pat. Nos. 6,040,177. Antigen-specific cells for use in the present invention may also be generated using any number of methods known in the art, for example, as described in Current Protocols in Immunology, or Current Protocols in Cell Biology, both published by John Wiley & Sons, Inc., Boston, Mass.

[0292] In a related embodiment, it may be desirable to sort or otherwise positively select (e.g. via magnetic selection) the antigen specific cells prior to or following one or two rounds of expansion. Sorting or positively selecting antigen-specific cells can be carried out using peptide-MHC tetramers (Altman, et al., Science. 1996 Oct. 4; 274(5284):94-6). In another embodiment, the adaptable tetramer technology approach is used (Andersen et al., 2012 Nat Protoc. 7:891-902). Tetramers are limited by the need to utilize predicted binding peptides based on prior hypotheses, and the restriction to specific HLAs. Peptide-MHC tetramers can be generated using techniques known in the art and can be made with any MHC molecule of interest and any antigen of interest as described herein. Specific epitopes to be used in this context can be identified using numerous assays known in the art. For example, the ability of a polypeptide to bind to MHC class I may be evaluated indirectly by monitoring the ability to promote incorporation of ^{125}I labeled β2-microglobulin (β2m) into MHC class I/β2m/peptide heterotrimeric complexes (see Parker et al., J. Immunol. 152:163, 1994).

[0293] In one embodiment cells are directly labeled with an epitope-specific reagent for isolation by flow cytometry followed by characterization of phenotype and TCRs. In one embodiment, T cells are isolated by contacting with T cell specific antibodies. Sorting of antigen-specific T cells, or generally any cells of the present invention, can be carried out using any of a variety of commercially available cell sorters, including, but not limited to, MoFlo sorter (DakoCytomation, Fort Collins, Colo.), FACSAria™, FACSArray™, FACSVantage™, BD™ LSR II, and FACSCalibur™ (BD Biosciences, San Jose, Calif.).

[0294] In a preferred embodiment, the method comprises selecting cells that also express CD3. The method may comprise specifically selecting the cells in any suitable manner. Preferably, the selecting is carried out using flow cytometry. The flow cytometry may be carried out using any suitable method known in the art. The flow cytometry may employ any suitable antibodies and stains. Preferably, the antibody is chosen such that it specifically recognizes and binds to the particular biomarker being selected. For example, the specific selection of CD3, CD8, TIM-3, LAG-3, 4-1BB, or PD-1 may be carried out using anti-CD3, anti-CD8, anti-TIM-3, anti-LAG-3, anti-4-lBB, or anti-PD-1 antibodies, respectively. The antibody or antibodies may be conjugated to a bead (e.g., a magnetic bead) or to a

fluorochrome. Preferably, the flow cytometry is fluorescence-activated cell sorting (FACS). TCRs expressed on T cells can be selected based on reactivity to autologous tumors. Additionally, T cells that are reactive to tumors can be selected for based on markers using the methods described in patent publication Nos. WO2014133567 and WO2014133568, herein incorporated by reference in their entirety. Additionally, activated T cells can be selected for based on surface expression of CD107a.

[0295] In one embodiment of the invention, the method further comprises expanding the numbers of T cells in the enriched cell population. Such methods are described in U.S. Patent No. 8,637,307 and is herein incorporated by reference in its entirety. The numbers of T cells may be increased at least about 3-fold (or 4-, 5-, 6-, 7-, 8-, or 9-fold), more preferably at least about 10-fold (or 20-, 30-, 40-, 50-, 60-, 70-, 80-, or 90-fold), more preferably at least about 100-fold, more preferably at least about 1,000 fold, or most preferably at least about 100,000-fold. The numbers of T cells may be expanded using any suitable method known in the art. Exemplary methods of expanding the numbers of cells are described in patent publication No. WO 2003057171, U.S. Patent No. 8,034,334, and U.S. Patent Application Publication No. 2012/0244133, each of which is incorporated herein by reference.

[0296] In one embodiment, *ex vivo* T cell expansion can be performed by isolation of T cells and subsequent stimulation or activation followed by further expansion. In one embodiment of the invention, the T cells may be stimulated or activated by a single agent. In another embodiment, T cells are stimulated or activated with two agents, one that induces a primary signal and a second that is a co-stimulatory signal. Ligands useful for stimulating a single signal or stimulating a primary signal and an accessory molecule that stimulates a second signal may be used in soluble form. Ligands may be attached to the surface of a cell, to an Engineered Multivalent Signaling Platform (EMSP), or immobilized on a surface. In a preferred embodiment both primary and secondary agents are co-immobilized on a surface, for example a bead or a cell. In one embodiment, the molecule providing the primary activation signal may be a CD3 ligand, and the co-stimulatory molecule may be a CD28 ligand or 4-1BB ligand.

[0297] In certain embodiments, T cells comprising a CAR or an exogenous TCR, may be manufactured as described in WO2015120096, by a method comprising: enriching a population of lymphocytes obtained from a donor subject; stimulating the population of lymphocytes with one or more T-cell stimulating agents to produce a population of activated T cells, wherein the stimulation is performed in a closed system using serum-free culture

medium; transducing the population of activated T cells with a viral vector comprising a nucleic acid molecule which encodes the CAR or TCR, using a single cycle transduction to produce a population of transduced T cells, wherein the transduction is performed in a closed system using serum-free culture medium; and expanding the population of transduced T cells for a predetermined time to produce a population of engineered T cells, wherein the expansion is performed in a closed system using serum-free culture medium. In certain embodiments, T cells comprising a CAR or an exogenous TCR, may be manufactured as described in WO2015120096, by a method comprising: obtaining a population of lymphocytes; stimulating the population of lymphocytes with one or more stimulating agents to produce a population of activated T cells, wherein the stimulation is performed in a closed system using serum-free culture medium; transducing the population of activated T cells with a viral vector comprising a nucleic acid molecule which encodes the CAR or TCR, using at least one cycle transduction to produce a population of transduced T cells, wherein the transduction is performed in a closed system using serum-free culture medium; and expanding the population of transduced T cells to produce a population of engineered T cells, wherein the expansion is performed in a closed system using serum-free culture medium. The predetermined time for expanding the population of transduced T cells may be 3 days. The time from enriching the population of lymphocytes to producing the engineered T cells may be 6 days. The closed system may be a closed bag system. Further provided is population of T cells comprising a CAR or an exogenous TCR obtainable or obtained by said method, and a pharmaceutical composition comprising such cells.

[0298] In certain embodiments, T cell maturation or differentiation in vitro may be delayed or inhibited by the method as described in WO2017070395, comprising contacting one or more T cells from a subject in need of a T cell therapy with an AKT inhibitor (such as, e.g., one or a combination of two or more AKT inhibitors disclosed in claim 8 of WO2017070395) and at least one of exogenous Interleukin-7 (IL-7) and exogenous Interleukin-15 (IL-15), wherein the resulting T cells exhibit delayed maturation or differentiation, and/or wherein the resulting T cells exhibit improved T cell function (such as, e.g., increased T cell proliferation; increased cytokine production; and/or increased cytolytic activity) relative to a T cell function of a T cell cultured in the absence of an AKT inhibitor.

[0299] In certain embodiments, a patient in need of a T cell therapy may be conditioned by a method as described in WO2016191756 comprising administering to the patient a dose

of cyclophosphamide between 200 mg/m2/day and 2000 mg/m2/day and a dose of fludarabine between 20 mg/m2/day and 900 mg/m^2/day.

Diseases

[0300] It will be understood by the skilled person that treating as referred to herein encompasses enhancing treatment, or improving treatment efficacy. Treatment may include inhibition of tumor regression as well as inhibition of tumor growth, metastasis or tumor cell proliferation, or inhibition or reduction of otherwise deleterious effects associated with the tumor.

[0301] Efficaciousness of treatment is determined in association with any known method for diagnosing or treating the particular disease. The invention comprehends a treatment method comprising any one of the methods or uses herein discussed.

[0302] The phrase "therapeutically effective amount" as used herein refers to a sufficient amount of a drug, agent, or compound to provide a desired therapeutic effect.

[0303] As used herein “patient” refers to any human being receiving or who may receive medical treatment and is used interchangeably herein with the term “subject”.

[0304] Therapy or treatment according to the invention may be performed alone or in conjunction with another therapy, and may be provided at home, the doctor’s office, a clinic, a hospital’s outpatient department, or a hospital. Treatment generally begins at a hospital so that the doctor can observe the therapy’s effects closely and make any adjustments that are needed. The duration of the therapy depends on the age and condition of the patient, the stage of the cancer, and how the patient responds to the treatment.

[0305] The disclosure also provides methods for reducing resistance to immunotherapy and treating disease. Not being bound by a theory, cancer cells have many strategies of avoiding the immune system and by reducing the signature of the present invention cancer cells may be unmasked to the immune system. Not being bound by a theory, reducing a gene signature of the present invention may be used to treat a subject who has not been administered an immunotherapy, such that the subject’s tumor becomes unmasked to their natural or unamplified immune system. In other embodiments, the cancer is resistant to therapies targeting the adaptive immune system (see e.g., Rooney et al., Molecular and genetic properties of tumors associated with local immune cytolytic activity, Cell. 2015 January 15; 160(1-2): 48–61). In one embodiment, modulation of one or more of the signature genes are used for reducing an immunotherapy resistant signature for the treatment

of a subpopulation of tumor cells that are linked to resistance to targeted therapies and progressive tumor growth.

[0306] In general, the immune system is involved with controlling all cancers and the present application is applicable to treatment of all cancers. Not being bound by a theory, the signature of the present invention is applicable to all cancers and may be used for treatment, as well as for determining a prognosis and stratifying patients. The cancer may include, without limitation, liquid tumors such as leukemia (e.g., acute leukemia, acute lymphocytic leukemia, acute myelocytic leukemia, acute myeloblastic leukemia, acute promyelocytic leukemia, acute myelomonocytic leukemia, acute monocytic leukemia, acute erythroleukemia, chronic leukemia, chronic myelocytic leukemia, chronic lymphocytic leukemia), polycythemia vera, lymphoma (e.g., Hodgkin's disease, non-Hodgkin's disease), Waldenstrom's macroglobulinemia, heavy chain disease, or multiple myeloma.

[0307] The cancer may include, without limitation, solid tumors such as sarcomas and carcinomas. Examples of solid tumors include, but are not limited to fibrosarcoma, myxosarcoma, liposarcoma, chondrosarcoma, osteogenic sarcoma, chordoma, angiosarcoma, endotheliosarcoma, lymphangiosarcoma, lymphangioendotheliosarcoma, synovioma, mesothelioma, Ewing's tumor, leiomyosarcoma, rhabdomyosarcoma, squamous cell carcinoma, basal cell carcinoma, adenocarcinoma, sweat gland carcinoma, sebaceous gland carcinoma, papillary carcinoma, papillary adenocarcinomas, cystadenocarcinoma, medullary carcinoma, epithelial carcinoma, bronchogenic carcinoma, hepatoma, colorectal cancer (e.g., colon cancer, rectal cancer), anal cancer, pancreatic cancer (e.g., pancreatic adenocarcinoma, islet cell carcinoma, neuroendocrine tumors), breast cancer (e.g., ductal carcinoma, lobular carcinoma, inflammatory breast cancer, clear cell carcinoma, mucinous carcinoma), ovarian carcinoma (e.g., ovarian epithelial carcinoma or surface epithelial-stromal tumour including serous tumour, endometrioid tumor and mucinous cystadenocarcinoma, sex-cord-stromal tumor), prostate cancer, liver and bile duct carcinoma (e.g., hepatocelluar carcinoma, cholangiocarcinoma, hemangioma), choriocarcinoma, seminoma, embryonal carcinoma, kidney cancer (e.g., renal cell carcinoma, clear cell carcinoma, Wilm's tumor, nephroblastoma), cervical cancer, uterine cancer (e.g., endometrial adenocarcinoma, uterine papillary serous carcinoma, uterine clear-cell carcinoma, uterine sarcomas and leiomyosarcomas, mixed mullerian tumors), testicular cancer, germ cell tumor, lung cancer (e.g., lung adenocarcinoma, squamous cell carcinoma, large cell carcinoma, bronchioloalveolar carcinoma, non-small-cell carcinoma, small cell carcinoma,

mesothelioma), bladder carcinoma, signet ring cell carcinoma, cancer of the head and neck (e.g., squamous cell carcinomas), esophageal carcinoma (e.g., esophageal adenocarcinoma), tumors of the brain (e.g., glioma, glioblastoma, medullablastoma, astrocytoma, medulloblastoma, craniopharyngioma, ependymoma, pinealoma, hemangioblastoma, acoustic neuroma, oligodenroglioma, schwannoma, meningioma), neuroblastoma, retinoblastoma, neuroendocrine tumor, melanoma, cancer of the stomach (e.g., stomach adenocarcinoma, gastrointestinal stromal tumor), or carcinoids. Lymphoproliferative disorders are also considered to be proliferative diseases.

AdministrationIt will be appreciated that administration of therapeutic entities in accordance with the invention will be administered with suitable carriers, excipients, and other agents that are incorporated into formulations to provide improved transfer, delivery, tolerance, and the like. A multitude of appropriate formulations can be found in the formulary known to all pharmaceutical chemists: Remington's Pharmaceutical Sciences (15th ed, Mack Publishing Company, Easton, PA (1975)), particularly Chapter 87 by Blaug, Seymour, therein. These formulations include, for example, powders, pastes, ointments, jellies, waxes, oils, lipids, lipid (cationic or anionic) containing vesicles (such as Lipofectin™), DNA conjugates, anhydrous absorption pastes, oil-in-water and water-in-oil emulsions, emulsions carbowax (polyethylene glycols of various molecular weights), semi-solid gels, and semi-solid mixtures containing carbowax. Any of the foregoing mixtures may be appropriate in treatments and therapies in accordance with the present invention, provided that the active ingredient in the formulation is not inactivated by the formulation and the formulation is physiologically compatible and tolerable with the route of administration. *See* also Baldrick P. "Pharmaceutical excipient development: the need for preclinical guidance." Regul. Toxicol Pharmacol. 32(2):210-8 (2000), Wang W. "Lyophilization and development of solid protein pharmaceuticals." Int. J. Pharm. 203(1-2):1-60 (2000), Charman WN "Lipids, lipophilic drugs, and oral drug delivery-some emerging concepts." J Pharm Sci. 89(8):967-78 (2000), Powell *et al.* "Compendium of excipients for parenteral formulations" PDA J Pharm Sci Technol. 52:238-311 (1998) and the citations therein for additional information related to formulations, excipients and carriers well known to pharmaceutical chemists.

[0309] The medicaments of the invention are prepared in a manner known to those skilled in the art, for example, by means of conventional dissolving, lyophilizing, mixing, granulating or confectioning processes. Methods well known in the art for making formulations are found, for example, in Remington: The Science and Practice of Pharmacy,

20th ed., ed. A. R. Gennaro, 2000, Lippincott Williams & Wilkins, Philadelphia, and Encyclopedia of Pharmaceutical Technology, eds. J. Swarbrick and J. C. Boylan, 1988-1999, Marcel Dekker, New York.

[0310] Administration of medicaments of the invention may be by any suitable means that results in a compound concentration that is effective for treating or inhibiting (e.g., by delaying) the development of a disease. The compound is admixed with a suitable carrier substance, e.g., a pharmaceutically acceptable excipient that preserves the therapeutic properties of the compound with which it is administered. One exemplary pharmaceutically acceptable excipient is physiological saline. The suitable carrier substance is generally present in an amount of 1-95% by weight of the total weight of the medicament. The medicament may be provided in a dosage form that is suitable for administration. Thus, the medicament may be in form of, e.g., tablets, capsules, pills, powders, granulates, suspensions, emulsions, solutions, gels including hydrogels, pastes, ointments, creams, plasters, drenches, delivery devices, injectables, implants, sprays, or aerosols.

[0311] The agents disclosed herein (e.g., antibodies) may be used in a pharmaceutical composition when combined with a pharmaceutically acceptable carrier. Such compositions comprise a therapeutically-effective amount of the agent and a pharmaceutically acceptable carrier. Such a composition may also further comprise (in addition to an agent and a carrier) diluents, fillers, salts, buffers, stabilizers, solubilizers, and other materials well known in the art. Compositions comprising the agent can be administered in the form of salts provided the salts are pharmaceutically acceptable. Salts may be prepared using standard procedures known to those skilled in the art of synthetic organic chemistry.

[0312] The term “pharmaceutically acceptable salts” refers to salts prepared from pharmaceutically acceptable non-toxic bases or acids including inorganic or organic bases and inorganic or organic acids. Salts derived from inorganic bases include aluminum, ammonium, calcium, copper, ferric, ferrous, lithium, magnesium, manganic salts, manganous, potassium, sodium, zinc, and the like. Particularly preferred are the ammonium, calcium, magnesium, potassium, and sodium salts. Salts derived from pharmaceutically acceptable organic non-toxic bases include salts of primary, secondary, and tertiary amines, substituted amines including naturally occurring substituted amines, cyclic amines, and basic ion exchange resins, such as arginine, betaine, caffeine, choline, N,N′-dibenzylethylenediamine, diethylamine, 2-diethylaminoethanol, 2-dimethylaminoethanol, ethanolamine, ethylenediamine, N-ethyl-morpholine, N-ethylpiperidine, glucamine,

glucosamine, histidine, hydrabamine, isopropylamine, lysine, methylglucamine, morpholine, piperazine, piperidine, polyamine resins, procaine, purines, theobromine, triethylamine, trimethylamine, tripropylamine, tromethamine, and the like. The term "pharmaceutically acceptable salt" further includes all acceptable salts such as acetate, lactobionate, benzenesulfonate, laurate, benzoate, malate, bicarbonate, maleate, bisulfate, mandelate, bitartrate, mesylate, borate, methylbromide, bromide, methylnitrate, calcium edetate, methylsulfate, camsylate, mucate, carbonate, napsylate, chloride, nitrate, clavulanate, N-methylglucamine, citrate, ammonium salt, dihydrochloride, oleate, edetate, oxalate, edisylate, pamoate (embonate), estolate, palmitate, esylate, pantothenate, fumarate, phosphate/diphosphate, gluceptate, polygalacturonate, gluconate, salicylate, glutamate, stearate, glycollylarsanilate, sulfate, hexylresorcinate, subacetate, hydrabamine, succinate, hydrobromide, tannate, hydrochloride, tartrate, hydroxynaphthoate, teoclate, iodide, tosylate, isothionate, triethiodide, lactate, panoate, valerate, and the like which can be used as a dosage form for modifying the solubility or hydrolysis characteristics or can be used in sustained release or pro-drug formulations. It will be understood that, as used herein, references to specific agents (e.g., neuromedin U receptor agonists or antagonists), also include the pharmaceutically acceptable salts thereof.

[0313] Methods of administrating the pharmacological compositions, including agonists, antagonists, antibodies or fragments thereof, to an individual include, but are not limited to, intradermal, intrathecal, intramuscular, intraperitoneal, intravenous, subcutaneous, intranasal, epidural, by inhalation, and oral routes. The compositions can be administered by any convenient route, for example by infusion or bolus injection, by absorption through epithelial or mucocutaneous linings (for example, oral mucosa, rectal and intestinal mucosa, and the like), ocular, and the like and can be administered together with other biologically-active agents. Administration can be systemic or local. In addition, it may be advantageous to administer the composition into the central nervous system by any suitable route, including intraventricular and intrathecal injection. Pulmonary administration may also be employed by use of an inhaler or nebulizer, and formulation with an aerosolizing agent. It may also be desirable to administer the agent locally to the area in need of treatment; this may be achieved by, for example, and not by way of limitation, local infusion during surgery, topical application, by injection, by means of a catheter, by means of a suppository, or by means of an implant.

[0314] Various delivery systems are known and can be used to administer the pharmacological compositions including, but not limited to, encapsulation in liposomes, microparticles, microcapsules; minicells; polymers; capsules; tablets; and the like. In one embodiment, the agent may be delivered in a vesicle, in particular a liposome. In a liposome, the agent is combined, in addition to other pharmaceutically acceptable carriers, with amphipathic agents such as lipids which exist in aggregated form as micelles, insoluble monolayers, liquid crystals, or lamellar layers in aqueous solution. Suitable lipids for liposomal formulation include, without limitation, monoglycerides, diglycerides, sulfatides, lysolecithin, phospholipids, saponin, bile acids, and the like. Preparation of such liposomal formulations is within the level of skill in the art, as disclosed, for example, in U.S. Pat. No. 4,837,028 and U.S. Pat. No. 4,737,323. In yet another embodiment, the pharmacological compositions can be delivered in a controlled release system including, but not limited to: a delivery pump (See, for example, Saudek, et al., New Engl. J. Med. 321: 574 (1989) and a semi-permeable polymeric material (See, for example, Howard, et al., J. Neurosurg. 71: 105 (1989)). Additionally, the controlled release system can be placed in proximity of the therapeutic target (e.g., a tumor), thus requiring only a fraction of the systemic dose. See, for example, Goodson, In: Medical Applications of Controlled Release, 1984. (CRC Press, Boca Raton, Fla.).

[0315] The amount of the agents which will be effective in the treatment of a particular disorder or condition will depend on the nature of the disorder or condition, and may be determined by standard clinical techniques by those of skill within the art. In addition, *in vitro* assays may optionally be employed to help identify optimal dosage ranges. The precise dose to be employed in the formulation will also depend on the route of administration, and the overall seriousness of the disease or disorder, and should be decided according to the judgment of the practitioner and each patient's circumstances. Ultimately, the attending physician will decide the amount of the agent with which to treat each individual patient. In certain embodiments, the attending physician will administer low doses of the agent and observe the patient's response. Larger doses of the agent may be administered until the optimal therapeutic effect is obtained for the patient, and at that point the dosage is not increased further. In general, the daily dose range of a drug lie within the range known in the art for a particular drug or biologic. Effective doses may be extrapolated from dose-response curves derived from *in vitro* or animal model test systems. Ultimately the attending physician will decide on the appropriate duration of therapy using compositions of the present

invention. Dosage will also vary according to the age, weight and response of the individual patient.

[0316] Methods for administering antibodies for therapeutic use is well known to one skilled in the art. In certain embodiments, small particle aerosols of antibodies or fragments thereof may be administered (see e.g., Piazza et al., J. Infect. Dis., Vol. 166, pp. 1422-1424, 1992; and Brown, Aerosol Science and Technology, Vol. 24, pp. 45-56, 1996). In certain embodiments, antibodies are administered in metered-dose propellant driven aerosols. In certain embodiments, antibodies may be administered in liposomes, i.e., immunoliposomes (see, e.g., Maruyama et al., Biochim. Biophys. Acta, Vol. 1234, pp. 74-80, 1995). In certain embodiments, immunoconjugates, immunoliposomes or immunomicrospheres containing an agent of the present invention is administered by inhalation.

[0317] In certain embodiments, antibodies may be topically administered to mucosa, such as the oropharynx, nasal cavity, respiratory tract, gastrointestinal tract, eye such as the conjunctival mucosa, vagina, urogenital mucosa, or for dermal application. In certain embodiments, antibodies are administered to the nasal, bronchial or pulmonary mucosa. In order to obtain optimal delivery of the antibodies to the pulmonary cavity in particular, it may be advantageous to add a surfactant such as a phosphoglyceride, e.g. phosphatidylcholine, and/or a hydrophilic or hydrophobic complex of a positively or negatively charged excipient and a charged antibody of the opposite charge.

[0318] Other excipients suitable for pharmaceutical compositions intended for delivery of antibodies to the respiratory tract mucosa may be a) carbohydrates, e.g., monosaccharides such as fructose, galactose, glucose. D-mannose, sorbiose, and the like; disaccharides, such as lactose, trehalose, cellobiose, and the like; cyclodextrins, such as 2-hydroxypropyl-β-cyclodextrin; and polysaccharides, such as raffinose, maltodextrins, dextrans, and the like; b) amino acids, such as glycine, arginine, aspartic acid, glutamic acid, cysteine, lysine and the like; c) organic salts prepared from organic acids and bases, such as sodium citrate, sodium ascorbate, magnesium gluconate, sodium gluconate, tromethamine hydrochloride, and the like: d) peptides and proteins, such as aspartame, human serum albumin, gelatin, and the like; e) alditols, such mannitol, xylitol, and the like, and f) polycationic polymers, such as chitosan or a chitosan salt or derivative.

[0319] For dermal application, the antibodies of the present invention may suitably be formulated with one or more of the following excipients: solvents, buffering agents, preservatives, humectants, chelating agents, antioxidants, stabilizers, emulsifying agents,

suspending agents, gel-forming agents, ointment bases, penetration enhancers, and skin protective agents.

[0320] Examples of solvents are e.g. water, alcohols, vegetable or marine oils (e.g. edible oils like almond oil, castor oil, cacao butter, coconut oil, corn oil, cottonseed oil, linseed oil, olive oil, palm oil, peanut oil, poppy seed oil, rapeseed oil, sesame oil, soybean oil, sunflower oil, and tea seed oil), mineral oils, fatty oils, liquid paraffin, polyethylene glycols, propylene glycols, glycerol, liquid polyalkylsiloxanes, and mixtures thereof.

[0321] Examples of buffering agents are e.g. citric acid, acetic acid, tartaric acid, lactic acid, hydrogenphosphoric acid, diethyl amine etc. Suitable examples of preservatives for use in compositions are parabenes, such as methyl, ethyl, propyl p-hydroxybenzoate, butylparaben, isobutylparaben, isopropylparaben, potassium sorbate, sorbic acid, benzoic acid, methyl benzoate, phenoxyethanol, bronopol, bronidox, MDM hydantoin, iodopropynyl butylcarbamate, EDTA, benzalconium chloride, and benzylalcohol, or mixtures of preservatives.

[0322] Examples of humectants are glycerin, propylene glycol, sorbitol, lactic acid, urea, and mixtures thereof.

[0323] Examples of antioxidants are butylated hydroxy anisole (BHA), ascorbic acid and derivatives thereof, tocopherol and derivatives thereof, cysteine, and mixtures thereof.

[0324] Examples of emulsifying agents are naturally occurring gums, e.g. gum acacia or gum tragacanth; naturally occurring phosphatides, e.g. soybean lecithin, sorbitan monooleate derivatives: wool fats; wool alcohols; sorbitan esters; monoglycerides; fatty alcohols; fatty acid esters (e.g. triglycerides of fatty acids); and mixtures thereof.

[0325] Examples of suspending agents are e.g. celluloses and cellulose derivatives such as, e.g., carboxymethyl cellulose, hydroxyethylcellulose, hydroxypropylcellulose, hydroxypropylmethylcellulose, carraghenan, acacia gum, arabic gum, tragacanth, and mixtures thereof.

[0326] Examples of gel bases, viscosity-increasing agents or components which are able to take up exudate from a wound are: liquid paraffin, polyethylene, fatty oils, colloidal silica or aluminum, zinc soaps, glycerol, propylene glycol, tragacanth, carboxyvinyl polymers, magnesium-aluminum silicates, Carbopol®, hydrophilic polymers such as, e.g. starch or cellulose derivatives such as, e.g., carboxymethylcellulose, hydroxyethylcellulose and other cellulose derivatives, water-swellable hydrocolloids, carragenans, hyaluronates (e.g.

hyaluronate gel optionally containing sodium chloride), and alginates including propylene glycol alginate.

[0327] Examples of ointment bases are e.g. beeswax, paraffin, cetanol, cetyl palmitate, vegetable oils, sorbitan esters of fatty acids (Span), polyethylene glycols, and condensation products between sorbitan esters of fatty acids and ethylene oxide, e.g. polyoxyethylene sorbitan monooleate (Tween).

[0328] Examples of hydrophobic or water-emulsifying ointment bases are paraffins, vegetable oils, animal fats, synthetic glycerides, waxes, lanolin, and liquid polyalkylsiloxanes. Examples of hydrophilic ointment bases are solid macrogols (polyethylene glycols). Other examples of ointment bases are triethanolamine soaps, sulphated fatty alcohol and polysorbates.

[0329] Examples of other excipients are polymers such as carmelose, sodium carmelose, hydroxypropylmethylcellulose, hydroxyethylcellulose, hydroxypropylcellulose, pectin, xanthan gum, locust bean gum, acacia gum, gelatin, carbomer, emulsifiers like vitamin E, glyceryl stearates, cetanyl glucoside, collagen, carrageenan, hyaluronates and alginates and chitosans.

[0330] The dose of antibody required in humans to be effective in the treatment of cancer differs with the type and severity of the cancer to be treated, the age and condition of the patient, etc. Typical doses of antibody to be administered are in the range of 1 μg to 1 g, preferably 1-1000 μg, more preferably 2-500, even more preferably 5-50, most preferably 10-20 μg per unit dosage form. In certain embodiments, infusion of antibodies of the present invention may range from 10-500 mg/m^2.

[0331] There are a variety of techniques available for introducing nucleic acids into viable cells. The techniques vary depending upon whether the nucleic acid is transferred into cultured cells *in vitro*, or *in vivo* in the cells of the intended host. Techniques suitable for the transfer of nucleic acid into mammalian cells in vitro include the use of liposomes, electroporation, microinjection, cell fusion, DEAE-dextran, the calcium phosphate precipitation method, etc. The currently preferred *in vivo* gene transfer techniques include transduction with viral (typically lentivirus, adeno associated virus (AAV) and adenovirus) vectors.

[0332] In certain embodiments, an agent that reduces a gene signature as described herein is used to treat a subject in need thereof having a cancer.

[0333] In one embodiment, the agent is a protein kinase C (PKC) activator. By "protein kinase C activator" is meant any compound that increases the catalytic activity of any protein kinase C (PKC) isoform (see, e.g., WO1998017299A1). The preferred catalytic activity that is enhanced is the kinase activity. Protein kinase C ("PKC") is a key enzyme in signal transduction involved in a variety of cellular functions, including cell growth, regulation of gene expression, and ion channel activity. The PKC family of isozymes includes at least 11 different protein kinases that can be divided into at least three subfamilies based on their homology and sensitivity to activators. Each isozyme includes a number of homologous ("conserved" or "C") domains interspersed with isozyme-unique ("variable" or "V") domains. Members of the "classical" or "cPKC" subfamily, α, βι, βM and yPKC, contain four homologous domains (C1 , C2, C3 and C4) and require calcium, phosphatidylserine, and diacylglycerol or phorbol esters for activation. In members of the "novel" or "nPKC" subfamily, δ, ε, η and θ PKC, a C2-like domain preceeds the C1 domain. However, that C2 domain does not bind calcium and therefore the nPKC subfamily does not require calcium for activation. Finally, members of the "atypical" or "αPKC" subfamily, ζ and λ/iPKC, lack both the C2 and one-half of the C1 homologous domains and are insensitive to diacylglycerol, phorbol esters and calcium. Studies on the subcellular distribution of PKC isozymes demonstrate that activation of PKC results in its redistribution in the cells (also termed trans location), such that activated PKC isozymes associate with the plasma membrane, cytoskeletal elements, nuclei, and other subcellular compartments (Saito, N. et al, Proc. Natl. Acad. Sci. USA 86:3409-3413 (1989); Papadopoulos, V. and Hall, P.F. J. Cell Biol. 108:553-567 (1989); Mochly-Rosen, D., et al., Molec. Biol. Cell (formerly Cell Reg.) 1 :693-706, (1990)).

[0334] Mochly-Rosen, D., et al. discusses activation of PKC (Nat Rev Drug Discov. 2012 Dec; 11(12): 937–957). PKC isozymes are activated by a variety of hormones, such as adrenalin and angiotensin, by growth factors, including epidermal growth factor and insulin, and by neurotransmitters such as dopamine and endorphin; these stimulators, when bound to their respective receptors, activate members of the phospholipase C family, which generates diacylglycerol, a lipid-derived second messenger. The novel isozymes (PKC δ, ε, θ and η) are activated by diacylglycerol alone, whereas the four conventional PKC isozymes (PKCα, βI, βII and γ) also require calcium for their activation. Cellular calcium levels are elevated along with diacylglycerol, because the latter is often co-produced with inositol trisphosphate (IP3), which triggers calcium release into the cytosol from internal stores. Activation of PKC can

also occur in the absence of the above second messengers. High levels of cytosolic calcium can directly activate phospholipase C, thus leading to PKC activation in the absence of receptor activation. A number of post-translational modifications of PKC were also found to lead to activation of select PKC isozymes both in normal and disease states. These include activation by proteolysis between the regulatory and the catalytic domain that was noted to occur for PKCδ, for example. Phosphorylation of a number of sites may be required for maturation of the newly synthesized enzyme, but also for activation of mature isozymes, e.g. H2O2-induced tyrosine phosphorylation of PKCδ. Other modifications including oxidation, acetylation and nitration have also been found to activate PKC.

[0335] In one embodiment, the agent is an inhibitor of the NFκB pathway. Inhibitors of the NFκB pathway have been described (see, e.g., Gilmore and Herscovitch, Inhibitors of NF-kappaB signaling: 785 and counting. Oncogene (2006) 25, 6887–6899). These compounds include chemicals, metals, metabolites, synthetic compounds, antioxidants, peptides, small RNA/DNA, microbial and viral proteins, small molecules, and engineered dominant-negative or constitutively active polypeptides.

[0336] In one embodiment, the agent is an IGF1R inhibitor. IGF1R inhibitors are well known in the art (see, e.g., King et al., Can we unlock the potential of IGF-1R inhibition in cancer therapy? Cancer Treat Rev. 2014 Oct; 40(9): 1096–1105). IGF1R inhibitors may include, but are not limited to monoclonal anti-IGF1R antibodies, small molecule tyrosine kinase inhibitors (TKIs), and IGF ligand antibodies.

[0337] In one embodiment, the agent is Reserpine (methyl 18β-hydroxy-11,17 α-dimethoxy-3β, 20α-yohimban-16β-carboxylate 3,4,5-trimethoxybenzoate) or derivative thereof. Reserpine is an alkaloid first isolated from *Rauwolfia serpentina*. Reserpine (also known by trade names Raudixin, Serpalan, Serpasil) is an indole alkaloid, antipsychotic, and antihypertensive drug that has been used for the control of high blood pressure and for the relief of psychotic symptoms, although because of the development of better drugs for these purposes and because of its numerous side-effects, it is rarely used today. The antihypertensive actions of reserpine are a result of its ability to deplete catecholamines (among other monoamine neurotransmitters) from peripheral sympathetic nerve endings. These substances are normally involved in controlling heart rate, force of cardiac contraction and peripheral vascular resistance. The daily dose of reserpine in antihypertensive treatment is as low as 0.1 to 0.25 mg. In certain embodiments, the dose is significantly higher for the treatment of cancer. A skilled practitioner would know to adjust the dose based on response

to the drug. For example, reduction of an immunotherapy resistance signature or decrease in tumor size and/or proliferation. In certain embodiments, Reserpine is administered directly to a tumor. In certain embodiments, reserpine is administered over the course of a single day or week or month.

[0338] Typical of the known rauwolfia alkaloids are deserpidine, alperaxylon, reserpine, and rauwolfia serpentina. Oral dosage of the rauwolfia alkaloid should be carefully adjusted according to individual tolerance and response, using the lowest possible effective dosage. Typically, the amount of rauwolfia alkaloid administered daily is from about 0.001 to about 0.01 mg per kg of body weight.

[0339] In certain embodiments, the agent capable of modulating a signature as described herein is a cell cycle inhibitor (see e.g., Dickson and Schwartz, Development of cell-cycle inhibitors for cancer therapy, Curr Oncol. 2009 Mar; 16(2): 36–43). In one embodiment, the agent capable of modulating a signature as described herein is a CDK4/6 inhibitor, such as LEE011, palbociclib (PD-0332991), and Abemaciclib (LY2835219) (see, e.g., US9259399B2; WO2016025650A1; US Patent Publication No. 20140031325; US Patent Publication No. 20140080838; US Patent Publication No. 20130303543; US Patent Publication No. 2007/0027147; US Patent Publication No. 2003/0229026; US Patent Publication No 2004/0048915; US Patent Publication No. 2004/0006074; US Patent Publication No. 2007/0179118; each of which is incorporated by reference herein in its entirety). Currently there are three CDK4/6 inhibitors that are either approved or in late-stage development: palbociclib (PD-0332991; Pfizer), ribociclib (LEE011; Novartis), and abemaciclib (LY2835219; Lilly) (see e.g., Hamilton and Infante, Targeting CDK4/6 in patients with cancer, Cancer Treatment Reviews, Volume 45, April 2016, Pages 129-138).

[0340] In certain embodiments, an agent that reduces an immunotherapy resistance signature is co-administered with an immunotherapy or is administered before or after administration of an immunotherapy. In certain embodiments, a subject in need thereof is treated with a phased combination therapy. The phased combination therapy may be a treatment regimen comprising checkpoint inhibition followed by a CDK4/6 inhibitor and checkpoint inhibitor combination. Checkpoint inhibitors may be administered every two weeks. The combination therapy may be administered when an immunotherapy resistance signature is detected. This may be after two weeks to six months after the initial checkpoint inhibition. The immunotherapy may be adoptive cell transfer therapy, as described herein or may be an inhibitor of any check point protein described herein. The checkpoint blockade

therapy may comprise anti-TIM3, anti-CTLA4, anti-PD-L1, anti-PD1, anti-TIGIT, anti-LAG3, or combinations thereof. Specific check point inhibitors include, but are not limited to anti-CTLA4 antibodies (e.g., Ipilimumab), anti-PD-1 antibodies (e.g., Nivolumab, Pembrolizumab), and anti-PD-L1 antibodies (e.g., Atezolizumab). Dosages for the immunotherapy and/or CDK4/6 inhibitors may be determined according to the standard of care for each therapy and may be incorporated into the standard of care (see, e.g., Rivalland et al., Standard of care in immunotherapy trials: Challenges and considerations, Hum Vaccin Immunother. 2017 Jul; 13(9): 2164–2178; and Pernas et al., CDK4/6 inhibition in breast cancer: current practice and future directions, Ther Adv Med Oncol. 2018). The standard of care is the current treatment that is accepted by medical experts as a proper treatment for a certain type of disease and that is widely used by healthcare professionals. Standard or care is also called best practice, standard medical care, and standard therapy.

[0341] In another aspect, provided is a pharmaceutical pack or kit, comprising one or more containers filled with one or more of the ingredients of the pharmaceutical compositions.

[0342] In another aspect, provided is a kit for detecting the gene signature as described herein.

[0343] With respect to general information on CRISPR-Cas Systems, components thereof, and delivery of such components, including methods, materials, delivery vehicles, vectors, particles, AAV, and making and using thereof, including as to amounts and formulations, all useful in the practice of the instant invention, reference is made to: US Patents Nos. 8,999,641, 8,993,233, 8,945,839, 8,932,814, 8,906,616, 8,895,308, 8,889,418, 8,889,356, 8,871,445, 8,865,406, 8,795,965, 8,771,945 and 8,697,359; US Patent Publications US 2014-0310830 (US APP. Ser. No. 14/105,031), US 2014-0287938 A1 (U.S. App. Ser. No. 14/213,991), US 2014-0273234 A1 (U.S. App. Ser. No. 14/293,674), US2014-0273232 A1 (U.S. App. Ser. No. 14/290,575), US 2014-0273231 (U.S. App. Ser. No. 14/259,420), US 2014-0256046 A1 (U.S. App. Ser. No. 14/226,274), US 2014-0248702 A1 (U.S. App. Ser. No. 14/258,458), US 2014-0242700 A1 (U.S. App. Ser. No. 14/222,930), US 2014-0242699 A1 (U.S. App. Ser. No. 14/183,512), US 2014-0242664 A1 (U.S. App. Ser. No. 14/104,990), US 2014-0234972 A1 (U.S. App. Ser. No. 14/183,471), US 2014-0227787 A1 (U.S. App. Ser. No. 14/256,912), US 2014-0189896 A1 (U.S. App. Ser. No. 14/105,035), US 2014-0186958 (U.S. App. Ser. No. 14/105,017), US 2014-0186919 A1 (U.S. App. Ser. No. 14/104,977), US 2014-0186843 A1 (U.S. App. Ser. No. 14/104,900), US 2014-0179770

A1 (U.S. App. Ser. No. 14/104,837) and US 2014-0179006 A1 (U.S. App. Ser. No. 14/183,486), US 2014-0170753 (US App Ser No 14/183,429); European Patents EP 2 784 162 B1 and EP 2 771 468 B1; European Patent Applications EP 2 771 468 (EP13818570.7), EP 2 764 103 (EP13824232.6), and EP 2 784 162 (EP14170383.5); and PCT Patent Publications PCT Patent Publications WO 2014/093661 (PCT/US2013/074743), WO 2014/093694 (PCT/US2013/074790), WO 2014/093595 (PCT/US2013/074611), WO 2014/093718 (PCT/US2013/074825), WO 2014/093709 (PCT/US2013/074812), WO 2014/093622 (PCT/US2013/074667), WO 2014/093635 (PCT/US2013/074691), WO 2014/093655 (PCT/US2013/074736), WO 2014/093712 (PCT/US2013/074819), WO2014/093701 (PCT/US2013/074800), WO2014/018423 (PCT/US2013/051418), WO 2014/204723 (PCT/US2014/041790), WO 2014/204724 (PCT/US2014/041800), WO 2014/204725 (PCT/US2014/041803), WO 2014/204726 (PCT/US2014/041804), WO 2014/204727 (PCT/US2014/041806), WO 2014/204728 (PCT/US2014/041808), WO 2014/204729 (PCT/US2014/041809). Reference is also made to US provisional patent applications 61/758,468; 61/802,174; 61/806,375; 61/814,263; 61/819,803 and 61/828,130, filed on January 30, 2013; March 15, 2013; March 28, 2013; April 20, 2013; May 6, 2013 and May 28, 2013 respectively. Reference is also made to US provisional patent application 61/836,123, filed on June 17, 2013. Reference is additionally made to US provisional patent applications 61/835,931, 61/835,936, 61/836,127, 61/836, 101, 61/836,080 and 61/835,973, each filed June 17, 2013. Further reference is made to US provisional patent applications 61/862,468 and 61/862,355 filed on August 5, 2013; 61/871,301 filed on August 28, 2013; 61/960,777 filed on September 25, 2013 and 61/961,980 filed on October 28, 2013. Reference is yet further made to: PCT Patent applications Nos: PCT/US2014/041803, PCT/US2014/041800, PCT/US2014/041809, PCT/US2014/041804 and PCT/US2014/041806, each filed June 10, 2014 6/10/14; PCT/US2014/041808 filed June 11, 2014; and PCT/US2014/62558 filed October 28, 2014, and US Provisional Patent Applications Serial Nos.: 61/915,150, 61/915,301, 61/915,267 and 61/915,260, each filed December 12, 2013; 61/757,972 and 61/768,959, filed on January 29, 2013 and February 25, 2013; 61/835,936, 61/836,127, 61/836,101, 61/836,080, 61/835,973, and 61/835,931, filed June 17, 2013; 62/010,888 and 62/010,879, both filed June 11, 2014; 62/010,329 and 62/010,441, each filed June 10, 2014; 61/939,228 and 61/939,242, each filed February 12, 2014; 61/980,012, filed April 15,2014; 62/038,358, filed August 17, 2014; 62/054,490, 62/055,484, 62/055,460 and 62/055,487, each filed September 25, 2014; and 62/069,243,

filed October 27, 2014. Reference is also made to US provisional patent applications Nos. 62/055,484, 62/055,460, and 62/055,487, filed September 25, 2014; US provisional patent application 61/980,012, filed April 15, 2014; and US provisional patent application 61/939,242 filed February 12, 2014. Reference is made to PCT application designating, inter alia, the United States, application No. PCT/US14/41806, filed June 10, 2014. Reference is made to US provisional patent application 61/930,214 filed on January 22, 2014. Reference is made to US provisional patent applications 61/915,251; 61/915,260 and 61/915,267, each filed on December 12, 2013. Reference is made to US provisional patent application USSN 61/980,012 filed April 15, 2014. Reference is made to PCT application designating, inter alia, the United States, application No. PCT/US14/41806, filed June 10, 2014. Reference is made to US provisional patent application 61/930,214 filed on January 22, 2014. Reference is made to US provisional patent applications 61/915,251; 61/915,260 and 61/915,267, each filed on December 12, 2013.

[0344] Mention is also made of US application 62/091,455, filed, 12-Dec-14, PROTECTED GUIDE RNAS (PGRNAS); US application 62/096,708, 24-Dec-14, PROTECTED GUIDE RNAS (PGRNAS); US application 62/091,462, 12-Dec-14, DEAD GUIDES FOR CRISPR TRANSCRIPTION FACTORS; US application 62/096,324, 23-Dec-14, DEAD GUIDES FOR CRISPR TRANSCRIPTION FACTORS; US application 62/091,456, 12-Dec-14, ESCORTED AND FUNCTIONALIZED GUIDES FOR CRISPR-CAS SYSTEMS; US application 62/091,461, 12-Dec-14, DELIVERY, USE AND THERAPEUTIC APPLICATIONS OF THE CRISPR-CAS SYSTEMS AND COMPOSITIONS FOR GENOME EDITING AS TO HEMATOPOETIC STEM CELLS (HSCs); US application 62/094,903, 19-Dec-14, UNBIASED IDENTIFICATION OF DOUBLE-STRAND BREAKS AND GENOMIC REARRANGEMENT BY GENOME-WISE INSERT CAPTURE SEQUENCING; US application 62/096,761, 24-Dec-14, ENGINEERING OF SYSTEMS, METHODS AND OPTIMIZED ENZYME AND GUIDE SCAFFOLDS FOR SEQUENCE MANIPULATION; US application 62/098,059, 30-Dec-14, RNA-TARGETING SYSTEM; US application 62/096,656, 24-Dec-14, CRISPR HAVING OR ASSOCIATED WITH DESTABILIZATION DOMAINS; US application 62/096,697, 24-Dec-14, CRISPR HAVING OR ASSOCIATED WITH AAV; US application 62/098,158, 30-Dec-14, ENGINEERED CRISPR COMPLEX INSERTIONAL TARGETING SYSTEMS; US application 62/151,052, 22-Apr-15, CELLULAR TARGETING FOR EXTRACELLULAR EXOSOMAL REPORTING; US application 62/054,490, 24-Sep-14,

DELIVERY, USE AND THERAPEUTIC APPLICATIONS OF THE CRISPR-CAS SYSTEMS AND COMPOSITIONS FOR TARGETING DISORDERS AND DISEASES USING PARTICLE DELIVERY COMPONENTS; US application 62/055,484, 25-Sep-14, SYSTEMS, METHODS AND COMPOSITIONS FOR SEQUENCE MANIPULATION WITH OPTIMIZED FUNCTIONAL CRISPR-CAS SYSTEMS; US application 62/087,537, 4-Dec-14, SYSTEMS, METHODS AND COMPOSITIONS FOR SEQUENCE MANIPULATION WITH OPTIMIZED FUNCTIONAL CRISPR-CAS SYSTEMS; US application 62/054,651, 24-Sep-14, DELIVERY, USE AND THERAPEUTIC APPLICATIONS OF THE CRISPR-CAS SYSTEMS AND COMPOSITIONS FOR MODELING COMPETITION OF MULTIPLE CANCER MUTATIONS *IN VIVO*; US application 62/067,886, 23-Oct-14, DELIVERY, USE AND THERAPEUTIC APPLICATIONS OF THE CRISPR-CAS SYSTEMS AND COMPOSITIONS FOR MODELING COMPETITION OF MULTIPLE CANCER MUTATIONS *IN VIVO*; US application 62/054,675, 24-Sep-14, DELIVERY, USE AND THERAPEUTIC APPLICATIONS OF THE CRISPR-CAS SYSTEMS AND COMPOSITIONS IN NEURONAL CELLS/TISSUES; US application 62/054,528, 24-Sep-14, DELIVERY, USE AND THERAPEUTIC APPLICATIONS OF THE CRISPR-CAS SYSTEMS AND COMPOSITIONS IN IMMUNE DISEASES OR DISORDERS; US application 62/055,454, 25-Sep-14, DELIVERY, USE AND THERAPEUTIC APPLICATIONS OF THE CRISPR-CAS SYSTEMS AND COMPOSITIONS FOR TARGETING DISORDERS AND DISEASES USING CELL PENETRATION PEPTIDES (CPP); US application 62/055,460, 25-Sep-14, MULTIFUNCTIONAL-CRISPR COMPLEXES AND/OR OPTIMIZED ENZYME LINKED FUNCTIONAL-CRISPR COMPLEXES; US application 62/087,475, 4-Dec-14, FUNCTIONAL SCREENING WITH OPTIMIZED FUNCTIONAL CRISPR-CAS SYSTEMS; US application 62/055,487, 25-Sep-14, FUNCTIONAL SCREENING WITH OPTIMIZED FUNCTIONAL CRISPR-CAS SYSTEMS; US application 62/087,546, 4-Dec-14, MULTIFUNCTIONAL CRISPR COMPLEXES AND/OR OPTIMIZED ENZYME LINKED FUNCTIONAL-CRISPR COMPLEXES; and US application 62/098,285, 30-Dec-14, CRISPR MEDIATED *IN VIVO* MODELING AND GENETIC SCREENING OF TUMOR GROWTH AND METASTASIS.

[0345] Each of these patents, patent publications, and applications, and all documents cited therein or during their prosecution ("appln cited documents") and all documents cited or referenced in the appln cited documents, together with any instructions, descriptions, product

specifications, and product sheets for any products mentioned therein or in any document therein and incorporated by reference herein, are hereby incorporated herein by reference, and may be employed in the practice of the invention. All documents (e.g., these patents, patent publications and applications and the appln cited documents) are incorporated herein by reference to the same extent as if each individual document was specifically and individually indicated to be incorporated by reference.

[0346] Also with respect to general information on CRISPR-Cas Systems, mention is made of the following (also hereby incorporated herein by reference):

- Multiplex genome engineering using CRISPR/Cas systems. Cong, L., Ran, F.A., Cox, D., Lin, S., Barretto, R., Habib, N., Hsu, P.D., Wu, X., Jiang, W., Marraffini, L.A., & Zhang, F. Science Feb 15;339(6121):819-23 (2013);
- RNA-guided editing of bacterial genomes using CRISPR-Cas systems. Jiang W., Bikard D., Cox D., Zhang F, Marraffini LA. Nat Biotechnol Mar;31(3):233-9 (2013);
- One-Step Generation of Mice Carrying Mutations in Multiple Genes by CRISPR/Cas-Mediated Genome Engineering. Wang H., Yang H., Shivalila CS., Dawlaty MM., Cheng AW., Zhang F., Jaenisch R. Cell May 9;153(4):910-8 (2013);
- Optical control of mammalian endogenous transcription and epigenetic states. Konermann S, Brigham MD, Trevino AE, Hsu PD, Heidenreich M, Cong L, Platt RJ, Scott DA, Church GM, Zhang F. Nature. Aug 22;500(7463):472-6. doi: 10.1038/Nature12466. Epub 2013 Aug 23 (2013);
- Double Nicking by RNA-Guided CRISPR Cas9 for Enhanced Genome Editing Specificity. Ran, FA., Hsu, PD., Lin, CY., Gootenberg, JS., Konermann, S., Trevino, AE., Scott, DA., Inoue, A., Matoba, S., Zhang, Y., & Zhang, F. Cell Aug 28. pii: S0092-8674(13)01015-5 (2013-A);
- DNA targeting specificity of RNA-guided Cas9 nucleases. Hsu, P., Scott, D., Weinstein, J., Ran, FA., Konermann, S., Agarwala, V., Li, Y., Fine, E., Wu, X., Shalem, O., Cradick, TJ., Marraffini, LA., Bao, G., & Zhang, F. Nat Biotechnol doi:10.1038/nbt.2647 (2013);
- Genome engineering using the CRISPR-Cas9 system. Ran, FA., Hsu, PD., Wright, J., Agarwala, V., Scott, DA., Zhang, F. Nature Protocols Nov;8(11):2281-308 (2013-B);

- Genome-Scale CRISPR-Cas9 Knockout Screening in Human Cells. Shalem, O., Sanjana, NE., Hartenian, E., Shi, X., Scott, DA., Mikkelson, T., Heckl, D., Ebert, BL., Root, DE., Doench, JG., Zhang, F. Science Dec 12. (2013). [Epub ahead of print];
- Crystal structure of cas9 in complex with guide RNA and target DNA. Nishimasu, H., Ran, FA., Hsu, PD., Konermann, S., Shehata, SI., Dohmae, N., Ishitani, R., Zhang, F., Nureki, O. Cell Feb 27, 156(5):935-49 (2014);
- Genome-wide binding of the CRISPR endonuclease Cas9 in mammalian cells. Wu X., Scott DA., Kriz AJ., Chiu AC., Hsu PD., Dadon DB., Cheng AW., Trevino AE., Konermann S., Chen S., Jaenisch R., Zhang F., Sharp PA. Nat Biotechnol. Apr 20. doi: 10.1038/nbt.2889 (2014);
- CRISPR-Cas9 Knockin Mice for Genome Editing and Cancer Modeling. Platt RJ, Chen S, Zhou Y, Yim MJ, Swiech L, Kempton HR, Dahlman JE, Parnas O, Eisenhaure TM, Jovanovic M, Graham DB, Jhunjhunwala S, Heidenreich M, Xavier RJ, Langer R, Anderson DG, Hacohen N, Regev A, Feng G, Sharp PA, Zhang F. Cell 159(2): 440-455 DOI: 10.1016/j.cell.2014.09.014(2014);
- Development and Applications of CRISPR-Cas9 for Genome Engineering, Hsu PD, Lander ES, Zhang F., Cell. Jun 5;157(6):1262-78 (2014).
- Genetic screens in human cells using the CRISPR/Cas9 system, Wang T, Wei JJ, Sabatini DM, Lander ES., Science. January 3; 343(6166): 80-84. doi:10.1126/science.1246981 (2014);
- Rational design of highly active sgRNAs for CRISPR-Cas9-mediated gene inactivation, Doench JG, Hartenian E, Graham DB, Tothova Z, Hegde M, Smith I, Sullender M, Ebert BL, Xavier RJ, Root DE., (published online 3 September 2014) Nat Biotechnol. Dec;32(12):1262-7 (2014);
- *In vivo* interrogation of gene function in the mammalian brain using CRISPR-Cas9, Swiech L, Heidenreich M, Banerjee A, Habib N, Li Y, Trombetta J, Sur M, Zhang F., (published online 19 October 2014) Nat Biotechnol. Jan;33(1):102-6 (2015);
- Genome-scale transcriptional activation by an engineered CRISPR-Cas9 complex, Konermann S, Brigham MD, Trevino AE, Joung J, Abudayyeh OO, Barcena C, Hsu PD, Habib N, Gootenberg JS, Nishimasu H, Nureki O, Zhang F., Nature. Jan 29;517(7536):583-8 (2015).

- A split-Cas9 architecture for inducible genome editing and transcription modulation, Zetsche B, Volz SE, Zhang F., (published online 02 February 2015) Nat Biotechnol. Feb;33(2):139-42 (2015);
- Genome-wide CRISPR Screen in a Mouse Model of Tumor Growth and Metastasis, Chen S, Sanjana NE, Zheng K, Shalem O, Lee K, Shi X, Scott DA, Song J, Pan JQ, Weissleder R, Lee H, Zhang F, Sharp PA. Cell 160, 1246-1260, March 12, 2015 (multiplex screen in mouse), and
- *In vivo* genome editing using Staphylococcus aureus Cas9, Ran FA, Cong L, Yan WX, Scott DA, Gootenberg JS, Kriz AJ, Zetsche B, Shalem O, Wu X, Makarova KS, Koonin EV, Sharp PA, Zhang F., (published online 01 April 2015), Nature. Apr 9;520(7546):186-91 (2015).
- Shalem et al., "High-throughput functional genomics using CRISPR-Cas9," Nature Reviews Genetics 16, 299-311 (May 2015).
- Xu et al., "Sequence determinants of improved CRISPR sgRNA design," Genome Research 25, 1147-1157 (August 2015).
- Parnas et al., "A Genome-wide CRISPR Screen in Primary Immune Cells to Dissect Regulatory Networks," Cell 162, 675-686 (July 30, 2015).
- Ramanan et al., CRISPR/Cas9 cleavage of viral DNA efficiently suppresses hepatitis B virus," Scientific Reports 5:10833. doi: 10.1038/srep10833 (June 2, 2015)
- Nishimasu et al., Crystal Structure of Staphylococcus aureus Cas9," Cell 162, 1113-1126 (Aug. 27, 2015)
- BCL11A enhancer dissection by Cas9-mediated in situ saturating mutagenesis, Canver et al., Nature 527(7577):192-7 (Nov. 12, 2015) doi: 10.1038/nature15521. Epub 2015 Sep 16.
- *Cpf1 Is a Single RNA-Guided Endonuclease of a Class 2 CRISPR-Cas System*, Zetsche et al., Cell 163, 759-71 (Sep 25, 2015).
- *Discovery and Functional Characterization of Diverse Class 2 CRISPR-Cas Systems*, Shmakov et al., Molecular Cell, 60(3), 385–397 doi: 10.1016/j.molcel.2015.10.008 Epub October 22, 2015.
- *Rationally engineered Cas9 nucleases with improved specificity*, Slaymaker et al., Science 2016 Jan 1 351(6268): 84-88 doi: 10.1126/science.aad5227. Epub 2015 Dec 1.

- Gao *et al*, "Engineered Cpf1 Enzymes with Altered PAM Specificities," bioRxiv 091611; doi: http://dx.doi.org/10.1101/091611 (Dec. 4, 2016).

each of which is incorporated herein by reference, may be considered in the practice of the instant invention, and discussed briefly below:

- Cong et al. engineered type II CRISPR-Cas systems for use in eukaryotic cells based on both Streptococcus thermophilus Cas9 and also Streptococcus pyogenes Cas9 and demonstrated that Cas9 nucleases can be directed by short RNAs to induce precise cleavage of DNA in human and mouse cells. Their study further showed that Cas9 as converted into a nicking enzyme can be used to facilitate homology-directed repair in eukaryotic cells with minimal mutagenic activity. Additionally, their study demonstrated that multiple guide sequences can be encoded into a single CRISPR array to enable simultaneous editing of several at endogenous genomic loci sites within the mammalian genome, demonstrating easy programmability and wide applicability of the RNA-guided nuclease technology. This ability to use RNA to program sequence specific DNA cleavage in cells defined a new class of genome engineering tools. These studies further showed that other CRISPR loci are likely to be transplantable into mammalian cells and can also mediate mammalian genome cleavage. Importantly, it can be envisaged that several aspects of the CRISPR-Cas system can be further improved to increase its efficiency and versatility.
- Jiang et al. used the clustered, regularly interspaced, short palindromic repeats (CRISPR)-associated Cas9 endonuclease complexed with dual-RNAs to introduce precise mutations in the genomes of Streptococcus pneumoniae and Escherichia coli. The approach relied on dual-RNA:Cas9-directed cleavage at the targeted genomic site to kill unmutated cells and circumvents the need for selectable markers or counter-selection systems. The study reported reprogramming dual-RNA:Cas9 specificity by changing the sequence of short CRISPR RNA (crRNA) to make single- and multinucleotide changes carried on editing templates. The study showed that simultaneous use of two crRNAs enabled multiplex mutagenesis. Furthermore, when the approach was used in combination with recombineering, in S. pneumoniae, nearly 100% of cells that were recovered using the described approach contained the desired mutation, and in E. coli, 65% that were recovered contained the mutation.

- Wang et al. (2013) used the CRISPR/Cas system for the one-step generation of mice carrying mutations in multiple genes which were traditionally generated in multiple steps by sequential recombination in embryonic stem cells and/or time-consuming intercrossing of mice with a single mutation. The CRISPR/Cas system will greatly accelerate the *in vivo* study of functionally redundant genes and of epistatic gene interactions.
- Konermann et al. (2013) addressed the need in the art for versatile and robust technologies that enable optical and chemical modulation of DNA-binding domains based CRISPR Cas9 enzyme and also Transcriptional Activator Like Effectors
- Ran et al. (2013-A) described an approach that combined a Cas9 nickase mutant with paired guide RNAs to introduce targeted double-strand breaks. This addresses the issue of the Cas9 nuclease from the microbial CRISPR-Cas system being targeted to specific genomic loci by a guide sequence, which can tolerate certain mismatches to the DNA target and thereby promote undesired off-target mutagenesis. Because individual nicks in the genome are repaired with high fidelity, simultaneous nicking via appropriately offset guide RNAs is required for double-stranded breaks and extends the number of specifically recognized bases for target cleavage. The authors demonstrated that using paired nicking can reduce off-target activity by 50- to 1,500-fold in cell lines and to facilitate gene knockout in mouse zygotes without sacrificing on-target cleavage efficiency. This versatile strategy enables a wide variety of genome editing applications that require high specificity.
- Hsu et al. (2013) characterized SpCas9 targeting specificity in human cells to inform the selection of target sites and avoid off-target effects. The study evaluated >700 guide RNA variants and SpCas9-induced indel mutation levels at >100 predicted genomic off-target loci in 293T and 293FT cells. The authors that SpCas9 tolerates mismatches between guide RNA and target DNA at different positions in a sequence-dependent manner, sensitive to the number, position and distribution of mismatches. The authors further showed that SpCas9-mediated cleavage is unaffected by DNA methylation and that the dosage of SpCas9 and sgRNA can be titrated to minimize off-target modification. Additionally, to facilitate mammalian genome engineering applications, the authors reported

providing a web-based software tool to guide the selection and validation of target sequences as well as off-target analyses.

- Ran et al. (2013-B) described a set of tools for Cas9-mediated genome editing via non-homologous end joining (NHEJ) or homology-directed repair (HDR) in mammalian cells, as well as generation of modified cell lines for downstream functional studies. To minimize off-target cleavage, the authors further described a double-nicking strategy using the Cas9 nickase mutant with paired guide RNAs. The protocol provided by the authors experimentally derived guidelines for the selection of target sites, evaluation of cleavage efficiency and analysis of off-target activity. The studies showed that beginning with target design, gene modifications can be achieved within as little as 1-2 weeks, and modified clonal cell lines can be derived within 2-3 weeks.
- Shalem et al. described a new way to interrogate gene function on a genome-wide scale. Their studies showed that delivery of a genome-scale CRISPR-Cas9 knockout (GeCKO) library targeted 18,080 genes with 64,751 unique guide sequences enabled both negative and positive selection screening in human cells. First, the authors showed use of the GeCKO library to identify genes essential for cell viability in cancer and pluripotent stem cells. Next, in a melanoma model, the authors screened for genes whose loss is involved in resistance to vemurafenib, a therapeutic that inhibits mutant protein kinase BRAF. Their studies showed that the highest-ranking candidates included previously validated genes NF1 and MED12 as well as novel hits NF2, CUL3, TADA2B, and TADA1. The authors observed a high level of consistency between independent guide RNAs targeting the same gene and a high rate of hit confirmation, and thus demonstrated the promise of genome-scale screening with Cas9.
- Nishimasu et al. reported the crystal structure of Streptococcus pyogenes Cas9 in complex with sgRNA and its target DNA at 2.5 A° resolution. The structure revealed a bilobed architecture composed of target recognition and nuclease lobes, accommodating the sgRNA:DNA heteroduplex in a positively charged groove at their interface. Whereas the recognition lobe is essential for binding sgRNA and DNA, the nuclease lobe contains the HNH and RuvC nuclease domains, which are properly positioned for cleavage of the complementary and non-complementary strands of the target DNA, respectively. The nuclease lobe also contains a

carboxyl-terminal domain responsible for the interaction with the protospacer adjacent motif (PAM). This high-resolution structure and accompanying functional analyses have revealed the molecular mechanism of RNA-guided DNA targeting by Cas9, thus paving the way for the rational design of new, versatile genome-editing technologies.

- Wu et al. mapped genome-wide binding sites of a catalytically inactive Cas9 (dCas9) from Streptococcus pyogenes loaded with single guide RNAs (sgRNAs) in mouse embryonic stem cells (mESCs). The authors showed that each of the four sgRNAs tested targets dCas9 to between tens and thousands of genomic sites, frequently characterized by a 5-nucleotide seed region in the sgRNA and an NGG protospacer adjacent motif (PAM). Chromatin inaccessibility decreases dCas9 binding to other sites with matching seed sequences; thus 70% of off-target sites are associated with genes. The authors showed that targeted sequencing of 295 dCas9 binding sites in mESCs transfected with catalytically active Cas9 identified only one site mutated above background levels. The authors proposed a two-state model for Cas9 binding and cleavage, in which a seed match triggers binding but extensive pairing with target DNA is required for cleavage.
- Platt et al. established a Cre-dependent Cas9 knockin mouse. The authors demonstrated *in vivo* as well as ex vivo genome editing using adeno-associated virus (AAV)-, lentivirus-, or particle-mediated delivery of guide RNA in neurons, immune cells, and endothelial cells.
- Hsu et al. (2014) is a review article that discusses generally CRISPR-Cas9 history from yogurt to genome editing, including genetic screening of cells.
- Wang et al. (2014) relates to a pooled, loss-of-function genetic screening approach suitable for both positive and negative selection that uses a genome-scale lentiviral single guide RNA (sgRNA) library.
- Doench et al. created a pool of sgRNAs, tiling across all possible target sites of a panel of six endogenous mouse and three endogenous human genes and quantitatively assessed their ability to produce null alleles of their target gene by antibody staining and flow cytometry. The authors showed that optimization of the PAM improved activity and also provided an on-line tool for designing sgRNAs.

- Swiech et al. demonstrate that AAV-mediated SpCas9 genome editing can enable reverse genetic studies of gene function in the brain.
- Konermann et al. (2015) discusses the ability to attach multiple effector domains, e.g., transcriptional activator, functional and epigenomic regulators at appropriate positions on the guide such as stem or tetraloop with and without linkers.
- Zetsche et al. demonstrates that the Cas9 enzyme can be split into two and hence the assembly of Cas9 for activation can be controlled.
- Chen et al. relates to multiplex screening by demonstrating that a genome-wide *in vivo* CRISPR-Cas9 screen in mice reveals genes regulating lung metastasis.
- Ran et al. (2015) relates to SaCas9 and its ability to edit genomes and demonstrates that one cannot extrapolate from biochemical assays.
- Shalem et al. (2015) described ways in which catalytically inactive Cas9 (dCas9) fusions are used to synthetically repress (CRISPRi) or activate (CRISPRa) expression, showing. advances using Cas9 for genome-scale screens, including arrayed and pooled screens, knockout approaches that inactivate genomic loci and strategies that modulate transcriptional activity.
- Xu et al. (2015) assessed the DNA sequence features that contribute to single guide RNA (sgRNA) efficiency in CRISPR-based screens. The authors explored efficiency of CRISPR/Cas9 knockout and nucleotide preference at the cleavage site. The authors also found that the sequence preference for CRISPRi/a is substantially different from that for CRISPR/Cas9 knockout.
- Parnas et al. (2015) introduced genome-wide pooled CRISPR-Cas9 libraries into dendritic cells (DCs) to identify genes that control the induction of tumor necrosis factor (Tnf) by bacterial lipopolysaccharide (LPS). Known regulators of Tlr4 signaling and previously unknown candidates were identified and classified into three functional modules with distinct effects on the canonical responses to LPS.
- Ramanan et al (2015) demonstrated cleavage of viral episomal DNA (cccDNA) in infected cells. The HBV genome exists in the nuclei of infected hepatocytes as a 3.2kb double-stranded episomal DNA species called covalently closed circular DNA (cccDNA), which is a key component in the HBV life cycle whose replication is not inhibited by current therapies. The authors showed that sgRNAs specifically targeting highly conserved regions of HBV robustly suppresses viral replication and depleted cccDNA.

- Nishimasu et al. (2015) reported the crystal structures of SaCas9 in complex with a single guide RNA (sgRNA) and its double-stranded DNA targets, containing the 5'-TTGAAT-3' PAM and the 5'-TTGGGT-3' PAM. A structural comparison of SaCas9 with SpCas9 highlighted both structural conservation and divergence, explaining their distinct PAM specificities and orthologous sgRNA recognition.
- Canver *et al.* (2015) demonstrated a CRISPR-Cas9-based functional investigation of non-coding genomic elements. The authors developed pooled CRISPR-Cas9 guide RNA libraries to perform *in situ* saturating mutagenesis of the human and mouse BCL11A enhancers which revealed critical features of the enhancers.
- Zetsche et al. (2015) reported characterization of Cpf1, a class 2 CRISPR nuclease from Francisella novicida U112 having features distinct from Cas9. Cpf1 is a single RNA-guided endonuclease lacking tracrRNA, utilizes a T-rich protospacer-adjacent motif, and cleaves DNA via a staggered DNA double-stranded break.
- Shmakov et al. (2015) reported three distinct Class 2 CRISPR-Cas systems. Two system CRISPR enzymes (C2c1 and C2c3) contain RuvC-like endonuclease domains distantly related to Cpf1. Unlike Cpf1, C2c1 depends on both crRNA and tracrRNA for DNA cleavage. The third enzyme (C2c2) contains two predicted HEPN RNase domains and is tracrRNA independent.
- Slaymaker et al (2016) reported the use of structure-guided protein engineering to improve the specificity of Streptococcus pyogenes Cas9 (SpCas9). The authors developed "enhanced specificity" SpCas9 (eSpCas9) variants which maintained robust on-target cleavage with reduced off-target effects.

[0347] Also, "Dimeric CRISPR RNA-guided FokI nucleases for highly specific genome editing", Shengdar Q. Tsai, Nicolas Wyvekens, Cyd Khayter, Jennifer A. Foden, Vishal Thapar, Deepak Reyon, Mathew J. Goodwin, Martin J. Aryee, J. Keith Joung Nature Biotechnology 32(6): 569-77 (2014), relates to dimeric RNA-guided FokI Nucleases that recognize extended sequences and can edit endogenous genes with high efficiencies in human cells.

[0348] The methods and tools provided herein are may be designed for use with or Cas13, a type II nuclease that does not make use of tracrRNA. Orthologs of Cas13 have been identified in different bacterial species as described herein. Further type II nucleases with similar properties can be identified using methods described in the art (Shmakov et al. 2015, 60:385–397; Abudayeh et al. 2016, Science, 5;353(6299)). In particular embodiments, such

methods for identifying novel CRISPR effector proteins may comprise the steps of selecting sequences from the database encoding a seed which identifies the presence of a CRISPR Cas locus, identifying loci located within 10 kb of the seed comprising Open Reading Frames (ORFs) in the selected sequences, selecting therefrom loci comprising ORFs of which only a single ORF encodes a novel CRISPR effector having greater than 700 amino acids and no more than 90% homology to a known CRISPR effector. In particular embodiments, the seed is a protein that is common to the CRISPR-Cas system, such as Cas1. In further embodiments, the CRISPR array is used as a seed to identify new effector proteins.

[0349] One type of programmable DNA-binding domain is provided by artificial zinc-finger (ZF) technology, which involves arrays of ZF modules to target new DNA-binding sites in the genome. Each finger module in a ZF array targets three DNA bases. A customized array of individual zinc finger domains is assembled into a ZF protein (ZFP).

[0350] ZFPs can comprise a functional domain. The first synthetic zinc finger nucleases (ZFNs) were developed by fusing a ZF protein to the catalytic domain of the Type IIS restriction enzyme FokI. (Kim, Y. G. et al., 1994, Chimeric restriction endonuclease, Proc. Natl. Acad. Sci. U.S.A. 91, 883−887; Kim, Y. G. et al., 1996, Hybrid restriction enzymes: zinc finger fusions to Fok I cleavage domain. Proc. Natl. Acad. Sci. U.S.A. 93, 1156−1160). Increased cleavage specificity can be attained with decreased off target activity by use of paired ZFN heterodimers, each targeting different nucleotide sequences separated by a short spacer. (Doyon, Y. et al., 2011, Enhancing zinc-finger-nuclease activity with improved obligate heterodimeric architectures. Nat. Methods 8, 74−79). ZFPs can also be designed as transcription activators and repressors and have been used to target many genes in a wide variety of organisms.

[0351] In advantageous embodiments of the invention, the methods provided herein use isolated, non-naturally occurring, recombinant or engineered DNA binding proteins that comprise TALE monomers or TALE monomers or half monomers as a part of their organizational structure that enable the targeting of nucleic acid sequences with improved efficiency and expanded specificity.

[0352] Naturally occurring TALEs or "wild type TALEs" are nucleic acid binding proteins secreted by numerous species of proteobacteria. TALE polypeptides contain a nucleic acid binding domain composed of tandem repeats of highly conserved monomer polypeptides that are predominantly 33, 34 or 35 amino acids in length and that differ from each other mainly in amino acid positions 12 and 13. In advantageous embodiments the

nucleic acid is DNA. As used herein, the term "polypeptide monomers", "TALE monomers" or "monomers" will be used to refer to the highly conserved repetitive polypeptide sequences within the TALE nucleic acid binding domain and the term "repeat variable di-residues" or "RVD" will be used to refer to the highly variable amino acids at positions 12 and 13 of the polypeptide monomers. As provided throughout the disclosure, the amino acid residues of the RVD are depicted using the IUPAC single letter code for amino acids. A general representation of a TALE monomer which is comprised within the DNA binding domain is X1-11-(X12X13)-X14-33 or 34 or 35, where the subscript indicates the amino acid position and X represents any amino acid. X12X13 indicate the RVDs. In some polypeptide monomers, the variable amino acid at position 13 is missing or absent and in such monomers, the RVD consists of a single amino acid. In such cases the RVD may be alternatively represented as X*, where X represents X12 and (*) indicates that X13 is absent. The DNA binding domain comprises several repeats of TALE monomers and this may be represented as (X1-11-(X12X13)-X14-33 or 34 or 35)z, where in an advantageous embodiment, z is at least 5 to 40. In a further advantageous embodiment, z is at least 10 to 26.

[0353] The TALE monomers have a nucleotide binding affinity that is determined by the identity of the amino acids in its RVD. For example, polypeptide monomers with an RVD of NI preferentially bind to adenine (A), monomers with an RVD of NG preferentially bind to thymine (T), monomers with an RVD of HD preferentially bind to cytosine (C) and monomers with an RVD of NN preferentially bind to both adenine (A) and guanine (G). In yet another embodiment of the invention, monomers with an RVD of IG preferentially bind to T. Thus, the number and order of the polypeptide monomer repeats in the nucleic acid binding domain of a TALE determines its nucleic acid target specificity. In still further embodiments of the invention, monomers with an RVD of NS recognize all four base pairs and may bind to A, T, G or C. The structure and function of TALEs is further described in, for example, Moscou et al., Science 326:1501 (2009); Boch et al., Science 326:1509-1512 (2009); and Zhang et al., Nature Biotechnology 29:149-153 (2011), each of which is incorporated by reference in its entirety.

[0354] The polypeptides used in methods of the invention are isolated, non-naturally occurring, recombinant or engineered nucleic acid-binding proteins that have nucleic acid or DNA binding regions containing polypeptide monomer repeats that are designed to target specific nucleic acid sequences.

[0355] As described herein, polypeptide monomers having an RVD of HN or NH preferentially bind to guanine and thereby allow the generation of TALE polypeptides with high binding specificity for guanine containing target nucleic acid sequences. In a preferred embodiment of the invention, polypeptide monomers having RVDs RN, NN, NK, SN, NH, KN, HN, NQ, HH, RG, KH, RH and SS preferentially bind to guanine. In a much more advantageous embodiment of the invention, polypeptide monomers having RVDs RN, NK, NQ, HH, KH, RH, SS and SN preferentially bind to guanine and thereby allow the generation of TALE polypeptides with high binding specificity for guanine containing target nucleic acid sequences. In an even more advantageous embodiment of the invention, polypeptide monomers having RVDs HH, KH, NH, NK, NQ, RH, RN and SS preferentially bind to guanine and thereby allow the generation of TALE polypeptides with high binding specificity for guanine containing target nucleic acid sequences. In a further advantageous embodiment, the RVDs that have high binding specificity for guanine are RN, NH RH and KH. Furthermore, polypeptide monomers having an RVD of NV preferentially bind to adenine and guanine. In more preferred embodiments of the invention, monomers having RVDs of H*, HA, KA, N*, NA, NC, NS, RA, and S* bind to adenine, guanine, cytosine and thymine with comparable affinity.

[0356] The predetermined N-terminal to C-terminal order of the one or more polypeptide monomers of the nucleic acid or DNA binding domain determines the corresponding predetermined target nucleic acid sequence to which the polypeptides of the invention will bind. As used herein the monomers and at least one or more half monomers are "specifically ordered to target" the genomic locus or gene of interest. In plant genomes, the natural TALE-binding sites always begin with a thymine (T), which may be specified by a cryptic signal within the non-repetitive N-terminus of the TALE polypeptide; in some cases, this region may be referred to as repeat 0. In animal genomes, TALE binding sites do not necessarily have to begin with a thymine (T) and polypeptides of the invention may target DNA sequences that begin with T, A, G or C. The tandem repeat of TALE monomers always ends with a half-length repeat or a stretch of sequence that may share identity with only the first 20 amino acids of a repetitive full length TALE monomer and this half repeat may be referred to as a half-monomer. Therefore, it follows that the length of the nucleic acid or DNA being targeted is equal to the number of full monomers plus two.

[0357] As described in Zhang et al., Nature Biotechnology 29:149-153 (2011), TALE polypeptide binding efficiency may be increased by including amino acid sequences from the

"capping regions" that are directly N-terminal or C-terminal of the DNA binding region of naturally occurring TALEs into the engineered TALEs at positions N-terminal or C-terminal of the engineered TALE DNA binding region. Thus, in certain embodiments, the TALE polypeptides described herein further comprise an N-terminal capping region and/or a C-terminal capping region.

[0358] As used herein the predetermined "N-terminus" to "C terminus" orientation of the N-terminal capping region, the DNA binding domain comprising the repeat TALE monomers and the C-terminal capping region provide structural basis for the organization of different domains in the d-TALEs or polypeptides of the invention.

[0359] The entire N-terminal and/or C-terminal capping regions are not necessary to enhance the binding activity of the DNA binding region. Therefore, in certain embodiments, fragments of the N-terminal and/or C-terminal capping regions are included in the TALE polypeptides described herein.

[0360] In certain embodiments, the TALE polypeptides described herein contain a N-terminal capping region fragment that included at least 10, 20, 30, 40, 50, 54, 60, 70, 80, 87, 90, 94, 100, 102, 110, 117, 120, 130, 140, 147, 150, 160, 170, 180, 190, 200, 210, 220, 230, 240, 250, 260 or 270 amino acids of an N-terminal capping region. In certain embodiments, the N-terminal capping region fragment amino acids are of the C-terminus (the DNA-binding region proximal end) of an N-terminal capping region. As described in Zhang et al., *Nature Biotechnology* 29:149-153 (2011), N-terminal capping region fragments that include the C-terminal 240 amino acids enhance binding activity equal to the full length capping region, while fragments that include the C-terminal 147 amino acids retain greater than 80% of the efficacy of the full length capping region, and fragments that include the C-terminal 117 amino acids retain greater than 50% of the activity of the full-length capping region.

[0361] In some embodiments, the TALE polypeptides described herein contain a C-terminal capping region fragment that included at least 6, 10, 20, 30, 37, 40, 50, 60, 68, 70, 80, 90, 100, 110, 120, 127, 130, 140, 150, 155, 160, 170, 180 amino acids of a C-terminal capping region. In certain embodiments, the C-terminal capping region fragment amino acids are of the N-terminus (the DNA-binding region proximal end) of a C-terminal capping region. As described in Zhang et al., Nature Biotechnology 29:149-153 (2011), C-terminal capping region fragments that include the C-terminal 68 amino acids enhance binding activity equal to the full length capping region, while fragments that include the C-terminal 20 amino acids retain greater than 50% of the efficacy of the full length capping region.

[0362] In certain embodiments, the capping regions of the TALE polypeptides described herein do not need to have identical sequences to the capping region sequences provided herein. Thus, in some embodiments, the capping region of the TALE polypeptides described herein have sequences that are at least 50%, 60%, 70%, 80%, 85%, 90%, 91%, 92%, 93%, 94%, 95%, 96%, 97%, 98% or 99% identical or share identity to the capping region amino acid sequences provided herein. Sequence identity is related to sequence homology. Homology comparisons may be conducted by eye, or more usually, with the aid of readily available sequence comparison programs. These commercially available computer programs may calculate percent (%) homology between two or more sequences and may also calculate the sequence identity shared by two or more amino acid or nucleic acid sequences. In some preferred embodiments, the capping region of the TALE polypeptides described herein have sequences that are at least 95% identical or share identity to the capping region amino acid sequences provided herein.

[0363] Sequence homologies may be generated by any of a number of computer programs known in the art, which include but are not limited to BLAST or FASTA. Suitable computer program for carrying out alignments like the GCG Wisconsin Bestfit package may also be used. Once the software has produced an optimal alignment, it is possible to calculate % homology, preferably % sequence identity. The software typically does this as part of the sequence comparison and generates a numerical result.

[0364] In advantageous embodiments described herein, the TALE polypeptides of the invention include a nucleic acid binding domain linked to the one or more effector domains. The terms “effector domain” or “regulatory and functional domain” refer to a polypeptide sequence that has an activity other than binding to the nucleic acid sequence recognized by the nucleic acid binding domain. By combining a nucleic acid binding domain with one or more effector domains, the polypeptides of the invention may be used to target the one or more functions or activities mediated by the effector domain to a particular target DNA sequence to which the nucleic acid binding domain specifically binds.

[0365] In some embodiments of the TALE polypeptides described herein, the activity mediated by the effector domain is a biological activity. For example, in some embodiments the effector domain is a transcriptional inhibitor (i.e., a repressor domain), such as an mSin interaction domain (SID). SID4X domain or a Krüppel-associated box (KRAB) or fragments of the KRAB domain. In some embodiments, the effector domain is an enhancer of transcription (i.e. an activation domain), such as the VP16, VP64 or p65 activation domain.

In some embodiments, the nucleic acid binding is linked, for example, with an effector domain that includes but is not limited to a transposase, integrase, recombinase, resolvase, invertase, protease, DNA methyltransferase, DNA demethylase, histone acetylase, histone deacetylase, nuclease, transcriptional repressor, transcriptional activator, transcription factor recruiting, protein nuclear-localization signal or cellular uptake signal.

[0366] In some embodiments, the effector domain is a protein domain which exhibits activities which include but are not limited to transposase activity, integrase activity, recombinase activity, resolvase activity, invertase activity, protease activity, DNA methyltransferase activity, DNA demethylase activity, histone acetylase activity, histone deacetylase activity, nuclease activity, nuclear-localization signaling activity, transcriptional repressor activity, transcriptional activator activity, transcription factor recruiting activity, or cellular uptake signaling activity. Other preferred embodiments of the invention may include any combination the activities described herein.

[0367] In certain embodiments, the invention involves targeted nucleic acid profiling (e.g., sequencing, quantitative reverse transcription polymerase chain reaction, and the like) (see e.g., Geiss GK, et al., Direct multiplexed measurement of gene expression with color-coded probe pairs. Nat Biotechnol. 2008 Mar;26(3):317–25). In certain embodiments, a target nucleic acid molecule (e.g., RNA molecule), may be sequenced by any method known in the art, for example, methods of high-throughput sequencing, also known as next generation sequencing or deep sequencing. A nucleic acid target molecule labeled with a barcode (for example, an origin-specific barcode) can be sequenced with the barcode to produce a single read and/or contig containing the sequence, or portions thereof, of both the target molecule and the barcode. Exemplary next generation sequencing technologies include, for example, Illumina sequencing, Ion Torrent sequencing, 454 sequencing, SOLiD sequencing, and nanopore sequencing amongst others. Methods for constructing sequencing libraries are known in the art (see, e.g., Head et al., Library construction for next-generation sequencing: Overviews and challenges. Biotechniques. 2014; 56(2): 61–77).

[0368] In certain embodiments, the invention involves plate based single cell RNA sequencing (see, e.g., Picelli, S. et al., 2014, “Full-length RNA-seq from single cells using Smart-seq2” Nature protocols 9, 171-181, doi:10.1038/nprot.2014.006).

[0369] In certain embodiments, the invention involves high-throughput single-cell RNA-seq and/or targeted nucleic acid profiling where the RNAs from different cells are tagged individually, allowing a single library to be created while retaining the cell identity of each

read. In this regard reference is made to Macosko et al., 2015, "Highly Parallel Genome-wide Expression Profiling of Individual Cells Using Nanoliter Droplets" Cell 161, 1202–1214; International patent application number PCT/US2015/049178, published as WO2016/040476 on March 17, 2016; Klein et al., 2015, "Droplet Barcoding for Single-Cell Transcriptomics Applied to Embryonic Stem Cells" Cell 161, 1187–1201; International patent application number PCT/US2016/027734, published as WO2016168584A1 on October 20, 2016; Zheng, et al., 2016, "Haplotyping germline and cancer genomes with high-throughput linked-read sequencing" Nature Biotechnology 34, 303–311; Zheng, et al., 2017, "Massively parallel digital transcriptional profiling of single cells" Nat. Commun. 8, 14049 doi: 10.1038/ncomms14049; International patent publication number WO 2014210353 A2; Zilionis, et al., 2017, "Single-cell barcoding and sequencing using droplet microfluidics" Nat Protoc. Jan;12(1):44-73; Cao et al., 2017, "Comprehensive single cell transcriptional profiling of a multicellular organism by combinatorial indexing" bioRxiv preprint first posted online Feb. 2, 2017, doi: dx.doi.org/10.1101/104844; Rosenberg et al., 2017, "Scaling single cell transcriptomics through split pool barcoding" bioRxiv preprint first posted online Feb. 2, 2017, doi: dx.doi.org/10.1101/105163; Vitak, et al., "Sequencing thousands of single-cell genomes with combinatorial indexing" Nature Methods, 14(3):302–308, 2017; Cao, et al., Comprehensive single-cell transcriptional profiling of a multicellular organism. Science, 357(6352):661–667, 2017; and Gierahn et al., "Seq-Well: portable, low-cost RNA sequencing of single cells at high throughput" Nature Methods 14, 395–398 (2017), all the contents and disclosure of each of which are herein incorporated by reference in their entirety.

[0370] In certain embodiments, the invention involves single nucleus RNA sequencing (sn-RNA-seq). In this regard reference is made to Swiech et al., 2014, "In vivo interrogation of gene function in the mammalian brain using CRISPR-Cas9" Nature Biotechnology Vol. 33, pp. 102–106; Habib et al., 2016, "Div-Seq: Single-nucleus RNA-Seq reveals dynamics of rare adult newborn neurons" Science, Vol. 353, Issue 6302, pp. 925-928; and Habib et al., 2017, "Massively parallel single-nucleus RNA-seq with DroNc-seq" Nat Methods. 2017 Oct;14(10):955-958, which are herein incorporated by reference in their entirety.

[0371] In certain embodiments, the immunotherapy resistance signature comprises EGR1 and/or MAZ. In other embodiments, EGR1 and/or MAZ are targeted for therapeutic intervention. In one embodiment, EGR1 and/or MAZ are targeted to reduce a resistance signature. EGR1 and MAZ are zinc finger transcription factors (TF). EGR1 is down

regulated in malignant cells of the post-treatment tumors, and MAZ (Myc-associated *zinc* finger protein) is up-regulated. These TFs may be connected to the decrease in metallothioneins post-treatment and availability to metal ions. Applicants saw an enrichment in EGR1 targets in the genes which are down-regulated post-treatment. Applicants also saw an overlap with a signature identified in synovial sarcoma. In synovial sarcoma EGR1 is repressed. Mutations in the BAF complex are strongly associated with the response to immunotherapy/resistance to T-cells, and is related to the present invention.

[0372] In certain embodiments, the gene signatures described herein are screened by perturbation of target genes within said signatures. In certain embodiments, perturbation of any signature gene or gene described herein may reduce or induce the immunotherapy resistance signature. In preferred embodiments, the perturbed genes include MAZ, NFKBIZ, MYC, ANXA1, SOX4, MT2A, PTP4A3, CD59, DLL3, SERPINE2, SERPINF1, PERP, EGR1, SERPINA3, IFNGR2, B2M, and PDL1. In certain embodiments, after perturbation, gene expression may be evaluated to determine whether the gene signature is reduced.

[0373] Methods and tools for genome-scale screening of perturbations in single cells using CRISPR-Cas9 have been described, herein referred to as perturb-seq (see e.g., Dixit et al., "Perturb-Seq: Dissecting Molecular Circuits with Scalable Single-Cell RNA Profiling of Pooled Genetic Screens" 2016, Cell 167, 1853–1866; Adamson et al., "A Multiplexed Single-Cell CRISPR Screening Platform Enables Systematic Dissection of the Unfolded Protein Response" 2016, Cell 167, 1867–1882; and International publication serial number WO/2017/075294). The present invention is compatible with perturb-seq, such that signature genes may be perturbed and the perturbation may be identified and assigned to the proteomic and gene expression readouts of single cells. In certain embodiments, signature genes may be perturbed in single cells and gene expression analyzed. Not being bound by a theory, networks of genes that are disrupted due to perturbation of a signature gene may be determined. Understanding the network of genes effected by a perturbation may allow for a gene to be linked to a specific pathway that may be targeted to modulate the signature and treat a cancer. Thus, in certain embodiments, perturb-seq is used to discover novel drug targets to allow treatment of specific cancer patients having the gene signature of the present invention.

[0374] The perturbation methods and tools allow reconstructing of a cellular network or circuit. In one embodiment, the method comprises (1) introducing single-order or combinatorial perturbations to a population of cells, (2) measuring genomic, genetic,

proteomic, epigenetic and/or phenotypic differences in single cells and (3) assigning a perturbation(s) to the single cells. Not being bound by a theory, a perturbation may be linked to a phenotypic change, preferably changes in gene or protein expression. In preferred embodiments, measured differences that are relevant to the perturbations are determined by applying a model accounting for co-variates to the measured differences. The model may include the capture rate of measured signals, whether the perturbation actually perturbed the cell (phenotypic impact), the presence of subpopulations of either different cells or cell states, and/or analysis of matched cells without any perturbation. In certain embodiments, the measuring of phenotypic differences and assigning a perturbation to a single cell is determined by performing single cell RNA sequencing (RNA-seq). In preferred embodiments, the single cell RNA-seq is performed by any method as described herein (e.g., Drop-seq, InDrop, 10X genomics). In certain embodiments, unique barcodes are used to perform Perturb-seq. In certain embodiments, a guide RNA is detected by RNA-seq using a transcript expressed from a vector encoding the guide RNA. The transcript may include a unique barcode specific to the guide RNA. Not being bound by a theory, a guide RNA and guide RNA barcode is expressed from the same vector and the barcode may be detected by RNA-seq. Not being bound by a theory, detection of a guide RNA barcode is more reliable than detecting a guide RNA sequence, reduces the chance of false guide RNA assignment and reduces the sequencing cost associated with executing these screens. Thus, a perturbation may be assigned to a single cell by detection of a guide RNA barcode in the cell. In certain embodiments, a cell barcode is added to the RNA in single cells, such that the RNA may be assigned to a single cell. Generating cell barcodes is described herein for single cell sequencing methods. In certain embodiments, a Unique Molecular Identifier (UMI) is added to each individual transcript and protein capture oligonucleotide. Not being bound by a theory, the UMI allows for determining the capture rate of measured signals, or preferably the binding events or the number of transcripts captured. Not being bound by a theory, the data is more significant if the signal observed is derived from more than one protein binding event or transcript. In preferred embodiments, Perturb-seq is performed using a guide RNA barcode expressed as a polyadenylated transcript, a cell barcode, and a UMI.

[0375] Perturb-seq combines emerging technologies in the field of genome engineering, single-cell analysis and immunology, in particular the CRISPR-Cas9 system and droplet single-cell sequencing analysis. In certain embodiments, a CRISPR system is used to create an INDEL at a target gene. In other embodiments, epigenetic screening is performed by

applying CRISPRa/i/x technology (see, e.g., Konermann et al. "Genome-scale transcriptional activation by an engineered CRISPR-Cas9 complex" Nature. 2014 Dec 10. doi: 10.1038/nature14136; Qi, L. S., et al. (2013). "Repurposing CRISPR as an RNA-guided platform for sequence-specific control of gene expression". Cell. 152 (5): 1173–83; Gilbert, L. A., et al., (2013). "CRISPR-mediated modular RNA-guided regulation of transcription in eukaryotes". Cell. 154 (2): 442–51; Komor et al., 2016, Programmable editing of a target base in genomic DNA without double-stranded DNA cleavage, Nature 533, 420–424; Nishida et al., 2016, Targeted nucleotide editing using hybrid prokaryotic and vertebrate adaptive immune systems, Science 353(6305); Yang et al., 2016, Engineering and optimising deaminase fusions for genome editing, Nat Commun. 7:13330; Hess et al., 2016, Directed evolution using dCas9-targeted somatic hypermutation in mammalian cells, Nature Methods 13, 1036–1042; and Ma et al., 2016, Targeted AID-mediated mutagenesis (TAM) enables efficient genomic diversification in mammalian cells, Nature Methods 13, 1029–1035). Numerous genetic variants associated with disease phenotypes are found to be in non-coding region of the genome, and frequently coincide with transcription factor (TF) binding sites and non-coding RNA genes. Not being bound by a theory, CRISPRa/i/x approaches may be used to achieve a more thorough and precise understanding of the implication of epigenetic regulation. In one embodiment, a CRISPR system may be used to activate gene transcription. A nuclease-dead RNA-guided DNA binding domain, dCas9, tethered to transcriptional repressor domains that promote epigenetic silencing (e.g., KRAB) may be used for "CRISPRi" that represses transcription. To use dCas9 as an activator (CRISPRa), a guide RNA is engineered to carry RNA binding motifs (e.g., MS2) that recruit effector domains fused to RNA-motif binding proteins, increasing transcription. A key dendritic cell molecule, p65, may be used as a signal amplifier, but is not required.

[0376] In certain embodiments, other CRISPR-based perturbations are readily compatible with Perturb-seq, including alternative editors such as CRISPR/Cpf1. In certain embodiments, Perturb-seq uses Cpf1 as the CRISPR enzyme for introducing perturbations. Not being bound by a theory, Cpf1 does not require Tracr RNA and is a smaller enzyme, thus allowing higher combinatorial perturbations to be tested.

[0377] The cell(s) may comprise a cell in a model non-human organism, a model non-human mammal that expresses a Cas protein, a mouse that expresses a Cas protein, a mouse that expresses Cpf1, a cell in vivo or a cell ex vivo or a cell in vitro (see e.g., WO 2014/093622 (PCT/US13/074667); US Patent Publication Nos. 20120017290 and

20110265198 assigned to Sangamo BioSciences, Inc.; US Patent Publication No. 20130236946 assigned to Cellectis; Platt et al., "CRISPR-Cas9 Knockin Mice for Genome Editing and Cancer Modeling" Cell (2014), 159(2): 440-455; "Oncogenic models based on delivery and use of the CRISPR-Cas systems, vectors and compositions" WO2014204723A1 "Delivery and use of the CRISPR-Cas systems, vectors and compositions for hepatic targeting and therapy" WO2014204726A1; "Delivery, use and therapeutic applications of the CRISPR-Cas systems and compositions for modeling mutations in leukocytes" WO2016049251; and Chen et al., "Genome-wide CRISPR Screen in a Mouse Model of Tumor Growth and Metastasis" 2015, Cell 160, 1246–1260). The cell(s) may also comprise a human cell. Mouse cell lines may include, but are not limited to neuro-2a cells and EL4 cell lines (ATCC TIB-39). Primary mouse T cells may be isolated from C57/BL6 mice. Primary mouse T cells may be isolated from Cas9-expressing mice.

[0378] In one embodiment, CRISPR/Cas9 may be used to perturb protein-coding genes or non-protein-coding DNA. CRISPR/Cas9 may be used to knockout protein-coding genes by frameshifts, point mutations, inserts, or deletions. An extensive toolbox may be used for efficient and specific CRISPR/Cas9 mediated knockout as described herein, including a double-nicking CRISPR to efficiently modify both alleles of a target gene or multiple target loci and a smaller Cas9 protein for delivery on smaller vectors (Ran, F.A., et al., In vivo genome editing using *Staphylococcus aureus* Cas9. Nature. 520, 186-191 (2015)). A genome-wide sgRNA mouse library (~10 sgRNAs/gene) may also be used in a mouse that expresses a Cas9 protein (see, e.g., WO2014204727A1).

[0379] In one embodiment, perturbation is by deletion of regulatory elements. Non-coding elements may be targeted by using pairs of guide RNAs to delete regions of a defined size, and by tiling deletions covering sets of regions in pools.

[0380] In one embodiment, perturbation of genes is by RNAi. The RNAi may be shRNA's targeting genes. The shRNA's may be delivered by any methods known in the art. In one embodiment, the shRNA's may be delivered by a viral vector. The viral vector may be a lentivirus, adenovirus, or adeno associated virus (AAV).

[0381] A CRISPR system may be delivered to primary mouse T-cells. Over 80% transduction efficiency may be achieved with Lenti-CRISPR constructs in CD4 and CD8 T-cells. Despite success with lentiviral delivery, recent work by Hendel et al, (Nature Biotechnology 33, 985–989 (2015) doi:10.1038/nbt.3290) showed the efficiency of editing human T-cells with chemically modified RNA, and direct RNA delivery to T-cells via

electroporation. In certain embodiments, perturbation in mouse primary T-cells may use these methods.

[0382] In certain embodiments, whole genome screens can be used for understanding the phenotypic readout of perturbing potential target genes. In preferred embodiments, perturbations target expressed genes as defined by a gene signature using a focused sgRNA library. Libraries may be focused on expressed genes in specific networks or pathways. In other preferred embodiments, regulatory drivers are perturbed. In certain embodiments, Applicants perform systematic perturbation of key genes that regulate T-cell function in a high-throughput fashion. In certain embodiments, Applicants perform systematic perturbation of key genes that regulate cancer cell function in a high-throughput fashion (e.g., immune resistance or immunotherapy resistance). Applicants can use gene expression profiling data to define the target of interest and perform follow-up single-cell and population RNA-seq analysis. Not being bound by a theory, this approach will accelerate the development of therapeutics for human disorders, in particular cancer. Not being bound by a theory, this approach will enhance the understanding of the biology of T-cells and tumor immunity, and accelerate the development of therapeutics for human disorders, in particular cancer, as described herein.

[0383] Not being bound by a theory, perturbation studies targeting the genes and gene signatures described herein could (1) generate new insights regarding regulation and interaction of molecules within the system that contribute to suppression of an immune response, such as in the case within the tumor microenvironment, and (2) establish potential therapeutic targets or pathways that could be translated into clinical application.

[0384] In certain embodiments, after determining Perturb-seq effects in cancer cells and/or primary T-cells, the cells are infused back to the tumor xenograft models (melanoma, such as B16F10 and colon cancer, such as CT26) to observe the phenotypic effects of genome editing. Not being bound by a theory, detailed characterization can be performed based on (1) the phenotypes related to tumor progression, tumor growth, immune response, etc. (2) the TILs that have been genetically perturbed by CRISPR-Cas9 can be isolated from tumor samples, subject to cytokine profiling, qPCR/RNA-seq, and single-cell analysis to understand the biological effects of perturbing the key driver genes within the tumor-immune cell contexts. Not being bound by a theory, this will lead to validation of TILs biology as well as lead to therapeutic targets.

[0385] The invention is further described in the following examples, which do not limit the scope of the invention described in the claims.

EXAMPLES

Example 1 - Identifying Signatures of Resistance

[0386] Applicants leveraged single-cell RNA-sequencing (scRNA-Seq) of thousands of cells from melanoma tumors and a novel data-driven method to systematically map cancer programs that promote ICR and T cell exclusion. Applicants collected 10,123 scRNA-seq profiles from the tumors of 31 patients, consisting of 15 treatment naïve (**TN**) patients, and 16 post-ICI tumors. Of these 16 post-ICI specimens, 15 had clinical resistance and were therefore termed ICI-resistant (**ICR**), and one had a partial response (PR) according to the RECIST criteria (Eisenhauer et al., 2009) (**Fig. 1A, table 1**), and was termed as having clinical benefit (**CB**). Applicants filtered lower-quality cells to retain 7,186 high-quality transcriptomes, including 4,199 cells from 16 patients that Applicants previously reported (Tirosh et al., 2016a), and 2,987 cells from 16 newly collected patient tumors (**table 1**).

[0387] Applicants first aimed to determine the effects ICI has on different cell types in the tumor at the time of post-ICI progression, by comparing between the ICR and TN tumors. Although the specimens in the different treatment groups were not from the same patients, Applicants reasoned that the high resolution and large number of cells profiled will provide sufficient power to detect some of these effects.

[0388] It revealed that, despite the lack of clinical response, CD8 T-cells in the ICR tumors manifested heterogeneous phenotypes of T-cell activation. Conversely, the malignant cells of ICR tumors had a distinct transcriptional state that was substantially less frequent in the TN tumors.

[0389] Next, for any such transcriptional program that may reflect ICI effects, Applicants examined its potential causal connection to immune evasion or resistance. Applicants acknowledged the possibility that malignant cells derived from TN tumors could contain both treatment-sensitive and intrinsically resistant cells. Thus, Applicants tested the malignant signatures in two independent validation cohorts (**Fig. 1A**), where pre-ICI patient biopsies were profiled with bulk RNA-Seq, and the response to ICI therapy was monitored. Applicants demonstrated that this oncogenic state is tightly linked to immune evasion and exclusion, and that it can be used to predict ICR based on the bulk RNA-seq of the pre-ICI biopsy.

[0390] Applicants collected scRNA-Seq of dissociated individual cells from fresh tumor resections, sorted into immune and non-immune cells based on the CD45 expression, and profiled them with a modified full-length SMART-Seq2 protocol (**materials and methods, table 2**). Applicants distinguished different cell subsets and clones both by their expression profiles and by their inferred genetic features. In the non-immune compartment (**Fig. 1B**), Applicants distinguished malignant from non-malignant cells (**materials and methods**) according to (1) their inferred CNV profiles (Tirosh et al., 2016a) (**fig. 5**); (2) under-expression of different non-malignant cell-type signatures (**fig. 5B**); and (3) high similarity to bulk RNA-Seq profiles of melanoma tumors compared to adjacent normal tissue. The cell assignments by the different criteria were highly consistent (hypergeometric p-value $< 10^{-17}$, **fig. 5, materials and methods**). Within non-malignant cells, Applicants used unsupervised clustering to identify (**materials and methods**) CD8 and CD4 T cells, B cells, NK cells, macrophages, Cancer Associated Fibroblasts (CAFs) and endothelial cells **(Fig. 1C, fig. 6, table 3**). Overall, malignant cells clustered first by their tumor of origin (**Fig. 1B**), while the non-malignant cells clustered primarily by their cell type, and only then by their tumor of origin (**Fig. 1C**).

[0391] Applicants identified transcriptional features that distinguish between the cells of TN and ICR tumors, analyzing separately each cell type with a sufficient number (>100) of cells: malignant cells, macrophages, B cells, CD8 T cells, and CD4 T cells. Applicants applied a subsampling procedure to prevent tumors with a particularly large number of cells of a given type from dominating the results and to mitigate the effects of outliers. For each cell type Applicants defined an ICR-up and ICR-down signature, consisting of genes that were significantly up or down regulated in the cells from the ICR tumors, respectively (Kharchenko, et al., 2014). Applicants used a mixed-effect model to test the ability of a given gene signature to distinguish between cells from ICR and TN tumors, while accounting for potential confounders, including other clinical characteristics and cell quality (**materials and methods**).

[0392] The CD8 T cells and malignant cells subset derived from ICR patients were markedly different from their TN counterparts (**fig. 7, tables 4 and 5**), and are the focus of this analysis. Macrophages also showed ICR associated expression programs (**table 4**), but due to their relatively small number in the dataset, Applicants did not pursue them further. Conversely, very few genes where differentially expressed between the ICR vs. TN groups

when analyzing B cells or CD4 T cells (**table 4**). Deeper sampling of these and other cell types might identify significant distinctions.

[0393] The CD8 T-cell-ICR signatures (**Fig. 1D**) revealed the induction of cytotoxicity genes and the repression of some exhaustion features. Compared to TN CD8 T cells, ICR CD8 T cells up regulated the T cell activation markers STAT1, GBP2, GBP5 and IRF1, and down regulated WNK1. Inhibition of WNK1 has been shown to increase T cell infiltration and accumulation in tumors in an in vivo shRNA screen (Zhou et al., 2014). Lactate dehydrogenase A (LDHA) was also up regulated in the ICR CD8 T cells, suggesting that the cells may have infiltrated the hypoxic tumor microenvironment. Among the immune checkpoints, HAVCR2 (TIM3) and CD27 are significantly, though modestly, down-regulated. Although the inhibitory checkpoints CTLA-4, TIGIT, LAG-3, PD-1, and TIM3 co-vary across cells (along with the transcription factor PRDM1), as Applicants previously reported (Tirosh et al., 2016a; and Singer et al., 2016), Applicants did not detect a significant difference in their expression between TN and ICR cells (**fig. 8A**). Rather, CD8 T cells from both TN and ICR tumor specimens spanned a spectrum of states in the exhaustion-cytotoxicity space, even within the CD8 T cells of the same tumor (Tirosh et al., 2016a), with a strong association between dysfunction ("exhaustion") and cytotoxicity scores at the single cell level (**Fig. 1E, fig. 8B**), as Applicants previously reported (Tirosh et al., 2016a). Notably, the CD8 T cells of the one ICI responder patient are both highly cytotoxic and significantly less dysfunctional than cells of other patients (**Fig. 1E**, $P = 1.31*10^{-6}$, hypergeometric test). However, since a similar trend was observed in one of the ICR patients (Mel126, $P = 4.08*10^{-13}$, hypergeometric test), such an enhanced cytotoxic state may not necessarily mark clinical response. These findings were robust when using different T cell dysfunction signatures (**materials and methods**), including single-cell signatures that were recently identified in T cells from hepatocellular carcinoma tumors (Zheng et al., 2017) (**fig. 8B**, $P < 2.46*10^{-4}$, hypergeometric test). A list of differentially expressed genes obtained when comparing the CD8 T cells of the CB patients to those from the ICR patients is provided in **table 6**.

[0394] To examine the association between CD8 T cell profiles and clonal expansion Applicants reconstructed full-length T cell receptors (TCR) and identified 137 CD8 T cell clones of varying sizes (Stubbington et al., 2016) (**Fig. 1F, fig. 9**). Three patients, all of them ICR, had exceptionally large clonal expansions, with 39-51% of the CD8 T cells in these tumors as members of large (>20 cells) clonotypes (Fig. 1F). These three ICR patients had

extremely expanded CD8 T cells, even after controlling for the number of CD8 T cells profiled and the success rate of TCR reconstruction (**materials and methods**, $P = 4.54*10^{-3}$, one-sided Wilcoxon ranksum, **fig. 9B**). For one ICR patient with extreme clonal expansions, Applicants obtained two lesions a year apart: 15 of the 28 clones identified in these specimens included cells from both lesions, such that 71% and 52% of the CD8 T cells in the early and late samples, respectively, were in the shared clones, demonstrating their stability and persistence (**fig. 9C,D**). T cell clonality pre-treatment has previously been identified as a potential predictive marker of response to anti-PD-1 therapy (6); the results herein suggest that the extent of clonal expansion post ICI may not be coupled to clinical response.

[0395] The expression of the ICR signature is higher in expanded CD8 T cells within each subset of patients, with the clonally expanded ICR CD8 T cells scoring highest (**Fig. 1D,G**, left, $P = 3.23*10^{-5}$, mixed-effects test). Nonetheless, even when completely removing the T cells of the three ICR patients with the large T cell clonal expansion, the T-cell-ICR signature still significantly distinguished between the TN and ICR CD8 T cells (**Fig. 1G**, right, $P = 5.56*10^{-53}$ and $7.41*10^{-3}$, t-test and mixed effects test, respectively). The expanded T cells had a gene signature that included significant down-regulation of KLRG1 (**table 10**).

[0396] According to the expression of cell cycle signatures in each cell (**materials and methods**), five patients had a significantly larger fraction of cycling CD8 T cells (hypergeometric p-value <0.01), four of them were ICR patients. Proliferating CD8 T cells expressed some unique genes compared to proliferating malignant cells (**Fig. 1H, table 7**), including induction of oxidative phosphorylation ($P = 7.89*10^{-6}$, hypergeometric test) and repression of the hematopoietic lineage genes CD37, IL11RA, and IL7R ($P = 1.28*10^{-4}$, hypergeometric test). Thus, it may be possible to perturb T cell proliferation specifically, without affecting tumor cells (i.e. tumor growth).

[0397] Taken together, these findings demonstrate that even in ICR patients CD8 T cells following ICI can show some indicators of enhanced functionality, such as expansion and transcriptional changes. In other words, these findings demonstrate that ICI can promote the expansion and functionality of the CD8 T cells without leading to a clinical response. Additional data from ICI responders is needed to examine if insufficient T cell functionality nonetheless limited the clinical response in such ICR patients. Nevertheless, Applicants hypothesized that the malignant cell compartment may contribute to ICR in these patients, at least in part.

[0398] Applicants thus turned to examine the effect of ICI on the malignant cell profiles, and identified signatures that distinguish malignant cells from ICR vs. TN tumors: oncogenic-ICR-up and oncogenic-ICR-down (**Fig. 2A,B, table 5**). The signatures were robust and generalizable in cross-validation (withholding data from each patient in turn and classifying the withheld test set; **materials and methods, Fig. 2A**, AUC=0.86). The variation in the expression of the oncogenic-ICR signatures in either this data or across TCGA melanoma bulk tumors was not significantly associated with potential confounders (**materials and methods**, mixed-effect model and ANOVA, respectively). Finally, a proportion of malignant cells in TN tumors manifested the oncogenic-ICR state (**Fig. 2B, right**), suggesting that it may precede ICI at least in some patients. This is discussed further below.

[0399] The oncogenic-ICR-down signature genes were enriched both in pathways that reflect established mechanisms of resistance, including downregulation of IFN- signaling and MHC class I presentation (Zaretsky et al., 2016), and in additional processes, not previously implicated in ICR (**Fig. 2B, tables 5 and 8, materials and methods**). These include suppression of other innate immune responses, such as TNF-αmediated NF B signaling, apoptosis, response to the complement system, IL2/STAT5 signaling, and the reduced expression of metallothioneins. NFκB pathway activation can induce expression of cytokines with either negative or positive immune-modulatory effects (Muthuswamy et al., 2012; and Pikarsky et al., 2004). The results suggest that under-expression of TNF-αmediated NFκB signaling genes may be detrimental for response. The oncogenic-ICR-up genes include several transcriptional and chromatin regulators (e.g., SNAI2, HMGA1), and are enriched for Myc and CDK7/8 targets ($P<10^{-11}$, hypergeometric p-value). Myc-activation has been previously linked to increased expression of immunosuppressive signals, including the upregulation of PD-L1 and β-catenin, which in turn inhibits dendritic cell recruitment to the tumor microenvironment via CCL4 (11). Similar results were obtained when comparing pre-defined gene modules directly between malignant cells of ICR and TN patients (**Fig. 2C, materials and methods**), including repression of the IL6/JAK/STAT3 pathway; mutations in this pathway were recently reported as an escape mechanism to anti-PD-1 therapy (Zaretsky et al., 2016).

[0400] Gene modules are more robust to noise and provide more coherent signals than the expression of single genes. Applicants thus applied the mixed-effect models to test which biological pathways are differentially expressed between the two groups. The analysis

revealed similar pathways to those outlined above, as well as the repression of the JAK/STAT pathway. Mutations in this pathway were previously reported as an escape mechanism to anti-PD-1 therapy.

[0401] Several lines of evidence suggest that the oncogenic-ICR-up and oncogenic-ICR-down signatures are under shared control by one or few master regulators with opposing effects on these two programs. First, the expression of the oncogenic-ICR-up and oncogenic-ICR-down signatures is anti-correlated within the malignant cells of the same tumor and across hundreds of (TCGA) melanoma tumors (**Fig. 2D,E**). Second, in the Connectivity Map (Lamb et al., 2006), there is a significant overlap between the genetic perturbations that induce the oncogenic-ICR-down signature and those that repress the oncogenic-ICR-up signature (hypergeometric p-value = $1.9*10^{-6}$), including overexpression of IFN-γ and IFN-β and the knockdown of MYC. Indeed, MYC knockdown is the top perturbation to repress oncogenic-ICR-up, which is enriched for Myc targets. Moreover, there are 1,583 protein-protein interactions within and between the genes in the two oncogenic-ICR signatures ($P < 10^{-3}$, empirical test), consistent with participation in convergent biological processes. Applicants therefore defined the oncogenic-ICR state as a concurrent induction of the oncogenic-ICR-up signature and repression of the oncogenic-ICR-down signature, which Applicants quantify by the overall expression (**materials and methods**) of the oncogenic-ICR-up signature minus the overall expression of the oncogenic-ICR-down signature.

[0402] Next, Applicants hypothesized that the oncogenic-ICR signatures reflect an active resistance program, rather than only a post-ICI malignant cell state. This would be consistent with the presence of cells expressing the program in TN patients. In particular, to resist ICI, malignant cells may not only evade the immune cells (e.g., through the repression of MHC I and IFN-γ in oncogenic- ICR-down) but may also actively exclude the immune cells. The latter will impact the extent of CD8 T cell infiltration, which is a known pre-treatment predictor of ICI response (Tumeh et al., 2014; and Taube et al., 2012). To explore this possibility, Applicants developed a data-driven approach that characterizes malignant cells in non-infiltrated niches or tumors (**Fig. 2F**). In this approach, Applicants combined single cell profiles (irrespective of treatment status) with 473 melanoma bulk expression profiles from TCGA. First, Applicants used the single-cell profiles to define a T cell specific signature of 143 genes, and a signature of 332 genes that were primarily expressed by malignant cells (**table 3**). Then Applicants estimated the T cell infiltration level of the TCGA tumors based on their expression of the T cell signature (**materials and methods**), and identified malignant

genes whose expression was correlated to the estimated T cell infiltration levels. Six and 20 of the 332 malignant cell genes were significantly correlated or anti-correlated to the T cell infiltration level, respectively, which Applicants termed the seed T cell exclusion (Exclusion)-down and -up modules, respectively. However, the seed modules would neglect genes that are expressed also by other, non-malignant cells in the tumor (as MHC I, IFN-γ). To recover these, Applicants correlated the expression of each gene to the expression of the seed Exclusion modules across the entire malignant single-cell profiles. This yielded the final Exclusion-up and down modules, with 101 and 134 genes, respectively (**table 5**).

[0403] The Exclusion-down module was enriched for antigen processing and presentation genes (B2M, CTSB, CTSL1, HLA-B/C/F, HSPA1A, HSPA1B, $P = 4.19*10^{-7}$, hypergeometric test), immune modulation genes ($P = 3.84*10^{-9}$, as CD58 and the NFκB inhibitor, NFKBIA), and genes involved in the response to the Complement system ($P = 2.26*10^{-7}$, e.g., CD59 and C4A). CD58 KO in malignant cells was recently shown to enhance the survival of melanoma cells in a genome-scale CRISPR screen of melanoma/T cell co-cultures (28), and its genetic loss or epigenetic inactivation are frequent immune evasion drivers in diffuse large B cell lymphoma (Challa-Malladi et al., 2011). The Exclusion-up module included MYC itself and Myc targets ($P = 6.8*10^{-12}$), as well as the transcription factors SNAI2 and SOX4.

[0404] Even though the Exclusion modules were identified without considering the treatment status of the tumors (TN or ICR), they significantly overlapped the corresponding oncogenic-ICR signatures (64 and 52 overlapping genes in oncogenic-ICR-up and -down, respectively, $P < 10^{-16}$, hypergeometric test, **Fig. 2G,H**). Both oncogenic-ICR (AUC = 0.83, in cross-validation) and the Exclusion signatures (AUC = 0.86) robustly classified individual cells as TN or ICR (**Fig. 2A,G**). In light of this congruence, Applicants defined a unified resistance program (uICR-up and uICRdown) as the union of the corresponding oncogenic-ICR and Exclusion signatures.

[0405] Importantly, there was no significant difference between the fraction of cycling cells in ICR vs. TN tumors ($P = 0.696$, t-test), and the oncogenic-ICR signatures were identical when identified only based on non-cycling cells. Interestingly however, the oncogenic-ICR state was more pronounced in cycling cells, both within the same patient group and among cells of the same tumor (**Fig. 2B,H, fig. 10A,B,** $P < 10^{-16}$, mixed effects model). Thus, cycling malignant cells may have induced stronger immune evasion capacities compared to their non-cycling counterparts. Moreover, CDK4 was a member of the of the

induced resistance program (uICRup). Applicants thus hypothesized that its targeted inhibition could shift the malignant cells to a less resistant state.

[0406] Unlike other biomarkers, such as PDL1 expression, mutational load, or T cell infiltration levels, the immune resistance signature could potentially provide a basis to develop novel treatment strategies. Next, Applicants explored therapeutic strategies to overcome resistance by reversing the uICR cell state in cancer cells. As CDK4 and multiple CDK target were members of the of the induced resistance program (uICR-up) and as the ICR state was more pronounced in cycling cells, Applicants hypothesized that cell cycle arrest through CDK4/6 inhibition could shift the malignant cells to a less resistant state. Additionally, CDK4/6 inhibitors could potentially increase tumor cell immunogenicity by inducing SASP, which was significantly repressed in the cancer cells from the ICR tumors compared to those from the untreated ones.

[0407] To test this assumption, Applicants first analyzed a recently published data set (Goel et al., 2017) in breast cancer cell lines and *in vivo* models and showed that CDK4/6 inhibition through abemaciclib treatment represses the ICR state defined by our signatures (**Fig. 3A-B, fig. 10C**). Applicants found that the CDK4/6 inhibitor abemaciclib strongly repressed uICR-up (which includes CDK4) and induced uICR-down (which includes the D-cyclin, CCND3). Indeed, abemaciclib, approved for the treatment of *BRCA*-mutated breast cancer, was recently shown to trigger anti-tumor activity by inducing type III interferon production and suppressing T regulatory cells (Goel et al., 2017). Furthermore it was shown to sensitize solid tumors to anti-PDL1 in mouse models (Goel et al., 2017) in an RB-dependent manner.

[0408] To determine this effect in melanoma, Applicants identified melanoma cell lines in the Cancer Cell Line Encyclopedia (CCLE) with the strongest expression of the uICR signature, including IGR37, UACC257 (both RB-sufficient) and A2058 (RB-deficient). Applicants performed scRNA-seq on these cell lines before and after treatment with abemaciclib for 1 week **(Fig. 41)**. In both IGR37 and UACC257, Applicants saw a decrease in the expression of the uICR state ($P < 3.59*10^{-34}$, one-sided t-test). The single-cell resolution of the data revealed that in IGR37 there was a subpopulation of cells with an exceptionally strong expression of the uICR signature prior to the treatment with abemaciclib **(Fig. 43)**. This population decreased from 10% before treatment (2,454 cells) to 2% in the post-treatment condition (1,570 cells). In contrast, the RB-deficient cell line A2058 did not

show changes in the uICR expression, consistent with the hypothesis that this effect depends on RB-sufficiency.

[0409] Interestingly, Applicants found that DNMT1 is repressed while ERV-3 is induced in IGR37 and UACC257 cells post-treatment. These findings support previous observations that CDK4/6 inhibition leads to DNMT1 repression, allowing the methylation of endogenous retroviral genes (ERVs). The induction of ERVs triggers 'viral mimicry' and a double-stranded RNA (dsRNA) response, which stimulates type III IFN production to activate IFN-stimulated genes. Interestingly, Applicants also find that abemaciclib induces the expression of an MITF signature (Tirosh I, et al., Science. 2016 Apr 8;352(6282):189-96) and of the SASP module **(Fig. 42)**. The resistant cells, which are eradicated or altered by abemaciclib, had the lowest expression of the MITF and SASP signatures. While this pattern is decoupled from the expression of the MITF gene itself, it nonetheless indicates that, unlike the mechanism described in breast cancer cells (Goel et al., 2017), abemaciclib might trigger SASP and cell differentiation in melanoma cells.

[0410] To explore the potential of abemaciclib to induce T cell mediated toxicity to tumor cells, Applicants leveraged a patient-derived co-culture model of melanoma cells and ex-vivo expanded tumor infiltrating lymphocytes (TILs) from a metastatic melanoma lesion. Following one week of treatment of tumor cells with abemaciclib, cells were treated with their autologous TILs vs. control, and surviving tumor cells were submitted to scRNA-seq. The exposure to TILs reduced the expression of the uICR signature, both in the control and abemaciclib-treated cells ($P < 4.91*10^{-13}$). The treatment with abemaciclib further intensifies these effects, such that in the abemaciclib-treated cells there was an increase in a sensitive (ICR-low) subpopulation of cells post-TILs (**Fig. 42**). These sensitive cells are also characterized by a low expression of DNMT1, overexpression of ERV-3, and higher expression of the MITF and SASP modules. Furthermore, Applicants measured 40 human cytokines/chemokines in the conditioned media of abemaciclib treated cancer cells (before co-culture) and found the induction of several secreted factors **(Fig. 42):** macrophage inhibition factor (MIF), CX3CL1 a chemokine that induces migration and adhesion of T and NK cells and is linked to clinical outcomes in immunotherapy treatment (Akbani, et al., 2015; and Ayers, et al., 2017), and CCL20, an important factor for T cell differentiation that may enhance immunity in melanoma (Barretina, et al., 2012).

[0411] The relevance of the uICR as a resistance program is further supported by several lines of evidence. First, the induced uICR is overexpressed in uveal melanoma, which resides

in an immune-privileged environment and has very low response rates to immunotherapy (Zimmer et al., 2015; and Algazi et al., 2016), compared to cutaneous melanoma (**Fig. 3D**). Second, perturbations of genes from the repressed resistance program (uICR-down) in malignant melanoma cells conferred resistance to cytotoxic CD8 T cells in a genome-wide CRISPR KO screen ($P = 6.37*10^{-3}$, hypergeometric test). Third, malignant cells in the resistant state substantially repress interaction routes with other cell types in the tumor (**Fig. 3E**), as defined by cognate pairs of interacting surface molecules (**materials and methods**), including MHC I:TCR (T cells), CD58:CD2 (T cells), and IL1RAP:IL1B (macrophages).

[0412] These results support a model, in which malignant cells from ICR tumors either had active resistance programs prior to treatment or induced the resistance program upon ICI exposure. Because some of the malignant cells from the TN patients expressed the resistance programs (**Fig. 2B,H**) Applicants next tested their prognostic value in independent datasets and cohorts. To this end, Applicants used both the full uICR and further filtered/refined uICR signatures. The refined signatures include only uICR genes that were also co-regulated with genes whose inhibition enhanced melanoma cell resistance to T cell mediated killing in functional screens (Patel et al., 2017) (**table5, materials and methods**); the oncogenic-ICR and Exclusion signatures show the same behavior (**Fig 4E-H, figs. 11-13**).

[0413] The uICR programs are prognostic and predictive for response in external data sets. First, the signatures strongly associated with survival in 431 TCGA melanoma patients (who did not receive ICI, **Fig. 4A, fig. 11**), even after controlling for tumor purity and T cell infiltration, a known prognostic marker in melanoma (Azimi et al., 2012; and Bogunovic et al., 2009). Furthermore, combining resistance signatures and T cell infiltration levels yielded a significantly stronger association of patient survival than either alone (COX p-value = $1.4*10^{-8}$, **Fig. 4A**, right). Other proposed mechanisms, such as dedifferentiation of melanoma cells (Landsberg et al., 2012), as reflected by an MITF-low signature, and other malignant signatures from the single cell profiles (e.g., cell cycle and the AXL program) (Tirosh et al., 2016a), did not show an association to patient survival, indicating that mere variation across malignant cells is insufficient as a prognostic signature. Second, the signatures were associated with benefit of ICI in published pre-treatment and early on-treatment bulk expression profiles. In a lung cancer mouse model, which was mostly free of confounding genetic variability, the uICR clearly separated anti-CTLA-4 responders from non-responders based on early on-treatment profiles ($P = 3.6*10^{-7}$, one-sided t-test, **Fig. 4B**) (Lesterhuis et al., 2015). In bulk pre-treatment RNA-Seq data from 27 melanoma patients that were

subsequently treated with Pembrolizumab (Hugo et al., 2016), the uICR program was lower in the five complete responders, though just above statistical significance ($P=6.3*10^{-2}$, **Fig. 4C**). In bulk pre-treatment RNA-Seq data from 42 melanoma patients that were subsequently treated with the CTLA-4 inhibitor ipilimumab (Van Allen et al., 2015), the uICR program was significantly lower in the two complete responders ($P = 5.2*10^{-3}$).

[0414] To test the predictive value of the resistance program in a larger independent setting, Applicants assembled a validation cohort of 112 patients with metastatic melanoma who underwent pretreatment biopsy and bulk RNA-Seq followed by Pembrolizumab (anti-PD-1) therapy (**Fig. 1A, table 1**). The cohort was collected in a different hospital and country (Germany), and samples were processed and sequenced on the same platform at the Broad Institute (**materials and methods**). Applicants evaluated the performances of the malignant resistance modules in predicting anti-PD-1 responses, with respect to three parameters (**materials and methods**): (1) progression-free survival (PFS, recorded for 104 of the 112 patients), (2) clinical benefit (CB, defined as either partial or complete response by RECIST criteria), and (3) complete response (CR). To compare the performance of the predictors to prior knowledge and clinically used markers, Applicants assembled a set of 32 other transcriptional signatures, including the top hits of two ICR functional CRISPR screens (Patel et al., 2017; and Manguso et al., 2017) (**table 9**).

[0415] Our malignant cell resistance signatures were predictive of PFS in the validation cohort (**Fig. 4D,E, figs. 12 and 13**). Their predictive value was significant even when accounting for other known predictors of ICI response, including inferred T cell infiltration levels and PD-L1 expression (**figs. 12E and 13E**). Although cell cycle alone is not associated with CB (COX $P > 0.25$), filtering the cell-cycle component from the uICR overexpression score (**materials and methods**) further improved the PFS predictions (**Fig. 4D, right**), suggesting that a tumor ICR level should be evaluated conditioning on its proliferation level. The additional predictive value of the malignant resistance signatures beyond T cell infiltration was significantly higher than that of other signatures ($P = 3.37*10^{-6}$, Wilcoxon-ranksum test), and they were the only ones negatively associated with PFS. Other alternative predictors were either not predictive or highly associated with T cell infiltration levels, such that they did not provide an additive predictive value once accounting for T cell infiltration levels (**Fig. 4E**).

[0416] The uICR state was overexpressed in patients with CB vs. no-CB (**Fig. 4F**). Applicants noted however that some CB patients had high pre-treatment uICR expression and

hypothesized that these patients, while experiencing an initial CB, might cease to respond quickly. Indeed, when stratifying patients with CB based on the duration of their response (>12 months, <12 months but >6 months, and <6 months), Applicants found that patients with an initial CB but high uICR score pretreatment were significantly more likely to experience subsequent progressive disease (**Fig. 4F**). Indeed, patients with rapid progression, that is CB<6 months had the highest uICR score, even compared to those with no-CB. Consistently, the resistance signatures were most accurate in predicting patients with complete responses ($P < 6.31*10^{-3}$, one-sided t-test, **Fig. 4G, fig. 14**). In this task, they were superior to all the other alternative predictors ($P = 1.64*10^{-8}$, Wilcoxon ranksum test), all of which, including the clinically used markers, failed to predict complete response (**Fig. 4H**).

[0417] Finally, Applicants explored intrinsic vs. acquired uICR programs in an additional independent cohort, collected in yet another hospital (**materials and methods**), consisting of 90 samples from 26 patients with metastatic melanoma who underwent both pre-treatment and post-progression biopsies with bulk RNA-Seq, including 17 patients with on-treatment biopsy (**Fig. 1A**). The ICR state was induced following ICI compared to pre-ICI lesions from the same patient ($P = 1.26*10^{-4}$ and 0.01, for the refined uICR and uICR-up, respectively; mixed-effect test, **materials and methods**). However, inter-patient variation in uICR expression was significantly higher than intra-patient changes ($P < 10^{-8}$, ANOVA). This suggests that one pre-treatment sample per patient may suffice to evaluate ICR for many patients, and that intrinsic resistance may be more prevalent than acquired resistance, consistent with clinical observations (Sharma, et al., 2017). Notably, Applicants did not observe an induction in uICR expression following RAF/MEK-inhibition (**materials and methods**), indicating that the ICR state is specific to ICI therapy and not merely a marker of a generally drug resistant tumor ecosystem.

Discussion

[0418] Applicants discovered new features linked to response and resistance to immunotherapy in metastatic melanoma with a strong prognostic and predictive value in independent patient cohorts. T cell profiles from ICR patients reflect variability in T cell responses, which are often decoupled from the clinical response. In some ICR patients, T cells manifest substantial clonal expansions, in others higher frequency of T cell proliferation, or a shift in the cytotoxicity/exhaustion balance. While more data is needed to distinguish between proper and insufficient T cell response to ICI, the results suggest that

malignant cell-autonomous programs may be another key contributor to ICR, even in the presence of properly activated T cells (**Fig. 4I**).

[0419] Malignant cell programs that suppress interactions with the tumor microenvironment, modulate key inflammatory pathways and activate mechanisms of T cell exclusion were distinguishing features of ICR tumors. These may be jointly controlled as a single coherent resistance program to confer ICR, through master regulators like Myc and CDK4/6. While these programs were initially identified in post-progression samples using scRNA-Seq, Applicants validated their predictive value in a pre-ICI cohort and explored their expression in matched pre/post specimens of ICI-treated patients. The ICR signatures Applicants identified were superior to a comprehensive and diverse set of alternative predictors in several ways, especially in predicting complete responders and patients that responded for more than 6 months. Unlike other predictors, the ICR signatures have a significant additional predictive value beyond pre-treatment T cell infiltration levels, indicating that they highlight new and yet unappreciated aspects of ICR. In light of these results, the signatures may help stratify patients for ICI beyond currently used biomarkers.

[0420] The pathways represented in the resistance program also highlight potential mechanistic causes of ICR that could be reversed by combining ICI with other drugs. Combination of ICI with CDK4/6 inhibitors (such as abemaciclib) may be particularly attractive in light of the findings that abemaciclib reverses the resistant oncogenic state and that there are distinctions between the cell cycle programs of malignant cells and T cells.

[0421] The malignant resistance programs may be relevant in other subtypes of melanoma and even in other lineage-independent cancer types. Among different types of melanoma, uveal melanoma has more active resistance programs compared to cutaneous melanoma (**Fig. 3D**); across cancers, the resistance program is higher in some cancer types that are less responsive to immunotherapy and/or arise from immune-privileged tissues (eye, testis) and lower in some of the more responsive tissues (head and neck, kidney, skin, lung) (**fig. 15**). This distinction, however, is imperfect, and additional, tumor-specific resistance programs may be discovered by similar strategies. Our study uncovers an improved, potentially clinically applicable biomarker for patient selection, provides a rationale to examine novel mechanisms of ICR, and reveals guiding principles to further dissect and repress mechanistic underpinnings that mediate ICI resistance.

[0422] Applicants demonstrated that cancer cell-autonomous ICR programs identified by scRNA-Seq predict clinical response (per RECIST criteria) and progression-free survival in

two independent cohorts: one of patients who underwent RNA-seq of matched pre-treatment and progression (ICR) specimens; and another of 112 melanoma patients with pre-treatment RNA-seq who receive anti-PD-1 monotherapy. Applicants also validated the prognostic value of these cell programs in TCGA. Lastly, Applicants demonstrated that pharmacological reversal of these oncogenic cell states can be achieved by CDK4/6-inhibition, and explored the impact of this treatment in melanoma at the single cell level. To determine the role of T cell exclusion from the TME as a potential mechanism of ICR, Applicants performed spatially resolved 30-plex single-cell protein analysis of matching FFPE specimens from 16 of the patients who also underwent scRNA-seq. Thus, the presented analytical platforms provide a promising approach to understanding drug resistance within preserved tumor ecosystems.

[0423] In conclusion, this study provides a high-resolution landscape of oncogenic ICR states, identifies clinically predictive signatures, and forms a basis to develop novel therapeutic strategies that could overcome immunotherapy resistance in melanoma.

Table 1. Clinical characteristics of the patients and samples in the scRNA-Seq cohort, and in the two validation cohorts.

scRNA-Seq cohort

Sample	Cohort	Age	Sex	Treatment	Treatment group	Lesion type	Site
Mel53	Tirosh et al. 2016	77	F	None	TN	metastasis	Subcutaneous back lesion
Mel58	Tirosh et al. 2016	83	M	Ipilimumab	ICR	metastasis	Subcutaneous leg lesion
Mel60	Tirosh et al. 2016	60	M	Trametinib, ipilimumab	ICR	metastasis	Spleen
Mel71	Tirosh et al. 2016	79	M	None	TN	metastasis	Transverse colon
Mel72	Tirosh et al. 2016	57	F	IL-2, nivolumab, ipilimumab + anti-KIR-Ab	ICR	metastasis	External iliac lymph node
Mel74	Tirosh et al. 2016	63	M	Nivolumab	ICR	metastasis	Terminal Ileum
Mel75	Tirosh et al. 2016	80	M	Ipilimumab + nivolumab, WDVAX	ICR	metastasis	Subcutaneous leg lesion
Mel78	Tirosh et al. 2016	73	M	WDVAX, ipilimumab + nivolumab	ICR	metastasis	Small bowel
Mel79	Tirosh et al. 2016	74	M	None	TN	metastasis	Axillary lymph node
Mel80	Tirosh et al. 2016	86	F	None	TN	metastasis	Axillary lymph node
Mel81	Tirosh et al. 2016	43	F	None	TN	metastasis	Axillary lymph node
Mel82	Tirosh et al. 2016	73	F	None	TN	metastasis	Axillary lymph node
Mel84	Tirosh et al. 2016	67	M	None	TN	primary tumor	Acral primary

Sample	Cohort	Age	Sex	Treatment	Treatment group	Lesion type	Site
Mel88	Tirosh et al. 2016	54	F	Tremelimumab + MEDI3617	ICR	metastasis	Cutanoues met
Mel89	Tirosh et al. 2016	67	M	None	TN	metastasis	Axillary lymph node
Mel94	Tirosh et al. 2016	54	F	IFN, ipilimumab + nivolumab	ICR	metastasis	Iliac lymph node
Mel126	Additional	63	M	Ipilimumab, nivolumab	ICR	metastasis	Soft tissue
Mel04.3	Additional	81	M	Ipilimumab	CB	metastasis	Skin
Mel110	Additional	74	M	ipilimumab + angiopoietin 2 inhibitor, Temezlolamide, Pembrolizumab	ICR	metastasis	R adrenal metastasis
Mel121.1	Additional	74	M	S/p Pembrolizumab	ICR	metastasis	Skin
Mel106	Additional	67	M	Prior treatment: nivolumab + ipilimumab	ICR	metastasis	Necrotic L axillary lymph nodes
Mel75.1	Additional	81	M	Ipilimumab + nivolumab, WDVAX, Pembrolizumab	ICR	metastasis	Soft tissue
Mel98	Additional	47	F	S/p IFN, s/p ipilimumab+GMCSF	ICR	metastasis	L thigh soft tissue metastasis
Mel102	Additional	72	F	S/p nivolumab + ipilimumab	ICR	metastasis	Fragmented pieces of (R) adrenal gland metastasis
Mel129PA	Additional	63	M	None	TN	primary tumor	Skin
Mel129PB	Additional	63	M	None	TN	primary tumor	Skin
Mel116	Additional	85	M	None	TN	metastasis	Lymph node
Mel103	Additional	58	M	None	TN	metastasis	Lymph node
Mel105	Additional	77	M	None	TN	primary tumor	Skin
Mel112	Additional	76	M	None	TN	metastasis	Bulky (L) axillary metastasis
Mel194	Additional	68	M	Nivolumab + lirilumab (anti-kit), Nivolumab, Ipilimumab, Pan-RAF-inhibitor, Pembrolizumab	ICR	metastasis	L anterior shoulder subcutaneous
Mel478	Additional	54	F	None	TN	metastasis	Transanal rectal mass
Mel128	Additional	37	M	None	TN	metastasis	Lymph node

Cohort 2	Sex, n	Number of therapies prior to anti-PD-1 therapy, n	RECIST category
Patients 1-112	Female, 49	No prior treatment, 49	PD, 49
	Male, 56	1, 34	SD, 13
	n/a, 7	2, 14	PR, 25
		3, 6	CR, 14
		7, 2	n/a, 11
		n/a, 7	

Cohort 1	Number of samples per patient, n
Patients 1-26	2, 10
90 samples	3, 8

	4, 3
	6, 2
	7, 2
	8, 1

Table 2

Table 2. Quality measures of scRNA-Seq experiments.

Cell type	Median no. of detected genes	Median no. of aligned reads	No. of TN cells	No. of ICR cells	Total no. of cells
B.cell	3774	164400	463	355	818
CAF	5518	357423	61	45	106
Endothelial cell	5057	304326	87	17	104
Macrophage	5670	654482	161	259	420
Mal	5482	335563	1193	825	2018
NK	3909	147376	44	48	92
CD4 T cell	4036	220614	420	436	856
CD8 T cell	4064	264494	720	1039	1759
T cell (unresolved)	3827	234410	298	408	706
Low quality cell	732	24991	1386	1551	2937
?	3433	221421	183	124	307
All cells	3559	377141	5016	5107	10123

Table 3

Table 3. Cell type signatures that were derived from the analysis of the scRNA-seq data (see section Data-driven signatures of specific cell-types).

B cell	CAF	Endothelial cell	Macrophage	Malignant cell	NK cell	T cell	CD4 T cell	CD8 T cell	Immune cell		Lymphocyte	Stroma cell
ADAM19	ABI3BP	A2M	ACP5	AATF	CCL4	AAK1	AQP3	AKAP5	AAK1	HLA-DRB6	AAK1	A2M
ADAM28	ACTA2	ADAM15	ACSL1	ACN9	CD244	ACAP1	CCR4	APOBEC3C	ACAP1	HMHA1	ACAP1	ABI3BP
AFF3	ADAM12	ADAMTS9	ADAMDEC1	ACSL3	CST7	AKNA	CD28	APOBEC3G	ACP5	HMOX1	ADAM19	ACTA2
BANK1	ADAMTS2	ADCY4	ADAP2	AHCY	CTSW	APOBEC3G	CD4	ARHGAP9	ACSL1	HNRNPA1P10	ADAM28	ADAM12
BCL11A	ANTXR1	AFAP1L1	ADORA3	AIF1L	GNLY	ARAP2	CD40LG	ATP8A1	ADAM19	HOPX	AFF3	ADAM15
BIRC3	ASPN	APLNR	ADPGK	AK2	GZMA	ARHGEF1	CD5	BTN3A1	ADAM28	HSH2D	AKAP5	ADAMTS2
BLK	C1S	AQP1	AIF1	ALX1	GZMB	ASB2	DGKA	CBLB	ADAMDEC1	HSPA6	AKNA	ADAMTS9
BLNK	CALD1	ARHGEF15	AKR1A1	AMD1	HOPX	ATHL1	F5	CCL4	ADAP2	HSPA7	ANKRD44	ADCY4
BTLA	CCDC80	CALCRL	ALDH2	ANKRD20A12P	ID2	BCL11B	FAAH2	CCL4L1	ADORA3	HVCN1	APOBEC3C	AFAP1L1
CCR6	CD248	CCL14	ALDH3B1	ANKRD54	IL2RB	BTN3A2	FOXP3	CCL4L2	ADPGK	ICOS	APOBEC3D	ANTXR1
CCR7	CDH11	CD200	AMICA1	AP1S2	KLRB1	CBLB	ICOS	CCL5	AFF3	ID2	APOBEC3G	APLNR
CD19	CERCAM	CD34	ANKRD22	APOA1BP	KLRC1	CCL4	IL6R	CD27	AIF1	IFI30	AQP3	APP
CD1C	COL12A1	CD93	AP1B1	APOC2	KLRD1	CCL5	IL7R	CD7	AKAP5	IFNG	ARAP2	AQP1

Table 3. Cell type signatures that were derived from the analysis of the scRNA-seq data (see section Data-driven signatures of specific cell-types).

B cell	CAF	Endothelial cell	Macrophage	Malignant cell	NK cell	T cell	CD4 T cell	CD8 T cell	Immune cell		Lymphocyte	Stroma cell
CD22	COL14A1	CDH5	AQP9	APOD	KLRF1	CD2	PASK	CD8A	AKNA	IFNGR1	ARHGAP15	ARHGEF15
CD24	COL1A1	CFI	ATF5	APOE	KLRK1	CD247	PBXIP1	CD8B	AKR1A1	IFNGR2	ARHGAP9	ASPN
CD37	COL1A2	CLDN5	ATG3	ATP1A1	NCAM1	CD27	SLAMF1	CD96	ALDH2	IGFLR1	ARHGEF1	BGN
CD52	COL3A1	CLEC14A	ATG7	ATP1B1	NKG7	CD28	SPOCK2	CLEC2D	ALDH3B1	IGLL1	ASB2	C1R
CD79A	COL5A1	COL15A1	ATP6V0B	ATP5C1	PRF1	CD3D	TCF7	CRTAM	ALOX5	IGLL3P	ATHL1	C1S
CD79B	COL5A2	COL4A1	ATP6V0D1	ATP5G1	PTGDR	CD3E	TNFSF8	CST7	ALOX5AP	IGLL5	ATP2A3	CALCRL
CD82	COL6A1	COL4A2	ATP6V1B2	ATP5G2	SH2D1B	CD3G		CTSW	AMICA1	IGSF6	ATP8A1	CALD1
CHMP7	COL6A2	CRIP2	BCL2A1	ATP6V0E2	XCL1	CD5		CXCL13	ANKRD22	IKZF1	BANK1	CCDC80
CIITA	COL6A3	CXorf36	BID	ATP6V1C1		CD6		CXCR6	ANKRD44	IKZF3	BCL11A	CCL14
CLEC17A	COL8A1	CYYR1	BLVRA	ATP6V1E1		CD7		DTHD1	AOAH	IL10RA	BCL11B	CD200
CNR2	CREB3L1	DARC	BLVRB	ATP6V1G1		CD8A		DUSP2	AP1B1	IL12RB1	BIRC3	CD248
COL19A1	CXCL14	DCHS1	C11orf75	AZGP1		CD8B		EOMES	APOBEC3C	IL16	BLK	CD34
COL4A3	CYBRD1	DOCK6	C15orf48	BAIAP2		CD96		FASLG	APOBEC3D	IL18	BLNK	CD93
CR2	DCN	DOCK9	C19orf38	BANCR		CDC42SE2		FYN	APOBEC3G	IL1B	BTLA	CDH11
CXCR5	DPT	DYSF	C1orf162	BCAN		CELF2		GPR171	AQP3	IL1RN	BTN3A1	CDH5
ELK2AP	EFEMP2	ECE1	C1QA	BCAS3		CLEC2D		GZMA	AQP9	IL2RB	BTN3A2	CERCAM
FAIM3	FBLN1	ECSCR	C1QB	BCHE		CNOT6L		GZMB	ARAP2	IL2RG	C16orf54	CFI
FAM129C	FBLN5	EGFL7	C1QC	BIRC7		CST7		GZMH	ARHGAP15	IL32	CBLB	CLDN5
FCER2	FGF7	ELK3	C2	BZW2		CTLA4		GZMK	ARHGAP30	IL4I1	CCL4	CLEC14A
FCRL1	GPR176	ELTD1	C3AR1	C10orf90		CTSW		ID2	ARHGAP4	IL6R	CCL4L1	COL12A1
FCRL2	HSPB6	EMCN	C5AR1	C11orf31		CXCL13		IFNG	ARHGAP9	IL7R	CCL4L2	COL14A1
FCRL5	INHBA	ENG	C9orf72	C12orf76		CXCR3		IKZF3	ARHGDIB	IL8	CCL5	COL15A1
FCRLA	ISLR	EPAS1	CAPG	C17orf89		CXCR6		IL2RB	ARHGEF1	INPP4B	CCR4	COL1A1
HLA-DOB	ITGA11	EPHB4	CARD9	C1orf43		DEF6		ITGA4	ARPC3	INPP5D	CCR6	COL1A2
HLA-DQA2	LOX	ERG	CASP1	C1orf85		DENND2D		ITGB7	ARRB2	IPCEF1	CCR7	COL3A1
HVCN1	LPAR1	ESAM	CCR1	C4orf48		DGKA		JAKMIP1	ASB2	IRF5	CD19	COL4A1
IGLL1	LTBP2	FGD5	CCR2	CA14		DTHD1		KIR2DL4	ATF5	IRF8	CD1C	COL4A2
IGLL3P	LUM	FKBP1A	CD14	CA8		DUSP2		KLRC1	ATG3	ISG20	CD2	COL5A1
IGLL5	MAP1A	FLT4	CD163	CACYBP		EMB		KLRC2	ATG7	ITGA4	CD22	COL5A2
IRF8	MEG3	GALNT18	CD274	CAPN3		EVL		KLRC3	ATHL1	ITGAL	CD24	COL6A1
KBTBD8	MIR100HG	GPR116	CD300C	CBX3		FASLG		KLRC4	ATP2A3	ITGAM	CD244	COL6A2
KIAA0125	MRC2	HERC2P2	CD300E	CCDC47		FYN		KLRC4-KLRK1	ATP6V0B	ITGAX	CD247	COL6A3

Table 3. Cell type signatures that were derived from the analysis of the scRNA-seq data (see section Data-driven signatures of specific cell-types).

B cell	CAF	Endothelial cell	Macrophage	Malignant cell	NK cell	T cell	CD4 T cell	CD8 T cell	Immune cell		Lymphocyte	Stroma cell
KIAA0226L	MXRA8	HSPG2	CD300LB	CCND1		GATA3		KLRD1	ATP6V0D1	ITGB2	CD27	COL8A1
LOC283663	MYL9	HYAL2	CD300LF	CCT2		GPR171		KLRK1	ATP6V1B2	ITGB7	CD28	CREB3L1
LRMP	NID2	ICA1	CD302	CCT3		GPR174		LAG3	ATP8A1	ITK	CD37	CRIP2
LTB	OLFML3	ID1	CD33	CCT6A		GPRIN3		LOC100506776	BANK1	JAK3	CD3D	CXCL14
MS4A1	PALLD	IL3RA	CD4	CCT8		GRAP2		LYST	BCL11A	JAKMIP1	CD3E	CXorf36
NAPSB	PCDH18	ITGB4	CD68	CDH19		GZMA		MIR155HG	BCL11B	KBTBD8	CD3G	CYBRD1
NCOA3	PCOLCE	KDR	CD80	CDH3		GZMB		NELL2	BCL2A1	KCNMA1	CD4	CYYR1
P2RX5	PDGFRA	LAMA5	CD86	CDK2		GZMH		NKG7	BID	KIAA0125	CD40LG	DARC
PAX5	PDGFRB	LDB2	CECR1	CHCHD6		GZMK		OASL	BIN2	KIAA0226L	CD5	DCHS1
PLEKHF2	PDGFRL	LOC100505495	CFP	CITED1		GZMM		PARP8	BIRC3	KIR2DL4	CD52	DCN
PNOC	PLAC9	MALL	CLEC10A	CLCN7		HNRNPA1P10		PDCD1	BLK	KLRB1	CD6	DOCK6
POLD4	PODN	MMRN1	CLEC12A	CLNS1A		ICOS		PIP4K2A	BLNK	KLRC1	CD69	DOCK9
POU2AF1	PRRX1	MMRN2	CLEC4A	CMC2		IFNG		PRF1	BLVRA	KLRC2	CD7	DPT
POU2F2	RARRES2	MYCT1	CLEC4E	COA6		IKZF1		PRKCH	BLVRB	KLRC3	CD79A	DYSF
QRSL1	RCN3	NOS3	CLEC5A	COX5B		IKZF3		PSTPIP1	BTK	KLRC4	CD79B	ECE1
RALGPS2	SDC2	NOTCH4	CLEC7A	COX7A2		IL12RB1		PTPN22	BTLA	KLRC4-KLRK1	CD82	ECSCR
RPL13	SFRP2	NPDC1	CMKLR1	COX7C		IL2RB		PVRIG	BTN3A1	KLRD1	CD8A	EFEMP2
RPS20	SLIT3	PALMD	CNPY3	CRYL1		IL2RG		PYHIN1	BTN3A2	KLRF1	CD8B	EGFL7
RPS23	SMOC2	PCDH17	COTL1	CSAG1		IL32		RAB27A	C11orf75	KLRK1	CD96	EHD2
SEL1L3	SPOCK1	PDE2A	CPVL	CSAG2		IL7R		RARRES3	C15orf48	KYNU	CDC42SE2	ELK3
SELL	SULF1	PDLIM1	CREG1	CSAG3		INPP4B		RUNX3	C16orf54	LAG3	CELF2	ELTD1
SMIM14	SVEP1	PECAM1	CSF1R	CSPG4		IPCEF1		SAMD3	C19orf38	LAIR1	CHMP7	EMCN
SNX29	TAGLN	PLVAP	CSF2RA	CTNNB1		ITGAL		SH2D1A	C1orf162	LAPTM5	CIITA	ENG
SNX29P1	THBS2	PLXND1	CSF3R	CYC1		ITK		SLA2	C1QA	LAT	CLEC17A	EPAS1
SPIB	THY1	PODXL	CSTA	CYP27A1		JAK3		SLAMF6	C1QB	LAT2	CLEC2D	EPHB4
ST6GAL1	TMEM119	PRCP	CTSB	DAAM2		JAKMIP1		SYTL3	C1QC	LBH	CNOT6L	ERG
STAG3	TPM1	PREX2	CTSC	DANCR		KLRC4		TARP	C2	LCK	CNR2	ESAM
STAP1	TPM2	PTPRB	CTSD	DAP3		KLRD1		THEMIS	C3AR1	LCP1	COL19A1	FBLN1
TCL1A		PVRL2	CTSH	DCT		KLRK1		TIGIT	C5AR1	LCP2	COL4A3	FBLN5
TLR10		RAMP2	CTSS	DCXR		LAG3		TNFRSF9	C9orf72	LEPROTL1	CORO1A	FBN1
TMEM154		RAMP3	CXCL10	DDIT3		LAT		TNIP3	CAPG	LGALS2	CR2	FGD5
TNFRSF13B		RHOJ	CXCL16	DDT		LCK		TOX	CARD9	LGMN	CRTAM	FGF7

Table 3. Cell type signatures that were derived from the analysis of the scRNA-seq data (see section Data-driven signatures of specific cell-types).

B cell	CAF	Endothelial cell	Macrophage	Malignant cell	NK cell	T cell	CD4 T cell	CD8 T cell	Immune cell		Lymphocyte	Stroma cell
VPREB3		ROBO4	CXCL9	DFNB31		LEPROTL1		TTC24	CASP1	LILRA1	CST7	FKBP1A
WDFY4		S1PR1	CXCR2P1	DLL3		LIME1		WIPF1	CBLB	LILRA2	CTLA4	FLT4
ZCCHC7		SDPR	CYBB	DNAH14		LOC100130231		XCL1	CCL3	LILRA3	CTSW	FSTL1
		SELP	CYP2S1	DNAJA4		MAP4K1		XCL2	CCL4	LILRA5	CXCL13	GALNT18
		SHROOM4	DAPK1	DSCR8		MIAT			CCL4L1	LILRA6	CXCR3	GNG11
		SLCO2A1	DHRS9	DUSP4		NELL2			CCL4L2	LILRB1	CXCR4	GPR116
		SMAD1	DMXL2	EDNRB		NKG7			CCL5	LILRB2	CXCR5	GPR176
		STOM	DNAJC5B	EIF3C		NLRC3			CCR1	LILRB3	CXCR6	HERC2P2
		SYNPO	EBI3	EIF3D		NLRC5			CCR2	LILRB4	CYFIP2	HSPB6
		TAOK2	EMR2	EIF3E		OXNAD1			CCR4	LILRB5	CYTIP	HSPG2
		TEK	EPSTI1	EIF3H		PAG1			CCR6	LIMD2	DEF6	HYAL2
		TENC1	F13A1	EIF3L		PARP8			CCR7	LIME1	DENND2D	ICA1
		TGFBR2	FAM157B	ENO1		PCED1B			CD14	LIPA	DGKA	ID1
		TGM2	FAM26F	ENO2		PCED1B-AS1			CD163	LITAF	DTHD1	ID3
		THBD	FBP1	ENTHD1		PDCD1			CD19	LOC100130231	DUSP2	IFITM3
		TIE1	FCER1G	ENTPD6		PIK3IP1			CD1C	LOC100506776	ELK2AP	IGFBP4
		TM4SF1	FCGR1A	ERBB3		PIM2			CD2	LOC283663	EMB	IGFBP7
		TM4SF18	FCGR1B	ESRP1		PIP4K2A			CD22	LOC729737	EOMES	IL3RA
		TMEM255B	FCGR1C	ETV4		PPP2R5C			CD24	LPXN	EVL	INHBA
		TSPAN18	FCGR2A	ETV5		PRDM1			CD244	LRMP	EZR	ISLR
		TSPAN7	FCGR2C	EXOSC4		PRF1			CD247	LRRC25	F5	ITGA11
		VWF	FCN1	EXTL1		PRKCQ			CD27	LSP1	FAAH2	ITGA5
		ZNF385D	FGL2	FAHD2B		PSTPIP1			CD274	LST1	FAIM3	ITGB4
			FOLR2	FAM103A1		PTPN22			CD28	LTA4H	FAM129C	KDR
			FPR1	FAM178B		PTPN7			CD300A	LTB	FAM65B	LAMA5
			FPR2	FANCL		PVRIG			CD300C	LY86	FASLG	LAMB1
			FPR3	FARP2		PYHIN1			CD300E	LY9	FCER2	LDB2
			FTH1	FASN		RAB27A			CD300LB	LYN	FCRL1	LOC100505495
			FTL	FBXO32		RAPGEF6			CD300LF	LYST	FCRL2	LOX
			FUCA1	FBXO7		RARRES3			CD302	LYZ	FCRL3	LPAR1
			FUOM	FDFT1		RASAL3			CD33	M6PR	FCRL5	LTBP2
			GABARAP	FKBP4		RASGRP1			CD37	MAFB	FCRLA	LUM

Table 3. Cell type signatures that were derived from the analysis of the scRNA-seq data (see section Data-driven signatures of specific cell-types).

B cell	CAF	Endothelial cell	Macrophage	Malignant cell	NK cell	T cell	CD4 T cell	CD8 T cell	Immune cell		Lymphocyte	Stroma cell
			GATM	FMN1		RGS1			CD38	MAN2B1	FOXP3	MALL
			GBP1	FXYD3		RHOF			CD3D	MAP4K1	FYB	MAP1A
			GCA	GALE		RNF213			CD3E	1-Mar	FYN	MEG3
			GK	GAPDH		RUNX3			CD3G	MARCO	GATA3	MIR100HG
			GLA	GAPDHS		SCML4			CD4	MFSD1	GNLY	MMP2
			GLRX	GAS2L3		SEMA4D			CD40LG	MIAT	GPR171	MMRN1
			GLUL	GAS5		1-Sep			CD48	MILR1	GPR174	MMRN2
			GM2A	GAS7		SH2D1A			CD5	MIR155HG	GPRIN3	MRC2
			GNA15	GDF15		SH2D2A			CD52	MNDA	GRAP2	MXRA8
			GPBAR1	GJB1		SIRPG			CD53	MOB1A	GZMA	MYCT1
			GPR34	GPATCH4		SIT1			CD6	MPEG1	GZMB	MYL9
			GPR84	GPM6B		SKAP1			CD68	MPP1	GZMH	NFIB
			GPX1	GPNMB		SLA2			CD69	MS4A1	GZMK	NID2
			GRN	GPR137B		SPATA13			CD7	MS4A4A	GZMM	NNMT
			HCAR2	GPR143		SPN			CD72	MS4A6A	HLA-DOB	NOS3
			HCAR3	GPS1		SPOCK2			CD74	MS4A7	HLA-DQA2	NOTCH4
			HCK	GSTP1		STAT4			CD79A	MSR1	HMHA1	NPDC1
			HK2	GYG2		SYTL3			CD79B	MTMR14	HNRNPA1P10	OLFML3
			HK3	H2AFZ		TARP			CD80	MYD88	HOPX	PALLD
			HLA-DMA	HAX1		TBC1D10C			CD82	MYO1F	HSH2D	PALMD
			HLA-DMB	HIST1H2BD		TC2N			CD83	NAAA	HVCN1	PCDH17
			HLA-DPA1	HIST3H2A		TESPA1			CD84	NADK	ICOS	PCDH18
			HLA-DPB1	HMG20B		THEMIS			CD86	NAGA	ID2	PCOLCE
			HLA-DPB2	HMGA1		TIGIT			CD8A	NAGK	IFNG	PDE2A
			HLA-DRA	HPGD		TNFAIP3			CD8B	NAIP	IGLL1	PDGFRA
			HLA-DRB1	HPS4		TNFRSF9			CD96	NAPSB	IGLL3P	PDGFRB
			HLA-DRB5	HPS5		TOX			CD97	NCAM1	IGLL5	PDGFRL
			HLA-DRB6	HSP90AA1		TRAF1			CDC42SE2	NCF1	IKZF1	PDLIM1
			HMOX1	HSP90AB1		TRAT1			CECR1	NCF1B	IKZF3	PECAM1
			HSPA6	HSPA9		TTC39C			CELF2	NCF1C	IL12RB1	PLAC9
			HSPA7	HSPD1		UBASH3A			CFP	NCF2	IL16	PLVAP
			IFI30	HSPE1		WIPF1			CHMP7	NCF4	IL2RB	PLXND1
			IFNGR	IGSF11		ZAP70			CIITA	NCKAP	IL2RG	PODN

Table 3. Cell type signatures that were derived from the analysis of the scRNA-seq data (see section Data-driven signatures of specific cell-types).

B cell	CAF	Endothelial cell	Macrophage	Malignant cell	NK cell	T cell	CD4 T cell	CD8 T cell	Immune cell		Lymphocyte	Stroma cell
			1							1L		
			IFNGR2	IGSF3		ZC3HAV1			CLEC10A	NCOA3	IL32	PODXL
			IGFLR1	IGSF8					CLEC12A	NCOA4	IL6R	PPIC
			IGSF6	INPP5F					CLEC17A	NELL2	IL7R	PRCP
			IL18	IRF4					CLEC2D	NFAM1	INPP4B	PREX2
			IL1B	ISYNA1					CLEC4A	NINJ1	IPCEF1	PRRX1
			IL1RN	KCNJ13					CLEC4E	NKG7	IRF8	PTPRB
			IL4I1	LAGE3					CLEC5A	NLRC3	ISG20	PTRF
			IL8	LDHB					CLEC7A	NLRC4	ITGA4	PVRL2
			IRF5	LDLRAD3					CMKLR1	NLRC5	ITGAL	PXDN
			KCNMA1	LEF1-AS1					CNOT6L	NLRP3	ITGB7	RAMP2
			KYNU	LHFPL3-AS1					CNPY3	NMI	ITK	RAMP3
			LAIR1	LINC00473					CNR2	NPC2	JAK3	RARRES2
			LGALS2	LINC00518					COL19A1	NPL	JAKMIP1	RCN3
			LGMN	LINC00673					COL4A3	OAS1	KBTBD8	RHOJ
			LILRA1	LOC100126784					CORO1A	OASL	KIAA0125	ROBO4
			LILRA2	LOC100127888					COTL1	OAZ1	KIAA0226L	S1PR1
			LILRA3	LOC100130370					CPVL	OLR1	KIR2DL4	SDC2
			LILRA5	LOC100133445					CR2	OSCAR	KLRB1	SDPR
			LILRA6	LOC100505865					CREG1	OXNAD1	KLRC1	SELP
			LILRB1	LOC146481					CRTAM	P2RX5	KLRC2	SFRP2
			LILRB2	LOC340357					CSF1R	P2RY12	KLRC3	SHROOM4
			LILRB3	LONP2					CSF2RA	P2RY13	KLRC4	SLCO2A1
			LILRB4	LOXL4					CSF3R	PAG1	KLRC4-KLRK1	SLIT3
			LILRB5	LZTS1					CST7	PAK1	KLRD1	SMAD1
			LIPA	MAGEA1					CSTA	PARP15	KLRF1	SMOC2
			LOC729737	MAGEA12					CTLA4	PARP8	KLRK1	SPARC
			LRRC25	MAGEA2					CTSB	PARVG	LAG3	SPARCL1
			LST1	MAGEA2B					CTSC	PASK	LAT	SPOCK1
			LTA4H	MAGEA3					CTSD	PAX5	LBH	STOM
			LYZ	MAGEA4					CTSH	PBXIP1	LCK	SULF1
			MAFB	MAGEA6					CTSS	PCED1B	LEPROTL1	SVEP1

Table 3. Cell type signatures that were derived from the analysis of the scRNA-seq data (see section Data-driven signatures of specific cell-types).

B cell	CAF	Endothelial cell	Macrophage	Malignant cell	NK cell	T cell	CD4 T cell	CD8 T cell	Immune cell		Lymphocyte	Stroma cell
			MAN2B1	MAGEC1					CTSW	PCED1B-AS1	LIMD2	SYNPO
			MARCO	MDH1					CXCL10	PCK2	LIME1	TAGLN
			MFSD1	MDH2					CXCL13	PDCD1	LOC100130231	TAOK2
			MILR1	MFI2					CXCL16	PIK3AP1	LOC100506776	TEK
			MNDA	MFSD12					CXCL9	PIK3IP1	LOC283663	TENC1
			MOB1A	MIA					CXCR2P1	PIK3R5	LRMP	TGFBR2
			MPEG1	MIF					CXCR3	PILRA	LTB	TGM2
			MPP1	MITF					CXCR4	PIM2	LY9	THBD
			MS4A4A	MLANA					CXCR5	PION	LYST	THBS2
			MS4A6A	MLPH					CXCR6	PIP4K2A	MAP4K1	THY1
			MS4A7	MOK					CYBA	PLA2G7	MIAT	TIE1
			MSR1	MRPS21					CYBB	PLAC8	MIR155HG	TM4SF1
			MTMR14	MRPS25					CYFIP2	PLAUR	MS4A1	TM4SF18
			MYD88	MRPS26					CYP2S1	PLBD1	NAPSB	TMEM119
			NAAA	MRPS6					CYTH4	PLCB2	NCAM1	TMEM255B
			NADK	MSI2					CYTIP	PLEK	NCOA3	TPM1
			NAGA	MXI1					DAPK1	PLEKHA2	NELL2	TPM2
			NAGK	MYO10					DAPP1	PLEKHF2	NKG7	TSPAN18
			NAIP	NAV2					DEF6	PLEKHO1	NLRC3	TSPAN7
			NCF2	NDUFA4					DENND2D	PLIN2	NLRC5	VWF
			NCF4	NDUFB9					DGKA	PNOC	OASL	ZNF385D
			NCOA4	NDUFS2					DHRS9	POLD4	OXNAD1	
			NFAM1	NEDD4L					DMXL2	POU2AF1	P2RX5	
			NINJ1	NELFCD					DNAJC5B	POU2F2	PAG1	
			NLRC4	NHP2					DOCK2	PPM1K	PARP15	
			NLRP3	NME1					DOCK8	PPP2R5C	PARP8	
			NMI	NOP58					DOK2	PPT1	PASK	
			NPC2	NPM1					DOK3	PRAM1	PAX5	
			NPL	NSG1					DTHD1	PRDM1	PBXIP1	
			OAS1	NT5C3					DUSP2	PRF1	PCED1B	
			OAZ1	NT5DC3					EBI3	PRKCB	PCED1B-AS1	
			OLR1	OSTM1					ELK2AP	PRKCD	PDCD1	

Table 3. Cell type signatures that were derived from the analysis of the scRNA-seq data (see section Data-driven signatures of specific cell-types).

B cell	CAF	Endothelial cell	Macrophage	Malignant cell	NK cell	T cell	CD4 T cell	CD8 T cell	Immune cell		Lymphocyte	Stroma cell
			OSCAR	PACSIN2					EMB	PRKCH	PIK3IP1	
			P2RY12	PAGE5					EMR2	PRKCQ	PIM2	
			P2RY13	PAICS					EOMES	PSAP	PIP4K2A	
			PAK1	PAX3					EPSTI1	PSMB10	PLAC8	
			PCK2	PEBP1					EVI2A	PSTPIP1	PLEKHA2	
			PILRA	PEG10					EVI2B	PTAFR	PLEKHF2	
			PLA2G7	PFDN2					EVL	PTGDR	PNOC	
			PLAUR	PHB					EZR	PTK2B	POLD4	
			PLBD1	PHLDA1					F13A1	PTPN22	POU2AF1	
			PLEKHO1	PIGY					F5	PTPN6	POU2F2	
			PLIN2	PIR					FAAH2	PTPN7	PPM1K	
			PPT1	PLEKHB1					FAIM3	PTPRC	PPP2R5C	
			PRAM1	PLP1					FAM105A	PTPRCAP	PRDM1	
			PRKCD	PMEL					FAM129C	PVRIG	PRF1	
			PSAP	POLR2F					FAM157B	PYCARD	PRKCH	
			PTAFR	PPIL1					FAM26F	PYHIN1	PRKCQ	
			PYCARD	PRAME					FAM49B	QRSL1	PSTPIP1	
			RAB20	PSMB4					FAM65B	RAB20	PTGDR	
			RASSF4	PSMD4					FASLG	RAB27A	PTPN22	
			RBM47	PUF60					FBP1	RAC2	PTPN7	
			RELT	PYGB					FCER1G	RALGPS2	PTPRC	
			RGS10	PYURF					FCER2	RAPGEF6	PTPRCAP	
			RGS18	QDPR					FCGR1A	RARRES3	PVRIG	
			RGS19	RAB17					FCGR1B	RASAL3	PYHIN1	
			RGS2	RAB38					FCGR1C	RASGRP1	QRSL1	
			RHBDF2	RAN					FCGR2A	RASSF4	RAB27A	
			RILPL2	RAP1GAP					FCGR2C	RASSF5	RAC2	
			RIPK2	RGS20					FCGR3A	RBM47	RALGPS2	
			RNASE6	ROPN1					FCGR3B	RCSD1	RAPGEF6	
			RNASET2	ROPN1B					FCN1	RELT	RARRES3	
			RNF13	RPL38					FCRL1	RGS1	RASAL3	
			RNF130	RPS6KA5					FCRL2	RGS10	RASGRP1	

Table 3. Cell type signatures that were derived from the analysis of the scRNA-seq data (see section Data-driven signatures of specific cell-types).

B cell	CAF	Endothelial cell	Macrophage	Malignant cell	NK cell	T cell	CD4 T cell	CD8 T cell	Immune cell		Lymphocyte	Stroma cell
			RNF144B	RSL1D1					FCRL3	RGS18	RGS1	
			RTN1	RTKN					FCRL5	RGS19	RHOF	
			S100A8	S100A1					FCRLA	RGS2	RHOH	
			S100A9	S100B					FERMT3	RHBDF2	RNF213	
			SAMHD1	SCD					FGD2	RHOF	RPL13	
			SAT1	SDC3					FGD3	RHOG	RPS20	
			SDS	SEC11C					FGL2	RHOH	RPS23	
			SECTM1	SEMA3B					FGR	RILPL2	RUNX3	
			SEMA4A	SERPINA3					FOLR2	RIPK2	SAMD3	
			SERPINA1	SERPINE2					FOXP3	RNASE6	SCML4	
			SIGLEC1	SGCD					FPR1	RNASET2	SEL1L3	
			SIGLEC5	SGK1					FPR2	RNF13	SELL	
			SIGLEC9	SHC4					FPR3	RNF130	SEMA4D	
			SIRPB1	SLC19A2					FTH1	RNF144B	1-Sep	
			SIRPB2	SLC24A5					FTL	RNF213	SH2D1A	
			SLAMF8	SLC25A13					FUCA1	RPL13	SH2D1B	
			SLC11A1	SLC25A4					FUOM	RPS20	SH2D2A	
			SLC15A3	SLC26A2					FYB	RPS23	SIRPG	
			SLC1A3	SLC3A2					FYN	RPS6KA1	SIT1	
			SLC29A3	SLC45A2					GABARAP	RTN1	SKAP1	
			SLC31A2	SLC5A3					GATA3	RUNX3	SLA2	
			SLC7A7	SLC6A15					GATM	S100A8	SLAMF1	
			SLCO2B1	SLC7A5					GBP1	S100A9	SLAMF6	
			SMPDL3A	SNCA					GBP5	SAMD3	SMIM14	
			SNX10	SNHG16					GCA	SAMHD1	SNX29	
			SOD2	SNHG6					GK	SAMSN1	SNX29P1	
			SPI1	SNRPC					GLA	SASH3	SP140	
			SPINT2	SNRPD1					GLRX	SAT1	SPATA13	
			STAT1	SNRPE					GLUL	SCIMP	SPIB	
			STX11	SOD1					GM2A	SCML4	SPN	
			TBXAS1	SORD					GNA15	SDS	SPOCK2	
			TGFBI	SORT1					GNLY	SECTM1	ST6GAL1	

Table 3. Cell type signatures that were derived from the analysis of the scRNA-seq data (see section Data-driven signatures of specific cell-types).

B cell	CAF	Endothelial cell	Macrophage	Malignant cell	NK cell	T cell	CD4 T cell	CD8 T cell	Immune cell		Lymphocyte	Stroma cell
			THEMIS2	SOX10					GPBAR1	SEL1L3	STAG3	
			TIFAB	SPCS1					GPR171	SELL	STAP1	
			TLR1	SPRY4					GPR174	SELPLG	STAT4	
			TLR2	ST13					GPR183	SEMA4A	STK17B	
			TLR5	ST3GAL4					GPR34	SEMA4D	STK4	
			TLR8	ST3GAL6					GPR84	1-Sep	SYTL3	
			TMEM106A	ST3GAL6-AS1					GPRIN3	SERPINA1	TARP	
			TMEM176A	ST6GALNAC2					GPSM3	SH2D1A	TBC1D10C	
			TMEM176B	STIP1					GPX1	SH2D1B	TC2N	
			TMEM37	STK32A					GRAP2	SH2D2A	TCF7	
			TNFAIP2	STMN1					GRB2	SIGLEC1	TCL1A	
			TNFAIP8L2	STX7					GRN	SIGLEC14	TESPA1	
			TNFSF13	STXBP1					GZMA	SIGLEC5	THEMIS	
			TNFSF13B	SYNGR1					GZMB	SIGLEC7	TIGIT	
			TPP1	TBC1D7					GZMH	SIGLEC9	TLR10	
			TREM1	TBCA					GZMK	SIRPB1	TMC8	
			TREM2	TEX2					GZMM	SIRPB2	TMEM154	
			TWF2	TFAP2A					HAVCR2	SIRPG	TNFAIP3	
			TYMP	TFAP2C					HCAR2	SIT1	TNFRSF13B	
			TYROBP	TMEM147					HCAR3	SKAP1	TNFRSF9	
			UBE2D1	TMEM14B					HCK	SLA	TNFSF8	
			VAMP8	TMEM177					HCLS1	SLA2	TNIP3	
			VMO1	TMEM251					HCST	SLAMF1	TOX	
			VSIG4	TMX4					HK2	SLAMF6	TRAF1	
			ZNF385A	TNFRSF21					HK3	SLAMF7	TRAF3IP3	
				TOM1L1					HLA-DMA	SLAMF8	TRAT1	
				TOMM20					HLA-DMB	SLC11A1	TSC22D3	
				TOMM22					HLA-DOB	SLC15A3	TTC24	
				TOMM6					HLA-DPA1	SLC1A3	TTC39C	
				TOMM7					HLA-DPB1	SLC29A3	UBASH3A	
				TOP1MT					HLA-DPB2	SLC31A2	VPREB3	
				TRIB2					HLA-DQA1	SLC7A7	WDFY4	

Table 3. Cell type signatures that were derived from the analysis of the scRNA-seq data (see section Data-driven signatures of specific cell-types).

B cell	CAF	Endothelial cell	Macrophage	Malignant cell	NK cell	T cell	CD4 T cell	CD8 T cell	Immune cell		Lymphocyte	Stroma cell
				TRIM2					HLA-DQA2	SLCO2B1	WIPF1	
				TRIM63					HLA-DQB1	SMAP2	XCL1	
				TRIML2					HLA-DQB2	SMIM14	XCL2	
				TRMT112					HLA-DRA	SMPDL3A	ZAP70	
				TSNAX					HLA-DRB1	SNX10	ZC3HAV1	
				TTLL4					HLA-DRB5	SNX20	ZCCHC7	
				TTYH2					SNX29	TMEM176A		
				TUBB2B					SNX29P1	TMEM176B		
				TUBB4A					SOD2	TMEM37		
				TYR					SP140	TNFAIP2		
				TYRP1					SPATA13	TNFAIP3		
				UBL3					SPI1	TNFAIP8		
				UQCRH					SPIB	TNFAIP8L2		
				UTP18					SPINT2	TNFRSF13B		
				VAT1					SPN	TNFRSF9		
				VDAC1					SPOCK2	TNFSF13		
				VPS72					SRGN	TNFSF13B		
				WBSCR22					ST6GAL1	TNFSF8		
				XAGE1A					STAG3	TNIP3		
				XAGE1B					STAP1	TOX		
				XAGE1C					STAT1	TPP1		
				XAGE1D					STAT4	TRAF1		
				XAGE1E					STK17B	TRAF3IP3		
				XRCC6					STK4	TRAT1		
				XYLB					STX11	TREM1		
				ZCCHC17					STXBP2	TREM2		
				ZFAS1					SYK	TSC22D3		
				ZFP106					SYTL3	TTC24		
				ZNF280B					TAGAP	TTC39C		
				ZNF330					TARP	TWF2		
				ZNF692					TBC1D10C	TYMP		
									TBXAS1	TYROBP		

Table 3. Cell type signatures that were derived from the analysis of the scRNA-seq data (see section Data-driven signatures of specific cell-types).

B cell	CAF	Endothelial cell	Macrophage	Malignant cell	NK cell	T cell	CD4 T cell	CD8 T cell	Immune cell		Lymphocyte	Stroma cell
									TC2N	UBASH3A		
									TCF7	UBE2D1		
									TCL1A	UCP2		
									TESPA1	VAMP8		
									TGFBI	VAV1		
									THEMIS	VMO1		
									THEMIS2	VPREB3		
									TIFAB	VSIG4		
									TIGIT	WDFY4		
									TLR1	WIPF1		
									TLR10	XCL1		
									TLR2	XCL2		
									TLR5	ZAP70		
									TLR8	ZC3HAV1		
									TMC8	ZCCHC7		
									TMEM106A	ZNF385A		
									TMEM154			

Table 4

Table 4. The ICR signatures of the different immune cell types: B-cells, macrophages, CD4 and CD8 T cells.

CD8-T-cell-up	CD8-T-cell-down	macrophage-up	macrophage-down	B-cell-up	B-cell-down	CD4-T-cell-up	CD4-T-cell-down
CEP19	ACP5	APOL1	A2M	C6orf62	MTRNR2L1	PRDM1	CHI3L2
EXO5	AKNA	CD274	ADAP2	CDC42	MTRNR2L10		RPL13A
FAM153C	BTN3A2	CSTB	ADORA3	CNN2	MTRNR2L3		
FCRL6	CCDC141	DCN	ARL4C	FOXP1	MTRNR2L4		
GBP2	CD27	HLA-DPB2	ASPH	FYB	RGS2		
GBP5	CDC42SE1	HLA-DQA1	BCAT1	GRB2			
HSPA1B	DDIT4	HLA-G	C11orf31				
IER2	FAU	HSPA8	C3				
IRF1	FKBP5	HSPB1	C3AR1				
KLRK1	GPR56	IL18BP	C6orf62				
LDHA	HAVCR2	TMEM176A	CAPN2				
LOC100506083	HLA-B	UBD	CD200R1				
MBOAT1	HLA-C		CD28				
SEMA4D	HLA-F		CD9				
SIRT3	IL6ST		CD99				
SPDYE2	ITGA4		COMT				
SPDYE2L	KIAA1551		CREM				

STAT1	KLF12		CRTAP				
STOM	MIR155HG		CYFIP1				
UBE2Q2P3	MTA2		DDOST				
	MTRNR2L1		DHRS3				
	MTRNR2L3		EGFL7				
	PIK3IP1		EIF1AY				
	RPL26		ETS2				
	RPL27		FCGR2A				
	RPL27A		FOLR2				
	RPL35A		GATM				
	RPS11		GBP3				
	RPS16		GNG2				
	RPS20		GSTT1				
	RPS26		GYPC				
	SPOCK2		HIST1H1E				
	SYTL3		HPGDS				
	TOB1		IFI44L				
	TPT1		IGFBP4				
	TTN		ITGA4				
	TXNIP		KCTD12				
	WNK1		LGMN				
	ZFP36L2		LOC441081				
			LTC4S				
			LYVE1				
			MERTK				
			METTL7B				
			MS4A4A				
			MS4A7				
			MTSS1				
			NLRP3				
			OLFML3				
			PLA2G15				
			PLXDC2				
			PMP22				
			POR				
			PRDX2				
			PTGS1				
			RNASE1				
			ROCK1				
			RPS4Y1				
			S100A9				
			SCAMP2				
			SEPP1				
			SESN1				
			SLC18B1				
			SLC39A1				
			SLC40A1				
			SLC7A8				
			SORL1				
			SPP1				
			STAB1				
			TMEM106C				
			TMEM86A				
			TMEM9				
			TNFRSF1B				
			TNFRSF21				
			TPD52L2				
			ULK3				
			ZFP36L2				

Table 5

Table 5. The oncogenic resistance signatures: oncogenic-ICR, exclusion, uICR, and the refined uICR.		
Genes up-regulated in ICR malignant cells (1 denotes the gene is included in the signature, and 0 otherwise)		**Genes down-regulated in ICR malignant cells (1 denotes the gene is included in the signature, and 0 otherwise)**

uICR-up genes (immune resistance)	oncogenic-ICR-up (post treatment)	Exclusion-up	uICR-up (refined)		uICR-down genes	oncogenic-ICR-down	Exclusion-down	uICR-down (refined)
ACAT1	0	1	0		A2M	1	1	0
ACP5	0	1	0		ACSL3	1	0	0
ACTB	1	0	0		ACSL4	1	0	0
ACTG1	0	1	0		ADM	1	0	0
ADSL	0	1	0		AEBP1	1	0	1
AEN	1	0	0		AGA	1	1	0
AK2	0	1	0		AHNAK	1	1	1
ANP32E	1	0	0		ANGPTL4	1	0	0
APP	0	1	0		ANXA1	1	1	0
ASAP1	0	1	0		ANXA2	1	0	0
ATP5A1	1	0	0		APLP2	1	1	0
ATP5D	0	1	0		APOC2	0	1	1
ATP5G2	1	0	0		APOD	1	0	1
BANCR	0	1	0		APOE	1	0	1
BCAN	0	1	0		ARF5	0	1	0
BZW2	1	1	0		ARL6IP5	1	0	0
C17orf76-AS1	1	1	0		ATF3	1	0	0
C1QBP	1	1	1		ATP1A1	1	1	0
C20orf112	1	0	0		ATP1B1	1	1	0
C6orf48	0	1	0		ATP1B3	1	0	0
CA14	1	1	0		ATRAID	0	1	0
CBX5	1	0	0		B2M	1	1	1
CCT2	1	0	1		BACE2	1	0	0
CCT3	1	1	0		BBX	1	0	0
CCT6A	0	1	1		BCL6	1	0	0
CDK4	1	0	0		C10orf54	0	1	1
CEP170	0	1	0		C4A	0	1	0
CFL1	1	0	0		CALU	1	0	0
CHP1	0	1	0		CASP1	1	0	0
CNRIP1	1	0	0		CAST	1	0	0
CRABP2	1	0	0		CAV1	1	0	0
CS	1	0	0		CBLB	0	1	0
CTPS1	1	1	0		CCND3	1	1	0
CYC1	0	1	0		CD151	1	1	0
DAP3	0	1	0		CD44	1	0	0
DCAF13	1	0	1		CD47	1	1	0
DCT	1	1	0		CD58	1	1	0
DDX21	0	1	0		CD59	1	1	0
DDX39B	1	0	0		CD63	1	0	1
DLL3	1	0	0		CD9	1	0	0
EDNRB	0	1	0		CDH19	1	1	0
EEF1D	0	1	0		CHI3L1	1	0	0
EEF1G	1	1	0		CHN1	0	1	0
EEF2	0	1	0		CLIC4	1	0	0
EIF1AX	0	1	0		CLU	0	1	0
EIF2S3	1	1	0		CPVL	0	1	0
EIF3E	0	1	0		CRELD1	1	0	0
EIF3K	1	1	0		CRYAB	1	0	0
EIF3L	0	1	0		CSGALNACT1	1	0	0
EIF4A1	1	1	1		CSPG4	1	0	0
EIF4EBP2	1	0	0		CST3	1	1	0
ESRP1	0	1	0		CTSA	1	0	0
FAM174B	1	0	0		CTSB	1	1	0
FAM178B	0	1	0		CTSD	1	1	1
FAM92A1	0	1	0		CTSL1	1	1	0
FBL	1	0	0		DAG1	1	0	0
FBLN1	1	0	0		DCBLD2	1	0	0
FOXRED2	1	0	0		DDR1	1	1	0
FTL	1	1	0		DDX5	1	0	0
FUS	1	0	0		DPYSL2	1	1	0
GABARAP	1	0	0		DSCR8	0	1	0
GAS5	1	1	0		DUSP4	1	0	0
GNB2L1	1	1	0		DUSP6	1	1	0
GPATCH4	1	0	0		DYNLRB1	0	1	0

Table 5. The oncogenic resistance signatures: oncogenic-ICR, exclusion, uICR, and the refined uICR.

Genes up-regulated in ICR malignant cells (1 denotes the gene is included in the signature, and 0 otherwise)					Genes down-regulated in ICR malignant cells (1 denotes the gene is included in the signature, and 0 otherwise)			
uICR-up genes (immune resistance)	oncogenic-ICR-up (post treatment)	Exclusion-up	uICR-up (refined)		uICR-down genes	oncogenic-ICR-down	Exclusion-down	uICR-down (refined)
GPI	1	1	0		ECM1	1	0	0
GRWD1	1	0	0		EEA1	1	0	1
GSTO1	0	1	0		EGR1	1	0	0
H3F3A	1	0	0		EMP1	1	1	1
H3F3AP4	1	0	0		EPHX2	1	0	0
HMGA1	1	0	0		ERBB3	1	0	0
HNRNPA1	1	0	0		EVA1A	1	0	0
HNRNPA1P10	1	0	0		EZH1	1	0	0
HNRNPC	1	0	0		EZR	0	1	0
HSPA8	1	0	0		FAM3C	1	1	0
IDH2	1	0	0		FBXO32	1	0	1
IFI16	0	1	0		FCGR2C	1	0	0
ILF2	1	1	1		FCRLA	1	0	0
IMPDH2	0	1	0		FGFR1	1	1	0
ISYNA1	1	0	0		FLJ43663	1	0	0
ITM2C	1	0	0		FOS	1	0	0
KIAA0101	1	0	0		FYB	0	1	1
LHFPL3-AS1	0	1	0		GAA	1	1	0
LOC100190986	0	1	0		GADD45B	1	0	0
LYPLA1	0	1	0		GATSL3	0	1	1
MAGEA4	1	0	1		GEM	1	0	0
MARCKS	0	1	0		GOLGB1	1	0	0
MDH2	1	1	0		GPNMB	1	0	0
METAP2	1	0	0		GRN	1	1	0
MID1	1	0	0		GSN	1	1	0
MIR4461	1	0	0		HCP5	0	1	1
MLLT11	1	0	0		HLA-A	1	0	1
MPZL1	1	0	0		HLA-B	1	1	1
MRPL37	0	1	0		HLA-C	1	1	1
MRPS12	0	1	0		HLA-E	1	0	1
MRPS21	1	0	0		HLA-F	1	1	1
MYC	0	1	0		HLA-H	1	1	1
NACA	1	0	0		HPCAL1	1	0	0
NCL	1	1	0		HSPA1A	1	1	0
NDUFS2	1	0	0		HSPA1B	0	1	0
NF2	0	1	0		HTATIP2	1	0	0
NID1	0	1	0		ID2	0	1	0
NOLC1	1	1	0		IFI27L2	0	1	0
NONO	1	0	1		IFI35	1	0	0
NPM1	0	1	0		IGF1R	1	0	0
NUCKS1	0	1	0		IL1RAP	1	0	0
OAT	0	1	0		IL6ST	1	0	0
PA2G4	1	0	1		ISCU	0	1	0
PABPC1	1	1	0		ITGA3	1	1	1
PAFAH1B3	1	0	0		ITGA6	1	0	0
PAICS	0	1	0		ITGA7	0	1	0
PFDN2	1	0	0		ITGB1	1	0	0
PFN1	1	0	0		ITGB3	1	1	0
PGAM1	1	0	1		ITM2B	1	0	0
PIH1D1	1	0	0		JUN	1	0	0
PLTP	0	1	0		KCNN4	1	1	0
PPA1	1	0	1		KLF4	1	0	0
PPIA	1	0	1		KLF6	1	0	0
PPP2R1A	1	0	0		KRT10	0	1	0
PSAT1	0	1	0		LAMP2	1	0	1
PSMD4	1	0	0		LEPROT	1	0	0
PTMA	1	0	0		LGALS1	1	0	0
PYCARD	0	1	0		LGALS3	1	0	0
RAN	1	0	0		LGALS3BP	1	0	0

Table 5. The oncogenic resistance signatures: oncogenic-ICR, exclusion, uICR, and the refined uICR.

Genes up-regulated in ICR malignant cells (1 denotes the gene is included in the signature, and 0 otherwise)					Genes down-regulated in ICR malignant cells (1 denotes the gene is included in the signature, and 0 otherwise)			
uICR-up genes (immune resistance)	oncogenic-ICR-up (post treatment)	Exclusion-up	uICR-up (refined)		uICR-down genes	oncogenic-ICR-down	Exclusion-down	uICR-down (refined)
RASA3	0	1	0		LOC100506190	0	1	0
RBM34	1	0	0		LPL	1	0	0
RNF2	1	0	0		LRPAP1	1	0	0
RPAIN	1	0	0		LTBP3	0	1	0
RPL10	0	1	0		LYRM9	0	1	1
RPL10A	1	1	0		MAEL	0	1	0
RPL11	1	1	0		MAGEC2	1	0	0
RPL12	1	1	0		MAP1B	0	1	0
RPL13	1	1	0		MATN2	0	1	0
RPL13A	1	1	0		MFGE8	1	1	1
RPL13AP5	1	1	0		MFI2	1	1	0
RPL14	0	1	0		MIA	1	1	1
RPL17	1	1	0		MRPS6	0	1	0
RPL18	1	1	0		MT1E	1	0	0
RPL18A	1	1	1		MT1M	1	0	0
RPL21	1	0	0		MT1X	1	0	0
RPL26	1	0	1		MT2A	1	1	0
RPL28	1	1	0		NDRG1	0	1	0
RPL29	1	1	0		NEAT1	1	0	0
RPL3	1	1	0		NFKBIA	1	1	0
RPL30	0	1	0		NFKBIZ	1	0	0
RPL31	1	0	1		NNMT	1	0	0
RPL35	0	1	0		NPC1	1	1	0
RPL36A	1	0	0		NPC2	1	0	1
RPL37	1	0	0		NR4A1	1	0	0
RPL37A	1	1	0		NSG1	1	0	1
RPL39	1	1	0		OCIAD2	0	1	0
RPL4	1	1	0		PAGE5	0	1	0
RPL41	1	0	0		PDK4	1	0	0
RPL5	1	1	0		PERP	0	1	0
RPL6	1	1	0		PKM	0	1	0
RPL7	0	1	0		PLP2	1	0	0
RPL7A	0	1	0		PRKCDBP	1	0	0
RPL8	1	1	0		PRNP	1	0	0
RPLP0	1	1	0		PROS1	1	0	1
RPLP1	1	1	0		PRSS23	1	0	0
RPS10	1	1	0		PSAP	1	0	0
RPS11	1	1	1		PSMB9	1	0	0
RPS12	1	0	0		PTRF	1	0	0
RPS15	0	1	1		RDH5	0	1	1
RPS15A	1	1	0		RNF145	1	0	0
RPS16	1	1	0		RPS4Y1	1	0	0
RPS17	1	1	0		S100A13	0	1	0
RPS17L	1	1	0		S100A6	1	1	0
RPS18	1	1	0		S100B	1	0	0
RPS19	1	1	0		SAT1	1	0	0
RPS2	0	1	0		SCARB2	1	0	0
RPS21	1	0	1		SCCPDH	1	0	0
RPS23	1	0	0		SDC3	1	0	0
RPS24	1	1	0		SEL1L	1	0	0
RPS26	1	0	0		SEMA3B	1	0	0
RPS27	1	1	0		SERPINA1	0	1	1
RPS27A	1	0	0		SERPINA3	1	1	0
RPS3	1	1	0		SERPINE2	1	1	0
RPS3A	0	1	0		SGCE	1	1	0
RPS4X	1	1	0		SGK1	1	0	0

Table 5. The oncogenic resistance signatures: oncogenic-ICR, exclusion, uICR, and the refined uICR.

Genes up-regulated in ICR malignant cells (1 denotes the gene is included in the signature, and 0 otherwise)					Genes down-regulated in ICR malignant cells (1 denotes the gene is included in the signature, and 0 otherwise)			
uICR-up genes (immune resistance)	oncogenic-ICR-up (post treatment)	Exclusion-up	uICR-up (refined)		uICR-down genes	oncogenic-ICR-down	Exclusion-down	uICR-down (refined)
RPS5	1	1	1		SLC20A1	1	0	0
RPS6	1	0	0		SLC26A2	1	1	0
RPS7	1	1	0		SLC39A14	1	0	0
RPS8	1	1	0		SLC5A3	1	1	0
RPS9	1	1	0		SNX9	0	1	0
RPSA	1	1	0		SOD1	1	0	0
RSL1D1	0	1	0		SPON2	0	1	0
RUVBL2	1	0	1		SPRY2	1	0	0
SAE1	1	0	1		SQSTM1	1	0	0
SCD	1	1	0		SRPX	1	0	0
SCNM1	1	0	0		STOM	1	0	0
SERBP1	0	1	0		SYNGR2	1	0	0
SERPINF1	1	1	0		SYPL1	1	0	0
SET	1	0	0		TAPBP	1	0	1
SF3B4	1	0	0		TAPBPL	1	0	0
SHMT2	1	0	0		TF	1	0	0
SKP2	1	0	0		TGOLN2	1	0	0
SLC19A1	0	1	0		THBD	0	1	0
SLC25A3	1	0	0		TIMP1	1	1	0
SLC25A5	0	1	0		TIMP2	1	0	1
SLC25A6	0	1	0		TIMP3	1	0	0
SMS	1	0	0		TIPARP	1	0	0
SNAI2	1	1	0		TM4SF1	1	1	0
SNHG16	0	1	0		TMBIM6	0	1	0
SNHG6	1	1	0		TMED10	1	0	0
SNRPE	1	0	1		TMED9	1	0	0
SORD	0	1	0		TMEM66	1	0	0
SOX4	1	1	0		TMX4	1	0	0
SRP14	1	0	0		TNC	1	0	0
SSR2	1	0	0		TNFSF4	0	1	1
TIMM13	0	1	0		TPP1	1	1	0
TIMM50	1	1	0		TRIML2	0	1	1
TMC6	1	0	0		TSC22D3	1	1	0
TOP1MT	0	1	0		TSPYL2	0	1	0
TP53	1	0	0		TXNIP	0	1	0
TRAP1	0	1	0		TYR	1	0	0
TRPM1	1	0	0		UBC	1	1	0
TSR1	1	0	0		UPP1	1	0	0
TUBA1B	1	0	0		XAGE1A	0	1	0
TUBB	1	0	0		XAGE1B	0	1	0
TUBB4A	0	1	0		XAGE1C	0	1	0
TULP4	1	0	0		XAGE1D	0	1	0
TXLNA	0	1	0		XAGE1E	0	1	0
TYRP1	0	1	0		ZBTB20	1	0	0
UBA52	1	0	1		ZBTB38	1	0	0
UCK2	0	1	0					
UQCRFS1	1	1	0					
UQCRH	1	0	1					
USP22	1	0	0					
VCY1B	1	0	0					
VDAC2	1	0	1					
VPS72	1	0	0					
YWHAE	1	0	0					
ZFAS1	0	1	0					
ZNF286A	1	0	0					

Table 6. Genes differentially expressed in CD8 T cells of the CB patient compared to those of the ICR patients.

Up-regulated in CB vs. ICR	Down-regulated in CB vs. ICR
ALOX5AP	AKIRIN2
C1D	APIP
C3orf14	ARL5A
CCL5	ASF1B
CCR2	ATP6V0C
CD52	ATP9B
CDC26	BRAT1
CIDECP	BRD7
CISH	C17orf89
COX5B	C1GALT1C1
CRIP1	C4orf48
CTSW	CALR
CXCR6	CCDC137
DDX3Y	CDC73
EDF1	CDCA7
EIF1AY	CDK1
FAM127B	CENPM
FASLG	CEP78
FAU	CHMP6
FCGR3A	CITED2
FTL	CLINT1
GZMA	CMTM7
GZMB	COTL1
GZMH	CRIPT
HCG26	CSNK1G3
HCST	CYB5R4
HLA-A	DCPS
HLA-C	DNAJB14
HLA-DQA2	DND1
HLA-H	DPH3
HSPA1B	EFR3A
ID2	EMC2
KDM5D	EML3
LAIR2	FAM160B1
MIR4461	FAM168B
MTRNR2L1	FAM46C
MTRNR2L10	FAM53C
MTRNR2L6	FAM69A
NACA	FARSB
NCF4	FBXO22
NDUFA13	FEM1A
NDUFS5	FTSJD1
NDUFV2	GATAD2A
RBPJ	GET4
RNASEK	GGA3
RPL10	GLTSCR2
RPL11	GNL3
RPL12	GOLT1B
RPL13	GPR137B
RPL13AP5	GTDC1
RPL15	HIST1H1E
RPL17	HMGA1
RPL18	HMHA1

Up-regulated in CB vs. ICR	Down-regulated in CB vs. ICR
RPL18A	HSF1
RPL19	IARS2
RPL21	IL6ST
RPL23	JUNB
RPL23A	KATNA1
RPL24	KIAA1429
RPL26	LATS1
RPL29	LOC100294145
RPL30	LRIG2
RPL32	MAN2A1
RPL35	MAP3K2
RPL35A	MB21D1
RPL36	MCM2
RPL36AL	MCM4
RPL37A	MED23
RPL4	MGEA5
RPL41	MPLKIP
RPL6	MRPS33
RPL7	MZT1
RPL7A	NAGK
RPL9	NEK1
RPLP1	NOA1
RPLP2	NPC2
RPS10	NUDT1
RPS11	NUP107
RPS12	OSGEP
RPS13	PARP10
RPS14	PELI1
RPS15	PGS1
RPS15A	PITHD1
RPS16	PLEKHF2
RPS18	POLR3E
RPS19	PPIF
RPS20	PPP1R21
RPS24	PRKAB1
RPS25	PSMD2
RPS27	PTGDR
RPS27A	PYGO2
RPS3	RAB11B
RPS3A	RABEP1
RPS4X	RALB
RPS4Y1	REC8
RPS5	REEP4
RPS6	RNF216P1
RPS8	RNF219
SAMD3	RPIA
SELM	RPS6KA5
SH3BGRL3	RPSAP58
SYMPK	SFSWAP
TMSB10	SGSM2
TMSB4X	SLC1A5
TNFSF4	SLC25A26
TPT1	SLC33A1
TXLNG2P	SLC39A3
	SLC7A5
	SMC1A
	SMC4

Up-regulated in CB vs. ICR	Down-regulated in CB vs. ICR
	SNX4
	SPPL2A
	STAT1
	STX17
	SYPL1
	TAF1B
	TAF6
	TCERG1
	TCF7
	TEKT4P2
	TERF2IP
	TIMM44
	TMEM161B
	TMEM170A
	TMEM189
	TMEM69
	TMX4
	TNIP1
	TNPO1
	TOP2A
	TPX2
	TRIB2
	TSC22D1
	TUBGCP3
	TYMS
	UBA5
	UBE2J1
	UBE2Q2
	UBE2T
	USP38
	UVRAG
	WDR18
	ZBED6
	ZBTB20
	ZFYVE28
	ZNF259
	ZNF511

Table 7

Table 7. Cell-cycle signatures specific to CD8 T cells.	
Up-regulated in cycling CD8 T cells	**Down-regulated in cycling CD8 T cells**
ACTG1	AOAH
ANXA5	ATHL1
ARHGDIB	C11orf21
ARL6IP1	CCL3L1
ARPC2	CD37
ATP5L	CISH
CD74	CX3CR1
CNTRL	DENND2D
CORO1A	GNPDA1
COTL1	GZMM
COX6A1	IL11RA
COX6C	IL7R
COX8A	KLRB1
DDOST	LDLRAP1

GALM	LINC00612
GMFG	LY9
GNG5	NR4A3
HLA-DRA	PDGFD
HP1BP3	PLCB2
LCP1	PTGDR
LRRFIP1	RAB37
MPC2	RPS27
MT2A	SORL1
NDUFA4	TRIM22
NDUFC2	TRMU
NUP50	TTN
PCBP1	UPRT
PKM	ZNF121
POLR2A	
PSMB2	
SNX1	
SRRM1	
TMA7	
VIM	
YWHAE	
YWHAQ	

Table 8. The topmost differentially expressed gene sets in the malignant cells from ICR vs. TN tumors

Gene set	t-test p-value (-log10(|p|), negative = lower in ICR, positive = higher in ICR)		N = No. of genes in the gene set	N.qc = No. of used genes	N/N.qc
	t-test p-value	mixed effects p-value			
GO_RESPONSE_TO_ENDOPLASMIC_RETICULUM_STRESS	-36.49	-4.05	233	147	0.63
GO_CELLULAR_COPPER_ION_HOMEOSTASIS	-44.3	-4.04	13	9	0.69
GO_CELLULAR_RESPONSE_TO_ZINC_ION	-215.84	-4	16	7	0.44
ENDOPLASMIC_RETICULUM_MEMBRANE	-42.56	-3.93	85	55	0.65
GO_REGULATION_OF_ENDOTHELIAL_CELL_APOPTOTIC_PROCESS	-52.39	-3.79	42	14	0.33
METALLOTHIONEINS	-208.11	-3.72	13	6	0.46
GO_INTRAMOLECULAR_OXIDOREDUCTASE_ACTIVITY_TRANSPOSING_S_S_BONDS	-40.53	-3.64	22	14	0.64
NUCLEAR_ENVELOPE_ENDOPLASMIC_RETICULUM_NETWORK	-38.41	-3.59	94	62	0.66
GO_CELLULAR_RESPONSE_TO_VITAMIN_D	-78.74	-3.56	14	4	0.29
KEGG_SNARE_INTERACTIONS_IN_VESICULAR_TRANSPORT	-17.6	-3.43	38	23	0.61
ENDOPLASMIC_RETICULUM_PART	-44.43	-3.43	97	65	0.67
GO_COPPER_ION_HOMEOSTASIS	-38.11	-3.38	16	12	0.75
KEGG_ECM_RECEPTOR_INTERACTION	-163.89	-3.35	84	35	0.42
GO_ENDOPLASMIC_RETICULUM_GOLGI_INTERMEDIATE_COMPARTMENT	-40.27	-3.3	105	64	0.61
GO_BLOOD_VESSEL_MORPHOGENESIS	-153.28	-3.3	364	117	0.32
GO_PLATELET_DERIVED_GROWTH_FACTOR_RECEPTOR_BINDING	-62.32	-3.24	15	5	0.33
GO_ANGIOGENESIS	-148.37	-3.23	293	102	0.35
GO_RESPONSE_TO_ZINC_ION	-76.24	-3.22	55	21	0.38
PID_INTEGRIN_CS_PATHWAY	-172.58	-3.19	26	9	0.35
GOLGI_MEMBRANE	-53.05	-3.13	45	26	0.58
GO_TRANSITION_METAL_ION_TRANSMEMBRANE_TRANSPORTER_ACTIVITY	-61.25	-3.12	39	19	0.49

Gene set	t-test p-value (-log10(|p|), positive = higher in ICR, negative = lower in ICR)		N = No. of genes in the gene set	N.qc = No. of used genes	N/N.qc
	t-test p-value	mixed effects p-value			
POSITIVE_REGULATION_OF_CELL_PROLIFERATION	-31.46	-3.11	149	48	0.32
GO_MUSCLE_CELL_MIGRATION	-164.41	-3.11	18	10	0.56
NUCLEAR ORPHAN RECEPTOR	-83.44	-3.09	3	2	0.67
GO_POSITIVE_REGULATION_OF_EXTRINSIC_APOPTOTIC_SIGNALING_PATHWAY_VIA_DEATH_DOMAIN_RECEPTORS	-75.37	-3.08	17	11	0.65
GO_PHOSPHOTRANSFERASE_ACTIVITY_FOR_OTHER_SUBSTITUTED_PHOSPHATE_GROUPS	-32.33	-3.07	19	11	0.58
ST_INTERLEUKIN_13_PATHWAY	-2.38	-3.03	7	2	0.29
WOUND_HEALING	-148	-3.02	54	13	0.24
C/EBP	-38.85	-3	10	3	0.3
GO_INSULIN_LIKE_GROWTH_FACTOR_BINDING	-62.71	-2.98	25	11	0.44
MUSCLE_DEVELOPMENT	-122.53	-2.98	93	29	0.31
GO_PLATELET_ALPHA_GRANULE_MEMBRANE	-104.99	-2.96	13	7	0.54
GO_MANNOSIDASE_ACTIVITY	-28.46	-2.95	15	5	0.33
GO_POSITIVE_REGULATION_OF_ADHERENS_JUNCTION_ORGANIZATION	-61.36	-2.95	21	9	0.43
GO_NEGATIVE_REGULATION_OF_EPITHELIAL_CELL_APOPTOTIC_PROCESS	-70.48	-2.95	35	8	0.23
ENDOPLASMIC_RETICULUM	-50.01	-2.94	294	180	0.61
CELL_FATE_COMMITMENT	-72.59	-2.94	13	3	0.23
GO_ENDOPLASMIC_RETICULUM_GOLGI_INTERMEDIATE_COMPARTMENT_MEMBRANE	-65.43	-2.93	63	38	0.6
GO_NEGATIVE_REGULATION_OF_INTERLEUKIN_8_PRODUCTION	-126.57	-2.93	15	5	0.33
PID_TNF_PATHWAY	-73	-2.92	46	22	0.48
GO_RECEPTOR_REGULATOR_ACTIVITY	-92.97	-2.92	45	10	0.22
GO_EXTRACELLULAR_STRUCTURE_ORGANIZATION	-107.25	-2.92	304	111	0.37
ER_GOLGI_INTERMEDIATE_COMPARTMENT	-12.41	-2.91	24	20	0.83
GO_RESPONSE_TO_CADMIUM_ION	-124.5	-2.9	40	25	0.62
GO_HEPARAN_SULFATE_PROTEOGLYCAN_BIOSYNTHETIC_PROCESS	-31.95	-2.89	23	8	0.35
GO_AXON_REGENERATION	-144.4	-2.88	24	9	0.38
ENDOMEMBRANE_SYSTEM	-21.95	-2.87	220	137	0.62
HALLMARK_IL6_JAK_STAT3_SIGNALING	-170.22	-2.87	87	40	0.46
GO_HEPARAN_SULFATE_PROTEOGLYCAN_METABOLIC_PROCESS	-30.74	-2.86	28	8	0.29
GO_POSITIVE_REGULATION_OF_CELL_JUNCTION_ASSEMBLY	-88.33	-2.85	24	11	0.46
GO_VASCULATURE_DEVELOPMENT	-143.79	-2.84	469	153	0.33
CELLULAR_CATION_HOMEOSTASIS	-96.84	-2.83	106	32	0.3
GO_CELL_SUBSTRATE_JUNCTION_ASSEMBLY	-79.64	-2.82	41	19	0.46
PID_FRA_PATHWAY	-55.92	-2.81	37	17	0.46
GO_REGULATION_OF_ADHERENS_JUNCTION_ORGANIZATION	-63.38	-2.81	50	22	0.44
GO_CELL_ADHESION_MEDIATED_BY_INTEGRIN	-81.75	-2.81	12	8	0.67
GO_SARCOLEMMA	-216.58	-2.81	125	37	0.3
GO_NEGATIVE_REGULATION_OF_ENDOTHELIAL_CELL_APOPTOTIC_PROCESS	-38.24	-2.8	27	7	0.26
GO_CORECEPTOR_ACTIVITY	-68.21	-2.79	38	11	0.29
GO_REGULATION_OF_INTERLEUKIN_8_BIOSYNTHETIC_PROCESS	-12.85	-2.78	12	3	0.25
REACTOME_EXTRINSIC_PATHWAY_FOR_APOPTOSIS	-55.38	-2.78	13	8	0.62
HALLMARK_HYPOXIA	-112.24	-2.78	200	116	0.58
GO_ER_NUCLEUS_SIGNALING_PATHWAY	-28.31	-2.75	34	25	0.74
HOMOPHILIC_CELL_ADHESION	-55	-2.74	16	4	0.25
GO_SNAP_RECEPTOR_ACTIVITY	-20.16	-2.73	38	22	0.58
HALLMARK_EPITHELIAL_MESENCHYMAL_TRANSITION	-128.55	-2.73	200	110	0.55
GO_CELLULAR_RESPONSE_TO_CADMIUM_ION	-155.05	-2.73	15	9	0.6
GO_BASAL_LAMINA	-27.9	-2.72	21	6	0.29
CELL_CELL_ADHESION	-40.27	-2.72	86	19	0.22
POSITIVE_REGULATION_OF_MULTICELLULAR_ORGANISMAL_PROCESS	-45.51	-2.71	66	18	0.27
FIBROBLAST	-73.88	-2.71	6	3	0.5
GO_ATPASE_COMPLEX	-80.46	-2.7	24	7	0.29
GO_INTRINSIC_COMPONENT_OF_EXTERNAL_SIDE_OF_PLASMA_MEMBRANE	-68.1	-2.69	27	7	0.26
PID_INTEGRIN3_PATHWAY	-78.14	-2.68	43	22	0.51
CATION_HOMEOSTASIS	-93.05	-2.68	109	32	0.29

Gene set	t-test p-value (-log10(|p|), positive = higher in ICR, negative = lower in ICR)		N = No. of genes in the gene set	N.qc = No. of used genes	N/N.qc
	t-test p-value	mixed effects p-value			
GO_CELL_SUBSTRATE_ADHESION	-162.02	-2.68	164	58	0.35
GO_INTRINSIC_APOPTOTIC_SIGNALING_PATHWAY_IN_RESPONSE_TO_ENDOPLASMIC_RETICULUM_STRESS	-37.62	-2.67	32	18	0.56
GO_POSITIVE_REGULATION_OF_CELL_MATRIX_ADHESION	-57.1	-2.66	40	15	0.38
GO_NEGATIVE_REGULATION_OF_GLYCOPROTEIN_METABOLIC_PROCESS	-60.19	-2.66	15	10	0.67
GO_NEGATIVE_REGULATION_OF_TYPE_2_IMMUNE_RESPONSE	-162.47	-2.66	11	4	0.36
REACTOME_ACTIVATION_OF_CHAPERONES_BY_ATF6_ALPHA	-22.85	-2.64	13	8	0.62
GO_NEGATIVE_REGULATION_OF_DNA_RECOMBINATION	-13.63	-2.63	16	8	0.5
GO_CELLULAR_RESPONSE_TO_TOPOLOGICALLY_INCORRECT_PROTEIN	-22.73	-2.63	122	81	0.66
GO_CELLULAR_RESPONSE_TO_CALCIUM_ION	-69.45	-2.63	49	18	0.37
GO_SECRETORY_GRANULE_MEMBRANE	-133.42	-2.63	78	28	0.36
GOLGI_VESICLE_TRANSPORT	-13.68	-2.62	48	37	0.77
REACTOME_DIABETES_PATHWAYS	-20.26	-2.62	133	80	0.6
GO_NEGATIVE_REGULATION_OF_GLYCOPROTEIN_BIOSYNTHETIC_PROCESS	-23.98	-2.61	12	9	0.75
CAHOY_ASTROGLIAL	-197.11	-2.61	100	37	0.37
GO_HEMIDESMOSOME_ASSEMBLY	-95.2	-2.6	12	5	0.42
GO_FIBRINOLYSIS	-98.47	-2.6	21	6	0.29
GO_PROTEIN_COMPLEX_INVOLVED_IN_CELL_ADHESION	-171.74	-2.6	30	10	0.33
ST_IL_13_PATHWAY	-1.56	-2.59	7	2	0.29
POSITIVE_REGULATION_OF_PROTEIN_MODIFICATION_PROCESS	-37.38	-2.58	29	9	0.31
HALLMARK_UV_RESPONSE_UP	-67.14	-2.57	158	93	0.59
CELL_MIGRATION	-87.02	-2.57	96	34	0.35
ATPASE_ACTIVITY_COUPLED_TO_TRANSMEMBRANE_MOVEMENT_OF_IONS_PHOSPHORYLATIVE_MECHANISM	-130.2	-2.57	20	5	0.25
GO_INTEGRIN_BINDING	-94.95	-2.56	105	48	0.46
HALLMARK_TNFA_SIGNALING_VIA_NFKB	-154.11	-2.56	200	108	0.54
GO_PLATELET_ALPHA_GRANULE	-164.05	-2.56	75	35	0.47
PID_INTEGRIN1_PATHWAY	-89.65	-2.55	66	34	0.52
GO_CATION_TRANSPORTING_ATPASE_COMPLEX	-119.68	-2.55	16	4	0.25
PROTEIN_AMINO_ACID_LIPIDATION	-35.59	-2.54	24	19	0.79
GO_NEGATIVE_REGULATION_OF_LIPID_STORAGE	-92.01	-2.54	17	6	0.35
GO_BASEMENT_MEMBRANE_ORGANIZATION	-26.24	-2.53	11	7	0.64
POSITIVE_REGULATION_OF_CYTOKINE_PRODUCTION	-41.65	-2.53	15	5	0.33
BIOCARTA_SODD_PATHWAY	-37.42	-2.52	10	8	0.8
GO_PERK_MEDIATED_UNFOLDED_PROTEIN_RESPONSE	-39.21	-2.52	12	10	0.83
PHOSPHOLIPID_METABOLIC_PROCESS	-44.83	-2.52	74	42	0.57
Targets of NFAT_Q6	-53.2	-2.52	246	80	0.33
BIOCARTA_STRESS_PATHWAY	-71.76	-2.52	25	10	0.4
CYTOPLASM_ORGANIZATION_AND_BIOGENESIS	-67.96	-2.51	15	7	0.47
Targets of FREAC3_01	-23.28	-2.5	251	65	0.26
GO_COLLAGEN_BINDING	-84.49	-2.5	65	27	0.42
PID_INTEGRIN4_PATHWAY	-35.75	-2.49	11	4	0.36
CELL_SURFACE	-42.55	-2.49	79	27	0.34
GO_PHOSPHATE_TRANSMEMBRANE_TRANSPORTER_ACTIVITY	-14.32	-2.48	30	16	0.53
NAIVE_VS_ACTIVATED_CD8_TCELL_DN	-38.5	-2.48	200	81	0.4
MEMBRANE_LIPID_BIOSYNTHETIC_PROCESS	-20.36	-2.47	49	29	0.59
GO_GLYCEROPHOSPHOLIPID_CATABOLIC_PROCESS	-27.95	-2.47	13	7	0.54
GO_INTERSTITIAL_MATRIX	-81.96	-2.47	14	3	0.21
GO_REGULATION_OF_EXTRINSIC_APOPTOTIC_SIGNALING_PATHWAY_VIA_DEATH_DOMAIN_RECEPTORS	-103.8	-2.47	55	32	0.58
INORGANIC_ANION_TRANSPORT	-151.85	-2.47	18	4	0.22
REACTOME_CLASS_B_2_SECRETIN_FAMILY_RECEPTORS	-62.64	-2.46	88	19	0.22
GO_DECIDUALIZATION	-99.39	-2.46	21	7	0.33
GO_MULTI_MULTICELLULAR_ORGANISM_PROCESS	-129.03	-2.46	213	62	0.29
NABA_BASEMENT_MEMBRANES	-19.18	-2.45	40	12	0.3
GO_PROTEINACEOUS_EXTRACELLULAR_MATRIX	-60.88	-2.45	356	86	0.24
GO_EXTRACELLULAR_MATRIX	-121.18	-2.45	426	116	0.27
GO_INTEGRIN_MEDIATED_SIGNALING_PATHWAY	-129.11	-2.45	82	36	0.44
SECRETION	-34.16	-2.44	178	68	0.38

Gene set	t-test p-value (-log10(|p|), positive = higher in ICR, negative = lower in ICR)		N = No. of genes in the gene set	N.qc = No. of used genes	N/N.qc
	t-test p-value	mixed effects p-value			
GO_CARBOHYDRATE_DERIVATIVE_CATABOLIC_PROCESS	-62.72	-2.44	174	76	0.44
HALLMARK_APOPTOSIS	-184.35	-2.44	161	111	0.69
LIPOPROTEIN_METABOLIC_PROCESS	-34.84	-2.43	33	21	0.64
LIPOPROTEIN_BIOSYNTHETIC_PROCESS	-36.48	-2.43	26	19	0.73
GO_BASEMENT_MEMBRANE	-54.56	-2.43	93	32	0.34
REACTOME_UNFOLDED_PROTEIN_RESPONSE	-13.89	-2.42	80	58	0.72
GO_LIPOPROTEIN_BIOSYNTHETIC_PROCESS	-63.03	-2.42	85	40	0.47
GO_HYDROLASE_ACTIVITY_ACTING_ON_GLYCOSYL_BONDS	-65.4	-2.42	122	44	0.36
GO_REGULATION_OF_VIRAL_ENTRY_INTO_HOST_CELL	-72.07	-2.42	28	12	0.43
BIOCARTA_IL1R_PATHWAY	-72.17	-2.41	33	12	0.36
HALLMARK_IL2_STAT5_SIGNALING	-199.12	-2.41	200	91	0.46
GO_NEGATIVE_REGULATION_OF_SMALL_GTPASE_MEDIATED_SIGNAL_TRANSDUCTION	-72.25	-2.4	40	14	0.35
GO_GROWTH_FACTOR_BINDING	-107.54	-2.39	123	46	0.37
GO_METALLOENDOPEPTIDASE_INHIBITOR_ACTIVITY	-118.81	-2.39	14	5	0.36
TTAYRTAA_Targets of E4BP4_01	-133.15	-2.39	265	74	0.28
GO_REGULATION_OF_T_HELPER_2_CELL_DIFFERENTIATION	-200.19	-2.39	11	3	0.27
CELL_ACTIVATION	-24.51	-2.38	77	17	0.22
GO_EXTRACELLULAR_MATRIX_COMPONENT	-46.21	-2.38	125	47	0.38
GO_RESPONSE_TO_AXON_INJURY	-138.03	-2.38	48	19	0.4
GO_FORMATION_OF_PRIMARY_GERM_LAYER	-93.37	-2.37	110	33	0.3
HYDROLASE_ACTIVITY_ACTING_ON_ACID_ANHYDRIDESCATALYZING_TRANSMEMBRANE_MOVEMENT_OF_SUBSTANCES	-126.69	-2.37	39	14	0.36
GO_CELLULAR_RESPONSE_TO_PROSTAGLANDIN_STIMULUS	-41.78	-2.36	24	10	0.42
GO_NEGATIVE_REGULATION_OF_MULTICELLULAR_ORGANISMAL_METABOLIC_PROCESS	-55.1	-2.36	12	6	0.5
GO_NEGATIVE_REGULATION_OF_GROWTH	-96.42	-2.36	236	85	0.36
GO_REGULATION_OF_ERK1_AND_ERK2_CASCADE	-121.13	-2.36	238	74	0.31
GO_CELL_MATRIX_ADHESION	-156.53	-2.36	119	42	0.35
PID_P38_MKK3_6PATHWAY	-11.76	-2.35	26	9	0.35
GO_ACROSOMAL_MEMBRANE	-98.54	-2.35	22	8	0.36
BLOOD_COAGULATION	-133.89	-2.35	43	12	0.28
GO_REGULATION_OF_INTERLEUKIN_2_PRODUCTION	-134.5	-2.35	48	19	0.4
GO_IRE1_MEDIATED_UNFOLDED_PROTEIN_RESPONSE	-17.39	-2.34	56	44	0.79
GO_PROTEIN_HETEROOLIGOMERIZATION	-31.48	-2.34	113	44	0.39
GO_NEGATIVE_REGULATION_OF_SODIUM_ION_TRANSPORT	-110.08	-2.34	11	4	0.36
MEMBRANE_FUSION	-27.59	-2.33	28	15	0.54
KEGG_GLYCOSPHINGOLIPID_BIOSYNTHESIS_GANGLIO_SERIES	-46.27	-2.33	15	6	0.4
GO_REGULATION_OF_CELL_SUBSTRATE_ADHESION	-62.07	-2.33	173	67	0.39
GO_REGULATION_OF_PROTEIN_GLYCOSYLATION	-18.5	-2.32	14	5	0.36
GO_PLASMA_MEMBRANE_FUSION	-40.77	-2.32	26	8	0.31
GO_COMPACT_MYELIN	-55.03	-2.31	15	8	0.53
Targets of CDPCR1_01	-74.82	-2.31	130	33	0.25
AMINO_ACID_DERIVATIVE_BIOSYNTHETIC_PROCESS	-10.41	-2.3	10	4	0.4
KEGG_GLYCOSAMINOGLYCAN_BIOSYNTHESIS_CHONDROITIN_SULFATE	-61.3	-2.3	22	6	0.27
GO_REGULATION_OF_CELL_MATRIX_ADHESION	-63.63	-2.3	90	34	0.38
GO_ANTIMICROBIAL_HUMORAL_RESPONSE	-81.25	-2.3	52	14	0.27
GO_NEGATIVE_REGULATION_OF_PROTEIN_KINASE_B_SIGNALING	-47.66	-2.29	36	16	0.44
GO_RESPONSE_TO_OXYGEN_LEVELS	-69.16	-2.29	311	127	0.41
GO_RESPONSE_TO_TRANSITION_METAL_NANOPARTICLE	-89.78	-2.29	148	63	0.43
GO_FIBRONECTIN_BINDING	-106.39	-2.29	28	16	0.57
GO_POSITIVE_REGULATION_OF_INTERLEUKIN_2_PRODUCTION	-147.35	-2.29	31	12	0.39
GO_ENDOPLASMIC_RETICULUM_LUMEN	-32.2	-2.28	201	84	0.42
GO_POSITIVE_REGULATION_OF_EXTRINSIC_APOPTOTIC_SIGNALING_PATHWAY	-52.86	-2.28	53	35	0.66
GO_CELLULAR_RESPONSE_TO_OXYGEN_LEVELS	-58.67	-2.28	143	55	0.38
REACTOME_INTEGRIN_CELL_SURFACE_INTERACTIONS	-89.69	-2.28	79	37	0.47
EXTRACELLULAR_REGION_PART	-125.68	-2.28	338	88	0.26
GO_SECRETORY_GRANULE_LUMEN	-157.29	-2.28	85	31	0.36
GO_SNARE_COMPLEX	-17.36	-2.27	53	28	0.53

Gene set	t-test p-value (-log10(|p|), positive = higher in ICR, negative = lower in ICR)		N = No. of genes in the gene set	N.qc = No. of used genes	N/N.qc
	t-test p-value	mixed effects p-value			
KEGG_GLYCOSAMINOGLYCAN_DEGRADATION	-47	-2.27	21	9	0.43
ATPASE_ACTIVITY_COUPLED_TO_TRANSMEMBRANE_MOVEMENT_OF_IONS	-133.35	-2.27	24	9	0.38
GO_NEGATIVE_REGULATION_OF_COAGULATION	-196.17	-2.27	48	13	0.27
REACTOME_TRANSPORT_OF_VITAMINS_NUCLEOSIDES_AND_RELATED_MOLECULES	-10.14	-2.26	31	9	0.29
GO_IRON_ION_BINDING	-18.16	-2.26	163	42	0.26
GO_ACETYLGLUCOSAMINYLTRANSFERASE_ACTIVITY	-38.97	-2.26	49	19	0.39
GO_POSITIVE_REGULATION_OF_RECEPTOR_MEDIATED_ENDOCYTOSIS	-75.46	-2.26	47	13	0.28
HALLMARK_UV_RESPONSE_DN	-95.37	-2.26	144	64	0.44
GO_CELL_ADHESION_MOLECULE_BINDING	-113.26	-2.26	186	74	0.4
REACTOME_CELL_SURFACE_INTERACTIONS_AT_THE_VASCULAR_WALL	-148.37	-2.26	91	38	0.42
GO_UBIQUITIN_UBIQUITIN_LIGASE_ACTIVITY	-10.5	-2.25	13	7	0.54
GO_N_GLYCAN_PROCESSING	-37.67	-2.25	20	5	0.25
GO_BRANCH_ELONGATION_OF_AN_EPITHELIUM	-38.53	-2.25	17	4	0.24
REACTOME_TRANSPORT_OF_GLUCOSE_AND_OTHER_SUGARS_BILE_SALTS_AND_ORGANIC_ACIDS_METAL_IONS_AND_AMINE_COMPOUNDS	-70.87	-2.25	89	18	0.2
GO_BASAL_PLASMA_MEMBRANE	-102.25	-2.25	33	9	0.27
GO_PLATELET_DEGRANULATION	-156.77	-2.25	107	51	0.48
PDZ_DOMAIN_BINDING	-29.47	-2.24	14	4	0.29
BIOCARTA_GATA3_PATHWAY	-52.32	-2.24	16	4	0.25
GO_NEGATIVE_REGULATION_OF_CELL_SUBSTRATE_ADHESION	-81.77	-2.24	53	25	0.47
AMINE_BIOSYNTHETIC_PROCESS	-12.25	-2.23	15	7	0.47
GO_REGULATION_OF_RECEPTOR_ACTIVITY	-13.59	-2.23	117	30	0.26
GO_PYRIMIDINE_NUCLEOSIDE_CATABOLIC_PROCESS	-79.61	-2.23	21	8	0.38
GO_CIRCULATORY_SYSTEM_DEVELOPMENT	-132.21	-2.23	788	233	0.3
GO_MATURE_B_CELL_DIFFERENTIATION	-21.54	-2.22	17	7	0.41
GO_OLIGOSACCHARIDE_CATABOLIC_PROCESS	-24.14	-2.22	12	7	0.58
GO_RESPONSE_TO_PROSTAGLANDIN	-38.47	-2.22	34	11	0.32
GO_OXIDOREDUCTASE_ACTIVITY_ACTING_ON_THE_CH_NH2_GROUP_OF_DONORS_OXYGEN_AS_ACCEPTOR	-60.87	-2.22	15	5	0.33
ST_TUMOR_NECROSIS_FACTOR_PATHWAY	-96.67	-2.22	29	17	0.59
GO_REGULATION_OF_INTERLEUKIN_8_SECRETION	-101.51	-2.22	19	8	0.42
GO_REGULATION_OF_MEMBRANE_PROTEIN_ECTODOMAIN_PROTEOLYSIS	-157.88	-2.22	21	9	0.43
ER_TO_GOLGI_VESICLE_MEDIATED_TRANSPORT	-4.83	-2.21	18	15	0.83
PID_TCR_JNK_PATHWAY	-26.53	-2.21	14	6	0.43
REACTOME_IL1_SIGNALING	-34.94	-2.21	39	16	0.41
GO_POSITIVE_REGULATION_OF_IMMUNOGLOBULIN_SECRETION	-97.18	-2.21	11	4	0.36
PID_AP1_PATHWAY	-129.76	-2.2	70	31	0.44
Targets of LMO2COM_01	-20.1	-2.19	264	72	0.27
GO_RESPONSE_TO_STARVATION	-41.8	-2.19	154	70	0.45
GO_MEMBRANE_RAFT_ORGANIZATION	-114.17	-2.19	17	12	0.71
COAGULATION	-131.28	-2.19	44	12	0.27
GO_SULFATE_TRANSPORT	-73.24	-2.18	14	3	0.21
Targets of STAT5A_02	-73.82	-2.18	141	42	0.3
GO_SECRETORY_GRANULE	-145.5	-2.18	352	114	0.32
GO_REGULATION_OF_COAGULATION	-149.09	-2.18	88	26	0.3
GO_CELL_SURFACE	-169.9	-2.18	757	217	0.29
GO_NUCLEOTIDE_TRANSMEMBRANE_TRANSPORT	-6.85	-2.17	12	7	0.58
PROTEIN_TRANSPORTER_ACTIVITY	-7.67	-2.17	14	7	0.5
ENDOPLASMIC_RETICULUM_LUMEN	-16.08	-2.17	14	12	0.86
GO_REGULATION_OF_PEPTIDYL_SERINE_PHOSPHORYLATION	-34.4	-2.17	118	37	0.31
LIPID_RAFT	-83.19	-2.17	29	16	0.55
GO_CELLULAR_RESPONSE_TO_EXTERNAL_STIMULUS	-74.77	-2.16	264	114	0.43
GO_REGULATION_OF_EXTRINSIC_APOPTOTIC_SIGNALING_PATHWAY	-97.55	-2.16	153	77	0.5
GO_RESPONSE_TO_DRUG	-144.63	-2.16	431	159	0.37
GO_REGULATION_OF_EXTRACELLULAR_MATRIX_DISASSEMBLY	-147.71	-2.16	14	4	0.29
REACTOME_ACTIVATION_OF_CHAPERONE_GENES_BY_XBP1S	-15.37	-2.15	46	35	0.76
GO_DENDRITE_MORPHOGENESIS	-17.1	-2.15	42	12	0.29
GO_MATURE_B_CELL_DIFFERENTIATION_INVOLVED_IN_IMMUNE_RES	-27.87	-2.15	13	6	0.46

Gene set	t-test p-value (-log10(|p|), positive = higher in ICR, negative = lower in ICR)		N = No. of genes in the gene set	N.qc = No. of used genes	N/N.qc
	t-test p-value	mixed effects p-value			
PONSE					
GO_CELLULAR_RESPONSE_TO_MECHANICAL_STIMULUS	-133.12	-2.15	80	32	0.4
GO_HETEROTYPIC_CELL_CELL_ADHESION	-138.66	-2.15	27	9	0.33
BIOCARTA_LYM_PATHWAY	-58.96	-2.14	11	7	0.64
HINATA_NFKB_MATRIX	-78.15	-2.14	10	7	0.7
GO_NEGATIVE_REGULATION_OF_RHO_PROTEIN_SIGNAL_TRANSDUCTION	-83.78	-2.14	14	8	0.57
GO_TELOMERE_LOCALIZATION	-8.52	-2.13	11	4	0.36
INTRINSIC_TO_ENDOPLASMIC_RETICULUM_MEMBRANE	-11.39	-2.13	24	14	0.58
CELLULAR_HOMEOSTASIS	-61.96	-2.13	147	45	0.31
GO_CELL_MIGRATION_INVOLVED_IN_SPROUTING_ANGIOGENESIS	-87.08	-2.13	15	4	0.27
GO_GASTRULATION	-36.59	-2.12	155	46	0.3
PID_IL1_PATHWAY	-68.25	-2.12	34	15	0.44
GO_ENDOPEPTIDASE_ACTIVITY	-81.63	-2.12	448	135	0.3
INTEGRAL_TO_ENDOPLASMIC_RETICULUM_MEMBRANE	-9.58	-2.11	24	14	0.58
REACTOME_ACTIVATION_OF_CHAPERONE_GENES_BY_ATF6_ALPHA	-16.39	-2.11	11	7	0.64
GO_ZINC_II_ION_TRANSPORT	-38.12	-2.11	26	13	0.5
RYAAAKNNNNNNTTGW_UNKNOWN	-51.33	-2.11	84	22	0.26
GGARNTKYCCA_UNKNOWN	-56.64	-2.11	78	24	0.31
GO_MEMBRANE_HYPERPOLARIZATION	-86.71	-2.11	11	3	0.27
PID_INTEGRIN_A9B1_PATHWAY	-88.11	-2.11	25	11	0.44
GO_MEMBRANE_ASSEMBLY	-113.44	-2.11	25	10	0.4
GO_ALCOHOL_TRANSMEMBRANE_TRANSPORTER_ACTIVITY	-135.7	-2.11	24	5	0.21
LEUKOCYTE_ACTIVATION	-21.62	-2.1	69	16	0.23
GO_POSITIVE_REGULATION_OF_PEPTIDYL_SERINE_PHOSPHORYLATION	-60.49	-2.1	88	29	0.33
GO_OXALATE_TRANSPORT	-81.43	-2.09	12	3	0.25
GO_MEMBRANE_BIOGENESIS	-92.93	-2.09	30	12	0.4
GO_SECRETORY_VESICLE	-133.02	-2.09	461	143	0.31
REACTOME_EXTRACELLULAR_MATRIX_ORGANIZATION	-29.23	-2.08	87	25	0.29
Targets of ATargets of 01	-45.86	-2.08	259	109	0.42
ATPASE_ACTIVITY_COUPLED_TO_MOVEMENT_OF_SUBSTANCES	-130.08	-2.08	40	14	0.35
GO_ENDOPLASMIC_RETICULUM_CHAPERONE_COMPLEX	-3.32	-2.07	11	8	0.73
GO_CIS_GOLGI_NETWORK	-25.98	-2.07	40	23	0.57
GO_RESPONSE_TO_OXIDATIVE_STRESS	-58.41	-2.07	352	165	0.47
Targets of FOXD3_01	-77.69	-2.07	199	45	0.23
HYDROLASE_ACTIVITY_HYDROLYZING_O_GLYCOSYL_COMPOUNDS	-37.78	-2.06	37	13	0.35
Targets of CEBP_Q2_01	-52.02	-2.06	267	76	0.28
GO_REGULATION_OF_CELL_JUNCTION_ASSEMBLY	-53.46	-2.06	68	27	0.4
GO_PEPTIDASE_ACTIVITY	-53.89	-2.06	663	202	0.3
GO_REGULATION_OF_EPITHELIAL_CELL_APOPTOTIC_PROCESS	-88.51	-2.06	59	20	0.34
ACTIVE_TRANSMEMBRANE_TRANSPORTER_ACTIVITY	-98.29	-2.06	122	31	0.25
GO_REGULATION_OF_PEPTIDASE_ACTIVITY	-127.28	-2.06	392	176	0.45
GO_RESPONSE_TO_FOOD	-15.02	-2.05	19	5	0.26
GO_PROTEIN_DEGLYCOSYLATION	-21.99	-2.05	21	13	0.62
GO_AMINOGLYCAN_CATABOLIC_PROCESS	-66.41	-2.05	68	27	0.4
INTEGRAL_TO_ORGANELLE_MEMBRANE	-12.43	-2.04	50	27	0.54
LYMPHOCYTE_ACTIVATION	-16.18	-2.04	61	15	0.25
BIOCARTA_VITCB_PATHWAY	-23.55	-2.04	11	6	0.55
NEGATIVE_REGULATION_OF_SECRETION	-25.56	-2.04	13	5	0.38
MEMBRANE_LIPID_METABOLIC_PROCESS	-61.37	-2.04	101	55	0.54
GO_CELL_CELL_CONTACT_ZONE	-91.65	-2.04	64	21	0.33
KEGG_COMPLEMENT_AND_COAGULATION_CASCADES	-112.22	-2.04	69	28	0.41
GO_NEGATIVE_REGULATION_OF_WOUND_HEALING	-182.92	-2.04	58	13	0.22
NUCLEOTIDE_KINASE_ACTIVITY	-0.4	-2.03	13	5	0.38
GO_ENDODERM_FORMATION	-52.71	-2.03	50	20	0.4
GO_GLYCOLIPID_BIOSYNTHETIC_PROCESS	-58.12	-2.03	62	33	0.53
M1_MACROPHAGES	-77.24	-2.03	54	25	0.46
RESPONSE_TO_WOUNDING	-137.23	-2.03	190	58	0.31
GO_REGULATION_OF_ASTROCYTE_DIFFERENTIATION	-149.91	-2.03	27	7	0.26
GO_HOST	-4.29	-2.02	12	8	0.67

Gene set	t-test p-value (-log10(|p|), positive = higher in ICR, negative = lower in ICR)		N = No. of genes in the gene set	N.qc = No. of used genes	N/N.qc
	t-test p-value	mixed effects p-value			
GO_REGULATION_OF_CHOLESTEROL_HOMEOSTASIS	-29.21	-2.02	11	4	0.36
GO_REGULATION_OF_SODIUM_ION_TRANSMEMBRANE_TRANSPORT	-67.2	-2.02	48	14	0.29
TIL_HCC_C9_CD4_GZMK	-75.21	-2.02	10	5	0.5
SUGAR_BINDING	-98.2	-2.02	34	7	0.21
GO_APICAL_PLASMA_MEMBRANE	-139.37	-2.02	292	74	0.25
GO_REGULATION_OF_SODIUM_ION_TRANSPORT	-143	-2.02	77	22	0.29
GO_UDP_GLYCOSYLTRANSFERASE_ACTIVITY	-33.38	-2.01	139	38	0.27
GO_OXIDOREDUCTASE_ACTIVITY_ACTING_ON_THE_CH_NH2_GROUP_OF_DONORS	-37.81	-2.01	19	6	0.32
GO_ENDODERM_DEVELOPMENT	-49.7	-2.01	71	21	0.3
GO_CARBOHYDRATE_BINDING	-65.62	-2.01	277	72	0.26
Targets of OCT1_Q5_01	-69.32	-2.01	273	64	0.23
GO_MATERNAL_PROCESS_INVOLVED_IN_FEMALE_PREGNANCY	-72.71	-2.01	60	21	0.35
GO_SODIUM_POTASSIUM_EXCHANGING_ATPASE_COMPLEX	-141.23	-2.01	11	3	0.27
HALLMARK_COAGULATION	-166.89	-2.01	138	64	0.46
SULFURIC_ESTER_HYDROLASE_ACTIVITY	-49.62	-2	16	4	0.25
GO_RESPONSE_TO_UV	39.84	2	126	60	0.48
FATTY_ACID_OXIDATION	17.45	2	18	12	0.67
GO_PROTEIN_SUMOYLATION	74.55	2.01	115	68	0.59
GO_POSITIVE_REGULATION_OF_DNA_REPAIR	59.89	2.01	38	17	0.45
GO_CHROMOSOMAL_REGION	54.33	2.01	330	159	0.48
GO_NEGATIVE_REGULATION_OF_DEFENSE_RESPONSE_TO_VIRUS	42.57	2.01	18	8	0.44
KEGG_LIMONENE_AND_PINENE_DEGRADATION	40.9	2.01	10	7	0.7
NUCLEAR_HORMONE_RECEPTOR_BINDING	39.05	2.01	28	15	0.54
CELLULAR_PROTEIN_COMPLEX_DISASSEMBLY	35.57	2.01	13	7	0.54
BIOCARTA_VEGF_PATHWAY	21.87	2.01	29	15	0.52
GO_FILAMENTOUS_ACTIN	8.26	2.01	20	6	0.3
GO_DNA_METHYLATION_OR_DEMETHYLATION	2.5	2.01	59	22	0.37
GO_REGULATION_OF_TELOMERASE_ACTIVITY	68.25	2.02	43	17	0.4
GO_HORMONE_RECEPTOR_BINDING	23.76	2.02	168	73	0.43
GO_REGULATION_OF_MITOCHONDRIAL_OUTER_MEMBRANE_PERMEABILIZATION_INVOLVED_IN_APOPTOTIC_SIGNALING_PATHWAY	17.67	2.02	43	23	0.53
GO_DNA_HELICASE_COMPLEX	50.82	2.03	14	9	0.64
GO_VIRAL_GENOME_REPLICATION	28.4	2.03	21	13	0.62
GO_REGULATION_OF_SPINDLE_ASSEMBLY	8.3	2.03	15	11	0.73
TAAYNRNNTCC_UNKNOWN	3.81	2.03	172	44	0.26
GO_REGULATION_OF_TELOMERE_MAINTENANCE_VIA_TELOMERE_LENGTHENING	108.58	2.04	50	26	0.52
BIOCARTA_EIF2_PATHWAY	19.87	2.04	11	7	0.64
GO_REGULATION_OF_CHROMATIN_SILENCING	70.9	2.05	21	9	0.43
GO_MICROTUBULE	70.74	2.05	405	173	0.43
GO_POSITIVE_REGULATION_OF_PROTEIN_LOCALIZATION_TO_NUCLEUS	60.95	2.05	129	53	0.41
GO_NEGATIVE_REGULATION_OF_TELOMERE_MAINTENANCE_VIA_TELOMERE_LENGTHENING	59.17	2.05	17	12	0.71
Targets of E2F_Q6_01	44.57	2.05	240	111	0.46
PROTEIN_COMPLEX_DISASSEMBLY	32.97	2.05	14	7	0.5
GO_PEROXISOME_PROLIFERATOR_ACTIVATED_RECEPTOR_BINDING	23	2.05	15	4	0.27
GO_FEMALE_MEIOTIC_DIVISION	19.4	2.05	26	10	0.38
GO_POSITIVE_REGULATION_OF_MRNA_PROCESSING	7.84	2.05	32	20	0.62
GO_MICROTUBULE_CYTOSKELETON_ORGANIZATION	7.79	2.05	348	134	0.39
Targets of AP4_Q6_01	21.61	2.06	255	71	0.28
REACTOME_TRANSPORT_OF_MATURE_MRNA_DERIVED_FROM_AN_INTRONLESS_TRANSCRIPT	36.77	2.07	33	26	0.79
AUXILIARY_TRANSPORT_PROTEIN_ACTIVITY	9.03	2.07	26	6	0.23
GO_POSITIVE_REGULATION_OF_TELOMERE_MAINTENANCE_VIA_TELOMERE_LENGTHENING	96.96	2.08	33	14	0.42
GO_NEGATIVE_REGULATION_OF_CHROMOSOME_ORGANIZATION	77.33	2.08	96	49	0.51
RNA_DEPENDENT_ATPASE_ACTIVITY	48.48	2.08	18	14	0.78
GO_MIRNA_BINDING	31.2	2.08	16	5	0.31
GO_G1_DNA_DAMAGE_CHECKPOINT	31.15	2.08	73	44	0.6

Gene set	t-test p-value (-log10(|p|), positive = higher in ICR, negative = lower in ICR)		N = No. of genes in the gene set	N.qc = No. of used genes	N/N.qc
	t-test p-value	mixed effects p-value			
GO_TELOMERE_ORGANIZATION	47.03	2.09	104	49	0.47
DNA_INTEGRITY_CHECKPOINT	25.86	2.09	24	11	0.46
GO_CYTOPLASMIC_MICROTUBULE	33.85	2.1	57	27	0.47
GO_UBIQUITIN_LIKE_PROTEIN_LIGASE_BINDING	27.06	2.1	264	154	0.58
GO_POSITIVE_REGULATION_OF_ERYTHROCYTE_DIFFERENTIATION	12.02	2.1	23	7	0.3
GO_REGULATION_OF_HISTONE_H3_K9_ACETYLATION	27.95	2.11	14	4	0.29
GO_DNA_BINDING_BENDING	19.1	2.11	20	6	0.3
GO_MACROPHAGE_ACTIVATION_INVOLVED_IN_IMMUNE_RESPONSE	10.16	2.11	11	3	0.27
NEGATIVE_REGULATION_OF_IMMUNE_SYSTEM_PROCESS	8.83	2.11	14	3	0.21
GO_DNA_INTEGRITY_CHECKPOINT	37.37	2.12	146	72	0.49
GO_REGULATION_OF_SPINDLE_ORGANIZATION	15.42	2.12	20	14	0.7
GO_CHROMATIN_BINDING	78.09	2.13	435	148	0.34
GO_VIRAL_LATENCY	68.81	2.13	11	9	0.82
DNA_HELICASE_ACTIVITY	52.6	2.13	25	15	0.6
GO_NUCLEAR_CHROMOSOME_TELOMERIC_REGION	62.34	2.14	132	66	0.5
GO_POSITIVE_REGULATION_OF_GLUCOSE_IMPORT_IN_RESPONSE_TO_INSULIN_STIMULUS	13.76	2.14	12	4	0.33
GO_CELL_CELL_RECOGNITION	92.12	2.15	60	13	0.22
GO_RIBONUCLEOPROTEIN_GRANULE	90.49	2.15	148	87	0.59
CONTRACTILE_FIBER_PART	82.69	2.15	23	8	0.35
GO_MITOTIC_NUCLEAR_DIVISION	44.49	2.15	361	187	0.52
GO_CELL_CYCLE_PHASE_TRANSITION	35.91	2.16	255	127	0.5
Targets of OCT1_02	29.34	2.16	214	50	0.23
GO_BINDING_OF_SPERM_TO_ZONA_PELLUCIDA	99.01	2.17	33	9	0.27
GO_POSITIVE_REGULATION_OF_DNA_BIOSYNTHETIC_PROCESS	81.19	2.17	59	23	0.39
TRANSLATION_FACTOR_ACTIVITY_NUCLEIC_ACID_BINDING	69.02	2.17	39	29	0.74
REACTOME_CELL_DEATH_SIGNALLING_VIA_NRAGE_NRIF_AND_NADE	32.08	2.17	60	22	0.37
GO_EMBRYONIC_HEMOPOIESIS	17.18	2.17	20	6	0.3
GO_POSITIVE_REGULATION_OF_TELOMERE_MAINTENANCE	98.25	2.18	47	24	0.51
GO_ADENYL_NUCLEOTIDE_BINDING	83.66	2.19	1514	548	0.36
GO_DAMAGED_DNA_BINDING	66.18	2.19	63	38	0.6
GO_SPINDLE_POLE	31.43	2.19	126	54	0.43
GO_CENTROSOME_CYCLE	7.5	2.19	45	18	0.4
CONTRACTILE_FIBER	88.84	2.2	25	8	0.32
AEROBIC_RESPIRATION	53.17	2.2	15	13	0.87
RESPONSE_TO_RADIATION	39	2.2	60	16	0.27
PID_IL3_PATHWAY	9.65	2.2	27	10	0.37
GO_TRANSCRIPTION_EXPORT_COMPLEX	52.59	2.21	13	12	0.92
GO_POSITIVE_REGULATION_OF_DNA_TEMPLATED_TRANSCRIPTION_ELONGATION	47.81	2.21	23	16	0.7
PID_INSULIN_GLUCOSE_PATHWAY	18.14	2.22	26	11	0.42
GO_POSITIVE_REGULATION_OF_MRNA_METABOLIC_PROCESS	17.19	2.22	45	27	0.6
ZF-MIZ	11.83	2.22	7	4	0.57
GO_MRNA_3_UTR_BINDING	52.16	2.23	48	26	0.54
REACTOME_PURINE_METABOLISM	48.02	2.23	33	22	0.67
DNA_REPLICATION_INITIATION	9.15	2.23	16	7	0.44
GO_REGULATION_OF_CHROMATIN_ORGANIZATION	70.88	2.24	152	61	0.4
GO_NEGATIVE_REGULATION_OF_GENE_SILENCING	42.63	2.24	19	5	0.26
BIOCARTA_G1_PATHWAY	41.82	2.24	28	10	0.36
GO_CELL_CYCLE_CHECKPOINT	54.94	2.25	194	93	0.48
GO_PROTEIN_N_TERMINUS_BINDING	25.88	2.25	103	64	0.62
GO_ENDODEOXYRIBONUCLEASE_ACTIVITY	48.57	2.26	51	21	0.41
GO_ASPARTATE_METABOLIC_PROCESS	31.42	2.26	11	5	0.45
GO_POSITIVE_REGULATION_OF_CELLULAR_RESPONSE_TO_INSULIN_STIMULUS	16.99	2.26	23	6	0.26
GO_RESPONSE_TO_ACIDIC_PH	16.79	2.26	21	5	0.24
GO_ENDOLYSOSOME_MEMBRANE	16.29	2.27	11	5	0.45
GO_MYOFILAMENT	82.74	2.28	24	6	0.25
GO_REGULATION_OF_SIGNAL_TRANSDUCTION_BY_P53_CLASS_MEDIATOR	53.98	2.28	162	73	0.45

Gene set	t-test p-value (-log10(|P|), positive = higher in ICR, negative = lower in ICR)		N = No. of genes in the gene set	N.qc = No. of used genes	N/N.qc
	t-test p-value	mixed effects p-value			
MACROMOLECULAR_COMPLEX_DISASSEMBLY	38.21	2.28	15	8	0.53
PID_P73PATHWAY	17.96	2.28	79	41	0.52
GO_RIBONUCLEOTIDE_BINDING	81.21	2.29	1860	694	0.37
GO_REGULATION_OF_PROTEIN_ACETYLATION	48.57	2.29	64	27	0.42
GO_NEGATIVE_REGULATION_OF_CELL_CYCLE_PROCESS	44.5	2.29	214	104	0.49
GO_MEIOTIC_CELL_CYCLE	22.02	2.3	186	58	0.31
GO_ALDEHYDE_CATABOLIC_PROCESS	17.84	2.3	13	9	0.69
M_PHASE_OF_MITOTIC_CELL_CYCLE	46.52	2.31	85	47	0.55
PID_CMYB_PATHWAY	41.73	2.31	84	36	0.43
REACTOME_DOUBLE_STRAND_BREAK_REPAIR	40.26	2.31	24	9	0.38
REGULATION_OF_MITOSIS	40.4	2.32	41	20	0.49
GO_CELL_CYCLE_G2_M_PHASE_TRANSITION	28.36	2.32	138	77	0.56
TCCCRNNRTGC_UNKNOWN	23.51	2.32	213	111	0.52
GO_NUCLEAR_CHROMOSOME	70.81	2.33	523	222	0.42
GO_CHROMATIN_DNA_BINDING	69.13	2.33	80	35	0.44
Targets of COUP_DR1_Q6	66.25	2.33	247	94	0.38
ATP_DEPENDENT_DNA_HELICASE_ACTIVITY	62.62	2.33	11	8	0.73
GO_MITOTIC_DNA_INTEGRITY_CHECKPOINT	39.42	2.33	100	56	0.56
GO_PROTEIN_C_TERMINUS_BINDING	25.24	2.33	186	81	0.44
GO_P53_BINDING	85.62	2.34	67	23	0.34
M_PHASE	45.04	2.35	114	55	0.48
GO_CORONARY_VASCULATURE_DEVELOPMENT	30.33	2.35	37	9	0.24
GO_NEGATIVE_REGULATION_OF_DNA_DEPENDENT_DNA_REPLICATIO N	9.47	2.35	16	5	0.31
Targets of E2F1_Q4_01	60.41	2.36	228	90	0.39
MICROTUBULE_CYTOSKELETON_ORGANIZATION_AND_BIOGENESIS	50.93	2.36	35	18	0.51
GO_NEGATIVE_REGULATION_OF_VIRAL_RELEASE_FROM_HOST_CELL	21.79	2.37	16	9	0.56
REACTOME_APOPTOSIS_INDUCED_DNA_FRAGMENTATION	13.69	2.37	13	8	0.62
GO_CHROMOSOME	75.27	2.38	880	390	0.44
DNA_DEPENDENT_ATPASE_ACTIVITY	64.91	2.38	22	13	0.59
GO_NUCLEOSOMAL_DNA_BINDING	79.26	2.39	30	22	0.73
GO_DNA_DOUBLE_STRAND_BREAK_PROCESSING	21.71	2.39	20	9	0.45
GO_MICROTUBULE_ORGANIZING_CENTER_ORGANIZATION	15.43	2.39	84	40	0.48
Targets of E2F_Q4_01	69.24	2.4	237	100	0.42
GO_ORGANELLE_ASSEMBLY	55.85	2.4	495	214	0.43
GO_REGULATION_OF_PROTEIN_INSERTION_INTO_MITOCHONDRIAL_M EMBRANE_INVOLVED_IN_APOPTOTIC_SIGNALING_PATHWAY	13.8	2.4	29	15	0.52
PID_PI3KCI_AKT_PATHWAY	5.36	2.41	35	16	0.46
REACTOME_DESTABILIZATION_OF_MRNA_BY_BRF1	57.41	2.42	17	13	0.76
GO_POSITIVE_REGULATION_OF_CHROMATIN_MODIFICATION	52.36	2.42	85	35	0.41
HISTONE_METHYLTRANSFERASE_ACTIVITY	26.67	2.42	11	4	0.36
REACTOME_PLATELET_SENSITIZATION_BY_LDL	22.83	2.42	16	6	0.38
PROTEIN_AMINO_ACID_ADP_RIBOSYLATION	20.94	2.42	10	3	0.3
PROTEIN_PHOSPHATASE_TYPE_2A_REGULATOR_ACTIVITY	37.57	2.43	14	7	0.5
CONDENSED_CHROMOSOME	47.3	2.44	34	16	0.47
GTTRYCATRR_UNKNOWN	16.7	2.44	172	45	0.26
MITOCHONDRIAL_TRANSPORT	44.92	2.45	21	19	0.9
REACTOME_INTEGRATION_OF_PROVIRUS	80.22	2.46	16	6	0.38
GO_POSITIVE_REGULATION_OF_MRNA_SPLICING_VIA_SPLICEOSOME	46.81	2.46	14	6	0.43
GO_NEGATIVE_REGULATION_OF_MITOTIC_CELL_CYCLE	36.32	2.46	199	100	0.5
ST_FAS_SIGNALING_PATHWAY	29.53	2.46	65	31	0.48
GO_POSITIVE_REGULATION_OF_DNA_REPLICATION	68.55	2.47	86	31	0.36
GO_NEGATIVE_REGULATION_OF_DNA_REPLICATION	64.35	2.47	55	25	0.45
RRCCGTTA_UNKNOWN	36.84	2.47	87	52	0.6
GO_CHROMATIN	66.61	2.48	441	168	0.38
GO_RESPONSE_TO_FUNGICIDE	17.51	2.48	11	4	0.36
GO_GLOBAL_GENOME_NUCLEOTIDE_EXCISION_REPAIR	16.24	2.49	32	25	0.78
GO_DNA_CATABOLIC_PROCESS	16.38	2.5	27	13	0.48
GO_ATP_DEPENDENT_DNA_HELICASE_ACTIVITY	54.77	2.51	34	19	0.56
MRNA_BINDING	90.95	2.52	23	17	0.74

Gene set	t-test p-value (-log10(|p|), positive = higher in ICR, negative = lower in ICR)		N = No. of genes in the gene set	N.qc = No. of used genes	N/N.qc
	t-test p-value	mixed effects p-value			
PID_AURORA_B_PATHWAY	31.45	2.52	39	19	0.49
CELL_CYCLE_PHASE	53	2.53	170	78	0.46
GO_AU_RICH_ELEMENT_BINDING	29.36	2.54	23	12	0.52
GO_REGULATION_OF_MICROTUBULE_POLYMERIZATION_OR_DEPOLYMERIZATION	19.11	2.54	178	88	0.49
GO_SUMO_BINDING	13.84	2.54	14	5	0.36
Targets of CEBPGAMMA_Q6	46.47	2.55	257	78	0.3
HMG	13.08	2.55	51	17	0.33
GO_REGULATION_OF_PROTEIN_PHOSPHATASE_TYPE_2A_ACTIVITY	33.51	2.57	24	11	0.46
KEGG_BETA_ALANINE_METABOLISM	64.25	2.58	22	11	0.5
GO_RNA_POLYMERASE_II_DISTAL_ENHANCER_SEQUENCE_SPECIFIC_DNA_BINDING	55.57	2.59	65	28	0.43
GO_PEPTIDYL_AMINO_ACID_MODIFICATION	43.76	2.59	841	340	0.4
GO_NEGATIVE_REGULATION_OF_TELOMERASE_ACTIVITY	29.05	2.59	15	7	0.47
Targets of AP2REP_01	27.21	2.61	178	57	0.32
GO_MITOTIC_SPINDLE_ORGANIZATION	21.78	2.61	69	32	0.46
KEGG_GLYOXYLATE_AND_DICARBOXYLATE_METABOLISM	60.42	2.62	16	10	0.62
GO_MITOTIC_CELL_CYCLE_CHECKPOINT	53.4	2.62	139	75	0.54
GO_REGULATION_OF_CELL_CYCLE_ARREST	50.41	2.62	108	52	0.48
GO_REGULATION_OF_DNA_TEMPLATED_TRANSCRIPTION_ELONGATION	46.41	2.62	44	25	0.57
GO_RESPONSE_TO_AMMONIUM_ION	32.19	2.62	51	11	0.22
GO_REGULATION_OF_THYMOCYTE_APOPTOTIC_PROCESS	49.18	2.63	12	4	0.33
GO_POSITIVE_REGULATION_OF_MITOCHONDRIAL_OUTER_MEMBRANE_PERMEABILIZATION_INVOLVED_IN_APOPTOTIC_SIGNALING_PATHWAY	19.54	2.63	36	19	0.53
GO_NEGATIVE_REGULATION_OF_TELOMERE_MAINTENANCE	62.11	2.64	26	17	0.65
GO_CHROMOSOME_TELOMERIC_REGION	64.33	2.65	162	79	0.49
GO_REGULATION_OF_GENE_SILENCING	48.57	2.65	52	16	0.31
PID_ATM_PATHWAY	33.28	2.66	34	12	0.35
REACTOME_E2F_ENABLED_INHIBITION_OF_PRE_REPLICATION_COMPLEX_FORMATION	17.78	2.66	10	6	0.6
GO_REGULATION_OF_EXECUTION_PHASE_OF_APOPTOSIS	88.61	2.67	24	11	0.46
MICROTUBULE	51.63	2.67	32	22	0.69
BIOCARTA_ATRBRCA_PATHWAY	37.5	2.67	21	8	0.38
GO_NEGATIVE_REGULATION_OF_RESPONSE_TO_BIOTIC_STIMULUS	20.91	2.68	30	14	0.47
GO_POSITIVE_REGULATION_OF_PROTEIN_IMPORT_INTO_NUCLEUS_TRANSLOCATION	7.78	2.69	13	5	0.38
GO_NEGATIVE_REGULATION_OF_EPITHELIAL_CELL_MIGRATION	6.17	2.7	53	21	0.4
Targets of E2F1_Q6_01	71.47	2.71	238	98	0.41
GO_ORGANIC_ACID_BINDING	25.77	2.71	209	68	0.33
GO_AMINO_ACID_BINDING	78.19	2.73	108	36	0.33
MITOTIC_SPINDLE_ORGANIZATION_AND_BIOGENESIS	41.3	2.73	10	5	0.5
CHROMOSOMEPERICENTRIC_REGION	29.45	2.74	31	14	0.45
GO_REGULATION_OF_DNA_REPLICATION	86.77	2.75	161	66	0.41
YAATNRNNNYNATT_UNKNOWN	70.49	2.75	104	27	0.26
GO_LYMPHOID_PROGENITOR_CELL_DIFFERENTIATION	77.56	2.78	11	3	0.27
Targets of E2F_Q3_01	60.66	2.79	235	89	0.38
PID_P38_MK2_PATHWAY	31.15	2.82	21	12	0.57
REACTOME_RECRUITMENT_OF_NUMA_TO_MITOTIC_CENTROSOMES	26.59	2.82	10	7	0.7
DNA_RECOMBINATION	70.64	2.85	47	18	0.38
GO_GLYOXYLATE_METABOLIC_PROCESS	55.35	2.86	28	14	0.5
MITOTIC_CELL_CYCLE_CHECKPOINT	22.04	2.86	21	10	0.48
Targets of EFC_Q6	17.64	2.86	268	84	0.31
Targets of E2F_Q3	45.09	2.87	227	91	0.4
REACTOME_E2F_MEDIATED_REGULATION_OF_DNA_REPLICATION	40.93	2.87	35	13	0.37
Targets of ER_Q6_02	15.46	2.87	252	79	0.31
GO_POSITIVE_REGULATION_OF_PROTEIN_ACETYLATION	43.79	2.88	36	12	0.33
CELL_CYCLE_PROCESS	52.7	2.89	193	87	0.45
Targets of E2F1_Q6	63.66	2.9	232	101	0.44
GO_MODULATION_BY_SYMBIONT_OF_HOST_CELLULAR_PROCESS	8.45	2.92	28	11	0.39

Gene set	t-test p-value (-log10(|P|), positive = higher in ICR, negative = lower in ICR)		N = No. of genes in the gene set	N.qc = No. of used genes	N/N.qc
	t-test p-value	mixed effects p-value			
REACTOME_EARLY_PHASE_OF_HIV_LIFE_CYCLE	76.06	2.94	21	10	0.48
SPINDLE_POLE	22.59	2.94	18	9	0.5
GO_POSITIVE_REGULATION_OF_PROTEIN_EXPORT_FROM_NUCLEUS	44.14	2.95	19	7	0.37
GO_GTPASE_ACTIVATING_PROTEIN_BINDING	21.58	2.95	14	7	0.5
TRANSCRIPTION_ELONGATION_REGULATOR_ACTIVITY	23.11	2.99	12	7	0.58
GO_POSITIVE_REGULATION_OF_DNA_METABOLIC_PROCESS	102.41	3.01	185	76	0.41
KEGG_BUTANOATE_METABOLISM	29.15	3.01	34	17	0.5
GO_NUCLEAR_CHROMATIN	52.27	3.03	291	111	0.38
GO_REGULATION_OF_MICROTUBULE_BASED_PROCESS	24.01	3.04	243	106	0.44
GO_FOLIC_ACID_BINDING	53.44	3.06	14	3	0.21
Targets of E2F1DP1RB_01	65.74	3.1	231	96	0.42
Targets of E2F4DP1_01	60.9	3.1	239	100	0.42
BIOCARTA_RB_PATHWAY	33.67	3.1	13	7	0.54
GO_POSITIVE_REGULATION_OF_PROTEIN_IMPORT	26.61	3.11	104	35	0.34
SGCGSSAAA_Targets of E2F1DP2_01	57.9	3.12	168	77	0.46
SPINDLE_ORGANIZATION_AND_BIOGENESIS	51.5	3.13	11	6	0.55
Targets of E2F1DP1_01	71.16	3.17	235	97	0.41
GO_POSITIVE_REGULATION_OF_NUCLEOCYTOPLASMIC_TRANSPORT	29.3	3.19	121	40	0.33
REACTOME_TGF_BETA_RECEPTOR_SIGNALING_IN_EMT_EPITHELIAL_TO_MESENCHYMAL_TRANSITION	66.6	3.2	16	6	0.38
BIOCARTA_TEL_PATHWAY	35.54	3.21	18	10	0.56
Targets of E2F1DP2_01	71.9	3.22	235	97	0.41
DNA_DAMAGE_RESPONSESIGNAL_TRANSDUCTION	42.9	3.24	35	13	0.37
Targets of E2F_02	70.15	3.28	235	98	0.42
BIOCARTA_CHREBP2_PATHWAY	19.81	3.28	42	17	0.4
PID_BARD1_PATHWAY	56.99	3.32	29	15	0.52
GO_NEGATIVE_REGULATION_OF_ORGANELLE_ORGANIZATION	54.33	3.34	387	184	0.48
REACTOME_MITOTIC_G2_G2_M_PHASES	45.21	3.36	81	47	0.58
Targets of E2F4DP2_01	72.15	3.4	235	97	0.41
DNA_DAMAGE_RESPONSESIGNAL_TRANSDUCTION_BY_P53_CLASS_MEDIATOR	39.26	3.44	13	7	0.54
REACTOME_TGF_BETA_RECEPTOR_SIGNALING_ACTIVATES_SMADS	40.84	3.46	26	12	0.46
Targets of E2F1_Q3	79.97	3.47	244	97	0.4
NEGATIVE_REGULATION_OF_ANGIOGENESIS	107.96	3.51	13	3	0.23
Targets of CMYB_01	41.11	3.52	249	106	0.43
GO_RNA_CAP_BINDING_COMPLEX	25.05	3.54	14	6	0.43
PROTEIN_N_TERMINUS_BINDING	65.41	3.56	38	22	0.58
GO_PRONUCLEUS	49.72	3.57	15	9	0.6
PID_DNA_PK_PATHWAY	69.37	3.63	16	9	0.56
GO_RESPONSE_TO_COBALT_ION	77.24	3.64	13	7	0.54
GGAMTNNNNNTCCY_UNKNOWN	108.65	3.67	117	41	0.35
Targets of SMAD3_Q6	25.73	3.74	239	56	0.23
Targets of E2F_Q4	70.57	3.77	234	99	0.42
REACTOME_LOSS_OF_NLP_FROM_MITOTIC_CENTROSOMES	64.59	3.84	59	34	0.58
REACTOME_RECRUITMENT_OF_MITOTIC_CENTROSOME_PROTEINS_AND_COMPLEXES	67.72	3.9	66	39	0.59
Targets of E2F_Q6	72.88	3.99	232	97	0.42
Targets of MYCMAX_B (Myc and MAX targets)	138.78	4.02	268	108	0.4
GO_NEGATIVE_REGULATION_OF_ENDOTHELIAL_CELL_MIGRATION	13.25	4.42	39	16	0.41
GO_RESPONSE_TO_ARSENIC_CONTAINING_SUBSTANCE	68.55	4.46	29	18	0.62
GO_REGULATION_OF_CIRCADIAN_RHYTHM	93.03	5.08	103	29	0.28
GO_ENDODEOXYRIBONUCLEASE_ACTIVITY_PRODUCING_5_PHOSPHOMONOESTERS	26.73	5.36	12	4	0.33

Table 9. Signatures that were used as alternative ICR predictors.

Description	
Signature name	**Reference**
AXL (Tirosh)	Tirosh et al Science 2016

Melanoma cell cycle (Tirosh)	Tirosh et al Science 2016
G1 S (Tirosh)	Tirosh et al Science 2016
G2 M (Tirosh)	Tirosh et al Science 2016
Melanoma cells (Tirosh)	Tirosh et al Science 2016
MITF (Tirosh)	Tirosh et al Science 2016
TME B cell	Tumor microenvironment (TME): Current study
TME CAF	TME: Current study
TME Endo	TME: Current study
TME Mal	TME: Current study
TME NK	TME: Current study
TME Neutrophil	TME: Current study
TME T cells	TME: Current study
TME T CD4	TME: Current study
TME T CD8	TME: Current study
TME Macrophage	TME: Current study
TME immune cells	TME: Current study
TME lymphocytes	TME: Current study
TME meyloid	TME: Current study
TME stroma	TME: Current study
Fluidgm Panel A	www.fluidigm.com/applications/advanta-immuno-oncology-gene-expression-assay
Fluidgm Panel B	www.fluidigm.com/applications/advanta-immuno-oncology-gene-expression-assay
in-vivo screen GVAXPD1 vs TCRaKO depleted	Manguso et al. Cell 2017
in-vivo screen GVAX vs TCRaKO depleted	Manguso et al. Cell 2017
in-vivo screen TCRaKO vs in-vitro depleted	Manguso et al. Cell 2017
in-vivo screen GVAXPD1 vs TCRaKO enriched	Manguso et al. Cell 2017
in-vivo screen GVAX vs TCRaKO enriched	Manguso et al. Cell 2017
in-vivo screen TCRaKO vs in-vitro enriched	Manguso et al. Cell 2017
co-culture screen top 10 hits	Patel et al. Nature 2017
co-culture screen top 50 hits	Patel et al. Nature 2017
Ayers IFNg sig	Ayers et al. JCI 2017
Ayers immune sig	Ayers et al. JCI 2017

TME B cell	TME CAF	TME Endo	TME Mal	TME NK	TME T cells	TME T CD4	TME T CD8	TME Macrophage	TME immune	TME lymphocytes	TME meyloid	TME stroma
ADAM19	ABI3BP	A2M	ABTB2	CCL4	CXCL13	AQP3	APOBEC3C	ACP5	ACAP1	ADAM28	ADAP2	ABI3BP
ADAM28	ACTA2	ADAM15	ACN9	CD244	CST7	CCR4	APOBEC3G	ACRBP	ADAM28	APOBEC3G	AIF1	ACTA2
AFF3	ADAM12	ADCY4	ACSL3	CST7	RARRES3	CCR8	CBLB	ADAMDEC1	ADAP2	BANK1	AMICA1	ADAM12
BANK1	ADAMTS2	AFAP1L1	AHCY	CTSW	KLRC4	CD28	CCL4	ADAP2	AFF3	BCL11A	BCL2A1	ADCY4
BCL11A	ANTXR1	AQP1	AIF1L	GNLY	EMB	CD4	CCL4L1	ADORA3	AIF1	BCL11B	C1orf162	AFAP1L1
BIRC3	ASPN	ARHGEF15	AK2	GZMA	TESPA1	CD40LG	CCL4L2	ALDH2	AKNA	BIRC3	C1QA	APP
BLK	AXL	CALCRL	ALX1	GZMB	LAT	CD5	CCL5	ANKRD22	ALOX5	BLK	C1QB	AQP1
BLNK	BGN	CCL14	ANKRD54	HOPX	CD28	DGKA	CD8A	C1QA	ALOX5AP	BLNK	C1QC	ARHGAP29
BTLA	C1R	CD200	AP1S2	ID2	IL2RG	FAAH2	CD8B	C1QB	AMICA1	CBLB	C3AR1	BGN
CCR6	C1S	CD34	APOA1BP	IL2RB	DUSP2	FOXP3	CRTAM	C1QC	ANKRD44	CCL4	C5AR1	C1R
CCR7	C3	CD93	APOC2	KLRB1	PAG1	ICOS	CST7	C1orf162	AOAH	CCL4L1	CASP1	C1S
CD19	CALD1	CDH5	APOD	KLRC1	TRAT1	IL7R	CTSW	C3AR1	APOBEC3G	CCL4L2	CCR1	CALCRL
CD1C	CCDC80	CFI	APOE	KLRD1	PPP2R5C	LOC100128420	CXCL13	CAPG	ARHGAP15	CCL5	CD14	CALD1
CD22	CD248	CLDN5	ATP1A1	KLRF1	SKAP1	MAL	DTHD1	CARD9	ARHGAP30	CD19	CD163	CCDC80
CD24	CDH11	CLEC14A	ATP1B1	KLRK1	CD96	PASK	DUSP2	CASP1	ARHGAP9	CD2	CD33	CD200
CD37	CERCAM	COL4A2	ATP5C1	NKG7	GPRIN3	PBXIP1	EOMES	CCR2	ARHGDIB	CD22	CD4	CD248
CD79A	CKAP4	CRIP2	ATP5G1	PRF1	CDC42SE2	SLAMF1	FCRL6	CD163	ARRB2	CD247	CD68	CD34
CD79B	COL12A1	CXorf36	ATP5G2	PTGDR	GRAP2	SPOCK2	GZMA	CD300C	B2M	CD27	CD86	CDH11

TME B cell	TME CAF	TME Endo	TME Mal	TME NK	TME T cells	TME T CD4	TME T CD8	TME Macrophage	TME immune	TME lymphocytes	TME meyloid	TME stroma
CHMP7	COL14A1	CYYR1	ATP6V0E2	SH2D1B	GZMM		GZMB	CD33	BANK1	CD28	CECR1	CDH5
CIITA	COL1A1	DARC	ATP6V1C1		RGS1		GZMH	CD4	BCL11A	CD37	CLEC4A	CFH
CLEC17A	COL1A2	DOCK6	ATP6V1E1		SLA2		GZMK	CD68	BCL11B	CD3D	CLEC7A	CFI
CNR2	COL3A1	DOCK9	ATP6V1G1		LOC100130231		ID2	CD86	BCL2A1	CD3E	CPVL	CLDN5
COL19A1	COL5A1	ECE1	AZGP1		PDCD1		IFNG	CEBPA	BIN2	CD3G	CSF1R	CLEC14A
CR2	COL5A2	ECSCR	BAIAP2		ICOS		IKZF3	CECR1	BIRC3	CD5	CSF2RA	COL12A1
CXCR5	COL6A1	EGFL7	BANCR		EVL		ITGAE	CLEC10A	BLK	CD52	CSF3R	COL14A1
ELK2AP	COL6A2	ELK3	BCAN		TC2N		JAKMIP1	CLEC5A	BLNK	CD6	CSTA	COL15A1
FAIM3	COL6A3	ELTD1	BCAS3		LAG3		KLRC4	CMKLR1	BTK	CD7	CTSB	COL1A1
FAM129C	COL8A1	EMCN	BCHE		CBLB		KLRC4-KLRK1	CPVL	C16orf54	CD79A	CTSS	COL1A2
FCER2	CREB3L1	ENG	BIRC7		LCK		KLRD1	CSF1R	C1orf162	CD79B	CXCL16	COL3A1
FCRL1	CTSK	EPHB4	BZW2		TTC39C		KLRK1	CTSB	C1QA	CD8A	CYBB	COL4A1
FCRL2	CXCL12	ERG	C10orf90		NLRC5		MIR155HG	CTSC	C1QB	CD8B	EPSTI1	COL4A2
FCRL5	CXCL14	ESAM	C11orf31		CD5		NKG7	CTSH	C1QC	CD96	FAM26F	COL5A1
FCRLA	CYBRD1	FGD5	C17orf89		ASB2		PRF1	CXCL10	C3AR1	CLEC2D	FBP1	COL5A2
HLA-DOB	CYP1B1	FLT4	C1orf43		PTPN22		RAB27A	CXCL9	C5AR1	CST7	FCGR1A	COL6A1
HLA-DQA2	DCLK1	GALNT18	C1orf85		RAPGEF6		RUNX3	CXCR2P1	CASP1	CTSW	FCGR1B	COL6A2
HVCN1	DCN	GNG11	C4orf48		TNFRSF9		TARP	CYBB	CBLB	CXCR5	FCGR2A	COL6A3
IGLL1	DPT	GPR116	CA14		SH2D2A		TNFRSF9	CYP2S1	CCL3	DENND2D	FCGR2C	CRIP2
IGLL3P	ECM2	GPR146	CA8		GPR174		TOX	DMXL2	CCL4	DGKA	FCGR3B	CTGF
IGLL5	EFEMP2	HSPG2	CACYBP		ITK			DNAJC5B	CCL4L1	DUSP2	FCN1	CXCL12
IRF8	FAM114A1	HYAL2	CAPN3		PCED1B			EBI3	CCL4L2	EEF1A1	FGL2	CXorf36
KIAA0125	FAT1	ICA1	CBX3		CD247			EPSTI1	CCL5	EZR	FPR1	CYBRD1
KIAA0226L	FBLN1	ID1	CCDC47		DGKA			F13A1	CCR1	FAIM3	FPR2	CYR61
LOC283663	FBLN2	IL3RA	CCT2		AAK1			FAM26F	CCR6	FAM129C	FPR3	DCHS1
LTB	FBLN5	ITGB4	CCT3		SH2D1A			FBP1	CD14	FCER2	FTH1	DCN
MS4A1	FGF7	KDR	CCT6A		BTN3A2			FCER1G	CD163	FCRL1	FTL	DOCK6
NAPSB	FSTL1	LAMA5	CCT8		PTPN7			FCGR1A	CD19	FCRLA	GOS2	DPT
P2RX5	GPR176	LDB2	CDH19		UBASH3A			FCGR1C	CD2	FYN	GLUL	ECSCR
PAX5	GPX8	LOC100505495	CDH3		ACAP1			FOLR2	CD22	GNLY	GPX1	EFEMP1
PLEKHF2	HSPB6	MALL	CDK2		FASLG			FPR3	CD244	GZMA	HCK	EFEMP2
PNOC	IGFBP6	MMRN1	CELSR2		INPP4B			FUCA1	CD247	GZMB	HK3	EGFL7
POU2AF1	INHBA	MMRN2	CHCHD6		ARAP2			FUOM	CD27	GZMK	HLA-C	EHD2
POU2F2	ISLR	MYCT1	CITED1		CD3G			GATM	CD28	HLA-DOB	HLA-DMA	ELK3
QRSL1	ITGA11	NOS3	CLCN7		IL7R			GM2A	CD300A	HOPX	HLA-DMB	ELN
RALGPS2	ITGBL1	NOTCH4	CLNS1A		1-Sep			GNA15	CD33	HVCN1	HLA-DRB1	ELTD1
SEL1L3	LOX	NPDC1	CMC2		SCML4			GPBAR1	CD37	ID2	HLA-DRB5	EMCN
SNX29P1	LPAR1	PALMD	COA6		IKZF3			GPR34	CD38	IGLL5	IFI30	ENG
SPIB	LRP1	PCDH17	COX7A2		GATA3			GPX1	CD3D	IKZF3	IGSF6	EPAS1
ST6GAL1	LTBP2	PDE2A	CRYL1		PIM2			HLA-DMA	CD3E	IL2RB	IL1RN	EPHB4
STAG3	LUM	PECAM1	CSAG1		NKG7			HLA-DMB	CD3G	IL32	IL4I1	ERG
STAP1	MAP1A	PLVAP	CSAG2		KLRK1			HLA-	CD4	IL7R	IL8	ESAM

TME B cell	TME CAF	TME Endo	TME Mal	TME NK	TME T cells	TME T CD4	TME T CD8	TME Macrophage	TME immune	TME lymphocytes	TME meyloid	TME stroma
								DPB2				
TCL1A	MEG3	PLXND1	CSAG3		SIT1			HLA-DRB1	CD48	IRF8	IRF5	FAM114A1
TLR10	MFAP4	PODXL	CSAG4		DEF6			HLA-DRB5	CD5	ITK	KYNU	FAP
VPREB3	MFAP5	PRCP	CSPG4		GZMH			HLA-DRB6	CD52	JAK3	LAIR1	FBLN1
WDFY4	MIR100HG	PTPRB	CYC1		LIME1			HMOX1	CD53	KLRB1	LILRA1	FBLN2
	MMP2	PVRL2	CYP27A1		GZMA			IFI30	CD6	KLRC4	LILRA2	FBLN5
	MRC2	RAMP2	DAAM2		JAK3			IL4I1	CD68	KLRD1	LILRA3	FBN1
	MXRA5	RAMP3	DANCR		DENND2D			IRF5	CD69	KLRK1	LILRA6	FGF7
	MXRA8	RHOJ	DAP3		SEMA4D			KCNMA1	CD7	LAG3	LILRB1	FHL1
	MYL9	ROBO4	DCT		SIRPG			KYNU	CD72	LAT	LILRB2	FN1
	NID2	S1PR1	DCXR		CLEC2D			LAIR1	CD74	LCK	LILRB3	FSTL1
	NUPR1	SDPR	DDT		CD8B			LGALS2	CD79A	LOC283663	LILRB4	GNG11
	OLFML2B	SELP	DLGAP1		THEMIS			LILRB1	CD79B	LTB	LRRC25	GPR116
	OLFML3	SHROOM4	DLL3		NLRC3			LILRB4	CD83	LY9	LST1	HSPG2
	PALLD	SLCO2A1	DNAH14		ZAP70			LILRB5	CD86	MAP4K1	LYZ	HTRA1
	PCDH18	SMAD1	DNAJA4		IL12RB1			LIPA	CD8A	MS4A1	MAFB	HYAL2
	PCOLCE	STOM	DSCR8		CTSW			MAFB	CD8B	NAPSB	MAN2B1	ID1
	PDGFRA	TEK	DUSP4		MAP4K1			MAN2B1	CD96	NKG7	MFSD1	ID3
	PDGFRB	TGM2	EDNRB		IFNG			MARCO	CDC42SE2	PARP15	MNDA	IFITM3
	PDGFRL	THBD	EIF3C		SPOCK2			MFSD1	CECR1	PAX5	MPEG1	IGFBP4
	PLAC9	TIE1	EIF3D		DTHD1			MPEG1	CELF2	PCED1B-AS1	MPP1	IGFBP7
	PODN	TM4SF1	EIF3E		APOBEC3G			MS4A4A	CIITA	PDCD1	MS4A4A	IL33
	PRRX1	TM4SF18	EIF3H		PSTPIP1			MS4A6A	CLEC2D	PLAC8	MS4A6A	ISLR
	RARRES2	TMEM255B	EIF3L		CD2			MS4A7	CLEC4A	POU2AF1	MS4A7	KDR
	RCN3	TSPAN18	ENO1		PRF1			MSR1	CLEC7A	POU2F2	MSR1	LAMA5
	SDC1	TSPAN7	ENO2		BCL11B			MTMR14	CORO1A	PRDM1	MXD1	LAMB1
	SDC2	VWF	ENTHD1		PARP8			NAGA	CPVL	PRF1	NAIP	LAMC1
	SEC24D	ZNF385D	ENTPD6		CXCR3			NPC2	CSF1R	PTPN7	NCF2	LDB2
	SERPINF1		ERBB3		CELF2			OAS1	CSF2RA	PTPRCAP	NINJ1	LHFP
	SFRP2		ESRP1		CCL5			OLR1	CSF3R	PYHIN1	NPC2	LIMA1
	SFRP4		ETV4		IL32			PLA2G7	CST7	RHOH	NPL	LIMS2
	SLIT3		ETV5		PRKCQ			PPT1	CSTA	RNF213	PILRA	LOX
	SMOC2		EXOSC4		WIPF1			PTPRO	CTSB	RPL13	PPT1	LOXL2
	SPARC		EXTL1		GZMK			RASSF4	CTSC	RPS27	PSAP	LPAR1
	SPOCK1		FAHD2B		ATHL1			RGS10	CTSD	RPS3A	PTAFR	LTBP2
	SPON1		FAM103A1		ZC3HAV1			RHBDF2	CTSS	RPS6	PYCARD	LUM
	SULF1		FAM178B		CD7			RNASE6	CTSW	RUNX3	RAB20	MAP1B
	SVEP1		FANCL		CD3D			RNASET2	CXCL16	1-Sep	RASSF4	MEG3
	TAGLN		FARP2		RASGRP1			RTN1	CXCR4	SH2D1A	RBM47	MFAP4
	THBS2		FASN		TBC1D10C			SDS	CXCR5	SH2D2A	RGS2	MGP
	THY1		FBXO32		TRAF1			SIGLEC1	CYBA	SIRPG	RNASE6	MMP2
	TMEM119		FBXO7		ARHGEF1			SLAMF8	CYBB	SIT1	RNF130	MXRA8
	TPM1		FDFT1		TARP			SLC15A3	CYFIP2	SKAP1	RNF144B	MYCT1
	TPM2		FKBP4		SPATA13			SLC6A12	CYTH4	SP140	S100A8	MYL9
	VCAN		FMN1		PCED1B-AS1			SLC7A7	CYTIP	SPOCK2	S100A9	NFIB
			FOXD3		RUNX3			SLCO2B1	DENND2D	STAP1	SAT1	NID2
			FXYD3		CD6			SPINT2	DGKA	STAT4	SERPINA1	NNMT
			GAPDH		CD8A			TFEC	DOCK2	TARP	SIGLEC1	NPDC1
			GAPDHS		NELL2			TIFAB	DOCK8	TIGIT	SIGLEC9	OLFML

TME B cell	TME CAF	TME Endo	TME Mal	TME NK	TME T cells	TME T CD4	TME T CD8	TME Macrophage	TME immune	TME lymphocytes	TME meyloid	TME stroma
												3
			GAS2L3		TNFAIP3			TNFSF13	DOK2	TMC8	SIRPB1	PALLD
			GAS5		IPCEF1			TPP1	DOK3	TOX	SLAMF8	PCOLCE
			GAS7		CXCR6			TREM2	DUSP2	VPREB3	SLC7A7	PDGFRA
			GDF15		ITGAL			TYMP	EEF1A1	ZAP70	SLCO2B1	PDGFRB
			GJB1		RHOF			VAMP8	EPSTI1		SPI1	PDLIM1
			GPATCH4		STAT4			VSIG4	EVI2A		SPINT2	PLAC9
			GPM6B		PVRIG			ZNF385A	EVI2B		TBXAS1	PLVAP
			GPNMB		TIGIT				EZR		TFEC	PLXND1
			GPR137B		CD27				FAIM3		THEMIS2	PODN
			GPR143		ZNF831				FAM129C		TLR2	PODXL
			GSTP1		RNF213				FAM26F		TNFRSF10C	PPAP2A
			GYG2		SYTL3				FAM49B		TNFSF13	PPIC
			H2AFZ		CNOT6L				FAM65B		TPP1	PRCP
			HIST1H2BD		SPN				FBP1		TREM1	PRRX1
			HIST3H2A		GPR171				FCER1G		VSIG4	PRSS23
			HMG20B		AKNA				FCER2		ZNF385A	PTPRB
			HMGA1		FYN				FCGR1A			PTRF
			HPGD		RASAL3				FCGR1B			PXDN
			HPS4		CCL4				FCGR2A			RAMP2
			HPS5		TOX				FCGR2C			RAMP3
			HSP90AA1		PRDM1				FCGR3A			RARRES2
			HSP90AB1		PIP4K2A				FCGR3B			RCN3
			HSPA9		CTLA4				FCN1			RHOJ
			HSPD1		GZMB				FCRL1			ROBO4
			HSPE1		HNRNPA1P10				FCRLA			S100A16
			IGSF11		CD3E				FERMT3			S1PR1
			IGSF3		IKZF1				FGD2			SELM
			IGSF8		JAKMIP1				FGD3			SERPINH1
			INPP5F		PYHIN1				FGL2			SLCO2A1
			ISYNA1		MIAT				FGR			SMAD1
			KCNJ13		LEPROTL1				FPR1			SPARC
			LAGE3		OXNAD1				FPR2			SPARCL1
			LDHB		RAB27A				FPR3			SULF1
			LDLRAD3		IL2RB				FTH1			SYNPO
			LEF1-AS1		KLRD1				FTL			TAGLN
			LHFPL3-AS1		PIK3IP1				FYB			TEK
			LINC00473						FYN			TFPI
			LINC00518						G0S2			TGFB1I1
			LINC00673						GBP5			THBS1
			LOC100126784						GLUL			THBS2
			LOC100127888						GNA15			THY1
			LOC100130370						GNLY			TIE1
			LOC100133445						GPR183			TM4SF1
			LOC100505865						GPSM3			TMEM204
			LOC146481						GPX1			TMEM255B
			LOC340357						GRB2			TNS1
			LONP2						GZMA			TPM1
			LOXL4						GZMB			TPM2

TME B cell	TME CAF	TME Endo	TME Mal	TME NK	TME T cells	TME T CD4	TME T CD8	TME Macrophage	TME immune	TME lymphocytes	TME meyloid	TME stroma
			LZTS1						GZMK			VCL
			MAGEA1						HAVCR2			VWF
			MAGEA12						HCK			
			MAGEA2						HCLS1			
			MAGEA2B						HCST			
			MAGEA3						HK3			
			MAGEA4						HLA-B			
			MAGEA6						HLA-C			
			MAGEC1						HLA-DMA			
			MDH1						HLA-DMB			
			MFI2						HLA-DOB			
			MFSD12						HLA-DPA1			
			MIA						HLA-DPB1			
			MIF						HLA-DPB2			
			MITF						HLA-DQA1			
			MLANA						HLA-DQA2			
			MLPH						HLA-DQB1			
			MOK						HLA-DQB2			
			MRPS21						HLA-DRA			
			MRPS25						HLA-DRB1			
			MRPS26						HLA-DRB5			
			MRPS6						HLA-G			
			MSI2						HMHA1			
			MXI1						HOPX			
			MYO10						HVCN1			
			NAV2						ID2			
			NDUFA4						IFI30			
			NDUFB9						IGFLR1			
			NEDD4L						IGLL5			
			NELFCD						IGSF6			
			NHP2						IKZF1			
			NME1						IKZF3			
			NOP58						IL10RA			
			NPM1						IL16			
			NSG1						IL1RN			
			NT5DC3						IL2RB			
			OSTM1						IL2RG			
			PACSIN2						IL32			
			PAGE5						IL4I1			
			PAICS						IL7R			
			PAX3						IL8			
			PEG10						INPP5D			
			PFDN2						IRF5			
			PHB						IRF8			
			PHLDA1						ITGAL			
			PIGY						ITGAM			
			PIR						ITGAX			
			PKNOX2						ITGB2			
			PLEKHB1						ITK			
			PLP1						JAK3			
			PLXNB3						KLRB1			
			PMEL						KLRC4			
			POLR2F						KLRD1			
			PPIL1						KLRK1			
			PPM1H						KYNU			
			PRAME						LAG3			
			PSMB4						LAIR1			
			PUF60						LAPTM5			
			PYGB						LAT			
			PYURF						LAT2			
			QDPR						LCK			
			RAB17						LCP1			
			RAB38						LCP2			
			RAP1GAP						LILRA1			
			RGS20						LILRA2			
			RNF43						LILRA3			
			ROPN1						LILRA6			
			ROPN1B						LILRB1			
			RPL38						LILRB2			
			RSL1D1						LILRB3			
			RTKN						LILRB4			
			S100A1						LIMD2			
			S100B						LITAF			
			SCD						LOC283663			
			SDC3						LRRC25			
			SEC11C						LSP1			
			SEMA3B						LST1			
			SERPINA						LTB			

TME B cell	TME CAF	TME Endo	TME Mal	TME NK	TME T cells	TME T CD4	TME T CD8	TME Macrophage	TME immune	TME lymphocytes	TME meyloid	TME stroma
			3									
			SERPINE2						LY86			
			SGCD						LY9			
			SGK1						LYN			
			SH3D21						LYST			
			SHC4						LYZ			
			SLC19A2						M6PR			
			SLC24A5						MAFB			
			SLC25A13						MAN2B1			
			SLC25A4						MAP4K1			
			SLC26A2						1-Mar			
			SLC3A2						MFSD1			
			SLC45A2						MNDA			
			SLC5A3						MPEG1			
			SLC6A15						MPP1			
			SLC6A8						MS4A1			
			SLC7A5						MS4A4A			
			SNCA						MS4A6A			
			SNHG16						MS4A7			
			SNHG6						MSR1			
			SNRPC						MXD1			
			SNRPD1						MYO1F			
			SNRPE						NAIP			
			SOD1						NAPSB			
			SORD						NCF1			
			SORT1						NCF1B			
			SOX10						NCF1C			
			SOX6						NCF2			
			SPCS1						NCF4			
			SPRY4						NCKAP1L			
			ST13						NINJ1			
			ST3GAL4						NKG7			
			ST3GAL6						NPC2			
			ST3GAL6-AS1						NPL			
			ST6GALNAC2						PAG1			
			STIP1						PARP15			
			STK32A						PARVG			
			STMN1						PAX5			
			STX7						PCED1B-AS1			
			STXBP1						PDCD1			
			SYNGR1						PIK3AP1			
			TBC1D7						PIK3R5			
			TBCA						PILRA			
			TEX2						PIM2			
			TFAP2A						PION			
			TFAP2C						PLAC8			
			TMEM147						PLCB2			
			TMEM14B						PLEK			
			TMEM177						PLEKHA2			
			TMEM251						POU2AF1			
			TMX4						POU2F2			
			TNFRSF21						PPT1			
			TOM1L1						PRDM1			
			TOMM20						PRF1			
			TOMM22						PSAP			
			TOMM6						PSMB10			
			TOMM7						PSTPIP1			
			TOP1MT						PTAFR			
			TRIB2						PTK2B			
			TRIM2						PTPN6			
			TRIM63						PTPN7			
			TRIM9						PTPRC			
			TRIML2						PTPRCAP			
			TRMT112						PYCARD			
			TSPAN10						PYHIN1			
			TTLL4						RAB20			
			TTYH2						RAC2			
			TUBB2B						RASSF4			
			TUBB4A						RBM47			
			TYR						RGS1			

TME B cell	TME CAF	TME Endo	TME Mal	TME NK	TME T cells	TME T CD4	TME T CD8	TME Macrophage	TME immune	TME lymphocytes	TME meyloid	TME stroma
			TYRP1						RGS19			
			UBL3						RGS2			
			UQCRH						RHOF			
			UTP18						RHOG			
			VAT1						RHOH			
			VDAC1						RNASE6			
			VPS72						RNASET2			
			WBSCR22						RNF130			
			XAGE1A						RNF144B			
			XAGE1B						RNF213			
			XAGE1C						RPL13			
			XAGE1D						RPS27			
			XAGE1E						RPS3A			
			XYLB						RPS6			
			ZCCHC17						RPS6KA1			
			ZFP106						RUNX3			
			ZNF280B						S100A8			
			ZNF330						S100A9			
									SAMHD1			
									SAMSN1			
									SASH3			
									SAT1			
									SCIMP			
									SELL			
									SELPLG			
									1-Sep			
									SERPINA1			
									SH2D1A			
									SH2D2A			
									SIGLEC1			
									SIGLEC14			
									SIGLEC7			
									SIGLEC9			
									SIRPB1			
									SIRPG			
									SIT1			
									SKAP1			
									SLA			
									SLAMF6			
									SLAMF7			
									SLAMF8			
									SLC7A7			
									SLCO2B1			
									SNX10			
									SP140			
									SPI1			
									SPINT2			
									SPN			
									SPOCK2			
									SRGN			
									STAP1			
									STAT4			
									STK17B			
									STXBP2			
									SYK			
									TAGAP			
									TARP			
									TBC1D10C			
									TBXAS1			
									TFEC			
									THEMIS2			
									TIGIT			
									TLR1			
									TLR2			
									TMC8			
									TNFRSF10C			
									TNFRSF9			
									TNFSF13			
									TOX			
									TPP1			
									TRAF3IP3			
									TREM1			
									TYROBP			
									UCP2			
									VAMP8			
									VAV1			
									VNN2			
									VPREB3			
									VSIG4			

TME B cell	TME CAF	TME Endo	TME Mal	TME NK	TME T cells	TME T CD4	TME T CD8	TME Macrophage	TME immune	TME lymphocytes	TME meyloid	TME stroma
									WIPF1			
									ZAP70			
									ZNF385A			

Table 10. Signatures of Expanded T cells

Up/down regulated in expanded T cells compared to non-expanded T cells.					
up (expanded)	down (expanded)	up (all)		down (all)	
ABCD2	ALOX5AP	ABCD2	NAB1	AAK1	MCM5
ADAM28	ANXA1	ADAM28	NCALD	AHNAK	MRPS24
AIM2	ARL4C	AIM2	NEK7	ALOX5AP	MRPS34
AKAP5	C12orf75	AKAP5	NFAT5	ANAPC15	MUTYH
AP1AR	CAMK4	AKAP8L	NMB	ANXA1	MXD4
ARID5A	CD200R1	ANAPC4	NOD2	AP5S1	MYH9
ARNT	CD44	AP1AR	NOTCH1	APOBEC3G	NDUFB9
ATHL1	CD5	AQR	NSUN2	ARL4C	NEDD8
ATP2C1	COX7A2	ARID5A	OPA1	ASF1B	NFKBIZ
BCOR	DBF4	ARNT	ORMDL3	ATG16L2	NR4A3
CADM1	EMP3	ATHL1	OSBPL3	AURKA	NUP37
CCL3L3	FAM46C	ATM	PAPOLA	BOLA3	PCK2
DGKD	FOSB	ATP2C1	PARP11	BUB1	PCNA
DTHD1	GZMH	ATXN7L1	PCED1B	C12orf75	PDCD5
ETV1	HMGA1	BCOR	PCM1	C3orf38	PDE4B
G3BP1	KIAA0101	C17orf59	PDE7B	CAMK4	PFDN2
HSPA1B	KLRG1	C18orf25	PDGFD	CARD16	PHLDA1
ID3	LIME1	CADM1	PDXDC2P	CCR5	POLR2K
ITM2A	LMNB1	CAV1	PIK3AP1	CCR7	PRDX3
KCNK5	MAB21L3	CCL3L3	PIKFYVE	CD200R1	PRPF4
KLRC2	NR4A3	CD200	PJA2	CD44	PRR5L
KLRC3	PCK2	CDC73	PRKCH	CD5	PXN
KLRC4	PCNA	CEP85L	PROSER1	CD97	RDH11
KLRK1	PDCD5	DDX3Y	PSTPIP1	CKS1B	REXO2
LOC220729	PDE4B	DDX6	PTPN6	COX7A2	RNASEH2C
LONP2	PFDN2	DGKD	PYHIN1	DBF4	RNASEK
LRBA	RDH11	DGKH	RALGDS	DNAJC9	RPUSD3
LYST	S100A10	DNAJA2	RCBTB2	DTYMK	RTCA
NAB1	S100A4	DTHD1	RGS2	ECE1	S100A10
NMB	SAMD3	ELF1	RGS4	ECHS1	S100A4
PAPOLA	SPOCK2	ELMO1	RHOB	ELL	S100A6
PDE7B	TKT	ETNK1	RIN3	EMP3	S1PR1
PIK3AP1	TNF	ETV1	RNF19A	F2R	SAMD3
PRKCH	TOB1	FAIM3	RWDD2B	FAM46C	SELL
PROSER1	TOMM7	FBXW11	S100PBP	FAM50B	SLIRP
PTPN6	TUBA1C	FCRL3	SATB1	FOSB	SPOCK2
PYHIN1	UGDH-AS1	FOXN2	SDAD1	FOXP1	STX16
RGS2		G3BP1	SEC24C	GMCL1	TANK
RGS4		GALT	SERINC3	GNPTAB	TKT
S100PBP		GFOD1	SFI1	GPR183	TMEM173
SH2D1B		GNG4	SH2D1B	GTF3C6	TNF
SNAP47		HIF1A	SKIV2L	GYPC	TNFAIP3
SPDYE8P		HIST1H2BG	SLC30A7	GZMA	TNFSF4
SPRY2		HIST2H2BE	SLC7A5P1	GZMH	TOB1
SYVN1		HSPA1B	SLFN11	HAUS4	TOMM5
TACO1		HSPB1	SNAP47	HMGA1	TOMM7
THADA		ID3	SOD1	HMOX2	TPT1
TP53INP1		IL6ST	SPATA13	INSIG1	TUBA1B
TSC22D1		INPP5B	SPDYE8P	ITM2C	TUBA1C
UBA7		INPP5F	SPRY2	KIAA0101	TUBB4B
ZMYM2		IRF8	STT3B	KLF6	TXN

Up/down regulated in expanded T cells compared to non-expanded T cells.					
up (expanded)	down (expanded)	up (all)		down (all)	
		ITM2A	SYVN1	KLRB1	UBE2Q2P3
		KCNK5	TACO1	KLRG1	UCHL3
		KDM4C	TBC1D23	LEF1	UGDH-AS1
		KLRC2	TBC1D4	LIME1	UQCRB
		KLRC3	THADA	LMNB1	VIM
		KLRC4	TNFRSF9	LTB	WBP11
		KLRD1	TNIP1	LY6E	ZNF683
		KLRK1	TP53INP1	MAB21L3	
		LOC100190986	TRAF5		
		LOC220729	TSC22D1		
		LOC374443	TTI2		
		LONP2	TTTY15		
		LRBA	TXNDC11		
		LRRC8D	UBA7		
		LSM14A	VMA21		
		LY9	VPRBP		
		LYST	WWC3		
		MBP	ZBED5		
		MED13	ZMYM2		
		MGA	ZMYM5		
		MGEA5	ZNF384		
		MS4A1	ZNF468		
		MST4	ZNF83		
		NAA16			

Example 2 – Immunotherapy Resistance Signature from 26 Melanoma Tumors

[0424] Applicants performed single-cell RNA-seq on 26 melanoma tumors (12 treatment naïve, 14 post immunotherapy) (**Figure 17**). Applicants discovered that immunotherapy leads to profound transcriptional alterations in both the malignant and immune cells. Applicants also discovered that these transcriptional programs are associated the response to immunotherapy by analyzing prior data sets (Hugo et al. Cell. 2016 Mar 24;165(1):35-44. doi: 10.1016/j.cell.2016.02.065; and Riaz et al. Nature Genetics 48, 1327–1329 (2016) doi:10.1038/ng.3677). Applicants also discovered that these transcriptional programs are associated Intra-tumor: heterogeneity, location, and antigen presentation. Applicants explored and characterized the effect immunotherapies have on different cell types within the tumor (i.e., Malignant cells, CD8/CD4 T-cells, B cells and Macrophages). The data includes twenty six samples (14 post immunotherapy, 8 anti-CTLA4 & anti-PD-1, 2 anti-PD1(Nivolumab), 4 anti-CTLA4 (Ipilimumab), and 12 treatment naïve (**Figure 17**).

[0425] Applicants performed principal component analysis on the expression data. The second Principle Component (PC) separates between immunotherapy resistant and untreated tumors (**Figure 18**). Applicants discovered that treatment is the main source of variation in malignant cells between tumors, reflected by the difference in the score of malignant cells from treatment naive and resistant tumors on the second principle component.

[0426] Applicants analyzed the transcriptome of the malignant cells to identify cell states that are associated with immunotherapy. To this end, Applicants identified differentially expressed genes and derived two post-immunotherapy (PIT) modules, consisting of genes that are up (PIT-up) or down (PIT-down) regulated in PIT malignant cells compared to the untreated ones. In comparison to the treatment naive tumors, all the PIT tumors overexpress the PIT-up module and underexpress the PIT-down module, such that there is a spectrum of expression levels also within each patient group and within the malignant cell population of a single tumor (**Figure 19**). The genes within each module are co-expressed, while the two modules are anti-correlated with each other, not only across tumors but also within the malignant cell population of a single tumor. Additionally, the two modules have heavy and opposite weights in the first principle components of the malignant single-cell expression profiles, indicating that immunotherapy is one of the main sources of inter-tumor heterogeneity in the data.

[0427] Applicants applied down sampling and cross-validation to confirm that the PIT modules are robust and generalizable (**Figure 20**). More specifically, Applicants repeatedly identified the signatures without accounting for the data of one of the tumors, and showed that the modules were similar to those derived with the full dataset. Furthermore, the modules that were derived based on a *training* data could still correctly classify the *test* tumor as either PIT or treatment naive. The signature is very robust. If Applicants leave out all the malignant cells from a given tumor, recalculate it and then assign the cells, Applicants make only one "error" when guessing if the tumor is treatment naive or ITR. This one tumor has a particularly high T cell infiltration. These results testify that, while more data and samples will enable us to refine these modules, the resulting modules are not likely to change substantially. The signature is also supported by the mutual exclusive expression of the up and down genes across malignant cells, and their anti-correlation in TCGA (**Figure 21**).

[0428] Gene set enrichment analysis of the PIT programs highlights well-established immune-evasion mechanisms as the down-regulation of MHC class I antigen presentation machinery and interferon gamma signaling in PIT cells (**Table 11**). Cells with less MHC-I expression are more resistant to immunotherapy (**Figure 22**). Additionally, it has been recently shown that melanoma tumors that are resistant to ipilimumab therapy contain genomic defects in IFN-gamma pathway genes, and that the knockdown of IFNGR1 promotes tumor growth and reduces mouse survival in response to anti-CTLA-4 therapy. The PIT-down program is also enriched with genes involved in coagulation, IL2-STAT5

signaling, TNFα signaling via NFkB, hypoxia, and apoptosis. The PIT-up program is tightly linked to MYC. It is enriched with MYC targets and according to the connectivity map data (c-map) – MYC knockout alone is able to repress the expression of the entire PIT-up signature. Supporting these findings, it has been shown that MYC modulates immune regulatory molecules, such that its inactivation in mouse tumors enhances the antitumor immune response. Interestingly, Applicants find that metalothionines (MTs) are overrepresented in the PIT-down program, and show that their expression alone separates between the PIT and untreated samples (**Figure 23**). MTs are a family of metal-binding proteins that function as immune modulators and zinc regulators. The secretion of MTs to the extracellular matrix can suppress T-cells and promote T-cell chemotaxis. Interestingly, it has been recently shown that MT2A is a key regulator of CD8 T-cells, such that its inhibition promotes T-cell functionality in the immunosuppressive tumor microenvironment (Singer et al. Cell. 2016 Sep 8;166(6):1500-1511). The underexpression of MTs in the malignant cells of post-immunotherapy tumors could potentially be linked to the role of MT2A in T-cells and to the abundance of zinc in the tumor microenvironment.

Table 11. Functional classification of PIT module genes.

Pathway	Genes
MHC class I antigen presentation machinery	*CTSB, HLA-A, HLA-C, HLA-E, HLA-F, PSME1, TAP1, TAPBP*
Coagulation	*ANXA1, CD9, CFB, CTSB, FN1, ITGB3, LAMP2, PROS1, PRSS23, SERPINE1, SPARC, TF*
TNFα signaling via NFkB	*ATF3, BCL6, BIRC3, CD44, EGR1, GADD45B, GEM, JUNB, KLF4, KLF6, NR4A1, PDE4B, SERPINE1, TAP1, TNC*
IL2/STAT5 signaling	*AHNAK, AHR, CCND3, CD44, EMP1, GADD45B, IFITM3, IGF1R, ITGA6, KLF6, NFKBIZ, PRNP, RNH1*
Metallothioneins	*MT1E, MT1F, MT1G, MT1M, MT1X, MT2A*
MYC targets	*EIF4A1, FBL, HDAC2, ILF2, NCBP1, NOLC1, PABPC1, PRDX3, RPS3, RUVBL2, SRSF7*

[0429] Applicants identified an immunotherapy resistance signature by identifying genes that were up and down regulated in immunotherapy treated subjects as compared to untreated subjects (**Table 12, 13**). The signature was compared to clinical data of subjects that were

complete responders to immunotherapy, partial responders and non-responders. The data was also compared to subjects with high survival and low survival.

Table 12. Analysis of all gene expression data and clinical data

	clinic.R.more	clinic.R.less	sc.All	sc.Old	sc.New	sc.Bulk	sc.Q.gene	tcga.Increased.risk	tcga.Increased.risk.beyond.T.cells
ANXA1	7.58E-02	8.19E-01	-202.40	-2.44	-200.00	-3.02	FALSE	-2.64	-1.37
EMP1	4.92E-01	8.96E-02	-189.84	-20.93	-75.82	-2.58	FALSE	0.69	0.60
TSC22D3	4.26E-01	4.63E-01	-175.14	-13.19	-82.60	-2.43	FALSE	-1.52	-0.32
MT2A	4.06E-02	7.81E-01	-174.76	-18.16	-67.52	-4.41	FALSE	-2.83	-1.80
CTSB	4.03E-01	5.87E-01	-165.96	-25.70	-112.90	-2.50	FALSE	-0.44	0.56
TM4SF1	1.76E-01	7.74E-01	-164.10	5.621836397	-165.5071875	-1.14	FALSE	0.45	0.32
CDH19	4.35E-02	4.15E-01	-155.59	-3.79	-42.42	-1.53	FALSE	-2.24	-1.86
MIA	3.62E-01	4.96E-01	-152.98	-4.22	-60.91	-1.53	FALSE	-1.60	-0.91
SERPINE2	2.27E-02	1.70E-01	-151.17	-31.78	-46.03	-1.68	FALSE	-3.66	-3.12
SERPINA3	1.43E-01	4.64E-01	-148.25	13.63	-229.59	-1.37	FALSE	-2.64	-2.04
S100A6	2.91E-01	2.01E-01	-128.57	-12.30	-49.34	-2.42	FALSE	-0.40	-0.47
ITGA3	3.35E-02	9.20E-01	-123.57	1.88215819	-83.80670184	-0.97	FALSE	-0.51	-0.49
SLC5A3	4.64E-01	4.71E-01	-119.83	1.06	-96.80	-1.71	FALSE	-6.19	-4.10
A2M	3.01E-02	4.38E-01	-118.06	-15.73720409	-30.29161959	-1.07	FALSE	-2.81	-1.47
MFI2	3.67E-01	4.22E-01	-117.29	-3.06	-44.01	-1.41	FALSE	0.46	0.38
CSPG4	7.50E-01	2.24E-01	-112.90	-5.56	-30.13	-1.87	FALSE	-1.60	-1.41
AHNAK	5.70E-02	7.09E-01	-112.83	-12.69	-13.16	-2.03	FALSE	-0.45	-0.38
APOC2	6.76E-01	1.57E-01	-111.01	4.108007818	-92.34012794	-0.52	FALSE	-0.55	0.51
ITGB3	1.66E-01	3.79E-01	-110.25	0.79	-109.99	-1.75	FALSE	-2.25	-1.42
NNMT	4.47E-01	6.63E-01	-110.12	-1.62	-122.65	-2.51	FALSE	-2.28	-0.87
ATP1A1	2.34E-01	4.92E-01	-107.58	-19.25	-26.63	-1.40	FALSE	0.52	0.30
SEMA3B	8.03E-02	9.69E-01	-106.75	-2.022007432	-74.18998319	-1.06	FALSE	-1.65	-1.08
CD59	3.34E-02	7.57E-01	-101.92	-16.59	-40.13	-1.86	FALSE	-1.71	-0.90
PERP	1.03E-01	9.58E-01	-99.65	-2.61892627	-123.0851115	-1.13	FALSE	0.78	-0.77
EGR1	1.98E-01	8.54E-01	-96.70	-1.43	-25.74	-1.30	FALSE	-0.80	0.30
LGALS3	2.66E-01	6.41E-01	-96.06	-57.79606403	1.174991366	-1.19	FALSE	-0.42	-0.50
SLC26A2	1.86E-01	2.65E-01	-95.69	0.615403346	-34.74613485	-0.92	FALSE	-3.62	-2.73
CRYAB	2.26E-02	5.72E-01	-94.74	0.85	-139.66	-1.89	FALSE	-0.84	-0.63
HLA-F	4.70E-02	9.62E-01	-94.42	-12.84	-23.07	-1.82	FALSE	-4.49	-1.03

	clinic.R.more	clinic.R.less	sc.All	sc.Old	sc.New	sc.Bulk	sc.Q.gene	tcga.Increased.risk	tcga.Increased.risk.beyond.T.cells
MT1E	1.78E-01	5.89E-01	-92.61	-14.66	-27.25	-3.00	FALSE	-1.20	-1.19
KCNN4	1.88E-01	7.63E-01	-92.09	-1.36	-108.90	-2.56	FALSE	-4.61	-2.92
CST3	1.87E-01	6.36E-01	-90.32	-3.11	-43.51	-2.19	FALSE	-1.31	0.32
CD9	6.23E-01	4.58E-01	-89.32	-9.57	-19.34	-2.77	FALSE	0.35	-0.79
TNC	3.59E-01	6.45E-01	-87.60	-6.21	-88.45	-1.78	FALSE	-2.72	-1.10
SGCE	2.19E-02	3.21E-01	-87.28	-0.302176627	-62.80958661	-1.02	FALSE	-3.12	-1.69
NFKBIZ	2.32E-02	9.71E-01	-86.67	-4.35	-30.64	-2.89	FALSE	-2.40	-1.85
PROS1	2.16E-02	4.37E-01	-86.35	-0.52	-28.78	-1.72	FALSE	-0.40	-0.71
CAV1	6.55E-02	3.13E-01	-85.42	-24.08	-6.13	-1.34	FALSE	-1.43	-0.72
MFGE8	2.64E-01	3.77E-01	-84.81	-12.26983949	-19.33461436	-1.07	FALSE	-1.84	-1.29
IGFBP7	7.97E-01	9.60E-02	-83.96	-22.46	-27.89	-1.37	FALSE	-0.37	0.88
SLC39A14	1.73E-01	8.74E-01	-83.65	0.52	-37.30	-1.97	FALSE	-0.52	-0.67
CD151	2.53E-01	3.98E-01	-83.63	-2.11	-33.44	-1.90	FALSE	-0.56	-0.63
SCCPDH	5.51E-01	3.85E-01	-83.37	-3.18	-20.08	-1.68	FALSE	-1.26	-1.07
MATN2	6.66E-01	2.81E-01	-82.90	-0.523529704	-70.365600 95	-1.17	FALSE	-0.34	0.68
DUSP4	2.30E-01	3.73E-01	-82.27	-6.19379111	-19.37401872	-1.18	FALSE	0.58	0.60
APOD	3.39E-01	5.42E-01	-81.89	-9.70	-15.76	-1.58	FALSE	-1.62	-1.49
GAA	1.72E-01	6.87E-01	-81.55	-2.56	-27.32	-1.50	FALSE	-1.23	-0.56
CD58	1.48E-01	5.02E-01	-81.12	-1.03	-40.89	-2.52	FALSE	-2.40	-3.24
HLA-E	5.00E-02	9.47E-01	-79.92	-25.19	-23.50	-1.86	FALSE	-3.54	0.48
TIMP3	4.17E-01	8.28E-02	-79.58	-6.278620205	-2.728290317	-1.11	FALSE	-1.13	-1.19
NR4A1	1.22E-01	6.52E-01	-79.47	-14.82	-8.42	-1.37	FALSE	0.32	-0.51
FXYD3	2.31E-02	8.64E-01	-78.83	-3.88	-17.90	-1.81	FALSE	-0.47	-0.96
TAPBP	9.56E-02	9.33E-01	-78.23	-9.90	-25.67	-1.40	FALSE	-3.06	0.45
CTSD	2.10E-01	4.50E-01	-76.29	-35.68	-12.15	-1.73	FALSE	0.51	1.21
NSG1	2.25E-01	5.26E-02	-75.54	-6.8850195	-45.25690934	-0.59	FALSE	NA	NA
DCBLD2	1.51E-01	3.97E-01	-75.17	-2.70	-30.36	-2.50	FALSE	-0.93	-1.69
GBP2	3.33E-02	4.65E-01	-74.58	-6.60	-112.34	-3.42	FALSE	-9.49	-2.53
FAM3C	2.17E-02	3.24E-01	-73.79	-1.099557442	-34.2099212	-0.80	FALSE	-4.22	-2.95
CALU	7.70E-01	2.45E-01	-73.21	-2.96	-22.58	-1.44	FALSE	0.34	-0.56
DDR1	1.30E-02	9.47E-01	-72.94	1.320302264	-41.93649931	-0.93	FALSE	-0.66	-1.98
TIMP1	2.44E-01	1.95E-01	-72.66	0.832732502	-44.3146	-1.27	FALSE	-2.53	-0.80

	clinic.R.more	clinic.R.less	sc.All	sc.Old	sc.New	sc.Bulk	sc.Q.gene	tcga.Increased.risk	tcga.Increased.risk.beyond.T.cells
					5375				
LRPAP1	3.26E-01	5.82E-01	-72.03	-8.741825947	-33.28409269	-1.12	FALSE	0.55	0.62
CD44	1.20E-01	7.83E-01	-71.20	-42.03	-7.56	-1.31	FALSE	-1.20	-0.70
GSN	1.83E-01	9.76E-02	-71.17	-7.066367901	-8.379109684	-1.25	FALSE	-0.48	-0.40
PTRF	1.20E-01	1.26E-01	-70.87	-11.99	-21.89	-2.19	FALSE	-0.81	-0.88
CAPG	3.42E-01	4.17E-01	-70.60	-17.12110776	-3.792804113	-1.21	FALSE	-0.42	0.69
CD47	1.14E-01	8.55E-01	-68.77	-5.84	-21.44	-2.75	FALSE	-5.65	-3.19
CCND3	1.48E-01	7.90E-01	-68.60	-0.85	-62.30	-2.43	FALSE	-0.65	0.43
HLA-C	1.63E-01	4.28E-01	-68.47	-22.92	-13.18	-1.33	FALSE	-4.97	-1.10
CARD16	3.15E-02	9.14E-01	-68.09	-1.20	-51.51	-1.48	FALSE	-0.65	0.50
DUSP6	3.52E-01	3.46E-01	-67.35	-1.443530586	-32.17071544	-0.53	FALSE	-4.33	-2.45
IL1RAP	6.76E-03	4.53E-01	-66.82	-2.25	-24.21	-3.64	FALSE	-1.77	-1.51
FGFR1	7.25E-02	1.31E-01	-66.47	-9.950506533	-57.92951091	-1.14	FALSE	-0.49	-0.62
TRIML2	8.90E-01	1.20E-01	-66.24	-21.84557542	-68.40922705	-0.49	FALSE	-1.47	-1.52
ZBTB38	7.00E-01	3.77E-01	-65.84	-6.25	-8.44	-1.64	FALSE	-3.18	-3.11
PRSS23	6.42E-01	8.53E-02	-63.62	-0.34	-35.59	-1.53	FALSE	-0.54	0.37
S100B	4.64E-01	6.74E-01	-63.21	-18.39689161	-0.989534032	-1.08	FALSE	-1.72	-0.73
PLP2	1.29E-02	7.48E-01	-63.01	-3.16	-7.46	-1.46	FALSE	0.34	-0.80
LAMP2	2.64E-01	6.13E-01	-62.96	-5.73	-13.68	-1.48	FALSE	-1.19	-1.06
FCGR2A	8.31E-04	8.38E-01	-62.40	-0.623470411	-28.64302633	-0.93	FALSE	-6.97	-2.82
LGALS1	7.24E-02	1.72E-01	-61.40	-12.41	-1.43	-1.38	FALSE	0.77	1.02
NPC1	9.96E-02	4.70E-01	-60.93	-2.330822107	-12.24708172	-0.83	FALSE	0.37	-0.31
UBC	6.96E-01	4.80E-01	-60.76	-6.83	-41.63	-1.69	FALSE	-1.71	-0.61
TNFRSF12A	8.03E-02	7.99E-01	-60.31	1.73	-37.68	-1.53	FALSE	-0.63	-0.66
SPON2	1.56E-01	2.67E-01	-59.94	-0.444813435	-54.28549635	-0.87	FALSE	-0.62	0.47
EEA1	4.38E-01	4.73E-01	-59.50	-0.680184335	-13.23401918	-1.02	FALSE	-1.33	-2.70
CD63	7.00E-01	2.67E-01	-59.49	-14.73233445	-14.29263209	-1.30	FALSE	1.10	0.65
SGK1	4.34E-01	3.83E-01	-59.42	-2.77588165	-13.57291112	-0.52	FALSE	0.63	0.68
HPCAL1	1.03E-01	6.53E-02	-59.22	-8.70	-10.48	-1.83	FALSE	-0.69	-0.91
HLA-B	5.22E-02	8.84E-01	-58.69	-16.77311	-7.71200	-1.18	FALSE	-5.85	-0.79

	clinic.R.more	clinic.R.less	sc.All	sc.Old	sc.New	sc.Bulk	sc.Q.gene	tcga.Increased.risk	tcga.Increased.risk.beyond.T.cells
				58	708				
SERPINA1	5.48E-01	4.51E-01	-58.50	4.67012442	-61.13154453	-0.74	FALSE	-2.78	0.47
JUN	3.03E-01	7.09E-01	-58.42	1.182777495	-17.43164065	-1.18	FALSE	-0.89	0.32
HLA-A	4.98E-02	9.30E-01	-58.18	-26.50	-18.12	-1.46	FALSE	-2.09	-0.34
RAMP1	5.43E-01	2.02E-01	-58.03	-11.93	-63.50	-1.60	FALSE	0.45	0.53
TPP1	7.54E-02	8.18E-01	-57.91	-18.16810565	-4.426800522	-1.02	FALSE	-0.70	-0.41
FYB	1.49E-01	7.19E-01	-57.13	-2.867192419	-45.734459 12	-0.52	FALSE	-4.33	-0.75
RDH5	1.02E-01	8.47E-01	-56.99	1.683618144	-39.48423368	-0.59	FALSE	-3.18	-2.30
SDC3	1.84E-01	4.92E-01	-56.80	-2.227320442	-7.930319849	-0.90	FALSE	-1.46	-0.67
PRKCDBP	2.03E-01	3.35E-01	-56.58	-3.45	-25.88	-2.48	FALSE	-0.69	-0.46
CSGALNACT1	3.14E-01	1.30E-01	-56.46	-1.005860494	-21.10234746	-1.19	FALSE	-5.34	-3.85
HLA-H	2.38E-01	7.55E-01	-56.36	-26.8522345	-2.691659575	-0.99	FALSE	-2.77	-0.44
CLEC2B	9.68E-04	1.64E-01	-55.69	-3.93	-40.47	-1.87	FALSE	-8.63	-4.19
ATP1B1	4.75E-01	9.93E-02	-55.53	3.790248535	-73.66520645	-0.74	FALSE	-3.09	-1.56
DAG1	2.86E-01	6.40E-01	-55.41	-3.15	-5.62	-1.66	FALSE	-0.71	-0.52
NFKBIA	5.25E-03	5.77E-01	-55.35	-7.315272323	-17.05872829	-1.05	FALSE	-4.18	-0.54
SRPX	3.36E-01	2.51E-01	-55.12	-7.37	-3.79	-2.09	FALSE	-0.80	-1.57
CASP1	6.92E-02	8.19E-01	-55.00	-1.031280571	-66.19783 81	-0.96	FALSE	-1.32	0.38
DPYSL2	1.23E-02	7.32E-01	-54.92	-1.056511462	-99.22916498	-1.14	FALSE	-0.77	0.34
S100A1	1.82E-01	1.09E-01	-54.68	-14.25397572	-14.42420921	-0.63	FALSE	-0.61	-0.78
FLJ43663	Inf	Inf	-54.67	-6.490292736	-10.57910257	-1.20	FALSE	-4.45	-4.16
UPP1	1.21E-01	7.67E-01	-54.34	-7.451372117	-2.528276372	-1.13	FALSE	1.67	1.17
APOE	3.46E-01	1.80E-01	-54.04	-4.357609216	-10.06500479	0.32	FALSE	0.31	1.11
LPL	1.87E-01	1.61E-01	-54.00	-6.59	-51.84	-2.19	FALSE	-0.45	-0.45
KLF4	3.63E-02	9.02E-01	-53.99	-0.31	-23.01	-2.34	FALSE	-0.55	-0.36
SLC20A1	3.66E-01	3.38E-01	-53.68	0.47	-18.37	-2.06	FALSE	-2.41	-1.61
LGALS3BP	1.92E-01	8.74E-01	-53.62	-12.98	-5.64	-1.68	FALSE	-0.61	0.43
LINC00116	4.39E-01	1.53E-01	-53.33	0.38	-29.09	-1.90	FALSE	NA	NA

	clinic.R.more	clinic.R.less	sc.All	sc.Old	sc.New	sc.Bulk	sc.Q.gene	tcga.Increased.risk	tcga.Increased.risk.beyond.T.cells
RPS4Y1	8.64E-02	9.11E-01	-53.11	-64.09755214	-3.82061851	-0.66	FALSE	1.34	1.23
SQRDL	9.82E-02	8.26E-01	-52.38	-5.25	-38.28	-3.08	FALSE	-3.94	-1.26
ITM2B	2.72E-02	7.97E-01	-52.21	-10.23	-13.51	-1.63	FALSE	-5.41	-2.59
TMX4	4.28E-01	2.58E-01	-52.20	-1.16	-13.17	-1.39	FALSE	-2.83	-1.33
IL6ST	1.01E-02	3.26E-01	-52.05	-2.89	-6.37	-1.61	FALSE	-1.92	-0.83
BIRC3	1.72E-01	7.32E-01	-51.42	-7.23	-41.19	-4.32	FALSE	-7.28	-2.50
ANXA2	4.45E-01	5.66E-01	-51.27	-12.18	-8.25	-2.15	FALSE	0.78	0.68
ZBTB20	2.19E-01	7.01E-01	-51.13	-1.09	-25.68	-1.43	FALSE	-0.42	0.31
GRN	9.79E-02	5.69E-01	-51.04	-3.33479904	-10.58500961	-0.92	FALSE	0.51	0.95
SERPINE1	2.26E-01	8.94E-02	-50.78	0.45	-45.37	-2.08	FALSE	-1.78	-0.47
MT1X	9.41E-02	7.92E-01	-50.16	-2.90	-20.02	-1.51	FALSE	-1.45	-2.13
FCGR2C	6.04E-04	3.75E-01	-50.04	-6.560207399	-28.23432948	-0.90	FALSE	-5.71	-2.00
ACSL3	4.57E-01	3.37E-01	-49.94	-3.939970091	-4.775352737	-0.49	FALSE	-0.93	-1.32
IFI27	2.77E-01	4.25E-01	-49.91	-24.12491388	-7.193933103	-1.12	FALSE	-3.69	-1.74
AEBP1	7.23E-03	7.36E-01	-49.86	-0.652064041	-9.791519511	-1.24	FALSE	-0.31	0.33
TIPARP	6.67E-02	5.81E-01	-49.73	-1.699010303	-20.128488456	-1.30	FALSE	-2.25	-1.20
VAMP8	7.89E-02	4.82E-01	-49.73	-5.340727074	-25.951535555	-0.78	FALSE	-0.77	1.19
DST	3.55E-01	6.19E-01	-48.89	-2.44	-3.35	-1.59	FALSE	0.47	0.55
IFI35	1.88E-01	7.91E-01	-48.67	-7.02	-6.98	-2.31	FALSE	-3.05	-1.00
ITGB1	3.60E-01	2.39E-01	-48.52	-3.58	-9.62	-2.66	FALSE	-1.85	-1.87
BCL6	8.45E-02	8.06E-01	-48.50	-4.89	-22.66	-3.13	FALSE	-4.25	-1.89
ERBB3	1.90E-01	6.37E-01	-48.36	-9.73134426	-0.4390782615	-0.73	FALSE	0.53	0.33
ZMYM6NB	6.10E-01	1.14E-01	-47.89	-1.77	-21.83	-1.45	FALSE	NA	NA
CLIC4	1.22E-01	3.15E-01	-47.81	-1.16	-17.42	-1.41	FALSE	-4.55	-3.87
FOS	4.13E-01	6.43E-01	-47.57	-6.386092681	-1.042139346	-0.73	FALSE	-0.87	-0.36
IGF1R	3.62E-01	4.41E-01	-47.19	-1.54	-23.75	-1.37	FALSE	-0.36	-0.58
PLEKHB1	2.57E-02	3.38E-01	-46.81	-6.095867912	-42.432086655	-0.54	FALSE	-1.60	-1.68
GOLGB1	5.56E-01	4.63E-01	-46.38	-4.661054566	-8.368284482	-1.24	FALSE	-2.84	-2.24
PSAP	1.12E-01	7.72E-01	-45.94	-17.73630528	0.396372679	-1.07	FALSE	-0.67	0.69
RNF145	4.06E-02	6.25E-01	-45.93	-4.00	-9.25	-2.29	FALSE	-2.59	-1.12

	clinic.R.more	clinic.R.less	sc.All	sc.Old	sc.New	sc.Bulk	sc.Q.gene	tcga.Increased.risk	tcga.Increased.risk.beyond.T.cells
CTSL1	5.49E-01	2.91E-01	-45.88	-13.12164871	-18.65717439	-0.84	FALSE	0.67	0.86
SYNGR2	2.82E-03	7.59E-01	-45.78	-5.09168104	-10.48190321	-0.94	FALSE	-1.25	0.81
HTATIP2	8.60E-01	1.13E-01	-45.69	-2.00	-19.85	-2.43	FALSE	-1.31	-1.68
KLF6	2.33E-02	6.52E-01	-45.62	-18.85	1.21	-1.57	FALSE	-0.45	-0.44
LOC541471	Inf	Inf	-45.38	-2.644136674	-11.14964202	-1.23	FALSE	1.16	1.08
SAT1	2.24E-01	3.62E-01	-44.81	-30.71664031	-1.26808839	-0.55	FALSE	-0.81	0.50
FBXO32	1.79E-01	2.88E-01	-44.73	0.322762583	-6.161648524	-0.32	FALSE	0.70	0.40
S100A10	5.31E-03	6.74E-01	-44.66	-22.95	0.42	-2.01	FALSE	0.38	0.48
ATF3	4.52E-01	3.92E-01	-44.63	1.63	-38.08	-2.50	FALSE	-1.55	0.34
SCARB2	8.77E-02	6.12E-01	-44.43	-2.576905156	-2.01525226	-1.16	FALSE	-1.06	-0.77
GPNMB	1.82E-01	7.59E-01	-44.30	-27.37333779	-0.672867612	-0.74	FALSE	0.44	0.73
FCRLA	7.03E-03	9.79E-01	-44.01	-10.35	-13.12	-1.87	FALSE	-0.40	0.40
CLU	6.77E-01	4.88E-01	-43.85	2.663183144	-40.06196504	-0.63	FALSE	-1.13	0.40
ADM	6.89E-01	6.95E-02	-43.84	-4.543551718	-28.969298 56	-0.76	FALSE	0.30	0.30
TF	5.05E-01	4.79E-01	-43.65	-8.72	-51.07	-1.33	FALSE	-1.03	-0.56
CAST	2.14E-02	8.85E-01	-43.40	-2.23	-9.80	-1.38	FALSE	-1.51	-1.09
C10orf54	2.37E-01	5.08E-01	-43.23	-1.005464269	-47.29182888	-1.01	FALSE	-3.61	0.82
ITGA6	4.78E-01	4.15E-01	-43.18	-3.18	-12.52	-2.60	FALSE	-3.43	-1.94
PSMB9	1.02E-01	7.61E-01	-43.08	-9.75	-11.68	-1.87	FALSE	-6.40	-1.66
BACE2	3.23E-01	6.02E-01	-43.02	-1.544458411	-3.818105651	-0.83	FALSE	2.35	1.69
GADD45B	4.04E-01	1.97E-01	-42.59	-1.28	-35.87	-1.53	FALSE	-1.56	0.60
IFI27L2	4.94E-01	1.42E-01	-42.51	-11.43	-4.73	-1.31	FALSE	-0.54	-0.68
FADS3	3.81E-01	5.31E-01	-42.38	-2.307281418	-10.48779629	-0.84	FALSE	-0.73	-0.64
GPR155	4.45E-01	3.44E-01	-42.36	-1.727392739	-9.730760161	-0.67	FALSE	-2.99	-1.44
IFNGR2	2.69E-02	5.64E-01	-42.34	-2.678730729	-5.824501595	-1.16	FALSE	-2.71	-1.79
NEAT1	1.24E-03	9.34E-01	-42.32	-3.957711442	-4.816575504	-0.65	FALSE	-2.07	-2.38
ARL6IP5	9.95E-02	8.05E-01	-42.03	-5.061500123	-6.026877076	-1.20	FALSE	-4.08	-2.21
GJB1	6.66E-02	6.60E-01	-42.02	-3.94868444	-3.639865415	-0.32	FALSE	-0.31	0.38

	clinic.R.more	clinic.R.less	sc.All	sc.Old	sc.New	sc.Bulk	sc.Q.gene	tcga.Increased.risk	tcga.Increased.risk.beyond.T.cells
ACSL4	6.24E-01	3.88E-01	-41.97	-1.75	-14.86	-2.59	FALSE	-6.05	-3.62
ATP1B3	2.92E-02	6.43E-01	-41.66	-2.82	-21.79	-3.00	FALSE	-0.52	-0.79
ECM1	1.35E-01	5.94E-01	-41.65	-2.62	-6.36	-1.47	FALSE	2.45	1.30
APLP2	4.94E-01	1.91E-01	-41.49	1.55753898	-32.79252137	-0.99	FALSE	-1.94	-2.11
ANGPTL4	4.14E-01	2.31E-01	-41.48	-0.66	-57.88	-1.62	FALSE	-0.39	0.38
GPR56	7.32E-03	6.52E-01	-41.45	-18.86181027	6.113225588	0.32	FALSE	1.27	1.10
SYPL1	2.59E-01	7.74E-01	-41.38	-2.204809487	-11.39626417	-1.08	FALSE	-1.57	-3.14
FNDC3B	2.11E-01	3.32E-01	-41.27	-1.78	-19.28	-1.86	FALSE	-4.21	-2.77
CYBRD1	3.43E-01	9.88E-02	-41.01	-3.84	-6.47	-1.37	FALSE	-1.60	-1.51
CTSA	1.55E-01	5.79E-01	-40.89	-3.17	-15.31	-1.86	FALSE	0.49	0.68
MCL1	4.84E-01	4.49E-01	-40.82	-0.665221316	-21.449244463	-1.22	FALSE	-4.37	-1.75
LEF1	1.84E-01	7.45E-01	-40.69	-0.409062265	-22.957591126	-0.36	FALSE	-0.88	-0.46
BBX	2.43E-01	5.39E-01	-40.61	-0.61	-21.43	-1.67	FALSE	-3.83	-2.98
FKBP5	5.46E-01	2.10E-01	-40.55	-9.020160799	-25.902858892	-1.24	FALSE	-1.88	-0.53
FAM114A1	7.76E-01	2.18E-01	-40.47	-3.16	-18.85	-1.90	FALSE	-0.54	-0.53
LTBP3	1.66E-01	4.22E-01	-40.27	3.20667713	-16.874364626	-0.99	FALSE	-2.15	-2.16
HSPA1A	9.37E-01	1.13E-01	-40.16	9.037838299	-41.236498866	-0.31	FALSE	1.23	1.55
EPHX2	1.42E-01	2.31E-01	-40.08	-1.222892988	-48.822458871	-1.07	FALSE	0.77	0.95
ITGA7	6.60E-01	3.30E-01	-40.03	15.86332961	-39.835924494	0.37	FALSE	0.61	-0.61
AGA	2.23E-01	7.32E-01	-39.91	0.536274519	-9.136581859	-0.68	FALSE	-1.38	-1.08
LYRM9	7.78E-03	8.61E-01	-39.80	1.964812062	-24.631025517	-0.69	FALSE	NA	NA
CREG1	2.30E-01	6.57E-01	-39.71	-1.46	-13.57	-1.52	FALSE	-3.57	-3.22
IFI6	4.46E-01	3.38E-01	-39.64	-15.10	0.69	-1.73	FALSE	-1.61	-0.66
JUNB	3.17E-01	3.06E-01	-39.64	1.25	-18.40	-1.74	FALSE	-1.43	-0.32
SPTBN1	6.95E-03	6.68E-02	-39.48	-10.19774666	1.9742265	-0.96	FALSE	0.37	-0.44
PRNP	1.27E-01	7.68E-01	-39.20	-0.86	-16.57	-1.55	FALSE	-2.85	-2.80
TNFSF4	9.86E-01	3.54E-03	-38.88	16.30016407	-42.882092111	-0.42	FALSE	-3.81	-2.50
C8orf40	2.61E-01	2.10E-01	-38.60	-0.90	-18.77	-2.97	FALSE	-0.99	-1.72
SEL1L	4.31E-01	4.74E-01	-38.58	-3.90	-1.91	-1.65	FALSE	-3.19	-2.36

	clinic.R.more	clinic.R.less	sc.All	sc.Old	sc.New	sc.Bulk	sc.Q.gene	tcga.Increased.risk	tcga.Increased.risk.beyond.T.cells
SNX9	8.39E-02	9.43E-01	-38.40	4.21773408	-17.87314667	-0.31	FALSE	-1.99	-2.10
KRT10	7.68E-01	1.86E-01	-38.33	6.615582665	-27.12457887	-1.01	FALSE	2.72	0.66
EPDR1	1.94E-01	1.86E-01	-37.93	4.58	-42.43	-1.53	FALSE	-0.35	-0.76
EGR2	2.42E-01	1.28E-01	-37.72	-0.332043956	-14.27003379	-1.16	FALSE	-2.88	-0.63
GATSL3	1.63E-01	1.34E-02	-37.61	7.800143337	-24.63977081	-0.35	FALSE	-0.94	-0.81
COL16A1	3.73E-01	3.56E-01	-37.54	-2.47	-38.81	-1.42	FALSE	-1.72	-0.87
CD55	5.71E-01	1.64E-01	-37.49	-1.97067768	-9.604169548	-0.97	FALSE	-1.46	-4.40
CRELD1	5.86E-01	6.12E-01	-37.35	5.47	-34.69	-1.57	FALSE	-1.13	-0.68
SVIP	5.84E-01	1.64E-01	-37.25	-0.974568455	-25.31871464	-0.74	FALSE	-1.56	-1.15
NFE2L1	8.30E-02	8.74E-01	-37.12	-0.70	-10.29	-1.42	FALSE	1.23	0.70
PRDX1	6.51E-01	4.55E-01	-36.94	-3.087427147	-24.82199094	-0.54	FALSE	0.70	0.62
B2M	4.43E-02	7.71E-01	-36.89	-21.10505197	-26.41773682	-1.10	FALSE	-7.29	-2.96
PDE4DIP	5.31E-01	5.09E-02	-36.89	-0.402602515	-9.208907424	-0.71	FALSE	0.49	0.41
APOL1	1.22E-01	6.68E-01	-36.88	-1.287252758	-17.14787261	-0.74	FALSE	-5.74	-1.36
CREB3L2	4.17E-01	4.63E-01	-36.84	0.358284954	-2.018391143	-0.49	FALSE	-0.60	-0.70
EVA1A	1.57E-01	6.76E-01	-36.71	-0.761040106	-18.07156414	-0.66	FALSE	NA	NA
TIMP2	1.13E-01	8.26E-01	-36.71	-0.626230588	-4.251996112	-0.64	FALSE	1.22	0.72
STAT3	1.90E-01	6.70E-01	-36.62	-0.369941565	-8.5293768	-1.07	FALSE	-3.12	-0.90
EZH1	5.10E-02	3.93E-01	-36.54	-0.417829156	-9.673454	-1.13	FALSE	-2.33	-2.81
SPRY2	1.85E-02	2.34E-01	-36.26	-1.08	-25.28	-1.61	FALSE	-2.42	-2.39
ITGA10	6.22E-01	1.93E-01	-36.13	-2.05617709	-7.093599209	-0.71	FALSE	-1.57	-1.75
TGOLN2	2.71E-01	6.43E-01	-35.99	-1.61	-8.04	-1.52	FALSE	-2.20	-1.14
NFAT5	3.84E-02	6.11E-01	-35.92	-0.97	-7.21	-1.45	FALSE	-2.99	-2.31
CD46	7.87E-01	3.15E-01	-35.83	-11.65	-0.60	-1.53	FALSE	-4.30	-4.97
HLA-G	1.55E-01	5.82E-01	-35.67	-28.13806449	-4.324585401	-1.15	FALSE	-2.09	-0.41
NPC2	4.63E-01	2.90E-01	-35.66	-14.30417724	0.495091905	-0.40	FALSE	0.54	1.18
LOC100127888	6.29E-02	8.12E-01	-35.63	-11.84	-3.62	-1.37	FALSE	0.83	-0.35

	clinic.R.more	clinic.R.less	sc.All	sc.Old	sc.New	sc.Bulk	sc.Q.gene	tcga.Increased.risk	tcga.Increased.risk.beyond.T.cells
LXN	1.66E-01	5.62E-01	-35.60	-4.54	-40.35	-2.72	FALSE	-0.74	-0.38
MT1M	3.49E-01	2.33E-01	-35.36	-14.10	-11.08	-3.18	FALSE	-0.69	-0.68
C16orf45	3.02E-03	6.46E-01	-35.32	-0.76	-48.53	-1.56	FALSE	-2.09	-1.93
LOXL3	8.91E-01	4.37E-02	-35.03	4.82	-40.56	-1.35	FALSE	-3.28	-1.82
LINC00152	5.34E-01	3.79E-01	-34.97	-5.73	-8.24	-1.32	FALSE	NA	NA
PDK4	6.52E-01	1.85E-01	-34.90	-5.780192629	-25.27607059	-0.98	FALSE	-0.86	-0.83
GEM	4.46E-01	1.12E-02	-34.88	1.13	-32.19	-1.60	FALSE	-1.36	-0.81
CCDC47	2.14E-01	1.23E-01	-34.85	0.460464013	-4.08009 3569	-0.82	FALSE	-0.76	-0.68
SAA1	2.70E-01	6.03E-01	-34.50	-14.25803074	-33.7718886	-1.07	FALSE	-0.63	-0.54
FAP	2.46E-01	1.13E-01	-34.42	4.359167404	-41.9045 5405	-0.39	FALSE	-0.67	-0.60
IER3	9.45E-02	7.96E-01	-34.39	1.561694536	-19.8124 9058	-1.06	FALSE	-1.68	-2.71
LEPROT	6.81E-02	4.29E-01	-34.35	-3.84	-3.79	-1.37	FALSE	-1.36	-1.01
SQSTM1	3.08E-01	5.29E-01	-34.34	-8.65	-2.82	-1.56	FALSE	-0.46	-0.44
TMEM66	1.03E-01	1.17E-01	-34.23	-6.335487056	-14.2478 9241	-1.11	FALSE	-2.58	-1.09
BIN3	7.84E-02	8.47E-01	-34.16	-1.04	-4.76	-1.88	FALSE	0.32	-0.68
H2AFJ	3.84E-02	5.04E-01	-34.07	-25.87241942	16.3668 4482	-1.06	FALSE	2.18	1.36
TAPBPL	1.34E-01	7.56E-01	-33.96	-0.367921789	-29.9760 1261	-1.09	FALSE	-2.88	-0.43
CHPF	6.61E-01	4.31E-01	-33.88	2.895612909	-13.0886 9319	-1.15	FALSE	0.71	-0.37
KIAA1551	3.03E-01	2.58E-01	-33.84	-2.17	-10.79	-2.28	FALSE	NA	NA
CCPG1	6.35E-01	5.74E-01	-33.73	-2.59	-3.53	-1.41	FALSE	-3.84	-3.38
CHI3L1	4.46E-01	4.28E-01	-33.64	0.396603931	-50.3233 9741	-1.07	FALSE	-3.88	-1.18
TNFRSF10B	2.48E-01	3.26E-01	-33.55	-1.29	-19.70	-1.58	FALSE	0.41	-0.32
ENDOD1	3.12E-01	7.77E-01	-33.51	-2.51853644	1.04123 2189	-1.04	FALSE	-0.45	-1.09
CLIP1	1.44E-02	6.78E-01	-33.48	-2.054976195	-6.35811 2418	-1.14	FALSE	-0.55	-0.44
TMBIM1	8.50E-02	9.38E-01	-33.46	-7.42	-1.80	-1.93	FALSE	0.33	-0.34
AHR	5.02E-02	6.01E-02	-33.45	-2.02	-16.52	-2.41	FALSE	-3.48	-1.81
TMED9	7.07E-01	4.41E-01	-33.43	3.860348819	-7.45232 1879	-0.87	FALSE	0.49	0.55
NPTN	1.61E-01	6.54E-01	-33.14	-0.52	-4.89	-1.37	FALSE	-2.34	-2.31
UBE2B	1.90E-01	3.56E-01	-33.08	-4.50	-9.49	-2.60	FALSE	-3.96	-3.73
SYNE2	8.23E-02	8.84E-01	-33.05	-8.739833	3.94233 7418	-0.55	FALSE	-0.81	0.32

	clinic.R.more	clinic.R.less	sc.All	sc.Old	sc.New	sc.Bulk	sc.Q.gene	tcga.Increased.risk	tcga.Increased.risk.beyond.T.cells
				095					
MBNL1	8.92E-02	5.79E-01	-32.82	-5.434241 63	0.46937 185	-1.05	FALSE	-5.55	-2.89
FAM46A	3.69E-01	2.02E-02	-32.69	3.82	-22.62	-1.63	FALSE	-1.06	-1.10
IL12RB2	4.14E-01	3.95E-01	-32.68	-16.46671 472	-5.37628 8421	-0.96	FALSE	-0.41	0.64
DDIT3	7.65E-01	3.64E-02	-32.63	1.447014 332	-19.2775 0288	-1.20	FALSE	-0.70	-2.12
FOSB	1.43E-01	8.00E-01	-32.49	-0.796475 507	-4.31272 261	-1.06	FALSE	-1.11	0.34
CAV2	1.80E-01	2.59E-01	-32.43	-3.08	-4.61	-1.36	FALSE	-1.69	-1.13
STOM	3.22E-01	4.73E-01	-32.40	-4.411700 006	-0.60124 6398	-0.40	FALSE	-0.52	1.09
SERINC1	6.29E-02	4.88E-01	-32.30	-3.03	-11.26	-1.69	FALSE	-1.80	-2.10
MT1F	5.29E-01	2.87E-01	-32.19	-10.67	-7.72	-1.67	FALSE	-0.35	0.31
FZD6	4.56E-02	4.75E-01	-32.14	-4.466223 946	-10.6108 4389	-0.42	FALSE	-2.55	-3.38
G6PD	4.37E-02	7.80E-01	-32.10	2.04	-13.40	-1.65	FALSE	-0.35	0.40
MVP	4.11E-02	9.36E-01	-32.00	-2.51	-3.07	-1.43	FALSE	-1.53	-0.51
TMED10	3.04E-01	4.70E-01	-31.94	-3.937577 051	-1.49110 1847	-0.72	FALSE	-0.78	-1.04
MCOLN3	5.15E-02	7.52E-01	-31.92	-1.592257 374	-34.9598 1505	-1.28	FALSE	0.56	0.63
C4A	5.68E-02	7.73E-01	-31.78	5.638375 4	-63.9558 7021	-0.57	FALSE	-3.86	-0.65
CHPT1	1.14E-01	7.16E-01	-31.65	-1.71	-8.66	-1.96	FALSE	-0.92	-0.97
TOB1	1.63E-01	2.88E-01	-31.63	-3.499775 851	-9.25731 9016	-0.60	FALSE	0.32	-0.67
ELK3	2.92E-01	4.28E-01	-31.32	0.690617 385	-15.6088 5115	-0.75	FALSE	-1.57	-1.23
RND3	3.53E-01	5.03E-01	-30.88	-4.70	-15.82	-2.44	FALSE	-1.33	-1.28
PHLDA1	1.23E-01	6.12E-01	-30.88	-3.554078 519	-12.0807 0285	-1.05	FALSE	-0.72	-1.27
TRIB1	2.16E-01	4.24E-01	-30.87	-4.102846 583	-7.01253 5992	-1.14	FALSE	-1.07	-0.49
PLOD3	6.85E-01	3.92E-01	-30.70	-4.529043 691	-0.52129 9179	-1.19	FALSE	0.50	-0.36
DUSP1	2.31E-01	1.61E-01	-30.66	0.662164 296	-14.2747 394	-0.77	FALSE	-1.45	-0.31
LAMA4	3.36E-01	1.86E-01	-30.65	1.304437 005	-13.7140 9326	-0.96	FALSE	-2.08	-1.15
ALCAM	1.39E-01	5.13E-01	-30.52	-0.324216 688	-7.23309 32	-1.26	FALSE	-0.64	0.45
PRKAR1A	6.16E-01	5.09E-01	-30.49	-2.995748 369	-5.80777 074	-0.36	FALSE	-2.49	-1.59

	clinic.R.more	clinic.R.less	sc.All	sc.Old	sc.New	sc.Bulk	sc.Q.gene	tcga.Increased.risk	tcga.Increased.risk.beyond.T.cells
CYSTM1	1.56E-01	6.62E-01	-30.37	-5.01	-1.52	-1.52	FALSE	NA	NA
MPZ	7.95E-01	3.44E-02	-30.22	3.827991239	-17.8589262	-0.79	FALSE	-0.98	-0.46
REEP5	4.44E-01	2.83E-01	-30.12	-5.08	-6.71	-2.22	FALSE	-0.94	-0.57
BCAP29	6.01E-02	2.85E-01	-30.07	-0.788569825	-8.452538217	-0.66	FALSE	-3.69	-3.59
PLEC	3.00E-01	1.49E-01	-29.99	0.32314	-11.40496196	-1.07	FALSE	-0.70	-0.48
CBLB	4.62E-02	6.91E-01	-29.96	1.160755876	-17.28521246	-0.37	FALSE	-0.90	-0.37
CHI3L2	4.24E-01	3.28E-01	-29.83	-4.908298993	-29.80387401	-1.50	FALSE	-2.40	-0.30
GRAMD3	2.24E-02	1.27E-01	-29.69	-3.175491376	-32.24829385	-2.48	FALSE	-1.28	-0.61
CAMP	2.58E-01	2.56E-01	-29.67	-6.537864387	-32.95941798	-1.04	FALSE	-1.50	-0.43
CSRP1	6.53E-01	4.51E-01	-29.65	-3.645548095	-4.555036259	-1.17	FALSE	-1.00	-1.12
ARMCX3	5.62E-01	4.06E-02	-29.33	-6.284817238	-0.591876729	-1.90	FALSE	-0.38	-0.36
CANX	2.70E-01	5.34E-01	-29.31	-1.780081404	-6.181232682	-0.92	FALSE	-0.75	-0.53
TXNIP	1.58E-01	8.52E-01	-29.27	-0.527598171	-4.214704474	0.37	FALSE	-0.70	1.02
S100A16	4.52E-01	6.89E-01	-29.26	0.688460885	-13.99697	-0.84	FALSE	-0.44	-1.03
HEXB	3.66E-01	1.28E-01	-29.23	-6.435524884	-0.371050963	-1.21	FALSE	-1.30	-0.79
WEE1	2.40E-02	3.83E-01	-29.22	-1.837664314	-10.457768818	-0.94	FALSE	-2.16	-1.20
CTSO	2.03E-01	3.03E-01	-29.18	-0.529135038	-10.257117093	-0.89	FALSE	-3.34	-0.64
PLOD2	2.29E-02	2.76E-01	-29.00	-1.038914654	-11.952619747	-0.82	FALSE	-1.68	-0.99
DAAM2	2.86E-01	8.20E-01	-28.93	0.995149536	-16.353413947	-0.37	FALSE	0.33	0.31
IQGAP1	2.26E-01	8.38E-01	-28.81	-5.892500327	-3.999796242	-1.01	FALSE	-1.12	-0.63
ATP6V1B2	3.12E-02	9.33E-01	-28.81	-1.236034151	-5.748568853	-1.57	FALSE	-0.42	-0.37
PSMB8	8.52E-02	7.24E-01	-28.67	-5.117567066	-8.854518735	-1.76	FALSE	-4.67	-1.59
TES	1.42E-01	5.00E-01	-28.64	-0.478011716	-32.215559921	-0.44	FALSE	-0.88	0.34
ABHD2	1.04E-01	6.28E-01	-28.54	-1.251595254	-10.618951132	-2.78	FALSE	-1.09	-0.84
AKAP9	6.09E-01	1.96E-01	-28.52	0.35918391	-5.461432538	-0.42	FALSE	-2.69	-2.68

	clinic.R.more	clinic.R.less	sc.All	sc.Old	sc.New	sc.Bulk	sc.Q.gene	tcga.Increased.risk	tcga.Increased.risk.beyond.T.cells
LIF	6.70E-01	3.44E-01	-28.52	3.073773887	-28.07039375	-1.10	FALSE	-4.32	-3.08
PLK3	1.38E-01	8.45E-01	-28.49	1.464108474	-11.44618117	-0.99	FALSE	-0.50	-0.36
OSBPL5	6.95E-01	3.31E-02	-28.46	-2.269849969	-8.980489184	-1.32	FALSE	-0.98	-1.54
ADIPOR2	1.68E-01	8.80E-01	-28.35	-0.839832233	-5.706827917	-1.02	FALSE	1.68	0.89
S100A4	7.37E-01	6.12E-02	-28.27	-3.380134016	-64.01199908	-1.03	FALSE	-1.02	-0.40
RTKN	6.89E-01	3.62E-01	-28.22	-0.492129374	-9.892228036	-0.92	FALSE	0.53	-0.68
NR4A2	4.92E-02	6.31E-01	-28.21	-3.780760282	-0.423389847	-1.30	FALSE	-2.24	-1.22
PPAPDC1B	2.33E-01	9.19E-02	-28.10	-1.533802908	-10.81399535	-1.87	FALSE	-1.98	-1.79
MAGEC2	6.50E-01	7.68E-02	-28.07	-2.1071117	-41.347003335	-1.46	FALSE	-1.05	-1.02
PDE4B	6.64E-01	2.67E-01	-28.03	-2.364902426	-35.009444346	-2.37	FALSE	-3.27	-0.50
AQP3	3.72E-01	7.16E-01	-28.03	-9.058871123	-22.680440058	-1.01	FALSE	0.58	1.50
RTP4	1.96E-02	8.07E-01	-27.94	-5.675337518	-6.019705486	-2.01	FALSE	-2.18	-0.74
NIPAL3	7.84E-02	7.37E-01	-27.58	-2.025738972	-2.559743987	-0.76	FALSE	-3.63	-3.63
PPP4R2	5.59E-01	3.37E-01	-27.53	-2.21758079	-3.375501383	-0.68	FALSE	-2.28	-1.72
NDRG1	3.17E-01	1.99E-01	-27.44	-2.248121009	-15.876895568	-0.56	FALSE	-3.88	-3.05
PFKP	3.56E-02	1.73E-01	-27.42	0.422114565	-4.660264324	-0.49	FALSE	1.20	0.49
CD200	2.69E-01	5.64E-01	-27.40	-2.559052299	-16.890136676	-2.02	FALSE	-2.30	-0.77
SLC2A3	5.69E-01	3.59E-01	-27.38	-1.861116025	-1.247312253	-0.79	FALSE	0.52	0.65
TRIM51	1.23E-02	9.86E-01	-27.38	-22.00677143	-5.876405839	-0.74	FALSE	NA	NA
TJP1	2.45E-01	2.61E-01	-27.23	0.387152694	-29.978507109	-0.85	FALSE	-0.81	0.36
CPVL	6.42E-01	1.96E-01	-27.04	0.662656107	-31.857370706	-0.59	FALSE	-1.29	-0.44
IFRD1	5.23E-02	1.74E-01	-27.01	4.489953381	-27.072407597	-0.51	FALSE	-1.74	-3.39
LMNA	2.61E-01	7.35E-01	-26.99	-14.85556789	5.149222622	-0.90	FALSE	0.57	0.39
TMEM30A	8.31E-02	1.20E-01	-26.95	-1.296738123	-9.650459473	-0.72	FALSE	-4.05	-4.59

	clinic.R.more	clinic.R.less	sc.All	sc.Old	sc.New	sc.Bulk	sc.Q.gene	tcga.Increased.risk	tcga.Increased.risk.beyond.T.cells
NAMPT	2.38E-01	8.88E-01	-26.92	-0.599957745	-8.35441204	-1.27	FALSE	-3.72	-2.18
INPP5F	1.79E-01	4.31E-01	-26.90	-4.825022902	0.536466924	-0.49	FALSE	-2.07	-1.43
DLGAP1-AS1	9.43E-01	5.69E-02	-26.86	-0.873888664	-5.983055739	-0.56	FALSE	NA	NA
ENTPD6	3.39E-01	2.81E-01	-26.81	0.918823136	-9.944809472	-0.69	FALSE	0.64	0.62
ANKRD36BP1	3.05E-01	8.29E-01	-26.74	-0.387440246	-1.450487926	-1.12	FALSE	-0.84	0.33
DNASE2	3.82E-01	3.30E-01	-26.66	-5.792710027	-3.087603241	-1.13	FALSE	-0.85	-0.45
PARP9	1.77E-02	9.10E-01	-26.62	-8.593426968	-3.79735601	-3.07	FALSE	-6.05	-2.17
ETV4	4.66E-01	4.90E-01	-26.48	2.154806287	-40.7905761	-0.37	FALSE	-0.31	-0.77
AKR1C3	1.43E-01	4.41E-01	-26.25	-4.534550779	-31.83008396	-1.29	FALSE	-0.42	0.41
PIGT	8.38E-01	1.37E-01	-26.24	0.796637157	-21.82796134	-1.98	FALSE	1.11	0.71
ANKRD28	6.58E-02	8.47E-01	-26.18	-0.835178911	-1.880605312	-1.05	FALSE	-0.34	-0.72
TCN1	2.30E-01	3.90E-01	-25.97	13.20783241	-24.95604114	-0.76	FALSE	0.85	0.51
SERINC5	2.86E-01	3.40E-01	-25.90	-1.367509487	-2.310450523	-0.56	FALSE	-0.35	0.98
SLC38A2	2.45E-01	6.32E-01	-25.84	5.887885708	-14.851784	-0.51	FALSE	-3.06	-2.13
SLC16A3	4.77E-01	5.69E-03	-25.80	-1.860338009	-2.425802885	-0.48	FALSE	-0.53	0.41
ENO2	7.06E-02	3.19E-01	-25.77	-5.890890828	-0.712932382	-0.60	FALSE	0.64	-0.60
ADAM9	2.70E-02	5.60E-01	-25.74	0.496294512	-4.870672147	-1.45	FALSE	-0.75	-0.46
P4HA2	2.45E-01	1.78E-01	-25.73	1.590533138	-10.68944038	-1.54	FALSE	0.67	0.58
TRIM47	7.98E-02	9.46E-01	-25.63	-1.850462382	-9.018178263	-0.70	FALSE	-0.52	0.36
S100A13	1.28E-01	8.69E-01	-25.59	-0.978590241	-3.665918361	-0.34	FALSE	0.38	-0.44
SUMF2	3.63E-01	4.64E-01	-25.55	1.576955308	-9.135832478	-1.47	FALSE	0.43	-0.50
LONP2	7.24E-02	6.03E-01	-25.52	-1.149798332	-2.114676254	-0.35	FALSE	-0.92	-0.99
PJA2	1.03E-01	1.27E-02	-25.34	0.664063647	-8.490295655	-1.46	FALSE	-4.51	-2.82
NOTCH2	6.53E-02	9.23E-01	-25.27	1.062830302	-18.145775992	-1.39	FALSE	1.89	1.93

	clinic.R.more	clinic.R.less	sc.All	sc.Old	sc.New	sc.Bulk	sc.Q.gene	tcga.Increased.risk	tcga.Increased.risk.beyond.T.cells
FLNA	1.85E-01	6.62E-01	-25.25	1.245245646	-6.641620967	-0.69	FALSE	1.17	1.24
ETV5	1.03E-01	7.28E-01	-25.16	-2.425088433	-2.095041157	-0.33	FALSE	0.56	0.31
IRF4	1.43E-01	1.55E-01	-25.14	-8.149769268	-1.664389215	-0.51	FALSE	1.06	1.71
RNF213	1.31E-01	8.83E-01	-25.03	-2.256625015	-0.442801921	-0.70	FALSE	-5.53	-0.81
ACTN1	8.63E-02	6.82E-01	-24.87	-2.392087133	-0.461493171	-0.63	FALSE	0.67	0.34
MAP1B	1.41E-01	3.16E-01	-24.85	16.48663287	-91.90376064	-0.75	FALSE	-1.34	-0.72
SIL1	7.50E-01	8.78E-02	-24.81	-0.575261468	-7.539668952	-2.88	FALSE	-0.51	0.38
PNPLA2	1.42E-02	9.22E-01	-24.79	-3.113307912	-6.394818612	-1.78	FALSE	-1.19	-0.63
TSPYL2	6.78E-01	1.52E-01	-24.72	3.778385825	-9.370339528	-0.51	FALSE	-0.61	0.31
SLC44A1	1.06E-01	6.28E-01	-24.69	-2.380864194	-0.349647359	-0.92	FALSE	-0.51	-0.39
PARP4	6.46E-02	8.01E-01	-24.68	-4.15933969	-4.597805687	-1.69	FALSE	-2.92	-1.43
THBD	3.74E-01	3.56E-01	-24.64	14.85253744	-8.817215143	-0.72	FALSE	0.36	0.50
ATP6AP2	2.46E-01	2.24E-01	-24.56	-2.737231423	-3.505213377	-1.49	FALSE	-4.10	-3.54
SLCO4A1	1.17E-01	4.29E-01	-24.54	-12.32577077	-2.491285662	-1.12	FALSE	0.53	0.32
QDPR	3.87E-01	3.01E-01	-24.46	0.848626308	-1.281479991	-0.58	FALSE	0.93	-0.37
ACSL1	3.34E-01	7.20E-01	-24.44	-1.343355398	-2.394218878	-0.74	FALSE	-0.52	-0.42
PHF17	1.88E-01	3.97E-01	-24.41	-2.536355562	-9.666960095	-0.67	FALSE	-1.39	-0.76
PKM	4.16E-01	3.42E-01	-24.35	2.779782869	-25.724554124	0.30	FALSE	NA	NA
SUMF1	4.47E-02	9.62E-01	-24.20	0.385589079	-18.617668978	-1.61	FALSE	-0.41	-0.67
DIP2C	1.36E-01	5.96E-01	-24.12	-0.89530856	-0.456829866	-0.77	FALSE	0.40	-0.78
CCDC109B	1.35E-01	5.33E-01	-24.12	-5.921564373	-20.897588313	-2.54	FALSE	-2.60	-1.01
CLCN3	3.24E-02	6.68E-01	-24.11	-1.199961056	-0.424869674	-1.19	FALSE	0.36	-0.49
UBE2L6	1.07E-01	9.31E-01	-24.10	-32.4126104	-8.305731147	-1.48	FALSE	-7.72	-2.59
SNCA	5.44E-02	5.43E-01	-24.09	-4.640547132	4.114790574	-0.52	FALSE	1.38	0.88

	clinic.R.more	clinic.R.less	sc.All	sc.Old	sc.New	sc.Bulk	sc.Q.gene	tcga.Increased.risk	tcga.Increased.risk.beyond.T.cells
PCM1	8.07E-03	3.32E-01	-24.08	0.54026566	0.72218 8884	-0.72	FALSE	-2.49	-2.26
GPR137B	6.68E-02	6.10E-01	-24.07	-11.24242878	4.38425 8609	-0.67	FALSE	0.75	-0.31
XPO7	2.20E-01	6.54E-01	-24.04	1.12830525	-11.7746 9529	-2.28	FALSE	0.54	-0.32
ACTN4	2.89E-01	6.30E-01	-23.85	1.040958249	-7.66818 6482	-1.69	FALSE	-1.41	-2.22
SERINC3	5.28E-01	6.88E-02	-23.84	0.812247624	-7.88097 1405	-1.79	FALSE	-2.22	-1.93
RCAN1	4.73E-01	4.75E-01	-23.82	-7.64834132	1.42444 6662	-1.57	FALSE	-1.78	-1.20
RHOB	1.81E-01	2.40E-01	-23.80	-1.511826677	-3.89608 0823	-1.25	FALSE	1.01	0.81
GNPTG	5.17E-01	5.84E-01	-23.63	-2.367199494	-5.62907 5389	-1.60	FALSE	0.40	-0.35
SHC4	8.71E-02	8.28E-01	-23.63	0.761842584	-1.21341 2465	-0.41	FALSE	-0.92	-0.56
RGS2	5.33E-01	2.47E-01	-23.60	0.640530514	-35.2694 8489	-0.86	FALSE	-1.66	-0.77
LOC729013	Inf	Inf	-23.34	-1.347015309	-7.73923 7399	-0.38	FALSE	NA	NA
SPTAN1	2.79E-01	6.02E-01	-23.28	-3.516248421	-0.93349 9052	-1.09	FALSE	1.33	1.92
ROPN1B	1.96E-01	5.51E-01	-23.25	-0.392244359	-3.75722 9083	-1.17	FALSE	-0.37	0.31
CD97	5.02E-02	6.09E-01	-23.17	-1.828424 99	-11.2144 0814	-2.60	FALSE	-4.58	-1.91
HIST1H2BD	1.36E-01	7.30E-02	-22.98	-1.015586013	-7.33602 1298	-0.59	FALSE	0.44	0.52
RNH1	3.44E-01	5.51E-01	-22.98	-15.57474178	-1.48976 8126	-2.73	FALSE	-0.36	-0.33
LAMB2	1.53E-01	7.07E-01	-22.88	-5.223327364	6.00551 1857	-0.66	FALSE	1.34	1.26
CFB	2.69E-01	6.21E-01	-22.75	-3.336017193	-33.8193 6425	-1.72	FALSE	-5.01	-1.30
APOC1	3.51E-01	2.53E-01	-22.72	-5.24845496	-10.9311 5237	0.56	FALSE	-0.97	0.35
CTTN	2.95E-02	8.62E-01	-22.68	-21.47838673	-14.3723 1691	-0.93	TRUE	1.79	1.06
SERPINI1	1.94E-01	3.95E-01	-22.64	7.367752032	-20.7152 515	-0.82	FALSE	-2.81	-2.79
AQP1	3.61E-01	1.34E-02	-22.54	-3.04043337	-24.5447 6544	-1.11	FALSE	-0.63	-0.40
C9orf89	1.20E-02	3.49E-01	-22.49	-0.827086987	-7.74480 6672	-2.09	FALSE	-1.25	-1.19
IGSF8	6.93E-01	1.66E-02	-22.42	-3.569587 79	3.52059 0252	-0.34	FALSE	1.85	0.62
LOXL4	3.71E-01	2.10E-01	-22.33	1.334897324	-7.47665	0.30	FALSE	-2.35	-1.86

	clinic.R.more	clinic.R.less	sc.All	sc.Old	sc.New	sc.Bulk	sc.Q.gene	tcga.Increased.risk	tcga.Increased.risk.beyond.T.cells
					9986				
PARP14	5.18E-02	9.01E-01	-22.19	-8.097178503	-0.328886759	-1.20	FALSE	-7.56	-1.95
METTL7B	8.30E-01	3.07E-01	-22.13	-5.765117863	-28.52875728	-0.53	FALSE	-2.27	-1.03
DDIT4	1.02E-01	3.25E-01	-22.11	-5.255322514	-6.526304 95	-0.30	FALSE	-0.73	0.42
ATP6AP1	6.86E-01	2.45E-01	-22.08	-2.478485511	-4.574014 32	-1.25	FALSE	2.24	1.59
EFCAB14	1.39E-01	7.38E-01	-22.08	-3.316119059	-1.515729612	-0.55	FALSE	NA	NA
HIPK3	9.45E-02	3.66E-01	-22.07	-2.821393944	-4.287750809	-2.31	FALSE	-2.16	-1.20
TRAM1	1.70E-01	3.45E-01	-22.00	-1.343023324	-5.818549856	-0.80	FALSE	-2.96	-0.93
GNG12	1.51E-01	4.34E-01	-21.98	-3.285765565	-0.610412559	-1.15	FALSE	-0.52	-1.19
HEXIM1	3.90E-01	6.89E-01	-21.98	0.494765627	-1.209847864	-0.53	FALSE	0.77	0.59
ARPC1B	4.19E-01	5.02E-01	-21.95	-5.014848929	-0.378721015	-0.51	FALSE	-0.44	0.43
TBC1D10A	7.46E-02	1.14E-01	-21.92	-0.552709866	-1.475904674	-0.40	FALSE	-0.67	-0.35
CELF2	1.04E-03	9.09E-01	-21.91	-11.30510408	4.398026966	-0.65	FALSE	0.72	1.32
AASS	2.27E-02	4.80E-01	-21.87	-2.59954819	-6.596863423	-0.58	FALSE	-1.59	-1.62
BTG1	3.04E-02	8.04E-01	-21.84	-2.240405471	-2.125110401	0.32	FALSE	-2.35	-2.87
ITGB5	2.13E-01	3.37E-01	-21.80	1.055482689	-7.664663167	-1.23	FALSE	-0.39	-0.59
LRP10	2.33E-03	9.26E-01	-21.76	-2.643825963	-0.575237992	-0.86	FALSE	0.59	0.83
APOBEC3G	3.50E-01	1.02E-01	-21.76	-1.435926819	-18.55196462	-1.19	FALSE	-7.99	-3.16
NBR1	1.91E-01	1.24E-01	-21.73	-0.401682359	-7.030124647	-1.45	FALSE	-2.31	-1.99
ARHGAP18	6.67E-02	5.56E-01	-21.70	1.549818958	-6.083078 45	-0.91	FALSE	-3.47	-1.51
RHBDF1	5.39E-01	3.26E-01	-21.64	-1.584125889	-5.041016329	-2.17	FALSE	0.56	-0.47
C2orf82	8.24E-01	1.09E-01	-21.54	-3.589476747	-36.07674841	-0.80	FALSE	-0.76	-1.03
MRPS6	8.46E-01	6.04E-02	-21.54	3.8198103	-31.19537764	-0.48	FALSE	-3.76	-2.64
MFSD12	7.75E-02	7.20E-01	-21.46	-10.32875944	0.847324385	-0.81	FALSE	NA	NA
IL17RC	3.20E-03	9.68E-01	-21.46	-0.950909	-6.90376	-1.33	FALSE	0.41	1.10

	clinic.R.more	clinic.R.less	sc.All	sc.Old	sc.New	sc.Bulk	sc.Q.gene	tcga.Increased.risk	tcga.Increased.risk.beyond.T.cells
				415	5831				
ORMDL3	2.42E-01	4.01E-01	-21.35	1.028831949	-12.12181027	-0.82	FALSE	-1.56	-0.43
ERAP1	8.92E-03	8.00E-01	-21.33	-2.020343036	-1.07433683	-1.32	FALSE	-4.25	-0.52
DHRS3	3.85E-01	1.49E-01	-21.32	-3.674737662	-36.77125122	-0.89	FALSE	-3.81	-1.01
SMIM3	4.40E-01	1.74E-01	-21.31	-0.533091389	-27.3010335	-1.51	FALSE	NA	NA
MTRNR2L7	9.55E-01	4.31E-01	-21.30	-0.641838996	-0.838254683	-0.36	FALSE	NA	NA
MAN2B2	8.41E-02	6.73E-01	-21.30	-3.188196571	-7.235940374	-2.17	FALSE	-0.67	0.35
UBA7	9.53E-03	9.62E-01	-21.16	-6.237460628	-12.06515012	-2.74	FALSE	-7.29	-1.47
LOC100126784	2.74E-01	6.97E-01	-21.12	0.617459169	1.538338712	-0.33	FALSE	0.91	0.40
ZMYND8	6.52E-01	4.23E-01	-21.09	8.46997889	-41.05985472	-0.84	FALSE	-0.71	-0.77
SERPINB1	7.69E-02	7.68E-01	-21.08	-7.082913363	-3.513176367	-1.08	FALSE	-2.14	-0.81
TUG1	7.67E-01	2.24E-01	-21.08	4.463316224	-0.484401657	-0.88	FALSE	-0.47	-0.64
TMEM123	4.50E-01	4.45E-01	-21.02	1.608148266	-24.282809986	-1.17	FALSE	-3.65	-3.37
OPTN	1.75E-02	9.00E-01	-21.01	-15.25331624	6.957858787	-1.28	FALSE	-1.82	-0.67
SPP1	1.58E-01	2.37E-01	-20.95	29.30414836	-15.67592791	-0.31	FALSE	-1.62	-0.80
VAMP5	2.01E-01	2.49E-01	-20.80	-18.92620281	-2.119672202	-2.52	TRUE	-4.70	-0.83
PFN1P2	2.26E-01	5.20E-01	-20.78	-4.251955922	0.435712066	-1.31	FALSE	NA	NA
STRIP2	2.90E-01	6.75E-01	-20.69	0.450218251	-16.83533974	0.68	FALSE	NA	NA
TERF2IP	4.19E-01	4.95E-01	-20.68	-0.523959722	-4.99899526	-1.15	FALSE	-2.47	-2.74
CALD1	4.76E-02	4.98E-01	-20.63	-0.95351804	-3.241925514	-0.49	FALSE	-1.72	-1.22
SDC4	1.32E-01	5.67E-02	-20.63	-1.191859966	-2.500483993	-0.76	FALSE	-1.75	-1.20
ST3GAL6	2.60E-02	4.09E-01	-20.62	-3.940416547	1.011466756	-0.39	FALSE	-1.54	-1.76
GABARAPL1	8.78E-02	5.78E-01	-20.60	0.899609729	-10.630729995	-1.03	FALSE	-1.21	-1.70
ATP2B4	3.11E-01	3.74E-01	-20.51	-4.945501045	-0.713728198	-0.82	FALSE	0.42	-0.73
TYR	1.62E-01	8.43E-01	-20.44	-5.806227943	8.573828698	0.35	FALSE	0.95	0.74

	clinic.R.more	clinic.R.less	sc.All	sc.Old	sc.New	sc.Bulk	sc.Q.gene	tcga.Increased.risk	tcga.Increased.risk.beyond.T.cells
LPXN	9.73E-02	5.50E-01	-20.32	-4.724249565	-6.69091907	-2.49	FALSE	-2.90	-0.99
NT5DC3	3.85E-01	7.50E-01	-20.30	-3.824113566	-9.439658069	0.87	FALSE	1.45	1.08
TMEM43	2.13E-01	7.61E-01	-20.29	-0.777872969	-10.65895763	-1.87	FALSE	-0.43	-0.78
PPFIBP1	4.24E-01	4.93E-01	-20.24	-1.128627461	-0.721079442	-0.79	FALSE	-1.32	-2.12
HPS5	1.63E-01	5.31E-01	-20.20	-4.91161177	-0.941788497	-0.87	FALSE	-1.99	-1.23
ST6GALNAC2	1.94E-01	4.17E-01	-20.18	-15.32664647	2.850160806	-0.52	FALSE	0.64	0.45
GANAB	4.65E-01	2.60E-01	-20.18	-6.760249926	-6.862001928	-0.43	FALSE	0.73	-0.34
UBE2Z	1.30E-01	7.08E-01	-20.12	-0.635275033	-4.157138659	-0.93	FALSE	-0.40	0.34
BHLHE40	2.74E-01	3.89E-01	-20.08	-15.75869206	0.460982512	-1.07	FALSE	0.49	0.41
ICAM1	1.40E-01	1.30E-01	-20.07	-5.42980278	-4.227678526	-0.90	FALSE	-2.94	-0.81
MT1G	2.64E-01	6.28E-01	-20.07	-6.619086183	-19.45360494	-1.78	FALSE	-1.25	-0.92
TNFRSF1A	1.73E-01	3.01E-01	-20.05	-1.213887782	-9.901384801	-2.19	FALSE	-0.58	-0.31
CEACAM1	8.88E-02	2.21E-01	-20.04	-7.679312791	-0.618868776	-0.70	FALSE	0.31	-0.35
ATP6V0E2	1.88E-02	4.01E-01	-20.03	-1.928199495	-14.26365141	-0.52	FALSE	0.57	0.41
IER2	6.61E-01	4.96E-01	-20.02	-4.109943558	-25.74745651	-0.51	FALSE	-0.30	0.35
PELI1	4.39E-01	3.28E-01	-20.00	-1.189921924	-35.64655558	-2.97	FALSE	-2.64	-1.15
GLCE	1.85E-01	3.72E-01	-19.98	-1.177969643	-8.825783231	-0.32	FALSE	-1.80	-2.12
AFAP1L2	6.59E-01	4.14E-02	-19.97	-1.073567177	-0.570275269	-1.36	FALSE	-2.23	-1.19
SRPR	6.59E-01	3.13E-01	-19.93	-0.531970765	-4.906202103	-2.01	FALSE	-0.93	-1.11
PEG10	6.25E-02	5.12E-01	-19.79	-9.864562142	-70.658863456	-0.36	FALSE	-1.59	-1.00
CCND1	2.58E-01	5.24E-01	-19.79	-44.94838696	9.144440051	-0.44	FALSE	0.93	0.81
PDLIM5	1.61E-01	8.65E-01	-19.73	-1.229814252	-4.441449396	-0.81	FALSE	-1.49	-0.84
PTTG1IP	4.37E-01	4.41E-01	-19.73	-5.840061211	31.816746616	-0.46	FALSE	1.42	0.70
PIM3	1.43E-01	4.70E-01	-19.67	-2.05856412	-2.93170429	-0.43	FALSE	-1.29	-0.88

	clinic.R.more	clinic.R.less	sc.All	sc.Old	sc.New	sc.Bulk	sc.Q.gene	tcga.Increased.risk	tcga.Increased.risk.beyond.T.cells
LOXL2	1.30E-01	5.07E-02	-19.66	-2.227721553	-17.75782926	-1.59	FALSE	0.63	0.59
CASP4	4.33E-02	5.13E-01	-19.66	-1.060183077	-8.339833791	-2.26	FALSE	-2.39	-0.56
SLC39A6	2.57E-01	2.62E-01	-19.62	-7.554501206	2.808826234	-0.42	FALSE	1.49	0.36
MICA	1.60E-02	3.12E-01	-19.54	-4.830115449	-3.599631309	-1.12	FALSE	1.47	1.02
PTPRM	4.72E-01	5.15E-01	-19.50	0.81484529	-4.358551311	-0.92	FALSE	0.73	0.87
IGFBP3	7.45E-01	6.80E-03	-19.50	-1.314794414	-34.097600334	-1.44	FALSE	-1.60	-1.31
OCIAD2	6.65E-01	2.76E-01	-19.49	1.305114076	-79.982500015	-0.31	FALSE	-1.69	-0.93
ASAH1	4.70E-01	3.55E-01	-19.40	-8.977291847	12.309690044	-0.54	FALSE	1.02	0.93
BAMBI	7.62E-02	4.89E-01	-19.40	-7.127650082	0.371125258	-0.66	FALSE	0.37	-0.67
CHN1	4.39E-01	1.42E-02	-19.28	4.899749645	-63.056446674	-1.01	FALSE	-2.08	-1.63
SORT1	2.69E-01	6.04E-01	-19.05	-0.346897384	4.214233311	0.30	FALSE	1.07	0.79
SPARCL1	2.75E-01	7.92E-02	-19.00	-5.863651519	-7.671589784	-0.45	FALSE	-0.51	0.84
TYMP	5.50E-02	7.40E-01	-18.99	-7.727093689	-2.343707718	-1.57	FALSE	-2.68	0.30
LYST	3.98E-01	5.38E-01	-18.94	-2.644630966	2.410020413	-0.84	FALSE	-0.74	0.57
PACSIN2	1.92E-01	4.29E-01	-18.93	-1.371299596	-1.411697598	-0.54	FALSE	-0.34	-0.40
GNS	6.32E-01	5.79E-01	-18.78	-4.823051083	-3.286157821	-1.51	FALSE	-0.32	0.38
CSTB	1.50E-01	8.41E-02	-18.77	-10.13996322	12.458988834	-0.64	FALSE	3.01	2.46
PRR4	5.94E-01	3.79E-02	-18.75	2.79869096	-29.635771458	-1.07	FALSE	-0.94	-1.61
MFNG	4.15E-01	6.44E-01	13.74	5.389614969	-7.877828514	0.76	FALSE	-3.24	1.32
RNMTL1	6.42E-01	2.90E-02	13.76	5.382060026	3.630827576	0.81	FALSE	1.85	0.97
6-Sep	3.42E-01	4.64E-01	13.79	4.196300143	5.140156942	1.00	FALSE	-1.09	1.29
TUBGCP4	1.83E-02	8.31E-01	13.81	3.017098753	1.78840835	1.56	FALSE	0.56	0.31
ARHGEF1	1.00E-01	4.17E-01	13.83	-0.583974655	21.570526633	1.53	FALSE	-0.81	0.82
11-Sep	1.16E-01	1.74E-01	13.88	1.430393629	24.223676679	0.89	FALSE	0.61	0.64
PCOLCE	2.45E-01	8.53E-02	13.90	60.72202561	-6.40674755	1.57	TRUE	-0.54	-0.79
SURF2	3.11E-01	8.17E-03	13.90	3.289195508	4.660965337	0.89	FALSE	1.86	0.96

	clinic.R.more	clinic.R.less	sc.All	sc.Old	sc.New	sc.Bulk	sc.Q.gene	tcga.Increased.risk	tcga.Increased.risk.beyond.T.cells
MRPL44	1.42E-01	2.49E-01	13.90	-0.452623362	9.001640945	0.59	FALSE	0.66	0.47
DCAF12	2.42E-01	2.44E-01	13.91	7.312065126	0.851451243	1.40	FALSE	-0.37	0.47
SAT2	5.10E-01	3.73E-01	13.92	12.75708283	5.628354728	1.21	FALSE	0.47	-0.33
TSNAX	2.90E-01	5.50E-01	13.92	1.805752837	12.12793854	1.33	FALSE	-1.86	-2.50
THOC3	8.77E-02	5.88E-01	13.92	4.098106348	1.957900047	0.65	FALSE	1.18	0.59
PDCD5	7.35E-01	4.07E-01	13.98	6.751326589	6.836586916	-0.35	FALSE	0.34	-1.77
MOCS3	3.15E-01	3.56E-02	14.00	1.434370227	2.043955951	0.95	FALSE	0.34	-0.66
RBM4B	6.30E-01	1.64E-02	14.11	6.906518123	12.538101823	0.59	FALSE	0.40	0.38
MTX1	6.94E-01	2.54E-01	14.12	5.91760368	2.667632146	1.24	FALSE	2.66	1.38
PRPF4	5.54E-01	1.41E-01	14.16	8.189088103	2.044969562	0.86	FALSE	2.38	1.76
HNRNPD	5.99E-01	2.59E-01	14.17	4.315130309	7.503641237	1.01	FALSE	-0.35	0.63
MCM4	4.36E-01	2.25E-01	14.19	1.664350763	0.953479445	0.93	FALSE	1.50	1.57
AP3M1	8.55E-02	5.45E-01	14.24	0.629153205	6.417423361	1.11	FALSE	0.51	0.84
XIST	7.44E-01	2.49E-02	14.30	29.59293181	7.697689322	0.45	FALSE	-1.93	-1.51
FAM64A	6.61E-01	8.41E-02	14.31	8.330570062	-0.351042029	0.83	FALSE	1.24	0.88
G3BP1	4.02E-01	3.85E-01	14.31	10.54566035	1.943806272	-0.40	FALSE	-0.40	0.45
SNCG	4.74E-01	1.77E-01	14.33	-18.24763977	-7.528207908	0.97	FALSE	0.76	2.26
PI4KB	6.25E-01	2.16E-01	14.34	-0.797031323	29.521177947	0.41	FALSE	4.66	3.87
DDX46	5.72E-01	7.29E-02	14.35	5.88404805	5.552908424	0.75	FALSE	-0.96	-0.52
NNT	3.32E-01	5.47E-01	14.37	14.45967163	6.905512186	1.70	FALSE	0.34	0.45
TIMM17A	8.05E-01	5.02E-02	14.40	4.529771377	5.274485432	0.98	FALSE	0.67	-0.48
FTSJ3	7.42E-01	2.64E-02	14.41	11.3059408	2.197523397	0.77	FALSE	1.50	1.16
HNRNPM	8.64E-01	8.82E-02	14.42	5.210267361	2.738024614	0.91	FALSE	0.90	1.26
EXOSC6	3.95E-01	7.85E-01	14.43	0.458097878	5.662862445	2.19	FALSE	1.75	0.76
IDH3B	8.23E-01	8.08E-02	14.43	-3.288279147	-0.694931133	0.49	TRUE	2.10	1.15
NHEJ1	6.12E-02	5.57E-01	14.45	0.7467667	10.013626284	2.85	FALSE	3.41	2.34
COPS5	4.72E-01	2.19E-01	14.49	-13.43972244	-1.109684877	1.29	FALSE	-3.27	-3.87
SBNO1	2.70E-01	6.76E-01	14.50	11.83280512	0.315307709	1.51	FALSE	-0.35	0.40
TXNDC17	8.75E-01	2.11E-01	14.51	19.93469228	1.537234956	0.37	FALSE	0.51	-0.73
HMG20A	4.15E-01	2.71E-01	14.51	8.768995629	3.138684411	1.23	FALSE	-0.42	-0.34
TRIB2	6.31E-01	4.40E-01	14.51	-1.325156749	36.783317778	1.14	FALSE	0.56	0.37
CSK	1.54E-01	1.13E-01	14.53	1.783684971	3.908601844	0.83	FALSE	0.84	3.57
B4GALT3	6.85E-01	3.24E-	14.53	2.984723	13.9929	2.23	FALSE	0.64	0.69

	clinic.R.more	clinic.R.less	sc.All	sc.Old	sc.New	sc.Bulk	sc.Q.gene	tcga.Increased.risk	tcga.Increased.risk.beyond.T.cells
		02		465	3996				
AIMP2	1.98E-01	2.26E-01	14.54	9.995109565	0.589234557	0.68	FALSE	3.46	1.01
SUPT5H	7.15E-01	1.21E-01	14.56	0.524094651	17.26213471	0.54	FALSE	2.66	1.82
POSTN	2.42E-01	9.71E-02	14.57	-25.61569592	-8.584718074	0.72	FALSE	0.46	0.73
GTF2H2C	6.04E-01	1.69E-01	14.58	-0.403995243	5.926998115	2.48	FALSE	-1.77	-1.09
GNL3	3.37E-01	4.02E-01	14.61	3.602849144	4.807218992	0.66	FALSE	-1.34	-1.91
GBAS	2.19E-01	2.58E-01	14.62	3.050038089	8.165505882	1.17	FALSE	-1.66	-2.61
MEST	4.42E-01	1.23E-01	14.64	-26.73500059	-1.521354639	0.45	FALSE	0.43	0.43
CDH3	6.93E-02	4.14E-02	14.67	-4.060021324	-27.37588719	0.38	FALSE	3.88	3.59
PLEKHJ1	5.88E-01	1.16E-01	14.68	3.793428817	7.780824818	0.33	FALSE	0.67	0.70
ECHS1	1.07E-01	2.20E-01	14.72	1.041998674	13.080422231	1.96	FALSE	2.27	1.81
SLC45A2	4.80E-01	3.24E-02	14.73	11.23157773	20.345005987	1.51	FALSE	2.62	2.58
NEUROD1	5.30E-01	1.52E-01	14.75	-11.86664298	-10.869079078	0.69	FALSE	-0.77	-1.69
ACTR1A	2.03E-01	2.17E-02	14.76	0.616928184	16.242002821	0.49	FALSE	3.57	3.89
CD24	2.14E-01	2.06E-01	14.78	1.079125614	1.079391239	0.79	FALSE	0.64	1.79
LOC388796	Inf	Inf	14.79	-0.443428997	8.562706973	-0.46	FALSE	1.60	0.61
CDC20	5.51E-01	4.34E-02	14.80	4.913073148	0.753666063	0.63	FALSE	2.89	2.24
TPI1	4.34E-01	1.30E-01	14.82	5.327916572	-0.744378475	0.77	TRUE	3.41	1.46
NOC2L	6.32E-01	2.28E-01	14.83	16.2653311	-1.958200998	1.14	TRUE	1.46	0.80
CHCHD1	1.48E-01	5.42E-03	14.88	2.622835248	9.473060062	0.94	FALSE	0.45	0.40
ALDH1B1	6.57E-01	3.31E-01	14.98	0.922296057	19.440116174	2.22	FALSE	0.94	0.33
NTHL1	3.95E-01	1.32E-01	15.01	10.15717558	2.446536902	1.34	FALSE	1.35	0.87
RARRES2	2.25E-01	5.11E-01	15.05	4.873224671	-0.301976127	0.91	FALSE	-1.43	-0.37
SLC25A44	2.69E-01	1.85E-01	15.12	1.806177902	12.427007653	0.82	FALSE	2.81	2.10
ECD	3.16E-02	3.29E-01	15.16	0.508216518	14.926002402	1.10	FALSE	-0.56	-0.81
ACBD6	4.72E-01	9.99E-02	15.18	4.54003142	6.492731101	0.49	FALSE	1.54	-0.33
AURKA	4.90E-01	5.48E-03	15.18	4.926437071	1.293700898	1.38	FALSE	1.99	1.32
PRMT1	5.78E-01	3.22E-01	15.18	7.87390675	2.414514677	0.56	FALSE	1.52	0.88
GNB2L1	3.13E-02	4.07E-01	15.22	0.754171752	3.352765588	0.35	TRUE	0.40	-0.33
TOMM5	2.75E-01	5.50E-02	15.24	16.83196592	1.221893499	1.00	FALSE	1.00	-0.31
SNRPF	2.17E-01	1.95E-01	15.27	15.00145479	3.094281947	0.67	FALSE	1.20	0.60
KLHL9	1.47E-01	7.18E-01	15.27	-0.397375	24.812899951	0.85	FALSE	-1.85	-1.54

	clinic.R.more	clinic.R.less	sc.All	sc.Old	sc.New	sc.Bulk	sc.Q.gene	tcga.Increased.risk	tcga.Increased.risk.beyond.T.cells
				031					
RNPS1	1.42E-01	4.75E-01	15.29	2.320398903	3.78227 1567	1.76	FALSE	1.11	0.72
RPL36	5.72E-02	3.71E-01	15.33	2.178512724	26.4170 9158	-0.33	FALSE	0.50	0.33
SLC25A11	6.01E-01	2.68E-01	15.38	12.13755268	0.76179 644	0.69	FALSE	1.65	1.15
FDPS	3.64E-01	1.03E-01	15.41	3.097761019	7.76264 8036	0.62	FALSE	4.01	2.54
PRPSAP2	4.16E-01	1.22E-01	15.41	9.218191038	2.29874 1055	1.45	FALSE	-0.83	-1.15
HAUS1	2.26E-01	3.37E-01	15.43	5.352399583	1.24736 9224	0.96	FALSE	-1.42	-1.32
POLR2A	2.03E-01	8.81E-01	15.51	13.15051816	22.8032 9056	2.32	FALSE	4.89	3.89
TDG	9.85E-01	3.25E-02	15.51	6.013013072	1.03069 4741	1.73	FALSE	-0.62	-0.69
EGLN2	1.62E-01	2.30E-01	15.51	4.254455956	6.34470 7044	1.09	FALSE	1.99	2.30
CDCA5	5.88E-01	1.06E-01	15.53	5.285026282	-0.30704 5502	0.82	FALSE	1.49	1.03
EIF2S2	6.74E-01	1.23E-02	15.55	8.293233204	-0.58456 1792	0.79	FALSE	-1.33	-2.61
CACYBP	5.67E-01	5.28E-02	15.56	2.448860208	6.78446 5091	1.43	FALSE	-0.90	-1.21
TOMM22	5.29E-01	3.03E-03	15.57	11.70143787	1.10512 845	1.41	FALSE	1.63	0.57
GLUL	4.19E-01	1.68E-01	15.60	-0.524584718	13.6220 7707	0.68	FALSE	-1.32	0.33
KPNA2	2.93E-01	5.18E-03	15.60	4.991817798	6.63982 0973	0.58	FALSE	3.86	3.97
GTF2E1	2.03E-01	5.56E-01	15.64	0.783473 28	2.04871 9802	1.04	FALSE	-1.63	-1.64
LINC00665	1.28E-01	8.43E-01	15.74	1.516171688	5.78048 6589	1.43	FALSE	NA	NA
TARS2	4.95E-01	1.64E-01	15.74	3.244718053	7.16795 3196	1.02	FALSE	2.01	1.13
ZSWIM7	4.97E-01	4.57E-01	15.77	5.395171027	2.00074 9052	0.66	FALSE	-0.62	-1.46
SPDYE5	2.06E-01	4.71E-01	15.80	0.748477234	8.22009 067	1.06	FALSE	-0.85	-0.64
LSM4	6.34E-01	1.59E-01	15.82	4.470623 28	2.25169 3195	0.39	FALSE	3.16	1.48
MYL9	4.21E-01	5.72E-02	15.88	0.696709556	7.75093 8059	0.63	FALSE	0.83	0.90
ATP5B	4.63E-01	7.46E-02	15.89	2.737412219	3.55705 0178	1.66	FALSE	3.60	1.19
RGS3	2.55E-01	4.95E-01	15.91	6.172391972	3.48462 9082	-0.38	FALSE	-0.57	0.57
CHTOP	6.15E-01	8.77E-02	15.91	10.10615811	5.69056 281	0.97	FALSE	NA	NA
SMG7	5.02E-01	6.60E-03	15.93	5.209483431	11.9910 1659	2.02	FALSE	1.66	1.06
EIF3J	2.68E-01	1.88E-01	16.00	14.28593134	-0.67422 3072	0.92	FALSE	-2.31	-3.82
MGC2752	Inf	Inf	16.00	2.904335761	2.48840 784	0.80	FALSE	1.05	0.69
PAM	3.98E-01	5.38E-03	16.04	0.837075 37	10.5175 5539	0.48	FALSE	-0.65	-0.55
GSTO1	6.07E-02	5.15E-01	16.05	-1.337030558	62.1927 9211	0.95	FALSE	1.72	0.92
RABEP1	8.74E-01	1.42E-01	16.06	21.29284 48	4.65628 2388	0.49	FALSE	-0.59	-0.83
KIF2C	7.82E-01	4.29E-02	16.11	6.859855363	1.85427 0407	0.97	FALSE	2.25	1.77
CCNB2	2.81E-01	2.26E-01	16.12	3.919230216	0.97304 1322	0.76	FALSE	1.37	0.69

	clinic.R.more	clinic.R.less	sc.All	sc.Old	sc.New	sc.Bulk	sc.Q.gene	tcga.Increased.risk	tcga.Increased.risk.beyond.T.cells
NEK5	1.56E-01	8.32E-01	16.17	-0.324543846	3.958302922	0.56	FALSE	0.47	-0.69
PPIF	3.27E-02	9.52E-02	16.22	4.347882752	2.129355273	0.32	FALSE	3.33	3.00
C17orf49	8.03E-01	3.47E-01	16.22	9.736718533	0.870053317	0.67	FALSE	-0.49	0.64
EXOSC5	5.33E-01	4.78E-01	16.26	4.490272348	1.542142828	0.38	FALSE	0.48	-0.45
MAP1LC3C	4.65E-01	1.06E-01	16.27	-1.592062983	3.554313965	1.34	FALSE	0.54	1.25
TUBB4A	9.06E-02	5.47E-01	16.29	-18.47518133	78.69139618	0.66	TRUE	NA	NA
EIF3G	2.66E-01	4.13E-01	16.30	0.485973534	14.911677008	-0.34	FALSE	0.45	0.32
KIRREL	7.10E-01	1.91E-01	16.31	1.457831877	23.609660921	1.24	FALSE	1.50	2.01
ID3	4.40E-01	4.62E-02	16.33	6.385801262	6.661876303	1.01	FALSE	-0.70	0.37
CCNB1IP1	9.37E-02	6.45E-01	16.37	1.083665256	8.087590455	0.98	FALSE	0.41	-0.93
IL6R	1.64E-01	1.16E-01	16.40	-1.548267241	43.852550904	1.24	FALSE	0.72	2.10
RPS10	1.11E-01	1.50E-01	16.42	3.683944948	16.303391108	0.76	FALSE	0.71	0.42
PKN1	5.51E-01	4.88E-01	16.42	13.74625835	3.306345432	0.70	FALSE	-0.75	-0.56
C10orf32	7.21E-02	4.78E-01	16.43	-1.253078131	10.418244098	1.99	FALSE	-1.13	-0.68
SKA1	9.28E-02	2.26E-02	16.59	0.563847042	6.4942639	1.74	FALSE	1.34	1.20
MRPS10	4.85E-01	8.68E-02	16.61	11.13816237	1.780643088	0.73	FALSE	-0.56	-1.54
CKB	7.19E-01	2.83E-01	16.62	-0.94366682	-0.673071985	0.87	TRUE	0.91	0.69
CDCA8	6.65E-01	4.59E-02	16.62	5.935347842	3.409036488	0.85	FALSE	3.42	2.98
ATP5A1	3.11E-02	3.82E-01	16.68	4.114811371	5.5164772	1.16	FALSE	2.11	1.65
TTYH3	8.19E-01	6.55E-02	16.68	-0.839172467	25.99819956	0.60	FALSE	6.36	5.75
WDR6	2.40E-01	6.41E-01	16.69	2.8454458	11.146822125	2.13	FALSE	0.52	0.72
SLC5A6	6.91E-01	2.34E-01	16.79	12.87746605	0.747794957	0.73	FALSE	1.64	1.27
FAM213A	2.19E-01	5.17E-02	16.83	0.649223104	18.382766775	1.31	FALSE	NA	NA
SNRPA1	9.48E-01	1.16E-01	16.88	8.418866258	1.511738171	1.59	FALSE	0.34	-0.32
MARCKSL1	6.64E-01	2.42E-01	16.89	-11.85693628	-0.322901855	0.35	FALSE	0.54	1.18
DDX39A	6.91E-01	1.20E-01	16.91	0.618867402	13.259938888	0.54	FALSE	NA	NA
BEX1	6.18E-01	4.03E-02	16.92	-15.14930944	-3.639527861	0.58	FALSE	0.98	0.40
ZNF526	3.02E-01	5.04E-01	16.95	0.4369126	4.005769467	1.12	FALSE	1.81	0.94
SMCR7L	2.03E-01	2.97E-01	17.02	7.881351856	5.194504892	2.41	FALSE	2.29	1.25
FAM126A	5.19E-01	3.75E-02	17.08	4.35274429	8.584972	0.63	FALSE	-1.33	-1.06
LSM14A	5.40E-01	3.49E-01	17.11	0.425148121	20.860399965	0.55	FALSE	-1.33	-1.39
FDXR	5.12E-01	4.05E-	17.12	1.673688	16.3833	1.47	FALSE	2.00	1.47

	clinic.R.more	clinic.R.less	sc.All	sc.Old	sc.New	sc.Bulk	sc.Q.gene	tcga.Increased.risk	tcga.Increased.risk.beyond.T.cells
		01		01	1044				
SLC19A1	5.55E-01	2.28E-01	17.15	5.585866639	14.84646384	0.81	FALSE	2.13	2.18
GAGE12J	1.82E-01	2.36E-01	17.16	17.96014408	-14.68096465	0.33	FALSE	-1.39	-2.77
OCA2	1.40E-01	2.52E-02	17.16	-5.354814935	28.51719977	1.11	FALSE	5.56	3.33
RBBP4	8.19E-01	1.59E-01	17.17	7.90217054	3.958262309	1.72	FALSE	-0.54	0.47
NIP7	1.48E-01	4.29E-01	17.34	7.740805625	3.790249229	0.73	FALSE	0.63	-0.54
PRPF31	6.36E-01	4.74E-01	17.37	3.746194298	5.153934765	0.79	FALSE	1.42	0.91
MKI67IP	4.95E-01	4.41E-01	17.46	5.342737904	3.950369618	0.74	FALSE	-0.37	-1.42
TRUB2	7.07E-01	7.54E-02	17.48	4.61575142	4.893775965	2.04	FALSE	2.77	1.68
METTL13	3.47E-01	4.85E-02	17.49	3.1052895	5.77183743	0.61	FALSE	2.17	1.65
HMGB1	3.33E-01	2.08E-01	17.50	6.146315189	2.060104614	0.82	FALSE	-1.52	-1.07
RCC1	6.07E-01	2.04E-01	17.52	6.917331724	3.981254561	0.87	FALSE	3.62	1.69
RPA1	3.28E-01	4.21E-01	17.53	5.961074344	5.617977147	1.25	FALSE	1.36	1.23
HNRNPUL1	1.01E-01	2.70E-01	17.55	0.680339536	16.426469971	0.56	FALSE	3.18	3.24
NDUFV3	4.85E-01	2.61E-01	17.56	2.992981728	18.75771812	1.14	FALSE	2.18	2.14
RQCD1	7.06E-01	1.40E-01	17.57	2.435033782	2.120791626	-0.41	FALSE	1.93	1.80
TCF4	3.80E-01	1.16E-01	17.62	-9.236103162	-2.679784236	0.53	FALSE	-1.45	-0.68
C20orf27	4.98E-01	4.60E-01	17.62	7.631118695	10.619499581	0.86	FALSE	3.11	2.07
CCT4	3.45E-01	9.10E-02	17.65	2.170402339	6.399317541	2.01	FALSE	0.42	-0.48
VPS53	1.15E-01	3.30E-01	17.69	0.335449031	37.019700924	1.02	FALSE	5.99	4.71
WDR46	2.26E-01	4.31E-01	17.76	8.702406207	1.725874114	1.39	FALSE	1.37	0.53
NEFL	7.01E-01	2.22E-02	17.76	-11.97364126	-5.921165572	0.60	FALSE	1.26	0.51
TCEA3	8.40E-01	7.29E-02	17.83	0.459042162	4.038014366	1.40	FALSE	0.52	-0.40
GAGE6	1.00E+00	1.00E+00	17.86	-16.08931781	-14.75860399	0.66	FALSE	NA	NA
GALT	1.33E-01	6.34E-01	17.87	1.976498011	20.981852221	2.04	FALSE	-0.54	0.38
SNRNP40	8.89E-01	5.60E-02	17.90	8.554249159	4.948734856	0.85	FALSE	0.87	1.24
CRK	8.58E-01	1.99E-01	17.94	3.670575611	7.55391113	0.91	FALSE	0.87	0.76
GNL3L	5.40E-01	2.97E-01	17.96	4.387265453	23.908147734	1.25	FALSE	2.02	2.37
NUF2	7.59E-01	7.74E-02	17.97	4.131933124	3.647607035	1.05	FALSE	-0.49	-0.70
SERPINB9	2.32E-01	9.95E-02	17.99	-2.38056198	-2.914786989	1.08	FALSE	-1.77	-0.41
ZFP36L1	1.21E-01	4.84E-01	18.01	5.938605734	19.429900388	1.51	FALSE	-0.55	0.31
MRPS2	3.15E-02	1.72E-01	18.02	4.542140417	7.779275401	2.47	FALSE	6.06	4.32
NENF	7.99E-01	2.86E-01	18.04	6.800958187	30.655988274	1.02	FALSE	1.98	0.56

	clinic.R.more	clinic.R.less	sc.All	sc.Old	sc.New	sc.Bulk	sc.Q.gene	tcga.Increased.risk	tcga.Increased.risk.beyond.T.cells
DUSP12	8.17E-01	2.93E-01	18.14	3.468611254	6.132917887	1.25	FALSE	-0.48	-1.03
FLJ30403	7.61E-02	8.71E-01	18.15	-0.598011003	3.407988308	1.44	FALSE	NA	NA
APEX1	7.41E-02	1.70E-01	18.19	5.445008003	9.919076697	0.96	FALSE	-0.31	-0.60
NUP62	5.48E-01	4.64E-01	18.22	2.387450184	4.822540016	1.22	FALSE	1.90	3.41
LYPLA2	4.25E-01	4.36E-01	18.23	13.82195911	2.615939526	1.18	FALSE	1.38	0.79
EEF1D	3.44E-01	6.12E-01	18.28	0.985759893	7.451311433	1.02	FALSE	-0.45	1.00
ABCF1	4.22E-01	1.35E-01	18.31	7.435248233	0.356070614	1.34	FALSE	3.23	2.37
SKAP2	2.81E-01	3.45E-01	18.37	0.456404247	23.72086612	0.76	TRUE	-5.45	-3.16
GPS2	6.67E-01	3.04E-01	18.40	4.308701037	7.881185647	0.55	FALSE	0.87	-0.37
SNRPA	2.81E-01	1.16E-01	18.50	3.411530561	7.835454232	1.66	FALSE	1.41	1.64
SNRPD1	5.32E-01	2.38E-02	18.60	21.15658975	-0.554113785	0.82	TRUE	0.74	-0.30
NR2F6	5.66E-01	3.63E-01	18.64	8.495360144	6.727710363	1.64	FALSE	3.63	2.14
IMPDH2	7.55E-02	4.30E-01	18.71	-0.535373592	30.685744445	1.02	FALSE	1.81	1.03
PSMC4	9.11E-01	1.04E-01	18.73	8.390998517	3.114001291	0.46	FALSE	1.33	0.75
GPM6B	3.21E-01	7.52E-01	18.77	4.862310428	33.472899854	0.32	FALSE	-0.57	-1.24
SNRPE	7.55E-01	3.43E-02	18.80	16.92686645	0.331937635	0.74	TRUE	1.03	-0.49
ASS1	4.62E-01	1.92E-01	18.80	14.90230724	-0.463357928	0.85	FALSE	0.92	1.15
SF3B2	2.20E-01	6.96E-01	18.81	10.70469624	15.015699271	0.94	FALSE	-0.31	-0.94
NDST1	3.03E-01	6.10E-02	18.82	7.522230908	12.727839941	0.34	FALSE	2.20	2.95
RBM4	5.21E-01	4.82E-01	18.84	12.59107638	10.000771396	1.52	FALSE	0.55	0.52
SERPINH1	9.28E-01	8.95E-03	18.85	37.928133	8.200485704	0.49	FALSE	0.99	0.91
RBP1	8.03E-01	2.16E-01	18.86	12.31936246	-4.522015287	-0.31	FALSE	0.36	-0.37
SCO1	8.30E-01	2.85E-01	18.86	12.77799115	2.974478737	0.72	FALSE	0.54	-0.48
RAB20	7.25E-01	1.55E-01	18.87	0.538124767	16.585255585	1.08	FALSE	-0.59	1.11
CRABP2	4.46E-01	4.25E-02	18.88	5.991748766	0.818296256	0.73	FALSE	2.76	1.86
AURKB	5.17E-01	1.81E-02	18.88	9.869762355	0.859165871	0.75	FALSE	2.28	1.41
DCTN5	1.03E-01	3.03E-01	18.90	3.150239057	6.140267676	1.32	FALSE	1.98	1.58
POLD1	4.07E-01	2.17E-01	18.90	2.322155697	4.865956872	0.55	FALSE	1.04	1.35
ENY2	6.49E-01	3.68E-01	18.91	24.95069297	-0.410508403	1.77	FALSE	-1.25	-1.00
QARS	4.42E-02	3.13E-01	18.96	3.706877301	9.488292408	2.20	FALSE	2.33	1.73
TOP1MT	7.94E-01	1.59E-01	19.00	2.138074483	7.061622399	1.01	FALSE	0.46	-0.34
MPDU1	2.78E-01	1.02E-01	19.02	12.07276379	5.758652693	1.46	FALSE	2.19	2.00
SMC3	1.43E-01	2.89E-01	19.04	2.200475748	26.655166067	1.37	FALSE	-1.26	-1.19

	clinic.R.more	clinic.R.less	sc.All	sc.Old	sc.New	sc.Bulk	sc.Q.gene	tcga.Increased.risk	tcga.Increased.risk.beyond.T.cells
DTD2	7.61E-02	7.38E-01	19.06	-0.454680038	11.47425732	1.86	FALSE	NA	NA
TATDN1	1.17E-01	6.67E-01	19.10	6.785825964	2.252004297	1.28	FALSE	-2.97	-3.70
UQCRC2	2.53E-02	3.72E-01	19.12	7.938348231	5.090440135	0.94	FALSE	0.45	-0.44
RPP30	1.91E-01	2.11E-01	19.13	0.301420634	11.77733863	1.87	FALSE	-0.60	-1.17
ATXN10	6.94E-01	2.97E-01	19.14	15.77144524	13.44735554	2.30	FALSE	0.57	-0.50
WDR81	9.64E-02	8.16E-01	19.17	1.702392177	25.939048876	1.27	FALSE	2.80	2.13
PEPD	5.58E-01	2.73E-01	19.18	4.936443511	11.49578245	1.14	FALSE	2.63	1.77
GAGE2B	2.57E-01	4.80E-01	19.18	-17.70105474	-15.35736178	0.61	FALSE	-0.98	-2.19
FEN1	1.07E-01	2.62E-01	19.24	8.650445933	5.653847713	0.63	FALSE	1.14	0.66
MRPS12	5.69E-01	1.66E-01	19.31	5.930175903	5.311619169	1.32	FALSE	2.84	1.58
FKBP4	6.18E-01	5.52E-02	19.36	10.29840259	1.108434516	1.06	FALSE	3.95	2.47
ALAS1	5.54E-01	3.19E-02	19.38	5.938125987	9.878635076	1.06	FALSE	1.02	1.71
DPP9	1.83E-01	1.89E-01	19.42	-0.678639926	18.41244692	0.58	FALSE	2.05	1.88
ELAC2	5.97E-01	2.82E-01	19.45	12.02634776	3.287839364	0.85	FALSE	3.04	1.34
RPS21	3.21E-01	5.10E-02	19.59	15.48074181	4.433652949	0.81	FALSE	-0.61	-0.82
HYPK	9.14E-02	8.26E-02	19.62	15.88253495	-0.541561047	0.94	TRUE	NA	NA
THEM4	3.55E-01	4.66E-01	19.63	2.641838036	14.1049993	1.04	FALSE	0.60	-0.35
NXN	9.91E-01	1.25E-02	19.72	-0.570380212	4.965390098	0.91	FALSE	0.84	1.70
ABR	3.48E-01	6.70E-01	19.73	1.706300196	19.361391 74	0.77	FALSE	2.16	1.33
DARS	3.52E-01	2.45E-01	19.76	5.49558121	7.54473926	1.48	FALSE	-1.49	-3.22
KCNAB2	6.30E-02	6.76E-01	19.79	-3.601301043	82.174982	1.14	FALSE	1.31	1.95
NUSAP1	1.31E-01	1.92E-01	19.90	4.885093685	2.576691979	0.97	FALSE	0.59	0.37
STOML2	3.74E-01	6.99E-02	20.04	8.770091625	2.098212208	1.02	FALSE	0.98	0.41
TOP2A	7.94E-01	4.05E-02	20.04	4.27101052	1.775930792	1.05	FALSE	0.51	0.43
INTS7	8.16E-01	4.00E-02	20.23	6.6444416	3.720076088	0.79	FALSE	0.71	0.87
MFAP4	2.69E-01	1.24E-01	20.27	17.64876071	-2.070632726	1.07	FALSE	0.53	2.01
MYADM	1.93E-01	6.15E-01	20.29	10.61246616	11.674757742	1.39	FALSE	0.56	0.81
POLR3C	8.17E-01	1.79E-01	20.29	1.698797211	13.48631224	1.26	FALSE	2.24	0.39
OXA1L	1.12E-02	3.08E-01	20.35	-0.321055708	42.387469 33	2.14	FALSE	1.48	0.84
RRP15	6.36E-01	1.43E-01	20.36	4.607755076	2.111990874	0.77	FALSE	-0.71	-2.44
GAS5	1.29E-01	5.14E-01	20.37	0.472735128	48.154625 74	0.76	FALSE	0.36	-0.61
HMGN1	6.43E-01	1.36E-01	20.39	6.749846284	4.090025383	2.61	FALSE	-1.19	-0.56

	clinic.R.more	clinic.R.less	sc.All	sc.Old	sc.New	sc.Bulk	sc.Q.gene	tcga.Increased.risk	tcga.Increased.risk.beyond.T.cells
BIRC5	4.62E-01	2.77E-01	20.53	3.988960147	2.589116396	0.84	FALSE	2.08	1.65
NEK2	8.14E-01	3.28E-02	20.55	5.416078429	2.176491052	1.71	FALSE	1.32	0.82
RRS1	8.28E-01	1.39E-01	20.58	10.21643123	1.580673648	0.47	FALSE	0.67	0.47
PPP5C	4.71E-01	2.16E-01	20.62	1.771526742	8.368988743	0.76	FALSE	1.43	0.61
ARPC5	1.89E-01	8.71E-02	20.70	1.972299705	13.38339241	1.47	FALSE	-3.00	-2.34
TMEM206	3.87E-01	7.69E-02	20.75	8.747393842	9.677672637	2.21	FALSE	0.45	-0.31
GAGE4	9.87E-02	9.02E-01	20.76	-20.72965183	-14.00709129	0.42	FALSE	-1.23	-2.28
EML4	9.25E-01	8.77E-02	20.79	12.05217543	6.934825832	1.60	FALSE	-0.36	0.76
NT5DC2	1.03E-01	3.47E-02	20.89	8.113534256	5.662342879	0.87	FALSE	4.32	1.93
GAGE12H	6.82E-01	2.28E-01	20.99	-18.51606224	-13.97338677	0.70	FALSE	NA	NA
PA2G4	1.68E-01	1.03E-01	21.05	5.49759507	1.679971385	1.66	FALSE	3.15	1.29
LOC100133445	5.36E-01	3.78E-01	21.09	-3.452678468	36.55092064	0.98	FALSE	NA	NA
RRM2	4.18E-01	5.40E-02	21.19	3.042468097	2.545029055	0.55	FALSE	0.92	0.82
GAGE2D	8.73E-03	3.59E-01	21.20	-20.08829393	-14.28059448	0.62	FALSE	-1.16	-2.67
MRPL9	8.73E-01	4.07E-03	21.35	5.97577942	6.146484827	1.12	FALSE	2.40	1.13
TMEM11	4.08E-01	1.35E-01	21.40	20.12015326	1.018469789	0.89	FALSE	2.30	0.92
TPM4	2.84E-01	6.94E-02	21.55	8.611761357	10.141009291	-0.31	FALSE	-0.32	-0.56
ESRG	1.86E-01	7.18E-01	21.56	-0.451092433	19.128552841	1.43	FALSE	NA	NA
SLC25A5	1.55E-01	6.97E-02	21.57	2.102500624	13.097551618	0.79	FALSE	1.48	1.20
CYP51A1	2.25E-01	6.21E-01	21.57	-1.084958837	-22.75159578	0.35	FALSE	0.48	-0.53
TBXA2R	7.68E-01	7.92E-02	21.58	-1.441369813	-22.29805571	1.63	FALSE	-0.58	-0.43
LOC100128252	Inf	Inf	21.59	-25.17189358	-14.09632693	0.36	FALSE	NA	NA
SKA2	8.87E-01	9.62E-02	21.67	5.316547277	9.937930469	1.05	FALSE	-0.60	0.37
RUSC1	4.21E-02	3.03E-01	21.75	1.660172441	20.893226619	0.95	FALSE	2.59	1.08
PSTPIP2	5.69E-01	3.55E-01	21.76	-1.750472311	-11.72131361	1.49	FALSE	-2.63	0.44
LMCD1	1.57E-01	9.29E-01	21.91	6.221082642	20.611722886	2.05	FALSE	-0.68	-0.33
TIMM23	6.53E-03	8.93E-02	21.92	5.327664989	21.550100632	2.07	FALSE	NA	NA
NARS2	5.28E-01	9.12E-02	21.93	7.661886481	16.673400475	1.86	FALSE	2.52	0.96
STRAP	6.79E-01	3.63E-01	21.97	4.999612565	3.189133343	1.85	FALSE	2.08	0.65
XRCC5	7.17E-01	2.58E-01	22.00	10.2024523	3.783862242	2.03	FALSE	0.45	-0.49
EEF1G	4.35E-03	6.07E-01	22.24	3.623195074	11.377855233	0.69	FALSE	0.57	0.44
FLAD1	2.73E-01	9.01E-	22.24	9.115959	4.88990	1.14	FALSE	5.30	3.34

	clinic.R.more	clinic.R.less	sc.All	sc.Old	sc.New	sc.Bulk	sc.Q.gene	tcga.Increased.risk	tcga.Increased.risk.beyond.T.cells
		02		046	0661				
PRDX3	1.28E-01	7.54E-01	22.26	1.506889444	32.24191804	1.77	FALSE	-2.28	-1.43
GAGE2E	1.19E-01	2.55E-01	22.36	-20.18764216	-14.80560626	0.69	FALSE	-1.21	-2.41
TUBGCP2	1.31E-01	5.85E-02	22.66	-0.633889067	43.15291198	0.99	FALSE	0.85	1.13
ORC6	7.21E-01	1.58E-01	22.71	0.700919811	7.219074042	1.94	FALSE	NA	NA
GAGE12G	4.76E-01	1.69E-01	22.73	-21.55374302	-14.04755971	0.65	FALSE	NA	NA
TSTD1	3.33E-02	9.76E-01	22.77	-4.022382197	28.17986342	0.77	FALSE	-1.68	-0.68
GAGE12E	8.00E-01	6.52E-01	22.80	-22.0897866	-14.2987637	0.63	FALSE	NA	NA
GAGE12C	6.13E-01	4.14E-01	22.81	-22.08782445	-14.30284956	0.63	FALSE	NA	NA
NOP56	2.92E-01	1.32E-01	22.85	5.832178979	12.65094704	0.93	FALSE	1.58	0.68
HNRNPA1P10	4.99E-01	2.94E-01	22.87	10.61174151	6.927854056	1.18	FALSE	NA	NA
H3F3AP4	3.96E-01	6.95E-01	22.91	11.05089081	0.790953059	1.18	FALSE	NA	NA
ALDH18A1	3.46E-01	2.20E-02	22.94	15.61796755	10.12846167	0.91	FALSE	1.76	1.87
HN1	1.94E-01	5.05E-02	23.04	12.03860552	3.775525297	0.96	FALSE	1.78	1.68
CPXM1	5.09E-01	3.38E-02	23.05	-34.54741553	-19.23570018	0.59	FALSE	2.24	1.64
SEMA6A	2.72E-01	2.53E-01	23.06	2.112698771	36.865866147	0.89	FALSE	5.02	3.59
PLTP	1.26E-01	1.21E-01	23.23	0.705496057	32.77700504	-0.35	FALSE	0.93	1.16
NAPRT1	1.05E-01	7.78E-01	23.49	-2.243806067	26.634181143	1.37	TRUE	0.57	0.58
CPSF1	4.77E-01	5.25E-01	23.53	4.938813475	18.99445597	2.32	FALSE	0.49	1.64
BUB3	5.98E-03	2.03E-01	23.57	3.787914349	14.66044954	0.94	FALSE	-0.59	-0.47
RGS16	7.20E-01	1.09E-01	23.66	24.77150312	1.061623763	0.59	FALSE	-1.88	-0.96
AFMID	4.63E-01	6.89E-01	23.73	3.422504125	5.089000714	1.48	FALSE	0.59	-0.43
SSR2	8.95E-01	3.81E-02	23.74	3.23295404	13.356007135	0.81	FALSE	1.29	0.98
NDUFAF6	1.88E-01	3.96E-01	23.75	10.7563607	2.527813066	1.97	FALSE	NA	NA
HSD17B14	6.74E-01	1.51E-01	23.76	0.434598607	25.175100233	1.72	FALSE	1.16	1.55
GPC3	5.12E-01	1.16E-02	23.81	-28.39313231	-5.633300805	1.17	TRUE	1.77	1.50
PGAM1	1.41E-01	1.70E-01	23.81	1.192883052	16.09900166	0.93	FALSE	2.85	2.14
C16orf88	7.89E-01	7.76E-02	23.89	16.56262336	4.404648103	2.01	FALSE	2.80	0.95
MSTO1	6.69E-01	1.41E-01	23.89	4.649573196	15.34721826	2.10	FALSE	2.66	2.24
TSTA3	3.55E-01	3.22E-01	23.94	3.15100581	16.378503925	2.68	FALSE	1.80	2.04
UBAP2L	1.55E-01	5.08E-01	23.97	1.815656305	18.648322265	1.97	FALSE	5.67	2.94
C1orf198	9.00E-01	5.96E-04	24.06	3.577483523	22.4333289	0.58	FALSE	0.91	0.42

	clinic.R.more	clinic.R.less	sc.All	sc.Old	sc.New	sc.Bulk	sc.Q.gene	tcga.Increased.risk	tcga.Increased.risk.beyond.T.cells
MAP1LC3A	9.31E-01	1.21E-01	24.10	3.104255127	16.39766697	0.32	FALSE	-0.39	-0.34
ISG20L2	4.82E-02	7.63E-02	24.21	5.979207631	5.765211543	2.61	FALSE	3.40	2.02
PHB2	2.37E-01	6.02E-01	24.23	5.049553302	6.970041892	0.90	FALSE	2.24	0.97
SETDB1	4.06E-01	2.32E-01	24.24	7.633068319	13.365923165	0.89	FALSE	2.05	1.23
MRPL15	7.82E-01	2.79E-01	24.35	14.96676665	0.581390132	0.63	FALSE	0.78	0.45
MRPS16	1.40E-02	1.52E-01	24.39	2.641804679	22.53091111	1.30	FALSE	2.35	1.47
EIF2S3	3.38E-01	1.48E-01	24.47	1.156094853	13.374977764	1.03	FALSE	-0.58	-0.91
ACAA2	4.20E-01	3.56E-01	24.48	15.52042436	6.988920199	3.83	FALSE	1.04	0.47
TYRP1	2.10E-01	6.41E-01	24.53	-1.989085889	12.274488658	0.37	TRUE	4.01	3.07
HDAC2	6.57E-01	4.07E-02	24.61	10.46242506	1.208332687	1.89	FALSE	-0.33	-0.87
PIH1D1	4.87E-01	3.31E-01	24.70	6.126480848	5.911744655	0.82	FALSE	0.33	-0.49
KLHDC3	5.70E-01	5.28E-01	24.75	-22.33788991	-0.664001516	1.15	FALSE	0.64	0.44
CBX5	3.09E-01	1.03E-01	24.89	9.713726735	-0.310128775	1.22	FALSE	0.56	0.91
GLOD4	4.51E-01	5.04E-01	25.00	7.219301782	20.689944046	1.38	FALSE	0.87	0.44
ZNF146	8.68E-01	5.38E-02	25.03	9.080673457	6.819875157	1.59	FALSE	-1.63	-1.82
NOP2	5.64E-01	7.22E-02	25.08	11.43230613	4.158086545	1.14	FALSE	4.00	1.65
TTC39A	7.10E-01	2.95E-01	25.13	0.597290641	46.838166572	1.24	FALSE	2.76	2.75
SRSF7	7.30E-01	9.45E-02	25.21	8.342370883	11.021466198	2.23	FALSE	NA	NA
LHFPL3-AS1	1.04E-01	8.00E-01	25.24	-1.251309555	100.2514925	1.11	FALSE	NA	NA
ARHGDIB	6.71E-01	4.56E-01	25.26	5.905664136	-2.352194126	0.72	FALSE	-3.46	0.38
CYC1	5.00E-01	3.51E-01	25.32	6.635231365	2.419386869	0.90	FALSE	1.34	1.07
ECH1	4.73E-01	6.23E-01	25.36	1.907500873	11.830827	0.92	FALSE	0.78	0.46
DECR1	2.26E-01	3.03E-01	25.39	7.937262507	8.725112226	1.50	FALSE	0.45	0.66
SET	6.42E-01	2.79E-01	25.45	-4.492009689	-0.831007838	0.72	TRUE	0.94	1.17
MTG1	9.69E-02	1.90E-01	25.55	2.947736591	23.272494486	1.53	FALSE	1.11	1.61
KIAA0020	1.64E-01	7.24E-02	25.57	9.60401931	20.8418105	3.17	FALSE	-0.87	-0.80
TMEM204	6.97E-01	1.75E-02	25.57	-1.118931472	23.082396672	1.12	FALSE	1.25	1.89
TPX2	5.81E-01	1.52E-02	25.77	6.760853407	2.944371134	1.10	FALSE	2.34	1.50
H19	5.96E-01	5.55E-02	25.91	23.61054168	-2.068122358	1.12	FALSE	2.09	1.92
CCT3	7.28E-01	3.59E-02	26.21	1.163472086	9.119575759	0.97	TRUE	2.53	1.55
MAZ	1.20E-01	6.09E-01	26.28	2.123839678	31.484304112	1.74	FALSE	3.12	2.51
UBE2T	4.62E-01	5.78E-03	26.39	5.398937996	6.613266871	1.01	FALSE	1.24	0.33

	clinic.R.more	clinic.R.less	sc.All	sc.Old	sc.New	sc.Bulk	sc.Q.gene	tcga.Increased.risk	tcga.Increased.risk.beyond.T.cells
FES	6.27E-01	4.01E-01	26.47	3.382276111	18.36046107	0.93	FALSE	-0.51	0.43
VPS72	6.31E-01	5.39E-02	26.53	3.539245137	18.53462929	2.49	FALSE	2.18	0.88
GAGE2A	8.47E-01	5.06E-01	26.66	26.34578486	-13.96862467	0.74	FALSE	-1.31	-2.19
TUFM	2.00E-01	4.80E-01	26.80	8.01239921	6.859267668	1.22	FALSE	3.70	2.18
ARHGAP4	5.56E-01	4.68E-01	26.84	0.711358224	23.06729832	0.64	FALSE	-2.39	0.44
CCT2	4.07E-01	1.05E-01	26.85	10.05194913	1.601942797	1.94	TRUE	-0.36	-1.08
CDK1	2.44E-01	1.98E-01	26.89	8.429749705	4.579575038	1.09	FALSE	0.50	0.37
TIMM22	7.29E-01	2.48E-01	27.00	11.76212824	8.691671484	2.40	FALSE	2.25	1.64
UHRF1	1.91E-01	7.94E-02	27.05	11.51644137	3.212636756	0.59	FALSE	1.58	1.23
PTGDS	1.81E-01	3.97E-02	27.10	1.823688286	19.02431831	1.54	FALSE	-0.48	2.64
RPSA	7.46E-02	4.38E-01	27.28	0.915567272	24.13544158	1.43	FALSE	0.54	0.86
RPL29	4.20E-02	3.07E-01	27.64	2.972270992	52.83468434	0.64	FALSE	0.92	0.78
CECR5	6.73E-02	2.16E-01	27.64	13.822315	12.734665581	1.44	FALSE	2.59	1.35
HENMT1	7.20E-01	1.17E-01	27.70	10.6271938	2.355018229	0.47	FALSE	NA	NA
SAMM50	7.10E-01	2.57E-02	27.73	5.612340388	28.916066056	1.76	FALSE	3.26	1.17
PPAP2C	6.46E-01	1.02E-01	27.88	13.08854512	13.326595581	0.63	FALSE	0.96	0.90
TRAF7	4.61E-02	5.61E-01	28.04	6.064625478	9.782204488	1.01	FALSE	2.88	2.20
NPL	5.63E-01	3.07E-01	28.07	0.304899232	41.139400087	0.67	FALSE	0.45	0.83
NOSIP	7.94E-01	2.53E-01	28.19	7.332252555	5.086418955	0.83	FALSE	0.65	0.73
UBE2C	4.15E-01	8.94E-03	28.23	9.149834832	3.062410476	1.03	FALSE	2.08	1.46
RPL13A	1.11E-01	4.09E-01	28.31	1.051589093	14.629363637	0.79	TRUE	-0.32	0.45
TUBA1B	4.48E-01	4.72E-01	28.35	7.11176895	4.011979889	1.64	FALSE	2.11	2.10
MPZL1	9.84E-01	1.31E-02	28.40	2.648030647	32.987166246	1.58	FALSE	1.65	0.74
LINC00439	8.10E-01	7.13E-02	28.43	11.2244352	1.289530792	0.65	FALSE	NA	NA
NCBP1	5.60E-01	4.63E-01	28.57	5.488108351	20.395001388	3.16	FALSE	0.36	0.42
SMIM15	5.85E-01	3.47E-01	28.60	6.23912759	8.28036221	0.36	FALSE	NA	NA
UQCRH	5.30E-01	2.97E-01	28.67	22.1641541	-0.337282219	1.11	TRUE	1.42	0.46
APP	7.36E-01	7.63E-02	28.72	9.599129023	18.698795539	0.43	FALSE	0.36	0.59
ADSL	3.60E-01	4.89E-02	28.74	6.11432109	24.626523135	2.18	FALSE	0.56	-0.90
UCK2	4.01E-01	2.08E-01	28.95	9.052578861	3.566943066	1.07	FALSE	1.80	0.82
TP53I11	7.37E-01	2.79E-01	29.06	17.31232856	3.337087794	1.14	FALSE	1.19	2.37
GPATCH4	5.94E-01	1.85E-01	29.10	12.26517954	11.030203118	1.48	FALSE	0.81	-0.34
C20orf112	5.78E-01	1.41E-01	29.13	30.6975856	2.959060323	3.54	FALSE	-0.60	-0.46
RPL17	4.53E-02	4.62E-01	29.30	5.134546488	21.691279968	1.41	FALSE	-0.53	-0.65
BGN	4.65E-01	1.30E-01	29.51	11.64816463	0.49018527	1.80	FALSE	1.45	2.25

	clinic.R.more	clinic.R.less	sc.All	sc.Old	sc.New	sc.Bulk	sc.Q.gene	tcga.Increased.risk	tcga.Increased.risk.beyond.T.cells
BCCIP	4.09E-01	9.82E-02	29.59	5.686214848	17.77614765	1.64	FALSE	-0.86	-1.00
CALM3	6.27E-01	2.48E-01	29.70	5.470474648	20.69905116	0.69	FALSE	2.37	2.29
FAM178B	7.63E-01	1.55E-02	29.73	-0.777212747	24.88791609	0.43	FALSE	0.77	0.55
PAICS	3.90E-01	5.41E-01	29.76	3.312032659	24.26869834	1.74	FALSE	1.52	0.48
TSR1	5.73E-01	1.43E-01	29.94	11.25783989	1.502635952	2.19	FALSE	0.94	0.32
DDX21	5.48E-02	4.82E-01	29.97	3.930072862	12.65700417	0.62	FALSE	-0.65	-0.52
METAP2	4.28E-01	4.93E-01	30.02	11.00208454	8.139440078	1.75	FALSE	-0.92	-2.24
TPM1	1.25E-01	3.35E-01	30.15	16.47245443	3.780545609	1.38	FALSE	-0.36	0.45
CHP1	1.28E-03	7.38E-01	30.25	-0.401031609	22.86929931	0.99	FALSE	NA	NA
DDX50	4.87E-02	6.45E-01	30.29	4.624495525	16.84678101	1.01	FALSE	-2.74	-2.56
RPL30	3.28E-01	5.91E-01	30.39	14.92031239	3.618436257	0.77	FALSE	-0.63	-0.43
FBLN2	3.82E-01	2.03E-03	30.66	7.803353827	7.695710285	1.55	FALSE	0.87	1.75
BANCR	1.42E-01	5.48E-01	30.82	3.861608173	8.402734173	0.46	FALSE	NA	NA
SCIN	6.93E-01	5.54E-02	31.02	-2.738650819	81.946582272	1.03	FALSE	0.70	1.60
C19orf48	7.07E-01	2.88E-01	31.11	6.190544609	6.038677728	1.17	FALSE	2.31	1.10
RPL5	2.21E-01	4.46E-01	31.16	6.752007916	6.997915457	1.15	FALSE	-0.84	-1.18
SCD	1.21E-01	6.04E-01	31.17	-18.67992188	88.984737766	0.55	TRUE	0.71	0.59
MDH2	2.90E-01	2.00E-01	31.18	7.906322813	3.895302932	1.76	TRUE	2.21	0.97
PRAME	4.80E-01	4.11E-01	31.19	9.259758737	33.892455342	2.16	FALSE	0.32	-0.41
HNRNPA1	3.07E-01	1.30E-01	31.31	4.371453406	3.269972055	1.46	TRUE	-0.33	-0.43
SCNM1	2.19E-01	1.06E-01	31.31	3.806661745	7.463417038	1.35	TRUE	1.13	0.51
TUBB	2.22E-01	2.35E-01	31.61	3.915227069	4.379109031	1.16	TRUE	2.41	1.48
KLHDC8B	1.33E-01	4.28E-01	31.64	2.496474168	41.315500213	1.51	FALSE	2.20	2.37
ASAP1	2.03E-01	3.78E-01	31.68	3.393690401	25.615227297	1.04	FALSE	0.31	1.36
CD68	1.98E-01	3.79E-01	31.75	1.979897879	50.211926829	0.57	FALSE	-1.06	0.58
ANP32E	4.92E-01	2.24E-01	31.96	12.31896695	6.597294926	0.68	FALSE	-1.10	-0.82
ITM2C	9.63E-01	1.39E-02	32.08	8.323594178	9.180730963	0.37	FALSE	0.59	0.59
VDAC2	8.01E-02	3.76E-01	32.24	-1.012942241	29.463978783	0.83	FALSE	1.61	0.74
EGFL8	4.52E-01	1.29E-01	32.55	12.73725487	42.564566272	1.01	FALSE	1.36	1.54
RPS11	1.39E-01	2.94E-01	32.62	6.172582657	42.702000252	0.39	FALSE	0.32	0.36
GRWD1	4.38E-01	5.24E-01	32.83	10.9143261	5.020040199	1.24	FALSE	5.62	3.78
CS	1.65E-01	7.41E-01	33.27	6.422065041	17.12335515	2.24	FALSE	5.08	2.61
FAM92A1	1.80E-01	1.18E-02	33.62	23.12776574	3.344554005	0.74	FALSE	-1.33	-2.16
NDUFS2	7.10E-01	9.12E-	34.33	3.683553	26.4960	2.86	FALSE	1.87	0.56

	clinic.R.more	clinic.R.less	sc.All	sc.Old	sc.New	sc.Bulk	sc.Q.gene	tcga.Increased.risk	tcga.Increased.risk.beyond.T.cells
		02		625	6832				
PPA1	1.68E-02	7.35E-01	34.57	4.191072237	36.24460964	1.33	FALSE	-3.57	-1.51
THOC5	4.22E-01	3.11E-01	34.76	23.72211148	8.655594417	1.61	FALSE	0.56	-0.39
NF2	2.21E-01	4.46E-01	35.44	5.935951855	29.68303947	1.87	FALSE	3.24	2.59
SMS	3.48E-01	3.36E-01	35.45	10.57117775	7.554385933	3.53	FALSE	0.82	0.45
MARCKS	2.18E-01	8.98E-01	35.55	1.393466011	26.71905725	0.42	TRUE	-0.60	-0.35
TRPM1	2.73E-02	4.37E-01	35.72	-18.29374495	70.90187013	0.92	TRUE	3.10	2.37
RPL10A	4.87E-02	3.71E-01	35.75	6.395271832	19.89595719	1.43	FALSE	0.56	0.44
LYPLA1	3.39E-01	5.06E-01	36.15	10.23638354	8.320184641	1.87	FALSE	-2.44	-1.87
FBL	5.03E-01	3.43E-01	36.53	4.637441097	24.85286255	1.35	FALSE	2.64	1.65
ZNF286A	9.41E-01	4.19E-02	36.53	14.1424198	2.768284631	1.36	FALSE	-0.47	-0.77
LIMD2	5.49E-01	1.46E-01	36.60	2.122873767	9.295102203	1.17	FALSE	-0.75	2.94
TULP4	2.15E-01	8.43E-02	36.72	3.566475392	21.11741429	1.35	FALSE	0.87	1.16
TIMM13	5.36E-01	2.65E-01	37.26	13.78610742	7.021803959	0.77	FALSE	2.20	1.24
RPAIN	5.60E-01	1.47E-01	37.35	20.39074062	4.484947614	1.21	FALSE	-0.81	-1.76
RBM34	3.24E-01	2.16E-01	37.89	2.249744298	18.86752144	2.58	FALSE	-1.41	-2.72
AHCY	3.78E-01	5.00E-02	38.02	10.5770466	15.468790045	2.09	FALSE	2.49	1.19
MLLT11	9.77E-01	1.52E-02	38.08	-44.02874412	-1.884444301	0.56	TRUE	0.76	0.55
MYBBP1A	6.00E-01	2.83E-01	38.23	29.53471619	4.324352219	1.57	FALSE	2.43	1.71
AEN	5.21E-02	2.42E-01	38.35	14.49457588	12.691077053	2.30	FALSE	3.38	2.32
TRIM28	3.81E-01	3.31E-01	38.48	14.93519938	7.650222211	1.28	FALSE	2.93	2.05
NOLC1	2.47E-02	2.92E-01	38.64	8.507240496	23.202488731	1.84	FALSE	3.61	2.77
SHMT2	2.12E-01	1.72E-01	38.82	7.77411114	5.099441692	0.97	FALSE	2.62	1.34
TYMS	4.65E-01	1.60E-01	38.85	5.796612685	6.721259278	1.64	FALSE	2.02	1.91
RPS12	3.71E-02	4.01E-01	38.95	6.384081023	4.082782447	1.08	FALSE	0.45	0.39
SORD	2.73E-02	3.55E-01	38.98	9.939454508	11.496665193	2.10	FALSE	3.16	1.05
RPL7	4.01E-01	3.36E-01	39.04	11.15340377	3.782743401	1.06	FALSE	-0.38	0.30
ESRP1	4.44E-01	4.55E-02	39.09	10.06244484	25.106977937	1.20	FALSE	2.42	1.76
BZW2	6.62E-01	1.05E-01	39.22	21.62172441	26.924442566	0.92	FALSE	1.37	0.90
RPL18A	8.24E-02	3.34E-01	39.43	2.878936474	36.698444039	0.51	TRUE	1.13	1.24
CA14	3.81E-02	1.81E-01	39.82	-3.998230163	67.430655241	0.77	FALSE	2.21	1.79
SKP2	9.82E-01	1.14E-02	39.93	21.51868872	1.283417716	1.83	FALSE	1.68	1.42
DCAF13	4.60E-01	2.72E-01	40.41	24.87612305	1.564297695	2.88	TRUE	-1.21	-1.72
HMGA1	6.81E-02	6.40E-01	40.42	19.74301642	5.936479134	0.83	FALSE	0.84	0.52
KIAA0101	4.38E-01	5.20E-	41.14	5.177374	9.34349	1.31	FALSE	-0.55	-0.59

	clinic.R.more	clinic.R.less	sc.All	sc.Old	sc.New	sc.Bulk	sc.Q.gene	tcga.Increased.risk	tcga.Increased.risk.beyond.T.cells
		02		736	1776				
CTPS1	8.43E-01	8.35E-02	41.34	24.76379084	7.765650207	1.78	FALSE	NA	NA
PPP2R1A	3.35E-01	5.52E-01	42.96	5.321317629	16.81313352	1.23	FALSE	5.38	2.24
FBLN1	5.09E-01	4.76E-03	43.12	7.246750299	20.27949953	1.92	FALSE	1.65	2.28
RNF2	8.06E-01	2.83E-02	43.71	8.672094386	7.736904785	2.07	FALSE	-0.38	-0.97
CDCA7	6.15E-01	3.99E-02	43.91	5.924051047	11.47163669	1.55	FALSE	0.55	0.97
RPS6	8.53E-02	5.20E-01	43.91	1.692897361	54.07563381	0.83	TRUE	-1.35	-1.38
ILF2	8.63E-01	1.77E-03	45.26	6.943339213	14.84972817	1.39	FALSE	1.31	0.79
RPL18	9.66E-02	2.25E-01	45.37	3.114484434	48.25066529	0.95	FALSE	1.39	1.27
UQCRFS1	4.79E-01	1.04E-01	45.94	2.40443746	31.0840894	0.72	FALSE	3.57	1.57
RUVBL2	7.03E-01	3.34E-01	46.06	9.456736484	13.39002528	1.57	FALSE	2.93	1.38
RPL26	1.01E-01	1.65E-01	46.82	16.99198955	14.09396856	0.84	FALSE	-2.08	-2.60
RPS27	1.47E-02	3.83E-01	47.85	6.873462208	48.31694024	0.66	FALSE	-0.90	0.30
CDKN2A	5.27E-01	6.49E-01	48.20	1.937507613	16.9016692	0.77	TRUE	-0.46	-0.33
MIR4461	9.23E-01	1.12E-02	48.20	5.488218285	21.56158776	1.49	FALSE	NA	NA
TPM2	5.40E-01	2.36E-02	48.33	47.15134153	0.452068271	0.90	TRUE	-0.30	0.49
CNRIP1	4.03E-01	5.26E-01	48.87	10.22154305	16.25935254	1.06	FALSE	-0.36	-0.36
PAFAH1B3	3.38E-01	4.49E-01	49.53	9.159237785	28.8635675	1.14	FALSE	1.48	0.86
FAM174B	6.29E-01	2.83E-01	50.07	15.22332615	36.22910751	1.63	FALSE	3.44	1.88
USP22	4.57E-01	4.65E-01	51.05	32.02385954	8.721171083	1.03	FALSE	2.18	1.05
GTSF1	8.47E-01	2.11E-01	51.20	-89.51451745	-29.39568184	1.35	TRUE	-3.43	-1.39
ISYNA1	5.19E-01	3.37E-01	51.20	8.162255211	38.33773761	3.05	FALSE	1.99	1.79
DLL3	8.77E-01	6.01E-02	51.70	14.88708119	20.30775936	3.27	FALSE	3.09	2.42
TMC6	3.36E-01	5.51E-02	52.13	5.290669679	67.71127702	2.25	FALSE	2.61	3.47
RPS18	7.25E-02	7.13E-01	52.28	27.56806633	18.63526549	0.69	FALSE	0.61	0.32
NREP	6.54E-01	6.71E-03	52.32	-66.79439813	-16.67629308	0.68	TRUE	NA	NA
RPL21	3.07E-01	2.13E-01	52.38	3.737360847	14.06619494	2.11	TRUE	-1.10	-1.33
RPS3	5.62E-02	3.60E-01	52.44	10.48799182	69.45371116	1.37	FALSE	0.97	0.76
RPS5	2.04E-02	3.71E-01	56.38	4.84715055	32.71260656	0.81	TRUE	1.33	0.83
EIF4A1	7.28E-01	1.85E-01	56.54	12.44176552	23.79777896	1.45	FALSE	1.80	0.60
GPI	1.17E-01	3.72E-01	57.12	1.130371128	45.76480744	1.30	TRUE	4.46	2.91
BCAN	7.45E-01	2.02E-01	57.20	2.308514409	72.97911384	0.48	FALSE	3.07	3.42
FTL	2.64E-01	3.99E-01	57.23	1.205064194	75.23699673	1.17	FALSE	0.51	2.31
DCT	3.01E-01	4.11E-01	58.58	-1.023830081	123.9360976	0.58	TRUE	1.78	2.06
RPS16	2.08E-01	4.47E-	58.91	5.580237	61.9000	1.24	FALSE	0.90	0.61

	clinic.R.more	clinic.R.less	sc.All	sc.Old	sc.New	sc.Bulk	sc.Q.gene	tcga.Increased.risk	tcga.Increased.risk.beyond.T.cells
		02		253	3741				
RPL6	1.02E-01	5.40E-01	60.07	16.14902123	9.904010704	2.18	TRUE	-0.35	-0.63
IDH2	6.45E-01	1.16E-01	60.71	11.44171851	14.05976702	1.57	FALSE	-0.31	1.14
H3F3A	3.97E-01	4.63E-01	61.79	14.22533613	3.667893274	1.73	TRUE	-0.70	-0.70
EIF3K	3.13E-01	9.04E-02	61.83	8.143610635	22.751266648	0.89	FALSE	2.25	1.49
SAE1	7.36E-01	1.87E-01	64.08	5.547424178	19.20099815	1.27	FALSE	3.78	2.16
TIMM50	6.48E-01	9.10E-02	65.03	5.084853086	35.29538079	1.29	FALSE	2.94	1.91
RPS24	8.85E-02	3.75E-01	66.05	3.716330306	98.779895575	1.30	FALSE	-0.64	-0.62
RPL28	1.50E-02	4.21E-01	67.31	5.83385988	54.9536147	0.71	TRUE	0.99	1.01
MID1	1.41E-01	5.75E-01	68.45	30.60224621	19.98794862	1.40	FALSE	1.53	1.43
MAGEA4	6.31E-01	2.50E-01	70.13	154.853259	-37.772688982	0.76	TRUE	-1.19	-1.25
SOX4	4.33E-01	3.28E-01	71.11	26.0610551	13.43061044	2.03	FALSE	1.15	0.82
EIF4EBP2	4.09E-02	5.48E-01	71.92	4.991883552	41.120877104	1.61	FALSE	0.57	1.03
SNAI2	3.83E-01	1.30E-01	75.43	7.149559432	49.171855344	1.36	FALSE	1.35	1.14
FOXRED2	2.26E-01	4.31E-01	75.45	12.49982549	58.213396609	3.02	FALSE	3.28	1.62
RPL13AP5	1.17E-01	2.55E-01	77.82	2.595272255	72.740299977	0.90	TRUE	NA	NA
PABPC1	1.84E-01	6.67E-01	79.27	7.945824677	66.885881105	1.76	FALSE	-0.44	0.64
RPL8	1.61E-01	5.12E-01	79.52	0.613777713	40.160800849	1.75	TRUE	0.73	1.10
RPS7	1.97E-01	2.87E-01	79.88	12.55655574	40.627101274	1.62	FALSE	-0.52	-0.79
C1QBP	4.72E-01	1.88E-01	84.82	24.30944797	14.370479936	1.82	TRUE	1.60	0.63
TP53	5.16E-01	4.69E-01	85.56	32.44957009	13.449900773	1.60	TRUE	0.40	0.47
C17orf76-AS1	7.92E-01	9.18E-02	87.51	6.678852726	62.538600033	1.51	FALSE	NA	NA
PTP4A3	5.09E-01	1.18E-01	94.12	18.75491086	26.974107247	3.61	FALSE	1.56	1.83
PFN1	3.26E-01	2.42E-01	96.68	20.383459	27.164877933	2.07	FALSE	1.34	2.82
RPLP0	5.66E-02	6.51E-01	102.20	8.883720005	57.644503707	1.97	TRUE	1.37	0.73
RPS19	1.31E-01	3.50E-01	116.49	8.842607397	97.092603286	1.07	TRUE	1.43	1.14
SERPINF1	1.90E-01	4.68E-01	138.29	45.36545505	71.246701866	3.31	FALSE	0.79	0.87

Table 13. Down-regulated and Up-regulated genes post-immunotherapy treatment in malignant cells

Down-regulated post-treatment		Up-regulated post-treatment	
ABHD2	ITM2B	ACAA2	PRDX3
ACSL4	JUNB	ADSL	PSTPIP2
AHNAK	KCNN4	AEN	PTGDS
AHR	KIAA1551	AHCY	PTP4A3
AIM2	KLF4	ALDH1B1	RBM34
ANGPTL4	KLF6	ARHGEF1	RBM4
ANXA1	LAMB1	ARPC5	RPL10A
ANXA2	LAMP2	ATXN10	RPL17

Down-regulated post-treatment		Up-regulated post-treatment	
APOD	LGALS1	ATXN2L	RPP30
ATF3	LGALS3BP	B4GALT3	RPS3
ATP1A1	LINC00116	BCCIP	RPS7
ATP1B3	LOC100127888	BGN	RPSA
BBX	LOXL2	C10orf32	RUVBL2
BCL6	LOXL3	C16orf88	SAMM50
BIRC3	LPL	C17orf76-AS1	SBNO1
BSG	LXN	C20orf112	SERPINF1
C16orf45	MAGEC2	CDCA7	SKP2
C8orf40	MFI2	CECR5	SLC45A2
CALU	MIA	CPSF1	SMC3
CARD16	MT1E	CS	SMG7
CAV1	MT1F	CTCFL	SMS
CBFB	MT1G	CTPS1	SNAI2
CCDC109B	MT1M	DLL3	SORD
CCND3	MT1X	DTD2	SOX4
CD151	MT2A	ECHDC1	SRCAP
CD200	NFE2L1	ECHS1	SRSF7
CD44	NFKBIZ	EIF4A1	STARD10
CD46	NNMT	EIF4EBP2	TBXA2R
CD47	NOTCH2	EIF6	THOC5
CD58	NR4A1	EML4	TIMM22
CD59	OS9	ENY2	TIMM23
CD9	P4HA2	ESRG	TMC6
CD97	PDE4B	FAM174B	TOMM22
CDH19	PELI1	FAM213A	TPM1
CERS5	PIGT	FBL	TSNAX
CFB	PMAIP1	FBLN1	TSR1
CHI3L2	PNPLA8	FDXR	TSTA3
CLEC2B	PPAPDC1B	FOXRED2	TULP4
CLIC4	PRKCDBP	FXN	UBAP2L
COL16A1	PRNP	GALT	UCHL5
COL5A2	PROS1	GEMIN8	UROS
CREG1	PRSS23	GLOD4	VPS72
CRELD1	PSMB9	GPATCH4	WDR6
CRYAB	PSME1	HDAC2	XPNPEP1
CSPG4	PTPMT1	HMGN3	XRCC5
CST3	PTRF	HSD17B14	YDJC
CTNNAL1	RAMP1	IDH2	ZFP36L1
CTSA	RND3	ILF2	ZNF286A
CTSB	RNH1	ISYNA1	
CTSD	RPN2	KIAA0020	
DCBLD2	S100A10	KLHDC8B	
DCTN6	S100A6	LMCD1	
EGR1	SCCPDH	LOC100505876	
EMP1	SERINC1	LYPLA1	
EPDR1	SERPINA3	LZTS2	
FAM114A1	SERPINE1	MAZ	
FAM46A	SERPINE2	METAP2	
FCRLA	SLC20A1	MID1	
FN1	SLC35A5	MIR4461	
FNDC3B	SLC39A14	MPDU1	
FXYD3	SLC5A3	MPZL1	
G6PD	SMIM3	MRPS16	
GAA	SPARC	MSTO1	
GADD45B	SPRY2	MTG1	
GALNS	SQRDL	MYADM	
GBP2	STAT1	MYBBP1A	
GEM	SUMF1	MYL6B	
GRAMD3	TAP1	NARS2	

Down-regulated post-treatment		Up-regulated post-treatment	
GSTM2	TAPBP	NCBP1	
HLA-A	TEKT4P2	NDUFAF6	
HLA-C	TF	NDUFS2	
HLA-E	TFAP2C	NF2	
HLA-F	TMEM43	NHEJ1	
HPCAL1	TMX4	NME6	
HSP90B1	TNC	NNT	
HTATIP2	TNFRSF10B	NOLC1	
IFI27L2	TNFRSF12A	NTHL1	
IFI44	TSC22D3	OAZ2	
IFI6	TSPAN31	OXA1L	
IFITM3	UBA7	PABPC1	
IGF1R	UBC	PAICS	
IGFBP3	UBE2L6	PAK1IP1	
IGFBP7	XPO7	PFN1	
IL1RAP	ZBTB20	POLR2A	
ITGA6	ZDHHC5	PPA1	
ITGB3	ZMYM6NB	PRAME	

[0430] The signature was down-regulated in resistant tumors for genes associated with coagulation, apoptosis, TNF-alpha signaling via NFKB (NFKBIZ), Antigen processing and presentation (e.g., MHC-I, HSPA1A), metallothioneins (e.g., MT2A, MT1E) involved in metal storage, transport, and detoxification, and IFNGR2 (Gao et al. *Cell* 2016).

[0431] The signature was up-regulated in resistant tumors for genes associated with negative regulation of angiogenesis and MYC targets.

[0432] **Ser**ine **p**rotease **in**hibitors (SERPINs), which are involved in protease inhibition and control of coagulation and inflammation were differentially expressed in the signature. Prior studies relate to recurrent *SERPINB3* and *SERPINB4* mutations in patients who respond to anti-CTLA4 immunotherapy (Riaz et al. *NG* 2016). SERPINA3, SERPINA1, SERPINE2 were down-regulated in resistant tumors. SERPINF1, SERPINB9 were up-regulated in resistant tumors.

[0433] The resistance signature also strongly correlated with MHC-I expression (**Figure 22**). One of the tumors in the cohort has a wide range of MHC-I expression in the malignant cells. Applicants filtered HLA genes from the resistance signature, and scored the malignant cells. The malignant cells with the highest resistance scores in this tumor under express MHC-I.

[0434] There are 13 different metallothioneins and 6 of them are moderately/highly expressed in the melanoma malignant cells. When Applicants scored the cells according to this mini-signature separation between the treated and untreated samples was observed

(**Figure 23**). Therefore, a signature only including metallothioneins may be used in the methods of the present invention.

The prognostic value of the post-immunotherapy modules

[0435] Applicants discovered that the immunotherapy resistance signature was also predictive of survival rates in tumors. The prognostic value of the signature is significant (P = 1.6e-05), even when accounting for T-cell infiltration scores as shown by analyzing samples in the cancer genome atlas (TCGA) (**Figure 24**). The resistance signature performs better than other single-cell based signatures in predicting high and low survival rates (**Figure 25**).

[0436] To further examine the generalizability of the PIT modules Applicants analyzed the bulk gene expression data of melanoma tumors from The Cancer Genome Atlas (TCGA). As Applicants saw at the single-cell level, Applicants find that the genes within each module are co-expressed across tumors, while the two modules are negatively correlated. Applicants postulated that higher expression of the PIT-up program and a lower expression of the PIT-down program might indicate that the tumor is more resilient against immune-mediated clearing, resulting in a more aggressive disease. To test this hypothesis, Applicants scored each tumor according to the immunotherapy modules and examined the prognostic value of these scores. Indeed, the immunotherapy scores are significantly associated with patient survival, such that the expression of the PIT-up (down) signature is associated with lower (higher) survival rates (**Figure 24, 25**).

[0437] To examine the significance of this finding Applicants performed the same analysis with signatures that were previously identified based on the analysis of the single cell melanoma data (Tirosh *et al.*, Dissecting the multicellular ecosystem of metastatic melanoma by single-cell RNA-seq. Science. 2016 Apr 8;352(6282):189-96). Applicants divided these signatures into two groups: (1) malignant signatures – signatures that describe the state of the malignant cells, as cell cycle, and the AXL and MITF signatures, which were previously shown to be associated with the response to targeted therapy; (2) tumor composition signatures that describe a specific cell type or the state of a non-malignant cell type within the tumor microenvironment. None of the malignant signatures is significantly associated with patient survival, indicating that mere variation across malignant cells is not sufficient to yield such results. The cell-type signatures are associated with patient survival, especially those that related to T-cell infiltration, though their prognostic signal is redundant when accounting for tumor purity. The latter is estimated based on CNVs.

[0438] Importantly, the prognostic value of the PIT scores is significant even when accounting for the tumor purity and T-cell infiltration scores. Interestingly, the PIT-up (down) scores are negatively (positively) correlated to the T-cell scores, as Applicants further describe herein. Nonetheless, the combination of the PIT and T-cell scores yields significantly more accurate predictions of patient survival compared to those obtained when using each score separately, indicating that the PIT modules capture tumor properties that cannot be explained just by T-cell infiltration levels.

The post-immunotherapy modules are associated with response to anti-PD1 and anti-CTLA4 in the clinic and in mouse models

[0439] Immunotherapy introduces selective pressures that, in case of an unsuccessful treatment, are likely to increase the abundance of immunotherapy-resistant cells. The post-immunotherapy signatures Applicants derived might capture these resistant cell states, and, as such, may help to detect innate resistance to anti-PD-1 or anti-CTLA4 therapy – pretreatment. To examine this concept Applicants analyzed the gene expression profiles of responding (n = 15) and non-responding (n = 13) tumors sampled prior to anti-PD-1 therapy. Indeed, the tumors of responders overexpressed the PIT-down signature and underexpressed the PIT-up signature, resulting in accurate predictors of response to anti-PD-1 (P = 3.38e-02 and 5.5e-04, Area Under the Receiver Operating Characteristic Curve (ROC-AUC) = 0.91 and 0.77. In another gene expression cohort of pre-anti-CTLA-4 melanoma tumors the signatures did not yield a significant separation between the responders and non-responders. Therefore, Applicants set out to test the signatures in a more controlled setting of a murine model, in which genetically identical mice that experienced the same environment and treatment display a dichotomous response to anti-CTLA4. Indeed, responders scored higher for the PIT-down signature and lower for the PIT-up signature, resulting in accurate predictors of response to anti-CTLA4 in this model (P = 1.2e-05, ROC-AUC = 0.99). The ITR signature was predictive of eventual outcome in both mouse and human data. First, in a bulk RNA-Seq study of anti-CTLA4 therapy in mouse, the malignant ITR score predicted well non-responders compared to responders. Applicants analyzed 27 patients associated with anti-PD1 response (Hugo et al., 2016). The malignant ITR was significantly lower in pre-treatment samples from patients with complete response compared to those with partial or no response (**Figure 26**). The (5) complete-responders in the data of Hugo et al. scored lower for the sc-resistance signature compared to the other 22 patients (P = 9.37e-04). These results indicate that the signatures identified capture cell states that are linked to anti-PD1 and

anti-CTLA4 resistance.

[0440] Genes that were up-regulated in the resistant tumors (single cell) were down-regulated in CR vs. others (P = 9.6e-14) and C/PR vs. NR (NS) (**Figure 27**). Genes that were down-regulated in the resistant tumors (single cell) were up-regulated in CR vs. others (P = 2.8e-11) and C/PR vs. NR (P = 2.8e-03) (**Figure 28**).

Associating melanoma-cell-intrinsic states with T-cell infiltration and exclusion.

[0441] Tumor infiltration with T cells is one of the strongest predictors of patient response to immune checkpoint inhibitors in various cancer types. Understanding the molecular mechanisms that underlie spontaneous T-cell infiltration could aid the development of therapeutic solutions for patients with non-inflamed tumors. Applicants leveraged the single-cell data and bulk gene expression cohorts of melanoma tumors to map malignant transcriptional states that are associated with T-cell infiltration or exclusion.

[0442] First, Applicants analyzed the single-cell data to derive a CD8 T-cell signature, consisting of genes that are primarily expressed by CD8 T-cells (Methods). Applicants used this signature to estimate the T-cell infiltration level of melanoma tumors based on their bulk gene expression profiles. Applicants show that patients with more T-cell infiltration, according to this measure, are more likely to respond to anti-CTLA4 and to MAGE-A3 antigen-specific immunotherapy, and have better overall survival. Next, Applicants identified based on the single-cell data genes that are expressed primarily by malignant melanoma cells. Applicants then searched for genes that are correlated with T cell abundance in the bulk TCGA gene expression cohort, while restricting the search only to the malignant-specific genes to derive an *initial* T-cell-infiltration signature (T cell exclusion signature (T-ex).

[0443] While the initial signature is informative, it is limited for two main reasons. First, there are only 384 genes that could be confidently defined as exclusively expressed by the malignant melanoma cells. Second, it cannot confidently identify genes whose expression in the malignant cells will exclude T-cells. To overcome these limitations, Applicants used the initial T-cell infiltration signature only as an anchor, and searched for genes whose expression level in the individual malignant cells is positively or negatively correlated to the overall expression of this initial signature. Applicants defined genes that are strongly positively (negatively) correlated to the initial signature as the infiltrated (non-infiltrated) module. Of note, non-malignant cells express most of the genes in these modules, and hence it would have been difficult to associate them with T-cell infiltration without leveraging the single-cell data.

[0444] The genes in the infiltrated module (exclusion-down) play a major role in antigen processing and presentation (HLA-A/B/C, B2M, TAPBP) and interferon gamma response (e.g., IFI27, IFI35, IRF4, IRF9, STAT2). In certain embodiments, the infiltrated module includes the following genes: A2M, AEBP1, AHNAK, ANXA1, APOC2, APOD, APOE, ATP1A1, ATP1B1, C4A, CAPN3, CAV1, CD151, CD59, CD63, CDH19, CRYAB, CSPG4, CSRP1, CST3, CTSB, CTSD, DAG1, DDR1, DUSP6, ETV5, EVA1A, FBXO32, FCGR2A, FGFR1, GAA, GATSL3, GJB1, GRN, GSN, HLA-B, HLA-C, HLA-F, HLA-H, IFI35, IGFBP7, IGSF8, ITGA3, ITGA7, ITGB3, LAMP2, LGALS3, LOXL4, LRPAP1, LY6E, LYRM9, MATN2, MFGE8, MIA, MPZ, MT2A, MTRNR2L3, MTRNR2L6, NPC1, NPC2, NSG1, PERP, PKM, PLEKHB1, PROS1, PRSS23, PYGB, RDH5, ROPN1, S100A1, S100A13, S100A6, S100B, SCARB2, SCCPDH, SDC3, SEMA3B, SERPINA1, SERPINA3, SERPINE2, SGCE, SGK1, SLC26A2, SLC5A3, SPON2, SPP1, TIMP1, TIMP2, TIMP3, TM4SF1, TMEM255A, TMX4, TNFSF4, TPP1, TRIML2, TSC22D3, TXNIP, TYR, UBC and WBP2.

[0445] The non-infiltrated module (exclusion-up) is mainly enriched with MYC targets and MYC itself. It also includes STRAP, which is an inhibitor of TGF-beta signaling, and SMARCA4 (or BRG1) – a subunit of the BAF complex that has a key role in mediating beta-catenin signaling. The latter has been shown to promote T-cell exclusion in mice. In certain embodiments, the non-infiltrated module includes the following genes: AHCY, BZW2, CCNB1IP1, CCT6A, EEF2, EIF3B, GGCT, ILF3, IMPDH2, MDH2, MYBBP1A, NT5DC2, PAICS, PFKM, POLD2, PTK7, SLC19A1, SMARCA4, STRAP, TIMM13, TOP1MT, TRAP1 and USP22.

[0446] Interestingly, these results mirror and overlap the PIT signatures. When scoring the malignant cells according to these infiltration signatures Applicants find that the treatment naïve malignant cells score significantly higher for infiltration compared to the post-treatment malignant cells. In other words, malignant cells having the ITR signature have higher exclusion signatures and treatment naïve malignant cells have higher infiltration signatures (**Figure 29**). These results indicate that cells which survive post-immunotherapy either reside in less infiltrated niches within the tumor or have increased capacity to exclude T-cells from their immediate microenvironment. Not being bound by a theory, malignant cells that survive immunotherapy are either to begin with are in a T cell excluded TME or became T cell excluding.

Immunotherapy triggers significant transcriptional changes in CD8 T-cells

[0447] Next Applicants set out to map the transcriptional landscape of the immune cells and examine the association of these states with immunotherapy. Applicants performed the analysis separately for each cell type (CD8 T-cells, CD4 T-cells, B-cells, and macrophages). First, Applicants performed an unbiased analysis to explore the main sources of heterogeneity in melanoma CD8 T-cells. To this end, Applicants applied Principle Component Analysis (PCA) followed by nonlinear dimensionality reduction (t-distributed stochastic neighbor embedding (t-SNE)). Interestingly, in the first PCs and the t-SNE dimensions, the CD8 T-cells are segregated according to their treatment history, such that post-treatment cells cluster together and apart from the treatment naïve cells. These findings demonstrate that immunotherapy triggers significant transcriptional changes in CD8 T-cells, and highlight two additional and orthogonal sources of heterogeneity: one that is attributed to cell cycle, and another that is attributed to the expression of inhibitory checkpoints (**Figure 30, 31**).

[0448] Applicants performed supervised analyses to identify the genes and pathways that are differentially expressed in the post-immunotherapy CD8 T-cells compared to the treatment naïve cells. The resulting signatures indicate that the post-treatment CD8 T-cells are more cytotoxic and exhausted, such that naïve T-cell markers are downregulated, while IL-2 signaling, T-cell exhaustion and activation-dysfunction pathways are up regulated. Applicants then scored the CD8 T-cells according to these two signatures, revealing a spectrum of phenotypes also within the PIT and treatment naive populations, and within the CD8 T-cell population of the same tumor.

[0449] Applicants speculated that this spectrum might be related to clonal expansion. Clonal expansion occurs when T cells that recognize a specific (tumor) antigen proliferate to generate discernible clonal subpopulations defined by an identical T cell receptor (TCR) sequence. Applicants applied TraCeR to reconstruct the TCR chains of the T-cells and identify cells that are likely to be a part of the same clone (Stubbington et al., Nature Methods 13, 329–332 (2016)). Overall, Applicants identified 113 clones of varying sizes, three of which consist of more than 20 cells (**Figure 32**). Specifically, Applicants used the TcR sequence to determine the clone of each T cell, and distinguished four categories: treatment naive or ITR, and expanded or not. Applicants analyzed their gene expression and saw that cells vary in two ways. First CD8 T cells from ITR patients have distinct expression, and this is especially pronounced in expanded cells. All the major expanded clones were in ITR samples, and only very few cells were expanded in treatment naive patients. These few

expanded cells look more like cells from the treated patients. Similar to results reported in mice there is an expanded population of Bcl6+Tcf7+ cells in the ITR samples, some also CXCR5+. When Applicants turn to their functional state, Applicants observed that across all patients, regardless of treatment, some cells are more exhausted and others more naive.

[0450] These large clones are from post-treatment patients, indicating that immunotherapy is triggering T-cell activation and proliferation even when no objective clinical response is observed. Moreover, Applicants find that clonal expansion is strongly associated with the PIT scores, not only across all patients, but also when considering only the post-immunotherapy or treatment naïve cells. Next Applicants compared clonally expanded T-cells to the other T-cells within the same tumor to derive signatures of clonal expansion. By leveraging intra-tumor T-cell heterogeneity in this manner Applicants were able to mitigate the problem of batch effects. In concordance with the previous results Applicants find that genes, which are over (under) expressed post-immunotherapy, are overrepresented in the up (down) regulated clonal-expansion module (**Figure 33**).

[0451] Not being bound by a theory, inhibition of genes, which are under expressed in the T-cells post immunotherapy, could potentially promote T-cell survival and expansion in the tumor microenvironment. Indeed, these genes are ranked significantly high in the results of an in-vivo shRNA screen that identified negative regulators of T-cell proliferation and survival in mice tumors (P = 4.98e-03). All in all, these results suggest that post-immunotherapy T-cells are more activated, even in this cohort of non-responders.

Table 14

Post-immunotherapy state in CD8 T-cells	Pathway	Genes
Up-regulated	Zinc TFs	*ZBTB24, ZNF526, ZNF528, ZNF543, ZNF620, ZNF652, ZSCAN2, ZSCAN22*
	IFN gamma signaling	*GBP2, GBP5, IRF1, PTPN2, STAT1*
	PD1 signaling	*CD3D, CD3E, CD3G, HLA-DQA1, HLA-DQA2, HLA-DRB5, PDCD1*
Down-regulated	Cell cycle	*BIRC5, BUB1, GMNN, MAD2L1, NDC80, TTN, UBE2C, ZWINT*
	Negative regulators of T-cell survival/proliferation in the TME	*CBLB, WNK1, PDCD1*

(Zhou et al. 2014)

[0452] Not being bound by a theory, immunotherapy is triggering transcriptional changes both in the malignant cells and in the CD8 T-cells. The results suggest that the T-cells become more effective, while the malignant cells become more "immune-edited" (e.g., evasion (MHC-1) vs. T-cell exclusion).

Example 3 - C-map analysis

[0453] Drugs that could reduce the resistance signature were analyzed by c-map analysis. The analysis showed that the following drugs could reduce the immunotherapy resistance signature:

- PKC activators;
- NFKB pathway inhibitors;
- IGF1R inhibitors; and
- Reserpine (Used to control high blood pressure & psychotic symptoms and blocks the vesicular monoamine transporter (VMAT)).

[0454] The signature is associated with drug response/effects. There was an association between the toxicity of different drugs and their resistance scores (according to the resistance signatures). C-map results indicated drugs that can sensitize/de-sensitize the cells to immunotherapy. The results of this analysis are summarized in Table 15-17.

Table 15. Drugs that modulate Gene Signature

The correlation between the resistance scores of the cell lines and their sensitivity (IC50) to the pertaining drug (based on the CCLE gene expression and the Garnett et al. Nature 2012)				
Negative R -> more toxic/selective to the immuno-resistant cells.				
Positive R -> less toxic/selective to the immuno-resistant cells.				
Drug	**All.R**	**All.P**	**melanoma.R**	**melanoma.P**
Pazopanib	-0.01	8.62E-01	-0.48	3.27E-02
Shikonin	-0.05	4.55E-01	-0.48	3.97E-02
Etoposide	-0.16	2.02E-02	-0.48	4.05E-02
JNK.9L	-0.13	4.97E-02	-0.39	1.00E-01
GSK.650394	-0.17	1.02E-02	-0.37	1.05E-01
X681640	-0.08	1.56E-01	-0.37	1.55E-01
Vinorelbine	-0.14	3.68E-02	-0.34	1.54E-01
AZD6482	0.16	1.46E-02	-0.34	1.56E-01
BIRB.0796	-0.11	6.17E-02	-0.33	2.13E-01
NVP.BEZ235	0.00	9.79E-01	-0.30	1.59E-01
Roscovitine	0.03	6.90E-01	-0.30	4.37E-01
Sunitinib	-0.04	6.12E-01	-0.30	4.37E-01
Gemcitabine	-0.05	4.18E-01	-0.29	2.19E-01
Epothilone.B	-0.05	4.40E-01	-0.29	2.21E-01
ATRA	-0.20	6.16E-04	-0.28	3.14E-01
VX.702	-0.16	6.16E-03	-0.27	2.62E-01
QS11	-0.17	7.40E-03	-0.27	2.50E-01
Lapatinib	0.29	4.69E-04	-0.27	4.93E-01
BMS.536924	0.32	7.64E-05	-0.25	5.21E-01
Vorinostat	-0.37	2.73E-11	-0.25	3.02E-01

PD.0332991	-0.06	2.82E-01	-0.22	3.75E-01
Parthenolide	0.08	3.55E-01	-0.22	5.81E-01
AZD.2281	-0.18	1.72E-03	-0.21	3.71E-01
FTI.277	0.18	6.29E-03	-0.21	3.85E-01
IPA.3	-0.08	2.14E-01	-0.21	3.75E-01
PF.562271	0.05	4.31E-01	-0.20	4.10E-01
PD.173074	-0.18	1.89E-03	-0.19	3.74E-01
Tipifarnib	-0.09	1.93E-01	-0.18	4.33E-01
A.770041	0.24	4.60E-03	-0.18	6.44E-01
Z.LLNle.CHO	0.23	5.71E-03	-0.18	6.44E-01
CEP.701	-0.10	9.73E-02	-0.17	4.75E-01
PAC.1	-0.09	1.52E-01	-0.17	4.76E-01
BI.2536	0.14	9.25E-02	-0.17	6.78E-01
GW843682X	0.05	5.52E-01	-0.17	6.78E-01
Midostaurin	0.06	3.70E-01	-0.16	5.03E-01
Metformin	-0.21	9.02E-05	-0.16	4.24E-01
ZM.447439	-0.09	1.27E-01	-0.14	5.21E-01
Elesclomol	0.07	2.48E-01	-0.14	6.21E-01
AZD7762	-0.08	1.48E-01	-0.14	5.68E-01
Sorafenib	-0.03	7.33E-01	-0.13	7.44E-01
XMD8.85	0.00	9.81E-01	-0.13	7.44E-01
BAY.61.3606	-0.05	4.84E-01	-0.13	5.81E-01
BI.D1870	-0.02	7.72E-01	-0.13	6.41E-01
Doxorubicin	-0.03	6.08E-01	-0.11	6.44E-01
DMOG	0.17	1.05E-02	-0.10	6.78E-01
BMS.509744	0.08	3.30E-01	-0.10	8.10E-01
Bosutinib	-0.05	3.91E-01	-0.09	7.05E-01
CMK	0.17	3.68E-02	-0.08	8.43E-01
KIN001.135	0.19	2.39E-02	-0.08	8.43E-01
WZ.1.84	0.21	1.47E-02	-0.08	8.43E-01
AZD8055	-0.11	5.79E-02	-0.08	7.33E-01
Paclitaxel	0.18	3.31E-02	-0.07	8.80E-01
VX.680	-0.01	9.30E-01	-0.07	8.80E-01
LFM.A13	0.12	5.87E-02	-0.06	8.11E-01
Methotrexate	-0.35	1.27E-09	-0.06	8.42E-01
NU.7441	0.10	1.02E-01	-0.06	8.39E-01
KU.55933	0.07	2.68E-01	-0.05	8.48E-01
JW.7.52.1	0.11	1.80E-01	-0.05	9.12E-01
OSI.906	0.06	3.67E-01	-0.05	8.36E-01
PD.0325901	0.23	4.75E-05	-0.04	8.51E-01
JNK.Inhibitor.VIII	0.03	6.13E-01	-0.04	9.00E-01
Gefitinib	-0.02	6.99E-01	-0.03	9.23E-01
BMS.754807	0.01	8.32E-01	-0.02	9.32E-01
BIBW2992	0.04	5.07E-01	-0.02	9.43E-01
Salubrinal	-0.11	1.93E-01	-0.02	9.82E-01
Camptothecin.3	0.03	6.44E-01	-0.01	9.57E-01
Camptothecin.5	0.03	6.44E-01	-0.01	9.57E-01
A.443654	0.14	9.40E-02	0.00	1.00E+00
Thapsigargin	-0.02	7.97E-01	0.00	9.92E-01
NSC.87877	-0.17	1.36E-02	0.01	9.86E-01
BX.795	0.03	6.53E-01	0.01	9.73E-01
X17.AAG	0.22	2.11E-04	0.03	9.26E-01
Mitomycin.C	-0.12	7.40E-02	0.03	9.11E-01
Temsirolimus	-0.12	4.14E-02	0.03	9.13E-01
Docetaxel	0.13	2.39E-02	0.03	8.84E-01
Cyclopamine	0.01	8.84E-01	0.03	9.48E-01
Camptothecin	-0.12	3.84E-02	0.04	8.74E-01
Camptothecin.4	-0.12	3.84E-02	0.04	8.74E-01
GDC0941	0.02	7.65E-01	0.04	8.41E-01
Obatoclax.Mesylate	-0.05	4.59E-01	0.05	8.41E-01
CGP.082996	-0.01	9.29E-01	0.07	8.80E-01
Bleomycin	-0.09	1.92E-01	0.08	7.53E-01
AS601245	-0.03	6.96E-01	0.08	7.29E-01
Bryostatin.1	-0.01	8.31E-01	0.08	7.29E-01
Embelin	-0.01	9.13E-01	0.09	7.05E-01
AKT.inhibitor.VIII	-0.10	1.35E-01	0.09	7.05E-01
AP.24534	0.13	6.29E-02	0.09	7.05E-01
RDEA119	0.27	1.44E-06	0.12	5.98E-01

Nilotinib	-0.09	1.34E-01	0.13	6.00E-01
CGP.60474	0.26	1.85E-03	0.13	7.44E-01
S.Trityl.L.cysteine	0.00	9.82E-01	0.13	7.44E-01
Erlotinib	0.18	4.08E-02	0.15	7.08E-01
ABT.888	-0.11	6.48E-02	0.15	5.17E-01
MK.2206	-0.09	1.47E-01	0.16	5.14E-01
Dasatinib	0.38	4.98E-06	0.17	6.78E-01
MG.132	0.25	2.24E-03	0.17	6.78E-01
PF.02341066	0.14	7.89E-02	0.17	6.78E-01
Cisplatin	-0.01	8.94E-01	0.18	5.12E-01
WH.4.023	0.23	5.25E-03	0.18	6.44E-01
CI.1040	0.09	1.24E-01	0.20	4.74E-01
SL.0101.1	-0.06	2.74E-01	0.20	4.56E-01
SB590885	-0.11	5.08E-02	0.21	3.61E-01
A.769662	0.06	3.85E-01	0.21	3.85E-01
AZ628	0.17	4.24E-02	0.22	5.81E-01
GSK269962A	0.21	1.14E-02	0.22	5.81E-01
MS.275	0.00	9.71E-01	0.22	5.81E-01
Cytarabine	-0.02	7.54E-01	0.22	4.10E-01
Axitinib	-0.19	1.11E-03	0.22	3.54E-01
Vinblastine	-0.07	2.38E-01	0.23	3.91E-01
Bicalutamide	0.02	7.59E-01	0.24	2.99E-01
PLX4720	0.07	2.41E-01	0.25	3.43E-01
RO.3306	0.11	6.07E-02	0.25	2.41E-01
AUY922	0.01	9.32E-01	0.26	2.75E-01
GNF.2	0.27	1.27E-03	0.27	4.93E-01
Lenalidomide	-0.11	5.30E-02	0.27	2.69E-01
GDC.0449	-0.12	3.17E-02	0.29	2.20E-01
AICAR	-0.16	3.97E-03	0.30	1.33E-01
AZD6244	0.17	4.19E-03	0.32	1.97E-01
Nutlin.3a	-0.09	1.18E-01	0.32	1.36E-01
Bexarotene	-0.01	9.08E-01	0.34	1.41E-01
Imatinib	0.15	6.78E-02	0.35	3.59E-01
Rapamycin	0.09	2.59E-01	0.35	3.59E-01
GW.441756	-0.09	1.17E-01	0.35	1.41E-01
ABT.263	-0.12	3.89E-02	0.37	8.43E-02
CHIR.99021	0.19	3.91E-03	0.38	1.10E-01
Bortezomib	0.36	6.13E-06	0.38	3.13E-01
Pyrimethamine	0.09	2.84E-01	0.38	3.13E-01
FH535	-0.24	1.51E-04	0.40	8.41E-02
AMG.706	-0.04	4.43E-01	0.45	3.14E-02
SB.216763	0.02	7.29E-01	0.46	4.84E-02
AZD.0530	0.31	1.05E-04	0.53	1.48E-01
PHA.665752	0.18	2.41E-02	0.68	5.03E-02
NVP.TAE684	0.21	8.27E-03	0.72	3.69E-02

Table 16. Top 200 drugs that induce downregulated genes in the signature

Rank	Score	Type (cp= compound, kd = knock-down, oe = over-expression, cc = cmap class)	ID	Name	Description
1	99.95	cc		PKC Activator	-
2	99.95	kd	CGS001-10538	BATF	basic leucine zipper proteins
3	99.95	kd	CGS001-25937	WWTR1	Hippo Signaling
4	99.95	kd	CGS001-7483	WNT9A	Wingless-type MMTV integration sites
5	99.95	kd	CGS001-2837	UTS2R	Urotensin receptor
6	99.95	kd	CGS001-7187	TRAF3	-
7	99.95	kd	CGS001-27242	TNFRSF21	Tumour necrosis factor (TNF) receptor family
8	99.95	kd	CGS001-7027	TFDP1	-
9	99.95	kd	CGS001-64783	RBM15	RNA binding motif (RRM) containing
10	99.95	kd	CGS001-8438	RAD54L	-
11	99.95	kd	CGS001-8624	PSMG1	-
12	99.95	kd	CGS001-53632	PRKAG3	AMPK subfamily

Rank	Score	Type (cp= compound, kd = knock-down, oe = over-expression, cc = cmap class)	ID	Name	Description
13	99.95	kd	CGS001-5184	PEPD	Methionyl aminopeptidase
14	99.95	kd	CGS001-4688	NCF2	Tetratricopeptide (TTC) repeat domain containing
15	99.95	kd	CGS001-11004	KIF2C	Kinesins
16	99.95	kd	CGS001-22832	KIAA1009	-
17	99.95	kd	CGS001-10014	HDAC5	Histone deacetylases
18	99.95	kd	CGS001-2355	FOSL2	basic leucine zipper proteins
19	99.95	kd	CGS001-2864	FFAR1	Fatty acid receptors
20	99.95	kd	CGS001-51719	CAB39	-
21	99.95	kd	CGS001-604	BCL6	BTB/POZ domain containing
22	99.95	kd	CGS001-326	AIRE	Zinc fingers, PHD-type
23	99.93	cp	BRD-K02526760	QS-11	ARFGAP inhibitor
24	99.92	kd	CGS001-23224	SYNE2	-
25	99.92	kd	CGS001-10267	RAMP1	Receptor (G protein-coupled) activity modifying proteins
26	99.92	kd	CGS001-4323	MMP14	Matrix metallopeptidase
27	99.92	kd	CGS001-9455	HOMER2	-
28	99.92	kd	CGS001-2852	GPER	-
29	99.92	kd	CGS001-694	BTG1	-
30	99.91	cc		NFKB Activation	-
31	99.91	oe	ccsbBroad304_00833	IFNG	Interferons
32	99.91	oe	ccsbBroad304_02889	WWTR1	Hippo Signaling
33	99.91	oe	ccsbBroad304_00832	IFNB1	Interferons
34	99.91	oe	ccsbBroad304_00259	CD40	Tumour necrosis factor (TNF) receptor family
35	99.91	oe	ccsbBroad304_05881	BCL2L2	Serine/threonine phosphatases / Protein phosphatase 1, regulatory subunits
36	99.91	oe	ccsbBroad304_05390	DUSP28	Protein tyrosine phosphatases / Class I Cys-based PTPs : Atypical dual specificity phosphatases
37	99.91	oe	ccsbBroad304_06021	KLF6	Kruppel-like transcription factors
38	99.91	oe	ccsbBroad304_00954	LYN	Src family
39	99.91	oe	ccsbBroad304_03926	SLC39A8	SLC39 family of metal ion transporters
40	99.89	cp	BRD-A52650764	ingenol	PKC activator
41	99.89	kd	CGS001-54472	TOLLIP	-
42	99.89	kd	CGS001-26472	PPP1R14B	Serine/threonine phosphatases / Protein phosphatase 1, regulatory subunits
43	99.89	kd	CGS001-6927	HNF1A	Homeoboxes / HNF class
44	99.87	kd	CGS001-79724	ZNF768	Zinc fingers, C2H2-type
45	99.87	kd	CGS001-6915	TBXA2R	GPCR / Class A : Prostanoid receptors
46	99.87	kd	CGS001-51588	PIAS4	Zinc fingers, MIZ-type
47	99.87	kd	CGS001-8974	P4HA2	-
48	99.87	kd	CGS001-283455	KSR2	RAF family
49	99.86	oe	ccsbBroad304_00880	IRF2	-
50	99.86	oe	ccsbBroad304_00771	HOXA5	Homeoboxes / ANTP class : HOXL subclass
51	99.86	oe	ccsbBroad304_06260	GATA3	GATA zinc finger domain containing
52	99.84	kd	CGS001-7106	TSPAN4	Tetraspanins
53	99.84	kd	CGS001-93487	MAPK1IP1L	-
54	99.84	kd	CGS001-10112	KIF20A	Kinesins
55	99.84	kd	CGS001-3784	KCNQ1	Voltage-gated potassium channels
56	99.84	kd	CGS001-182	JAG1	CD molecules

Rank	Score	Type (cp= compound, kd = knock-down, oe = over-expression, cc = cmap class)	ID	Name	Description
57	99.84	kd	CGS001-1440	CSF3	Endogenous ligands
58	99.82	cp	BRD-K91145395	prostratin	PKC activator
59	99.82	cp	BRD-K32744045	disulfiram	Aldehyde dehydrogenase inhibitor
60	99.82	kd	CGS001-7525	YES1	Src family
61	99.82	kd	CGS001-7849	PAX8	Paired boxes
62	99.82	kd	CGS001-1845	DUSP3	Protein tyrosine phosphatases / Class I Cys-based PTPs : Atypical dual specificity phosphatases
63	99.82	kd	CGS001-1154	CISH	SH2 domain containing
64	99.81	oe	ccsbBroad304_04728	TWIST2	Basic helix-loop-helix proteins
65	99.81	oe	ccsbBroad304_02048	BCL10	-
66	99.8	kd	CGS001-10196	PRMT3	Protein arginine N-methyltransferases
67	99.79	cp	BRD-A15079084	phorbol-12-myristate-13-acetate	PKC activator
68	99.79	kd	CGS001-7090	TLE3	WD repeat domain containing
69	99.79	kd	CGS001-21	ABCA3	ATP binding cassette transporters / subfamily A
70	99.78	cc		Ribonucleotide Reductase Inhibitor	-
71	99.78	kd	CGS001-23057	NMNAT2	-
72	99.77	oe	ccsbBroad304_03232	VPS28	-
73	99.76	kd	CGS001-115509	ZNF689	Zinc fingers, C2H2-type
74	99.76	kd	CGS001-9928	KIF14	Kinesins
75	99.76	kd	CGS001-3417	IDH1	-
76	99.75	cp	BRD-K88429204	pyrimethamine	Dihydrofolate reductase inhibitor
77	99.75	cp	BRD-K25504083	cytochalasin-d	Actin polymerization inhibitor
78	99.75	cp	BRD-K47983010	BX-795	IKK inhibitor
79	99.74	kd	CGS001-6909	TBX2	T-boxes
80	99.74	kd	CGS001-5577	PRKAR2B	Protein kinase A
81	99.73	kd	CGS001-5469	MED1	-
82	99.72	oe	ccsbBroad304_07680	NEK6	NIMA (never in mitosis gene a)- related kinase (NEK) family
83	99.72	cp	BRD-A15010982	HU-211	Glutamate receptor antagonist
84	99.72	cp	BRD-K33106058	cytarabine	Ribonucleotide reductase inhibitor
85	99.71	kd	CGS001-6857	SYT1	Synaptotagmins
86	99.71	kd	CGS001-4482	MSRA	-
87	99.71	kd	CGS001-8321	FZD1	GPCR / Class F : Frizzled receptors
88	99.71	kd	CGS001-124583	CANT1	-
89	99.71	kd	CGS001-8312	AXIN1	Serine/threonine phosphatases / Protein phosphatase 1, regulatory subunits
90	99.71	kd	CGS001-8874	ARHGEF7	Rho guanine nucleotide exchange factors
91	99.68	oe	ccsbBroad304_03556	SMU1	WD repeat domain containing
92	99.68	oe	ccsbBroad304_06557	MAOA	Catecholamine turnover
93	99.68	oe	ccsbBroad304_08282	ATP6V1D	ATPases / V-type
94	99.66	kd	CGS001-8738	CRADD	-
95	99.65	kd	CGS001-29890	RBM15B	RNA binding motif (RRM) containing
96	99.63	kd	CGS001-3397	ID1	Basic helix-loop-helix proteins

Rank	Score	Type (cp= compound, kd = knock-down, oe = over-expression, cc = cmap class)	ID	Name	Description
97	99.63	kd	CGS001-26036	ZNF451	Zinc fingers, C2H2-type
98	99.63	kd	CGS001-9375	TM9SF2	-
99	99.63	kd	CGS001-10287	RGS19	Regulators of G-protein signaling
100	99.63	kd	CGS001-374291	NDUFS7	Mitochondrial respiratory chain complex / Complex I
101	99.63	kd	CGS001-51001	MTERFD1	-
102	99.63	oe	ccsbBroad304_06542	LTBR	Tumor necrosis factor receptor superfamily
103	99.61	cp	BRD-A54632525	BRD-A54632525	-
104	99.61	kd	CGS001-5654	HTRA1	Serine peptidases / Serine peptidases
105	99.61	kd	CGS001-2673	GFPT1	-
106	99.6	kd	CGS001-11057	ABHD2	Abhydrolase domain containing
107	99.58	kd	CGS001-4835	NQO2	-
108	99.58	kd	CGS001-11329	STK38	NDR family
109	99.58	kd	CGS001-1666	DECR1	Short chain dehydrogenase/reductase superfamily / Classical SDR fold cluster 1
110	99.58	kd	CGS001-4299	AFF1	-
111	99.58	oe	ccsbBroad304_07137	WT1	Zinc fingers, C2H2-type
112	99.55	kd	CGS001-22949	PTGR1	-
113	99.55	kd	CGS001-2071	ERCC3	General transcription factors
114	99.55	kd	CGS001-10668	CGRRF1	RING-type (C3HC4) zinc fingers
115	99.55	kd	CGS001-348	APOE	Apolipoproteins
116	99.54	oe	ccsbBroad304_00282	CDKN1A	-
117	99.54	oe	ccsbBroad304_01010	MGST2	Glutathione S-transferases / Microsomal
118	99.51	cp	BRD-K77908580	entinostat	HDAC inhibitor
119	99.5	kd	CGS001-7371	UCK2	-
120	99.5	kd	CGS001-5198	PFAS	-
121	99.5	kd	CGS001-51005	AMDHD2	-
122	99.47	kd	CGS001-5188	PET112	-
123	99.47	kd	CGS001-25836	NIPBL	-
124	99.47	kd	CGS001-5891	MOK	RCK family
125	99.47	kd	CGS001-1994	ELAVL1	RNA binding motif (RRM) containing
126	99.45	oe	ccsbBroad304_04891	TMEM174	-
127	99.44	cp	BRD-K73610817	BRD-K73610817	-
128	99.44	cp	BRD-K65814004	diphenyleneiodonium	Nitric oxide synthase inhibitor
129	99.44	oe	ccsbBroad304_01388	RELB	NFkappaB transcription factor family
130	99.42	kd	CGS001-8996	NOL3	-
131	99.42	kd	CGS001-64223	MLST8	WD repeat domain containing
132	99.41	kd	CGS001-929	CD14	CD molecules
133	99.4	oe	ccsbBroad304_07306	TNFRSF10A	Tumour necrosis factor (TNF) receptor family
134	99.4	cp	BRD-K26818574	BIX-01294	Histone lysine methyltransferase inhibitor
135	99.4	cp	BRD-K92991072	PAC-1	Caspase activator
136	99.39	cc		ATPase Inhibitor	-
137	99.37	kd	CGS001-1955	MEGF9	-
138	99.37	cp	BRD-K93034159	cladribine	Adenosine deaminase inhibitor
139	99.34	kd	CGS001-2063	NR2F6	COUP-TF-like receptors
140	99.33	cp	BRD-K50841342	PAC-1	-

Rank	Score	Type (cp= compound, kd = knock-down, oe = over-expression, cc = cmap class)	ID	Name	Description
141	99.32	cc		BCL2 And Related Protein Inhibitor	-
142	99.32	kd	CGS001-54386	TERF2IP	-
143	99.32	kd	CGS001-1852	DUSP9	Protein tyrosine phosphatases / Class I Cys-based PTPs : MAP kinase phosphatases
144	99.32	kd	CGS001-1212	CLTB	-
145	99.32	kd	CGS001-9459	ARHGEF6	Rho guanine nucleotide exchange factors
146	99.31	oe	ccsbBroad304_08010	FBXO5	F-boxes / other
147	99.3	kd	CGS001-9643	MORF4L2	-
148	99.29	kd	CGS001-22827	PUF60	RNA binding motif (RRM) containing
149	99.29	kd	CGS001-1349	COX7B	Mitochondrial respiratory chain complex
150	99.26	kd	CGS001-79885	HDAC11	Histone deacetylases
151	99.26	kd	CGS001-4046	LSP1	-
152	99.25	kd	CGS001-3177	SLC29A2	SLC29 family
153	99.24	kd	CGS001-3326	HSP90AB1	Heat shock proteins / HSPC
154	99.23	kd	CGS001-1643	DDB2	WD repeat domain containing
155	99.22	kd	CGS001-8986	RPS6KA4	MSK subfamily
156	99.22	cp	BRD-K26664453	cytochalasin-b	Microtubule inhibitor
157	99.21	cc		Aldo Keto Reductase	-
158	99.21	oe	ccsbBroad304_01710	TRAF2	RING-type (C3HC4) zinc fingers
159	99.21	oe	ccsbBroad304_05941	CBR3	Short chain dehydrogenase/reductase superfamily / Classical SDR fold cluster 1
160	99.21	kd	CGS001-5096	PCCB	Carboxylases
161	99.21	oe	ccsbBroad304_06392	HOXB7	Homeoboxes / ANTP class : HOXL subclass
162	99.18	kd	CGS001-22955	SCMH1	Sterile alpha motif (SAM) domain containing
163	99.17	oe	ccsbBroad304_00773	HOXA9	Homeoboxes / ANTP class : HOXL subclass
164	99.17	kd	CGS001-3108	HLA-DMA	Immunoglobulin superfamily / C1-set domain containing
165	99.17	oe	ccsbBroad304_05098	MAGEB6	-
166	99.14	oe	ccsbBroad304_01686	TNFAIP3	OTU domain containing
167	99.13	kd	CGS001-7690	ZNF131	BTB/POZ domain containing
168	99.13	kd	CGS001-23011	RAB21	RAB, member RAS oncogene
169	99.13	kd	CGS001-5106	PCK2	-
170	99.13	kd	CGS001-85315	PAQR8	-
171	99.12	oe	ccsbBroad304_01858	FOSL1	basic leucine zipper proteins
172	99.12	cp	BRD-K23984367	sorafenib	-
173	99.12	cp	BRD-K72264770	QW-BI-011	Histone lysine methyltransferase inhibitor
174	99.11	kd	CGS001-11116	FGFR1OP	-
175	99.1	kd	CGS001-4804	NGFR	Tumour necrosis factor (TNF) receptor family
176	99.08	kd	CGS001-6676	SPAG4	-
177	99.08	kd	CGS001-63874	ABHD4	Abhydrolase domain containing
178	99.07	oe	ccsbBroad304_00389	CTBP1	-

Rank	Score	Type (cp= compound, kd = knock-down, oe = over-expression, cc = cmap class)	ID	Name	Description
179	99.05	kd	CGS001-7480	WNT10B	Wingless-type MMTV integration sites
180	99.05	kd	CGS001-80351	TNKS2	Ankyrin repeat domain containing
181	99.05	kd	CGS001-2264	FGFR4	Type V RTKs: FGF (fibroblast growth factor) receptor family
182	99.05	kd	CGS001-1725	DHPS	-
183	99.05	kd	CGS001-64170	CARD9	-
184	99.03	kd	CGS001-6259	RYK	Type XV RTKs: RYK
185	99.03	kd	CGS001-54566	EPB41L4B	-
186	99.02	kd	CGS001-308	ANXA5	Annexins
187	99.01	kd	CGS001-5257	PHKB	-
188	99	kd	CGS001-7764	ZNF217	Zinc fingers, C2H2-type
189	99	kd	CGS001-5451	POU2F1	Homeoboxes / POU class
190	98.98	cp	BRD-K30677119	PP-30	RAF inhibitor
191	98.98	kd	CGS001-23368	PPP1R13B	Ankyrin repeat domain containing
192	98.98	cp	BRD-A34208323	VU-0404997-2	Glutamate receptor modulator
193	98.97	kd	CGS001-4601	MXI1	Basic helix-loop-helix proteins
194	98.97	kd	CGS001-10247	HRSP12	-
195	98.95	kd	CGS001-8295	TRRAP	TRRAP subfamily
196	98.95	kd	CGS001-26064	RAI14	Ankyrin repeat domain containing
197	98.95	kd	CGS001-5710	PSMD4	Proteasome (prosome, macropain) subunits
198	98.95	kd	CGS001-3312	HSPA8	Heat shock proteins / HSP70
199	98.93	cp	BRD-K59456551	methotrexate	Dihydrofolate reductase inhibitor
200	98.93	kd	CGS001-10327	AKR1A1	Aldo-keto reductases

Table 17. Top 200 drugs that repress upregulated genes in the signature

Rank	Score	Type (cp= compound, kd = knock-down, oe = over-expression, cc = cmap class)	ID	Name	Description
8875	-99.95	kd	CGS001-10254	STAM2	-
8876	-99.95	kd	CGS001-5966	REL	NFkappaB transcription factor family
8877	-99.95	kd	CGS001-4609	MYC	Basic helix-loop-helix proteins
8878	-99.95	kd	CGS001-2079	ERH	-
8879	-99.95	kd	CGS001-2683	B4GALT1	Beta 4-glycosyltransferases
8880	-99.95	kd	CGS001-406	ARNTL	Basic helix-loop-helix proteins
8872	-99.92	cc		Aldo Keto Reductase	-
8873	-99.92	kd	CGS001-8644	AKR1C3	Prostaglandin synthases
8874	-99.92	kd	CGS001-2863	GPR39	GPCR / Class A : Orphans
8870	-99.91	oe	ccsbBroad304_03864	OVOL2	Zinc fingers, C2H2-type
8871	-99.91	oe	ccsbBroad304_08418	FBXL12	F-boxes / Leucine-rich repeats
8866	-99.89	kd	CGS001-114026	ZIM3	Zinc fingers, C2H2-type
8867	-99.89	kd	CGS001-51021	MRPS16	Mitochondrial ribosomal proteins / small subunits
8868	-99.89	kd	CGS001-3265	HRAS	RAS subfamily
8869	-99.89	kd	CGS001-1643	DDB2	WD repeat domain containing
8864	-99.88	kd	CGS001-6337	SCNN1A	Epithelial sodium channels (ENaC)

Rank	Score	Type (cp= compound, kd = knock-down, oe = over-expression, cc = cmap class)	ID	Name	Description
8865	-99.88	kd	CGS001-4191	MDH2	-
8861	-99.87	kd	CGS001-26137	ZBTB20	BTB/POZ domain containing
8862	-99.87	kd	CGS001-7227	TRPS1	GATA zinc finger domain containing
8863	-99.87	kd	CGS001-95	ACY1	-
8856	-99.86	oe	ccsbBroad304_00832	IFNB1	Interferons
8857	-99.86	oe	ccsbBroad304_05982	CDX2	Homeoboxes / ANTP class : HOXL subclass
8858	-99.86	oe	ccsbBroad304_06021	KLF6	Kruppel-like transcription factors
8859	-99.86	oe	ccsbBroad304_01249	PPARG	Peroxisome proliferator-activated receptors
8860	-99.86	oe	ccsbBroad304_00472	EBF1	-
8854	-99.84	kd	CGS001-7185	TRAF1	-
8855	-99.84	kd	CGS001-5562	PRKAA1	AMPK subfamily
8853	-99.83	kd	CGS001-7775	ZNF232	Zinc fingers, C2H2-type
8852	-99.82	kd	CGS001-10525	HYOU1	Heat shock proteins / HSP70
8851	-99.81	oe	ccsbBroad304_07363	AIFM1	-
8850	-99.79	cp	BRD-A81772229	simvastatin	HMGCR inhibitor
8847	-99.77	oe	ccsbBroad304_00747	HLF	-
8848	-99.77	oe	ccsbBroad304_00487	EGR1	Zinc fingers, C2H2-type
8849	-99.77	oe	ccsbBroad304_04271	MXD3	Basic helix-loop-helix proteins
8846	-99.76	kd	CGS001-5608	MAP2K6	MAPKK:STE7 family
8844	-99.75	cc		JAK Inhibitor	-
8845	-99.75	cp	BRD-K91290917	amodiaquine	Histamine receptor agonist
8843	-99.74	kd	CGS001-9296	ATP6V1F	ATPases / V-type
8841	-99.71	kd	CGS001-6389	SDHA	Mitochondrial respiratory chain complex
8842	-99.71	kd	CGS001-6275	S100A4	EF-hand domain containing
8839	-99.68	oe	ccsbBroad304_00833	IFNG	Interferons
8840	-99.68	oe	ccsbBroad304_07117	UGCG	Glycosyltransferase family 2 domain containing
8838	-99.67	kd	CGS001-8031	NCOA4	-
8836	-99.66	kd	CGS001-7167	TPI1	-
8837	-99.66	kd	CGS001-3419	IDH3A	-
8835	-99.63	kd	CGS001-5469	MED1	-
8830	-99.61	cp	BRD-K52850071	JAK3-Inhibitor-II	JAK inhibitor
8831	-99.61	cp	BRD-K49049886	CGS-15943	Adenosine receptor antagonist
8832	-99.61	kd	CGS001-115650	TNFRSF13C	Tumour necrosis factor (TNF) receptor family
8833	-99.61	kd	CGS001-6493	SIM2	Basic helix-loop-helix proteins
8834	-99.61	kd	CGS001-7803	PTP4A1	Protein tyrosine phosphatases / Class I Cys-based PTPs : PRLs
8829	-99.59	cc		Aurora Kinase Inhibitor Grp2	-
8825	-99.58	cp	BRD-K37691127	hinokitiol	Tyrosinase inhibitor
8826	-99.58	kd	CGS001-5170	PDPK1	PDK1 family
8827	-99.58	kd	CGS001-4199	ME1	-
8828	-99.58	kd	CGS001-51295	ECSIT	Mitochondrial respiratory chain

Rank	Score	Type (cp= compound, kd = knock-down, oe = over-expression, cc = cmap class)	ID	Name	Description
					complex assembly factors
8822	-99.55	kd	CGS001-51520	LARS	Aminoacyl tRNA synthetases / Class I
8823	-99.55	kd	CGS001-2538	G6PC	-
8824	-99.55	kd	CGS001-2059	EPS8	-
8819	-99.54	cp	BRD-K58299615	RO-90-7501	Beta amyloid inhibitor
8820	-99.54	kd	CGS001-3485	IGFBP2	insulin-like growth factor (IGF) binding proteins
8821	-99.54	cp	BRD-K85606544	neratinib	EGFR inhibitor
8813	-99.53	kd	CGS001-54472	TOLLIP	-
8814	-99.53	kd	CGS001-4998	ORC1	ATPases / AAA-type
8815	-99.53	kd	CGS001-9020	MAP3K14	MAPKKK:STE-unique family
8816	-99.53	kd	CGS001-355	FAS	Tumour necrosis factor (TNF) receptor family
8817	-99.53	kd	CGS001-10327	AKR1A1	Aldo-keto reductases
8818	-99.53	kd	CGS001-178	AGL	-
8812	-99.52	cc		HOX Gene	-
8810	-99.51	cp	BRD-A19633847	perhexiline	Carnitine palmitoyltransferase inhibitor
8811	-99.51	cp	BRD-K47105409	AG-490	-
8809	-99.49	oe	ccsbBroad304_00706	GTF2B	General transcription factors
8806	-99.47	oe	ccsbBroad304_05980	CDKN1B	-
8807	-99.47	kd	CGS001-8226	HDHD1	-
8808	-99.47	kd	CGS001-5045	FURIN	Subtilisin
8805	-99.45	oe	ccsbBroad304_00772	HOXA6	Homeoboxes / ANTP class : HOXL subclass
8804	-99.44	kd	CGS001-3309	HSPA5	Heat shock proteins / HSP70
8803	-99.43	oe	ccsbBroad304_00838	IGFBP5	insulin-like growth factor (IGF) binding proteins
8802	-99.4	cp	BRD-K92991072	PAC-1	Caspase activator
8801	-99.39	kd	CGS001-35	ACADS	-
8800	-99.38	kd	CGS001-3122	HLA-DRA	Immunoglobulin superfamily / C1-set domain containing
8799	-99.37	cp	BRD-K66296774	fluvastatin	HMGCR inhibitor
8798	-99.36	kd	CGS001-7525	YES1	Src family
8797	-99.35	kd	CGS001-57178	ZMIZ1	Zinc fingers, MIZ-type
8795	-99.34	kd	CGS001-3635	INPP5D	Inositol polyphosphate phosphatases
8796	-99.34	kd	CGS001-3416	IDE	Pitrilysin
8794	-99.33	cp	BRD-K07881437	danusertib	Aurora kinase inhibitor
8793	-99.32	cp	BRD-A50675702	fipronil	GABA gated chloride channel blocker
8792	-99.29	kd	CGS001-998	CDC42	-
8791	-99.28	cc		PI3K Inhibitor	-
8787	-99.26	cc		DNA-dependent Protein Kinase	-
8788	-99.26	cp	BRD-K94441233	mevastatin	HMGCR inhibitor
8789	-99.26	oe	ccsbBroad304_02571	TOMM34	Tetratricopeptide (TTC) repeat domain containing
8790	-99.26	oe	ccsbBroad304_01579	SOX2	SRY (sex determining region Y)-boxes
8784	-99.24	kd	CGS001-5682	PSMA1	Proteasome subunits
8785	-99.24	kd	CGS001-53347	UBASH3A	-
8786	-99.24	kd	CGS001-2782	GNB1	WD repeat domain containing
8782	-99.23	oe	ccsbBroad304_1127	HAT1	Histone

Rank	Score	Type (cp= compound, kd = knock-down, oe = over-expression, cc = cmap class)	ID	Name	Description
			7		acetyltransferases (HATs)
8783	-99.23	kd	CGS001-4323	MMP14	Matrix metallopeptidase
8780	-99.2	kd	CGS001-79142	PHF23	Zinc fingers, PHD-type
8781	-99.2	kd	CGS001-2664	GDI1	-
8778	-99.19	cp	BRD-K48974000	BRD-K48974000	-
8779	-99.19	kd	CGS001-4817	NIT1	-
8777	-99.18	kd	CGS001-7126	TNFAIP1	BTB/POZ domain containing
8775	-99.17	kd	CGS001-10497	UNC13B	-
8776	-99.17	kd	CGS001-57448	BIRC6	Inhibitors of apoptosis (IAP) protein family
8772	-99.15	cp	BRD-K13514097	everolimus	MTOR inhibitor
8773	-99.15	cp	BRD-K59331372	SB-366791	TRPV antagonist
8774	-99.15	cp	BRD-K78373679	RO-3306	CDK inhibitor
8770	-99.13	oe	ccsbBroad304_02451	HOXB13	Homeoboxes / ANTP class : HOXL subclass
8771	-99.13	kd	CGS001-7405	UVRAG	-
8769	-99.12	cp	BRD-K06217810	BRD-K06217810	-
8768	-99.11	cc		HMGCR Inhibitor	-
8765	-99.08	kd	CGS001-55781	RIOK2	RIO2 subfamily
8766	-99.08	kd	CGS001-7026	NR2F2	COUP-TF-like receptors
8767	-99.08	kd	CGS001-7994	KAT6A	Histone acetyltransferases (HATs)
8762	-99.07	oe	ccsbBroad304_06131	DUSP6	Protein tyrosine phosphatases / Class I Cys-based PTPs : MAP kinase phosphatases
8763	-99.07	kd	CGS001-4916	NTRK3	Type VII RTKs: Neurotrophin receptor/Trk family
8764	-99.07	oe	ccsbBroad304_06394	HOXC9	Homeoboxes / ANTP class : HOXL subclass
8761	-99.06	cp	BRD-K60623809	SU-11652	Tyrosine kinase inhibitor
8758	-99.03	oe	ccsbBroad304_03574	FBXW7	F-boxes / WD-40 domains
8759	-99.03	kd	CGS001-6772	STAT1	SH2 domain containing
8760	-99.03	kd	CGS001-6768	ST14	Serine peptidases / Transmembrane
8757	-99.02	kd	CGS001-64170	CARD9	-
8753	-98.98	oe	ccsbBroad304_02048	BCL10	-
8754	-98.98	cp	BRD-K50836978	purvalanol-a	CDK inhibitor
8755	-98.98	kd	CGS001-9601	PDIA4	Protein disulfide isomerases
8756	-98.98	cp	BRD-K46056750	AZD-7762	CHK inhibitor
8751	-98.97	kd	CGS001-1936	EEF1D	-
8752	-98.97	kd	CGS001-8192	CLPP	ATPases / AAA-type
8750	-98.96	kd	CGS001-5211	PFKL	-
8749	-98.95	kd	CGS001-23476	BRD4	Bromodomain kinase (BRDK) family
8746	-98.94	cp	BRD-K97399794	quercetin	Polar auxin transport inhibitor
8747	-98.94	oe	ccsbBroad304_10487	BPHL	-
8748	-98.94	cp	BRD-K64890080	BI-2536	PLK inhibitor
8745	-98.93	kd	CGS001-3927	LASP1	-
8742	-98.92	kd	CGS001-7541	ZFP161	-
8743	-98.92	kd	CGS001-56993	TOMM22	-
8744	-98.92	kd	CGS001-1326	MAP3K8	MAPKKK:STE-unique family
8739	-98.91	kd	CGS001-55038	CDCA4	-
8740	-98.91	kd	CGS001-7840	ALMS1	-
8741	-98.91	cp	BRD-A31159102	fluoxetine	Selective serotonin reuptake inhibitor (SSRI)

Rank	Score	Type (cp= compound, kd = knock-down, oe = over-expression, cc = cmap class)	ID	Name	Description
8736	-98.89	cc		MTOR Inhibitor	-
8737	-98.89	cc		IGF1R Inhibitor	-
8738	-98.89	oe	ccsbBroad304_01545	SLC3A2	SLC3 family
8735	-98.88	cp	BRD-A75769826	SDM25N	Opioid receptor antagonist
8733	-98.87	cc		EGFR Inhibitor	-
8734	-98.87	cp	BRD-K64881305	ispinesib	Kinesin-like spindle protein inhibitor
8731	-98.8	oe	ccsbBroad304_00100	RHOA	-
8732	-98.8	cp	BRD-K05350981	oligomycin-c	ATPase inhibitor
8730	-98.79	kd	CGS001-949	SCARB1	-
8729	-98.78	kd	CGS001-2114	ETS2	ETS Transcription Factors
8728	-98.77	cp	BRD-K73610817	BRD-K73610817	-
8725	-98.74	kd	CGS001-166793	ZBTB49	BTB/POZ domain containing
8726	-98.74	kd	CGS001-55176	SEC61A2	-
8727	-98.74	kd	CGS001-8313	AXIN2	-
8723	-98.73	cp	BRD-A81177136	KN-62	Calcium-calmodulin dependent protein kinase inhibitor
8724	-98.73	kd	CGS001-8792	TNFRSF11A	Tumour necrosis factor (TNF) receptor family
8722	-98.72	kd	CGS001-10600	USP16	Ubiquitin-specific peptidases
8720	-98.71	kd	CGS001-117289	TAGAP	Rho GTPase activating proteins
8721	-98.71	kd	CGS001-11230	PRAF2	-
8717	-98.7	oe	ccsbBroad304_06257	GATA2	GATA zinc finger domain containing
8718	-98.7	cp	BRD-K55070890	thiothixene	-
8719	-98.7	cp	BRD-K09499853	KU-0060648	DNA dependent protein kinase inhibitor
8715	-98.69	kd	CGS001-6777	STAT5B	SH2 domain containing
8716	-98.69	kd	CGS001-5184	PEPD	Methionyl aminopeptidase
8710	-98.66	oe	ccsbBroad304_06639	NFYB	-
8711	-98.66	cp	BRD-K68065987	MK-2206	AKT inhibitor
8712	-98.66	kd	CGS001-55872	PBK	TOPK family
8713	-98.66	kd	CGS001-1482	NKX2-5	Homeoboxes / ANTP class : NKL subclass
8714	-98.66	oe	ccsbBroad304_06393	HOXC4	Homeoboxes / ANTP class : HOXL subclass
8709	-98.62	cc		NFKB Pathway Inhibitor	-
8705	-98.61	kd	CGS001-6256	RXRA	Retinoid X receptors
8706	-98.61	kd	CGS001-8833	GMPS	-
8707	-98.61	kd	CGS001-2021	ENDOG	-
8708	-98.61	oe	ccsbBroad304_01291	MAP2K6	MAPKK:STE7 family
8703	-98.6	oe	ccsbBroad304_11796	ULK3	Unc-51-like kinase (ULK) family
8704	-98.6	kd	CGS001-5524	PPP2R4	Serine/threonine phosphatases / Protein phosphatase 2, regulatory subunits
8702	-98.59	kd	CGS001-27	ABL2	Abl family
8701	-98.58	kd	CGS001-54623	PAF1	-
8699	-98.57	kd	CGS001-11105	PRDM7	Zinc fingers, C2H2-type
8700	-98.57	oe	ccsbBroad304_08681	ADCK3	ABC1-B subfamily
8697	-98.52	kd	CGS001-5777	PTPN6	Protein tyrosine phosphatases

Rank	Score	Type (cp= compound, kd = knock-down, oe = over-expression, cc = cmap class)	ID	Name	Description
8698	-98.52	cp	BRD-K02130563	panobinostat	HDAC inhibitor
8696	-98.51	kd	CGS001-4223	MEOX2	Homeoboxes / ANTP class : HOXL subclass
8694	-98.5	oe	ccsbBroad304_00498	ELK1	ETS Transcription Factors
8695	-98.5	kd	CGS001-47	ACLY	-
8693	-98.48	kd	CGS001-5434	POLR2E	RNA polymerase subunits
8692	-98.47	kd	CGS001-4351	MPI	-
8691	-98.45	kd	CGS001-5710	PSMD4	Proteasome (prosome, macropain) subunits
8687	-98.43	cc		HSP90 Inhibitor	-
8688	-98.43	kd	CGS001-6259	RYK	Type XV RTKs: RYK
8689	-98.43	oe	ccsbBroad304_08879	CASD1	-
8690	-98.43	oe	ccsbBroad304_00283	CDKN2C	Ankyrin repeat domain containing
8686	-98.42	kd	CGS001-29957	SLC25A24	Mitochondrial nucleotide transporter subfamily
8683	-98.41	kd	CGS001-3312	HSPA8	Heat shock proteins / HSP70
8684	-98.41	cp	BRD-K36740062	GSK-1070916	Aurora kinase inhibitor
8685	-98.41	cp	BRD-K98548675	parthenolide	NFkB pathway inhibitor
8681	-98.39	kd	CGS001-527	ATP6V0C	ATPases / V-type
8682	-98.39	kd	CGS001-513	ATP5D	ATPases / F-type
8678	-98.38	oe	ccsbBroad304_02864	PRDX5	-
8679	-98.38	oe	ccsbBroad304_00817	IDH2	-
8680	-98.38	oe	ccsbBroad304_03232	VPS28	-
8677	-98.37	kd	CGS001-481	ATP1B1	ATPases / P-type
8676	-98.35	kd	CGS001-3113	HLA-DPA1	Immunoglobulin superfamily / C1-set domain containing
8672	-98.34	cp	BRD-K06147391	telenzepine	Acetylcholine receptor antagonist
8673	-98.34	cp	BRD-K78122587	NNC-55-0396	T-type calcium channel blocker
8674	-98.34	cp	BRD-K14618467	IKK-16	IKK inhibitor
8675	-98.34	kd	CGS001-26574	AATF	-

[0455] Applicants can also identify novel immunotherapy targets by looking for genes which are co-regulated with the immune-checkpoints (PDCD1, TIGIT, HAVCR2, LAG3, CTLA4) in CD4 and CD8 T-cells. For example, Applicants found CD27, an immune checkpoint and the target of an experimental cancer treatment (Varlilumab). The results of this analysis are for the top 200 genes summarized in Table 18.

Table 18. Top 200 genes that are co-regulated with immune-checkpoints

	CD8.R	CD8.P	CD4.R	CD4.P
PDCD1	0.66	1.59E-215	0.60	1.03E-119
CTLA4	0.63	4.88E-193	0.65	2.60E-145
TIGIT	0.63	1.11E-191	0.73	8.03E-204
HAVCR2	0.62	1.39E-183	0.32	7.85E-30
LAG3	0.55	7.66E-136		
LYST	0.42	5.22E-76	0.26	1.67E-20
CD8A	0.40	3.93E-66	-0.08	0.007523193
TNFRSF9	0.39	1.13E-64	0.09	0.001435974
CD27	0.39	6.38E-64	0.22	3.99E-15

FAM3C	0.34	1.47E-48		
CXCL13	0.34	1.47E-47	0.27	2.41E-21
SP47	0.33	1.43E-46	0.11	0.000202982
CBLB	0.33	7.16E-46	0.20	1.64E-12
SNX9	0.33	1.35E-45	0.11	6.89E-05
SIRPG	0.33	5.21E-45	0.33	2.62E-31
TNFRSF1B	0.33	1.09E-44	0.22	3.31E-15
FCRL3	0.32	1.36E-41	0.26	9.32E-20
VCAM1	0.31	3.44E-41		
DGKH	0.31	1.67E-39		
PRDM1	0.30	3.07E-38	0.20	2.24E-12
IGFLR1	0.30	6.12E-38	0.21	7.66E-14
ETV1	0.30	1.03E-37		
RGS1	0.30	4.15E-37	0.30	3.35E-27
WARS	0.30	1.32E-36	0.14	4.98E-07
MYO7A	0.30	3.10E-36		
ITM2A	0.29	2.65E-35	0.31	1.30E-27
GBP2	0.29	1.24E-34	0.21	3.93E-13
ENTPD1	0.28	1.21E-33	0.12	4.17E-05
TOX	0.28	2.39E-32	0.44	2.27E-58
DUSP4	0.28	2.48E-32	0.36	1.94E-38
TP53INP1	0.28	7.24E-32	0.23	2.04E-16
GAPDH	0.28	1.57E-31	0.36	1.21E-37
DFNB31	0.27	6.10E-31		
ATHL1	0.27	1.19E-30	0.01	0.71761873
TRAF5	0.27	2.83E-30	0.10	0.000897484
CLEC2D	0.27	5.88E-30	-0.02	0.535704689
SLA	0.26	6.03E-29	0.20	1.37E-12
CCL3	0.26	1.26E-28	0.04	0.161249379
IL6ST	0.26	2.25E-28	0.02	0.440674275
PCED1B	0.26	3.01E-28	0.21	3.65E-13
RAB27A	0.26	3.09E-28	0.13	6.49E-06
CD7	0.26	3.23E-28	0.06	0.049851187
ICOS	0.25	3.99E-27	0.31	2.87E-28
FUT8	0.25	1.41E-26	0.10	0.000314275
RNF19A	0.25	4.44E-26	0.29	1.51E-24
TBC1D4	0.25	1.16E-25	0.31	6.28E-29
FABP5	0.25	1.63E-25	0.18	2.19E-10
B1	0.24	3.89E-24	0.24	9.16E-18
TTN	0.24	6.97E-24		
SRGN	0.24	9.35E-24	0.36	1.61E-37
SARDH	0.24	2.50E-23	0.19	3.48E-11
IFNG	0.24	3.00E-23	0.14	4.84E-07
INPP5F	0.23	3.38E-23	0.14	4.75E-07
RGS2	0.23	4.50E-23	0.18	7.21E-10
CD38	0.23	5.61E-23	0.15	1.54E-07
ID3	0.23	1.34E-22	0.05	0.066457964
PHLDA1	0.23	1.35E-22	0.11	0.000184209
TIMD4	0.23	3.53E-22		
PAM	0.23	3.69E-22	0.28	2.82E-23
PTMS	0.23	1.99E-21		
CXCR6	0.22	6.84E-21	0.26	6.42E-20
LBH	0.22	1.48E-20	0.18	3.85E-10
PRF1	0.22	1.90E-20	0.09	0.001065922
ASB2	0.22	1.90E-20	0.29	8.22E-25
KIR2DL4	0.22	2.29E-20		
STAT3	0.22	4.75E-20	0.05	0.063080818
GLDC	0.22	5.92E-20		
MIR155HG	0.22	8.11E-20	0.15	9.54E-08
CD8B	0.22	1.10E-19	-0.14	2.30E-06
CD200	0.22	1.25E-19	0.25	1.49E-18
CD2BP2	0.21	1.79E-19	0.17	5.47E-09
CD84	0.21	2.59E-19	0.11	0.000105368
CD2	0.21	3.46E-19	0.32	5.24E-31
UBE2F	0.21	3.72E-19	0.06	0.035820564
TNS3	0.21	6.38E-19		
ATXN1	0.21	1.35E-18		
HNRPLL	0.21	1.51E-18	0.26	1.96E-20

FKBP1A	0.21	2.34E-18	0.19	2.16E-11
GALM	0.21	2.95E-18	0.19	3.98E-11
TOX2	0.20	6.98E-18	0.35	2.14E-35
AFAP1L2	0.20	1.90E-17		
GEM	0.20	2.64E-17	0.16	5.19E-08
HSPB1	0.20	2.75E-17	0.09	0.002636939
CCL3L3	0.20	3.71E-17		
CADM1	0.20	3.76E-17		
GFOD1	0.20	3.88E-17		
SH2D2A	0.20	3.90E-17	0.13	6.62E-06
PKM	0.20	4.16E-17	0.26	1.71E-19
HAPLN3	0.20	9.31E-17	-0.02	0.483961847
MTSS1	0.20	1.03E-16		
ZNF79	0.20	1.79E-16	0.03	0.275651913
EID1	0.19	2.53E-16	0.09	0.003034835
ZBED2	0.19	2.96E-16	0.14	1.69E-06
PTPN6	0.19	1.31E-15	0.04	0.210702886
HMOX1	0.19	1.51E-15		
SAMSN1	0.19	1.97E-15	0.10	0.00025252
SIT1	0.19	2.34E-15	0.08	0.007781849
CCDC64	0.19	2.65E-15	0.09	0.000993524
PTPN7	0.19	4.49E-15	0.25	3.66E-18
NDFIP2	0.19	6.66E-15	0.17	6.39E-09
CD74	0.19	7.63E-15	0.28	1.23E-22
CREM	0.18	1.94E-14	0.05	0.106041668
IRF4	0.18	1.98E-14	0.16	4.09E-08
ARNT	0.18	2.23E-14	0.10	0.000571869
TRPS1	0.18	2.93E-14		
ZC3H7A	0.18	3.28E-14	0.14	1.33E-06
RHOB	0.18	3.58E-14		
ASXL2	0.18	3.99E-14		
ITGA4	0.18	4.04E-14	0.08	0.008613713
CCL4L2	0.18	5.53E-14	0.11	0.000238679
CCL4L1	0.18	5.69E-14	0.11	0.000238679
IGF2R	0.18	1.06E-13		
SOD1	0.18	1.26E-13	0.18	4.99E-10
SYNGR2	0.18	1.31E-13	0.11	0.00010303
PDE3B	0.18	1.38E-13	-0.11	0.000178183
IFI16	0.18	1.43E-13	0.20	5.81E-12
PDE7B	0.18	1.46E-13		
SLC2A8	0.18	1.59E-13		
FYN	0.17	2.58E-13	0.23	2.55E-16
ARID5B	0.17	4.06E-13	0.22	2.72E-15
NFATC1	0.17	4.72E-13	0.10	0.000521207
TPI1	0.17	4.96E-13	0.17	2.07E-09
DTHD1	0.17	6.29E-13		
CD3E	0.17	7.13E-13	0.03	0.271016862
CRIM1	0.17	7.24E-13		
TMEM155	0.17	1.02E-12		
INPP4B	0.17	1.66E-12	-0.06	0.035577188
OSBPL3	0.17	1.74E-12	0.16	4.35E-08
LIMS1	0.17	1.76E-12	0.17	1.29E-09
KCNK5	0.17	1.76E-12		
KLRC2	0.17	2.17E-12		
RGS4	0.17	3.04E-12		
ACP5	0.17	3.13E-12	0.19	5.03E-11
DENND2D	0.17	3.30E-12	0.01	0.631199717
FAIM3	0.17	3.53E-12	0.04	0.189542882
DDX3Y	0.17	4.25E-12	0.00	0.907797482
HLA-H	0.16	4.66E-12	0.21	1.54E-13
GPR56	0.16	5.64E-12	0.11	6.30E-05
MAF	0.16	5.82E-12	0.36	2.14E-38
TRIM69	0.16	7.34E-12		
SEMA4A	0.16	9.52E-12		
IL2RG	0.16	1.04E-11	0.18	6.51E-10
TMEM140	0.16	1.11E-11	0.09	0.00163736
GMDS	0.16	1.18E-11	0.08	0.008326449
LITAF	0.16	1.19E-11	-0.05	0.063294972

HSPA1A	0.16	1.56E-11	0.11	0.000172577
PAPOLA	0.16	1.56E-11	-0.01	0.70579933
AHI1	0.16	2.36E-11	0.16	9.85E-09
EZR	0.16	2.40E-11	0.14	1.92E-06
MIS18BP1	0.16	2.58E-11	0.17	6.15E-09
HLA-A	0.16	2.74E-11	0.32	9.78E-31
PSTPIP1	0.16	3.27E-11	0.11	9.40E-05
GBP5	0.16	3.71E-11	0.13	5.66E-06
RIN3	0.16	3.77E-11		
HIF1A	0.16	3.97E-11	0.06	0.048813828
HLA-DRB6	0.16	4.67E-11		
PAG1	0.16	5.87E-11	-0.08	0.003384546
AKAP5	0.16	6.76E-11		
KLRC3	0.16	6.90E-11		
RFX5	0.16	8.25E-11	0.07	0.014179979
UBB	0.15	8.74E-11	0.13	5.13E-06
TXNDC11	0.15	9.85E-11	0.14	1.74E-06
FOXN2	0.15	1.00E-10	0.05	0.082411107
DUSP16	0.15	1.15E-10	0.13	1.07E-05
CD82	0.15	1.38E-10	0.18	1.30E-10
PELI1	0.15	1.40E-10	0.20	6.92E-13
AMIGO2	0.15	2.03E-10		
CCDC141	0.15	2.42E-10	0.06	0.036155173
TNIP3	0.15	2.63E-10	0.10	0.000563452
SAT1	0.15	2.71E-10	0.26	2.07E-20
LRBA	0.15	3.00E-10	0.12	2.66E-05
HLA-DMA	0.15	3.36E-10	0.20	2.02E-12
MAPRE2	0.15	3.48E-10	0.10	0.000867905
BIRC3	0.15	3.71E-10	-0.01	0.720398325
EPSTI1	0.15	4.13E-10	0.18	5.86E-10
NCALD	0.15	4.21E-10	0.22	5.12E-15
ID2	0.15	4.32E-10	-0.04	0.201480439
NFAT5	0.15	4.95E-10	0.14	5.55E-07
GOLIM4	0.15	6.33E-10		
ZBTB32	0.15	6.70E-10		
NDUFB3	0.15	6.70E-10	0.13	3.74E-06
CALM3	0.15	7.24E-10	0.22	2.32E-14
SHFM1	0.15	8.32E-10	0.09	0.000949937
HLA-DRB5	0.15	9.22E-10	0.17	1.46E-09
C21orf91	0.15	9.87E-10	0.07	0.011223721
CCND2	0.15	1.09E-09	0.02	0.530718461
BTLA	0.14	1.29E-09	0.16	1.30E-08
PRKCH	0.14	1.31E-09	0.12	3.11E-05
GALNT2	0.14	1.53E-09		
IKZF3	0.14	1.77E-09	0.12	3.13E-05
AMICA1	0.14	2.14E-09	-0.06	0.026070815
STAT1	0.14	2.64E-09	0.05	0.064028082
IRF8	0.14	2.81E-09		
ELF1	0.14	2.91E-09	0.02	0.548742854
CD3D	0.14	2.93E-09	0.16	5.77E-08
RBPJ	0.14	3.26E-09	0.12	2.32E-05
BATF	0.14	3.46E-09	0.34	3.15E-33
LRRC8D	0.14	3.57E-09	0.07	0.014705554
PMF1	0.14	3.60E-09	0.10	0.000379898
TNFSF4	0.14	4.01E-09		

Example 4 – Tumor microenvironment analysis in melanoma tumors

[0456] T cells were also analyzed and the T cells contributed to the predicative value of the signature of the present invention (**Figure 30**).

[0457] The novel microenvironment cell-type signatures were very much associated with survival in both immunotherapy treated patients, and in general. The genes which are

up/down regulated in the immune cells after immunotherapy (CD4 T-cells, CD8 T-cells, B cells, and macrophages) are shown in Table 19.

Table 19. All Cell Type Signatures

B cells	Macrophage	Malignant		T cells cd4	T cells cd8
ADAM19	AIF1	ACOT7	MFGE8	AIM1	APOBEC3G
AKAP2	ALDH2	ACSL3	MFI2	ANK3	CBLB
BACH2	ANPEP	ACTN1	MGST3	AQP3	CCL4
BANK1	C15orf48	ADAM15	MIA	CAMK4	CCL4L1
BCL11A	C1orf162	ADI1	MIF	CCR4	CCL4L2
BLK	C1QA	AEBP1	MITF	CCR8	CCL5
CD19	C1QB	AGPAT1	MLANA	CD28	CD27
CD1C	C1QC	AGRN	MLPH	CD40LG	CD8A
CD22	C3AR1	AHCY	MMP14	DGKA	CD8B
CD79A	CCR1	AIF1L	MORF4L2	EML4	CST7
CD79B	CD14	AKAP12	MORN2	FAAH2	CTSW
CLEC17A	CD163	AKT3	MPZL1	FBLN7	CXCL13
CNR2	CD300A	ANXA5	MRPL24	FKBP5	CXCR6
COL19A1	CD300C	APOA1BP	MT2A	FLT3LG	DTHD1
COL4A3	CD300LF	APOD	MTUS1	FOXP3	DUSP2
CPNE5	CD33	APOE	MXI1	FXYD5	EOMES
CR2	CD86	ARL2	MYH10	IL6R	FASLG
CXCR5	CFP	ARNT2	MYO10	IL7R	FCRL3
EBF1	CLEC10A	ARPC1A	MYO1D	ITGB2-AS1	GBP5
ELK2AP	CLEC12A	ASPH	NAV2	JUNB	GZMA
FAM129C	CLEC4A	ATP1A1	NCKAP1	KLRB1	GZMB
FAM177B	CLEC5A	ATP1B1	NDST1	LEPROTL1	GZMH
FCER2	CMKLR1	ATP6V0A1	NENF	LOC100128420	GZMK
FCRL1	CSF1R	B3GNT1	NES	MAL	HCST
FCRL2	CSF2RB	BACE2	NGFRAP1	OXNAD1	HLA-A
FCRL5	CSF3R	BAIAP2	NGRN	PBXIP1	HLA-B
FCRLA	CSTA	BCAN	NHSL1	PIK3IP1	HLA-H
HLA-DOB	CXCL9	BIRC7	NID1	PIM2	ID2
IGJ	CXCR2P1	BTBD3	NME1	PRKCQ-AS1	IFNG
IGLL1	DSC2	C11orf24	NME2	RORA	IL2RB
IGLL3P	FAM26F	C17orf89	NME4	RPL35A	KLRC3
IGLL5	FBP1	C1orf198	NRP2	RPL4	KLRC4
KIAA0125	FCER1G	C1orf21	NRSN2	RPL6	KLRC4-KLRK1
KIAA0226L	FCGR1A	C1orf85	NSG1	RPS15A	KLRD1
LOC283663	FCGR1B	CALD1	OSBPL1A	RPS27	KLRK1
MS4A1	FCGR1C	CALU	P4HA2	RPS28	LAG3
P2RX5	FCGR3A	CAPN3	PACSIN2	SEPT6	LSP1
PAX5	FCGR3B	CAV1	PAX3	SLAMF1	LYST
PNOC	FCN1	CBR1	PCDHGC3	SORL1	NKG7
POU2AF1	FOLR2	CCND1	PEG10	SPOCK2	PDCD1
POU2F2	FPR1	CCT3	PFDN2	SUSD3	PRF1
RASGRP3	FPR2	CD151	PFKM	TCF7	PSTPIP1
SEL1L3	FPR3	CD276	PFN2	TMEM66	PYHIN1
SNX29P1	GGTA1P	CD59	PGRMC1	TNFRSF18	RARRES3
ST6GAL1	GNA15	CD63	PHB	TNFRSF25	SH2D1A
STAP1	GPR84	CD9	PHLDB1	TNFRSF4	SH2D2A
SWAP70	HCK	CDC42BPA	PIR	TNFSF8	TARP
TCL1A	HK3	CDC42EP4	PKNOX2	TRABD2A	TIGIT
TMEM154	IGSF6	CDH19	PLEKHB1	TSC22D3	TNFRSF9
VPREB3	IL1B	CDK2	PLK2	TXK	TOX
	IL1RN	CDK2AP1	PLOD1		
	IL4I1	CECR7	PLOD3		
	ITGAM	CELSR2	PLP1		
	KYNU	CERCAM	PLS3		
	LGALS2	CERS2	PLXNA1		
	LILRA1	CHCHD6	PLXNB3		
	LILRA2	CHL1	PMEL		
	LILRA3	CHPF	PMP22		
	LILRA4	CLDN12	POLR2F		
	LILRB2	CLIC4	POLR2L		
	LILRB4	CNIH4	PON2		

B cells	Macrophage	Malignant		T cells cd4	T cells cd8
	LILRB5	CNN3	PPT2		
	LST1	CNP	PRAME		
	MAFB	CNPY2	PRDX4		
	MARCO	COA3	PRDX6		
	MNDA	COL16A1	PRKCDBP		
	MRC1	COMT	PROS1		
	MS4A4A	CRIP2	PRSS23		
	MS4A6A	CRNDE	PSMB5		
	MSR1	CRTAP	PTGFRN		
	NCF2	CRYAB	PTGR1		
	OLR1	CSAG1	PTK2		
	P2RY13	CSAG3	PTPLAD1		
	PILRA	CSPG4	PTPRM		
	PLAU	CSRP1	PTPRS		
	PLBD1	CTDSPL	PTRH2		
	PLXDC2	CTHRC1	PTTG1IP		
	PRAM1	CTNNAL1	PYCR1		
	RAB20	CTNNB1	PYGB		
	RAB31	CTSF	PYGL		
	RASSF4	CTSK	QDPR		
	RBM47	CTTN	QPCT		
	RGS18	CYB5R1	RAB13		
	S100A8	CYP27A1	RAB17		
	S100A9	CYSTM1	RAB34		
	SECTM1	CYTH3	RAB38		
	SIGLEC1	DAAM2	RAI14		
	SIGLEC7	DCBLD2	RBFOX2		
	SIGLEC9	DCT	RCAN1		
	SLAMF8	DDR1	RCN1		
	SLC31A2	DDR2	RCN2		
	SLC43A2	DIP2C	RDX		
	SLC7A7	DLC1	RGS20		
	SLC8A1	DNAH14	RND3		
	SLCO2B1	DOCK7	ROBO1		
	SPI1	DST	ROPN1		
	STAB1	DSTN	ROPN1B		
	TBXAS1	DUSP6	RTKN		
	TFEC	ECM1	S100A1		
	TGFBI	EDNRB	S100A13		
	TLR2	EFNA5	S100A16		
	TLR4	EIF4EBP1	S100B		
	TLR8	EMP1	SCARB1		
	TMEM176A	ENTPD6	SCCPDH		
	TMEM176B	EPS8	SCD		
	TNFSF13	ERBB3	SDC3		
	TNFSF13B	ETV4	SDC4		
	TREM2	ETV5	SDCBP		
	TYROBP	EVA1A	SELENBP1		
	VSIG4	EXOSC4	SEMA3B		
	ZNF385A	FAM127A	SEMA3C		
		FAM127B	SEMA6A		
		FAM167B	SEPT10		
		FARP1	SERPINA3		
		FARP2	SERPINE2		
		FASN	SERPINH1		
		FKBP10	SGCD		
		FKBP4	SGCE		
		FKBP9	SHC1		
		FN1	SHC4		
		FNBP1L	SLC19A2		
		FRMD6	SLC24A5		
		FSTL1	SLC25A13		
		FXYD3	SLC25A4		
		G6PC3	SLC35B2		
		GALE	SLC39A1		
		GCSH	SLC39A6		
		GDF15	SLC45A2		

B cells	Macrophage	Malignant		T cells cd4	T cells cd8
		GJB1	SLC6A15		
		GLI3	SLC7A8		
		GNG12	SMARCA1		
		GOLM1	SNAI2		
		GPM6B	SNCA		
		GPR143	SNHG16		
		GPRC5B	SNRPE		
		GSTA4	SORT1		
		GSTP1	SOX10		
		GULP1	SOX13		
		GYG2	SOX4		
		H1F0	SPARC		
		HIBADH	SPR		
		HMCN1	SPRY4		
		HMG20B	SPTBN1		
		HOXB7	SRPX		
		HOXC10	SSFA2		
		HSBP1	ST3GAL4		
		HSP90AB1	ST5		
		HSPB1	ST6GALNAC2		
		HSPD1	STK32A		
		HSPG2	STMN1		
		IFI27	STXBP1		
		IGF1R	SYNGR1		
		IGFBP7	TANC1		
		IGSF11	TBC1D16		
		IGSF3	TBC1D7		
		IGSF8	TCEAL4		
		IMPDH2	TEAD1		
		ISYNA1	TENC1		
		ITFG3	TEX2		
		ITGA3	TFAP2A		
		ITGB3	TIMP2		
		KIRREL	TIMP3		
		LAMB1	TJP1		
		LAMB2	TMEM147		
		LAMC1	TMEM14C		
		LAPTM4A	TMEM9		
		LAPTM4B	TMEM98		
		LDLRAD3	TNFRSF19		
		LGALS1	TOM1L1		
		LGALS3BP	TRIM2		
		LINC00473	TRIM63		
		LINC00673	TSC22D1		
		LMNA	TSPAN3		
		LOC100126784	TSPAN4		
		LOC100130370	TSPAN6		
		LOC645166	TTLL4		
		LOXL4	TUBB2A		
		LRP6	TUBB2B		
		MAGEA12	TUBB3		
		MAGEA2B	TYR		
		MAGEA3	UBL3		
		MAGEA6	VAT1		
		MAGED1	VIM		
		MAGED2	VKORC1		
		MAP1B	WASL		
		MARCKSL1	WBP5		
		MDK	WIPI1		
		MFAP2	WLS		
			XAGE1A		
			XAGE1B		
			XAGE1C		
			XAGE1D		
			XAGE1E		
			XYLB		
			YWHAE		

B cells	Macrophage	Malignant		T cells cd4	T cells cd8
			ZNF462		

Table 20. Down-regulated and Up-regulated genes post-immunotherapy treatment in microenvironment

T.cd8.up		T.cd8.down		T.cd4.up	T.cd4.down	Macro.up	Macro.down
AARS2	LYRM7	ACTN4	MAL	AARS2	ACTR2	APOC1	AREG
ABHD15	MAP3K13	ADAM10	MAP1LC3A	ABI2	ADRBK1	APOE	ARF1
ABI2	MAP7D3	AEN	MED21	APOBEC3A	ANAPC11	C17orf76-AS1	BRE-AS1
AK3	MAPK13	AIM1	MGMT	APOL2	ANKRD36BP1	C1orf56	CD55
AKAP5	MBOAT1	AIP	MKNK2	ARF6	ARAP2	CA2	CREM
AKIP1	ME2	AKAP13	MPG	C17orf76-AS1	ASCC3	CD81	DUSP2
ALG1	MED18	AKNA	MRPL47	C1orf56	ASMTL	CSTB	EREG
ANKRD40	METTL16	AMD1	MRPL53	C1QB	ATXN2L	CXCL9	ETS2
AP1G2	METTL2B	ANKRD11	MRPL54	CASP10	BCL6	DBNDD2	FKBP5
AP3M1	MFSD11	ANKRD36BP1	MSI2	CCL5	C22orf34	DHRS4L2	FOSB
AP3S2	MIAT	APBB1IP	MT2A	CCND2	CALM3	DNAJC5B	GAPT
APOL2	MLANA	APH1A	MXD4	CD68	CCNG1	DYNC1I2	HIF1A
ARF6	MMS22L	APOBEC3G	MYCBP2	CEP41	CD200	DYNLL1	ICAM3
ARIH2OS	MOCS3	ARID1A	MYEOV2	CLUAP1	CD226	FABP3	IFI44L
ARMC10	MREG	ARID2	MYH9	CNNM3	CD3E	FOLR2	IL1B
ARSA	MRPL44	ARL1	NACA	CTBP1	CD40LG	FTL	LOC100130476
ASB8	MS4A1	ARL4C	NAP1L1	CXCR3	CD58	FUCA1	MEF2C
ATP6V0A2	MSH3	ASF1B	NDC80	CXCR6	CD6	GPNMB	NFIL3
B2M	MTFMT	ATAD1	NDE1	DCAF10	CDC42EP3	HLA-J	NFKBIA
BCL6	NAA16	ATP5E	NDUFA12	DNAJC14	CHI3L2	HSD11B1	NFKBIZ
BLOC1S6	NDNL2	ATP5L	NDUFA13	FAM126B	COX7C	HSD3B7	NLRP3
BMS1P1	NEK2	ATP5O	NDUFA2	FAM134A	CPSF1	HSPA7	NR4A2
BMS1P4	NFKBIB	ATP6V0C	NDUFA4	FAM153C	CTSA	HSPB1	PPP1R15B
BMS1P5	NME6	ATP6V0E2	NDUFA6	FGD5-AS1	CXCR5	KLHDC8B	REL
BRIP1	NOL9	ATXN2L	NFATC2	GBP4	DDX39B	MGLL	RPSAP58
C10orf32	NPIPL3	ATXN7L1	NFKBIA	GBP5	DDX3Y	MIR4461	THBS1
C12orf65	NQO1	AURKB	NFKBIZ	GNRHR2	DHRS7	MRPS15	TNFAIP3
C19orf40	NT5DC3	BCL11B	NINJ2	GPR56	EHD1	NOP10	ZBTB16
C1orf174	NUAK2	BCL2	NIPBL	GSTM3	EIF3L	NUPR1	ZFP36
C1orf210	OCLN	BHLHE40-AS1	NIT2	GZMA	ERGIC3	PCBD1	
C1orf56	OPHN1	BIRC5	NOP56	HAUS2	EXOC1	PLA2G2D	
C1orf63	ORC6	BLMH	NPM1	HERC2P4	FAM172A	PLA2G7	
C1QTNF6	PACS2	BLVRA	ORMDL3	HLA-DRA	GNG5	RAB20	
C5orf24	PAFAH1B2	BRK1	OST4	HLA-DRB1	GPRIN3	SCARB1	
C5orf55	PAICS	BTF3	PABPC1	HNRNPH1	HDDC2	SLIRP	
C9orf3	PAN3	BTN3A2	PAIP2	INADL	HINT1	ST3GAL5	
C9orf85	PAR-SN	BUB1	PAM	KLRD1	HIST1H1D	TIMP2	
CACUL1	PARP11	BUB3	PARK7	LINC00439	HIST1H1E	TMSB10	
CAMLG	PARP3	C1D	PARP8	LOC100506469	HIVEP2	TRNAU1AP	
CCDC122	PARP9	CARD16	PCBP1	LOC284379	HNRNPC	UBD	
CCR6	PCGF5	CARS	PCBP2	LOC389641	HS3ST3B1	WSB2	
CD160	PDE12	CASP4	PDCD1	LOC644961	ICA1	XIST	
CD24	PER2	CASP8	PDCD5	LOC727896	ITM2A	YTHDF2	
CD68	PEX13	CBLB	PER1	MAP3K13	ITPR1		
CENPN	PIGX	CCDC141	PET117	MCTS1	KLF12		
CEP104	PKNOX1	CCDC167	PFDN5	NANOG	LCMT1		
CHP1	PMEL	CCDC23	PIK3IP1	NXNL2	LOC100216545		
CLCC1	POU2AF1	CCL4	PIK3R5	PIP4K2A	LOC100271836		
CLUAP1	PPP1R3B	CCNB2	PIN4	PLEKHA2	LOC285740		

T.cd8.up		T.cd8.down		T.cd4.up	T.cd4.down	Macro.up	Macro.down
CNNM3	PQLC2	CCND1	PLCB2	PPID	MAEA		
COA1	PRMT2	CCND3	PLEK	PRDM1	MAP2K3		
COX10-AS1	PSTPIP2	CCNH	PLEKHM1	PSTPIP2	MAP4K1		
COX18	PTPN2	CCNK	PLIN2	QRSL1	MED21		
CPPED1	QPRT	CCR1	POGZ	RASSF3	MKNK2		
CPT1A	RAB21	CCR4	PPIA	RBM43	MRPL33		
CRK	RAB33B	CCR5	PPM1G	RGS1	MRPS2		
CSAD	RAD1	CD2	PRDM1	RPP14	MTERFD2		
CSNK1G1	RASSF1	CD200R1	PRDX6	RUNX1-IT1	MTMR6		
CWC25	RBBP5	CD27	PRMT10	SBF2-AS1	MYEOV2		
CYB5D2	RBL1	CD320	PRPF8	SCAI	NAB1		
CYP4V2	RBMS2	CD37	PRR14L	SGOL1	NDUFA4		
DCP1A	RDH10	CD3D	PRRC2B	SLC25A51	NEK7		
DESI1	REL	CD3E	PTBP3	SLC35E1	NFATC1		
DGKD	RFC2	CD3G	PTPN4	SPDYE1	NFATC2		
DHODH	RFT1	CD4	PTRHD1	SPDYE2	NINJ2		
DIP2A	RHD	CD7	RAB1B	SPDYE2L	OST4		
DIS3	RIOK3	CD79A	RAPGEF1	SPDYE7P	P2RX5		
DIS3L	RNF14	CD81	RASA1	SWSAP1	PAPD4		
DNASE1	RNF141	CDC42SE1	RASA2	THAP5	PARL		
DND1	RPS6KA3	CDK1	RBM38	TMEM120B	PASK		
DTD2	RUNDC1	CENPK	RGS1	TMEM192	PCBP1		
EEF2K	S1PR2	CHCHD2	RGS10	TP53RK	PDCD1		
EIF5A2	SATB1	CHI3L2	RHBDD3	TRMT10B	PFKL		
ELMSAN1	SCAI	CIRBP	RHOA	TSNAX	PHF3		
ESYT2	SCAMP1	CITED2	RNASEK	TXNDC15	PHF8		
EYA3	SCML4	CLASP1	RPA3	UGT8	PIK3CG		
F11R	SEC23IP	CLDND1	RPL13A	UPK3BL	PLP2		
FAM126B	SEMA4D	CLECL1	RPL14	XIST	PON2		
FAM210B	SENP5	COX17	RPL18	ZNF253	PPP1CA		
FAM215A	SERPINB1	COX4I1	RPL22	ZNF276	PRKCH		
FAM217B	SERPINB6	COX6A1	RPL23	ZSWIM7	PRNP		
FAM73A	SGCB	COX7A2L	RPL27		PRRC2B		
FANCD2	SGK3	COX7C	RPL27A		PTBP3		
FASTKD2	SGOL1	COX8A	RPL29		RBM25		
FBLIM1	SH2D1B	CREB3L2	RPL31		RERE		
FBXL18	SIRT5	CSNK1D	RPL32		RGS3		
FBXW2	SKP2	CST7	RPL34		RPL13A		
FCRL3	SLAMF7	CTSC	RPL35		RPL14		
FCRL6	SLC25A15	CTSD	RPL35A		RPL27		
FDPSL2A	SLC25A32	CXCL13	RPL36		RPL37		
FLCN	SLC25A51	CXCR4	RPL36A		RPS26		
FLOT1	SLC2A3	CXCR6	RPL36AL		RPS4Y1		
FOXK1	SLC30A6	CYTIP	RPL37		RPS5		
FTO	SLC30A7	DDIT4	RPL37A		SARDH		
FXN	SLC31A1	DDX6	RPL38		SEC11C		
GALNT6	SLC35A3	DNAJB12	RPL39		SEC16A		
GATAD1	SLC48A1	DNAJC9	RPLP0		SELT		
GBP1	SLC50A1	DPM3	RPRD2		SF3B1		
GBP2	SLC7A5P2	DTHD1	RPS10		SFI1		
GBP4	SMIM14	DUSP4	RPS13		SMARCE1		
GBP5	SMYD4	EBP	RPS16		SMG1P1		
GCLM	SNAPC3	EEF1B2	RPS17		SNHG5		
GDAP2	SNHG7	EEF1D	RPS17L		SNRPN		
GEMIN8	SNIP1	EEF2	RPS20		SRRM2		
GGPS1	SOAT1	EHMT1	RPS21		SSH2		
GLIPR1L2	SPAST	EIF3F	RPS23		STAU1		
GLUD1P7	SPRYD4	EIF3G	RPS24		TATDN1		
GMEB1	SRSF8	EIF4B	RPS26		TCF7		
GNE	SS18	ELK2AP	RPS28		THADA		
GNG4	STAT1	EMB	RPS29		TIAM1		
GNRHR2	STAT5B	ENSA	RPS4X		TIGIT		
GOLGA3	STOM	ERAP2	RPS5		TMEM59		
GPCPD1	STYX	ERGIC3	RPS7		TOX		
GPR82	SWSAP1	ERH	RPS9		TOX2		
GTF2H2C	TADA2B	ERN1	RPSA		TYK2		

T.cd8.up		T.cd8.down		T.cd4.up	T.cd4.down	Macro.up	Macro.down
GTPBP5	TADA3	ETS1	RSBN1		UBQLN1		
HAUS3	TANGO2	EVL	RUNX2		UQCR10		
HERC2P7	TARS2	FAM102A	RUNX3		UQCRH		
HIST1H2BG	TATDN3	FAM129A	S100A6		UTRN		
HIVEP3	TBC1D24	FAM53B	SELL		UXT		
HMHA1	TBCCD1	FAM78A	SF3A1		WNK1		
HOGA1	TERF1	FAU	SHISA9		WWP2		
HOPX	TERF2	FBXO5	SIRPG		ZFP36		
HSPA1B	THAP5	FKBP5	SLA		ZNF217		
ICA1L	TLE3	FNDC3A	SLC39A7				
ID3	TM7SF3	FOSB	SLC4A7				
IDO1	TMEM123	FOXP1	SMG7				
IER2	TMEM209	FRYL	SNORD10				
IFITM3	TMEM41A	G6PD	SNRNP200				
IFNAR1	TMEM41B	GAS5	SON				
IFNLR1	TNFAIP8L2-SCNM1	GINS2	SPOCK2				
IKBIP	TNFSF14	GLRX	SRRM2				
IL10	TPMT	GMCL1	SSR4				
INIP	TRIM5	GMFG	STK16				
INPP4B	TRIOBP	GMNN	SUMO2				
INPP5F	TSNAX	GNG5	SUPV3L1				
IRAK4	TTC39C	GNLY	SYNGR2				
IRF1	TUBGCP4	GOLGA8B	SYTL3				
IRF2BP2	TYMP	GPR183	TAF15				
ITGAX	UBE2Q2	GPR56	TAOK3				
ITK	UBOX5	GRN	TAP2				
KCNK5	UBXN2B	GSTM1	TK1				
KDELC2	UTP23	GSTP1	TLN1				
KDSR	VMP1	GTF2B	TMED9				
KIAA0355	WAC-AS1	GTF3C6	TMEM155				
KIAA1324	WDR92	GZMK	TMEM2				
KIAA1919	XIAP	H2AFZ	TNFAIP3				
KIF18B	XKR9	HDAC8	TNFSF4				
KIF3A	ZBTB24	HERC2P2	TNFSF8				
KIN	ZBTB43	HERPUD1	TOB1				
KLHL28	ZCCHC4	HINT1	TOMM7				
KLRC2	ZFP14	HIST1H1E	TOX				
KLRC3	ZFP36L1	HIST1H3G	TP53INP1				
KLRD1	ZMYM5	HIST1H4C	TPX2				
KRAS	ZNF100	HLA-DQA1	TSC22D3				
LAIR1	ZNF124	HLA-DQA2	TSPAN14				
LDHA	ZNF160	HLA-DRB5	TSPYL2				
LDLR	ZNF321P	HLA-F	TSTD1				
LIAS	ZNF333	HLA-H	TTN				
LINC00476	ZNF37BP	HMBOX1	TUBA4A				
LLGL1	ZNF483	HUWE1	TXK				
LOC100131067	ZNF526	IFIT5	TXNIP				
LOC100131089	ZNF528	IL6ST	TYMS				
LOC100132247	ZNF529	IQGAP1	UBA52				
LOC100190986	ZNF543	IQGAP2	UBE2C				
LOC100268168	ZNF548	ISCU	UBE2T				
LOC100271836	ZNF549	ISG20	UCP2				
LOC100505812	ZNF620	ITGAD	UGDH-AS1				
LOC100505876	ZNF652	ITGB1	UQCR11				
LOC100506083	ZNF665	ITGB2	UQCRB				

T.cd8.up		T.cd8.down		T.cd4.up	T.cd4.down	Macro.up	Macro.down
LOC100652772	ZNF669	ITM2B	UQCRH				
LOC202781	ZNF683	KDM5C	USB1				
LOC284023	ZNF721	KIAA1551	UXT				
LOC389641	ZNF793	KIR2DL4	VCAM1				
LOC727896	ZNF805	KLF12	VRK1				
LOC729603	ZNF814	KPNB1	WDR83OS				
LOC90834	ZSCAN2	LDHB	WNK1				
LRRC57	ZSCAN22	LENG8	YEATS4				
LRRC58	ZSCAN29	LINC00493	YWHAB				
LY9	ZSWIM7	LINC00612	ZBTB38				
		LNPEP	ZC3H12A				
		LOC643406	ZC3HC1				
		LOC643733	ZDHHC24				
		LOC646214	ZFP36L2				
		LRRC37A4P	ZMYND8				
		LSM6	ZNF638				
		MAD2L1	ZWINT				
		MAEA					

Table 21. Top Genes from Table 20

T.cd8.up	T.cd8.down	T.cd4.up	T.cd4.down	Macro.up	Macro.down
AP1G2	AKNA	CASP10	CHI3L2	NUPR1	FKBP5
AP3M1	BCL2	CXCR3	COX7C		LOC100130476
APOL2	CARD16	CXCR6	CXCR5		NLRP3
ARF6	CCDC141	FAM153C	HIST1H1E		THBS1
C12orf65	COX4I1	FGD5-AS1	HIVEP2		TNFAIP3
CCDC122	COX8A	GBP5	ICA1		
CSAD	EIF3G	LOC727896	NEK7		
CWC25	FAU	NXNL2	NFATC2		
DHODH	G6PD	RBM43	NINJ2		
DIS3L	GLRX	RGS1	PASK		
FAM217B	GNLY	SLC35E1	RPL13A		
GBP2	GPR56	SPDYE1	TCF7		
GDAP2	HIST1H4C				
HOPX	HLA-DRB5				
IKBIP	HUWE1				
KIAA1919	ITGB2				
LOC727896	MGMT				
LOC90834	MKNK2				
LRRC58	NDC80				
MAP7D3	NDUFA6				
MFSD11	PIK3R5				
MOCS3	RPL35A				
PER2	SYTL3				
POU2AF1	TNFSF4				
PQLC2	TOB1				
RAD1	UCP2				
SGCB	WNK1				
SGOL1					
SLC2A3					
SNAPC3					
SRSF8					
SS18					
STOM					
SWSAP1					
TANGO2					
TERF2					
TMEM123					
TMEM209					
ZBTB43					
ZNF160					
ZNF528					
ZNF543					

Example 5

Protein-Protein interactions between genes in the resistance signatures

[0458] In line with the co/anti-regulatory patterns of the PIT-Up (ICR-Up, post-treatment-up) and PIT-Down (ICR-down, post-treatment-down) modules, a significantly large number of protein-protein interactions occur within and between the two modules (253 interactions, P = <1e-3,) (Table 22). The number of interactions is ~7 times more than expected (empirical p-value)

Table 22.

GeneA	GeneB
ACAA2	PFN1
ACAA2	ATP1B3
ACAA2	ISYNA1
ACSL4	PTPMT1
ACSL4	HTATIP2
ADSL	UBC
ADSL	XPNPEP1
ADSL	PAICS
AEN	LZTS2
AHNAK	FN1
AHNAK	S100A10
ALDH1B1	UBC
ALDH1B1	FN1
ALDH1B1	XPNPEP1
ANXA1	UCHL5
ANXA1	FN1
ANXA2	CTSB
ANXA2	S100A10
ANXA2	MID1
ANXA2	FN1
ANXA2	LGALS1
ARHGEF1	CD44
ARHGEF1	FN1
ATF3	STAT1
ATF3	JUNB
ATP1A1	UBC
ATP1A1	ATP1B3
ATP1B3	PTP4A3
ATP1B3	HLA-C
ATP1B3	RPL17
ATXN10	BSG
ATXN10	FN1
ATXN10	MRPS16
ATXN2L	GALNS
ATXN2L	PABPC1
BCCIP	EIF6
BCCIP	FAM46A
BCCIP	SORD
BCCIP	SMS
BCL6	JUNB

GeneA	GeneB
FOXRED2	OS9
FXYD3	NR4A1
G6PD	GBP2
G6PD	TSTA3
G6PD	IDH2
GEM	LZTS2
GLOD4	NR4A1
GLOD4	NNMT
GLOD4	PAICS
HDAC2	SMC3
HDAC2	KLF4
HDAC2	RUVBL2
HDAC2	SNAI2
HDAC2	TSC22D3
HLA-A	TAPBP
HLA-A	TAP1
HLA-A	UBC
HLA-A	ITM2B
HLA-A	HLA-C
HLA-A	HLA-E
HLA-C	UBC
HLA-C	HLA-F
HLA-C	HLA-E
HLA-C	ITGA6
HLA-E	HLA-F
HLA-E	ITGA6
HSP90B1	OS9
HSP90B1	TPM1
HSP90B1	RPN2
HSP90B1	TSR1
HSP90B1	STAT1
IDH2	UBC
IGF1R	IGFBP3
IGFBP3	TF
ILF2	XRCC5
ILF2	RPL17
ILF2	RPL10A
ILF2	RPS3
ILF2	SRSF7
ILF2	PRKCDBP

GeneA	GeneB
BCL6	HDAC2
BCL6	PELI1
BIRC3	UBC
BSG	OS9
BSG	MYBBP1A
BSG	XPO7
BSG	METAP2
BSG	PTPMT1
CALU	GAA
CALU	PRKCDBP
CALU	CTNNAL1
CALU	HSP90B1
CAV1	CD44
CAV1	PTRF
CD151	CD46
CD44	IGFBP3
CD44	FN1
CD44	NF2
CD46	CD9
CD9	LGALS3BP
CFB	FN1
CPSF1	POLR2A
CRELD1	EIF6
CRYAB	CS
CRYAB	SORD
CS	CTPS1
CST3	CTSB
CTSA	CTSD
CTSB	S100A10
CTSB	SPRY2
CTSD	UCHL5
CTSD	HSP90B1
DCBLD2	ITM2B
DCTN6	RPSA
ECHS1	UCHL5
ECHS1	ISYNA1
EGR1	JUNB
EIF4A1	PABPC1
EIF4A1	UCHL5
EIF4A1	RPSA
EIF4A1	TMEM43
EIF4A1	ILF2
EIF4A1	FN1
EIF6	PAICS
EIF6	PSME1
EIF6	FBL
EIF6	RPL17
EIF6	RUVBL2
EIF6	TSNAX
EIF6	KIAA0020
EMP1	SMIM3
EPDR1	NF2
FAM213A	HLA-C
FAM46A	PRSS23
FAM46A	SQRDL
FAM46A	FNDC3B
FBL	RUVBL2

GeneA	GeneB
ILF2	TOMM22
ILF2	PTRF
ILF2	RUVBL2
ILF2	MYBBP1A
ILF2	KIAA0020
ITGA6	LGALS3BP
KLF4	KLF6
LAMB1	UBC
LGALS1	LGALS3BP
LZTS2	TSNAX
LZTS2	SMIM3
MID1	RPS3
MID1	UBC
MTG1	PRNP
MYBBP1A	NR4A1
MYBBP1A	RPS3
MYBBP1A	PTRF
NCBP1	THOC5
NCBP1	SERPINE2
NF2	XRCC5
NF2	RPS3
NF2	RPS7
NF2	SMC3
NOLC1	PTRF
OXA1L	PTPMT1
PABPC1	RPSA
PABPC1	RBM4
PABPC1	RPL10A
PABPC1	RPL17
PELI1	UBC
PFN1	UCHL5
POLR2A	XRCC5
POLR2A	SMC3
POLR2A	PSMB9
POLR2A	RUVBL2
PRAME	UBC
PRDX3	UCHL5
PRDX3	PSME1
PROS1	RPSA
PSMB9	PSME1
PSMB9	UCHL5
PTP4A3	XPO7
RND3	SKP2
RPL10A	RPS3
RPL10A	RPL17
RPL10A	RPSA
RPL10A	S100A10
RPL10A	RPS7
RPL17	RPS3
RPL17	RPSA
RPN2	UBC
RPS3	RPS7
RPS3	RPSA
RPS3	TPM1
RPS3	TSR1
RPS3	UBC
RPS3	TSNAX

GeneA	GeneB
FBL	KLF6
FBL	UBC
FBL	NOLC1
FBL	RPL17
FBL	RPS7
FBL	RPS3
FBL	FN1
FBL	GPATCH4
FBL	KIAA0020
FBLN1	FN1
FN1	IGFBP3
FN1	MIA
FN1	TNC
FN1	LGALS1
FN1	LYPLA1
FN1	RPL17
FN1	RNH1
FN1	G6PD
FN1	PAICS
FN1	SLC5A3
FN1	NCBP1
FN1	PPA1
FN1	XRCC5
FN1	RPSA
FN1	RUVBL2
FN1	PRDX3
FN1	RPL10A
FN1	RPS7
FN1	ILF2
FN1	PFN1
FN1	UBAP2L
FN1	PABPC1
FN1	RPS3
FN1	UBC
FN1	RBM4
FN1	TF

GeneA	GeneB
RPS7	RPSA
RPS7	TSR1
RPSA	TSR1
RUVBL2	SRCAP
RUVBL2	UCHL5
RUVBL2	UBC
RUVBL2	VPS72
SAMM50	TOMM22
SAMM50	SQRDL
SAMM50	SERINC1
SMG7	TSNAX
SMS	SORD
SORD	TPM1
SRCAP	VPS72
STAT1	TSNAX
TAP1	TAPBP
TPM1	UBC
TSC22D3	UBC
TSTA3	UBC
UBA7	UBE2L6
UBC	UCHL5
UBC	XPNPEP1
UCHL5	XPNPEP1

Example 6 - Tumor microenvironment interaction analysis

[0459] The ITR-down genes and ITR-up genes interact with stromal and immune genes. The ITR-down genes interact with more genes (**Figure 34, 35**). Figure 33 shows that genes that are down in malignant cells in immunotherapy resistant samples are rich in interactors of immune and stromal cells. Conversely, few such interaction genes are induced in malignant cells in immunotherapy resistant samples.

Example 7 –ITR signature scores from melanoma tumors in different cancers

[0460] The ITR scores are different in different cancers (**Figure 36, 37**). Bladder cancer has the highest. Thymoma has the lowest. Uveal melanoma has the fourth highest. Applicants observed a difference in score between two melanomas (uveal and skin cutaneous). Not being bound by a theory, cancers with the highest ITR scores are more resistant to immunotherapy

than cancers with a lower score. Not being bound by a theory, cancers with the highest ITR scores have a worse prognosis. The cancers on the right are more sensitive to immunotherapy (**Figure 36**). Furthermore, they have less of an anti-correlation between ITR and T cell infiltration.

Example 8 –Analysis of Single Cells from ER+ Metastatic Breast Cancer and Colon Cancer

[0461] Applicants also analyzed single cells in other cancers having an ICR signature, (see, e.g., **Figure 15A, B**). Applicants further extended the melanoma ecosystem studies to study response to immunotherapy, using massively parallel droplet scRNA-Seq to analyze cells from colon tumors, using snRNA-Seq methods to profile metastatic breast cancer samples and profiling pancreatic tumors. Cancer cells may be more or less resistant to immunotherapy based on uICR scores. Single cells in other cancers may be shifted to an immunotherapy sensitive signature by treating with CDK4/6 inhibitors. Analysis of this signature and measuring shifts in the signature after CDK4/6 inhibition can allow the proper administration of an immunotherapy in a combination treatment.

[0462] Applicants analyzed ER+ metastatic breast cancer using single nuclei RNA-seq (snRNA-seq) on fresh and frozen tissue samples (**Figure 38**). snRNA-seq as described herein is compatible with frozen tissue samples. Non-malignant cells clustered by cell type in both frozen and fresh tissue samples. Malignant cells clustered by patient.

[0463] Applicants analyzed 22 colon cancer samples using scRNA-seq (**Figure 39**). With strict quality control (QC) on the 22 samples analyzed Applicants obtained 12,215 epithelial cells and 17,143 non-epithelial cells.

Example 9 – Immunotherapy Resistance Signature

[0464] Immunotherapies have transformed the therapeutic landscape of several cancer types (Sharma and Allison, 2015). However, despite the durable responses in some patients, most patients' tumors manifest unpredictable resistance to immunotherapies (Gibney et al., 2016; Sharma et al., 2017). This hampers appropriate selection of patients for therapies, rational enrollment to clinical trials and the development of new therapeutic strategies that could overcome resistance (Sharma and Allison, 2015). Most non-responding patients manifest intrinsic resistance, reflected as continued tumor growth or occurrence of new metastatic lesions despite therapy, whereas some patients develop acquired resistance following an initial clinical disease regression. It is unknown whether these clinically discrete

manifestations are associated with shared or distinct molecular mechanisms of resistance (Sharma et al., 2017).

[0465] Recent studies characterized resistance to immune checkpoint inhibitors (ICI) by analyzing Whole Exome Sequencing (WES) and transcriptional profiles of bulk tumors (Hugo et al., 2016; Mariathasan et al., 2018; Van Allen et al., 2015). These studies demonstrated that tumors with a high mutational load (Van Allen et al., 2015) and a high level of immune cell infiltration (Riaz et al., 2017; Tumeh et al., 2014) are more likely to respond, and linked ICI resistance in patients to functional immune evasion phenotypes, including defects in the JAK/STAT pathway (Zaretsky et al., 2016) and interferon gamma (IFN-γ) response (Gao et al., 2016; Zaretsky et al., 2016), impaired antigen presentation (Hugo et al., 2016; Zaretsky et al., 2016), and PTEN loss (Peng et al., 2016). While these studies significantly contributed to the understanding of the cancer-immune interplay, the resulting biomarkers where only partially predictive (Sharma et al., 2017). This may be due to the fact that they only reflect some facets of the causes of resistance (WES) or combine signals from malignant and non-malignant (immune and stroma) cells (RNA and copy-number variations).

[0466] Because immune checkpoint inhibitors target the interactions between different cells in the tumor, their impact depends on multicellular circuits between malignant and non-malignant cells (Tirosh et al., 2016a). In principle, resistance can stem from different compartment of the tumor's ecosystem, for example, the proportion of different cell types (*e.g.*, T cells, macrophages, fibroblasts), the intrinsic state of each cell (*e.g.*, memory or dysfunctional T cell), and the impact of one cell on the proportions and states of other cells in the tumor (*e.g.*, malignant cells inducing T cell dysfunction by expressing PD-L1 or promoting T cell memory formation by presenting neoantigens). These different facets are inter-connected through the cellular ecosystem: intrinsic cellular states control the expression of secreted factors and cell surface receptors that in turn affect the presence and state of other cells, and vice versa. In particular, brisk tumor infiltration with T cell has been associated with patient survival and improved immunotherapy responses (Fridman et al., 2012), but the determinants that dictate if a tumor will have high ("hot") or low ("cold") levels of T cell infiltration are only partially understood. Among multiple factors, malignant cells may play an important role in determining this phenotype (Spranger et al., 2015). Resolving this relationship with bulk genomics approaches has been challenging; single-cell RNA-seq

(scRNA-seq) of tumors (Li et al., 2017; Patel et al., 2014; Tirosh et al., 2016a, 2016b; Venteicher et al., 2017) has the potential to shed light on a wide range of immune evasion mechanisms and immune suppression programs.

[0467] Here, Applicants used scRNA-seq and a new computational approach to identify immune evasion or suppression mechanisms in the melanoma ecosystem (**Figure 44A,B**). Applicants developed a data-driven approach that integrates scRNA-seq with other data sources to characterize malignant cell states that drive immune resistance in melanoma (**Figure 44B**). Applicants identified a program in malignant cells that is associated with T cell exclusion prior to immunotherapy, and with the melanoma cell states in patients who were resistant to immunotherapies. Applicants confirmed its presence *in situ* in tumors with multiplex protein imaging. This program predominantly reflects intrinsic resistance to immune checkpoint inhibitors (but not to RAF/MEK-targeted therapy) and its expression predicts responses to ICI and clinical outcomes in independent patient cohorts. Applicants further associated the CDK4/6 pathway with control of this program and showed that treatment with CDK4/6 inhibitors reverses it and promotes a senescent-like state and when combined with immunotherapies, may even overcome resistance *in vivo*.. This work provides a new predictive biomarker for ICI response, suggests a new therapeutic modality that may re-sensitize malignant melanoma cells to ICI, and provides a general framework to study the effect of immunotherapies and other drugs on complex tumor ecosystems.

RESULTS

Systematic approach to discover malignant cell programs associated with immune cell infiltration or exclusion

[0468] To identify malignant cell programs that characterize "cold" melanoma tumors, Applicants devised a new strategy that combines scRNA-seq and bulk RNA-Seq data to relate the cellular state of one cell type (*e.g.*, malignant cell states) to the cellular composition of the tumors (*e.g.*, T cell infiltration *vs.* exclusion) (**Figure 44B**). For clarity, Applicants describe the strategy in this specific context, though it can be applied to any two cell-types of interest. Applicants first use scRNA-seq profiles to define cell type specific signatures of T cells and of malignant cells in melanoma tumors. Next, Applicants use the T cell signature to estimate T cell infiltration levels in each of hundreds of tumors, based on their bulk RNA-Seq profile. For the analysis outlined here, Applicants focused on CD8+ T cells, but Applicants have inferred the relationship between cancer cells and other T cell populations, including

pan-T cells ($CD3^+$), $CD8^+$ T cells, and $CD4^+$ T cells; naïve, cytotoxic, and exhausted $CD8^+$ T cell; and naïve, exhausted, and regulatory $CD4^+$ T cells (Methods).

[0469] Applicants then define a "seed exclusion program" by identifying genes from the *malignant* cell signature whose expression is strongly correlated (positively or negatively) with the T cell infiltration level across those bulk tumors. Because the seed program is identified only among a few hundred genes that are exclusively expressed by scRNA-Seq in malignant cells, it avoids contamination from the tumor microenvironment; however, important genes that promote exclusion or infiltration may also be expressed by non-malignant cells (*e.g.*, MHC class I molecules). To recover these genes, Applicants finally return to the scRNA-seq data of the malignant cells and expand the seed program by searching for genes that are correlated with it across the single malignant cells, irrespective of their expression in other cell types. In this way, Applicants derive a genome-scale, malignant-cell exclusion program, consisting of genes induced ("up") or repressed ("down") by malignant cells in "cold" *vs.* "hot" tumors. Applicants can then score each cell or tumor for expression of the program, such that overexpression of the program is defined as the overexpression of its induced part and underexpression of its repressed part, and vice versa (**Methods**).

Analysis of clinical scRNA-seq identifies a malignant cell program associated with T cell exclusion from melanoma tumors

[0470] Applicants applied the approach to 7,186 high-quality scRNA-seq profiles from the tumors of 31 melanoma patients, comprised of 2,987 cells from 16 newly collected patient tumors (**Figure 44A, Table 1**), and 4,199 cells from 16 patients that Applicants previously reported (Tirosh et al., 2016a), along with 473 bulk RNA-seq melanoma profiles from The Cancer Genome Atlas (TCGA) (Akbani et al., 2015). Applicants dissociated individual cells from fresh tumor resections, isolated immune and non-immune cells by FACS based on CD45 staining, and profiled them with a modified full-length SMART-Seq2 protocol (**Methods, Table 2**). Applicants distinguished different cell subsets and genetic clones both by their expression profiles and by their inferred CNV profiles (Tirosh et al., 2016a) (**Methods**), identifying: malignant cells, CD8 and CD4 T cells, B cells, NK cells, macrophages, Cancer Associated Fibroblasts (CAFs) and endothelial cells (**Figures 44C,D and 51, Tables 26C and 3**). Overall, malignant cells primarily grouped by their tumor of origin (**Figure 44C**), while the non-malignant cells grouped primarily by their cell type, and

only then by their tumor of origin (**Figure 44D**), as Applicants have previously reported for melanoma and other tumor types (Puram et al., 2017; Tirosh et al., 2016a; Venteicher et al., 2017).

[0471] The resulting exclusion program (**Figure 44E, Table 5**) highlights the repression of diverse immune response pathways and the induction of a co-regulated gene module of Myc and CDK targets. The repressed genes were enriched for antigen processing and presentation genes (*B2M*, *CTSB*, *CTSL1*, *HLA-B/C/F*, *HSPA1A*, *HSPA1B*, $P = 4.19*10^{-7}$, hypergeometric test), immune modulation genes ($P = 3.84*10^{-9}$, *e.g.*, *CD58* and the NFκB inhibitor, *NFKBIA*), and genes involved in the response to the complement system ($P = 2.26*10^{-7}$, *e.g.*, *CD59* and *C4A*). *CD58* KO in malignant cells was recently shown to enhance the survival of melanoma cells in a genome-scale CRISPR screen of melanoma/T cell co-cultures (Patel et al., 2017), and its genetic loss or epigenetic inactivation are frequent immune evasion drivers in diffuse large B cell lymphoma (Challa-Malladi et al., 2011). The induced genes included *MYC* and Myc targets ($P = 2.8*10^{-14}$), many *CDK7/8* targets ($P < 3*10^{-9}$) (Oki et al., 2018), and transcription factors, such as *SNAI2* and *SOX4*. Myc-activation has been previously linked to increased expression of immunosuppressive signals, including the upregulation of *PD-L1* and β-catenin, which in turn inhibits dendritic cell recruitment to the tumor microenvironment via *CCL4* (Spranger et al., 2015).

[0472] Applicants tested whether other cell populations with sufficient scRNA-seq profiles, including macrophages and B cells, contributed to T cell exclusion/infiltration, but did not find significant impact on regulating T cell abundance.

The exclusion program characterizes individual malignant cells from patients who developed progressive disease on immunotherapy

[0473] To determine whether the malignant T cell exclusion program manifests in the context of immune checkpoint inhibitor therapy, Applicants leveraged the fact that the scRNA-seq cohort included both untreated patients and post-ICI patients who manifested intrinsic resistance. As clinical response rates to ICI vary, with up to 61% responders with combination therapies (Hodi et al., 2010; Larkin et al., 2015; Postow et al., 2015; Ribas et al., 2015), the untreated tumors Applicants profiled likely include both ICI sensitive and ICI resistant tumors, whereas the tumors from ICI resistant patients are expected to include primarily resistant malignant cells. Applicants thus turned to examine if the exclusion program is more pronounced in the malignant cells from ICI resistant *vs.* untreated patients.

ScRNA-seq data provide particular power for such inter-patient comparisons, even when considering only a small number of tumors, because of the larger number of cells per tumor and because non-malignant cells in the tumor microenvironment do not confound the analyses.

[0474] Applicants thus independently identified a post-treatment transcriptional program, consisting of features that distinguish individual malignant cells from post-ICI resistant tumors compared to malignant cells from untreated tumors (**Table 5**). Applicants found a robust post-treatment program, consisting of genes induced (up) and repressed (down) by malignant cells from the post-treatment resistant *vs.* untreated patients, which is stable and generalizable in cross-validation (**Methods**, **Figure 45A**, AUC=0.83). In principle, the program might reflect both the overall impact of ICI therapy and intrinsic ICI resistance *per se*, but those cannot be directly distinguished based on the single-cell cohort, where Applicants did not have matched samples from the same patient or pre-treatment tumors from responders and non-responders. Applicants address this below by analyzing two independent validation cohorts.

[0475] The post-treatment program substantially overlapped the exclusion program (**Figures 44E and 45B,C, Table 5;** $P < 10^{-16}$, hypergeometric test, Jaccard index = 0.27 and 0.23, for induced and repressed genes, respectively) and highlighted similar modules and pathways (**Figure 45D**), even though the exclusion program was identified without considering the treatment status of the tumors in the scRNA-seq data and with bulk RNA-Seq data of untreated patients. Both programs robustly classified individual cells as untreated or post-treatment (AUC = 0.83 and 0.86 for cross-validation post-treatment and exclusion, respectively, **Figure 45A,E**). Notably, a number of overlapping genes encode for ribosomal proteins (including 46 genes in the upregulated components of both signatures). This is consistent with the observation of Myc upregulation in both signatures, which is a major regulator of ribosome biogenesis (Kress et al., 2015), and whose knockdown is among the top perturbations predicted to repress the program according to the Connectivity map (Subramanian et al.). To exclude the possibility that the overlap was dominated only by this signal, Applicants removed the ribosomal genes from the signatures altogether, but observed a preserved significant overlap ($P < 10^{-17}$) between both signatures with 41 and 77 overlapping genes out of a total of 197 and 244 induced or repressed compartments, respectively. Overall, in light of the congruence of the signatures, Applicants defined a

unified immune resistance program as the union of the corresponding post-treatment and exclusion programs, and used it in all subsequent analyses, unless indicated otherwise.

The immune resistance program reflects a coherent multifaceted state of immune evasion

[0476] The program is consistent with several hallmarks of active immune evasion, suppression and exclusion. First, even though the program was derived in cutaneous melanoma, it is more pronounced in uveal melanoma, which resides in an immune-privileged environment and has very low response rates to immunotherapy, compared to cutaneous melanoma (**Figure 46A**) (Algazi et al., 2016; Zimmer et al., 2015). Second, the inhibition of genes from the repressed component of the program in malignant melanoma cells conferred resistance to CD8 T cells in a genome-wide CRISPR KO screen ($P = 6.37*10^{-3}$, hypergeometric test) (Patel et al., 2017). Third, malignant cells which express the program substantially repress a significant number of interaction routes with other cell types in the tumor microenvironment, including MHC I:TCR (T cells), *CD58:CD2* (T cells), and *IL1RAP:IL1B* (macrophages) (**Figure 46B, Methods**), as well as the overall Senescence Associated Secretory Phenotype (SASP) ($P = 4.3*10^{-166}$ and $3.6*10^{-3}$, one-sided t-test and mixed effects, respectively, **Figure 45D, right**).

[0477] The program genes appear to be under shared control by one or a few master regulators, with opposing effects on the repressed and induced components of the program. There was a strong positive correlation within the induced or repressed genes, and a strong anti-correlation between the induced and repressed genes, both across single cells in the same tumor and across TCGA tumors (**Figures 46C,D**). The co-variation patterns were remarkably reproducible within each one of the tumors in the cohort (**Figure 52**), such that any given aspect of the program (*e.g.*, under-expression of MHC-1 genes in a cell) is coupled to the state of the entire program. Moreover, there is a significant overlap between the perturbations that reverse the expression of the program's repressed and induced components (p-value=$2.33*10^{-14}$, hypergeometric test), including the overexpression of IFN-γ and IFN-β and the knockdown of *MYC* (Subramanian et al., 2017). Indeed, *MYC* knockdown is among the top perturbation to repress the program, which is enriched for Myc targets.

Expression of resistance program features in malignant cells in T cell-depleted niches *in situ*

[0478] If the immune resistance program in malignant cells is associated with T cell exclusion, malignant and T cells should vary in their relative spatial distribution in tumors depending on the activity of the program. To explore this, Applicants used multiplexed immunofluorescence (t-CyCIF) (Lin et al., 2017) to stain histological sections of 19 tumors from the single-cell cohort for 14 proteins: six cell type markers (CD3, CD8, MHC-II, FOXP3, S100, and MITF) and eight members of the immune resistance program (induced: p53, CEP170, Myc, DLL3; repressed: HLA-A, c-Jun, SQSTM1, LAMP2). Following cell segmentation and estimation of antibody staining intensities (**Methods**), Applicants assigned cells (424,000 cells/image on average) into malignant cells ($S100^+$, $MITF^+$), T cells ($CD3^+$) and cytotoxic T cells ($CD8^+$); the rest were defined as uncharacterized.

[0479] To explore the association between the program markers and the "cold" phenotype, Applicants first generated a Delaunay neighborhood graph for each image (linking cells that are immediate neighbors) and computed the observed frequency of cell-to-cell interaction compared to that expected by chance, as recently described (Goltsev et al., 2017). Malignant cells were significantly more likely to reside next to other malignant cells, and significantly less likely to reside next to T cells ($P < 1*10^{-16}$, binomial test, **Methods**). Next, for each frame in the imaged section (1,377 cells/frame on average; **Methods**), Applicants computed the fraction of T cells and the average expression of the different markers in the malignant cells. Applicants then quantified the association between expression of the immune resistance program markers and T cell infiltration levels across frames from the different images (**Methods**). Confirming this analysis approach, malignant cells in highly infiltrated niches had significantly higher levels of HLA-A (**Figure 47A**, $P = 2.61*10^{-46}$, mixed-effects). Moreover, in line with the predictions, malignant cells in cold/hot niches had significantly lower/higher levels of c-Jun (repressed in the resistance program), respectively (**Figure 47B**, $P = 2.85*10^{-12}$, mixed-effects), whereas p53, induced in the resistance program) characterized cold niches ($P = 6.16*10^{-7}$, mixed-effects). Applicants do note, however, that LAMP2 expression (repressed in the resistance program) was also associated with cold niches, potentially due to its post-transcriptional regulation (Feng et al., 2015).

[0480] Finally, since only a few markers were analyzed *in situ*, Applicants tested whether scRNA-seq and multiplex *in situ* protein profiles can be combined to jointly learn cell states, using a variant of canonical correlation analysis (CCA) (Butler and Satija, 2017) (**Methods**). The cells were primarily embedded and clustered based on their cell types, and not according to source, confirming the congruence of the two datasets, and that the markers tested can link

global transcriptional cell states to spatial organization in tissue (**Figures 47C,D and 53**). Taken together, these results support the association between the expression of the immune resistance program and the cold phenotype.

The immune resistance program is intrinsic in melanoma cells prior to treatment and is enhanced specifically post-immunotherapy

[0481] Applicants hypothesized that the immune resistance program, while more pronounced in the malignant cell of patients after ICI, in fact reflects an intrinsic resistance mechanism, present even before immunotherapy. First, the program is detected in TCGA tumors, which were all untreated. Second, while the program is more predominant in the malignant cells of the post-treatment resistant patients, it is also overexpressed in a subset of the malignant cells from untreated patients (**Figure 44E and 45C**, right plots). This is aligned with clinical observations that intrinsic ICI resistance is more prevalent than acquired ICI resistance (Sharma et al., 2017). However, because the scRNA-seq cohort did not include matched samples from the same patient or pre-treatment tumors from subsequent responders vs. non-responders, Applicants could not directly distinguish intrinsic resistance from post-treatment effects.

[0482] To test this hypothesis, Applicants therefore analyzed an independent cohort of 90 specimens collected from 26 patients with metastatic melanoma who underwent ICI therapy, with bulk RNA-Seq from biopsies collected pre-treatment (n = 29), on-treatment (n = 35), and at the time of progression (n = 26) (**Figure 44A, validation cohort 1**). Applicants tested for changes in the program score during the course of treatment, while accounting for tumor composition (**Methods**). The program was induced in on- and post-treatment samples compared to pre-treatment samples from the same patient ($P = 1.36*10^{-4}$ and $4.98*10^{-2}$, immune resistance program, refined and non-refined, respectively, mixed-effect test, **Methods**), consistent with its overexpression in individual post-ICI malignant cells in the unmatched single-cell cohort (**Figures 44E and 45C**). However, *inter-patient variation* in the program's expression was significantly higher than these intra-patient changes ($P < 10^{-8}$, ANOVA). This suggested that the major differences between the post-treatment and untreated tumors in the single-cell cohort reflect, at least in part, intrinsic differences between the two groups, which preceded the treatment, which Applicants turned to assess in a second validation cohort (below). Notably, Applicants did not observe an induction in the program following RAF/MEK-inhibition, indicating that the immune resistance state it defines is specific to ICI therapy and not merely a generic marker of any drug resistant tumor.

The immune resistance program predicts patient survival and clinical responses to ICI

[0483] The association of the program with T cell infiltration, its functional enrichment with immune evasion and exclusion mechanisms, its intrinsic expression in some malignant cells prior to treatment, and its further induction in post-ICI resistant lesions could make it a compelling biomarker for response to immunotherapy. To test this hypothesis, Applicants examined the program in multiple independent cohorts. Applicants used both the full program and one refined to the subset of genes that are co-regulated (positively) or anti-regulated (negatively) with genes whose inhibition desensitized melanoma cells to T cell mediated killing in functional screens (Patel et al., 2017) (**Table 5**, **Methods**) (The exclusion and post-treatment programs show similar signals and trends; **Figures 48E-H and 54-55**).

[0484] The underexpression of the program was strongly associated with improved survival in 473 TCGA melanoma patients (who did not receive ICI immunotherapy, **Figures 48A and 54**), even after controlling for tumor purity and inferred T cell infiltration (Azimi et al., 2012; Bogunovic et al., 2009). Furthermore, combining the program with inferred T cell infiltration levels yielded significantly more accurate predictions of patient survival than either alone (COX p-value = $1.4*10^{-8}$, **Figure 48A, right**). Other proposed mechanisms, such as de-differentiation of melanoma cells (Landsberg et al., 2012), as reflected by an MITF-low signature, and other malignant cell signatures (*e.g.*, cell cycle or the AXL program) (Tirosh et al., 2016a), did not show an association with patient survival, indicating that mere biological variation across malignant cells is insufficient as a prognostic signature.

[0485] The program expression in published pre-treatment and early on-treatment bulk expression profiles also distinguished eventual ICI responders from non-responders in those studies (**Figures 48B,C**). In a lung cancer mouse model, the program expression in early on-treatment profiles clearly separated anti-CTLA-4 responders from non-responders (P = $3.6*10^{-7}$, one-sided *t*-test, **Figure 48B**) (Lesterhuis et al., 2015). In bulk pre-treatment RNA-Seq data from 27 melanoma patients that were subsequently treated with Pembrolizumab (anti-PD-1) (Hugo et al., 2016), the program was underexpressed in the five complete responders, though just above statistical significance (P = $6.3*10^{-2}$, one-sided *t*-test, **Figure 48C**). In bulk pre-treatment RNA-Seq data from 42 melanoma patients that were subsequently treated with the CTLA-4 inhibitor ipilimumab (Van Allen et al., 2015), the program was significantly lower in the two complete responders (P = $5.2*10^{-3}$, one-sided *t*-test).

[0486] To test the predictive value of the program in a larger independent setting, Applicants assembled a validation cohort of 112 patients with metastatic melanoma who underwent a pre-treatment biopsy and bulk RNA-Seq followed by Pembrolizumab (anti-PD-1) therapy (**Figure 44A, validation cohort 2, Table 1**). The cohort was collected in a different hospital and country (Germany; **Methods**), and samples were processed and sequenced on the same platform (**Methods**). Applicants evaluated the program's performance in predicting anti-PD-1 responses as reflected by: **(1)** progression-free survival (PFS, recorded for 104 of the 112 patients), **(2)** clinical benefit (CB, defined as either partial or complete response by RECIST criteria), and **(3)** complete response (CR) (**Methods**). Applicants also compared the performance of the predictors to those of 32 other signatures, including the top hits of two functional CRISPR screens of resistance to T cells and ICI (Manguso et al., 2017; Patel et al., 2017) (**Table 9, Methods**).

[0487] The programs were predictive of PFS in the validation cohort (**Figures 48D and 55A-E**), even when accounting for other known predictors of ICI response, including inferred T cell infiltration levels and PD-L1 expression (**Figure 55E**). Although cell cycle alone is not associated with PFS (COX $P > 0.25$), filtering the cell-cycle component from the program score (**Methods**, and below) further improved PFS predictions (**Figure 48D, right**), suggesting that a tumor's immune resistance should be evaluated conditioning on its proliferation level. The program had a strong predictive value beyond T cell infiltration ($P = 3.37*10^{-6}$, Wilcoxon-ranksum test), and was the only one negatively associated with PFS. Other alternative signatures were either not predictive or did not provide any additive predictive value once accounting for T cell infiltration levels (**Figure 48E**).

[0488] The program was underexpressed in patients with clinical benefit (CB) compared to those without benefit (no-CB) (**Figure 48F**). Nevertheless, some patients with clinical benefit had high pre-treatment expression of the program. Applicants hypothesized that these patients might cease to respond quickly, due to pre-existing intrinsically resistant cells, like those Applicants observed in the single-cell cohort and in validation cohort 1. Indeed, among patients with clinical benefit, those with high expression of the program pre-treatment were significantly more likely to experience subsequent progressive disease (**Figure 48F**), and those with rapid progression (CB<6 months) had the highest scores of the program, even compared to those with no clinical benefit. Consistently, the program was most accurate in predicting patients with complete responses ($P < 6.31*10^{-3}$, one-sided t-test, **Figures 48G and 55F**), outperforming all the other predictors ($P = 1.64*10^{-8}$, Wilcoxon ranksum test), all

of which, including clinically-used markers and inferred T cell infiltration levels, failed to predict complete response (**Figure 48H**).

The immune resistance program is coherently controlled by CDK4/6

[0489] Applicants reasoned that the program could be a compelling drug target: it was identified by its association with a critical process – T cell exclusion – that affects resistance to immunotherapy; it is a significantly predictive biomarker of ICI resistance; and it appears to be coherently regulated, such that a shared control mechanism could be targeted to reverse it.

[0490] To this end, Applicants identified drugs that were significantly more toxic to cell lines overexpressing the immune resistance program (controlling for cancer types, **Methods**), according to the efficacy measures of 131 drugs across 639 human cancer cell lines (Garnett et al., 2012). The top scoring drug was a CDK4/6-inhibitor (palbociclib) ($P = 6.28*10^{-6}$, mixed-effects). Furthermore, the efficacy of CDK4/6 inhibition and the expression of the resistance program were also correlated in a study where the efficacies of CDK4/6 inhibitors palbociclib and abemaciclib were measured across a collection of cancer cell lines ($P = 7.15*10^{-6}$, mixed-effects) (Gong et al., 2017).

[0491] Applicants further hypothesized that CDK4 and 6 may act as the master regulators of the immune resistance program. First, both CDK4 itself and multiple CDK target genes, are members of the of the induced program (**Figure 45C**, **Table 5**). Second, the program is more pronounced in cycling cells (where CDK4/6 are active), both within the same patient group and among cells of the same tumor (**Figures 44E, 45C**, and **56A,B**, $P < 10^{-16}$, mixed effects model). Importantly, the program is not merely a proxy of the cell's proliferation state: there was no significant difference between the fraction of cycling cells in untreated *vs.* post-treatment tumors ($P = 0.696$, t-test), the program was nearly identical when identified only based on non-cycling cells, and – unlike the expression of the resistance program – the expression of cell cycle signatures was not associated with the efficacy of CDK4/6 inhibitors across the cell lines. Finally, Applicants analyzed recently published expression profiles (Goel et al., 2017) of breast cancer cell lines and *in vivo* mouse models and found that CDK4/6 inhibition by abemaciclib represses the program (**Figures 49A-C** and **56C**). Thus, multiple lines of evidence suggest that CDK4/6 inhibition could repress the expression of the immune resistance program and shift the cancer cell population to a less immune resistant state.

The immune resistance program can be intrinsically expressed and repressed by CDK4/6 inhibitors in melanoma cells

[0492] To test this hypothesis, Applicants studied the effect of abemaciclib on the immune resistance program in melanoma cell lines. Applicants selected three melanoma cell lines from the Cancer Cell Line Encyclopedia (Barretina et al., 2012) that exhibited strong expression of the resistance program (**Table 23**), two of which are RB1-sufficient (IGR37, UACC257) and one is RB1-deficient (A2058). Notably, these cells expressed the resistance program in the absence of microenvironmental cues, indicating the importance of intrinsic expression of this program in cancer cells. Applicants profiled each cell line with scRNA-seq before and after treatment with abemaciclib for 1 week (**Figures 49D-E**), analyzing over 23,000 cells in these and follow-up conditions (below).

[0493] **Table 23. The overall expression (OE) of the immune resistance signature across the CCLE melanoma cell lines.**

Melanoma cell line	Immune resistance OE
HMCB	0.818
LOXIMVI	0.72
UACC257	0.706
CHL1	0.698
IGR37	0.57
MELHO	0.522
COLO741	0.5
G361	0.476
COLO679	0.468
A2058	0.465
SKMEL3	0.443
GRM	0.431
SKMEL30	0.405
MEWO	0.371
A375	0.368
HS936T	0.339
K029AX	0.308
IPC298	0.261
IGR1	0.243
SKMEL1	0.238
SKMEL5	0.182
COLO783	0.174
COLO849	0.082
CJM	0.06
MELJUSO	0.049
COLO792	0.041
UACC62	0.015
MDAMB435S	0.005
IGR39	0
WM2664	-0.015

WM88	-0.045
HS944T	-0.053
RPMI7951	-0.067
WM983B	-0.09
WM1799	-0.091
A101D	-0.097
HS895T	-0.126
SKMEL28	-0.152
SH4	-0.226
RVH421	-0.227
HT144	-0.23
SKMEL2	-0.242
COLO800	-0.251
HS294T	-0.264
WM793	-0.265
HS852T	-0.341
HS934T	-0.368
COLO829	-0.377
HS839T	-0.386
C32	-0.427
HS940T	-0.434
HS688AT	-0.435
HS939T	-0.464
HS600T	-0.464
COLO818	-0.466
HS695T	-0.5
WM115	-0.513
MALME3M	-0.607
SKMEL31	-0.759
SKMEL24	-0.975

[0494] Consistent with the hypothesis, only in the RB-sufficient cell lines, abemaciclib dramatically decreased the proportion of cells overexpressing the immune resistance program and induced an immune response in the surviving cells. In the RB1-sufficient lines, IGR37 and UACC257, 10% of the cells had exceptionally strong expression of the immune resistance program ("immune resistant" cells) prior to treatment, decreasing to 2% and 1% of cells post-treatment, respectively ($P < 1*10^{-30}$, hypergeometric test) (**Figures 49D,E**). In contrast, in the RB1-deficient line A2058 the treatment did not repress the immune resistant state ($P > 0.5$, one-sided t-test), consistent with the hypothesis that the effects of CDK4/6 inhibitors are RB-dependent.

[0495] Moreover, in the two RB-sufficient lines, the remaining cells that underexpressed the immune resistance program, underwent substantial transcriptional changes, including the induction of key repressed component of the immune resistance program, such as the senescence-associated secretory phenotype (SASP). In particular, abemaciclib repressed the

expression of DNMT1 ($P < 2.23*10^{-106}$, likelihood-ratio test), consistent with previous observations (Goel et al., 2017) that CDK4/6 inhibition leads to DNMT1 repression, allowing the methylation of endogenous retroviral genes (ERVs), which in turn triggers a double-stranded RNA (dsRNA) response and stimulates type III IFN production (Goel et al., 2017). Following abemaciclib treatment there was also a higher portion of cells with induction of a MITF program (Tirosh et al., 2016a), which is repressed in "immune resistant" cells ($P < 3.33*10^{-15}$, hypergeometric test, **Figure 49D,E**).

[0496] In particular, abemaciclib induced SASP, which is a major repressed component in the resistance program. First, the SASP module was significantly induced at the transcriptional level ($P < 3.91*10^{-12}$, hypergeometric test, **Figures 49D,E**). Moreover, when Applicants measured 40 human cytokines and chemokines in the conditioned media of abemaciclib treated cancer cells, Applicants found it induced several secreted factors (**Figure 49F**), including macrophage inhibition factor (MIF), CX3CL1 (which induces migration and adhesion of T and NK cells and is linked to clinical outcomes in immunotherapy treatment (Herbst et al., 2014; Nelson and Muenchmeier, 2013)), and CCL20 (an important factor for T cell differentiation, which may enhance immunity in melanoma (Gordy et al., 2016)). Consistently, abemaciclib also induced alpha-galactosidase activity and morphological alterations that reflect cellular senescence (**Figure 49G**). Thus, unlike the mechanism described in breast cancer cells (Goel et al., 2017), abemaciclib might trigger SASP and cell differentiation in malignant melanoma cells. In line with this hypothesis, Applicants do not find significant cytotoxic effects of abemaciclib, but only a reduced rate of proliferation compared to DMSO (0.3 doublings/24 hrs vs. 0.64 doublings/24 hrs, $P < 0.0001$, two-tailed t test).

[0497] Finally, Applicants tested if the effect of abemaciclib treatment on malignant cells is impacted by the presence of tumor infiltrating lymphocytes (TILs) in a patient-derived co-culture model of melanoma cells and *ex vivo* expanded TILs from the same metastatic melanoma lesion. After treating the malignant cells with abemaciclib for one week, Applicants added autologous TILs to the cultures. Applicants compared scRNA-seq profiles between these melanoma cells to co-cultured cells without prior abemaciclib treatment cells with neither abemaciclib treatment nor co-culture with TILs. Exposure to TILs reduced the expression of the immune resistance program, both in the control and in the abemaciclib-treated cells ($P < 9.85*10^{-14}$, one-sided t-test). Abemaciclib further intensified these effects, as it further repressed the immune resistance program in both conditions (with and without

the exposure to TILs, $P < 3.60*10^{-7}$, one-sided t-test). Together with observations above, these results indicate that the resistance program can be intrinsically expressed and modulated by CDK4/6 inhibition and tumor-immune interactions.

[0498] Phased combination with CDK4/6 inhibitor enhances immune checkpoint blockade *in vivo.*

[0499] Applicants next sought to determine the efficacy of abemaciclib in promoting anti-tumor activity in a syngeneic mouse model. To determine the expression of the resistance signature identified in humans in commonly used immunocompetent mouse models of solid tumors, Applicants performed scRNA-seq on B16 (melanoma, relatively resistant to immune checkpoint inhibition), MC38 and CT26 cells (both colorectal cancer, partially sensitive to anti-PD1 and anti-CTLA-4 therapy, respectively). Applicants found strong expression of the resistance signature in B16 cells, while CT26 and MC38 had a mixture of high and low expressing cells, recapitulating their partial sensitivity to checkpoint inhibition. In line with results above, this analysis indicated that the resistance signature was strongly expressed in the absence of any microenvironmental cues. Next, Applicants tested whether addition of CDK4/6 inhibition could overcome resistance to immune checkpoint blockade *in vivo*. Applicants implanted B16 tumors in C57BL/6 mice and treated with either vehicle control, combination immune checkpoint blockade, abemaciclib monotherapy, or a combination of immune checkpoint blockade and abemaciclib with different dosing schedules (**Figure 58**). Compared to vehicle, abemaciclib monotherapy had no impact on the rate of tumor outgrowth, but when used in a phased combination (that is ICB followed by ICB plus abemaciclib), there was a strong reduction in the rate of developing tumors compared to all other groups, including ICB alone (**Figure 59**). Compared to vehicle, abemaciclib monotherapy had no impact on survival, but when used in a phased combination (that is ICB followed by ICB plus abemaciclib), there was a strong survival compared to all other groups, including ICB alone (**Figure 60**). Together, these results indicate that addition of abemaciclib may improve the sensitivity to immune checkpoint inhibitors, even in otherwise highly resistant models of immunotherapy. Future studies can pursue both the underlying mechanisms by which CDK4/6 inhibition is repressing the resistance program and sensitizing the tumor to immunotherapy, and could apply high throughput genetic screening methods to identify other regulators that repress the program.

Discussion

[0500] Most melanoma patients have either intrinsic or acquired resistance to ICI, yet the systematic characterization of molecular resistance mechanisms has been limited. Here, Applicants leverage clinical scRNA-seq data and multiple cohorts to map malignant cell states associated with resistance to ICI, revealing a coherently co-regulated program that may be therapeutically targeted to overcome immune evasion and suppression.

[0501] The malignant cell resistance program showed prognostic and predictive power in several independent ICI cohorts, including a large new clinically annotated cohort of patients with pre-treatment (anti-PD-1) biopsies profiled by RNA-seq. The program outperformed other published biomarkers in the space, and may help to prospectively stratify patients to clinical trials and therapies. Even though the program was initially derived, in part, based on associations with inferred T cell infiltration levels, unlike many other biomarkers, it has a significant predictive value beyond T cell infiltration.

[0502] The program Applicants uncovered is primarily associated with intrinsic ICI resistance. It is manifested also in malignant cells of untreated patients in the single-cell cohort, and in bulk RNA-seq data from three independent cohorts of untreated patients: TCGA, a longitudinal cohort of ICI-treated patients (validation cohort 1), and a cohort of 112 pre-ICI patients (validation cohort 2). Among single cells of pre-treated patients, a subset (20.9% cells from 10 different patients) already overexpresses the program. In bulk samples collected before and after ICI, inter-patient variation exceeded intra-patient variation, further supporting an intrinsic role. In 112 melanoma patients, this pre-ICI inter-patient variation is tightly associated with ICI responses. Notably, while the resistance signature was derived from scRNA-seq data in patients with prior treatment with either monotherapy (anti-CTLA-4 or anti-PD1) or a combination, it validated in previously published and newly added data sets of patients who were treated with any immune checkpoint inhibitor. Finally, the program is more pronounced after ICI failure, but not post targeted therapy as Applicants show in previously published data sets (Hugo et al.) and validation cohort 1 in this study., and thus it is unlikely to merely reflect the impact of any therapeutic intervention. However, whether the ICR signature may be more pronounced in RAF/MEK-resistant melanoma cannot be conclusively determined from these, and should be addressed in future work. This may be of particular clinical interest for patients with RAF/MEK-resistant melanoma, who appear to be less likely to respond to subsequent therapy with ICI (Ackerman et al., 2014).

[0503] Some of the concepts established for drug resistance to targeted cancer therapies with RAF/MEK-inhibitors in melanoma may also be applicable to immunotherapies. Similar

to the presence of a small sub-population of cells expressing a MITF-low program, which confers resistance to RAF/MEK-inhibitors, and rises in frequency under the pressure of a drug (Shaffer et al., 2017; Tirosh et al., 2016a, Hangauer et al., 2017; Viswanathan et al., 2017), patient tumors who have not been treated with ICI contain some cells expressing the immune resistance program. It is plausible that these cells are responsible for either intrinsic resistance to ICI or lie in protected niches, and thus emerge in the context of ICI resistance. Selective targeting of these cells in combination with ICI may delay or prevent ICI resistance.

[0504] Applicants have focused on malignant cells, but T cell states or clones, beyond their extent of infiltration, might also predict the success of ICI. Within the limitation of the unmatched single-cell cohort, comparing the individual T cells of untreated *vs.* post-treatment (resistant) patients, suggested that treatment has activated the T cells and caused their expansion (data not shown). While Applicants cannot rule out the presence of other intrinsic T cell dysfunction mechanisms, this is consistent with a model where, at least partly, malignant cells cause ICI resistance despite at least some T cell functionality.

[0505] Because of the potential functional role of the program and its coherent underlying regulation, compounds that repress it may sensitize malignant cells to immunotherapy and/or T-cell mediated killing (**Figure 50**), especially in patients with a high intrinsic (pre-ICI) expression of the immune resistance program. Based on a systematic analysis of drug efficacies and the program features Applicants hypothesized that CDK4/6 inhibition could have such a sensitizing effect, and tested this in malignant melanoma cell lines and in co-cultures of patient cells with autologous TILs. CDK4/6 inhibition reversed the resistant transcriptional state: subpopulations of highly immune resistant cancer cells were dramatically reduced, either because the drug selectively eradicated them or because it triggered them to adopt a less immune resistant state. In parallel, CDK4/6 inhibition triggered the melanoma cells to adopt a senescent-like phenotype accompanied by secretion of key chemokines, which have been previously shown to enhance T cell responses (Gordy et al., 2016; Herbst et al., 2014; Nelson and Muenchmeier, 2013). Phased combination of ICB with abemaciclib reduced the rate of tumor outgrowth in an otherwise ICB-resistant syngeneic mouse model (B16), which exhibits strong intrinsic expression of the resistance program, indicating that this may be a potential therapeutic avenue for patients with intrinsic or acquired resistance to immune checkpoint inhibition.

[0506] The malignant resistance programs may be relevant in other subtypes of melanoma as well as in other tumor types. Among different types of melanoma, uveal melanoma has more active resistance programs compared to cutaneous melanoma (**Figure 46A**); across cancers, the immune resistance program is lower in some of the more responsive tumors (head and neck, kidney, skin, lung) and higher in tumor types that are less responsive to immunotherapy and/or arise from immune-privileged tissues (eye, testis) (**Figure 57**). Interestingly, synovial sarcoma, which is driven by a single genomic aberration in the BAF complex, has the highest resistance scores. The BAF complex has been recently shown to play a key role in resistance to ICI immunotherapy (Miao et al., 2018; Pan et al., 2018). While this pan-cancer analysis is intriguing, it may still be impacted by the composition of the tumor microenvironment, which is challenging to control without single-cell data.

[0507] Future similar studies of other tumors could apply the approach to identify other tumor-specific resistance programs. For example, Applicants performed such analysis with the recent head and neck cancer single cell cohort (Puram et al., 2017) and found that CAFs in cold tumors overexpressed genes up-regulated by TGFB1 ($P = 1.70*10^{-7}$, hypergeometric test). Indeed, TGFB1 and TGFB signaling has been recently shown to be highly associated with lack of response to anti-PD-L1 treatment in urothelial cancer patients (Mariathasan et al., 2018). In line with the findings, co-administration of TGFβ-blocking and anti-PD-L1 has been shown to modulated the tumor CAFs, which in turn facilitated T cell infiltration and tumor regression in mouse models (Mariathasan et al., 2018).

[0508] Overall, the analysis sheds light on the way cells shape and are being shaped by their microenvironment in tumors, and the approaches can be applied in other tumors to systematically map immune resistant malignant cell states, uncover improved biomarkers for patient selection, and reveal principles for the development of new therapeutics.

Example 10 – Mechanisms of Immune Resistance and Immunotherapy Resistance Signature

[0509] Immune checkpoint inhibitors (ICI) have transformed the therapeutic landscape of several cancer types (Sharma and Allison, 2015), especially in melanoma. Nonetheless, many patients manifest resistance, which is often intrinsic (Sharma et al., 2017). Because ICI targets cell-cell interactions, resistance can stem from different cells and their interactions in the tumor ecosystem. Recent studies illuminated ICI resistance with Whole Exome Sequencing (WES) and transcriptional profiles of bulk tumors (Hugo et al., 2016; Riaz et al.,

2017; Van Allen et al., 2015), but had limited ability to dissect the cancer-immune interplay and generate reliable response biomarkers. Single-cell RNA-seq (scRNA-seq) of patient tumors (Tirosh et al., 2016) can alleviate this limitation.

[0510] Infiltration of the tumor with T cells has been associated with patient survival and improved immunotherapy responses (Fridman et al., 2012), but the determinants that dictate if a tumor will have high ("hot") or low ("cold") levels of T cell infiltration are only partially understood. Among multiple factors, malignant cells may play an important role in determining this phenotype. However, while current methods use bulk genomics to deconvolve the tumor's composition (Newman et al., 2015), they cannot recover the salient intracellular programs of malignant cells. Hence linking malignant cell states to T cell infiltration levels has been challenging.

[0511] Here, using an integrative data-driven approach (**Figure 62A,B**), Applicants identified a malignant cell program that is associated with T cell exclusion and is predictive of ICI resistance. Applicants demonstrated that CDK4/6 inhibitors repress this program and sensitize melanoma tumors to ICI in mouse models. This work provides a predictive biomarker for ICI response, suggests a new therapeutic modality that may sensitize melanoma tumors to ICI, and provides a framework to study cell-cell interactions and drug effects in other tumor ecosystems.

RESULTS

Systematic approach to discover cancer cell-autonomous programs associated with T cell exclusion

[0512] To identify malignant cell programs that characterize "cold" tumors, Applicants combined scRNA-seq and bulk RNA-Seq data to relate the state of one cell type to the tumor composition (**Figure 62B**, **Methods**). Applicants describe the strategy in a specific context, but it can be applied to other pairs of cell types. First, Applicants use scRNA-seq profiles to define cell type specific signatures of T cells and malignant cells in melanoma. Using the T cell signature and bulk RNA-Seq profiles, Applicants infer T cell infiltration levels in hundreds of tumors. Applicants then define a "seed exclusion program": genes from the malignant cell signature whose expression is strongly correlated (positively or negatively) with T cell abundance across those bulk tumors. To avoid mRNA contamination by the tumor microenvironment Applicants restrict the seed program only to a few hundred genes that are exclusively expressed by malignant cells. To recover potentially important genes which are also expressed by non-malignant cells (*e.g.*, MHC class I), Applicants search for

genes that are correlated with the seed program across the malignant cells in the scRNA-seq data, irrespective of their expression in other cell types. Finally, Applicants define a genome-scale, malignant-cell exclusion program, consisting of genes induced or repressed by malignant cells in "cold" *vs.* "hot" tumors. Applicants then score each cell or tumor based on its Overall Expression (OE) of the program, defined as the overexpression of its induced part and underexpression of its repressed part (**Methods**).

Analysis of clinical scRNA-seq identifies a malignant cell program associated with T cell exclusion

[0513] Applicants applied the approach to 7,186 high-quality scRNA-seq profiles from 33 human melanoma tumors (from 31 patients), comprised of 2,987 cells from 17 newly collected patient tumors, and 4,199 cells from 16 patient tumors that Applicants previously reported (Tirosh et al., 2016) (**Figure 62A, Tables 24A** and **25, Methods**; one patient overlaps), along with 473 bulk RNA-seq melanoma profiles from The Cancer Genome Atlas (TCGA) (Akbani et al., 2015). Fifteen of the tumors in the single-cell cohort are post-ICI resistant tumors (**Table 24A**).

[0514] Applicants distinguished different cell subsets based on their expression profiles and inferred Copy Number Variation (CNV) profiles (**Methods**), identifying: malignant cells, $CD8^+$ and $CD4^+$ T cells, B cells, NK cells, macrophages, Cancer Associated Fibroblasts (CAFs) and endothelial cells (**Figures 62C,D and 69, Table 26**). Malignant cells primarily grouped by their tumor of origin (**Figure 62C**), and non-malignant cells by their cell type (**Figure 62D**), as Applicants previously observed (Tirosh et al., 2016).

[0515] Applicants applied the approach to delineate the relationship between malignant cell states and $CD8^+$ T cell infiltration, identifying a T cell exclusion program (**Figure 62E**, **Table 27A**). The repressed part of the program was enriched for genes involved in antigen processing and presentation (*e.g.*, *B2M*, *CTSB*, *HLA-A/B/C*, *TAPBP*, $P = 3.26*10^{-10}$, hypergeometric test), IFN-γ signaling pathways ($P = 2.94*10^{-9}$), response to the complement system ($P = 1.13*10^{-8}$, *e.g.*, *CD59* and *C4A*), and immune modulation ($P = 2.10*10^{-7}$, *e.g.*, *CD47* and *CD58*). The induced part included *CDK4* and its downstream E2F targets ($P = 3.97*10^{-5}$), transcriptional regulators (*e.g.*, *SOX4, SMARCA4*), and numerous CDK7 and Myc targets ($P < 1*10^{-17}$; **Table 27A**). Notably, the malignant cell programs associated with exclusion of different T cell subsets were highly overlapping (**Figures 70A-C**, **Tables 26B** and **27B**, **Methods**).

The exclusion program characterizes malignant cells from patients who progressed on immunotherapy

[0516] To determine whether the exclusion program is associated with ICI resistance, Applicants tested if it is more pronounced in malignant cells from ICI resistant *vs.* untreated patients in the scRNA-seq cohort. As clinical response rates to ICI vary, with up to ~57% responders to ICI combinations (Larkin et al., 2015), the untreated tumors Applicants profiled likely include both ICI sensitive and ICI resistant ones, whereas the ICI resistant tumors likely include mostly resistant malignant cells. Comparing malignant cells from post-ICI resistant tumors to malignant cells from untreated tumors, Applicants found a robust and generalizable post-treatment transcriptional program (cross-validation AUC=0.83; **Figure 63A**, **Table 27A**, **Methods**). This program might reflect both the overall impact of ICI therapy and intrinsic ICI resistance *per se*, but those cannot be distinguished based on the single-cell cohort, which neither includes matched samples from the same patient nor pre-treatment tumors from responders and non-responders. Applicants address this later in two validation cohorts (**Tables 24B-C**).

[0517] The post-treatment and exclusion programs substantially overlapped (**Figures 62E** and **63B,C**, **Table 27A**; $P < 10^{-16}$, hypergeometric test) and highlighted similar modules and pathways (**Figure 63D**, **Table 28**). Both programs were more pronounced in the post-treatment malignant cells, and robustly classified malignant cells as untreated or post-treatment (AUC = 0.83 and 0.81 for cross- validation post-treatment and exclusion, respectively, **Figure 63A,E**). The upregulated components of both programs include 46 ribosomal protein (RPs) genes, but their overlap remains significant even after removing RPs ($P < 10^{-16}$, hypergeometric test, **Figure 63B**). As Myc is a master regulator of ribosome biogenesis (Kress et al., 2015), the induced RP genes might reflect Myc activation. Indeed, the programs are enriched for Myc targets, even after removing RP genes ($P < 7.18*10^{-10}$), and are predicted to be repressed by MYC knockdown according to the Connectivity map (Subramanian et al., 2017).

[0518] In light of the congruence of the programs, Applicants defined a unified immune resistance program as the union of the post-treatment and exclusion programs (**Table 27A**), and used it in all subsequent analyses, unless indicated otherwise (**Methods**).

The immune resistance program reflects a coherent state of immune evasion

[0519] The immune resistance program manifests hallmarks of immune evasion, suppression and exclusion. First, compared to cutaneous melanoma (where Applicants

initially identified it), the program is more pronounced in uveal melanoma (**Figure 64A**), which resides in an immune-privileged environment and has very low response rates to immunotherapy (Algazi et al., 2016). Second, inhibition of genes from the repressed component of the program in malignant melanoma cells conferred resistance to $CD8^+$ T cells in a genome-wide CRISPR screen ($P = 1.67*10^{-3}$, hypergeometric test) (Patel et al., 2017). Third, the program marks the suppression of physical interactions between resistant malignant cells and other cell types in the tumor microenvironment, including MHC I:TCR (T cells), *CD58:CD2* (T cells), and *IL1RAP:IL1B* (macrophages) (**Figure 64B**, **Methods**), and of the Senescence Associated Secretory Phenotype (SASP) ($P = 4.3*10^{-166}$ and $3.6*10^{-3}$, one-sided t-test and mixed-effects, respectively, **Figure 63D**), which has been shown to enhance T cell responses (Gordy et al., 2016).

[0520] The program's genes appear to be under shared control by a few master regulators. The expression of genes within each components (induced or repressed) is positively correlated, while the induced genes are anti-correlated with the repressed genes, both across single cells in one tumor and across TCGA tumors (**Figures 64C,D** and **71**). Thus, any given aspect of the program (*e.g.*, under-expression of antigen presentation) is coupled to the state of the entire program. Moreover, there is a significant overlap between the perturbations that reverse the expression of the program's repressed and induced components ($P = 4.35*10^{-6}$, hypergeometric test), including the overexpression of IFN-γ and IFN-β and the knockdown of *MYC* and *CDK7* (Subramanian et al., 2017). The latter mirrors the significantly large number of Myc and CDK7 (direct) targets (Oki et al., 2018; Subramanian et al., 2005) in the program ($P < 1*10^{-17}$, hypergeometric test). Further supporting the role of CDKs as regulators, the program is more pronounced in cycling cells, albeit present and detectable in non-cycling cells (**Figures 62E,** $P < 8.42*10^{-27}$, mixed-effects). Notably, the association between cellular proliferation and the resistant program is only partial, and the two cell states can be decoupled (**Methods**, **Table 27B**, **Figures 70D-H**).

[0521] Applicants compared the immune resistance program to 12 signatures (**Table 29**) previously associated with the response to immunotherapy (Ayers et al., 2017; Hugo et al., 2016; Riaz et al., 2017) or targeted therapy (RAF and MEK inhibitors) (Hugo et al., 2015; Tirosh et al., 2016) in melanoma patients. Four of the six signatures that characterize immunotherapy sensitive melanoma were enriched with one or more of the T cell signatures

($P < 1*10^{-3}$, hypergeometric test), suggesting that they capture tumor composition and not malignant cell states. The induced component of the resistance program was not enriched in any of the previous 12 signatures. The repressed component was enriched in two signatures of immunotherapy sensitivity ($P < 2.65*10^{-3}$, hypergeometric test), and with signatures associated with sensitivity and resistance to targeted therapy ($P < 1.48*10^{-4}$) (Tirosh et al., 2016).

Malignant cells in T cell-depleted niches express features of the resistance program *in situ*

[0522] To test if the resistance program in malignant cells is associated with T cell exclusion *in situ*, Applicants used multiplexed immunofluorescence (t-CyCIF) (Lin et al., 2018). Applicants stained histological sections of 19 tumors (472,771 cells/image on average) from the single-cell cohort for 14 proteins: six cell type markers (CD3, CD8, MHC-II, FOXP3, S100, and MITF) and seven resistance program members (induced: p53, Myc, DLL3; repressed: HLA-A, c-Jun, SQSTM1, LAMP2). Following cell segmentation and intensity quantification (**Methods**), Applicants assigned malignant cells ($S100^+$, $MITF^+$), T cells ($CD3^+$) and cytotoxic T cells ($CD8^+$); the rest were defined as uncharacterized.

[0523] The scRNA-seq and multiplex *in situ* protein profiles were congruent by cell type assignment and by resistance program assessment. First, combining the two data sets using a variant of canonical correlation analysis (CCA) (Butler and Satija, 2017) (**Methods**) successfully embedded and clustered cells primarily by type and not by method (**Figures 65A,B** and **72**). Second, the average immune resistance scores of the different tumors according to their *in situ* images were correlated with their scores according to scRNA-seq ($R = 0.57$, $P = 0.041$) (**Methods**), even though the scRNA-seq and the *in situ* image of each tumor were obtained from separated specimens, measuring RNA *vs.* protein, respectively. Additionally, in both cases, the inter-tumor variation of the program was significantly greater than its intra-tumor variation ($P < 1*10^{-30}$, ANOVA).

[0524] As predicted, the resistance score Applicants computed from all seven program markers (**Methods**) was significantly higher in malignant cells that reside in cold niches ($P = 1.18*10^{-6}$, mixed-effects). Aside from LAMP2, individual markers also showed the predicted trend: Malignant cells in cold niches had significantly lower levels of markers repressed in the resistance program (**Figures 65C-D**, $P = 1.41*10^{-13}$ and $8.35*10^{-18}$, mixed-effects, for c-Jun and HLA-A, respectively), whereas p53 (induced in the resistance program)

characterized cold niches ($P = 5.25*10^{-3}$, mixed-effects). Thus, this analysis validates the signature and its association with cold niches at the protein level *in situ*.

The resistance program is expressed prior to treatment and is enhanced following immunotherapy in resistant lesions

[0525] Applicants hypothesized that the immune resistance program, while more pronounced in the malignant cells of resistant patients after ICI, in fact reflects intrinsic resistance. Supporting this, the program is detected in untreated TCGA melanoma tumors and in a subset of malignant cells from untreated patients (**Figures 62E** and **63C**, right plots).

[0526] To test this hypothesis, Applicants analyzed an independent RNA-Seq cohort of 90 specimens collected from 26 metastatic melanoma patients throughout the course of treatment. Fourteen patients received ICI therapy (anti-PD1 or anti-CTLA4) without prior targeted therapy, and 12 patients first received targeted therapy (BRAF/MEK inhibitors) followed by ICI after tumor progression (**Figure 62A**, **Table 24B**, **validation cohort 1**). The cohort has several partially overlapping sets (**Table 24B**): treatment naïve (n = 18), on targeted therapy (n = 17), post targeted therapy (n = 25), on ICI (n = 35), and post-ICI (n = 50). Given this composition, Applicants used a mixed-effects model to determine the effects of the different treatments. As expected, Applicants found a significant induction in the (inferred) T cell fraction of tumors on ICI treatment ($P = 1.85*10^{-3}$, mixed-effects test), but not on targeted therapy.

[0527] The program was induced in on- and post-ICI samples compared to pre-ICI samples from the same patient ($P = 7.41*10^{-3}$, mixed-effect test, controlling for tumor composition; **Methods**). However, inter-patient variation in the program's expression was significantly higher than these intra-patient changes ($P < 4.98*10^{-14}$, ANOVA). This suggested that the major differences between the post-ICI and untreated tumors in the single-cell cohort reflect, at least in part, intrinsic differences between the two groups, which preceded the treatment.

[0528] Applicants did not observe an induction of the program following RAF/MEK-inhibition. Applicants confirmed this in another cohort of patient-matched melanoma tumors biopsied before MAPK-inhibition and during disease progression (Hugo et al., 2015) ($P > 0.1$, mixed-effects).

The resistance program predicts ICI responses in melanoma patients

[0529] Next, Applicants used the Overall Expression (OE) of the program (with and without an additional refinement, **Table 27A**, **Methods**) to estimate the immune resistance

level of a given tumor, and tested its ability to predict clinical outcomes (**Figures 66, 73 and 74**).

[0530] The program's expression was associated with poor survival in 473 TCGA melanoma patients (**Figures 66A** and **73**), also when controlling for tumor purity and inferred T cell infiltration. Combining the program with inferred T cell infiltration levels yielded significantly more accurate predictions than either alone ($P = 9.1*10^{-8}$, COX regression, **Figure 66A**, **right**). Other proposed mechanisms, such as de-differentiation of melanoma cells reflected by an MITF-low state, and other malignant cell signatures (Tirosh et al., 2016), were not associated with survival, indicating that mere biological variation across malignant cells is insufficient for prognosis.

[0531] To test if the program can predict clinical responses to ICI, Applicants analyzed five RNA-Seq cohorts collected from melanoma patients prior to ICI treatment: Validation cohort 2 collected by us across 112 patients (validation cohort 2; **Figure 62A**), Validation Cohort 1 (pre-ICI samples; **Figure 62A**), and three published cohorts of less than 50 patients each (Hugo et al., 2015; Riaz et al., 2017; Van Allen et al., 2015). Applicants compared the predictors to 47 other gene signatures (**Table 29**, **Methods**), which Applicants tested as alternative predictors, including: commercial immune panels, the top hits of two CRISPR screens of resistance to T cells and anti-PD-1 (Manguso et al., 2017; Patel et al., 2017), and signatures generated by analyzing previous melanoma ICI cohorts (Hugo et al., 2016; Riaz et al., 2017).

[0532] The program's expression distinguished ICI responders from non-responders (**Figures 66B,C**). In a lung cancer mouse model, its expression early on-treatment separated anti-CTLA-4 non-responders from responders ($P = 4.89*10^{-7}$, one-sided *t*-test, **Figure 66B**) (Lesterhuis et al., 2015). In 27 melanoma patients treated with Pembrolizumab (anti-PD-1) (Hugo et al., 2016), underexpression of the program pre-treatment distinguished the five complete responders ($P = 5.80*10^{-3}$ and $1.89*10^{-2}$, one-sided *t*-test, refined and non-refined version, respectively, **Figure 66C**). In 42 melanoma patients treated with CTLA-4 blockade using Ipilimumab (Van Allen et al., 2015), it was lower in the two complete responders pre-treatment. In 43 melanoma patients profiled before and early on treatment with Nivolumab (anti-PD-1) (Riaz et al., 2017), it was down- regulated early on-treatment specifically in responders ($P < 9.60*10^{-6}$, hypergeometric test). However, in this specific cohort, the pre-treatment expression of the program (and of all other alternative predictors) was not associated with response, possibly due to the small number (3) of complete responders. In

validation cohort 1, the program was under-expressed in the 7 pre-ICI samples from patients with an objective response (OR, including partial or complete response; in some examples OR is also referred to as CB, clinical benefit) compared to 12 pre-ICI samples from non-responders (progressive disease; $P = 7.88*10^{-3}$, one-sided t-test).

[0533] Finally, Applicants tested the predictive value of the program in 112 patients with metastatic melanoma who underwent a pre-treatment biopsy and RNA-Seq followed by anti-PD-1 therapy (**Figure 62A**, **validation cohort 2**, **Tables 24C**). Applicants evaluated the program's performance in predicting **(1)** progression-free survival (PFS, available for 104 patients; **Figure 66D**), **(2)** objective response (OR, including partial or complete response; **Figure 66E**), and **(3)** complete response (**Figure 66F**; **Methods**).

[0534] The program was predictive of PFS (**Figures 66D** and **74**), including when accounting for other potential biomarkers (T cell infiltration levels and PD-L1 expression) (**Figure 74E**). It outperformed all the alternative predictors Applicants tested (**Table 29**, $P = 1.75*10^{-8}$, Wilcoxon-ranksum test), which were either not predictive or did not provide additional predictive value once accounting for T cell infiltration levels of the tested tumors (**Figure 66G**). Although the program was more pronounced in cycling cells, cell cycle alone was not associated with PFS ($P > 0.25$, COX regression), nor was a signature of malignant-specific genes that characterizes cycling malignant cells ($P > 0.05$, COX regression). Filtering the cell-cycle component from the resistance program score (**Methods**) further improved PFS predictions (**Figure 66D**), suggesting that a tumor's immune resistance profile should be evaluated conditioning on its proliferation level.

[0535] The program was strongly underexpressed in patients with OR compared to those without response (PD, progressive disease) (**Figure 66E**). Moreover, patients with OR that nonetheless had high pre-treatment expression of the program were significantly more likely to rapidly (<6 months) develop progressive disease (**Figure 66E**). Consistently, the program was most accurate in predicting complete responses ($P = 1.34*10^{-4}$, one-sided t-test, **Figure 66F**), outperforming all other tested predictors ($P = 1.24*10^{-7}$, Wilcoxon ranksum test) (**Figure 66H**).

The resistance program is coherently controlled by CDK4/6

[0536] Next, Applicants sought to pharmacologically target the program. Applicants first identified drugs that were significantly more toxic to cell lines intrinsically overexpressing the program in a screen of 131 drugs across 639 human cell lines (**Methods**) (Garnett et al., 2012). The 3rd highest scoring drug was the CDK4/6 inhibitor (CDK4/6i) palbociclib (P =

$1.01*10^{-4}$, mixed-effects). Applicants confirmed this in another screen of two CDK4/6i (palbociclib and abemaciclib) across hundreds of cell lines (Gong et al., 2017) ($P = 3.96*10^{-5}$, mixed-effects, **Figure 67A**).

[0537] Applicants hypothesized that CDK4/6 may act as master regulators of the program. Multiple CDK target genes are members of the induced program (**Table 27A**), and CDK4 is a member of the induced component of both the exclusion and the post-treatment programs (**Figures 62E, 63C**). Three genes (*CDKN2C*/p18, *CDKN1B*/p27, *CDKN1A*/p21) that inhibit CDK4 represses the program when overexpressed (Subramanian et al., 2017) (**Methods**), and the program is more pronounced in cycling cells (**Figures 62E**, **63C**, and **70E**), where CDK4/6 are active. Finally, analysis of published gene expression profiles of breast cancer cell lines and mouse models (Goel et al., 2017) showed that CDK4/6i represses the resistance program (**Figures 67B-D**).

CDK4/6 inhibitors repress the resistance program in melanoma cells

[0538] Applicants therefore tested if CDK4/6i could shift the malignant cell population to a less immune resistant state. Applicants selected three melanoma cell lines that strongly expressed the program (**Table 30A**), two of which are RB1-sufficient (IGR37, UACC257) and one is RB1-deficient (A2058). Applicants profiled each cell line with scRNA-seq before and after treatment with abemaciclib, analyzing >23,000 cells (**Figures 67E,F**, **Table 25**). The program's expression varied between cells within each line, despite the absence of non-malignant cells, suggesting cell intrinsic regulation (**Figures 67E,F panel 4**). In the RB-sufficient cell lines, IGR37 and UACC257, 10% of cells had exceptionally strong expression of the program ("immune resistant" cells) prior to treatment. Post-treatment the relative abundance of these cells decreased to 2% and 0.6% of the total population, respectively (**Figures 67E,F panel 4**). In the RB1-deficient cell line A2058 the treatment did not repress the resistant state, consistent with the fact that the impact of CDK4/6i is RB1-dependent (Goel et al., 2017) (**Figure 75A**). In the two RB-sufficient cell lines, post-treatment cells showed substantial transcriptional changes linked to the resistance program. Abemaciclib induced the MITF program (Tirosh et al., 2016) ($P < 1*10^{-17}$, hypergeometric test, **Figures 67E,F**, **panel 5**), which is repressed in "immune resistant" cells and is associated with melanocytic differentiation. Abemaciclib also repressed the expression of DNMT1 ($P < 2.23*10^{-106}$, likelihood-ratio test, **Figures 67E,F**, **panel 7**), which has been shown to confer an immunogenic phenotype (Goel et al., 2017).

[0539] Expression of the SASP – a repressed component in the resistance program – was induced in abemaciclib-treated cells ($P < 3.33*10^{-16}$, hypergeometric test, **Figures 67E,F**, **panel 6**). Abemaciclib also increased cytokine secretion (**Figure 67G, Table 30B**), β-galactosidase activity, and morphological alterations that reflect cellular senescence (**Figure 67H**). It reduced proliferation rates compared to DMSO (0.3 vs. 0.64 doublings/24 hours, $P < 1*10^{-4}$, t-test; **Figures 67E,F**, **panel 3**), but was not cytotoxic.

[0540] Next, Applicants tested abemaciclib effects on malignant cells in the presence of tumor infiltrating T lymphocytes (TILs) in a patient-derived co-culture of melanoma cells and autologous *ex vivo* expanded TILs. While TIL exposure alone represses the immune resistance program in both conditions ($P < 7.94*10^{-7}$, one-sided t-test), this effect was smaller compared to the intrinsic variation between cells of the same cell line (IGR37, **Figure 67E, panel 4**, $P < 8.17*10^{-12}$, F-test). Treatment with abemaciclib alone or with additional TIL exposure significantly repressed the resistance program ($P < 7.72*10^{-3}$, one-sided t-test, **Figure 75B**). Overall, these results indicate that the resistance program is mostly intrinsically regulated, and can be repressed by CDK4/6i.

CDK4/6 inhibition enhances ICI efficacy *in vivo*

[0541] To determine abemaciclib's efficacy in promoting anti-tumor activity *in vivo*, Applicants tested its effect in the context of ICI therapy in the B16 melanoma model, which is relatively resistant to immune checkpoint inhibitors (Curran et al., 2010). scRNA-seq of B16, MC38 and CT26 cell lines *in vitro* showed that the resistance program is intrinsically expressed in most B16 cells, but only in a portion of CT26 and MC38 cells (**Figures 75C,D**), corresponding to the responses of these models to ICI *in vivo*. Applicants implanted B16 tumors in C57BL/6 mice and treated with different therapy arms (**Figure 68A**). Compared to vehicle, abemaciclib monotherapy had no impact on the rate of tumor outgrowth, but when used in a phased combination (ICI followed by ICI plus abemaciclib), there was a significant reduction in the rate of tumor outgrowth and improved survival (**Figures 68B,C**). Depletion of $CD8^+$ T cells resulted in loss of the beneficial effect of phased combination therapy (**Figures 75E,F**) and the effect was at least in part RB-dependent in the malignant cells (data not shown). Thus, abemaciclib may sensitize melanoma tumors to immunotherapies, even in the case of intrinsic resistance.

DISCUSSION

[0542] By leveraging clinical scRNA-seq data and multiple patient cohorts, Applicants mapped malignant cell states associated with ICI resistance, revealing a coherent program that has a prognostic and predictive value and may be therapeutically targeted.

[0543] The program predicted ICI responses in several independent cohorts, outperforming other published signature-based biomarkers. Unlike the program described herein, many of the existing biomarkers capture the tumor composition, and do not have an additive predictive value once accounting for the inferred T cell levels. The program described herein predicts responses to anti-PD-1, and to some extent also to anti-CTLA-4 therapy, yet additional studies are required to dissect treatment-specific effects and predict ICI in all patients/cohorts.

[0544] The program is primarily associated with intrinsic ICI resistance. It is observed in bulk RNA-Seq of untreated tumors, and in a subset of ~24% of malignant cells of ~80% of untreated tumors. Applicants predict that these malignant cells will have a selective advantage during ICI treatment. Indeed, the program is more pronounced after ICI failure, but not post targeted therapy, indicating that it does not merely reflect the impact of any therapeutic intervention.

[0545] By integrating scRNA-seq and *in situ* images of matched tissue slides Applicants showed that the program is robustly detected and consistent across data modalities and patient samples, and is associated with cold niches within tumors. A key question is whether the program merely captures the response of malignant cells to immune infiltrates, or marks an intrinsic mechanism that allows malignant cells to escape immunity and shape their microenvironment. As Applicants show, the program expression varies across malignant human cell lines, which are not exposed to cues from non-malignant cells. Such intrinsic expression *in vitro* across mouse cell lines is aligned with their *in vivo* response to ICI.

[0546] Compounds that repress the program may sensitize malignant cells to immunotherapy and T-cell mediated killing (**Figure 68D**). Applicants demonstrated that a CDK4/6i reverses the resistant cell state, induces SASP, and improves responses to ICI *in vivo*. These mechanisms are distinct from previously described immune enhancing mechanisms of CDK4/6i (Deng et al., 2018; Goel et al., 2017), and indicate a potential role of CDK4/6, and specifically CDK4, as one of the master regulators of the program. Thus, CDK4/6i administered in a phased fashion, could potentially alleviate ICI resistance in some melanoma patients, consistently with a recent observation (Schaer et al., 2018). More

generally, the program's repression *in vitro* could be a readout to screen for other compounds that sensitize melanoma tumors to ICI.

[0547] The program may be relevant in other tumor types. It is lower in some of the more ICI-responsive tumors (kidney, skin, lung) and higher in tumor types that are less responsive and/or arise from immune-privileged tissues (eye, testis) (**Figures 75G,H**). Synovial sarcoma, which is driven by a single genomic aberration in the BAF complex, has the highest resistance scores. The BAF complex plays a key role in ICI resistance (Pan et al., 2018), and one of its subunits (SMARCA4) is up-regulated in the resistance program.

[0548] While Applicants focused on malignant cell-intrinsic mechanisms, Applicants also tested for association of T cell abundance with the state of macrophages and B cells (**Table 27C**). Applicants found a significant association only with macrophages: In cold niches/tumors, macrophages underexpress PD-L2, MHC class II genes ($P < 1*10^{-17}$, hypergeometric test), and IFN-γ response genes ($P = 9.76*10^{-10}$), and up-regulate immunosuppressants, such as hypoxia genes ($P = 4.55*10^{-6}$) and IL-8. Unlike the malignant cell program, the macrophage program was not associated with ICI resistance. Hence, it may represent the response of macrophages to T cell abundance, rather than a cause of T cell exclusion.

[0549] Overall, the work sheds light on the interplay between cells and their microenvironment in tumors, uncovers improved biomarkers for patient selection, and reveals principles for new therapeutics.

[0550] **Table 24.** Clinical characteristics of the patients and samples in **(A)** the scRNA-seq cohort, and in **(B-C)** the validation cohorts; related to **Figure 62**.

Table 24A

Discovery cohort: scRNA-seq								
Cohort	**Sample**	**Patient**	**Age**	**Sex**	**Treatment**	**Treatment group**	**Lesion type**	**Site**
Tirosh et al. 2016	Mel53	Mel53	77	F	None	Untreated	metastasis	Subcutaneous back lesion
	Mel58	Mel58	83	M	Ipilimumab	Post-ICI (resistant)	metastasis	Subcutaneous leg lesion
	Mel60	Mel60	60	M	Trametinib, ipilimumab	Post-ICI (resistant)	metastasis	Spleen
	Mel71	Mel71	79	M	None	Untreated	metastasis	Transverse colon
	Mel72	Mel72	57	F	IL-2, nivolumab, ipilimumab + anti-KIR-Ab	Post-ICI (resistant)	metastasis	External iliac lymph node
	Mel74	Mel74	63	M	Nivolumab	Post-ICI (resistant)	metastasis	Terminal Ileum
	Mel75	Mel75	80	M	Ipilimumab +	Post-ICI	metastasis	Subcutaneous

					nivolumab, WDVAX	(resistant)		leg lesion
	Mel78	Mel78	73	M	WDVAX, ipilimumab + nivolumab	Post-ICI (resistant)	metastasis	Small bowel
	Mel79	Mel79	74	M	None	Untreated	metastasis	Axillary lymph node
	Mel80	Mel80	86	F	None	Untreated	metastasis	Axillary lymph node
	Mel81	Mel81	43	F	None	Untreated	metastasis	Axillary lymph node
	Mel82	Mel82	73	F	None	Untreated	metastasis	Axillary lymph node
	Mel84	Mel84	67	M	None	Untreated	primary tumor	Acral primary
	Mel88	Mel88	54	F	Tremelimumab + MEDI3617	Post-ICI (resistant)	metastasis	Cutanoues met
	Mel89	Mel89	67	M	None	Untreated	metastasis	Axillary lymph node
	Mel94	Mel94	54	F	IFN, ipilimumab + nivolumab	Post-ICI (resistant)	metastasis	Iliac lymph node
Additional	Mel126	Mel126	63	M	Ipilimumab, nivolumab	Post-ICI (resistant)	metastasis	Soft tissue
	Mel04.3	Mel04.3	81	M	Ipilimumab	OR	metastasis	Skin
	Mel110	Mel110	74	M	ipilimumab + angiopoietin 2 inhibitor, Temezlolamide, Pembrolizumab	Post-ICI (resistant)	metastasis	R adrenal metastasis
	Mel121.1	Mel121.1	74	M	S/p Pembrolizumab	Post-ICI (resistant)	metastasis	Skin
	Mel106	Mel106	67	M	Prior treatment: nivolumab + ipilimumab	Post-ICI (resistant)	metastasis	Necrotic L axillary lymph nodes
	Mel75.1	Mel75	81	M	Ipilimumab + nivolumab, WDVAX, Pembrolizumab	Post-ICI (resistant)	metastasis	Soft tissue
	Mel98	Mel98	47	F	S/p IFN, s/p ipilimumab+GMCSF	Post-ICI (resistant)	metastasis	L thigh soft tissue metastasis
	Mel102	Mel102	72	F	S/p nivolumab + ipilimumab	Post-ICI (resistant)	metastasis	Fragmented pieces of (R) adrenal gland metastasis
	Mel129PA	Mel129	63	M	None	Untreated	primary tumor	Skin
	Mel129PB	Mel129	63	M	None	Untreated	primary tumor	Skin
	Mel116	Mel116	85	M	None	Untreated	metastasis	Lymph node
	Mel103	Mel103	58	M	None	Untreated	metastasis	Lymph node
	Mel105	Mel105	77	M	None	Untreated	primary tumor	Skin
	Mel112	Mel112	76	M	None	Untreated	metastasis	Bulky (L) axillary metastasis
	Mel194	Mel194	68	M	Nivolumab + lirilumab (anti-kit), Nivolumab, Ipilimumab, Pan-	Post-ICI (resistant)	metastasis	L anterior shoulder subcutaneous

					RAF-inhibitor, Pembrolizumab			
	Mel478	Mel478	54	F	None	Untreated	metastasis	Transanal rectal mass
	Mel128	Mel128	37	M	None	Untreated	metastasis	Lymph node

Table 24B. Clinical characteristics of the patients and samples Validation Cohort 1

Patient	Sample	ICI		Targeted therapy		Other therapy	
		on	post	on	post	on	post
Pat1	Pat1_s1	FALSE	FALSE	FALSE	FALSE	FALSE	FALSE
Pat1	Pat1_s2	FALSE	TRUE	FALSE	FALSE	FALSE	TRUE
Pat2	Pat2_s3	FALSE	FALSE	FALSE	FALSE	FALSE	FALSE
Pat2	Pat2_s4	TRUE	FALSE	FALSE	FALSE	FALSE	FALSE
Pat2	Pat2_s5	FALSE	TRUE	FALSE	FALSE	FALSE	FALSE
Pat2	Pat2_s6	TRUE	TRUE	FALSE	FALSE	FALSE	FALSE
Pat3	Pat3_s7	FALSE	FALSE	TRUE	FALSE	FALSE	FALSE
Pat3	Pat3_s8	TRUE	FALSE	FALSE	TRUE	FALSE	FALSE
Pat4	Pat4_s9	FALSE	TRUE	FALSE	TRUE	FALSE	TRUE
Pat4	Pat4_s10	TRUE	TRUE	FALSE	TRUE	FALSE	TRUE
Pat4	Pat4_s11	TRUE	TRUE	FALSE	TRUE	FALSE	TRUE
Pat5	Pat5_s12	FALSE	FALSE	FALSE	FALSE	FALSE	FALSE
Pat5	Pat5_s13	TRUE	TRUE	FALSE	FALSE	FALSE	FALSE
Pat5	Pat5_s14	TRUE	TRUE	FALSE	FALSE	FALSE	FALSE
Pat6	Pat6_s15	FALSE	FALSE	FALSE	FALSE	FALSE	FALSE
Pat6	Pat6_s16	FALSE	TRUE	FALSE	FALSE	FALSE	FALSE
Pat7	Pat7_s17	FALSE	FALSE	FALSE	FALSE	FALSE	FALSE
Pat7	Pat7_s18	FALSE	TRUE	FALSE	FALSE	FALSE	FALSE
Pat7	Pat7_s19	FALSE	TRUE	FALSE	FALSE	FALSE	FALSE
Pat8	Pat8_s20	FALSE	FALSE	FALSE	FALSE	FALSE	FALSE
Pat8	Pat8_s21	TRUE	FALSE	FALSE	FALSE	FALSE	FALSE
Pat9	Pat9_s22	TRUE	FALSE	FALSE	FALSE	FALSE	FALSE
Pat9	Pat9_s23	TRUE	FALSE	FALSE	FALSE	FALSE	FALSE
Pat10	Pat10_s24	FALSE	TRUE	FALSE	FALSE	FALSE	FALSE
Pat10	Pat10_s25	TRUE	TRUE	FALSE	FALSE	FALSE	FALSE
Pat10	Pat10_s26	TRUE	TRUE	FALSE	FALSE	FALSE	FALSE
Pat11	Pat11_s27	FALSE	FALSE	FALSE	FALSE	FALSE	FALSE
Pat11	Pat11_s28	TRUE	FALSE	FALSE	FALSE	FALSE	FALSE
Pat12	Pat12_s29	FALSE	TRUE	FALSE	FALSE	FALSE	FALSE
Pat12	Pat12_s30	TRUE	TRUE	FALSE	FALSE	FALSE	FALSE
Pat12	Pat12_s31	FALSE	TRUE	FALSE	FALSE	FALSE	FALSE
Pat13	Pat13_s32	FALSE	TRUE	FALSE	TRUE	FALSE	TRUE
Pat13	Pat13_s33	TRUE	TRUE	FALSE	TRUE	FALSE	TRUE
Pat13	Pat13_s34	TRUE	TRUE	FALSE	TRUE	FALSE	TRUE
Pat13	Pat13_s35	TRUE	TRUE	FALSE	TRUE	FALSE	TRUE
Pat13	Pat13_s36	TRUE	TRUE	FALSE	TRUE	FALSE	TRUE
Pat13	Pat13_s37	TRUE	TRUE	FALSE	TRUE	FALSE	TRUE
Pat13	Pat13_s38	TRUE	TRUE	FALSE	TRUE	FALSE	TRUE
Pat14	Pat14_s39	FALSE	FALSE	TRUE	FALSE	FALSE	FALSE
Pat14	Pat14_s40	TRUE	FALSE	FALSE	TRUE	FALSE	FALSE
Pat15	Pat15_s41	FALSE	FALSE	FALSE	FALSE	FALSE	FALSE
Pat15	Pat15_s42	TRUE	FALSE	FALSE	FALSE	FALSE	FALSE
Pat15	Pat15_s43	FALSE	TRUE	FALSE	FALSE	FALSE	FALSE

Pat16	Pat16_s44	FALSE	FALSE	FALSE	FALSE	FALSE	FALSE
Pat16	Pat16_s45	TRUE	FALSE	FALSE	FALSE	FALSE	FALSE
Pat16	Pat16_s46	FALSE	TRUE	FALSE	FALSE	FALSE	FALSE
Pat16	Pat16_s47	FALSE	TRUE	FALSE	FALSE	FALSE	FALSE
Pat16	Pat16_s48	TRUE	TRUE	FALSE	FALSE	FALSE	FALSE
Pat16	Pat16_s49	TRUE	TRUE	FALSE	FALSE	FALSE	FALSE
Pat17	Pat17_s50	FALSE	FALSE	FALSE	FALSE	FALSE	FALSE
Pat17	Pat17_s51	FALSE	FALSE	FALSE	TRUE	FALSE	FALSE
Pat17	Pat17_s52	FALSE	FALSE	FALSE	TRUE	FALSE	FALSE
Pat17	Pat17_s53	FALSE	TRUE	FALSE	TRUE	FALSE	FALSE
Pat18	Pat18_s54	FALSE	FALSE	FALSE	FALSE	FALSE	FALSE
Pat18	Pat18_s55	FALSE	TRUE	FALSE	FALSE	FALSE	FALSE
Pat18	Pat18_s56	FALSE	TRUE	FALSE	FALSE	FALSE	FALSE
Pat18	Pat18_s57	FALSE	TRUE	FALSE	FALSE	FALSE	FALSE
Pat19	Pat19_s58	FALSE	FALSE	FALSE	FALSE	FALSE	TRUE
Pat19	Pat19_s59	FALSE	FALSE	TRUE	FALSE	FALSE	TRUE
Pat19	Pat19_s60	TRUE	FALSE	TRUE	FALSE	FALSE	TRUE
Pat20	Pat20_s61	FALSE	FALSE	FALSE	FALSE	FALSE	FALSE
Pat20	Pat20_s62	FALSE	TRUE	FALSE	TRUE	FALSE	TRUE
Pat21	Pat21_s63	FALSE	FALSE	FALSE	FALSE	FALSE	FALSE
Pat21	Pat21_s64	FALSE	FALSE	TRUE	FALSE	TRUE	FALSE
Pat22	Pat22_s65	FALSE	FALSE	FALSE	FALSE	FALSE	FALSE
Pat22	Pat22_s66	FALSE	FALSE	TRUE	FALSE	TRUE	FALSE
Pat23	Pat23_s67	FALSE	FALSE	FALSE	FALSE	FALSE	FALSE
Pat23	Pat23_s68	FALSE	FALSE	FALSE	FALSE	FALSE	FALSE
Pat23	Pat23_s69	FALSE	FALSE	TRUE	FALSE	TRUE	FALSE
Pat24	Pat24_s70	TRUE	TRUE	FALSE	FALSE	FALSE	TRUE
Pat24	Pat24_s71	TRUE	TRUE	FALSE	FALSE	FALSE	TRUE
Pat24	Pat24_s72	TRUE	TRUE	TRUE	FALSE	FALSE	TRUE
Pat24	Pat24_s73	TRUE	TRUE	TRUE	FALSE	FALSE	TRUE
Pat24	Pat24_s74	TRUE	TRUE	TRUE	FALSE	FALSE	TRUE
Pat24	Pat24_s75	TRUE	TRUE	TRUE	FALSE	FALSE	TRUE
Pat24	Pat24_s76	TRUE	TRUE	TRUE	FALSE	FALSE	TRUE
Pat25	Pat25_s77	FALSE	FALSE	FALSE	FALSE	FALSE	TRUE
Pat25	Pat25_s78	FALSE	FALSE	TRUE	FALSE	FALSE	TRUE
Pat25	Pat25_s79	TRUE	FALSE	TRUE	FALSE	FALSE	TRUE
Pat25	Pat25_s80	FALSE	TRUE	FALSE	TRUE	FALSE	TRUE
Pat25	Pat25_s81	FALSE	TRUE	TRUE	TRUE	FALSE	TRUE
Pat25	Pat25_s82	FALSE	TRUE	TRUE	TRUE	FALSE	TRUE
Pat25	Pat25_s83	FALSE	TRUE	TRUE	TRUE	FALSE	TRUE
Pat25	Pat25_s84	FALSE	TRUE	FALSE	TRUE	FALSE	TRUE
Pat26	Pat26_s85	FALSE	FALSE	FALSE	FALSE	FALSE	FALSE
Pat26	Pat26_s86	FALSE	FALSE	FALSE	FALSE	FALSE	FALSE
Pat26	Pat26_s87	FALSE	TRUE	FALSE	TRUE	FALSE	FALSE
Pat26	Pat26_s88	TRUE	TRUE	FALSE	TRUE	FALSE	FALSE
Pat26	Pat26_s89	FALSE	TRUE	FALSE	TRUE	FALSE	FALSE
Pat26	Pat26_s90	FALSE	TRUE	FALSE	TRUE	FALSE	FALSE

Table 24C. Clinical characteristics of the patients and samples Validation Cohort 2

Sample	RECIST	PFS (years)	PFS (status, 1 = progression, 0 = no progression)
Patient185_T	NA	NA	NA

Patient168_T	PR	0.539726027	0
Patient102_T_P	MR	0.482191781	1
Patient169_T	PR	1.487671233	0
Patient156_T	PD	0.219178082	1
Patient48_T_M	PD	0.136986301	1
Patient150_T	NA	NA	NA
Patient63_T_P	PD	0.243835616	1
Patient155_T	PD	0.309589041	1
Patient125_T_P	CR	1.326027397	0
Patient135_T	CR	0.909589041	0
Patient148_T	PR	1.589041096	0
Patient15_T_M	PR	0.287671233	1
Patient152_T	PD	0.123287671	1
Patient21_T_M	PR	1.443835616	0
Patient133_T	PD	0.17260274	1
Patient163_T	PD	0.131506849	1
Patient8_T_M	SD	2.616438356	1
Patient4_T_M	CR	1.57260274	1
Patient99_T_P	PR	0.873972603	1
Patient105_T_P	MR	1.035616438	0
Patient165_T	PD	0.035616438	1
Patient38_T_M	PD	0.268493151	1
Patient126_T_P	PR	1.145205479	0
Patient10_T_M	PR	0.463013699	1
Patient22_T_M	PD	0.249315068	1
Patient16_T_M	PD	0.126027397	1
Patient72_T_P	PD	0.183561644	1
Patient6_T_M	SD	0.339726027	1
Patient23_T_M	PD	0.210958904	1
Patient134_T	PD	0.17260274	1
Patient83_T_P	PD	0.194520548	1
Patient121_T_P	PR	2.112328767	0
Patient18_T_M	PD	0.235616438	1
Patient132_T	CR	1.065753425	1
Patient184_T	NA	NA	NA
Patient77_T_P	PD	0.260273973	1
Patient131_T	PR	1.526027397	0
Patient9_T_M	PD	0.057534247	1
Patient79_T_P	PD	0.230136986	1
Patient74_T_P	NA	NA	NA
Patient141_T	PR	0.221917808	0
Patient34_T_M	PR	0.657534247	1
Patient187_T	CR	0.887671233	0
Patient146_T	CR	0.890410959	0
Patient116_T_P	PD	0.175342466	1
Patient82_T_P	PD	0.243835616	1
Patient94_T_P	PD	0.109589041	1
Patient183_T	NA	NA	NA
Patient166_T	PR	0.364383562	0
Patient170_T	SD	0.950684932	0
Patient173_T	PD	0.043835616	1
Patient7_T_M	SD	0.594520548	1
Patient11_T_M	PD	0.232876712	1
Patient151_T	CR	1.153424658	0
Patient31_T_M	PD	0.232876712	1
Patient67_T_P	PD	0.257534247	1
Patient36_T_M	PD	0.17260274	1
Patient17_T_M	SD	0.553424658	1

Patient154_T	SD	0.687671233	1
Patient87_T_P	PR	3.128767123	1
Patient1_T_M	PD	0.246575342	1
Patient100_T_P	PR	1.449315068	0
Patient153_T	PR	0.567123288	1
Patient75_T_P	PR	1.232876712	0
Patient61_T_P	SD	1.879452055	0
Patient35_T_M	SD	0.791780822	1
Patient32_T_M	PD	0.134246575	1
Patient25_T_M	PR	2.060273973	1
Patient98_T_P	PD	0.2	1
Patient117_T_P	PD	0.273972603	1
Patient14_T_M	PD	0.208219178	1
Patient58_T_M	PD	0.210958904	1
Patient108_T_P	PD	0.210958904	1
Patient147_T	CR	1.693150685	0
Patient24_T_M	PD	0.084931507	1
Patient47_T_M	PD	0.202739726	1
Patient179_T	PR	0.920547945	1
Patient45_T_M	PR	3.350684932	0
Patient140_T	PD	0.183561644	1
Patient112_T_P	PD	0.249315068	1
Patient96_T_P	CR	1.545205479	0
Patient62_T_P	PR	1.898630137	0
Patient144_T	PR	1.120547945	0
Patient188_T	PD	0.063013699	1
Patient130_T_P	PD	0.301369863	1
Patient27_T_M	PD	0.257534247	1
Patient162_T	PD	0.145205479	1
Patient142_T	SD	0.515068493	1
Patient127_T_P	CR	1.24109589	0
Patient33_T_M	PR	3.506849315	0
Patient20_T_M	PD	0.230136986	1
Patient30_T_M	SD	0.364383562	1
Patient13_T_M	PD	0.120547945	1
Patient78_T_P	PD	0.235616438	1
Patient44_T_M	PR	1.317808219	0
Patient172_T	SD	0.745205479	1
Patient19_T_M	na	NA	0
Patient40_T_M	PD	0.17260274	1
Patient42_T_M	CR	0.821917808	0
Patient73_T_P	PD	0.232876712	1
Patient86_T_P	SD	2.753424658	0
Patient137_T	CR	1.323287671	0
Patient37_T_M	PD	0.210958904	1
Patient159_T	SD	0.591780822	1
Patient158_T	PR	0.443835616	1
Patient181_T	NA	NA	NA
Patient76_T_P	na	0.123287671	1
Patient145_T	CR	1.375342466	0
Patient167_T	PD	0.156164384	1
Patient106_T_P	CR	1.005479452	0
Patient149_T	NA	NA	NA

[0551] **Table 25.** Quality measures of scRNA-seq experiments; related to **Figure 62**.

Clinical data					
Cell type	**Median no. of detected**	**Median no. of aligned**	**No. of TN**	**No. of ICR**	**Total no. of**

	genes	reads	cells	cells	cells
B cell	3774	164400	355	463	818
CAF	5518	357423	45	61	106
Endothelial cell	5057	304326	17	87	104
Macrophage	5670	654482	259	161	420
Malignant cells	5482	335563	825	1193	2018
NK	3909	147376	48	44	92
CD4 T cell	4036	220614	436	420	856
CD8 T cell	4064	264494	1039	720	1759
T cell	3827	234410	408	298	706
Low quality cell	732	24991	1551	1386	2937
UD	3433	221421	124	183	307
All cells	3655	176595	5107	5016	10123

Experimental data (in vitro)				
Type	**Cell line and condition**	**Median no. of detected genes**	**Median no. of aligned reads**	**Total no. of cells**
Human melanoma cell lines	**A2058 Abemaciclib**	4270	19144	2769
	A2058 DMSO	3510	12945	2607
	UACC257 Abemaciclib	4044	25271	2939
	UACC257 DMSO	3286	14174	4401
	IGR37 Abemaciclib	4259	26184	1570
	IGR37 DMSO	3990	16972	2454
Patient-derived co-culture	**Monoculture Abemaciclib**	4492	34414	2064
	Monoculture DMSO	3708	20337	3865
	TIL coculture Abemaciclib	5719	65130	102
	TIL coculture DMSO	4824	40700	124
Mouse cell lines	**B16**	2044	5254	3031
	CT26	2369	7365	3208
	MC38	2406	6865	3424

[0552] **Table 26. (A)** Cell type signatures and markers used for cell classification; **(B)** cell type signatures derived from the analysis of scRNA-seq data; related to **Figure 62**; **(C)** Alternative cell type signatures and markers used for cell classification.

Table 26A.

ENDOTHELIAL CELL	STROMAL CELL	CAF	BASOPHILE	B CELL	EOSINOPHIL	ERYTHROCYTE	MAST CELL	MDSC	MEGAKARYOCYTE	MYELOID DENDRITIC CELL
CD34	*ICAM1*	*COL1A1*	*ANPEP*	*BLK*	*C3AR1*	*CD24*	*ENPP3*	*CCR7*	*CD9*	*CCR7*
CDH5	*ICAM2*	*COL1A2*	*CCR3*	*CD19*	*C5AR1*	*GYPA*	*KIT*	*CD1A*	*GP1BA*	*CD1A*
ENG	*ICAM3*	*COL6A1*	*CD44*	*CD2*	*CCR1*	*PTPRC*		*CD1B*	*ITGA2B*	*CD1B*
FLT4	*ITGA4*	*COL6A2*	*CD63*	*CD22*	*CCR3*			*CD1C*	*ITGAV*	*CD1C*
ICAM1	*ITGB1*	*COL6A3*	*CD69*	*CD40*	*CD244*			*CD207*	*ITGB3*	*CD207*
ITGB3	*KIT*	*DCN*	*ENPP3*	*CD5*	*CD52*			*CD209*	*PECAM1*	*CD209*
KDR	*MADCA*	*FAP*	*ICAM1*	*CD69*	*CD53*			*CD4*	*SELP*	*CD4*

	M1									
MCAM	MME	THY1	IL3RA	CD70	CXCR3			CD40		CD40
PECAM1	MMP1		LAMP1	CD79A	FCER2			CD80		CD80
PROCR	MMP2		TLR4	CD79B	FUT4			CD83		CD83
SELE	MMP9			CD80	IL9R			CD86		CD86
TEK	PDGFRA			CD86	ITGA4			CMKLR1		CMKLR1
VCAM1	PDGFRB			CD93	LAIR1			HLA-DOA		DCX
VWF	PECAM1			FCER2	PTGDR2			HLA-DOB		ITGA4
	THY1			MS4A1	S100A9			HLA-DRA		ITGAM
	TIMP1			PAX5	SIGLEC10			HLA-DRB1		ITGAX
	TIMP2			PDCD1	SIGLEC8			HLA-DRB5		LY75
	TLR1			SDC1				HLA-DRB6		NRP1
	TLR2			TNFRSF13B				ITGA4		PDCD1LG2
	TLR3			TNFRSF13C				ITGAM		
	TLR4			TNFRSF9				ITGAX		
	VCAM1			TNFSF4				LY75		
								NRP1		
								PDCD1LG2		

NAIVE CD4 T CELL	NEUTROPHIL	NK CELL	PLASMACYTOID DENDRITIC CELL	PLATELET	T FOLLICULAR HELPER	TH1	TH2	TH9	TH17
CCR7	ANPEP	B3GAT1	CCR7	BSG	BCL6	CCR1	CCR3	CD3D	CCR4
CD3D	C5AR1	CD244	CD1A	CCL5	CD3D	CCR5	CCR4	CD3E	CCR6
CD3E	CD14	CD69	CD1B	CCR3	CD3E	CD4	CCR7	CD3G	CD38
CD3G	CD33	IL2RB	CD1C	CD109	CD3G	CSF2	CCR8	CD4	CD3D
CD4	CEACAM8	ITGA2	CD4	CD151	CD4	CXCR3	CD4	GATA3	CD3E
SELL	CSF3R	ITGAM	CD40	CD226	CD40LG	DPP4	CSF2	IRF4	CD3G
	CXCR1	ITGAX	CD80	CD36	CD84	HAVCR2	CXCR4	STAT6	CD4
	CXCR2	KLRA1	CD83	CD46	CXCR5	IFNA1	GATA3		IL17A
	FCGR1A	KLRB1	CD86	CD47	ICOS	IFNGR1	HAVCR1		IL17F
	FUT4	KLRD1	CD8A	CD48	IL6R	IL2	ICOS		IL1R1
	ITGAM	KLRK1	CLEC4C	CD63	PDCD1	KLRD1	IL10		IL21
	ITGAX	NCAM1	CMKLR1	CD69	SLAMF1	TNF	IL13		IL22
	MME	NCR1	IL3RA	CD84	STAT3	TNFSF11	IL1R1		KLRB1
	PECAM1	NKG2	ITGA4	CD9	TNFSF4		IL4		LINC-ROR
	SELL	SIGLEC7	ITGAM	CNGB1			IL5		STAT3
	TLR2	SLAMF6	ITGAX	CSF3R			IL6		
		SLAMF7	NRP1	FCGR2A			PTGDR2		

			PDCD1LG2	*FCGR2B*					
			TLR9	*GP1BA*					
				ICAM2					
				ITGA2					
				ITGA2B					
				ITGA6					
				ITGAV					
				ITGB1					
				ITGB3					
				JAM3					
				LAMP2					
				LRRC32					
				LYN					
				PECAM1					
				SELP					
				SPN					
				TNFSF14					
				VEGFA					

TH22	**TREG**	**CYTOTOXIC CD8 T CELL**	**MACROPHAGE**	**CYTOTOXIC T CELL (SPECIFIC MARKERS)**	**EXHAUSTED T CELL (SPECIFIC MARKERS)**	**NAIVE T CELL (SPECIFIC MARKERS)**	**TREG (SPECIFIC MARKERS)**	**CELL CYCLE: G1/S**	**CELL CYCLE: G2/M**
AHR	*CCR4*	*CCL3*	*CCR5*	*CCL3*	*CTLA4*	*CCR7*	*FOXP3*	*ATAD2*	*ANLN*
CCR10	*CD4*	*CCL4*	*CD14*	*CCL4*	*HAVCR2*	*LEF1*	*IL2RA*	*BLM*	*ANP32E*
CCR4	*CNGB1*	*CD2*	*CD163*	*CST7*	*LAG3*	*SELL*		*BRIP1*	*AURKA*
CCR6	*CTLA4*	*CD3D*	*CD33*	*GZMA*	*PDCD1*	*TCF7*		*CASP8AP2*	*AURKB*
CD3D	*ENTPD1*	*CD3E*	*CD68*	*GZMB*	*TIGIT*			*CCNE2*	*BIRC5*
CD3E	*FOXP3*	*CD3G*	*CD80*	*IFNG*				*CDC45*	*BUB1*
CD3G	*IKZF2*	*CD8A*	*CD86*	*NKG7*				*CDC6*	*CBX5*
CD4	*IL2RA*	*CD8B*	*CSF1R*	*PRF1*				*CDCA7*	*CCNB2*
	ISG20	*CST7*	*ENG*					*CHAF1B*	*CDC20*
	ITGAE	*GZMA*	*FCGR1A*					*CLSPN*	*CDC25C*
	LAG3	*GZMB*	*FUT4*					*DSCC1*	*CDCA2*
	LRRC32	*IFNG*	*ITGAL*					*DTL*	*CDCA3*
	NT5E	*NKG7*	*ITGAM*					*E2F8*	*CDCA8*
	SELL	*PRF1*	*ITGAX*					*EXO1*	*CDK1*
	TNFRSF18		*LAMP2*					*FEN1*	*CENPA*
	TNFRSF4		*LILRB4*					*GINS2*	*CENPE*
			TLR2					*GMNN*	*CENPF*
			TLR4					*HELLS*	*CKAP2*
								MCM2	*CKAP2L*
								MCM4	*CKAP5*
								MCM5	*CKS1B*
								MCM6	*CKS2*
								MLF1IP	*CTCF*
								MSH2	*DLGAP5*
								NASP	*ECT2*
								PCNA	*FAM64A*
								POLA1	*G2E3*
								POLD3	*GAS2L3*
								PRIM1	*GTSE1*
								RAD51	*HJURP*
								RAD51A	*HMGB2*

								P1	
								RFC2	HMMR
								RPA2	HN1
								RRM1	KIF11
								RRM2	KIF20B
								SLBP	KIF23
								TIPIN	KIF2C
								TYMS	LBR
								UBR7	MKI67
								UHRF1	NCAPD2
								UNG	NDC80
								USP1	NEK2
								WDR76	NUF2
									NUSAP1
									PSRC1
									RANGAP 1
									SMC4
									TACC3
									TMPO
									TOP2A
									TPX2
									TTK
									TUBB4B
									UBE2C

Table 26B.

B CELL	CAF	ENDOTHELIAL	MACROPHAGE		MALIGNANT		NK
ADAM19	ABCA6	A2M	ABCA1	KYNU	AASDHPPT	NAV2	ALOX5AP
ADAM28	ABCA8	ABCD4	ABI1	LAIR1	AATF	NDUFA4	APMAP
AFF3	ABI3BP	ADAM15	ACAA1	LAP3	ACN9	NDUFAF3	CALM1
ATF7IP	ACTA2	ADAMTS9	ACER3	LGALS2	ACOT7	NDUFB9	CD160
BACH2	ACVR1	ADCY4	ACP2	LGALS9	ACSL3	NDUFS2	CD244
BANK1	ADAM12	ADM5	ACP5	LGMN	ADIPOR1	NEDD4L	CD247
BCL11A	ADAMTS12	AFAP1L1	ACSL1	LILRA1	ADSL	NELFCD	CLIC3
BLK	ADAMTS2	APLNR	ADAMDEC1	LILRA2	AHCY	NFYA	CTSW
BLNK	ANTXR1	AQP1	ADAP2	LILRA3	AIF1L	NGRN	FCRL6
BTLA	AOX1	ARHGAP29	ADORA3	LILRA4	AK2	NHP2	FGFBP2
CCR6	ARMCX2	ARHGAP31	ADPGK	LILRA5	ALDOA	NME1	GNLY
CD19	ASPN	ARHGEF15	AIF1	LILRA6	ALX1	NOP58	GZMB
CD1C	BACE1	ASAP1	AKR1A1	LILRB1	AMZ2	NPM1	GZMM
CD22	BAG2	BCAM	ALDH2	LILRB2	ANAPC11	NSG1	HOPX
CD24	BGN	BCL6B	ALDH3B1	LILRB3	ANKRD54	NT5DC3	ID2
CD37	C1R	BCR	AMICA1	LILRB4	ANP32A	NUP93	IL18RAP
CD52	C1S	BMPR2	AMPD3	LILRB5	AP1S2	OCA2	IL2RB
CD79A	CALD1	BMX	ANKRD22	LIPA	APEH	PACSIN2	KIR2DL3
CD79B	CCDC80	CALCRL	AP1B1	LOC338758	APOA1BP	PAFAH1B3	KIR3DL2
CHMP7	CD248	CARD10	APOC1	LOC729737	APOC2	PAGE5	KLRB1
CIITA	CDH11	CASKIN2	AQP9	LRRC25	APOD	PAICS	KLRC1
CLEC17A	CDR1	CCL14	ARAP1	LST1	APOO	PAX3	KLRD1
CNR2	CERCAM	CD200	ARHGAP18	LTA4H	ARPC1A	PEBP1	KLRF1
COL19A1	CILP	CD34	ARHGAP27	LYN	ATIC	PEG10	MATK
COL4A3	CKAP4	CD93	ARHGEF10L	LYZ	ATP1A1	PEX19	MYBL1
CR2	CLEC11A	CDH5	ARPC1B	M6PR	ATP5C1	PFDN2	NCAM1
CXCR5	CLIP3	CFI	ARRB2	MAFB	ATP5G1	PHACTR1	NCR1
CYBASC3	CNN1	CLDN15	ASAH1	MAN2B1	ATP5G2	PHB	NCR3
EEF1B2	COL11A1	CLDN5	ATF5	MAPKAPK3	ATP5G3	PHF5A	NKG7

EEF1G	*COL12A1*	*CLEC14A*	*ATG3*	*MARCO*	*ATP6V1C1*	*PHLDA1*	*NMUR1*
EIF2S3	*COL14A1*	*CLEC1A*	*ATG7*	*MERTK*	*ATP6V1E1*	*PIGY*	*PRF1*
ELK2AP	*COL16A1*	*CNTNAP3B*	*ATP6AP1*	*MFSD1*	*ATP6V1G1*	*PIR*	*PTGDR*
FAIM3	*COL1A1*	*COL15A1*	*ATP6V0B*	*MGAT1*	*BAIAP2*	*PLEKHB1*	*PTPN4*
FAM129C	*COL1A2*	*COL4A1*	*ATP6V0D1*	*MIF4GD*	*BANCR*	*PLP1*	*SAMD3*
FAM65B	*COL3A1*	*COL4A2*	*ATP6V1B2*	*MIIP*	*BCAN*	*PMEL*	*SH2D1B*
FCER2	*COL5A1*	*CRIP2*	*ATP6V1F*	*MILR1*	*BCAS3*	*POLD2*	*TXK*
FCRL1	*COL5A2*	*CXorf36*	*BACH1*	*MKNK1*	*BCL2L13*	*POLR2F*	*XCL1*
FCRL2	*COL6A1*	*CYYR1*	*BCKDHA*	*MNDA*	*BIRC7*	*POMGNT1*	*XCL2*
FCRL5	*COL6A2*	*DARC*	*BCL2A1*	*MOB1A*	*BZW2*	*PPIL1*	
FCRLA	*COL6A3*	*DCHS1*	*BID*	*MPEG1*	*C10orf90*	*PRAME*	
GGA2	*COL8A1*	*DLL4*	*BLOC1S1*	*MPP1*	*C11orf31*	*PRDX6*	
GNB2L1	*COMP*	*DOCK6*	*BLVRA*	*MRC1*	*C17orf89*	*PSMB4*	
HLA-DOB	*CPE*	*DOCK9*	*BLVRB*	*MS4A4A*	*C1orf43*	*PSMB7*	
HLA-DQA2	*CPXM1*	*DYSF*	*C10orf54*	*MS4A6A*	*C1orf85*	*PSMD4*	
HVCN1	*CPZ*	*ECE1*	*C11orf75*	*MS4A7*	*C1QBP*	*PTTG1*	
IGJ	*CRABP2*	*ECSCR*	*C15orf48*	*MSR1*	*C22orf32*	*PUF60*	
IGLL1	*CREB3L1*	*EFNA1*	*C19orf38*	*MTHFD2*	*C4orf48*	*PYGB*	
IGLL3P	*CRISPLD2*	*EFNB2*	*C1orf162*	*MTMR14*	*CA14*	*PYURF*	
IGLL5	*CTSK*	*EGFL7*	*C1QA*	*MX1*	*CA8*	*QDPR*	
IRF8	*CXCL12*	*ELK3*	*C1QB*	*MX2*	*CACYBP*	*QPCT*	
KBTBD8	*CXCL14*	*ELTD1*	*C1QC*	*MXD1*	*CAPN3*	*RAB17*	
KIAA0125	*CYBRD1*	*EMCN*	*C2*	*MYD88*	*CBX3*	*RAB38*	
KIAA0226L	*CYGB*	*ENG*	*C3AR1*	*N4BP2L1*	*CCND1*	*RABGGTB*	
LOC283663	*CYP1B1*	*EPAS1*	*C5AR1*	*NAAA*	*CCT2*	*RAD51C*	
LRMP	*DCN*	*EPB41L4A*	*C9orf72*	*NADK*	*CCT3*	*RAE1*	
MS4A1	*DDAH1*	*EPHB4*	*CAPG*	*NAGA*	*CCT4*	*RAN*	
NAPSB	*DDR2*	*ERG*	*CAPZA2*	*NAGK*	*CCT6A*	*RAP1GAP*	
NCF1C	*DEPTOR*	*ESAM*	*CARD9*	*NAIP*	*CCT8*	*RGS20*	
NCOA3	*DKK3*	*EXOC3L1*	*CASP1*	*NCF2*	*CDH19*	*ROPN1*	
P2RX5	*DPT*	*F11R*	*CAT*	*NCF4*	*CDH3*	*ROPN1B*	
PAX5	*EBF2*	*FABP4*	*CCDC88A*	*NCKAP1L*	*CDK2*	*RRS1*	
PLEKHF2	*ECM2*	*FAM107A*	*CCR1*	*NCOA4*	*CDK4*	*RSL1D1*	
PNOC	*EDNRA*	*FAM65A*	*CCR2*	*NFAM1*	*CEP170*	*RTKN*	
POLD4	*EFEMP2*	*FAT4*	*CCRL2*	*NFKBID*	*CHCHD6*	*RUVBL2*	
POU2AF1	*EGFLAM*	*FGD5*	*CD14*	*NINJ1*	*CHD1L*	*S100A1*	
POU2F2	*EGFR*	*FKBP1A*	*CD163*	*NLRC4*	*CLCN7*	*S100B*	
PRKCB	*EMILIN1*	*FLI1*	*CD1D*	*NLRP3*	*CLNS1A*	*SAMM50*	
QRSL1	*FAT1*	*FLT4*	*CD274*	*NMI*	*CMC2*	*SCD*	
RALGPS2	*FBLN1*	*FZD6*	*CD300C*	*NOD2*	*COA3*	*SDC3*	
RHOH	*FBLN2*	*GALNT18*	*CD300E*	*NPC2*	*COA4*	*SDCBP*	
SEL1L3	*FBLN5*	*GATA2*	*CD300LB*	*NPL*	*COA6*	*SDHC*	
SELL	*FGF7*	*GIPC2*	*CD300LF*	*NR1H3*	*COX5B*	*SEC11C*	
SMIM14	*FIBIN*	*GNG11*	*CD302*	*OAS1*	*COX6A1*	*SF3A1*	
SNX29	*FMOD*	*GPR116*	*CD33*	*OAZ1*	*COX7A2*	*SGCD*	
SNX29P1	*FN1*	*GPR146*	*CD68*	*OLR1*	*COX7A2L*	*SHC4*	
SP110	*FNDC1*	*GRB10*	*CD80*	*OSCAR*	*COX7C*	*SKP1*	
SP140	*FRMD6*	*GUK1*	*CD86*	*P2RX4*	*COX8A*	*SLC19A1*	
SPIB	*FST*	*HECW2*	*CECR1*	*P2RY12*	*CSAG1*	*SLC19A2*	
ST6GAL1	*FSTL1*	*HERC2P2*	*CFD*	*P2RY13*	*CSAG2*	*SLC24A5*	
STAG3	*GEM*	*HID1*	*CFP*	*P2RY14*	*CSAG3*	*SLC25A13*	
STAP1	*GFPT2*	*HSPG2*	*CLEC10A*	*P2RY6*	*CSPG4*	*SLC25A4*	
STRBP	*GFRA1*	*HYAL2*	*CLEC12A*	*PAK1*	*CYC1*	*SLC39A4*	
TCL1A	*GLT8D2*	*ICA1*	*CLEC4A*	*PCK2*	*CYP27A1*	*SLC45A2*	
TLR10	*GPC1*	*ID1*	*CLEC4E*	*PFKFB3*	*DAAM2*	*SLC5A3*	
TLR9	*GPC4*	*ID3*	*CLEC5A*	*PGD*	*DANCR*	*SLC6A15*	
TMEM154	*GPC6*	*IFITM3*	*CLEC7A*	*PILRA*	*DAP3*	*SLC7A5*	
TNFRSF13B	*GPR133*	*IGFBP7*	*CMKLR1*	*PLA2G15*	*DCT*	*SLMO2*	

TP53INP1	*GPR176*	*IL33*	*CMTM6*	*PLA2G7*	*DCXR*	*SMS*	
VPREB3	*GPX8*	*IL3RA*	*CNDP2*	*PLAUR*	*DDIT3*	*SNCA*	
WDFY4	*HSPB2*	*IPO11-LRRC70*	*CNPY3*	*PLBD1*	*DDT*	*SNHG16*	
ZCCHC7	*HSPB6*	*ITGA5*	*CORO7*	*PLEK*	*DLL3*	*SNHG6*	
	HSPB7	*ITGA6*	*CPVL*	*PLEKHO1*	*DNAH14*	*SNRPC*	
	HTRA3	*ITGB4*	*CREG1*	*PLEKHO2*	*DNAJA4*	*SNRPD1*	
	IGFBP6	*JAG2*	*CSF1R*	*PLIN2*	*DRG1*	*SNRPE*	
	INHBA	*JAM2*	*CSF2RA*	*PLXDC2*	*EDNRB*	*SOD1*	
	ISLR	*JUP*	*CSF3R*	*PPM1M*	*EIF3C*	*SORD*	
	ITGA11	*KANK3*	*CST3*	*PPT1*	*EIF3D*	*SORT1*	
	ITGB5	*KDR*	*CSTA*	*PRAM1*	*EIF3E*	*SOX10*	
	ITGBL1	*KLHL3*	*CTSA*	*PRKCD*	*EIF3H*	*SPCS1*	
	KDELR2	*LAMA5*	*CTSB*	*PSAP*	*EIF3L*	*SRP9*	
	KDELR3	*LDB2*	*CTSC*	*PSME2*	*EIF3M*	*ST13*	
	LARP6	*LOC100505495*	*CTSD*	*PTAFR*	*ENO1*	*ST3GAL4*	
	LEPREL2	*LRRC70*	*CTSH*	*PTPRE*	*ENO2*	*ST3GAL6*	
	LMO7	*LUZP1*	*CTSL1*	*PYCARD*	*ENTPD6*	*ST6GALNAC2*	
	LMOD1	*LYVE1*	*CTSS*	*RAB20*	*EPB41L4A-AS1*	*STAM*	
	LOX	*MALL*	*CXCL10*	*RAB4B*	*ERBB3*	*STIP1*	
	LOXL1	*MANSC1*	*CXCL16*	*RAB8A*	*ESRP1*	*STK32A*	
	LPAR1	*MECOM*	*CXCL9*	*RASGEF1B*	*ETV4*	*STMN1*	
	LTBP2	*MEOX1*	*CXCR2P1*	*RASSF4*	*ETV5*	*STOML2*	
	LUM	*MKL2*	*CYB5R4*	*RBM47*	*EXOSC4*	*STRA13*	
	LURAP1L	*MMRN1*	*CYBA*	*RBPJ*	*FAH*	*STRADB*	
	MAP1A	*MMRN2*	*CYBB*	*REEP4*	*FAHD2B*	*STX7*	
	MEG3	*MPZL2*	*CYP2S1*	*RELT*	*FAM103A1*	*STXBP1*	
	MFAP4	*MTUS1*	*DAPK1*	*RGS10*	*FAM162A*	*SUPT4H1*	
	MGST1	*MYCT1*	*DBNL*	*RGS18*	*FAM178B*	*SYNGR1*	
	MIR100HG	*MYO15B*	*DENND1A*	*RGS19*	*FARP2*	*TBC1D10A*	
	MMP2	*NOS3*	*DHRS9*	*RGS2*	*FASN*	*TBC1D16*	
	MOXD1	*NOSTRIN*	*DMXL2*	*RHBDF2*	*FBXO32*	*TBC1D7*	
	MRC2	*NOTCH4*	*DNAJC5B*	*RHOG*	*FBXO7*	*TBCA*	
	MRGPRF	*NPDC1*	*DOK1*	*RILPL2*	*FDFT1*	*TBRG4*	
	MSC	*NPR1*	*DOK3*	*RIPK2*	*FKBP4*	*TEX2*	
	MT1M	*NR5A2*	*DPYD*	*RNASE6*	*FMN1*	*TFAP2A*	
	MXRA5	*PALD1*	*EBI3*	*RNASEK*	*FXYD3*	*TIMM50*	
	MXRA8	*PALMD*	*EMR2*	*RNASET2*	*GALE*	*TMED10*	
	MYL9	*PCDH1*	*EPSTI1*	*RNF13*	*GAPDH*	*TMEM147*	
	NEXN	*PCDH12*	*ETV6*	*RNF130*	*GAPDHS*	*TMEM177*	
	NID2	*PCDH17*	*EVI2A*	*RNF144B*	*GAS2L3*	*TMEM255A*	
	NOTCH3	*PDE2A*	*F13A1*	*RNF149*	*GAS5*	*TMX4*	
	NTM	*PDLIM1*	*FAM105A*	*RTN1*	*GAS7*	*TOM1L1*	
	NTRK2	*PECAM1*	*FAM157B*	*S100A11*	*GCSH*	*TOMM20*	
	NUPR1	*PGM5*	*FAM26F*	*S100A8*	*GDF15*	*TOMM22*	
	OGN	*PIEZO1*	*FAM49A*	*S100A9*	*GJB1*	*TOMM6*	
	OLFML1	*PIK3R3*	*FAM96A*	*SAMHD1*	*GMNN*	*TOMM7*	
	OLFML2B	*PKP4*	*FBP1*	*SAT1*	*GMPR*	*TOP1MT*	
	OLFML3	*PLEKHA7*	*FCER1G*	*SCAMP2*	*GPATCH4*	*TRIM2*	
	OMD	*PLVAP*	*FCGR1A*	*SCIMP*	*GPM6B*	*TRIM63*	
	OSR2	*PLXNA2*	*FCGR1B*	*SCO2*	*GPR137B*	*TRMT112*	
	PALLD	*PLXND1*	*FCGR1C*	*SCPEP1*	*GPR143*	*TSNAX*	
	PAMR1	*PODXL*	*FCGR2A*	*SDS*	*GPS1*	*TTLL4*	
	PAPSS2	*PPM1F*	*FCGR2C*	*SECTM1*	*GSTP1*	*TUBB2A*	
	PCDH18	*PPP1R13B*	*FCGR3B*	*SEMA4A*	*GTF2F2*	*TUBB2B*	
	PCOLCE	*PRCP*	*FCGRT*	*SERPINA1*	*GYG2*	*TUBB4A*	
	PCOLCE2	*PREX2*	*FCN1*	*SERPINB1*	*H2AFZ*	*TYR*	
	PDGFRA	*PTPRB*	*FERMT3*	*SFT2D1*	*HAX1*	*TYRP1*	
	PDGFRB	*PVRL2*	*FES*	*SGPL1*	*HDDC2*	*UBA2*	

	PDGFRL	*PXN*	*FGL2*	*SH3BGRL*	*HIST1H2AC*	*UBL3*	
	PDLIM2	*RALGAPA2*	*FKBP15*	*SHKBP1*	*HIST1H2BD*	*UCHL5*	
	PLA2G2A	*RAMP2*	*FLVCR2*	*SIGLEC1*	*HIST3H2A*	*UQCRH*	
	PLAC9	*RAMP3*	*FOLR2*	*SIGLEC14*	*HMG20B*	*UTP18*	
	PLOD2	*RAPGEF3*	*FPR1*	*SIGLEC5*	*HMGA1*	*VAT1*	
	PODN	*RAPGEF4*	*FPR2*	*SIGLEC7*	*HPS4*	*VDAC1*	
	POSTN	*RASIP1*	*FPR3*	*SIGLEC9*	*HPS5*	*WBP11*	
	PPIB	*RBP7*	*FTH1*	*SIRPA*	*HSBP1*	*WBP2*	
	PRR16	*RGL2*	*FTL*	*SIRPB1*	*HSP90AA1*	*WBSCR22*	
	PRR24	*RHOJ*	*FUCA1*	*SIRPB2*	*HSP90AB1*	*WDFY1*	
	PRRX1	*ROBO4*	*FUOM*	*SKAP2*	*HSPA4*	*WDR43*	
	PRRX2	*S1PR1*	*GAA*	*SLAMF8*	*HSPA9*	*XAGE1A*	
	PTN	*SCARF1*	*GABARAP*	*SLC11A1*	*HSPD1*	*XAGE1B*	
	RARRES2	*SDPR*	*GALC*	*SLC15A3*	*HSPE1*	*XAGE1C*	
	RCN3	*SELE*	*GATM*	*SLC16A3*	*HSPH1*	*XAGE1D*	
	ROR2	*SELP*	*GBP1*	*SLC1A3*	*IGSF11*	*XAGE1E*	
	SCUBE3	*SH3BGRL2*	*GCA*	*SLC25A19*	*IGSF3*	*XYLB*	
	SDC1	*SHROOM4*	*GGTA1P*	*SLC29A3*	*IGSF8*	*ZCCHC17*	
	SDC2	*SLC29A1*	*GK*	*SLC2A5*	*ILF2*	*ZFAS1*	
	SEC24D	*SLC9A3R2*	*GLA*	*SLC2A8*	*IMMP2L*	*ZFP106*	
	SEMA5A	*SLCO2A1*	*GLB1*	*SLC2A9*	*INPP5F*	*ZNF280B*	
	SERPINF1	*SMAD1*	*GLRX*	*SLC31A2*	*IRF4*		
	SFRP2	*SNCG*	*GLUL*	*SLC43A2*	*ISYNA1*		
	SFRP4	*SOCS2*	*GM2A*	*SLC46A3*	*KCNJ13*		
	SH2D4A	*SOX18*	*GNA13*	*SLC7A7*	*LAGE3*		
	SH3D19	*SPNS2*	*GNA15*	*SLC9A9*	*LDHB*		
	SH3PXD2A	*STOM*	*GPBAR1*	*SLCO2B1*	*LHFPL3-AS1*		
	SLIT2	*SULF2*	*GPR34*	*SMPDL3A*	*LINC00473*		
	SLIT3	*SYNPO*	*GPR84*	*SNX10*	*LINC00518*		
	SMOC2	*TACR1*	*GPX1*	*SNX6*	*LINC00673*		
	SOD3	*TAOK2*	*GRN*	*SOD2*	*LOC100126784*		
	SPARC	*TEAD4*	*GSTO1*	*SPI1*	*LOC100127888*		
	SPOCK1	*TEK*	*H2AFY*	*SPINT2*	*LOC100130370*		
	SPON1	*TENC1*	*HCAR2*	*SQRDL*	*LOC100133445*		
	SRPX2	*TFF3*	*HCAR3*	*SRC*	*LOC100505865*		
	STEAP1	*TGFBR2*	*HCK*	*STX11*	*LOC146481*		
	SULF1	*TGM2*	*HEIH*	*STXBP2*	*LOC340357*		
	SUSD2	*THBD*	*HERPUD1*	*TALDO1*	*LOXL4*		
	SVEP1	*THSD1*	*HIST2H2BF*	*TBXAS1*	*LSM2*		
	TAGLN	*TIE1*	*HK2*	*TFRC*	*LZTS1*		
	TBX15	*TLL1*	*HK3*	*TGFBI*	*MAD2L1BP*		
	TCEAL7	*TM4SF1*	*HLA-DMA*	*THEMIS2*	*MAGEA12*		
	TGFB3	*TM4SF18*	*HLA-DMB*	*TIFAB*	*MAGEA2*		
	THBS2	*TMEM204*	*HLA-DPA1*	*TLR1*	*MAGEA2B*		
	THY1	*TMEM255B*	*HLA-DPB1*	*TLR2*	*MAGEA3*		
	TIMP1	*TNFAIP1*	*HLA-DPB2*	*TLR4*	*MAGEA4*		
	TMEM119	*TNFRSF10B*	*HLA-DQA1*	*TLR5*	*MAGEA6*		
	TMEM45A	*TSPAN12*	*HLA-DQB1*	*TLR8*	*MAGEC1*		
	TPM1	*TSPAN15*	*HLA-DRA*	*TMEM106A*	*MAGED2*		
	TPM2	*TSPAN18*	*HLA-DRB1*	*TMEM144*	*MDH1*		
	TWIST1	*TSPAN7*	*HLA-DRB5*	*TMEM176A*	*MDH2*		
	TWIST2	*USHBP1*	*HLA-DRB6*	*TMEM176B*	*METTL23*		
	UCHL1	*VWA1*	*HMOX1*	*TMEM37*	*METTL9*		
	VASN	*VWF*	*HN1*	*TMEM51*	*MFI2*		
	VCAN	*ZNF366*	*HPS1*	*TMEM86A*	*MIA*		
	WISP2	*ZNF385D*	*HSPA6*	*TNFAIP2*	*MIF*		
	WNT2		*HSPA7*	*TNFAIP8L2*	*MITF*		
			HSPBAP1	*TNFSF13*	*MKI67IP*		

			IDH1	*TNFSF13B*	*MLANA*		
			IFI30	*TPP1*	*MLPH*		
			IFI35	*TRAFD1*	*MOK*		
			IFIT2	*TREM1*	*MORN2*		
			IFNGR1	*TREM2*	*MRPL12*		
			IFNGR2	*TRPM2*	*MRPL21*		
			IGFLR1	*TTYH3*	*MRPL23*		
			IGSF6	*TWF2*	*MRPL24*		
			IL10RB	*TYMP*	*MRPL38*		
			IL18	*TYROBP*	*MRPL40*		
			IL1B	*UBE2D1*	*MRPS21*		
			IL1RN	*UBXN11*	*MRPS23*		
			IL4I1	*UNC93B1*	*MRPS25*		
			IL8	*VAMP8*	*MRPS26*		
			IRF5	*VMO1*	*MRPS6*		
			IRF7	*VSIG4*	*MSI2*		
			ITGAX	*WDFY2*	*MTHFS*		
			JAK2	*ZEB2*	*MXI1*		
			KCNMA1	*ZNF267*	*MYO10*		
			KCNMB1	*ZNF385A*	*NARS2*		

T CD4	T CD8	T CELL	STROMA	IMMUNE	T CD4 EXHAUSTED
AIM1	*ADORA2A*	*ARHGEF1*	*A4GALT*	*ACAP1*	*C9orf16*
AQP3	*ASB2*	*ASB2*	*ADAMTS1*	*AKNA*	*CDK5R1*
BCL11B	*ASXL2*	*ATHL1*	*ADAMTSL1*	*ALOX5AP*	*CTLA4*
CAMK4	*CBLB*	*BCL11B*	*ADIRF*	*ANKRD44*	*DDX5*
CCR4	*CCDC141*	*C16orf54*	*ANGPTL2*	*APOBEC3G*	*HLA-J*
CCR8	*CCDC64*	*CASP8*	*APP*	*ARHGAP15*	*ICA1*
CD28	*CD27*	*CCDC64*	*ARHGAP29*	*ARHGAP25*	*IGFLR1*
CD4	*CD3E*	*CCND2*	*BGN*	*ARHGAP30*	*IL21*
CD40LG	*CD84*	*CD2*	*BMP1*	*ARHGAP4*	*ITGB2-AS1*
CD5	*CD8A*	*CD247*	*C1R*	*ARHGAP9*	*ITM2A*
CD6	*CD8B*	*CD27*	*CCDC80*	*ARHGDIB*	*KCNK5*
DGKA	*CLEC2D*	*CD28*	*CFH*	*ATP2A3*	*KIAA0247*
DUSP16	*CRTAM*	*CD3D*	*CLU*	*BIN2*	*LIMS1*
EML4	*CXCL13*	*CD3E*	*COL15A1*	*C16orf54*	*LY6G5C*
F5	*DNAJB1*	*CD3G*	*COL18A1*	*CCDC88B*	*MAF*
FAAH2	*GPR171*	*CD5*	*COL4A1*	*CD37*	*METTL8*
FAM102A	*GZMK*	*CD6*	*COL4A2*	*CD48*	*MRP63*
FBLN7	*IFNG*	*CD7*	*COL6A2*	*CD52*	*NFATC1*
FLT3LG	*ITGA4*	*CD96*	*COX7A1*	*CD53*	*NR3C1*
FOXP3	*ITGAE*	*CDC42SE2*	*CTGF*	*CD69*	*PDCD1*
FYB	*ITM2A*	*CELF2*	*CYB5R3*	*CD84*	*PTPN11*
ICOS	*JAKMIP1*	*CNOT6L*	*CYR61*	*CDC42SE2*	*PTPRC*
IL6R	*KLHL28*	*CORO1A*	*DCHS1*	*CELF2*	*RNF19A*
IL7R	*LAG3*	*CST7*	*DPYSL3*	*CNTRL*	*SARDH*
ITGB2-AS1	*LYST*	*CTLA4*	*EFEMP1*	*CORO1A*	*SLA*
ITK	*MAP4K1*	*CXCR3*	*EHD2*	*CSK*	*SRGN*
LAT	*MCOLN2*	*CXCR6*	*ELN*	*CXCR4*	*TBC1D4*
LEPROTL1	*MIAT*	*CYTIP*	*EPAS1*	*CYTH4*	*THADA*
LOC100128420	*MIR155HG*	*DEF6*	*FAM171A1*	*CYTIP*	*TIGIT*
LOC285740	*NELL2*	*DENND2D*	*FAP*	*DEF6*	*TSPYL2*
MAF	*PAG1*	*EMB*	*FAT4*	*DENND1C*	*ZNF211*
MAL	*PCED1B*	*EVL*	*FBN1*	*DOCK2*	
PASK	*PDCD1*	*FYB*	*FLRT2*	*DOCK8*	
PBX4	*PRDM1*	*FYN*	*FSCN1*	*DUSP2*	
PBXIP1	*PTPN7*	*GATA3*	*FSTL1*	*EVI2B*	

PIK3IP1	*RAB27A*	*GNG2*	*GJA1*	*FERMT3*	
PIM2	*RNF19A*	*GPR171*	*GNG11*	*FGD3*	
SEPT6	*SIRPG*	*GPR174*	*HSPG2*	*FNBP1*	
SLAMF1	*SIT1*	*GPRIN3*	*HTRA1*	*GBP5*	
SPOCK2	*SNAP47*	*GRAP2*	*IFITM3*	*GPR65*	
SUSD3	*THEMIS*	*GZMA*	*IGF2*	*GPSM3*	
TBC1D4	*TIGIT*	*GZMM*	*IGFBP4*	*HCLS1*	
TCF7	*TIMD4*	*HNRNPA1P10*	*IGFBP7*	*HMHA1*	
TESPA1	*TMEM155*	*ICOS*	*JAG1*	*IKZF1*	
TIAM1	*TNFRSF9*	*IL12RB1*	*KIAA1217*	*IL10RA*	
TMEM66	*TNIP3*	*IL21R*	*LAMB1*	*IL16*	
TNFAIP3	*TOX*	*IL2RB*	*LAMB2*	*IL2RG*	
TNFSF8	*TTC24*	*IL2RG*	*LAMC1*	*INPP5D*	
TNIK	*TTN*	*IL32*	*LEPROT*	*ITGA4*	
TPT1	*ZBED2*	*INPP4B*	*LHFP*	*ITGAL*	
		IPCEF1	*LIMCH1*	*ITGB2*	
		ITGAL	*LIMS2*	*LAIR1*	
		ITK	*LMCD1*	*LAPTM5*	
		JAK3	*LOXL2*	*LCP1*	
		KCNA3	*LPHN2*	*LILRB3*	
		LAT	*LRRC32*	*LIMD2*	
		LCK	*MAP1B*	*LPXN*	
		LIME1	*MEOX2*	*LSP1*	
		LOC100130231	*MGP*	*LY9*	
		MBOAT1	*MMP2*	*MAP4K1*	
		MIAT	*NFIB*	*MYO1G*	
		NLRC5	*NID1*	*NCKAP1L*	
		PAG1	*NNMT*	*NR4A2*	
		PARP8	*NPDC1*	*PARP8*	
		PCED1B	*NR2F2*	*PARVG*	
		PCED1B-AS1	*NT5E*	*PIK3CD*	
		PDCD1	*NUAK1*	*PIM2*	
		PIP4K2A	*PEAR1*	*PLCB2*	
		PRDM1	*PHLDB2*	*PLEKHA2*	
		PRF1	*PLSCR4*	*PRKCB*	
		PRKCQ	*PPAP2A*	*PSD4*	
		PTPN22	*PPAP2B*	*PSTPIP2*	
		PTPN7	*PPIC*	*PTK2B*	
		PTPRC	*PRKCDBP*	*PTPN22*	
		PYHIN1	*PROCR*	*PTPN6*	
		RASAL3	*PRSS23*	*PTPN7*	
		RASGRP1	*PTRF*	*PTPRC*	
		RGS1	*PXDN*	*RAC2*	
		RHOF	*RAB11FIP5*	*RASSF5*	
		RNF213	*RABAC1*	*RCSD1*	
		SCML4	*RBPMS*	*RGS1*	
		SEPT1	*RUNX1T1*	*RHOH*	
		SH2D1A	*S100A16*	*RPS6KA1*	
		SH2D2A	*SERPINH1*	*SAMSN1*	
		SH3KBP1	*SPARC*	*SASH3*	
		SIRPG	*SPARCL1*	*SLA*	
		SIT1	*STC2*	*SNX20*	
		SKAP1	*TFPI*	*SP140*	
		SLC9A3R1	*TGFB1I1*	*STK17B*	
		SPATA13	*THBS1*	*TAGAP*	
		SPN	*THY1*	*TBC1D10C*	
		SPOCK2	*TMEM204*	*TMC6*	
		STAT4	*TNKS1BP1*	*TMC8*	

		SYTL3	*TNXB*	*TMSB4X*	
		TBC1D10C	*TPBG*	*TRAF3IP3*	
		TC2N	*UNC5B*	*TSC22D3*	
		TESPA1	*VCL*	*TSTD1*	
		THEMIS	*ZEB1*	*UCP2*	
		TIGIT	*ZNF423*	*VAV1*	
		TMEM66	*ZNF521*	*WIPF1*	
		TNFAIP3			
		TOX			
		TRAF1			
		TRAT1			
		TTC39C			
		TUBA4A			
		UBASH3A			
		WIPF1			
		ZAP70			
		ZC3HAV1			

T CD4 NAIVE	T CD4 TREG	T CD8 CYTOTOXIC	T CD8 EXHAUSTED	T CD8 NAIVE
ABLIM1	*ARID3B*	*APOBEC3C*	*ABCC9*	*ATM*
ATM	*CARD16*	*B2M*	*AKAP5*	*ATXN7*
CAMK4	*CCR4*	*CCL3*	*ANKLE1*	*CAMK4*
CCR7	*CCR8*	*CCL4*	*AP4B1-AS1*	*CCR7*
EEF1A1	*CD177*	*CCL5*	*APOBEC3A*	*EEF1A1*
EEF1B2	*DDX60*	*CSF1*	*ARHGEF26-AS1*	*FAM102A*
EEF1G	*ERI1*	*CST7*	*ASXL2*	*FKBP5*
FAM65B	*EZH2*	*FASLG*	*ATHL1*	*GPR155*
FHIT	*FAS*	*GZMB*	*ATXN1*	*IL7R*
GIMAP5	*FOXP3*	*GZMH*	*CBLB*	*LEF1*
IL7R	*GATA3*	*HLA-C*	*CD3E*	*NELL2*
LDHB	*GBP5*	*IFNG*	*CD8A*	*PIK3IP1*
LDLRAP1	*GCHFR*	*PRF1*	*CDKN1B*	*PPP1R2*
LEF1	*HNRNPC*		*CLEC2D*	*PRKCQ-AS1*
LOC100130231	*HPRT1*		*CNOT6L*	*SELL*
NAP1L1	*IL10RA*		*CTLA4*	*SORL1*
NOSIP	*IL1R2*		*CXCL13*	*TCF7*
PABPC1	*IL2RA*		*DENND2D*	*TSC22D3*
PIK3IP1	*IL2RG*		*DFNB31*	*UBA52*
SELL	*IL32*		*DGKH*	
SERINC5	*LAIR2*		*DOCK8*	
SF1	*LAYN*		*DTHD1*	
TCF7	*LOC541471*		*DUSP4*	
TMEM66	*LTB*		*ELF1*	
TPT1	*PARK7*		*ENTPD1*	
TRABD2A	*PIM2*		*FAM122C*	
TSC22D3	*PMAIP1*		*FAM3C*	
TXNIP	*PPP2CA*		*FAM73A*	
UBA52	*RASGRP1*		*FBXL18*	
	RORA		*FCRL3*	
	RTKN2		*GBP2*	
	S100A4		*GDPD1*	
	SAMD9		*GLUD1P7*	
	STAM		*HAVCR2*	
	SUMO2		*HINT3*	
	TNFRSF18		*HNRPLL*	
	USP15		*IFNLR1*	
	WDR1		*IL10*	
	ZBTB32		*INPP4B*	

			INPP5F	
			ITGA4	
			ITM2A	
			ITPKB	
			KIAA1324	
			LAG3	
			LINC00294	
			LOC100131257	
			LOC100190986	
			LOC100271836	
			LOC286186	
			LOC440354	
			LOC728558	
			LYST	
			MAPK13	
			MCL1	
			MTX3	
			NFATC1	
			NXNL2	
			ODF2L	
			OSBPL3	
			PCED1B	
			PCGF5	
			PDCD1	
			PDE4D	
			PER2	
			PLEKHG2	
			PRICKLE2-AS3	
			PTPRC	
			RAB27A	
			RAMP2-AS1	
			RGS1	
			RNF19A	
			SCD5	
			SF3B3	
			SH2D2A	
			SMG1P1	
			STAT1	
			STAT3	
			TANGO2	
			TATDN3	
			TBXA2R	
			TIGIT	
			TMEM136	
			TMEM212	
			TNFRSF1B	
			TNFRSF9	
			TP53INP1	
			TRAF5	
			TTN	
			TXNDC11	
			USP33	
			VSIG1	
			VSTM4	
			ZNF620	
			ZNF79	

Table 26C.

Table 26C. Cell type signatures that were used for cell classification.

Macrophage	CCR5	CD14	CD163	CD33	CD68	CD86	CSF1R	ENG	FCGR1A	FUT4	ITGAL	ITGAM	ITGAX	LAMP2	LILRB4
Cytotoxic_T_cell	CCL3	CCL4	CD2	CD3D	CD3E	CD3G	CD8A	CD8B	GST7	GZMA	GZMB	IFNG	NKG7	PRF1		
Treg	CCR4	CD4	CNGB1	CTLA4	ENTPD1	FOXP3	IKZF2	IL2RA	IS620	ITGAE	LAG3	LRRC32	NT5E	SELL	TNFRSF18	TNFRSF4
Th22	AHR	CCR10	CCR4	CCR6	CD3D	CD3E	CD3G	CD4								
Th17	CCR4	CCR6	CD38	CD3D	CD3E	CD3G	CD4	IL17A	IL17F	IL1R1	IL21	IL22	KLRB1	LINC-ROR	STAT3	
Th9	CD3D	CD3E	CD3G	CD4	GATA3	IRF4	STAT6									
Th2	CCR3	CCR4	CCR7	CCR8	CD4	CSF2	CXCR4	GATA3	HAVCR1	ICOS	IL10	IL13	IL1R1	IL4	IL5	IL6
Th1	CCR1	CCR5	CD4	CSF2	CXCR3	DPP4	HAVCR2	IFNA1	IFNGR1	IL2	KLRD1	TNF	TNFSF11			
T Follicular Helper	BCL6	CD3D	CD3E	CD3G	CD4	CD40LG	CD84	CXCR5	ICOS	IL6R	PDCD1	SLAMF1	STAT3	TNFSF4		
Platelet	BSG	CCL5	CCR3	CD109	CD151	CD226	CD36	CD46	CD47	CD48	CD63	CD69	CD84	CD9	CNGB1	CSF3R
Plasmacytoid Dendritic Cell	CCR7	CD1A	CD1B	CD1C	CD4	CD40	CD80	CD83	CD86	CD8A	CLEC4C	CMKLR1	IL3RA	ITGA4	ITGAM	ITGAX
NK Cell	B3GAT1	CD244	CD69	IL2RB	ITGA2	ITGAM	ITGAX	KLRA1	KLRB1	KLRD1	KLRK1	NCAM1	NCR1	NKG2	SIGLEC7	SLAMF6
Neutrophil	ANPEP	CSAR1	CD14	CD33	CEACAM8	CSF3R	CXCR1	CXCR2	FCGR1A	FUT4	ITGAM	ITGAX	MME	PECAM1	SELL	TLR2
Naive T Cell	CCR7	CD3D	CD3E	CD3G	CD4	SELL										
Myeloid Dendritic Cell	CCR7	CD1A	CD1B	CD1C	CD207	CD209	CD4	CD40	CD80	CD83	CD86	CMKLR1	DCX	ITGA4	ITGAM	ITGAX
Megakaryocyte	CD9	GP1BA	ITGA2B	ITGAV	ITGB3	PECAM1	SELP									HLA-DRB1
MDSC	CCR7	CD1A	CD1B	CD1C	CD207	CD209	CD4	CD40	CD80	CD83	CD86	CMKLR1	HLA-DOA	HLA-DOB	HLA-DRA	
Mast Cell	ENPP3	KIT														
Erythrocyte	CD24	GYPA	PTPRC													
Eosinophil	C3AR1	CSAR1	CCR1	CCR3	CD244	CD52	CD53	CXCR3	FCER2	FUT4	IL9R	ITGA4	LAIR1	PTGDR2	S100A9	SIGLEC10
B cell	BLK	CD19	CD2	CD22	CD40	CD5	CD69	CD70	CD79A	CD79B	CD80	CD86	CD93	FCER2	MS4A1	PAX5
Basophile	ANPEP	CCR3	CD44	CD63	CD69	ENPP3	ICAM1	IL3RA	LAMP1	TLR4						
CAF	FAP	THY1	DCN	COL1A1	COL1A2	COL6A1	COL6A2	COL6A3								
Stromal Cell	MMP2	ICAM3	TLR3	MADCAM 1	MMP1	PDGFRA	TLR4	THY1	KIT	TIMP1	ITGA4	MMP9	PDGFRB	MME	PECAM1	TIMP2
Endothelial Cell	VWF	TEK	MCAM	CD34	ITGB3	PROCR	CDH5	KDR	SELE	PECAM1	ENG	ICAM1	FLT4	VCAM1		

																								TLR2
																							TLR4	
																						PTGDR2		
																					FCGR2A			
																				NRP1	FCGR2B			
																			SLAMF7		GP1BA			
																					ICAM2			
																					ITGA2			
																					ITGA2B			
																					ITGA6			
																					ITGAV			
																					ITGB1			
																					ITGB3			
																					IAM3			
																					LAMP2			
																					LRRC32			
																					LYN			
																					PECAM1			
																					SELP			
																					SPN			
																					TNFSF14			
																					HLA-DRB5			
																				LY75	NRP1			
																					PDCD1LG2			
																					ITGA4			
																					ITGAM			
																					ITGAX			
																					LY75			
																					NRP1			
																					PDCD1LG2			
																					ITGB1			
																					ICAM1			
																					ICAM2			
																					TLR2			
																					VCAM1			
																					TLR1			



[0553] **Table 27. (A)** The immune resistance program; **(B)** alternative T cell exclusion and post-treatment signatures; **(C)** T cell exclusion and post-treatment signatures identified in macrophages; related to **Figures 62.**

Table 27A. The immune resistance program

Induced						
GENE (up)	Number of supporting evidences (up)	Exclusion (up)	Exclusion seed (up)	Post-treatment (up)	Functional immune resistance (up)	CDK7 targets
BZW2	3	1	1	1	0	0
CCT3	3	1	1	1	0	0
CDK4	3	1	1	1	0	0
GPATCH4	3	1	1	1	0	1
ISYNA1	3	1	1	1	0	0
MDH2	3	1	1	1	0	0
PPIA	3	1	0	1	1	0
RPL31	3	1	0	1	1	1
RPL37A	3	1	0	1	1	0
RPL41	3	1	0	1	1	1
RPS21	3	1	0	1	1	0
RPS27A	3	1	0	1	1	0
RUVBL2	3	1	1	1	0	0
SAE1	3	1	0	1	1	0
UBA52	3	1	0	1	1	0
AHCY	2	1	1	0	0	0
C17orf76-AS1	2	1	0	1	0	0
C19orf48	2	1	0	0	1	1
C1QBP	2	1	0	1	0	0
CCT6A	2	1	1	0	0	0
CHCHD2	2	1	0	0	1	0
CTPS1	2	1	0	1	0	0
EEF1G	2	1	0	1	0	0
EIF2S3	2	1	0	1	0	0
EIF3K	2	1	0	1	0	0
EIF4A1	2	1	0	1	0	1
FARSA	2	1	0	0	1	0
FBL	2	1	0	1	0	0
FKBP4	2	1	1	0	0	0
GAS5	2	1	0	1	0	0
GNB2L1	2	1	0	1	0	0
GPI	2	1	0	1	0	0
HNRNPA1	2	1	0	1	0	0
HNRNPC	2	1	0	1	0	0
IDH2	2	1	0	1	0	0
ILF2	2	1	0	1	0	0

NACA	2	1	0	1	0	0
NCL	2	1	0	1	0	0
NME1	2	1	1	0	0	1
NOLC1	2	1	0	1	0	0
NONO	2	0	0	1	1	0
PABPC1	2	1	0	1	0	1
PAICS	2	1	1	0	0	0
PFN1	2	1	0	1	0	0
POLD2	2	1	1	0	0	0
PPA1	2	1	0	1	0	0
PTMA	2	1	0	1	0	1
PUF60	2	1	1	0	0	0
RPL10A	2	1	0	1	0	1
RPL11	2	1	0	1	0	0
RPL12	2	1	0	1	0	0
RPL13	2	1	0	1	0	1
RPL13A	2	1	0	1	0	0
RPL13AP5	2	1	0	1	0	0
RPL17	2	1	0	1	0	0
RPL18	2	1	0	1	0	0
RPL18A	2	1	0	1	0	0
RPL21	2	1	0	1	0	0
RPL26	2	1	0	1	0	0
RPL27	2	1	0	0	1	0
RPL28	2	1	0	1	0	1
RPL29	2	1	0	1	0	1
RPL3	2	1	0	1	0	1
RPL36	2	1	0	0	1	1
RPL36A	2	1	0	1	0	0
RPL37	2	1	0	1	0	0
RPL4	2	1	0	1	0	0
RPL5	2	1	0	1	0	1
RPL6	2	1	0	1	0	0
RPL8	2	1	0	1	0	0
RPLP0	2	1	0	1	0	1
RPLP1	2	1	0	1	0	1
RPS10	2	1	0	1	0	0
RPS11	2	1	0	1	0	1
RPS13	2	1	0	0	1	0
RPS14	2	1	0	0	1	0
RPS15	2	1	0	0	1	1
RPS15A	2	1	0	1	0	1
RPS16	2	1	0	1	0	0
RPS17	2	1	0	1	0	0
RPS17L	2	1	0	1	0	0
RPS18	2	1	0	1	0	0
RPS19	2	1	0	1	0	0
RPS23	2	1	0	1	0	0
RPS24	2	1	0	1	0	0
RPS27	2	1	0	1	0	1
RPS28	2	1	0	0	1	1
RPS3	2	1	0	1	0	1
RPS4X	2	1	0	1	0	0

RPS5	2	1	0	1	0	1
RPS6	2	1	0	1	0	1
RPS7	2	1	0	1	0	1
RPS8	2	1	0	1	0	1
RPS9	2	1	0	1	0	1
RPSA	2	1	0	1	0	0
RRS1	2	1	1	0	0	0
SERPINF1	2	1	0	1	0	0
SET	2	1	0	1	0	0
SHMT2	2	1	0	1	0	0
SLC19A1	2	1	1	0	0	0
SLC25A13	2	1	1	0	0	0
SNHG6	2	1	0	1	0	0
SNRPE	2	1	0	1	0	1
SOX4	2	1	0	1	0	1
SSR2	2	1	0	1	0	0
TIMM50	2	1	0	1	0	0
TOP1MT	2	1	1	0	0	0
TUBB	2	1	0	1	0	0
UQCRFS1	2	1	0	1	0	0
UQCRH	2	1	0	1	0	0
VDAC2	2	1	0	1	0	0
ACTB	1	0	0	1	0	1
AEN	1	0	0	1	0	0
ANP32E	1	0	0	1	0	1
APP	1	1	0	0	0	0
ARMC6	1	0	0	0	1	0
ATP5A1	1	0	0	1	0	0
ATP5D	1	1	0	0	0	0
ATP5G2	1	0	0	1	0	0
ATP5G3	1	1	0	0	0	0
BOLA2	1	0	0	0	1	0
BOLA2B	1	0	0	0	1	0
BOP1	1	1	0	0	0	0
BTF3	1	1	0	0	0	0
C20orf112	1	0	0	1	0	0
C6orf48	1	1	0	0	0	1
CA14	1	0	0	1	0	0
CACYBP	1	1	0	0	0	0
CBX5	1	0	0	1	0	0
CCT2	1	0	0	1	0	0
CCT4	1	1	0	0	0	1
CCT7	1	1	0	0	0	0
CDC123	1	0	0	0	1	0
CDCA7	1	1	0	0	0	0
CFL1	1	0	0	1	0	0
CKS1B	1	0	0	0	1	0
CMSS1	1	0	0	0	1	0
CNRIP1	1	0	0	1	0	0
CS	1	0	0	1	0	0
DARS	1	1	0	0	0	0
DCAF13	1	0	0	1	0	0
DCT	1	0	0	1	0	0

DCTPP1	1	1	0	0	0	0
DDX21	1	1	0	0	0	0
DDX39A	1	0	0	0	1	0
DDX39B	1	0	0	1	0	1
DLL3	1	0	0	1	0	0
DNAJC9	1	0	0	0	1	0
EEF1B2	1	1	0	0	0	0
EEF1D	1	1	0	0	0	0
EEF2	1	1	0	0	0	0
EIF3E	1	1	0	0	0	0
EIF3F	1	1	0	0	0	0
EIF3G	1	1	0	0	0	1
EIF3M	1	1	0	0	0	0
EIF4EBP2	1	0	0	1	0	0
ENO1	1	1	0	0	0	0
EXOSC5	1	1	0	0	0	0
FAM174B	1	0	0	1	0	0
FAM60A	1	0	0	0	1	0
FAM92A1	1	1	0	0	0	0
FBLN1	1	0	0	1	0	0
FOXRED2	1	0	0	1	0	0
FTL	1	0	0	1	0	1
FUS	1	0	0	1	0	0
GABARAP	1	0	0	1	0	0
GGH	1	1	0	0	0	0
GNL3	1	1	0	0	0	0
GRWD1	1	0	0	1	0	0
H3F3A	1	0	0	1	0	0
H3F3AP4	1	0	0	1	0	0
HMGA1	1	0	0	1	0	0
HMGB1	1	1	0	0	0	0
HN1	1	0	0	0	1	0
HNRNPA1P10	1	0	0	1	0	0
HNRNPH1	1	1	0	0	0	1
HNRNPM	1	1	0	0	0	0
HSP90AB1	1	0	1	0	0	1
HSPA8	1	0	0	1	0	1
HSPD1	1	1	0	0	0	0
IFRD2	1	1	0	0	0	0
ILF3	1	1	0	0	0	0
IMPDH2	1	1	0	0	0	1
ITM2C	1	0	0	1	0	0
KIAA0101	1	0	0	1	0	0
LDHB	1	1	0	0	0	0
LSM4	1	1	0	0	0	0
LSM7	1	1	0	0	0	1
LYPLA1	1	1	0	0	0	0
MAGEA4	1	0	0	1	0	0
MAGEC1	1	1	0	0	0	0
MCM7	1	1	0	0	0	0
METAP2	1	0	0	1	0	0
MID1	1	0	0	1	0	0
MIR4461	1	0	0	1	0	0

MKI67IP	1	1	0	0	0	0
MLLT11	1	0	0	1	0	0
MPZL1	1	0	0	1	0	0
MRPL15	1	1	0	0	0	1
MRPL37	1	1	0	0	0	0
MRPL4	1	1	0	0	0	0
MRPL47	1	0	0	0	1	1
MRPS12	1	1	0	0	0	0
MRPS21	1	0	0	1	0	0
NDUFA11	1	1	0	0	0	0
NDUFA13	1	0	0	0	1	0
NDUFS2	1	0	0	1	0	1
NME2	1	1	0	0	0	0
NOP16	1	1	0	0	0	0
NPM1	1	1	0	0	0	1
NREP	1	1	0	0	0	0
PA2G4	1	0	0	1	0	0
PAFAH1B3	1	0	0	1	0	0
PET100	1	0	0	0	1	0
PFDN2	1	0	0	1	0	0
PFDN4	1	0	0	0	1	0
PGAM1	1	0	0	1	0	0
PIH1D1	1	0	0	1	0	0
PLEKHJ1	1	1	0	0	0	0
POLR1D	1	1	0	0	0	0
POLR2E	1	1	0	0	0	0
PPP2R1A	1	0	0	1	0	0
PRMT1	1	1	0	0	0	0
PSMA7	1	0	0	0	1	0
PSMD4	1	0	0	1	0	0
RAN	1	0	0	1	0	0
RBM34	1	0	0	1	0	0
RNASEH2A	1	0	0	0	1	0
RNF2	1	0	0	1	0	0
ROMO1	1	0	0	0	1	0
RPAIN	1	0	0	1	0	0
RPL10	1	1	0	0	0	1
RPL14	1	1	0	0	0	0
RPL15	1	1	0	0	0	0
RPL19	1	1	0	0	0	0
RPL22	1	1	0	0	0	0
RPL27A	1	1	0	0	0	0
RPL30	1	1	0	0	0	0
RPL32	1	1	0	0	0	0
RPL35	1	1	0	0	0	0
RPL35A	1	0	0	0	1	0
RPL39	1	1	0	0	0	0
RPL7	1	1	0	0	0	0
RPL7A	1	1	0	0	0	1
RPL9	1	1	0	0	0	0
RPLP2	1	1	0	0	0	0
RPS12	1	0	0	1	0	1
RPS2	1	1	0	0	0	1

RPS20	1	1	0	0	0	1
RPS25	1	1	0	0	0	0
RPS3A	1	1	0	0	0	1
RQCD1	1	1	0	0	0	0
RSL1D1	1	1	0	0	0	1
RTKN	1	0	1	0	0	0
SCD	1	0	0	1	0	0
SCNM1	1	0	0	1	0	1
SERBP1	1	1	0	0	0	0
SF3B4	1	0	0	1	0	0
SKP2	1	0	0	1	0	0
SLC25A3	1	0	0	1	0	0
SLC25A6	1	1	0	0	0	0
SLIRP	1	0	0	0	1	0
SLMO2	1	0	0	0	1	0
SMARCA4	1	1	0	0	0	0
SMIM15	1	1	0	0	0	0
SMS	1	0	0	1	0	0
SNAI2	1	0	0	1	0	0
SNHG15	1	1	0	0	0	0
SNRPB	1	1	0	0	0	0
SNRPC	1	1	0	0	0	1
SNRPD1	1	1	0	0	0	0
SNRPD2	1	1	0	0	0	0
SNRPF	1	0	0	0	1	0
SNRPG	1	0	0	0	1	0
SRM	1	1	0	0	0	0
SRP14	1	0	0	1	0	0
SSB	1	1	0	0	0	0
TIMM13	1	1	0	0	0	0
TIMM44	1	1	0	0	0	0
TMC6	1	0	0	1	0	0
TP53	1	0	0	1	0	0
TPI1	1	1	0	0	0	1
TPRKB	1	0	0	0	1	0
TRAP1	1	1	0	0	0	0
TRIM28	1	1	0	0	0	1
TRPM1	1	0	0	1	0	0
TSR1	1	0	0	1	0	0
TUBA1B	1	0	0	1	0	1
TULP4	1	0	0	1	0	0
TXNDC17	1	0	0	0	1	0
TYMS	1	1	0	0	0	0
UBL5	1	0	0	0	1	0
UCK2	1	1	0	0	0	0
UHRF1	1	1	0	0	0	0
USMG5	1	0	0	0	1	0
USP22	1	0	0	1	0	0
VCY1B	1	0	0	1	0	0
VPS72	1	0	0	1	0	0
XIST	1	1	0	0	0	0
YWHAE	1	0	0	1	0	1
ZFAS1	1	1	0	0	0	0

ZNF286A	1	0	0	1	0	0

Repressed					
GENE (down)	**Number of supporting evidences (down)**	**Exclusion (down)**	**Exclusion seed (down)**	**Post-treatment (down)**	**Functional immune resistance (down)**
AHNAK	3	1	0	1	1
APOD	3	1	0	1	1
ATP1A1	3	1	0	1	1
B2M	3	1	0	1	1
CD44	3	1	0	1	1
CD63	3	1	0	1	1
CTSB	3	1	0	1	1
CTSD	3	1	0	1	1
FOS	3	1	0	1	1
GRN	3	1	0	1	1
HLA-A	3	1	0	1	1
HLA-B	3	1	0	1	1
HLA-C	3	1	0	1	1
HLA-E	3	1	0	1	1
HLA-H	3	1	0	1	1
LAMP2	3	1	0	1	1
LGALS3	3	1	0	1	1
LGALS3BP	3	1	0	1	1
NPC2	3	1	0	1	1
PSAP	3	1	0	1	1
SERPINE2	3	1	0	1	1
TAPBP	3	1	0	1	1
TIMP2	3	1	0	1	1
A2M	2	1	0	1	0
ACSL3	2	1	0	1	0
AEBP1	2	1	0	1	0
AGA	2	1	0	1	0
APOC2	2	1	1	0	0
APOE	2	1	0	1	0
ATP1B1	2	1	0	1	0
CD151	2	1	0	1	0
CD47	2	1	0	1	0
CD58	2	1	0	1	0
CD59	2	1	0	1	0
CDH19	2	1	0	1	0
CSPG4	2	1	0	1	0
CST3	2	1	0	1	0
CTSA	2	1	0	1	0
CTSL1	2	1	0	1	0
CTSO	2	1	0	0	1
CYP27A1	2	1	1	0	0
DAG1	2	1	0	1	0
DDR1	2	1	0	1	0
EEA1	2	1	0	1	0
EMP1	2	1	0	1	0
EVA1A	2	1	0	1	0

FBXO32	2	1	0	1	0
FGFR1	2	1	0	1	0
GAA	2	1	0	1	0
GPNMB	2	1	0	1	0
GSN	2	1	0	1	0
HLA-F	2	1	0	1	0
HSPA1A	2	1	0	1	0
IRF4	2	1	1	0	0
ITGA3	2	1	0	1	0
KCNN4	2	1	0	1	0
KLF4	2	0	0	1	1
LEF1-AS1	2	1	0	0	1
LRPAP1	2	1	0	1	0
MFGE8	2	1	0	1	0
MIA	2	1	0	1	0
MT2A	2	1	0	1	0
NEAT1	2	1	0	1	0
NPC1	2	1	0	1	0
NSG1	2	1	0	1	0
PROS1	2	1	0	1	0
S100A6	2	1	0	1	0
S100B	2	1	0	1	0
SAT1	2	1	0	1	0
SCARB2	2	1	0	1	0
SDC3	2	1	0	1	0
SEC11C	2	1	1	0	0
SERPINA3	2	1	0	1	0
SGK1	2	1	0	1	0
SLC26A2	2	1	0	1	0
SLC5A3	2	1	0	1	0
STOM	2	0	0	1	1
STX7	2	1	1	0	0
TAPBPL	2	0	0	1	1
TIMP1	2	1	0	1	0
TIMP3	2	1	0	1	0
TM4SF1	2	1	0	1	0
TMED10	2	1	0	1	0
TPP1	2	1	0	1	0
TSC22D3	2	1	0	1	0
TYR	2	1	0	1	0
UBC	2	1	0	1	0
VAT1	2	1	0	0	1
WBP2	2	1	1	0	0
XAGE1D	2	1	1	0	0
ACSL4	1	0	0	1	0
ACTA2	1	0	0	0	1
ADM	1	0	0	1	0
ANGPTL4	1	0	0	1	0
ANXA1	1	0	0	1	0
ANXA2	1	0	0	1	0
APLP2	1	0	0	1	0
APOL1	1	1	0	0	0
ARL6IP5	1	0	0	1	0

ARSA	1	1	0	0	0
ATF3	1	0	0	1	0
ATP1B3	1	0	0	1	0
ATP6V0C	1	1	0	0	0
BACE2	1	0	0	1	0
BBX	1	0	0	1	0
BCL6	1	0	0	1	0
C4A	1	1	0	0	0
C6orf226	1	0	0	0	1
CALU	1	0	0	1	0
CARD16	1	1	0	0	0
CASP1	1	0	0	1	0
CAST	1	0	0	1	0
CAV1	1	0	0	1	0
CAV2	1	1	0	0	0
CCND3	1	0	0	1	0
CCR10	1	0	0	0	1
CD9	1	0	0	1	0
CDH1	1	1	0	0	0
CHI3L1	1	0	0	1	0
CITED1	1	0	0	0	1
CLIC4	1	0	0	1	0
CORO1A	1	0	0	0	1
CRELD1	1	0	0	1	0
CRYAB	1	0	0	1	0
CSGALNACT1	1	0	0	1	0
CXCR4	1	0	0	0	1
CYP4V2	1	1	0	0	0
DCBLD2	1	0	0	1	0
DDX17	1	0	0	0	1
DDX5	1	0	0	1	0
DPYSL2	1	0	0	1	0
DUSP4	1	0	0	1	0
DUSP6	1	0	0	1	0
ECM1	1	0	0	1	0
EGR1	1	0	0	1	0
EPHX2	1	0	0	1	0
ERBB3	1	0	0	1	0
EZH1	1	0	0	1	0
FAM3C	1	0	0	1	0
FCGR2C	1	0	0	1	0
FCRLA	1	0	0	1	0
FLJ39051	1	0	0	0	1
FLJ43663	1	0	0	1	0
FLNA	1	1	0	0	0
FMN1	1	0	0	0	1
FRZB	1	0	0	0	1
FSTL3	1	0	0	0	1
FTH1	1	0	0	0	1
GADD45B	1	0	0	1	0
GATSL3	1	1	0	0	0
GEM	1	0	0	1	0
GJB1	1	1	0	0	0

GOLGB1	1	0	0	1	0
GPR155	1	1	0	0	0
GPR56	1	1	0	0	0
HLA-DRB5	1	0	0	0	1
HLA-G	1	1	0	0	0
HPCAL1	1	0	0	1	0
HTATIP2	1	0	0	1	0
IDI2-AS1	1	0	0	0	1
IFI27	1	1	0	0	0
IFI27L2	1	1	0	0	0
IFI35	1	0	0	1	0
IFI6	1	1	0	0	0
IGF1R	1	0	0	1	0
IGFBP7	1	1	0	0	0
IGSF8	1	1	0	0	0
IL1RAP	1	0	0	1	0
IL6ST	1	0	0	1	0
ITGA6	1	0	0	1	0
ITGA7	1	1	0	0	0
ITGB1	1	0	0	1	0
ITGB3	1	0	0	1	0
ITM2B	1	0	0	1	0
JMJD7	1	0	0	0	1
JUN	1	0	0	1	0
KLF6	1	0	0	1	0
LAMB2	1	1	0	0	0
LCP1	1	0	0	0	1
LEPROT	1	0	0	1	0
LGALS1	1	0	0	1	0
LGMN	1	1	0	0	0
LINC00518	1	0	0	0	1
LOC100126784	1	1	0	0	0
LOC100506190	1	1	0	0	0
LOC100506714	1	0	0	0	1
LOC100507463	1	0	0	0	1
LPL	1	0	0	1	0
LY6E	1	1	0	0	0
LY96	1	0	0	0	1
LYRM9	1	1	0	0	0
MAGEC2	1	0	0	1	0
MALAT1	1	1	0	0	0
MATN2	1	1	0	0	0
MCAM	1	1	0	0	0
MFI2	1	0	0	1	0
MMP14	1	1	0	0	0
MPZ	1	1	0	0	0
MT1E	1	0	0	1	0
MT1M	1	0	0	1	0
MT1X	1	0	0	1	0
MTRNR2L1	1	1	0	0	0
MTRNR2L10	1	1	0	0	0
MTRNR2L2	1	1	0	0	0
MTRNR2L3	1	1	0	0	0

MTRNR2L4	1	1	0	0	0
MTRNR2L5	1	1	0	0	0
MTRNR2L6	1	1	0	0	0
MTRNR2L7	1	1	0	0	0
MTRNR2L8	1	1	0	0	0
MYO1D	1	1	0	0	0
NAV2	1	1	0	0	0
NFE2L1	1	1	0	0	0
NFKBIA	1	0	0	1	0
NFKBIZ	1	0	0	1	0
NMRK1	1	0	0	0	1
NNMT	1	0	0	1	0
NR4A1	1	0	0	1	0
P2RX4	1	0	0	0	1
PAGE5	1	0	1	0	0
PDE4DIP	1	1	0	0	0
PDK4	1	0	0	1	0
PERP	1	1	0	0	0
PIK3IP1	1	0	0	0	1
PLP2	1	0	0	1	0
PRKCDBP	1	0	0	1	0
PRNP	1	0	0	1	0
PRSS23	1	0	0	1	0
PSMB9	1	0	0	1	0
PTRF	1	0	0	1	0
PYGB	1	0	0	0	1
QPCT	1	1	0	0	0
RAB27A	1	0	0	0	1
RBP7	1	0	0	0	1
RDH5	1	1	0	0	0
RNF145	1	0	0	1	0
RNF213	1	0	0	0	1
RPS4Y1	1	0	0	1	0
RTP4	1	0	0	0	1
S100A1	1	1	0	0	0
S100A13	1	1	0	0	0
SCCPDH	1	0	0	1	0
SDCBP	1	0	0	0	1
SEL1L	1	0	0	1	0
SEMA3B	1	0	0	1	0
SERINC1	1	1	0	0	0
SERPINA1	1	1	0	0	0
SGCE	1	0	0	1	0
SHC4	1	1	0	0	0
SLC20A1	1	0	0	1	0
SLC22A18	1	0	0	0	1
SLC39A14	1	0	0	1	0
SLC7A5P1	1	0	0	0	1
SLC7A8	1	1	0	0	0
SNX9	1	1	0	0	0
SOD1	1	0	0	1	0
SORT1	1	1	0	0	0
SP100	1	0	0	0	1

SPESP1	1	0	0	0	1
SPINT1	1	0	0	0	1
SPON2	1	1	0	0	0
SPP1	1	1	0	0	0
SPRY2	1	0	0	1	0
SQSTM1	1	0	0	1	0
SRPX	1	0	0	1	0
ST3GAL6-AS1	1	0	0	0	1
ST6GALNAC2	1	0	0	0	1
STRIP2	1	1	0	0	0
SYNE2	1	1	0	0	0
SYNGR2	1	0	0	1	0
SYPL1	1	0	0	1	0
TF	1	0	0	1	0
TFAP2A	1	0	0	0	1
TGOLN2	1	0	0	1	0
THBD	1	1	0	0	0
TMBIM6	1	1	0	0	0
TMED9	1	0	0	1	0
TMEM255A	1	1	0	0	0
TMEM66	1	0	0	1	0
TMX4	1	0	0	1	0
TNC	1	0	0	1	0
TNFSF4	1	1	0	0	0
TRIM22	1	0	0	0	1
TRIML2	1	1	0	0	0
TSPYL2	1	1	0	0	0
TTLL1	1	0	0	0	1
TXNIP	1	1	0	0	0
UCN2	1	0	0	0	1
UPP1	1	0	0	1	0
WDFY1	1	0	1	0	0
ZBTB20	1	0	0	1	0
ZBTB38	1	0	0	1	0

Table 27B. Alternative T cell exclusion and post-treatment signatures

Table 27B.1

CELL CYCLE FILTERED					
POST TREATMENT	**POST TREATMENT DOWN**	**T CD8 EXC. (UP)**	**T CD8 EXC. (DOWN)**	**RELATIVE T CD8 EXC. (UP)**	**RELATIVE T CD8 EXC. (DOWN)**
ABR	*A2M*	*AASDHPPT*	*A2M*	*ATIC*	*APOD*
ANXA13	*ACSL3*	*AHCY*	*AEBP1*	*BTF3*	*APOE*
ATP5A1	*AEBP1*	*APP*	*AGA*	*CHCHD2*	*ATP1A1*
BCAN	*AHNAK*	*ATP5D*	*AHNAK*	*EEF1G*	*B2M*
BZW2	*ANXA1*	*BTF3*	*APOC2*	*EIF3G*	*CAPN3*
C17orf76-AS1	*ANXA2*	*BZW2*	*APOD*	*EIF3M*	*CD63*
C1QBP	*APLP2*	*C17orf76-AS1*	*APOE*	*EIF4A1*	*CDH1*
C20orf112	*APOC2*	*C1QBP*	*APOL1*	*ENO1*	*CTSD*
CD68	*APOD*	*C6orf48*	*ARSA*	*EXOSC4*	*DAAM2*
CDH3	*APOE*	*CCT3*	*ATP1A1*	*FARSA*	*GPNMB*
CHP1	*ARL6IP5*	*CCT6A*	*ATP1B1*	*GAPDH*	*GPR56*

CS	*ATP1A1*	*DAP3*	*ATP6V0B*	*H19*	*HLA-A*
DCT	*ATP1B1*	*DARS*	*ATP6V0C*	*HNRNPA1*	*HLA-B*
DDX39B	*ATP1B3*	*DDX21*	*B2M*	*LSM7*	*HLA-C*
EEF1A1	*B2M*	*EEF1B2*	*C4A*	*MAGEA4*	*HLA-F*
EEF1G	*BBX*	*EEF1G*	*CAV2*	*MAGEC1*	*HLA-H*
EGFL8	*CALU*	*EEF2*	*CCND3*	*MDH2*	*HPS5*
EIF2S3	*CAV1*	*EIF2S3*	*CD151*	*MKI67IP*	*HSP90AA1*
EIF3K	*CCND3*	*EIF3G*	*CD47*	*MLLT11*	*IFI27*
EIF4A1	*CD151*	*EIF3I*	*CD58*	*MRPS24*	*IRF4*
EIF4EBP2	*CD44*	*EIF3M*	*CD59*	*NACA*	*LGALS3*
FAM174B	*CD47*	*EIF4A1*	*CD63*	*NDUFB9*	*LGALS3BP*
FOXRED2	*CD58*	*FARSA*	*CDH1*	*NME1*	*MCAM*
FTL	*CD59*	*FBL*	*CDH19*	*NREP*	*MTRNR2L1*
GABARAP	*CD63*	*FKBP4*	*CSPG4*	*RPL13AP5*	*MTRNR2L10*
GAS5	*CD9*	*GAS5*	*CTSA*	*RPL18A*	*MTRNR2L2*
GNB2L1	*CDH19*	*GNB2L1*	*CTSB*	*RPL19*	*MTRNR2L3*
GPI	*CLIC4*	*GPATCH4*	*CTSD*	*RPL26*	*MTRNR2L4*
H3F3A	*CRYAB*	*GPI*	*CTSL1*	*RPL27A*	*MTRNR2L6*
HHATL	*CSPG4*	*HNRNPA1*	*DAG1*	*RPL31*	*MTRNR2L8*
HMGA1	*CST3*	*HNRNPC*	*DDR1*	*RPL32*	*NSG1*
HNRNPC	*CTSB*	*ILF2*	*DDX5*	*RPL35A*	*PLXNC1*
IDH2	*CTSD*	*IMPDH2*	*EEA1*	*RPL36*	*PSAP*
ILF2	*CTSL1*	*ISYNA1*	*EMP1*	*RPL37*	*QPCT*
ISYNA1	*DAG1*	*LSM7*	*EVA1A*	*RPL37A*	*RAB5B*
ITM2C	*DCBLD2*	*MDH2*	*EZR*	*RPL39*	*S100A1*
KCNAB2	*DDR1*	*MKI67IP*	*FBXO32*	*RPL6*	*S100B*
KLHDC8B	*DDX5*	*MRPL4*	*FGFR1*	*RPL7*	*SAT1*
LHFPL3-AS1	*DPYSL2*	*NAPRT1*	*FOS*	*RPLP2*	*SEC11C*
MAGEA4	*DUSP4*	*NME1*	*GAA*	*RPS11*	*SLC7A8*
MID1	*DUSP6*	*NOLC1*	*GATSL3*	*RPS13*	*ST3GAL6*
MIR4461	*EEA1*	*NPM1*	*GJB1*	*RPS14*	*TMED10*
MPZL1	*EGR1*	*PABPC1*	*GPR155*	*RPS15*	*TMEM255A*
NACA	*EMP1*	*PAICS*	*GRN*	*RPS16*	*TYR*
NDUFS2	*FAM114A1*	*PFN1*	*GSN*	*RPS17*	*VAT1*
NENF	*FAM3C*	*PLEKHJ1*	*HLA-A*	*RPS17L*	
NONO	*FCRLA*	*PLTP*	*HLA-B*	*RPS18*	
PABPC1	*FGFR1*	*POLD2*	*HLA-C*	*RPS20*	
PFDN2	*FOS*	*POLR1D*	*HLA-E*	*RPS21*	
PFN1	*FXYD3*	*POLR2E*	*HLA-F*	*RPS23*	
PLTP	*GAA*	*QTRT1*	*HLA-G*	*RPS25*	
PPP2R1A	*GRN*	*RPL10*	*HLA-H*	*RPS27A*	
PRAME	*GSN*	*RPL10A*	*HSPA1A*	*RPS28*	
PTMA	*HLA-A*	*RPL11*	*ID2*	*RPS4X*	
RAB38	*HLA-B*	*RPL12*	*IFI27*	*RPS5*	
RBM34	*HLA-C*	*RPL13*	*IFI27L2*	*RPS6*	
RPL10A	*HLA-E*	*RPL13A*	*IGFBP7*	*SMARCA4*	
RPL11	*HLA-F*	*RPL13AP5*	*IGSF8*	*SNRPD2*	
RPL13	*HLA-H*	*RPL14*	*IRF4*	*STOML2*	
RPL13AP5	*HPCAL1*	*RPL15*	*ITGA3*	*TIMM13*	
RPL17	*HSPA1A*	*RPL17*	*ITGA7*	*TPI1*	
RPL18	*IGF1R*	*RPL18*	*LAMP2*	*UBA52*	
RPL18A	*IGFBP7*	*RPL18A*	*LEF1-AS1*	*WBSCR22*	
RPL26	*IL6ST*	*RPL21*	*LGALS3*		
RPL28	*ITGA3*	*RPL23*	*LGMN*		
RPL29	*ITGB1*	*RPL26*	*LOC100126784*		
RPL31	*ITGB3*	*RPL27*	*LOC100506190*		
RPL36A	*ITM2B*	*RPL27A*	*LRPAP1*		
RPL37A	*JUN*	*RPL28*	*LYRM9*		

RPL4	*LAMP2*	*RPL29*	*MALAT1*		
RPL41	*LGALS3*	*RPL31*	*MATN2*		
RPL5	*LOXL3*	*RPL32*	*MFGE8*		
RPL6	*LPL*	*RPL35*	*MIA*		
RPL8	*LRPAP1*	*RPL36*	*MPZ*		
RPLP0	*MAGEC2*	*RPL36A*	*MT2A*		
RPLP1	*MCL1*	*RPL37*	*MTRNR2L1*		
RPS10	*MFGE8*	*RPL37A*	*MTRNR2L10*		
RPS11	*MFI2*	*RPL39*	*MTRNR2L2*		
RPS12	*MIA*	*RPL4*	*MTRNR2L3*		
RPS15	*MRPS6*	*RPL41*	*MTRNR2L4*		
RPS15A	*MT2A*	*RPL5*	*MTRNR2L5*		
RPS16	*NFKBIA*	*RPL6*	*MTRNR2L6*		
RPS17	*NFKBIZ*	*RPL7*	*MTRNR2L8*		
RPS17L	*NNMT*	*RPL7A*	*MYH9*		
RPS18	*NPC1*	*RPL8*	*MYO1D*		
RPS19	*NPC2*	*RPL9*	*NAV2*		
RPS23	*NR4A1*	*RPLP0*	*NEAT1*		
RPS24	*NSG1*	*RPLP2*	*NFE2L1*		
RPS27	*PERP*	*RPS10*	*NPC1*		
RPS27A	*PKM*	*RPS11*	*NPC2*		
RPS3	*PRKCDBP*	*RPS13*	*NSG1*		
RPS4X	*PROS1*	*RPS14*	*PDE4DIP*		
RPS5	*PRSS23*	*RPS15*	*PERP*		
RPS6	*PSAP*	*RPS15A*	*PROS1*		
RPS7	*PTRF*	*RPS16*	*PSAP*		
RPS8	*RPS4Y1*	*RPS17*	*RDH5*		
RPS9	*S100A6*	*RPS17L*	*S100A1*		
RPSA	*S100B*	*RPS18*	*S100A6*		
SAE1	*SCCPDH*	*RPS19*	*SDC3*		
SCD	*SDC3*	*RPS21*	*SEC11C*		
SCIN	*SEMA3B*	*RPS23*	*SERINC1*		
SERPINF1	*SERPINA3*	*RPS24*	*SERPINA1*		
SERPINH1	*SERPINE2*	*RPS25*	*SERPINA3*		
SHMT2	*SGCE*	*RPS27*	*SERPINE2*		
SLC25A3	*SGK1*	*RPS27A*	*SGK1*		
SLC45A2	*SLC20A1*	*RPS28*	*SLC26A2*		
SNAI2	*SLC26A2*	*RPS3*	*SLC5A3*		
SNHG6	*SLC39A14*	*RPS3A*	*SNX9*		
SOX4	*SLC5A3*	*RPS4X*	*SPON2*		
SRP14	*SYPL1*	*RPS5*	*SPP1*		
SSR2	*TAPBP*	*RPS6*	*STRIP2*		
TIMM50	*TIMP1*	*RPS7*	*SVIP*		
TMC6	*TIMP2*	*RPS8*	*THBD*		
TP53	*TIMP3*	*RPS9*	*TIMP2*		
TRIB2	*TM4SF1*	*RPSA*	*TM4SF1*		
TRPM1	*TNC*	*RRS1*	*TMBIM6*		
TUBB4A	*TOB1*	*RSL1D1*	*TMEM255A*		
TULP4	*TPP1*	*RUVBL2*	*TNFSF4*		
UBA52	*TSC22D3*	*SAE1*	*TPP1*		
USP22	*UBC*	*SERBP1*	*TRIML2*		
ZFP36L1	*ZBTB38*	*SERPINF1*	*TSC22D3*		
		SHMT2	*TSPYL2*		
		SLC19A1	*TXNIP*		
		SLC25A6	*TYR*		
		SMARCA4	*UBC*		
		SMIM15	*VAT1*		
		SNHG16	*XAGE1D*		

		SNHG6	*ZNF331*		
		SRM			
		SSR2			
		TIMM13			
		TIMM44			
		TOP1MT			
		TPI1			
		TRIM28			
		UBA52			
		UQCRFS1			
		WDR12			
		XIST			
		ZFAS1			

Table 27B.2

DIFFERENT T CELL SIGNATURES							
RELATIVE T CD8 EXC. (UP)	**RELATIVE T CD8 EXC. (DOWN)**	**T CD4 EXC. (UP)**	**T CD4 EXC. (DOWN)**	**T CD8 EXC. (UP)**	**T CD8 EXC. (DOWN)**	**T CELL EXC. (UP)**	**T CELL EXC. (DOWN)**
BTF3	*APOD*	*AHCY*	*A2M*	*AHCY*	*A2M*	*AHCY*	*A2M*
CHCHD2	*APOE*	*APP*	*AGA*	*APP*	*ACSL3*	*ALDH18A1*	*AEBP1*
CYC1	*ATP1A1*	*BANCR*	*AHNAK*	*ATP5D*	*AEBP1*	*APP*	*AGA*
EEF1B2	*ATP6V0C*	*BZW2*	*ANXA1*	*ATP5G3*	*AGA*	*ASAP1*	*AHNAK*
EEF1G	*B2M*	*C17orf76-AS1*	*APOC2*	*BOP1*	*AHNAK*	*ATP5D*	*ANXA1*
EIF3G	*CAPN3*	*C1QBP*	*APOD*	*BTF3*	*APOC2*	*ATP5G2*	*APOC2*
EIF3M	*CD59*	*C6orf48*	*APOE*	*BZW2*	*APOD*	*BANCR*	*APOD*
EIF4A1	*CD63*	*CCT3*	*ARSA*	*C17orf76-AS1*	*APOE*	*BCAN*	*APOE*
ENO1	*CDH1*	*CCT6A*	*ATP1A1*	*C19orf48*	*APOL1*	*BOP1*	*ARSA*
FARSA	*CTSD*	*CDCA7*	*ATP1B1*	*C1QBP*	*ARSA*	*BTF3*	*ATP1A1*
GAPDH	*DAAM2*	*CYC1*	*ATP6V0C*	*C6orf48*	*ATP1A1*	*BZW2*	*ATP1B1*
H19	*GPNMB*	*DAP3*	*B2M*	*CACYBP*	*ATP1B1*	*C17orf76-AS1*	*ATP6V0C*
HNRNPA1	*GPR56*	*EEF1A1*	*C4A*	*CCT3*	*ATP6V0C*	*C19orf48*	*B2M*
HSPE1	*HLA-A*	*EEF1B2*	*CAPN3*	*CCT4*	*B2M*	*C1QBP*	*C4A*
LDHB	*HLA-B*	*EEF1D*	*CARD16*	*CCT6A*	*C4A*	*C6orf48*	*CAPG*
LSM4	*HLA-C*	*EEF1G*	*CD151*	*CCT7*	*CARD16*	*CACYBP*	*CARD16*
LSM7	*HLA-E*	*EEF2*	*CD47*	*CDCA7*	*CAV2*	*CCT3*	*CAV1*
MAGEA4	*HLA-F*	*EIF2S3*	*CD58*	*CDK4*	*CD151*	*CCT6A*	*CAV2*
MAGEC1	*HLA-G*	*EIF3E*	*CD59*	*CHCHD2*	*CD44*	*CCT7*	*CCND3*
MDH2	*HLA-H*	*EIF3G*	*CD63*	*CTPS1*	*CD47*	*CDCA7*	*CD151*
MKI67IP	*HPS5*	*EIF3K*	*CDH1*	*DARS*	*CD58*	*CPXM1*	*CD47*
MLLT11	*HSP90AA1*	*EIF3L*	*CDH19*	*DCTPP1*	*CD59*	*CTPS1*	*CD58*
MRPS24	*IFI27*	*EIF4A1*	*CREB3L2*	*DDX21*	*CD63*	*CYC1*	*CD59*
NACA	*IFI6*	*FBL*	*CSPG4*	*EEF1B2*	*CDH1*	*CYP51A1*	*CD63*
NDUFB9	*IGSF8*	*FKBP4*	*CST3*	*EEF1D*	*CDH19*	*DARS*	*CDH19*
NHP2	*IRF4*	*GAS5*	*CTSB*	*EEF1G*	*CSPG4*	*DCAF13*	*CREB3L2*
NME1	*LAMP2*	*GCSH*	*CTSD*	*EEF2*	*CST3*	*DCT*	*CSPG4*
NREP	*LGALS3*	*GNB2L1*	*CTSL1*	*EIF2S3*	*CTSA*	*DDX21*	*CST3*
PPIA	*LGALS3BP*	*GNL3*	*DAG1*	*EIF3E*	*CTSB*	*EEF1A1*	*CTSA*
RPL13AP5	*LONP2*	*GPATCH4*	*DDR1*	*EIF3F*	*CTSD*	*EEF1B2*	*CTSB*
RPL18A	*MCAM*	*GPI*	*EEA1*	*EIF3G*	*CTSL1*	*EEF1D*	*CTSD*
RPL19	*MLPH*	*HMGB1*	*EMP1*	*EIF3K*	*CTSO*	*EEF1G*	*CTSL1*

RPL26	*MTRNR2L1*	*HNRNPA1*	*EVA1A*	*EIF3M*	*CYP27A1*	*EEF2*	*DAG1*
RPL27A	*MTRNR2L10*	*HNRNPC*	*FBXO32*	*EIF4A1*	*CYP4V2*	*EIF2S3*	*DDR1*
RPL31	*MTRNR2L2*	*HNRNPH1*	*FGFR1*	*ENO1*	*DAG1*	*EIF3E*	*DUSP4*
RPL32	*MTRNR2L3*	*HNRNPM*	*GAA*	*EXOSC5*	*DDR1*	*EIF3G*	*EEA1*
RPL36	*MTRNR2L4*	*HSPD1*	*GATSL3*	*FAM92A1*	*EEA1*	*EIF3H*	*EMP1*
RPL37	*MTRNR2L6*	*IDH2*	*GJB1*	*FARSA*	*EMP1*	*EIF3I*	*EVA1A*
RPL37A	*MTRNR2L8*	*IFRD2*	*GPR56*	*FBL*	*EVA1A*	*EIF3K*	*EZR*
RPL39	*NSG1*	*ILF2*	*GRN*	*FKBP4*	*FBXO32*	*EIF3L*	*FBXO32*
RPL6	*PLXNC1*	*IMPDH2*	*GSN*	*GAS5*	*FGFR1*	*EIF3M*	*FGFR1*
RPL7	*PSAP*	*LSM7*	*HCP5*	*GGH*	*FLNA*	*EIF4A1*	*GAA*
RPLP0	*QPCT*	*LYPLA1*	*HLA-A*	*GNB2L1*	*FOS*	*ENO1*	*GATSL3*
RPLP2	*RAB5B*	*MDH2*	*HLA-B*	*GNL3*	*GAA*	*FAM92A1*	*GJB1*
RPS10	*S100A1*	*MRPL15*	*HLA-C*	*GPATCH4*	*GATSL3*	*FBL*	*GPR155*
RPS11	*S100B*	*MRPL4*	*HLA-F*	*GPI*	*GJB1*	*FKBP4*	*GRN*
RPS13	*SAT1*	*NCL*	*HLA-G*	*HMGB1*	*GPNMB*	*GAS5*	*GSN*
RPS14	*SEC11C*	*NDUFA11*	*HLA-H*	*HNRNPA1*	*GPR155*	*GCSH*	*HCP5*
RPS15	*SHC4*	*NDUFS7*	*IFI27*	*HNRNPC*	*GPR56*	*GNB2L1*	*HLA-A*
RPS16	*SLC7A8*	*NME1*	*IFI27L2*	*HNRNPH1*	*GRN*	*GNL3*	*HLA-B*
RPS17	*SORT1*	*NOP16*	*IGFBP7*	*HNRNPM*	*GSN*	*GPATCH4*	*HLA-C*
RPS17L	*ST3GAL6*	*NPM1*	*IRF4*	*HSPD1*	*HLA-A*	*GPI*	*HLA-E*
RPS18	*STX7*	*PABPC1*	*ITGA3*	*IDH2*	*HLA-B*	*GPM6B*	*HLA-F*
RPS20	*TMED10*	*PAICS*	*ITGA7*	*IFRD2*	*HLA-C*	*HMGB1*	*HLA-G*
RPS21	*TMEM255A*	*PFN1*	*ITGB3*	*ILF2*	*HLA-E*	*HNRNPA1*	*HLA-H*
RPS23	*TYR*	*PLEKHJ1*	*KCNN4*	*ILF3*	*HLA-F*	*HNRNPC*	*HSPA1A*
RPS25		*POLD2*	*LAMP2*	*IMPDH2*	*HLA-G*	*HNRNPH1*	*IFI27*
RPS27A		*POLR1D*	*LEF1-AS1*	*ISYNA1*	*HLA-H*	*HNRNPM*	*IFI27L2*
RPS28		*POLR2E*	*LGALS3*	*LDHB*	*HSPA1A*	*HNRPDL*	*IFI35*
RPS5		*RPL10*	*LOC100126784*	*LSM4*	*IFI27*	*HSPD1*	*IFI6*
RPS6		*RPL10A*	*LOC100506190*	*LSM7*	*IFI27L2*	*IDH2*	*IGFBP7*
RPS7		*RPL11*	*LRPAP1*	*LYPLA1*	*IFI6*	*ILF2*	*IRF4*
RPSA		*RPL12*	*LYRM9*	*MAGEC1*	*IGFBP7*	*ILF3*	*ITGA3*
RUVBL2		*RPL13*	*MATN2*	*MCM7*	*IGSF8*	*IMPDH2*	*ITGA7*
SMARCA4		*RPL13A*	*MFGE8*	*MDH2*	*IRF4*	*LDHB*	*ITGB3*
SNRPD2		*RPL13AP5*	*MIA*	*MKI67IP*	*ITGA3*	*LIMD2*	*KCNN4*
SNRPE		*RPL14*	*MPZ*	*MRPL15*	*ITGA7*	*LSM7*	*LAMP2*
STOML2		*RPL15*	*MT2A*	*MRPL37*	*KCNN4*	*LYPLA1*	*LEF1-AS1*
TIMM13		*RPL17*	*MTRNR2L1*	*MRPL4*	*LAMB2*	*MAGEA4*	*LGALS1*
TPI1		*RPL18*	*MTRNR2L10*	*MRPS12*	*LAMP2*	*MARCKS*	*LGALS3*
UBA52		*RPL18A*	*MTRNR2L2*	*NACA*	*LEF1-AS1*	*MARCKSL1*	*LOC100126784*
UHRF1		*RPL21*	*MTRNR2L3*	*NCL*	*LGALS3*	*MDH2*	*LOC100506190*
UQCRH		*RPL22*	*MTRNR2L4*	*NDUFA11*	*LGALS3BP*	*MEST*	*LRP10*
WBSCR22		*RPL26*	*MTRNR2L5*	*NME1*	*LGMN*	*MID1*	*LRPAP1*
		RPL27A	*MTRNR2L6*	*NME2*	*LOC100126784*	*MKI67IP*	*LY6E*
		RPL28	*MTRNR2L7*	*NOLC1*	*LOC100506190*	*MPZL1*	*LYRM9*
		RPL29	*MTRNR2L8*	*NOP16*	*LRPAP1*	*MRPL15*	*MATN2*
		RPL3	*MYO1D*	*NPM1*	*LY6E*	*MRPL4*	*MFGE8*
		RPL30	*NEAT1*	*NREP*	*LYRM9*	*NACA*	*MFI2*
		RPL31	*NFKBIA*	*PABPC1*	*MALAT1*	*NAP1L1*	*MIA*
		RPL32	*NPC1*	*PAICS*	*MATN2*	*NCL*	*MMP14*

		RPL35	*NPC2*	*PFN1*	*MCAM*	*NHP2*	*MPZ*
		RPL36	*NSG1*	*PLEKHJ1*	*MFGE8*	*NME2*	*MT2A*
		RPL36A	*PDE4DIP*	*POLD2*	*MIA*	*NOLC1*	*MTRNR2L1*
		RPL37	*PERP*	*POLR1D*	*MMP14*	*NONO*	*MTRNR2L10*
		RPL37A	*PROS1*	*POLR2E*	*MPZ*	*NOP58*	*MTRNR2L2*
		RPL39	*PSAP*	*PPA1*	*MT2A*	*NPM1*	*MTRNR2L3*
		RPL4	*RDH5*	*PPIA*	*MTRNR2L1*	*NREP*	*MTRNR2L4*
		RPL41	*S100A1*	*PRMT1*	*MTRNR2L10*	*PABPC1*	*MTRNR2L5*
		RPL5	*S100A13*	*PTMA*	*MTRNR2L2*	*PAICS*	*MTRNR2L6*
		RPL6	*S100A6*	*PUF60*	*MTRNR2L3*	*PFDN2*	*MTRNR2L7*
		RPL7	*SAT1*	*RPL10*	*MTRNR2L4*	*PFN1*	*MTRNR2L8*
		RPL7A	*SDC3*	*RPL10A*	*MTRNR2L5*	*PHB2*	*MYO1D*
		RPL8	*SERINC1*	*RPL11*	*MTRNR2L6*	*PLTP*	*NEAT1*
		RPL9	*SERPINA1*	*RPL12*	*MTRNR2L7*	*POLD2*	*NFKBIA*
		RPLP0	*SERPINA3*	*RPL13*	*MTRNR2L8*	*POLR1D*	*NPC1*
		RPLP1	*SERPINE2*	*RPL13A*	*MYO1D*	*POLR2E*	*NPC2*
		RPLP2	*SGCE*	*RPL13AP5*	*NAV2*	*PPIA*	*NSG1*
		RPS10	*SGK1*	*RPL14*	*NEAT1*	*PTMA*	*PAGE5*
		RPS11	*SLC26A2*	*RPL15*	*NFE2L1*	*PTP4A3*	*PDE4DIP*
		RPS13	*SLC5A3*	*RPL17*	*NPC1*	*RPL10*	*PERP*
		RPS14	*SPON2*	*RPL18*	*NPC2*	*RPL10A*	*PKM*
		RPS15	*SPP1*	*RPL18A*	*NSG1*	*RPL11*	*PROS1*
		RPS15A	*STRIP2*	*RPL19*	*PDE4DIP*	*RPL12*	*PSAP*
		RPS16	*SYNE2*	*RPL21*	*PERP*	*RPL13*	*RDH5*
		RPS17	*THBD*	*RPL22*	*PROS1*	*RPL13A*	*RTP4*
		RPS17L	*TIMP1*	*RPL26*	*PSAP*	*RPL13AP5*	*S100A1*
		RPS18	*TIMP2*	*RPL27*	*QPCT*	*RPL14*	*S100A13*
		RPS19	*TM4SF1*	*RPL27A*	*RDH5*	*RPL15*	*S100A6*
		RPS20	*TMBIM6*	*RPL28*	*S100A1*	*RPL17*	*S100B*
		RPS21	*TMEM255A*	*RPL29*	*S100A13*	*RPL18*	*SAT1*
		RPS23	*TNFRSF12A*	*RPL3*	*S100A6*	*RPL18A*	*SCARB2*
		RPS24	*TNFSF4*	*RPL30*	*S100B*	*RPL19*	*SCCPDH*
		RPS25	*TPP1*	*RPL31*	*SAT1*	*RPL21*	*SDC3*
		RPS27	*TRIML2*	*RPL32*	*SCARB2*	*RPL22*	*SERINC1*
		RPS27A	*TSC22D3*	*RPL35*	*SDC3*	*RPL26*	*SERPINA1*
		RPS28	*TSPYL2*	*RPL36*	*SEC11C*	*RPL27*	*SERPINA3*
		RPS3	*TXNIP*	*RPL36A*	*SERINC1*	*RPL27A*	*SERPINE2*
		RPS3A	*TYR*	*RPL37*	*SERPINA1*	*RPL28*	*SGCE*
		RPS4X	*UBC*	*RPL37A*	*SERPINA3*	*RPL29*	*SGK1*
		RPS5	*WBP2*	*RPL39*	*SERPINE2*	*RPL3*	*SLC26A2*
		RPS6	*WSB1*	*RPL4*	*SGK1*	*RPL30*	*SLC5A3*
		RPS7		*RPL41*	*SHC4*	*RPL31*	*SNX9*
		RPS8		*RPL5*	*SLC26A2*	*RPL32*	*SPON2*
		RPS9		*RPL6*	*SLC5A3*	*RPL35*	*SPP1*
		RPSA		*RPL7*	*SLC7A8*	*RPL36*	*SQSTM1*
		RQCD1		*RPL7A*	*SNX9*	*RPL36A*	*STRIP2*
		RRS1		*RPL8*	*SORT1*	*RPL37*	*SYNE2*
		RSL1D1		*RPL9*	*SPON2*	*RPL37A*	*THBD*
		SAE1		*RPLP0*	*SPP1*	*RPL38*	*TIMP1*
		SERBP1		*RPLP1*	*STRIP2*	*RPL39*	*TIMP3*
		SERPINF1		*RPLP2*	*STX7*	*RPL4*	*TM4SF1*
		SET		*RPS10*	*SYNE2*	*RPL41*	*TMBIM6*
		SHMT2		*RPS11*	*TAPBP*	*RPL5*	*TMEM255A*
		SLC25A13		*RPS13*	*THBD*	*RPL6*	*TNFRSF12A*
		SLC25A5		*RPS14*	*TIMP1*	*RPL7*	*TNFSF4*
		SLC25A6		*RPS15*	*TIMP2*	*RPL7A*	*TPP1*
		SMARCA4		*RPS15A*	*TIMP3*	*RPL8*	*TRIML2*
		SMIM15		*RPS16*	*TM4SF1*	*RPL9*	*TSC22D3*

		SNHG15		*RPS17*	*TMBIM6*	*RPLP0*	*TSPYL2*
		SNHG16		*RPS17L*	*TMED10*	*RPLP1*	*TXNIP*
		SNHG6		*RPS18*	*TMEM255A*	*RPLP2*	*UBC*
		SNRPE		*RPS19*	*TNFSF4*	*RPS10*	*WBP2*
		SORD		*RPS2*	*TPP1*	*RPS11*	*ZBTB38*
		SOX4		*RPS20*	*TRIML2*	*RPS12*	
		SRM		*RPS21*	*TSC22D3*	*RPS13*	
		TIMM13		*RPS23*	*TSPYL2*	*RPS14*	
		TIMM44		*RPS24*	*TXNIP*	*RPS15*	
		TIMM50		*RPS25*	*TYR*	*RPS15A*	
		TOMM20		*RPS27*	*UBC*	*RPS16*	
		TOP1MT		*RPS27A*	*VAT1*	*RPS17*	
		TUFM		*RPS28*	*WBP2*	*RPS17L*	
		UBA52		*RPS3*	*XAGE1D*	*RPS18*	
		UCK2		*RPS3A*		*RPS19*	
		UQCR11		*RPS4X*		*RPS2*	
		UQCRFS1		*RPS5*		*RPS20*	
		ZFAS1		*RPS6*		*RPS21*	
				RPS7		*RPS23*	
				RPS8		*RPS24*	
				RPS9		*RPS25*	
				RPSA		*RPS27*	
				RQCD1		*RPS27A*	
				RRS1		*RPS28*	
				RSL1D1		*RPS3*	
				RUVBL2		*RPS3A*	
				SAE1		*RPS4X*	
				SERBP1		*RPS5*	
				SERPINF1		*RPS6*	
				SET		*RPS7*	
				SHMT2		*RPS8*	
				SLC19A1		*RPS9*	
				SLC25A13		*RPSA*	
				SLC25A6		*RQCD1*	
				SMARCA4		*RRP15*	
				SMIM15		*RRS1*	
				SNHG15		*RSL1D1*	
				SNHG6		*RUVBL2*	
				SNRPB		*SAE1*	
				SNRPC		*SERBP1*	
				SNRPD1		*SERPINF1*	
				SNRPD2		*SET*	
				SNRPE		*SHMT2*	
				SOX4		*SLC19A1*	
				SRM		*SLC25A13*	
				SSB		*SLC25A5*	
				SSR2		*SLC25A6*	
				TIMM13		*SMARCA4*	
				TIMM44		*SMIM15*	
				TIMM50		*SNAI2*	
				TOP1MT		*SNHG15*	
				TPI1		*SNHG6*	
				TRAP1		*SNRPD1*	
				TRIM28		*SNRPD2*	
				TUBB		*SNRPE*	
				TYMS		*SORD*	
				UBA52		*SOX4*	
				UCK2		*SRM*	

				UHRF1		*SSR2*	
				UQCRFS1		*STOML2*	
				UQCRH		*STRAP*	
				VDAC2		*TIMM13*	
				XIST		*TIMM44*	
				ZFAS1		*TIMM50*	
						TOMM20	
						TOP1MT	
						TP53	
						TRAP1	
						TUBB	
						TUFM	
						TYMS	
						TYRP1	
						UBA52	
						UCK2	
						UQCRFS1	
						UQCRH	
						USP22	
						XIST	
						YWHAE	
						ZFAS1	

DIFFERENT T CELL SIGNATURES							
T CD4 EXHAUSTED EXC. (UP)	**T CD4 EXHAUSTED EXC. (DOWN)**	**T CD4 TREG EXC. (UP)**	**T CD4 TREG EXC. (DOWN)**	**T CD8 CYTOTOXIC EXC. (UP)**	**T CD8 CYTOTOXIC EXC. (DOWN)**	**T CD8 NAIVE EXC. (UP)**	**T CD8 NAIVE EXC. (DOWN)**
ACP5	*A2M*	*ABR*	*A2M*	*ADCK3*	*A2M*	*ADSL*	*A2M*
ACTG1	*AKAP12*	*ACP5*	*AGA*	*ADSL*	*AEBP1*	*AHCY*	*ACSL3*
AK2	*ANGPTL4*	*ACTG1*	*AHNAK*	*AHCY*	*AGA*	*APEX1*	*AEBP1*
AP1S2	*ANXA1*	*AHCY*	*ANXA1*	*APEX1*	*AHNAK*	*ATP5D*	*AGA*
APOA1BP	*APLP2*	*ANKRD10*	*APLP2*	*APP*	*ANXA1*	*BANCR*	*AHNAK*
ASAH1	*APOC2*	*APP*	*APOC2*	*ATP5D*	*APOC2*	*BTF3*	*ANXA1*
ASAP1	*APOD*	*ASAP1*	*APOD*	*ATP5G2*	*APOD*	*C17orf76-AS1*	*APOC2*
ATP5D	*ATP1B1*	*ATP5D*	*ATP1A1*	*BANCR*	*APOE*	*C19orf48*	*APOD*
BAIAP2	*ATP6V0E2*	*BANCR*	*ATP1B1*	*BTF3*	*ARSA*	*C1QBP*	*APOE*
BCAN	*ATRAID*	*BCAN*	*ATP6V0E2*	*BZW2*	*ATP1A1*	*C6orf48*	*ATP1A1*
C11orf24	*C16orf45*	*BZW2*	*ATRAID*	*C17orf76-AS1*	*ATP6V0C*	*CACYBP*	*ATP1B1*
C17orf76-AS1	*C4A*	*C17orf76-AS1*	*B2M*	*C19orf48*	*ATP6V1E1*	*CCT2*	*B2M*
C1orf43	*CALM2*	*C6orf48*	*C4A*	*C1QBP*	*B2M*	*CCT3*	*C4A*
CA14	*CBLB*	*CA14*	*CBLB*	*C6orf48*	*C4A*	*CCT4*	*CALU*
CCT3	*CCND3*	*CCNG1*	*CCND3*	*CACYBP*	*CALU*	*CCT7*	*CARD16*
CDC16	*CD151*	*CCT3*	*CD151*	*CCNB1IP1*	*CAPG*	*CDCA7*	*CAV1*
CDH3	*CD47*	*CDH3*	*CD47*	*CCT2*	*CARD16*	*CDK4*	*CAV2*
CDK2	*CD58*	*CDR1*	*CD58*	*CCT3*	*CAV1*	*CPXM1*	*CCPG1*
CEP170	*CD59*	*CEP170*	*CD59*	*CCT4*	*CAV2*	*CYC1*	*CD151*
CERS4	*CDH19*	*CHP1*	*CD63*	*CCT5*	*CD151*	*DAP3*	*CD47*
CHCHD6	*CFI*	*CPXM1*	*CDH19*	*CCT6A*	*CD47*	*DDX21*	*CD58*
CTSK	*CHI3L1*	*CRISPLD1*	*CHI3L1*	*CCT7*	*CD58*	*EEF1A1*	*CD59*
DAP3	*CHN1*	*CYP51A1*	*CHN1*	*CDCA7*	*CD59*	*EEF1B2*	*CD63*
DCT	*CHRM3*	*DAP3*	*CLU*	*CDR1*	*CD63*	*EEF1D*	*CDH1*
DPP7	*CLU*	*DCT*	*COX17*	*CPXM1*	*CDH1*	*EEF1G*	*CDH19*
EDNRB	*CPVL*	*EDNRB*	*CPVL*	*CYC1*	*CDH19*	*EEF2*	*CLU*
EEF1D	*CRELD1*	*EEF1A1*	*CREB3L2*	*DARS*	*CREB3L2*	*EIF2S3*	*CREB3L2*
EEF2	*CRYAB*	*EEF1B2*	*CRELD1*	*DCAF13*	*CSPG4*	*EIF3E*	*CSPG4*

EIF2S3	*CSPG4*	*EEF1D*	*CSPG4*	*DDX21*	*CST3*	*EIF3F*	*CST3*
EIF3D	*CST3*	*EEF1G*	*CST3*	*EEF1A1*	*CTSA*	*EIF3G*	*CTSA*
EIF3I	*CTSB*	*EEF2*	*CTHRC1*	*EEF1B2*	*CTSB*	*EIF3H*	*CTSB*
EIF3L	*DDR1*	*EIF2S3*	*CTSB*	*EEF1D*	*CTSD*	*EIF3I*	*CTSD*
EPS15	*DPYSL2*	*EIF3E*	*CTSD*	*EEF1G*	*CYP27A1*	*EIF3K*	*DAG1*
ESRP1	*DSCR8*	*EIF3H*	*DAG1*	*EEF2*	*CYSTM1*	*EIF3L*	*DDR1*
FAM167B	*DUSP6*	*EIF3K*	*DDR1*	*EIF2S3*	*DAG1*	*EIF3M*	*DUSP4*
FAM174B	*DYNLRB1*	*EIF3L*	*DPYSL2*	*EIF3E*	*DDR1*	*EIF4A1*	*DUSP6*
FAM178B	*EFNA5*	*EIF4A1*	*DSCR8*	*EIF3F*	*ECM1*	*ENO1*	*ECM1*
FMN1	*EGR1*	*ESRP1*	*DUSP6*	*EIF3G*	*EEA1*	*ESRP1*	*EEA1*
FTL	*ERRFI1*	*FAM174B*	*DYNLRB1*	*EIF3H*	*EMP1*	*EXOSC4*	*EGR1*
FXYD5	*FAM3C*	*FAM178B*	*EEA1*	*EIF3K*	*ENDOD1*	*EXOSC5*	*ERBB3*
GAS5	*FAM46A*	*FAM92A1*	*EMP1*	*EIF3L*	*EVA1A*	*FAM178B*	*EVA1A*
GCNT2	*FCGR2A*	*FBL*	*ETV4*	*EIF3M*	*FBXO32*	*FAM92A1*	*FAM3C*
GGA1	*FGFR1*	*FKBP4*	*EVA1A*	*EIF4A1*	*FLNA*	*FARSA*	*FBXO32*
GMPR	*GAA*	*FOXRED2*	*EZR*	*EIF4B*	*GAA*	*FBL*	*FGFR1*
GNB2L1	*GAGE12G*	*FTL*	*FAM3C*	*ENO1*	*GATSL3*	*FKBP4*	*FLNA*
GPI	*GAGE4*	*GAS5*	*FCGR2A*	*EPB41L4A-AS1*	*GJB1*	*FRZB*	*FXYD3*
GPM6B	*GAGE6*	*GNB2L1*	*FGFR1*	*FARSA*	*GNPTG*	*GAS5*	*GAA*
GPR143	*GATSL3*	*GNL3*	*GAA*	*FBL*	*GPR155*	*GGH*	*GATSL3*
GRSF1	*GBP2*	*GPATCH4*	*GATSL3*	*FKBP4*	*GPR56*	*GNB2L1*	*GJB1*
GSTO1	*H3F3B*	*GPI*	*GJB1*	*GAS5*	*GRN*	*GNL3*	*GNPTG*
GSTP1	*HSPA1A*	*GPM6B*	*GRN*	*GCSH*	*GSN*	*GPI*	*GPR155*
HAGHL	*HSPA1B*	*GPR143*	*GSN*	*GNB2L1*	*HLA-A*	*H19*	*GPR56*
HAS2	*IER3*	*HAS2*	*H3F3B*	*GNL3*	*HLA-B*	*HMGA1*	*GRN*
HMG20B	*IGF1R*	*HMCN1*	*HCP5*	*GPATCH4*	*HLA-C*	*HMGB1*	*GSN*
HNRNPC	*ISCU*	*HNRNPA1*	*HLA-F*	*GPI*	*HLA-F*	*HNRNPA1*	*HLA-B*
HPS4	*ITGA10*	*HNRNPC*	*HSPA1A*	*HMGB1*	*HLA-G*	*HNRNPC*	*HLA-C*
HSPA2	*ITGA3*	*IFI16*	*IFI35*	*HNRNPA1*	*HLA-H*	*HNRNPH1*	*HLA-F*
IFI16	*ITGA7*	*IGSF11*	*ISCU*	*HNRNPA1P10*	*IFI27*	*HNRNPM*	*HLA-H*
ILVBL	*ITGB3*	*ILF2*	*ITGA3*	*HNRNPC*	*IFI27L2*	*HSP90AB1*	*HSPA1A*
IMPDH2	*KCNN4*	*ILVBL*	*ITGA7*	*HNRNPH1*	*IFI35*	*HSPD1*	*IFI27*
INPP4B	*KRT18*	*IMPDH2*	*ITGB3*	*HNRNPM*	*IFI6*	*IDH2*	*IFI35*
ISOC2	*LEF1-AS1*	*ISYNA1*	*KCNN4*	*HNRPDL*	*IGFBP7*	*ILF2*	*IFI6*
ITPKB	*LIF*	*ITM2C*	*LEF1-AS1*	*HSP90AB1*	*IGSF8*	*ILF3*	*IGFBP7*
KCNAB2	*LINC00623*	*KCNJ13*	*LGALS3*	*HSPD1*	*IRF4*	*IMPDH2*	*IGSF8*
KIT	*LOXL3*	*LHFPL3-AS1*	*LIF*	*ILF2*	*ITGA3*	*ISYNA1*	*ITGA3*
LHFPL3-AS1	*LOXL4*	*LIMD2*	*LINC00116*	*ILF3*	*ITGA7*	*LDHB*	*ITGA7*
LINC00518	*LRPAP1*	*LOC100133445*	*LRPAP1*	*IMPDH2*	*ITGB3*	*LIMD2*	*ITGB3*
LMNA	*LTBP3*	*LOC100190986*	*LTBP3*	*LDHB*	*LAMP2*	*LSM4*	*KCNN4*
LOC100133445	*LYRM9*	*LYPLA1*	*LYRM9*	*LIMD2*	*LEF1-AS1*	*LSM7*	*LAMP2*
MARCKS	*MAEL*	*MARCKS*	*MAEL*	*LSM7*	*LGALS1*	*LYPLA1*	*LEF1-AS1*
MAZ	*MAGEA10*	*MCC*	*MAP1B*	*LYPLA1*	*LGALS3*	*MAGEA4*	*LGALS3*
MC1R	*MAGEA3*	*MEST*	*MATN2*	*MAGEA4*	*LGALS3BP*	*MDH2*	*LGALS3BP*
MCC	*MAGEA4*	*MITF*	*METTL7B*	*MARCKS*	*LOC100126784*	*MEST*	*LOC100126784*
METTL9	*MAP1B*	*MPZL1*	*MFGE8*	*MARCKSL1*	*LRPAP1*	*MID1*	*LOC100506190*
MITF	*MATN2*	*MYC*	*MFI2*	*MDH2*	*LY6E*	*MRPL15*	*LOXL4*
MLANA	*MDK*	*MYO5A*	*MIA*	*MEST*	*LYRM9*	*MRPL37*	*LRPAP1*
MLPH	*METTL7B*	*NAP1L1*	*MPZ*	*MKI67IP*	*MATN2*	*MRPS12*	*LY6E*
MRPL24	*MFGE8*	*NAPRT1*	*MT2A*	*MPZL1*	*MFGE8*	*NACA*	*LYRM9*
MRPL44	*MFI2*	*NCL*	*MTRNR2L1*	*MRPL15*	*MIA*	*NCL*	*MATN2*
MXI1	*MIA*	*NID1*	*MTRNR2L1*	*NACA*	*MMP14*	*NDUFB9*	*MCAM*

			0				
MYC	MPZ	NOA1	MTRNR2L2	NAP1L1	MPZ	NME1	MFGE8
MYO10	MRPS6	NPIPL3	MTRNR2L3	NFYA	MT2A	NME2	MIA
MYO5A	MT2A	NPM1	MTRNR2L5	NHP2	MTRNR2L1	NOLC1	MMP14
NAPRT1	MTRNR2L6	P2RX7	MTRNR2L6	NME1	MTRNR2L10	NONO	MPZ
NCL	NDRG1	PABPC1	MTRNR2L7	NME2	MTRNR2L2	NPM1	MT2A
NDUFS2	NNMT	PAICS	MTRNR2L8	NOLC1	MTRNR2L3	NREP	MTRNR2L1
OAT	OCIAD2	PAX3	NDRG1	NONO	MTRNR2L4	PABPC1	MTRNR2L10
P2RX7	PAGE2	PEX19	NDUFB2	NPM1	MTRNR2L5	PAICS	MTRNR2L2
PABPC1	PAGE2B	PI4KB	NNMT	NREP	MTRNR2L6	PFN1	MTRNR2L3
PAICS	PAGE5	PIR	NPC1	PABPC1	MTRNR2L7	PHB2	MTRNR2L4
PAX3	PDK4	PLP1	NSG1	PAICS	MTRNR2L8	POLD2	MTRNR2L5
PHACTR1	PERP	PLTP	OCIAD2	PAN3	MYO1D	POLR1D	MTRNR2L6
PI4KB	PLEKHB1	POLR1D	PAGE5	PFN1	NDUFAF3	POLR2E	MTRNR2L7
PIR	PRR4	PRRC2C	PERP	PHB2	NPC1	PPIA	MTRNR2L8
PLP1	PSMB1	RAB38	PKM	PLEKHJ1	NPC2	PTMA	MYO1D
PLTP	RAB34	RAP1GAP	PROS1	POLR1D	NSG1	PTP4A3	NPC1
PMEL	RDH5	RPL10	PRSS23	POLR2E	PAGE5	PUF60	NPC2
POLD2	S100A16	RPL10A	RDH5	PPA1	PDE4DIP	RAN	NSG1
PSMB4	S100A6	RPL11	S100A1	PPIA	PERP	RPL10	PERP
PTTG1IP	SAA1	RPL12	S100A13	PRMT1	PKM	RPL10A	PROS1
PYCARD	SEMA3B	RPL13	S100A16	PTMA	PROS1	RPL11	PRSS23
RAB32	SEPP1	RPL13A	S100A6	PTP4A3	PRSS23	RPL12	PSAP
RAB38	SERPINA1	RPL13AP5	SDC3	RBMX	PSAP	RPL13	QPCT
RAP1GAP	SERPINA3	RPL14	SEC11C	RNF2	RDH5	RPL13A	RDH5
RAP2B	SERPINE2	RPL15	SERPINA1	RPL10	ROPN1	RPL13AP5	S100A1
RPL10	SERPINI1	RPL17	SERPINA3	RPL10A	S100A1	RPL14	S100A13
RPL10A	SFRP1	RPL18	SERPINE2	RPL11	S100A13	RPL15	S100A6
RPL11	SGCE	RPL18A	SGCE	RPL12	S100A6	RPL17	S100B
RPL12	SLC26A2	RPL21	SLC26A2	RPL13	S100B	RPL18	SAT1
RPL13	SLC39A14	RPL22	SLC39A14	RPL13A	SAT1	RPL18A	SCARB2
RPL13A	SLC5A3	RPL26	SLC5A3	RPL13AP5	SCARB2	RPL19	SCCPDH
RPL13AP5	SNX9	RPL27A	SNX9	RPL14	SCCPDH	RPL21	SDC3
RPL14	SPON2	RPL28	SPON2	RPL15	SDC3	RPL21P28	SEMA3B
RPL17	SPP1	RPL29	SPP1	RPL17	SEC11C	RPL22	SERPINA1
RPL18	SSBP1	RPL3	SVIP	RPL18	SEMA3B	RPL26	SERPINA3
RPL18A	SSBP2	RPL30	TAPBPL	RPL18A	SERPINA1	RPL27	SERPINE2
RPL28	TCN1	RPL31	TCN1	RPL19	SERPINA3	RPL27A	SGCE
RPL29	THBD	RPL32	THBD	RPL21	SERPINE2	RPL28	SGK1
RPL3	TIMP1	RPL35	TIMP1	RPL21P28	SGK1	RPL29	SHC4
RPL35	TJP1	RPL36	TJP1	RPL22	SHC4	RPL3	SLC26A2
RPL5	TM4SF1	RPL36A	TM4SF1	RPL23	SLC26A2	RPL30	SLC5A3
RPL7A	TMBIM4	RPL37	TNFRSF12A	RPL23A	SLC5A3	RPL31	SNX9
RPL8	TMX4	RPL37A	TNFSF4	RPL26	SLC7A8	RPL32	SPON2
RPLP0	TNFSF4	RPL39	TPP1	RPL27	SNX9	RPL35	SPP1
RPS10	TRIML2	RPL4	TRIML2	RPL27A	SPON2	RPL36	THBD
RPS11	TSC22D3	RPL5	TSC22D3	RPL28	SPP1	RPL36A	TIMP1
RPS16	TSPAN13	RPL6	UBC	RPL29	SQSTM1	RPL37	TIMP2
RPS18	TXNIP	RPL7	WBP2	RPL3	SYNE2	RPL37A	TIMP3
RPS19	UBC	RPL7A	WEE1	RPL30	THBD	RPL39	TM4SF1
RPS24	WSB1	RPL8	XAGE1A	RPL31	TIMP1	RPL4	TMEM255A
RPS3	XAGE1A	RPL9	XAGE1B	RPL32	TIMP2	RPL41	TMX4
RPS3A	XAGE1B	RPLP0	XAGE1C	RPL34	TIMP3	RPL5	TNFSF4
RPS5	XAGE1C	RPLP1	XAGE1D	RPL35	TM4SF1	RPL6	TPP1
RPS7	XAGE1D	RPLP2	XAGE1E	RPL35A	TMED10	RPL7	TRIML2
RPS8	XAGE1E	RPS10		RPL36	TMEM255A	RPL7A	TSC22D3
RPS9	ZBTB20	RPS11		RPL36A	TMEM59	RPL8	TXNIP

RPSA	*ZMYND8*	*RPS15*		*RPL37*	*TMX4*	*RPL9*	*TYR*
RUVBL2		*RPS15A*		*RPL37A*	*TNFSF4*	*RPLP0*	*UBC*
SAMM50		*RPS16*		*RPL38*	*TPP1*	*RPLP1*	*ZBTB20*
SCARB1		*RPS17*		*RPL39*	*TRIML2*	*RPLP2*	*ZBTB38*
SCD		*RPS17L*		*RPL4*	*TSC22D3*	*RPS10*	
SCIN		*RPS18*		*RPL41*	*TXNIP*	*RPS11*	
SDCBP		*RPS19*		*RPL5*	*TYR*	*RPS12*	
SEMA6A		*RPS20*		*RPL6*	*UBC*	*RPS13*	
SLC19A1		*RPS23*		*RPL7*	*WBP2*	*RPS14*	
SLC25A5		*RPS24*		*RPL7A*	*ZBTB38*	*RPS15*	
SLC25A6		*RPS25*		*RPL8*		*RPS15A*	
SLC45A2		*RPS27*		*RPL9*		*RPS16*	
SLC7A5P1		*RPS27A*		*RPLP0*		*RPS17*	
SNAI2		*RPS28*		*RPLP1*		*RPS17L*	
SNHG16		*RPS3*		*RPLP2*		*RPS18*	
SOAT1		*RPS3A*		*RPS10*		*RPS19*	
ST3GAL4		*RPS4X*		*RPS11*		*RPS2*	
STXBP1		*RPS5*		*RPS12*		*RPS20*	
TBC1D16		*RPS6*		*RPS13*		*RPS21*	
TDRD3		*RPS7*		*RPS14*		*RPS23*	
TFAP2A		*RPS8*		*RPS15*		*RPS24*	
TIMM50		*RPS9*		*RPS15A*		*RPS25*	
TNFRSF14		*RPSA*		*RPS16*		*RPS27*	
TPCN2		*RSL1D1*		*RPS17*		*RPS27A*	
TRAK2		*SAE1*		*RPS17L*		*RPS28*	
TRIB2		*SCD*		*RPS18*		*RPS3*	
TRIM63		*SDCBP*		*RPS19*		*RPS3A*	
TRPM1		*SERBP1*		*RPS2*		*RPS4X*	
TTC39A		*SERPINF1*		*RPS20*		*RPS5*	
TTYH2		*SET*		*RPS21*		*RPS6*	
TTYH3		*SLC19A1*		*RPS23*		*RPS7*	
TUBB4A		*SLC25A5*		*RPS24*		*RPS8*	
TXLNA		*SLC25A6*		*RPS25*		*RPS9*	
TYRP1		*SNAI2*		*RPS27*		*RPSA*	
UBL3		*SNHG16*		*RPS27A*		*RRS1*	
UGCG		*SNHG6*		*RPS28*		*RSL1D1*	
UQCRFS1		*SOX4*		*RPS3*		*RUVBL2*	
VAT1		*SSR2*		*RPS3A*		*SAE1*	
VIM		*TFAP2A*		*RPS4X*		*SERBP1*	
WDFY1		*TIMM13*		*RPS5*		*SERPINF1*	
		TIMM50		*RPS6*		*SET*	
		TMEM204		*RPS7*		*SHMT2*	
		TNFRSF14		*RPS8*		*SLC19A1*	
		TOMM20		*RPS9*		*SLC25A6*	
		TOP1MT		*RPSA*		*SMARCA4*	
		TPCN2		*RQCD1*		*SMIM15*	
		TPT1		*RRP15*		*SNAI2*	
		TRIB2		*RSL1D1*		*SNHG6*	
		TRPM1		*RUVBL2*		*SNRPB*	
		TUBB4A		*SAE1*		*SNRPD1*	
		TYRP1		*SERBP1*		*SNRPD2*	
		UBA52		*SERPINF1*		*SNRPE*	
		UQCRFS1		*SET*		*SOX4*	
		WDFY1		*SHMT2*		*SSR2*	
		XIST		*SLC25A6*		*STOML2*	
		ZEB2		*SMARCA4*		*STRAP*	
		ZFAS1		*SMIM15*		*TIMM13*	
				SNAI2		*TIMM44*	

				SNHG15		*TIMM50*	
				SNHG6		*TOMM22*	
				SNRPD1		*TOP1MT*	
				SNRPD2		*TP53*	
				SNRPE		*TPI1*	
				SOX4		*TPM2*	
				SSB		*TRIM28*	
				SSR2		*TUBB*	
				STOML2		*TYRP1*	
				STRAP		*UBA52*	
				TIMM13		*UHRF1*	
				TIMM44		*UQCRFS1*	
				TOMM20		*UQCRH*	
				TOP1MT		*ZFAS1*	
				TP53		*ZNF146*	
				TRIM28			
				TUBB			
				TUFM			
				TYRP1			
				UBA2			
				UBA52			
				UCK2			
				UQCRH			
				USP22			
				VDAC2			
				XIST			
				YWHAE			
				ZFAS1			
				ZNF146			

Table 27C. T cell exclusion and post-treatment signatures identified in macrophages

Macrophages in cold tumors		Post-treatment macrophages	
Up-regulated	**Down-regulated**	**Up-regulated**	**Down-regulated**
ADAM8	*AKR1A1*	*CSTB*	*ADORA3*
ALDOA	*ALDH1A1*	*HLA-DQA1*	*ASPH*
ANGPTL4	*APOC1*	*HSD11B1*	*C3AR1*
C19orf59	*APOE*	*HSP90AA1*	*CD200R1*
CD300E	*APOL3*	*IL18BP*	*CD28*
CD55	*AXL*	*LGALS2*	*CD99*
CD82	*B2M*	*NR1H3*	*COMT*
CDA	*C1orf54*	*PPA1*	*CREM*
CYTIP	*C1QA*	*SLAMF7*	*CRTAP*
DDIT4	*C1QB*	*TMSB4X*	*DDOST*
DUSP6	*C1QC*	*UBD*	*EGFL7*
EIF1	*C2*		*EIF1AY*
EMP3	*CD38*		*FCGR2A*
ENO2	*CD4*		*FCGRT*
FLNA	*CD74*		*GATM*
FXYD5	*CIITA*		*GNG2*
GAPDH	*CLIC2*		*GSTT1*
GPI	*CMKLR1*		*GYPC*
IL8	*CTSC*		*HIST1H1E*
LGALS1	*CXCL9*		*HPGDS*
LSP1	*EBI3*		*IFI44*
MTHFS	*ENPP2*		*LRP1*
MYADM	*EPB41L2*		*MEF2C*
MYO1G	*FAM26F*		*MS4A4A*

PGAM1	*FGD2*		*MS4A7*
S100A10	*GBP4*		*MTSS1*
S100A12	*GIMAP5*		*NAIP*
S100A4	*GM2A*		*NQO2*
S100A6	*HAPLN3*		*OLFML3*
S100A8	*HLA-DMA*		*PMP22*
S100A9	*HLA-DMB*		*PRDX2*
SLC11A1	*HLA-DOA*		*RNASE1*
STK10	*HLA-DPA1*		*RPS4Y1*
STK17B	*HLA-DPB1*		*SEPP1*
TREM1	*HLA-DPB2*		*SLC18B1*
VCAN	*HLA-DQA1*		*SLC40A1*
VIM	*HLA-DQB1*		*SPP1*
	HLA-DQB2		*STAB1*
	HLA-DRA		*TGFBI*
	HLA-DRB1		*TMEM106C*
	HLA-DRB5		*TMEM9*
	LGALS3BP		*TPD52L2*
	LILRB4		*ULK3*
	MS4A6A		
	NAGK		
	NR1H3		
	P2RY12		
	P2RY6		
	PDCD1LG2		
	PLA2G2D		
	PLEKHO1		
	PPA1		
	PRDX1		
	PSME2		
	RARRES3		
	SDC3		
	SERPING1		
	SLAMF7		
	SLAMF8		
	TIFAB		
	TMSB4X		
	TRAFD1		
	UBD		
	VOPP1		

[0554] **Table 28.** Differentially expressed gene sets in the malignant cells from post-treatment *vs.* untreated tumors; related to **Figure 63**.

Gene set	t-test p-value (-log10(|P|), positive = higher post-treatment, negative = lower in post-treatment)		N = No. of genes in the gene set	N.qc = No. of used genes	N/N.qc
	t-test p-value	mixed effects p-value			
GO_RESPONSE_TO_ENDOPLASMIC_RETICULUM_STRESS	-	-	233	147	0.63

	36.5	4.05			
GO_CELLULAR_COPPER_ION_HOMEOSTASIS	-44.3	-4.04	13	9	0.69
GO_CELLULAR_RESPONSE_TO_ZINC_ION	-215.8	-4	16	7	0.44
ENDOPLASMIC_RETICULUM_MEMBRANE	-42.6	-3.93	85	55	0.65
GO_REGULATION_OF_ENDOTHELIAL_CELL_APOPTOTIC_PROCESS	-52.4	-3.79	42	14	0.33
METALLOTHIONEINS	-208.1	-3.72	13	6	0.46
GO_INTRAMOLECULAR_OXIDOREDUCTASE_ACTIVITY_TRANSPOSING_S_S_BONDS	-40.5	-3.64	22	14	0.64
NUCLEAR_ENVELOPE_ENDOPLASMIC_RETICULUM_NETWORK	-38.4	-3.59	94	62	0.66
GO_CELLULAR_RESPONSE_TO_VITAMIN_D	-78.7	-3.56	14	4	0.29
KEGG_SNARE_INTERACTIONS_IN_VESICULAR_TRANSPORT	-17.6	-3.43	38	23	0.61
ENDOPLASMIC_RETICULUM_PART	-44.4	-3.43	97	65	0.67
GO_COPPER_ION_HOMEOSTASIS	-38.1	-3.38	16	12	0.75
KEGG_ECM_RECEPTOR_INTERACTION	-163.9	-3.35	84	35	0.42
GO_ENDOPLASMIC_RETICULUM_GOLGI_INTERMEDIATE_COMPARTMENT	-40.3	-3.3	105	64	0.61
GO_BLOOD_VESSEL_MORPHOGENESIS	-153.3	-3.3	364	117	0.32
GO_PLATELET_DERIVED_GROWTH_FACTOR_RECEPTOR_BINDING	-62.3	-3.24	15	5	0.33
GO_ANGIOGENESIS	-148.4	-3.23	293	102	0.35
GO_RESPONSE_TO_ZINC_ION	-76.2	-3.22	55	21	0.38
PID_INTEGRIN_CS_PATHWAY	-172.6	-3.19	26	9	0.35
GOLGI_MEMBRANE	-53.1	-3.13	45	26	0.58
GO_TRANSITION_METAL_ION_TRANSMEMBRANE_TRANSPORTER_ACTIVITY	-61.3	-3.12	39	19	0.49
POSITIVE_REGULATION_OF_CELL_PROLIFERATION	-31.5	-3.11	149	48	0.32
GO_MUSCLE_CELL_MIGRATION	-164.4	-3.11	18	10	0.56
NUCLEAR ORPHAN RECEPTOR	-83.4	-3.09	3	2	0.67
GO_POSITIVE_REGULATION_OF_EXTRINSIC_APOPTOTIC_SIGNALING_PATHWAY_VIA_DEATH_DOMAIN_RECEPTORS	-75.4	-3.08	17	11	0.65
GO_PHOSPHOTRANSFERASE_ACTIVITY_FOR_OTHER_SUBSTITUTED_PHOSPHATE_GROUPS	-32.3	-3.07	19	11	0.58
ST_INTERLEUKIN_13_PATHWAY	-2.4	-3.03	7	2	0.29
WOUND_HEALING	-148.0	-3.02	54	13	0.24
C/EBP	-38.9	-3	10	3	0.3
GO_INSULIN_LIKE_GROWTH_FACTOR_BINDING	-62.7	-2.98	25	11	0.44
MUSCLE_DEVELOPMENT	-122.5	-2.98	93	29	0.31
GO_PLATELET_ALPHA_GRANULE_MEMBRANE	-105.	-2.96	13	7	0.54

	0				
GO_MANNOSIDASE_ACTIVITY	-28.5	-2.95	15	5	0.33
GO_POSITIVE_REGULATION_OF_ADHERENS_JUNCTION_ORGANIZATION	-61.4	-2.95	21	9	0.43
GO_NEGATIVE_REGULATION_OF_EPITHELIAL_CELL_APOPTOTIC_PROCESS	-70.5	-2.95	35	8	0.23
ENDOPLASMIC_RETICULUM	-50.0	-2.94	294	180	0.61
CELL_FATE_COMMITMENT	-72.6	-2.94	13	3	0.23
GO_ENDOPLASMIC_RETICULUM_GOLGI_INTERMEDIATE_COMPARTMENT_MEMBRANE	-65.4	-2.93	63	38	0.6
GO_NEGATIVE_REGULATION_OF_INTERLEUKIN_8_PRODUCTION	-126.6	-2.93	15	5	0.33
PID_TNF_PATHWAY	-73.0	-2.92	46	22	0.48
GO_RECEPTOR_REGULATOR_ACTIVITY	-93.0	-2.92	45	10	0.22
GO_EXTRACELLULAR_STRUCTURE_ORGANIZATION	-107.3	-2.92	304	111	0.37
ER_GOLGI_INTERMEDIATE_COMPARTMENT	-12.4	-2.91	24	20	0.83
GO_RESPONSE_TO_CADMIUM_ION	-124.5	-2.9	40	25	0.62
GO_HEPARAN_SULFATE_PROTEOGLYCAN_BIOSYNTHETIC_PROCESS	-32.0	-2.89	23	8	0.35
GO_AXON_REGENERATION	-144.4	-2.88	24	9	0.38
ENDOMEMBRANE_SYSTEM	-22.0	-2.87	220	137	0.62
HALLMARK_IL6_JAK_STAT3_SIGNALING	-170.2	-2.87	87	40	0.46
GO_HEPARAN_SULFATE_PROTEOGLYCAN_METABOLIC_PROCESS	-30.7	-2.86	28	8	0.29
GO_POSITIVE_REGULATION_OF_CELL_JUNCTION_ASSEMBLY	-88.3	-2.85	24	11	0.46
GO_VASCULATURE_DEVELOPMENT	-143.8	-2.84	469	153	0.33
CELLULAR_CATION_HOMEOSTASIS	-96.8	-2.83	106	32	0.3
GO_CELL_SUBSTRATE_JUNCTION_ASSEMBLY	-79.6	-2.82	41	19	0.46
PID_FRA_PATHWAY	-55.9	-2.81	37	17	0.46
GO_REGULATION_OF_ADHERENS_JUNCTION_ORGANIZATION	-63.4	-2.81	50	22	0.44
GO_CELL_ADHESION_MEDIATED_BY_INTEGRIN	-81.8	-2.81	12	8	0.67
GO_SARCOLEMMA	-216.6	-2.81	125	37	0.3
GO_NEGATIVE_REGULATION_OF_ENDOTHELIAL_CELL_APOPTOTIC_PROCESS	-38.2	-2.8	27	7	0.26
GO_CORECEPTOR_ACTIVITY	-68.2	-2.79	38	11	0.29
GO_REGULATION_OF_INTERLEUKIN_8_BIOSYNTHETIC_PROCESS	-12.9	-2.78	12	3	0.25
REACTOME_EXTRINSIC_PATHWAY_FOR_APOPTOSIS	-55.4	-2.78	13	8	0.62
HALLMARK_HYPOXIA	-112.2	-2.78	200	116	0.58
GO_ER_NUCLEUS_SIGNALING_PATHWAY	-28.3	-2.75	34	25	0.74
HOMOPHILIC_CELL_ADHESION	-	-	16	4	0.25

	55.0	2.74			
GO_SNAP_RECEPTOR_ACTIVITY	-20.2	-2.73	38	22	0.58
HALLMARK_EPITHELIAL_MESENCHYMAL_TRANSITION	-128.6	-2.73	200	110	0.55
GO_CELLULAR_RESPONSE_TO_CADMIUM_ION	-155.1	-2.73	15	9	0.6
GO_BASAL_LAMINA	-27.9	-2.72	21	6	0.29
CELL_CELL_ADHESION	-40.3	-2.72	86	19	0.22
POSITIVE_REGULATION_OF_MULTICELLULAR_ORGANISMAL_PROCESS	-45.5	-2.71	66	18	0.27
FIBROBLAST	-73.9	-2.71	6	3	0.5
GO_ATPASE_COMPLEX	-80.5	-2.7	24	7	0.29
GO_INTRINSIC_COMPONENT_OF_EXTERNAL_SIDE_OF_PLASMA_MEMBRANE	-68.1	-2.69	27	7	0.26
PID_INTEGRIN3_PATHWAY	-78.1	-2.68	43	22	0.51
CATION_HOMEOSTASIS	-93.1	-2.68	109	32	0.29
GO_CELL_SUBSTRATE_ADHESION	-162.0	-2.68	164	58	0.35
GO_INTRINSIC_APOPTOTIC_SIGNALING_PATHWAY_IN_RESPONSE_TO_ENDOPLASMIC_RETICULUM_STRESS	-37.6	-2.67	32	18	0.56
GO_POSITIVE_REGULATION_OF_CELL_MATRIX_ADHESION	-57.1	-2.66	40	15	0.38
GO_NEGATIVE_REGULATION_OF_GLYCOPROTEIN_METABOLIC_PROCESS	-60.2	-2.66	15	10	0.67
GO_NEGATIVE_REGULATION_OF_TYPE_2_IMMUNE_RESPONSE	-162.5	-2.66	11	4	0.36
REACTOME_ACTIVATION_OF_CHAPERONES_BY_ATF6_ALPHA	-22.9	-2.64	13	8	0.62
GO_NEGATIVE_REGULATION_OF_DNA_RECOMBINATION	-13.6	-2.63	16	8	0.5
GO_CELLULAR_RESPONSE_TO_TOPOLOGICALLY_INCORRECT_PROTEIN	-22.7	-2.63	122	81	0.66
GO_CELLULAR_RESPONSE_TO_CALCIUM_ION	-69.5	-2.63	49	18	0.37
GO_SECRETORY_GRANULE_MEMBRANE	-133.4	-2.63	78	28	0.36
GOLGI_VESICLE_TRANSPORT	-13.7	-2.62	48	37	0.77
REACTOME_DIABETES_PATHWAYS	-20.3	-2.62	133	80	0.6
GO_NEGATIVE_REGULATION_OF_GLYCOPROTEIN_BIOSYNTHETIC_PROCESS	-24.0	-2.61	12	9	0.75
CAHOY_ASTROGLIAL	-197.1	-2.61	100	37	0.37
GO_HEMIDESMOSOME_ASSEMBLY	-95.2	-2.6	12	5	0.42
GO_FIBRINOLYSIS	-98.5	-2.6	21	6	0.29
GO_PROTEIN_COMPLEX_INVOLVED_IN_CELL_ADHESION	-171.7	-2.6	30	10	0.33
ST_IL_13_PATHWAY	-1.6	-2.59	7	2	0.29
POSITIVE_REGULATION_OF_PROTEIN_MODIFICATION_PROCESS	-37.4	-2.58	29	9	0.31
HALLMARK_UV_RESPONSE_UP	-67.1	-2.57	158	93	0.59
CELL_MIGRATION	-87.0	-2.57	96	34	0.35

ATPASE_ACTIVITY_COUPLED_TO_TRANSMEMBRANE_MOVEMENT_OF_IONS_PHOSPHORYLATIVE_MECHANISM	-130.2	-2.57	20	5	0.25
GO_INTEGRIN_BINDING	-95.0	-2.56	105	48	0.46
HALLMARK_TNFA_SIGNALING_VIA_NFKB	-154.1	-2.56	200	108	0.54
GO_PLATELET_ALPHA_GRANULE	-164.1	-2.56	75	35	0.47
PID_INTEGRIN1_PATHWAY	-89.7	-2.55	66	34	0.52
GO_CATION_TRANSPORTING_ATPASE_COMPLEX	-119.7	-2.55	16	4	0.25
PROTEIN_AMINO_ACID_LIPIDATION	-35.6	-2.54	24	19	0.79
GO_NEGATIVE_REGULATION_OF_LIPID_STORAGE	-92.0	-2.54	17	6	0.35
GO_BASEMENT_MEMBRANE_ORGANIZATION	-26.2	-2.53	11	7	0.64
POSITIVE_REGULATION_OF_CYTOKINE_PRODUCTION	-41.7	-2.53	15	5	0.33
BIOCARTA_SODD_PATHWAY	-37.4	-2.52	10	8	0.8
GO_PERK_MEDIATED_UNFOLDED_PROTEIN_RESPONSE	-39.2	-2.52	12	10	0.83
PHOSPHOLIPID_METABOLIC_PROCESS	-44.8	-2.52	74	42	0.57
Targets of NFAT_Q6	-53.2	-2.52	246	80	0.33
BIOCARTA_STRESS_PATHWAY	-71.8	-2.52	25	10	0.4
CYTOPLASM_ORGANIZATION_AND_BIOGENESIS	-68.0	-2.51	15	7	0.47
Targets of FREAC3_01	-23.3	-2.5	251	65	0.26
GO_COLLAGEN_BINDING	-84.5	-2.5	65	27	0.42
PID_INTEGRIN4_PATHWAY	-35.8	-2.49	11	4	0.36
CELL_SURFACE	-42.6	-2.49	79	27	0.34
GO_PHOSPHATE_TRANSMEMBRANE_TRANSPORTER_ACTIVITY	-14.3	-2.48	30	16	0.53
NAIVE_VS_ACTIVATED_CD8_TCELL_DN	-38.5	-2.48	200	81	0.4
MEMBRANE_LIPID_BIOSYNTHETIC_PROCESS	-20.4	-2.47	49	29	0.59
GO_GLYCEROPHOSPHOLIPID_CATABOLIC_PROCESS	-28.0	-2.47	13	7	0.54
GO_INTERSTITIAL_MATRIX	-82.0	-2.47	14	3	0.21
GO_REGULATION_OF_EXTRINSIC_APOPTOTIC_SIGNALING_PATHWAY_VIA_DEATH_DOMAIN_RECEPTORS	-103.8	-2.47	55	32	0.58
INORGANIC_ANION_TRANSPORT	-151.9	-2.47	18	4	0.22
REACTOME_CLASS_B_2_SECRETIN_FAMILY_RECEPTORS	-62.6	-2.46	88	19	0.22
GO_DECIDUALIZATION	-99.4	-2.46	21	7	0.33
GO_MULTI_MULTICELLULAR_ORGANISM_PROCESS	-129.0	-2.46	213	62	0.29
NABA_BASEMENT_MEMBRANES	-19.2	-2.45	40	12	0.3
GO_PROTEINACEOUS_EXTRACELLULAR_MATRIX	-60.9	-2.45	356	86	0.24
GO_EXTRACELLULAR_MATRIX	-	-	426	116	0.27

	121.2	2.45			
GO_INTEGRIN_MEDIATED_SIGNALING_PATHWAY	-129.1	-2.45	82	36	0.44
SECRETION	-34.2	-2.44	178	68	0.38
GO_CARBOHYDRATE_DERIVATIVE_CATABOLIC_PROCESS	-62.7	-2.44	174	76	0.44
HALLMARK_APOPTOSIS	-184.4	-2.44	161	111	0.69
LIPOPROTEIN_METABOLIC_PROCESS	-34.8	-2.43	33	21	0.64
LIPOPROTEIN_BIOSYNTHETIC_PROCESS	-36.5	-2.43	26	19	0.73
GO_BASEMENT_MEMBRANE	-54.6	-2.43	93	32	0.34
REACTOME_UNFOLDED_PROTEIN_RESPONSE	-13.9	-2.42	80	58	0.72
GO_LIPOPROTEIN_BIOSYNTHETIC_PROCESS	-63.0	-2.42	85	40	0.47
GO_HYDROLASE_ACTIVITY_ACTING_ON_GLYCOSYL_BONDS	-65.4	-2.42	122	44	0.36
GO_REGULATION_OF_VIRAL_ENTRY_INTO_HOST_CELL	-72.1	-2.42	28	12	0.43
BIOCARTA_IL1R_PATHWAY	-72.2	-2.41	33	12	0.36
HALLMARK_IL2_STAT5_SIGNALING	-199.1	-2.41	200	91	0.46
GO_NEGATIVE_REGULATION_OF_SMALL_GTPASE_MEDIATED_SIGNAL_TRANSDUCTION	-72.3	-2.4	40	14	0.35
GO_GROWTH_FACTOR_BINDING	-107.5	-2.39	123	46	0.37
GO_METALLOENDOPEPTIDASE_INHIBITOR_ACTIVITY	-118.8	-2.39	14	5	0.36
TTAYRTAA_Targets of E4BP4_01	-133.2	-2.39	265	74	0.28
GO_REGULATION_OF_T_HELPER_2_CELL_DIFFERENTIATION	-200.2	-2.39	11	3	0.27
CELL_ACTIVATION	-24.5	-2.38	77	17	0.22
GO_EXTRACELLULAR_MATRIX_COMPONENT	-46.2	-2.38	125	47	0.38
GO_RESPONSE_TO_AXON_INJURY	-138.0	-2.38	48	19	0.4
GO_FORMATION_OF_PRIMARY_GERM_LAYER	-93.4	-2.37	110	33	0.3
HYDROLASE_ACTIVITY_ACTING_ON_ACID_ANHYDRIDESCATALYZING_TRANSMEMBRANE_MOVEMENT_OF_SUBSTANCES	-126.7	-2.37	39	14	0.36
GO_CELLULAR_RESPONSE_TO_PROSTAGLANDIN_STIMULUS	-41.8	-2.36	24	10	0.42
GO_NEGATIVE_REGULATION_OF_MULTICELLULAR_ORGANISMAL_METABOLIC_PROCESS	-55.1	-2.36	12	6	0.5
GO_NEGATIVE_REGULATION_OF_GROWTH	-96.4	-2.36	236	85	0.36
GO_REGULATION_OF_ERK1_AND_ERK2_CASCADE	-121.1	-2.36	238	74	0.31
GO_CELL_MATRIX_ADHESION	-156.5	-2.36	119	42	0.35
PID_P38_MKK3_6PATHWAY	-11.8	-2.35	26	9	0.35
GO_ACROSOMAL_MEMBRANE	-	-	22	8	0.36

	98.5	2.35			
BLOOD_COAGULATION	-133.9	-2.35	43	12	0.28
GO_REGULATION_OF_INTERLEUKIN_2_PRODUCTION	-134.5	-2.35	48	19	0.4
GO_IRE1_MEDIATED_UNFOLDED_PROTEIN_RESPONSE	-17.4	-2.34	56	44	0.79
GO_PROTEIN_HETEROOLIGOMERIZATION	-31.5	-2.34	113	44	0.39
GO_NEGATIVE_REGULATION_OF_SODIUM_ION_TRANSPORT	-110.1	-2.34	11	4	0.36
MEMBRANE_FUSION	-27.6	-2.33	28	15	0.54
KEGG_GLYCOSPHINGOLIPID_BIOSYNTHESIS_GANGLIO_SERIES	-46.3	-2.33	15	6	0.4
GO_REGULATION_OF_CELL_SUBSTRATE_ADHESION	-62.1	-2.33	173	67	0.39
GO_REGULATION_OF_PROTEIN_GLYCOSYLATION	-18.5	-2.32	14	5	0.36
GO_PLASMA_MEMBRANE_FUSION	-40.8	-2.32	26	8	0.31
GO_COMPACT_MYELIN	-55.0	-2.31	15	8	0.53
Targets of CDPCR1_01	-74.8	-2.31	130	33	0.25
AMINO_ACID_DERIVATIVE_BIOSYNTHETIC_PROCESS	-10.4	-2.3	10	4	0.4
KEGG_GLYCOSAMINOGLYCAN_BIOSYNTHESIS_CHONDROITIN_SULFATE	-61.3	-2.3	22	6	0.27
GO_REGULATION_OF_CELL_MATRIX_ADHESION	-63.6	-2.3	90	34	0.38
GO_ANTIMICROBIAL_HUMORAL_RESPONSE	-81.3	-2.3	52	14	0.27
GO_NEGATIVE_REGULATION_OF_PROTEIN_KINASE_B_SIGNALING	-47.7	-2.29	36	16	0.44
GO_RESPONSE_TO_OXYGEN_LEVELS	-69.2	-2.29	311	127	0.41
GO_RESPONSE_TO_TRANSITION_METAL_NANOPARTICLE	-89.8	-2.29	148	63	0.43
GO_FIBRONECTIN_BINDING	-106.4	-2.29	28	16	0.57
GO_POSITIVE_REGULATION_OF_INTERLEUKIN_2_PRODUCTION	-147.4	-2.29	31	12	0.39
GO_ENDOPLASMIC_RETICULUM_LUMEN	-32.2	-2.28	201	84	0.42
GO_POSITIVE_REGULATION_OF_EXTRINSIC_APOPTOTIC_SIGNALING_PATHWAY	-52.9	-2.28	53	35	0.66
GO_CELLULAR_RESPONSE_TO_OXYGEN_LEVELS	-58.7	-2.28	143	55	0.38
REACTOME_INTEGRIN_CELL_SURFACE_INTERACTIONS	-89.7	-2.28	79	37	0.47
EXTRACELLULAR_REGION_PART	-125.7	-2.28	338	88	0.26
GO_SECRETORY_GRANULE_LUMEN	-157.3	-2.28	85	31	0.36
GO_SNARE_COMPLEX	-17.4	-2.27	53	28	0.53
KEGG_GLYCOSAMINOGLYCAN_DEGRADATION	-47.0	-2.27	21	9	0.43
ATPASE_ACTIVITY_COUPLED_TO_TRANSMEMBRANE_MOVEMENT_OF_IONS	-133.4	-2.27	24	9	0.38
GO_NEGATIVE_REGULATION_OF_COAGULATION	-196.2	-2.27	48	13	0.27

REACTOME_TRANSPORT_OF_VITAMINS_NUCLEOSIDES_AND_RELATED_MOLECULES	-10.1	-2.26	31	9	0.29
GO_IRON_ION_BINDING	-18.2	-2.26	163	42	0.26
GO_ACETYLGLUCOSAMINYLTRANSFERASE_ACTIVITY	-39.0	-2.26	49	19	0.39
GO_POSITIVE_REGULATION_OF_RECEPTOR_MEDIATED_ENDOCYTOSIS	-75.5	-2.26	47	13	0.28
HALLMARK_UV_RESPONSE_DN	-95.4	-2.26	144	64	0.44
GO_CELL_ADHESION_MOLECULE_BINDING	-113.3	-2.26	186	74	0.4
REACTOME_CELL_SURFACE_INTERACTIONS_AT_THE_VASCULAR_WALL	-148.4	-2.26	91	38	0.42
GO_UBIQUITIN_UBIQUITIN_LIGASE_ACTIVITY	-10.5	-2.25	13	7	0.54
GO_N_GLYCAN_PROCESSING	-37.7	-2.25	20	5	0.25
GO_BRANCH_ELONGATION_OF_AN_EPITHELIUM	-38.5	-2.25	17	4	0.24
REACTOME_TRANSPORT_OF_GLUCOSE_AND_OTHER_SUGARS_BILE_SALTS_AND_ORGANIC_ACIDS_METAL_IONS_AND_AMINE_COMPOUNDS	-70.9	-2.25	89	18	0.2
GO_BASAL_PLASMA_MEMBRANE	-102.3	-2.25	33	9	0.27
GO_PLATELET_DEGRANULATION	-156.8	-2.25	107	51	0.48
PDZ_DOMAIN_BINDING	-29.5	-2.24	14	4	0.29
BIOCARTA_GATA3_PATHWAY	-52.3	-2.24	16	4	0.25
GO_NEGATIVE_REGULATION_OF_CELL_SUBSTRATE_ADHESION	-81.8	-2.24	53	25	0.47
AMINE_BIOSYNTHETIC_PROCESS	-12.3	-2.23	15	7	0.47
GO_REGULATION_OF_RECEPTOR_ACTIVITY	-13.6	-2.23	117	30	0.26
GO_PYRIMIDINE_NUCLEOSIDE_CATABOLIC_PROCESS	-79.6	-2.23	21	8	0.38
GO_CIRCULATORY_SYSTEM_DEVELOPMENT	-132.2	-2.23	788	233	0.3
GO_MATURE_B_CELL_DIFFERENTIATION	-21.5	-2.22	17	7	0.41
GO_OLIGOSACCHARIDE_CATABOLIC_PROCESS	-24.1	-2.22	12	7	0.58
GO_RESPONSE_TO_PROSTAGLANDIN	-38.5	-2.22	34	11	0.32
GO_OXIDOREDUCTASE_ACTIVITY_ACTING_ON_THE_CH_NH2_GROUP_OF_DONORS_OXYGEN_AS_ACCEPTOR	-60.9	-2.22	15	5	0.33
ST_TUMOR_NECROSIS_FACTOR_PATHWAY	-96.7	-2.22	29	17	0.59
GO_REGULATION_OF_INTERLEUKIN_8_SECRETION	-101.5	-2.22	19	8	0.42
GO_REGULATION_OF_MEMBRANE_PROTEIN_ECTODOMAIN_PROTEOLYSIS	-157.9	-2.22	21	9	0.43
ER_TO_GOLGI_VESICLE_MEDIATED_TRANSPORT	-4.8	-2.21	18	15	0.83
PID_TCR_JNK_PATHWAY	-26.5	-2.21	14	6	0.43
REACTOME_IL1_SIGNALING	-34.9	-2.21	39	16	0.41
GO_POSITIVE_REGULATION_OF_IMMUNOGLOBULIN_SECRETION	-97.2	-2.21	11	4	0.36
PID_AP1_PATHWAY	-129.8	-2.2	70	31	0.44

Targets of LMO2COM_01	-20.1	-2.19	264	72	0.27
GO_RESPONSE_TO_STARVATION	-41.8	-2.19	154	70	0.45
GO_MEMBRANE_RAFT_ORGANIZATION	-114.2	-2.19	17	12	0.71
COAGULATION	-131.3	-2.19	44	12	0.27
GO_SULFATE_TRANSPORT	-73.2	-2.18	14	3	0.21
Targets of STAT5A_02	-73.8	-2.18	141	42	0.3
GO_SECRETORY_GRANULE	-145.5	-2.18	352	114	0.32
GO_REGULATION_OF_COAGULATION	-149.1	-2.18	88	26	0.3
GO_CELL_SURFACE	-169.9	-2.18	757	217	0.29
GO_NUCLEOTIDE_TRANSMEMBRANE_TRANSPORT	-6.9	-2.17	12	7	0.58
PROTEIN_TRANSPORTER_ACTIVITY	-7.7	-2.17	14	7	0.5
ENDOPLASMIC_RETICULUM_LUMEN	-16.1	-2.17	14	12	0.86
GO_REGULATION_OF_PEPTIDYL_SERINE_PHOSPHORYLATION	-34.4	-2.17	118	37	0.31
LIPID_RAFT	-83.2	-2.17	29	16	0.55
GO_CELLULAR_RESPONSE_TO_EXTERNAL_STIMULUS	-74.8	-2.16	264	114	0.43
GO_REGULATION_OF_EXTRINSIC_APOPTOTIC_SIGNALING_PATHWAY	-97.6	-2.16	153	77	0.5
GO_RESPONSE_TO_DRUG	-144.6	-2.16	431	159	0.37
GO_REGULATION_OF_EXTRACELLULAR_MATRIX_DISASSEMBLY	-147.7	-2.16	14	4	0.29
REACTOME_ACTIVATION_OF_CHAPERONE_GENES_BY_XBP1S	-15.4	-2.15	46	35	0.76
GO_DENDRITE_MORPHOGENESIS	-17.1	-2.15	42	12	0.29
GO_MATURE_B_CELL_DIFFERENTIATION_INVOLVED_IN_IMMUNE_RESPONSE	-27.9	-2.15	13	6	0.46
GO_CELLULAR_RESPONSE_TO_MECHANICAL_STIMULUS	-133.1	-2.15	80	32	0.4
GO_HETEROTYPIC_CELL_CELL_ADHESION	-138.7	-2.15	27	9	0.33
BIOCARTA_LYM_PATHWAY	-59.0	-2.14	11	7	0.64
HINATA_NFKB_MATRIX	-78.2	-2.14	10	7	0.7
GO_NEGATIVE_REGULATION_OF_RHO_PROTEIN_SIGNAL_TRANSDUCTION	-83.8	-2.14	14	8	0.57
GO_TELOMERE_LOCALIZATION	-8.5	-2.13	11	4	0.36
INTRINSIC_TO_ENDOPLASMIC_RETICULUM_MEMBRANE	-11.4	-2.13	24	14	0.58
CELLULAR_HOMEOSTASIS	-62.0	-2.13	147	45	0.31
GO_CELL_MIGRATION_INVOLVED_IN_SPROUTING_ANGIOGENESIS	-87.1	-2.13	15	4	0.27
GO_GASTRULATION	-36.6	-2.12	155	46	0.3
PID_IL1_PATHWAY	-	-	34	15	0.44

	68.3	2.12			
GO_ENDOPEPTIDASE_ACTIVITY	-81.6	-2.12	448	135	0.3
INTEGRAL_TO_ENDOPLASMIC_RETICULUM_MEMBRANE	-9.6	-2.11	24	14	0.58
REACTOME_ACTIVATION_OF_CHAPERONE_GENES_BY_ATF6_ALPHA	-16.4	-2.11	11	7	0.64
GO_ZINC_II_ION_TRANSPORT	-38.1	-2.11	26	13	0.5
RYAAAKNNNNNNTTGW_UNKNOWN	-51.3	-2.11	84	22	0.26
GGARNTKYCCA_UNKNOWN	-56.6	-2.11	78	24	0.31
GO_MEMBRANE_HYPERPOLARIZATION	-86.7	-2.11	11	3	0.27
PID_INTEGRIN_A9B1_PATHWAY	-88.1	-2.11	25	11	0.44
GO_MEMBRANE_ASSEMBLY	-113.4	-2.11	25	10	0.4
GO_ALCOHOL_TRANSMEMBRANE_TRANSPORTER_ACTIVITY	-135.7	-2.11	24	5	0.21
LEUKOCYTE_ACTIVATION	-21.6	-2.1	69	16	0.23
GO_POSITIVE_REGULATION_OF_PEPTIDYL_SERINE_PHOSPHORYLATION	-60.5	-2.1	88	29	0.33
GO_OXALATE_TRANSPORT	-81.4	-2.09	12	3	0.25
GO_MEMBRANE_BIOGENESIS	-92.9	-2.09	30	12	0.4
GO_SECRETORY_VESICLE	-133.0	-2.09	461	143	0.31
REACTOME_EXTRACELLULAR_MATRIX_ORGANIZATION	-29.2	-2.08	87	25	0.29
Targets of ATargets of 01	-45.9	-2.08	259	109	0.42
ATPASE_ACTIVITY_COUPLED_TO_MOVEMENT_OF_SUBSTANCES	-130.1	-2.08	40	14	0.35
GO_ENDOPLASMIC_RETICULUM_CHAPERONE_COMPLEX	-3.3	-2.07	11	8	0.73
GO_CIS_GOLGI_NETWORK	-26.0	-2.07	40	23	0.57
GO_RESPONSE_TO_OXIDATIVE_STRESS	-58.4	-2.07	352	165	0.47
Targets of FOXD3_01	-77.7	-2.07	199	45	0.23
HYDROLASE_ACTIVITY_HYDROLYZING_O_GLYCOSYL_COMPOUNDS	-37.8	-2.06	37	13	0.35
Targets of CEBP_Q2_01	-52.0	-2.06	267	76	0.28
GO_REGULATION_OF_CELL_JUNCTION_ASSEMBLY	-53.5	-2.06	68	27	0.4
GO_PEPTIDASE_ACTIVITY	-53.9	-2.06	663	202	0.3
GO_REGULATION_OF_EPITHELIAL_CELL_APOPTOTIC_PROCESS	-88.5	-2.06	59	20	0.34
ACTIVE_TRANSMEMBRANE_TRANSPORTER_ACTIVITY	-98.3	-2.06	122	31	0.25
GO_REGULATION_OF_PEPTIDASE_ACTIVITY	-127.3	-2.06	392	176	0.45
GO_RESPONSE_TO_FOOD	-15.0	-2.05	19	5	0.26
GO_PROTEIN_DEGLYCOSYLATION	-22.0	-2.05	21	13	0.62
GO_AMINOGLYCAN_CATABOLIC_PROCESS	-66.4	-2.05	68	27	0.4
INTEGRAL_TO_ORGANELLE_MEMBRANE	-12.4	-2.04	50	27	0.54

LYMPHOCYTE_ACTIVATION	-16.2	-2.04	61	15	0.25
BIOCARTA_VITCB_PATHWAY	-23.6	-2.04	11	6	0.55
NEGATIVE_REGULATION_OF_SECRETION	-25.6	-2.04	13	5	0.38
MEMBRANE_LIPID_METABOLIC_PROCESS	-61.4	-2.04	101	55	0.54
GO_CELL_CELL_CONTACT_ZONE	-91.7	-2.04	64	21	0.33
KEGG_COMPLEMENT_AND_COAGULATION_CASCADES	-112.2	-2.04	69	28	0.41
GO_NEGATIVE_REGULATION_OF_WOUND_HEALING	-182.9	-2.04	58	13	0.22
NUCLEOTIDE_KINASE_ACTIVITY	-0.4	-2.03	13	5	0.38
GO_ENDODERM_FORMATION	-52.7	-2.03	50	20	0.4
GO_GLYCOLIPID_BIOSYNTHETIC_PROCESS	-58.1	-2.03	62	33	0.53
M1_MACROPHAGES	-77.2	-2.03	54	25	0.46
RESPONSE_TO_WOUNDING	-137.2	-2.03	190	58	0.31
GO_REGULATION_OF_ASTROCYTE_DIFFERENTIATION	-149.9	-2.03	27	7	0.26
GO_HOST	-4.3	-2.02	12	8	0.67
GO_REGULATION_OF_CHOLESTEROL_HOMEOSTASIS	-29.2	-2.02	11	4	0.36
GO_REGULATION_OF_SODIUM_ION_TRANSMEMBRANE_TRANSPORT	-67.2	-2.02	48	14	0.29
TIL_HCC_C9_CD4_GZMK	-75.2	-2.02	10	5	0.5
SUGAR_BINDING	-98.2	-2.02	34	7	0.21
GO_APICAL_PLASMA_MEMBRANE	-139.4	-2.02	292	74	0.25
GO_REGULATION_OF_SODIUM_ION_TRANSPORT	-143.0	-2.02	77	22	0.29
GO_UDP_GLYCOSYLTRANSFERASE_ACTIVITY	-33.4	-2.01	139	38	0.27
GO_OXIDOREDUCTASE_ACTIVITY_ACTING_ON_THE_CH_NH2_GROUP_OF_DONORS	-37.8	-2.01	19	6	0.32
GO_ENDODERM_DEVELOPMENT	-49.7	-2.01	71	21	0.3
GO_CARBOHYDRATE_BINDING	-65.6	-2.01	277	72	0.26
Targets of OCT1_Q5_01	-69.3	-2.01	273	64	0.23
GO_MATERNAL_PROCESS_INVOLVED_IN_FEMALE_PREGNANCY	-72.7	-2.01	60	21	0.35
GO_SODIUM_POTASSIUM_EXCHANGING_ATPASE_COMPLEX	-141.2	-2.01	11	3	0.27
HALLMARK_COAGULATION	-166.9	-2.01	138	64	0.46
SULFURIC_ESTER_HYDROLASE_ACTIVITY	-49.6	-2	16	4	0.25
GO_RESPONSE_TO_UV	39.8	2	126	60	0.48
FATTY_ACID_OXIDATION	17.5	2	18	12	0.67
GO_PROTEIN_SUMOYLATION	74.6	2.01	115	68	0.59
GO_POSITIVE_REGULATION_OF_DNA_REPAIR	59.9	2.01	38	17	0.45
GO_CHROMOSOMAL_REGION	54.3	2.01	330	159	0.48

GO_NEGATIVE_REGULATION_OF_DEFENSE_RESPONSE_TO_VIRUS	42.6	2.01	18	8	0.44
KEGG_LIMONENE_AND_PINENE_DEGRADATION	40.9	2.01	10	7	0.7
NUCLEAR_HORMONE_RECEPTOR_BINDING	39.1	2.01	28	15	0.54
CELLULAR_PROTEIN_COMPLEX_DISASSEMBLY	35.6	2.01	13	7	0.54
BIOCARTA_VEGF_PATHWAY	21.9	2.01	29	15	0.52
GO_FILAMENTOUS_ACTIN	8.3	2.01	20	6	0.3
GO_DNA_METHYLATION_OR_DEMETHYLATION	2.5	2.01	59	22	0.37
GO_REGULATION_OF_TELOMERASE_ACTIVITY	68.3	2.02	43	17	0.4
GO_HORMONE_RECEPTOR_BINDING	23.8	2.02	168	73	0.43
GO_REGULATION_OF_MITOCHONDRIAL_OUTER_MEMBRANE_PERMEABILIZATION_INVOLVED_IN_APOPTOTIC_SIGNALING_PATHWAY	17.7	2.02	43	23	0.53
GO_DNA_HELICASE_COMPLEX	50.8	2.03	14	9	0.64
GO_VIRAL_GENOME_REPLICATION	28.4	2.03	21	13	0.62
GO_REGULATION_OF_SPINDLE_ASSEMBLY	8.3	2.03	15	11	0.73
TAAYNRNNTCC_UNKNOWN	3.8	2.03	172	44	0.26
GO_REGULATION_OF_TELOMERE_MAINTENANCE_VIA_TELOMERE_LENGTHENING	108.6	2.04	50	26	0.52
BIOCARTA_EIF2_PATHWAY	19.9	2.04	11	7	0.64
GO_REGULATION_OF_CHROMATIN_SILENCING	70.9	2.05	21	9	0.43
GO_MICROTUBULE	70.7	2.05	405	173	0.43
GO_POSITIVE_REGULATION_OF_PROTEIN_LOCALIZATION_TO_NUCLEUS	61.0	2.05	129	53	0.41
GO_NEGATIVE_REGULATION_OF_TELOMERE_MAINTENANCE_VIA_TELOMERE_LENGTHENING	59.2	2.05	17	12	0.71
Targets of E2F_Q6_01	44.6	2.05	240	111	0.46
PROTEIN_COMPLEX_DISASSEMBLY	33.0	2.05	14	7	0.5
GO_PEROXISOME_PROLIFERATOR_ACTIVATED_RECEPTOR_BINDING	23.0	2.05	15	4	0.27
GO_FEMALE_MEIOTIC_DIVISION	19.4	2.05	26	10	0.38
GO_POSITIVE_REGULATION_OF_MRNA_PROCESSING	7.8	2.05	32	20	0.62
GO_MICROTUBULE_CYTOSKELETON_ORGANIZATION	7.8	2.05	348	134	0.39
Targets of AP4_Q6_01	21.6	2.06	255	71	0.28
REACTOME_TRANSPORT_OF_MATURE_MRNA_DERIVED_FROM_AN_INTRONLESS_TRANSCRIPT	36.8	2.07	33	26	0.79
AUXILIARY_TRANSPORT_PROTEIN_ACTIVITY	9.0	2.07	26	6	0.23
GO_POSITIVE_REGULATION_OF_TELOMERE_MAINTENANCE_VIA_TELOMERE_LENGTHENING	97.0	2.08	33	14	0.42
GO_NEGATIVE_REGULATION_OF_CHROMOSOME_ORGANIZATION	77.3	2.08	96	49	0.51
RNA_DEPENDENT_ATPASE_ACTIVITY	48.5	2.08	18	14	0.78
GO_MIRNA_BINDING	31.2	2.08	16	5	0.31
GO_G1_DNA_DAMAGE_CHECKPOINT	31.2	2.08	73	44	0.6
GO_TELOMERE_ORGANIZATION	47.0	2.09	104	49	0.47
DNA_INTEGRITY_CHECKPOINT	25.9	2.09	24	11	0.46
GO_CYTOPLASMIC_MICROTUBULE	33.9	2.1	57	27	0.47
GO_UBIQUITIN_LIKE_PROTEIN_LIGASE_BINDING	27.1	2.1	264	154	0.58
GO_POSITIVE_REGULATION_OF_ERYTHROCYTE_DIFFERENTIATION	12.0	2.1	23	7	0.3
GO_REGULATION_OF_HISTONE_H3_K9_ACETYLATION	28.0	2.11	14	4	0.29
GO_DNA_BINDING_BENDING	19.1	2.11	20	6	0.3
GO_MACROPHAGE_ACTIVATION_INVOLVED_IN_IMMUNE_RESPONSE	10.2	2.11	11	3	0.27
NEGATIVE_REGULATION_OF_IMMUNE_SYSTEM_PROCESS	8.8	2.11	14	3	0.21
GO_DNA_INTEGRITY_CHECKPOINT	37.4	2.12	146	72	0.49
GO_REGULATION_OF_SPINDLE_ORGANIZATION	15.4	2.12	20	14	0.7
GO_CHROMATIN_BINDING	78.1	2.13	435	148	0.34
GO_VIRAL_LATENCY	68.8	2.13	11	9	0.82
DNA_HELICASE_ACTIVITY	52.6	2.13	25	15	0.6
GO_NUCLEAR_CHROMOSOME_TELOMERIC_REGION	62.3	2.14	132	66	0.5
GO_POSITIVE_REGULATION_OF_GLUCOSE_IMPORT_IN_RESPONSE_TO_INSULIN_STIMULUS	13.8	2.14	12	4	0.33
GO_CELL_CELL_RECOGNITION	92.1	2.15	60	13	0.22
GO_RIBONUCLEOPROTEIN_GRANULE	90.5	2.15	148	87	0.59
CONTRACTILE_FIBER_PART	82.7	2.15	23	8	0.35
GO_MITOTIC_NUCLEAR_DIVISION	44.5	2.15	361	187	0.52
GO_CELL_CYCLE_PHASE_TRANSITION	35.9	2.16	255	127	0.5
Targets of OCT1_02	29.3	2.16	214	50	0.23
GO_BINDING_OF_SPERM_TO_ZONA_PELLUCIDA	99.0	2.17	33	9	0.27
GO_POSITIVE_REGULATION_OF_DNA_BIOSYNTHETIC_PROCESS	81.2	2.17	59	23	0.39
TRANSLATION_FACTOR_ACTIVITY_NUCLEIC_ACID_BINDING	69.0	2.17	39	29	0.74
REACTOME_CELL_DEATH_SIGNALLING_VIA_NRAGE_NRIF_AND_NADE	32.1	2.17	60	22	0.37
GO_EMBRYONIC_HEMOPOIESIS	17.2	2.17	20	6	0.3
GO_POSITIVE_REGULATION_OF_TELOMERE_MAINTENANCE	98.3	2.18	47	24	0.51
GO_ADENYL_NUCLEOTIDE_BINDING	83.7	2.19	1514	548	0.36
GO_DAMAGED_DNA_BINDING	66.2	2.19	63	38	0.6
GO_SPINDLE_POLE	31.4	2.19	126	54	0.43
GO_CENTROSOME_CYCLE	7.5	2.19	45	18	0.4
CONTRACTILE_FIBER	88.8	2.2	25	8	0.32

AEROBIC_RESPIRATION	53.2	2.2	15	13	0.87
RESPONSE_TO_RADIATION	39.0	2.2	60	16	0.27
PID_IL3_PATHWAY	9.7	2.2	27	10	0.37
GO_TRANSCRIPTION_EXPORT_COMPLEX	52.6	2.21	13	12	0.92
GO_POSITIVE_REGULATION_OF_DNA_TEMPLATED_TRANSCRIPTION_ELONGATION	47.8	2.21	23	16	0.7
PID_INSULIN_GLUCOSE_PATHWAY	18.1	2.22	26	11	0.42
GO_POSITIVE_REGULATION_OF_MRNA_METABOLIC_PROCESS	17.2	2.22	45	27	0.6
ZF-MIZ	11.8	2.22	7	4	0.57
GO_MRNA_3_UTR_BINDING	52.2	2.23	48	26	0.54
REACTOME_PURINE_METABOLISM	48.0	2.23	33	22	0.67
DNA_REPLICATION_INITIATION	9.2	2.23	16	7	0.44
GO_REGULATION_OF_CHROMATIN_ORGANIZATION	70.9	2.24	152	61	0.4
GO_NEGATIVE_REGULATION_OF_GENE_SILENCING	42.6	2.24	19	5	0.26
BIOCARTA_G1_PATHWAY	41.8	2.24	28	10	0.36
GO_CELL_CYCLE_CHECKPOINT	54.9	2.25	194	93	0.48
GO_PROTEIN_N_TERMINUS_BINDING	25.9	2.25	103	64	0.62
GO_ENDODEOXYRIBONUCLEASE_ACTIVITY	48.6	2.26	51	21	0.41
GO_ASPARTATE_METABOLIC_PROCESS	31.4	2.26	11	5	0.45
GO_POSITIVE_REGULATION_OF_CELLULAR_RESPONSE_TO_INSULIN_STIMULUS	17.0	2.26	23	6	0.26
GO_RESPONSE_TO_ACIDIC_PH	16.8	2.26	21	5	0.24
GO_ENDOLYSOSOME_MEMBRANE	16.3	2.27	11	5	0.45
GO_MYOFILAMENT	82.7	2.28	24	6	0.25
GO_REGULATION_OF_SIGNAL_TRANSDUCTION_BY_P53_CLASS_MEDIATOR	54.0	2.28	162	73	0.45
MACROMOLECULAR_COMPLEX_DISASSEMBLY	38.2	2.28	15	8	0.53
PID_P73PATHWAY	18.0	2.28	79	41	0.52
GO_RIBONUCLEOTIDE_BINDING	81.2	2.29	1860	694	0.37
GO_REGULATION_OF_PROTEIN_ACETYLATION	48.6	2.29	64	27	0.42
GO_NEGATIVE_REGULATION_OF_CELL_CYCLE_PROCESS	44.5	2.29	214	104	0.49
GO_MEIOTIC_CELL_CYCLE	22.0	2.3	186	58	0.31
GO_ALDEHYDE_CATABOLIC_PROCESS	17.8	2.3	13	9	0.69
M_PHASE_OF_MITOTIC_CELL_CYCLE	46.5	2.31	85	47	0.55
PID_CMYB_PATHWAY	41.7	2.31	84	36	0.43
REACTOME_DOUBLE_STRAND_BREAK_REPAIR	40.3	2.31	24	9	0.38
REGULATION_OF_MITOSIS	40.4	2.32	41	20	0.49
GO_CELL_CYCLE_G2_M_PHASE_TRANSITION	28.4	2.32	138	77	0.56
TCCCRNNRTGC_UNKNOWN	23.5	2.32	213	111	0.52
GO_NUCLEAR_CHROMOSOME	70.8	2.33	523	222	0.42
GO_CHROMATIN_DNA_BINDING	69.1	2.33	80	35	0.44
Targets of COUP_DR1_Q6	66.3	2.33	247	94	0.38
ATP_DEPENDENT_DNA_HELICASE_ACTIVITY	62.6	2.33	11	8	0.73
GO_MITOTIC_DNA_INTEGRITY_CHECKPOINT	39.4	2.33	100	56	0.56
GO_PROTEIN_C_TERMINUS_BINDING	25.2	2.33	186	81	0.44
GO_P53_BINDING	85.6	2.34	67	23	0.34
M_PHASE	45.0	2.35	114	55	0.48
GO_CORONARY_VASCULATURE_DEVELOPMENT	30.3	2.35	37	9	0.24
GO_NEGATIVE_REGULATION_OF_DNA_DEPENDENT_DNA_REPLICATION	9.5	2.35	16	5	0.31
Targets of E2F1_Q4_01	60.4	2.36	228	90	0.39
MICROTUBULE_CYTOSKELETON_ORGANIZATION_AND_BIOGENESIS	50.9	2.36	35	18	0.51
GO_NEGATIVE_REGULATION_OF_VIRAL_RELEASE_FROM_HOST_CELL	21.8	2.37	16	9	0.56
REACTOME_APOPTOSIS_INDUCED_DNA_FRAGMENTATION	13.7	2.37	13	8	0.62
GO_CHROMOSOME	75.3	2.38	880	390	0.44
DNA_DEPENDENT_ATPASE_ACTIVITY	64.9	2.38	22	13	0.59
GO_NUCLEOSOMAL_DNA_BINDING	79.3	2.39	30	22	0.73
GO_DNA_DOUBLE_STRAND_BREAK_PROCESSING	21.7	2.39	20	9	0.45
GO_MICROTUBULE_ORGANIZING_CENTER_ORGANIZATION	15.4	2.39	84	40	0.48
Targets of E2F_Q4_01	69.2	2.4	237	100	0.42
GO_ORGANELLE_ASSEMBLY	55.9	2.4	495	214	0.43
GO_REGULATION_OF_PROTEIN_INSERTION_INTO_MITOCHONDRIAL_MEMBRANE_INVOLVED_IN_APOPTOTIC_SIGNALING_PATHWAY	13.8	2.4	29	15	0.52
PID_PI3KCI_AKT_PATHWAY	5.4	2.41	35	16	0.46
REACTOME_DESTABILIZATION_OF_MRNA_BY_BRF1	57.4	2.42	17	13	0.76
GO_POSITIVE_REGULATION_OF_CHROMATIN_MODIFICATION	52.4	2.42	85	35	0.41
HISTONE_METHYLTRANSFERASE_ACTIVITY	26.7	2.42	11	4	0.36
REACTOME_PLATELET_SENSITIZATION_BY_LDL	22.8	2.42	16	6	0.38
PROTEIN_AMINO_ACID_ADP_RIBOSYLATION	20.9	2.42	10	3	0.3
PROTEIN_PHOSPHATASE_TYPE_2A_REGULATOR_ACTIVITY	37.6	2.43	14	7	0.5
CONDENSED_CHROMOSOME	47.3	2.44	34	16	0.47
GTTRYCATRR_UNKNOWN	16.7	2.44	172	45	0.26
MITOCHONDRIAL_TRANSPORT	44.9	2.45	21	19	0.9

REACTOME_INTEGRATION_OF_PROVIRUS	80.2	2.46	16	6	0.38
GO_POSITIVE_REGULATION_OF_MRNA_SPLICING_VIA_SPLICEOSOME	46.8	2.46	14	6	0.43
GO_NEGATIVE_REGULATION_OF_MITOTIC_CELL_CYCLE	36.3	2.46	199	100	0.5
ST_FAS_SIGNALING_PATHWAY	29.5	2.46	65	31	0.48
GO_POSITIVE_REGULATION_OF_DNA_REPLICATION	68.6	2.47	86	31	0.36
GO_NEGATIVE_REGULATION_OF_DNA_REPLICATION	64.4	2.47	55	25	0.45
RRCCGTTA_UNKNOWN	36.8	2.47	87	52	0.6
GO_CHROMATIN	66.6	2.48	441	168	0.38
GO_RESPONSE_TO_FUNGICIDE	17.5	2.48	11	4	0.36
GO_GLOBAL_GENOME_NUCLEOTIDE_EXCISION_REPAIR	16.2	2.49	32	25	0.78
GO_DNA_CATABOLIC_PROCESS	16.4	2.5	27	13	0.48
GO_ATP_DEPENDENT_DNA_HELICASE_ACTIVITY	54.8	2.51	34	19	0.56
MRNA_BINDING	91.0	2.52	23	17	0.74
PID_AURORA_B_PATHWAY	31.5	2.52	39	19	0.49
CELL_CYCLE_PHASE	53.0	2.53	170	78	0.46
GO_AU_RICH_ELEMENT_BINDING	29.4	2.54	23	12	0.52
GO_REGULATION_OF_MICROTUBULE_POLYMERIZATION_OR_DEPOLYMERIZATION	19.1	2.54	178	88	0.49
GO_SUMO_BINDING	13.8	2.54	14	5	0.36
Targets of CEBPGAMMA_Q6	46.5	2.55	257	78	0.3
HMG	13.1	2.55	51	17	0.33
GO_REGULATION_OF_PROTEIN_PHOSPHATASE_TYPE_2A_ACTIVITY	33.5	2.57	24	11	0.46
KEGG_BETA_ALANINE_METABOLISM	64.3	2.58	22	11	0.5
GO_RNA_POLYMERASE_II_DISTAL_ENHANCER_SEQUENCE_SPECIFIC_DNA_BINDING	55.6	2.59	65	28	0.43
GO_PEPTIDYL_AMINO_ACID_MODIFICATION	43.8	2.59	841	340	0.4
GO_NEGATIVE_REGULATION_OF_TELOMERASE_ACTIVITY	29.1	2.59	15	7	0.47
Targets of AP2REP_01	27.2	2.61	178	57	0.32
GO_MITOTIC_SPINDLE_ORGANIZATION	21.8	2.61	69	32	0.46
KEGG_GLYOXYLATE_AND_DICARBOXYLATE_METABOLISM	60.4	2.62	16	10	0.62
GO_MITOTIC_CELL_CYCLE_CHECKPOINT	53.4	2.62	139	75	0.54
GO_REGULATION_OF_CELL_CYCLE_ARREST	50.4	2.62	108	52	0.48
GO_REGULATION_OF_DNA_TEMPLATED_TRANSCRIPTION_ELONGATION	46.4	2.62	44	25	0.57
GO_RESPONSE_TO_AMMONIUM_ION	32.2	2.62	51	11	0.22
GO_REGULATION_OF_THYMOCYTE_APOPTOTIC_PROCESS	49.2	2.63	12	4	0.33
GO_POSITIVE_REGULATION_OF_MITOCHONDRIAL_OUTER_MEMBRANE_PERMEABILIZATION_INVOLVED_IN_APOPTOTIC_SIGNALING_PATHWAY	19.5	2.63	36	19	0.53
GO_NEGATIVE_REGULATION_OF_TELOMERE_MAINTENANCE	62.1	2.64	26	17	0.65
GO_CHROMOSOME_TELOMERIC_REGION	64.3	2.65	162	79	0.49
GO_REGULATION_OF_GENE_SILENCING	48.6	2.65	52	16	0.31
PID_ATM_PATHWAY	33.3	2.66	34	12	0.35
REACTOME_E2F_ENABLED_INHIBITION_OF_PRE_REPLICATION_COMPLEX_FORMATION	17.8	2.66	10	6	0.6
GO_REGULATION_OF_EXECUTION_PHASE_OF_APOPTOSIS	88.6	2.67	24	11	0.46
MICROTUBULE	51.6	2.67	32	22	0.69
BIOCARTA_ATRBRCA_PATHWAY	37.5	2.67	21	8	0.38
GO_NEGATIVE_REGULATION_OF_RESPONSE_TO_BIOTIC_STIMULUS	20.9	2.68	30	14	0.47
GO_POSITIVE_REGULATION_OF_PROTEIN_IMPORT_INTO_NUCLEUS_TRANSLOCATION	7.8	2.69	13	5	0.38
GO_NEGATIVE_REGULATION_OF_EPITHELIAL_CELL_MIGRATION	6.2	2.7	53	21	0.4
Targets of E2F1_Q6_01	71.5	2.71	238	98	0.41
GO_ORGANIC_ACID_BINDING	25.8	2.71	209	68	0.33
GO_AMINO_ACID_BINDING	78.2	2.73	108	36	0.33
MITOTIC_SPINDLE_ORGANIZATION_AND_BIOGENESIS	41.3	2.73	10	5	0.5
CHROMOSOMEPERICENTRIC_REGION	29.5	2.74	31	14	0.45
GO_REGULATION_OF_DNA_REPLICATION	86.8	2.75	161	66	0.41
YAATNRNNNYNATT_UNKNOWN	70.5	2.75	104	27	0.26
GO_LYMPHOID_PROGENITOR_CELL_DIFFERENTIATION	77.6	2.78	11	3	0.27
Targets of E2F_Q3_01	60.7	2.79	235	89	0.38
PID_P38_MK2_PATHWAY	31.2	2.82	21	12	0.57
REACTOME_RECRUITMENT_OF_NUMA_TO_MITOTIC_CENTROSOMES	26.6	2.82	10	7	0.7
DNA_RECOMBINATION	70.6	2.85	47	18	0.38
GO_GLYOXYLATE_METABOLIC_PROCESS	55.4	2.86	28	14	0.5
MITOTIC_CELL_CYCLE_CHECKPOINT	22.0	2.86	21	10	0.48
Targets of EFC_Q6	17.6	2.86	268	84	0.31
Targets of E2F_Q3	45.1	2.87	227	91	0.4
REACTOME_E2F_MEDIATED_REGULATION_OF_DNA_REPLICATION	40.9	2.87	35	13	0.37
Targets of ER_Q6_02	15.5	2.87	252	79	0.31
GO_POSITIVE_REGULATION_OF_PROTEIN_ACETYLATION	43.8	2.88	36	12	0.33
CELL_CYCLE_PROCESS	52.7	2.89	193	87	0.45
Targets of E2F1_Q6	63.7	2.9	232	101	0.44
GO_MODULATION_BY_SYMBIONT_OF_HOST_CELLULAR_PROCESS	8.5	2.92	28	11	0.39
REACTOME_EARLY_PHASE_OF_HIV_LIFE_CYCLE	76.1	2.94	21	10	0.48
SPINDLE_POLE	22.6	2.94	18	9	0.5

GO_POSITIVE_REGULATION_OF_PROTEIN_EXPORT_FROM_NUCLEUS	44.1	2.95	19	7	0.37
GO_GTPASE_ACTIVATING_PROTEIN_BINDING	21.6	2.95	14	7	0.5
TRANSCRIPTION_ELONGATION_REGULATOR_ACTIVITY	23.1	2.99	12	7	0.58
GO_POSITIVE_REGULATION_OF_DNA_METABOLIC_PROCESS	102.4	3.01	185	76	0.41
KEGG_BUTANOATE_METABOLISM	29.2	3.01	34	17	0.5
GO_NUCLEAR_CHROMATIN	52.3	3.03	291	111	0.38
GO_REGULATION_OF_MICROTUBULE_BASED_PROCESS	24.0	3.04	243	106	0.44
GO_FOLIC_ACID_BINDING	53.4	3.06	14	3	0.21
Targets of E2F1DP1RB_01	65.7	3.1	231	96	0.42
Targets of E2F4DP1_01	60.9	3.1	239	100	0.42
BIOCARTA_RB_PATHWAY	33.7	3.1	13	7	0.54
GO_POSITIVE_REGULATION_OF_PROTEIN_IMPORT	26.6	3.11	104	35	0.34
SGCGSSAAA_Targets of E2F1DP2_01	57.9	3.12	168	77	0.46
SPINDLE_ORGANIZATION_AND_BIOGENESIS	51.5	3.13	11	6	0.55
Targets of E2F1DP1_01	71.2	3.17	235	97	0.41
GO_POSITIVE_REGULATION_OF_NUCLEOCYTOPLASMIC_TRANSPORT	29.3	3.19	121	40	0.33
REACTOME_TGF_BETA_RECEPTOR_SIGNALING_IN_EMT_EPITHELIAL_TO_MESENCHYMAL_TRANSITION	66.6	3.2	16	6	0.38
BIOCARTA_TEL_PATHWAY	35.5	3.21	18	10	0.56
Targets of E2F1DP2_01	71.9	3.22	235	97	0.41
DNA_DAMAGE_RESPONSESIGNAL_TRANSDUCTION	42.9	3.24	35	13	0.37
Targets of E2F_02	70.2	3.28	235	98	0.42
BIOCARTA_CHREBP2_PATHWAY	19.8	3.28	42	17	0.4
PID_BARD1_PATHWAY	57.0	3.32	29	15	0.52
GO_NEGATIVE_REGULATION_OF_ORGANELLE_ORGANIZATION	54.3	3.34	387	184	0.48
REACTOME_MITOTIC_G2_G2_M_PHASES	45.2	3.36	81	47	0.58
Targets of E2F4DP2_01	72.2	3.4	235	97	0.41
DNA_DAMAGE_RESPONSESIGNAL_TRANSDUCTION_BY_P53_CLASS_MEDIATOR	39.3	3.44	13	7	0.54
REACTOME_TGF_BETA_RECEPTOR_SIGNALING_ACTIVATES_SMADS	40.8	3.46	26	12	0.46
Targets of E2F1_Q3	80.0	3.47	244	97	0.4
NEGATIVE_REGULATION_OF_ANGIOGENESIS	108.0	3.51	13	3	0.23
Targets of CMYB_01	41.1	3.52	249	106	0.43
GO_RNA_CAP_BINDING_COMPLEX	25.1	3.54	14	6	0.43
PROTEIN_N_TERMINUS_BINDING	65.4	3.56	38	22	0.58
GO_PRONUCLEUS	49.7	3.57	15	9	0.6
PID_DNA_PK_PATHWAY	69.4	3.63	16	9	0.56
GO_RESPONSE_TO_COBALT_ION	77.2	3.64	13	7	0.54
GGAMTNNNNNTCCY_UNKNOWN	108.7	3.67	117	41	0.35
Targets of SMAD3_Q6	25.7	3.74	239	56	0.23
Targets of E2F_Q4	70.6	3.77	234	99	0.42
REACTOME_LOSS_OF_NLP_FROM_MITOTIC_CENTROSOMES	64.6	3.84	59	34	0.58
REACTOME_RECRUITMENT_OF_MITOTIC_CENTROSOME_PROTEINS_AND_COMPLEXES	67.7	3.9	66	39	0.59
Targets of E2F_Q6	72.9	3.99	232	97	0.42
Targets of MYCMAX_B (Myc and MAX targets)	138.8	4.02	268	108	0.4
GO_NEGATIVE_REGULATION_OF_ENDOTHELIAL_CELL_MIGRATION	13.3	4.42	39	16	0.41
GO_RESPONSE_TO_ARSENIC_CONTAINING_SUBSTANCE	68.6	4.46	29	18	0.62
GO_REGULATION_OF_CIRCADIAN_RHYTHM	93.0	5.08	103	29	0.28
GO_ENDODEOXYRIBONUCLEASE_ACTIVITY_PRODUCING_5_PHOSPHOMONOESTERS	26.7	5.36	12	4	0.33

[0555] **Table 29.** ICI predictors: Forty-seven signatures used as alternative ICI response predictors; related to **Figure 66**.

Description	
Reference	**Name**
Tirosh et al Science 2016	AXL (Tirosh)
	Melanoma cell cycle (Tirosh)
	G1 S (Tirosh)
	G2 M (Tirosh)
	Melanoma cells (Tirosh)
	MITF (Tirosh)
TME: Current study	TME B cell

	TME CAF
	TME Endo
	TME Macrophage
	TME Mal
	TME NK
	TME T CD4
	TME T CD8
	TME T cell
	TME stroma
	TME immune
	TME T CD4 exhausted
	TME T CD4 naive
	TME T CD4 Treg
	TME T CD8 cytotoxic
	TME T CD8 exhausted
	TME T CD8 naive
https://www.fluidigm.com/applications/advanta-immuno-oncology-gene-expression-assay	Fluidgm Panel A
	Fluidgm Panel B
Manguso et al. Cell 2017	in-vivo screen GVAXPD1 vs TCRaKO depleted
	in-vivo screen GVAX vs TCRaKO depleted
	in-vivo screen TCRaKO vs invitro depleted
	in-vivo screen GVAXPD1 vs TCRaKO enriched
	in-vivo screen GVAX vs TCRaKO enriched
	in-vivo screen TCRaKO vs invitro enriched
Patel et al. Nature 2017	co-culture screen hits10
	co-culture screen hits50
Ayers et al. JCI 2017	Ayers IFNg sig
	Ayers immune sig
Riaz et al. Cell 2017	Nivolumab (molecular) resistant melanoma up
	Nivolumab (molecular) resistant melanoma down
	Nivolumab resistant melanoma up
	Nivolumab resistant melanoma down
	On Nivolumab up
	On Nivolumab down
	Responders on Nivolumab up
	Responders on Nivolumab down
Hugo et al. Cell 2016	Anti-PD-1 resistant melanoma .up
	Anti-PD-1 resistant melanoma .down
Hugo et al. Cell 2015	MAPKi resistant melanoma up
	MAPKi resistant melanoma down

Signatures								
TME B cell	**TME CAF**	**TME Endo**	**TME Macrophage**	**TME Mal**	**TME NK**	**TME T CD4**	**TME T CD8**	**TME T cell**
ADAM19	*ABCA6*	*A2M*	*ABCA1*	*AASDHPPT*	*ALOX5AP*	*AIM1*	*ADORA2A*	*ARHGEF1*
ADAM28	*ABCA8*	*ABCD4*	*ABI1*	*AATF*	*APMAP*	*AQP3*	*ASB2*	*ASB2*
AFF3	*ABI3BP*	*ADAM15*	*ACAA1*	*ACN9*	*CALM1*	*BCL11B*	*ASXL2*	*ATHL1*
ATF7IP	*ACTA2*	*ADAMTS9*	*ACER3*	*ACOT7*	*CD160*	*CAMK4*	*CBLB*	*BCL11B*
BACH2	*ACVR1*	*ADCY4*	*ACP2*	*ACSL3*	*CD244*	*CCR4*	*CCDC141*	*C16orf54*
BANK1	*ADAM12*	*ADM5*	*ACP5*	*ADIPOR1*	*CD247*	*CCR8*	*CCDC64*	*CASP8*
BCL11A	*ADAMTS12*	*AFAP1L1*	*ACSL1*	*ADSL*	*CLIC3*	*CD28*	*CD27*	*CCDC64*
BLK	*ADAMTS2*	*APLNR*	*ADAMDEC1*	*AHCY*	*CTSW*	*CD4*	*CD3E*	*CCND2*
BLNK	*ANTXR1*	*AQP1*	*ADAP2*	*AIF1L*	*FCRL6*	*CD40LG*	*CD84*	*CD2*
BTLA	*AOX1*	*ARHGAP29*	*ADORA3*	*AK2*	*FGFBP*	*CD5*	*CD8A*	*CD247*

					2			
CCR6	ARMCX2	ARHGAP31	ADPGK	ALDOA	GNLY	CD6	CD8B	CD27
CD19	ASPN	ARHGEF15	AIF1	ALX1	GZMB	DGKA	CLEC2D	CD28
CD1C	BACE1	ASAP1	AKR1A1	AMZ2	GZMM	DUSP16	CRTAM	CD3D
CD22	BAG2	BCAM	ALDH2	ANAPC11	HOPX	EML4	CXCL13	CD3E
CD24	BGN	BCL6B	ALDH3B1	ANKRD54	ID2	F5	DNAJB1	CD3G
CD37	C1R	BCR	AMICA1	ANP32A	IL18RAP	FAAH2	GPR171	CD5
CD52	C1S	BMPR2	AMPD3	AP1S2	IL2RB	FAM102A	GZMK	CD6
CD79A	CALD1	BMX	ANKRD22	APEH	KIR2DL3	FBLN7	IFNG	CD7
CD79B	CCDC80	CALCRL	AP1B1	APOA1BP	KIR3DL2	FLT3LG	ITGA4	CD96
CHMP7	CD248	CARD10	APOC1	APOC2	KLRB1	FOXP3	ITGAE	CDC42SE2
CIITA	CDH11	CASKIN2	AQP9	APOD	KLRC1	FYB	ITM2A	CELF2
CLEC17A	CDR1	CCL14	ARAP1	APOO	KLRD1	ICOS	JAKMIP1	CNOT6L
CNR2	CERCAM	CD200	ARHGAP18	ARPC1A	KLRF1	IL6R	KLHL28	CORO1A
COL19A1	CILP	CD34	ARHGAP27	ATIC	MATK	IL7R	LAG3	CST7
COL4A3	CKAP4	CD93	ARHGEF10L	ATP1A1	MYBL1	ITGB2-AS1	LYST	CTLA4
CR2	CLEC11A	CDH5	ARPC1B	ATP5C1	NCAM1	ITK	MAP4K1	CXCR3
CXCR5	CLIP3	CFI	ARRB2	ATP5G1	NCR1	LAT	MCOLN2	CXCR6
CYBASC3	CNN1	CLDN15	ASAH1	ATP5G2	NCR3	LEPROTL1	MIAT	CYTIP
EEF1B2	COL11A1	CLDN5	ATF5	ATP5G3	NKG7	LOC100128420	MIR155HG	DEF6
EEF1G	COL12A1	CLEC14A	ATG3	ATP6V1C1	NMUR1	LOC285740	NELL2	DENND2D
EIF2S3	COL14A1	CLEC1A	ATG7	ATP6V1E1	PRF1	MAF	PAG1	EMB
ELK2AP	COL16A1	CNTNAP3B	ATP6AP1	ATP6V1G1	PTGDR	MAL	PCED1B	EVL
FAIM3	COL1A1	COL15A1	ATP6V0B	BAIAP2	PTPN4	PASK	PDCD1	FYB
FAM129C	COL1A2	COL4A1	ATP6V0D1	BANCR	SAMD3	PBX4	PRDM1	FYN
FAM65B	COL3A1	COL4A2	ATP6V1B2	BCAN	SH2D1B	PBXIP1	PTPN7	GATA3
FCER2	COL5A1	CRIP2	ATP6V1F	BCAS3	TXK	PIK3IP1	RAB27A	GNG2
FCRL1	COL5A2	CXorf36	BACH1	BCL2L13	XCL1	PIM2	RNF19A	GPR171
FCRL2	COL6A1	CYYR1	BCKDHA	BIRC7	XCL2	SEPT6	SIRPG	GPR174
FCRL5	COL6A2	DARC	BCL2A1	BZW2		SLAMF1	SIT1	GPRIN3
FCRLA	COL6A3	DCHS1	BID	C10orf90		SPOCK2	SNAP47	GRAP2
GGA2	COL8A1	DLL4	BLOC1S1	C11orf31		SUSD3	THEMIS	GZMA
GNB2L1	COMP	DOCK6	BLVRA	C17orf89		TBC1D4	TIGIT	GZMM
HLA-DOB	CPE	DOCK9	BLVRB	C1orf43		TCF7	TIMD4	HNRNPA1P10
HLA-DQA2	CPXM1	DYSF	C10orf54	C1orf85		TESPA1	TMEM155	ICOS
HVCN1	CPZ	ECE1	C11orf75	C1QBP		TIAM1	TNFRSF9	IL12RB1
IGJ	CRABP2	ECSCR	C15orf48	C22orf32		TMEM66	TNIP3	IL21R
IGLL1	CREB3L1	EFNA1	C19orf38	C4orf48		TNFAIP3	TOX	IL2RB
IGLL3P	CRISPLD2	EFNB2	C1orf162	CA14		TNFSF8	TTC24	IL2RG
IGLL5	CTSK	EGFL7	C1QA	CA8		TNIK	TTN	IL32
IRF8	CXCL12	ELK3	C1QB	CACYBP		TPT1	ZBED2	INPP4B
KBTBD8	CXCL14	ELTD1	C1QC	CAPN3				IPCEF1
KIAA0125	CYBRD1	EMCN	C2	CBX3				ITGAL
KIAA0226L	CYGB	ENG	C3AR1	CCND1				ITK
LOC283663	CYP1B1	EPAS1	C5AR1	CCT2				JAK3

LRMP	DCN	EPB41L4A	C9orf72	CCT3				KCNA3
MS4A1	DDAH1	EPHB4	CAPG	CCT4				LAT
NAPSB	DDR2	ERG	CAPZA2	CCT6A				LCK
NCF1C	DEPTOR	ESAM	CARD9	CCT8				LIME1
NCOA3	DKK3	EXOC3L1	CASP1	CDH19				LOC100130231
P2RX5	DPT	F11R	CAT	CDH3				MBOAT1
PAX5	EBF2	FABP4	CCDC88A	CDK2				MIAT
PLEKHF2	ECM2	FAM107A	CCR1	CDK4				NLRC5
PNOC	EDNRA	FAM65A	CCR2	CEP170				PAG1
POLD4	EFEMP2	FAT4	CCRL2	CHCHD6				PARP8
POU2AF1	EGFLAM	FGD5	CD14	CHD1L				PCED1B
POU2F2	EGFR	FKBP1A	CD163	CLCN7				PCED1B-AS1
PRKCB	EMILIN1	FLI1	CD1D	CLNS1A				PDCD1
QRSL1	FAT1	FLT4	CD274	CMC2				PIP4K2A
RALGPS2	FBLN1	FZD6	CD300C	COA3				PRDM1
RHOH	FBLN2	GALNT18	CD300E	COA4				PRF1
SEL1L3	FBLN5	GATA2	CD300LB	COA6				PRKCQ
SELL	FGF7	GIPC2	CD300LF	COX5B				PTPN22
SMIM14	FIBIN	GNG11	CD302	COX6A1				PTPN7
SNX29	FMOD	GPR116	CD33	COX7A2				PTPRC
SNX29P1	FN1	GPR146	CD68	COX7A2L				PYHIN1
SP110	FNDC1	GRB10	CD80	COX7C				RASAL3
SP140	FRMD6	GUK1	CD86	COX8A				RASGRP1
SPIB	FST	HECW2	CECR1	CSAG1				RGS1
ST6GAL1	FSTL1	HERC2P2	CFD	CSAG2				RHOF
STAG3	GEM	HID1	CFP	CSAG3				RNF213
STAP1	GFPT2	HSPG2	CLEC10A	CSPG4				SCML4
STRBP	GFRA1	HYAL2	CLEC12A	CYC1				1-Sep
TCL1A	GLT8D2	ICA1	CLEC4A	CYP27A1				SH2D1A
TLR10	GPC1	ID1	CLEC4E	DAAM2				SH2D2A
TLR9	GPC4	ID3	CLEC5A	DANCR				SH3KBP1
TMEM154	GPC6	IFITM3	CLEC7A	DAP3				SIRPG
TNFRSF13B	GPR133	IGFBP7	CMKLR1	DCT				SIT1
TP53INP1	GPR176	IL33	CMTM6	DCXR				SKAP1
VPREB3	GPX8	IL3RA	CNDP2	DDIT3				SLC9A3R1
WDFY4	HSPB2	IPO11-LRRC70	CNPY3	DDT				SPATA13
ZCCHC7	HSPB6	ITGA5	CORO7	DLL3				SPN
	HSPB7	ITGA6	CPVL	DNAH14				SPOCK2
	HTRA3	ITGB4	CREG1	DNAJA4				STAT4
	IGFBP6	JAG2	CSF1R	DRG1				SYTL3
	INHBA	JAM2	CSF2RA	EDNRB				TBC1D10C
	ISLR	JUP	CSF3R	EIF3C				TC2N
	ITGA11	KANK3	CST3	EIF3D				TESPA1
	ITGB5	KDR	CSTA	EIF3E				THEMIS
	ITGBL1	KLHL3	CTSA	EIF3H				TIGIT
	KDELR2	LAMA5	CTSB	EIF3L				TMEM66
	KDELR3	LDB2	CTSC	EIF3M				TNFAIP3
	LARP6	LOC100505495	CTSD	ENO1				TOX
	LEPREL2	LRRC70	CTSH	ENO2				TRAF1
	LMO7	LUZP1	CTSL1	ENTPD6				TRAT1
	LMOD1	LYVE1	CTSS	EPB41L4A-AS1				TTC39C

	LOX	*MALL*	*CXCL10*	*ERBB3*				*TUBA4A*
	LOXL1	*MANSC1*	*CXCL16*	*ESRP1*				*UBASH3A*
	LPAR1	*MECOM*	*CXCL9*	*ETV4*				*WIPF1*
	LTBP2	*MEOX1*	*CXCR2P1*	*ETV5*				*ZAP70*
	LUM	*MKL2*	*CYB5R4*	*EXOSC4*				*ZC3HAV1*
	LURAP1L	*MMRN1*	*CYBA*	*FAH*				
	MAP1A	*MMRN2*	*CYBB*	*FAHD2B*				
	MEG3	*MPZL2*	*CYP2S1*	*FAM103A1*				
	MFAP4	*MTUS1*	*DAPK1*	*FAM162A*				
	MGST1	*MYCT1*	*DBNL*	*FAM178B*				
	MIR100HG	*MYO15B*	*DENND1A*	*FARP2*				
	MMP2	*NOS3*	*DHRS9*	*FASN*				
	MOXD1	*NOSTRIN*	*DMXL2*	*FBXO32*				
	MRC2	*NOTCH4*	*DNAJC5B*	*FBXO7*				
	MRGPRF	*NPDC1*	*DOK1*	*FDFT1*				
	MSC	*NPR1*	*DOK3*	*FKBP4*				
	MT1M	*NR5A2*	*DPYD*	*FMN1*				
	MXRA5	*PALD1*	*EBI3*	*FXYD3*				
	MXRA8	*PALMD*	*EMR2*	*GALE*				
	MYL9	*PCDH1*	*EPSTI1*	*GAPDH*				
	NEXN	*PCDH12*	*ETV6*	*GAPDHS*				
	NID2	*PCDH17*	*EVI2A*	*GAS2L3*				
	NOTCH3	*PDE2A*	*F13A1*	*GAS5*				
	NTM	*PDLIM1*	*FAM105A*	*GAS7*				
	NTRK2	*PECAM1*	*FAM157B*	*GCSH*				
	NUPR1	*PGM5*	*FAM26F*	*GDF15*				
	OGN	*PIEZO1*	*FAM49A*	*GJB1*				
	OLFML1	*PIK3R3*	*FAM96A*	*GMNN*				
	OLFML2B	*PKP4*	*FBP1*	*GMPR*				
	OLFML3	*PLEKHA7*	*FCER1G*	*GPATCH4*				
	OMD	*PLVAP*	*FCGR1A*	*GPM6B*				
	OSR2	*PLXNA2*	*FCGR1B*	*GPR137B*				
	PALLD	*PLXND1*	*FCGR1C*	*GPR143*				
	PAMR1	*PODXL*	*FCGR2A*	*GPS1*				
	PAPSS2	*PPM1F*	*FCGR2C*	*GSTP1*				
	PCDH18	*PPP1R13B*	*FCGR3B*	*GTF2F2*				
	PCOLCE	*PRCP*	*FCGRT*	*GYG2*				
	PCOLCE2	*PREX2*	*FCN1*	*H2AFZ*				
	PDGFRA	*PTPRB*	*FERMT3*	*HAX1*				
	PDGFRB	*PVRL2*	*FES*	*HDDC2*				
	PDGFRL	*PXN*	*FGL2*	*HIST1H2AC*				
	PDLIM2	*RALGAPA2*	*FKBP15*	*HIST1H2BD*				
	PLA2G2A	*RAMP2*	*FLVCR2*	*HIST3H2A*				
	PLAC9	*RAMP3*	*FOLR2*	*HMG20B*				
	PLOD2	*RAPGEF3*	*FPR1*	*HMGA1*				
	PODN	*RAPGEF4*	*FPR2*	*HPS4*				
	POSTN	*RASIP1*	*FPR3*	*HPS5*				
	PPIB	*RBP7*	*FTH1*	*HSBP1*				
	PRR16	*RGL2*	*FTL*	*HSP90AA1*				
	PRR24	*RHOJ*	*FUCA1*	*HSP90AB1*				
	PRRX1	*ROBO4*	*FUOM*	*HSPA4*				
	PRRX2	*S1PR1*	*GAA*	*HSPA9*				
	PTN	*SCARF1*	*GABARAP*	*HSPD1*				
	RARRES2	*SDPR*	*GALC*	*HSPE1*				
	RCN3	*SELE*	*GATM*	*HSPH1*				
	ROR2	*SELP*	*GBP1*	*IGSF11*				

	SCUBE3	SH3BGRL2	GCA	IGSF3				
	SDC1	SHROOM4	GGTA1P	IGSF8				
	SDC2	SLC29A1	GK	ILF2				
	SEC24D	SLC9A3R2	GLA	IMMP2L				
	SEMA5A	SLCO2A1	GLB1	INPP5F				
	SERPINF1	SMAD1	GLRX	IRF4				
	SFRP2	SNCG	GLUL	ISYNA1				
	SFRP4	SOCS2	GM2A	KCNJ13				
	SH2D4A	SOX18	GNA13	LAGE3				
	SH3D19	SPNS2	GNA15	LDHB				
	SH3PXD2A	STOM	GPBAR1	LHFPL3-AS1				
	SLIT2	SULF2	GPR34	LINC00473				
	SLIT3	SYNPO	GPR84	LINC00518				
	SMOC2	TACR1	GPX1	LINC00673				
	SOD3	TAOK2	GRN	LOC100126784				
	SPARC	TEAD4	GSTO1	LOC100127888				
	SPOCK1	TEK	H2AFY	LOC100130370				
	SPON1	TENC1	HCAR2	LOC100133445				
	SRPX2	TFF3	HCAR3	LOC100505865				
	STEAP1	TGFBR2	HCK	LOC146481				
	SULF1	TGM2	HEIH	LOC340357				
	SUSD2	THBD	HERPUD1	LOXL4				
	SVEP1	THSD1	HIST2H2BF	LSM2				
	TAGLN	TIE1	HK2	LZTS1				
	TBX15	TLL1	HK3	MAD2L1BP				
	TCEAL7	TM4SF1	HLA-DMA	MAGEA12				
	TGFB3	TM4SF18	HLA-DMB	MAGEA2				
	THBS2	TMEM204	HLA-DPA1	MAGEA2B				
	THY1	TMEM255B	HLA-DPB1	MAGEA3				
	TIMP1	TNFAIP1	HLA-DPB2	MAGEA4				
	TMEM119	TNFRSF10B	HLA-DQA1	MAGEA6				
	TMEM45A	TSPAN12	HLA-DQB1	MAGEC1				
	TPM1	TSPAN15	HLA-DRA	MAGED2				
	TPM2	TSPAN18	HLA-DRB1	MDH1				
	TWIST1	TSPAN7	HLA-DRB5	MDH2				
	TWIST2	USHBP1	HLA-DRB6	METTL23				
	UCHL1	VWA1	HMOX1	METTL9				
	VASN	VWF	HN1	MFI2				
	VCAN	ZNF366	HPS1	MIA				
	WISP2	ZNF385D	HSPA6	MIF				
	WNT2		HSPA7	MITF				
			HSPBAP1	MKI67IP				
			IDH1	MLANA				
			IFI30	MLPH				
			IFI35	MOK				
			IFIT2	MORN2				
			IFNGR1	MRPL12				
			IFNGR2	MRPL21				
			IGFLR1	MRPL23				
			IGSF6	MRPL24				

			IL10RB	*MRPL38*				
			IL18	*MRPL40*				
			IL1B	*MRPS21*				
			IL1RN	*MRPS23*				
			IL4I1	*MRPS25*				
			IL8	*MRPS26*				
			IRF5	*MRPS6*				
			IRF7	*MSI2*				
			ITGAX	*MTHFS*				
			JAK2	*MXI1*				
			KCNMA1	*MYO10*				
			KCNMB1	*NARS2*				
			KYNU	*NAV2*				
			LAIR1	*NDUFA4*				
			LAP3	*NDUFAF3*				
			LGALS2	*NDUFB9*				
			LGALS9	*NDUFS2*				
			LGMN	*NEDD4L*				
			LILRA1	*NELFCD*				
			LILRA2	*NFYA*				
			LILRA3	*NGRN*				
			LILRA4	*NHP2*				
			LILRA5	*NME1*				
			LILRA6	*NOP58*				
			LILRB1	*NPM1*				
			LILRB2	*NSG1*				
			LILRB3	*NT5DC3*				
			LILRB4	*NUP93*				
			LILRB5	*OCA2*				
			LIPA	*PACSIN2*				
			LOC338758	*PAFAH1B3*				
			LOC729737	*PAGE5*				
			LRRC25	*PAICS*				
			LST1	*PAX3*				
			LTA4H	*PEBP1*				
			LYN	*PEG10*				
			LYZ	*PEX19*				
			M6PR	*PFDN2*				
			MAFB	*PHACTR1*				
			MAN2B1	*PHB*				
			MAPKAPK3	*PHF5A*				
			MARCO	*PHLDA1*				
			MERTK	*PIGY*				
			MFSD1	*PIR*				
			MGAT1	*PLEKHB1*				
			MIF4GD	*PLP1*				
			MIIP	*PMEL*				
			MILR1	*POLD2*				
			MKNK1	*POLR2F*				
			MNDA	*POMGNT1*				
			MOB1A	*PPIL1*				
			MPEG1	*PRAME*				
			MPP1	*PRDX6*				
			MRC1	*PSMB4*				
			MS4A4A	*PSMB7*				
			MS4A6A	*PSMD4*				
			MS4A7	*PTTG1*				
			MSR1	*PUF60*				

			MTHFD2	*PYGB*				
			MTMR14	*PYURF*				
			MX1	*QDPR*				
			MX2	*QPCT*				
			MXD1	*RAB17*				
			MYD88	*RAB38*				
			N4BP2L1	*RABGGTB*				
			NAAA	*RAD51C*				
			NADK	*RAE1*				
			NAGA	*RAN*				
			NAGK	*RAP1GAP*				
			NAIP	*RGS20*				
			NCF2	*ROPN1*				
			NCF4	*ROPN1B*				
			NCKAP1L	*RRS1*				
			NCOA4	*RSL1D1*				
			NFAM1	*RTKN*				
			NFKBID	*RUVBL2*				
			NINJ1	*S100A1*				
			NLRC4	*S100B*				
			NLRP3	*SAMM50*				
			NMI	*SCD*				
			NOD2	*SDC3*				
			NPC2	*SDCBP*				
			NPL	*SDHC*				
			NR1H3	*SEC11C*				
			OAS1	*SF3A1*				
			OAZ1	*SGCD*				
			OLR1	*SHC4*				
			OSCAR	*SKP1*				
			P2RX4	*SLC19A1*				
			P2RY12	*SLC19A2*				
			P2RY13	*SLC24A5*				
			P2RY14	*SLC25A13*				
			P2RY6	*SLC25A4*				
			PAK1	*SLC39A4*				
			PCK2	*SLC45A2*				
			PFKFB3	*SLC5A3*				
			PGD	*SLC6A15*				
			PILRA	*SLC7A5*				
			PLA2G15	*SLMO2*				
			PLA2G7	*SMS*				
			PLAUR	*SNCA*				
			PLBD1	*SNHG16*				
			PLEK	*SNHG6*				
			PLEKHO1	*SNRPC*				
			PLEKHO2	*SNRPD1*				
			PLIN2	*SNRPE*				
			PLXDC2	*SOD1*				
			PPM1M	*SORD*				
			PPT1	*SORT1*				
			PRAM1	*SOX10*				
			PRKCD	*SPCS1*				
			PSAP	*SRP9*				
			PSME2	*ST13*				
			PTAFR	*ST3GAL4*				
			PTPRE	*ST3GAL6*				
			PYCARD	*ST6GALNAC*				

				2				
			RAB20	STAM				
			RAB4B	STIP1				
			RAB8A	STK32A				
			RASGEF1B	STMN1				
			RASSF4	STOML2				
			RBM47	STRA13				
			RBPJ	STRADB				
			REEP4	STX7				
			RELT	STXBP1				
			RGS10	SUPT4H1				
			RGS18	SYNGR1				
			RGS19	TBC1D10A				
			RGS2	TBC1D16				
			RHBDF2	TBC1D7				
			RHOG	TBCA				
			RILPL2	TBRG4				
			RIPK2	TEX2				
			RNASE6	TFAP2A				
			RNASEK	TIMM50				
			RNASET2	TMED10				
			RNF13	TMEM147				
			RNF130	TMEM177				
			RNF144B	TMEM255A				
			RNF149	TMX4				
			RTN1	TOM1L1				
			S100A11	TOMM20				
			S100A8	TOMM22				
			S100A9	TOMM6				
			SAMHD1	TOMM7				
			SAT1	TOP1MT				
			SCAMP2	TRIM2				
			SCIMP	TRIM63				
			SCO2	TRMT112				
			SCPEP1	TSNAX				
			SDS	TTLL4				
			SECTM1	TUBB2A				
			SEMA4A	TUBB2B				
			SERPINA1	TUBB4A				
			SERPINB1	TYR				
			SFT2D1	TYRP1				
			SGPL1	UBA2				
			SH3BGRL	UBL3				
			SHKBP1	UCHL5				
			SIGLEC1	UQCRH				
			SIGLEC14	UTP18				
			SIGLEC5	VAT1				
			SIGLEC7	VDAC1				
			SIGLEC9	WBP11				
			SIRPA	WBP2				
			SIRPB1	WBSCR22				
			SIRPB2	WDFY1				
			SKAP2	WDR43				
			SLAMF8	XAGE1A				
			SLC11A1	XAGE1B				
			SLC15A3	XAGE1C				
			SLC16A3	XAGE1D				
			SLC1A3	XAGE1E				

			SLC25A19	*XYLB*				
			SLC29A3	*ZCCHC17*				
			SLC2A5	*ZFAS1*				
			SLC2A8	*ZFP106*				
			SLC2A9	*ZNF280B*				
			SLC31A2					
			SLC43A2					
			SLC46A3					
			SLC7A7					
			SLC9A9					
			SLCO2B1					
			SMPDL3A					
			SNX10					
			SNX6					
			SOD2					
			SPI1					
			SPINT2					
			SQRDL					
			SRC					
			STX11					
			STXBP2					
			TALDO1					
			TBXAS1					
			TFRC					
			TGFBI					
			THEMIS2					
			TIFAB					
			TLR1					
			TLR2					
			TLR4					
			TLR5					
			TLR8					
			TMEM106A					
			TMEM144					
			TMEM176A					
			TMEM176B					
			TMEM37					
			TMEM51					
			TMEM86A					
			TNFAIP2					
			TNFAIP8L2					
			TNFSF13					
			TNFSF13B					
			TPP1					
			TRAFD1					
			TREM1					
			TREM2					
			TRPM2					
			TTYH3					
			TWF2					
			TYMP					
			TYROBP					
			UBE2D1					
			UBXN11					
			UNC93B1					
			VAMP8					
			VMO1					
			VSIG4					

			WDFY2					
			ZEB2					
			ZNF267					
			ZNF385A					

Signatures							
TME stroma	**TME immune**	**TME T CD4 exhausted**	**TME T CD4 naive**	**TME T CD4 Treg**	**TME T CD8 cytotoxic**	**TME T CD8 exhausted**	**TME T CD8 naive**
A4GALT	*ACAP1*	*C9orf16*	*ABLIM1*	*ARID3B*	*APOBEC3C*	*ABCC9*	*ATM*
ADAMTS 1	*AKNA*	*CDK5R1*	*ATM*	*CARD16*	*B2M*	*AKAP5*	*ATXN7*
ADAMTS L1	*ALOX5AP*	*CTLA4*	*CAMK4*	*CCR4*	*CCL3*	*ANKLE1*	*CAMK4*
ADIRF	*ANKRD44*	*DDX5*	*CCR7*	*CCR8*	*CCL4*	*AP4B1-AS1*	*CCR7*
ANGPTL 2	*APOBEC3 G*	*HLA-J*	*EEF1A1*	*CD177*	*CCL5*	*APOBEC3A*	*EEF1A1*
APP	*ARHGAP1 5*	*ICA1*	*EEF1B2*	*DDX60*	*CSF1*	*ARHGEF26-AS1*	*FAM102A*
ARHGAP 29	*ARHGAP2 5*	*IGFLR1*	*EEF1G*	*ERI1*	*CST7*	*ASXL2*	*FKBP5*
BGN	*ARHGAP3 0*	*IL21*	*FAM65B*	*EZH2*	*FASLG*	*ATHL1*	*GPR155*
BMP1	*ARHGAP4*	*ITGB2-AS1*	*FHIT*	*FAS*	*GZMB*	*ATXN1*	*IL7R*
C1R	*ARHGAP9*	*ITM2A*	*GIMAP5*	*FOXP3*	*GZMH*	*CBLB*	*LEF1*
CCDC80	*ARHGDIB*	*KCNK5*	*IL7R*	*GATA3*	*HLA-C*	*CD3E*	*NELL2*
CFH	*ATP2A3*	*KIAA0247*	*LDHB*	*GBP5*	*IFNG*	*CD8A*	*PIK3IP1*
CLU	*BIN2*	*LIMS1*	*LDLRAP1*	*GCHFR*	*PRF1*	*CDKN1B*	*PPP1R2*
COL15A 1	*C16orf54*	*LY6G5C*	*LEF1*	*HNRNPC*		*CLEC2D*	*PRKCQ-AS1*
COL18A 1	*CCDC88B*	*MAF*	*LOC100130 231*	*HPRT1*		*CNOT6L*	*SELL*
COL4A1	*CD37*	*METTL8*	*NAP1L1*	*IL10RA*		*CTLA4*	*SORL1*
COL4A2	*CD48*	*MRP63*	*NOSIP*	*IL1R2*		*CXCL13*	*TCF7*
COL6A2	*CD52*	*NFATC1*	*PABPC1*	*IL2RA*		*DENND2D*	*TSC22D3*
COX7A1	*CD53*	*NR3C1*	*PIK3IP1*	*IL2RG*		*DFNB31*	*UBA52*
CTGF	*CD69*	*PDCD1*	*SELL*	*IL32*		*DGKH*	
CYB5R3	*CD84*	*PTPN11*	*SERINC5*	*LAIR2*		*DOCK8*	
CYR61	*CDC42SE 2*	*PTPRC*	*SF1*	*LAYN*		*DTHD1*	
DCHS1	*CELF2*	*RNF19A*	*TCF7*	*LOC541471*		*DUSP4*	
DPYSL3	*CNTRL*	*SARDH*	*TMEM66*	*LTB*		*ELF1*	
EFEMP1	*CORO1A*	*SLA*	*TPT1*	*PARK7*		*ENTPD1*	
EHD2	*CSK*	*SRGN*	*TRABD2A*	*PIM2*		*FAM122C*	
ELN	*CXCR4*	*TBC1D4*	*TSC22D3*	*PMAIP1*		*FAM3C*	
EPAS1	*CYTH4*	*THADA*	*TXNIP*	*PPP2CA*		*FAM73A*	
FAM171 A1	*CYTIP*	*TIGIT*	*UBA52*	*RASGRP1*		*FBXL18*	
FAP	*DEF6*	*TSPYL2*		*RORA*		*FCRL3*	
FAT4	*DENND1 C*	*ZNF211*		*RTKN2*		*GBP2*	
FBN1	*DOCK2*			*S100A4*		*GDPD1*	
FLRT2	*DOCK8*			*SAMD9*		*GLUD1P7*	
FSCN1	*DUSP2*			*STAM*		*HAVCR2*	
FSTL1	*EVI2B*			*SUMO2*		*HINT3*	
GJA1	*FERMT3*			*TNFRSF18*		*HNRPLL*	
GNG11	*FGD3*			*USP15*		*IFNLR1*	
HSPG2	*FNBP1*			*WDR1*		*IL10*	
HTRA1	*GBP5*			*ZBTB32*		*INPP4B*	
IFITM3	*GPR65*					*INPP5F*	

IGF2	*GPSM3*					*ITGA4*	
IGFBP4	*HCLS1*					*ITM2A*	
IGFBP7	*HMHA1*					*ITPKB*	
JAG1	*IKZF1*					*KIAA1324*	
KIAA1217	*IL10RA*					*LAG3*	
LAMB1	*IL16*					*LINC00294*	
LAMB2	*IL2RG*					*LOC100131257*	
LAMC1	*INPP5D*					*LOC100190986*	
LEPROT	*ITGA4*					*LOC100271836*	
LHFP	*ITGAL*					*LOC286186*	
LIMCH1	*ITGB2*					*LOC440354*	
LIMS2	*LAIR1*					*LOC728558*	
LMCD1	*LAPTM5*					*LYST*	
LOXL2	*LCP1*					*MAPK13*	
LPHN2	*LILRB3*					*MCL1*	
LRRC32	*LIMD2*					*MTX3*	
MAP1B	*LPXN*					*NFATC1*	
MEOX2	*LSP1*					*NXNL2*	
MGP	*LY9*					*ODF2L*	
MMP2	*MAP4K1*					*OSBPL3*	
NFIB	*MYO1G*					*PCED1B*	
NID1	*NCKAP1L*					*PCGF5*	
NNMT	*NR4A2*					*PDCD1*	
NPDC1	*PARP8*					*PDE4D*	
NR2F2	*PARVG*					*PER2*	
NT5E	*PIK3CD*					*PLEKHG2*	
NUAK1	*PIM2*					*PRICKLE2-AS3*	
PEAR1	*PLCB2*					*PTPRC*	
PHLDB2	*PLEKHA2*					*RAB27A*	
PLSCR4	*PRKCB*					*RAMP2-AS1*	
PPAP2A	*PSD4*					*RGS1*	
PPAP2B	*PSTPIP2*					*RNF19A*	
PPIC	*PTK2B*					*SCD5*	
PRKCDBP	*PTPN22*					*SF3B3*	
PROCR	*PTPN6*					*SH2D2A*	
PRSS23	*PTPN7*					*SMG1P1*	
PTRF	*PTPRC*					*STAT1*	
PXDN	*RAC2*					*STAT3*	
RAB11FIP5	*RASSF5*					*TANGO2*	
RABAC1	*RCSD1*					*TATDN3*	
RBPMS	*RGS1*					*TBXA2R*	
RUNX1T1	*RHOH*					*TIGIT*	
S100A16	*RPS6KA1*					*TMEM136*	
SERPINH1	*SAMSN1*					*TMEM212*	
SPARC	*SASH3*					*TNFRSF1B*	
SPARCL1	*SLA*					*TNFRSF9*	
STC2	*SNX20*					*TP53INP1*	
TFPI	*SP140*					*TRAF5*	
TGFB1I1	*STK17B*					*TTN*	
THBS1	*TAGAP*					*TXNDC11*	
THY1	*TBC1D10C*					*USP33*	
TMEM204	*TMC6*					*VSIG1*	

TNKS1BP1	*TMC8*					*VSTM4*	
TNXB	*TMSB4X*					*ZNF620*	
TPBG	*TRAF3IP3*					*ZNF79*	
UNC5B	*TSC22D3*						
VCL	*TSTD1*						
ZEB1	*UCP2*						
ZNF423	*VAV1*						
ZNF521	*WIPF1*						

[0556] **Table 30. (A)** Overall Expression of the resistance program across CCLE melanoma cell lines; **(B)** measurements of 40 cytokines and chemokines in the conditioned media of DMSO and abemaciclib treated cancer cells; related to **Figure 67**.

Table 30A. Overall Expression of the resistance program across CCLE melanoma cell lines

Cell line	Immune resistance Overall expression (OE)					
	Final	Up	Down	Final (refined)	Up (refined)	Down (refined)
HMCB	1.036	0.357	-0.68	2.307	0.81	-1.497
LOXIMVI	1.021	0.318	-0.703	2.083	0.654	-1.428
A375	0.983	0.352	-0.631	2.221	0.89	-1.331
GRM	0.972	0.296	-0.675	2.218	0.842	-1.376
CHL1	0.841	0.341	-0.5	1.876	0.694	-1.183
A2058	0.596	0.299	-0.297	1.219	0.37	-0.85
IGR39	0.493	-0.014	-0.507	1.1	0.25	-0.85
UACC62	0.383	0.27	-0.114	0.854	0.413	-0.441
G361	0.38	0.276	-0.104	0.81	0.385	-0.424
CJM	0.361	-0.219	-0.58	0.66	-0.047	-0.706
RPMI7951	0.354	-0.17	-0.525	0.626	-0.124	-0.749
MDAMB435S	0.346	-0.115	-0.461	0.775	0.143	-0.632
MEWO	0.316	0.09	-0.226	0.552	0.104	-0.448
COLO679	0.254	0.239	-0.015	0.646	0.335	-0.311
A101D	0.248	0.075	-0.173	0.612	0.158	-0.454
MELJUSO	0.229	0.176	-0.053	0.439	0.327	-0.112
COLO741	0.215	0.214	-0.001	0.255	0.282	0.027
HT144	0.212	0.112	-0.1	0.499	0.263	-0.237
WM793	0.16	-0.089	-0.249	0.318	-0.268	-0.587
IGR1	0.144	0.096	-0.048	0.376	0.143	-0.233
UACC257	0.142	0.335	0.193	0.124	0.522	0.398
HS294T	0.115	0.123	0.007	0.236	0.223	-0.013
HS944T	0.088	0.162	0.074	0.213	0.371	0.158
WM88	0.038	0.037	-0.001	-0.07	-0.056	0.014
HS695T	0.037	0.031	-0.006	0.412	0.137	-0.276
HS895T	0.035	-0.417	-0.451	0.32	-0.41	-0.731
IGR37	0.006	0.269	0.263	0.188	0.442	0.254
COLO849	-0.002	0.137	0.139	-0.179	0.165	0.344
SKMEL3	-0.019	0.196	0.214	-0.084	0.384	0.469
SKMEL30	-0.043	0.102	0.145	0.146	0.203	0.057
SKMEL1	-0.049	0.114	0.163	-0.035	0.313	0.348
MELHO	-0.05	0.153	0.203	-0.236	0.207	0.443
COLO783	-0.062	-0.001	0.061	-0.269	-0.134	0.136

K029AX	-0.065	0.129	0.194	-0.21	0.133	0.343
SKMEL2	-0.081	0.074	0.155	0.101	0.322	0.221
IPC298	-0.103	0.101	0.204	-0.104	0.296	0.399
WM983B	-0.112	-0.157	-0.045	-0.253	-0.286	-0.032
SKMEL5	-0.12	0.185	0.305	-0.317	0.188	0.506
HS936T	-0.144	-0.03	0.114	-0.495	-0.079	0.416
HS839T	-0.181	-0.48	-0.299	-0.39	-0.808	-0.418
HS934T	-0.196	-0.421	-0.225	-0.369	-0.684	-0.314
WM1799	-0.234	-0.061	0.173	-0.554	-0.374	0.18
WM115	-0.244	-0.227	0.018	-0.676	-0.428	0.247
HS940T	-0.253	-0.391	-0.139	-0.697	-0.755	-0.058
HS688AT	-0.303	-0.496	-0.192	-0.677	-0.889	-0.212
RVH421	-0.327	-0.056	0.271	-0.615	-0.144	0.472
SH4	-0.328	-0.05	0.277	-0.77	-0.174	0.596
WM2664	-0.335	0.043	0.378	-0.756	0.075	0.831
HS852T	-0.352	-0.234	0.118	-0.951	-0.571	0.38
HS600T	-0.401	-0.562	-0.161	-0.842	-0.97	-0.129
COLO800	-0.404	-0.111	0.293	-0.67	-0.214	0.456
COLO818	-0.406	-0.209	0.198	-0.768	-0.561	0.207
COLO792	-0.407	0.018	0.426	-0.965	-0.116	0.849
HS939T	-0.445	-0.136	0.309	-1.223	-0.437	0.786
C32	-0.5	-0.087	0.413	-1.167	-0.446	0.721
COLO829	-0.526	-0.067	0.459	-1.321	-0.23	1.091
SKMEL31	-0.726	-0.37	0.356	-1.63	-0.809	0.821
SKMEL28	-0.814	-0.183	0.631	-1.259	-0.221	1.039
SKMEL24	-0.833	-0.298	0.535	-1.567	-0.512	1.055
MALME3M	-0.941	-0.068	0.872	-2.067	-0.298	1.769

Table 30B. Measurements of 40 cytokines and chemokines in the conditioned media of DMSO and abemaciclib treated cancer cells

Analyte	Fold change (abemaciclib vs. DMSO treatment)
Hu MIF	2.9587
Hu IL-8	0.7253
Hu IL-6	0.3788
Hu MCP-1/CCL2	0.7175
Hu ENA-78/CXCL5	1.0188
Hu Gro-a/CXCL1	0.9135
Hu SDF1a+b/CXCL12	0.8885
Hu TECK/CCL25	1.5510
Hu GM-CSF	1.0191
Hu Gro-b/CXCL2	0.7471
Hu Fractalkine/CX3CL1	2.1863
Hu SCYB16/CXCL16	1.1278
Hu 6Ckine/CCL21	0.9700
Hu IL-10	1.0079
Hu IP-10/CXCL10	0.9103
Hu MIP-3a/CCL20	3.4000
Hu IL-16	0.8482
Hu MIP-3b/CCL19	0.8717
Hu I-309/CCL1	1.0389

Hu MCP-3/CCL7	1.0422
Hu MIP-1d/CCL15	1.0809
Hu Eotaxin/CCL11	0.9599
Hu MCP-4/CCL13	0.8887
Hu TNF-a	0.7465
Hu IL-1b	1.0719
Hu IL-4	1.6605
Hu TARC/CCL17	1.0104
Hu IL-2	0.5882
Hu MDC/CCL22	1.1142
Hu Eotaxin-3/CCL26	3.0279
Hu GCP-2/CXCL6	0.6386
Hu CTACK/CCL27	1.0834
Hu MIP-1a/CCL3	1.0350
Hu MCP-2/CCL8	1.0388
Hu I-TAC/CXCL11	0.9524
Hu IFN-g	Below the detection threshold
Hu BCA-1/CXCL13	Below the detection threshold
Hu MIG/CXCL9	Below the detection threshold
Hu MPIF-1/CCL23	Below the detection threshold
Hu Eotaxin-2/CCL24	Below the detection threshold

Example 11 – Clinical Trial Design

[0557] Applicants have designed an exemplary clinical trial based on the present disclosure. The study design includes a Phase I/II clinical trial combining abemaciclib plus LY3300054 for patients with melanoma with ICB resistance. LY3300054 is a monoclonal antibody that has been shown in vitro to target the PD-L1 expressed on tumor cells and tumor-infiltrating immune cells, preventing its binding to PD-1 and CD80 (B7-1) receptors on the T cells.

[0558] The patients to be recruited include patients that are post-PD-1 and/or post-CTLA-4 treatment with advanced/metastatic cutaneous melanoma. Phase I will include up to 24 patients. Phase I patients will be administered Anti-PD-L1 therapy plus oral abemaciclib. Abemaciclib will be administered according to the present disclosure in doses of 75, 100, 150, and 200 mg BID (i.e., twice daily). The primary goals of the phase I trial are safety and recommended phase 2 dose (RP2D). The secondary goal of the phase I trial is clinical benefit. The trial also includes a single-arm Phase II trial. The phase II trial will include n=30 patients and be two stage. The phase II trial will administer Anti-PD-L1 therapy plus oral abemaciclib at the RP2D. The primary goal of the phase II trial is clinical benefit. The secondary goal of the phase II trial is measuring immune phenotypes. Pre-treatment and on-treatment biopsy samples will be analyzed as described herein. Samples will be analyzed by one or more of scRNA-sequencing, immune resistance biomarker score, multiplexed immune

profiling, immuno-phenotyping (e.g., flow-cytometry) and/or tumor infiltrating lymphocytes activity (e.g., flow cytometry). The Trial will use a statistical plan.

[0559] Table 31. Statistical Plan

Number of Participants with DLT (dose limiting toxicity) at a Given Dose Level	Escalation Decision Rule
0 out of 3	Enter 3 participants at the next dose level.
>2	Dose escalation will be stopped. This dose level will be declared the maximally administered dose (highest dose administered). Three (3) additional participants will be entered at the next lowest dose level if only 3 participants were treated previously at that dose.
1 out of 3	Enter 3 participants at this dose level. • If 0 of these 3 participants experience DLT, proceed to the next dose level. • If 1 or more of this group suffer DLT, then dose escalation is stopped, and this dose is declared the maximally administered dose. Three (3) additional participants will be entered at the next lowest dose level if only 3 participants were treated previously at that dose.
≤1 out of 6 at highest dose level below the maximally administered dose	This is generally the recommended phase 2 dose. At least 6 participants must be entered at the recommended phase 2 dose.

[0560] Part 1 is a single arm, Phase I study with 3+3 design to identify the RP2D of abemaciclib. The total number of patients to be enrolled in the Part 1 is dependent upon the observed safety profile. The expected enrollment is between 3 and 24 patients for evaluating 4 dose levels. If 1 patient experiences a DLT in the first 3 patients, then 3 more patients will be recruited for a total of six in a dose cohort. The following table summarizes the probability of stopping accrual after the first 3 patients in a dose cohort (2 or more patients experience a DLT) for various true DLT rates.

[0561] Table 32

True Rate of DLT	0.1	0.2	0.3	0.4	0.5	0.6	0.7
Probability of Stopping Accrual	0.03	0.10	0.22	0.35	0.50	0.65	0.78

[0562] In addition, the exact 90% confidence interval for toxicity (or any other binomial parameter) will be no wider than 36% among 24 patients.

[0563] Sample size calculations for Part 2 take into consideration patients treated at the RP2D in Part 1.

[0564] For Part 2, abemaciclib plus anti-PD-L1 therapy will be considered worthy of further investigation in advanced/metastatic melanoma patients with resistance to PD-L1 if a clinical benefit rate (CBR) of at least 20% is observed. To achieve this, the study will employ a Simon two-stage design with a total sample of 30 patients to compare a null CBR of 5% against the alternative of 22%.

[0565] Including patients treated at the RP2D in Part1, thirteen patients in total will be enrolled in the first stage. If 1 or more patients achieve the primary endpoint of CBR, then 17 additional patients will be enrolled. If 4 or more of the total of 30 patients achieve the primary endpoint, then abemaciclib plus anti-PD-L1 therapy will be considered promising. This design has at least 90% power and a 6% one-sided type 1 error (target 10%). If the null hypothesis is true, the probability is 0.51 that the trial will stop at the end of stage 1.

[0566] In stage 1, the probability of observing one or more toxicity events given a true toxicity rate as low as 12%, with 13 patients, is at least 80%. If the Part 2 portion of the study is expanded to stage 2, the probability of observing one or more toxicity events given a true toxicity rate as low as 6%, with 30 patients, is at least 80%.

[0567] Correlative and biomarker objectives will be considered exploratory. Assuming the study moves to the second stage, the maximal width of a 90% confidence interval for any binomial parameter will be no wider than 32%, hence estimation of binomial quantities will be fairly accurate. Estimation of continuous biomarker measures will be via mean or median as appropriate and standard deviation. There will be limited power to correlate clinical measures with biomarker endpoints with this limited phase II sample size, hence those analyses will be considered exploratory.

Example 12 – *In vivo* and *ex vivo* studies

[0568] As described herein, Applicants can study the gene signatures in vivo and ex vivo. The studies can provide for information regarding how different treatment regimens can modulate the resistance signatures, tumor lymphocyte infiltration, and/or immune phenotypes. The studies can also provide for key genes required for resistance to the adaptive immune response (e.g., TILs). **Figure 76** shows tSNE analysis after scRNA-seq of B16 cells

implanted subcutaneously into B6 animals followed by treatment with either vehicle, abemaciclib alone, immune checkpoint inhibitors (ICI) alone or ICI plus abema. The cells were "perturbed" in vivo after implantation. Using the data obtained, Applicants can analyze the expression of the resistance signature, tumor infiltration and immune states of the in vivo tumor under each condition.

[0569] **Figure 77** shows ex vivo melanoma cells obtained from a single human patient perturbed with barcoded guide sequences targeting the indicated genes. The barcodes from this experiment were isolated and sequenced. The result shows that Applicants have successfully introduced a perturb-seq library that targets genes of resistance in human cells, and that the perturb-seq barcodes could be isolated and sequenced from this experiment. The names are the different channels that were loaded for sequencing. Applicants can perform a co-culture experiment with the patient's own (autologous) tumor-infiltrating lymphocytes after confirming that single-cell transcriptomes can be obtained from the same experiment in addition to the barcodes.

Example 13 – Materials and Methods

Human tumor specimens

[0570] For the discovery scRNA-seq cohort, tissue was procured under Institutional Review Board (IRB) approved protocols at Brigham and Women's Hospital and Dana-Farber Cancer Institute, Boston, MA. Patients were consented to these protocols (11-104) in clinic visits prior to surgery/biopsy. Patients included in the earlier study (Tirosh et al., 2016), and those specimens newly collected here are annotated in **Tables 1 and 24A**.

[0571] For validation cohorts (bulk-RNA-Seq), patient tissue was collected under IRB protocols of the University Hospital Essen, Germany and Massachusetts General Hospital, Boston, MA (protocol 11-181) and The Wistar Institute, Philadelphia, PA (Human subjects protocol 2802240). Validation Cohort 1 included 90 samples from 26 patients, with multiple biopsies per patient, taken before, during, and/or after various treatment regimens, including both targeted therapies and immunotherapies (see, e.g., **Table 24B**). Validation Cohort 2 included 112 samples collected before treatment with pembrolizumab (clinical information is provided in **Tables 24C**).

Single-cell cohort: Tissue handling and tumor disaggregation

[0572] Resected tumors were transported in DMEM (ThermoFisher Scientific, Waltham, MA) on ice immediately after surgical procurement. Tumors were rinsed with PBS (Life Technologies, Carlsbad, CA). A small fragment was stored in RNA-Protect (Qiagen, Hilden,

Germany) for bulk RNA and DNA isolation. Using scalpels, the remainder of the tumor was minced into tiny cubes <1 mm^3 and transferred into a 50 ml conical tube (BD Falcon, Franklin Lakes, NJ) containing 10 ml pre-warmed M199-media (ThermoFisher Scientific), 2 mg/ml collagenase P (Roche, Basel, Switzerland) and 10U/µl DNase I (Roche). Tumor pieces were digested in this media for 10 minutes at 37°C, then vortexed for 10 seconds and pipetted up and down for 1 minute using pipettes of descending sizes (25 ml, 10 ml and 5 ml). As needed, this was repeated twice more until a single-cell suspension was obtained. This suspension was then filtered using a 70µm nylon mesh (ThermoFisher Scientific) and residual cell clumps were discarded. The suspension was supplemented with 30 ml PBS (Life Technologies) with 2% fetal calf serum (FCS) (Gemini Bioproducts, West Sacramento, CA) and immediately placed on ice. After centrifuging at 580g at 4°C for 6 minutes, the supernatant was discarded and the cell pellet was re-suspended in PBS with 1% FCS and placed on ice prior to staining for FACS.

Single-cell cohort: FACS

[0573] Single-cell suspensions were stained with CD45-FITC (VWR, Radnor, PA) and live/dead stain using Zombie Aqua (BioLegend, San Diego, CA) per manufacturer recommendations. First, doublets were excluded based on forward and sideward scatter, then Applicants gated on viable cells ($Aqua^{low}$) and sorted single cells ($CD45^+$ or $CD45^-$) into 96-well plates chilled to 4°C, pre-prepared with 10µl TCL buffer (Qiagen) supplemented with 1% beta- mercaptoethanol (lysis buffer). Single-cell lysates were sealed, vortexed, spun down at 3,700 rpm at 4°C for 2 minutes, placed on dry ice and transferred for storage at -80°C.

scRNA-seq

[0574] For plate-based scRNA-seq, whole Transcriptome Amplification (WTA) was performed with a modified SMART-Seq2 protocol, as described previously (Trombetta et al., 2014) with Maxima Reverse Transcriptase (Life Technologies) instead of Superscript II. Next, WTA products were cleaned with Agencourt XP DNA beads and 70% ethanol (Beckman Coulter, Brea, CA) and Illumina sequencing libraries were prepared using Nextera XT (Illumina, San Diego, CA), as previously described (Trombetta et al., 2014). The 96 samples of a multiwell plates were pooled, and cleaned with two 0.8X DNA SPRIs (Beckman Coulter). Library quality was assessed with a high sensitivity DNA chip (Agilent) and quantified with a high sensitivity dsDNA Quant Kit (Life Technologies).

[0575] For droplet-based scRNA-seq, experiments were performed on the 10x Genomics Chromium platform, with the Chromium Single Cell 3′ Library & Gel Bead Kit v2 and Chromium Single Cell 3′ Chip kit v2 according to the manufacturer's instructions in the Chromium Single Cell 3′ Reagents Kits V2 User Guide. Briefly, ~6,000 cells were re-suspended in PBS supplemented with 0.04% BSA and loaded to each channel. The cells were then partitioned into Gel Beads in Emulsion in the GemCode instrument, where cell lysis and barcoded reverse transcription of RNA occurred, followed by amplification, shearing and 5′ adaptor and sample index attachment.

[0576] Barcoded single cell transcriptome libraries were sequenced with 38bp paired end reads on an Illumina NextSeq 500 Instrument.

Validation cohorts: RNA-capture and bulk RNA-Seq

[0577] RNA extraction from formalin-fixed, paraffin-embedded (FFPE) tissue slides was performed by the Genomics Platform of the Broad Institute (Cambridge, MA). For cDNA library construction total RNA was assessed for quality using the Caliper LabChip GX2 (Perkin Elmer). The percentage of fragments with a size greater than 200nt (DV200) was calculated and an aliquot of 200ng of RNA was used as the input for first strand cDNA synthesis using Illumina's TruSeq RNA Access Library Prep Kit. Synthesis of the second strand of cDNA was followed by indexed adapter ligation. Subsequent PCR amplification enriched for adapted fragments. The amplified libraries were quantified using an automated PicoGreen assay (Thermo Fisher Scientific, Cambridge, MA). 200ng of each cDNA library, not including controls, were combined into 4-plex pools. Capture probes that target the exome were added, and hybridized for the recommended time. Following hybridization, streptavidin magnetic beads were used to capture the library-bound probes from the previous step. Two wash steps effectively remove any nonspecifically bound products. These same hybridization, capture and wash steps are repeated to assure high specificity. A second round of amplification enriches the captured libraries. After enrichment, the libraries were quantified with qPCR using the KAPA Library Quantification Kit for Illumina Sequencing Platforms (Illumina) and then pooled equimolarly. The entire process was performed in 96-well format and all pipetting was done by either Agilent Bravo or Hamilton Starlet. Pooled libraries were normalized to 2nM and denatured using 0.1 N NaOH prior to sequencing. Flowcell cluster amplification and sequencing were performed according to the manufacturer's protocols using Illumina HiSeq 2000 or 2500 (Illumina). Each run was a 76bp

paired-end with an eight-base index barcode read. Data was analyzed using the Broad Picard Pipeline (broadinstitute.github.io/picard/), which includes de-multiplexing and data aggregation.

scRNA-seq data pre-processing

[0578] BAM files were converted to merged, demultiplexed FASTQ files. The paired-end reads obtained with the SMART-Seq2 protocol were mapped to the UCSC hg19 human transcriptome using Bowtie (Langmead et al., 2009), and transcript-per-million (TPM) values were calculated with RSEM v1.2.8 in paired-end mode (Li and Dewey, 2011). The paired-end reads obtained with the 10x Genomics platform were mapped to the UCSC hg19 human transcriptome using STAR (Dobin et al., 2013), and gene counts/TPM values were obtained using the 10x Genomics computational pipeline (cellranger-2.1.0).

[0579] For bulk RNA-Seq data, expression levels of genes were quantified as $E_{i,j}=log_2(TPM_{i,j}+1)$, where $TPM_{i,j}$ denotes the TPM value of gene i in sample j. For scRNA-seq data, expression levels were quantified as $E_{i,j}=log_2(TPM_{i,j}/10+1)$, where $TPM_{i,j}$ denotes the TPM value of gene i in cell j. TPM values were divided by 10 because the complexity of the single-cell libraries is estimated to be within the order of 100,000 transcripts. The 10^{-1} factoring prevents counting each transcript ~10 times, which would have resulted in overestimating the differences between positive and zero TPM values. The average expression of a gene i across a population of N cells, denoted here as P, was defined as

$$E_{i,p} = \log_2\left(1 + \frac{\sum_{j \in P} TPM_{i,j}}{N}\right)$$

[0580] For each cell, Applicants quantified the number of genes with at least one mapped read, and the average expression level of a curated list of housekeeping genes (Tirosh et al., 2016a). Applicants excluded all cells with either fewer than 1,700 detected genes or an average housekeeping expression (E, as defined above) below 3 (see, e.g., **Tables 2 and 25**). For the remaining cells, Applicants calculated the average expression of each gene (E_p), and excluded genes with an average expression below 4, which defined a different set of genes in different analyses depending on the subset of cells included. In cases where Applicants analyzed different cell types together, Applicants removed genes only if they had an average E_p below 4 in each of the different cell types that were included in the analysis. When analyzing $CD45^+$ cells, Applicants excluded genes as described above only after the

assignment of cells to cell types in order to prevent the filtering of genes that were expressed by less abundant cell types.

Data imputation and normalization

[0581] In all differential expression analyses of SMART-Seq2, Applicants first modeled the read counts as a mixture of a negative binomial (NB) and Poisson components to estimate the expression levels, using SCDE (Fan et al., 2016) with the code provided in github.com/hms-dbmi/scde. The resulting normalized and imputed expression matrix, denoted as *E'*, was used in the differential expression analyses. Analysis of droplet-based scRNA-seq data (10X Genomics Chromium, above) was performed with the Seurat package (www.satijalab.org/seurat), using the likelihood-ratio test for differential gene expression analyses (McDavid et al., 2013).

Identifying cell states associated with specific tumor compositions

[0582] Applicants combined scRNA-seq and bulk RNA-Seq data to characterize the state of a specific cell type in tumors with a specific cellular composition (See, e.g. **Figures 44B and 62B**). The method takes as input scRNA-seq data and a cohort of bulk RNA-Seq data, both collected from tumors of the same cancer type. The implementation of the approach is provided via GitHub (github.com/livnatje/ImmuneResistance/wiki/Mapping-immune-resistance-in-melanoma; *ImmRes2_immuneResistanceProgram.R*), and can be applied to regenerate the results reported here and facilitate new discoveries. For clarity Applicants describe the approach for malignant cells and T cells as applied here, although it can be applied to any pair of cell types, depending on data availability.

[0583] **STEP 1. Analyses of the input scRNA-seq data**: (**a**) assign cells to cell types (see sections: ***Classification of malignant and stromal cells*** and ***Classification of immune cells***); and (**b**) define a signature of malignant cells and a signature of T cells, consisting of genes which are primarily (specifically) expressed by malignant cells or T cells, respectively (see section: ***Data-driven signatures of specific cell types***).

[0584] **STEP 2. Analyses of the input bulk RNA-Seq data**: (**a**) estimate the T cell infiltration level in each tumor by computing the overall expression (OE, see section: ***Computing the OE of gene signatures***) of the T cell signature in each bulk sample; (**b**) compute the Pearson correlation coefficient between the expression of the genes in the malignant signature and the OE of the T cell signature across the bulk tumors; and (**c**) define the **seed exclusion-up (down)** signature as the top 20 malignant genes that are significantly

negatively (positively) correlated in (b) (adjusted P < 0.1, using Benjamini-Hochberg correction for multiple hypotheses testing (Benjamini and Hochberg, 1995)).

[0585] If confounding factors in the bulk RNA-Seq data should be controlled for, *partial* Pearson correlation is used in (**2.b**).

[0586] **STEP 3. Analyses of the input scRNA-seq data of the *malignant cells***: (**a**) compute the OE of the seed exclusion signatures in each of the malignant cells; (**b**) compute the partial Spearman correlation coefficient between the expression of each gene and the OE of the seed exclusion signatures across the single malignant cells, while controlling for technical quality (the number of reads and genes that were detected in the cells). Other confounding factors, besides technical variation, can also be controlled for, for example, cell cycle (see below).

[0587] Of note, to examine whether the seed signatures capture the two opposing transcriptional components of a malignant cell state, Applicants test whether their OE across the malignant cells is negatively correlated.

[0588] **STEP 4. Derive the final genome-scale exclusion signatures**, defined as: (**i**) **exclusion-up**: genes which were significantly positively correlated with the seed exclusion-up signature and significantly negatively correlated with the seed exclusion-down signature in the analysis described in (STEP 3); and (**ii**) **exclusion-down**: genes which were significantly positively correlated with the seed exclusion-down signature and significantly negatively correlated with the seed exclusion-up signature in the analysis described in (STEP 3). In this analysis, a gene is defined as significantly correlated with a signature if it was among the 200 topmost correlated genes, with Spearman correlation coefficient $|\rho| > 0.1$ and adjusted p-value < 10^{-10} (Benjamini-Hochberg correction for multiple hypotheses testing (Benjamini and Hochberg, 1995)).

[0589] To generate the exclusion program reported in the manuscript, Applicants applied the approach to the clinical scRNA-seq melanoma data and bulk RNA-Seq data of 473 Skin Cutaneous Melanoma (SKCM) tumors from TCGA (as provided in xenabrowser.net/datapages/). In (STEP 2) Applicants used the $CD8^+$ T cell signature Applicants generated (**Table 26B**).

[0590] Applicants also performed several additional analyses. First, for comparison, Applicants also applied the approach to other T cell populations, by using other T cell signatures (**Table 26B**) in (STEP 2): pan-T cells ($CD3^+$), $CD4^+$ T cells; naïve, cytotoxic, and

exhausted $CD8^+$ T cell subsets; and naïve, exhausted, and regulatory $CD4^+$ T cell subsets. Second, to compute the relative abundance of $CD8^+$ T cells *among the non-malignant cells* Applicants used the $CD8^+$ T cell signature and tumor purity that was previously assessed by genetic variations with ABSULOTE (Akbani et al., 2015; Carter et al., 2012). Of note, in this setting the resulting "up" and "down" seed signatures were *less* anti-correlated with each other across the single malignant cells (Pearson r = -0.22, P = $1.40*10^{-24}$, compared to $r = -0.58$, $P = 6.19*10^{-183}$, in the original setting). These findings indicate that the association between the state of the malignant cells and the *relative* proportion of T cells out of the non-malignant compartment may be more complex than the connection between malignant cells states and the proportion of T cells in the overall tumor. Tumor purity was provided in (STEP 2) as a confounding factor. Third, Applicants applied the approach when controlling for tumor and cellular proliferation. To do so, Applicants computed the OE of two cell cycle signatures (G1/S and G2/M, **Table 26A** (Tirosh et al., 2016)) across the bulk tumors and single malignant cells. Applicants then provided these values as confounding factors in (STEP 2) and (STEP 3), to control for the tumor proliferation rate and cell cycling, respectively.

[0591] In cases where the approach is applied to two cell types whose abundance in the tumor is highly correlated, for example macrophages and T cells, the seed exclusion-up signature can be identified in a more permissive manner. Otherwise, it may include very few genes. In the case of macrophages and T cells, the (more permissive) seed exclusion-up signature includes macrophage specific genes that fulfill the following requirements: (1) in comparison to other macrophage specific genes, their expression across bulk tumors has a low correlation to T cell abundance (conditional probability < 0.1); and (2) their expression across macrophages in the scRNA-seq data is negatively correlated to the OE of the exclusion-down seed signature. The analysis then proceeds in the same manner as described above.

Computing the OE of gene signatures

[0592] Gene modules are more robust to noise and provide more coherent signals than the expression of single genes (Shalek et al., 2013, 2014; Wagner et al., 2016). To compute the OE of a gene module or signature Applicants used a scheme that filters technical variation and highlights biologically meaningful patterns. The procedure is based on the notion that the measured expression of a specific gene is correlated with its true expression (signal), but also contains a technical (noise) component. The latter may be due to various

stochastic processes in the capture and amplification of the gene's transcripts, sample quality, as well as variation in sequencing depth (Wagner et al., 2016). The signal-to-noise ratio varies, depending, among other variables, on gene transcript abundance.

[0593] Applicants therefore computed the OE of gene signatures in a way that accounts for the variation in the signal-to-noise ratio across genes and cells. Given a gene signature and a gene expression matrix E (as defined above), Applicants first binned the genes into 50 expression bins according to their average expression across the cells or samples. The average expression of a gene across a set of cells *within* a sample is $E_{i,p}$ (see: ***RNA-Seq data pre-processing***) and the average expression of a gene *across* a set of N tumor samples was defined as: $\mathbb{E}_j[E_{ij}] = \sum_j \frac{E_{ij}}{N}$. Given a gene signature S that consists of K genes, with k_b genes in bin b, Applicants sample random *S-compatible* signatures for normalization. A random signature is *S-compatible* with signature S if it consists of overall K genes, such that in each bin (b) it has exactly k_b genes. The OE of signature S in cell or sample j is then defined as:

$$OE_j = \frac{\sum_{i \in S} C_{ij}}{\mathbb{E}_{\tilde{S}}[\sum_{i \in \tilde{S}} C_{ij}]}$$

[0594] Where $\tilde{S}$ is a random *S-compatible* signature, and C_{ij} is the centered expression of gene i in cell or sample j, defined as $\mathrm{C_{ij}} = \mathrm{E_{ij}} - \mathbb{E}[E_{ij}]$. Because the computation is based on the centered gene expression matrix C, genes that generally have a higher expression compared to other genes will not skew or dominate the signal.

[0595] Applicants found that 1,000 random *S-compatible* signatures are sufficient to yield a robust estimate of the expected value $\mathbb{E}_{\tilde{S}}[\sum_{i \in \tilde{S}} C_{ij}]$. The distribution of the OE values was normal or a mixture of normal distributions, and, unlike the expression of a single gene, fulfilled the assumptions of the mixed effects models or hierarchal linear models that Applicants applied to study the differential expression of gene signatures (as described in the ***Identifying differentially expressed gene sets*** section).

[0596] In cases where the OE of a given signature has a bimodal distribution across the cell population, it can be used to naturally separate the cells into two subsets. To this end, Applicants applied the Expectation Maximization (EM) algorithm for mixtures of normal distributions to define the two underlying normal distributions. Applicants then assigned cells to the two subsets, depending on the distribution (high or low) that they were assigned to.

[0597] Applicants use the term a transcriptional *program* (e.g., the immune resistant program) to characterize cell states which are defined by a pair of signatures, such that one

(*S-up*) is overexpressed and the other (*S-down*) is underexpressed. Applicants define the OE of such cell states as the OE of *S-up* minus the OE of *S-down*.

[0598] To compute the OE of gene signatures in bulk tumors or single cell data one can apply the R code Applicants provide via GitHub (github.com/livnatje/ImmuneResistance; ImmRes_OE.R).

Classification of malignant and stromal cells

[0599] In the non-immune compartment ($CD45^-$ cells), Applicants distinguished malignant and nonmalignant cells according to three criteria: (**1**) their inferred CNV profiles (Tirosh et al., 2016); (**2**) under-expression of different nonmalignant cell type signatures; and (**3**) higher similarity to melanoma tumors than to adjacent normal tissue, based on the comparison to bulk RNA-Seq profiles. Specifically: **(1)** to infer CNVs from the scRNA-seq data Applicants used the approach described in (Tirosh et al., 2016) as implemented in the R code provided in github.com/broadinstitute/inferCNV with the default parameters. Cells with an average absolute CNV level that was below the 0.1 quantile of the entire $CD45^-$ cell population were considered as potentially nonmalignant according to this criterion. **(2)** Applicants used signatures of endothelial cells, stromal cells, and Cancer Associated Fibroblasts (CAFs), as provided in **Table 26A and C**. The signatures combine well-established markers from two sources (www.biolegend.com/cell_markers and (Tirosh et al., 2016)). Applicants computed the OE of these three signatures in each of the $CD45^-$ cells, while controlling for the impact of technical cell quality (as described in section ***Computing the OE of gene signatures***). $CD45^-$ cells that expressed any one of these three signatures above the 0.95 quantile were considered as potentially nonmalignant according to this criterion. **(3)** Applicants downloaded the pan-cancer TCGA RNA-SeqV2 expression data from xena.ucsc.edu, and $\log^2$-transformed the RSEM-based gene quantifications. For each cell, Applicants computed the correlation (e.g., Spearman correlation) between its profile (in TPM) and each bulk profile (in TPM) of 473 skin cutaneous melanoma samples and 727 normal solid tissues. Applicants then tested, for each cell, if it was more similar to the melanoma tumors compared to the normal tissues, by applying a one-sided Wilcoxon ranksum test on the correlation coefficients that were obtained for that cell. Cells that were more similar to the normal tissues ($P < 0.05$, Wilcoxon ranksum test) were considered as potentially nonmalignant according to this criterion.

[0600] The cell assignments that were obtained by these three different criteria were highly consistent (see, e.g., **Figures 69A**,**B**, hypergeometric p-value < 10^{-17}). Cells that were

identified as potentially nonmalignant according to one or more of these three criteria were defined as nonmalignant, and were omitted from further analyses of the malignant cells. The nonmalignant $CD45^-$ cells were further classified into CAFs and endothelial cells, if they overexpressed only one of the corresponding gene signatures, and as unresolved cells otherwise.

Classification of immune cells

[0601] To classify immune cells, Applicants first filtered $CD45^+$ cells that were potentially malignant or doublets of immune and malignant cells based on their inferred CNV profiles. To this end, Applicants defined the *overall CNV level* of a given cell as the sum of the absolute CNV estimates across all genomic windows. For each tumor, Applicants generated its *CNV profile* by averaging the CNV profiles of its malignant cells, when considering only those with the highest *overall CNV level* (top 10%). Applicants then evaluated each cell by two values: (**1**) its *overall CNV level*, and (**2**) its *CNV-R-score*, that is, the Spearman correlation coefficient obtained when comparing its CNV profile to the CNV profile of its tumor. These two values were used to classify cells as malignant, nonmalignant, and unresolved cells that were excluded from further analysis (see, e.g., **Figures 69C-E**).

[0602] Next, Applicants applied two different clustering approaches to assign immune ($CD45^+$) cells into cell types. In the first approach, Applicants clustered the $CD45^+$ cells according to 194 well-established markers of 22 immune cell subtypes (**Table 26A**; assembled from www.biolegend.com/cell_markers and (Tirosh et al., 2016)). The clustering was performed in three steps: **(1)** Applicants computed the Principal Components (PCs) of the scRNA-seq profiles, while restricting the analysis to the 194 biomarker genes. Applicants used the top PCs that captured more than 50% of the cell-cell variation. In the presented analyses, 10 PCs were used, but the results were robust and stable when using the first 5-15 PCs. **(2)** Applicants applied t-SNE (t-Distributed Stochastic Neighbor Embedding) (van der Maaten and Hinton, 2008) to transform these first PCs to a two-dimensional embedding, using the R implementation of the t-SNE method with the default parameters, as provided in lvdmaaten.github.io/tsne/. **(3)** Applicants applied a density clustering method, DBscan (Ester et al., 1996), on the two-dimensional t-SNE embedding that was obtained in (2). This process resulted in four clusters for which the top preferentially expressed genes included multiple known markers of particular cell types (see, e.g., **Figures 69F,G**). Alternatively, this process resulted in six clusters for which the top preferentially expressed genes included multiple known markers of particular cell types.

[0603] To map between clusters and cell types Applicants compared each cluster to the other clusters according to the OE of the different cell type signatures (one sided *t*-test, **Table 26A**). The cell type signature that was most significantly (t-test p-value $<10^{-10}$) overexpressed in the cluster compared to all other clusters was used to define the cluster identity. In this manner, Applicants annotated the clusters as $CD8^+$ and $CD4^+$ T cells, B cells, and macrophages (see, e.g., **Figure 62D**). Alternatively, Applicants annotated the clusters as CD8 and CD4 T cells, B cells, macrophages, and neutrophils **(Fig. 1C)**. Cells that clustered with the $CD8^+$ T cells and did not express CD8A or CD8B were labeled as NK cells if they overexpressed NK markers, otherwise they were considered as unresolved T cells. T cells that were clustered together with the CD4 T cells and expressed CD8A or CD8B were also considered as unresolved T cells. Unresolved T cells were not used in further analyses.

[0604] To assess the robustness of the assignments, Applicants applied another approach, and determined the concordance between the two assignments. In the second approach, Applicants first made initial cell assignments based on the OE of well-established cell type markers: T cells (CD2, CD3D, CD3E, CD3G), B cells (CD19, CD79A, CD79B, BLK), and macrophages (CD163, CD14, CSF1R). Across all the $CD45^+$ cells, the OE levels of these signatures had bimodal distributions. Applicants used the bimodal OE of each signature to assign cells to cell types (see ***Computing OE of gene signatures***). Cells that were assigned to more than one cell type at this point were considered as unresolved. Cells that were defined as T cells according to this measure were further classified as $CD8^+$ or $CD4^+$ T cells if they expressed CD8 (CD8A or CD8B) or CD4, respectively. T cells that expressed both CD4 and CD8 were considered as unresolved. As a result, 67.3% of the cells had an initial cell type assignment.

[0605] Next, Applicants clustered the cells with the Infomap algorithm (Rosvall and Bergstrom, 2008). Infomap decomposes an input graph into modules by deriving a compressive description of random walks on the graph. The input to the algorithm was an unweighted *k*-NN graph ($k = 50$) that Applicants generated based on the expression of the 194 biomarker genes across the $CD45^+$ cells. Infomap produced 22 clusters, separating the different $CD45^+$ cells not only according to cell types but also according to various cell states. For each cluster, Applicants examined if it was enriched with cells of a specific cell type, according to the initial assignments. Nineteen clusters were enriched with only one cell type. The cells within these clusters were assigned to the cell type of their cluster, unless their initial assignment was different, and in this case, they were considered as unresolved.

[0606] The cell type assignments that were obtained by the two approaches were highly concordant: 97% of the cells had the same assignment with both approaches.

[0607] Interactive visualization of the immune cells' tSNE plots are provided in portals.broadinstitute.org/single_cell/study/melanoma-immunotherapy-resistance.

Data-driven signatures of specific cell types

[0608] To identify cell type signatures Applicants performed pairwise comparisons between the eight cell types that Applicants identified: malignant cells, CAFs, endothelial cells, NK cells, B cells, macrophages, and $CD8^+$ and $CD4^+$ T cells. Applicants performed these comparisons via one-sided Wilcoxon ranksum-tests on the normalized data *E*. Genes were considered as cell type specific if they were overexpressed in a particular cell type compared to all other cell types (Wilcoxon ranksum-test p-value $<10^{-5}$). For T cell types ($CD8^+$ and $CD4^+$) Applicants used more permissive cutoffs, as the transcriptional differences between these cell types are more subtle. To ensure that the genes are significantly higher in the specific T cell type across all pairwise comparisons, for each T cell type Applicants: (**1**) computed the least significant (maximal) p-value for each gene, when comparing its expression in the T cell type ($CD8^+$ or $CD4^+$) to its expression in each of the other cell types, (**2**) used the genes with the lowest maximal p-values to construct the signature (at most 50 genes with maximal $P<2*10^{-3}$). To derive a Pan-T cell signature that characterizes both $CD8^+$ and $CD4^+$ T cells, Applicants used genes that were overexpressed in $CD8^+$ and $CD4^+$ T cells ($P<10^{-5}$) compared to all other cell types, when disregarding T cells and NK cells.

[0609] To derive $CD8^+$ T cell state signatures Applicants: (**1**) classified $CD8^+$ T cells as cytotoxic, exhausted, naïve, or 'undetermined' based on well-established markers of these cell states (**Table 26A**); (**2**) performed pairwise comparisons between the different $CD8^+$ T cell subsets to derive initial $CD8^+$ T cell state signatures; (**3**) compared each $CD8^+$ T cell subset to all other cell types (*e.g.*, B cells, macrophages, etc.), and (**4**) filtered non-specific genes from the initial $CD8^+$ T cell state signatures. Applicants performed the same analysis with $CD4^+$ T cells to derive signatures of cytotoxic, exhausted, naïve, and regulatory $CD4^+$ T cells. The cytotoxic $CD4^+$ T cells signature included only four genes and thus was not used in subsequent analyses.

[0610] Applicants also identified signatures of three broader cell type categories: immune cells, lymphocytes, and stromal cells. The immune cell signature includes genes that are overexpressed by all the immune cell types compared to all other non-immune cells, and

likewise for the other two cell categories. The lymphocyte signature included only five genes and thus was not used in subsequent analyses.

[0611] The lists of cell subtype specific genes, which were identified as described above, are provided in **Table 26B**. The implementation of these analyses is provided via GitHub (github.com/livnatje/ImmuneResistance/wiki/Mapping-immune-resistance-in-melanoma**;** see *ImmRes1_denovoCellTypeSig.R*), and can be applied to reproduce the cell subtype signatures and generate cell subtype signatures based on other scRNA-seq cohorts.

[0612] Alternatively, to identify cell-type signatures Applicants performed pairwise comparisons between the nine different cell types that Applicants identified: malignant cells, CD8 and CD4 T-cells, NK cells, B-cells, macrophages, neutrophils, CAFs, and endothelial cells. Applicants then performed pairwise comparisons between the different cell types via one-sided Wilcoxon ranksum-tests on the imputed and normalized data *E'*. Genes that were overexpressed in a particular cell subtype compared to all other cell subtypes (Wilcoxon ranksum-test p-value $<10^{-5}$) were considered as cell-type specific. For cell types with less than 1,000 cells Applicants also ranked the genes based on the maximal p-value that was obtained when comparing the cell type to each of the other cell types; the bottom 100 genes that also passed the first filter were considered as cell type specific. As CD8 T-cells and NK cells had similar expression patterns, Applicants excluded NK cells from the analysis when identifying T-cell specific genes. In the analyses described above Applicants considered the CD4 and CD8 as one entity of T-cells, but also derived CD4 and CD8 specific signatures, by considering as separated entities. The lists of cell-type specific genes are provided in **table 3**.

Identifying the post-treatment program

[0613] To identify potential signatures of resistance, Applicants searched for transcriptional features that distinguish between the cells of TN (i.e., treatment naïve, or untreated) and ICR patients (i.e., post-treatment), for each cell category separately. In certain examples, Applicants analyzed each cell type that had a sufficient number (>100) of cells: malignant cells, macrophages, B cells, CD8 and CD4 T cells.

[0614] Applicants identified genes differentially expressed between the malignant cells of untreated and post-treatment tumors by using a subsampling approach that mitigates the effects of outliers and prevents tumors with a particularly large number of sequenced malignant cells from dominating the results. In each subsample, Applicants selected a subset of the tumors, subsampled at most 30 malignant cells from each tumor, and identified differentially expressed genes between the post-treatment and untreated cells. Differentially

expressed genes were identified by applying SCDE (Kharchenko et al., 2014), a Bayesian method that was developed specifically to detect single-cell differential expression. As input to SCDE Applicants used the normalized and imputed expression matrix E' (see ***Data imputation and normalization***).

[0615] Applicants repeated the subsampling procedure 500 times, and computed for each gene g the fraction of subsamples in which it was found to be significantly under ($F_{down,g}$) or over ($F_{up,g}$) expressed in the post-treatment population compared to the untreated population (|z-score| > 1.96). Genes with $F_{down,g}$ values larger than the 0.9 quantile of the F_{down} distribution were considered as potentially down-regulated in the post-treatment malignant cells. Likewise, genes with $F_{up,g}$ values larger than the 0.9 quantile were considered as potentially up-regulated in the respective post-treatment malignant cells.

[0616] Applicants further filtered the signatures with two additional statistical tests that Applicants applied on the full scRNA-seq data (E') of the malignant cells. The first test was SCDE followed by multiple hypotheses correction (Holm–Bonferroni (Holm, 1979)). The second was a non-parametric empirical test, where Applicants performed a Wilcoxon ranksum test to examine if a given gene is differentially expressed in the post-treatment *vs.* untreated cells, based on E'. Applicants corrected for multiple hypotheses testing using the Benjamini-Hochberg False Discovery Rate (FDR) (Benjamini and Hochberg, 1995), and obtained empirical p-values to ensure the differences in expression were not merely reflecting differences in cell quality (*i.e.*, the number of aligned reads per cell). To this end, Applicants generated 1,000 random permutations of the gene expression matrix E', such that each permutation preserves the overall distribution of each gene, as well as the association between the expression of each gene and cell quality. Applicants performed the Wilcoxon ranksum test on the permuted E' matrixes to compute empirical p-values.

[0617] To assemble the final post-treatment signatures, Applicants selected genes that fulfilled the subsampling criteria described above and were most significantly differentially expressed according to both the SCDE and empirical tests (top 200 genes with corrected P <0.05).

[0618] The implementation of these analyses is provided via GitHub (github.com/livnatje/ImmuneResistance/wiki/Mapping-immune-resistance-in-melanoma; *ImmRes2_immuneResistanceProgram.R*), and can be applied to regenerate the post-treatment signatures from the data.

Identifying differentially expressed gene sets

[0619] To test the ability of a given gene signature to distinguish between the malignant cells collected from post-treatment vs. untreated patients Applicants modeled the data with a mixed-effects model that accounts for the dependencies and structure of the data. The model had overall five covariates and two levels: (**1**) a cell-level, and (**2**) a sample-level. Level-1 covariates controlled for cell quality by providing the number of reads (log-transformed) and the number of genes that were detected in each malignant cell, and denoted which cells were cycling, based on the bimodal OE of the cell cycle signatures defined in (Tirosh et al., 2016). Level-2 covariates were the patient's gender, age, and treatment group, and a binary covariate that denotes if the sample was a metastatic or a primary lesion. The sample-level controlled for the dependency between the scRNA-seq profiles of malignant cells that were obtained from the same patient, having a sample-specific intercept. Using this model Applicants quantified the significance of the association between the treatment covariate and the OE of a given signature across the malignant cells. Applicants implemented the mixed-effects model in R, using the *lme4* and *lmerTest* packages (CRAN.R-project.org/package=lme4, CRAN.R-project.org/package=lmerTest).

[0620] Applicants applied this approach to test the post-treatment and exclusion programs defined here, as well as annotated pre-defined gene sets downloaded from MSigDB v6.0 (Subramanian et al., 2005). The results are provided in **Tables 4, 8** and **Figures 2C and 63D**.

Cross validation analysis

[0621] To examine the generalizability of the post-treatment signatures Applicants performed a cross-validation procedure. In each cross-validation round the test set consisted of all the cells of one patient, and the training set consisted of the data from all the other patients in the cohort. In each round, Applicants used only the training data to generate post-treatment signatures (as described in ***Identifying the post-treatment program***), and computed the OE of the resulting post-treatment program. To center the expression matrix for the computation of the OE values, Applicants used all the malignant cells in the data, such that the OE scores of one patient were relative to those of the other patients. Finally, Applicants computed Receiver Operating Characteristic (ROC) curves based on the resulting post-treatment OE scores, obtained for the test set. In an example, Applicants computed the OE of the resulting mICR (post-treatment) signatures in the cells of the test patient to obtain their resistance scores (mICR-up minus mICR-down).

Integrating the exclusion and post-treatment programs

[0622] Applicants combined the post-treatment and exclusion programs with a simple union of the matching signatures, into the immune resistance program (**Table 27A and Table 28**). To give more weight to genes that are included in both signatures Applicants compute the OE of the resistance program by averaging the OE of the exclusion and post-treatment programs.

[0623] Applicants further refined the immune resistance program by integrating the scRNA-seq data with the results of a genome-scale CRISPR screen that identified gene KOs which sensitize malignant melanoma cells to T cell killing (Patel et al., 2017). Applicants defined the single malignant cells as putatively *"resistant"* if they underexpressed (lowest 1%) one of the top hits of the screen: *B2M*, *CD58*, *HLA-A*, *MLANA*, *SOX10*, *SRP54*, *TAP2*, *TAPBP*. This underexpression did not reflect low cell quality, because these *"resistant"* cells had a higher number of genes and reads. These cells had significantly higher immune resistance scores ($P = 2.24*10^{-18}$ and $1.59*10^{-3}$, t-test and mixed-effects, respectively), and were enriched with cycling cells ($P = 1.74*10^{-13}$, hypergeometric test). Applicants derived a *functional resistance program* that consists of differentially expressed genes when comparing the "resistant" cells to other malignant cells (**Table 27A**). Applicants then refined the resistance score by adding to it also the OE of this functional program (note that this purposely increases the contribution to the score of genes that are both in the original resistance program and are identified by this additional comparison). In another example, Applicants identified the topmost differentially expressed genes by comparing the "resistant" cells to other malignant cells, and included in the refined immune resistance-up (down) signature only 25 immune resistance-up (down) genes that pass this additional differential expression test.

[0624] Applicants report the performances of all the resistance program subsets: exclusion, post-treatment, and their (weighted) union, with and without the functional refinement (**Figures 73 and 74 and Tables 27-28**). As comparators, Applicants used the hits of the co-culture screen along with other potentially prognostic signatures, to generate competing predictors of patient survival and response (**Figures 66G,H, 4E,H and 5E,H; and Tables 29A, 30 and 9** see section ***Competing ICI response predictors***).

Exploring the association between the immune resistance program and cell cycle

[0625] Applicants applied two approaches to examine the association between the immune resistance program and cell cycle: (1) Applicants detected immune resistance genes when using only non-cycling malignant cells, and (2) Applicants used all the data after

filtering cell cycle effects. Applicants start by computing the OE of two cell cycle signatures (G1/S and G2/M, **Table 26A**) (Tirosh et al., 2016) across the malignant cells and bulk melanoma TCGA tumors.

[0626] In the first approach Applicants classified malignant cell as cycling or non-cycling, and confirmed that the immune resistance program can be recovered also when excluding all cycling cells from consideration. More specifically, when analyzing only the non-cycling malignant cells, all but two of the genes in the post-treatment signatures were still significantly differentially expressed between the untreated and post-treatment tumors, and all genes from the exclusion program were still significantly associated with T cell exclusion.

[0627] In the second approach Applicants re-generated the program based on all the data while controlling for cell cycle as a potential confounder. In the case of the exclusion signatures, Applicants provided these cell cycle scores as confounding factors in the partial correlation analyses (see steps 2 and 3 in ***Identifying cell states associated with specific tumor compositions***). In the case of the post-treatment signatures, Applicants filtered out the cell cycle features from the data using PAGODA (Fan et al., 2016) (using *pagoda.subtract.aspect*) and regenerated the post-treatment signature. This regression successfully masked the differences between cycling and non-cycling cells, for example, when considering cell cycle genes (**Figure 70F**). However, it did not mask the association between cycling cells and the expression of the *immune resistance* genes (**Figures 70G-H**).

[0628] The resistance program that Applicants generated after filtering cell cycle effects (**Table 27B**) was very similar to the original one ($P < 1*10^{-17}$, hypergeometric test, Jaccard index = 0.56 and 0.66, induced and repressed signatures, respectively; **Figure 70D**). Lastly, the OE of the two programs was highly correlated across the malignant cells ($r = 0.99$, $P < 1*10^{-17}$), such that cycling cells overexpressed both programs ($P < 3.48*10^{-7}$, mixed-effects; **Figure 70E**).

[0629] In another example, Applicants performed the following analysis to identify gene modules that characterize cycling cells specifically in CD8 T-cells (**table 7**). First, Applicants identified cycling cells in the CD8 T-cells and in the malignant cells based on the bimodal OE of a cell-cycle signature (the GO gene set *cell cycle process*, as defined in the ***Overall Expression (OE) of gene signatures*** section). Applicants then identified differentially expressed genes (with SCDE (*13*)) between the cycling and non-cycling cells, separately in the CD8 T-cells and in the malignant cells. Lastly, Applicants filtered from the resulting CD8

T-cell cycling signatures the genes that were also included in the corresponding malignant signatures.

Cell-cell interaction network

[0630] Applicants generated genome-scale cell-cell interactions networks by integrating (**1**) protein-protein interactions that were previously assembled by (Ramilowski et al., 2015) as cognate ligand-receptor pairs, with (**2**) cell subtype specific signatures from the single-cell profiles, identified as described above in ***Data-driven signatures of specific cell types***. The resulting network maps the physical interactions between the different cell subtypes that Applicants characterized. Each cell subtype and protein are represented by a node in the network. An edge between a cell subtype node and a ligand or receptor node denotes that this protein is included in the cell-subtype signatures. An edge between two proteins denotes that they can physically bind to each other and mediate cell-cell interactions. A path from one cell subtype to another represents a potential route by which the cells can interact. For each cell subtype, Applicants defined a 'communication signature', which includes all the surface proteins that can bind to this cell subtype signature proteins. To examine if the immune resistant malignant cells suppress their interactions with other cell subtypes Applicants examined if the different immune resistance signatures were enriched (hypergeometric test) with genes from the different immune and stroma 'communication signatures' (see, e.g., **Figure 3E and 64B**). An interactive map of the cell-cell interaction network is provided in portals.broadinstitute.org/single_cell/study/melanoma-immunotherapy-resistance#study-download, and can be explored with Cytoscape www.cytoscape.org.

Clinical longitudinal analysis (validation cohort 1)

[0631] Applicants used a mixed-effects model to represent the longitudinal treatment data (**Figure 62A, validation cohort 1**) and examine the association between the expression of various gene signatures and different treatment categories. The model included two levels: a sample-level and a patient-level. The sample-level had overall 8 covariates: three treatment covariates and five tumor microenvironment covariates. The sample-level treatment covariates denote in this case whether the sample was exposed to: **(1)** targeted therapy (on/post RAF/MEK-inhibitors), **(2)** ICI (on/post), or **(3)** non-ICI immunotherapy (NK antibodies, IL2, IFN, or GM CSF) without ICI. The five sample-level tumor microenvironment covariates control for potential changes in the tumor composition by providing the OE of the different nonmalignant cell type signatures that Applicants identified (**Table 26B**). The patient-level controlled for the dependency between the scRNA-seq

profiles of samples that were obtained from the same patient, having a patient-specific intercept. The dependent variable was the OE of a given signature, which enabled us to quantify the association between the immune resistance program (or any other signature) and the exposure to ICI or targeted therapy (the second and first sample-level covariates, respectively). The implementation of this model is provided via GitHub (github.com/livnatje/ImmuneResistance/wiki/Predicting-immunotherapy-resistance; *ImmRes3_longitudinal.R*).

[0632] In another example, Applicants used a mixed-effects model to represent the data and examine the association between the expression of various gene signatures and different treatment categories. The model included two levels. The first, sample-level, had 12 covariates, the first three denote whether the sample was exposed to: (1) targeted therapy (on/post RAF/MEK-inhibitors), (2) ICI (on/post), with or without an additional immunotherapy, (3) non-ICI immunotherapy (NK antibodies, IL2, IFN, or GM CSF) without ICI. The other 9 sample-level covariates control for potential changes in the tumor microenvironment by providing the OE of the different non-malignant cell subtype signatures that Applicants identified (**table 3**). The second, patient-level, controlled for the dependency between the scRNA-seq profiles of samples that were obtained from the same patient, having a patient-specific intercept that provided the baseline level for each patient.

[0633] Applicants used the mixed effects model to quantify the association between the different ICR signatures and the exposure to ICI or targeted therapy (the second and first sample-level covariates, respectively). When testing the association between the tumor composition and the treatments Applicants used the model described above without the 9 TME covariates.

[0634] Applicants implemented the HLM model in R, using the lme4 and lmerTest packages (CRAN.R-project.org/package=lme4, CRAN.R-project.org/package=lmerTest).

[0635] For each resistance signature, Applicants applied ANOVA to test if the inter-patient variation in the OE values was significantly greater than the intra-patient variation, and reported the least significant ANOVA p-value that was obtained.

The immune resistance program *vs.* resistance to MAPK inhibitors

[0636] To test if the immune resistance program is related to resistance to MAPK inhibitors Applicants analyzed a published clinical cohort of patient-matched melanoma tumors biopsied before MAPK inhibitor therapy and during disease progression (Hugo et al., 2015). Applicants used the same mixed-effects model described above (***Clinical longitudinal***

analysis (validation cohort 1)), except that instead of three treatment covariates Applicants had only one, denoting if the sample was pre or post MAPKi treatment. The implementation of this analysis and its application to this published cohort is provided via GitHub (github.com/livnatje/ImmuneResistance/wiki/Predicting-immunotherapy-resistance; ImmRes3_longitudinal.R).

Multiplexed, tissue cyclic immunofluorescence (t-CyCIF) of FFPE tissue slides

[0637] Formalin-fixed, paraffin-embedded (FFPE) tissue slides, 5 μm in thickness, were generated at the Brigham and Women's Hospital Pathology Core Facility from tissue blocks collected from patients under IRB-approved protocols (DFCI 11-104). Multiplexed, tissue cyclic immunofluorescence (t-CyCIF) was performed as described recently (Lin et al., 2018). For direct immunofluorescence, Applicants used the following antibodies: CEP170 (Abcam, ab84545), LAMP2 (R&D technologies, AF6228), MITF (Abcam, ab3201), DLL3 (Abcam, ab103102, Rab), MITF (Abcam, ab3201, Ms), S100α-488 (Abcam, ab207367), CD3-555 (Abcam, ab208514), CD8a-660 (eBioscience, 50-0008-80), cJUN-488 (Abcam, ab193780), cMyc-555 (Abcam, ab201780), HLAA-647 (Abcam, ab199837), TP53-488 (Cell Signaling, 5429), SQSTM1-555 (Abcam, ab203430). Stained slides from each round of CycIF were imaged with a CyteFinder slide scanning fluorescence microscope (RareCyte Inc. Seattle WA) using either a 10X (NA=0.3) or 40X long-working distance objective (NA = 0.6). Imager5 software (RareCyte Inc.) was used to sequentially scan the region of interest in 4 fluorescence channels. Image processing, background subtraction, image registration, single-cell segmentation and quantification were performed as previously described (Lin et al., 2018).

Mapping cell-cell interactions based on *in situ* imaging data

[0638] Given the processed imaging data, Applicants assigned cells into cell types by discretizing the log-transformed expression levels of the cell type markers (S100, MITF, CD3, and CD8). Applicants applied the EM algorithm for mixtures of normal distributions to characterize the two normal distributions for each of these cell type marker intensities. $S100^+/MITF^+/CD3^-/CD8^-$ cells were defined as malignant cells; $S100^-/MITF^-/CD3^+/CD8^-$ cells were defined as T cells, and $S100^-/MITF^-/CD3^+/CD8^+$ cells were defined as $CD8^+$ T cells; other cells were defined as uncharacterized.

[0639] For each image Applicants constructed a Delaunay (Gabriel) graph, where two cells are connected to each other if there is no other cell between them. Following the approach presented in (Goltsev et al., 2017), Applicants examined if cells of certain types

were less/more likely to be connected to each other in the graph. To this end, Applicants computed the odds ratio of cell-cell interactions of cell type A and cell type B by computing the observed frequency of interactions divided by the expected theoretical frequency (calculated as the total frequency of edges incident to type A multiplied by the total frequency of edges incident to type B). Two cell types are less or more likely to interact than expected by chance if the log-transformed odds ratio is less or more than 0, respectively. The significance of the deviation from zero was tested using the binomial distribution test.

[0640] For each malignant cell, Applicants computed an immune resistance score based on the *in situ* protein levels of the immune resistance markers. First, Applicants centered and scaled the log-transformed expression of each protein across the malignant cells from all images (to have a zero average and a standard deviation of 1). Using this normalized data, Applicants computed the resistance-up score as the sum expression of p53, DLL3, and Myc, the resistance-down score as the sum of HLA-A, Jun, LAMP2, and SQSTM1, and the final resistance score by subtracting the resistance-down score from the resistance-up score. The average resistance score of the malignant cells in each image was used as the *in situ* resistance score of the corresponding tumor. Applicants then compared these tumor resistance scores to those computed based on the scRNA-seq data from the same patient.

[0641] Next, Applicants examined the association between the expression of the individual markers and the overall resistance score in the malignant cells and the level of T cell infiltration. Each image in the data was composed of a few hundred frames (119-648 frames/image), where each frame consists of 1,502 cells on average. In each frame, Applicants computed: (1) the fraction of T cells, (2) the average expression of the individual markers in the malignant cells, and (3) the average immune resistance (as above) across the malignant cells. Applicants used a hierarchical logistic regression model to quantify the associations between the expression of the individual markers (or overall resistance score) in the malignant cells (2-3) and the fraction of T cells (1). The independent variables included the average expression of the marker (or the average immune resistance score) in the malignant cells of the frame (level-1), the average expression of normalization markers in the malignant cells of the frame (level-1), and the image the frame was sampled from (level-2). The dependent variable was the discretized T cell infiltration level of the frame, defining frames with high/low lymphocyte-fraction as “hot”/”cold”, respectively. Applicants used different cutoffs to define hot/cold frames, such that a frame with a T cell fraction below the *Q* quantile was defined as cold, and a T cell fraction above the *1-Q* quantile was defined as

hot. Applicants report only markers that showed a consistent association with the "hot" or "cold" niche, when starting with a cutoff of Q = median (0.5), and then using increasingly more stringent cutoffs (0.4, 0.3, 0.2 and 0.1). Applicants provide the p-values obtained with $Q = 0.2$.

Integrating scRNA-seq and spatial data

[0642] Applicants integrated the scRNA-seq and multiplexed immunofluorescence (t-CyCIF) data via a variant of Canonical Correlation Analysis (CCA), using the code provided in the R toolkit Seurat (Butler and Satija, 2017). CCA aims to identify shared correlation structures across datasets, such that each dataset provides multiple measurements of a gene-gene covariance structure, and patterns which are common to both datasets are identified. Cells from both sources are then represented in an aligned-CCA space (Butler and Satija, 2017).

[0643] In the application, each cell in the t-CyCIF data was represented by the log-transformed intensities of 14 markers. Each cell in the scRNA-seq data was represented by the imputed expression of the genes encoding the same 14 proteins. To impute the scRNA-seq data Applicants identified a signature for each marker, consisting of the top 50 genes which were mostly correlated with the marker expression across the cell population in the scRNA-seq data. Applicants then used the OE of the marker signature as a measure of its activity in the scRNA-seq data.

[0644] The cells from both sources were represented in the resulting aligned-CCA space. Next, Applicants used the first five aligned-CCA dimensions to cluster the cells and represented them in a 2D t-SNE embedding (van der Maaten and Hinton, 2008). Clustering was preformed using a shared nearest neighbor (SNN) modularity optimization based clustering algorithm, which calculates k-nearest neighbors, constructs an SNN graph, and optimizes the modularity function to determine clusters (Waltman and van Eck, 2013).

[0645] To examine if cells clustered according to cell type or according to source Applicants computed the expected number of cells from each two categories to be assigned to the same cluster by chance, assuming a random distribution of cells into clusters. Applicants then used the observed *vs.* expected co-clustering ratio to quantify the deviation from the random distribution, and used the binomial test to compute the statistical significance of this deviation from random.

Survival and ICI-response predictions

[0646] To test if a given signature predicts survival or progression free-survival (PFS) Applicants first computed the OE of the signature in each tumor based on the bulk RNA-Seq data. Next, Applicants used a Cox regression model with censored data to compute the significance of the association between the OE values and prognosis. To examine if the signature's predictive value was significant beyond T cell infiltration levels Applicants computed for each sample the OE of the $CD8^+$ T cell signature (above), used this as another covariate in the Cox regression model, and computed another p-value for each signature, based on its association with survival or PFS in this two-covariate model.

[0647] To visualize the predictions of a specific signature in a Kaplan Meier (KM) plot, Applicants stratified the patients into three groups according to the OE of the signature: high or low expression correspond to the top or bottom 25% of the population, respectively, and intermediate otherwise. Applicants used a one-sided log-rank test to examine if there was a significant difference between these three patient groups in terms of their survival or PFS rates.

[0648] OR (or CB) was defined according to RESICT criteria, such that patients with a complete or partial response were defined as OR patients. Patients with progressive disease were defined as PD, and patients with more ill-defined response, such as stable disease or marginal responses, were excluded from this analysis. Applicants further stratified the OR patients according to the duration of the response: (**1**) less than 6 months, (**2**) more than 6 months and less than a year, and (**3**) more than a year (long-term OR). Applicants applied one-sided t-tests to examine if the OE of the different signatures were differentially expressed in the OR *vs.* PD patients, or in the long-term OR patients compared to the PD patients. Finally, Applicants tested the ability of the different signatures to predict complete response by comparing (t-test) between the complete responders and all other patients with a RECIST annotation (n = 101, see, e.g., **Figures 4H, 14, 48H and 66H**), and computing the Area Under the Curve (AUC) of the resulting ROC curve.

[0649] To reproduce this analysis and results see *ImmRes_valCohort2.R* provided in github.com/livnatje/ImmuneResistance/wiki/Predicting-immunotherapy-resistance (relevant functions are included in *ImmRes5_valCohort2.R*).

Controlling for cell cycle effects in the immune resistance OE scores

[0650] The single-cell data demonstrated that cycling cells have higher expression of the immune resistant program. Since the tumor proliferation rate may be a dynamic and context-dependent property, it might be advisable to compare between tumors based on their *basal*

resistance level, namely, after controlling for the cell cycle effect. To this end, Applicants compute for each tumor the OE of two cell cycle signatures (G1/S and G2/M signatures in **Table 26A and 9**). Applicants then fitted a linear model to estimate the expected OE of the resistance signature, when using the OE of the two cell cycle signatures as covariates. The residuals of this linear model, which quantify the deviation from the expected resistance OE values, were considered as the *basal resistance level*. In an example, Applicants preformed this analysis with different resistance signatures (e.g., uICR, exclusion, etc.).

Alternative ICI response predictors

[0651] To compare the predictive value of the resistance signatures to that of other signatures, Applicants repeated the prediction process, as describe in ***Survival and ICI response predictions***, for each of the following gene signatures (**Table 29 and 9**): (**1**) cell type specific signatures identified from the scRNA-seq data (as described in the ***Data-driven signatures of specific cell types*** section); (**2**) signatures that characterize melanoma cell states (the AXL-high, MITF-high, and cell cycle states from (Tirosh et al., 2016)); (**3**) six sets of genes whose CRISPR knockout in melanoma cells conferred resistance or sensitivity (FDR < 0.05) to different types of immune killing according to a genome-scale *in vivo* screen (Manguso et al., 2017); (**4**) genes whose CRISPR knockout in melanoma cells conferred resistance to T cell killing (top 10 and top 50) in a genome-scale co-culture screen (Patel et al., 2017); (**5**) immune-related signatures that were identified based on the analysis of multiple pembrolizumab clinical datasets, and were shown to predict the response to pembrolizumab in an independent cohort (Ayers et al., 2017); **(6)** the Fluidigm Advanta™ Immuno-Oncology Gene Expression signatures (www.fluidigm.com/applications/advanta-immuno-oncology-gene-expression-assay); **(7)** immunotherapy resistance signatures identified in a clinical cohort of pre and post nivolumab treated melanomas (Riaz et al., 2017); **(8)** immune related signatures identified in a clinical melanoma cohort (Hugo et al., 2015) **(9)** immunotherapy resistance signatures identified in a clinical cohort of pre-anti-PD1 melanoma tumors (Hugo et al., 2016) and **(10)** PD-L1 expression.

[0652] Applicants summarize in **table 9** the predictive value of each of these signatures when applied to predict melanoma (TCGA) patient survival, and the PFS, clinical benefit (CB), and complete response in the melanoma patients of the aPD1 cohort.

Searching for immune sensitizing drugs

[0653] Applicants performed the following analysis to identify drugs that could selectively eradicate malignant cells with a high expression of the resistance program, using

efficacy measures of 131 drugs across 639 human cancer cell lines (Garnett et al., 2012). For each drug, Applicants defined sensitive cell lines as those with the lowest (bottom 25%, however, the bottom 10% were previously used to define sensitive cell lines) IC50 values. Applicants then used the gene expression provided in (Garnett et al., 2012), computed the OE of the resistance program in each of the 639 cells, and defined "resistant" cell lines as those with the highest OE values (top 25%, or previously, top 10%). Next, for each drug Applicants built a hierarchical logistic regression model, where the dependent variable is the cell line's (drug-specific) binary sensitivity assignment, and the independent variables are the cell lines' "resistance" assignments (level-1) and cancer types (level-2). Drugs then were ranked based on the one-tailed p-values that quantify the significance of the positive association between the drug sensitivity (dependent) variable and the immune resistance (independent) variable.

[0654] To reproduce this analysis and results see github.com/livnatje/ImmuneResistance/wiki/Repressing-the-immune-resistance-program.

Abemaciclib treatment of melanoma cell lines

[0655] Established melanoma cell lines IGR39, UACC62 and A2058 were acquired from the Cancer Cell Line Encyplopedia (CCLE) from the Broad Institute. Cells were treated every 3 days with 500 nM abemacilib (LY2835219, MedChemExpress) or DMSO control. The doubling time of each cell line was established and lines were seeded such that cells collected for scRNA-seq were derived from culture dishes with ~50-60% confluency on day 7 of treatment. Cells were lifted off culture dishes using Versene solution (Life Technologies), washed twice in 1x PBS, counted and resuspended in PBS supplemented with 0.04% BSA for loading for scRNA-seq with the 10X Genomics platform.

Melanoma-TIL co-culture

[0656] An autologous pair of melanoma and TIL culture was provided by MD Anderson Cancer Center and were established using previously described protocols (Peng et al., 2016). Melanoma cells were pre-treated with 500 nM abemaciclib or DMSO control for 7 days followed by co-culture with autologous TILs (with an effector to target ratio of 5:1) for 48 hours. TILs were removed by pipetting of the supernatant, and the remaining melanoma cells were washed twice with PBS, lifted off the culture dish, and resuspended in PBS supplemented with 0.04% BSA for loading for scRNA-seq with the 10X Genomics platform.

Mouse experiments

[0657] All experiments were performed in accordance with the Dana-Farber Cancer Institute (DFCI) IACUC guidelines at the DFCI Longwood Center Animal Resource Facility per protocol 08-049. 5.0 * 10^5 B16F10 cells were subcutaneously injected into 6 weeks old female C57BL/6 mice (The Jackson Laboratory). Four or seven days after injection, animals were treated with either (**1**) isotype control antibody injected intraperitoneally (2A3 and polyclonal syrian hamster IgG, 200μg/mouse and 100μg/mouse, respectively) every 3 days for a total of 4 doses; (**2**) abemaciclib 90 mg/kg daily administered by oral gavage (LY2835219, MedChemExpress) for a total of 10 doses; (**3**) combination immune checkpoint blockade (ICI) with αPD-1 (clone 29F.1A12, 200μg/mouse) plus αCTLA-4 (clone 9H10, #BP0131, 100μg/mouse) every 3 days for a total of 4 doses; (**4**) abemaciclib (90mg/kg) daily for 4 days followed by ICI every 3 days for a total of 4 doses; (**5**) ICI for one initial dose followed 3 days later by abemaciclib (90mg/kg) daily combined with ICI every 3 days for an additional 3 doses; or (**6**) upfront combination of ICI and abemaciclib (75mg/kg) every 3 days for a total of 4 doses. $CD8^+$ T cell depletion was achieved using CD8b mAb (clone53-5.8, #BE0223, 100μg/mouse) that was administered on day-1, day 0 once a week until the end of the experiment. Tumor size was measured using digital calipers every 3 days. Tumor volume was determined by calculating (length x $width^2$)/2. Growth curves and survival curves were generated using GraphPad Prism v8.

Abemaciclib doubling time and cytostatic effect

[0658] 5 x 10^4 human melanoma cells (Melanoma cell line 2686, provided by MDACC) were seeded and treated with either DMSO or 500 nM abemaciclib (LY2835219, MedChemExpress) daily for a total of 6 days. Cell number and viability were determined using the Countess™ II FL Automated Cell Counter (ThermoFisher) on days 2, 4 and 6. All experiments were performed in triplicates. Cell doubling per 24 hours was determined based on cell numbers comparing cells seeded and on day 6 using the following formula: duration (in days) x log(2)/log(final cell number) – log(initial cell number).

Mouse melanoma cell line culture and profiling

[0659] B16F10, MC38 and CT26 cell line were obtained from American Type Culture Collection (ATCC). B16F10 cells were maintained in complete DMEM media (10% FBS and 50U/ml of Penicillin-Streptomycin). MC38 and CT26 were maintained in RPMI-1640 (10% FBS and 50U/ml of Penicillin-Streptomycin). For scRNA-seq, cells were washed twice with PBS, incubated with trypsin 0.05% for 2 minutes at 37ºC, quenched with complete media, and resuspended in PBS supplemented with 0.04% BSA prior to loading onto the

Chromium 10X platform and processed as described above. All cell lines were tested for Mycoplasma.

Data and code availability

[0660] Processed scRNA-seq data generated for this study, and the Overall Expression of the different signatures that were used in the analysis of the two clinical validation cohorts, are provided through the Single Cell Portal along with interactive plots at the following URL: portals.broadinstitute.org/single_cell/study/melanoma-immunotherapy-resistance. The processed scRNA-seq data is also provided via the Gene Expression Omnibus (GEO), accession number GSE115978. The raw scRNA-seq data is being deposited in dbGAP.

[0661] All the relevant code, with instructions is provided via GitHub github.com/livnatje/ImmuneResistance. The code enables one to repeat the analyses that were performed, reproduce the results, figures, and tables, and apply the computational approaches to other datasets.

T cell cytotoxicity and exhaustion signature analysis

[0662] The analysis of T-cell exhaustion *vs.* T-cell cytotoxicity was performed as previously described (Hugo et al., 2016), with six different exhaustion signatures, as provided in (Sharma, et al., 2015) and (Li et al., 2017). First, Applicants computed the cytotoxicity and exhaustion scores of each CD8 T cell. Next, to control for the association between the expression of exhaustion and cytotoxicity markers, Applicants estimated the relationship between the cytotoxicity and exhaustion scores using locally-weighted polynomial regression (LOWESS, black line in **Fig. 1E and 8B**). Based on these values, Applicants defined T cells as functional if they fulfilled two criteria: (1) their cytotoxicity score was at the top 20% of the CD8 T cell population (across all patients), and (2) their exhaustion scores were lower than expected given their cytotoxicity scores (below the dashed line in **Fig. 1E and 8B**). Applicants then applied a hypergeometric test to examine if the CD8 T cells of a given patient were enriched with functional cells.

Identifying T cell clones and estimating the fraction of clonally expanded T-cells

[0663] Applicants reconstructed the T-cell Receptors (TCRs) using TraCeR (Eisenhauer et al., 2009), with the Python package provided in github.com/Teichlab/tracer. TCR reconstruction significantly improved in the new cohort compared to previously analyzed patients (**table 1**): 92% CD8 T-cells had reconstructed TCRs, compared to only 50% such cells in the previously published cohort (**fig. 9A**). This is likely due to shorter read length and lower sequencing depth in the previous study (Sharma, et al., 2015). Applicants assigned T

cells to the clones defined in the TraCeR output. Reassuringly, cells from different patients were never falsely assigned to the same clone, and CD8 and CD4 T-cells were always assigned to different clones, even when they were obtained from the same tumor. In the CD8 T-cells Applicants detected 137 clones (**Fig. 1F**). In the CD4 T-cells Applicants detected only 29 clones, with at most 3 cells per clone.

[0664] The size and number of clones that Applicants identified in each tumor is affected by the number of T-cells that were sequenced from that tumor, and the success rate of TCR reconstruction. To estimate the fraction of clonally expanded T-cells in a given tumor Applicants therefore sampled its T-cells as follows. First, Applicants restricted the analysis to tumors with at least 20 CD8 T-cells with a full-length reconstructed TCR. Next, Applicants repeatedly sampled 20 cells from each tumor, such that, in each iteration, Applicants computed for every tumor the fraction of clonally expanded cells, namely, the fraction of sampled cells that shared their TCR with another cell within the sampled population. The average fraction of clonally expanded cells was used as an estimate of the T-cell clonal expansion level (**fig. 9B**).

References

Akbani, R., Akdemir, K.C., Aksoy, B.A., Albert, M., Ally, A., Amin, S.B., Arachchi, H., Arora, A., Auman, J.T., Ayala, B., et al. (2015). Genomic Classification of Cutaneous Melanoma. Cell *161*, 1681–1696.

Algazi, A.P., Tsai, K.K., Shoushtari, A.N., Munhoz, R.R., Eroglu, Z., Piulats, J.M., Ott, P.A., Johnson, D.B., Hwang, J., Daud, A.I., et al. (2016). Clinical outcomes in metastatic uveal melanoma treated with PD-1 and PD-L1 antibodies. Cancer *122*, 3344–3353.

Ayers, M., Lunceford, J., Nebozhyn, M., Murphy, E., Loboda, A., Kaufman, D.R., Albright, A., Cheng, J.D., Kang, S.P., Shankaran, V., et al. (2017). IFN-γ –related mRNA profile predicts clinical response to PD-1 blockade. J. Clin. Invest. *127*, 2930–2940.

F. Azimi et al., Tumor-Infiltrating Lymphocyte Grade Is an Independent Predictor of Sentinel Lymph Node Status and Survival in Patients With Cutaneous Melanoma. J. Clin. Oncol. 30, 2678–2683 (2012).

Barretina, J., Caponigro, G., Stransky, N., Venkatesan, K., Margolin, A.A., Kim, S., Wilson, C.J., Lehár, J., Kryukov, G.V., Sonkin, D., et benjal. (2012). The Cancer Cell Line

Encyclopedia enables predictive modelling of anticancer drug sensitivity. Nature *483*, 603–607.

Benjamini, Y., and Hochberg, Y. (1995). Controlling the False Discovery Rate: A Practical and Powerful Approach to Multiple Testing. J. R. Stat. Soc. Ser. B Methodol. *57*, 289–300.

D. Bogunovic et al., Immune profile and mitotic index of metastatic melanoma lesions enhance clinical staging in predicting patient survival. Proc. Natl. Acad. Sci. U. S. A. 106, 20429–20434 (2009).

Butler, A., and Satija, R. (2017). Integrated analysis of single cell transcriptomic data across conditions, technologies, and species. BioRxiv 164889.

Carter, S.L., Cibulskis, K., Helman, E., McKenna, A., Shen, H., Zack, T., Laird, P.W., Onofrio, R.C., Winckler, W., Weir, B.A., et al. (2012). Absolute quantification of somatic DNA alterations in human cancer. Nat. Biotechnol. *30*, 413–421.

M. Challa-Malladi et al., Combined genetic inactivation of β2-Microglobulin and CD58 reveals frequent escape from immune recognition in diffuse large B cell lymphoma. Cancer Cell. 20, 728–740 (2011).

Curran, M.A., Montalvo, W., Yagita, H., and Allison, J.P. (2010). PD-1 and CTLA-4 combination blockade expands infiltrating T cells and reduces regulatory T and myeloid cells within B16 melanoma tumors. Proc. Natl. Acad. Sci. U. S. A. *107*, 4275–4280.

Deng, J., Wang, E.S., Jenkins, R.W., Li, S., Dries, R., Yates, K., Chhabra, S., Huang, W., Liu, H., Aref, A.R., et al. (2018). CDK4/6 Inhibition Augments Antitumor Immunity by Enhancing T-cell Activation. Cancer Discov. *8*, 216–233.

Dobin, A., Davis, C.A., Schlesinger, F., Drenkow, J., Zaleski, C., Jha, S., Batut, P., Chaisson, M., and Gingeras, T.R. (2013). STAR: ultrafast universal RNA-seq aligner. Bioinforma. Oxf. Engl. *29*, 15–21.

E. A. Eisenhauer et al., New response evaluation criteria in solid tumours: revised RECIST guideline (version 1.1). Eur. J. Cancer Oxf. Engl. 1990. 45, 228–247 (2009).

Ester, M., Kriegel, H.-P., Sander, J., and Xu, X. (1996). A density-based algorithm for discovering clusters a density-based algorithm for discovering clusters in large spatial databases with noise. In Proceedings of the Second International Conference on Knowledge Discovery and Data Mining, (Portland, Oregon: AAAI Press), pp. 226–231.

Fan, J., Salathia, N., Liu, R., Kaeser, G.E., Yung, Y.C., Herman, J.L., Kaper, F., Fan, J.-B., Zhang, K., Chun, J., et al. (2016). Characterizing transcriptional heterogeneity through pathway and gene set overdispersion analysis. Nat. Methods *13*, 241–244.

Feng, Y., Yao, Z., and Klionsky, D.J. (2015). How to control self-digestion: transcriptional, post-transcriptional, and post-translational regulation of autophagy. Trends Cell Biol. *25*, 354–363.

Fridman, W.H., Pagès, F., Sautès-Fridman, C., and Galon, J. (2012). The immune contexture in human tumours: impact on clinical outcome. Nat. Rev. Cancer *12*, 298–306.

J. Gao et al., Loss of IFN-γ Pathway Genes in Tumor Cells as a Mechanism of Resistance to Anti-CTLA-4 Therapy. Cell. 167, 397–404.e9 (2016).

Garnett, M.J., Edelman, E.J., Heidorn, S.J., Greenman, C.D., Dastur, A., Lau, K.W., Greninger, P., Thompson, I.R., Luo, X., Soares, J., et al. (2012). Systematic identification of genomic markers of drug sensitivity in cancer cells. Nature *483*, 570–575.

G. T. Gibney, L. M. Weiner, M. B. Atkins, Predictive biomarkers for checkpoint inhibitor based immunotherapy. Lancet Oncol. 17, e542–e551 (2016).

Goel, S., DeCristo, M.J., Watt, A.C., BrinJones, H., Sceneay, J., Li, B.B., Khan, N., Ubellacker, J.M., Xie, S., Metzger-Filho, O., et al. (2017). CDK4/6 inhibition triggers anti-tumour immunity. Nature *548*, 471–475.

Goltsev, Y., Samusik, N., Kennedy-Darling, J., Bhate, S., Hale, M., Vasquez, G., and Nolan, G. (2017). Deep profiling of mouse splenic architecture with CODEX multiplexed imaging. BioRxiv 203166.

Gong, X., Litchfield, L.M., Webster, Y., Chio, L.-C., Wong, S.S., Stewart, T.R., Dowless, M., Dempsey, J., Zeng, Y., Torres, R., et al. (2017). Genomic Aberrations that Activate D-type Cyclins Are Associated with Enhanced Sensitivity to the CDK4 and CDK6 Inhibitor Abemaciclib. Cancer Cell *32*, 761-776.e6.

Gordy, J.T., Luo, K., Zhang, H., Biragyn, A., and Markham, R.B. (2016). Fusion of the dendritic cell-targeting chemokine MIP3 α to melanoma antigen Gp100 in a therapeutic DNA vaccine significantly enhances immunogenicity and survival in a mouse melanoma model. J. Immunother. Cancer *4*, 96.

Hangauer, M.J., Viswanathan, V.S., Ryan, M.J., Bole, D., Eaton, J.K., Matov, A., Galeas, J., Dhruv, H.D., Berens, M.E., Schreiber, S.L., et al. (2017). Drug-tolerant persister cancer cells are vulnerable to GPX4 inhibition. Nature *551*, 247.

Herbst, R.S., Soria, J.-C., Kowanetz, M., Fine, G.D., Hamid, O., Gordon, M.S., Sosman, J.A., McDermott, D.F., Powderly, J.D., Gettinger, S.N., et al. (2014). Predictive correlates of response to the anti-PD-L1 antibody MPDL3280A in cancer patients. Nature *515*, 563–567.

Hodi, F.S., O'Day, S.J., McDermott, D.F., Weber, R.W., Sosman, J.A., Haanen, J.B., Gonzalez, R., Robert, C., Schadendorf, D., Hassel, J.C., et al. (2010). Improved survival with ipilimumab in patients with metastatic melanoma. N. Engl. J. Med. *363*, 711–723.

F. S. Hodi, Kluger HM, Sznol M, Durable, long-term survival in previously treated patients with advanced melanoma who received nivolumab monotherapy in a phase I trial. 2016 AACR Annu. Meet. Abstr. CT001 Present. April 17 2016.

Holm, S. (1979). A Simple Sequentially Rejective Multiple Test Procedure. Scand. J. Stat. *6*, 65–70.

Hugo, W., Shi, H., Sun, L., Piva, M., Song, C., Kong, X., Moriceau, G., Hong, A., Dahlman, K.B., Johnson, D.B., et al. (2015). Non-genomic and Immune Evolution of Melanoma Acquiring MAPKi Resistance. Cell *162*, 1271–1285.

Hugo, W., Zaretsky, J.M., Sun, L., Song, C., Moreno, B.H., Hu-Lieskovan, S., Berent-Maoz, B., Pang, J., Chmielowski, B., Cherry, G., et al. (2016). Genomic and Transcriptomic Features of Response to Anti-PD-1 Therapy in Metastatic Melanoma. Cell *165*, 35–44.

Kharchenko, P.V., Silberstein, L., and Scadden, D.T. (2014). Bayesian approach to single-cell differential expression analysis. Nat. Methods *11*, 740–742.

Kress, T.R., Sabo, A., and Amati, B. (2015). MYC: connecting selective transcriptional control to global RNA production. Nat. Rev. Cancer *15*, 593–607.

J. Lamb et al., The Connectivity Map: using gene-expression signatures to connect small molecules, genes, and disease. Science. 313, 1929–1935 (2006).

J. Landsberg et al., Melanomas resist T-cell therapy through inflammation-induced reversible dedifferentiation. Nature. 490, 412–416 (2012).

Langmead, B., Trapnell, C., Pop, M., and Salzberg, S.L. (2009). Ultrafast and memory-efficient alignment of short DNA sequences to the human genome. Genome Biol. *10*, R25.

Larkin, J., Chiarion-Sileni, V., Gonzalez, R., Grob, J.J., Cowey, C.L., Lao, C.D., Schadendorf, D., Dummer, R., Smylie, M., Rutkowski, P., et al. (2015). Combined Nivolumab and Ipilimumab or Monotherapy in Untreated Melanoma. N. Engl. J. Med. *373*, 23–34.

Laurens Maaten (2009). Learning a Parametric Embedding by Preserving Local Structure. In Proceedings of the Twelth International Conference on Artificial Intelligence and Statistics, David van Dyk, and Max Welling, eds. (PMLR), pp. 384–391.

Lesterhuis, W.J., Rinaldi, C., Jones, A., Rozali, E.N., Dick, I.M., Khong, A., Boon, L., Robinson, B.W., Nowak, A.K., Bosco, A., et al. (2015). Network analysis of immunotherapy-induced regressing tumours identifies novel synergistic drug combinations. Sci. Rep. *5*, srep12298.

Li, B., and Dewey, C.N. (2011). RSEM: accurate transcript quantification from RNA-Seq data with or without a reference genome. BMC Bioinformatics *12*, 323.

H. Li et al., Reference component analysis of single-cell transcriptomes elucidates cellular heterogeneity in human colorectal tumors. Nat. Genet. 49, 708–718 (2017).

Lin, J.-R., Izar, B., Mei, S., Wang, S., Shah, P., and Sorger, P. (2017). A simple open-source method for highly multiplexed imaging of single cells in tissues and tumours. BioRxiv 151738.

Lin, J.-R., Izar, B., Wang, S., Yapp, C., Mei, S., Shah, P.M., Santagata, S., and Sorger, P.K. (2018). Highly multiplexed immunofluorescence imaging of human tissues and tumors using t-CyCIF and conventional optical microscopes. ELife *7*.

van der Maaten, L., and Hinton, G. (2008). Visualizing Data using t-SNE. *9*, 2579-2605.

Manguso, R.T., Pope, H.W., Zimmer, M.D., Brown, F.D., Yates, K.B., Miller, B.C., Collins, N.B., Bi, K., LaFleur, M.W., Juneja, V.R., et al. (2017). In vivo CRISPR screening identifies Ptpn2 as a cancer immunotherapy target. Nature *547*, 413–418.

Mariathasan, S., Turley, S.J., Nickles, D., Castiglioni, A., Yuen, K., Wang, Y., Kadel Iii, E.E., Koeppen, H., Astarita, J.L., Cubas, R., et al. (2018). TGFβ attenuates tumour response to PD-L1 blockade by contributing to exclusion of T cells. Nature *554*, 544–548.

McDavid, A., Finak, G., Chattopadyay, P.K., Dominguez, M., Lamoreaux, L., Ma, S.S., Roederer, M., and Gottardo, R. (2013). Data exploration, quality control and testing in single-cell qPCR-based gene expression experiments. Bioinforma. Oxf. Engl. *29*, 461–467.

Miao, D., Margolis, C.A., Gao, W., Voss, M.H., Li, W., Martini, D.J., Norton, C., Bosse, D., Wankowicz, S.M., Cullen, D., et al. (2018). Genomic correlates of response to immune checkpoint therapies in clear cell renal cell carcinoma. Science *359*, 801–806.

R. Muthuswamy et al., NF-κB hyperactivation in tumor tissues allows tumor-selective reprogramming of the chemokine microenvironment to enhance the recruitment of cytolytic T effector cells. Cancer Res. 72, 3735–3743 (2012).

Nelson, P.J., and Muenchmeier, N. (2013). Membrane-anchored chemokine fusion proteins: A novel class of adjuvants for immunotherapy. Oncoimmunology *2*, e26619.

Newman, A.M., Liu, C.L., Green, M.R., Gentles, A.J., Feng, W., Xu, Y., Hoang, C.D., Diehn, M., and Alizadeh, A.A. (2015). Robust enumeration of cell subsets from tissue expression profiles. Nat. Methods *12*, 453–457.

Oki, S., Ohta, T., Shioi, G., Hatanaka, H., Ogasawara, O., Okuda, Y., Kawaji, H., Nakaki, R., Sese, J., and Meno, C. (2018). Integrative analysis of transcription factor occupancy at enhancers and disease risk loci in noncoding genomic regions.

Pan, D., Kobayashi, A., Jiang, P., Ferrari de Andrade, L., Tay, R.E., Luoma, A.M., Tsoucas, D., Qiu, X., Lim, K., Rao, P., et al. (2018). A major chromatin regulator determines resistance of tumor cells to T cell-mediated killing. Science *359*, 770–775.

A. P. Patel et al., Single-cell RNA-seq highlights intratumoral heterogeneity in primary glioblastoma. Science. 344, 1396–1401 (2014).

Patel, S.J., Sanjana, N.E., Kishton, R.J., Eidizadeh, A., Vodnala, S.K., Cam, M., Gartner, J.J., Jia, L., Steinberg, S.M., Yamamoto, T.N., et al. (2017). Identification of essential genes for cancer immunotherapy. Nature *548*, 537–542.

Peng, W., Chen, J.Q., Liu, C., Malu, S., Creasy, C., Tetzlaff, M.T., Xu, C., McKenzie, J.A., Zhang, C., Liang, X., et al. (2016). Loss of PTEN Promotes Resistance to T Cell-Mediated Immunotherapy. Cancer Discov. *6*, 202–216.

S. Picelli et al., Smart-seq2 for sensitive full-length transcriptome profiling in single cells.

E. Pikarsky et al., NF-kappaB functions as a tumour promoter in inflammation-associated cancer. Nature. 431, 461–466 (2004).

Postow, M.A., Chesney, J., Pavlick, A.C., Robert, C., Grossmann, K., McDermott, D., Linette, G.P., Meyer, N., Giguere, J.K., Agarwala, S.S., et al. (2015). Nivolumab and ipilimumab versus ipilimumab in untreated melanoma. N. Engl. J. Med. *372*, 2006–2017.

Puram, S.V., Tirosh, I., Parikh, A.S., Patel, A.P., Yizhak, K., Gillespie, S., Rodman, C., Luo, C.L., Mroz, E.A., Emerick, K.S., et al. (2017). Single-Cell Transcriptomic Analysis of Primary and Metastatic Tumor Ecosystems in Head and Neck Cancer. Cell *171*, 1611-1624.e24.

Ramilowski, J.A., Goldberg, T., Harshbarger, J., Kloppmann, E., Lizio, M., Satagopam, V.P., Itoh, M., Kawaji, H., Carninci, P., Rost, B., et al. (2015). A draft network of ligand–receptor-mediated multicellular signalling in human. Nat. Commun. *6*, 7866.

Ribas, A., Puzanov, I., Dummer, R., Schadendorf, D., Hamid, O., Robert, C., Hodi, F.S., Schachter, J., Pavlick, A.C., Lewis, K.D., et al. (2015). Pembrolizumab versus investigator-choice chemotherapy for ipilimumab-refractory melanoma (KEYNOTE-002): a randomised, controlled, phase 2 trial. Lancet Oncol. *16*, 908–918.

Riaz, N., Havel, J.J., Makarov, V., Desrichard, A., Urba, W.J., Sims, J.S., Hodi, F.S., Martín-Algarra, S., Mandal, R., Sharfman, W.H., et al. (2017). Tumor and Microenvironment Evolution during Immunotherapy with Nivolumab. Cell *171*.

Rosvall, M., and Bergstrom, C.T. (2008). Maps of random walks on complex networks reveal community structure. Proc. Natl. Acad. Sci. U. S. A. *105*, 1118–1123.

Schaer, D.A., Beckmann, R.P., Dempsey, J.A., Huber, L., Forest, A., Amaladas, N., Li, Y., Wang, Y.C., Rasmussen, E.R., Chin, D., et al. (2018). The CDK4/6 Inhibitor Abemaciclib Induces a T Cell Inflamed Tumor Microenvironment and Enhances the Efficacy of PD-L1 Checkpoint Blockade. Cell Rep. *22*, 2978–2994.

Shaffer, S.M., Dunagin, M.C., Torborg, S.R., Torre, E.A., Emert, B., Krepler, C., Beqiri, M., Sproesser, K., Brafford, P.A., Xiao, M., et al. (2017). Rare cell variability and drug-induced reprogramming as a mode of cancer drug resistance. Nature *546*, 431–435.

Shalek, A.K., Satija, R., Adiconis, X., Gertner, R.S., Gaublomme, J.T., Raychowdhury, R., Schwartz, S., Yosef, N., Malboeuf, C., Lu, D., et al. (2013). Single-cell transcriptomics reveals bimodality in expression and splicing in immune cells. Nature *498*, 236–240.

Shalek, A.K., Satija, R., Shuga, J., Trombetta, J.J., Gennert, D., Lu, D., Chen, P., Gertner, R.S., Gaublomme, J.T., Yosef, N., et al. (2014). Single-cell RNA-seq reveals dynamic paracrine control of cellular variation. Nature *510*, 363–369.

Shannon, P., Markiel, A., Ozier, O., Baliga, N.S., Wang, J.T., Ramage, D., Amin, N., Schwikowski, B., and Ideker, T. (2003). Cytoscape: a software environment for integrated models of biomolecular interaction networks. Genome Res. *13*, 2498–2504.

Sharma, P., and Allison, J.P. (2015). The future of immune checkpoint therapy. Science *348*, 56–61.

Sharma, P., Hu-Lieskovan, S., Wargo, J.A., and Ribas, A. (2017). Primary, Adaptive, and Acquired Resistance to Cancer Immunotherapy. Cell *168*, 707–723.

M. Singer et al., A Distinct Gene Module for Dysfunction Uncoupled from Activation in Tumor-Infiltrating T Cells. Cell. 166, 1500–1511.e9 (2016).

S. Spranger, R. Bao, T. F. Gajewski, Melanoma-intrinsic β-catenin signalling prevents antitumour immunity. Nature. 523, 231–235 (2015).

M. J. T. Stubbington et al., T cell fate and clonality inference from single-cell transcriptomes. Nat. Methods. 13, 329–332 (2016).

Subramanian, A., Tamayo, P., Mootha, V.K., Mukherjee, S., Ebert, B.L., Gillette, M.A., Paulovich, A., Pomeroy, S.L., Golub, T.R., Lander, E.S., et al. (2005). Gene set enrichment analysis: a knowledge-based approach for interpreting genome-wide expression profiles. Proc. Natl. Acad. Sci. U. S. A. *102*, 15545–15550.

Subramanian, A., Narayan, R., Corsello, S.M., Peck, D.D., Natoli, T.E., Lu, X., Gould, J., Davis, J.F., Tubelli, A.A., Asiedu, J.K., et al. (2017). A Next Generation Connectivity Map: L1000 Platform and the First 1,000,000 Profiles. Cell *171*, 1437-1452.e17.

J. M. Taube et al., Sci. Transl. Med., in press, doi:10.1126/scitranslmed.3003689.

Tirosh, I., Izar, B., Prakadan, S.M., Wadsworth, M.H., Treacy, D., Trombetta, J.J., Rotem, A., Rodman, C., Lian, C., Murphy, G., et al. (2016a). Dissecting the multicellular ecosystem of metastatic melanoma by single-cell RNA-seq. Science *352*, 189–196.

I. Tirosh et al., Single-cell RNA-seq supports a developmental hierarchy in human oligodendroglioma. Nature. 539, 309–313 (2016b).

Trombetta, J.J., Gennert, D., Lu, D., Satija, R., Shalek, A.K., and Regev, A. (2014). Preparation of Single-Cell RNA-Seq Libraries for Next Generation Sequencing. Curr. Protoc. Mol. Biol. Ed. Frederick M Ausubel Al *107*, 4.22.1-4.22.17.

P. C. Tumeh et al., PD-1 blockade induces responses by inhibiting adaptive immune resistance. Nature. 515, 568–571 (2014).

Van Allen, E.M., Miao, D., Schilling, B., Shukla, S.A., Blank, C., Zimmer, L., Sucker, A., Hillen, U., Foppen, M.H.G., Goldinger, S.M., et al. (2015). Genomic correlates of response to CTLA-4 blockade in metastatic melanoma. Science *350*, 207–211.

A. S. Venteicher et al., Decoupling genetics, lineages, and microenvironment in IDH mutant gliomas by single-cell RNA-seq. Science. 355 (2017), doi:10.1126/science.aai8478.

Viswanathan, V.S., Ryan, M.J., Dhruv, H.D., Gill, S., Eichhoff, O.M., Seashore-Ludlow, B., Kaffenberger, S.D., Eaton, J.K., Shimada, K., Aguirre, A.J., et al. (2017). Dependency of a therapy-resistant state of cancer cells on a lipid peroxidase pathway. Nature *547*, 453.

Wagner, A., Regev, A., and Yosef, N. (2016). Revealing the vectors of cellular identity with single-cell genomics. Nat. Biotechnol. *34*, 1145–1160.

Waltman, L., and van Eck, N.J. (2013). A smart local moving algorithm for large-scale modularity-based community detection. Eur. Phys. J. B *86*.

J. M. Zaretsky et al., Mutations Associated with Acquired Resistance to PD-1 Blockade in Melanoma. N. Engl. J. Med. 375, 819–829 (2016).

C. Zheng et al., Landscape of Infiltrating T Cells in Liver Cancer Revealed by Single-Cell Sequencing. Cell. 169, 1342–1356.e16 (2017).

L. Zimmer et al., Phase II DeCOG-study of ipilimumab in pretreated and treatment-naïve patients with metastatic uveal melanoma. PloS One. 10, e0118564 (2015).

P. Zhou et al., In vivo discovery of immunotherapy targets in the tumour microenvironment. Nature. 506, 52–57 (2014).

* * *

[0665] Various modifications and variations of the described methods, pharmaceutical compositions, and kits of the invention will be apparent to those skilled in the art without departing from the scope and spirit of the invention. Although the invention has been described in connection with specific embodiments, it will be understood that it is capable of further modifications and that the invention as claimed should not be unduly limited to such specific embodiments. Indeed, various modifications of the described modes for carrying out the invention that are obvious to those skilled in the art are intended to be within the scope of the invention. This application is intended to cover any variations, uses, or adaptations of the invention following, in general, the principles of the invention and including such departures from the present disclosure come within known customary practice within the art to which the invention pertains and may be applied to the essential features herein before set forth.

CLAIMS

What is claimed is:

1. A method of detecting an immune checkpoint inhibitor resistance (ICR) gene signature in a tumor comprising, detecting in tumor cells obtained from a subject in need thereof the expression or activity of a malignant cell gene signature comprising:

a) one or more genes or polypeptides selected from the group consisting of PPIA, RPL31, RPL37A, RPL41, RPS21, RPS27A, SAE1, UBA52, C19orf48, CHCHD2, FARSA, NONO, RPL27, RPL36, RPS13, RPS14, RPS15, RPS28, ARMC6, BOLA2, BOLA2B, CDC123, CKS1B, CMSS1, DDX39A, DNAJC9, FAM60A, HN1, MRPL47, NDUFA13, PET100, PFDN4, PSMA7, RNASEH2A, ROMO1, RPL35A, SLIRP, SLMO2, SNRPF, SNRPG, TPRKB, TXNDC17, UBL5, USMG5, AHNAK, APOD, ATP1A1, B2M, CD44, CD63, CTSB, CTSD, FOS, GRN, HLA-A, HLA-B, HLA-C, HLA-E, HLA-H, LAMP2, LGALS3, LGALS3BP, NPC2, PSAP, SERPINE2, TAPBP, TIMP2, CTSO, KLF4, LEF1-AS1, STOM, TAPBPL, VAT1, ACTA2, C6orf226, CCR10, CITED1, CORO1A, CXCR4, DDX17, FLJ39051, FMN1, FRZB, FSTL3, FTH1, HLA-DRB5, IDI2-AS1, JMJD7, LCP1, LINC00518, LOC100506714, LOC100507463, LY96, NMRK1, P2RX4, PIK3IP1, PYGB, RAB27A, RBP7, RNF213, RTP4, SDCBP, SLC22A18, SLC7A5P1, SP100, SPESP1, SPINT1, ST3GAL6-AS1, ST6GALNAC2, TFAP2A, TRIM22, TTLL1 and UCN2; or

b) one or more genes or polypeptides selected from the group consisting of BZW2, CCT3, CDK4, GPATCH4, ISYNA1, MDH2, PPIA, RPL31, RPL37A, RPL41, RPS21, RPS27A, RUVBL2, SAE1, UBA52, AHCY, C17orf76-AS1, C19orf48, C1QBP, CCT6A, CHCHD2, CTPS1, EEF1G, EIF2S3, EIF3K, EIF4A1, FARSA, FBL, FKBP4, GAS5, GNB2L1, GPI, HNRNPA1, HNRNPC, IDH2, ILF2, NACA, NCL, NME1, NOLC1, NONO, PABPC1, PAICS, PFN1, POLD2, PPA1, PTMA, PUF60, RPL10A, RPL11, RPL12, RPL13, RPL13A, RPL13AP5, RPL17, RPL18, RPL18A, RPL21, RPL26, RPL27, RPL28, RPL29, RPL3, RPL36, RPL36A, RPL37, RPL4, RPL5, RPL6, RPL8, RPLP0, RPLP1, RPS10, RPS11, RPS13, RPS14, RPS15, RPS15A, RPS16, RPS17, RPS17L, RPS18, RPS19, RPS23, RPS24, RPS27, RPS28, RPS3, RPS4X, RPS5, RPS6, RPS7, RPS8, RPS9, RPSA, RRS1, SERPINF1, SET, SHMT2, SLC19A1, SLC25A13, SNHG6, SNRPE, SOX4, SSR2, TIMM50, TOP1MT, TUBB, UQCRFS1, UQCRH, VDAC2, ACTB, AEN, ANP32E, APP,

ARMC6, ATP5A1, ATP5D, ATP5G2, ATP5G3, BOLA2, BOLA2B, BOP1, BTF3, C20orf112, C6orf48, CA14, CACYBP, CBX5, CCT2, CCT4, CCT7, CDC123, CDCA7, CFL1, CKS1B, CMSS1, CNRIP1, CS, DARS, DCAF13, DCT, DCTPP1, DDX21, DDX39A, DDX39B, DLL3, DNAJC9, EEF1B2, EEF1D, EEF2, EIF3E, EIF3F, EIF3G, EIF3M, EIF4EBP2, ENO1, EXOSC5, FAM174B, FAM60A, FAM92A1, FBLN1, FOXRED2, FTL, FUS, GABARAP, GGH, GNL3, GRWD1, H3F3A, H3F3AP4, HMGA1, HMGB1, HN1, HNRNPA1P10, HNRNPH1, HNRNPM, HSP90AB1, HSPA8, HSPD1, IFRD2, ILF3, IMPDH2, ITM2C, KIAA0101, LDHB, LSM4, LSM7, LYPLA1, MAGEA4, MAGEC1, MCM7, METAP2, MID1, MIR4461, MKI67IP, MLLT11, MPZL1, MRPL15, MRPL37, MRPL4, MRPL47, MRPS12, MRPS21, NDUFA11, NDUFA13, NDUFS2, NME2, NOP16, NPM1, NREP, PA2G4, PAFAH1B3, PET100, PFDN2, PFDN4, PGAM1, PIH1D1, PLEKHJ1, POLR1D, POLR2E, PPP2R1A, PRMT1, PSMA7, PSMD4, RAN, RBM34, RNASEH2A, RNF2, ROMO1, RPAIN, RPL10, RPL14, RPL15, RPL19, RPL22, RPL27A, RPL30, RPL32, RPL35, RPL35A, RPL39, RPL7, RPL7A, RPL9, RPLP2, RPS12, RPS2, RPS20, RPS25, RPS3A, RQCD1, RSL1D1, RTKN, SCD, SCNM1, SERBP1, SF3B4, SKP2, SLC25A3, SLC25A6, SLIRP, SLMO2, SMARCA4, SMIM15, SMS, SNAI2, SNHG15, SNRPB, SNRPC, SNRPD1, SNRPD2, SNRPF, SNRPG, SRM, SRP14, SSB, TIMM13, TIMM44, TMC6, TP53, TPI1, TPRKB, TRAP1, TRIM28, TRPM1, TSR1, TUBA1B, TULP4, TXNDC17, TYMS, UBL5, UCK2, UHRF1, USMG5, USP22, VCY1B, VPS72, XIST, YWHAE, ZFAS1, ZNF286A, AHNAK, APOD, ATP1A1, B2M, CD44, CD63, CTSB, CTSD, FOS, GRN, HLA-A, HLA-B, HLA-C, HLA-E, HLA-H, LAMP2, LGALS3, LGALS3BP, NPC2, PSAP, SERPINE2, TAPBP, TIMP2, A2M, ACSL3, AEBP1, AGA, APOC2, APOE, ATP1B1, CD151, CD47, CD58, CD59, CDH19, CSPG4, CST3, CTSA, CTSL1, CTSO, CYP27A1, DAG1, DDR1, EEA1, EMP1, EVA1A, FBXO32, FGFR1, GAA, GPNMB, GSN, HLA-F, HSPA1A, IRF4, ITGA3, KCNN4, KLF4, LEF1-AS1, LRPAP1, MFGE8, MIA, MT2A, NEAT1, NPC1, NSG1, PROS1, S100A6, S100B, SAT1, SCARB2, SDC3, SEC11C, SERPINA3, SGK1, SLC26A2, SLC5A3, STOM, STX7, TAPBPL, TIMP1, TIMP3, TM4SF1, TMED10, TPP1, TSC22D3, TYR, UBC, VAT1, WBP2, XAGE1D, ACSL4, ACTA2, ADM, ANGPTL4, ANXA1, ANXA2, APLP2, APOL1, ARL6IP5, ARSA, ATF3, ATP1B3, ATP6V0C, BACE2, BBX, BCL6, C4A, C6orf226, CALU, CARD16, CASP1, CAST, CAV1, CAV2, CCND3, CCR10, CD9, CDH1, CHI3L1, CITED1, CLIC4, CORO1A, CRELD1, CRYAB, CSGALNACT1, CXCR4, CYP4V2, DCBLD2, DDX17, DDX5, DPYSL2, DUSP4, DUSP6, ECM1, EGR1, EPHX2, ERBB3, EZH1, FAM3C,

FCGR2C, FCRLA, FLJ39051, FLJ43663, FLNA, FMN1, FRZB, FSTL3, FTH1, GADD45B, GATSL3, GEM, GJB1, GOLGB1, GPR155, GPR56, HLA-DRB5, HLA-G, HPCAL1, HTATIP2, IDI2-AS1, IFI27, IFI27L2, IFI35, IFI6, IGF1R, IGFBP7, IGSF8, IL1RAP, IL6ST, ITGA6, ITGA7, ITGB1, ITGB3, ITM2B, JMJD7, JUN, KLF6, LAMB2, LCP1, LEPROT, LGALS1, LGMN, LINC00518, LOC100126784, LOC100506190, LOC100506714, LOC100507463, LPL, LY6E, LY96, LYRM9, MAGEC2, MALAT1, MATN2, MCAM, MFI2, MMP14, MPZ, MT1E, MT1M, MT1X, MTRNR2L1, MTRNR2L10, MTRNR2L2, MTRNR2L3, MTRNR2L4, MTRNR2L5, MTRNR2L6, MTRNR2L7, MTRNR2L8, MYO1D, NAV2, NFE2L1, NFKBIA, NFKBIZ, NMRK1, NNMT, NR4A1, P2RX4, PAGE5, PDE4DIP, PDK4, PERP, PIK3IP1, PLP2, PRKCDBP, PRNP, PRSS23, PSMB9, PTRF, PYGB, QPCT, RAB27A, RBP7, RDH5, RNF145, RNF213, RPS4Y1, RTP4, S100A1, S100A13, SCCPDH, SDCBP, SEL1L, SEMA3B, SERINC1, SERPINA1, SGCE, SHC4, SLC20A1, SLC22A18, SLC39A14, SLC7A5P1, SLC7A8, SNX9, SOD1, SORT1, SP100, SPESP1, SPINT1, SPON2, SPP1, SPRY2, SQSTM1, SRPX, ST3GAL6-AS1, ST6GALNAC2, STRIP2, SYNE2, SYNGR2, SYPL1, TF, TFAP2A, TGOLN2, THBD, TMBIM6, TMED9, TMEM255A, TMEM66, TMX4, TNC, TNFSF4, TRIM22, TRIML2, TSPYL2, TTLL1, TXNIP, UCN2, UPP1, WDFY1, ZBTB20 and ZBTB38; or

c) one or more genes or polypeptides selected from Table 27B.1.

2. The method according to claim 1, wherein said ICR signature comprises a ICR-down signature, said signature comprising one or more genes selected from the group consisting of:

a) AHNAK, APOD, ATP1A1, B2M, CD44, CD63, CTSB, CTSD, FOS, GRN, HLA-A, HLA-B, HLA-C, HLA-E, HLA-H, LAMP2, LGALS3, LGALS3BP, NPC2, PSAP, SERPINE2, TAPBP, TIMP2, CTSO, KLF4, LEF1-AS1, STOM, TAPBPL, VAT1, ACTA2, C6orf226, CCR10, CITED1, CORO1A, CXCR4, DDX17, FLJ39051, FMN1, FRZB, FSTL3, FTH1, HLA-DRB5, IDI2-AS1, JMJD7, LCP1, LINC00518, LOC100506714, LOC100507463, LY96, NMRK1, P2RX4, PIK3IP1, PYGB, RAB27A, RBP7, RNF213, RTP4, SDCBP, SLC22A18, SLC7A5P1, SP100, SPESP1, SPINT1, ST3GAL6-AS1, ST6GALNAC2, TFAP2A, TRIM22, TTLL1 and UCN2; or

b) AHNAK, APOD, ATP1A1, B2M, CD44, CD63, CTSB, CTSD, FOS, GRN,

HLA-A, HLA-B, HLA-C, HLA-E, HLA-H, LAMP2, LGALS3, LGALS3BP, NPC2, PSAP, SERPINE2, TAPBP, TIMP2, A2M, ACSL3, AEBP1, AGA, APOC2, APOE, ATP1B1, CD151, CD47, CD58, CD59, CDH19, CSPG4, CST3, CTSA, CTSL1, CTSO, CYP27A1, DAG1, DDR1, EEA1, EMP1, EVA1A, FBXO32, FGFR1, GAA, GPNMB, GSN, HLA-F, HSPA1A, IRF4, ITGA3, KCNN4, KLF4, LEF1-AS1, LRPAP1, MFGE8, MIA, MT2A, NEAT1, NPC1, NSG1, PROS1, S100A6, S100B, SAT1, SCARB2, SDC3, SEC11C, SERPINA3, SGK1, SLC26A2, SLC5A3, STOM, STX7, TAPBPL, TIMP1, TIMP3, TM4SF1, TMED10, TPP1, TSC22D3, TYR, UBC, VAT1, WBP2, XAGE1D, ACSL4, ACTA2, ADM, ANGPTL4, ANXA1, ANXA2, APLP2, APOL1, ARL6IP5, ARSA, ATF3, ATP1B3, ATP6V0C, BACE2, BBX, BCL6, C4A, C6orf226, CALU, CARD16, CASP1, CAST, CAV1, CAV2, CCND3, CCR10, CD9, CDH1, CHI3L1, CITED1, CLIC4, CORO1A, CRELD1, CRYAB, CSGALNACT1, CXCR4, CYP4V2, DCBLD2, DDX17, DDX5, DPYSL2, DUSP4, DUSP6, ECM1, EGR1, EPHX2, ERBB3, EZH1, FAM3C, FCGR2C, FCRLA, FLJ39051, FLJ43663, FLNA, FMN1, FRZB, FSTL3, FTH1, GADD45B, GATSL3, GEM, GJB1, GOLGB1, GPR155, GPR56, HLA-DRB5, HLA-G, HPCAL1, HTATIP2, IDI2-AS1, IFI27, IFI27L2, IFI35, IFI6, IGF1R, IGFBP7, IGSF8, IL1RAP, IL6ST, ITGA6, ITGA7, ITGB1, ITGB3, ITM2B, JMJD7, JUN, KLF6, LAMB2, LCP1, LEPROT, LGALS1, LGMN, LINC00518, LOC100126784, LOC100506190, LOC100506714, LOC100507463, LPL, LY6E, LY96, LYRM9, MAGEC2, MALAT1, MATN2, MCAM, MFI2, MMP14, MPZ, MT1E, MT1M, MT1X, MTRNR2L1, MTRNR2L10, MTRNR2L2, MTRNR2L3, MTRNR2L4, MTRNR2L5, MTRNR2L6, MTRNR2L7, MTRNR2L8, MYO1D, NAV2, NFE2L1, NFKBIA, NFKBIZ, NMRK1, NNMT, NR4A1, P2RX4, PAGE5, PDE4DIP, PDK4, PERP, PIK3IP1, PLP2, PRKCDBP, PRNP, PRSS23, PSMB9, PTRF, PYGB, QPCT, RAB27A, RBP7, RDH5, RNF145, RNF213, RPS4Y1, RTP4, S100A1, S100A13, SCCPDH, SDCBP, SEL1L, SEMA3B, SERINC1, SERPINA1, SGCE, SHC4, SLC20A1, SLC22A18, SLC39A14, SLC7A5P1, SLC7A8, SNX9, SOD1, SORT1, SP100, SPESP1, SPINT1, SPON2, SPP1, SPRY2, SQSTM1, SRPX, ST3GAL6-AS1, ST6GALNAC2, STRIP2, SYNE2, SYNGR2, SYPL1, TF, TFAP2A, TGOLN2, THBD, TMBIM6, TMED9, TMEM255A, TMEM66, TMX4, TNC, TNFSF4, TRIM22, TRIML2, TSPYL2, TTLL1, TXNIP, UCN2, UPP1, WDFY1, ZBTB20 and ZBTB38,

wherein said ICR-down signature is downregulated in a tumor with a high ICR score and upregulated in a tumor with a low ICR score.

3. The method according to claim 1, wherein said ICR signature comprises a ICR-up signature, said signature comprising one or more genes selected from the group consisting of:

a) PPIA, RPL31, RPL37A, RPL41, RPS21, RPS27A, SAE1, UBA52, C19orf48, CHCHD2, FARSA, NONO, RPL27, RPL36, RPS13, RPS14, RPS15, RPS28, ARMC6, BOLA2, BOLA2B, CDC123, CKS1B, CMSS1, DDX39A, DNAJC9, FAM60A, HN1, MRPL47, NDUFA13, PET100, PFDN4, PSMA7, RNASEH2A, ROMO1, RPL35A, SLIRP, SLMO2, SNRPF, SNRPG, TPRKB, TXNDC17, UBL5 and USMG5; or

b) BZW2, CCT3, CDK4, GPATCH4, ISYNA1, MDH2, PPIA, RPL31, RPL37A, RPL41, RPS21, RPS27A, RUVBL2, SAE1, UBA52, AHCY, C17orf76-AS1, C19orf48, C1QBP, CCT6A, CHCHD2, CTPS1, EEF1G, EIF2S3, EIF3K, EIF4A1, FARSA, FBL, FKBP4, GAS5, GNB2L1, GPI, HNRNPA1, HNRNPC, IDH2, ILF2, NACA, NCL, NME1, NOLC1, NONO, PABPC1, PAICS, PFN1, POLD2, PPA1, PTMA, PUF60, RPL10A, RPL11, RPL12, RPL13, RPL13A, RPL13AP5, RPL17, RPL18, RPL18A, RPL21, RPL26, RPL27, RPL28, RPL29, RPL3, RPL36, RPL36A, RPL37, RPL4, RPL5, RPL6, RPL8, RPLP0, RPLP1, RPS10, RPS11, RPS13, RPS14, RPS15, RPS15A, RPS16, RPS17, RPS17L, RPS18, RPS19, RPS23, RPS24, RPS27, RPS28, RPS3, RPS4X, RPS5, RPS6, RPS7, RPS8, RPS9, RPSA, RRS1, SERPINF1, SET, SHMT2, SLC19A1, SLC25A13, SNHG6, SNRPE, SOX4, SSR2, TIMM50, TOP1MT, TUBB, UQCRFS1, UQCRH, VDAC2, ACTB, AEN, ANP32E, APP, ARMC6, ATP5A1, ATP5D, ATP5G2, ATP5G3, BOLA2, BOLA2B, BOP1, BTF3, C20orf112, C6orf48, CA14, CACYBP, CBX5, CCT2, CCT4, CCT7, CDC123, CDCA7, CFL1, CKS1B, CMSS1, CNRIP1, CS, DARS, DCAF13, DCT, DCTPP1, DDX21, DDX39A, DDX39B, DLL3, DNAJC9, EEF1B2, EEF1D, EEF2, EIF3E, EIF3F, EIF3G, EIF3M, EIF4EBP2, ENO1, EXOSC5, FAM174B, FAM60A, FAM92A1, FBLN1, FOXRED2, FTL, FUS, GABARAP, GGH, GNL3, GRWD1, H3F3A, H3F3AP4, HMGA1, HMGB1, HN1, HNRNPA1P10, HNRNPH1, HNRNPM, HSP90AB1, HSPA8, HSPD1, IFRD2, ILF3, IMPDH2, ITM2C, KIAA0101, LDHB, LSM4, LSM7, LYPLA1, MAGEA4, MAGEC1, MCM7, METAP2, MID1, MIR4461, MKI67IP, MLLT11, MPZL1, MRPL15, MRPL37, MRPL4, MRPL47, MRPS12, MRPS21, NDUFA11, NDUFA13, NDUFS2, NME2, NOP16, NPM1, NREP, PA2G4, PAFAH1B3, PET100, PFDN2, PFDN4, PGAM1, PIH1D1, PLEKHJ1, POLR1D, POLR2E, PPP2R1A, PRMT1, PSMA7, PSMD4, RAN, RBM34, RNASEH2A, RNF2, ROMO1, RPAIN, RPL10, RPL14, RPL15, RPL19, RPL22,

RPL27A, RPL30, RPL32, RPL35, RPL35A, RPL39, RPL7, RPL7A, RPL9, RPLP2, RPS12, RPS2, RPS20, RPS25, RPS3A, RQCD1, RSL1D1, RTKN, SCD, SCNM1, SERBP1, SF3B4, SKP2, SLC25A3, SLC25A6, SLIRP, SLMO2, SMARCA4, SMIM15, SMS, SNAI2, SNHG15, SNRPB, SNRPC, SNRPD1, SNRPD2, SNRPF, SNRPG, SRM, SRP14, SSB, TIMM13, TIMM44, TMC6, TP53, TPI1, TPRKB, TRAP1, TRIM28, TRPM1, TSR1, TUBA1B, TULP4, TXNDC17, TYMS, UBL5, UCK2, UHRF1, USMG5, USP22, VCY1B, VPS72, XIST, YWHAE, ZFAS1 and ZNF286A,

wherein said ICR-up signature is upregulated in a tumor with a high ICR score and downregulated in a tumor with a low ICR score.

4. A method of detecting an immune checkpoint inhibitor resistance (ICR) gene signature in a tumor comprising, detecting in tumor cells obtained from a subject in need thereof the expression or activity of a malignant cell gene signature comprising one or more genes or polypeptides selected from the group consisting of BZW2, CCT3, CDK4, GPATCH4, ISYNA1, MDH2, PPIA, RPL31, RPL37A, RPL41, RPS21, RPS27A, RUVBL2, SAE1, UBA52, C17orf76-AS1, C1QBP, CTPS1, EEF1G, EIF2S3, EIF3K, EIF4A1, FBL, GAS5, GNB2L1, GPI, HNRNPA1, HNRNPC, IDH2, ILF2, NACA, NCL, NOLC1, NONO, PABPC1, PFN1, PPA1, PTMA, RPL10A, RPL11, RPL12, RPL13, RPL13A, RPL13AP5, RPL17, RPL18, RPL18A, RPL21, RPL26, RPL28, RPL29, RPL3, RPL36A, RPL37, RPL4, RPL5, RPL6, RPL8, RPLP0, RPLP1, RPS10, RPS11, RPS15A, RPS16, RPS17, RPS17L, RPS18, RPS19, RPS23, RPS24, RPS27, RPS3, RPS4X, RPS5, RPS6, RPS7, RPS8, RPS9, RPSA, SERPINF1, SET, SHMT2, SNHG6, SNRPE, SOX4, SSR2, TIMM50, TUBB, UQCRFS1, UQCRH, VDAC2, ACTB, AEN, ANP32E, ATP5A1, ATP5G2, C20orf112, CA14, CBX5, CCT2, CFL1, CNRIP1, CS, DCAF13, DCT, DDX39B, DLL3, EIF4EBP2, FAM174B, FBLN1, FOXRED2, FTL, FUS, GABARAP, GRWD1, H3F3A, H3F3AP4, HMGA1, HNRNPA1P10, HSPA8, ITM2C, KIAA0101, MAGEA4, METAP2, MID1, MIR4461, MLLT11, MPZL1, MRPS21, NDUFS2, PA2G4, PAFAH1B3, PFDN2, PGAM1, PIH1D1, PPP2R1A, PSMD4, RAN, RBM34, RNF2, RPAIN, RPS12, SCD, SCNM1, SF3B4, SKP2, SLC25A3, SMS, SNAI2, SRP14, TMC6, TP53, TRPM1, TSR1, TUBA1B, TULP4, USP22, VCY1B, VPS72, YWHAE, ZNF286A, AHNAK, APOD, ATP1A1, B2M, CD44, CD63, CTSB, CTSD, FOS, GRN, HLA-A, HLA-B, HLA-C, HLA-E, HLA-H, LAMP2, LGALS3, LGALS3BP, NPC2, PSAP, SERPINE2, TAPBP, TIMP2, A2M, ACSL3, AEBP1, AGA, APOE, ATP1B1, CD151, CD47, CD58, CD59, CDH19, CSPG4, CST3, CTSA,

CTSL1, DAG1, DDR1, EEA1, EMP1, EVA1A, FBXO32, FGFR1, GAA, GPNMB, GSN, HLA-F, HSPA1A, ITGA3, KCNN4, KLF4, LRPAP1, MFGE8, MIA, MT2A, NEAT1, NPC1, NSG1, PROS1, S100A6, S100B, SAT1, SCARB2, SDC3, SERPINA3, SGK1, SLC26A2, SLC5A3, STOM, TAPBPL, TIMP1, TIMP3, TM4SF1, TMED10, TPP1, TSC22D3, TYR, UBC, ACSL4, ADM, ANGPTL4, ANXA1, ANXA2, APLP2, ARL6IP5, ATF3, ATP1B3, BACE2, BBX, BCL6, CALU, CASP1, CAST, CAV1, CCND3, CD9, CHI3L1, CLIC4, CRELD1, CRYAB, CSGALNACT1, DCBLD2, DDX5, DPYSL2, DUSP4, DUSP6, ECM1, EGR1, EPHX2, ERBB3, EZH1, FAM3C, FCGR2C, FCRLA, FLJ43663, GADD45B, GEM, GOLGB1, HPCAL1, HTATIP2, IFI35, IGF1R, IL1RAP, IL6ST, ITGA6, ITGB1, ITGB3, ITM2B, JUN, KLF6, LEPROT, LGALS1, LPL, MAGEC2, MFI2, MT1E, MT1M, MT1X, NFKBIA, NFKBIZ, NNMT, NR4A1, PDK4, PLP2, PRKCDBP, PRNP, PRSS23, PSMB9, PTRF, RNF145, RPS4Y1, SCCPDH, SEL1L, SEMA3B, SGCE, SLC20A1, SLC39A14, SOD1, SPRY2, SQSTM1, SRPX, SYNGR2, SYPL1, TF, TGOLN2, TMED9, TMEM66, TMX4, TNC, UPP1, ZBTB20 and ZBTB38.

5. The method according to claim 4, wherein said ICR signature comprises an ICR-down signature, said signature comprising one or more genes selected from the group consisting of AHNAK, APOD, ATP1A1, B2M, CD44, CD63, CTSB, CTSD, FOS, GRN, HLA-A, HLA-B, HLA-C, HLA-E, HLA-H, LAMP2, LGALS3, LGALS3BP, NPC2, PSAP, SERPINE2, TAPBP, TIMP2, A2M, ACSL3, AEBP1, AGA, APOE, ATP1B1, CD151, CD47, CD58, CD59, CDH19, CSPG4, CST3, CTSA, CTSL1, DAG1, DDR1, EEA1, EMP1, EVA1A, FBXO32, FGFR1, GAA, GPNMB, GSN, HLA-F, HSPA1A, ITGA3, KCNN4, KLF4, LRPAP1, MFGE8, MIA, MT2A, NEAT1, NPC1, NSG1, PROS1, S100A6, S100B, SAT1, SCARB2, SDC3, SERPINA3, SGK1, SLC26A2, SLC5A3, STOM, TAPBPL, TIMP1, TIMP3, TM4SF1, TMED10, TPP1, TSC22D3, TYR, UBC, ACSL4, ADM, ANGPTL4, ANXA1, ANXA2, APLP2, ARL6IP5, ATF3, ATP1B3, BACE2, BBX, BCL6, CALU, CASP1, CAST, CAV1, CCND3, CD9, CHI3L1, CLIC4, CRELD1, CRYAB, CSGALNACT1, DCBLD2, DDX5, DPYSL2, DUSP4, DUSP6, ECM1, EGR1, EPHX2, ERBB3, EZH1, FAM3C, FCGR2C, FCRLA, FLJ43663, GADD45B, GEM, GOLGB1, HPCAL1, HTATIP2, IFI35, IGF1R, IL1RAP, IL6ST, ITGA6, ITGB1, ITGB3, ITM2B, JUN, KLF6, LEPROT, LGALS1, LPL, MAGEC2, MFI2, MT1E, MT1M, MT1X, NFKBIA, NFKBIZ, NNMT, NR4A1, PDK4, PLP2, PRKCDBP, PRNP, PRSS23, PSMB9, PTRF, RNF145, RPS4Y1, SCCPDH, SEL1L, SEMA3B, SGCE, SLC20A1, SLC39A14, SOD1,

SPRY2, SQSTM1, SRPX, SYNGR2, SYPL1, TF, TGOLN2, TMED9, TMEM66, TMX4, TNC, UPP1, ZBTB20 and ZBTB38,

wherein said ICR-down signature is downregulated in a tumor with a high ICR score and upregulated in a tumor with a low ICR score.

6. The method according to claim 4, wherein said ICR signature comprises an ICR-up signature, said signature comprising one or more genes selected from the group consisting of BZW2, CCT3, CDK4, GPATCH4, ISYNA1, MDH2, PPIA, RPL31, RPL37A, RPL41, RPS21, RPS27A, RUVBL2, SAE1, UBA52, C17orf76-AS1, C1QBP, CTPS1, EEF1G, EIF2S3, EIF3K, EIF4A1, FBL, GAS5, GNB2L1, GPI, HNRNPA1, HNRNPC, IDH2, ILF2, NACA, NCL, NOLC1, NONO, PABPC1, PFN1, PPA1, PTMA, RPL10A, RPL11, RPL12, RPL13, RPL13A, RPL13AP5, RPL17, RPL18, RPL18A, RPL21, RPL26, RPL28, RPL29, RPL3, RPL36A, RPL37, RPL4, RPL5, RPL6, RPL8, RPLP0, RPLP1, RPS10, RPS11, RPS15A, RPS16, RPS17, RPS17L, RPS18, RPS19, RPS23, RPS24, RPS27, RPS3, RPS4X, RPS5, RPS6, RPS7, RPS8, RPS9, RPSA, SERPINF1, SET, SHMT2, SNHG6, SNRPE, SOX4, SSR2, TIMM50, TUBB, UQCRFS1, UQCRH, VDAC2, ACTB, AEN, ANP32E, ATP5A1, ATP5G2, C20orf112, CA14, CBX5, CCT2, CFL1, CNRIP1, CS, DCAF13, DCT, DDX39B, DLL3, EIF4EBP2, FAM174B, FBLN1, FOXRED2, FTL, FUS, GABARAP, GRWD1, H3F3A, H3F3AP4, HMGA1, HNRNPA1P10, HSPA8, ITM2C, KIAA0101, MAGEA4, METAP2, MID1, MIR4461, MLLT11, MPZL1, MRPS21, NDUFS2, PA2G4, PAFAH1B3, PFDN2, PGAM1, PIH1D1, PPP2R1A, PSMD4, RAN, RBM34, RNF2, RPAIN, RPS12, SCD, SCNM1, SF3B4, SKP2, SLC25A3, SMS, SNAI2, SRP14, TMC6, TP53, TRPM1, TSR1, TUBA1B, TULP4, USP22, VCY1B, VPS72, YWHAE and ZNF286A,

wherein said ICR-up signature is upregulated in a tumor with a high ICR score and downregulated in a tumor with a low ICR score.

7. The method according to any of claims 1 to 6, wherein the ICR signature is detected in cycling cells and/or expanded cells.

8. A method of detecting an immune cell exclusion gene signature in a tumor comprising, detecting in tumor cells obtained from a subject in need thereof the expression or activity of a malignant cell gene signature comprising:

a) one or more genes or polypeptides selected from the group consisting of BZW2, CCT3, CDK4, GPATCH4, ISYNA1, MDH2, RUVBL2, AHCY, CCT6A, FKBP4, NME1, PAICS, POLD2, PUF60, RRS1, SLC19A1, SLC25A13, TOP1MT, HSP90AB1, RTKN, APOC2, CYP27A1, IRF4, SEC11C, STX7, WBP2, XAGE1D, PAGE5 and WDFY1; or

b) one or more genes or polypeptides selected from the group consisting of BZW2, CCT3, CDK4, GPATCH4, ISYNA1, MDH2, PPIA, RPL31, RPL37A, RPL41, RPS21, RPS27A, RUVBL2, SAE1, UBA52, AHCY, C17orf76-AS1, C19orf48, C1QBP, CCT6A, CHCHD2, CTPS1, EEF1G, EIF2S3, EIF3K, EIF4A1, FARSA, FBL, FKBP4, GAS5, GNB2L1, GPI, HNRNPA1, HNRNPC, IDH2, ILF2, NACA, NCL, NME1, NOLC1, PABPC1, PAICS, PFN1, POLD2, PPA1, PTMA, PUF60, RPL10A, RPL11, RPL12, RPL13, RPL13A, RPL13AP5, RPL17, RPL18, RPL18A, RPL21, RPL26, RPL27, RPL28, RPL29, RPL3, RPL36, RPL36A, RPL37, RPL4, RPL5, RPL6, RPL8, RPLP0, RPLP1, RPS10, RPS11, RPS13, RPS14, RPS15, RPS15A, RPS16, RPS17, RPS17L, RPS18, RPS19, RPS23, RPS24, RPS27, RPS28, RPS3, RPS4X, RPS5, RPS6, RPS7, RPS8, RPS9, RPSA, RRS1, SERPINF1, SET, SHMT2, SLC19A1, SLC25A13, SNHG6, SNRPE, SOX4, SSR2, TIMM50, TOP1MT, TUBB, UQCRFS1, UQCRH, VDAC2, APP, ATP5D, ATP5G3, BOP1, BTF3, C6orf48, CACYBP, CCT4, CCT7, CDCA7, DARS, DCTPP1, DDX21, EEF1B2, EEF1D, EEF2, EIF3E, EIF3F, EIF3G, EIF3M, ENO1, EXOSC5, FAM92A1, GGH, GNL3, HMGB1, HNRNPH1, HNRNPM, HSPD1, IFRD2, ILF3, IMPDH2, LDHB, LSM4, LSM7, LYPLA1, MAGEC1, MCM7, MKI67IP, MRPL15, MRPL37, MRPL4, MRPS12, NDUFA11, NME2, NOP16, NPM1, NREP, PLEKHJ1, POLR1D, POLR2E, PRMT1, RPL10, RPL14, RPL15, RPL19, RPL22, RPL27A, RPL30, RPL32, RPL35, RPL39, RPL7, RPL7A, RPL9, RPLP2, RPS2, RPS20, RPS25, RPS3A, RQCD1, RSL1D1, SERBP1, SLC25A6, SMARCA4, SMIM15, SNHG15, SNRPB, SNRPC, SNRPD1, SNRPD2, SRM, SSB, TIMM13, TIMM44, TPI1, TRAP1, TRIM28, TYMS, UCK2, UHRF1, XIST, ZFAS1, AHNAK, APOD, ATP1A1, B2M, CD44, CD63, CTSB, CTSD, FOS, GRN, HLA-A, HLA-B, HLA-C, HLA-E, HLA-H, LAMP2, LGALS3, LGALS3BP, NPC2, PSAP, SERPINE2, TAPBP, TIMP2, A2M, ACSL3, AEBP1, AGA, APOC2, APOE, ATP1B1, CD151, CD47, CD58, CD59, CDH19, CSPG4, CST3, CTSA, CTSL1, CTSO, CYP27A1, DAG1, DDR1, EEA1, EMP1, EVA1A, FBXO32, FGFR1, GAA, GPNMB, GSN, HLA-F, HSPA1A, IRF4, ITGA3, KCNN4, LEF1-AS1, LRPAP1, MFGE8, MIA, MT2A, NEAT1, NPC1, NSG1,

PROS1, S100A6, S100B, SAT1, SCARB2, SDC3, SEC11C, SERPINA3, SGK1, SLC26A2, SLC5A3, STX7, TIMP1, TIMP3, TM4SF1, TMED10, TPP1, TSC22D3, TYR, UBC, VAT1, WBP2, XAGE1D, APOL1, ARSA, ATP6V0C, C4A, CARD16, CAV2, CDH1, CYP4V2, FLNA, GATSL3, GJB1, GPR155, GPR56, HLA-G, IFI27, IFI27L2, IFI6, IGFBP7, IGSF8, ITGA7, LAMB2, LGMN, LOC100126784, LOC100506190, LY6E, LYRM9, MALAT1, MATN2, MCAM, MMP14, MPZ, MTRNR2L1, MTRNR2L10, MTRNR2L2, MTRNR2L3, MTRNR2L4, MTRNR2L5, MTRNR2L6, MTRNR2L7, MTRNR2L8, MYO1D, NAV2, NFE2L1, PDE4DIP, PERP, QPCT, RDH5, S100A1, S100A13, SERINC1, SERPINA1, SHC4, SLC7A8, SNX9, SORT1, SPON2, SPP1, STRIP2, SYNE2, THBD, TMBIM6, TMEM255A, TNFSF4, TRIML2, TSPYL2 and TXNIP.

9. The method according to claim 8, wherein said exclusion signature comprises an exclusion-down signature, said signature comprising one or more genes selected from the group consisting of:

a) APOC2, CYP27A1, IRF4, SEC11C, STX7, WBP2, XAGE1D, PAGE5 and WDFY1; or

b) AHNAK, APOD, ATP1A1, B2M, CD44, CD63, CTSB, CTSD, FOS, GRN, HLA-A, HLA-B, HLA-C, HLA-E, HLA-H, LAMP2, LGALS3, LGALS3BP, NPC2, PSAP, SERPINE2, TAPBP, TIMP2, A2M, ACSL3, AEBP1, AGA, APOC2, APOE, ATP1B1, CD151, CD47, CD58, CD59, CDH19, CSPG4, CST3, CTSA, CTSL1, CTSO, CYP27A1, DAG1, DDR1, EEA1, EMP1, EVA1A, FBXO32, FGFR1, GAA, GPNMB, GSN, HLA-F, HSPA1A, IRF4, ITGA3, KCNN4, LEF1-AS1, LRPAP1, MFGE8, MIA, MT2A, NEAT1, NPC1, NSG1, PROS1, S100A6, S100B, SAT1, SCARB2, SDC3, SEC11C, SERPINA3, SGK1, SLC26A2, SLC5A3, STX7, TIMP1, TIMP3, TM4SF1, TMED10, TPP1, TSC22D3, TYR, UBC, VAT1, WBP2, XAGE1D, APOL1, ARSA, ATP6V0C, C4A, CARD16, CAV2, CDH1, CYP4V2, FLNA, GATSL3, GJB1, GPR155, GPR56, HLA-G, IFI27, IFI27L2, IFI6, IGFBP7, IGSF8, ITGA7, LAMB2, LGMN, LOC100126784, LOC100506190, LY6E, LYRM9, MALAT1, MATN2, MCAM, MMP14, MPZ, MTRNR2L1, MTRNR2L10, MTRNR2L2, MTRNR2L3, MTRNR2L4, MTRNR2L5, MTRNR2L6, MTRNR2L7, MTRNR2L8, MYO1D, NAV2, NFE2L1, PDE4DIP, PERP, QPCT, RDH5, S100A1, S100A13, SERINC1, SERPINA1, SHC4, SLC7A8, SNX9, SORT1, SPON2, SPP1, STRIP2, SYNE2, THBD, TMBIM6, TMEM255A, TNFSF4, TRIML2, TSPYL2 and TXNIP,

wherein said exclusion-down signature is downregulated in a tumor with T cell exclusion and is upregulated in a tumor with T cell infiltration.

10. The method according to claim 8, wherein said exclusion signature comprises an exclusion-up signature, said signature comprising one or more genes selected from the group consisting of:

a) BZW2, CCT3, CDK4, GPATCH4, ISYNA1, MDH2, RUVBL2, AHCY, CCT6A, FKBP4, NME1, PAICS, POLD2, PUF60, RRS1, SLC19A1, SLC25A13, TOP1MT, HSP90AB1 and RTKN; or

b) BZW2, CCT3, CDK4, GPATCH4, ISYNA1, MDH2, PPIA, RPL31, RPL37A, RPL41, RPS21, RPS27A, RUVBL2, SAE1, UBA52, AHCY, C17orf76-AS1, C19orf48, C1QBP, CCT6A, CHCHD2, CTPS1, EEF1G, EIF2S3, EIF3K, EIF4A1, FARSA, FBL, FKBP4, GAS5, GNB2L1, GPI, HNRNPA1, HNRNPC, IDH2, ILF2, NACA, NCL, NME1, NOLC1, PABPC1, PAICS, PFN1, POLD2, PPA1, PTMA, PUF60, RPL10A, RPL11, RPL12, RPL13, RPL13A, RPL13AP5, RPL17, RPL18, RPL18A, RPL21, RPL26, RPL27, RPL28, RPL29, RPL3, RPL36, RPL36A, RPL37, RPL4, RPL5, RPL6, RPL8, RPLP0, RPLP1, RPS10, RPS11, RPS13, RPS14, RPS15, RPS15A, RPS16, RPS17, RPS17L, RPS18, RPS19, RPS23, RPS24, RPS27, RPS28, RPS3, RPS4X, RPS5, RPS6, RPS7, RPS8, RPS9, RPSA, RRS1, SERPINF1, SET, SHMT2, SLC19A1, SLC25A13, SNHG6, SNRPE, SOX4, SSR2, TIMM50, TOP1MT, TUBB, UQCRFS1, UQCRH, VDAC2, APP, ATP5D, ATP5G3, BOP1, BTF3, C6orf48, CACYBP, CCT4, CCT7, CDCA7, DARS, DCTPP1, DDX21, EEF1B2, EEF1D, EEF2, EIF3E, EIF3F, EIF3G, EIF3M, ENO1, EXOSC5, FAM92A1, GGH, GNL3, HMGB1, HNRNPH1, HNRNPM, HSPD1, IFRD2, ILF3, IMPDH2, LDHB, LSM4, LSM7, LYPLA1, MAGEC1, MCM7, MKI67IP, MRPL15, MRPL37, MRPL4, MRPS12, NDUFA11, NME2, NOP16, NPM1, NREP, PLEKHJ1, POLR1D, POLR2E, PRMT1, RPL10, RPL14, RPL15, RPL19, RPL22, RPL27A, RPL30, RPL32, RPL35, RPL39, RPL7, RPL7A, RPL9, RPLP2, RPS2, RPS20, RPS25, RPS3A, RQCD1, RSL1D1, SERBP1, SLC25A6, SMARCA4, SMIM15, SNHG15, SNRPB, SNRPC, SNRPD1, SNRPD2, SRM, SSB, TIMM13, TIMM44, TPI1, TRAP1, TRIM28, TYMS, UCK2, UHRF1, XIST and ZFAS1,

wherein said exclusion-up signature is upregulated in a tumor with T cell exclusion and is downregulated in a tumor with T cell infiltration.

11. The method according to any of claims 1 to 10, further comprising detecting the abundance of tumor infiltrating lymphocytes (TIL).

12. The method according to any of claims 1 to 11, wherein the gene signature is detected in a bulk tumor sample, whereby the gene signature is detected by deconvolution of bulk expression data such that gene expression is assigned to malignant cells and non-malignant cells in said tumor sample.

13. The method according to any of claims 1 to 12, wherein detecting the gene signature comprises detecting downregulation of the down signature and/or upregulation of the up signature, and wherein not detecting the gene signature comprises detecting upregulation of the down signature and/or downregulation of the up signature.

14. The method according to any of claims 1 to 13, wherein detecting the signature and/or TILs indicates lower progression free survival and/or resistance to checkpoint blockade therapy, and wherein not detecting the signature and/or TILs indicates higher progression free survival and/or sensitivity to checkpoint blockade therapy.

15. The method according to any of claims 1 to 14, wherein detecting the gene signature indicates a 10-year survival rate less than 40% and wherein not detecting the signature indicates a 10-year survival rate greater than 60%.

16. The method according to any of claims 1 to 15, wherein detecting an ICR signature in a tumor further comprises detecting in tumor infiltrating lymphocytes (TIL) obtained from the subject in need thereof the expression or activity of a CD8 T cell gene signature, said signature comprising one or more genes or polypeptides selected from Table 27B.2.

17. The method according to any of claims 1 to 16, wherein detecting an ICR signature in a tumor further comprises detecting in macrophages obtained from the subject in need thereof the expression or activity of a macrophage gene signature, said signature comprising one or more genes or polypeptides selected from Table 27C.

18. A method of stratifying cancer patients into a high survival group and a low survival group comprising detecting the expression or activity of an ICR and/or exclusion

signature in a tumor according to any of claims 1 to 17, wherein if the signature is detected the patient is in the low survival group and if the signature is not detected the patient is in the high survival group.

19. The method according to claim 18, wherein patients in the high survival group are immunotherapy responders and patients in the low survival group are immunotherapy non-responders.

20. A method of treating a cancer in a subject in need thereof comprising detecting the expression or activity of an ICR and/or exclusion signature according to any of claims 1 to 17 in a tumor obtained from the subject and administering a treatment,

wherein if an ICR and/or exclusion signature is detected the treatment comprises administering a treatment regimen comprising an immunotherapy followed by a CDK4/6 inhibitor and an immunotherapy.

21. A method of treating a cancer in a subject in need thereof comprising administering a treatment regimen comprising an immunotherapy followed by a CDK4/6 inhibitor and an immunotherapy.

22. The method according to any of claims 20 to 21, wherein the CDK4/6 inhibitor comprises abemaciclib.

23. The method according to any of claims 20 to 22, wherein the CDK4/6 inhibitor inhibits the expression or activity of one or more CDK7 targets selected from the group consisting of GPATCH4, RPL31, RPL41, C19orf48, EIF4A1, NME1, PABPC1, PTMA, RPL10A, RPL13, RPL28, RPL29, RPL3, RPL36, RPL5, RPLP0, RPLP1, RPS11, RPS15, RPS15A, RPS27, RPS28, RPS3, RPS5, RPS6, RPS7, RPS8, RPS9, SNRPE, SOX4, ACTB, ANP32E, C6orf48, CCT4, DDX39B, EIF3G, FTL, HNRNPH1, HSP90AB1, HSPA8, IMPDH2, LSM7, MRPL15, MRPL47, NDUFS2, NPM1, RPL10, RPL7A, RPS12, RPS2, RPS20, RPS3A, RSL1D1, SCNM1, SNRPC, TPI1, TRIM28, TUBA1B and YWHAE.

24. The method according to any of claims 20 to 23, wherein the immunotherapy comprises a check point inhibitor.

25. The method according to claim 23, wherein the checkpoint inhibitor

comprises anti-CTLA4, anti-PD-L1, anti-PD1, anti-TIM3, anti-TIGIT, anti-LAG3 or a combination thereof.

26. The method of any one of claims 1 to 25, wherein the cancer is melanoma or breast cancer.

27. The method of any one of claims 1 to 26, wherein the checkpoint inhibitors are administered and the CDK4/6 inhibitor and checkpoint inhibitor are administered between 14 days and 6 months after the first checkpoint inhibitors are administered.

28. A method of treating a cancer in a subject in need thereof comprising administering a combination treatment regimen comprising an immunotherapy and one or more drugs selected from Table 16.

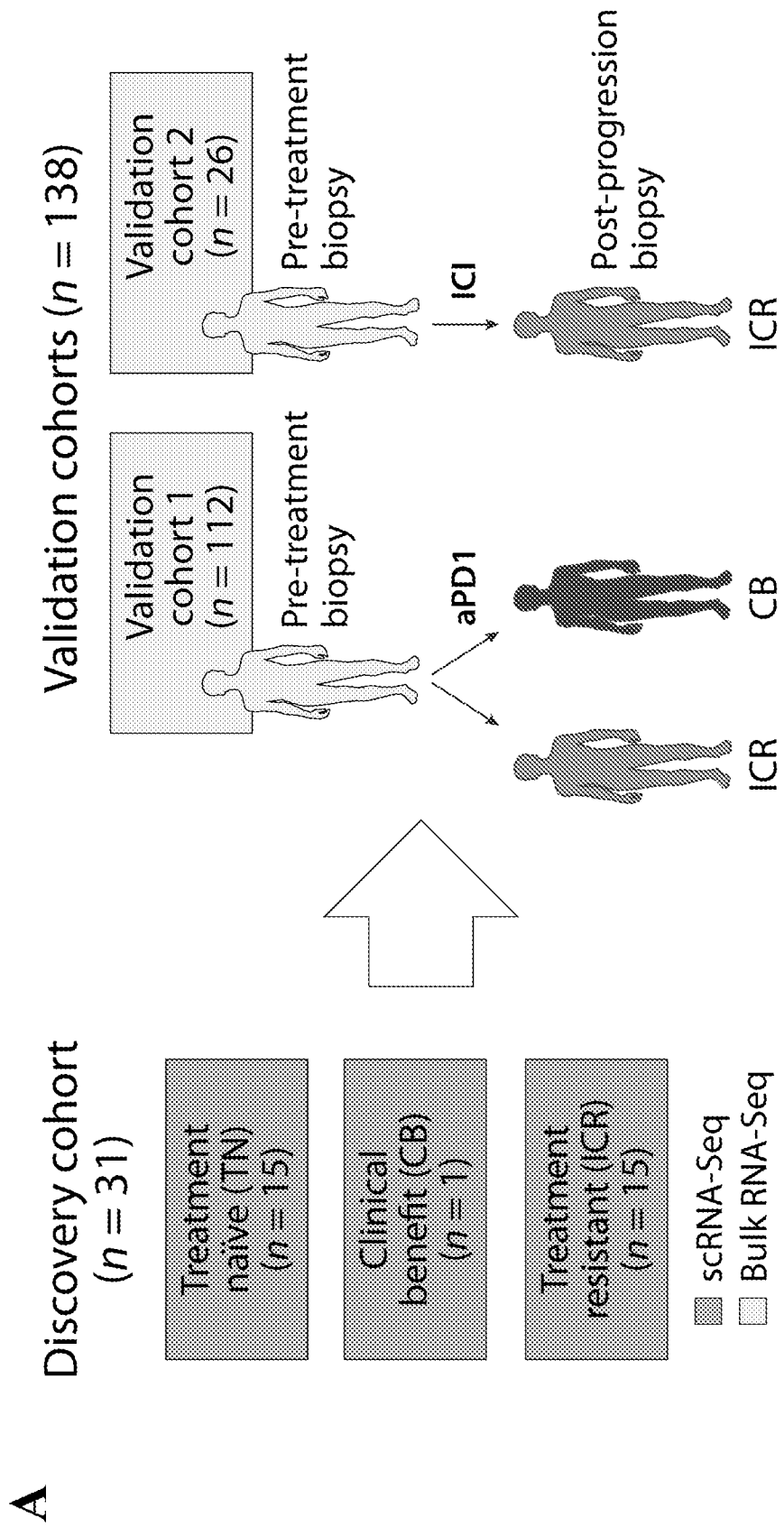

A
Discovery cohort
(n = 31)
Treatment naive (TN) (n = 15)
Clinical benefit (CB) (n = 1)
Treatment resistant (ICR) (n = 15)
scRNA-Seq
Bulk RNA-Seq
Validation cohorts (n = 138)
Validation cohort 1 (n = 112)
Pre-treatment biopsy
aPD1
ICR
CB
Validation cohort 2 (n = 26)
Pre-treatment biopsy
ICI
Post-progression biopsy
ICR

FIG. 1A

B

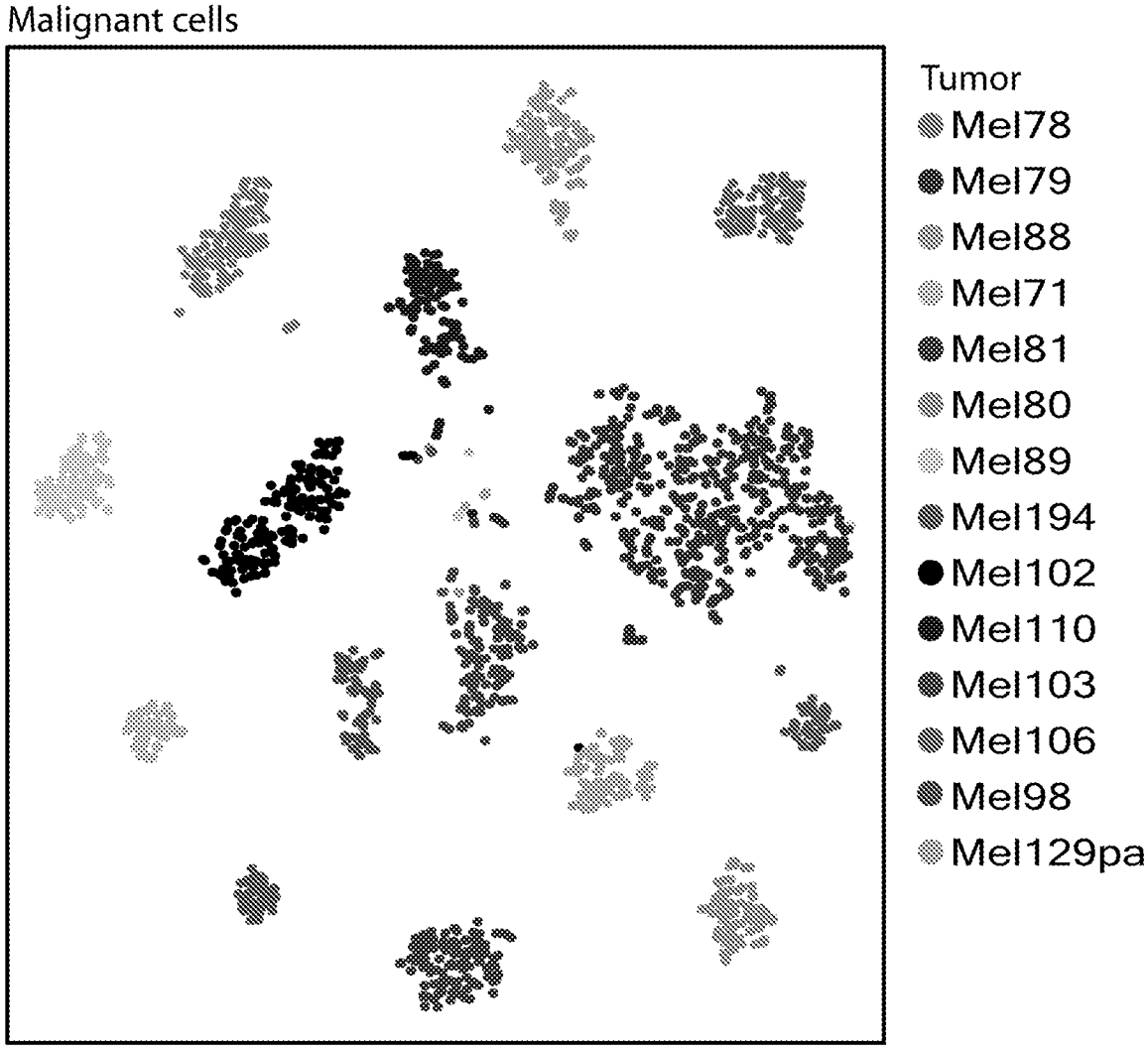

Malignant cells
Tumor
Mel78
Mel79
Mel88
Mel71
Mel81
Mel80
Mel89
Mel194
Mel102
Mel110
Mel103
Mel106
Mel98
Mel129pa

FIG. 1B

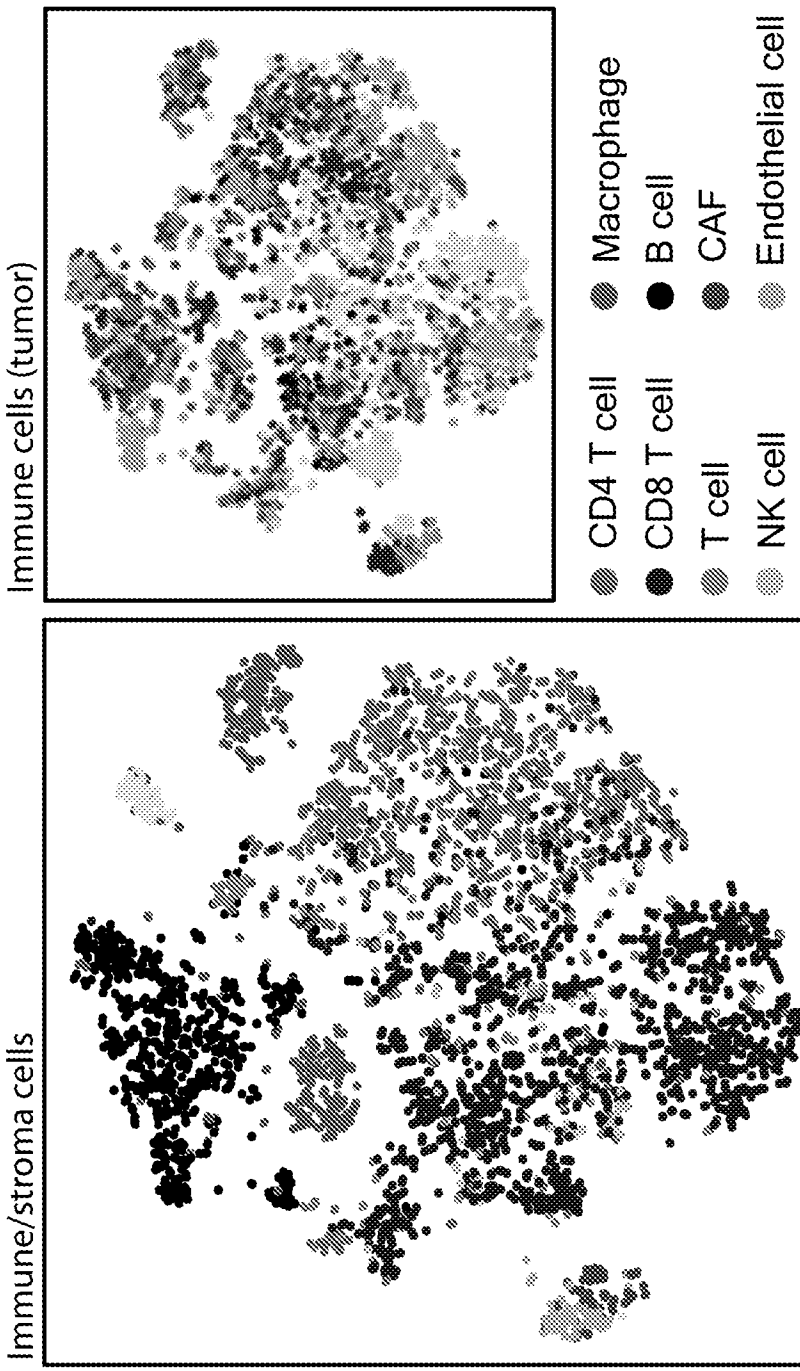

C
Immune/stroma cells
Immune cells (tumor)
CD4 T cell
CD8 T cell
T cell
NK cell
Macrophage
B cell
CAF
Endothelial cell

FIG. 1C

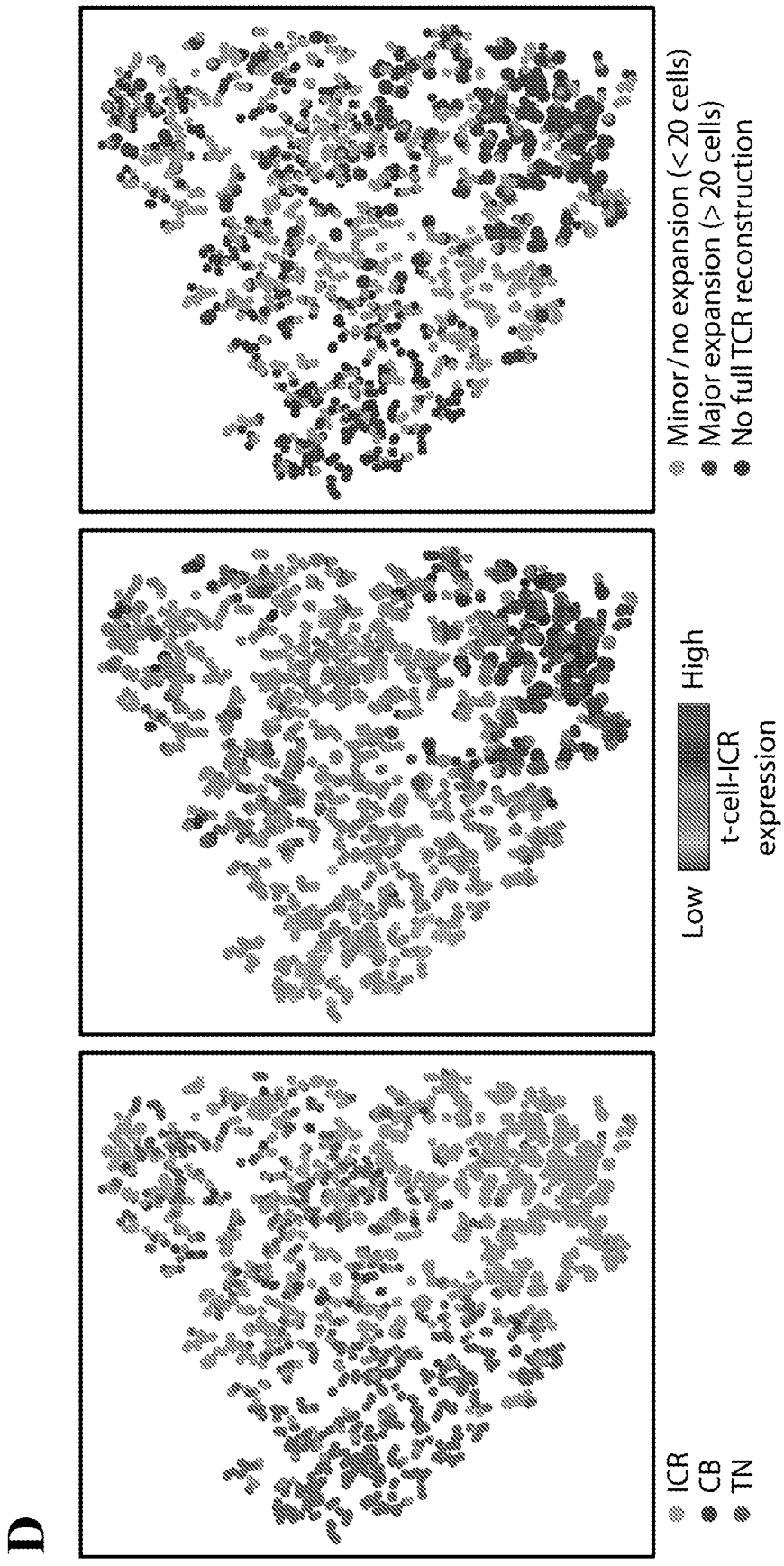

D
ICR
CB
TN
Low
High
t-cell-ICR
expression
Minor / no expansion (< 20 cells)
Major expansion (> 20 cells)
No full TCR reconstruction

FIG. 1D

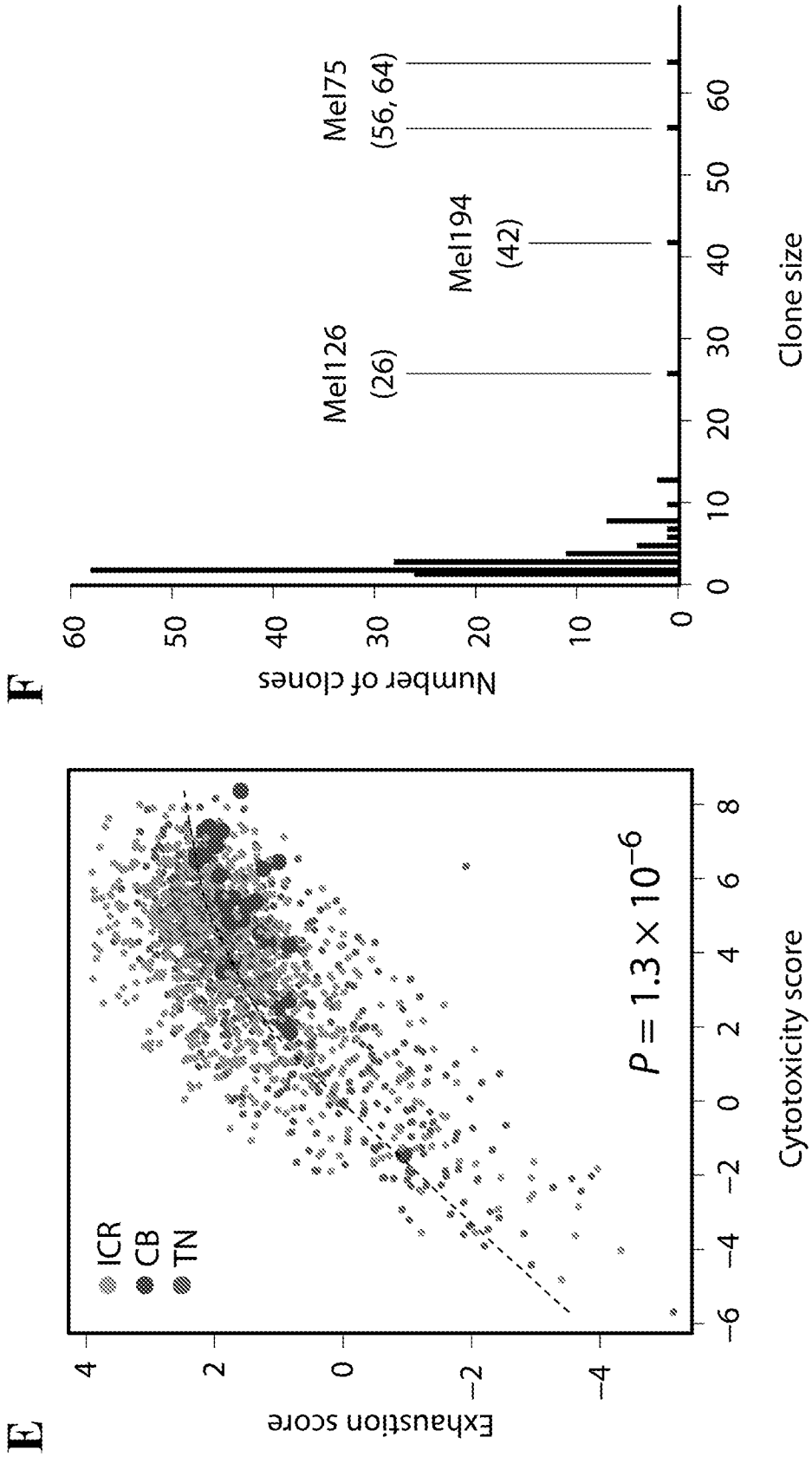

F
Number of clones
Clone size
Mel126
(26)
Mel194
(42)
Mel75
(56, 64)
E
Exhaustion score
Cytotoxicity score
ICR
CB
TN
$P = 1.3 \times 10^{-6}$

FIG. 1E-F

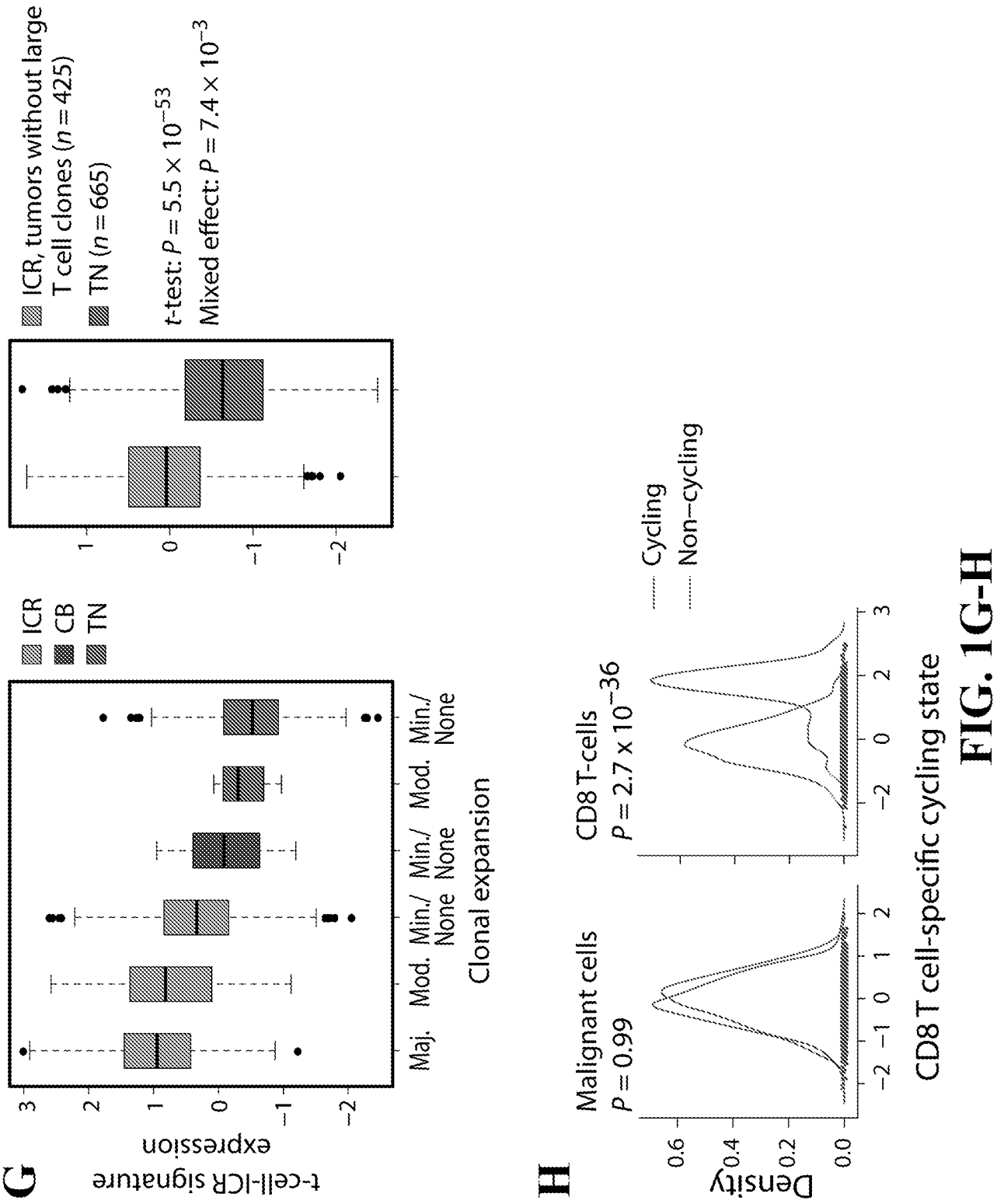

G
t-cell-ICR signature expression
ICR
CB
TN
Maj.
Mod.
Min./ None
Min./ None
Mod.
Min./ None
Clonal expansion
ICR, tumors without large T cell clones (n = 425)
TN (n = 665)
t-test: P = 5.5 × 10−53
Mixed effect: P = 7.4 × 10−3
H
Malignant cells
P = 0.99
CD8 T-cells
P = 2.7 x 10−36
Cycling
Non−cycling
Density
CD8 T cell-specific cycling state

FIG. 1G-H

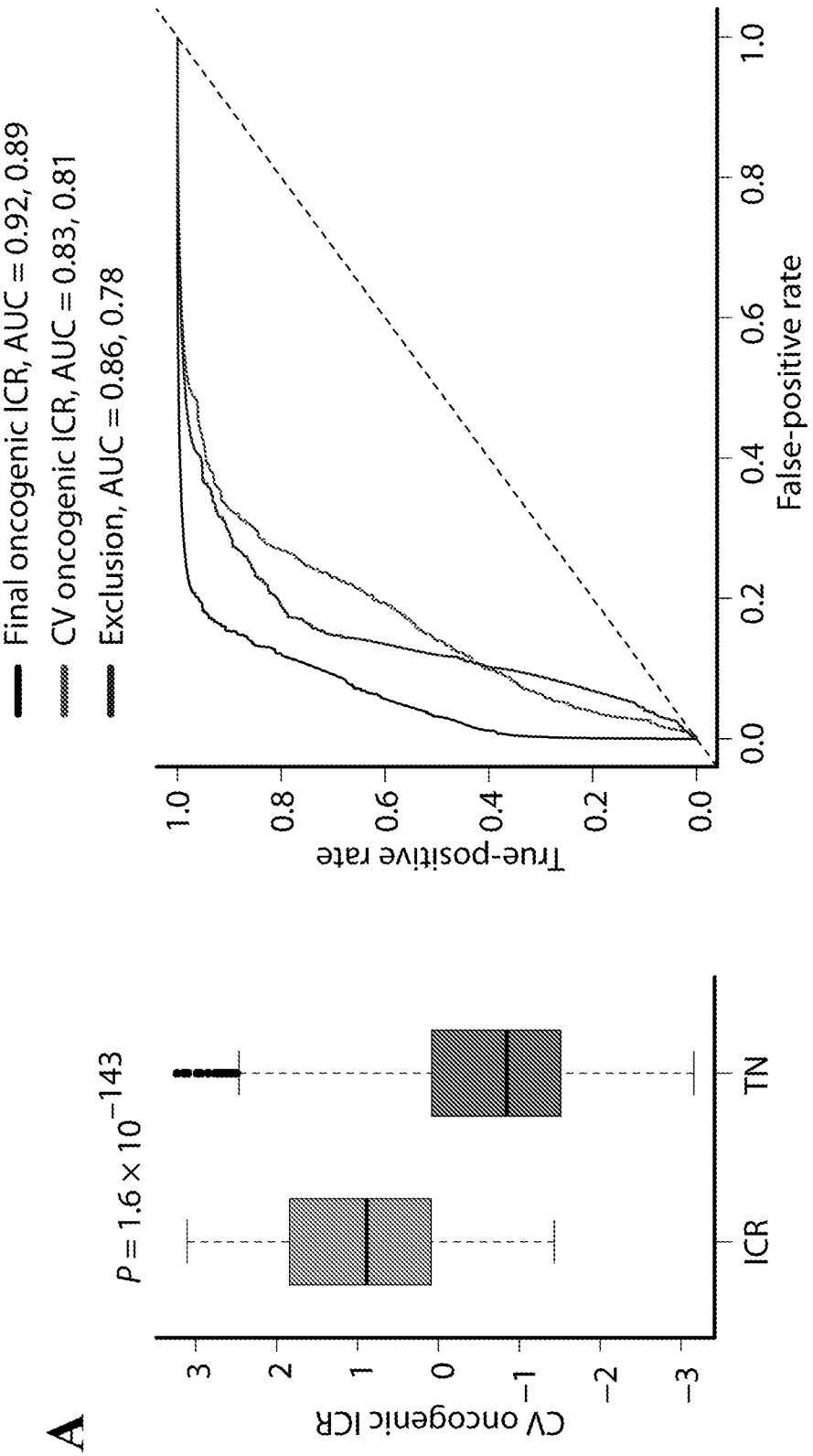

A
CV oncogenic ICR
3
2
1
0
−1
−2
−3
ICR
TN
$P = 1.6 \times 10^{-143}$
True-positive rate
0.0
0.2
0.4
0.6
0.8
1.0
False-positive rate
Final oncogenic ICR, AUC = 0.92, 0.89
CV oncogenic ICR, AUC = 0.83, 0.81
Exclusion, AUC = 0.86, 0.78

FIG. 2A

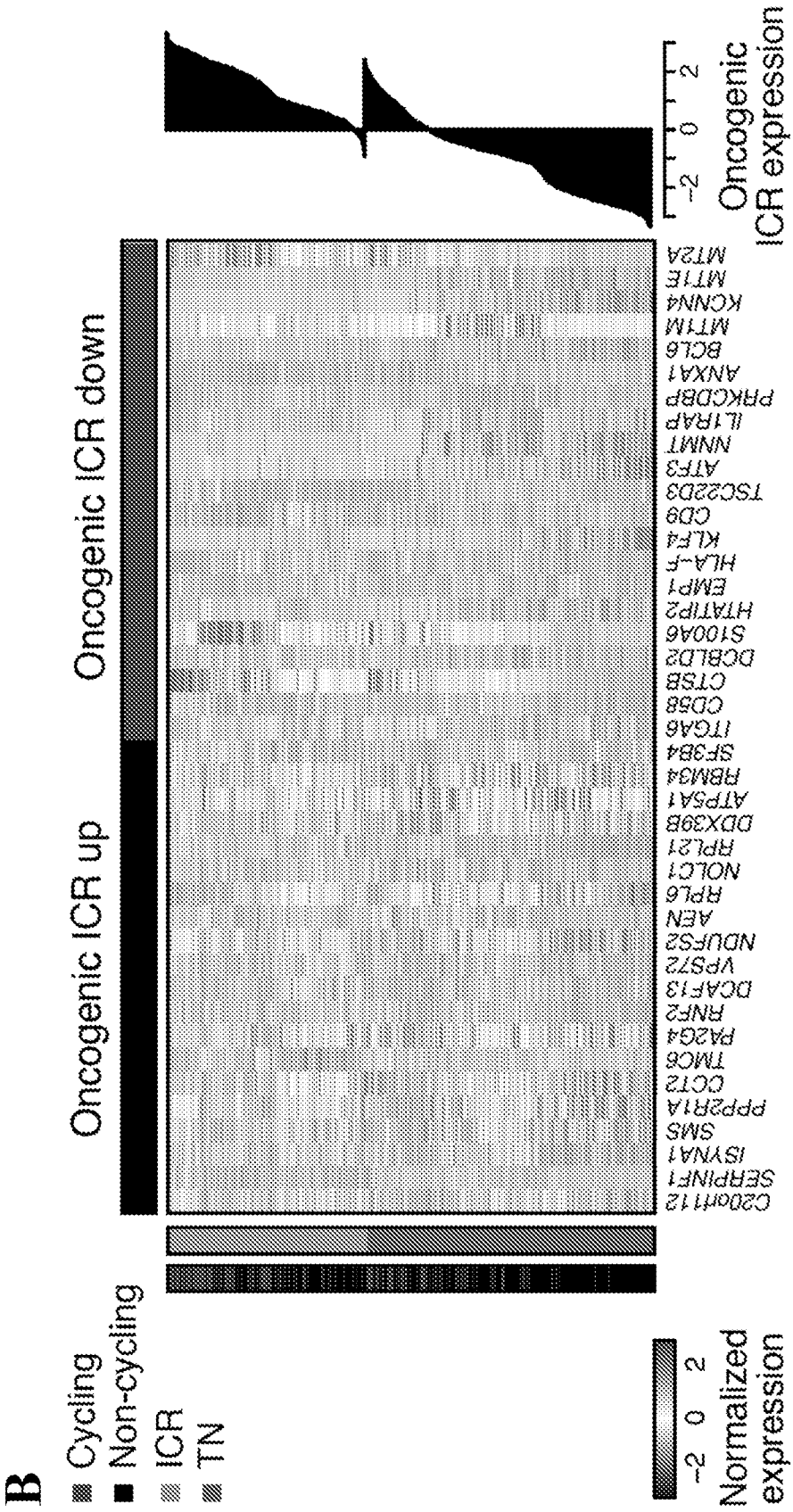

B
Cycling
Non-cycling
ICR
TN
Oncogenic ICR up
Oncogenic ICR down
Oncogenic ICR expression
−2 0 2
Normalized expression
C20orf112
SERPINF1
ISYNA1
SMS
PPP2R1A
CCT2
TMC8
PA2G4
RNF2
DCAF13
VPS72
NDUFS2
AEN
RPL6
NOLC1
RPL21
DDX39B
ATP5A1
RBM34
SF3B4
ITGA6
CD58
CTSB
DCBLD2
S100A6
HTATIP2
EMP1
HLA-F
KLF4
CD9
TSC22D3
ATF3
NNMT
IL1RAP
PRKCDBP
ANXA1
BCL6
MT1M
KCNN4
MT1E
MT2A

FIG. 2B

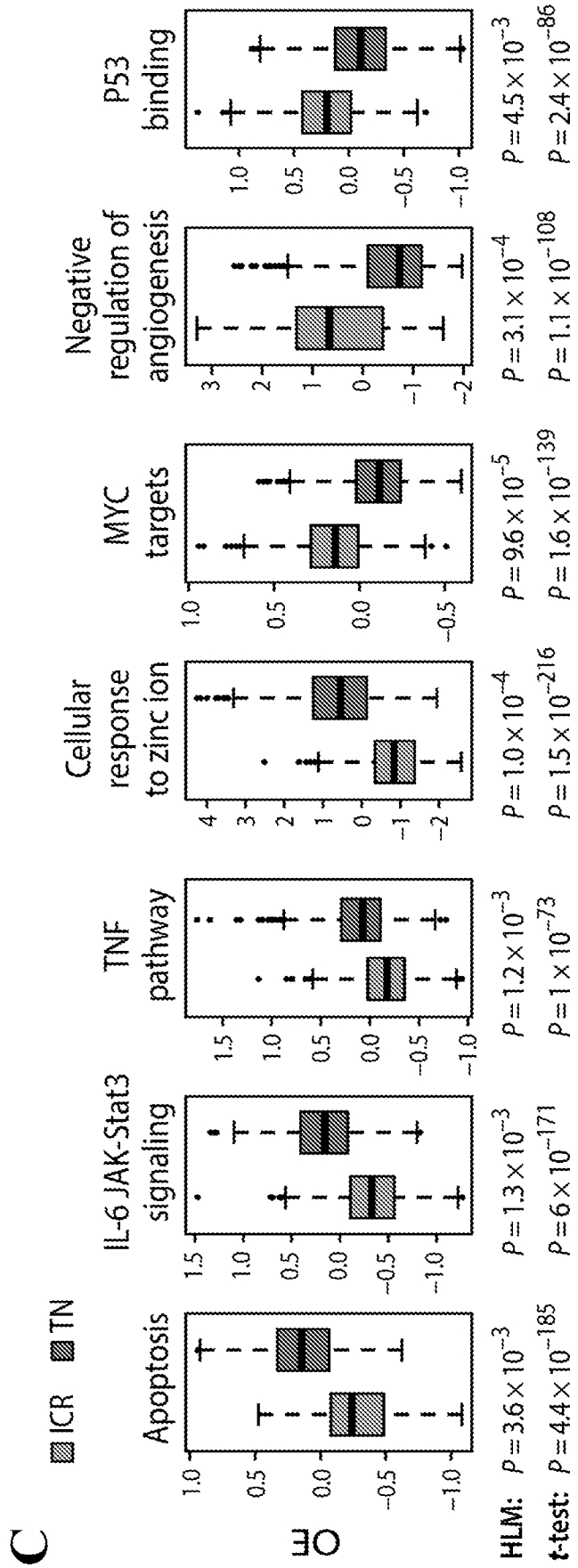

C
ICR
TN
OE
Apoptosis
IL-6 JAK-Stat3 signaling
TNF pathway
Cellular response to zinc ion
MYC targets
Negative regulation of angiogenesis
P53 binding
HLM: P = 3.6 × 10^−3 P = 1.3 × 10^−3 P = 1.2 × 10^−3 P = 1.0 × 10^−4 P = 9.6 × 10^−5 P = 3.1 × 10^−4 P = 4.5 × 10^−3
t-test: P = 4.4 × 10^−185 P = 6 × 10^−171 P = 1 × 10^−73 P = 1.5 × 10^−216 P = 1.6 × 10^−139 P = 1.1 × 10^−108 P = 2.4 × 10^−86

FIG. 2C

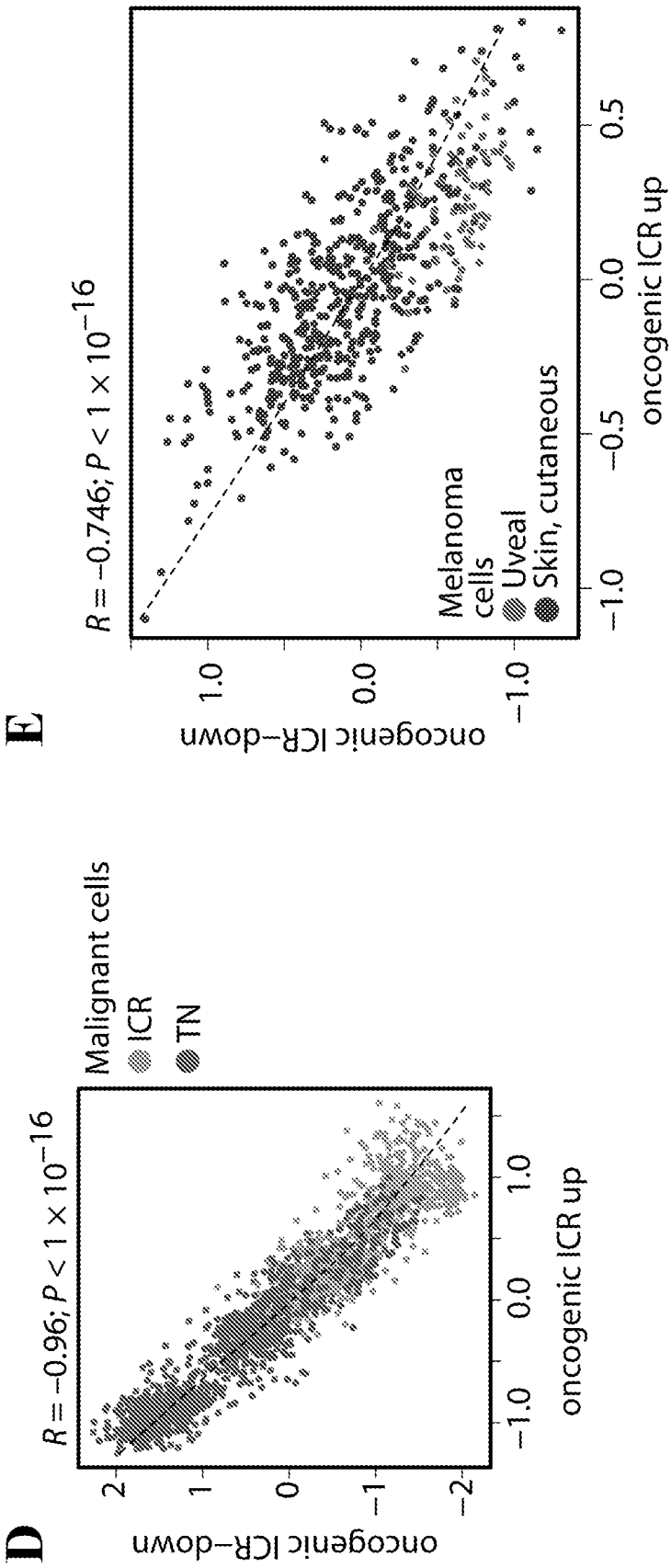

D
R = −0.96; P < 1 × 10−16
Malignant cells
ICR
TN
oncogenic ICR–down
oncogenic ICR up
2
1
0
−1
−2
−1.0
0.0
1.0
E
R = −0.746; P < 1 × 10−16
Melanoma cells
Uveal
Skin, cutaneous
oncogenic ICR–down
oncogenic ICR up
1.0
0.0
−1.0
−1.0
−0.5
0.0
0.5

FIG. 2D-E

F

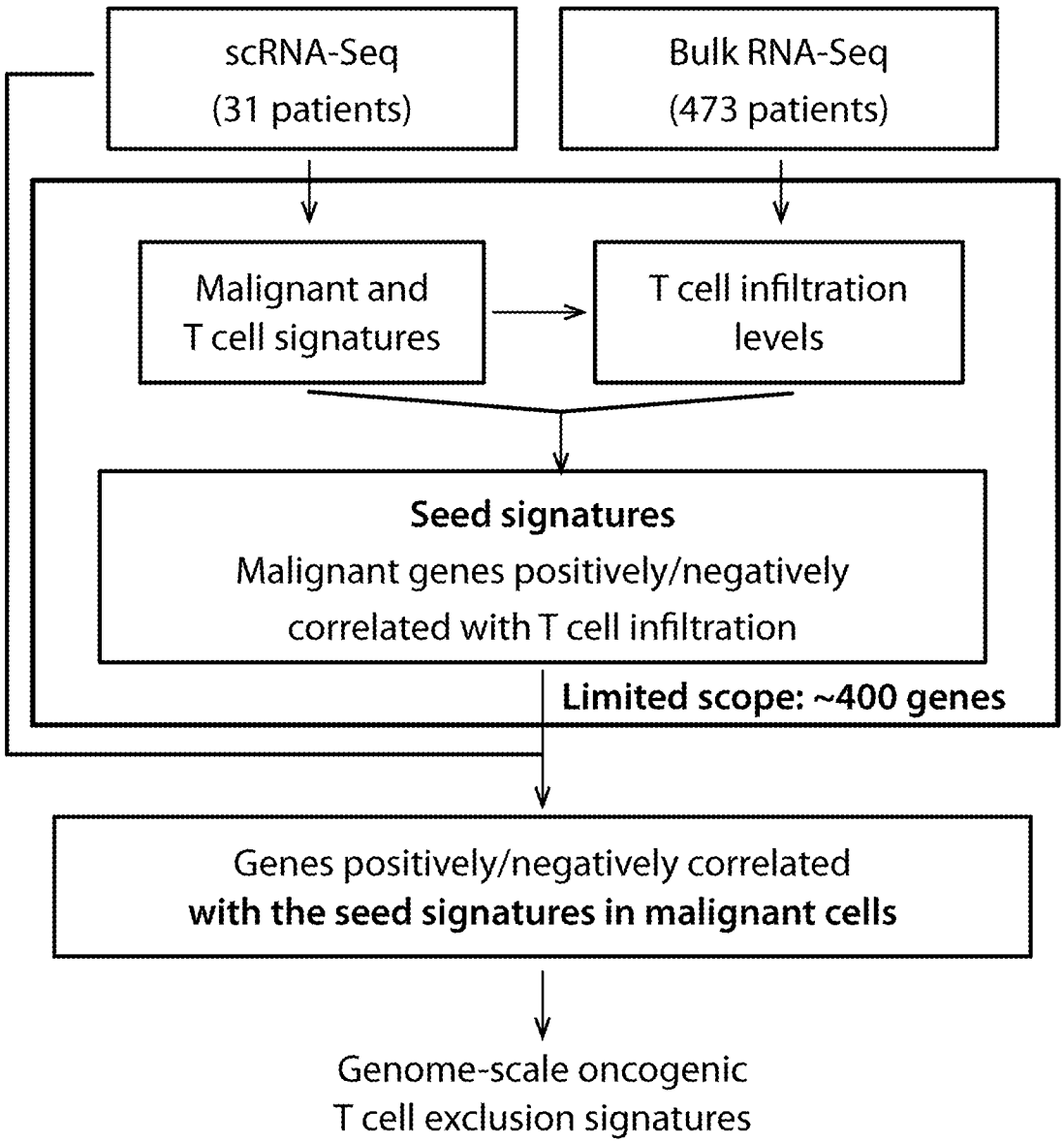

scRNA-Seq
(31 patients)
Bulk RNA-Seq
(473 patients)
Malignant and
T cell signatures
T cell infiltration
levels
Seed signatures
Malignant genes positively/negatively
correlated with T cell infiltration
Limited scope: ~400 genes
Genes positively/negatively correlated
with the seed signatures in malignant cells
Genome-scale oncogenic
T cell exclusion signatures

FIG. 2F

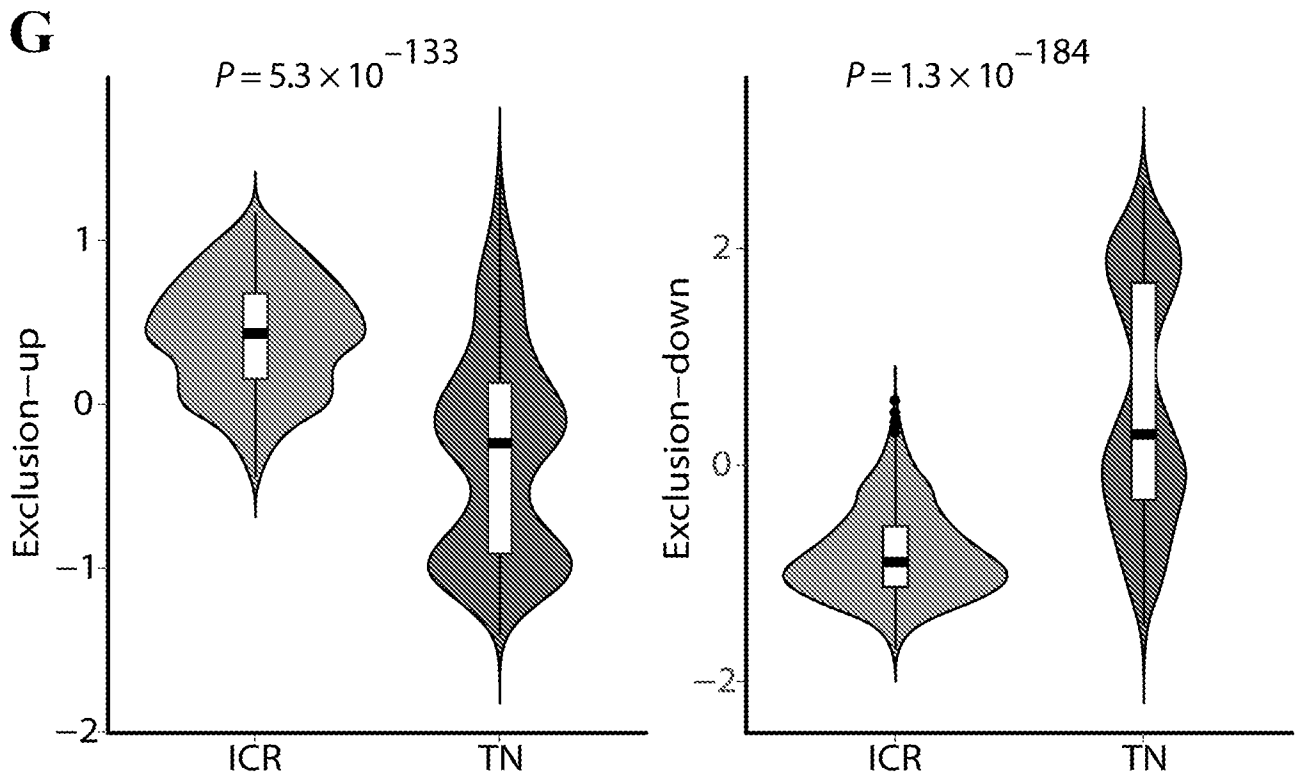

G
P = 5.3 × 10−133
P = 1.3 × 10−184
Exclusion−up
Exclusion−down
1
0
−1
−2
2
0
−2
ICR
TN
ICR
TN

FIG. 2G

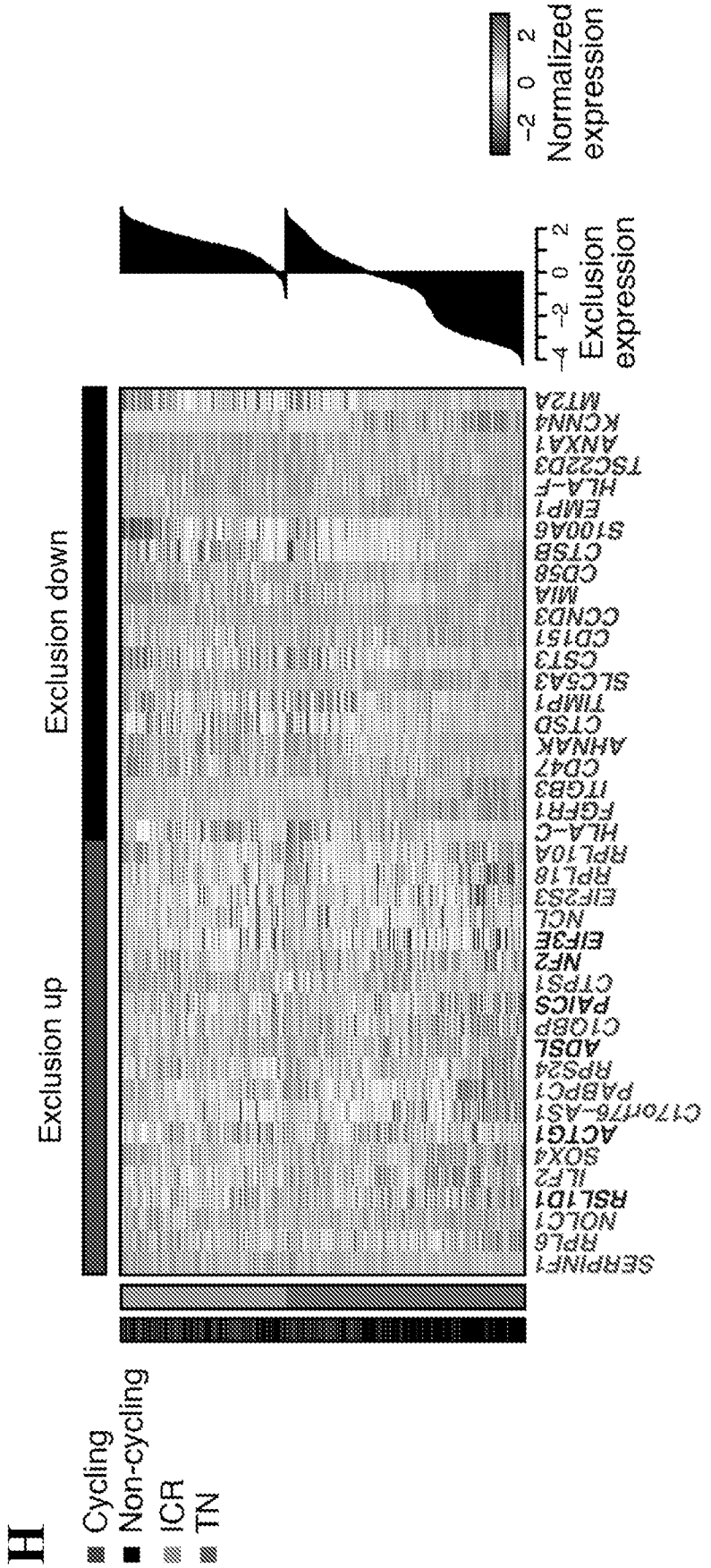

H
Cycling
Non-cycling
ICR
TN
Exclusion up
Exclusion down
Normalized expression
−2 0 2
Exclusion expression
−4 −2 0 2
SERPINF1
RPL6
NOLC1
RSL1D1
ILF2
SOX4
ACTG1
C17orf76-AS1
PABPC1
RPS24
ADSL
C1QBP
PAICS
CTPS1
NF2
EIF3E
NCL
EIF2S3
RPL18
RPL10A
HLA-C
FGFR1
ITGB3
CD47
AHNAK
CTSD
TIMP1
SLC6A3
CST3
CD151
CCND3
IMIA
CD58
CTSB
S100A6
EMP1
HLA-F
TSC22D3
ANXA1
KCNN4
MT2A

FIG. 2H

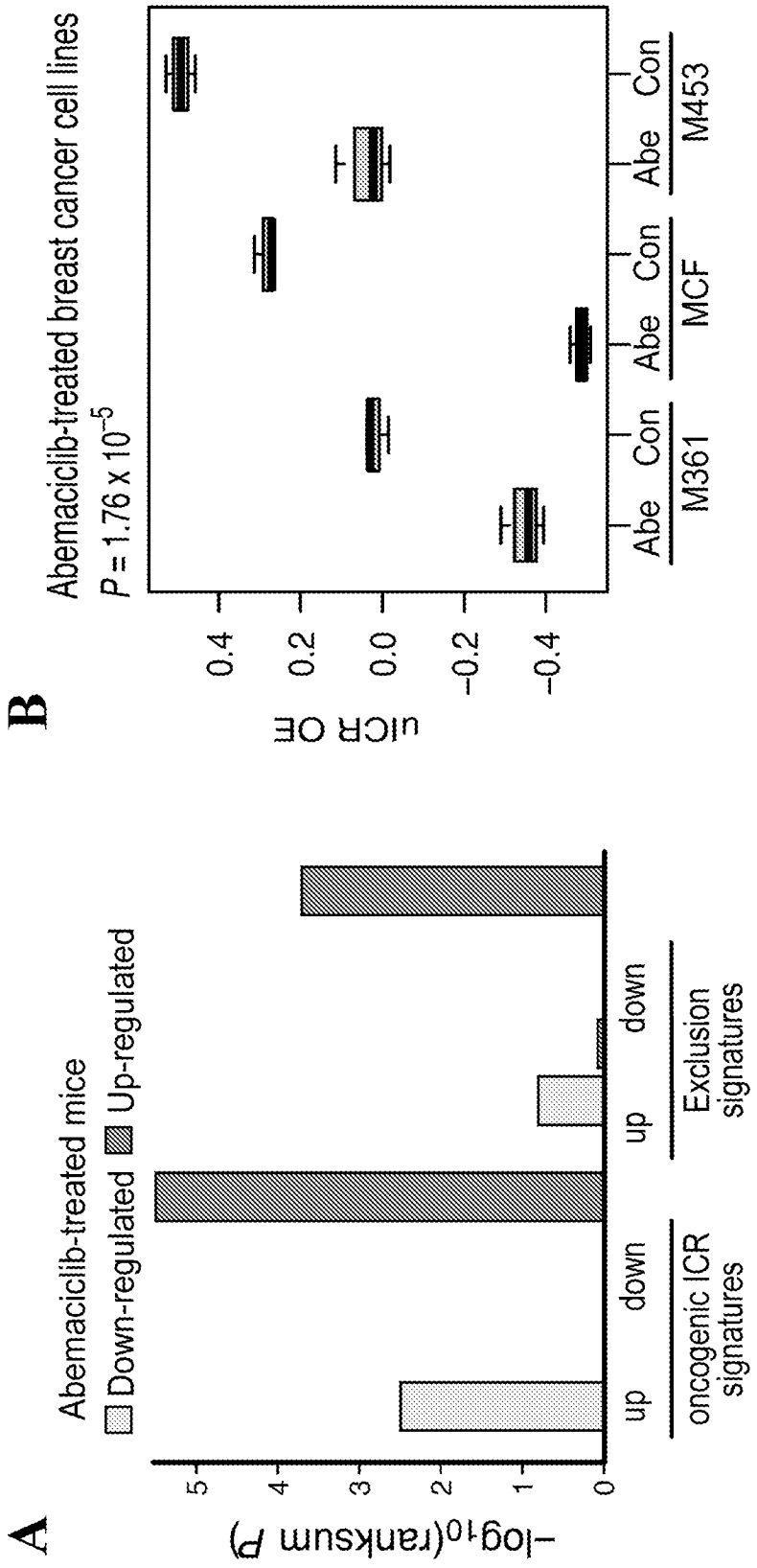

A
Abemaciclib-treated mice
Down-regulated
Up-regulated
−log10(ranksum P)
0
1
2
3
4
5
up
down
up
down
oncogenic ICR signatures
Exclusion signatures
B
Abemaciclib-treated breast cancer cell lines
P = 1.76 x 10−5
uICR OE
0.4
0.2
0.0
−0.2
−0.4
Abe
Con
Abe
Con
Abe
Con
M361
MCF
M453

FIG. 3A-B

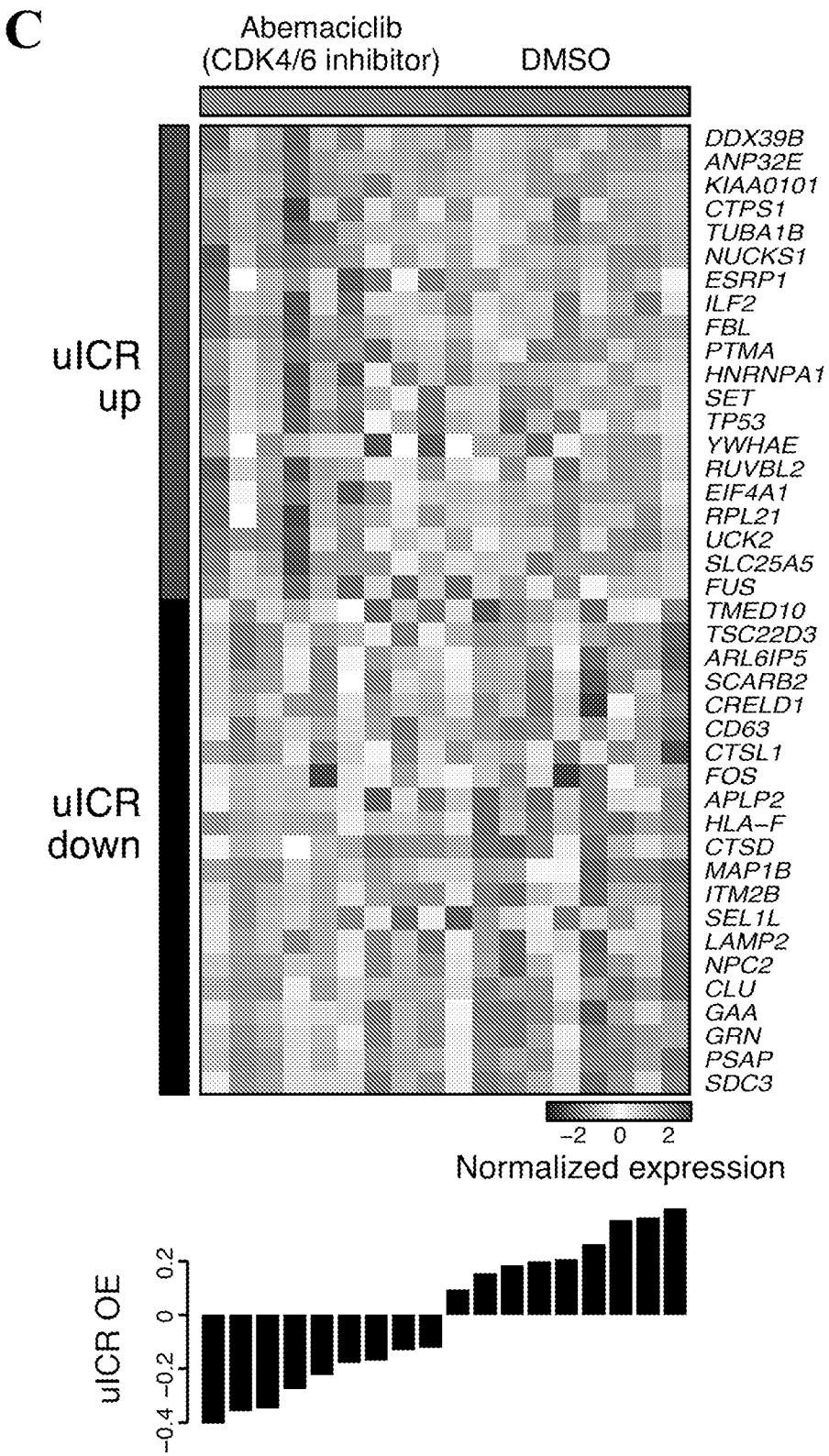

C
Abemaciclib
(CDK4/6 inhibitor)
DMSO
uICR
up
uICR
down
DDX39B
ANP32E
KIAA0101
CTPS1
TUBA1B
NUCKS1
ESRP1
ILF2
FBL
PTMA
HNRNPA1
SET
TP53
YWHAE
RUVBL2
EIF4A1
RPL21
UCK2
SLC25A5
FUS
TMED10
TSC22D3
ARL6IP5
SCARB2
CRELD1
CD63
CTSL1
FOS
APLP2
HLA-F
CTSD
MAP1B
ITM2B
SEL1L
LAMP2
NPC2
CLU
GAA
GRN
PSAP
SDC3
−2 0 2
Normalized expression
uICR OE
0.2
0
−0.2
−0.4

FIG. 3C

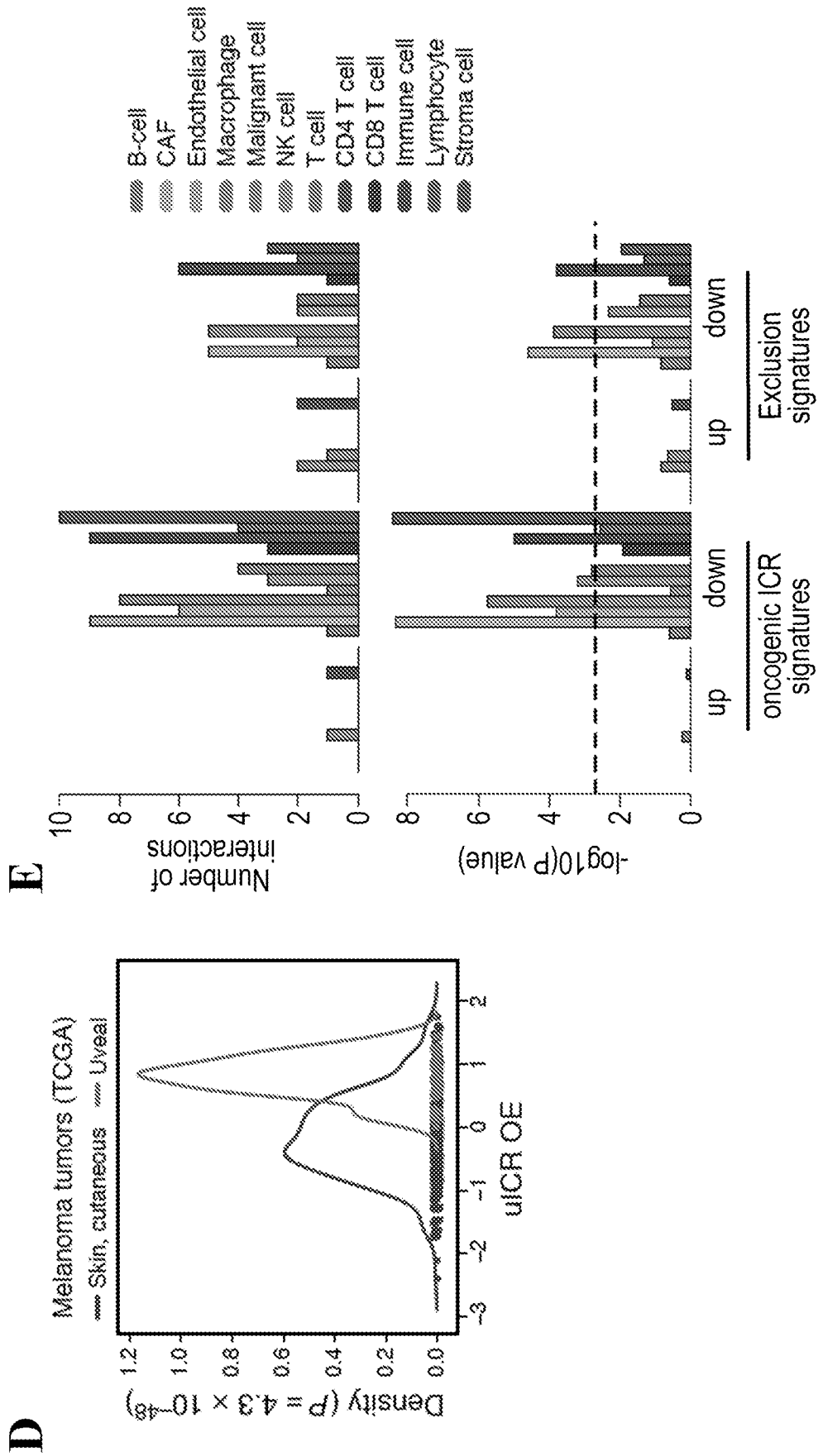

D
Melanoma tumors (TCGA)
Skin, cutaneous
Uveal
Density ($P = 4.3 \times 10^{-48}$)
1.2
1.0
0.8
0.6
0.4
0.2
0.0
−3
−2
−1
0
1
2
uICR OE
E
Number of interactions
10
8
6
4
2
0
B-cell
CAF
Endothelial cell
Macrophage
Malignant cell
NK cell
T cell
CD4 T cell
CD8 T cell
Immune cell
Lymphocyte
Stroma cell
-log10(P value)
8
6
4
2
0
up
down
oncogenic ICR signatures
up
down
Exclusion signatures

FIG. 3D-E

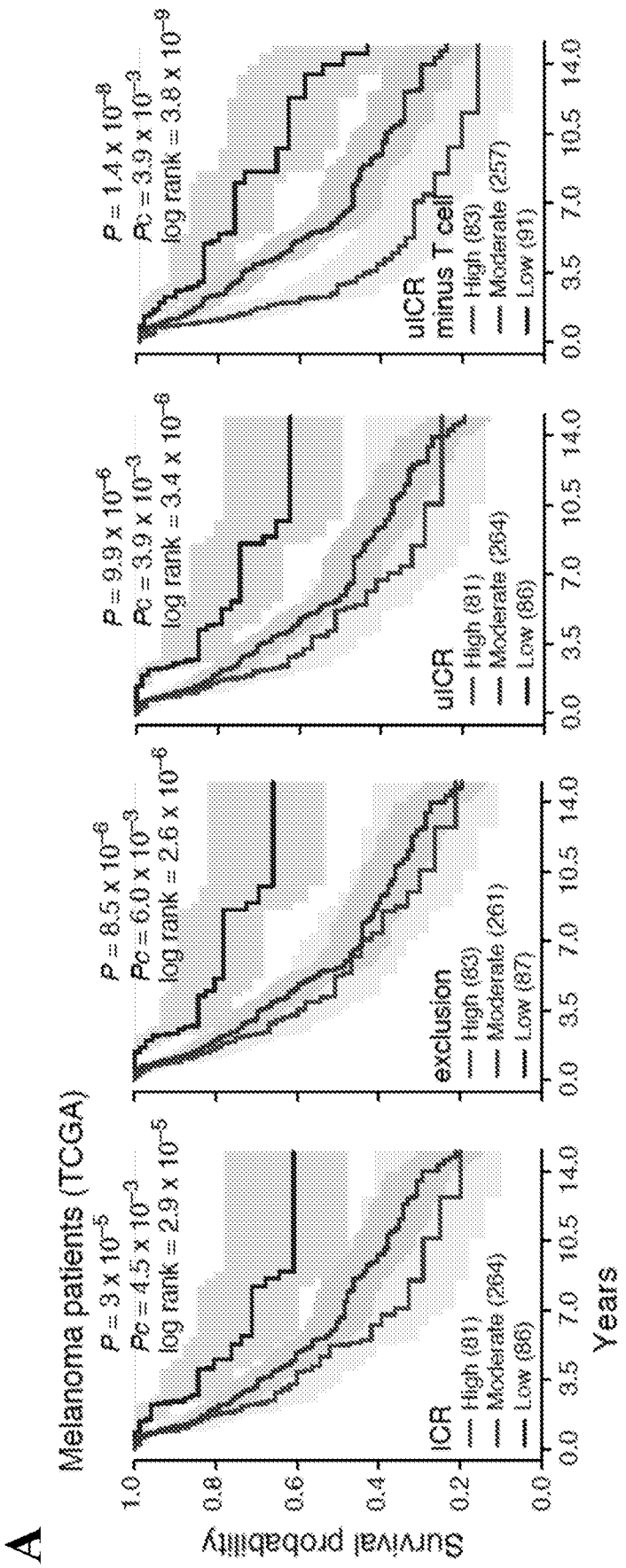

A
Melanoma patients (TCGA)
Survival probability
Years
ICR
High (81)
Moderate (264)
Low (86)
P = 3 x 10^-5
Pc = 4.5 x 10^-3
log rank = 2.9 x 10^-5
exclusion
High (83)
Moderate (261)
Low (87)
P = 8.5 x 10^-6
Pc = 6.0 x 10^-3
log rank = 2.6 x 10^-6
uICR
High (81)
Moderate (264)
Low (86)
P = 9.9 x 10^-6
Pc = 3.9 x 10^-3
log rank = 3.4 x 10^-6
uICR
minus T cell
High (83)
Moderate (257)
Low (91)
P = 1.4 x 10^-8
Pc = 3.9 x 10^-3
log rank = 3.8 x 10^-9
0.0
0.2
0.4
0.6
0.8
1.0
0.0
3.5
7.0
10.5
14.0

FIG. 4A

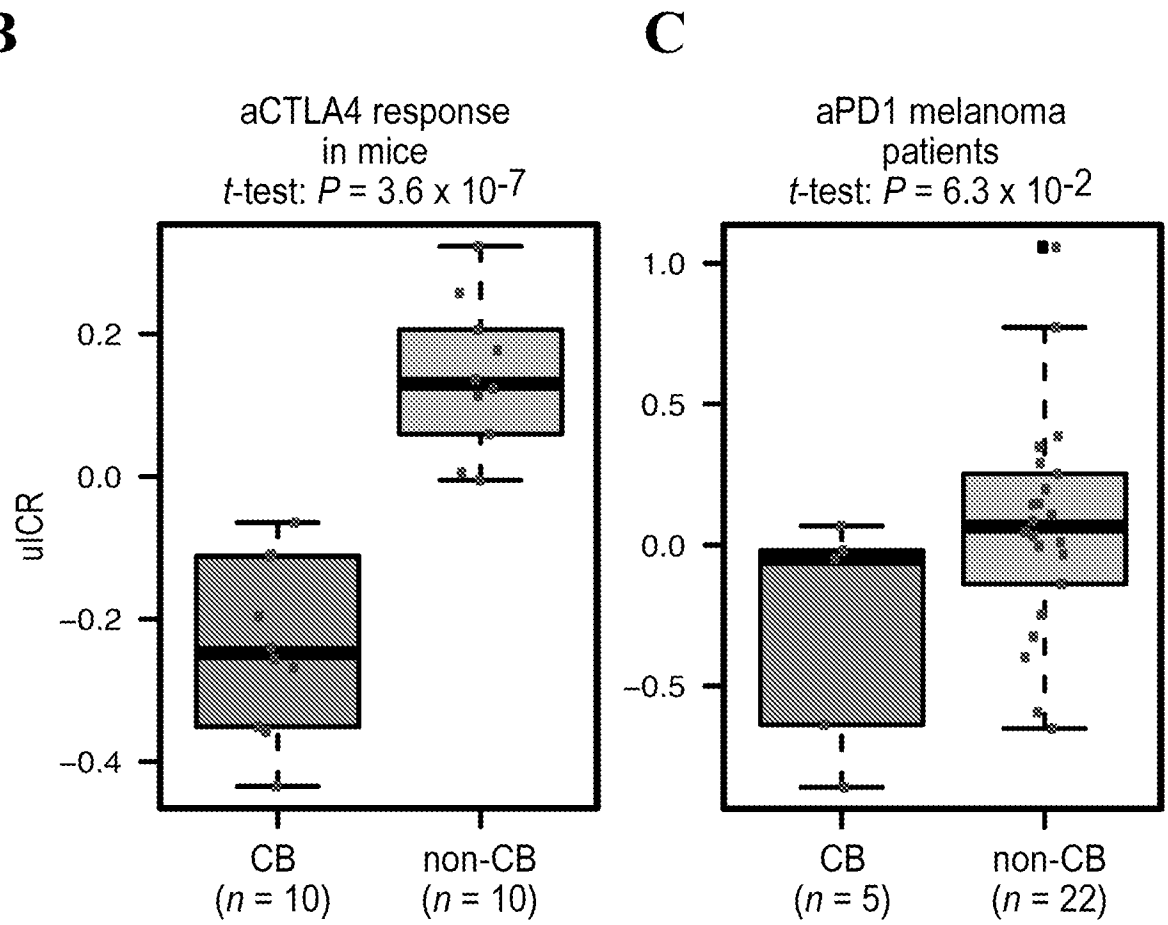

B
aCTLA4 response
in mice
t-test: P = 3.6 x 10-7
uICR
0.2
0.0
−0.2
−0.4
CB
(n = 10)
non-CB
(n = 10)
C
aPD1 melanoma
patients
t-test: P = 6.3 x 10-2
1.0
0.5
0.0
−0.5
CB
(n = 5)
non-CB
(n = 22)

FIG. 4B-C

D

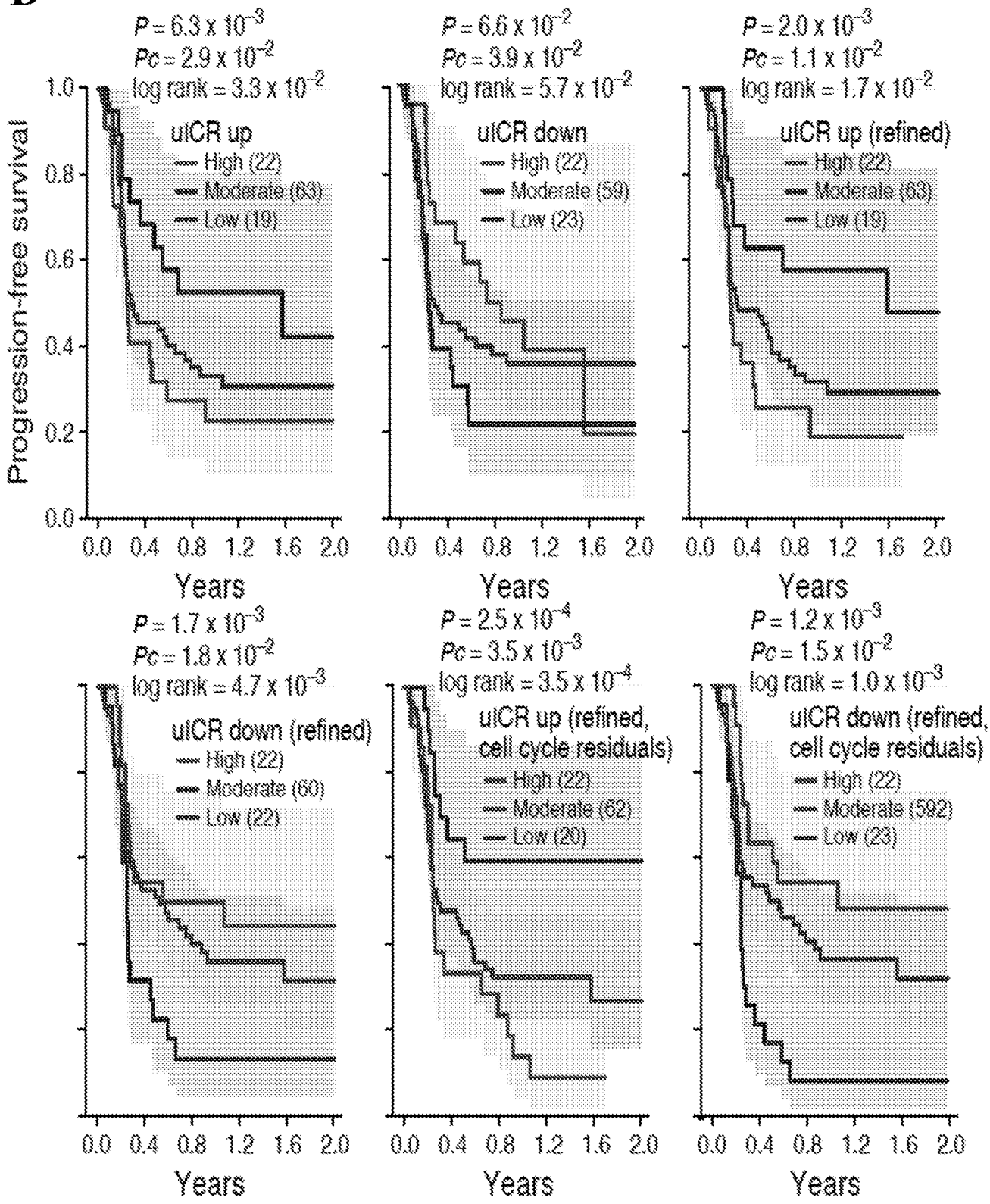

P = 6.3 x 10-3
Pc = 2.9 x 10-2
log rank = 3.3 x 10-2
ulCR up
High (22)
Moderate (63)
Low (19)
P = 6.6 x 10-2
Pc = 3.9 x 10-2
log rank = 5.7 x 10-2
ulCR down
High (22)
Moderate (59)
Low (23)
P = 2.0 x 10-3
Pc = 1.1 x 10-2
log rank = 1.7 x 10-2
ulCR up (refined)
High (22)
Moderate (63)
Low (19)
P = 1.7 x 10-3
Pc = 1.8 x 10-2
log rank = 4.7 x 10-3
ulCR down (refined)
High (22)
Moderate (60)
Low (22)
P = 2.5 x 10-4
Pc = 3.5 x 10-3
log rank = 3.5 x 10-4
ulCR up (refined, cell cycle residuals)
High (22)
Moderate (62)
Low (20)
P = 1.2 x 10-3
Pc = 1.5 x 10-2
log rank = 1.0 x 10-3
ulCR down (refined, cell cycle residuals)
High (22)
Moderate (592)
Low (23)
Progression-free survival
1.0
0.8
0.6
0.4
0.2
0.0
0.0 0.4 0.8 1.2 1.6 2.0
Years

FIG. 4D

E

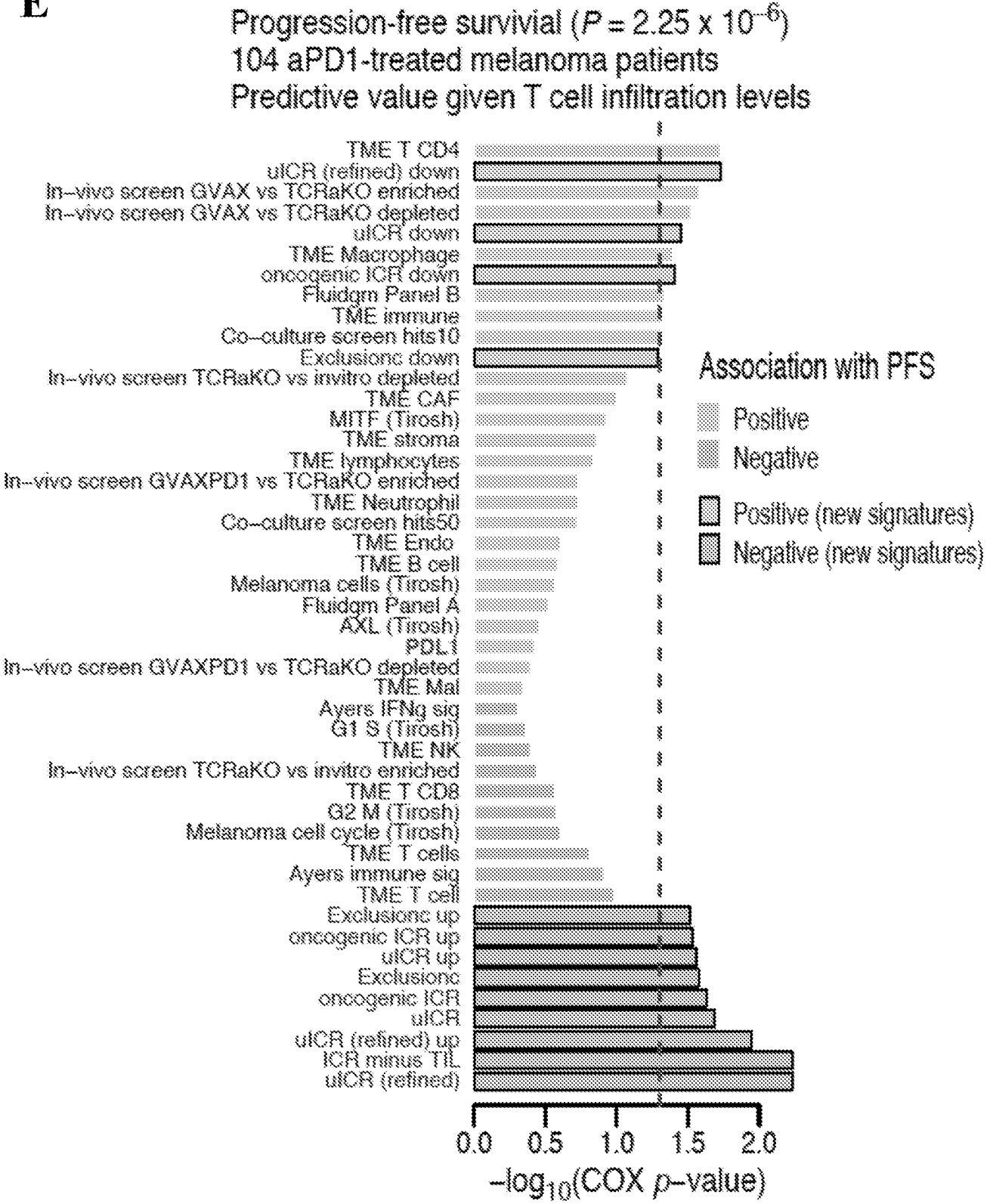

Progression-free survivial (P = 2.25 x 10−6)
104 aPD1-treated melanoma patients
Predictive value given T cell infiltration levels
TME T CD4
ulCR (refined) down
In−vivo screen GVAX vs TCRaKO enriched
In−vivo screen GVAX vs TCRaKO depleted
ulCR down
TME Macrophage
oncogenic ICR down
Fluidgm Panel B
TME immune
Co−culture screen hits10
Exclusionc down
In−vivo screen TCRaKO vs invitro depleted
TME CAF
MITF (Tirosh)
TME stroma
TME lymphocytes
In−vivo screen GVAXPD1 vs TCRaKO enriched
TME Neutrophil
Co−culture screen hits50
TME Endo
TME B cell
Melanoma cells (Tirosh)
Fluidgm Panel A
AXL (Tirosh)
PDL1
In−vivo screen GVAXPD1 vs TCRaKO depleted
TME Mal
Ayers IFNg sig
G1 S (Tirosh)
TME NK
In−vivo screen TCRaKO vs invitro enriched
TME T CD8
G2 M (Tirosh)
Melanoma cell cycle (Tirosh)
TME T cells
Ayers immune sig
TME T cell
Exclusionc up
oncogenic ICR up
ulCR up
Exclusionc
oncogenic ICR
ulCR
ulCR (refined) up
ICR minus TIL
ulCR (refined)
Association with PFS
Positive
Negative
Positive (new signatures)
Negative (new signatures)
0.0
0.5
1.0
1.5
2.0
−log10(COX p−value)

FIG. 4E

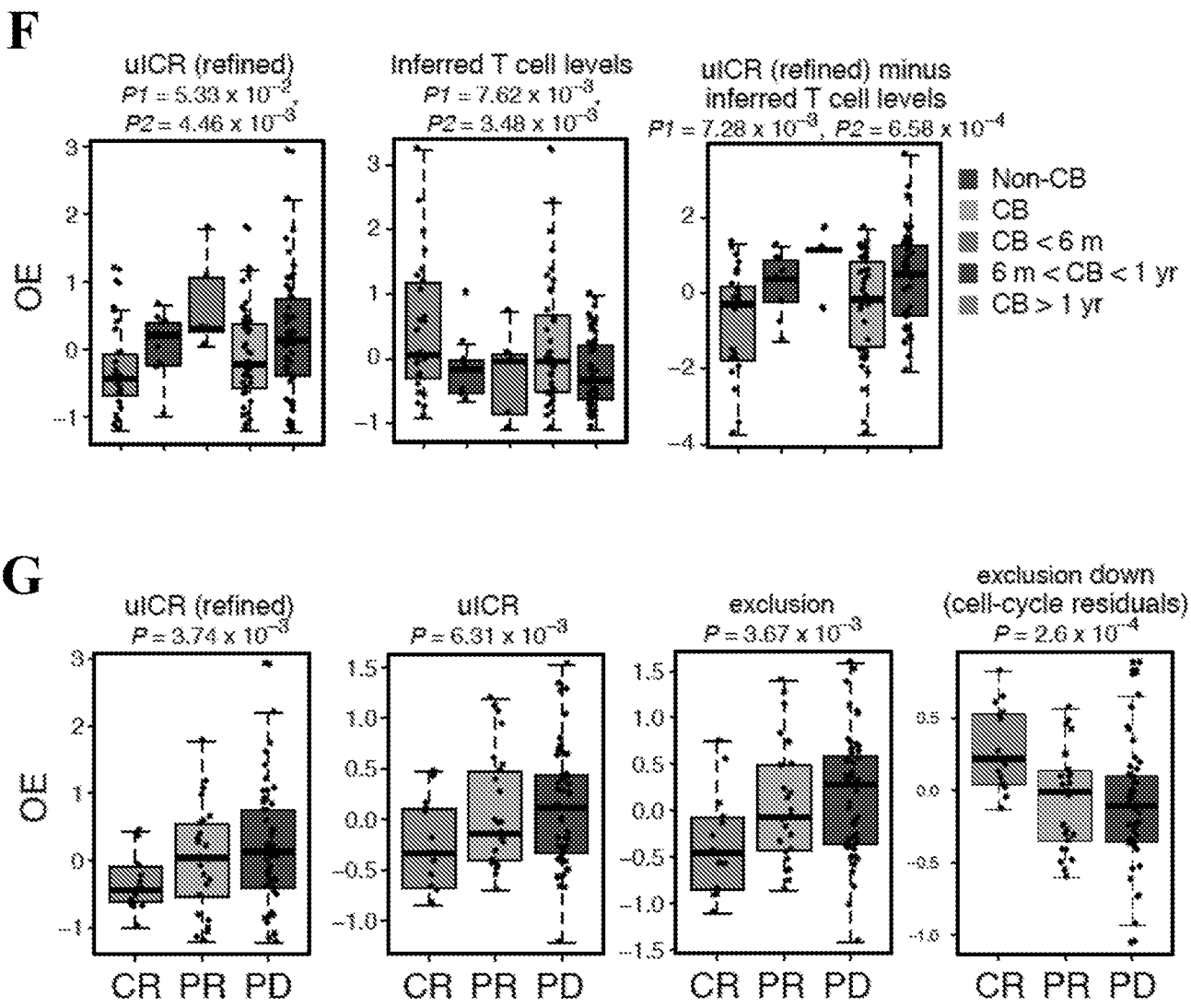

F
ulCR (refined)
P1 = 5.33 x 10^-3,
P2 = 4.46 x 10^-3
Inferred T cell levels
P1 = 7.62 x 10^-3,
P2 = 3.48 x 10^-3
ulCR (refined) minus
inferred T cell levels
P1 = 7.28 x 10^-3, P2 = 6.58 x 10^-4
OE
Non-CB
CB
CB < 6 m
6 m < CB < 1 yr
CB > 1 yr
G
ulCR (refined)
P = 3.74 x 10^-3
ulCR
P = 6.31 x 10^-3
exclusion
P = 3.67 x 10^-3
exclusion down
(cell-cycle residuals)
P = 2.6 x 10^-4
OE
CR PR PD
CR PR PD
CR PR PD
CR PR PD

FIG. 4F-G

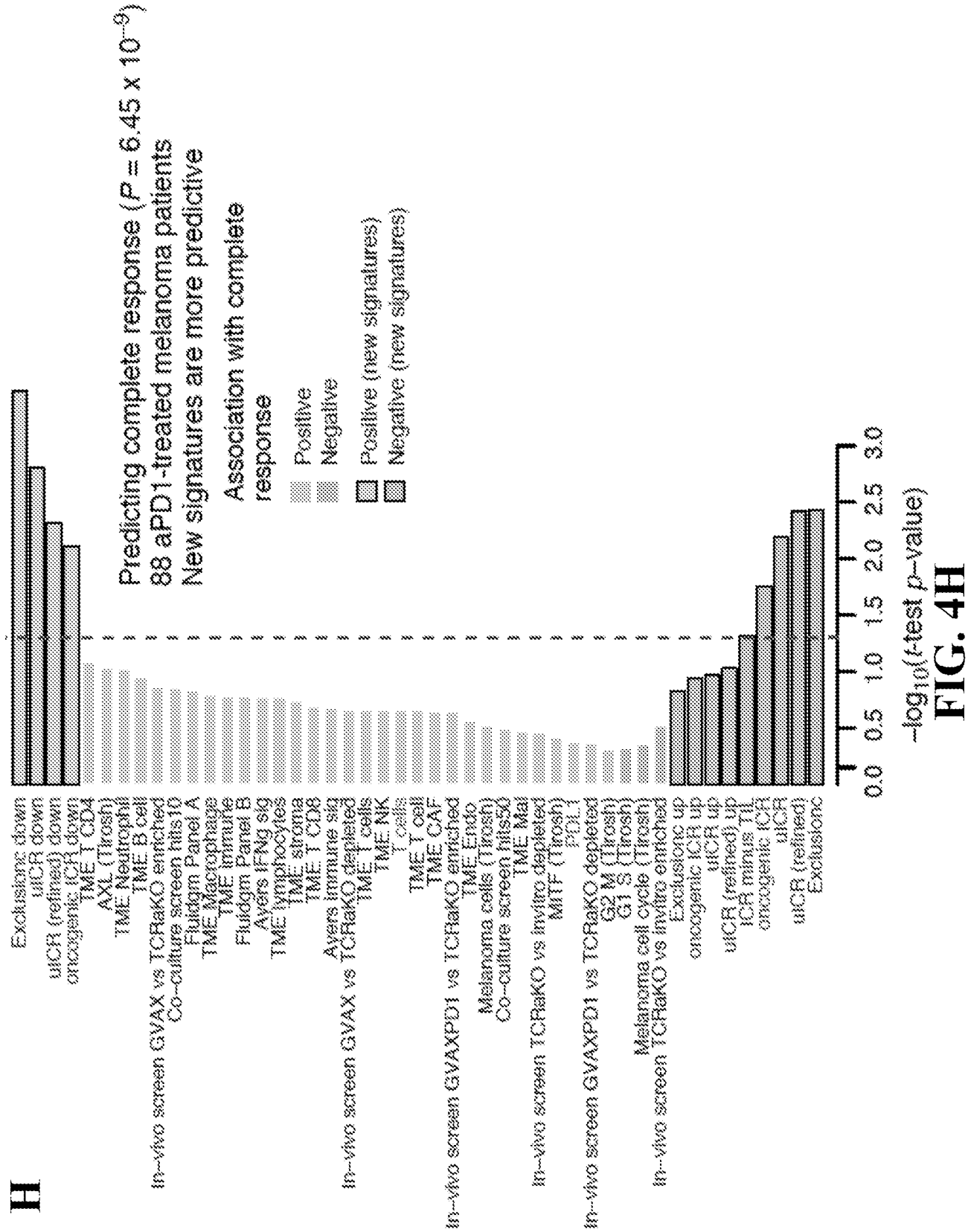

H
Predicting complete response ($P = 6.45 \times 10^{-9}$)
88 aPD1-treated melanoma patients
New signatures are more predictive
Association with complete response
Positive
Negative
Positive (new signatures)
Negative (new signatures)
Exclusionc down
uICR down
uICR (refined) down
oncogenic ICR down
TME T CD4
AXL (Tirosh)
TME Neutrophil
TME B cell
In–vivo screen GVAX vs TCRaKO enriched
Co–culture screen hits10
Fluidgm Panel A
TME Macrophage
TME immune
Fluidgm Panel B
Ayers IFNg sig
TME lymphocytes
TME stroma
TME T CD8
Ayers immune sig
In–vivo screen GVAX vs TCRaKO depleted
TME T cells
TME NK
T cells
TME T cell
TME CAF
In–vivo screen GVAXPD1 vs TCRaKO enriched
TME Endo
Melanoma cells (Tirosh)
Co–culture screen hits50
TME Mal
In–vivo screen TCRaKO vs invitro depleted
MITF (Tirosh)
FOL1
In–vivo screen GVAXPD1 vs TCRaKO depletet
G2 M (Tirosh)
G1 S (Tirosh)
Melanoma cell cycle (Tirosh)
In–vivo screen TCRaKO vs invitro enriched
Exclusionc up
oncogenic ICR up
uICR up
uICR (refined) up
ICR minus TIL
oncogenic ICR
uICR
uICR (refined)
Exclusionc
0.0 0.5 1.0 1.5 2.0 2.5 3.0
$-\log_{10}$(t-test p–value)

FIG. 4H

I

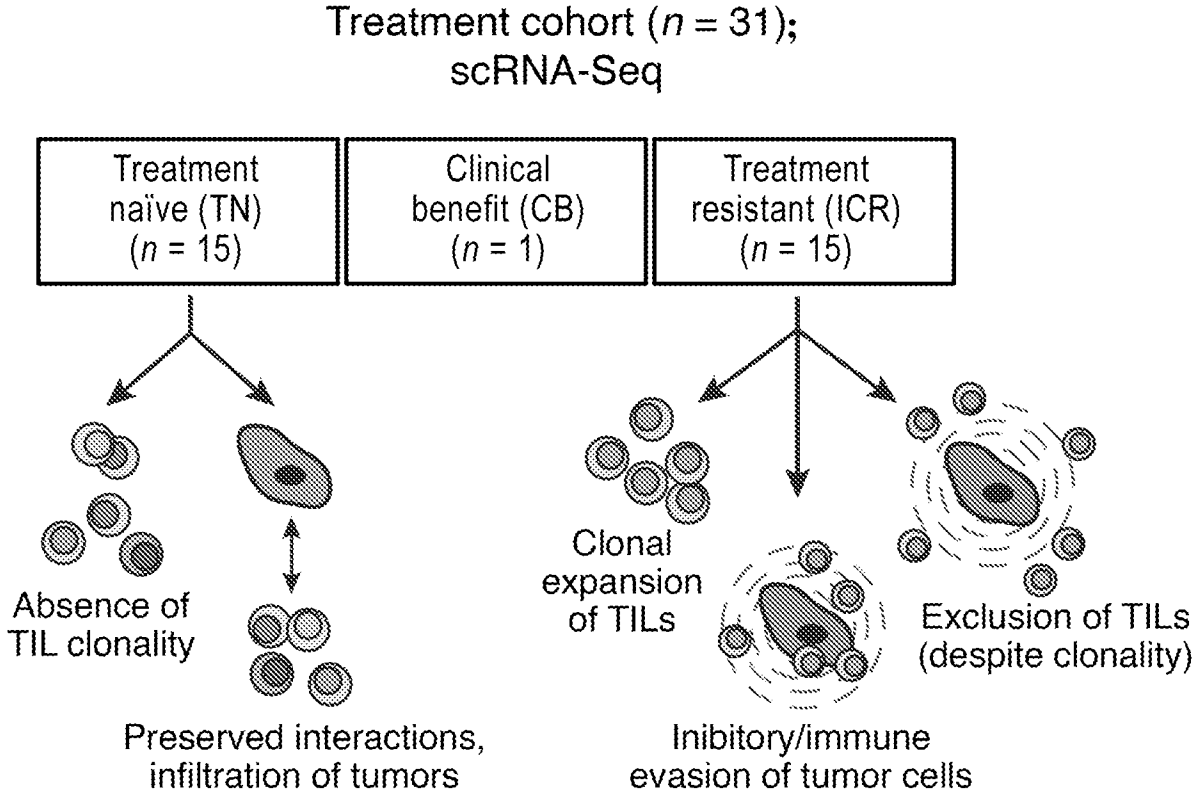

Treatment cohort (n = 31);
scRNA-Seq
Treatment naïve (TN) (n = 15)
Clinical benefit (CB) (n = 1)
Treatment resistant (ICR) (n = 15)
Absence of TIL clonality
Preserved interactions, infiltration of tumors
Clonal expansion of TILs
Exclusion of TILs (despite clonality)
Inibitory/immune evasion of tumor cells

FIG. 4I

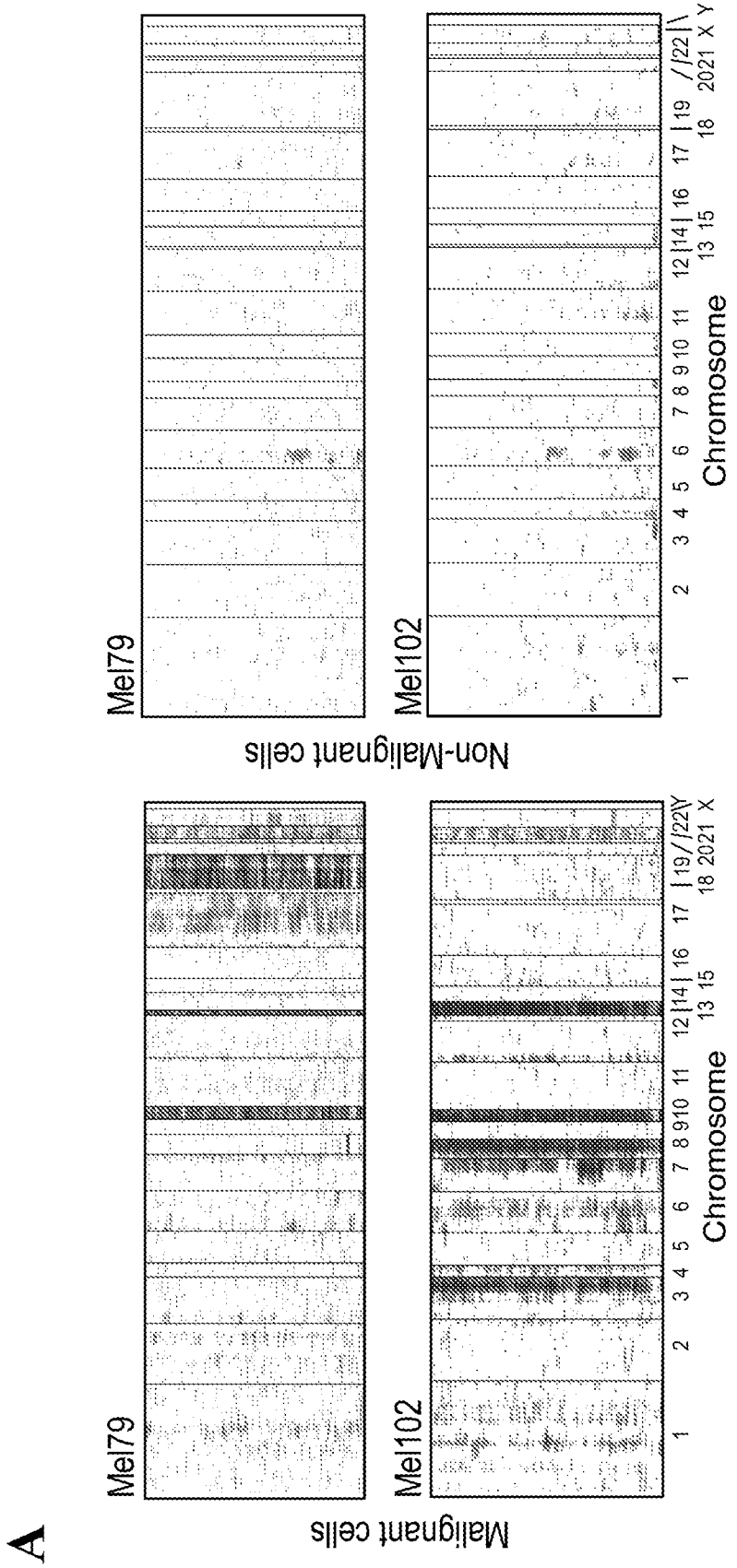

A
Malignant cells
Mel79
Mel102
1 2 3 4 5 6 7 8 9 10 11 12 13 14 15 16 17 18 19 20 21 22 X Y
Chromosome
Non-Malignant cells
Mel79
Mel102
1 2 3 4 5 6 7 8 9 10 11 12 13 14 15 16 17 18 19 20 21 22 X Y
Chromosome

FIG. 5A

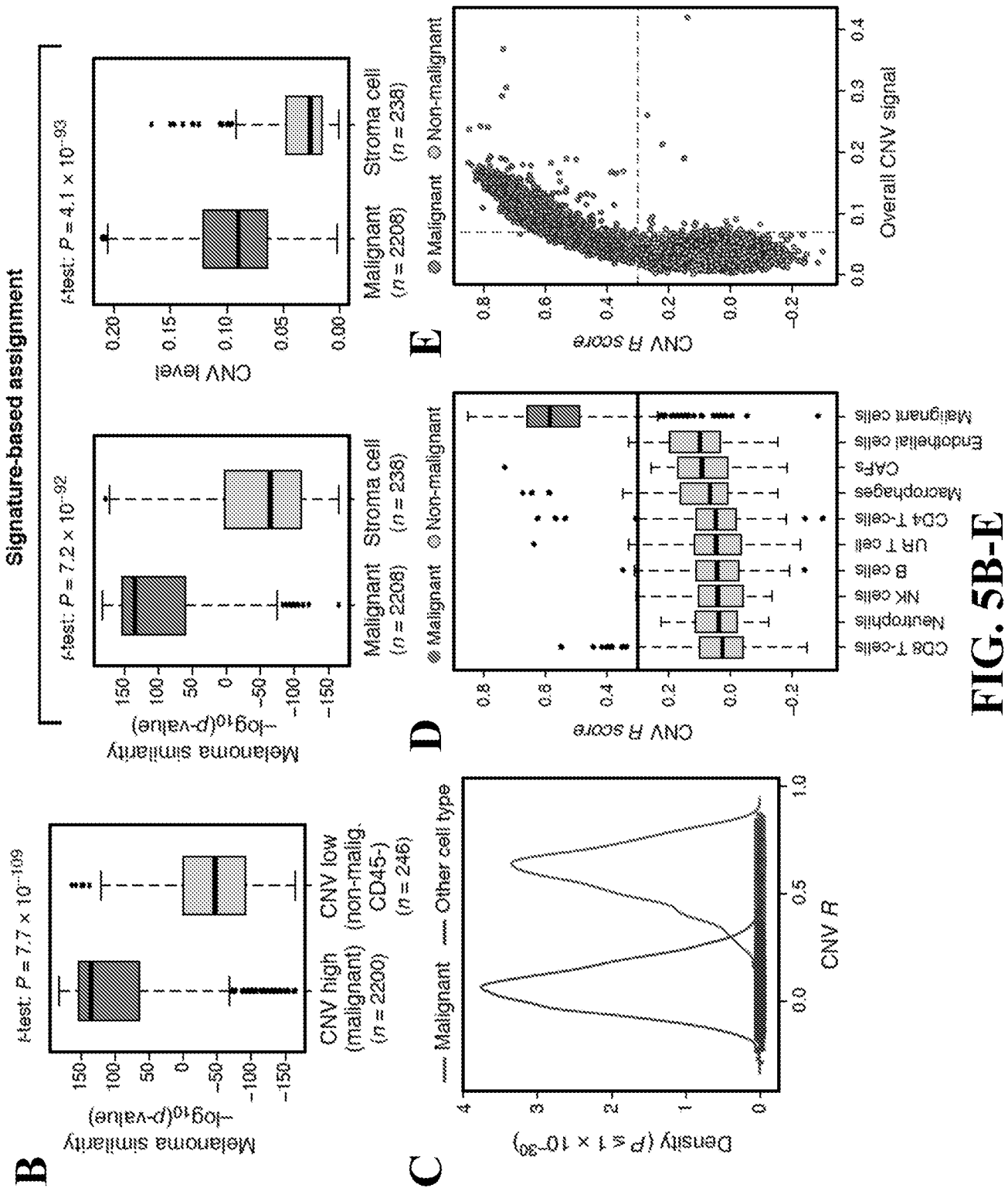

Signature-based assignment
B
t-test: P = 7.7 × 10⁻¹⁰⁹
Melanoma similarity −log10(p-value)
CNV high (malignant) (n = 2200)
CNV low (non-malig. CD45-) (n = 246)
t-test: P = 7.2 × 10⁻⁹²
Malignant (n = 2208)
Stroma cell (n = 238)
t-test: P = 4.1 × 10⁻⁹³
CNV level
C
Malignant
Other cell type
Density (P ≤ 1 × 10⁻³⁰)
CNV R
D
Malignant
Non-malignant
CNV R score
CD8 T-cells
Neutrophils
NK cells
B cells
UR T cell
CD4 T-cells
Macrophages
CAFs
Endothelial cells
Malignant cells
E
Malignant
Non-malignant
CNV R score
Overall CNV signal

FIG. 5B-E

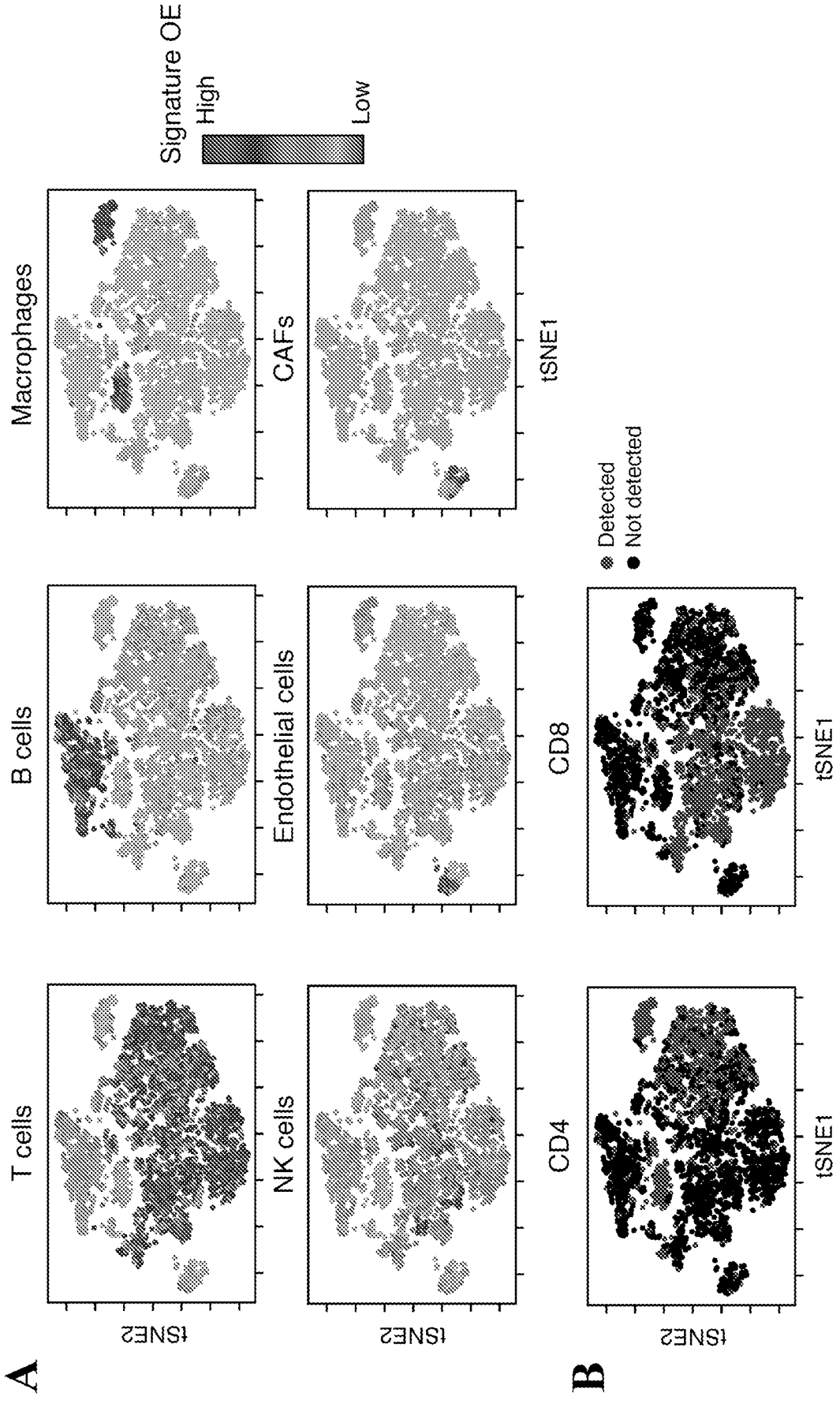

A
B
T cells
NK cells
B cells
Endothelial cells
Macrophages
CAFs
CD4
CD8
tSNE1
tSNE2
Signature OE
High
Low
Detected
Not detected

FIG. 6A-B

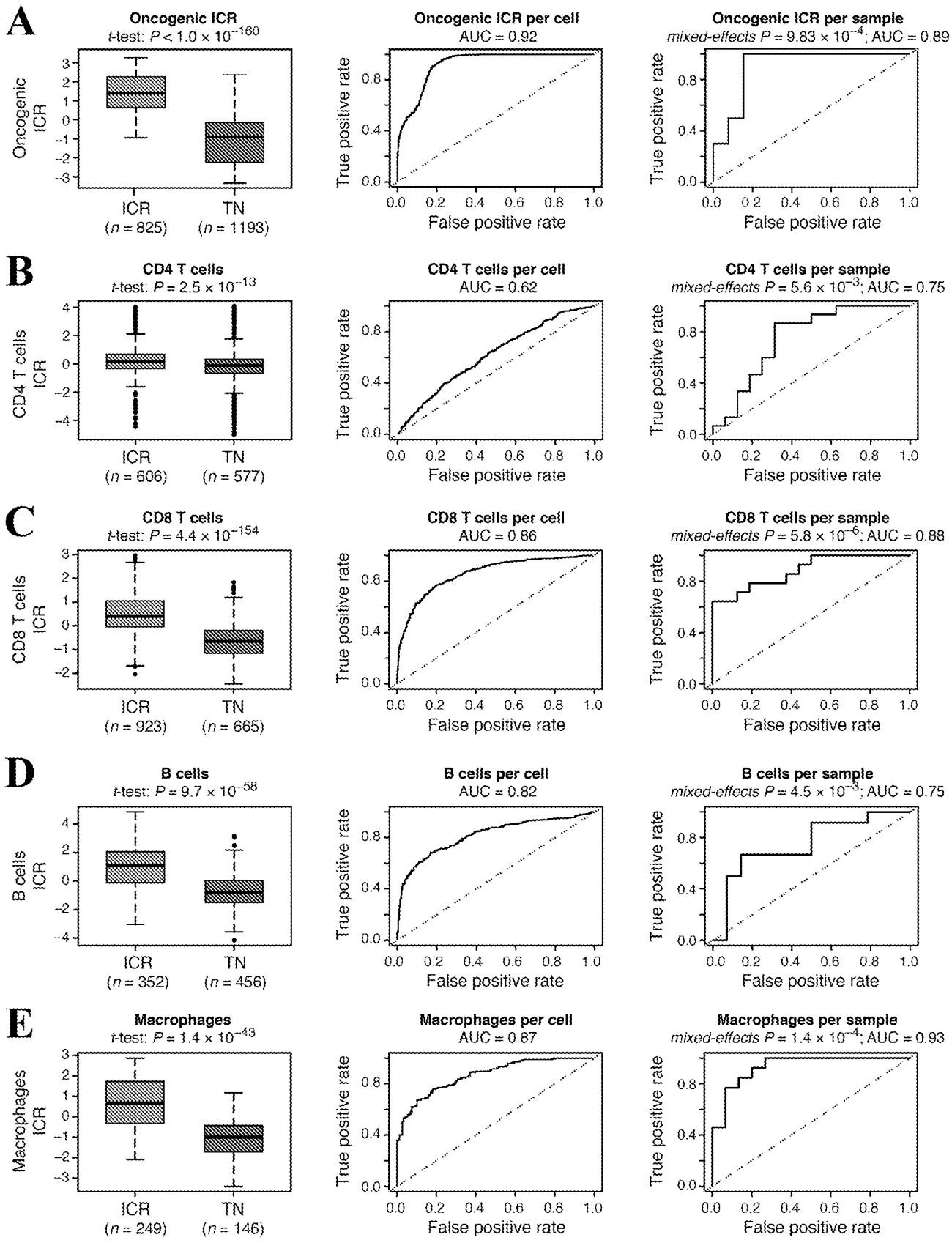

A
Oncogenic ICR
t-test: P < 1.0 × 10−160
Oncogenic ICR
ICR (n = 825)
TN (n = 1193)
Oncogenic ICR per cell
AUC = 0.92
Oncogenic ICR per sample
mixed-effects P = 9.83 × 10−4; AUC = 0.89
B
CD4 T cells
t-test: P = 2.5 × 10−13
CD4 T cells ICR
ICR (n = 606)
TN (n = 577)
CD4 T cells per cell
AUC = 0.62
CD4 T cells per sample
mixed-effects P = 5.6 × 10−3; AUC = 0.75
C
CD8 T cells
t-test: P = 4.4 × 10−154
CD8 T cells ICR
ICR (n = 923)
TN (n = 665)
CD8 T cells per cell
AUC = 0.86
CD8 T cells per sample
mixed-effects P = 5.8 × 10−6; AUC = 0.88
D
B cells
t-test: P = 9.7 × 10−58
B cells ICR
ICR (n = 352)
TN (n = 456)
B cells per cell
AUC = 0.82
B cells per sample
mixed-effects P = 4.5 × 10−3; AUC = 0.75
E
Macrophages
t-test: P = 1.4 × 10−43
Macrophages ICR
ICR (n = 249)
TN (n = 146)
Macrophages per cell
AUC = 0.87
Macrophages per sample
mixed-effects P = 1.4 × 10−4; AUC = 0.93
True positive rate
False positive rate

FIG. 7A-E

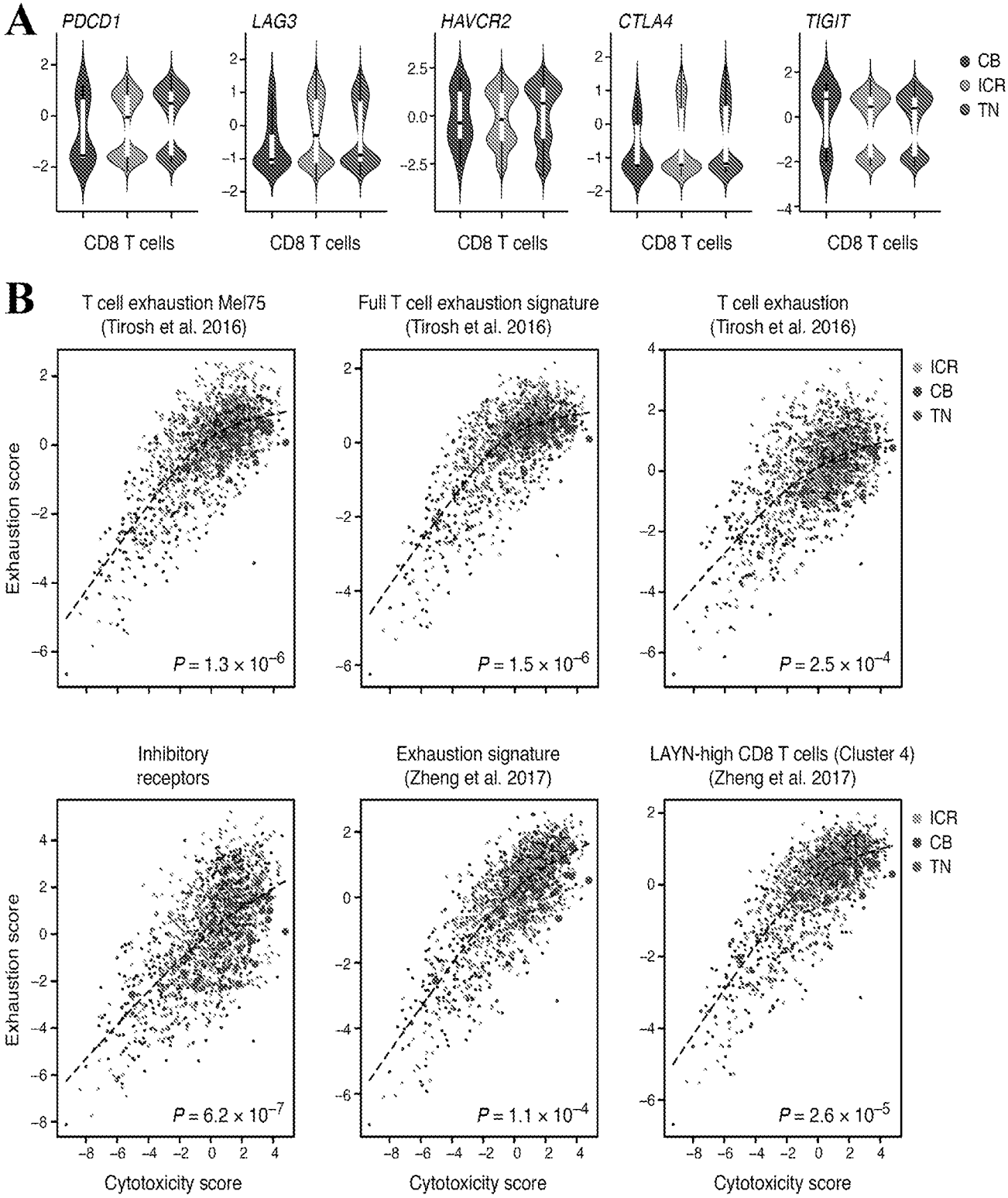

A
PDCD1
LAG3
HAVCR2
CTLA4
TIGIT
CD8 T cells
CB
ICR
TN
B
T cell exhaustion Mel75 (Tirosh et al. 2016)
Full T cell exhaustion signature (Tirosh et al. 2016)
T cell exhaustion (Tirosh et al. 2016)
Inhibitory receptors
Exhaustion signature (Zheng et al. 2017)
LAYN-high CD8 T cells (Cluster 4) (Zheng et al. 2017)
Exhaustion score
Cytotoxicity score
P = 1.3 × 10−6
P = 1.5 × 10−6
P = 2.5 × 10−4
P = 6.2 × 10−7
P = 1.1 × 10−4
P = 2.6 × 10−5

FIG. 8A-B

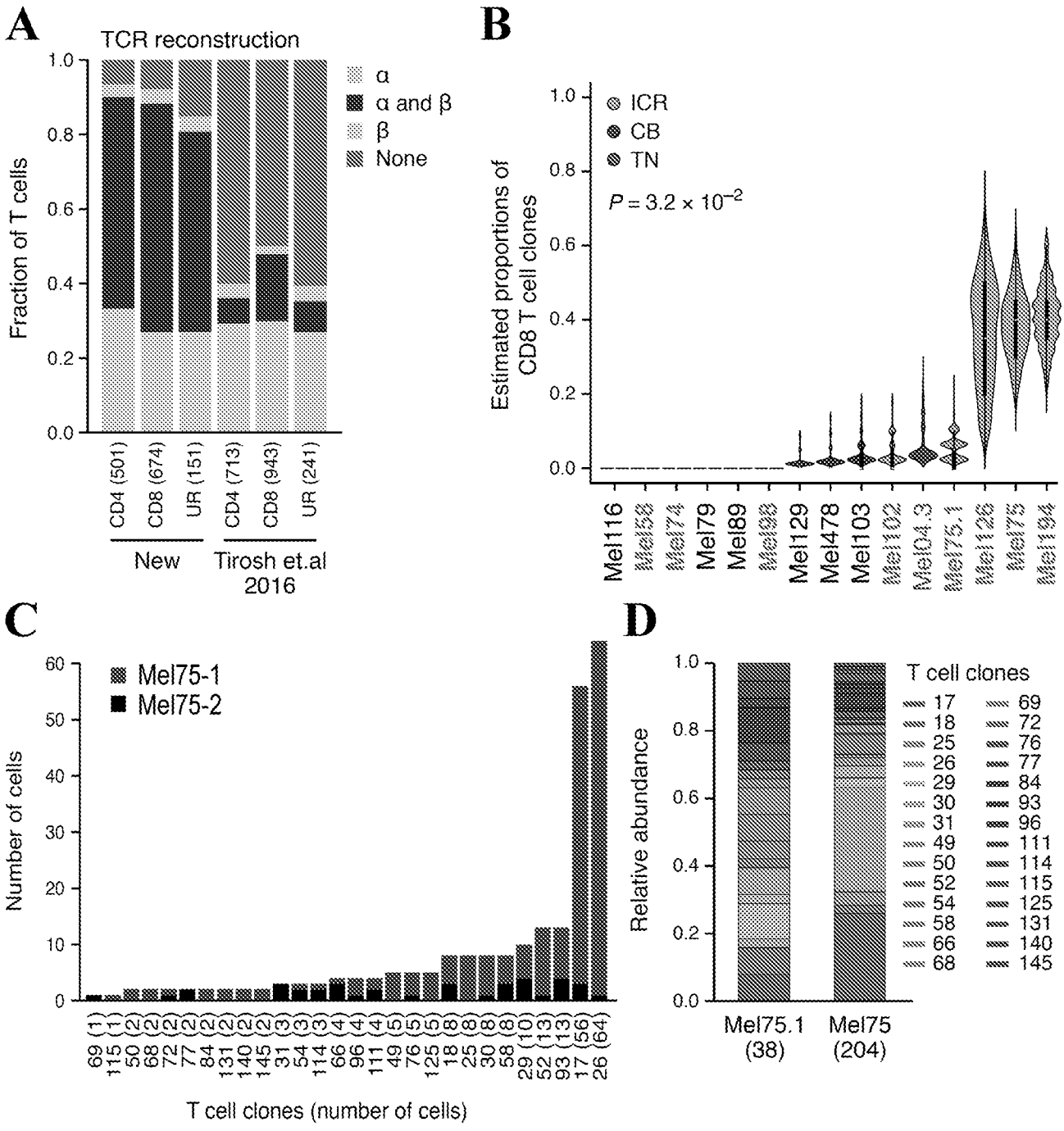

A
TCR reconstruction
Fraction of T cells
α
α and β
β
None
CD4 (501)
CD8 (674)
UR (151)
CD4 (713)
CD8 (943)
UR (241)
New
Tirosh et.al 2016
B
Estimated proportions of CD8 T cell clones
ICR
CB
TN
P = 3.2 × 10−2
Mel116
Mel58
Mel74
Mel79
Mel89
Mel93
Mel129
Mel478
Mel103
Mel102
Mel04.3
Mel75.1
Mel126
Mel75
Mel194
C
Number of cells
Mel75-1
Mel75-2
T cell clones (number of cells)
D
Relative abundance
T cell clones
Mel75.1 (38)
Mel75 (204)

FIG. 9A-D

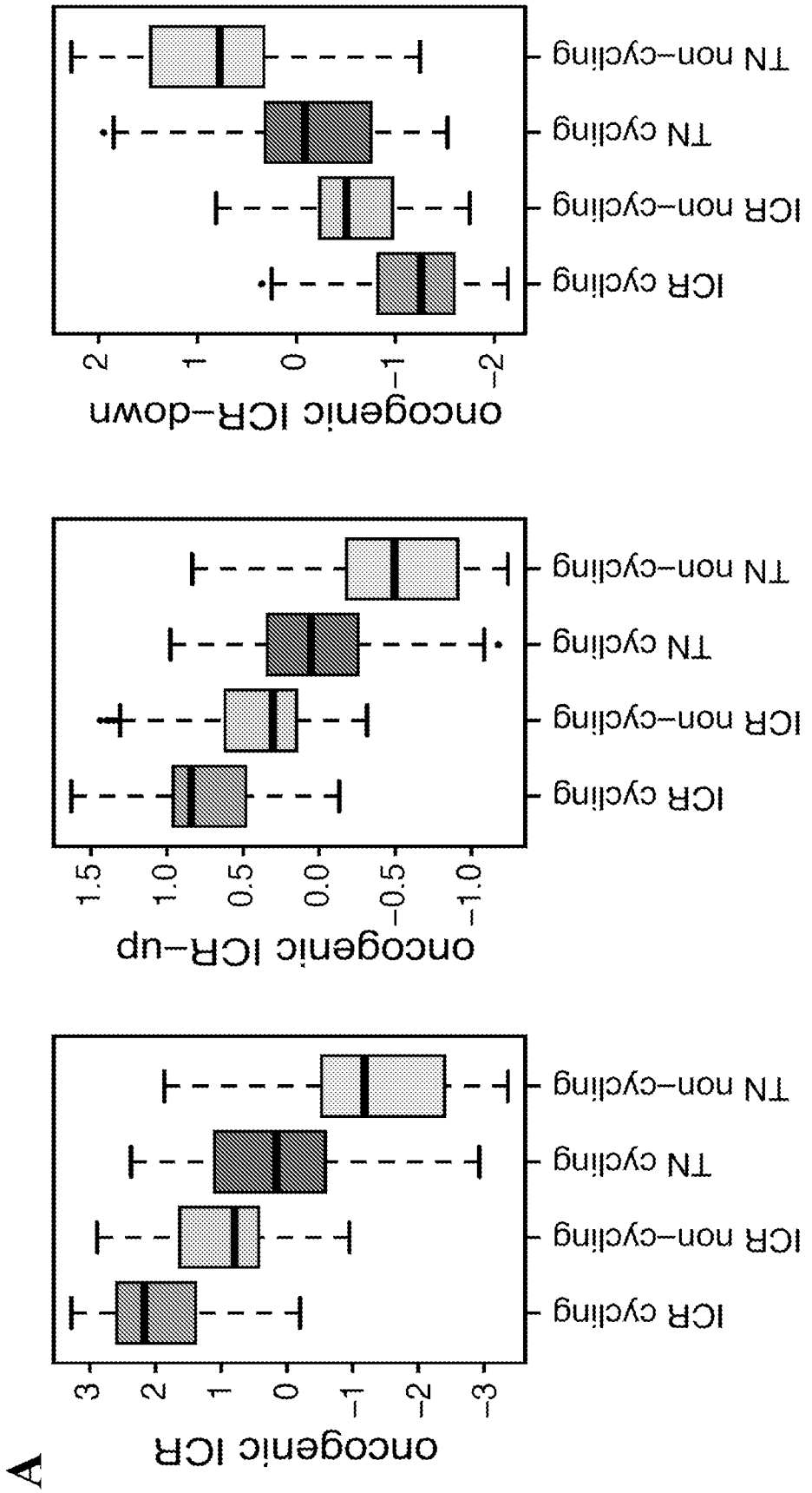

A
oncogenic ICR
3
2
1
0
−1
−2
−3
ICR cycling
ICR non−cycling
TN cycling
TN non−cycling
oncogenic ICR−up
1.5
1.0
0.5
0.0
−0.5
−1.0
ICR cycling
ICR non−cycling
TN cycling
TN non−cycling
oncogenic ICR−down
2
1
0
−1
−2
ICR cycling
ICR non−cycling
TN cycling
TN non−cycling

FIG. 10A

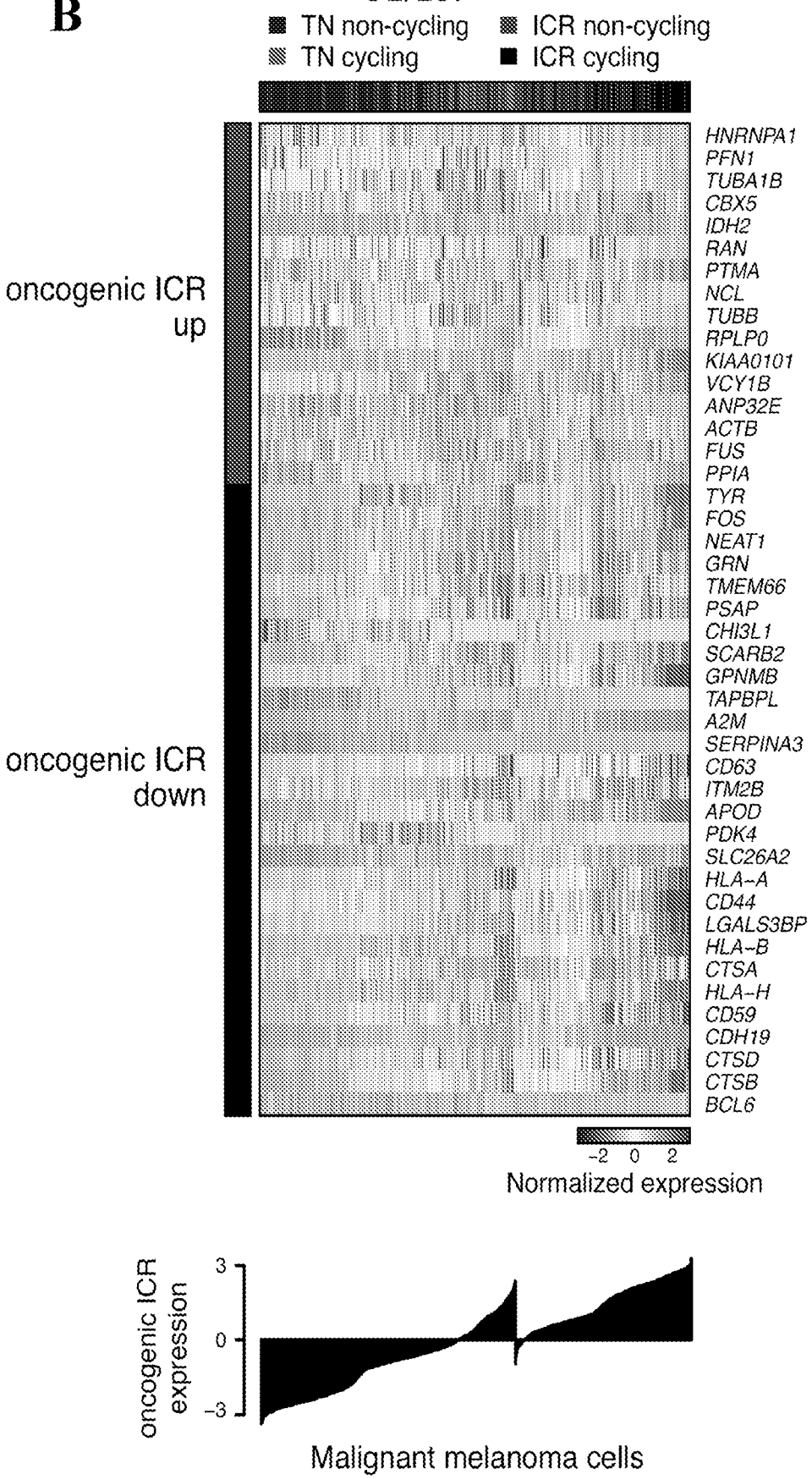

B
TN non-cycling
ICR non-cycling
TN cycling
ICR cycling
oncogenic ICR up
oncogenic ICR down
HNRNPA1
PFN1
TUBA1B
CBX5
IDH2
RAN
PTMA
NCL
TUBB
RPLP0
KIAA0101
VCY1B
ANP32E
ACTB
FUS
PPIA
TYR
FOS
NEAT1
GRN
TMEM66
PSAP
CHI3L1
SCARB2
GPNMB
TAPBPL
A2M
SERPINA3
CD63
ITM2B
APOD
PDK4
SLC26A2
HLA-A
CD44
LGALS3BP
HLA-B
CTSA
HLA-H
CD59
CDH19
CTSD
CTSB
BCL6
-2 0 2
Normalized expression
oncogenic ICR expression
3
0
-3
Malignant melanoma cells

FIG. 10B

C

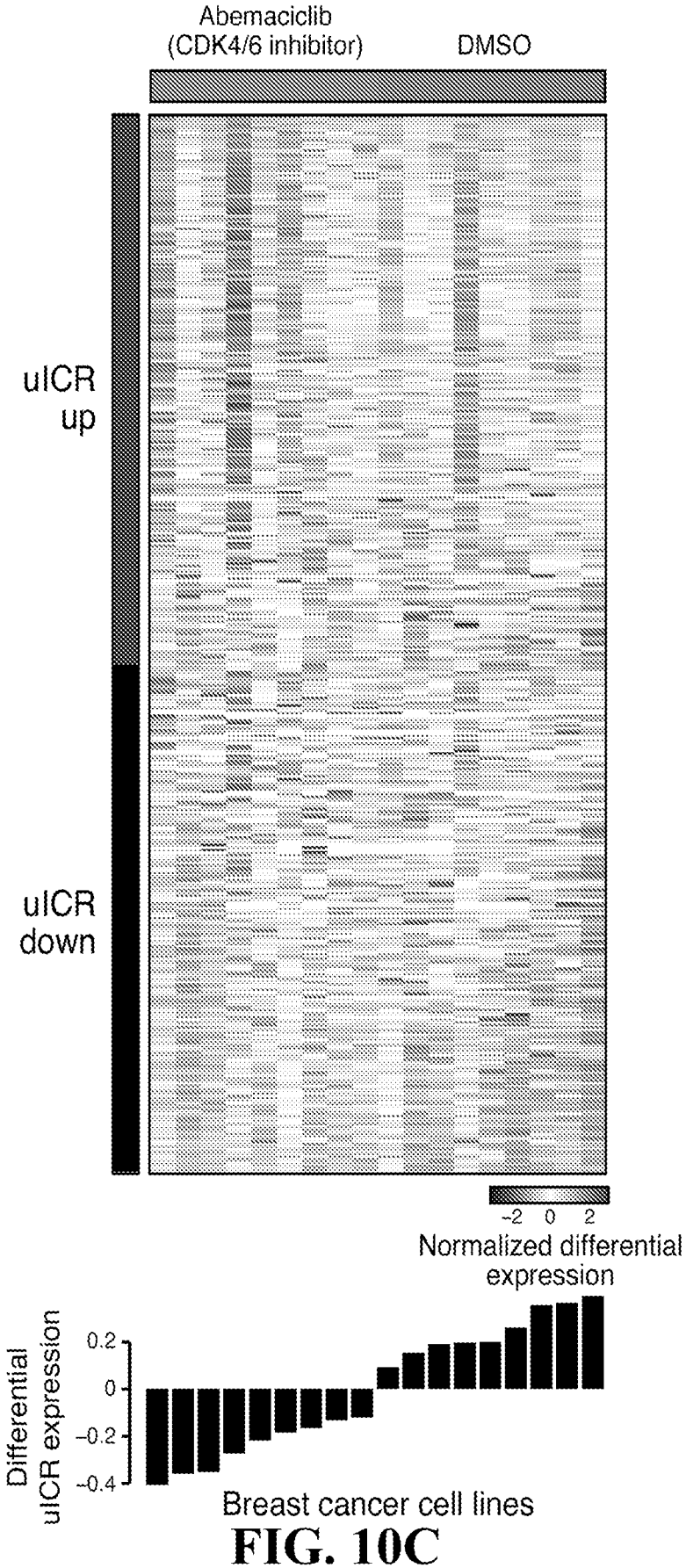

Abemaciclib
(CDK4/6 inhibitor)
DMSO
uICR
up
uICR
down
-2 0 2
Normalized differential
expression
Differential
uICR expression
0.2
0
-0.2
-0.4
Breast cancer cell lines

FIG. 10C

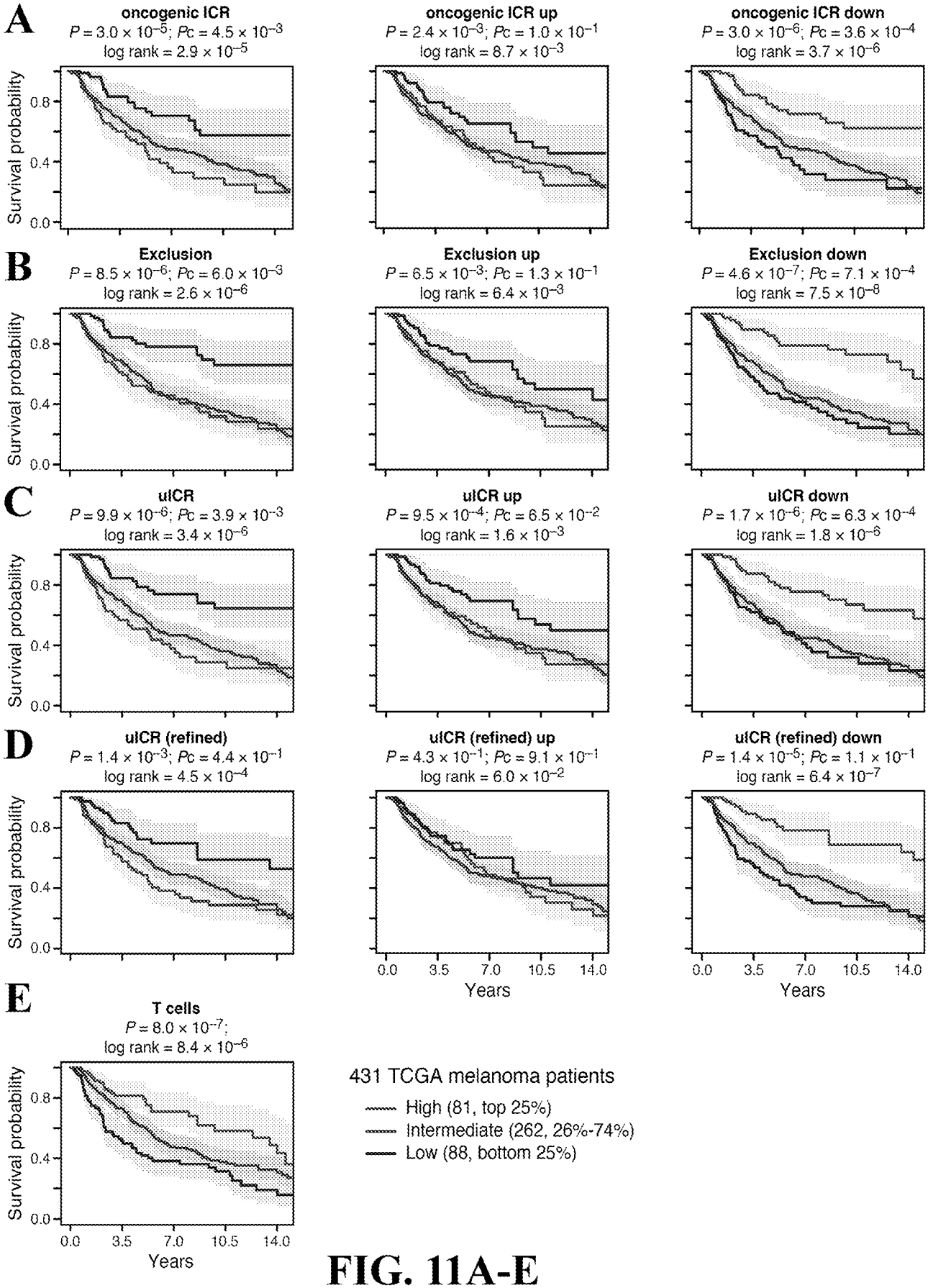

A
oncogenic ICR
P = 3.0 × 10−5; Pc = 4.5 × 10−3
log rank = 2.9 × 10−5
oncogenic ICR up
P = 2.4 × 10−3; Pc = 1.0 × 10−1
log rank = 8.7 × 10−3
oncogenic ICR down
P = 3.0 × 10−6; Pc = 3.6 × 10−4
log rank = 3.7 × 10−6
B
Exclusion
P = 8.5 × 10−6; Pc = 6.0 × 10−3
log rank = 2.6 × 10−6
Exclusion up
P = 6.5 × 10−3; Pc = 1.3 × 10−1
log rank = 6.4 × 10−3
Exclusion down
P = 4.6 × 10−7; Pc = 7.1 × 10−4
log rank = 7.5 × 10−8
C
ulCR
P = 9.9 × 10−6; Pc = 3.9 × 10−3
log rank = 3.4 × 10−6
ulCR up
P = 9.5 × 10−4; Pc = 6.5 × 10−2
log rank = 1.6 × 10−3
ulCR down
P = 1.7 × 10−6; Pc = 6.3 × 10−4
log rank = 1.8 × 10−6
D
ulCR (refined)
P = 1.4 × 10−3; Pc = 4.4 × 10−1
log rank = 4.5 × 10−4
ulCR (refined) up
P = 4.3 × 10−1; Pc = 9.1 × 10−1
log rank = 6.0 × 10−2
ulCR (refined) down
P = 1.4 × 10−5; Pc = 1.1 × 10−1
log rank = 6.4 × 10−7
E
T cells
P = 8.0 × 10−7;
log rank = 8.4 × 10−6
Survival probability
0.0
0.4
0.8
0.0 3.5 7.0 10.5 14.0
Years
431 TCGA melanoma patients
High (81, top 25%)
Intermediate (262, 26%-74%)
Low (88, bottom 25%)

FIG. 11A-E

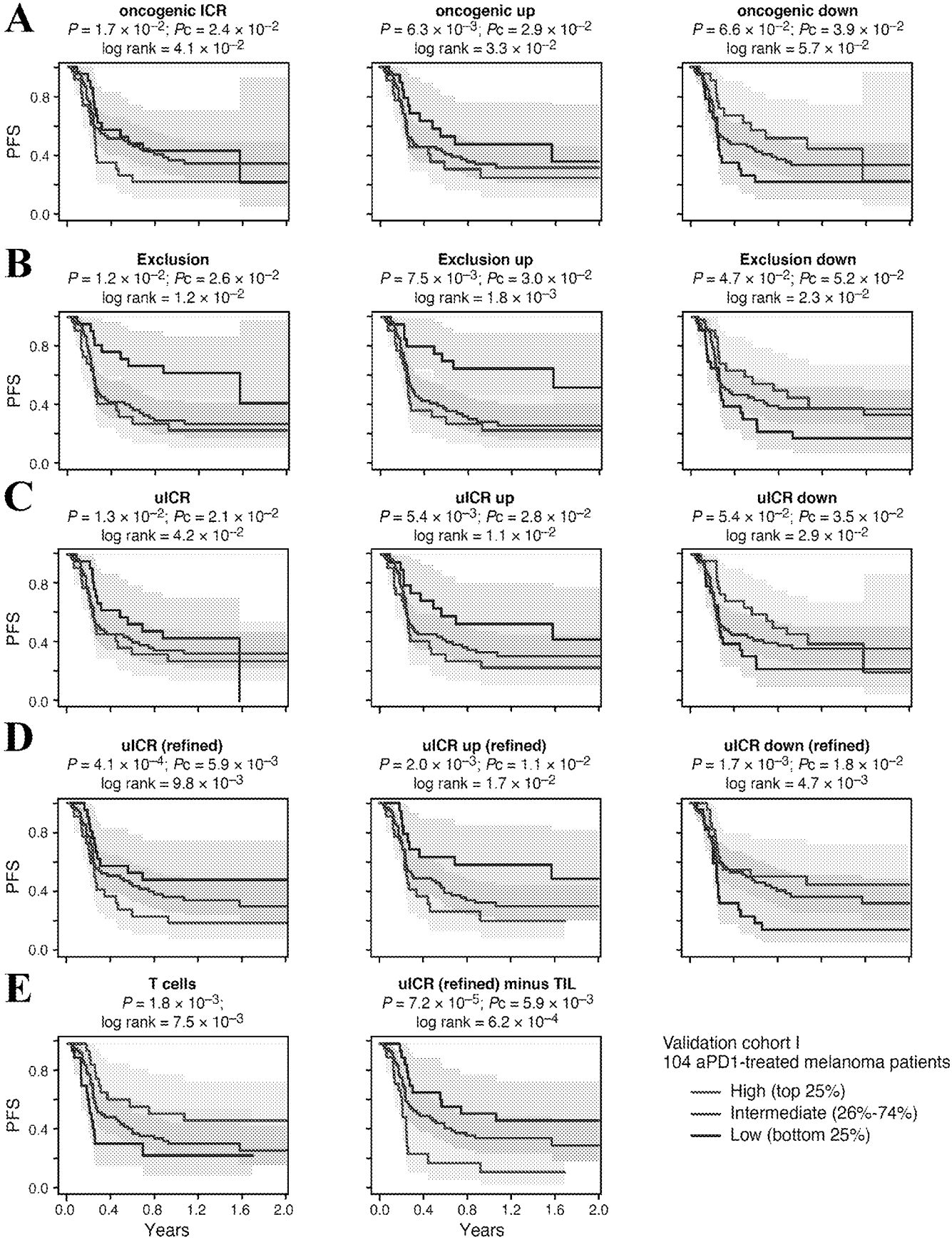

A
oncogenic ICR
P = 1.7 × 10−2; Pc = 2.4 × 10−2
log rank = 4.1 × 10−2
oncogenic up
P = 6.3 × 10−3; Pc = 2.9 × 10−2
log rank = 3.3 × 10−2
oncogenic down
P = 6.6 × 10−2; Pc = 3.9 × 10−2
log rank = 5.7 × 10−2
B
Exclusion
P = 1.2 × 10−2; Pc = 2.6 × 10−2
log rank = 1.2 × 10−2
Exclusion up
P = 7.5 × 10−3; Pc = 3.0 × 10−2
log rank = 1.8 × 10−3
Exclusion down
P = 4.7 × 10−2; Pc = 5.2 × 10−2
log rank = 2.3 × 10−2
C
uICR
P = 1.3 × 10−2; Pc = 2.1 × 10−2
log rank = 4.2 × 10−2
uICR up
P = 5.4 × 10−3; Pc = 2.8 × 10−2
log rank = 1.1 × 10−2
uICR down
P = 5.4 × 10−2; Pc = 3.5 × 10−2
log rank = 2.9 × 10−2
D
uICR (refined)
P = 4.1 × 10−4; Pc = 5.9 × 10−3
log rank = 9.8 × 10−3
uICR up (refined)
P = 2.0 × 10−3; Pc = 1.1 × 10−2
log rank = 1.7 × 10−2
uICR down (refined)
P = 1.7 × 10−3; Pc = 1.8 × 10−2
log rank = 4.7 × 10−3
E
T cells
P = 1.8 × 10−3;
log rank = 7.5 × 10−3
uICR (refined) minus TIL
P = 7.2 × 10−5; Pc = 5.9 × 10−3
log rank = 6.2 × 10−4
PFS
0.0
0.4
0.8
0.0 0.4 0.8 1.2 1.6 2.0
Years
Validation cohort I
104 aPD1-treated melanoma patients
High (top 25%)
Intermediate (26%-74%)
Low (bottom 25%)

FIG. 12A-E

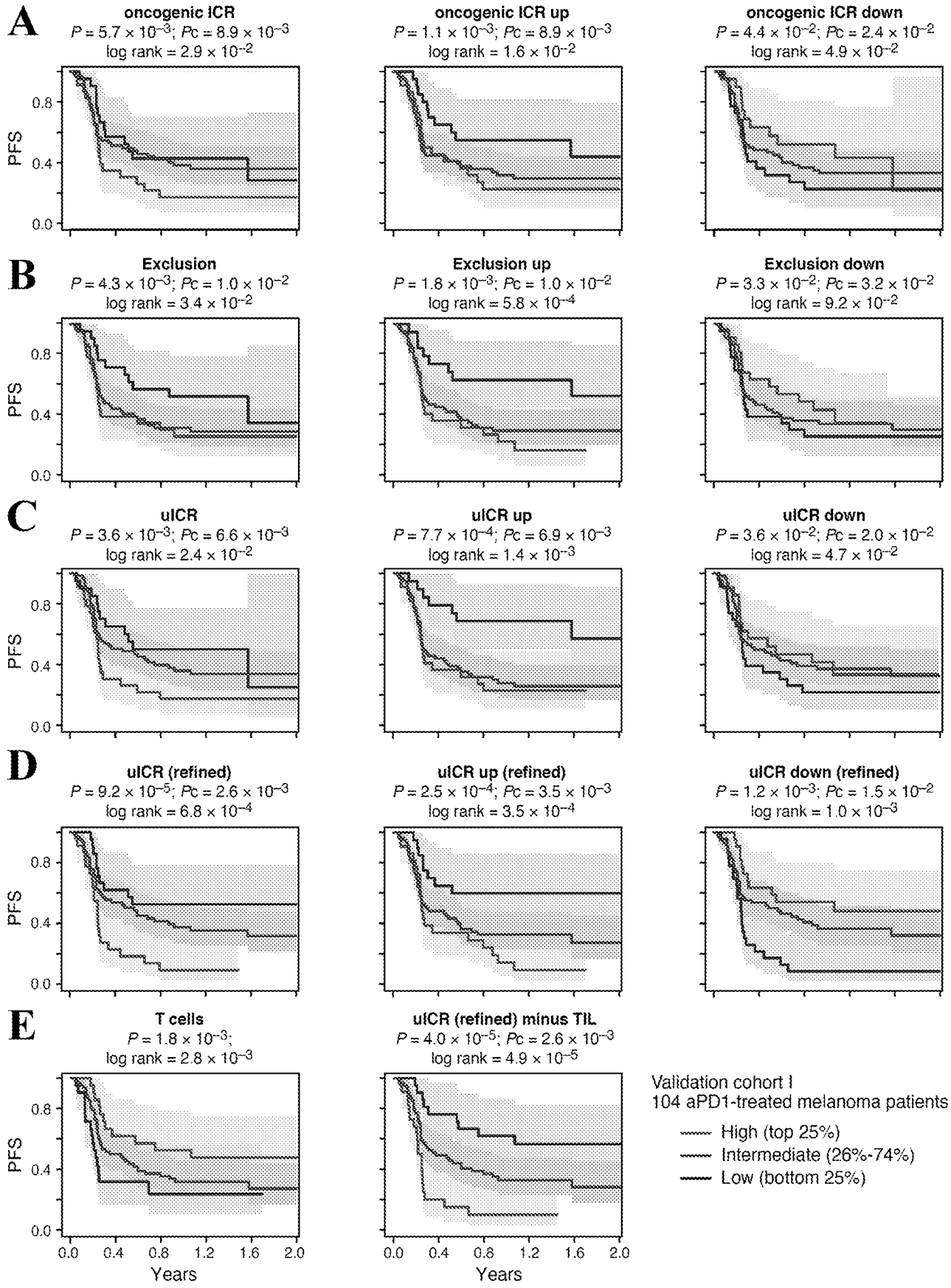

A
oncogenic ICR
P = 5.7 × 10−3; Pc = 8.9 × 10−3
log rank = 2.9 × 10−2
oncogenic ICR up
P = 1.1 × 10−3; Pc = 8.9 × 10−3
log rank = 1.6 × 10−2
oncogenic ICR down
P = 4.4 × 10−2; Pc = 2.4 × 10−2
log rank = 4.9 × 10−2
B
Exclusion
P = 4.3 × 10−3; Pc = 1.0 × 10−2
log rank = 3.4 × 10−2
Exclusion up
P = 1.8 × 10−3; Pc = 1.0 × 10−2
log rank = 5.8 × 10−4
Exclusion down
P = 3.3 × 10−2; Pc = 3.2 × 10−2
log rank = 9.2 × 10−2
C
uICR
P = 3.6 × 10−3; Pc = 6.6 × 10−3
log rank = 2.4 × 10−2
uICR up
P = 7.7 × 10−4; Pc = 6.9 × 10−3
log rank = 1.4 × 10−3
uICR down
P = 3.6 × 10−2; Pc = 2.0 × 10−2
log rank = 4.7 × 10−2
D
uICR (refined)
P = 9.2 × 10−5; Pc = 2.6 × 10−3
log rank = 6.8 × 10−4
uICR up (refined)
P = 2.5 × 10−4; Pc = 3.5 × 10−3
log rank = 3.5 × 10−4
uICR down (refined)
P = 1.2 × 10−3; Pc = 1.5 × 10−2
log rank = 1.0 × 10−3
E
T cells
P = 1.8 × 10−3;
log rank = 2.8 × 10−3
uICR (refined) minus TIL
P = 4.0 × 10−5; Pc = 2.6 × 10−3
log rank = 4.9 × 10−5
PFS
0.0
0.4
0.8
0.0 0.4 0.8 1.2 1.6 2.0
Years
Validation cohort I
104 aPD1-treated melanoma patients
High (top 25%)
Intermediate (26%-74%)
Low (bottom 25%)

FIG. 13A-E

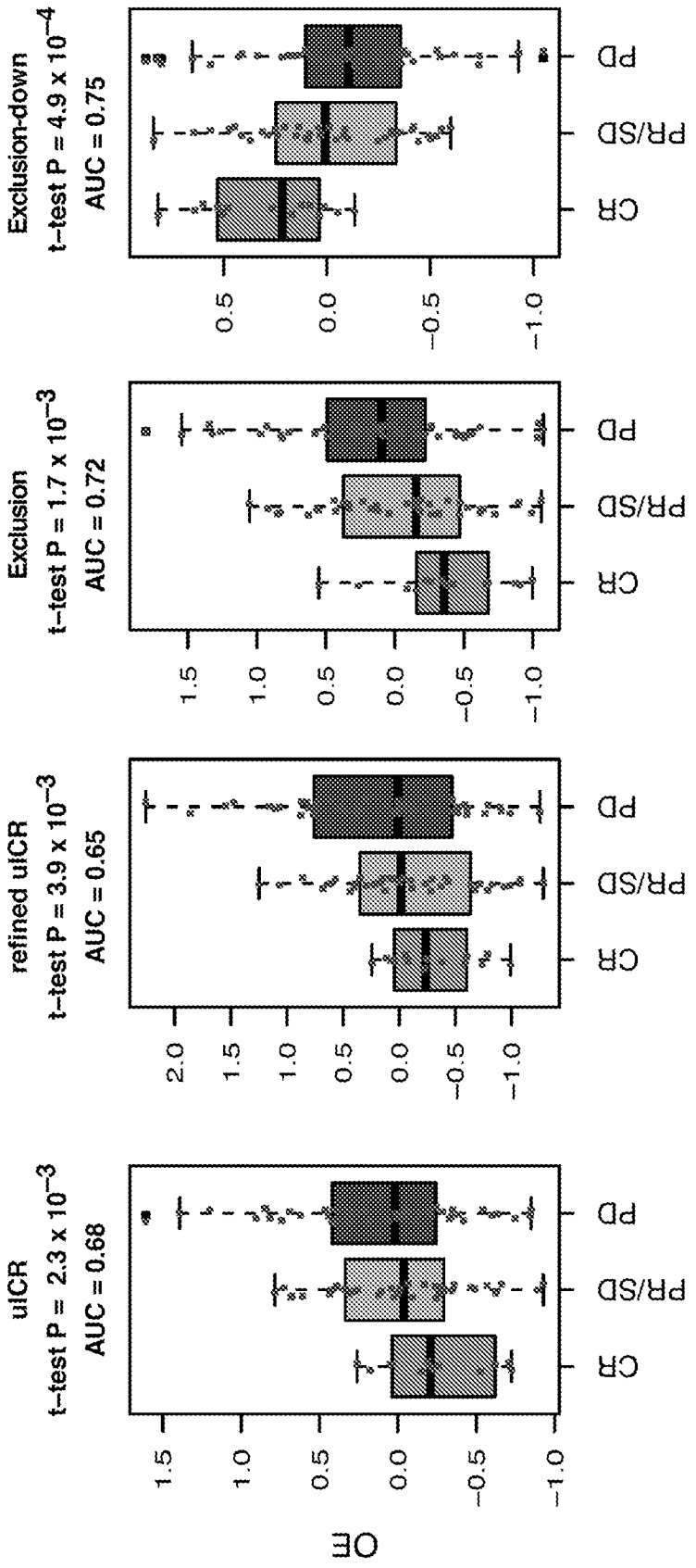

ulCR
t–test P = 2.3 x 10^{-3}
AUC = 0.68
refined ulCR
t–test P = 3.9 x 10^{-3}
AUC = 0.65
Exclusion
t–test P = 1.7 x 10^{-3}
AUC = 0.72
Exclusion-down
t–test P = 4.9 x 10^{-4}
AUC = 0.75
CR
PR/SD
PD
OE

FIG. 14

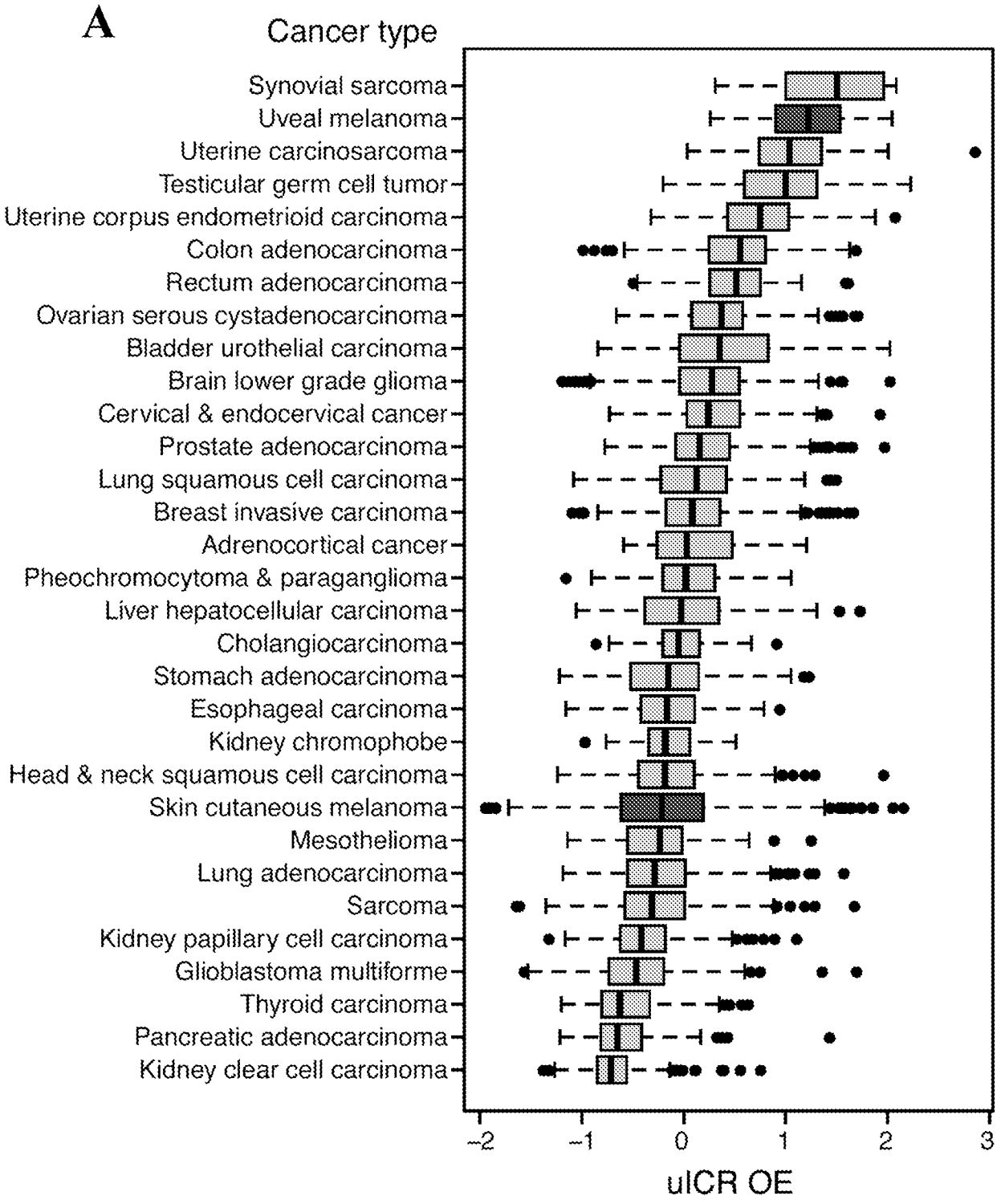

A
Cancer type
Synovial sarcoma
Uveal melanoma
Uterine carcinosarcoma
Testicular germ cell tumor
Uterine corpus endometrioid carcinoma
Colon adenocarcinoma
Rectum adenocarcinoma
Ovarian serous cystadenocarcinoma
Bladder urothelial carcinoma
Brain lower grade glioma
Cervical & endocervical cancer
Prostate adenocarcinoma
Lung squamous cell carcinoma
Breast invasive carcinoma
Adrenocortical cancer
Pheochromocytoma & paraganglioma
Liver hepatocellular carcinoma
Cholangiocarcinoma
Stomach adenocarcinoma
Esophageal carcinoma
Kidney chromophobe
Head & neck squamous cell carcinoma
Skin cutaneous melanoma
Mesothelioma
Lung adenocarcinoma
Sarcoma
Kidney papillary cell carcinoma
Glioblastoma multiforme
Thyroid carcinoma
Pancreatic adenocarcinoma
Kidney clear cell carcinoma
−2
−1
0
1
2
3
ulCR OE

FIG. 15A

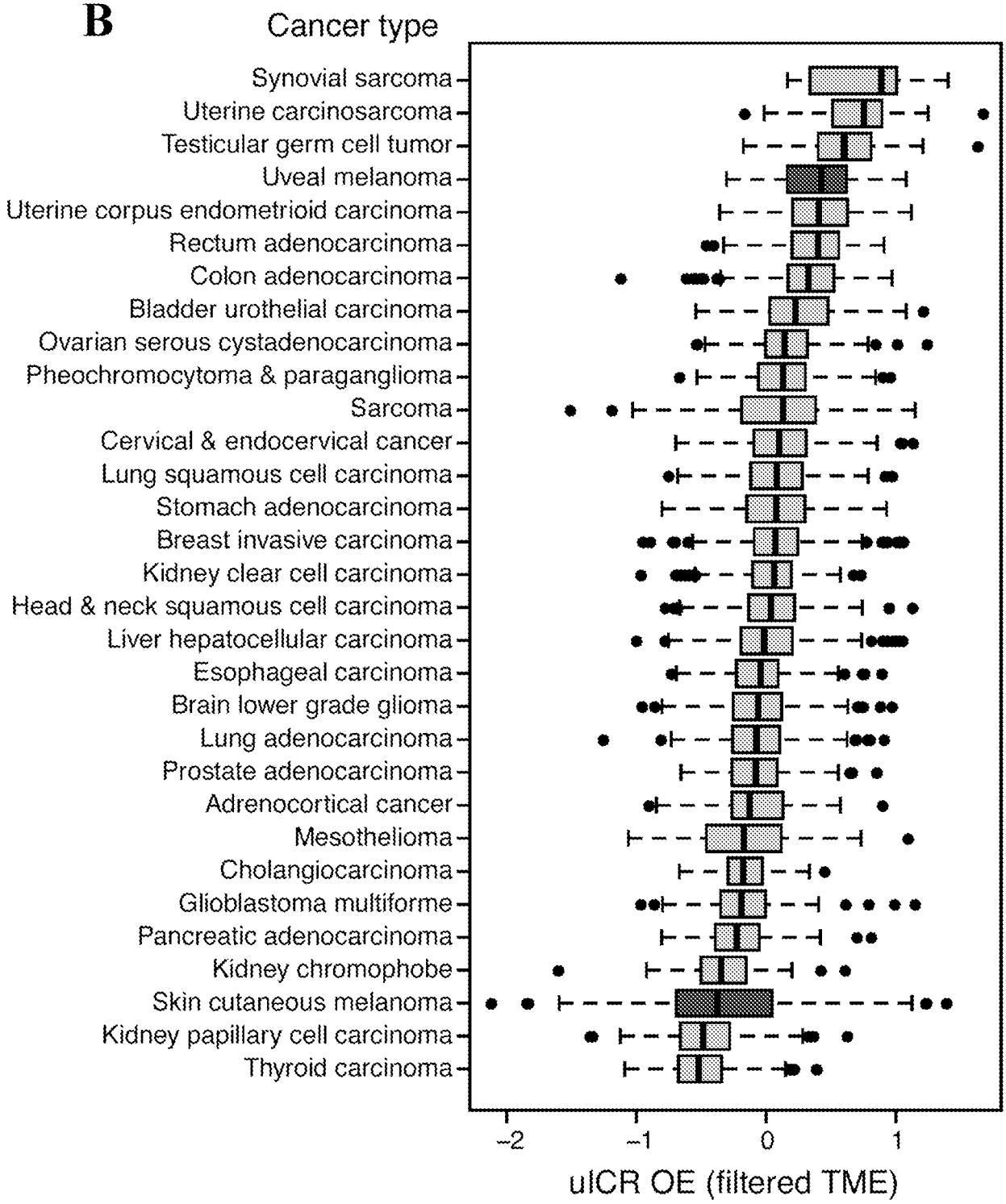

B
Cancer type
Synovial sarcoma
Uterine carcinosarcoma
Testicular germ cell tumor
Uveal melanoma
Uterine corpus endometrioid carcinoma
Rectum adenocarcinoma
Colon adenocarcinoma
Bladder urothelial carcinoma
Ovarian serous cystadenocarcinoma
Pheochromocytoma & paraganglioma
Sarcoma
Cervical & endocervical cancer
Lung squamous cell carcinoma
Stomach adenocarcinoma
Breast invasive carcinoma
Kidney clear cell carcinoma
Head & neck squamous cell carcinoma
Liver hepatocellular carcinoma
Esophageal carcinoma
Brain lower grade glioma
Lung adenocarcinoma
Prostate adenocarcinoma
Adrenocortical cancer
Mesothelioma
Cholangiocarcinoma
Glioblastoma multiforme
Pancreatic adenocarcinoma
Kidney chromophobe
Skin cutaneous melanoma
Kidney papillary cell carcinoma
Thyroid carcinoma
−2
−1
0
1
uICR OE (filtered TME)

FIG. 15B

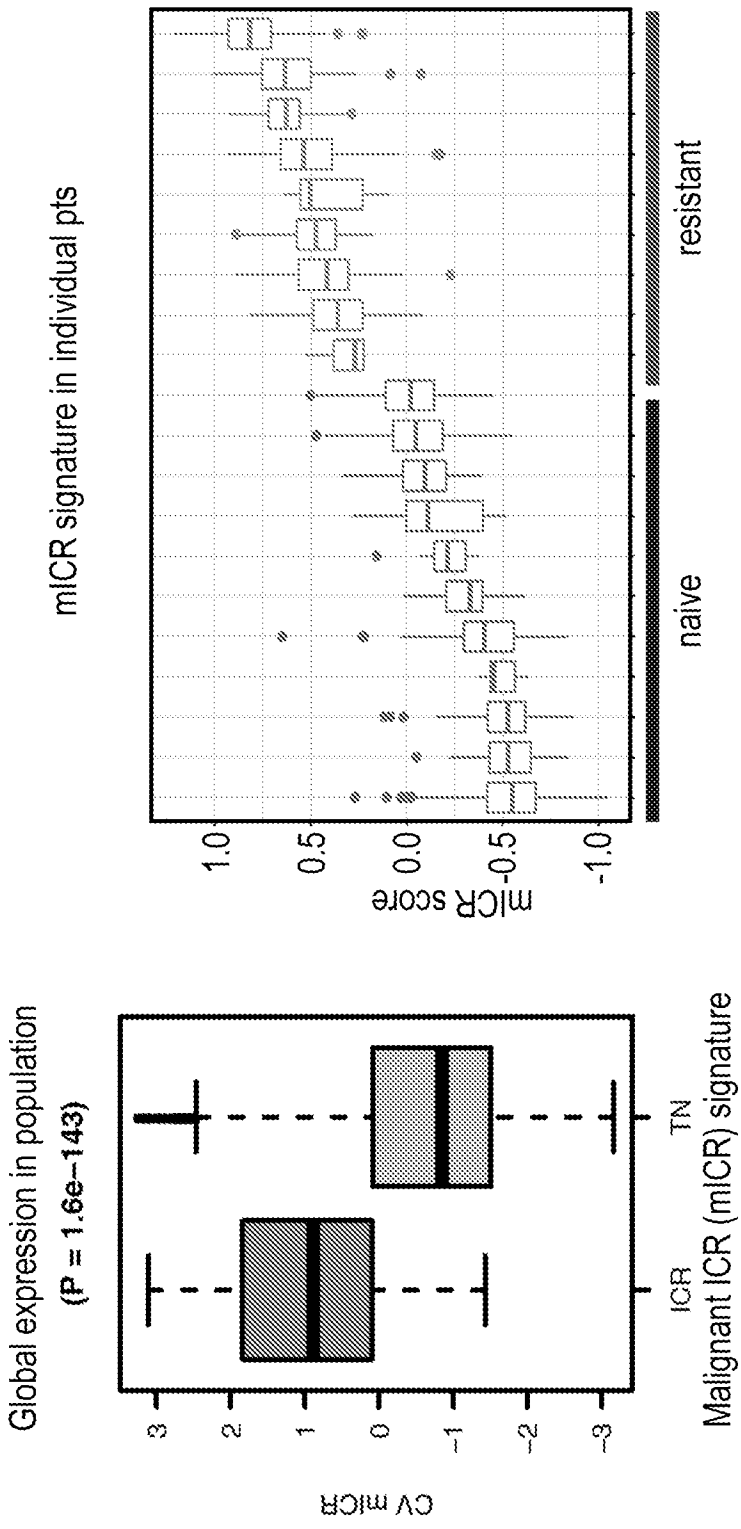

mICR signature in individual pts
mICR score
1.0
0.5
0.0
-0.5
-1.0
naive
resistant
Global expression in population
(P = 1.6e−143)
CV mICR
3
2
1
0
−1
−2
−3
ICR
TN
Malignant ICR (mICR) signature

FIG. 16

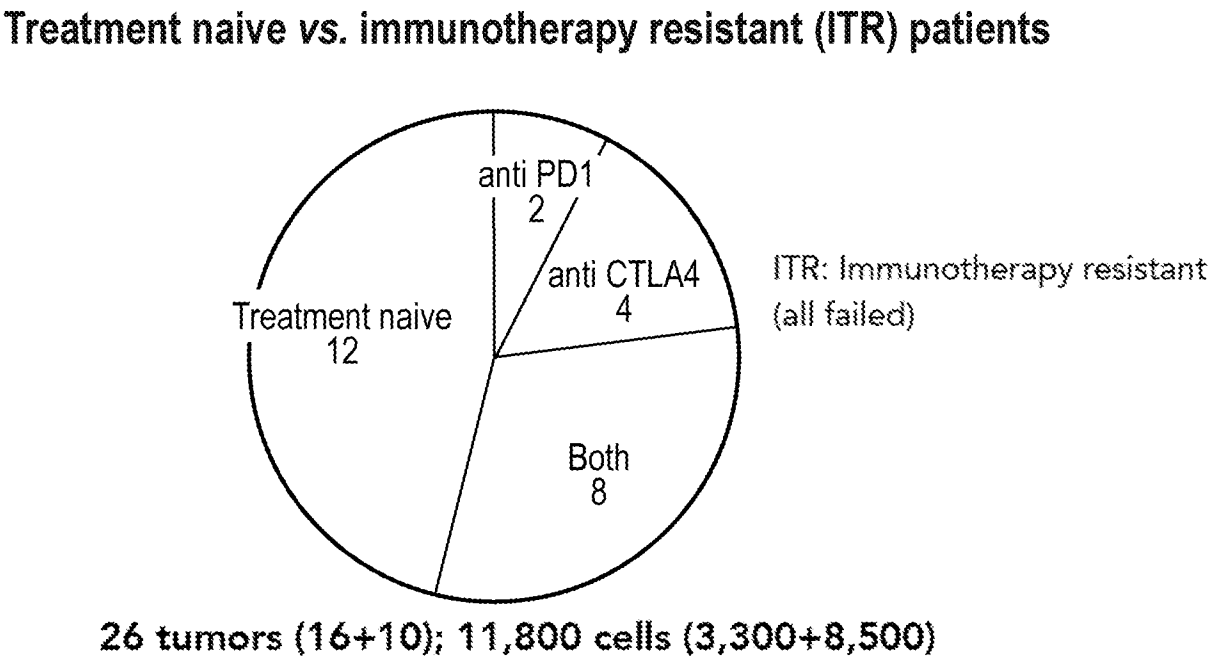

Treatment naive vs. immunotherapy resistant (ITR) patients
anti PD1
2
anti CTLA4
4
Treatment naive
12
Both
8
ITR: Immunotherapy resistant
(all failed)
26 tumors (16+10); 11,800 cells (3,300+8,500)

FIG. 17

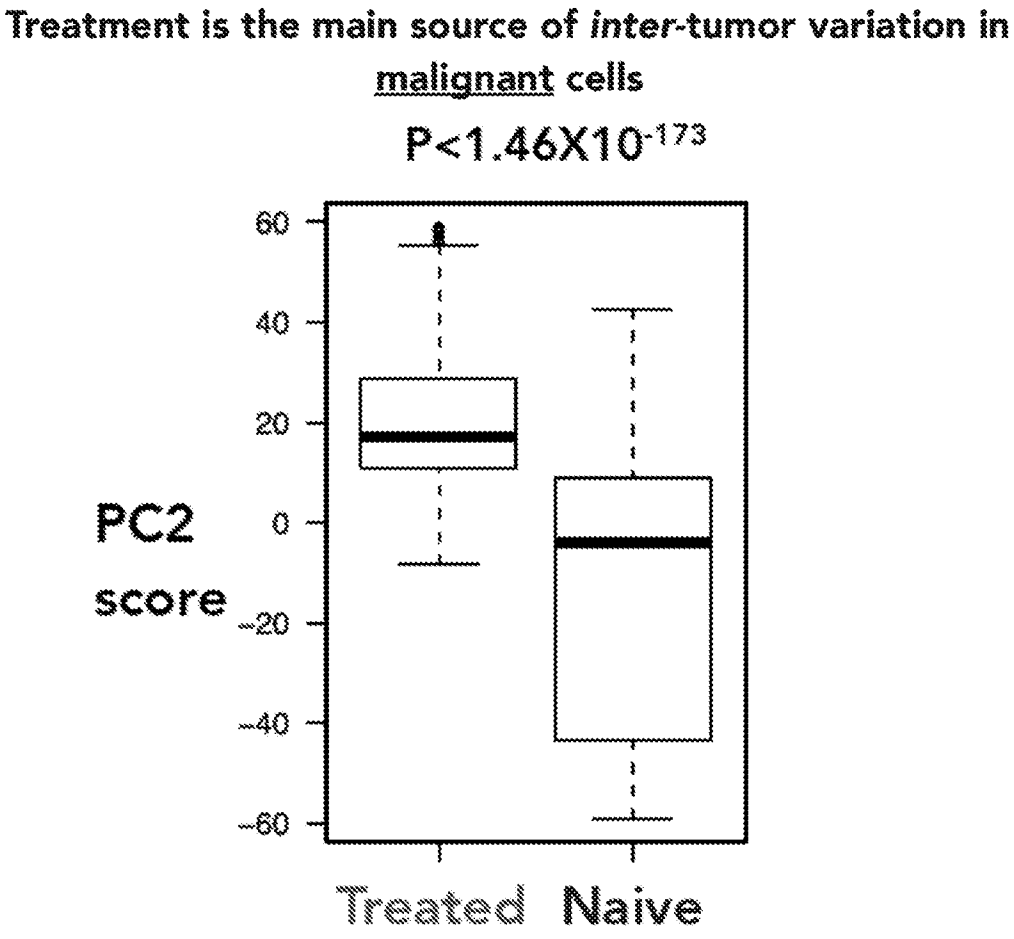

Treatment is the main source of inter-tumor variation in malignant cells
P<1.46X10-173
PC2 score
60
40
20
0
-20
-40
-60
Treated
Naive

FIG. 18

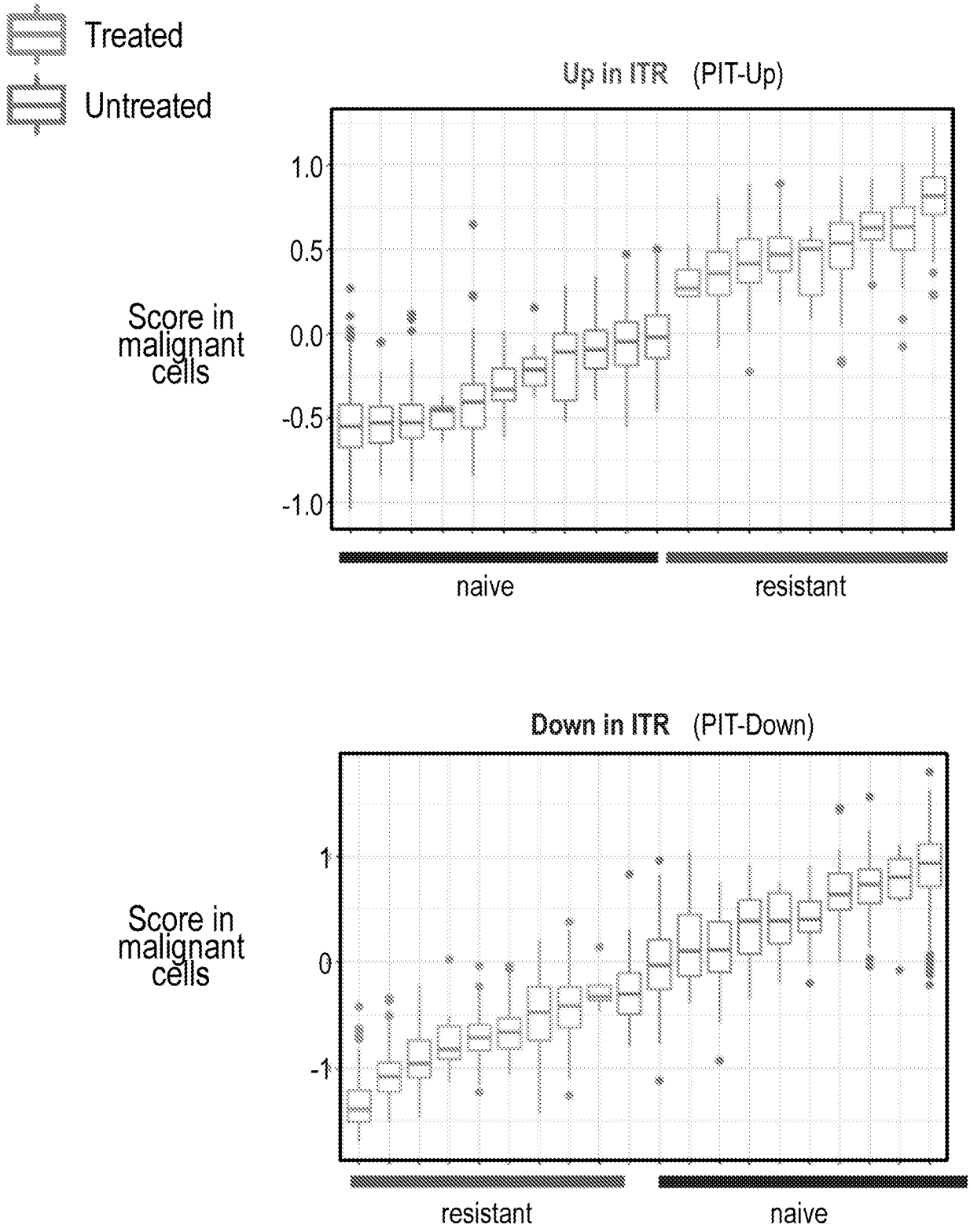

Treated
Untreated
Up in ITR (PIT-Up)
Score in malignant cells
1.0
0.5
0.0
-0.5
-1.0
naive
resistant
Down in ITR (PIT-Down)
Score in malignant cells
1
0
-1
resistant
naive

FIG. 19

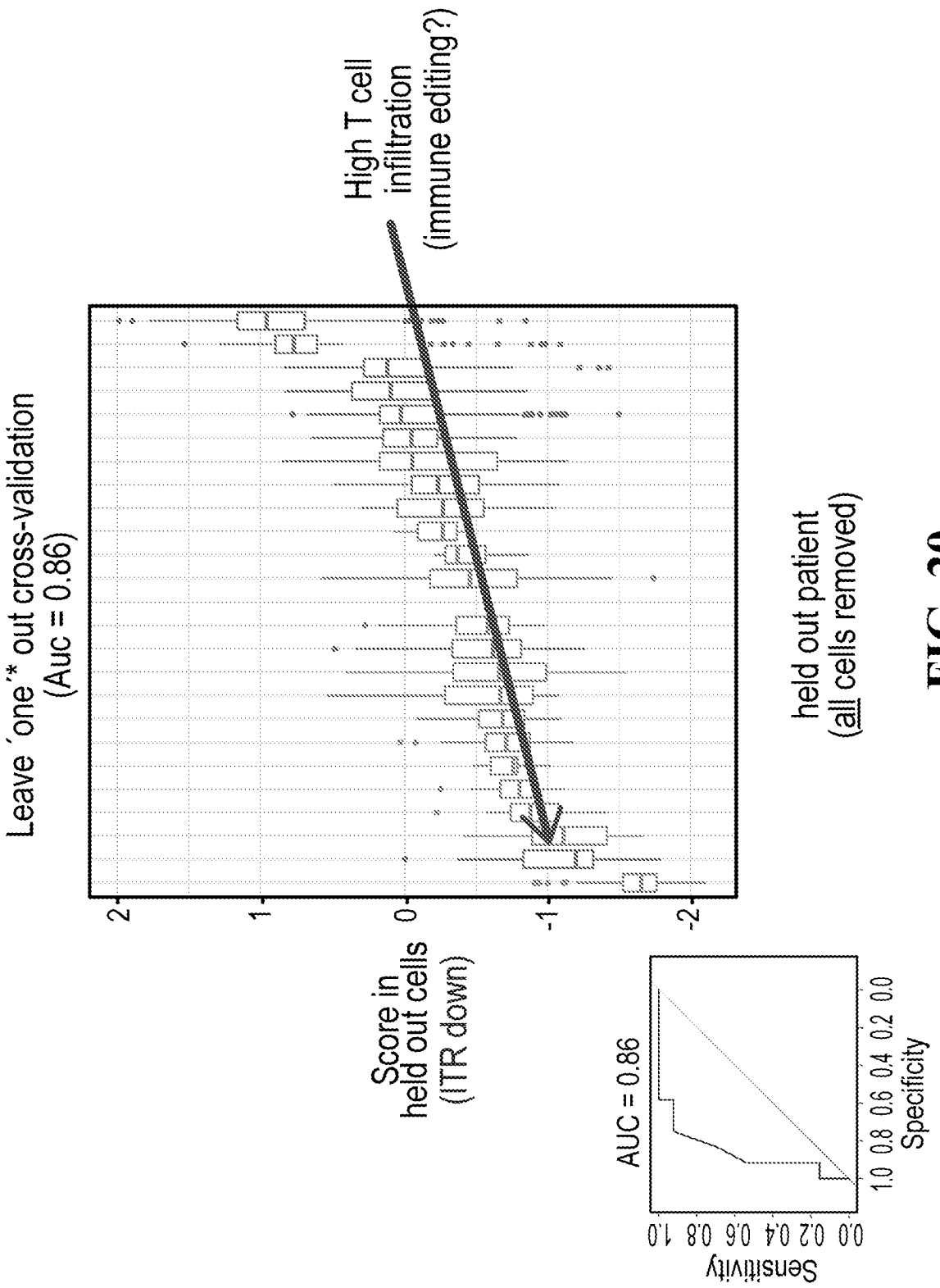

Leave ´one´* out cross-validation
(Auc = 0.86)
High T cell
infiltration
(immune editing?)
Score in
held out cells
(ITR down)
held out patient
(all cells removed)
AUC = 0.86
Sensitivity
Specificity
0.0 0.2 0.4 0.6 0.8 1.0
1.0 0.8 0.6 0.4 0.2 0.0
2
1
0
-1
-2

FIG. 20

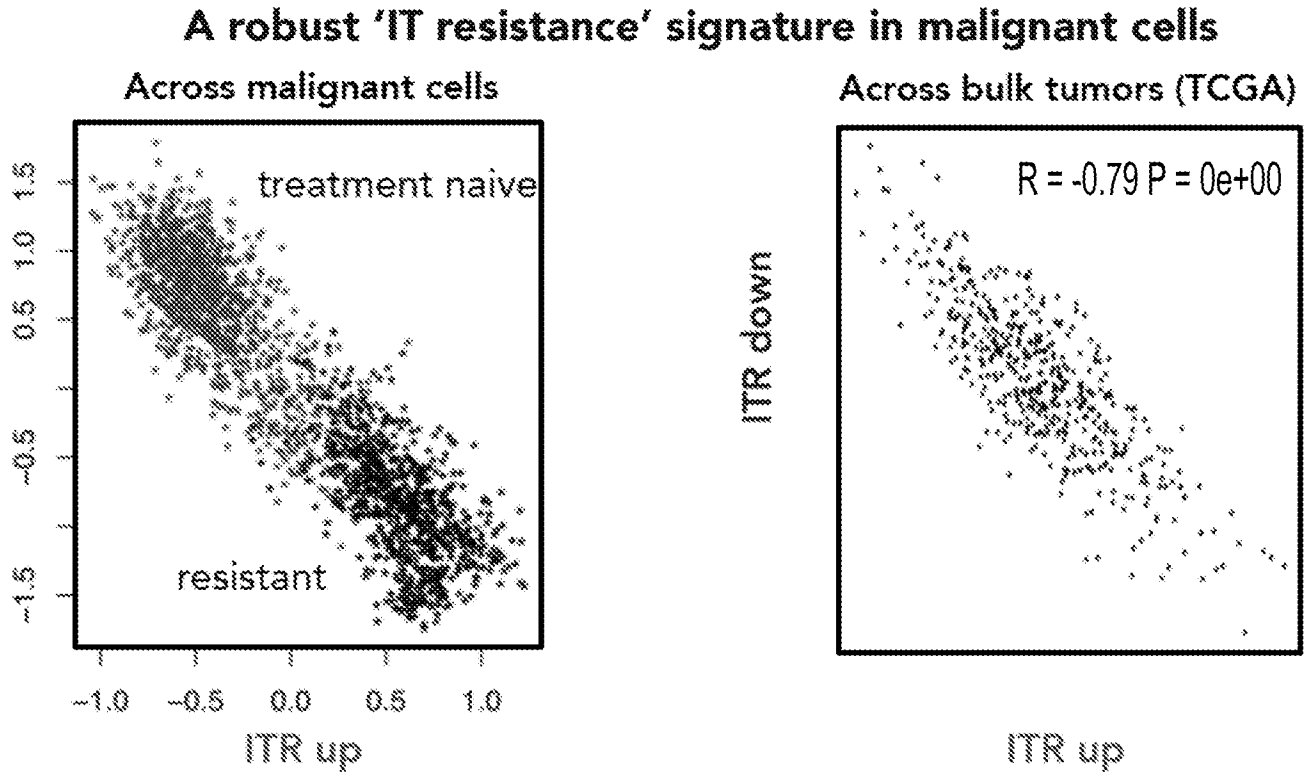

A robust 'IT resistance' signature in malignant cells
Across malignant cells
treatment naive
resistant
1.5
1.0
0.5
−0.5
−1.5
−1.0
−0.5
0.0
0.5
1.0
ITR up
Across bulk tumors (TCGA)
R = -0.79 P = 0e+00
ITR down
ITR up

FIG. 21

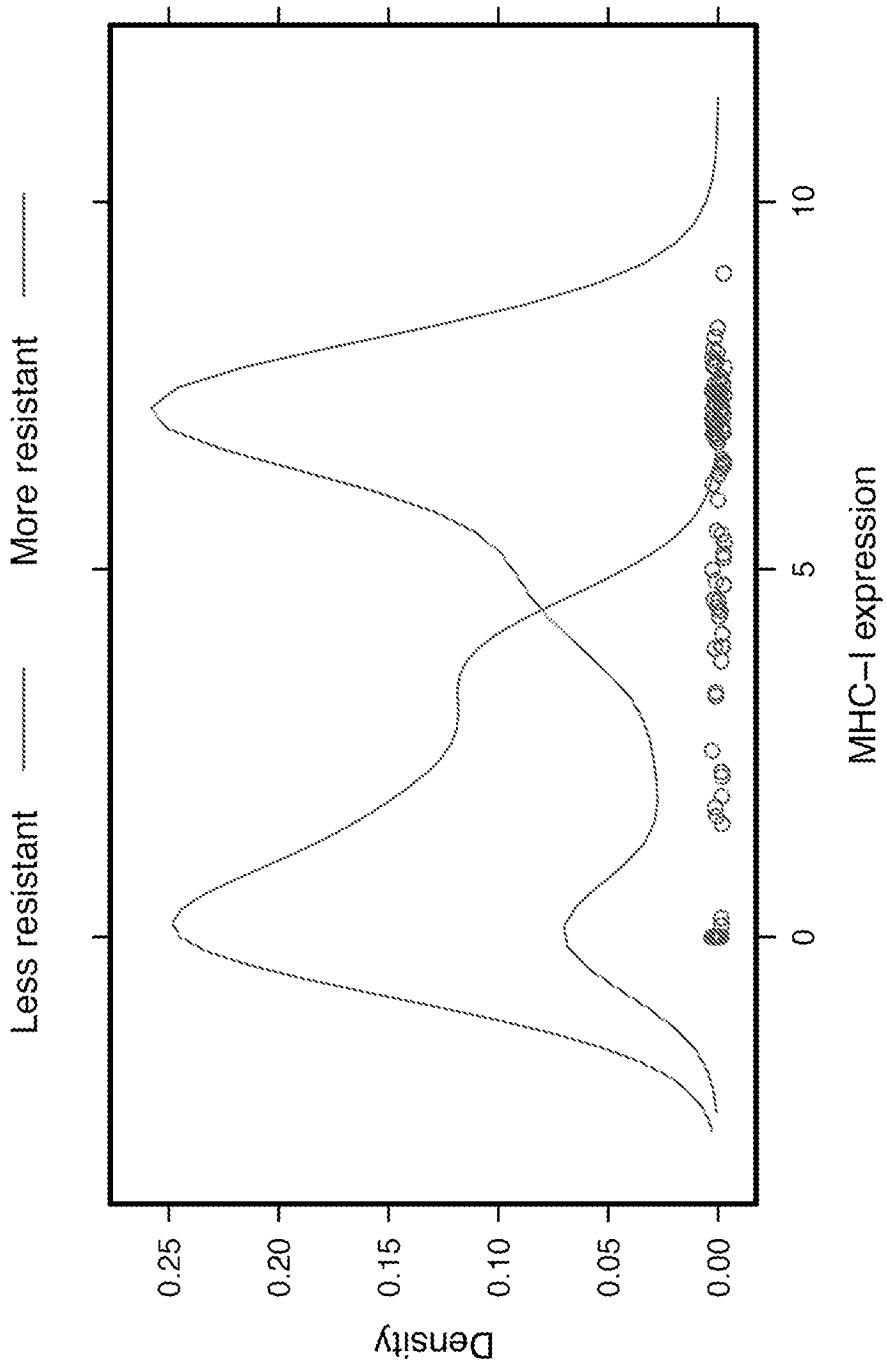

Less resistant
More resistant
Density
0.25
0.20
0.15
0.10
0.05
0.00
0
5
10
MHC−I expression

FIG. 22

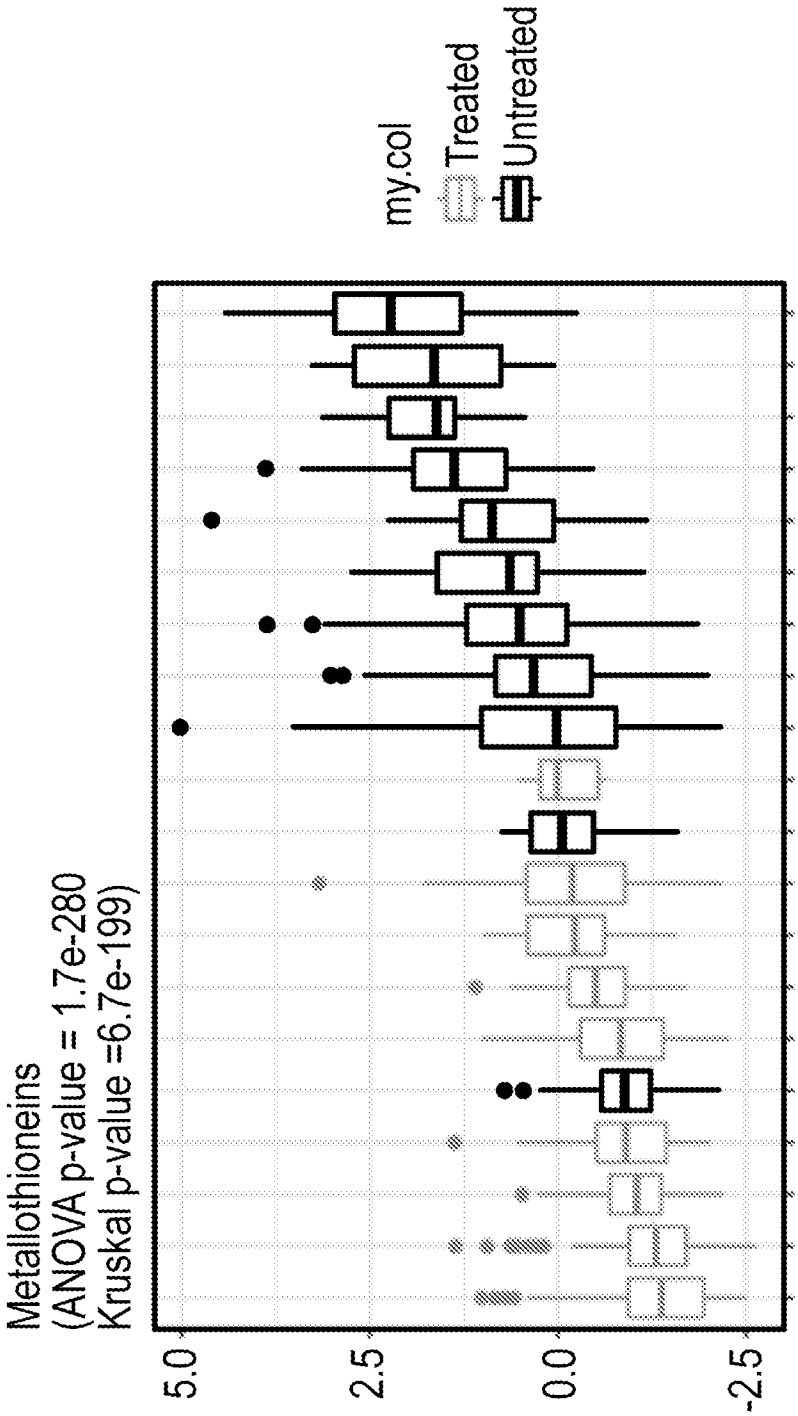

my.col
Treated
Untreated
Metallothioneins
(ANOVA p-value = 1.7e-280
Kruskal p-value =6.7e-199)
5.0
2.5
0.0
-2.5

FIG. 23

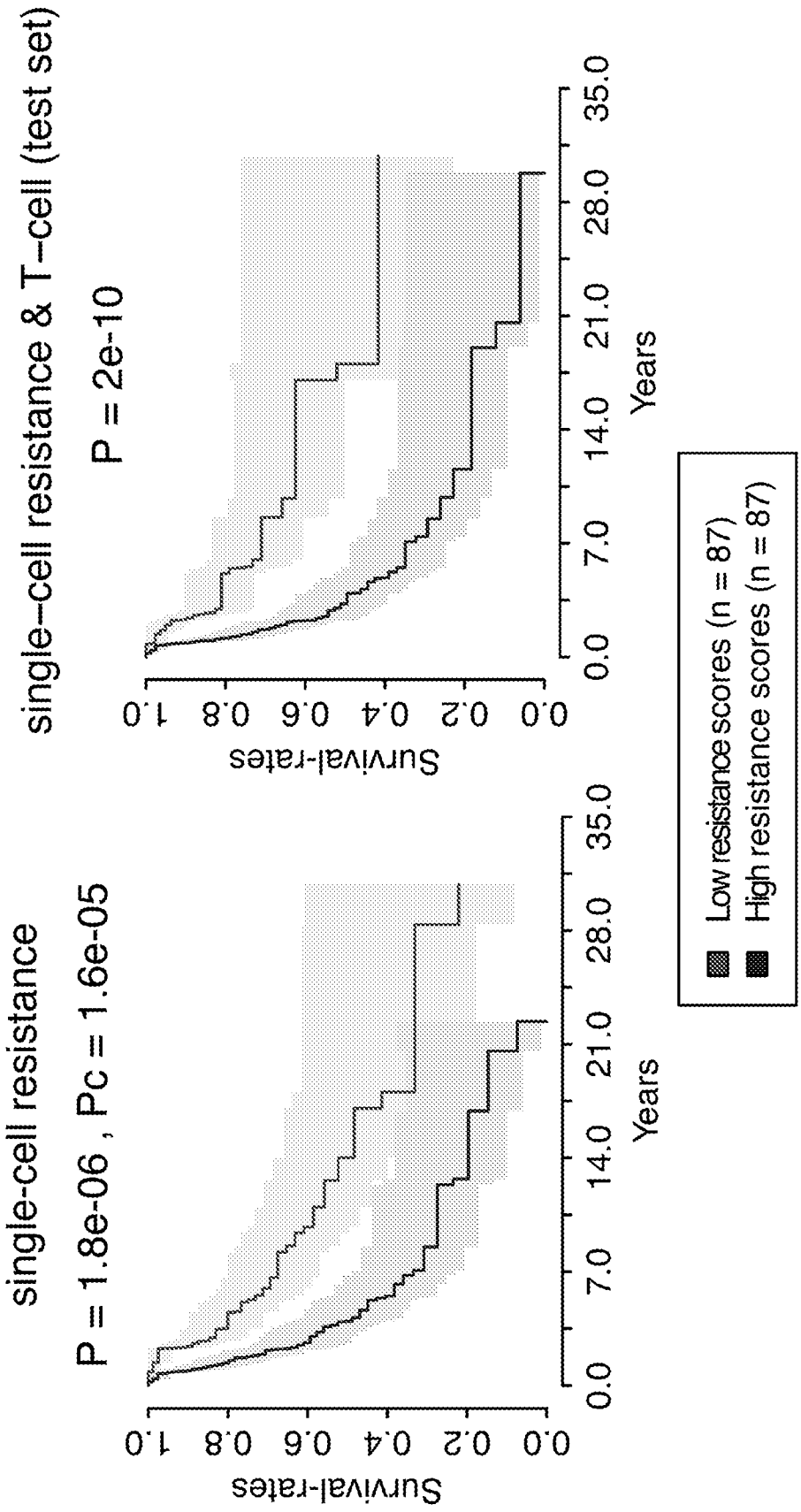

single−cell resistance & T−cell (test set)
P = 2e-10
Survival-rates
0.0
0.2
0.4
0.6
0.8
1.0
0.0
7.0
14.0
21.0
28.0
35.0
Years
single-cell resistance
P = 1.8e-06 , Pc = 1.6e-05
Survival-rates
0.0
0.2
0.4
0.6
0.8
1.0
0.0
7.0
14.0
21.0
28.0
35.0
Years
Low resistance scores (n = 87)
High resistance scores (n = 87)

FIG. 24

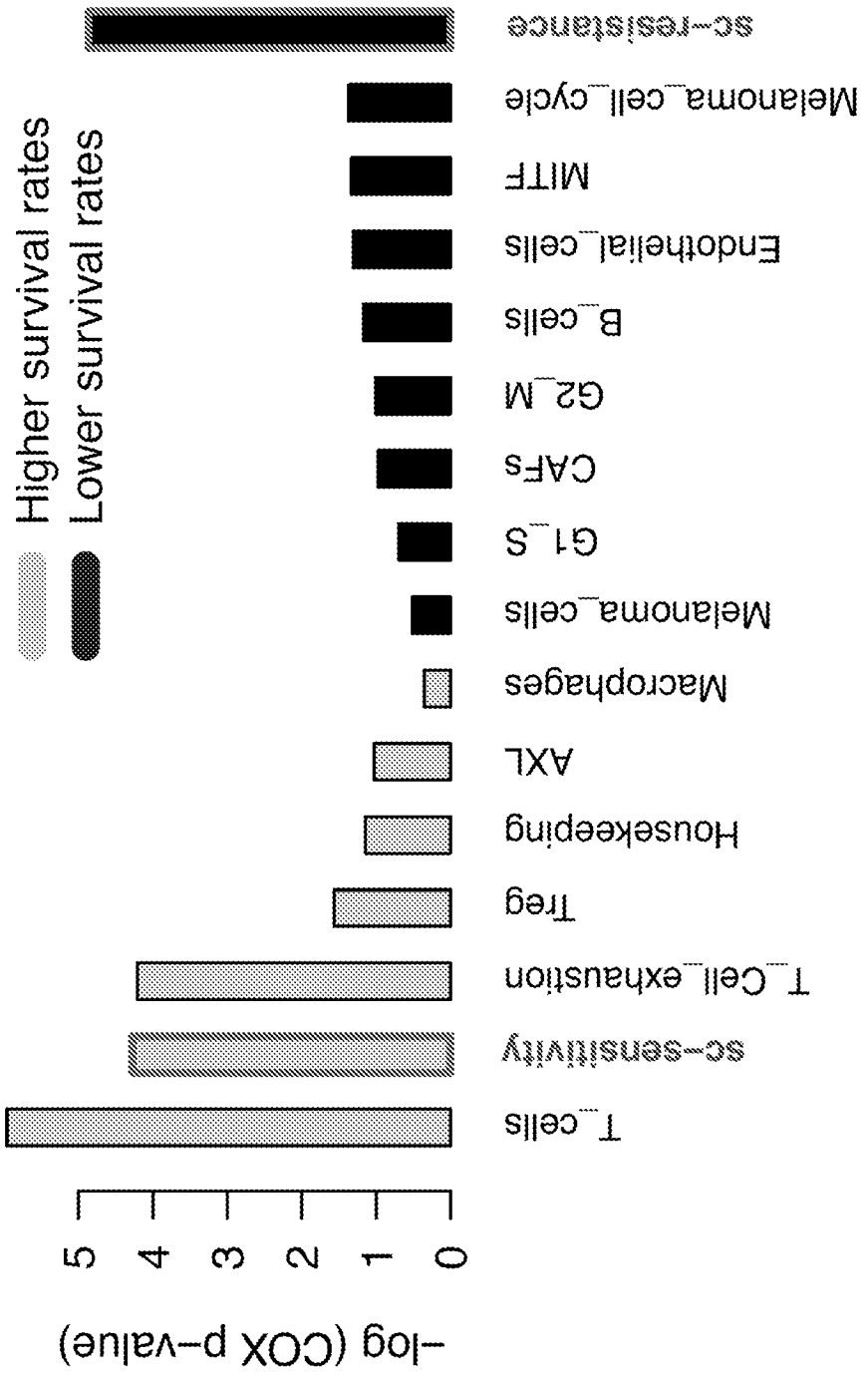

Higher survival rates
Lower survival rates
T_cells
sc-sensitivity
T_Cell_exhaustion
Treg
Housekeeping
AXL
Macrophages
Melanoma_cells
G1_S
CAFs
G2_M
B_cells
Endothelial_cells
MITF
Melanoma_cell_cycle
sc-resistance
5
4
3
2
1
0
-log (COX p-value)

FIG. 25

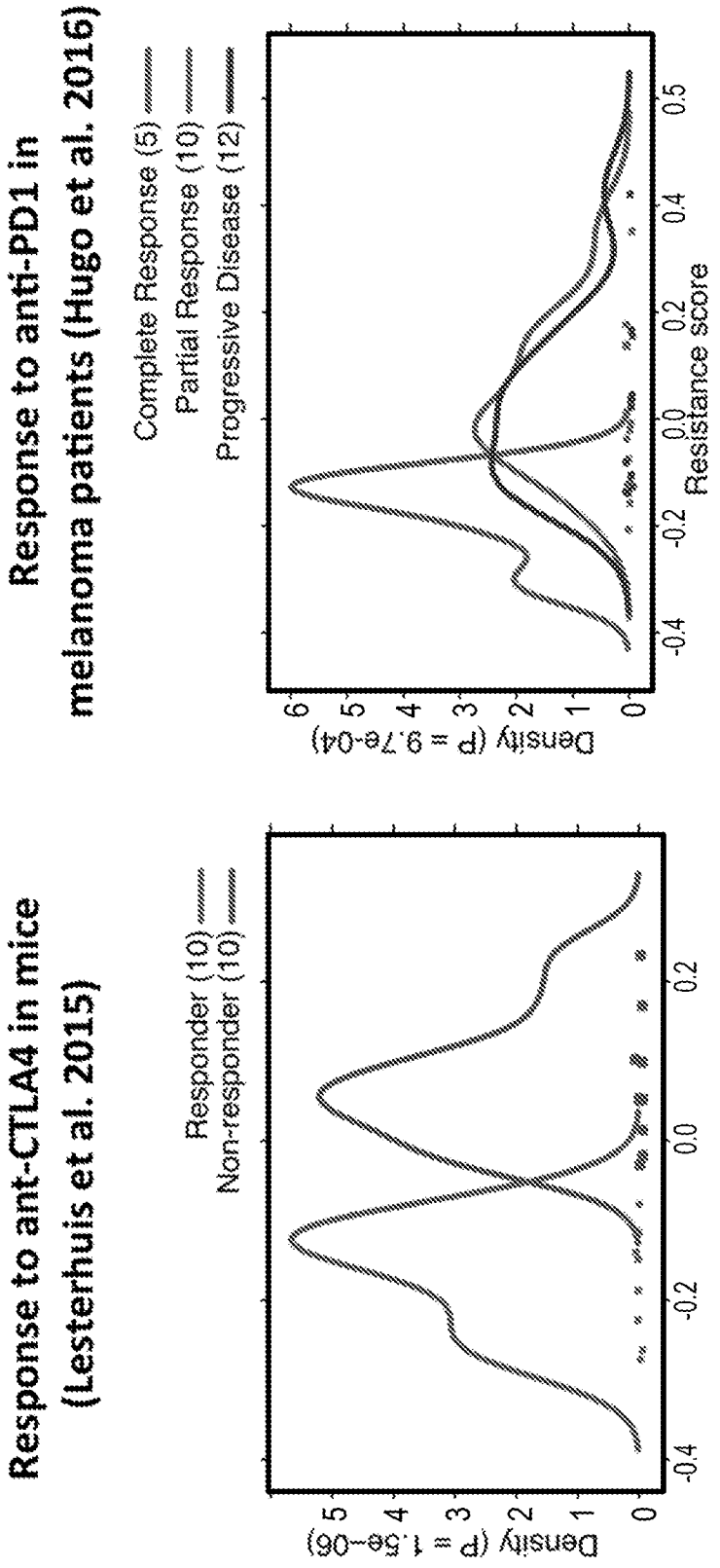

Response to anti-PD1 in melanoma patients (Hugo et al. 2016)
Complete Response (5)
Partial Response (10)
Progressive Disease (12)
Density (P = 9.7e-04)
Resistance score
Response to ant-CTLA4 in mice (Lesterhuis et al. 2015)
Responder (10)
Non-responder (10)
Density (P = 1.5e-06)

FIG. 26

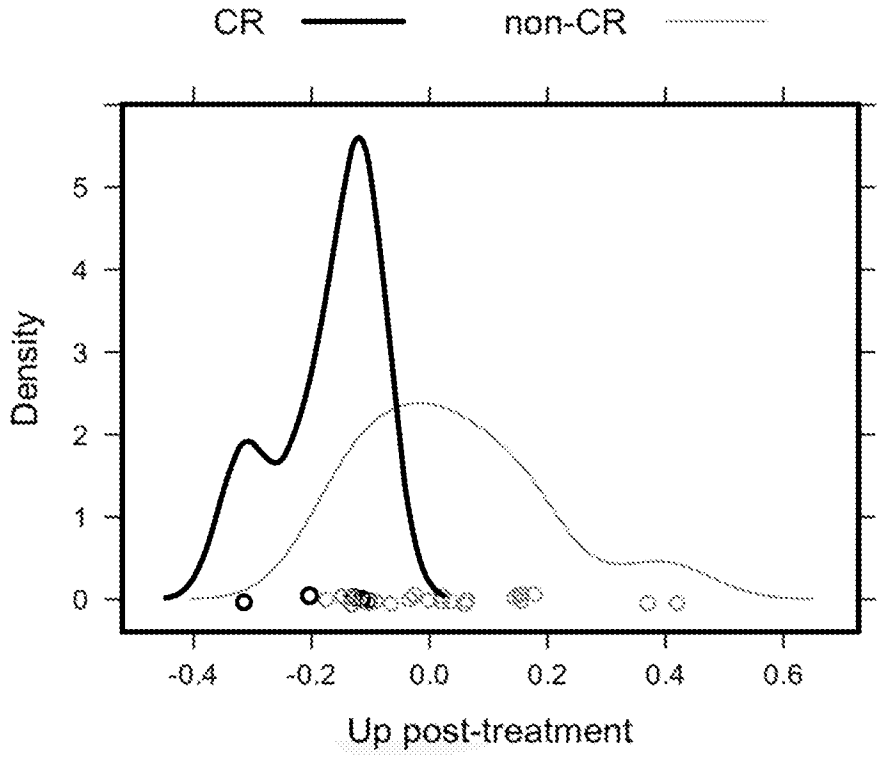


FIG. 27

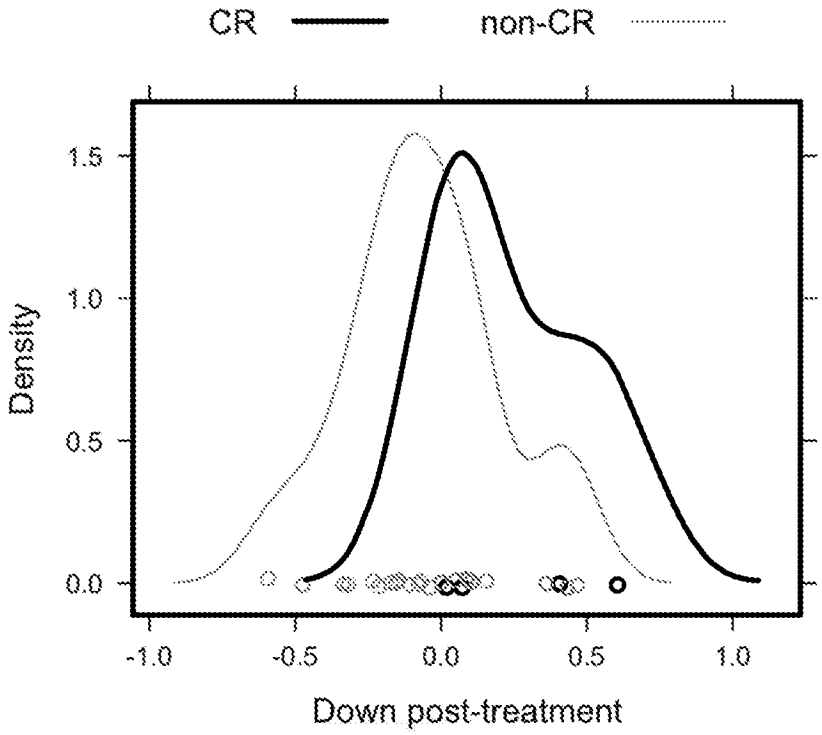


FIG. 28

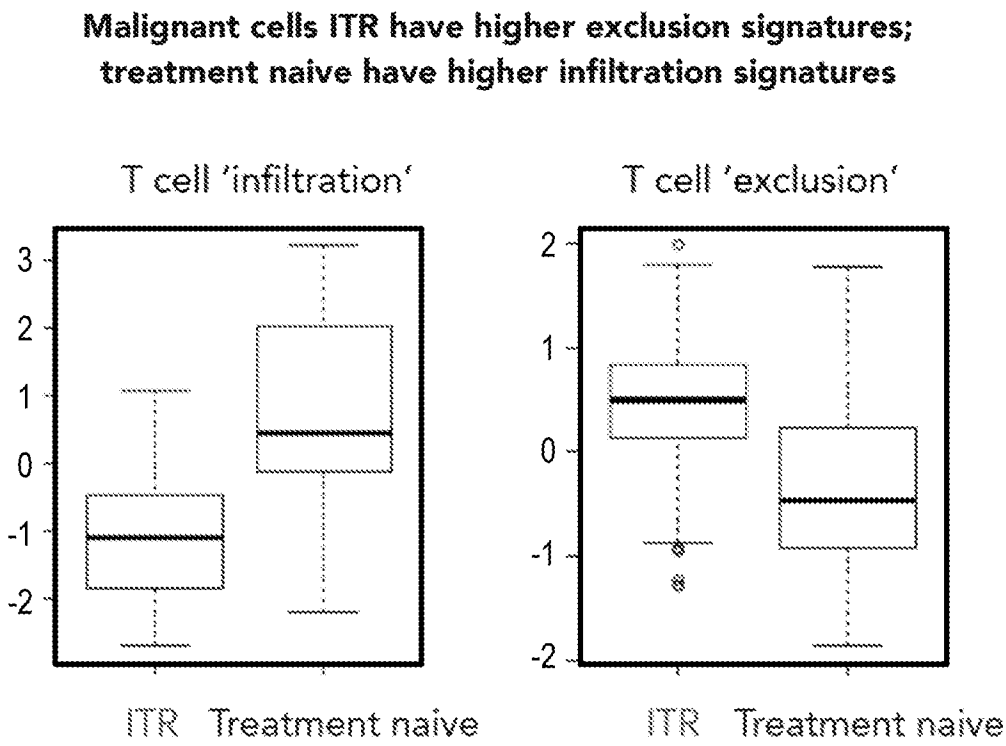

Malignant cells ITR have higher exclusion signatures;
treatment naive have higher infiltration signatures
T cell 'infiltration'
T cell 'exclusion'
3
2
1
0
-1
-2
2
1
0
-1
-2
ITR
Treatment naive
ITR
Treatment naive

FIG. 29

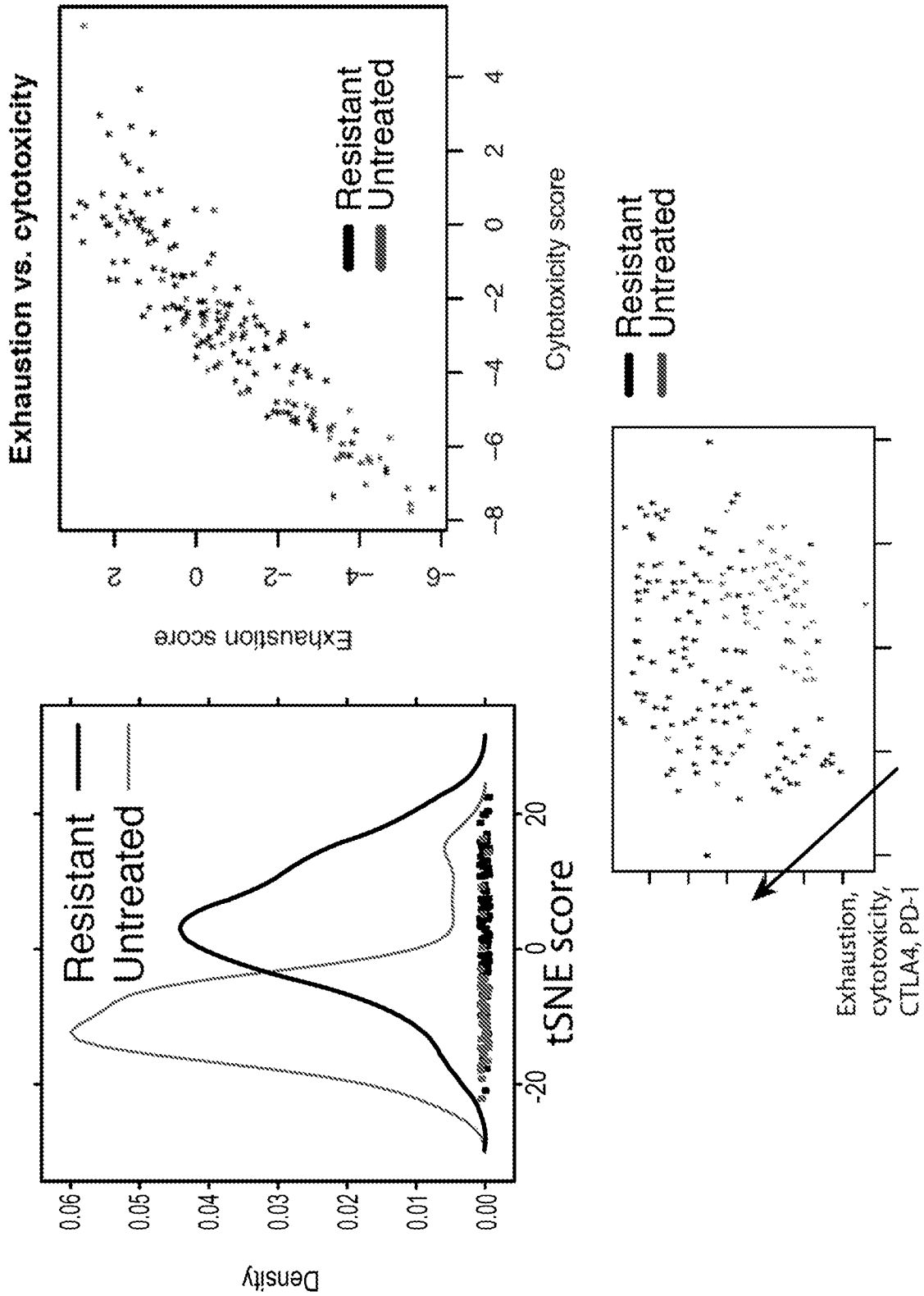

Exhaustion vs. cytotoxicity
Resistant
Untreated
Exhaustion score
Cytotoxicity score
Density
tSNE score
Exhaustion, cytotoxicity, CTLA4, PD-1

FIG. 30

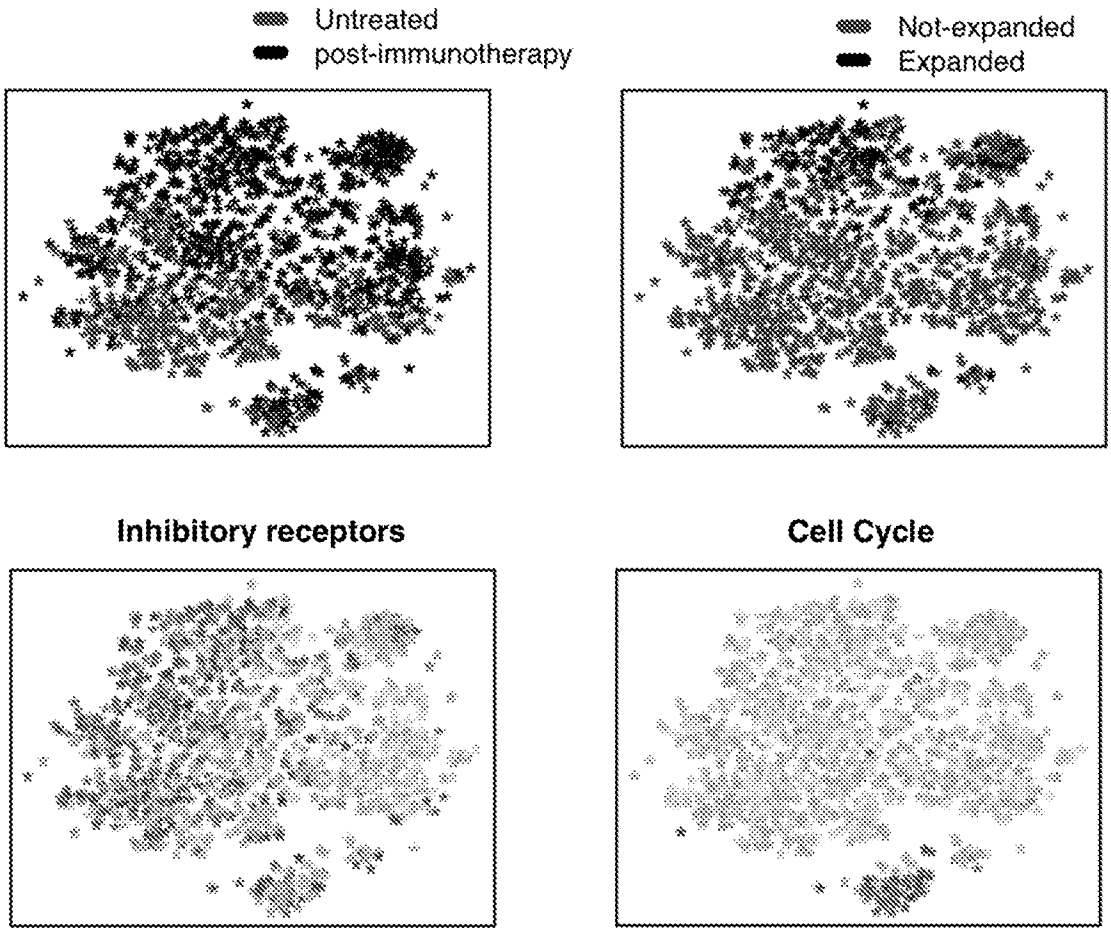

Untreated
post-immunotherapy
Not-expanded
Expanded
Inhibitory receptors
Cell Cycle

FIG. 31

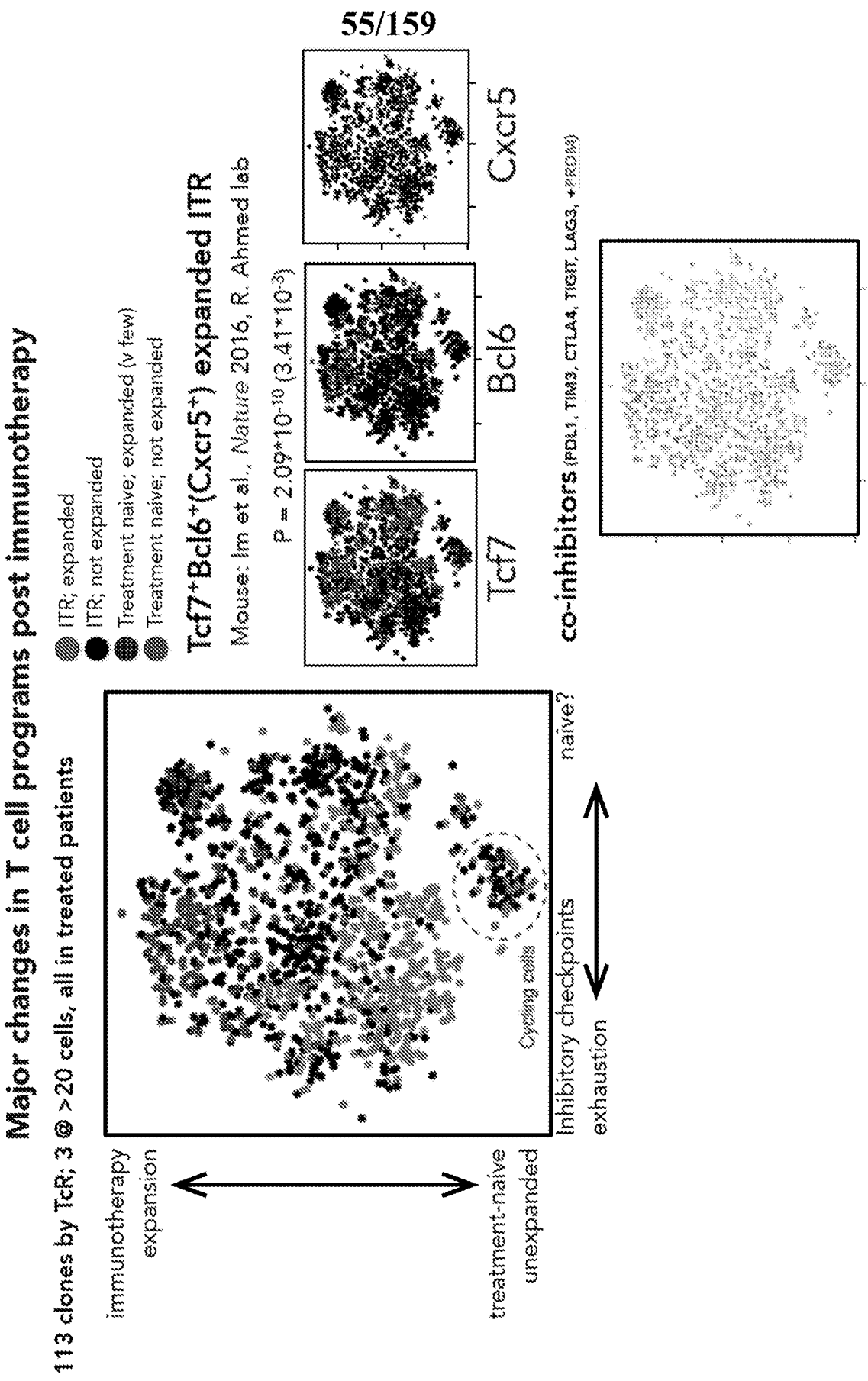

Major changes in T cell programs post immunotherapy
113 clones by TcR; 3 @ >20 cells, all in treated patients
ITR; expanded
ITR; not expanded
Treatment naive; expanded (v few)
Treatment naive; not expanded
immunotherapy expansion
treatment-naive unexpanded
Cycling cells
Inhibitory checkpoints
exhaustion
naive?
Tcf7+Bcl6+(Cxcr5+) expanded ITR
Mouse: Im et al., Nature 2016, R. Ahmed lab
P = 2.09*10-10 (3.41*10-3)
Tcf7
Bcl6
Cxcr5
co-inhibitors (PDL1, TIM3, CTLA4, TIGIT, LAG3, +PD1)

FIG. 32

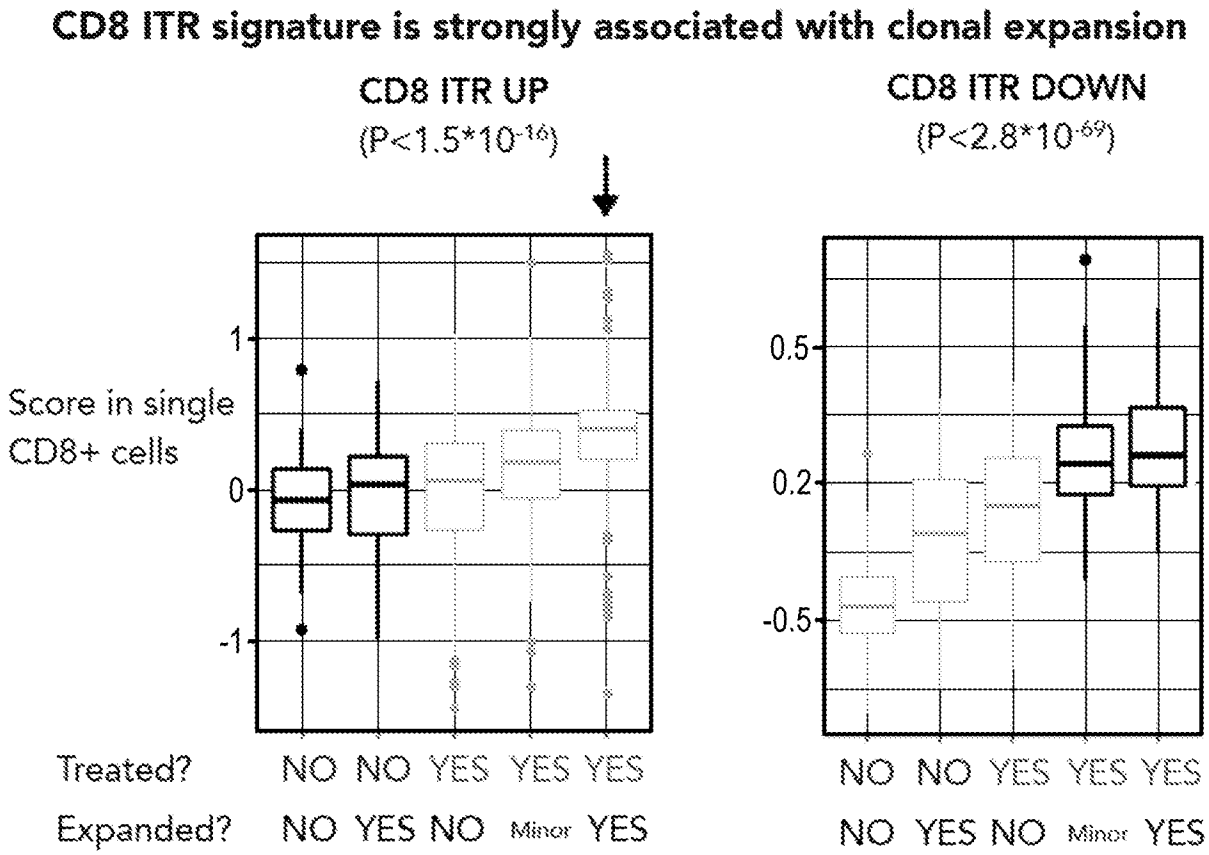

CD8 ITR signature is strongly associated with clonal expansion
CD8 ITR UP
(P<1.5*10-16)
CD8 ITR DOWN
(P<2.8*10-69)
Score in single CD8+ cells
1
0
-1
0.5
0.2
-0.5
Treated? NO NO YES YES YES
Expanded? NO YES NO Minor YES
NO NO YES YES YES
NO YES NO Minor YES

FIG. 33

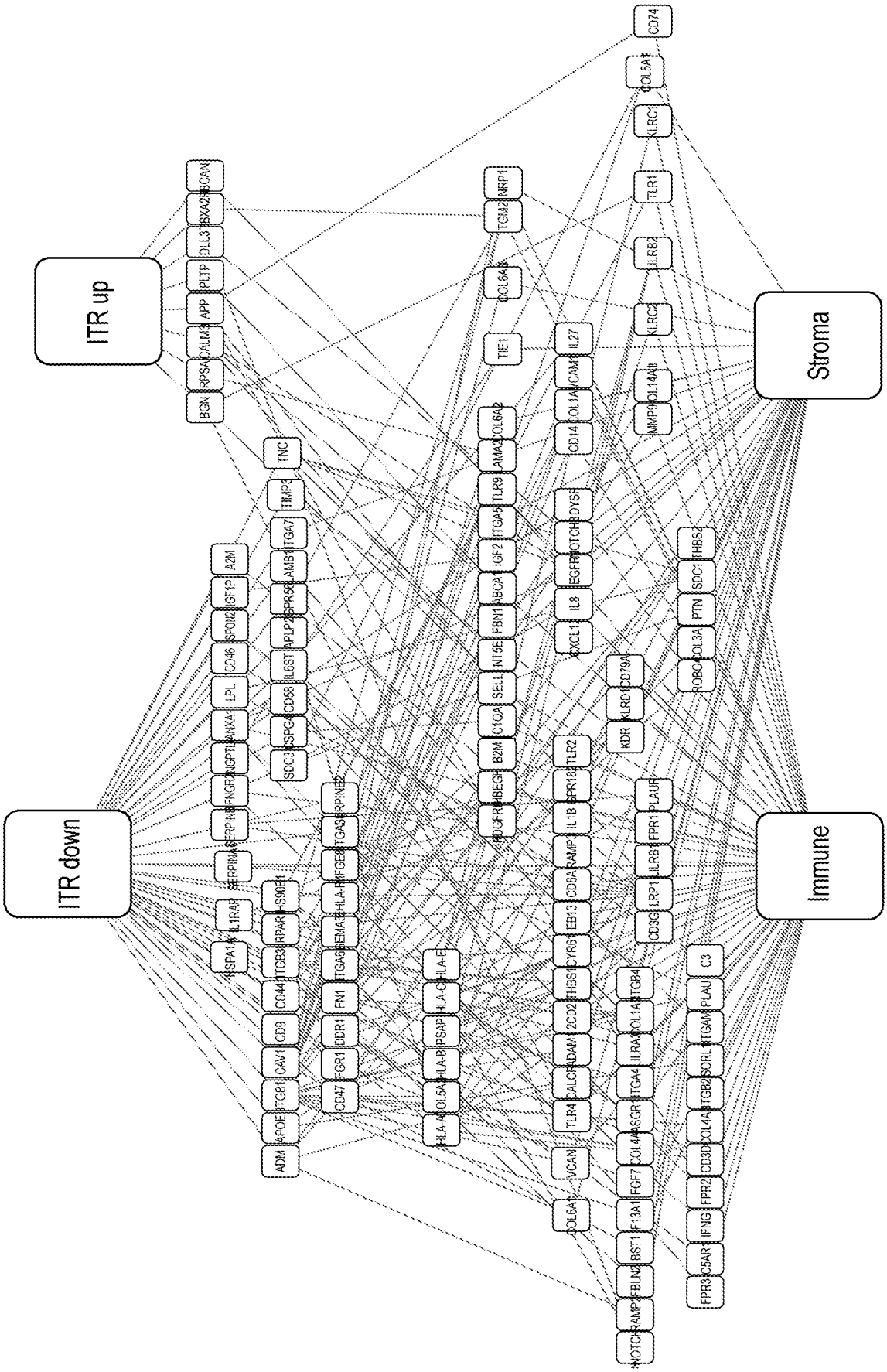

ITR up
ITR down
Stroma
Immune
BGN
RPSA
CALM3
APP
PLTP
DLL3
BXA2
CAN
TNC
TIMP3
TGA7
AMB1
PPRC1
APLP2
L6ST
CD58
SPG1
SDC3
A2M
GF1P
SPON2
CD46
LPL
ANX4
GPTL
FNGR
ERPIN
ERPIN
L1RAP
HSPA1A
IS90B1
RPAP3
TGB3
CD44
CD9
CAV1
TGB1
APOE
ADM
TGA5
RPIN2
TGA6
HMGB1
EMA1
TGA6
FN1
DDR1
FGR1
CD47
HLA-C
HLA-E
PSAP
HLA-B
COL5A
HLA-A
NRP1
TGM2
COL6A3
TIE1
COL6A2
AMA1
TLR9
ITGA5
IGF2
ABCA1
FBN1
NT5E
SELL
C1QA
B2M
EGFR
BEGF
TLR2
FPR1B
IL1B
CAMP1
CD8A
EB13
CYR6
HBS1
2CD2
CALCR
DAM1
TLR4
VCAN
COL6A1
IL27
ICAM1
COL1A1
CD14
EGFR
ROTOR
DYSF
IL8
CXCL1
KDR
LRD1
CD79A
TLR2
FPR1
LRB1
LRP1
CD3G
CD74
COL5A1
KLRC1
TLR1
ILRB2
KLRC2
IL14A0
MMP9
THBS1
SDC1
PTN
COL3A1
ROBO4
PLAUR
FPR1
ILRB1
LRP1
CD3G
ITGB4
ILRA2
COL1A2
ITGA4
SGR1
COL4A1
FGF7
F13A1
BST1
FBLN2
CAMP1
NOTCH
C3
PLAU
ITGAM
SORL1
ITGB2
COL4A2
CD3D
FPR2
IFNG
C5AR1
FPR3

FIG. 34

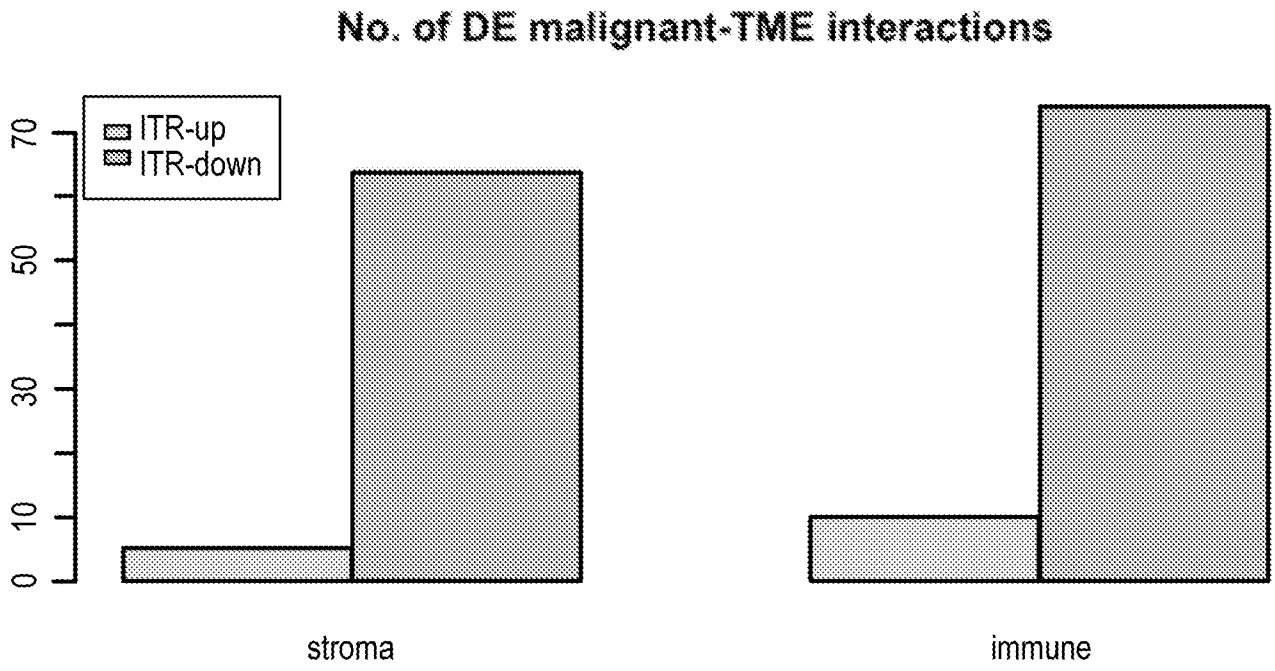

No. of DE malignant-TME interactions
ITR-up
ITR-down
0
10
30
50
70
stroma
immune

FIG. 35

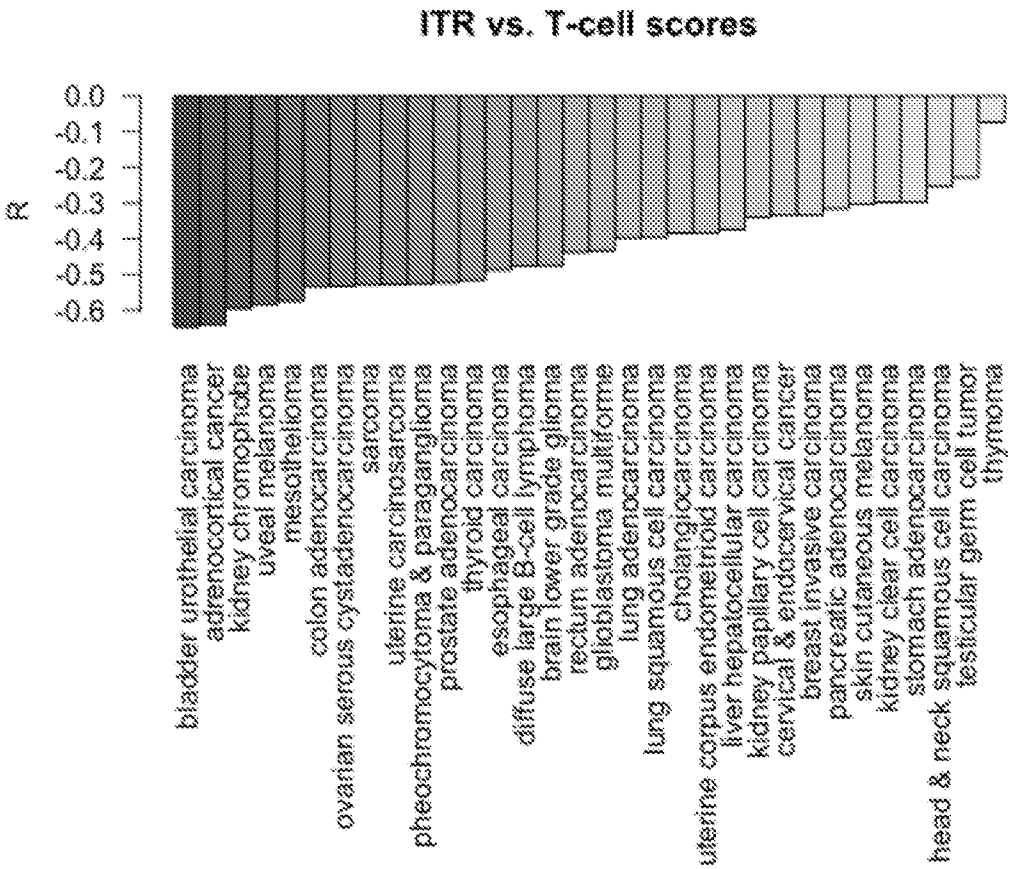

ITR vs. T-cell scores
R
0.0
-0.1
-0.2
-0.3
-0.4
-0.5
-0.6
bladder urothelial carcinoma
adrenocortical cancer
kidney chromophobe
uveal melanoma
mesothelioma
colon adenocarcinoma
ovarian serous cystadenocarcinoma
sarcoma
uterine carcinosarcoma
pheochromocytoma & paraganglioma
prostate adenocarcinoma
thyroid carcinoma
esophageal carcinoma
diffuse large B-cell lymphoma
brain lower grade glioma
rectum adenocarcinoma
glioblastoma multiforme
lung adenocarcinoma
lung squamous cell carcinoma
cholangiocarcinoma
uterine corpus endometrioid carcinoma
liver hepatocellular carcinoma
kidney papillary cell carcinoma
cervical & endocervical cancer
breast invasive carcinoma
pancreatic adenocarcinoma
skin cutaneous melanoma
kidney clear cell carcinoma
stomach adenocarcinoma
head & neck squamous cell carcinoma
testicular germ cell tumor
thymoma

FIG. 36

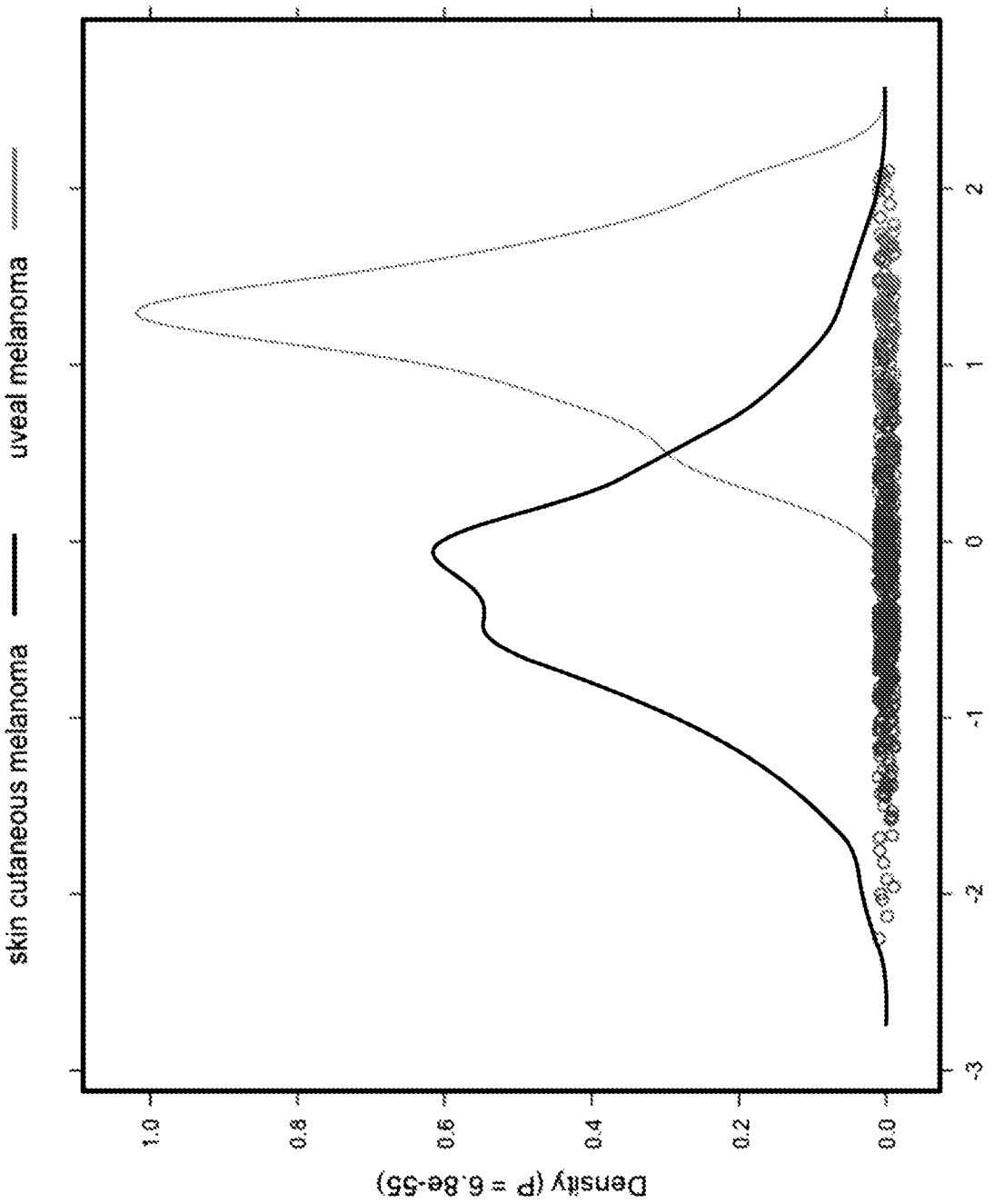

skin cutaneous melanoma
uveal melanoma
Density (P = 6.8e-55)
0.0
0.2
0.4
0.6
0.8
1.0
-3
-2
-1
0
1
2
ITR-scores

FIG. 37

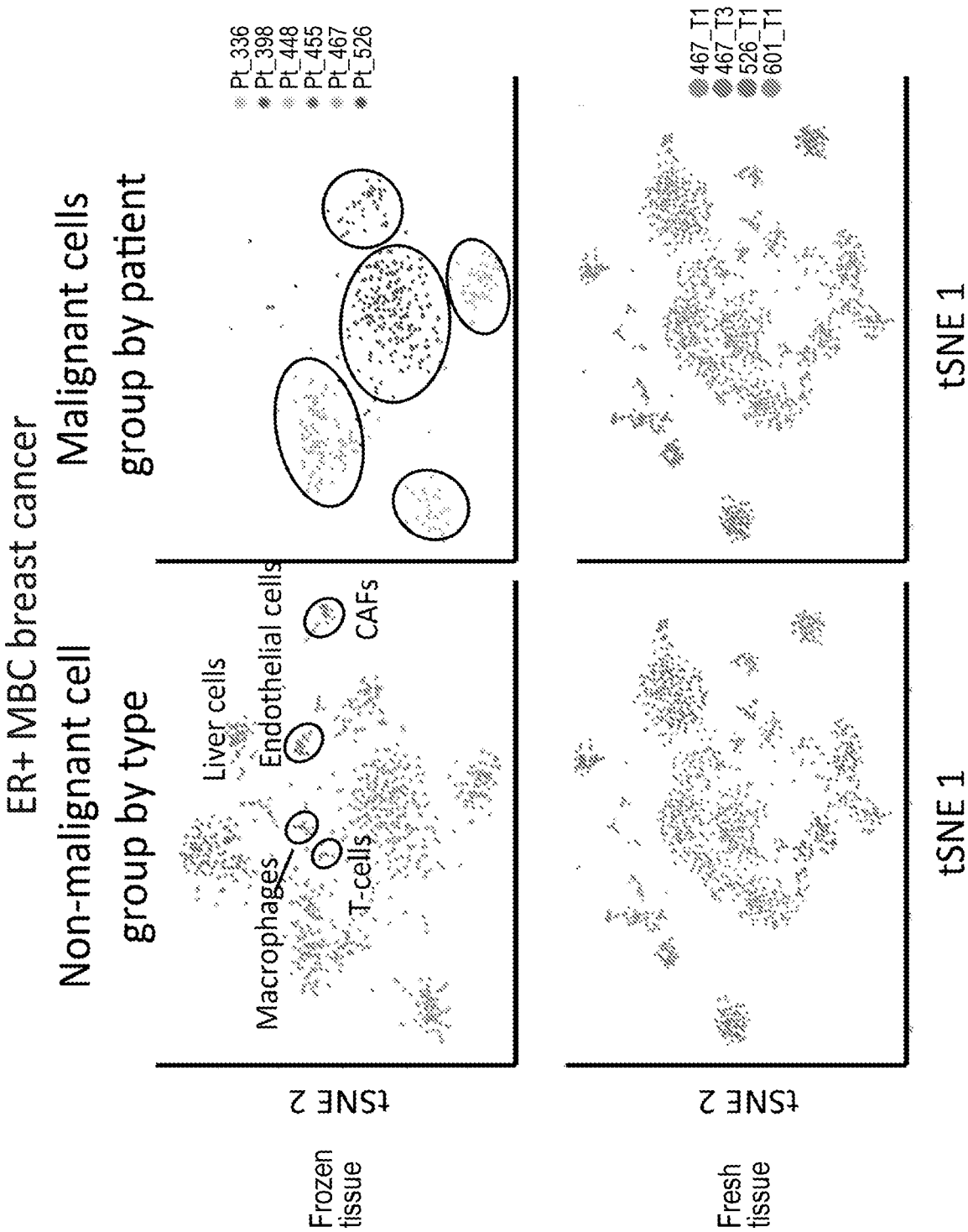

ER+ MBC breast cancer
Non-malignant cell group by type
Malignant cells group by patient
Pt_336
Pt_398
Pt_448
Pt_455
Pt_467
Pt_526
467_T1
467_T3
526_T1
601_T1
Liver cells
Endothelial cells
CAFs
Macrophages
T-cells
tSNE 2
tSNE 1
Frozen tissue
Fresh tissue

FIG. 38

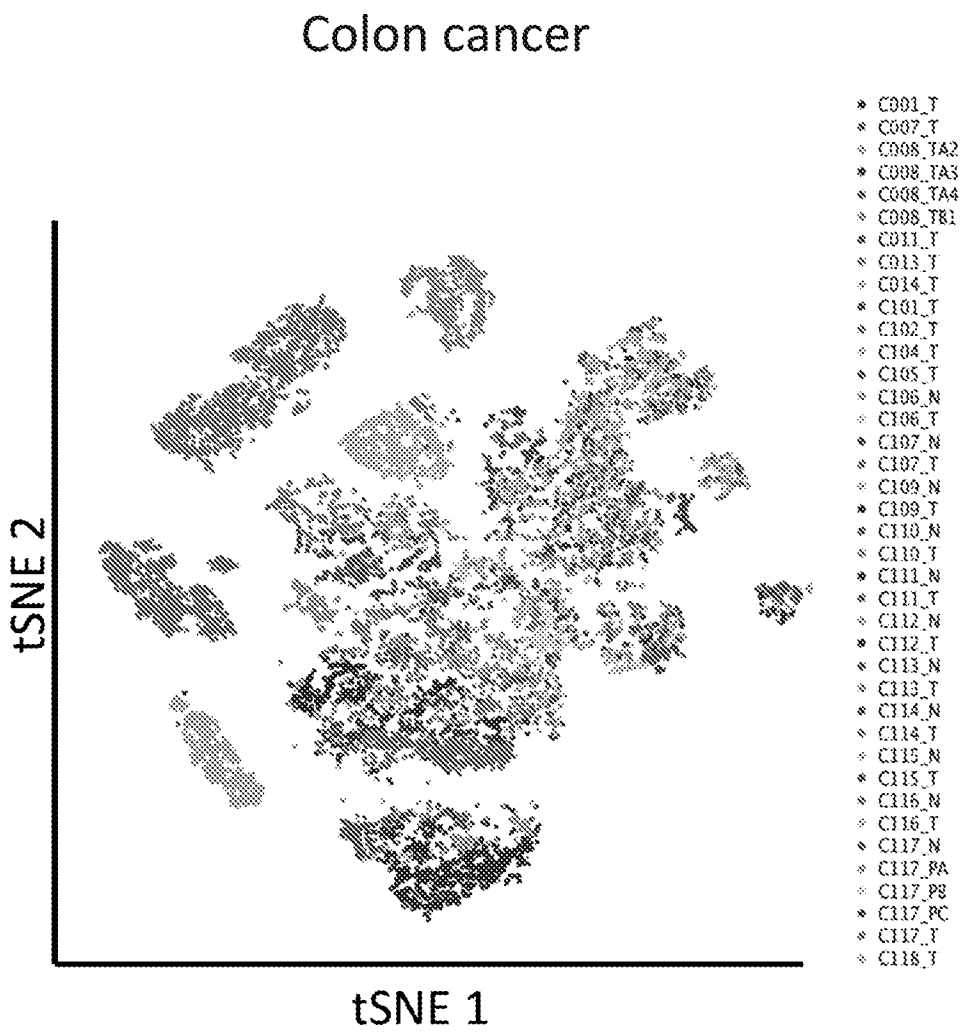

Colon cancer
tSNE 2
tSNE 1
C001_T
C007_T
C008_TA2
C008_TA3
C008_TA4
C008_TB1
C011_T
C013_T
C014_T
C101_T
C102_T
C104_T
C105_T
C106_N
C106_T
C107_N
C107_T
C109_N
C109_T
C110_N
C110_T
C111_N
C111_T
C112_N
C112_T
C113_N
C113_T
C114_N
C114_T
C115_N
C115_T
C116_N
C116_T
C117_N
C117_PA
C117_PB
C117_PC
C117_T
C118_T

FIG. 39

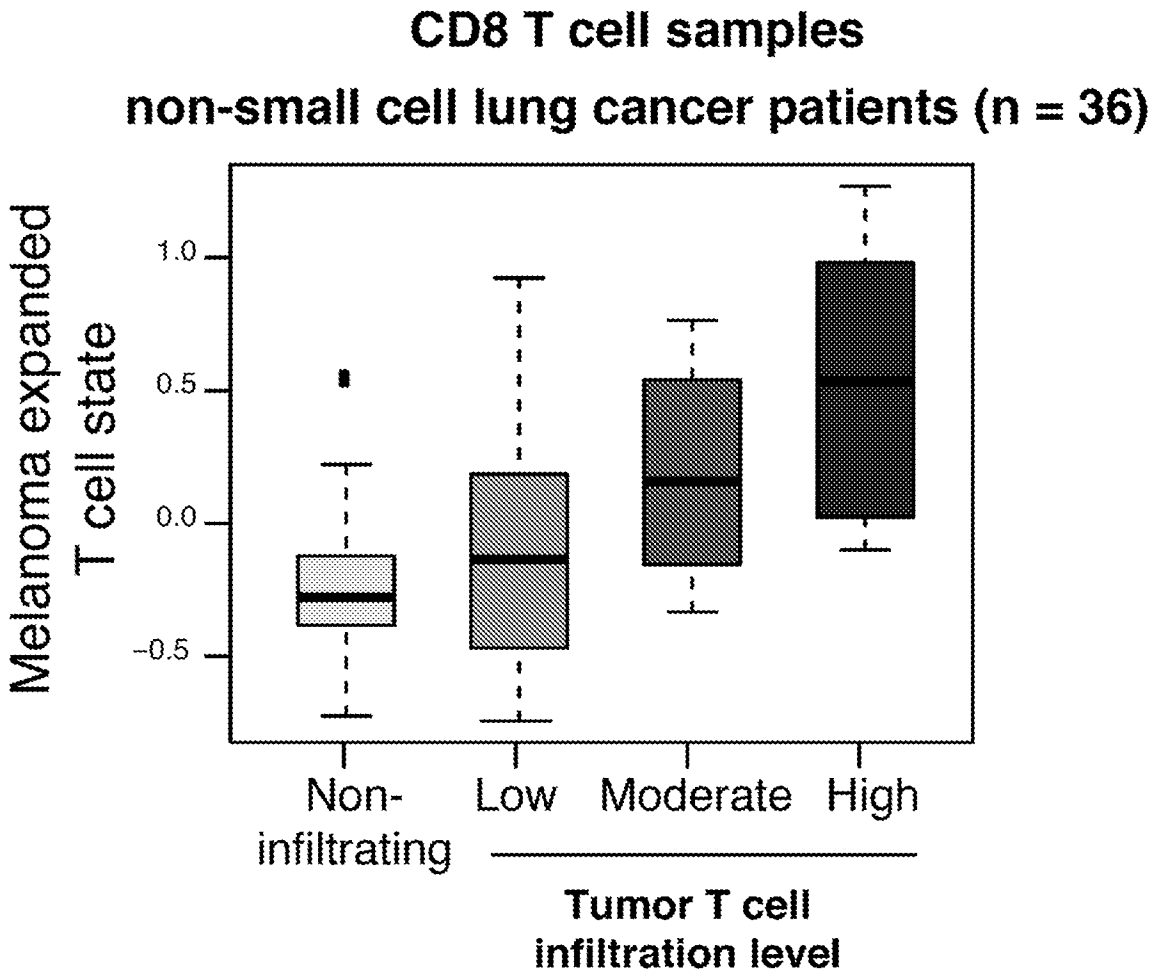

CD8 T cell samples
non-small cell lung cancer patients (n = 36)
Melanoma expanded T cell state
1.0
0.5
0.0
−0.5
Non-infiltrating
Low
Moderate
High
Tumor T cell infiltration level

FIG. 40

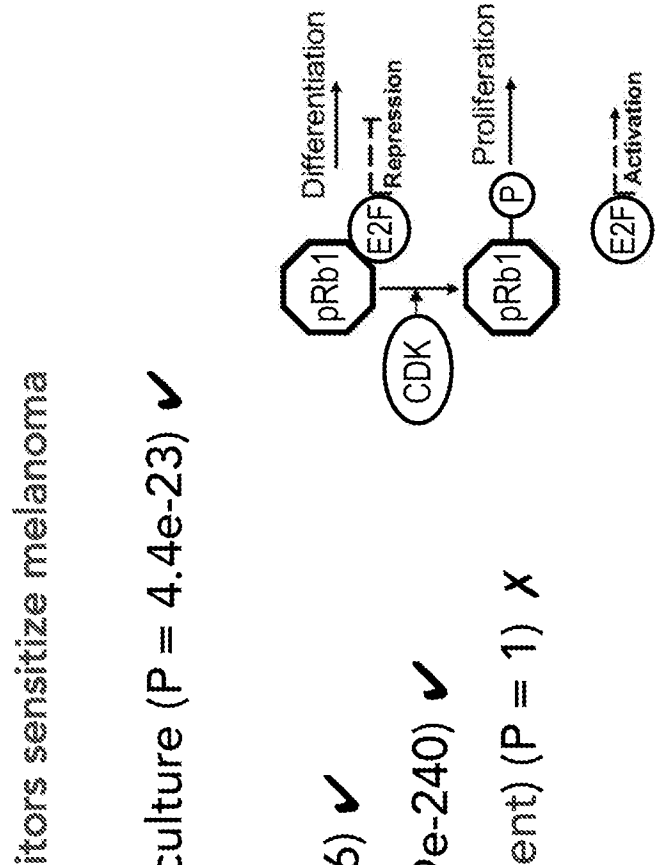

CDK4/6 inhibitors sensitize melanoma cells
• Short term melanoma culture (P = 4.4e-23) ✔
• Melanoma cell lines
1. IGR37 (P = 1.7e-36) ✔
2. UACC257 (P = 4.9e-240) ✔
3. A2058 (RB1-deficient) (P = 1) ✗
Differentiation
pRb1
E2F
Repression
CDK
pRb1
P
Proliferation
E2F
Activation

FIG. 41

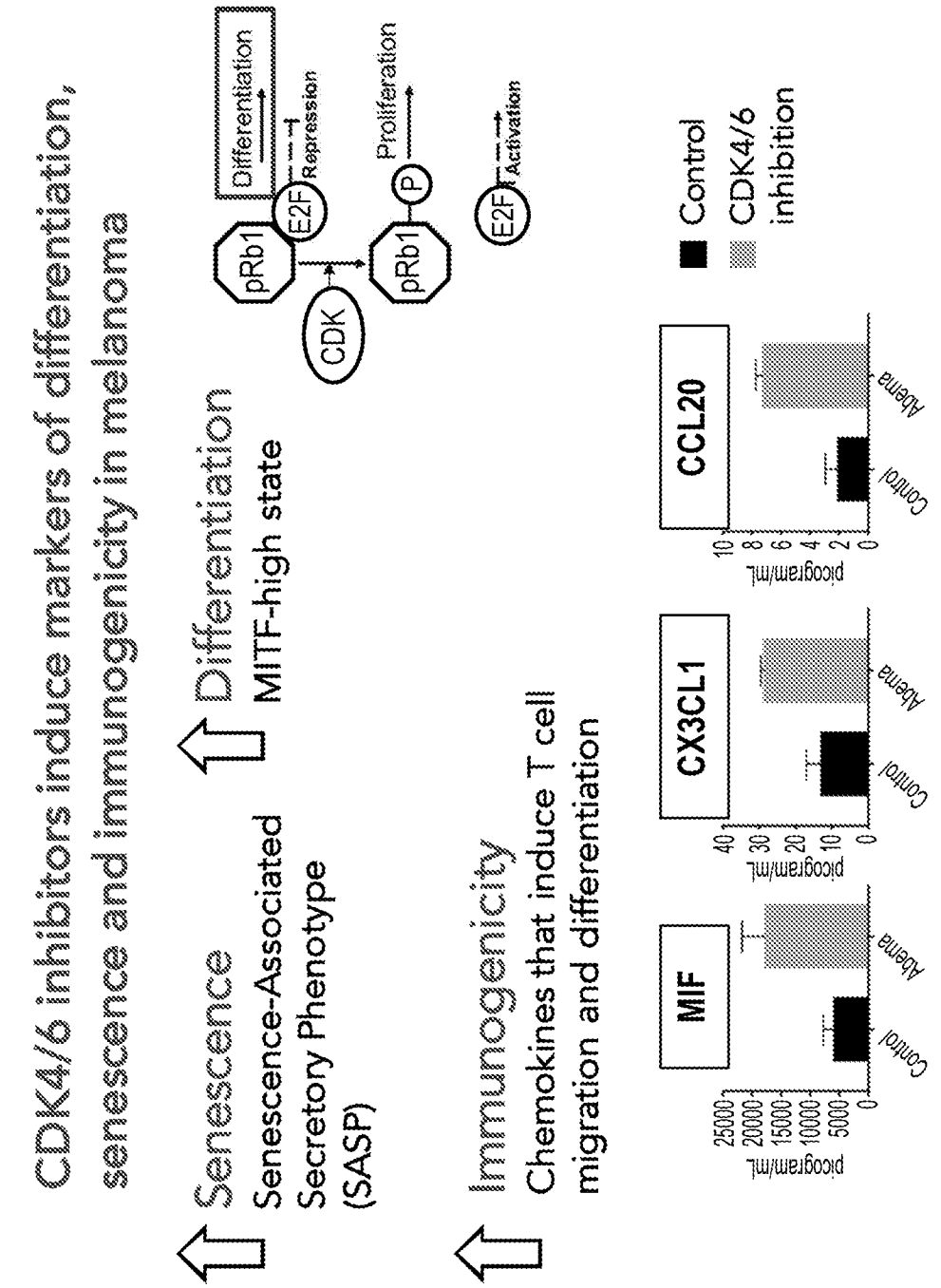

CDK4/6 inhibitors induce markers of differentiation, senescence and immunogenicity in melanoma
Senescence
Senescence-Associated Secretory Phenotype (SASP)
Differentiation
MITF-high state
Differentiation
pRb1
E2F
Repression
CDK
pRb1
P
Proliferation
E2F
Activation
Immunogenicity
Chemokines that induce T cell migration and differentiation
MIF
CX3CL1
CCL20
picogram/mL
Control
Abema
Control
CDK4/6 inhibition

FIG. 42

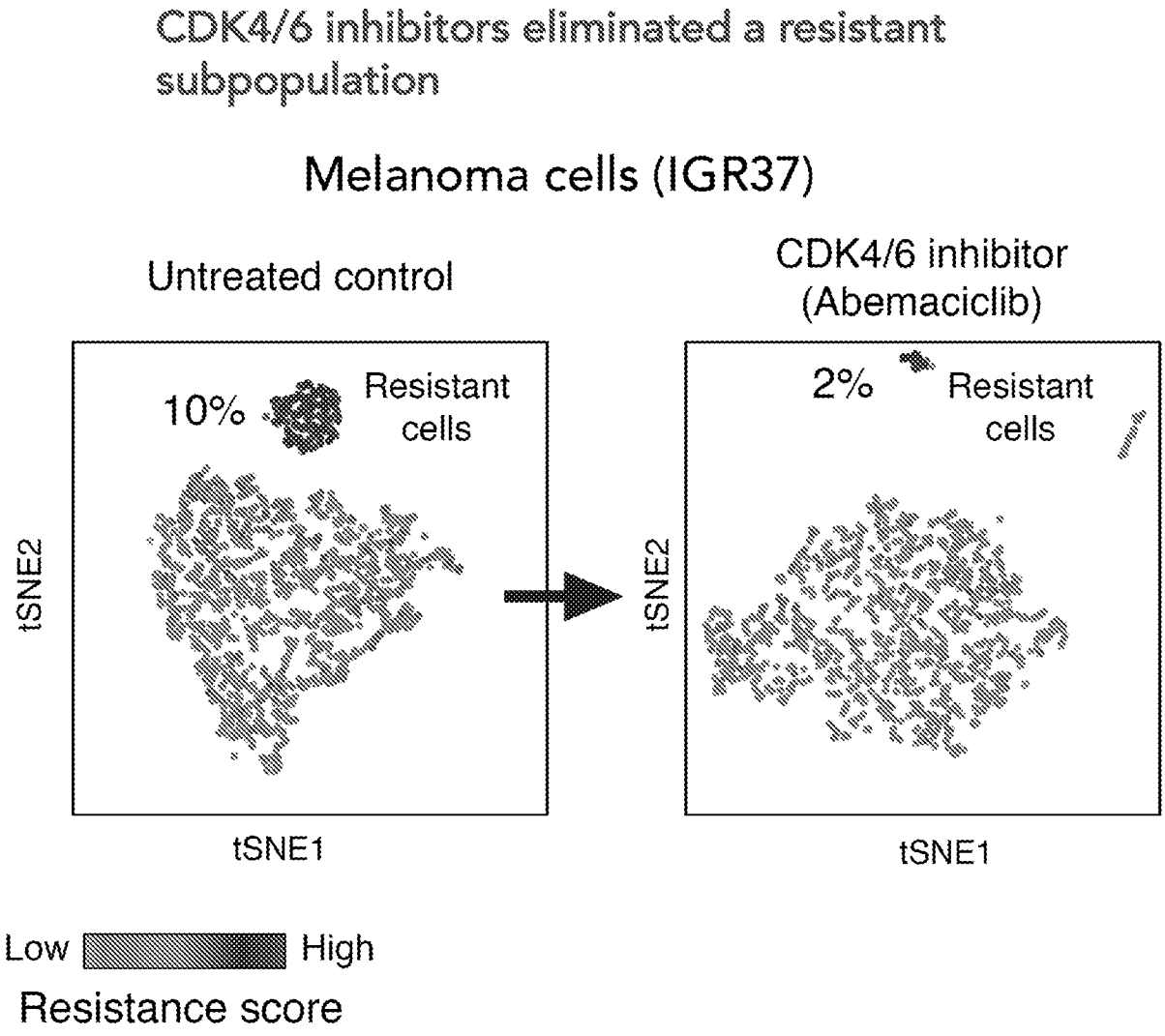

CDK4/6 inhibitors eliminated a resistant subpopulation
Melanoma cells (IGR37)
Untreated control
CDK4/6 inhibitor (Abemaciclib)
10%
Resistant cells
2%
Resistant cells
tSNE2
tSNE1
tSNE2
tSNE1
Low
High
Resistance score

FIG. 43

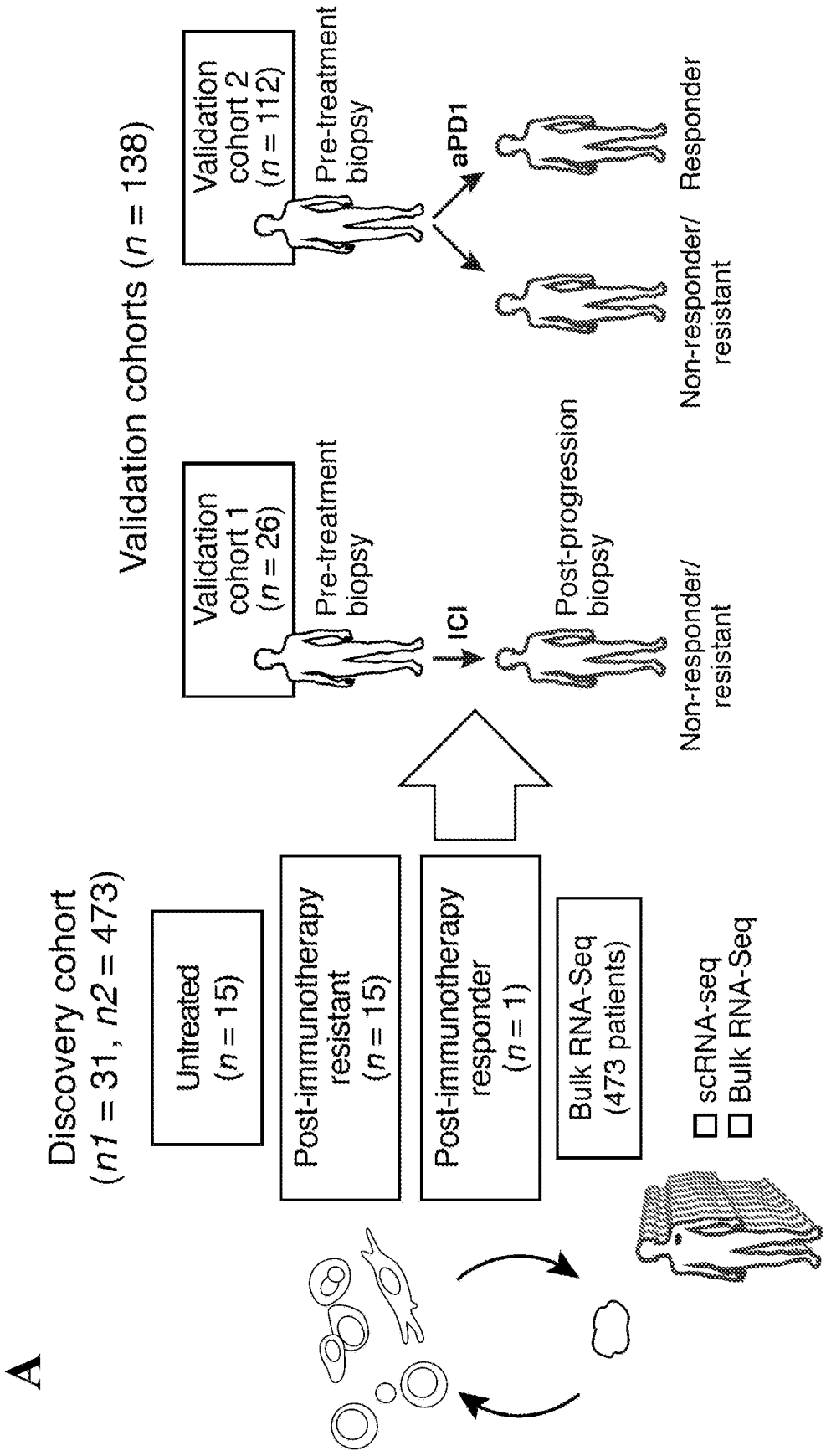

A
Discovery cohort
(n1 = 31, n2 = 473)
Untreated
(n = 15)
Post-immunotherapy
resistant
(n = 15)
Post-immunotherapy
responder
(n = 1)
Bulk RNA-Seq
(473 patients)
scRNA-seq
Bulk RNA-Seq
Validation cohorts (n = 138)
Validation
cohort 1
(n = 26)
Pre-treatment
biopsy
ICI
Post-progression
biopsy
Non-responder/
resistant
Validation
cohort 2
(n = 112)
Pre-treatment
biopsy
aPD1
Non-responder/
resistant
Responder

FIG. 44A

B

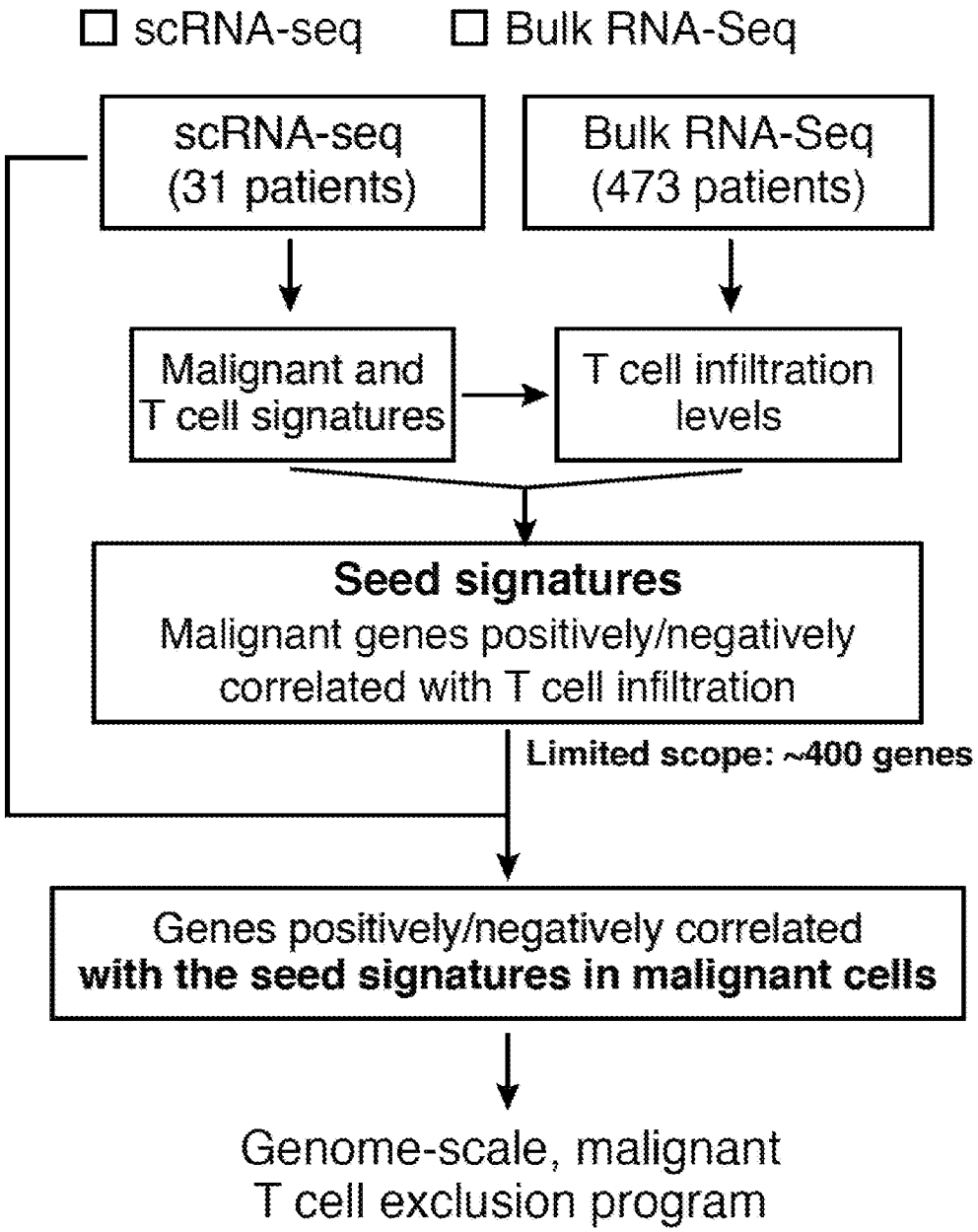

scRNA-seq
Bulk RNA-Seq
scRNA-seq (31 patients)
Bulk RNA-Seq (473 patients)
Malignant and T cell signatures
T cell infiltration levels
Seed signatures
Malignant genes positively/negatively correlated with T cell infiltration
Limited scope: ~400 genes
Genes positively/negatively correlated with the seed signatures in malignant cells
Genome-scale, malignant T cell exclusion program

FIG. 44B

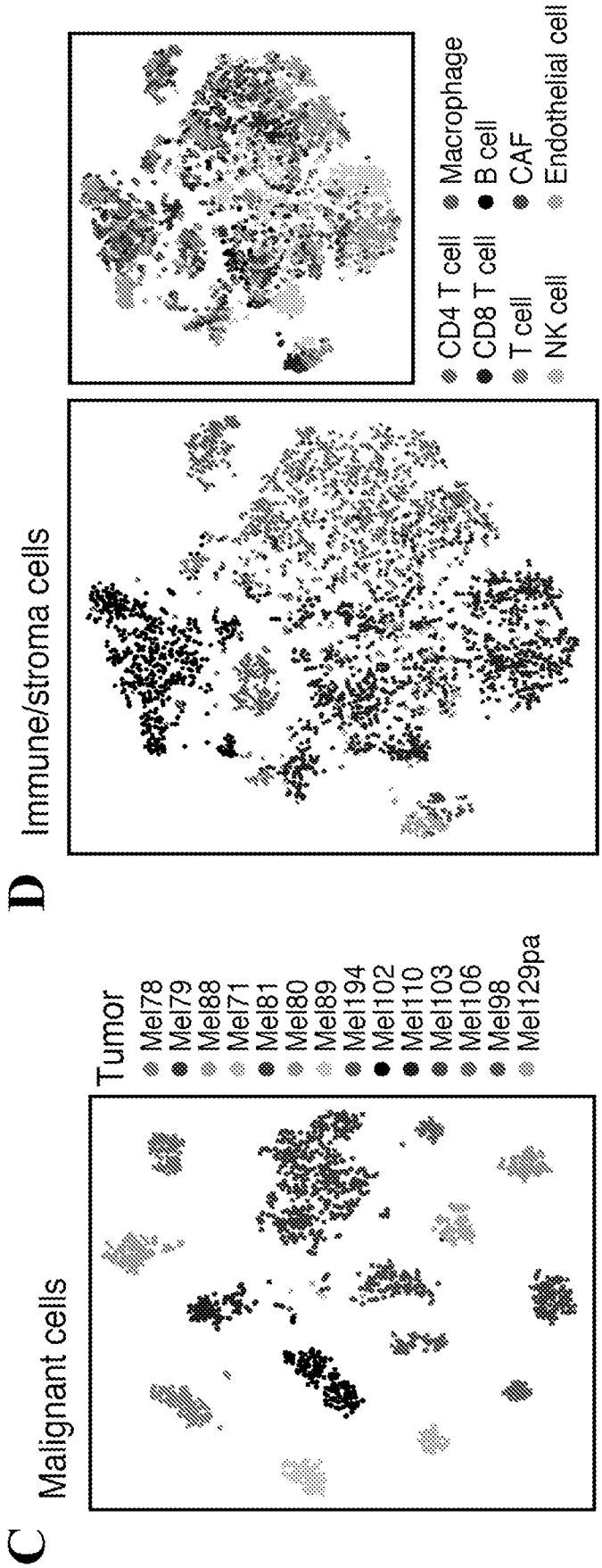

C
Malignant cells
Tumor
Mel78
Mel79
Mel88
Mel71
Mel81
Mel80
Mel89
Mel194
Mel102
Mel110
Mel103
Mel106
Mel98
Mel129pa
D
Immune/stroma cells
CD4 T cell
Macrophage
CD8 T cell
B cell
T cell
CAF
NK cell
Endothelial cell

FIG. 44C-D

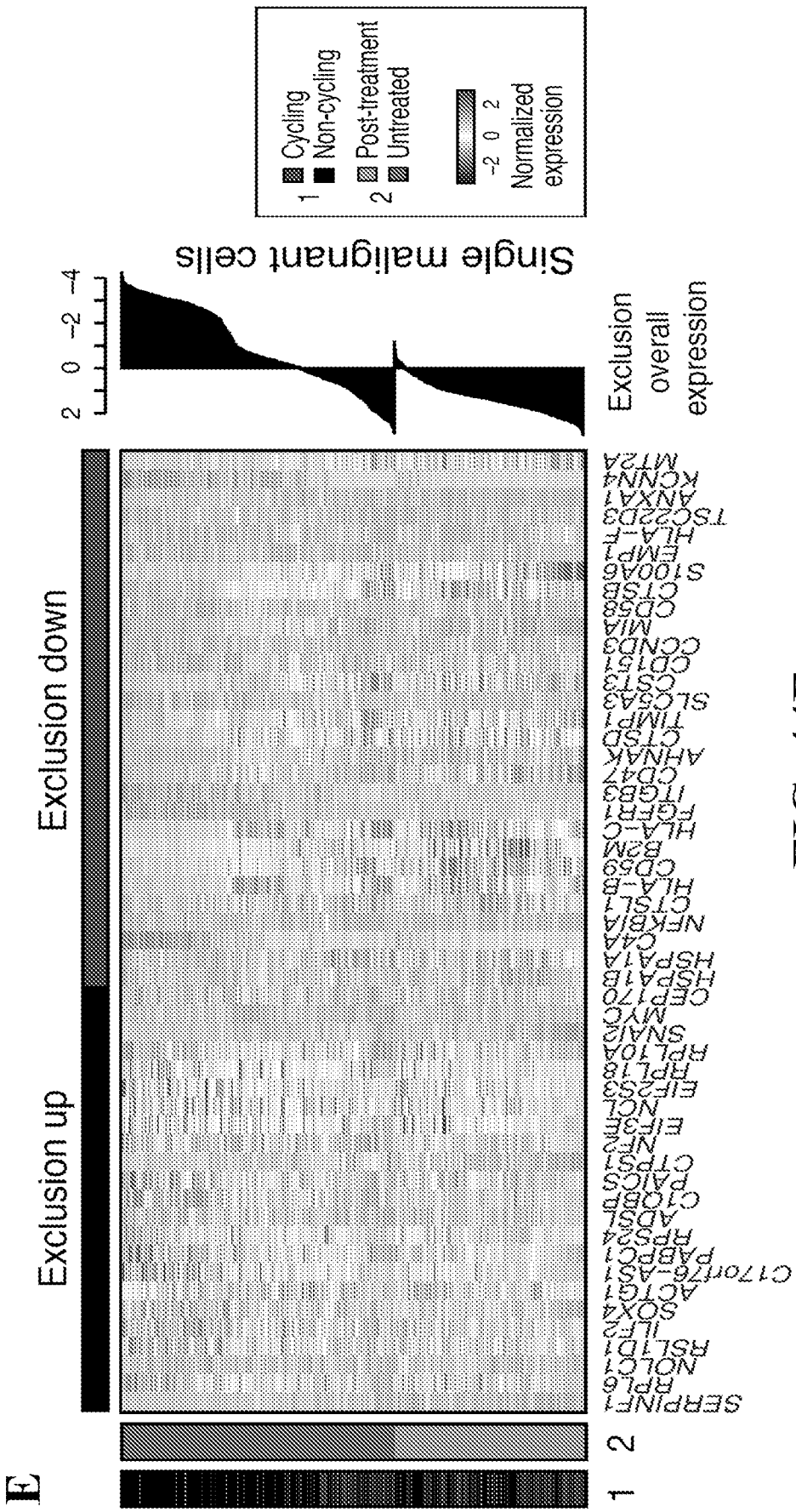

E
Exclusion up
Exclusion down
Single malignant cells
2 0 −2 −4
Exclusion overall expression
1 Cycling
2 Non-cycling
1 Post-treatment
2 Untreated
−2 0 2
Normalized expression
1
2
SERPINF1
RPL6
NOLC1
RSL1D1
ILF3
SOX4
ACTG1
C17orf76-AS1
PABPC1
RPS3A
ADSL
C1QBP
PAICS
CTPS1
NPM3
EIF3M
NCL
EIF2S3
RPL18
RPL10A
SNAI2
MYC
CEP170
HSPA1B
HSPA1A
C4A
NFKBIA
CITED2
HLA-B
CD59
B2M
HLA-C
FGFR1
ITGB3
CD47
AHNAK
CTSD
TIMP1
SLC9A3
CST3
CD151
CCND3
M1A
CD58
CTSB
S100A6
EMP1
HLA-F
TSC22D3
ANXA1
KCNN4
MT2A

FIG. 44E

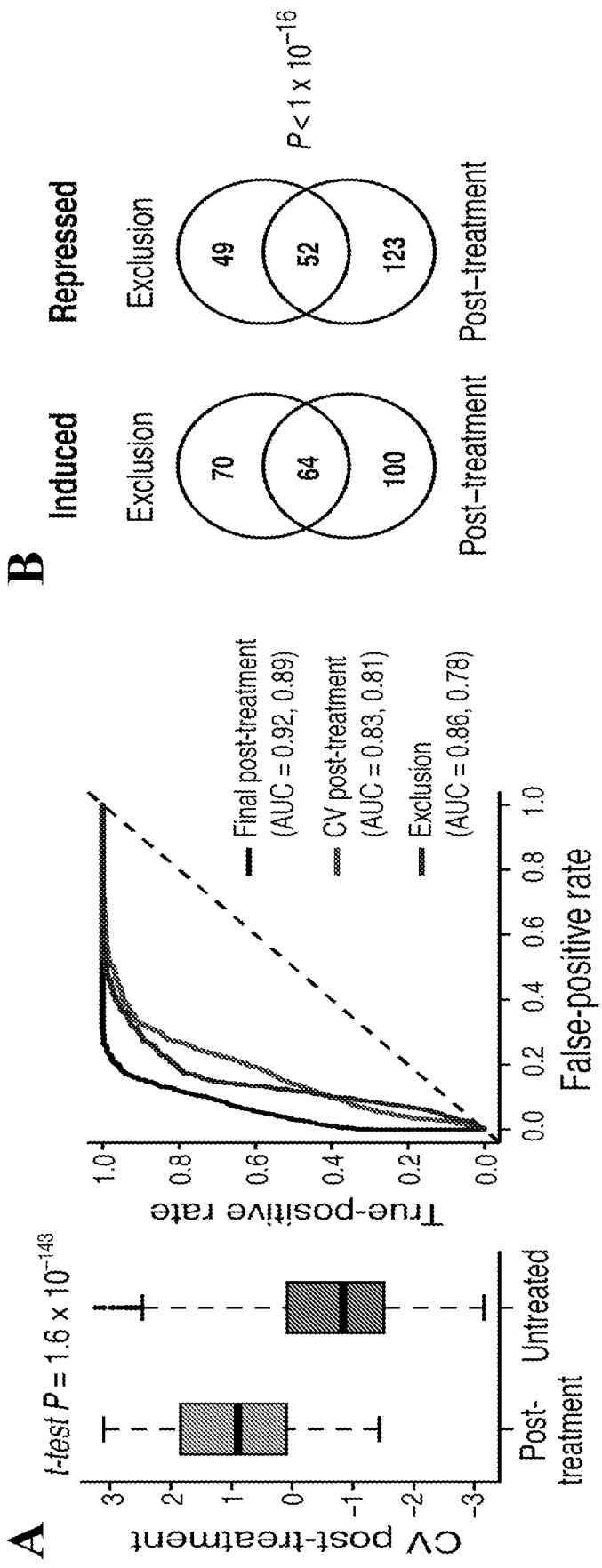

A
CV post-treatment
t-test P = 1.6 x 10^-143
Post-treatment
Untreated
True-positive rate
False-positive rate
Final post-treatment (AUC = 0.92, 0.89)
CV post-treatment (AUC = 0.83, 0.81)
Exclusion (AUC = 0.86, 0.78)
B
Induced
Exclusion
Post–treatment
70
64
100
P < 1 x 10^-16
Repressed
Exclusion
Post–treatment
49
52
123

FIG. 45A-B

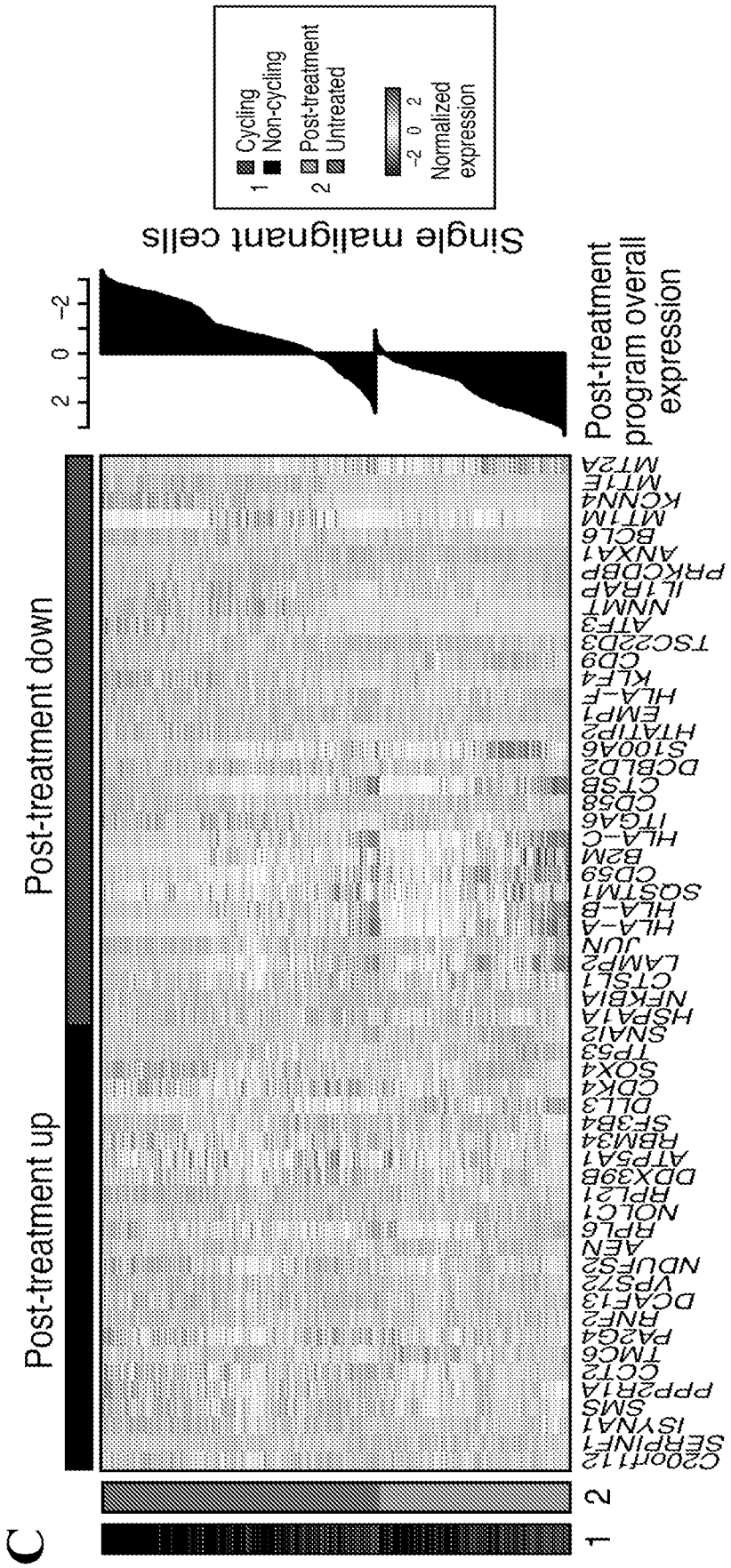

C
Post-treatment up
Post-treatment down
Single malignant cells
2 0 −2
Post-treatment program overall expression
1 Cycling
Non-cycling
2 Post-treatment
Untreated
−2 0 2
Normalized expression
1
2
C20orf112
SERPINF1
ISYNA1
SMS
PPP2R1A
CCT2
TMC6
PA2G4
RNF2
DCAF13
VPS72
NDUFS2
AEN
RPL6
NOLC1
RPL21
DDX39B
ATP5A1
RBM34
SF3B4
DLL3
CDK4
SOX4
TP53
SNAI2
HSPA1A
NFKBIA
CTSL1
LAMP2
JUN
HLA-A
HLA-B
SOSTM1
CD59
B2M
HLA-C
ITGA6
CD58
CTSB
DCBLD2
S100A6
HTATIP2
EMP1
HLA-F
KLF4
CD9
TSC22D3
ATF3
NNMT
IL1RAP
PRKCDBP
ANXA1
BCL6
MT1M
KCNN4
MT1E
MT2A

FIG. 45C

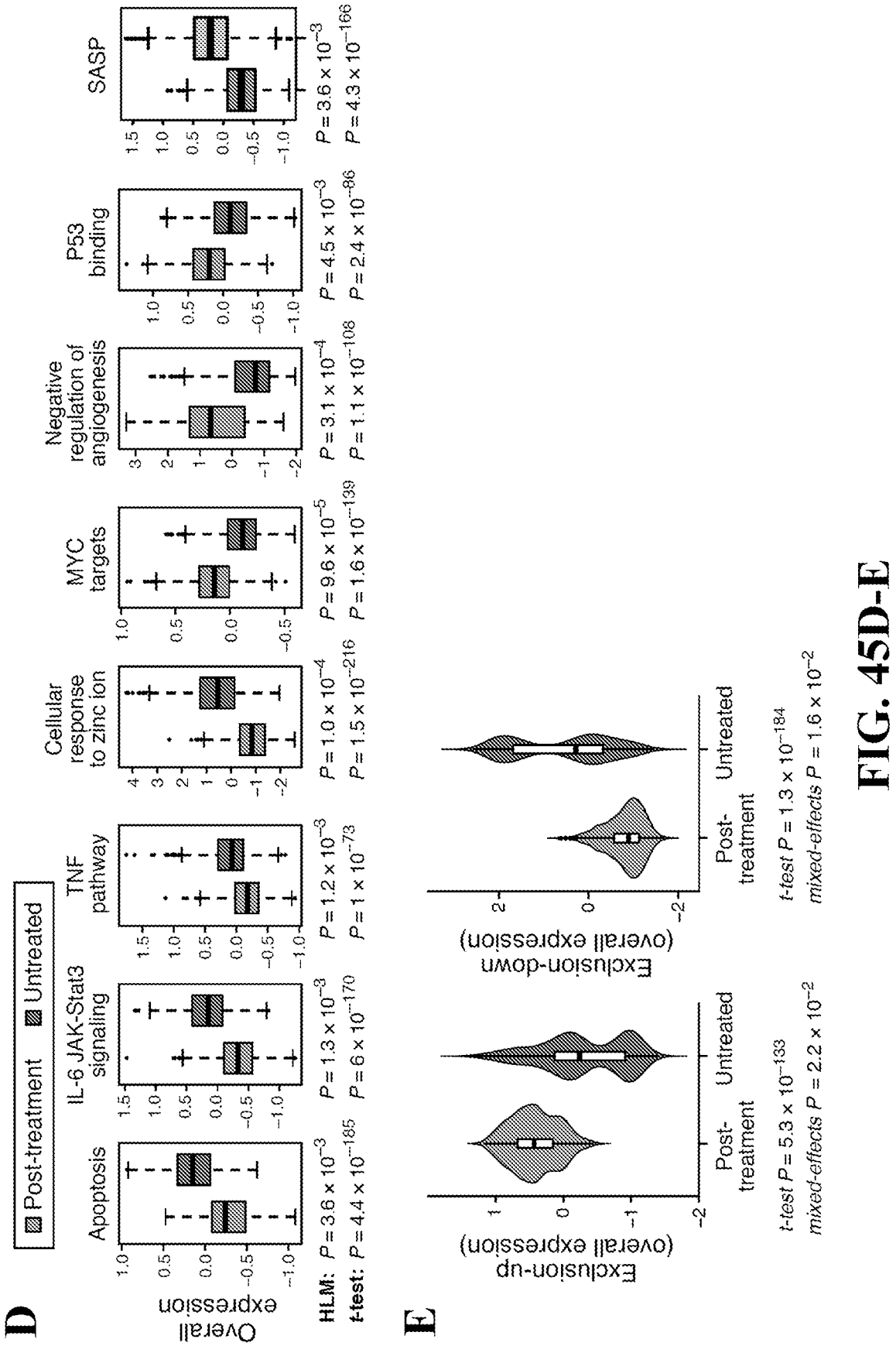

D
Post-treatment
Untreated
Overall expression
Apoptosis
IL-6 JAK-Stat3 signaling
TNF pathway
Cellular response to zinc ion
MYC targets
Negative regulation of angiogenesis
P53 binding
SASP
HLM: P = 3.6 × 10−3 P = 1.3 × 10−3 P = 1.2 × 10−3 P = 1.0 × 10−4 P = 9.6 × 10−5 P = 3.1 × 10−4 P = 4.5 × 10−3 P = 3.6 × 10−3
t-test: P = 4.4 × 10−185 P = 6 × 10−170 P = 1 × 10−73 P = 1.5 × 10−216 P = 1.6 × 10−139 P = 1.1 × 10−108 P = 2.4 × 10−86 P = 4.3 × 10−166
E
Exclusion-up (overall expression)
Exclusion-down (overall expression)
Post-treatment
Untreated
t-test P = 5.3 × 10−133
mixed-effects P = 2.2 × 10−2
t-test P = 1.3 × 10−184
mixed-effects P = 1.6 × 10−2

FIG. 45D-E

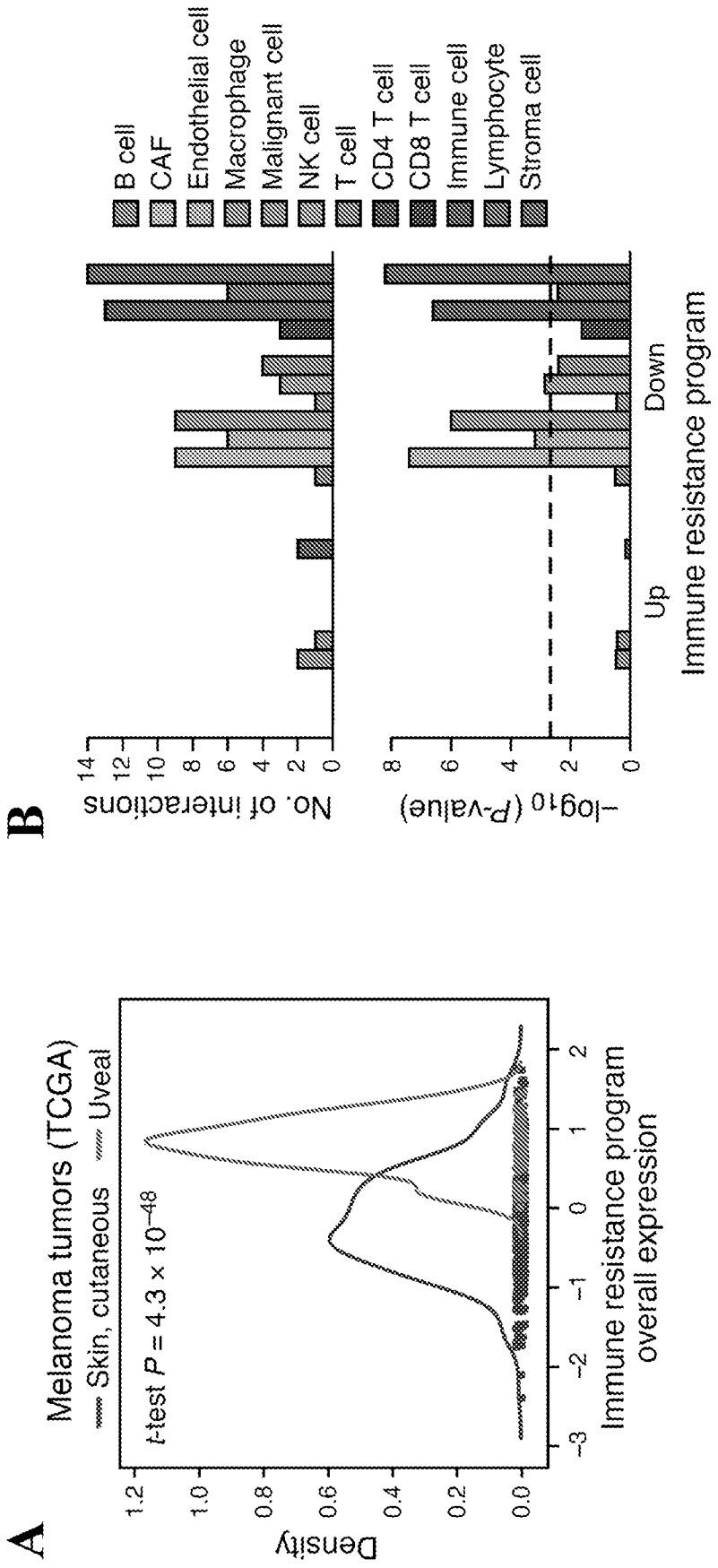

A
Melanoma tumors (TCGA)
Skin, cutaneous
Uveal
t-test P = 4.3 × 10−48
Density
1.2
1.0
0.8
0.6
0.4
0.2
0.0
−3
−2
−1
0
1
2
Immune resistance program
overall expression
B
B cell
CAF
Endothelial cell
Macrophage
Malignant cell
NK cell
T cell
CD4 T cell
CD8 T cell
Immune cell
Lymphocyte
Stroma cell
No. of interactions
14
12
10
8
6
4
2
0
−log10 (P-value)
8
6
4
2
0
Up
Down
Immune resistance program

FIG. 46A-B

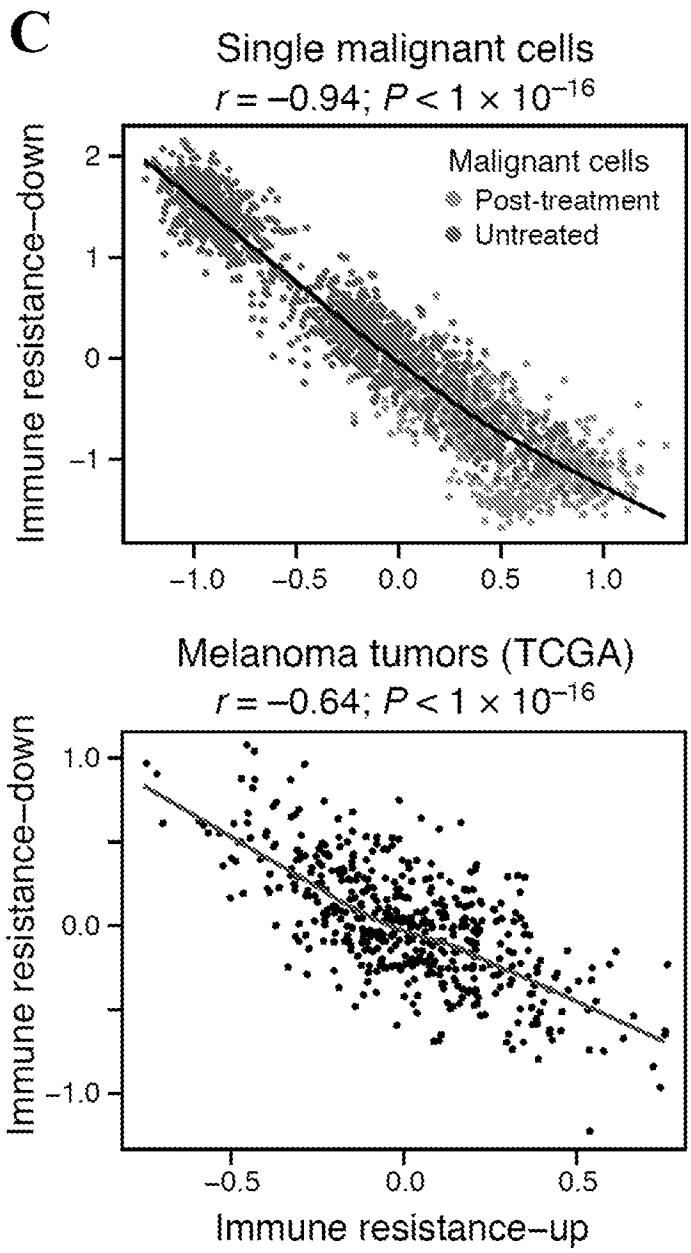

C
Single malignant cells
r = –0.94; P < 1 × 10–16
Malignant cells
Post-treatment
Untreated
Immune resistance–down
2
1
0
–1
–1.0
–0.5
0.0
0.5
1.0
Melanoma tumors (TCGA)
r = –0.64; P < 1 × 10–16
Immune resistance–down
1.0
0.0
–1.0
–0.5
0.0
0.5
Immune resistance–up

FIG. 46C

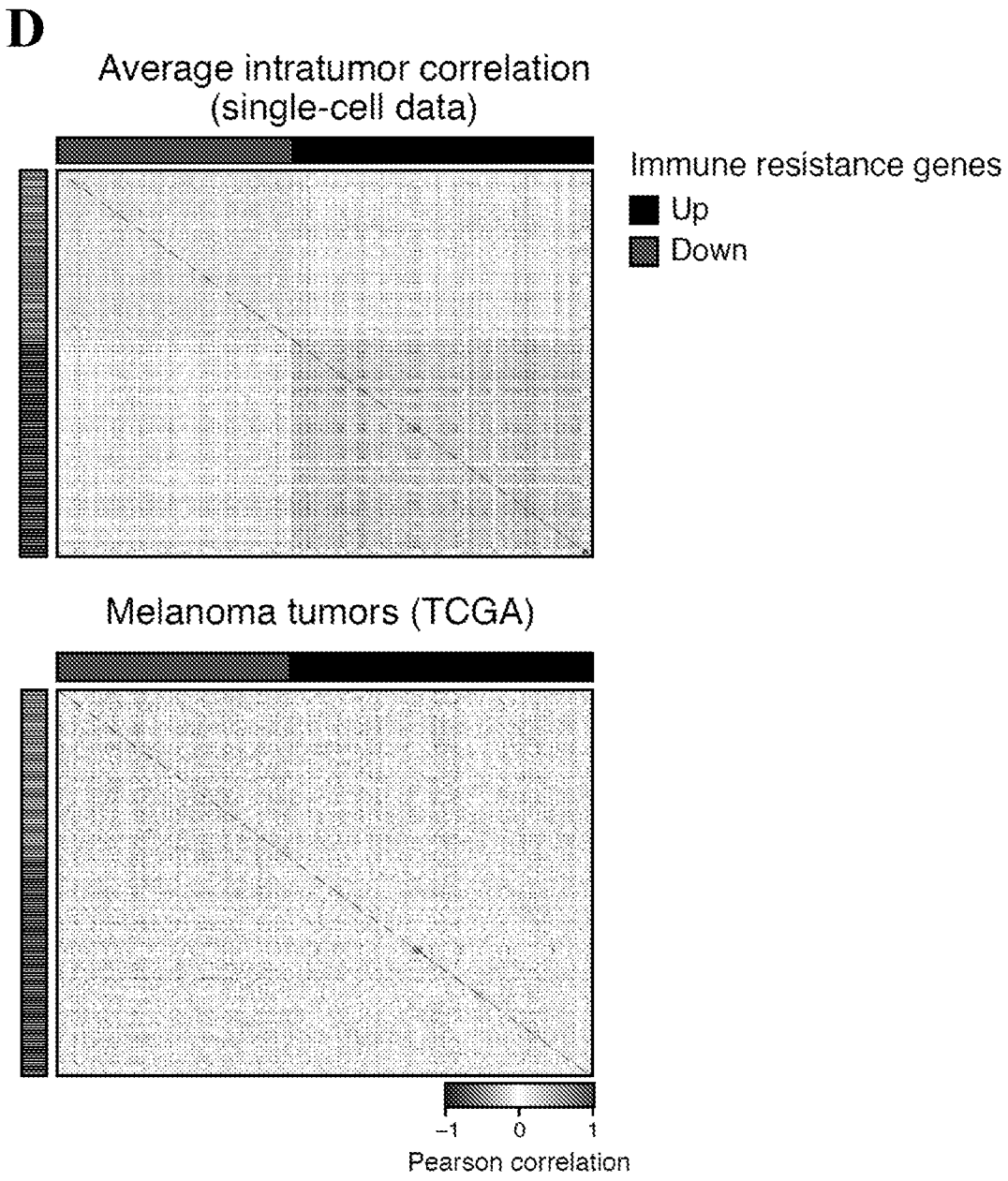

D
Average intratumor correlation
(single-cell data)
Immune resistance genes
Up
Down
Melanoma tumors (TCGA)
−1
0
1
Pearson correlation

FIG. 46D

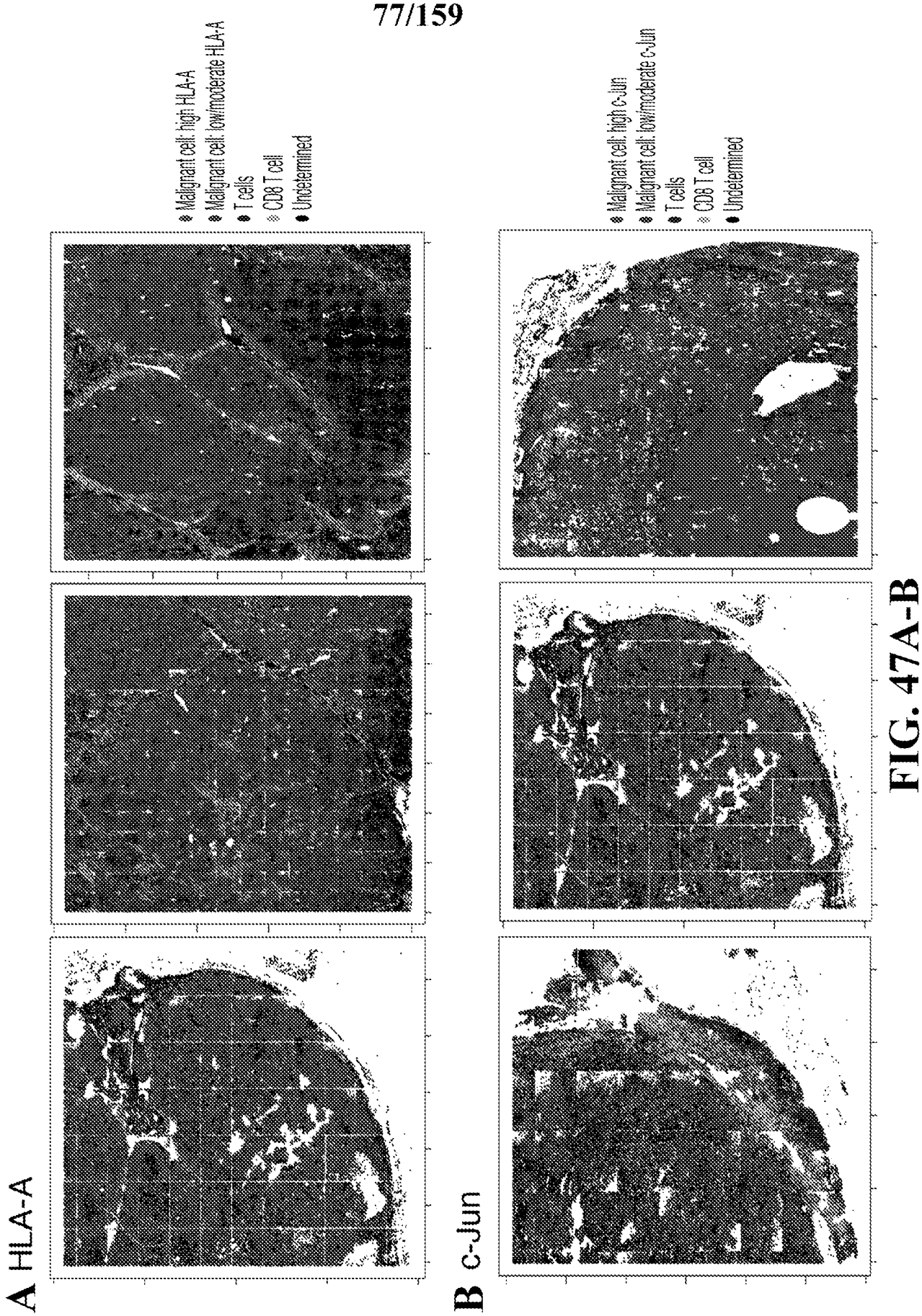

A HLA-A
Malignant cell: high HLA-A
Malignant cell: low/moderate HLA-A
T cells
CD8 T cell
Undetermined
B c-Jun
Malignant cell: high c-Jun
Malignant cell: low/moderate c-Jun
T cells
CD8 T cell
Undetermined

FIG. 47A-B

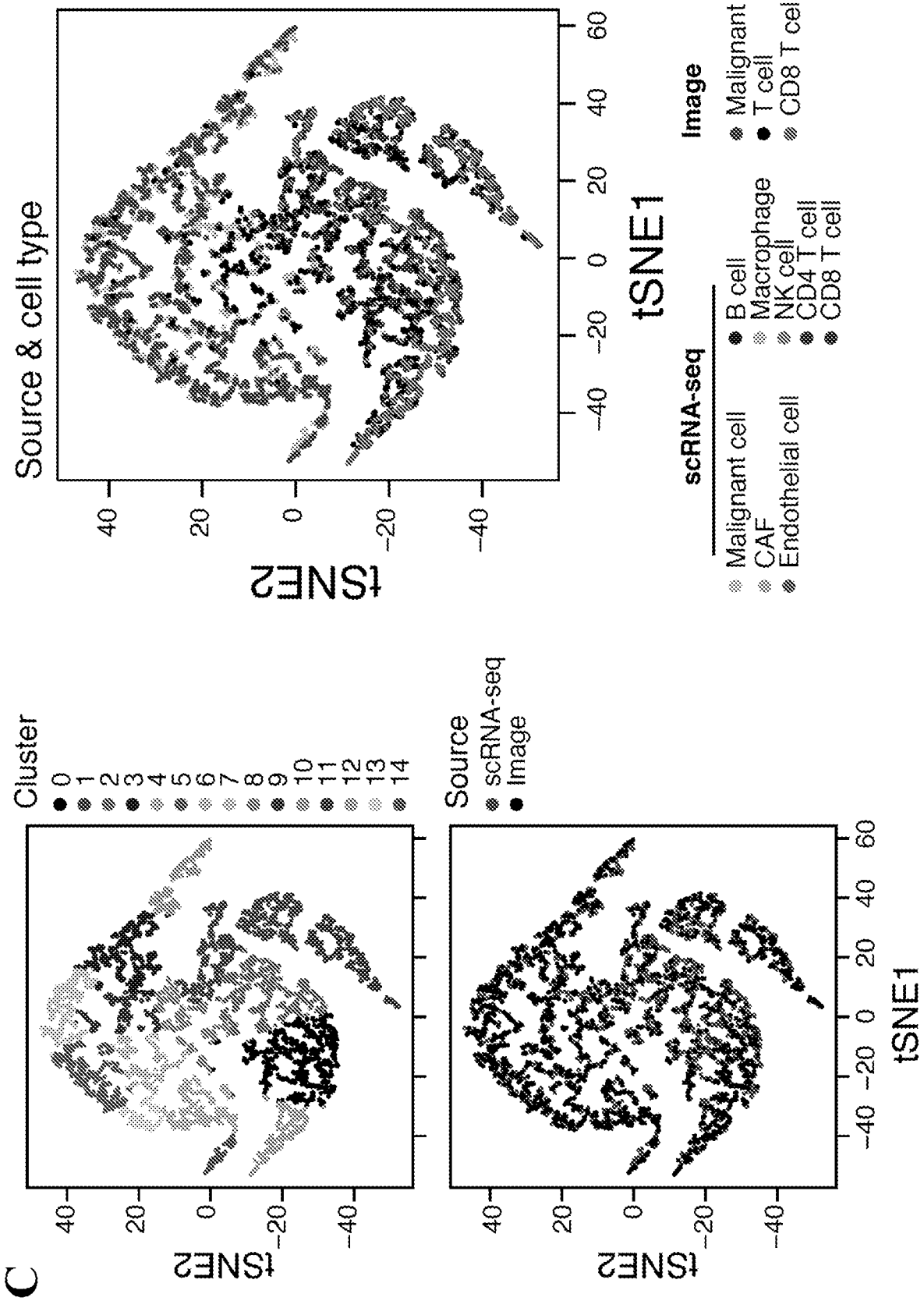

C
Cluster
0
1
2
3
4
5
6
7
8
9
10
11
12
13
14
tSNE2
tSNE1
Source
scRNA-seq
Image
Source & cell type
scRNA-seq
Malignant cell
CAF
Endothelial cell
B cell
Macrophage
NK cell
CD4 T cell
CD8 T cell
Image
Malignant cell
T cell
CD8 T cell

FIG. 47C

D

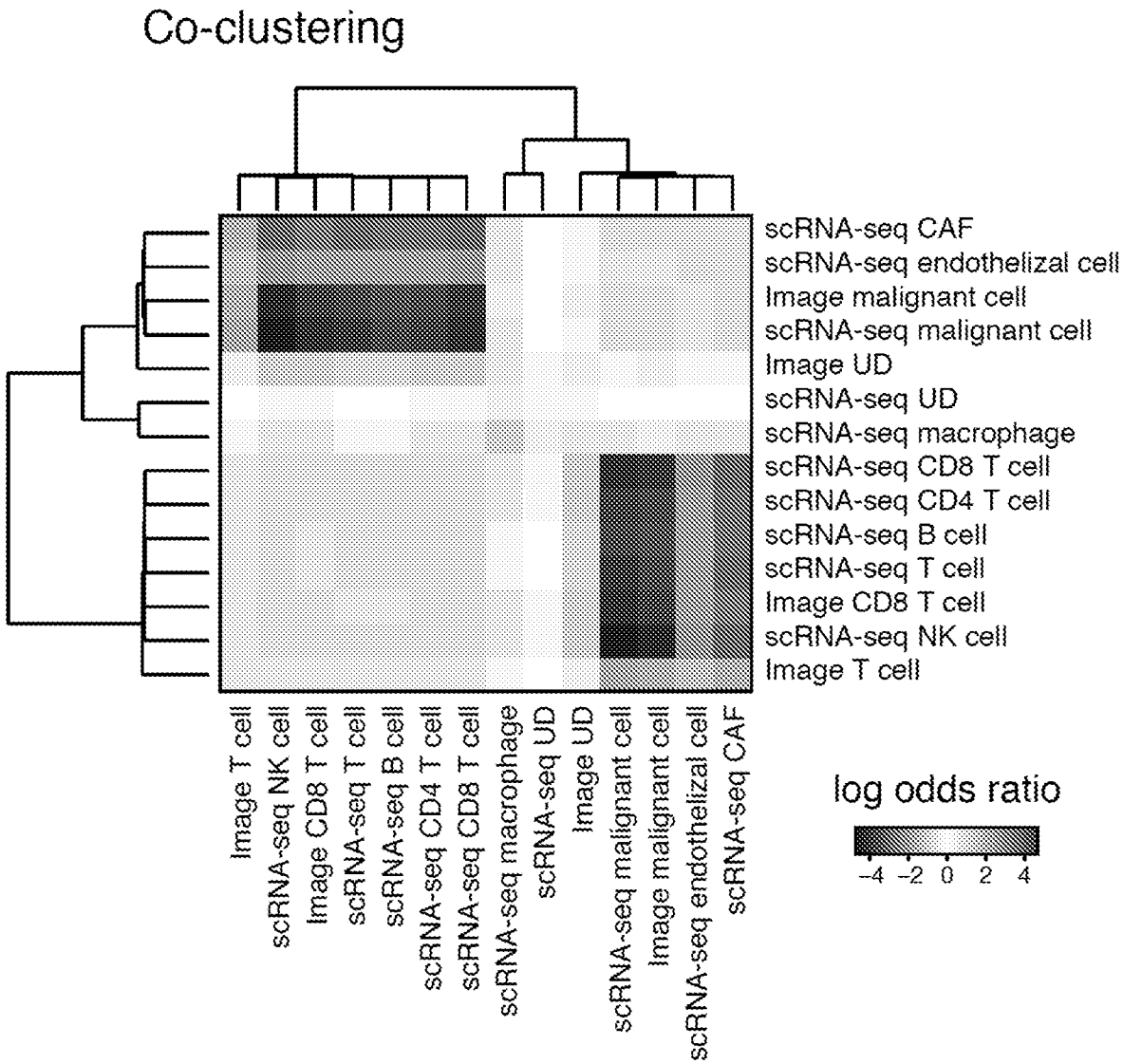

Co-clustering
scRNA-seq CAF
scRNA-seq endothelizal cell
Image malignant cell
scRNA-seq malignant cell
Image UD
scRNA-seq UD
scRNA-seq macrophage
scRNA-seq CD8 T cell
scRNA-seq CD4 T cell
scRNA-seq B cell
scRNA-seq T cell
Image CD8 T cell
scRNA-seq NK cell
Image T cell
Image T cell
scRNA-seq NK cell
Image CD8 T cell
scRNA-seq T cell
scRNA-seq B cell
scRNA-seq CD4 T cell
scRNA-seq CD8 T cell
scRNA-seq macrophage
scRNA-seq UD
Image UD
scRNA-seq malignant cell
Image malignant cell
scRNA-seq endothelizal cell
scRNA-seq CAF
log odds ratio
−4 −2 0 2 4

FIG. 47D

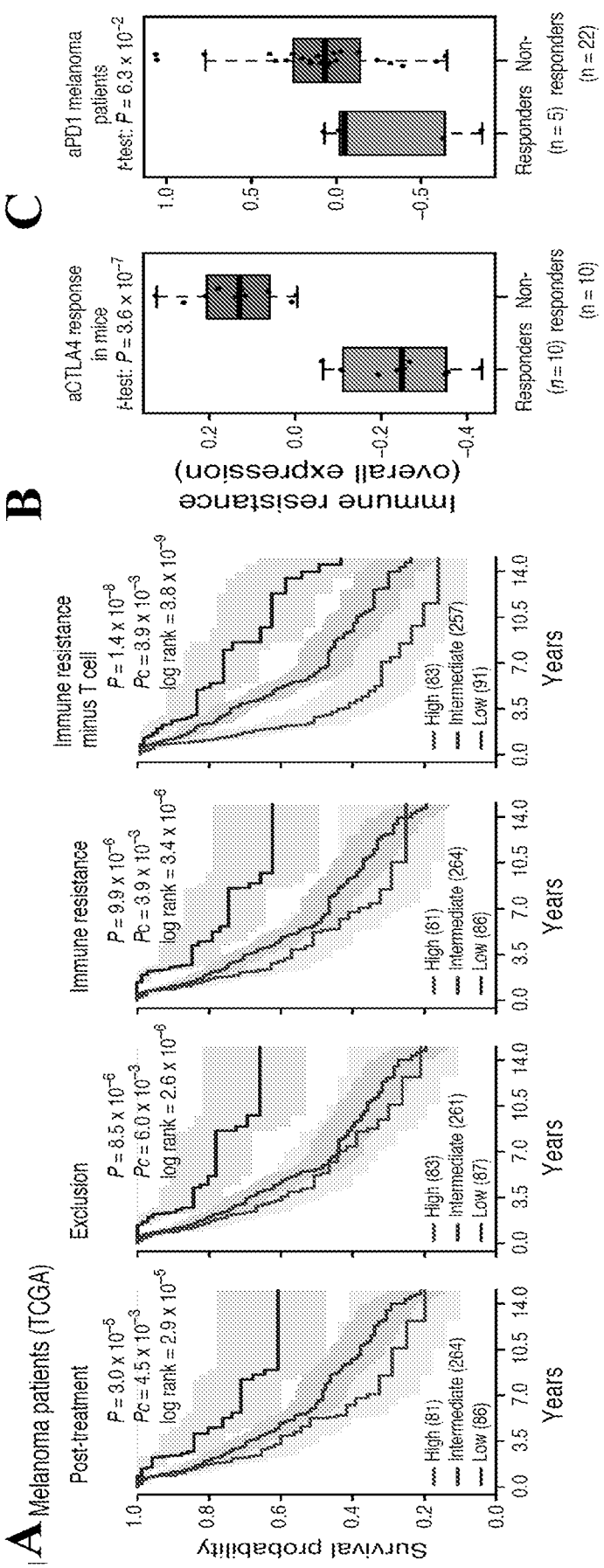

A
Melanoma patients (TCGA)
Post-treatment
Exclusion
Immune resistance
Immune resistance minus T cell
Survival probability
Years
High (81)
Intermediate (264)
Low (86)
High (83)
Intermediate (261)
Low (87)
High (61)
Intermediate (264)
Low (86)
High (83)
Intermediate (257)
Low (91)
B
Immune resistance (overall expression)
aCTLA4 response in mice
aPD1 melanoma patients
Responders (n = 10)
Non-responders (n = 10)
Responders (n = 5)
Non-responders (n = 22)
C

FIG. 48A-C

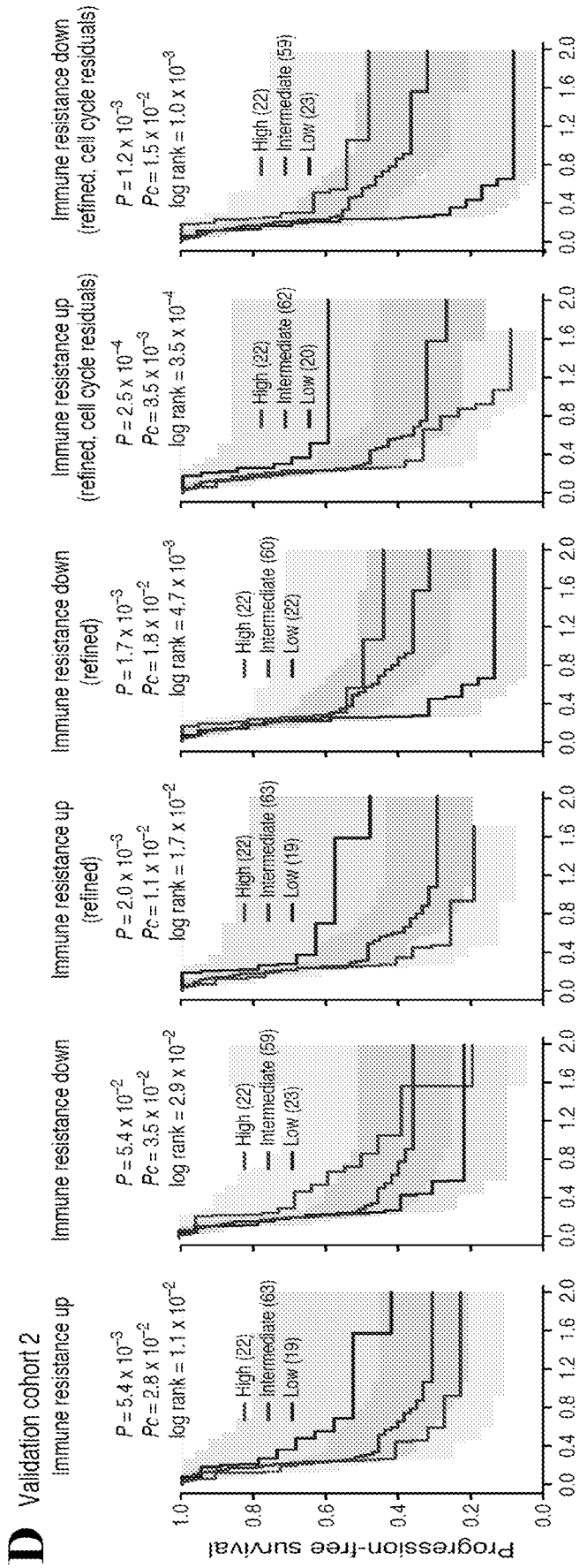

D
Validation cohort 2
Immune resistance up
P = 5.4 x 10−3
Pc = 2.8 x 10−2
log rank = 1.1 x 10−2
High (22)
Intermediate (63)
Low (19)
Immune resistance down
P = 5.4 x 10−2
Pc = 3.5 x 10−2
log rank = 2.9 x 10−2
High (22)
Intermediate (59)
Low (23)
Immune resistance up (refined)
P = 2.0 x 10−3
Pc = 1.1 x 10−2
log rank = 1.7 x 10−2
High (22)
Intermediate (63)
Low (19)
Immune resistance down (refined)
P = 1.7 x 10−3
Pc = 1.8 x 10−2
log rank = 4.7 x 10−3
High (22)
Intermediate (60)
Low (22)
Immune resistance up (refined, cell cycle residuals)
P = 2.5 x 10−4
Pc = 3.5 x 10−3
log rank = 3.5 x 10−4
High (22)
Intermediate (62)
Low (20)
Immune resistance down (refined, cell cycle residuals)
P = 1.2 x 10−3
Pc = 1.5 x 10−2
log rank = 1.0 x 10−3
High (22)
Intermediate (53)
Low (23)
Progression-free survival
1.0
0.8
0.6
0.4
0.2
0.0
0.0 0.4 0.8 1.2 1.6 2.0
Years

FIG. 48D

E

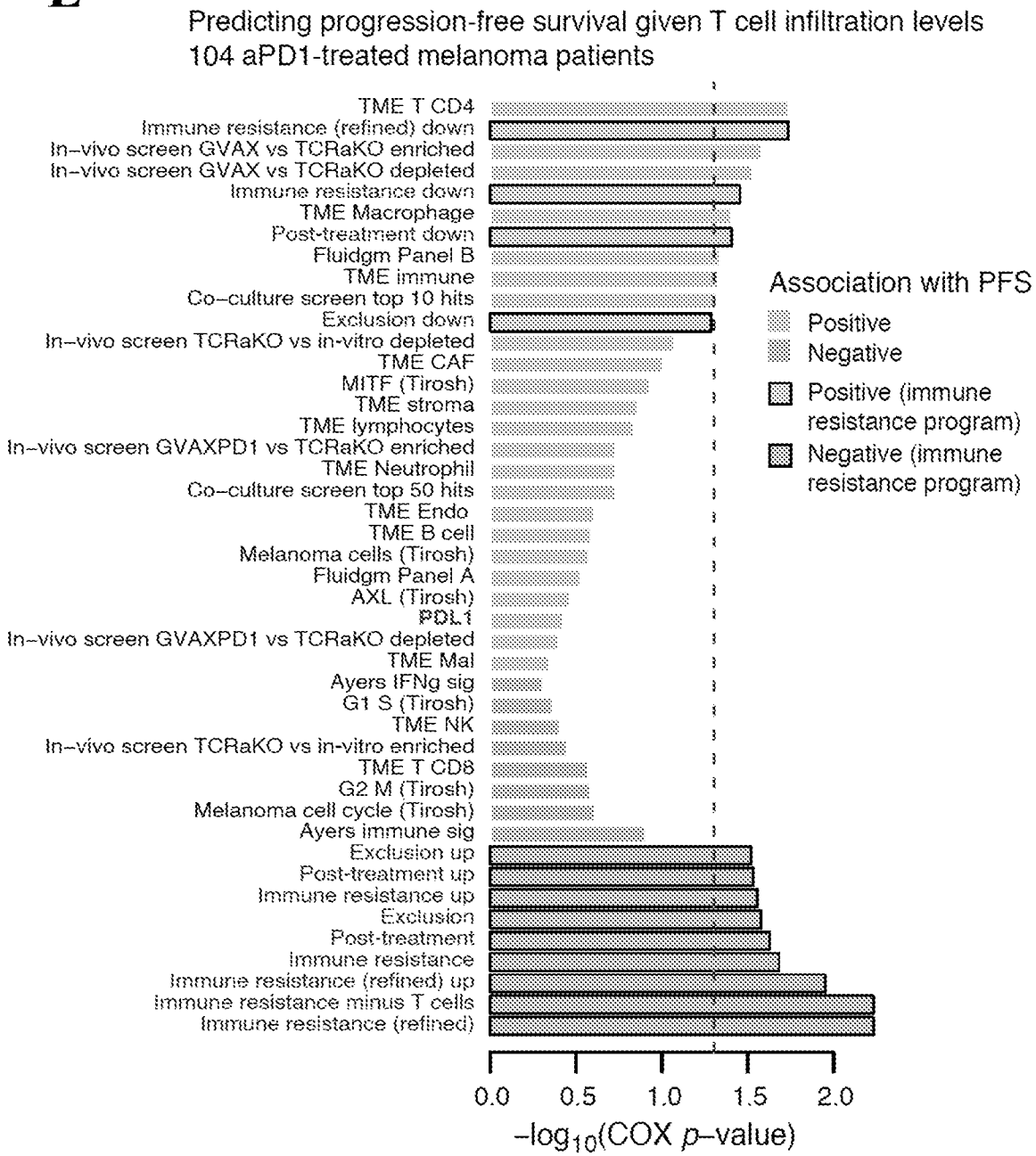

Predicting progression-free survival given T cell infiltration levels
104 aPD1-treated melanoma patients
TME T CD4
Immune resistance (refined) down
In−vivo screen GVAX vs TCRaKO enriched
In−vivo screen GVAX vs TCRaKO depleted
Immune resistance down
TME Macrophage
Post-treatment down
Fluidgm Panel B
TME immune
Co−culture screen top 10 hits
Exclusion down
In−vivo screen TCRaKO vs in-vitro depleted
TME CAF
MITF (Tirosh)
TME stroma
TME lymphocytes
In−vivo screen GVAXPD1 vs TCRaKO enriched
TME Neutrophil
Co−culture screen top 50 hits
TME Endo
TME B cell
Melanoma cells (Tirosh)
Fluidgm Panel A
AXL (Tirosh)
PDL1
In−vivo screen GVAXPD1 vs TCRaKO depleted
TME Mal
Ayers IFNg sig
G1 S (Tirosh)
TME NK
In−vivo screen TCRaKO vs in-vitro enriched
TME T CD8
G2 M (Tirosh)
Melanoma cell cycle (Tirosh)
Ayers immune sig
Exclusion up
Post-treatment up
Immune resistance up
Exclusion
Post-treatment
Immune resistance
Immune resistance (refined) up
Immune resistance minus T cells
Immune resistance (refined)
Association with PFS
Positive
Negative
Positive (immune resistance program)
Negative (immune resistance program)
0.0
0.5
1.0
1.5
2.0
−log10(COX p−value)

FIG. 48E

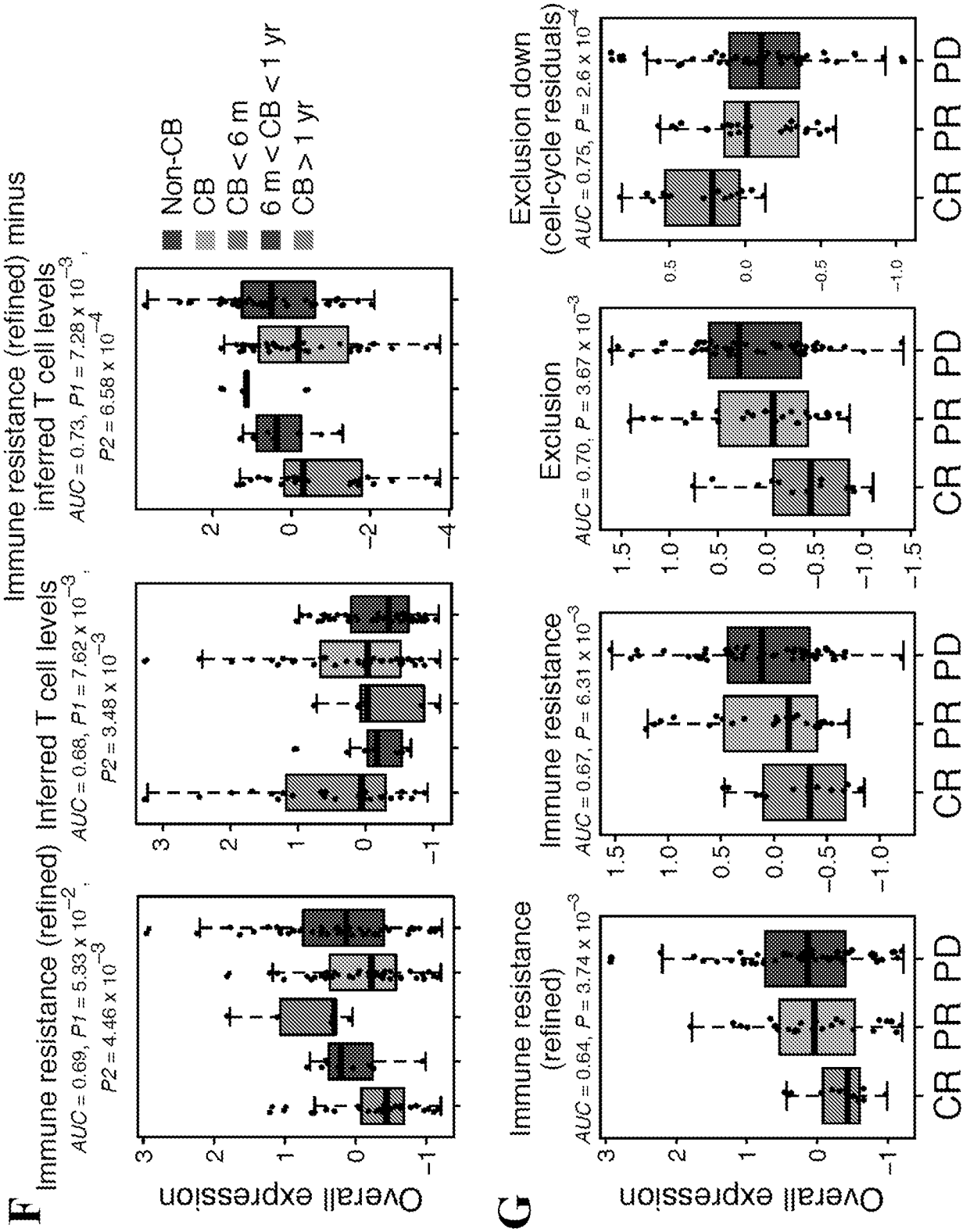

F
Immune resistance (refined) minus inferred T cell levels
AUC = 0.69, P1 = 5.33 x 10−2, P2 = 4.46 x 10−3
AUC = 0.68, P1 = 7.62 x 10−3, P2 = 3.48 x 10−3
AUC = 0.73, P1 = 7.28 x 10−3, P2 = 6.58 x 10−4
Non-CB
CB
CB < 6 m
6 m < CB < 1 yr
CB > 1 yr
Overall expression
G
Immune resistance (refined)
AUC = 0.64, P = 3.74 x 10−3
Immune resistance
AUC = 0.67, P = 6.31 x 10−3
Exclusion
AUC = 0.70, P = 3.67 x 10−3
Exclusion down (cell-cycle residuals)
AUC = 0.75, P = 2.6 x 10−4
CR PR PD

FIG. 48F-G

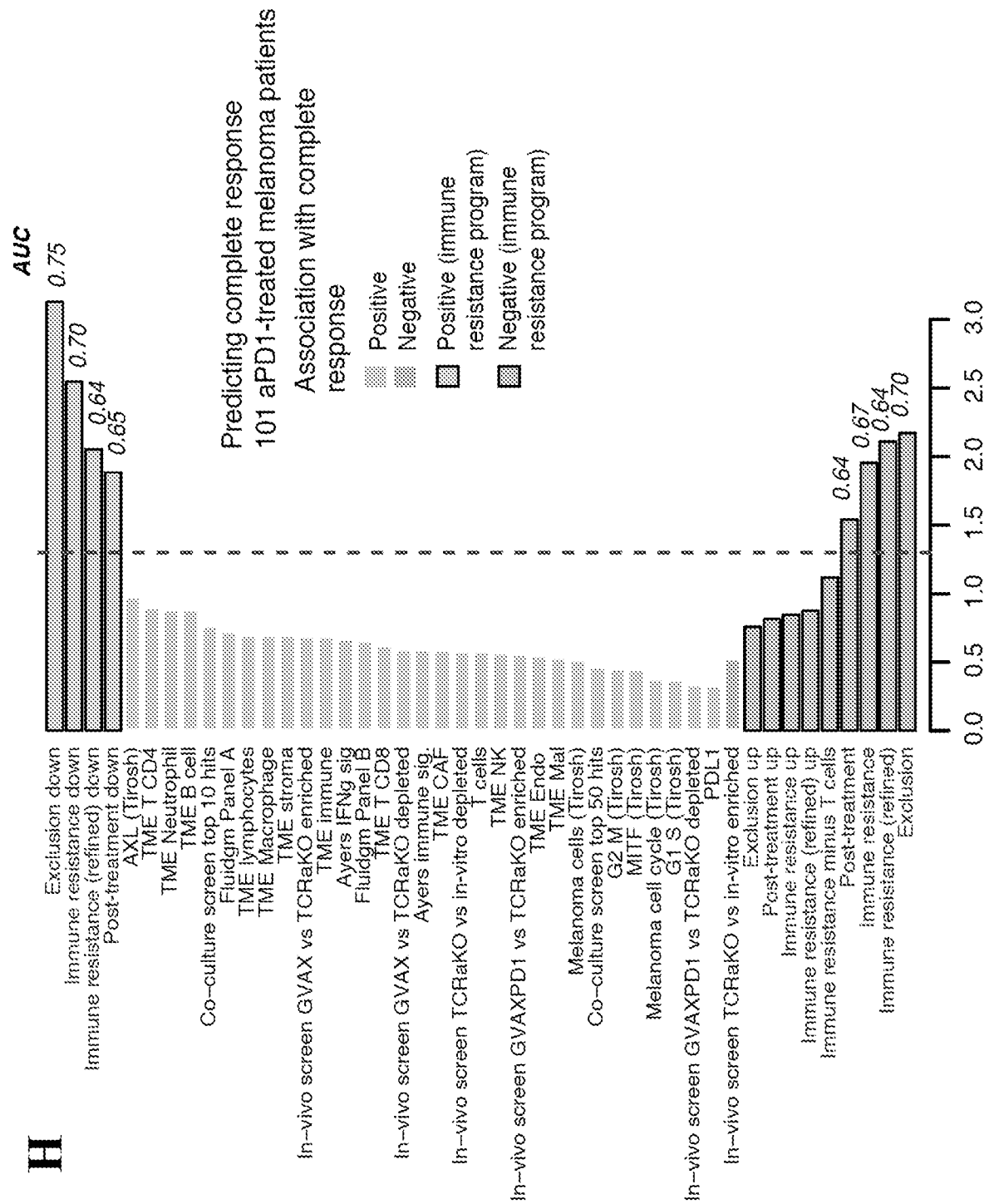

H
AUC
0.75
0.70
0.64
0.65
Predicting complete response
101 aPD1-treated melanoma patients
Association with complete response
Positive
Negative
Positive (immune resistance program)
Negative (immune resistance program)
Exclusion down
Immune resistance down
Immune resistance (refined) down
Post-treatment down
AXL (Tirosh)
TME T CD4
TME Neutrophil
TME B cell
Co-culture screen top 10 hits
Fluidgm Panel A
TME lymphocytes
TME Macrophage
TME stroma
In-vivo screen GVAX vs TCRaKO enriched
TME immune
Ayers IFNg sig
Fluidgm Panel B
TME T CD8
In-vivo screen GVAX vs TCRaKO depleted
Ayers immune sig.
TME CAF
In-vivo screen TCRaKO vs in-vitro depleted
T cells
TME NK
In-vivo screen GVAXPD1 vs TCRaKO enriched
TME Endo
TME Mal
Melanoma cells (Tirosh)
Co-culture screen top 50 hits
G2 M (Tirosh)
MITF (Tirosh)
Melanoma cell cycle (Tirosh)
G1 S (Tirosh)
In-vivo screen GVAXPD1 vs TCRaKO depleted
PDL1
In-vivo screen TCRaKO vs in-vitro enriched
Exclusion up
Post-treatment up
Immune resistance up
Immune resistance (refined) up
Immune resistance minus T cells
Post-treatment
Immune resistance
Immune resistance (refined)
Exclusion
0.64
0.67
0.64
0.70
0.0
0.5
1.0
1.5
2.0
2.5
3.0
−log10(t-test p−value)

FIG. 48H

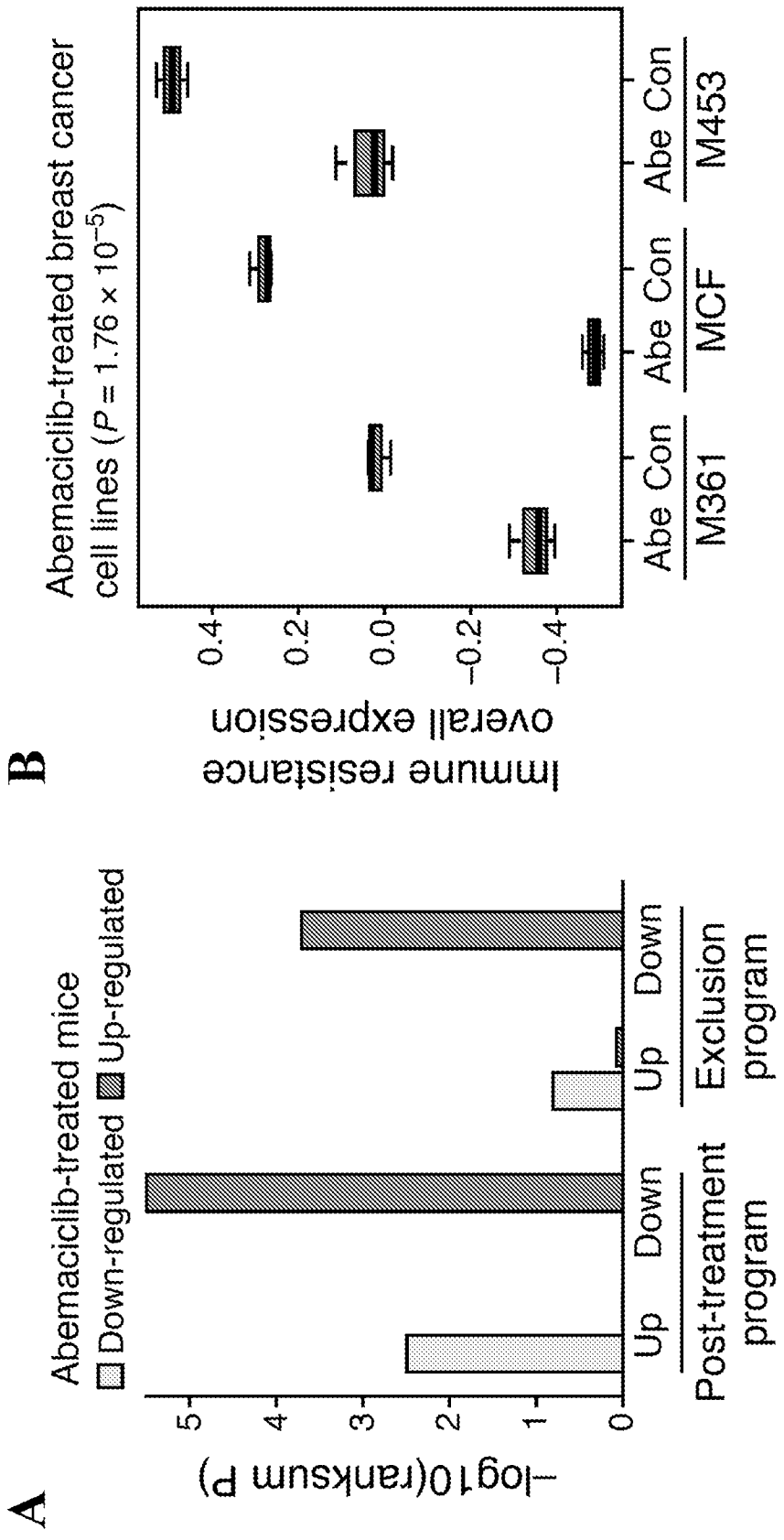

A
Abemaciclib-treated mice
Down-regulated
Up-regulated
−log10(ranksum P)
0
1
2
3
4
5
Up
Down
Up
Down
Post-treatment program
Exclusion program
B
Abemaciclib-treated breast cancer cell lines (P = 1.76 × 10−5)
Immune resistance overall expression
0.4
0.2
0.0
−0.2
−0.4
Abe
Con
Abe
Con
Abe
Con
M361
MCF
M453

FIG. 49A-B


C
DMSO
Abemaciclib
(CDK4/6 inhibitor)
Immune resistance up
Immune resistance down
Immune resistance
overall expression
0.2 0 −0.2
Breast cancer cell lines
−2 0 2
Normalized
expression
DDX39B
ANP32E
KIAA0101
CTPS1
TUBA1B
NUCKS1
ESRP1
ILF2
FBL
PTMA
HNRNPA1
SET
TP53
YWHAE
RUVBL2
EIF4A1
RPL21
UCK2
SLC25A5
FUS
TMED10
TSC22D3
ARL6IP5
SCARB2
CRELD1
CD63
CTSL1
FOS
APLP2
HLA−F
CTSD
MAP1B
ITM2B
SEL1L
LAMP2
NPC2
CLU
GAA
GRN
PSAP
SDC3

FIG. 49C

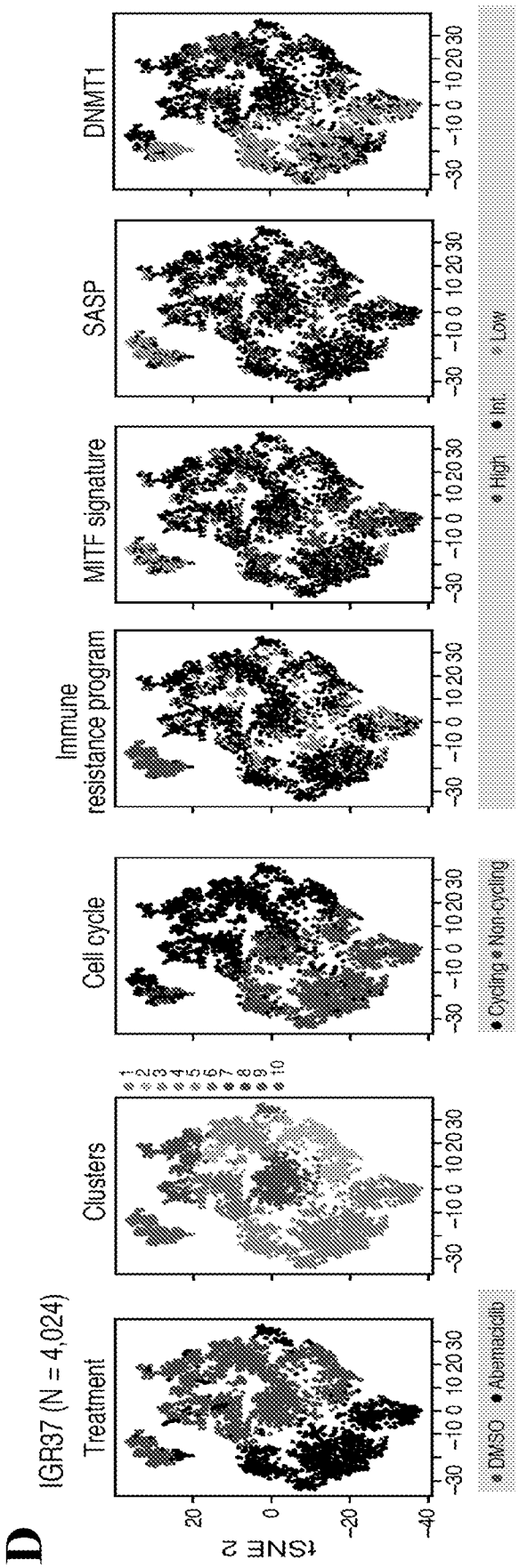

D
IGR37 (N = 4,024)
Treatment
Clusters
Cell cycle
Immune resistance program
MITF signature
SASP
DNMT1
tSNE 2
20
0
-20
-40
-30 -10 0 10 20 30
DMSO
Abemaciclib
1
2
3
4
5
6
7
8
9
10
Cycling
Non-cycling
High
Int
Low

FIG. 49D

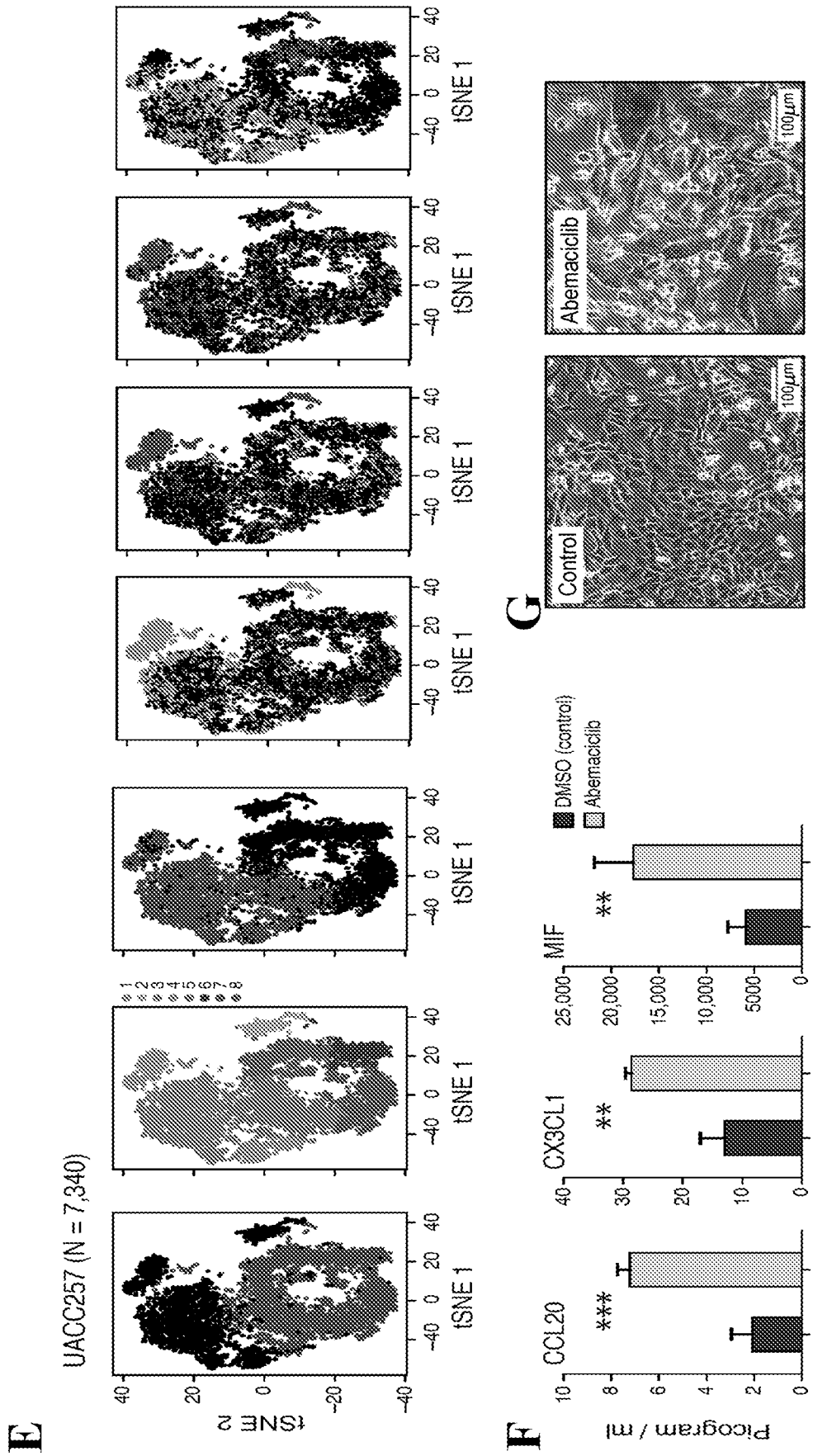

E
UACC257 (N = 7,340)
tSNE 2
tSNE 1
F
CCL20
CX3CL1
MIF
Picogram / ml
DMSO (control)
Abemaciclib
***
**
**
G
Control
Abemaciclib
100μm

FIG. 49E-G

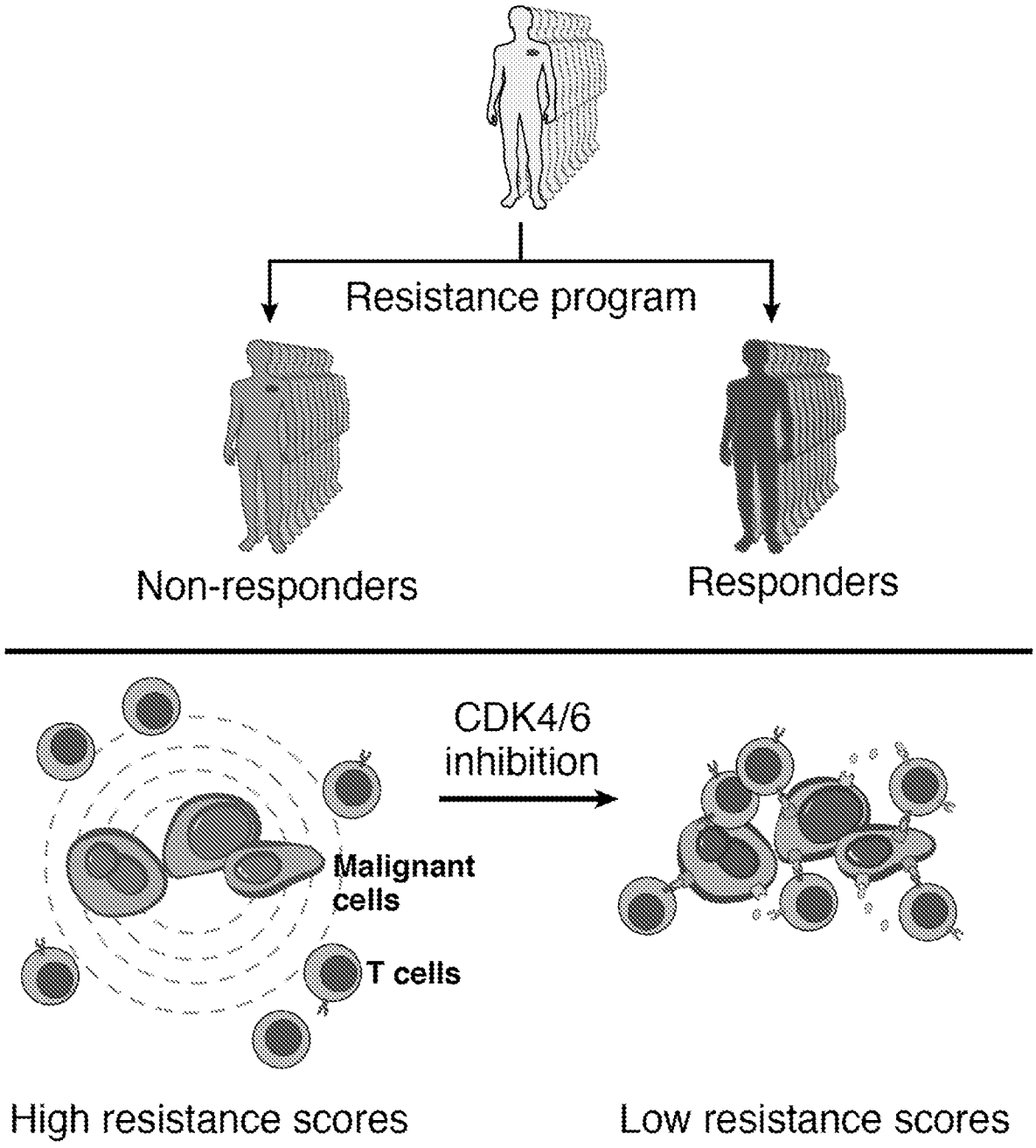

Resistance program
Non-responders
Responders
CDK4/6
inhibition
Malignant
cells
T cells
High resistance scores
Low resistance scores

FIG. 50

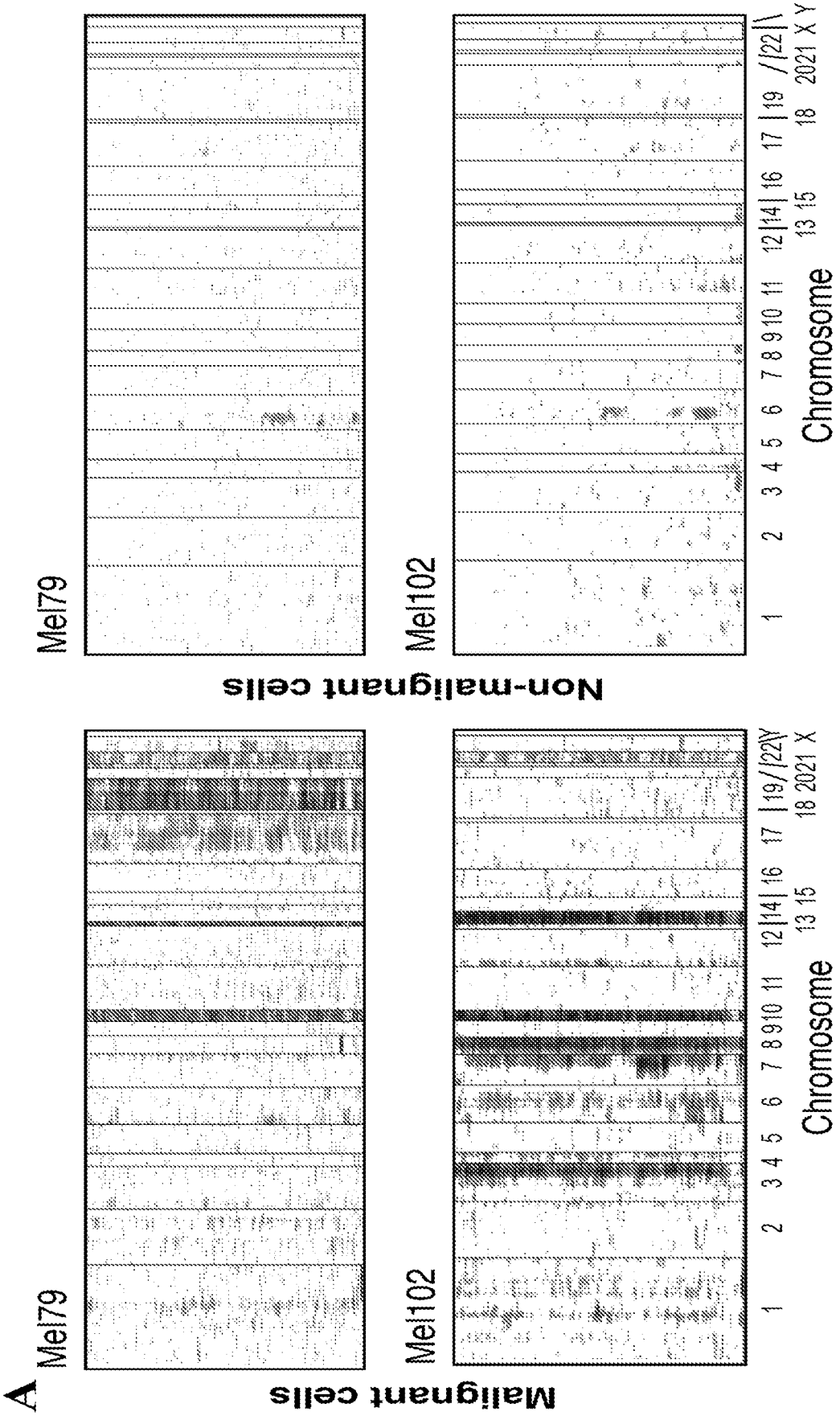

A
Mel79
Mel102
Malignant cells
Chromosome
1 2 3 4 5 6 7 8 9 10 11 12 13 14 15 16 17 18 19 20 21 22 X Y
Mel79
Mel102
Non-malignant cells
Chromosome
1 2 3 4 5 6 7 8 9 10 11 12 13 14 15 16 17 18 19 20 21 22 X Y

FIG. 51A

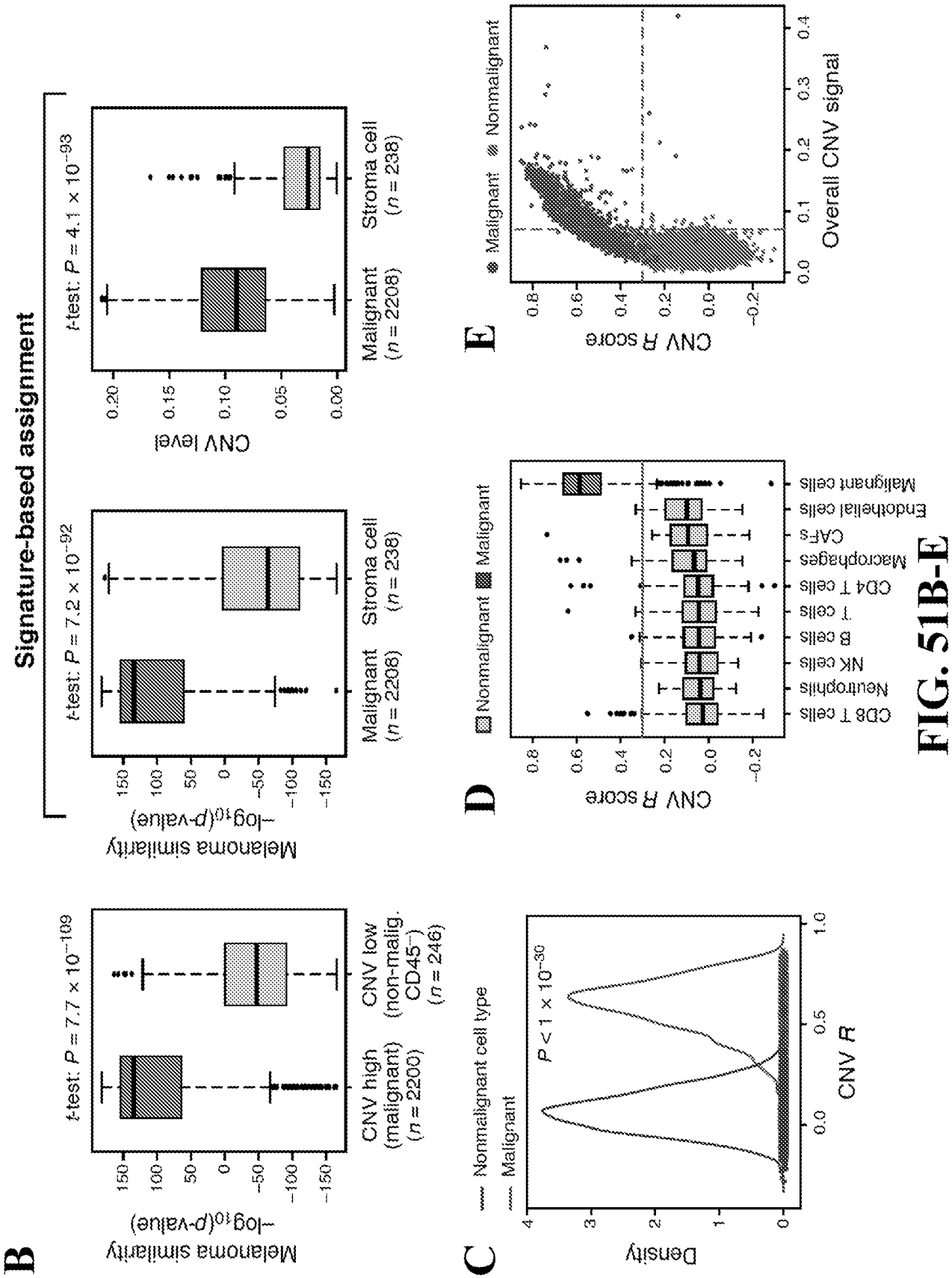

B
Signature-based assignment
t-test: P = 7.7 × 10−109
Melanoma similarity
−log10(p-value)
150
100
50
0
−50
−100
−150
CNV high (malignant) (n = 2200)
CNV low (non-malig. CD45−) (n = 246)
t-test: P = 7.2 × 10−92
Malignant (n = 2208)
Stroma cell (n = 238)
t-test: P = 4.1 × 10−93
CNV level
0.20
0.15
0.10
0.05
0.00
C
Nonmalignant cell type
Malignant
P < 1 × 10−30
Density
CNV R
D
Nonmalignant
Malignant
CNV R score
CD8 T cells
Neutrophils
NK cells
B cells
T cells
CD4 T cells
Macrophages
CAFs
Endothelial cells
Malignant cells
E
Malignant
Nonmalignant
CNV R score
Overall CNV signal

FIG. 51B-E

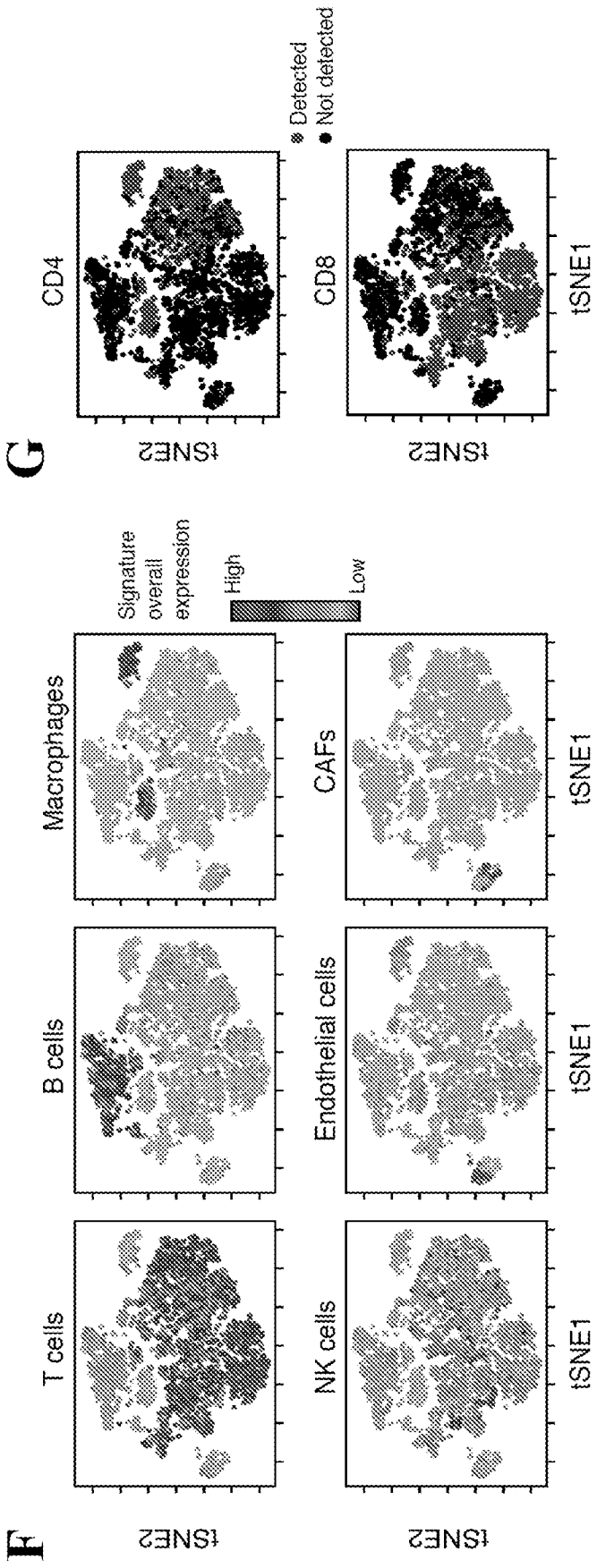

G
CD4
CD8
Detected
Not detected
tSNE1
tSNE2
F
Signature overall expression
High
Low
Macrophages
CAFs
B cells
Endothelial cells
T cells
NK cells

FIG. 51F-G

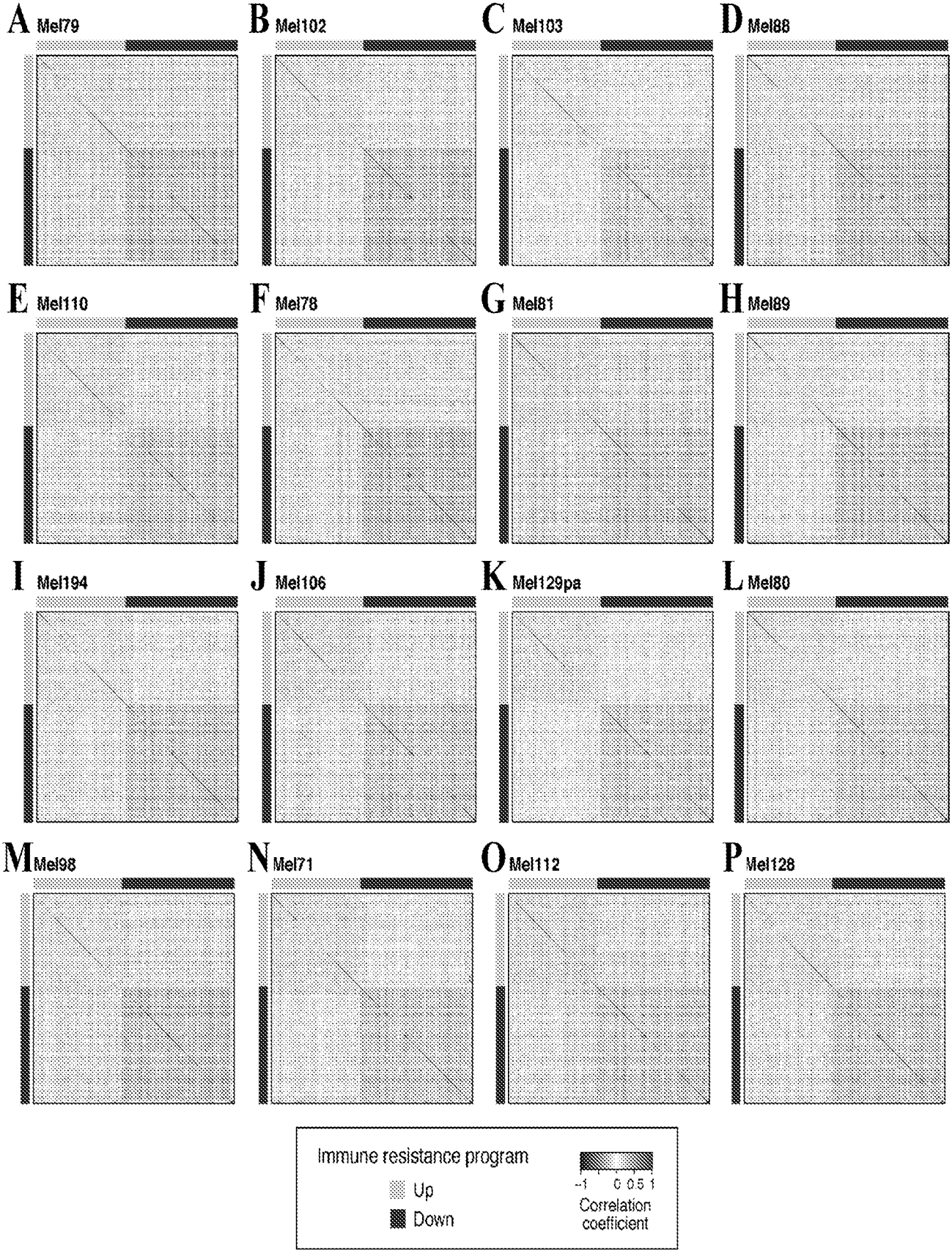

A Mel79
B Mel102
C Mel103
D Mel88
E Mel110
F Mel78
G Mel81
H Mel89
I Mel194
J Mel106
K Mel129pa
L Mel80
M Mel98
N Mel71
O Mel112
P Mel128
Immune resistance program
Up
Down
-1 0 0.5 1
Correlation coefficient

FIG. 52A-P

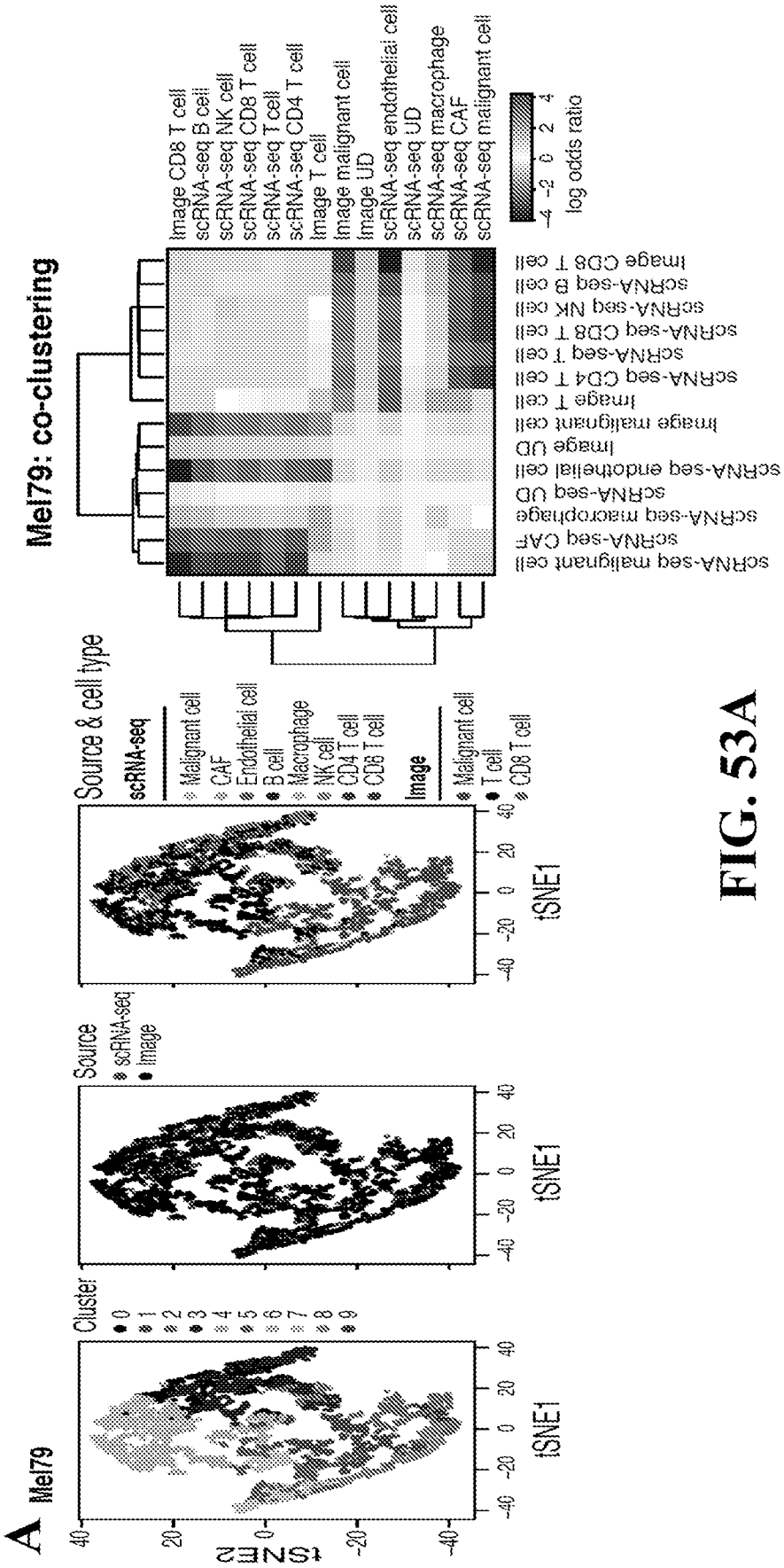

A
Mel79
Cluster
0
1
2
3
4
5
6
7
8
9
tSNE2
tSNE1
Source
scRNA-seq
Image
Source & cell type
scRNA-seq
Malignant cell
CAF
Endothelial cell
B cell
Macrophage
NK cell
CD4 T cell
CD8 T cell
Image
Malignant cell
T cell
CD8 T cell
Mel79: co-clustering
Image CD8 T cell
scRNA-seq B cell
scRNA-seq NK cell
scRNA-seq CD8 T cell
scRNA-seq T cell
scRNA-seq CD4 T cell
Image T cell
Image malignant cell
Image UD
scRNA-seq endothelial cell
scRNA-seq UD
scRNA-seq macrophage
scRNA-seq CAF
scRNA-seq malignant cell
log odds ratio

FIG. 53A

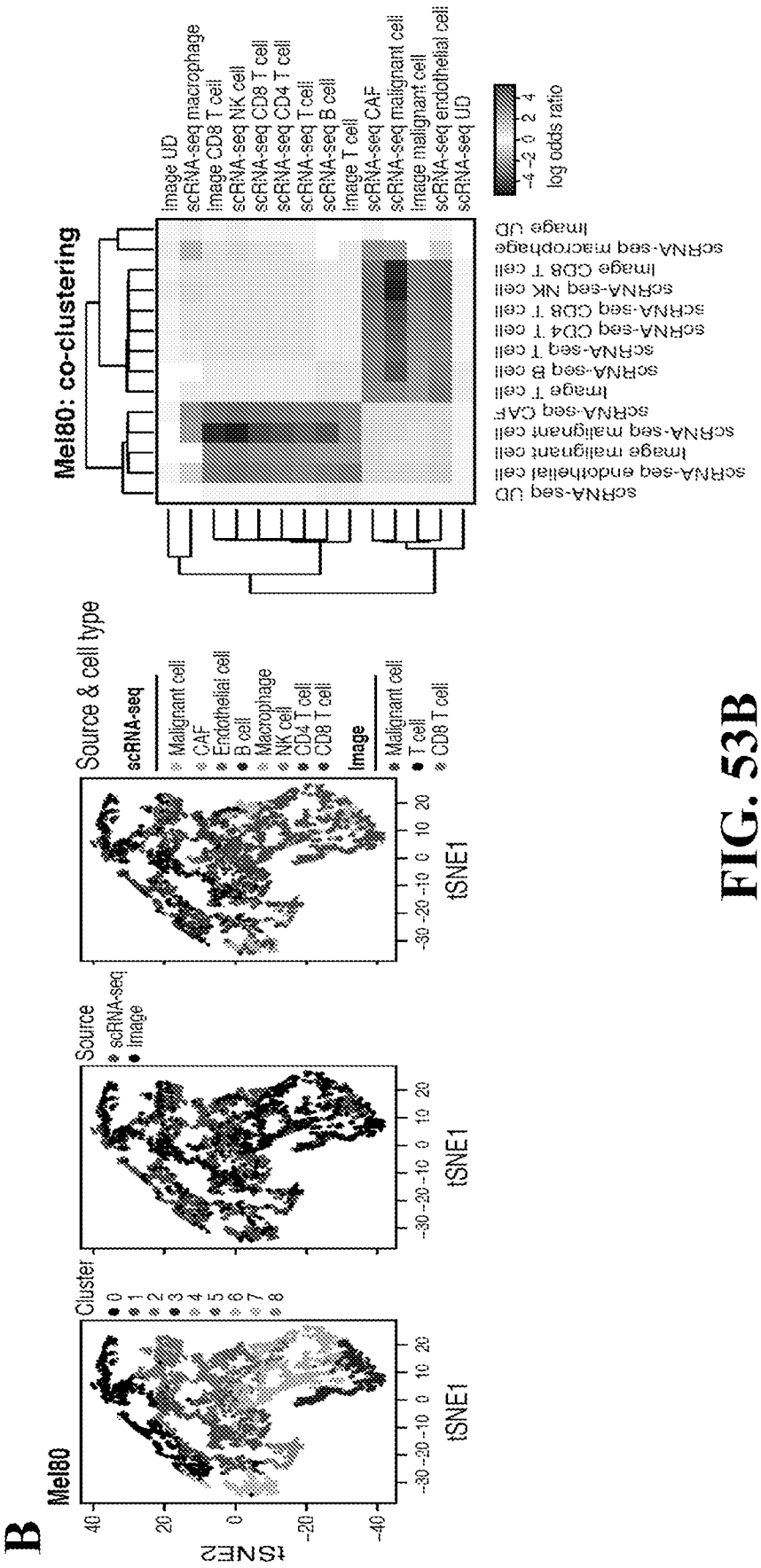

B
Mel80
tSNE2
tSNE1
Cluster
Source
scRNA-seq
image
Source & cell type
scRNA-seq
Malignant cell
CAF
Endothelial cell
B cell
Macrophage
NK cell
CD4 T cell
CD8 T cell
Image
Malignant cell
T cell
CD8 T cell
Mel80: co-clustering
image UD
scRNA-seq macrophage
image CD8 T cell
scRNA-seq NK cell
scRNA-seq CD8 T cell
scRNA-seq CD4 T cell
scRNA-seq T cell
scRNA-seq B cell
image T cell
scRNA-seq CAF
scRNA-seq malignant cell
image malignant cell
scRNA-seq endothelial cell
scRNA-seq UD
log odds ratio

FIG. 53B

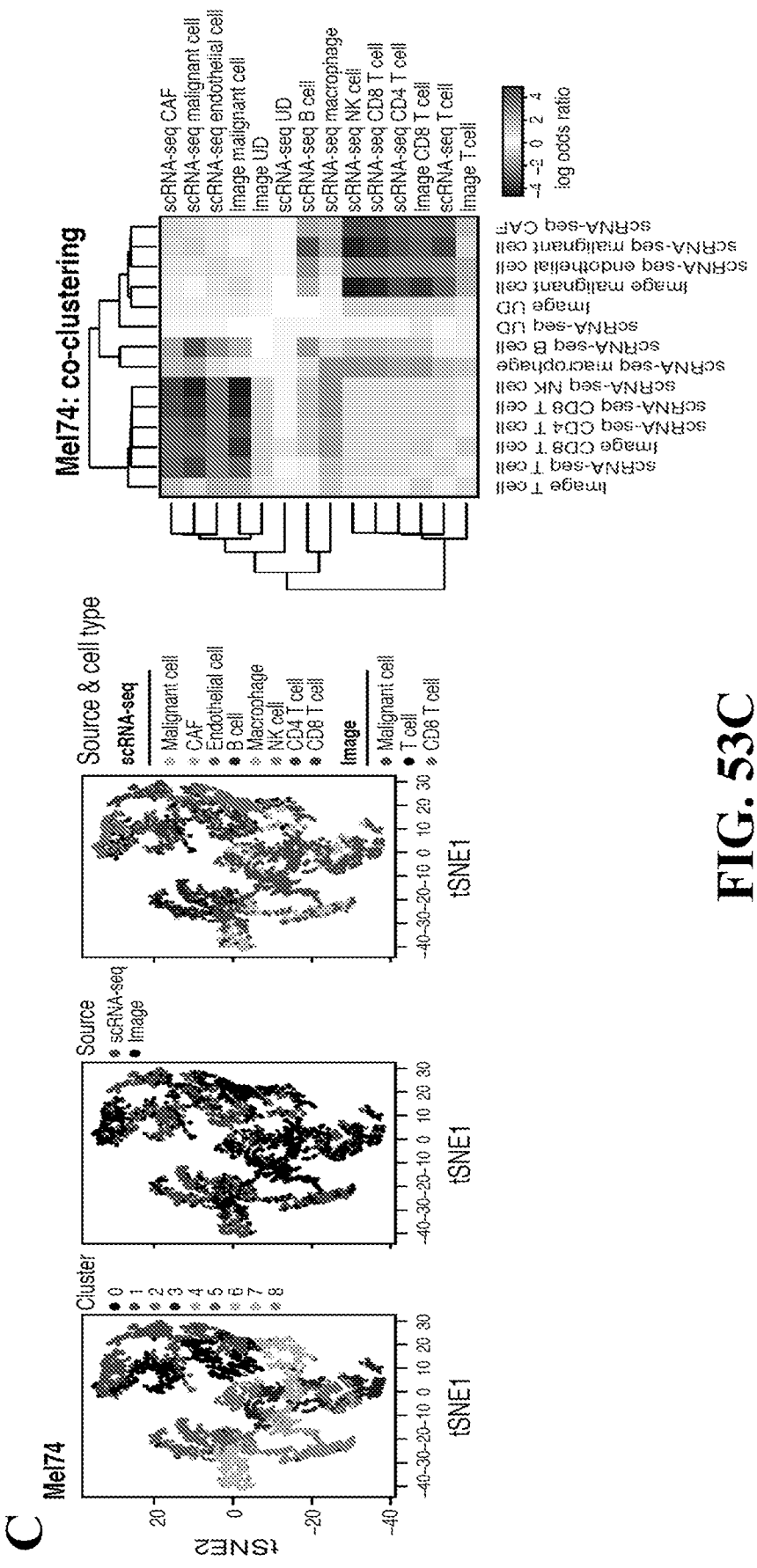

C
Mel74
tSNE2
tSNE1
Cluster
Source
scRNA-seq
Image
Source & cell type
scRNA-seq
Malignant cell
CAF
Endothelial cell
B cell
Macrophage
NK cell
CD4 T cell
CD8 T cell
Image
Malignant cell
T cell
CD8 T cell
Mel74: co-clustering
scRNA-seq CAF
scRNA-seq malignant cell
scRNA-seq endothelial cell
image malignant cell
image UD
scRNA-seq UD
scRNA-seq B cell
scRNA-seq macrophage
scRNA-seq NK cell
scRNA-seq CD8 T cell
scRNA-seq CD4 T cell
image CD8 T cell
scRNA-seq T cell
image T cell
log ccds ratio

FIG. 53C

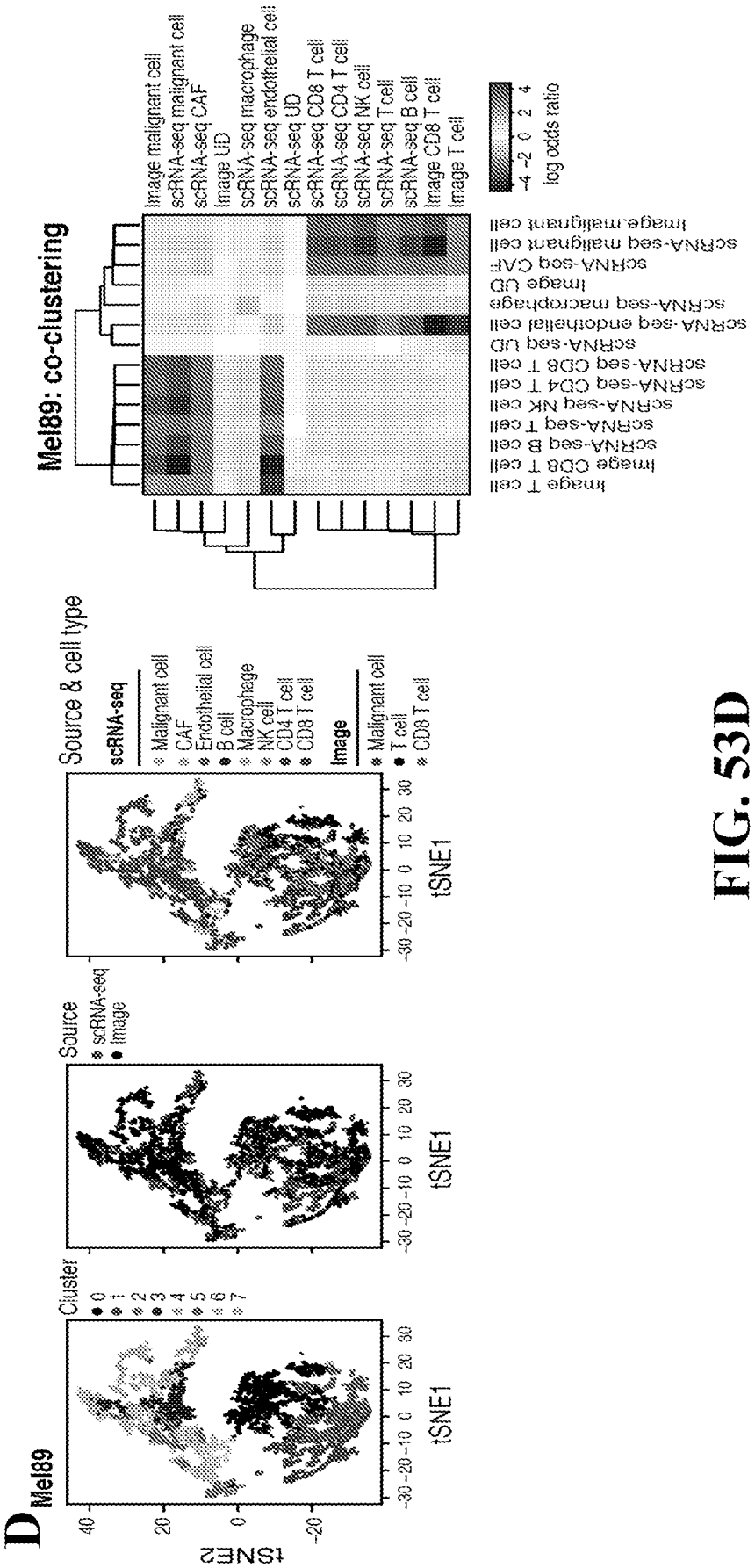

D
Mel89
tSNE2
tSNE1
Cluster
0
1
2
3
4
5
6
7
Source
scRNA-seq
Image
Source & cell type
scRNA-seq
Malignant cell
CAF
Endothelial cell
B cell
Macrophage
NK cell
CD4 T cell
CD8 T cell
Image
Malignant cell
T cell
CD8 T cell
Mel89: co-clustering
Image malignant cell
scRNA-seq malignant cell
scRNA-seq CAF
Image UD
scRNA-seq macrophage
scRNA-seq endothelial cell
scRNA-seq UD
scRNA-seq CD8 T cell
scRNA-seq CD4 T cell
scRNA-seq NK cell
scRNA-seq T cell
scRNA-seq B cell
Image CD8 T cell
Image T cell
log odds ratio

FIG. 53D

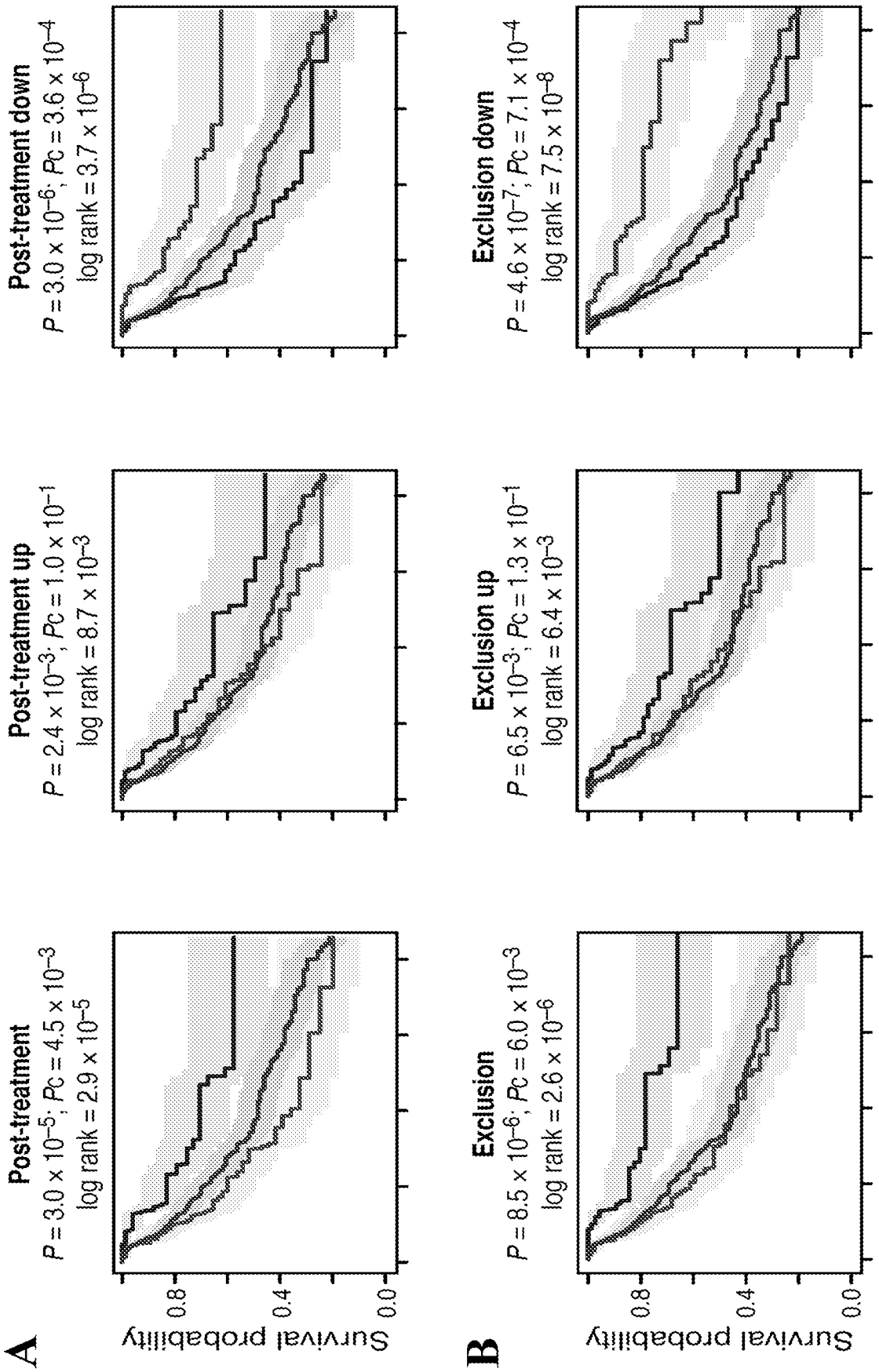

A
Post-treatment
P = 3.0 x 10−5; Pc = 4.5 x 10−3
log rank = 2.9 x 10−5
Post-treatment up
P = 2.4 x 10−3; Pc = 1.0 x 10−1
log rank = 8.7 x 10−3
Post-treatment down
P = 3.0 x 10−6; Pc = 3.6 x 10−4
log rank = 3.7 x 10−6
B
Exclusion
P = 8.5 x 10−6; Pc = 6.0 x 10−3
log rank = 2.6 x 10−6
Exclusion up
P = 6.5 x 10−3; Pc = 1.3 x 10−1
log rank = 6.4 x 10−3
Exclusion down
P = 4.6 x 10−7; Pc = 7.1 x 10−4
log rank = 7.5 x 10−8
Survival probability
0.0
0.4
0.8

FIG. 54A-B

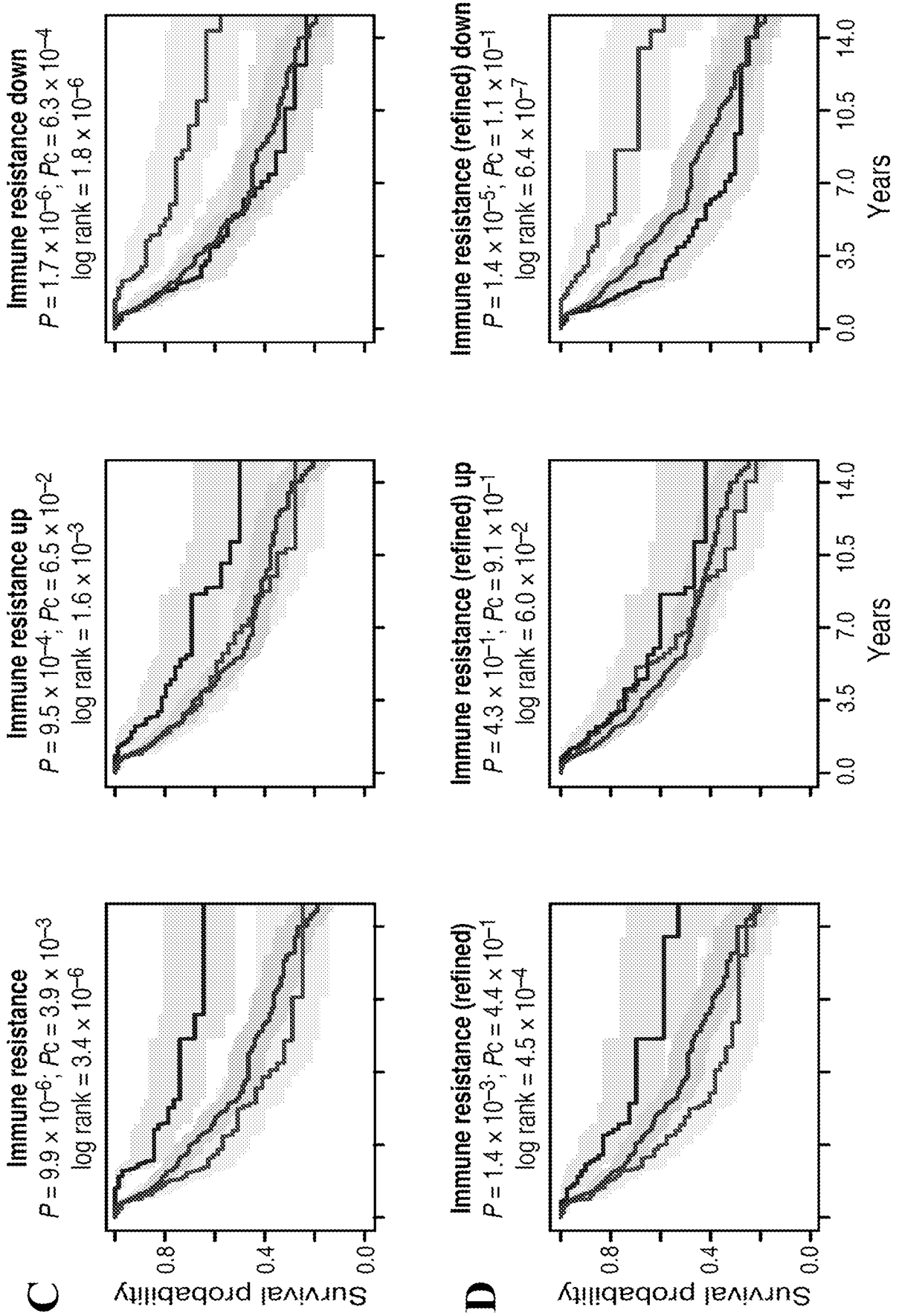

C
Immune resistance
P = 9.9 x 10−6; Pc = 3.9 x 10−3
log rank = 3.4 x 10−6
Immune resistance up
P = 9.5 x 10−4; Pc = 6.5 x 10−2
log rank = 1.6 x 10−3
Immune resistance down
P = 1.7 x 10−6; Pc = 6.3 x 10−4
log rank = 1.8 x 10−6
D
Immune resistance (refined)
P = 1.4 x 10−3; Pc = 4.4 x 10−1
log rank = 4.5 x 10−4
Immune resistance (refined) up
P = 4.3 x 10−1; Pc = 9.1 x 10−1
log rank = 6.0 x 10−2
Immune resistance (refined) down
P = 1.4 x 10−5; Pc = 1.1 x 10−1
log rank = 6.4 x 10−7
Survival probability
0.0
0.4
0.8
0.0
3.5
7.0
10.5
14.0
Years

FIG. 54C-D

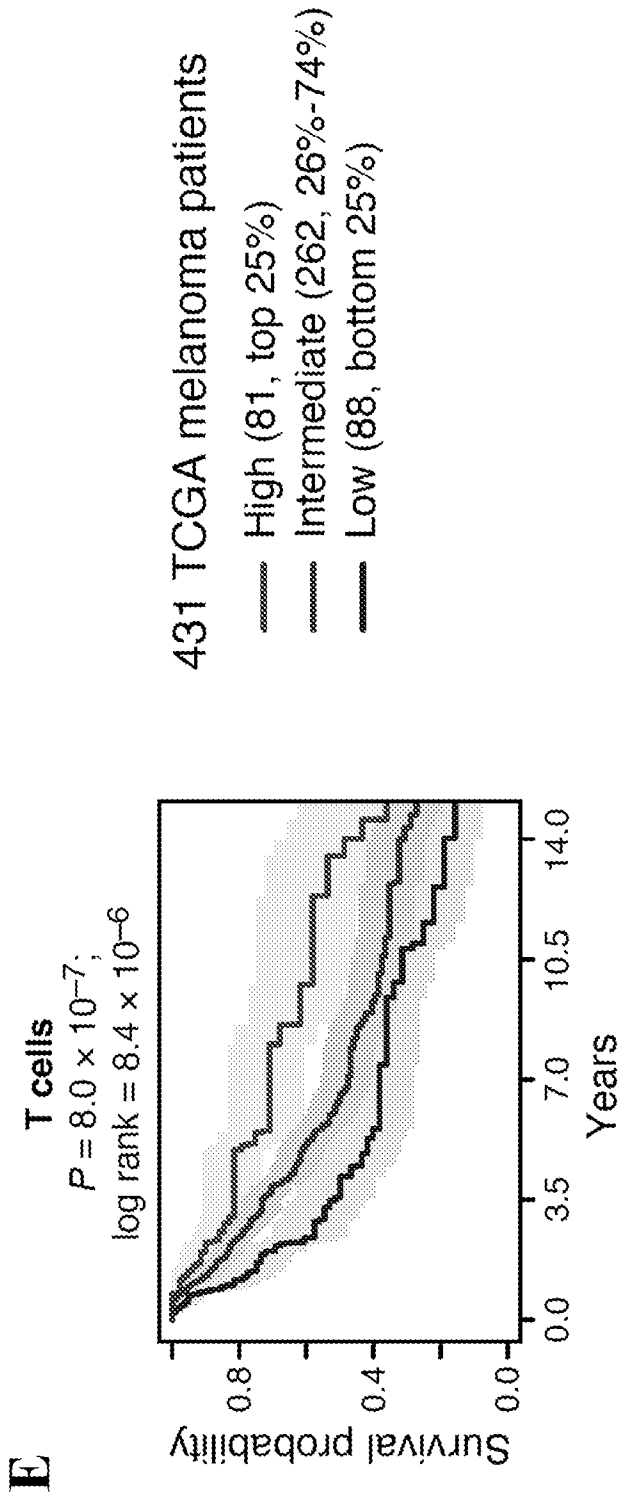

E
T cells
P = 8.0 × 10−7;
log rank = 8.4 × 10−6
Survival probability
0.0
0.4
0.8
0.0
3.5
7.0
10.5
14.0
Years
431 TCGA melanoma patients
High (81, top 25%)
Intermediate (262, 26%-74%)
Low (88, bottom 25%)

FIG. 54E

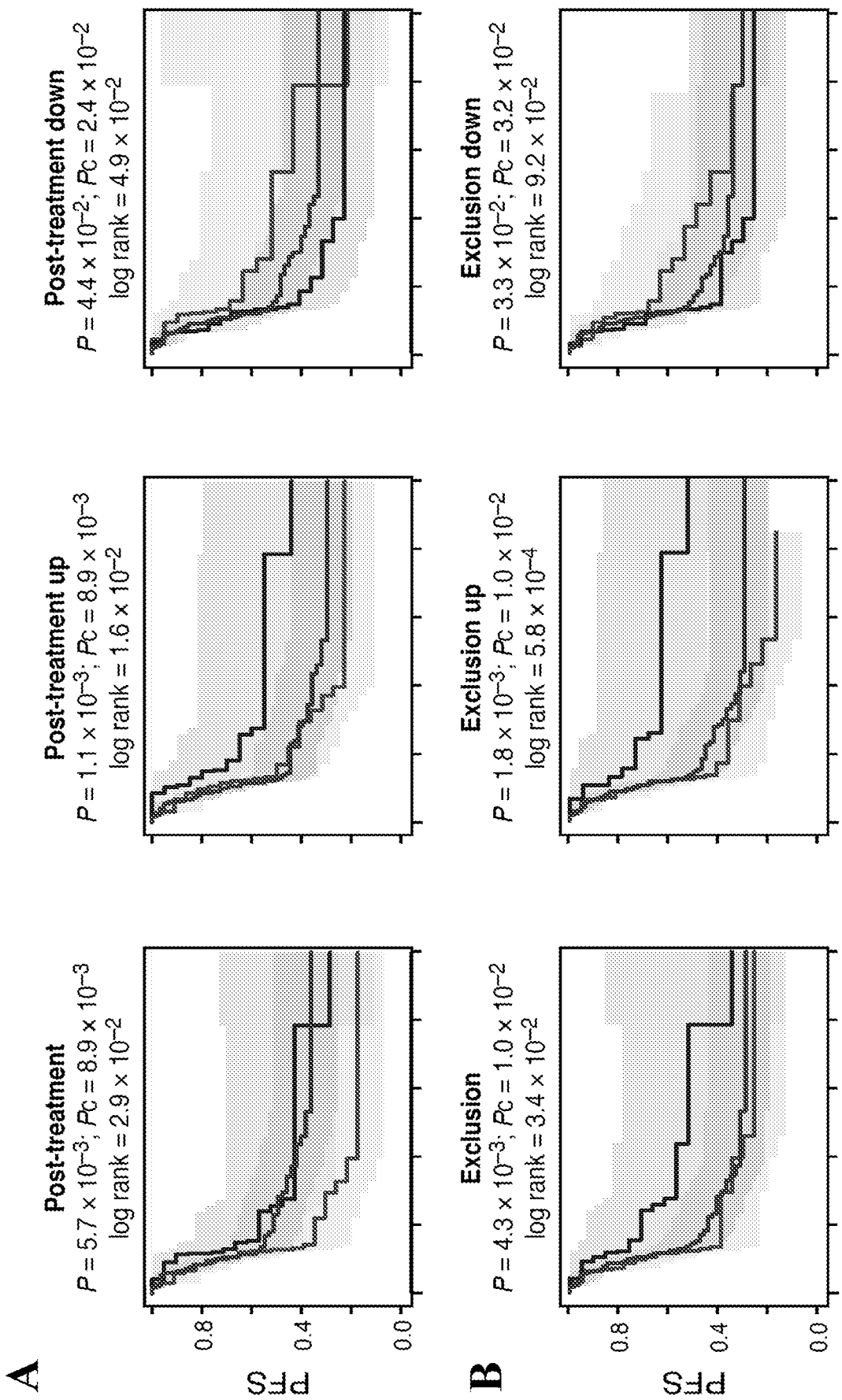

A
B
Post-treatment
P = 5.7 x 10−3; Pc = 8.9 x 10−3
log rank = 2.9 x 10−2
Post-treatment up
P = 1.1 x 10−3; Pc = 8.9 x 10−3
log rank = 1.6 x 10−2
Post-treatment down
P = 4.4 x 10−2; Pc = 2.4 x 10−2
log rank = 4.9 x 10−2
Exclusion
P = 4.3 x 10−3; Pc = 1.0 x 10−2
log rank = 3.4 x 10−2
Exclusion up
P = 1.8 x 10−3; Pc = 1.0 x 10−2
log rank = 5.8 x 10−4
Exclusion down
P = 3.3 x 10−2; Pc = 3.2 x 10−2
log rank = 9.2 x 10−2
PFS
0.0
0.4
0.8

FIG. 55A-B

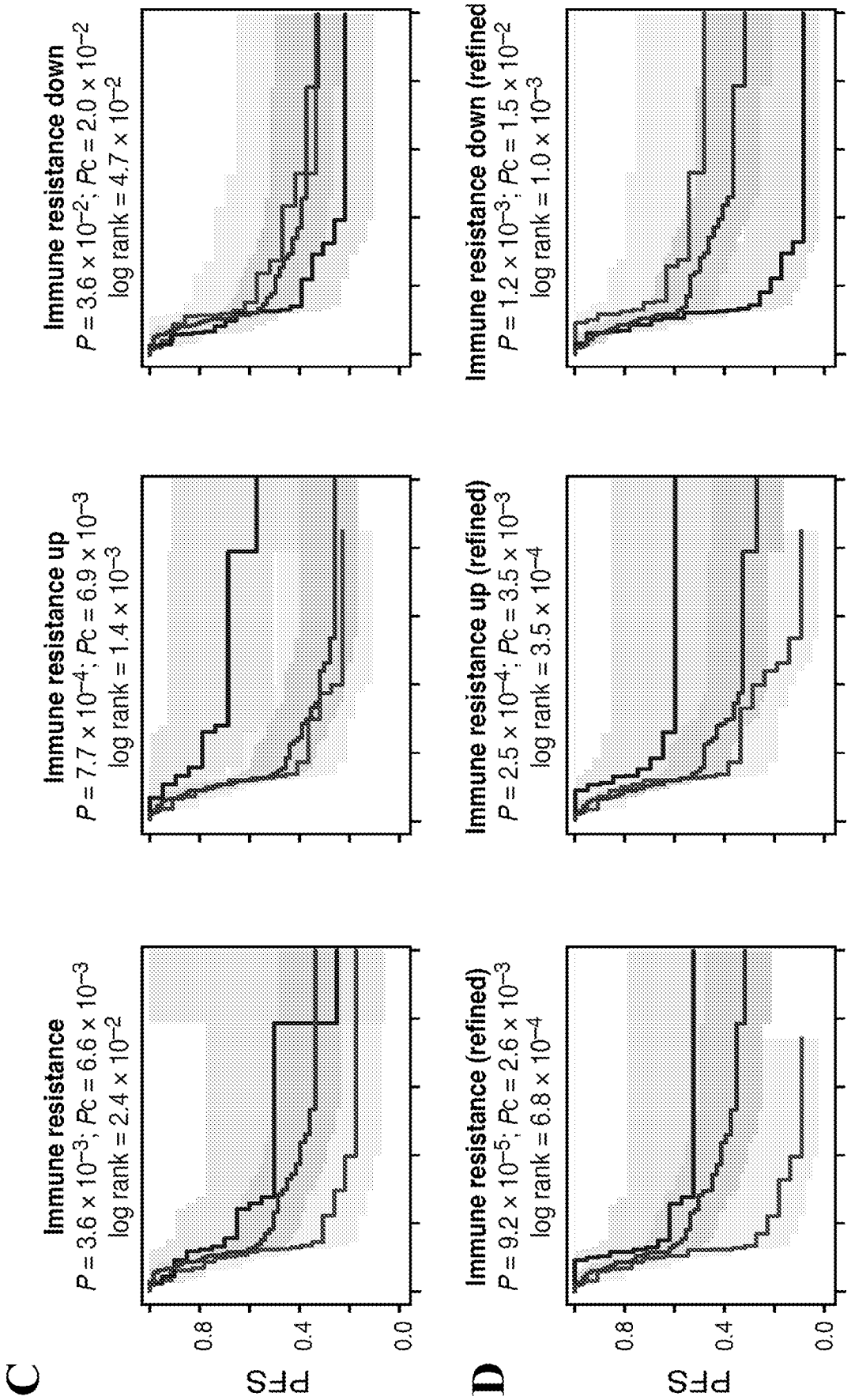

C
D
PFS
0.0
0.4
0.8
Immune resistance
P = 3.6 x 10−3; Pc = 6.6 x 10−3
log rank = 2.4 x 10−2
Immune resistance up
P = 7.7 x 10−4; Pc = 6.9 x 10−3
log rank = 1.4 x 10−3
Immune resistance down
P = 3.6 x 10−2; Pc = 2.0 x 10−2
log rank = 4.7 x 10−2
Immune resistance (refined)
P = 9.2 x 10−5; Pc = 2.6 x 10−3
log rank = 6.8 x 10−4
Immune resistance up (refined)
P = 2.5 x 10−4; Pc = 3.5 x 10−3
log rank = 3.5 x 10−4
Immune resistance down (refined
P = 1.2 x 10−3; Pc = 1.5 x 10−2
log rank = 1.0 x 10−3

FIG. 55C-D

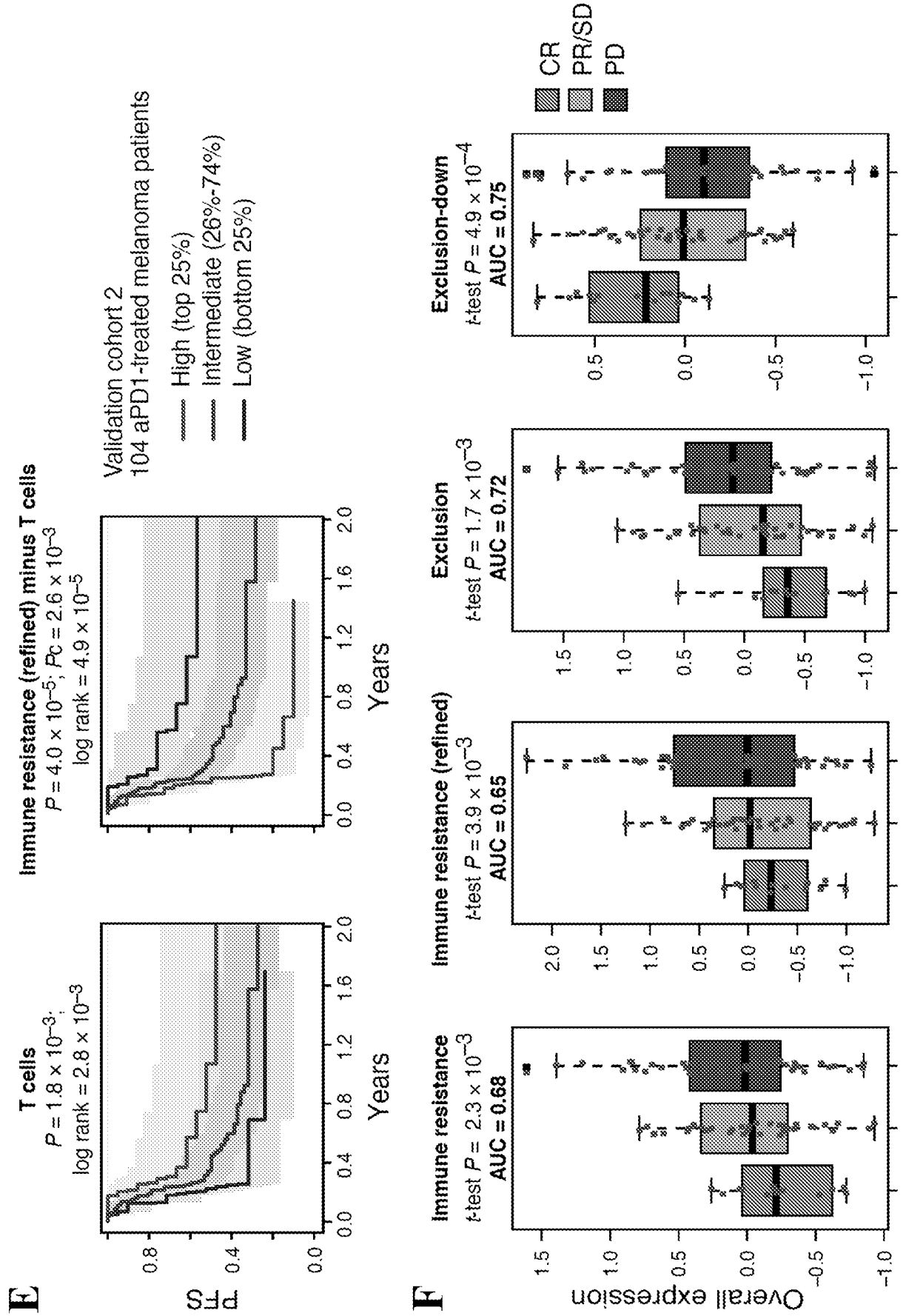

E
T cells
P = 1.8 × 10−3;
log rank = 2.8 × 10−3
Immune resistance (refined) minus T cells
P = 4.0 × 10−5; Pc = 2.6 × 10−3
log rank = 4.9 × 10−5
Validation cohort 2
104 aPD1-treated melanoma patients
High (top 25%)
Intermediate (26%-74%)
Low (bottom 25%)
PFS
Years
F
Immune resistance
t-test P = 2.3 × 10−3
AUC = 0.68
Immune resistance (refined)
t-test P = 3.9 × 10−3
AUC = 0.65
Exclusion
t-test P = 1.7 × 10−3
AUC = 0.72
Exclusion-down
t-test P = 4.9 × 10−4
AUC = 0.75
CR
PR/SD
PD
Overall expression

FIG. 55E-F

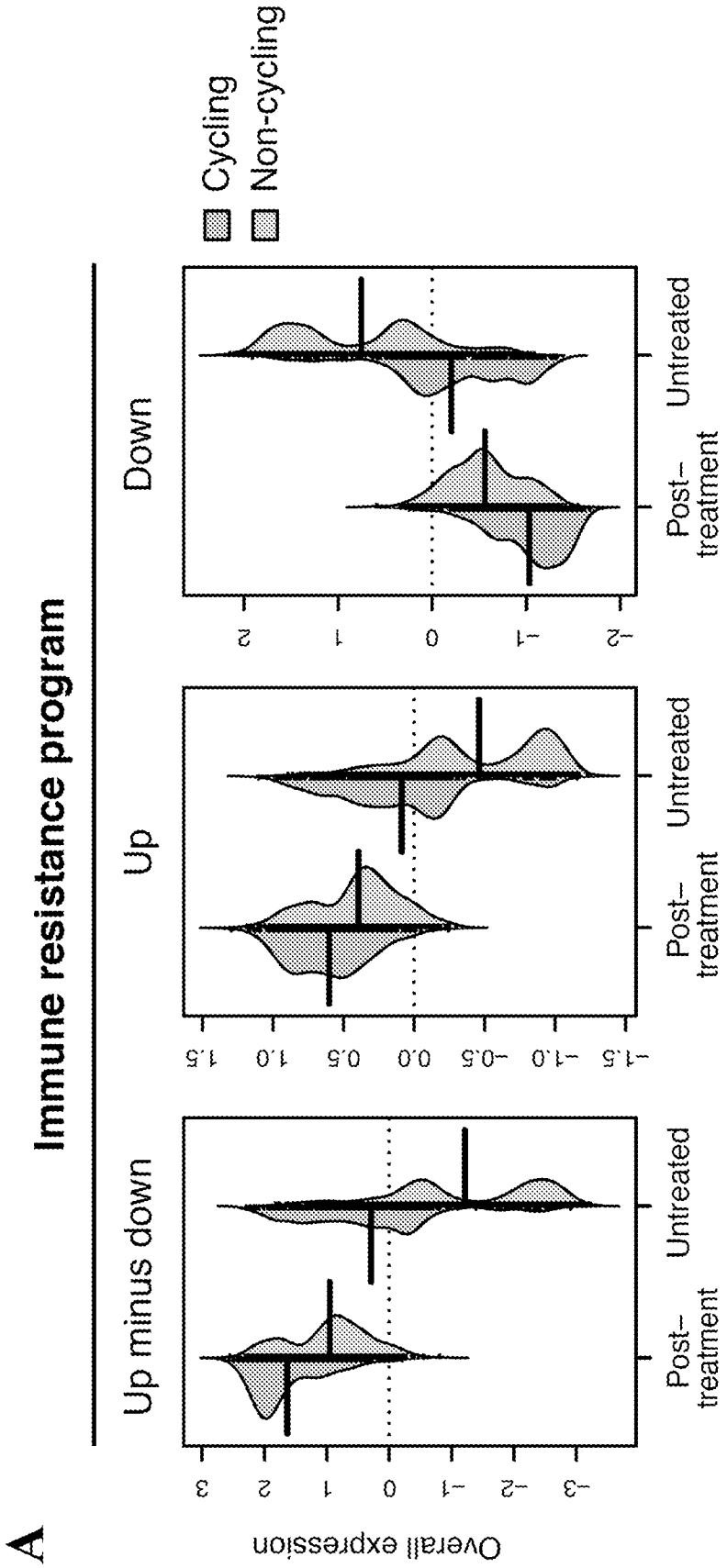

A
Immune resistance program
Up minus down
Up
Down
Cycling
Non-cycling
Overall expression
Untreated
Post-treatment

FIG. 56A

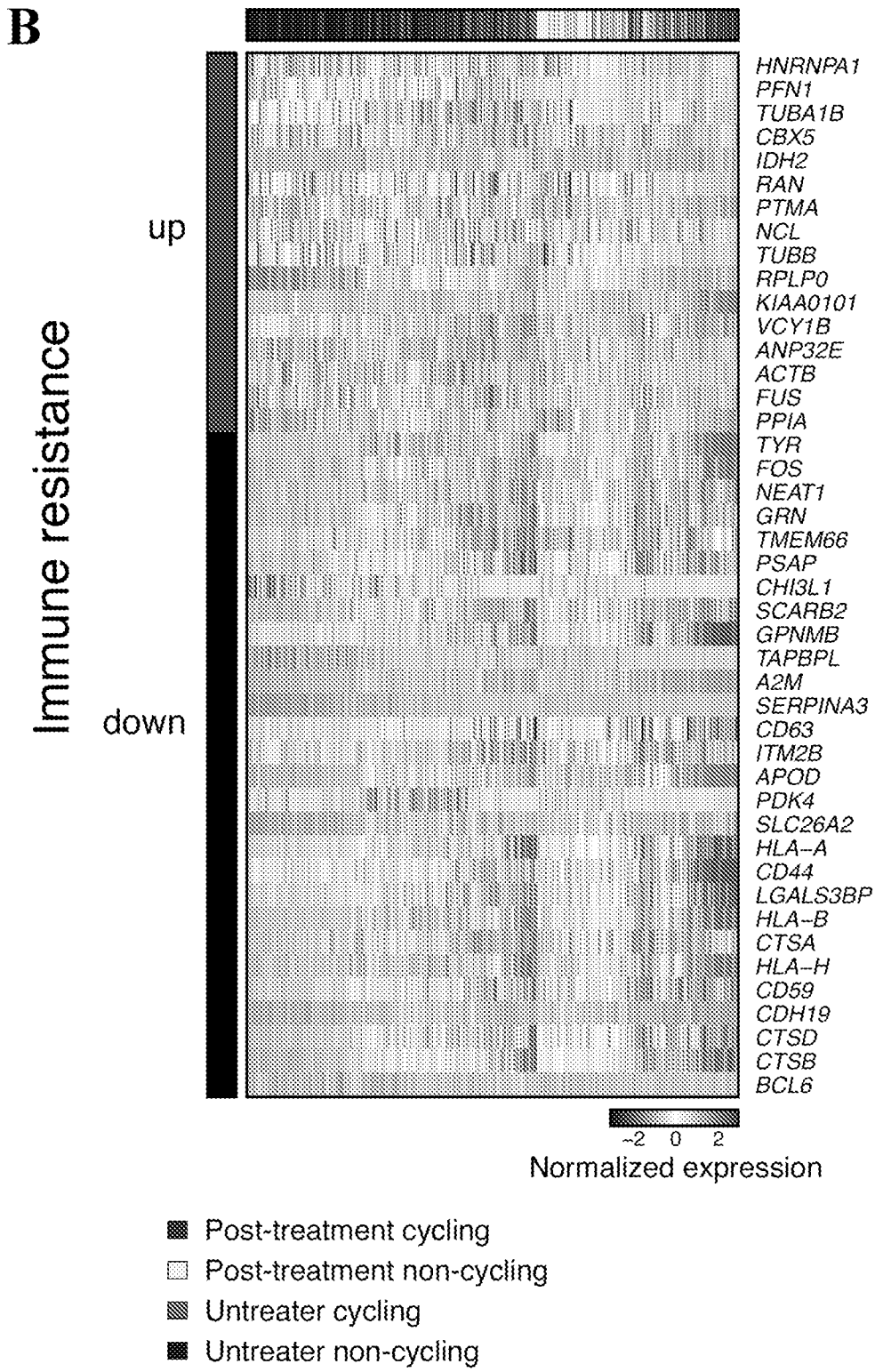

B
Immune resistance
up
down
HNRNPA1
PFN1
TUBA1B
CBX5
IDH2
RAN
PTMA
NCL
TUBB
RPLP0
KIAA0101
VCY1B
ANP32E
ACTB
FUS
PPIA
TYR
FOS
NEAT1
GRN
TMEM66
PSAP
CHI3L1
SCARB2
GPNMB
TAPBPL
A2M
SERPINA3
CD63
ITM2B
APOD
PDK4
SLC26A2
HLA-A
CD44
LGALS3BP
HLA-B
CTSA
HLA-H
CD59
CDH19
CTSD
CTSB
BCL6
-2 0 2
Normalized expression
Post-treatment cycling
Post-treatment non-cycling
Untreater cycling
Untreater non-cycling

FIG. 56B

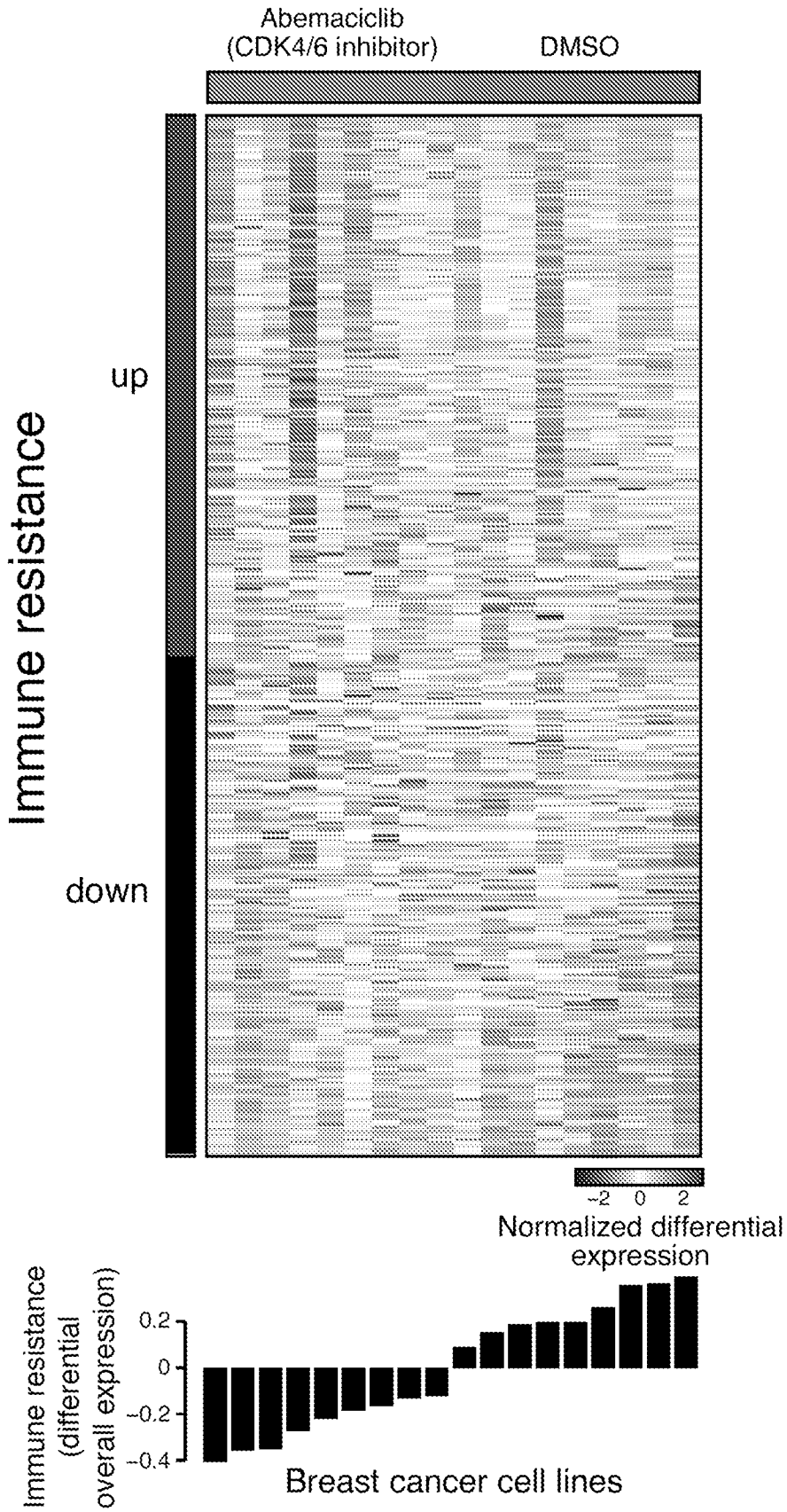

C
Abemaciclib
(CDK4/6 inhibitor)
DMSO
Immune resistance
up
down
−2 0 2
Normalized differential
expression
Immune resistance
(differential
overall expression)
0.2
0
−0.2
−0.4
Breast cancer cell lines

FIG. 56C

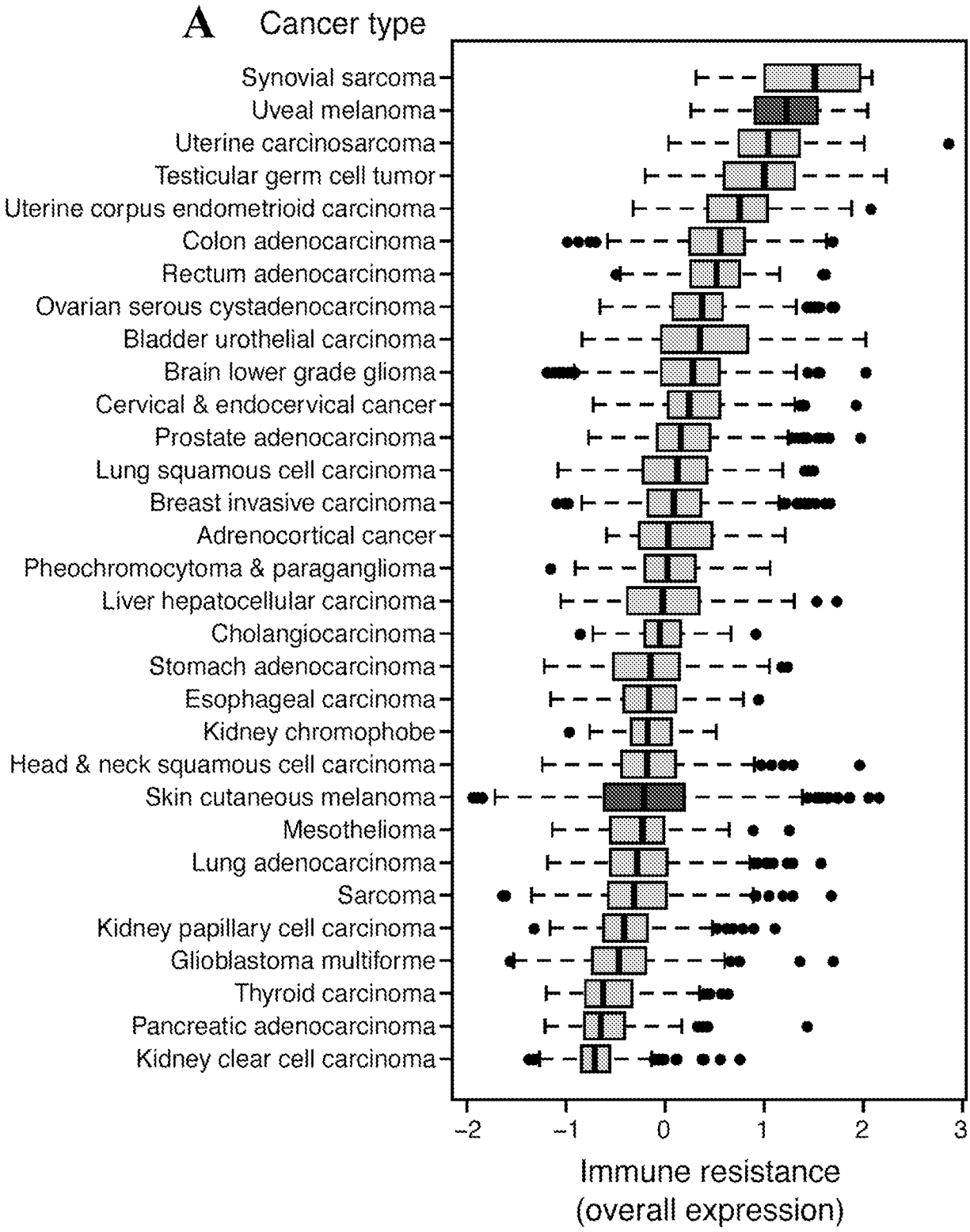

A
Cancer type
Synovial sarcoma
Uveal melanoma
Uterine carcinosarcoma
Testicular germ cell tumor
Uterine corpus endometrioid carcinoma
Colon adenocarcinoma
Rectum adenocarcinoma
Ovarian serous cystadenocarcinoma
Bladder urothelial carcinoma
Brain lower grade glioma
Cervical & endocervical cancer
Prostate adenocarcinoma
Lung squamous cell carcinoma
Breast invasive carcinoma
Adrenocortical cancer
Pheochromocytoma & paraganglioma
Liver hepatocellular carcinoma
Cholangiocarcinoma
Stomach adenocarcinoma
Esophageal carcinoma
Kidney chromophobe
Head & neck squamous cell carcinoma
Skin cutaneous melanoma
Mesothelioma
Lung adenocarcinoma
Sarcoma
Kidney papillary cell carcinoma
Glioblastoma multiforme
Thyroid carcinoma
Pancreatic adenocarcinoma
Kidney clear cell carcinoma
−2
−1
0
1
2
3
Immune resistance
(overall expression)

FIG. 57A

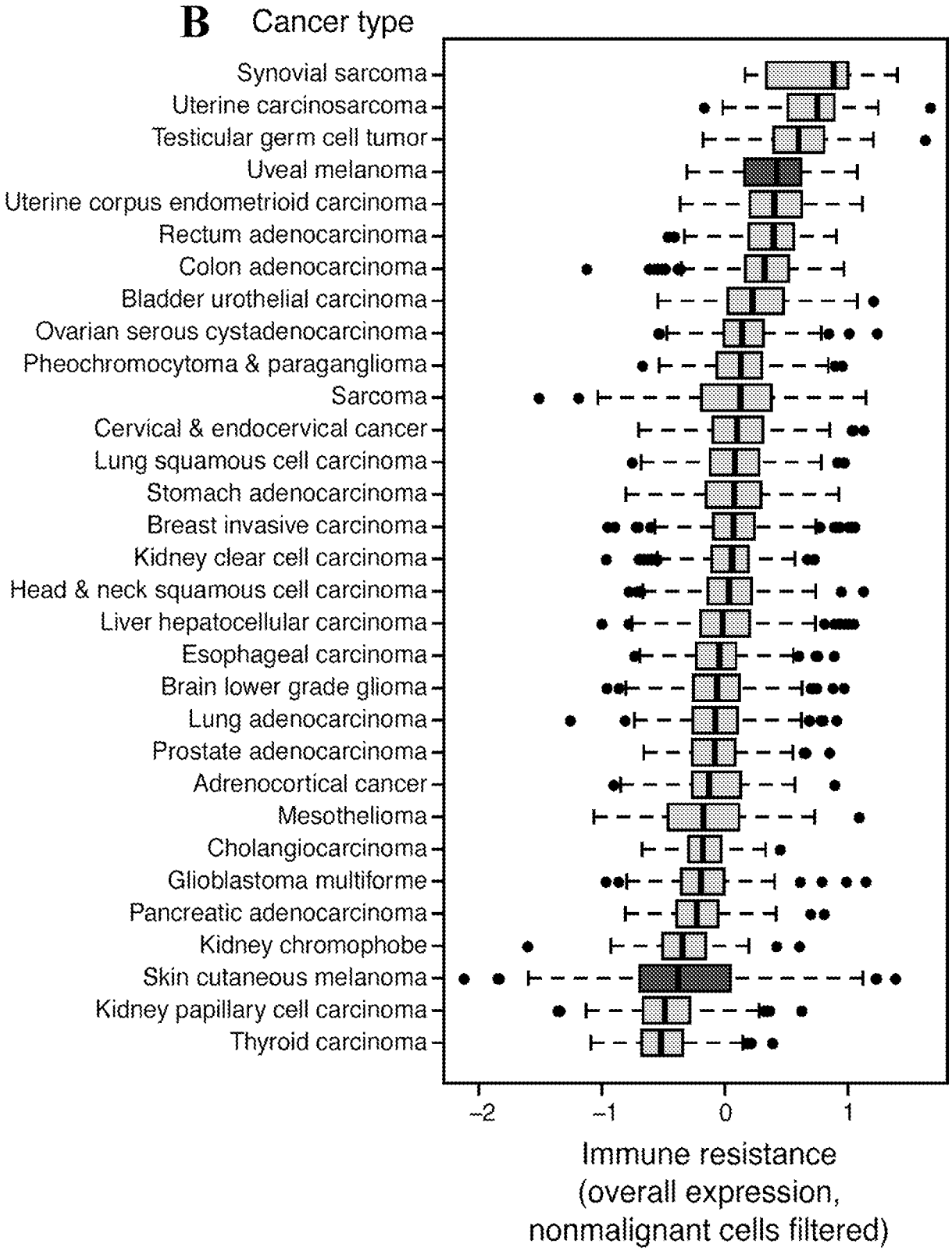

B
Cancer type
Synovial sarcoma
Uterine carcinosarcoma
Testicular germ cell tumor
Uveal melanoma
Uterine corpus endometrioid carcinoma
Rectum adenocarcinoma
Colon adenocarcinoma
Bladder urothelial carcinoma
Ovarian serous cystadenocarcinoma
Pheochromocytoma & paraganglioma
Sarcoma
Cervical & endocervical cancer
Lung squamous cell carcinoma
Stomach adenocarcinoma
Breast invasive carcinoma
Kidney clear cell carcinoma
Head & neck squamous cell carcinoma
Liver hepatocellular carcinoma
Esophageal carcinoma
Brain lower grade glioma
Lung adenocarcinoma
Prostate adenocarcinoma
Adrenocortical cancer
Mesothelioma
Cholangiocarcinoma
Glioblastoma multiforme
Pancreatic adenocarcinoma
Kidney chromophobe
Skin cutaneous melanoma
Kidney papillary cell carcinoma
Thyroid carcinoma
−2
−1
0
1
Immune resistance
(overall expression,
nonmalignant cells filtered)

FIG. 57B

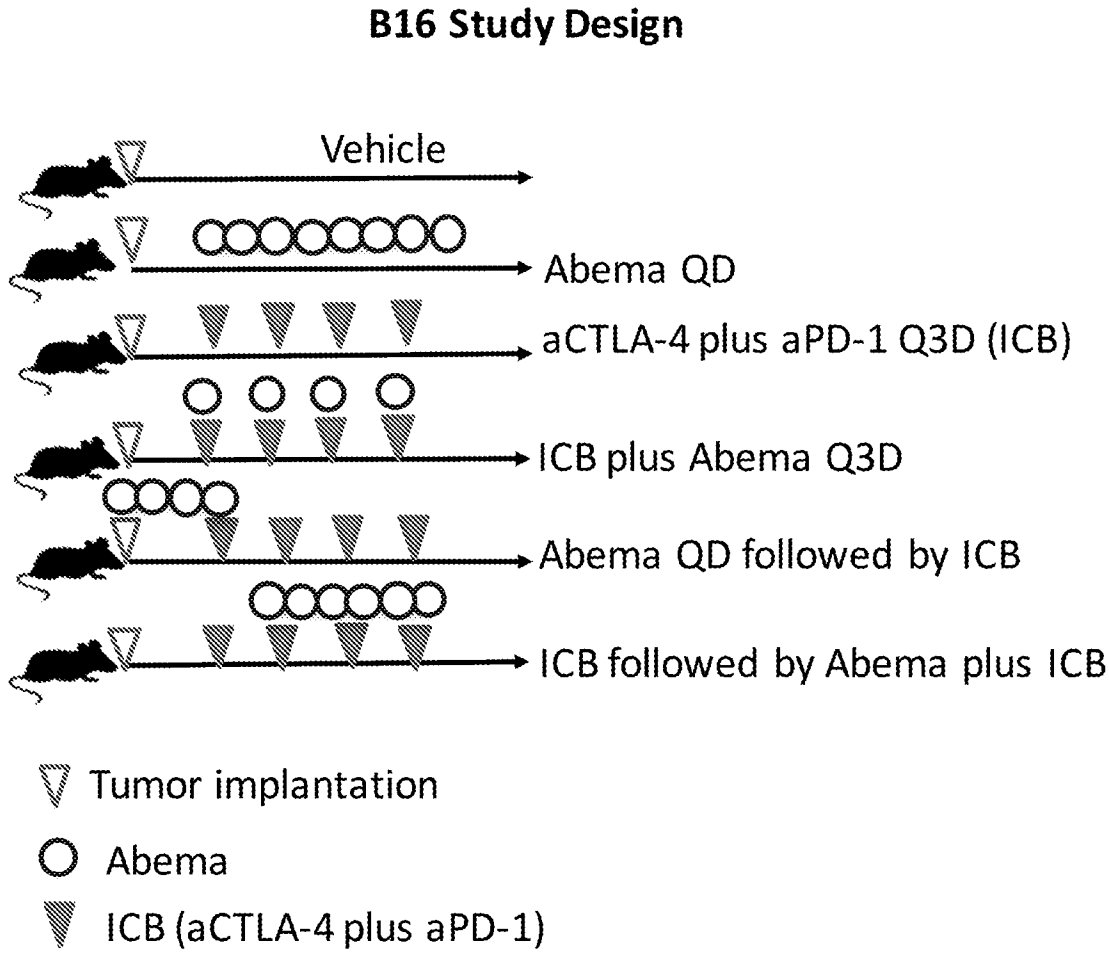

B16 Study Design
Vehicle
Abema QD
aCTLA-4 plus aPD-1 Q3D (ICB)
ICB plus Abema Q3D
Abema QD followed by ICB
ICB followed by Abema plus ICB
Tumor implantation
Abema
ICB (aCTLA-4 plus aPD-1)

FIG. 58

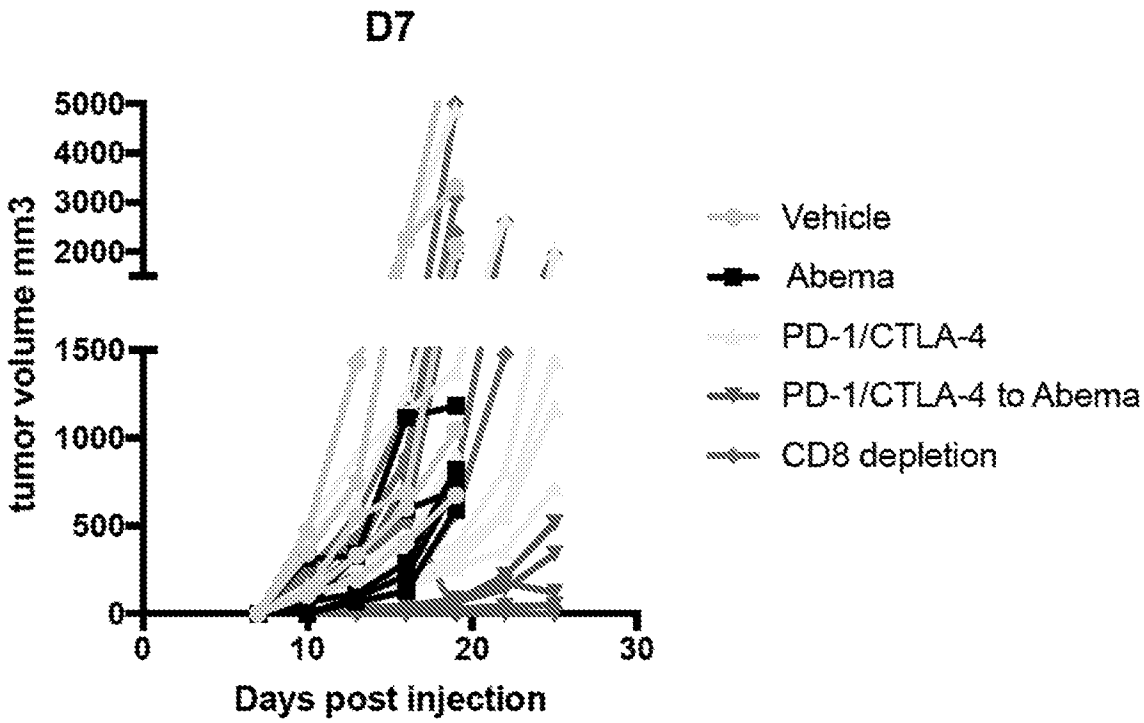

D7
5000
4000
3000
2000
1500
1000
500
0
tumor volume mm3
0
10
20
30
Days post injection
Vehicle
Abema
PD-1/CTLA-4
PD-1/CTLA-4 to Abema
CD8 depletion

FIG. 59

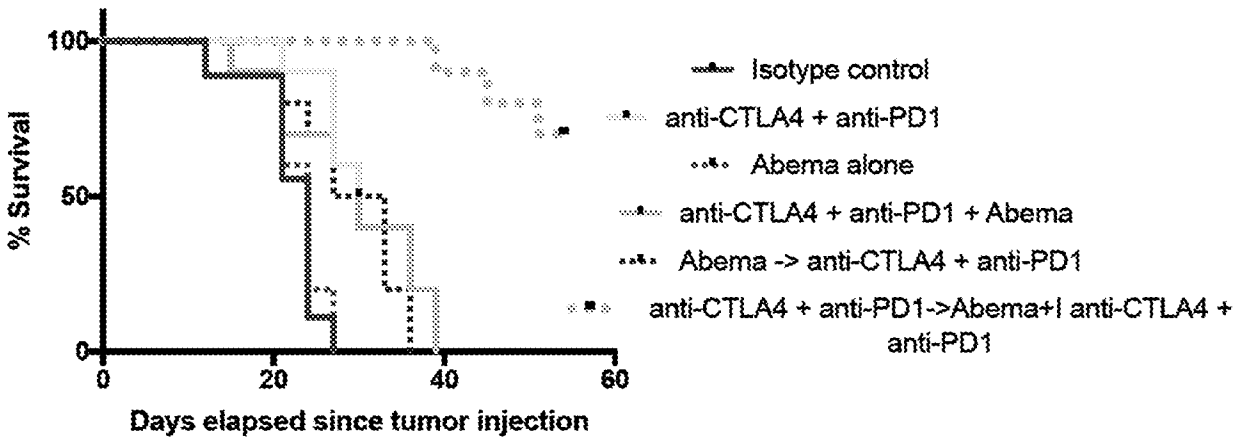

100
50
0
% Survival
0
20
40
60
Days elapsed since tumor injection
Isotype control
anti-CTLA4 + anti-PD1
Abema alone
anti-CTLA4 + anti-PD1 + Abema
Abema -> anti-CTLA4 + anti-PD1
anti-CTLA4 + anti-PD1->Abema+l anti-CTLA4 + anti-PD1

FIG. 60

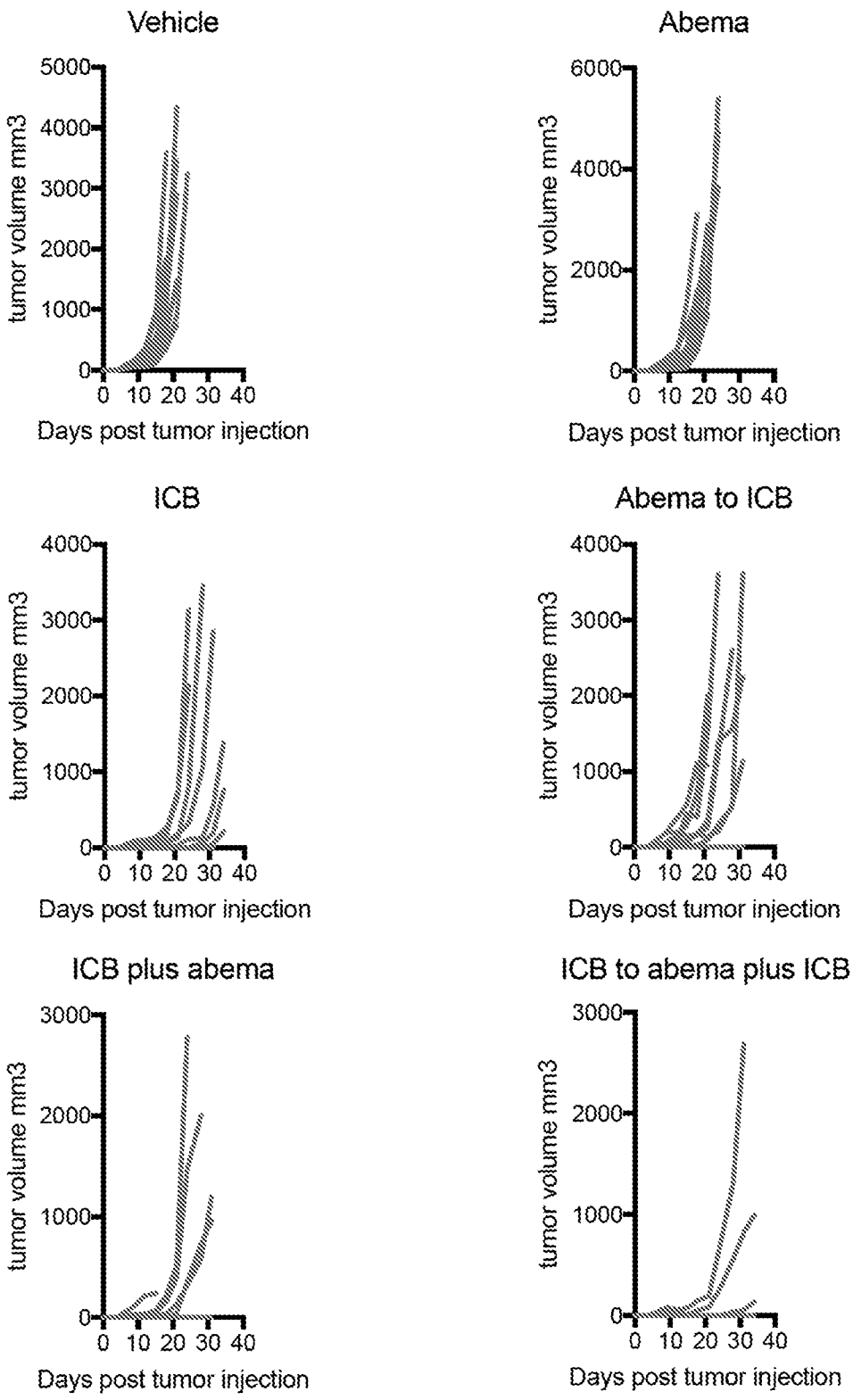

Vehicle
tumor volume mm3
5000
4000
3000
2000
1000
0
0 10 20 30 40
Days post tumor injection
Abema
tumor volume mm3
6000
4000
2000
0
0 10 20 30 40
Days post tumor injection
ICB
tumor volume mm3
4000
3000
2000
1000
0
0 10 20 30 40
Days post tumor injection
Abema to ICB
tumor volume mm3
4000
3000
2000
1000
0
0 10 20 30 40
Days post tumor injection
ICB plus abema
tumor volume mm3
3000
2000
1000
0
0 10 20 30 40
Days post tumor injection
ICB to abema plus ICB
tumor volume mm3
3000
2000
1000
0
0 10 20 30 40
Days post tumor injection

FIG. 61A

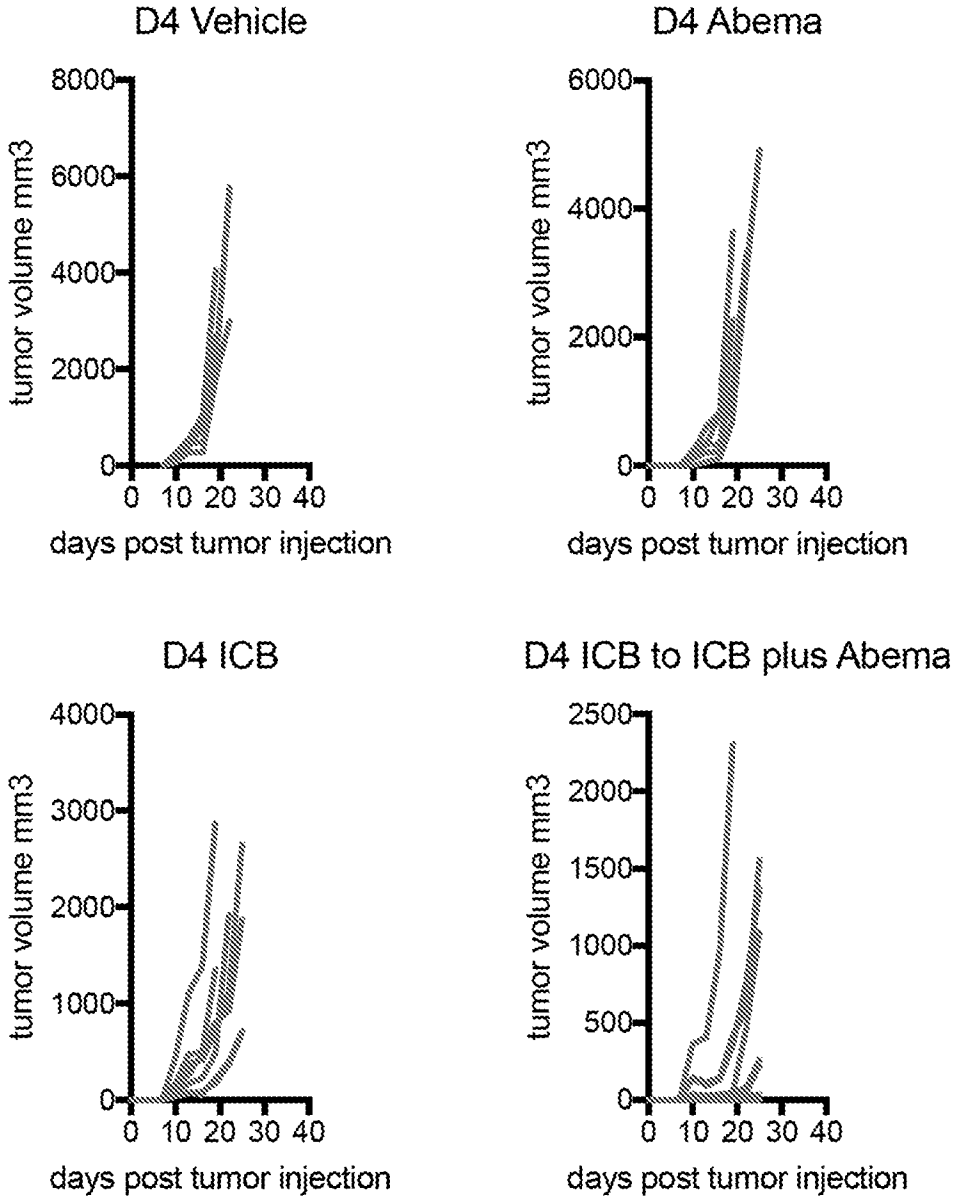

D4 Vehicle
tumor volume mm3
8000
6000
4000
2000
0
0 10 20 30 40
days post tumor injection
D4 Abema
tumor volume mm3
6000
4000
2000
0
0 10 20 30 40
days post tumor injection
D4 ICB
tumor volume mm3
4000
3000
2000
1000
0
0 10 20 30 40
days post tumor injection
D4 ICB to ICB plus Abema
tumor volume mm3
2500
2000
1500
1000
500
0
0 10 20 30 40
days post tumor injection

FIG. 61B

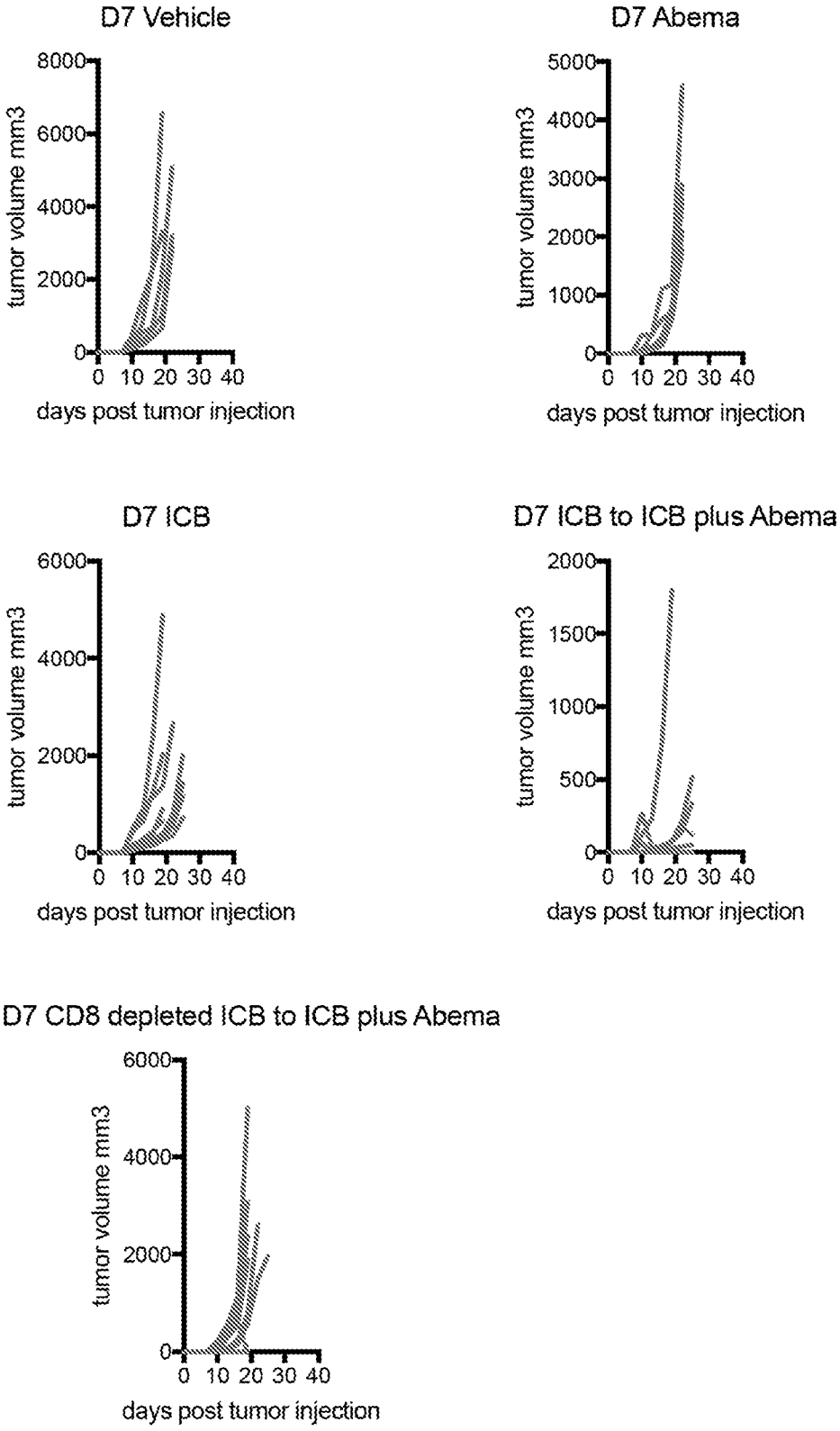

D7 Vehicle
8000
6000
4000
2000
0
tumor volume mm3
0 10 20 30 40
days post tumor injection
D7 Abema
5000
4000
3000
2000
1000
0
tumor volume mm3
0 10 20 30 40
days post tumor injection
D7 ICB
6000
4000
2000
0
tumor volume mm3
0 10 20 30 40
days post tumor injection
D7 ICB to ICB plus Abema
2000
1500
1000
500
0
tumor volume mm3
0 10 20 30 40
days post tumor injection
D7 CD8 depleted ICB to ICB plus Abema
6000
4000
2000
0
tumor volume mm3
0 10 20 30 40
days post tumor injection

FIG. 61C

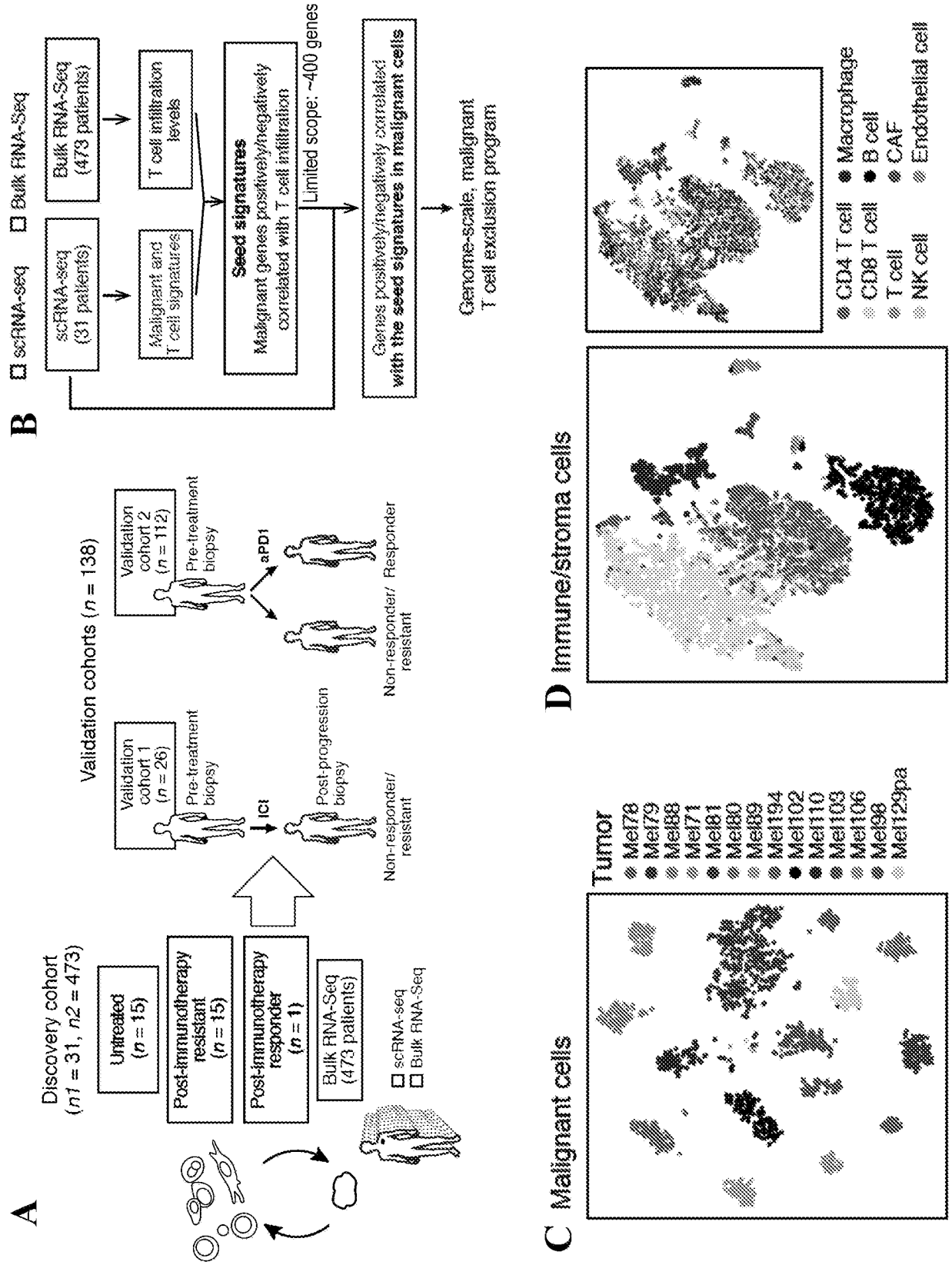

A
Discovery cohort
(n1 = 31, n2 = 473)
Untreated (n = 15)
Post-immunotherapy resistant (n = 15)
Post-immunotherapy responder (n = 1)
Bulk RNA-Seq (473 patients)
scRNA-seq
Bulk RNA-Seq
ICI
Pre-treatment biopsy
Post-progression biopsy
Non-responder/ resistant
Validation cohorts (n = 138)
Validation cohort 1 (n = 26)
Pre-treatment biopsy
aPD1
Non-responder/ resistant
Responder
Validation cohort 2 (n = 112)
Pre-treatment biopsy
B
scRNA-seq
Bulk RNA-Seq
scRNA-seq (31 patients)
Bulk RNA-Seq (473 patients)
Malignant and T cell signatures
T cell infiltration levels
Seed signatures
Malignant genes positively/negatively correlated with T cell infiltration
Limited scope: ~400 genes
Genes positively/negatively correlated with the seed signatures in malignant cells
Genome-scale, malignant T cell exclusion program
C Malignant cells
Tumor
Mel78
Mel79
Mel88
Mel71
Mel81
Mel80
Mel89
Mel194
Mel102
Mel110
Mel103
Mel106
Mel98
Mel129pa
D Immune/stroma cells
CD4 T cell
Macrophage
CD8 T cell
B cell
T cell
CAF
NK cell
Endothelial cell

FIG. 62A-D

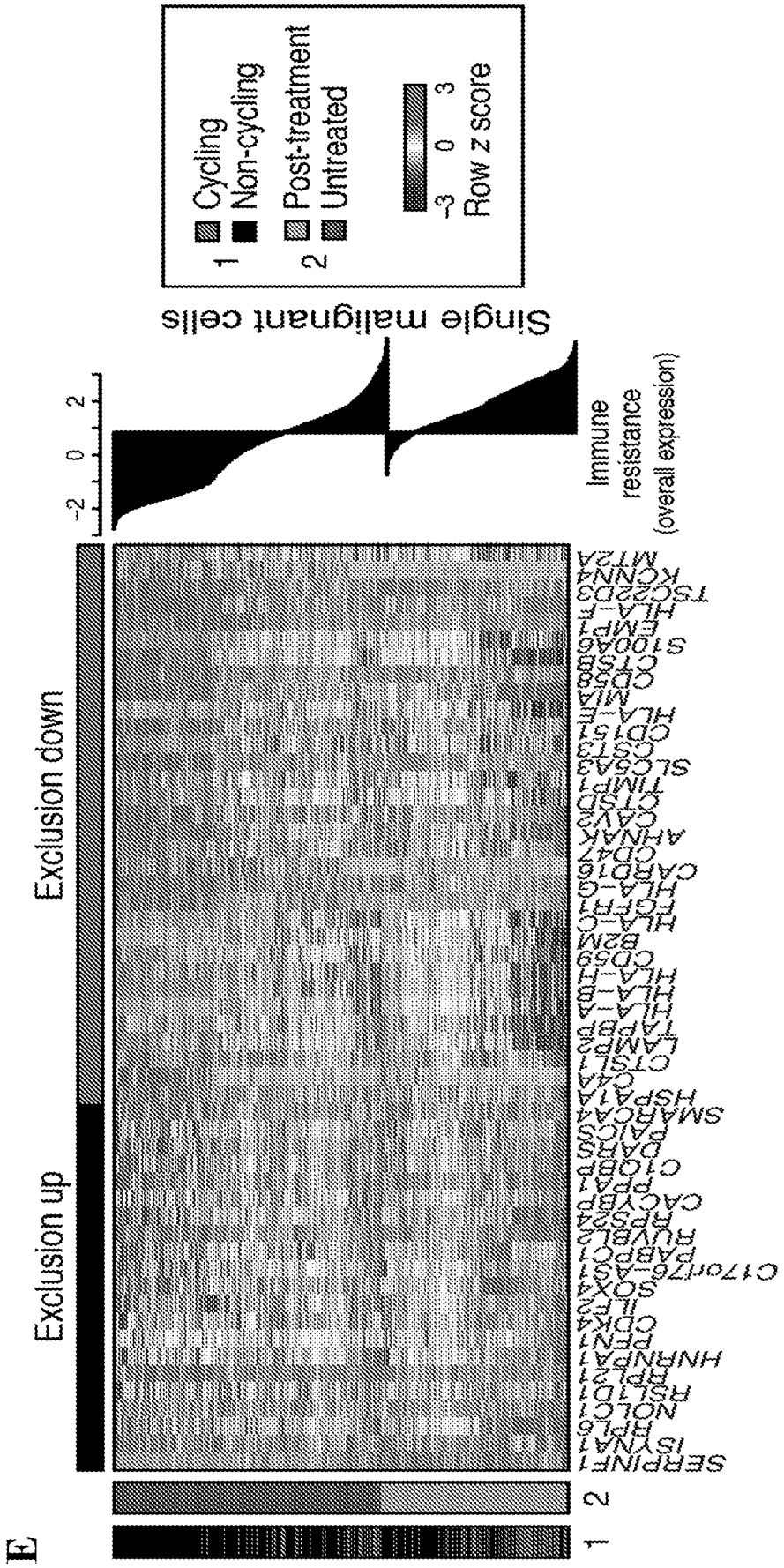

E
Exclusion up
Exclusion down
Single malignant cells
1 Cycling Non-cycling
2 Post-treatment Untreated
-3 0 3
Row z score
-2 0 2
Immune resistance (overall expression)
1
2
SERPINF1
ISYNA1
RPL6
NOLC1
RSL1D1
PRPF21
HNRNPA1
PENK1
CDK4
ILF2
SOX4
C17orf76-AS1
BABP C1
RUVBL2
RPS24
CACYBP
PPA1
C1QBP
DAHS
PAICS
SMARCA4
HSPA14
CA4
CTSL1
LAMP2
TAPBP
HLA-A
HLA-B
HLA-H
CD59
B2M
HLA-C
TGFR1
HLA-G
CARD16
CD47
AHNAK
CAV2
CTSD
TIMP1
SLC34A3
CST3
CD151
HLA-E
MIA
CD58
CTSB
S100A6
EMP1
HLA-F
TSC22D3
KCNN4
MT2A

FIG. 62E

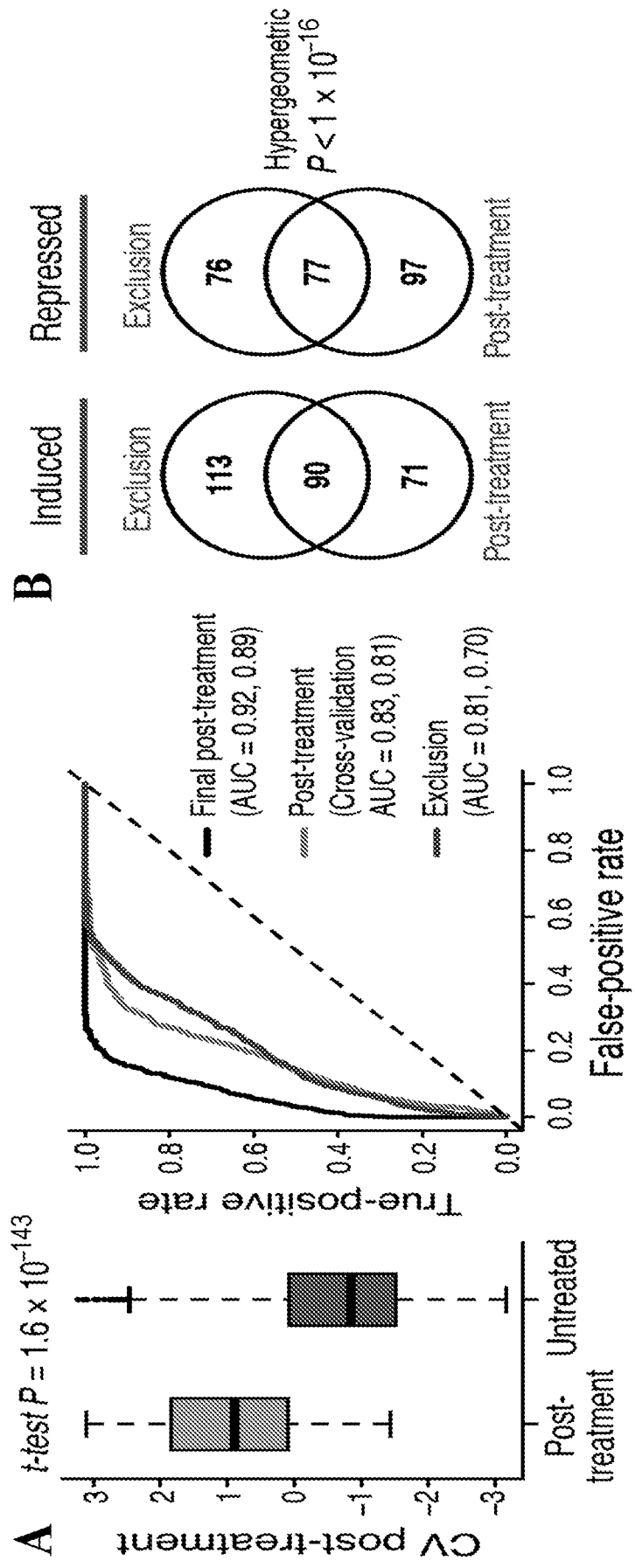

A
CV post-treatment
t-test P = 1.6 x 10^-143
Post-treatment
Untreated
True-positive rate
False-positive rate
Final post-treatment (AUC = 0.92, 0.89)
Post-treatment (Cross-validation AUC = 0.83, 0.81)
Exclusion (AUC = 0.81, 0.70)
B
Induced
Repressed
Exclusion
Post-treatment
113
90
71
76
77
97
Hypergeometric P < 1 x 10^-16

FIG. 63A-B

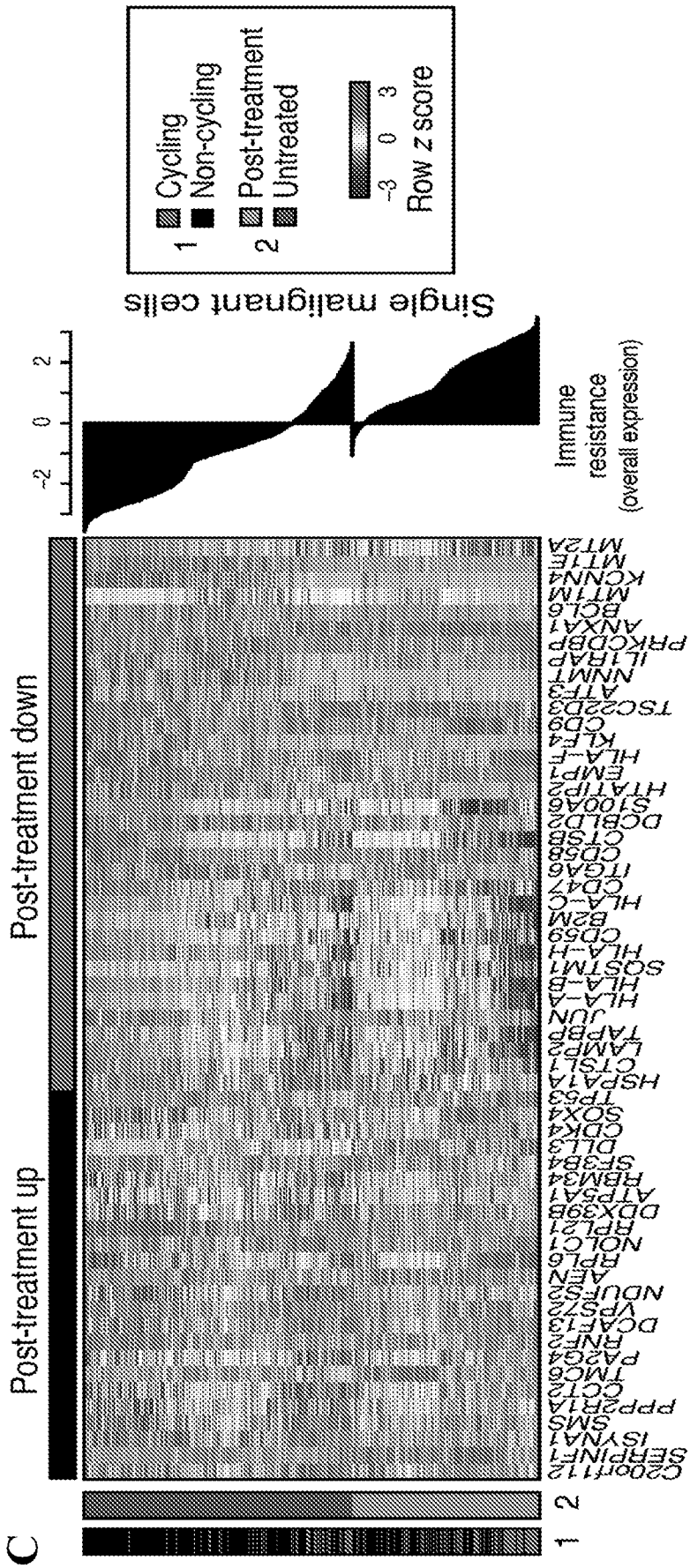

C
1 2
Post-treatment up
Post-treatment down
Single malignant cells
Cycling
Non-cycling
Post-treatment
Untreated
Row z score
-3 0 3
-2 0 2
Immune resistance (overall expression)
C20orf112
SERPINF1
ISYNA1
SMS
PPP2R1A
CCT2
TMC6
PA2G4
RNF2
DCAF13
VPS72
NDUFS2
AEN
RPL6
NOLC1
RPL21
DDX39B
ATP5A1
RBM34
SF3B4
DLL3
CDK4
SOX4
TP53
HSPA1A
CTSL1
LAMP2
TAPBP
JUN
HLA-A
HLA-B
SOSTM1
HLA-H
CD59
B2M
HLA-C
CD47
ITGA6
CD58
CTSB
DCBLD2
S100A6
HTATIP2
EMP1
HLA-F
KLF4
CD9
TSC22D3
ATF3
NNMT
IL1RAP
PRKCDBP
ANXA1
BCL6
MT1M
KCNN4
MT1E
MT2A

FIG. 63C

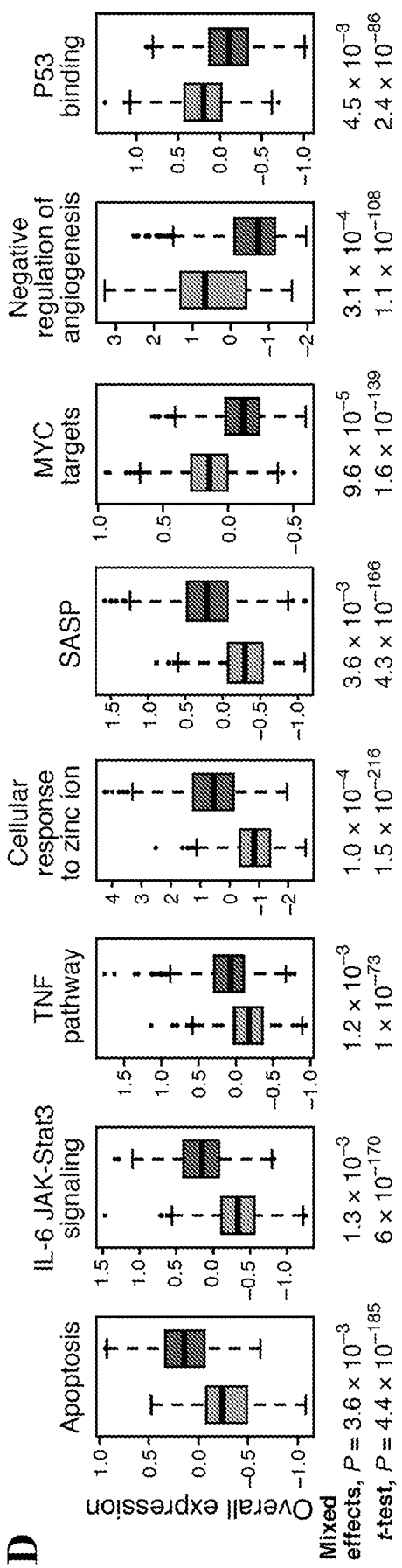

D
Overall expression
Apoptosis
IL-6 JAK-Stat3 signaling
TNF pathway
Cellular response to zinc ion
SASP
MYC targets
Negative regulation of angiogenesis
P53 binding
Mixed effects, P = 3.6 × 10−3
t-test, P = 4.4 × 10−185
1.3 × 10−3
6 × 10−170
1.2 × 10−3
1 × 10−73
1.0 × 10−4
1.5 × 10−216
3.6 × 10−3
4.3 × 10−166
9.6 × 10−5
1.6 × 10−139
3.1 × 10−4
1.1 × 10−108
4.5 × 10−3
2.4 × 10−86
E
Exclusion-up (overall expression)
t-test P = 1 × 10−157
Exclusion-down (overall expression)
t-test P = 3.9 × 10−179
Post-treatment
Untreated

FIG. 63D-E

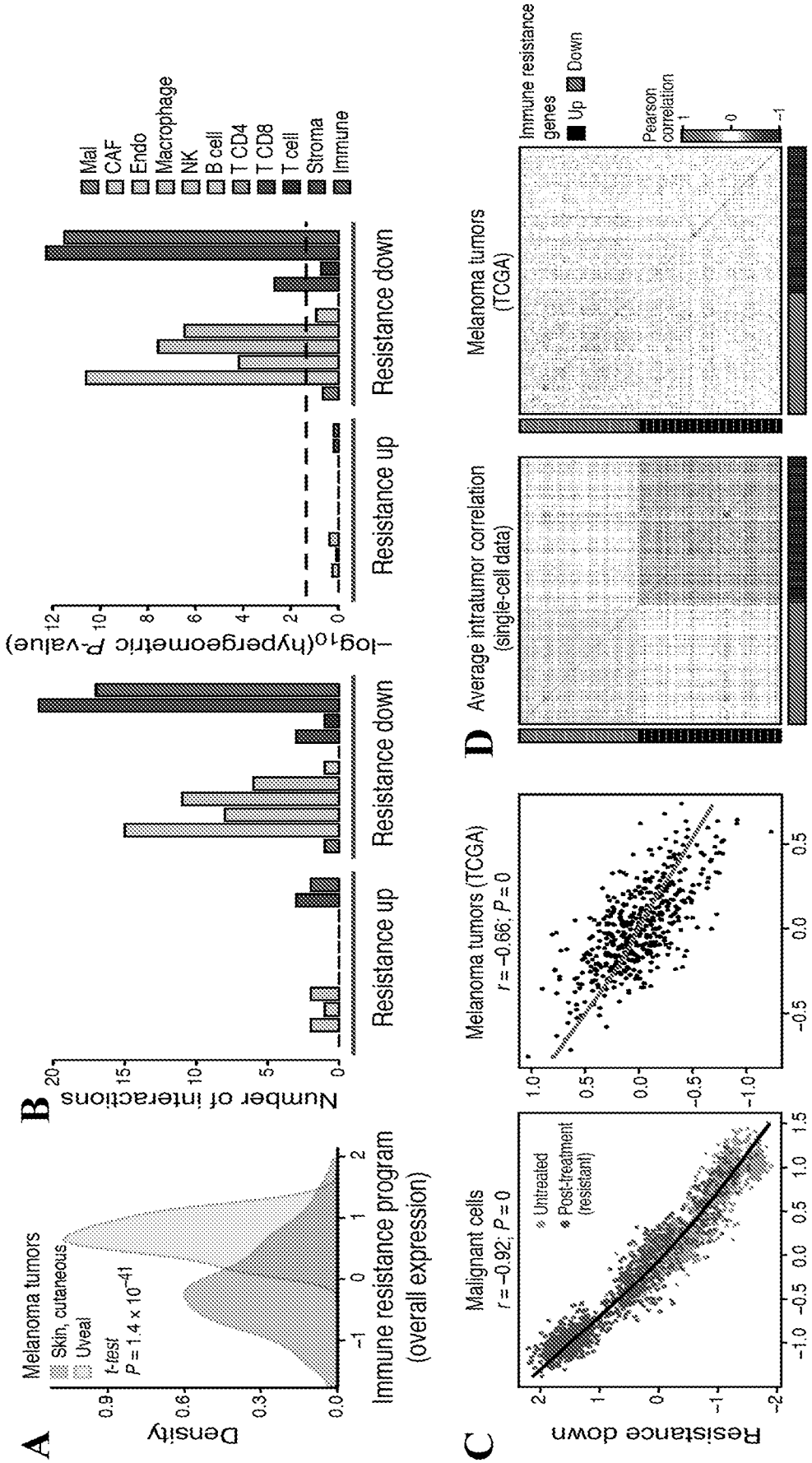

A
Melanoma tumors
Skin, cutaneous
Uveal
t-test
P = 1.4 × 10−41
Density
Immune resistance program
(overall expression)
B
Number of interactions
log10(hypergeometric P-value)
Resistance up
Resistance down
Mal
CAF
Endo
Macrophage
NK
B cell
T CD4
T CD8
T cell
Stroma
Immune
C
Malignant cells
r = −0.92; P = 0
Untreated
Post-treatment (resistant)
Resistance down
Resistance up
Melanoma tumors (TCGA)
r = −0.66; P = 0
Resistance up
D
Average intratumor correlation (single-cell data)
Melanoma tumors (TCGA)
Immune resistance genes
Up
Down
Pearson correlation

FIG. 64A-D

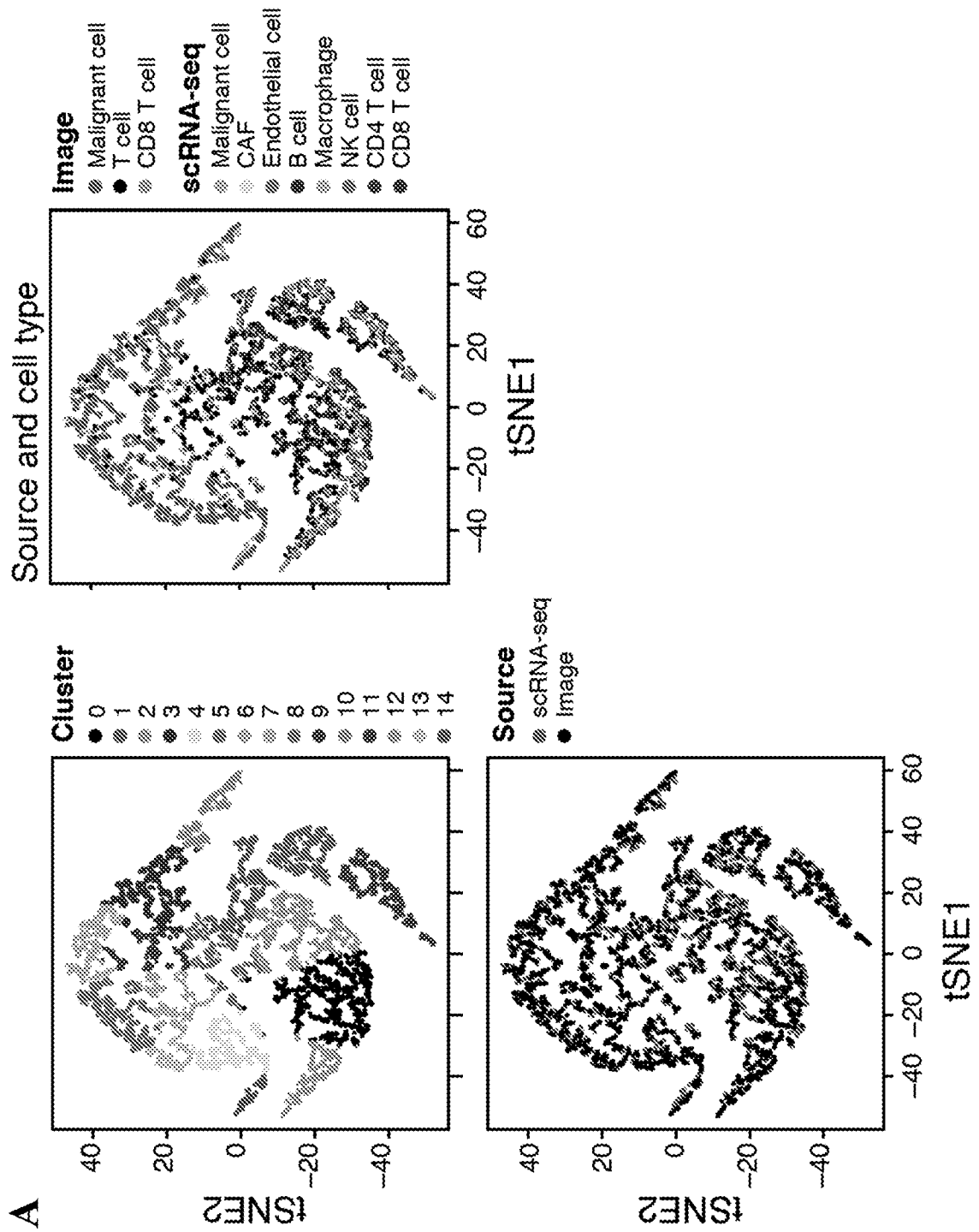

A
Cluster
0
1
2
3
4
5
6
7
8
9
10
11
12
13
14
Source and cell type
image
Malignant cell
T cell
CD8 T cell
scRNA-seq
Malignant cell
CAF
Endothelial cell
B cell
Macrophage
NK cell
CD4 T cell
CD8 T cell
Source
scRNA-seq
Image
tSNE1
tSNE2
40
20
0
−20
−40
−40
−20
0
20
40
60

FIG. 65A

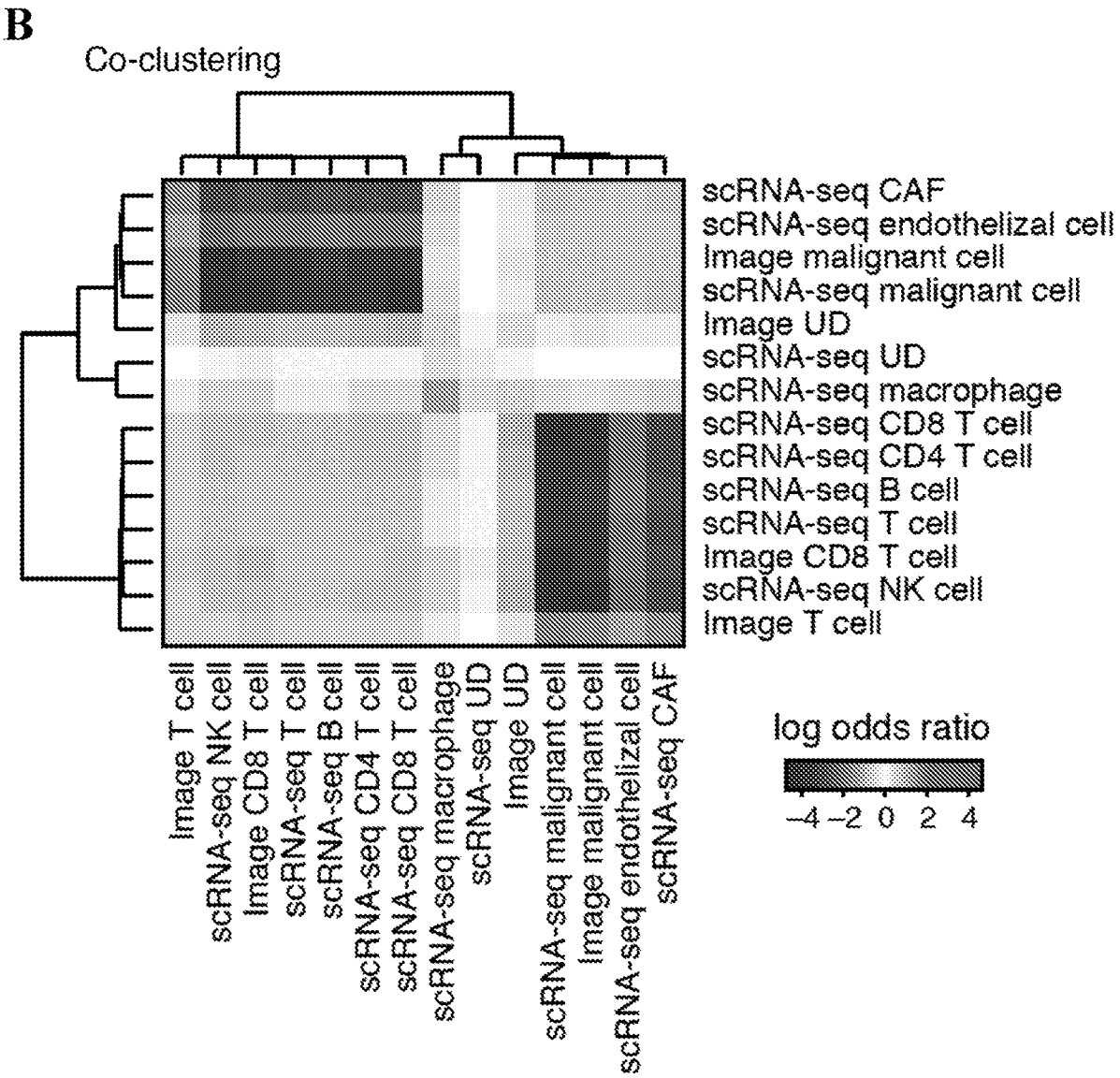

B
Co-clustering
scRNA-seq CAF
scRNA-seq endothelizal cell
Image malignant cell
scRNA-seq malignant cell
Image UD
scRNA-seq UD
scRNA-seq macrophage
scRNA-seq CD8 T cell
scRNA-seq CD4 T cell
scRNA-seq B cell
scRNA-seq T cell
Image CD8 T cell
scRNA-seq NK cell
Image T cell
Image T cell
scRNA-seq NK cell
Image CD8 T cell
scRNA-seq T cell
scRNA-seq B cell
scRNA-seq CD4 T cell
scRNA-seq CD8 T cell
scRNA-seq macrophage
scRNA-seq UD
Image UD
scRNA-seq malignant cell
Image malignant cell
scRNA-seq endothelizal cell
scRNA-seq CAF
log odds ratio
−4 −2 0 2 4

FIG. 65B

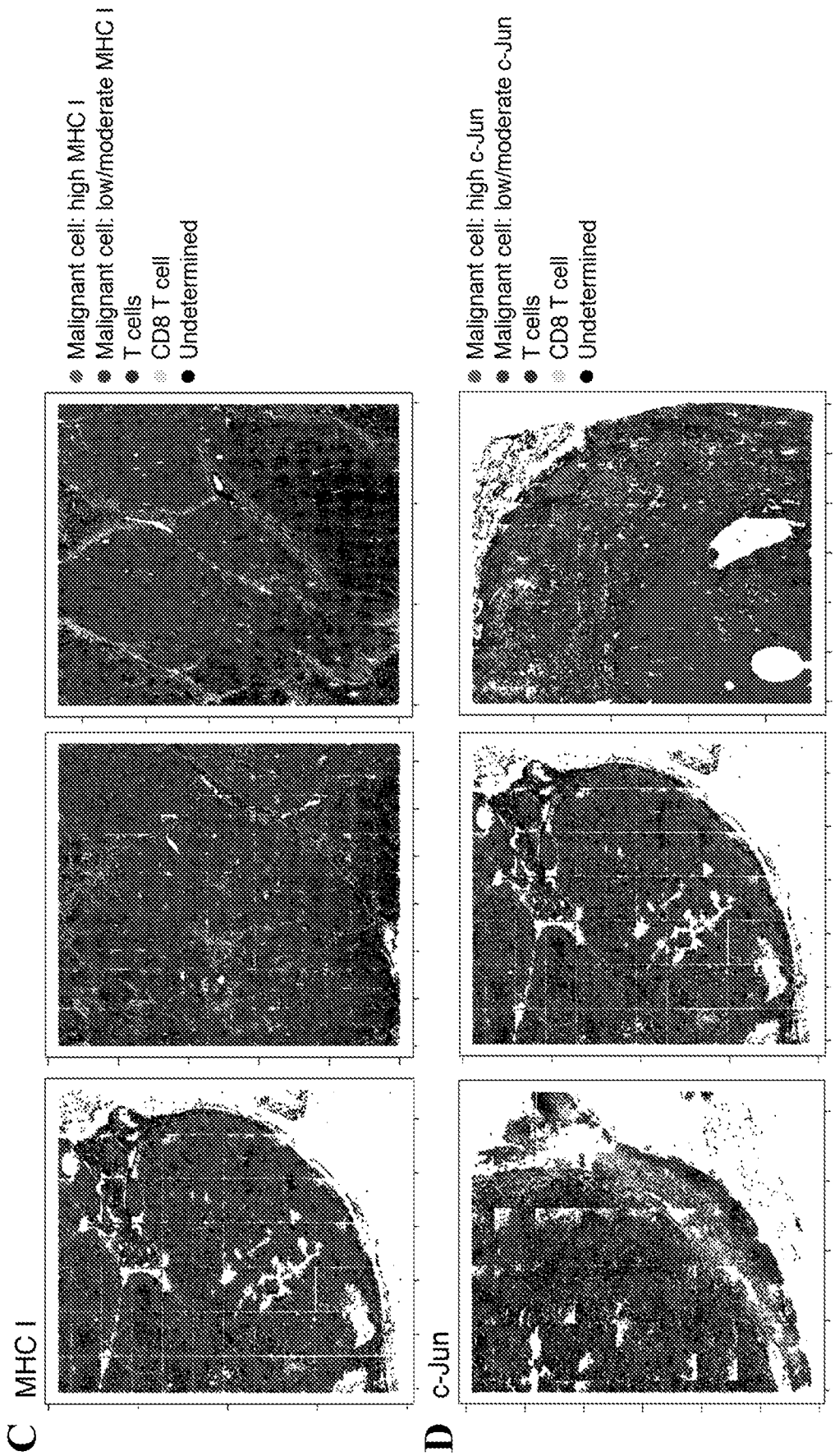

C
MHC I
Malignant cell: high MHC I
Malignant cell: low/moderate MHC I
T cells
CD8 T cell
Undetermined
D
c-Jun
Malignant cell: high c-Jun
Malignant cell: low/moderate c-Jun
T cells
CD8 T cell
Undetermined

FIG. 65C-D

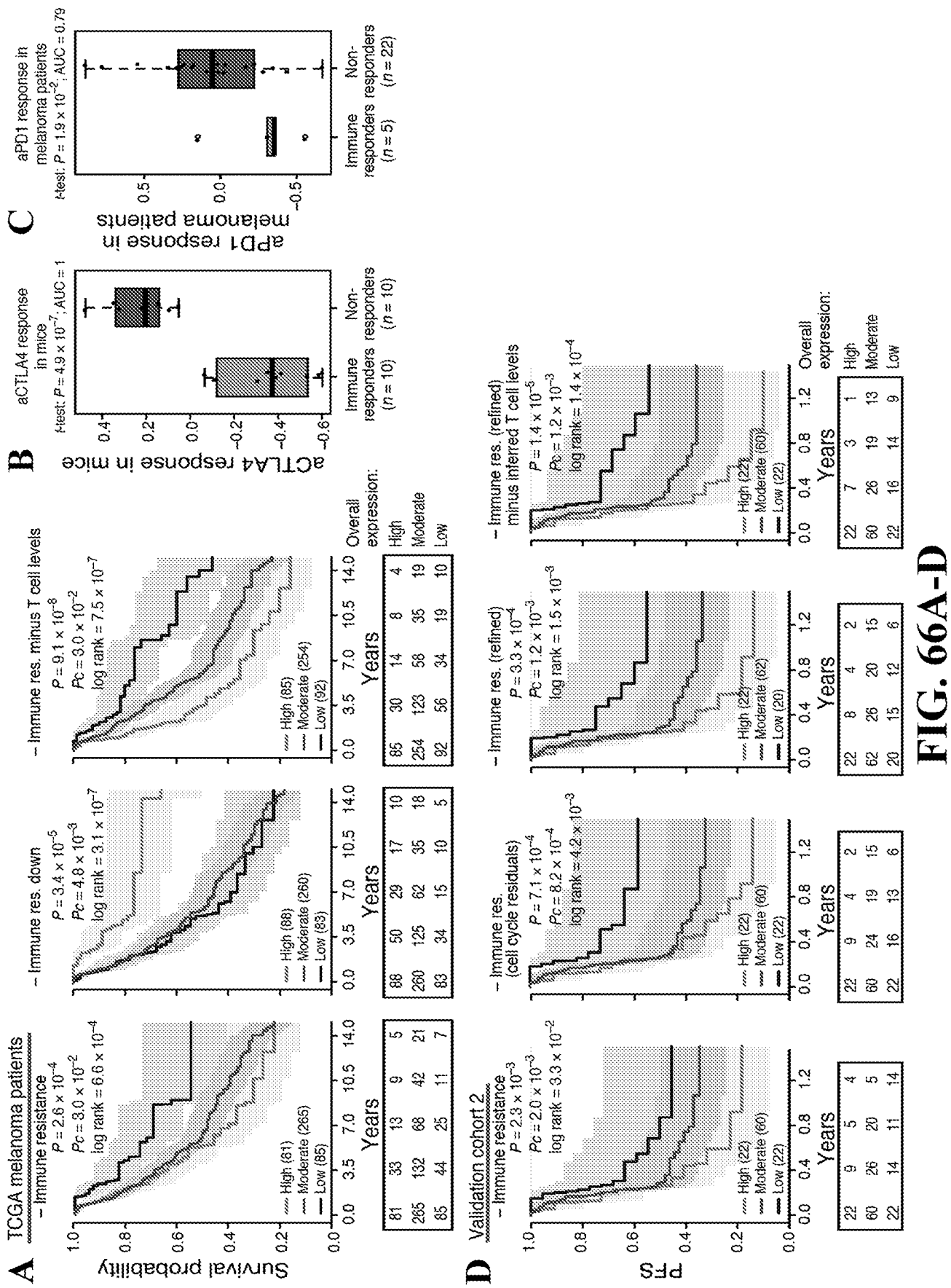

A
TCGA melanoma patients
– Immune resistance
P = 2.6 × 10⁻⁴
Pc = 3.0 × 10⁻²
log rank = 6.6 × 10⁻⁴
Survival probability
High (61)
Moderate (265)
Low (85)
Years
81 33 13 9 5
265 132 68 42 21
85 44 25 11 7
– Immune res. down
P = 3.4 × 10⁻⁵
Pc = 4.8 × 10⁻³
log rank = 3.1 × 10⁻⁷
High (88)
Moderate (260)
Low (83)
Years
88 50 29 17 10
260 125 62 35 18
83 34 15 10 5
– Immune res. minus T cell levels
P = 9.1 × 10⁻⁸
Pc = 3.0 × 10⁻²
log rank = 7.5 × 10⁻⁷
High (85)
Moderate (254)
Low (92)
Years
85 30 14 8 4
254 123 58 35 19
92 56 34 19 10
Overall expression:
High
Moderate
Low
B
aCTLA4 response in mice
Mest: P = 4.9 × 10⁻⁷; AUC = 1
aCTLA4 response in mice
Immune responders (n = 10)
Non-responders (n = 10)
C
aPD1 response in melanoma patients
Mest: P = 1.9 × 10⁻²; AUC = 0.79
aPD1 response in melanoma patients
Immune responders (n = 5)
Non-responders (n = 22)
D
Validation cohort 2
– Immune resistance
P = 2.3 × 10⁻³
Pc = 2.0 × 10⁻³
log rank = 3.3 × 10⁻²
PFS
High (22)
Moderate (60)
Low (22)
Years
22 9 5 4
60 26 20 5
22 14 11 14
– Immune res. (cell cycle residuals)
P = 7.1 × 10⁻⁴
Pc = 8.2 × 10⁻⁴
log rank = 4.2 × 10⁻³
High (22)
Moderate (60)
Low (22)
Years
22 9 4 2
60 24 19 15
22 16 13 6
– Immune res. (refined)
P = 3.3 × 10⁻⁴
Pc = 1.2 × 10⁻³
log rank = 1.5 × 10⁻³
High (22)
Moderate (62)
Low (20)
Years
22 8 4 2
62 26 20 15
20 15 12 6
– Immune res. (refined) minus inferred T cell levels
P = 1.4 × 10⁻⁵
Pc = 1.2 × 10⁻³
log rank = 1.4 × 10⁻⁴
High (22)
Moderate (60)
Low (22)
Years
22 7 3 1
60 26 19 13
22 16 14 9
Overall expression:
High
Moderate
Low

FIG. 66A-D

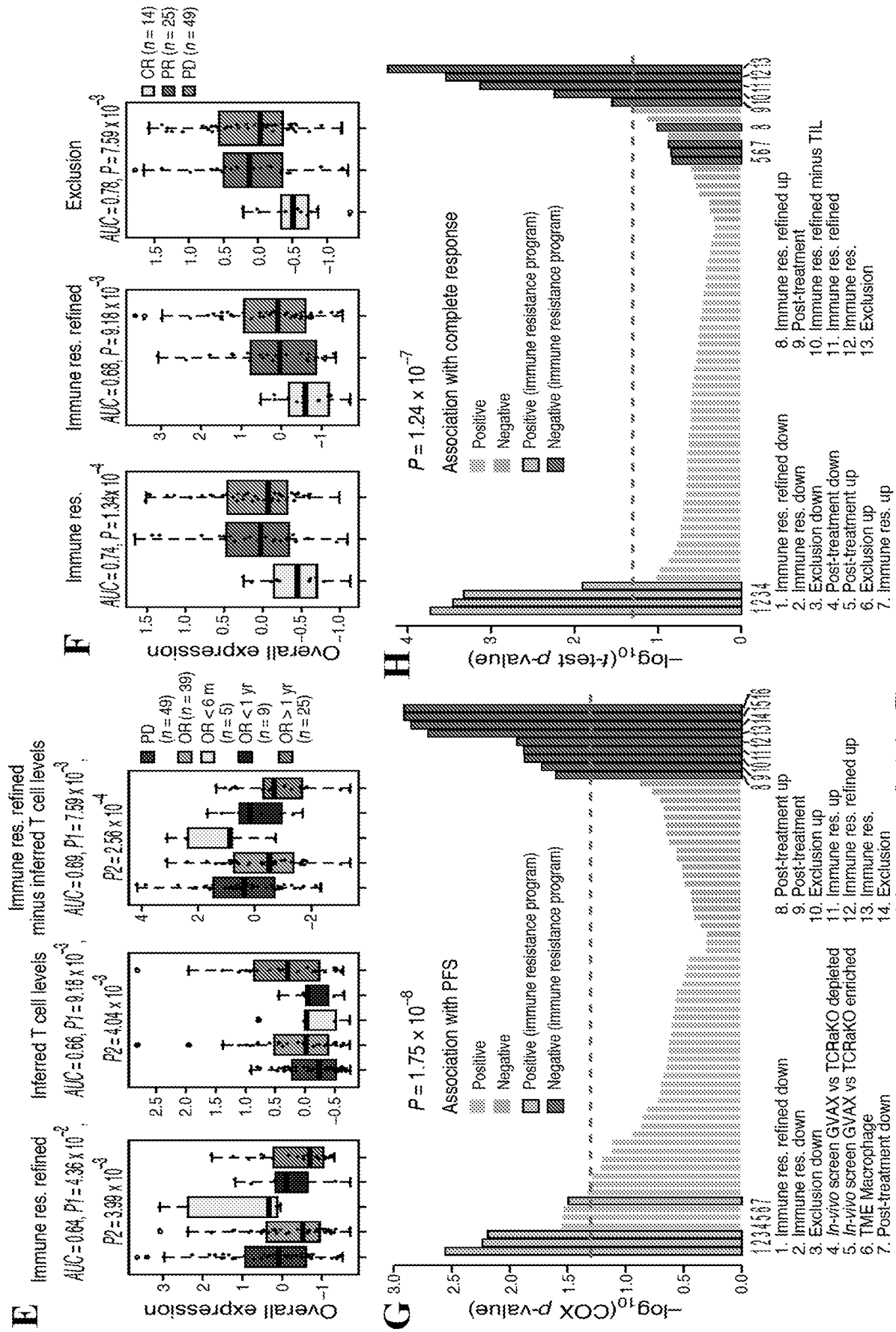

E
Immune res. refined
AUC = 0.64, P1 = 4.36 x 10^-2
P2 = 3.99 x 10^-3
Inferred T cell levels
AUC = 0.66, P1 = 9.16 x 10^-3
P2 = 4.04 x 10^-3
Immune res. refined minus inferred T cell levels
AUC = 0.69, P1 = 7.59 x 10^-3
P2 = 2.56 x 10^-4
Overall expression
PD (n = 49)
OR (n = 39)
OR < 6 m (n = 5)
OR < 1 yr (n = 9)
OR > 1 yr (n = 25)
F
Immune res.
AUC = 0.74, P = 1.34 x 10^-4
Immune res. refined
AUC = 0.68, P = 9.18 x 10^-3
Exclusion
AUC = 0.78, P = 7.59 x 10^-3
Overall expression
CR (n = 14)
PR (n = 25)
PD (n = 49)
G
P = 1.75 x 10^-8
Association with PFS
Positive
Negative
Positive (immune resistance program)
Negative (immune resistance program)
−log10(COX p-value)
1. Immune res. refined down
2. Immune res. down
3. Exclusion down
4. In-vivo screen GVAX vs TCRaKO depleted
5. In-vivo screen GVAX vs TCRaKO enriched
6. TME Macrophage
7. Post-treatment down
8. Post-treatment up
9. Post-treatment
10. Exclusion up
11. Immune res. up
12. Immune res. refined up
13. Immune res.
14. Exclusion
15. Immune res. refined minus TIL
16. Immune res. refined
H
P = 1.24 x 10^-7
Association with complete response
Positive
Negative
Positive (immune resistance program)
Negative (immune resistance program)
−log10(t-test p-value)
1. Immune res. refined down
2. Immune res. down
3. Exclusion down
4. Post-treatment down
5. Post-treatment up
6. Exclusion up
7. Immune res. up
8. Immune res. refined up
9. Post-treatment
10. Immune res. refined minus TIL
11. Immune res. refined
12. Immune res.
13. Exclusion

FIG. 66E-H

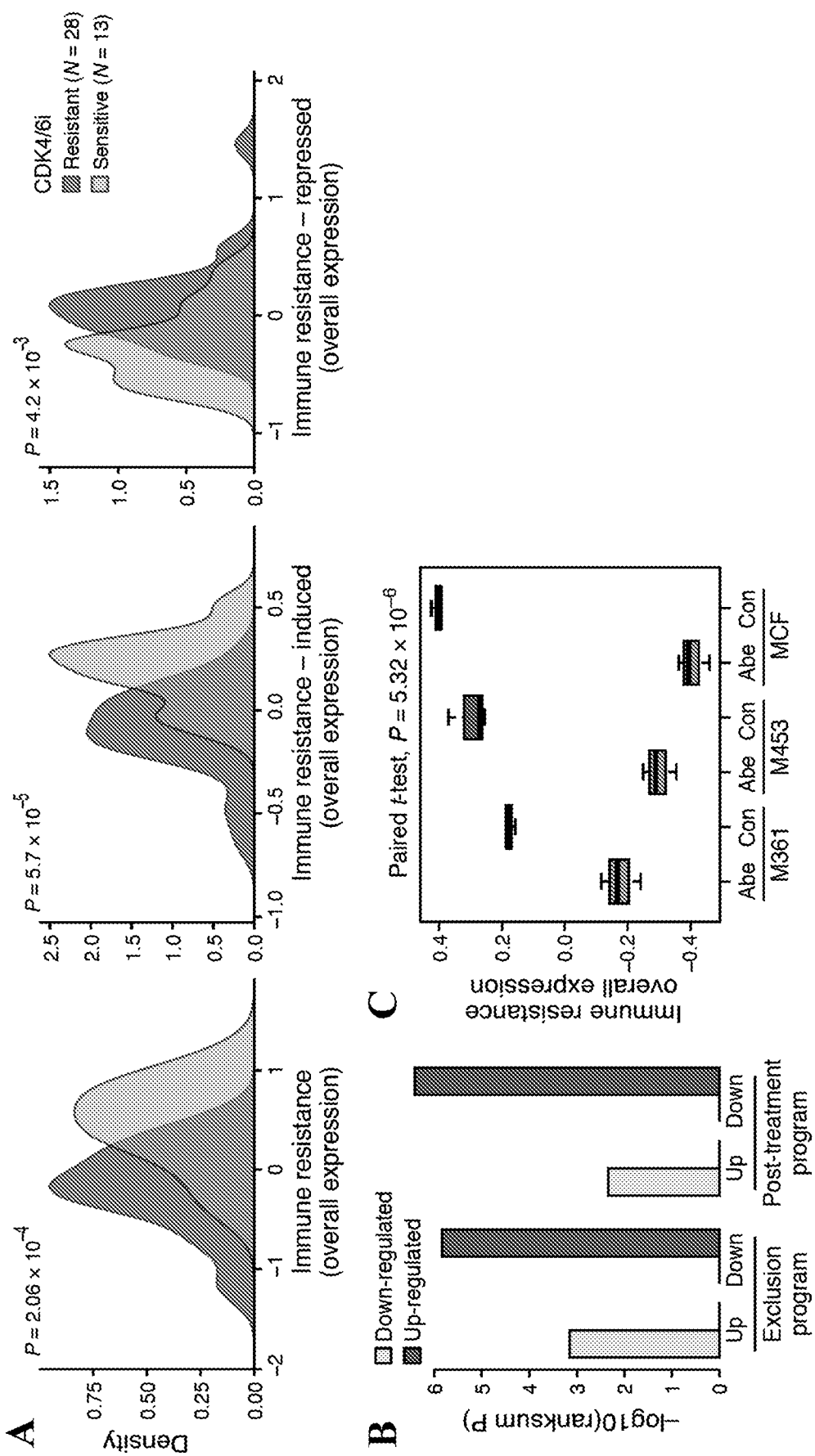

A
Density
P = 2.06 × 10−4
Immune resistance (overall expression)
P = 5.7 × 10−5
Immune resistance – induced (overall expression)
P = 4.2 × 10−3
Immune resistance – repressed (overall expression)
CDK4/6i
Resistant (N = 28)
Sensitive (N = 13)
B
Down-regulated
Up-regulated
−log10(ranksum P)
Up
Down
Exclusion program
Post-treatment program
C
Paired t-test, P = 5.32 × 10−6
Immune resistance overall expression
Abe Con
M361
M453
MCF

FIG. 67A-C


D
DMSO
Abemaciclib
(CDK4/6 inhibitor)
Immune resistance up
Immune resistance down
Immune resistance
(overall expression)
−0.4
0.0
0.4
Breast cancer cell lines
−2
0
2
Row Z score
DDX39B
UHRF1
HMGB1
ANP32E
MCM7
KIAA0101
CTPS1
SNRPD1
SNRPB
HNRNPH1
TUBA1B
IL F2
FBL
PTMA
A1PHNRN
SET
CYBPAC
LSM4
TP53
YWHAE
IGSF8
ARL6IP5
SCARB2
CRELD1
CTSO
CD63
CTSL1
FOS
APLP2
HLA−F
ARSA
CTSD
GPR155
ITM2B
SEL1L
LAMP2
NPC2
GAA
GRN
PSAP
SDC3

FIG. 67D

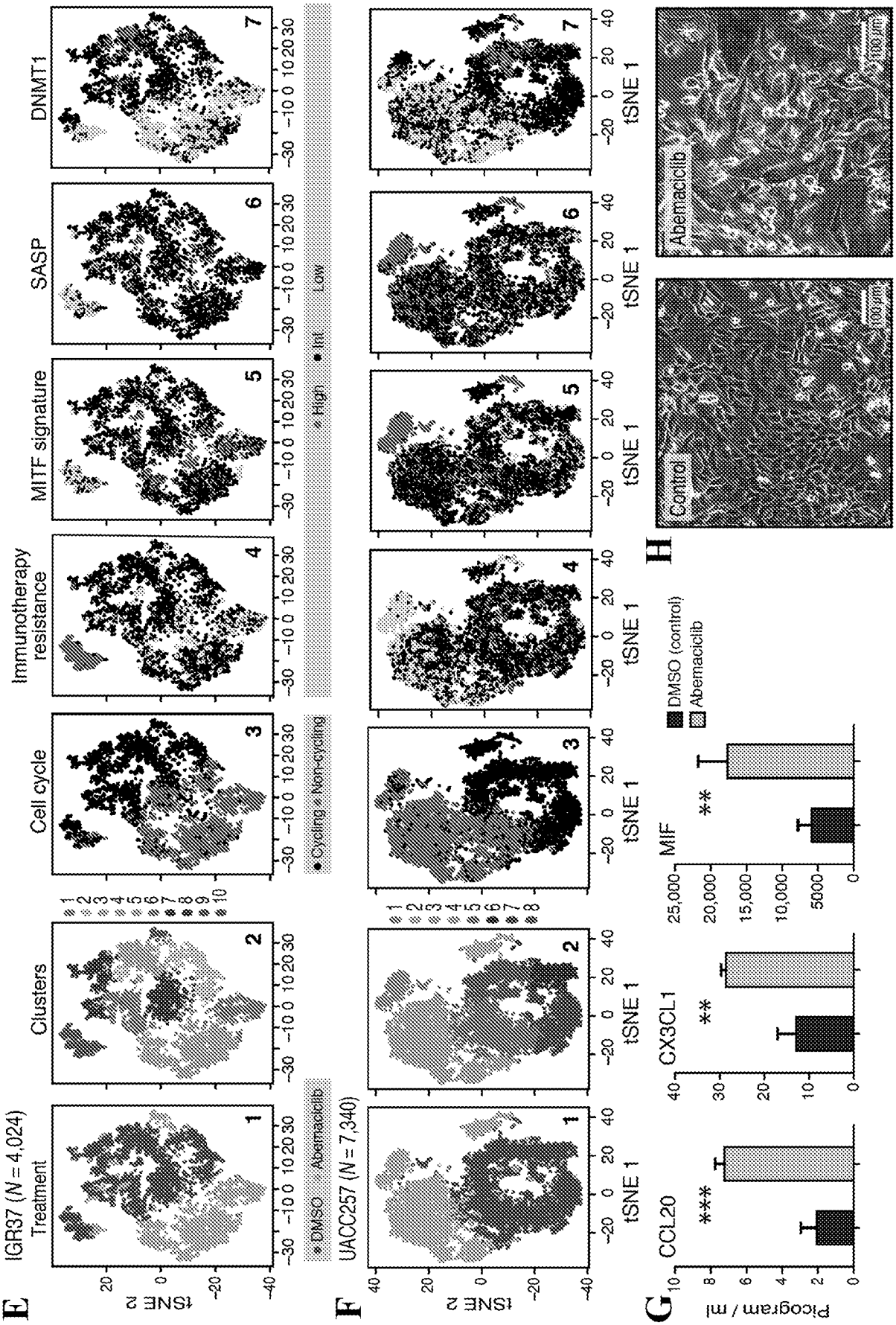

E
IGR37 (N = 4,024)
Treatment
Clusters
Cell cycle
Immunotherapy resistance
MITF signature
SASP
DNMT1
DMSO
Abemaciclib
Cycling
Non-cycling
High
Int
Low
tSNE 1
tSNE 2
F
UACC257 (N = 7,340)
G
CCL20
CX3CL1
MIF
DMSO (control)
Abemaciclib
Picogram / ml
H
Control
Abemaciclib
100 µm

FIG. 67E-H

A

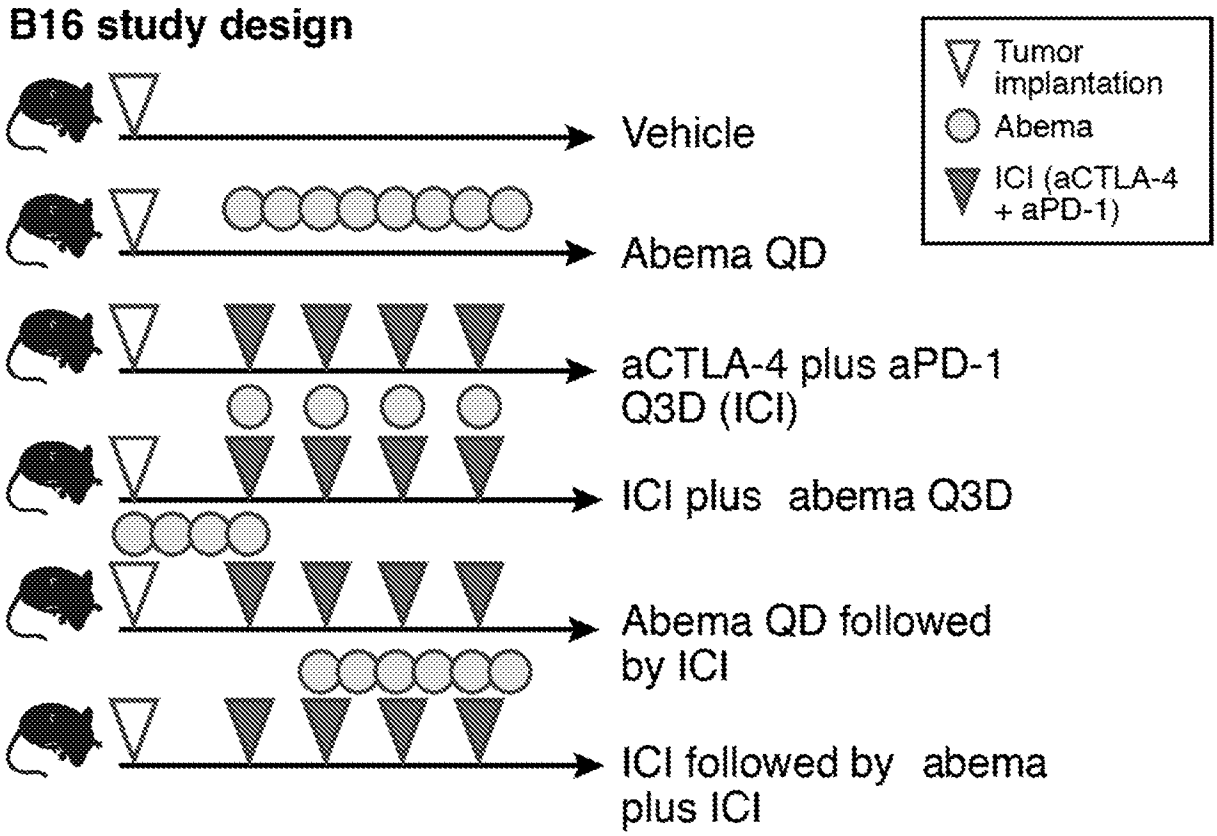

B16 study design
Tumor implantation
Abema
ICI (aCTLA-4 + aPD-1)
Vehicle
Abema QD
aCTLA-4 plus aPD-1 Q3D (ICI)
ICI plus abema Q3D
Abema QD followed by ICI
ICI followed by abema plus ICI

FIG. 68A

B

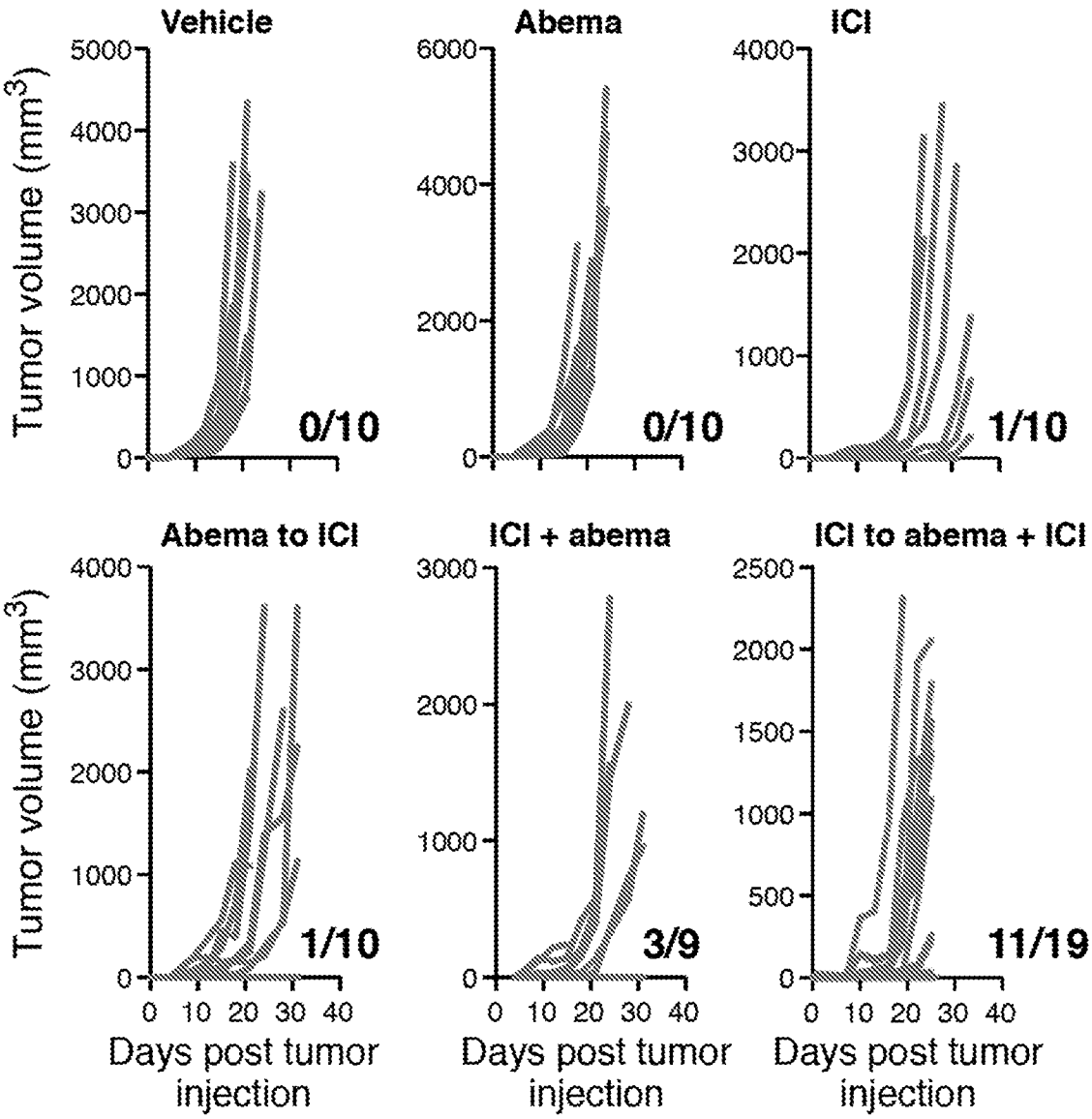

Vehicle
Abema
ICI
Abema to ICI
ICI + abema
ICI to abema + ICI
Tumor volume (mm3)
0/10
0/10
1/10
1/10
3/9
11/19
Days post tumor injection

FIG. 68B

C

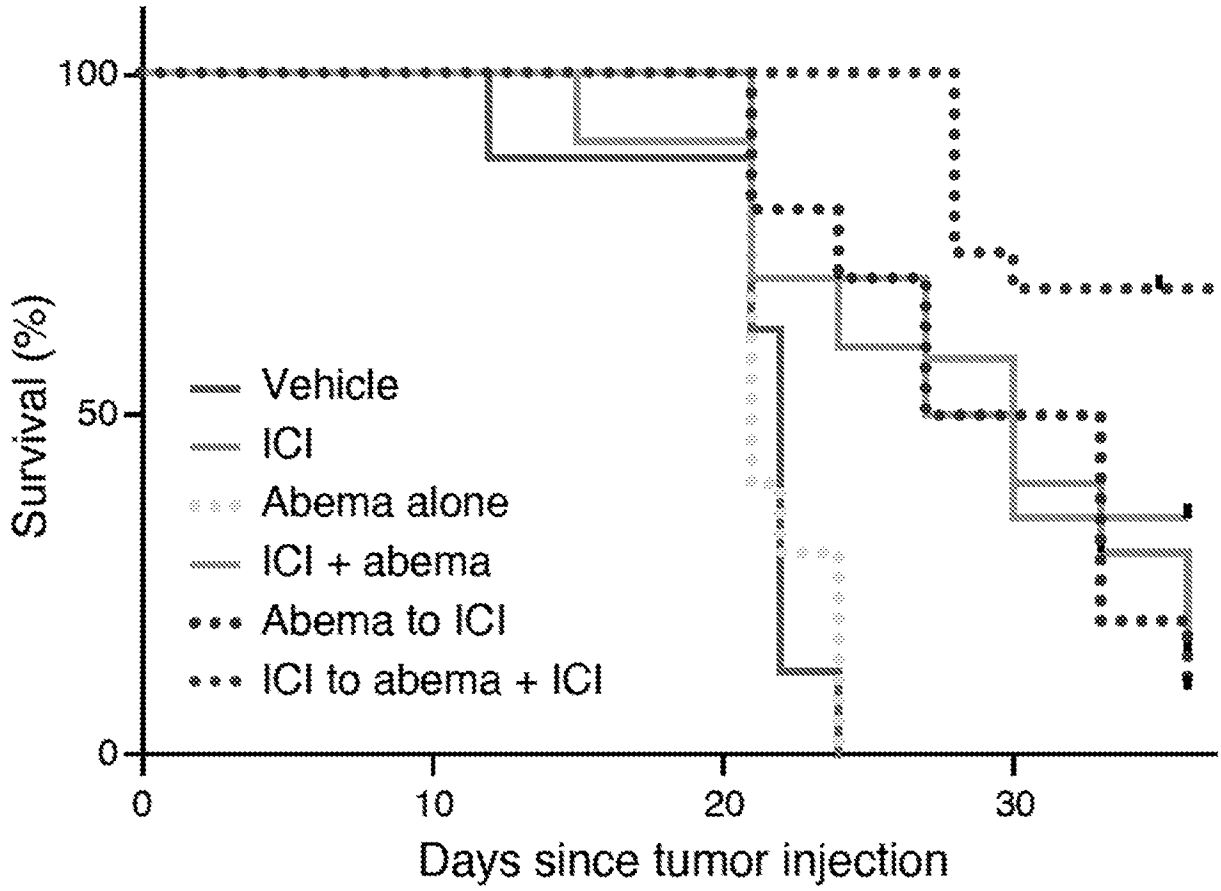

100
50
0
Survival (%)
Vehicle
ICI
Abema alone
ICI + abema
Abema to ICI
ICI to abema + ICI
0
10
20
30
Days since tumor injection

FIG. 68C

D

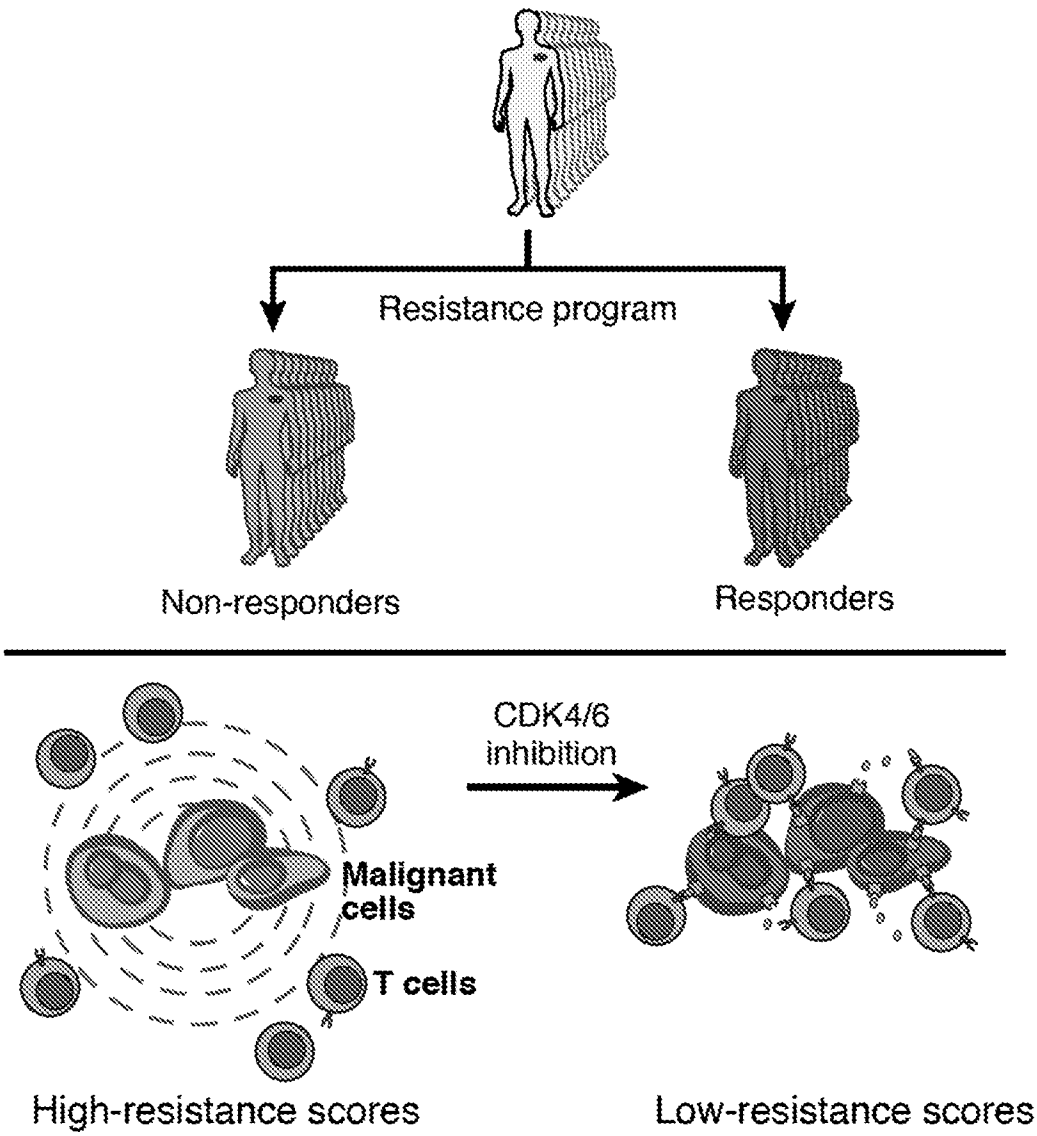

Resistance program
Non-responders
Responders
CDK4/6
inhibition
Malignant
cells
T cells
High-resistance scores
Low-resistance scores

FIG. 68D

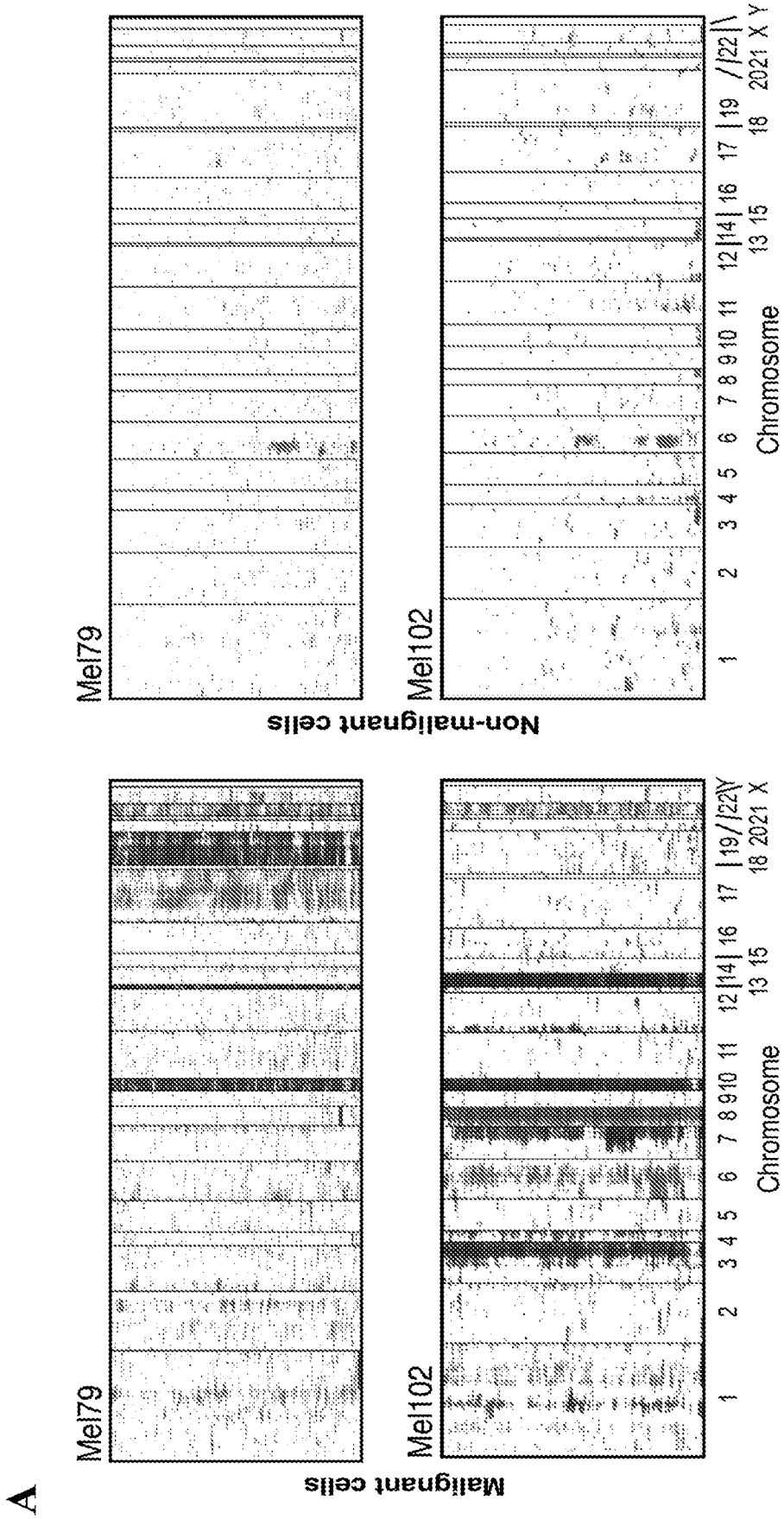

A
Malignant cells
Mel79
Mel102
1 2 3 4 5 6 7 8 9 10 11 12 13 14 15 16 17 18 19/22Y 2021 X
Chromosome
Non-malignant cells
Mel79
Mel102
1 2 3 4 5 6 7 8 9 10 11 12 13 14 15 16 17 18 19 /22 2021 X Y
Chromosome

FIG. 69A

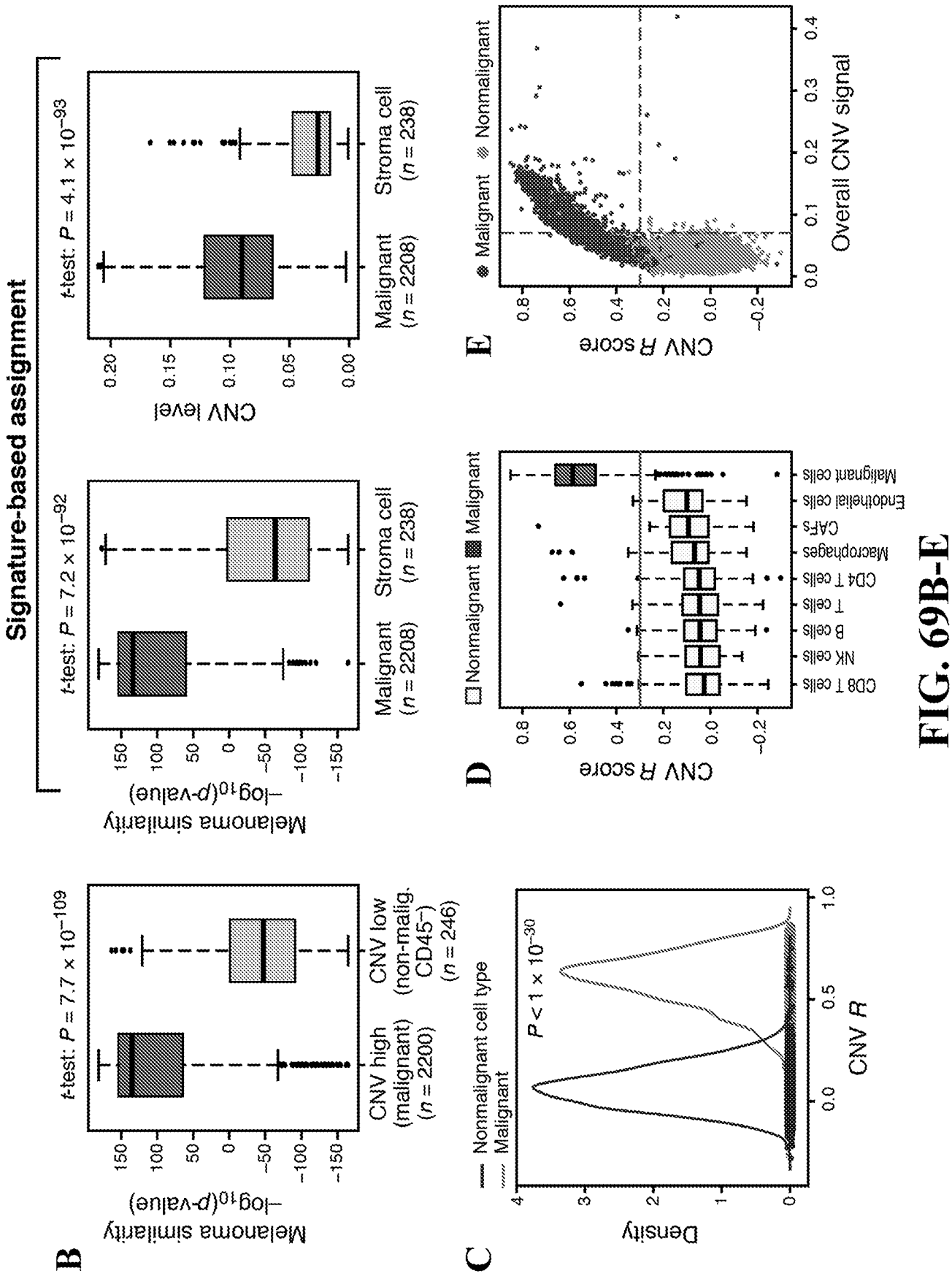

Signature-based assignment
B
t-test: P = 7.7 × 10−109
Melanoma similarity −log10(p-value)
CNV high (malignant) (n = 2200)
CNV low (non-malig. CD45−) (n = 246)
t-test: P = 7.2 × 10−92
Malignant (n = 2208)
Stroma cell (n = 238)
t-test: P = 4.1 × 10−93
CNV level
C
Nonmalignant cell type
Malignant
P < 1 × 10−30
Density
CNV R
D
Nonmalignant
Malignant
CNV R score
CD8 T cells
NK cells
B cells
T cells
CD4 T cells
Macrophages
CAFs
Endothelial cells
Malignant cells
E
Malignant
Nonmalignant
CNV R score
Overall CNV signal

FIG. 69B-E

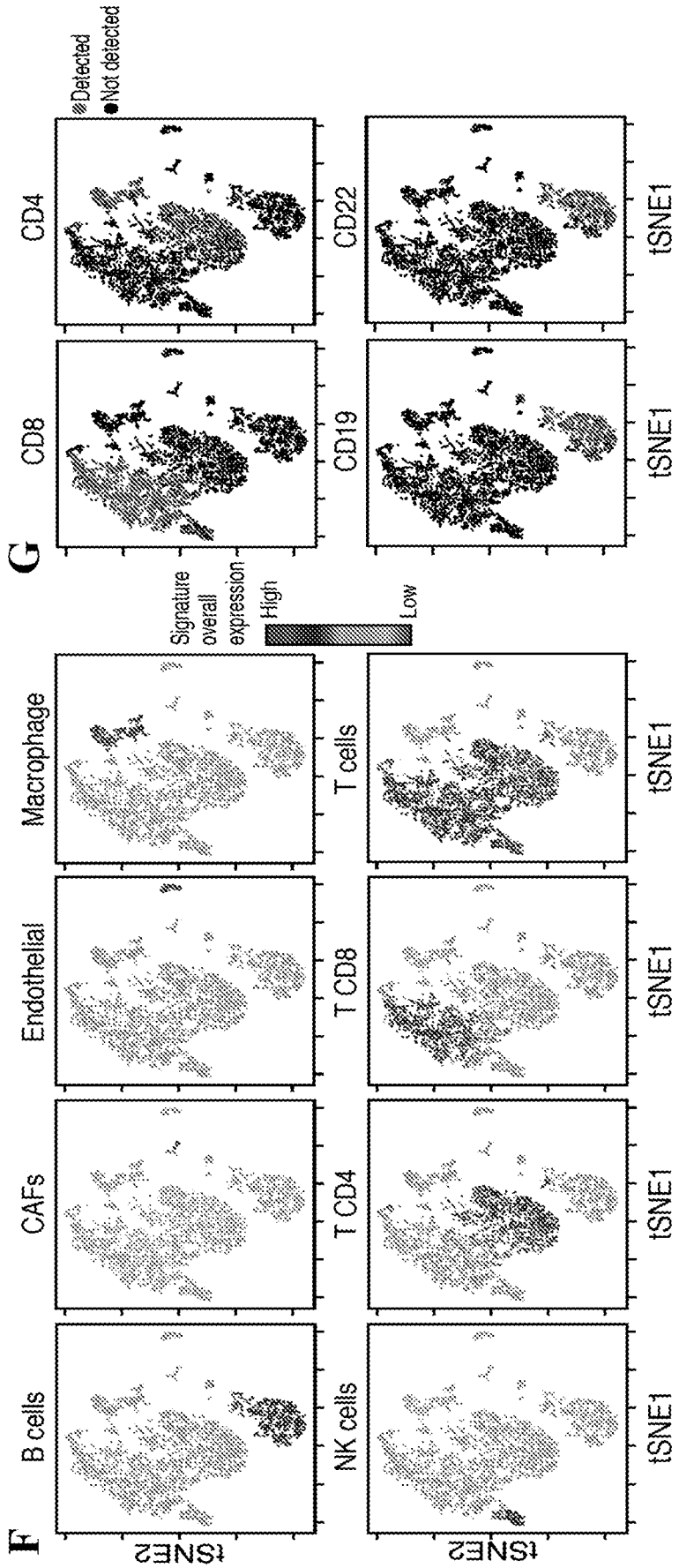

F
B cells
CAFs
Endothelial
Macrophage
NK cells
T CD4
T CD8
T cells
tSNE1
tSNE2
Signature overall expression
High
Low
G
CD4
CD8
CD22
CD19
Detected
Not detected

FIG. 69F-G

A

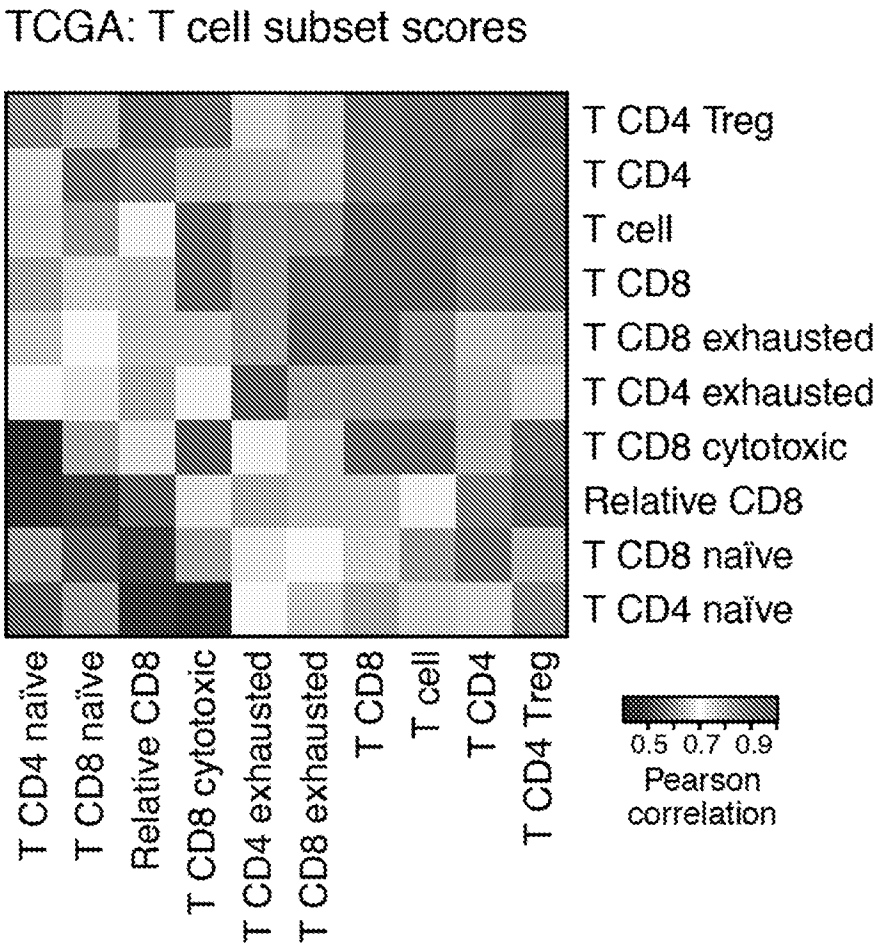

TCGA: T cell subset scores
T CD4 Treg
T CD4
T cell
T CD8
T CD8 exhausted
T CD4 exhausted
T CD8 cytotoxic
Relative CD8
T CD8 naïve
T CD4 naïve
T CD4 naïve
T CD8 naïve
Relative CD8
T CD8 cytotoxic
T CD4 exhausted
T CD8 exhausted
T CD8
T cell
T CD4
T CD4 Treg
0.5 0.7 0.9
Pearson correlation

FIG. 70A

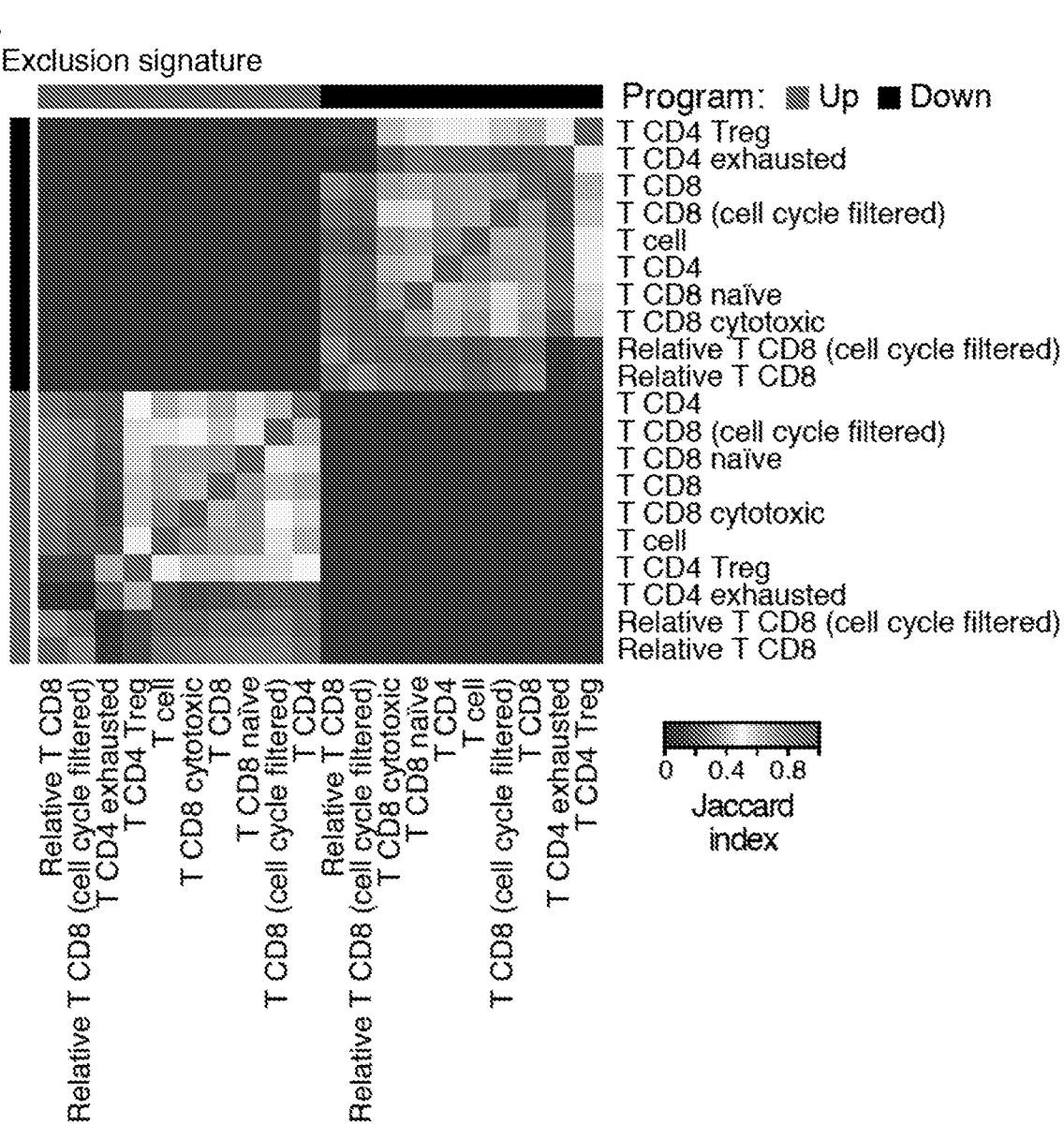

B
Exclusion signature
Program: Up Down
T CD4 Treg
T CD4 exhausted
T CD8
T CD8 (cell cycle filtered)
T cell
T CD4
T CD8 naïve
T CD8 cytotoxic
Relative T CD8 (cell cycle filtered)
Relative T CD8
T CD4
T CD8 (cell cycle filtered)
T CD8 naïve
T CD8
T CD8 cytotoxic
T cell
T CD4 Treg
T CD4 exhausted
Relative T CD8 (cell cycle filtered)
Relative T CD8
Relative T CD8
Relative T CD8 (cell cycle filtered)
T CD4 exhausted
T CD4 Treg
T cell
T CD8 cytotoxic
T CD8
T CD8 naïve
T CD8 (cell cycle filtered)
T CD4
Relative T CD8
Relative T CD8 (cell cycle filtered)
T CD8 cytotoxic
T CD8 naïve
T CD4
T cell
T CD8 (cell cycle filtered)
T CD8
T CD4 exhausted
T CD4 Treg
0 0.4 0.8
Jaccard index

FIG. 70B

C

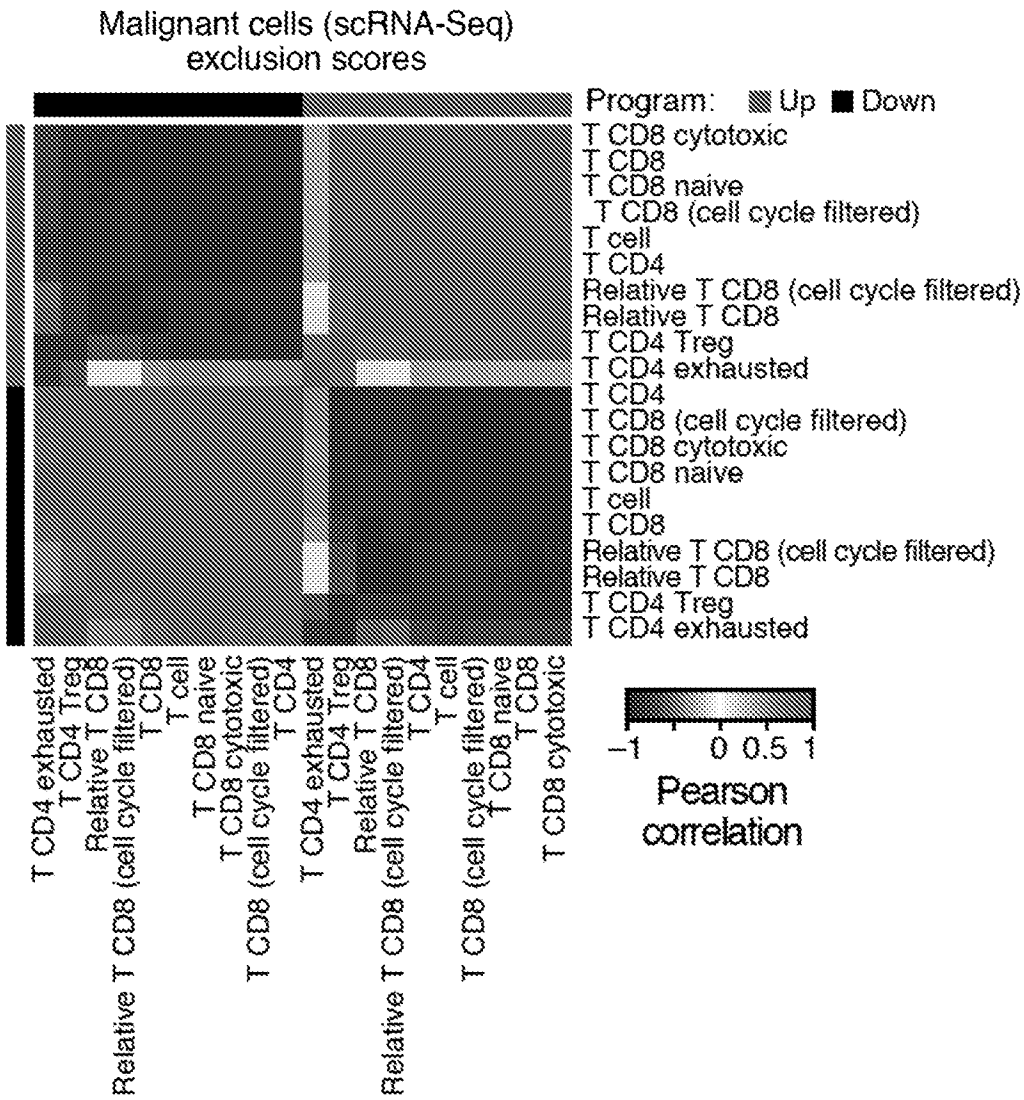

Malignant cells (scRNA-Seq)
exclusion scores
Program: Up Down
T CD8 cytotoxic
T CD8
T CD8 naive
T CD8 (cell cycle filtered)
T cell
T CD4
Relative T CD8 (cell cycle filtered)
Relative T CD8
T CD4 Treg
T CD4 exhausted
T CD4
T CD8 (cell cycle filtered)
T CD8 cytotoxic
T CD8 naive
T cell
T CD8
Relative T CD8 (cell cycle filtered)
Relative T CD8
T CD4 Treg
T CD4 exhausted
T CD4 exhausted
T CD4 Treg
Relative T CD8
Relative T CD8 (cell cycle filtered)
T CD8
T CD4
T cell
T CD8 (cell cycle filtered)
T CD8 naive
T CD8
T CD8 cytotoxic
T CD8 cytotoxic
T CD8 (cell cycle filtered)
T CD4
T CD8 naive
T cell
T CD8
Relative T CD8 (cell cycle filtered)
Relative T CD8
T CD4 Treg
T CD4 exhausted
−1 0 0.5 1
Pearson
correlation

FIG. 70C

C

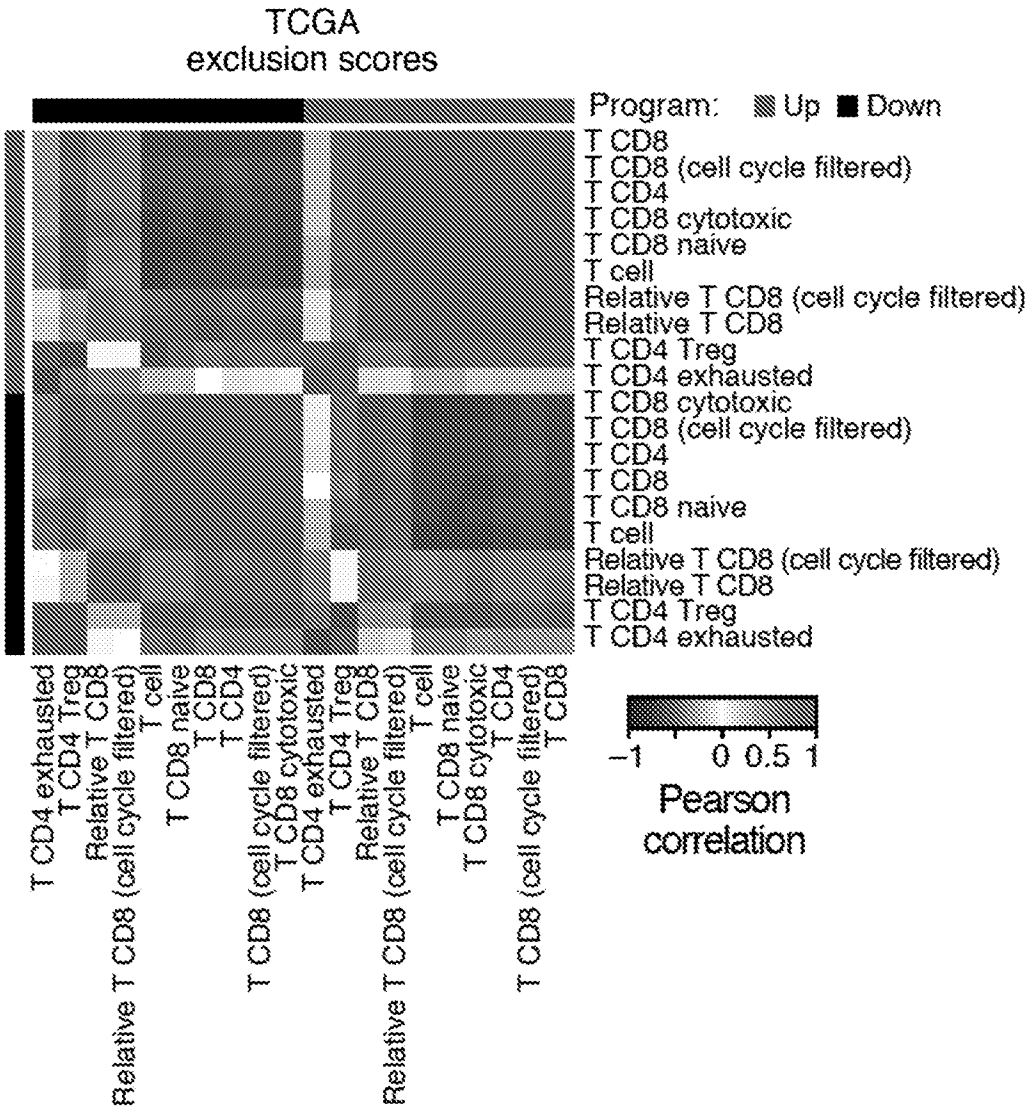


FIG. 70C continued

C

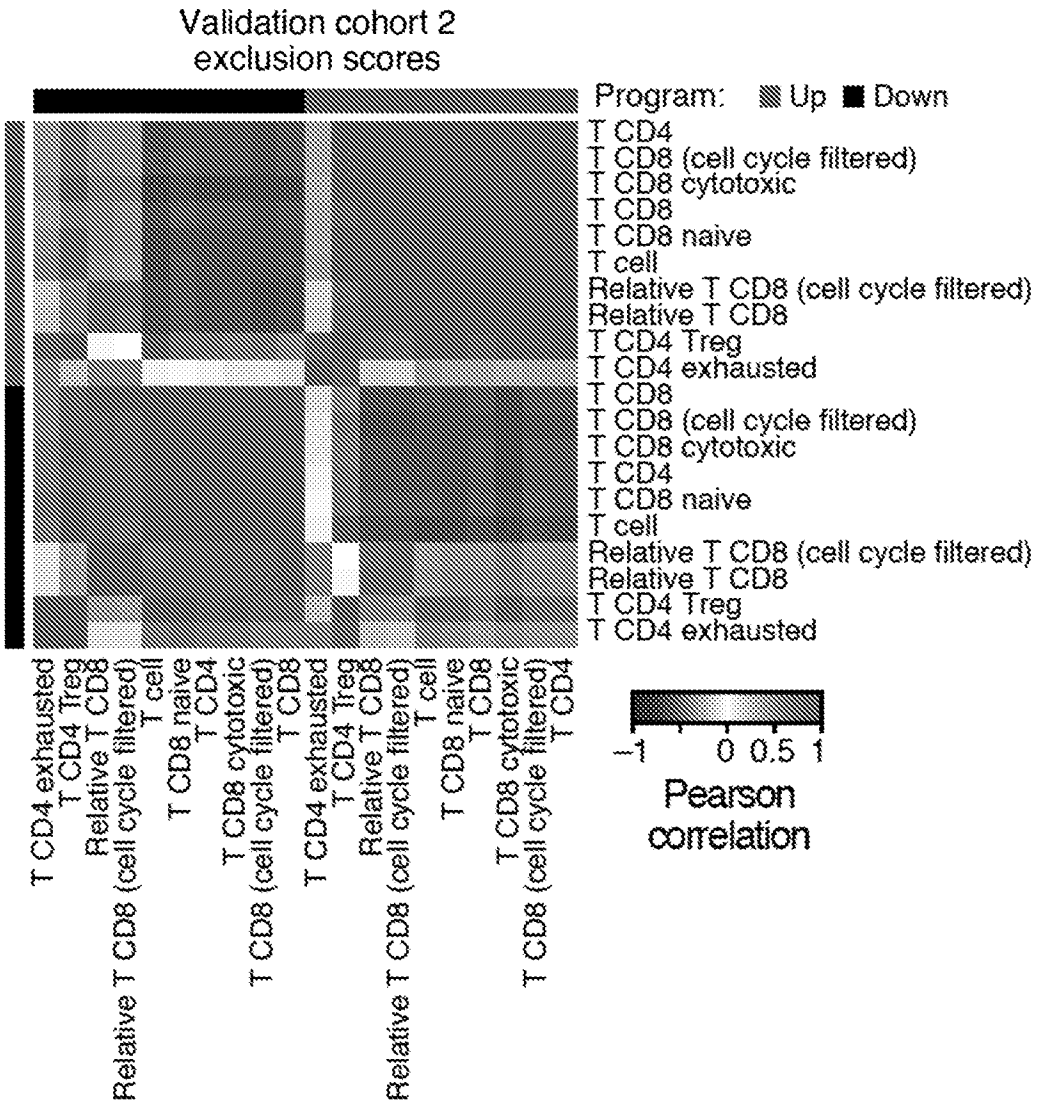


FIG. 70C continued

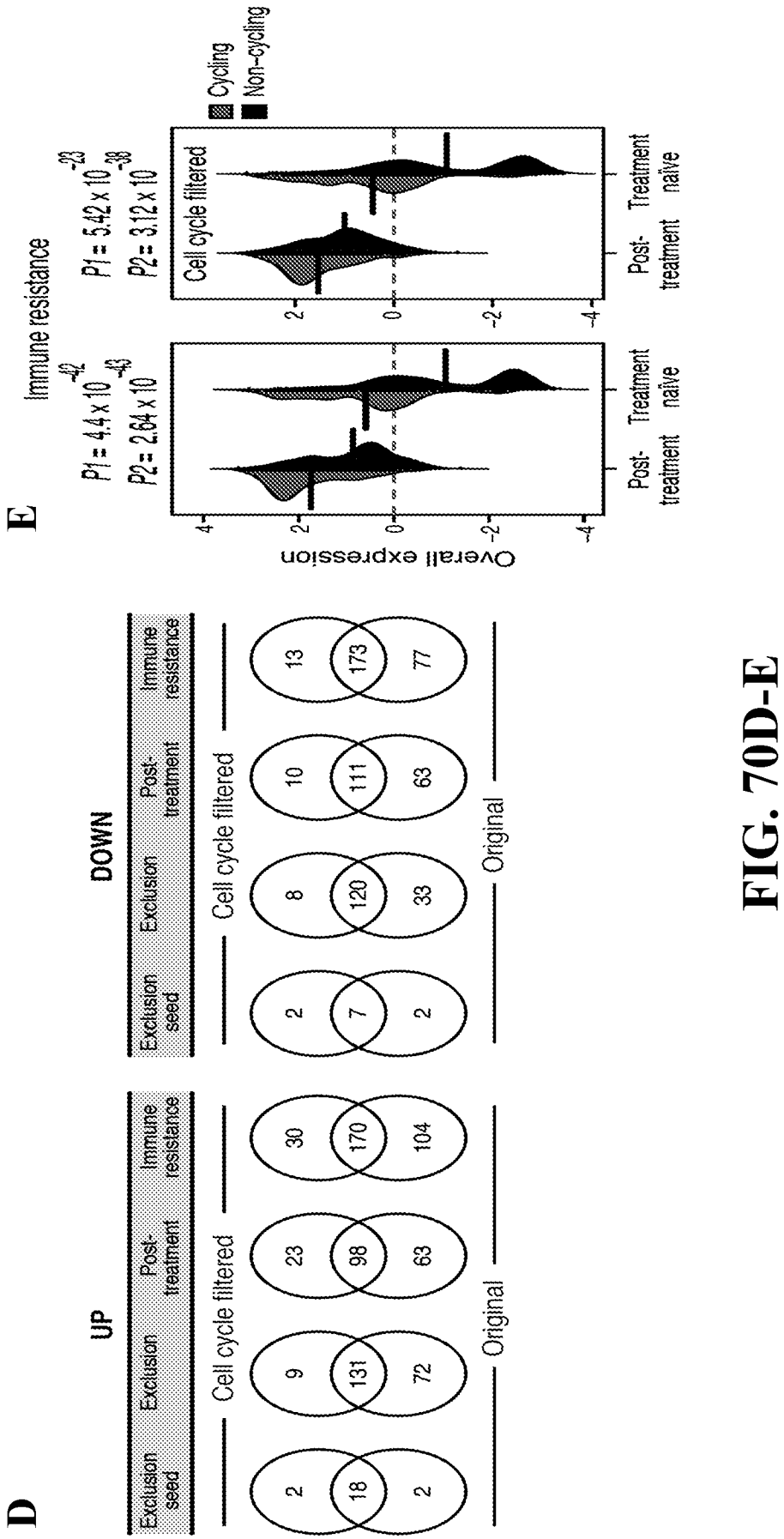

D
UP
Exclusion seed
Exclusion
Post-treatment
Immune resistance
Cell cycle filtered
Original
2
18
9
131
23
98
30
170
2
72
63
104
DOWN
Exclusion seed
Exclusion
Post-treatment
Immune resistance
Cell cycle filtered
Original
2
7
8
120
10
111
13
173
2
33
63
77
E
Immune resistance
P1 = 4.4 x 10^-42
P2 = 2.64 x 10^-43
P1 = 5.42 x 10^-23
P2 = 3.12 x 10^-38
Cycling
Non-cycling
Cell cycle filtered
Overall expression
4
2
0
-2
-4
Post-treatment
Treatment naive

FIG. 70D-E

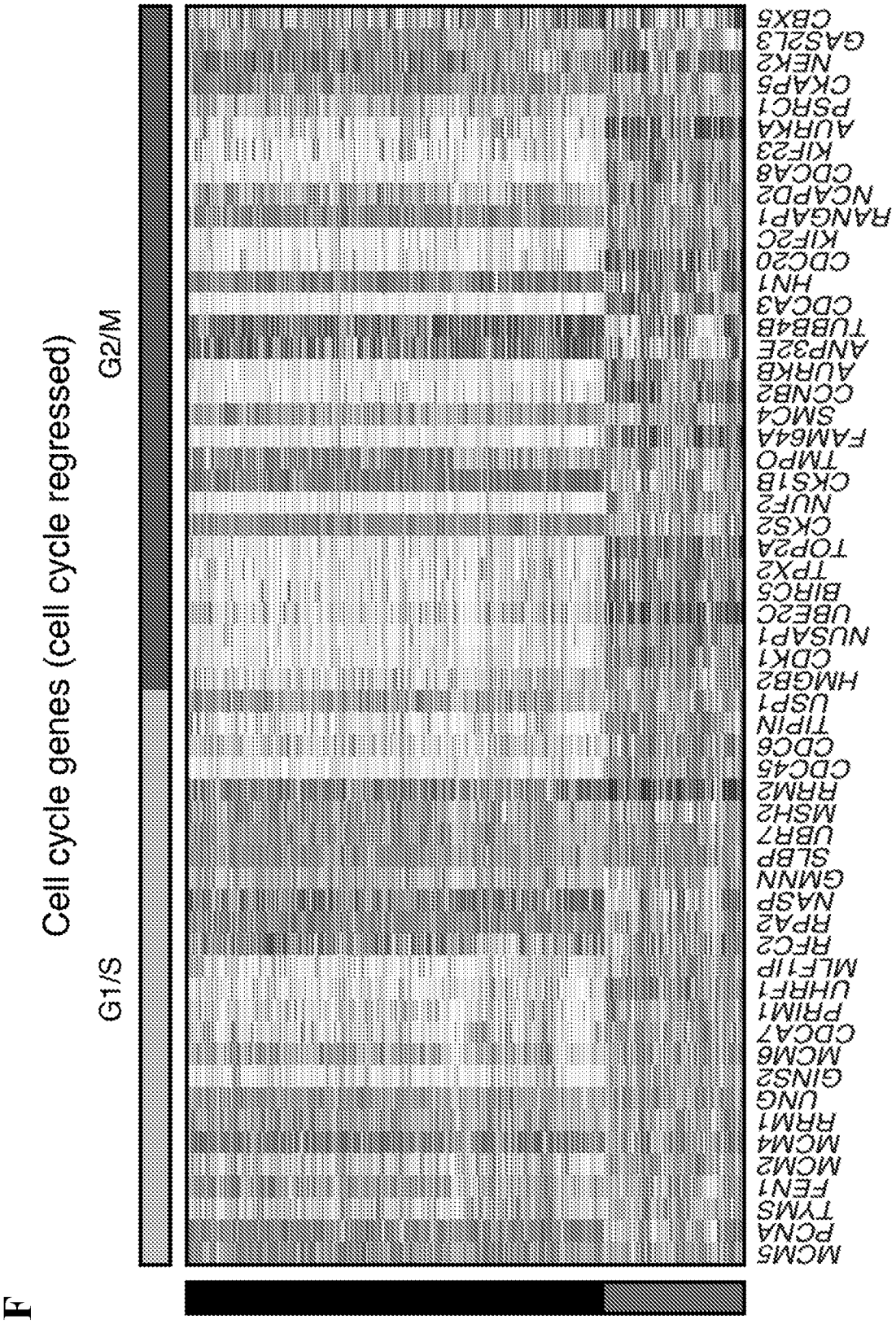

F
Cell cycle genes (cell cycle regressed)
G1/S
G2/M
MCM5
PCNA
TYMS
FEN1
MCM2
MCM4
RRM1
UNG
GINS2
MCM6
CDCA7
PRIM1
UHRF1
MLF1IP
RFC2
RPA2
NASP
GMNN
SLBP
UBR7
MSH2
RRM2
CDC45
CDC6
TIPIN
USP1
HMGB2
CDK1
NUSAP1
UBE2C
BIRC5
TPX2
TOP2A
CKS2
NUF2
CKS1B
TMPO
FAM64A
SMC4
CCNB2
AURKB
ANP32E
TUBB4B
CDCA3
HN1
CDC20
KIF2C
RANGAP1
NCAPD2
CDCA8
KIF23
AURKA
PSRC1
CKAP5
NEK2
GAS2L3
CBX5

FIG. 70F

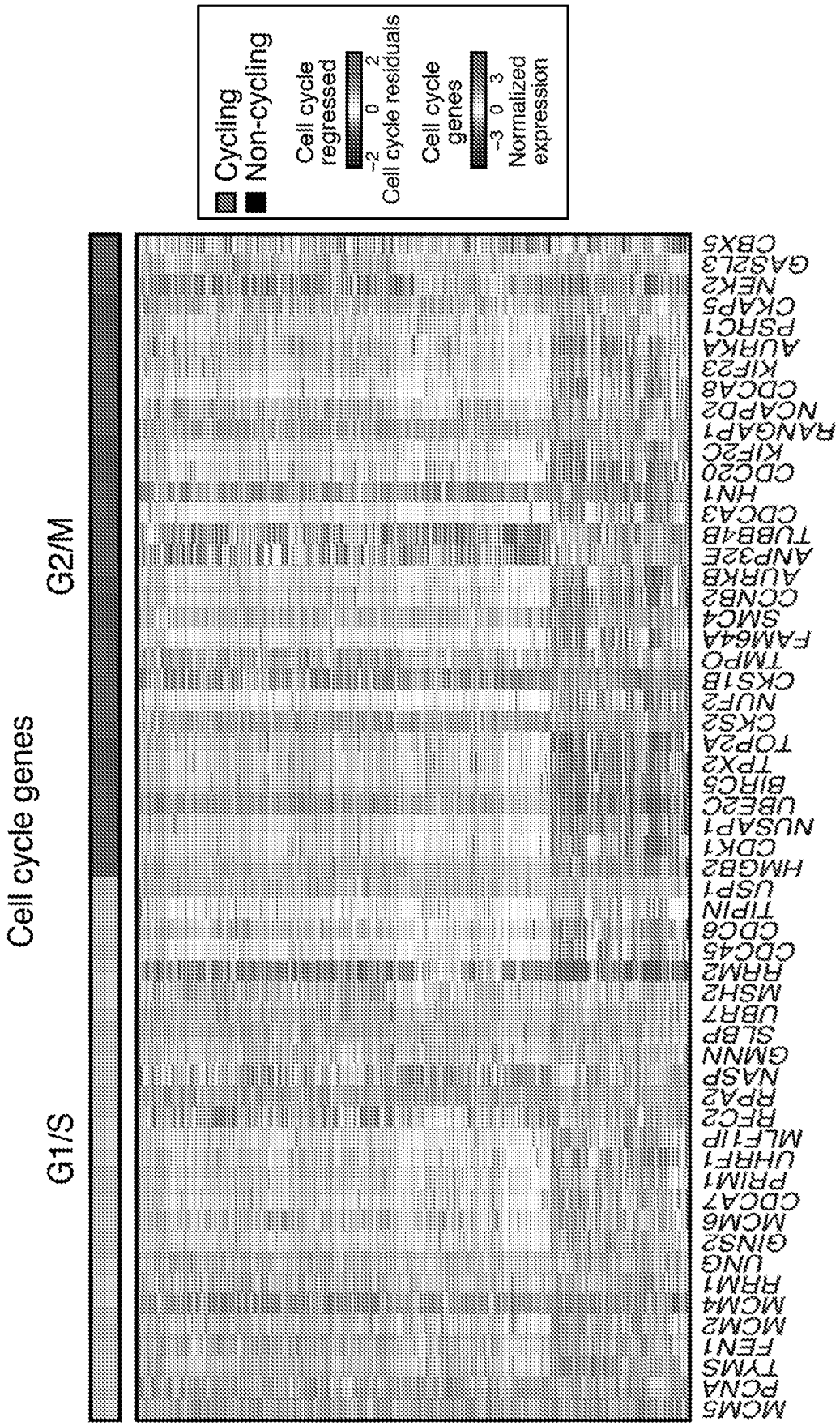


FIG. 70F continued

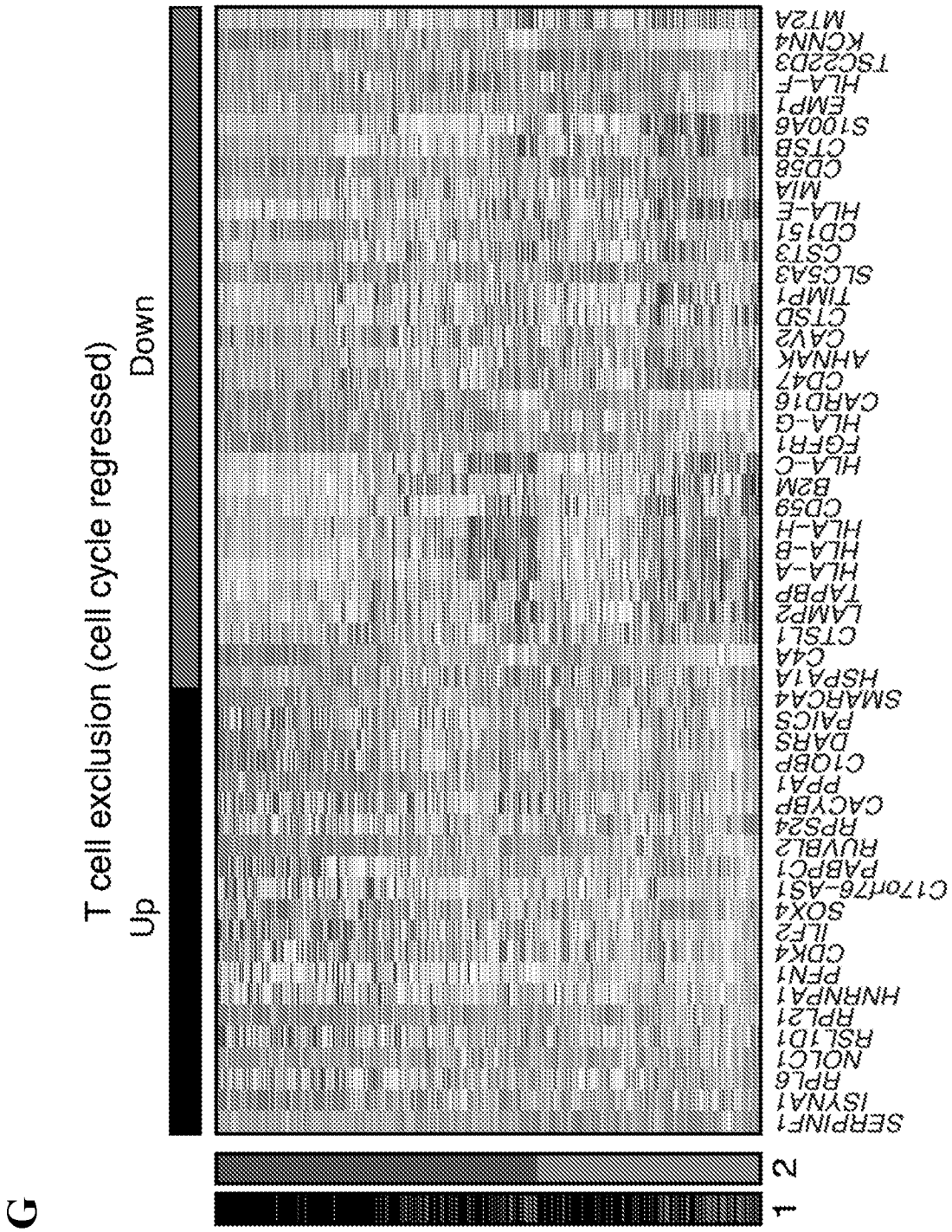

G
T cell exclusion (cell cycle regressed)
Up
Down
1
2
SERPINF1
ISYNA1
RPL6
NOLC1
RSL1D1
RPL21
HNRNPA1
PFN1
CDK4
JLF2
SOX4
C17orf76-AS1
PABPC1
RUVBL2
RPS24
CACYBP
PPA1
C1QBP
DARS
PAICS
SMARCA4
HSPA1A
C4A
CTSL1
LAMP2
TAPBP
HLA-A
HLA-B
HLA-H
CD59
B2M
HLA-C
FGFR1
HLA-G
CARD16
CD47
AHNAK
CAV2
CTSD
TIMP1
SLC5A3
CST3
CD151
HLA-E
MIA
CD58
CTSB
S100A6
EMP1
HLA-F
TSC22D3
KCNN4
MT2A

FIG. 70G

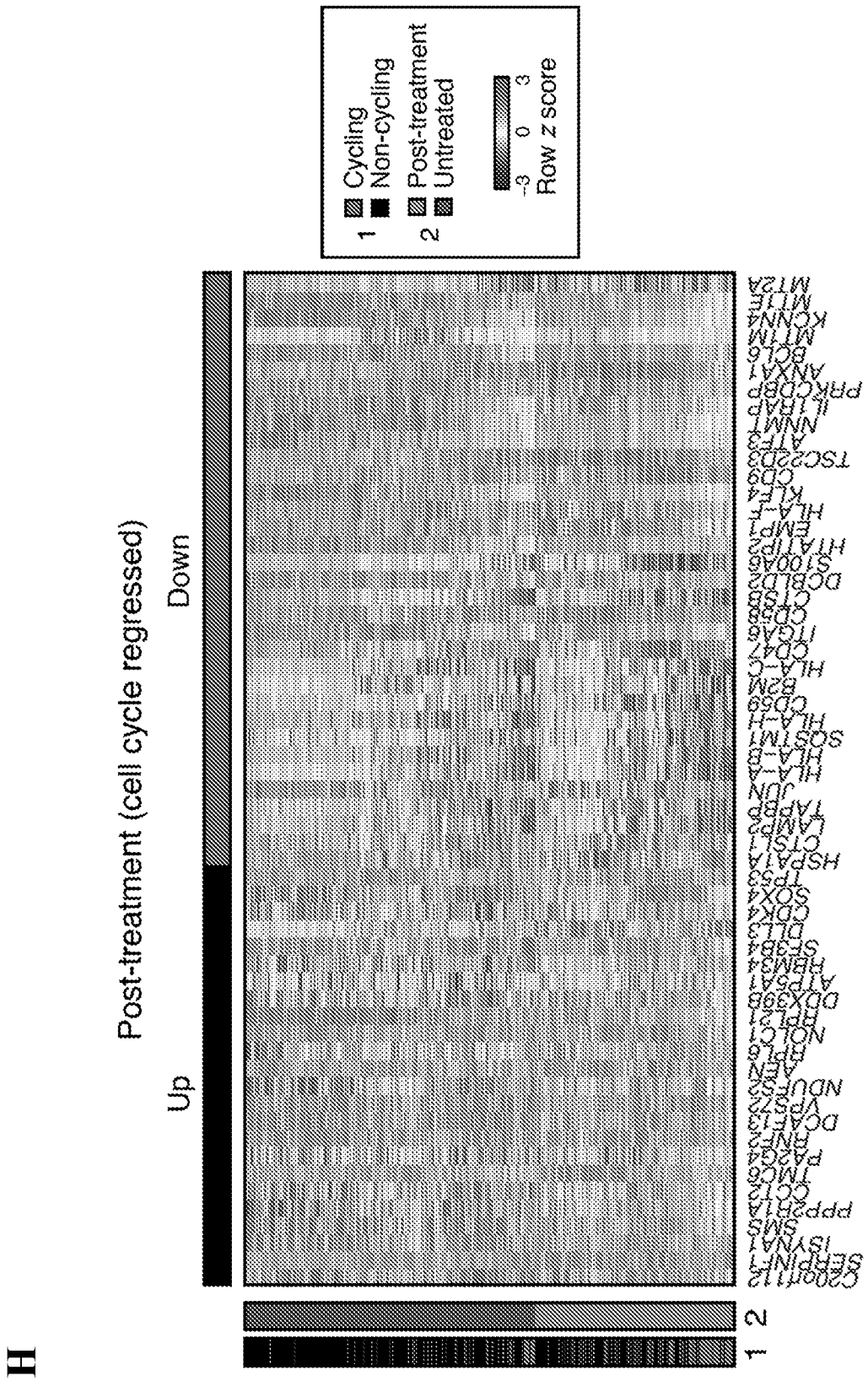

H
Post-treatment (cell cycle regressed)
Up
Down
1 Cycling
Non-cycling
2 Post-treatment
Untreated
−3 0 3
Row z score
1 2
C20orf112
SERPINH1
ISYNA1
SMS
PPP2R1A
CCT2
TMC6
P42G4
RNF2
DCAF13
VPS72
NDUFS2
AEN
RPL6
NOLC1
RPL31
DDX39B
ATP5A1
HEMK1
SF3B4
DLL3
CDK4
SOX4
TP53
HSPA1A
CTSL1
UAMP2
TAPBP
JUN
HLA-A
HLA-B
SOSTM1
HLA-H
CD59
B2M
HLA-C
CD47
ITGA6
CD58
CTSB
DCBLD2
S100A6
HNRNPA2B1
EMP1
HLA-F
KLF4
CD9
TSC22D3
ATF3
NNMT
IL1RAP
PRKCDBP
ANXA1
BCL6
MT1M
KCNN4
MT1E
MT2A

FIG. 70H

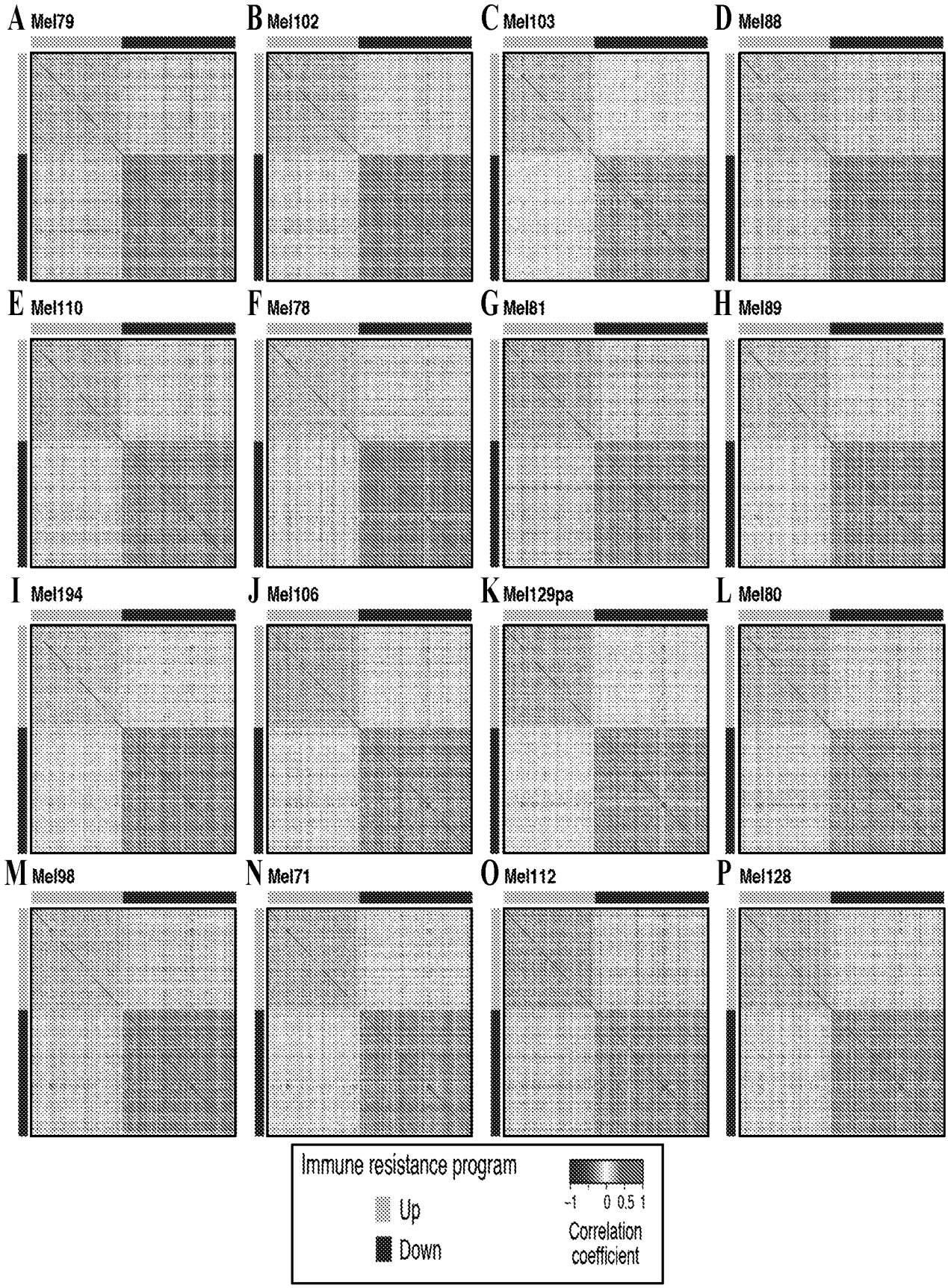

A Mel79
B Mel102
C Mel103
D Mel88
E Mel110
F Mel78
G Mel81
H Mel89
I Mel194
J Mel106
K Mel129pa
L Mel80
M Mel98
N Mel71
O Mel112
P Mel128
Immune resistance program
Up
Down
-1 0 0.5 1
Correlation coefficient

FIG. 71A-P

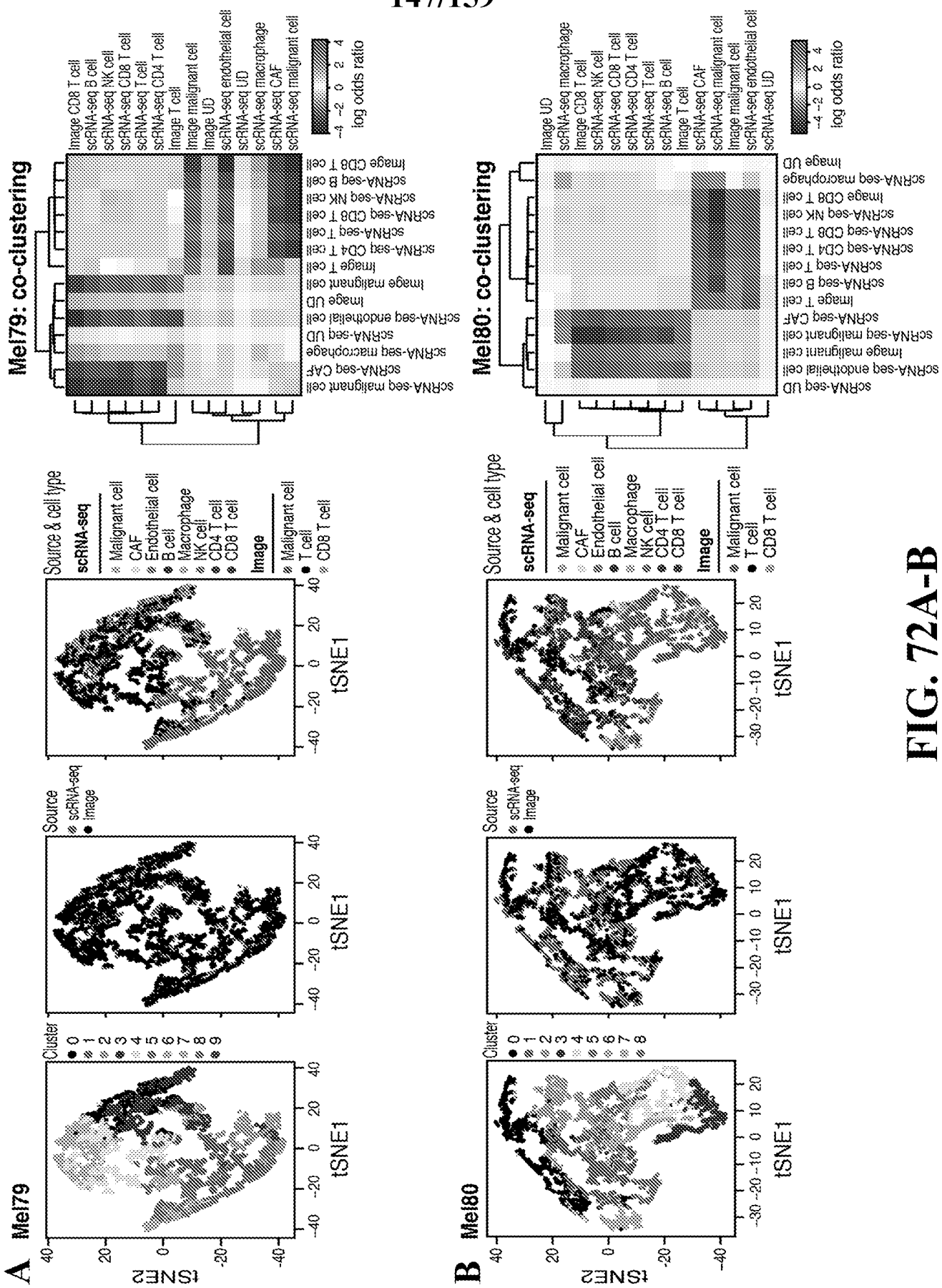

A
Mel79
tSNE2
tSNE1
Cluster
Source
scRNA-seq
image
Source & cell type
scRNA-seq
Malignant cell
CAF
Endothelial cell
B cell
Macrophage
NK cell
CD4 T cell
CD8 T cell
Image
Malignant cell
T cell
CD8 T cell
Mel79: co-clustering
Image CD8 T cell
scRNA-seq B cell
scRNA-seq NK cell
scRNA-seq CD8 T cell
scRNA-seq T cell
scRNA-seq CD4 T cell
Image T cell
Image malignant cell
Image UD
scRNA-seq endothelial cell
scRNA-seq UD
scRNA-seq macrophage
scRNA-seq CAF
scRNA-seq malignant cell
log odds ratio
B
Mel80
Mel80: co-clustering
Image UD
scRNA-seq macrophage
Image CD8 T cell
scRNA-seq NK cell
scRNA-seq CD8 T cell
scRNA-seq CD4 T cell
scRNA-seq T cell
scRNA-seq B cell
Image T cell
scRNA-seq CAF
scRNA-seq malignant cell
Image malignant cell
scRNA-seq endothelial cell
scRNA-seq UD

FIG. 72A-B

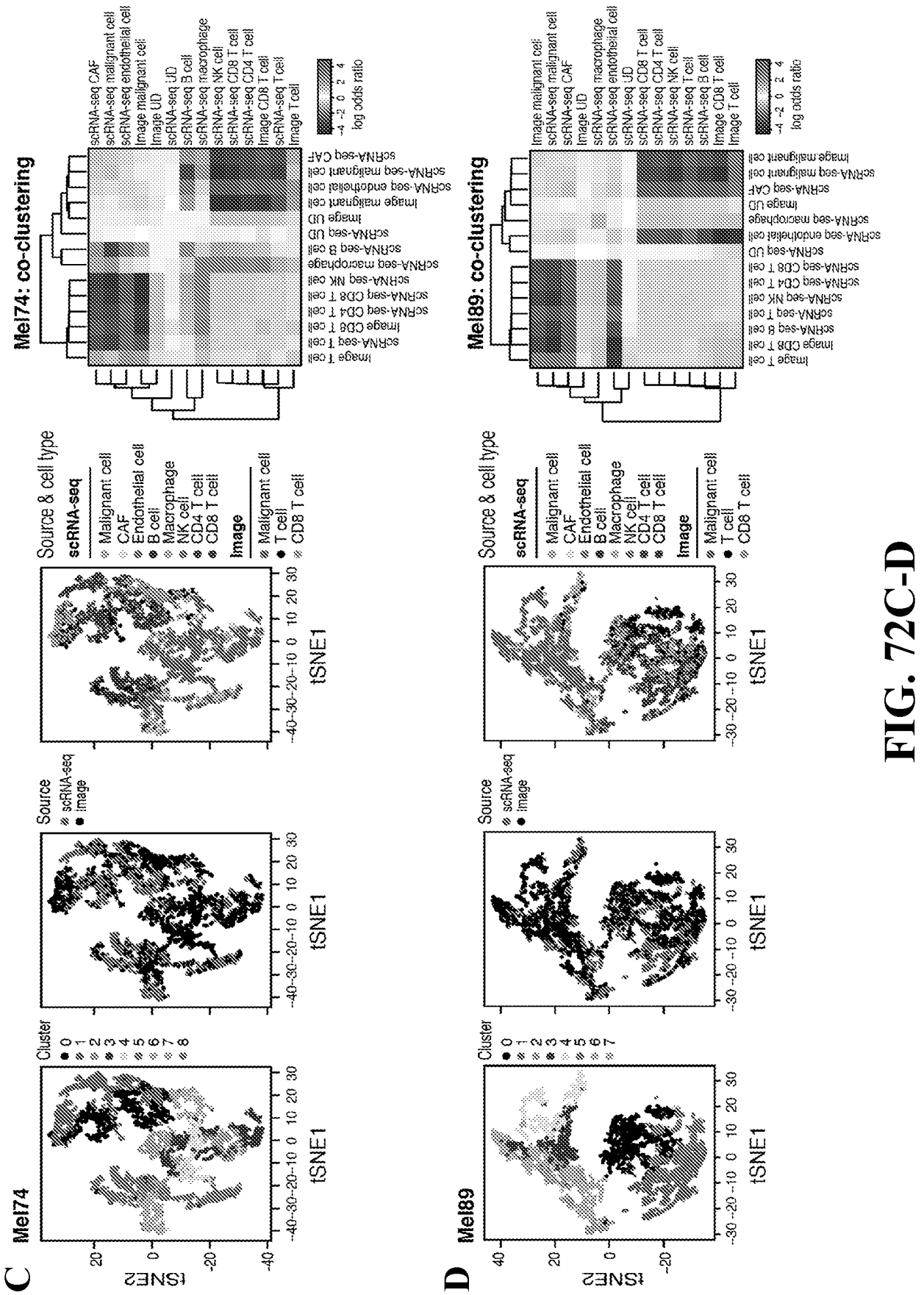

C
Mel74
Cluster
Source
scRNA-seq
image
Source & cell type
scRNA-seq
Malignant cell
CAF
Endothelial cell
B cell
Macrophage
NK cell
CD4 T cell
CD8 T cell
Image
Malignant cell
T cell
CD8 T cell
tSNE1
tSNE2
Mel74: co-clustering
scRNA-seq CAF
scRNA-seq malignant cell
scRNA-seq endothelial cell
Image malignant cell
Image UD
scRNA-seq B cell
scRNA-seq macrophage
scRNA-seq NK cell
scRNA-seq CD8 T cell
scRNA-seq CD4 T cell
Image CD8 T cell
scRNA-seq T cell
Image T cell
log odds ratio
D
Mel89
Mel89: co-clustering

FIG. 72C-D

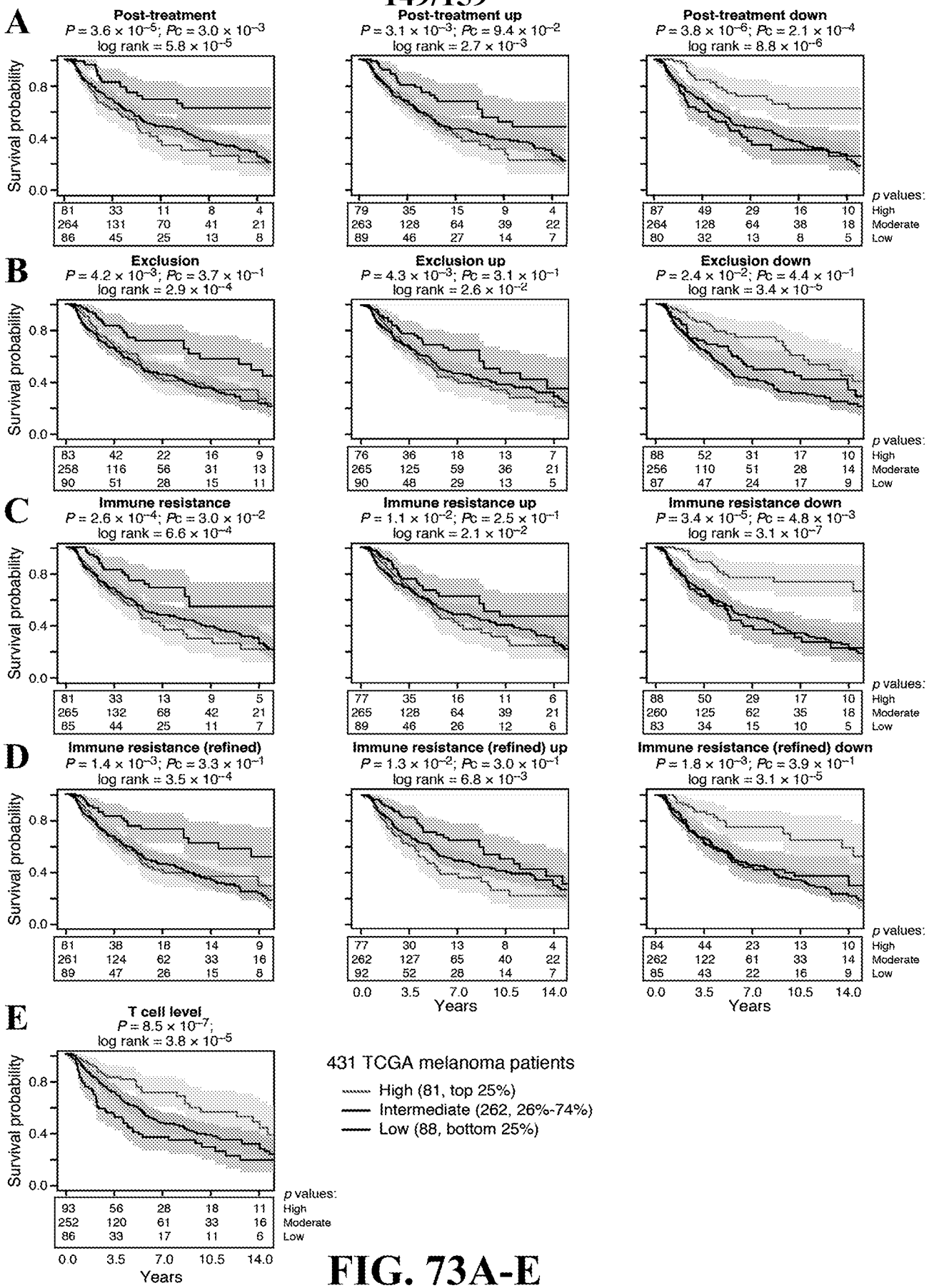

A
Post-treatment
P = 3.6 × 10−5; Pc = 3.0 × 10−3
log rank = 5.8 × 10−5
Post-treatment up
P = 3.1 × 10−3; Pc = 9.4 × 10−2
log rank = 2.7 × 10−3
Post-treatment down
P = 3.8 × 10−6; Pc = 2.1 × 10−4
log rank = 8.8 × 10−6
B
Exclusion
P = 4.2 × 10−3; Pc = 3.7 × 10−1
log rank = 2.9 × 10−4
Exclusion up
P = 4.3 × 10−3; Pc = 3.1 × 10−1
log rank = 2.6 × 10−2
Exclusion down
P = 2.4 × 10−2; Pc = 4.4 × 10−1
log rank = 3.4 × 10−5
C
Immune resistance
P = 2.6 × 10−4; Pc = 3.0 × 10−2
log rank = 6.6 × 10−4
Immune resistance up
P = 1.1 × 10−2; Pc = 2.5 × 10−1
log rank = 2.1 × 10−2
Immune resistance down
P = 3.4 × 10−5; Pc = 4.8 × 10−3
log rank = 3.1 × 10−7
D
Immune resistance (refined)
P = 1.4 × 10−3; Pc = 3.3 × 10−1
log rank = 3.5 × 10−4
Immune resistance (refined) up
P = 1.3 × 10−2; Pc = 3.0 × 10−1
log rank = 6.8 × 10−3
Immune resistance (refined) down
P = 1.8 × 10−3; Pc = 3.9 × 10−1
log rank = 3.1 × 10−5
E
T cell level
P = 8.5 × 10−7;
log rank = 3.8 × 10−5
Survival probability
0.0
0.4
0.8
p values:
High
Moderate
Low
0.0 3.5 7.0 10.5 14.0
Years
431 TCGA melanoma patients
High (81, top 25%)
Intermediate (262, 26%-74%)
Low (88, bottom 25%)

FIG. 73A-E

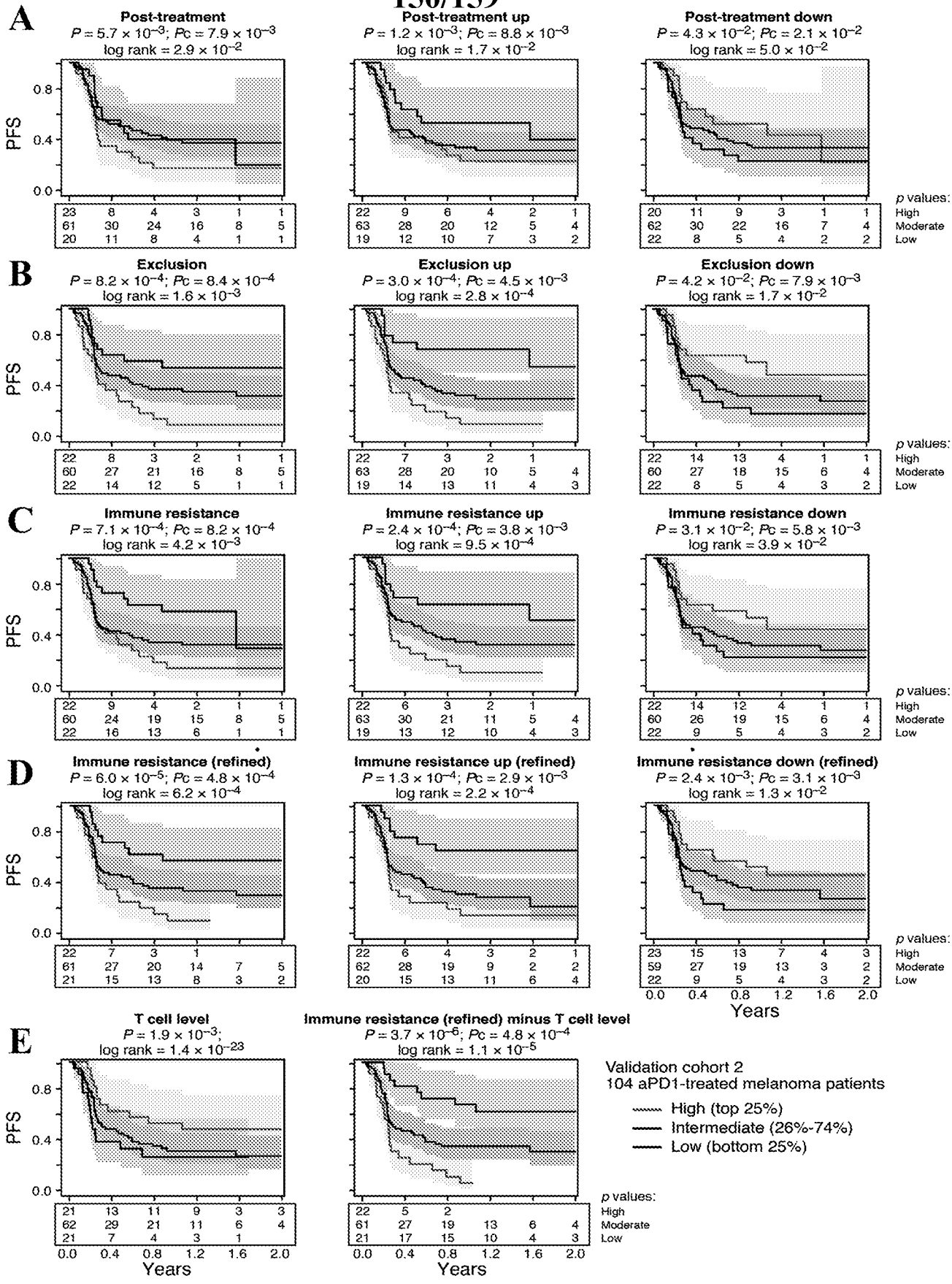

A
Post-treatment
P = 5.7 × 10−3; Pc = 7.9 × 10−3
log rank = 2.9 × 10−2
Post-treatment up
P = 1.2 × 10−3; Pc = 8.8 × 10−3
log rank = 1.7 × 10−2
Post-treatment down
P = 4.3 × 10−2; Pc = 2.1 × 10−2
log rank = 5.0 × 10−2
B
Exclusion
P = 8.2 × 10−4; Pc = 8.4 × 10−4
log rank = 1.6 × 10−3
Exclusion up
P = 3.0 × 10−4; Pc = 4.5 × 10−3
log rank = 2.8 × 10−4
Exclusion down
P = 4.2 × 10−2; Pc = 7.9 × 10−3
log rank = 1.7 × 10−2
C
Immune resistance
P = 7.1 × 10−4; Pc = 8.2 × 10−4
log rank = 4.2 × 10−3
Immune resistance up
P = 2.4 × 10−4; Pc = 3.8 × 10−3
log rank = 9.5 × 10−4
Immune resistance down
P = 3.1 × 10−2; Pc = 5.8 × 10−3
log rank = 3.9 × 10−2
D
Immune resistance (refined)
P = 6.0 × 10−5; Pc = 4.8 × 10−4
log rank = 6.2 × 10−4
Immune resistance up (refined)
P = 1.3 × 10−4; Pc = 2.9 × 10−3
log rank = 2.2 × 10−4
Immune resistance down (refined)
P = 2.4 × 10−3; Pc = 3.1 × 10−3
log rank = 1.3 × 10−2
E
T cell level
P = 1.9 × 10−3;
log rank = 1.4 × 10−23
Immune resistance (refined) minus T cell level
P = 3.7 × 10−6; Pc = 4.8 × 10−4
log rank = 1.1 × 10−5
PFS
p values:
High
Moderate
Low
Years
Validation cohort 2
104 aPD1-treated melanoma patients
High (top 25%)
Intermediate (26%-74%)
Low (bottom 25%)

FIG. 74A-E

A

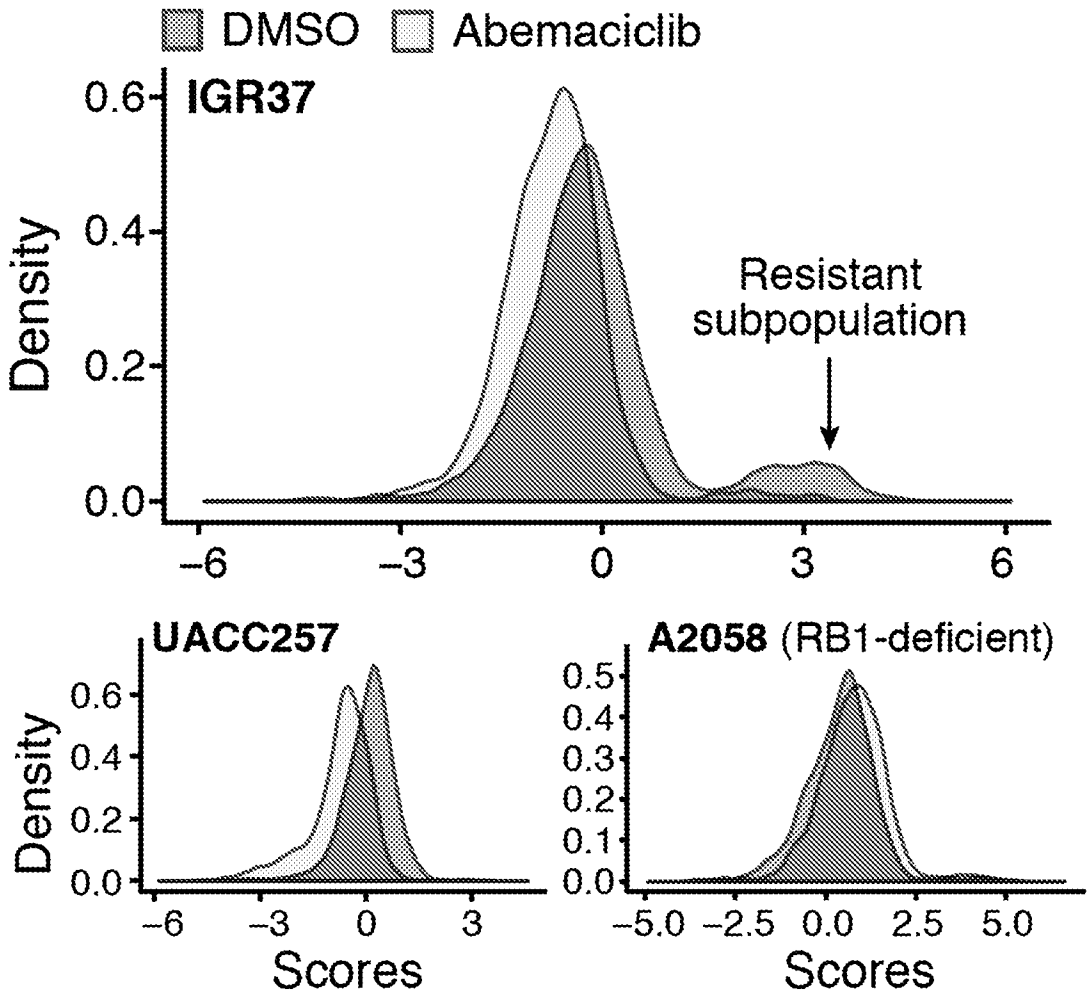

DMSO
Abemaciclib
IGR37
Density
0.6
0.4
0.2
0.0
Resistant subpopulation
−6
−3
0
3
6
UACC257
A2058 (RB1-deficient)
0.5
0.4
0.3
0.2
0.1
0.0
−5.0
−2.5
0.0
2.5
5.0
Scores

FIG. 75A

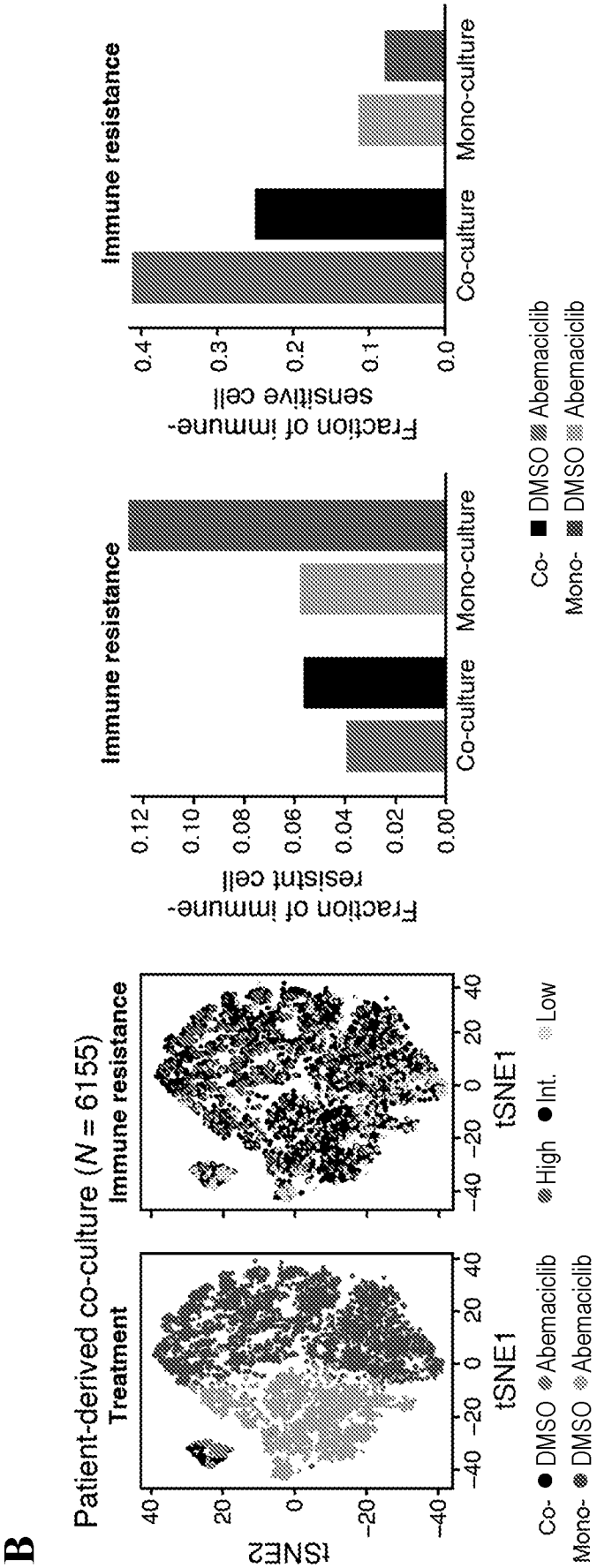

B
Patient-derived co-culture (N = 6155)
Treatment
Immune resistance
tSNE2
tSNE1
Co- ● DMSO ● Abemaciclib
Mono- ● DMSO ● Abemaciclib
● High ● Int. ● Low
Fraction of immune-resistnt cell
Immune resistance
Co-culture
Mono-culture
Co- ■ DMSO ■ Abemaciclib
Mono- ■ DMSO ■ Abemaciclib
Fraction of immune-sensitive cell
Immune resistance
Co-culture
Mono-culture

FIG. 75B

C

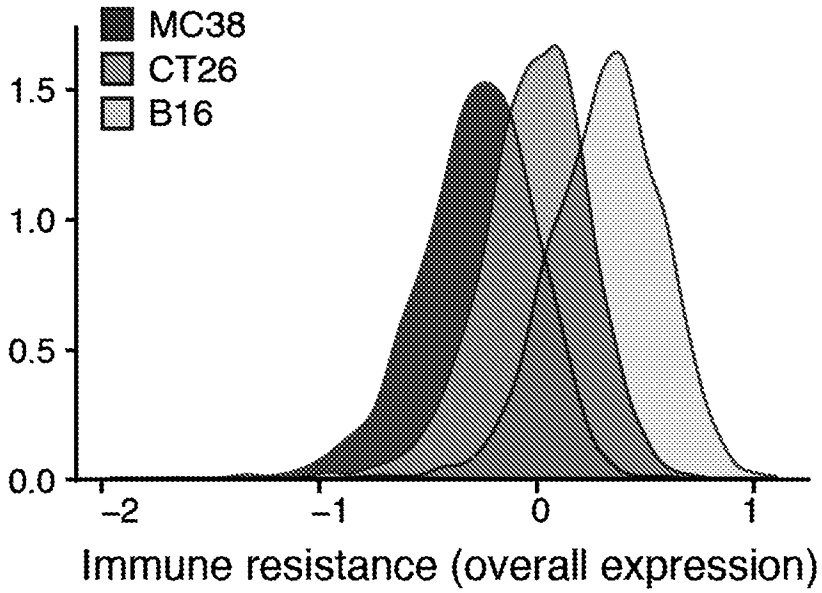

MC38
CT26
B16
1.5
1.0
0.5
0.0
−2
−1
0
1
Immune resistance (overall expression)

FIG. 75C

D

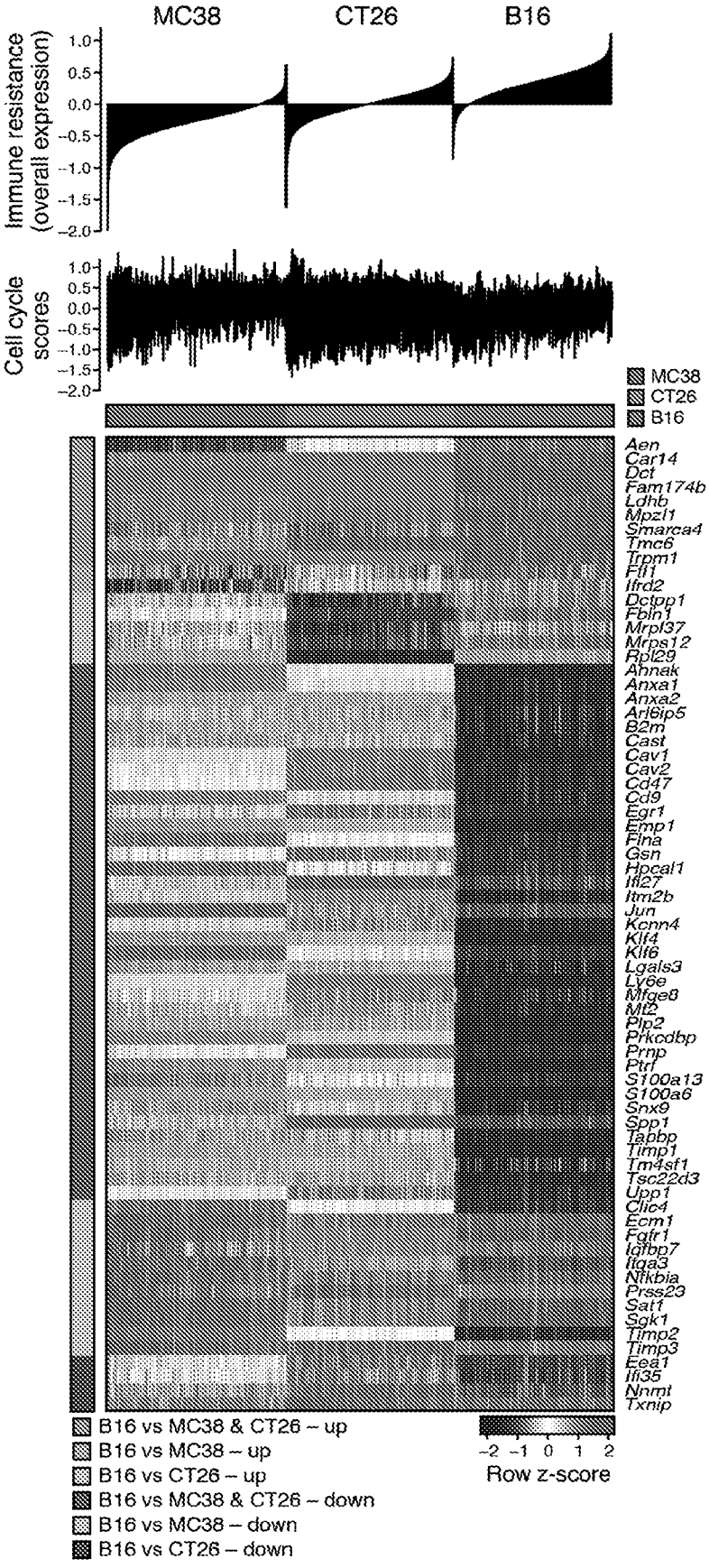

MC38
CT26
B16
Immune resistance (overall expression)
1.0
0.5
0.0
−0.5
−1.0
−1.5
−2.0
Cell cycle scores
MC38
CT26
B16
Aen
Car14
Dct
Fam174b
Ldhb
Mpzl1
Smarca4
Tmc6
Trpm1
Ffl1
Ifrd2
Dctpp1
Fbln1
Mrpl37
Mrps12
Rpl29
Ahnak
Anxa1
Anxa2
Arl6ip5
B2m
Cast
Cav1
Cav2
Cd47
Cd9
Egr1
Emp1
Fina
Gsn
Hpcal1
Ifi27
Itm2b
Jun
Kcnn4
Klf4
Klf6
Lgals3
Ly6e
Mfge8
Mt2
Plp2
Pfkcdbp
Prnp
Ptrf
S100a13
S100a6
Snx9
Spp1
Tapbp
Timp1
Tm4sf1
Tsc22d3
Upp1
Clic4
Ecm1
Fgfr1
Idfbp7
Itga3
Nfkbia
Prss23
Sat1
Sgk1
Timp2
Timp3
Eea1
Ifi35
Nnmt
Txnip
B16 vs MC38 & CT26 – up
B16 vs MC38 – up
B16 vs CT26 – up
B16 vs MC38 & CT26 – down
B16 vs MC38 – down
B16 vs CT26 – down
−2 −1 0 1 2
Row z-score

FIG. 75D

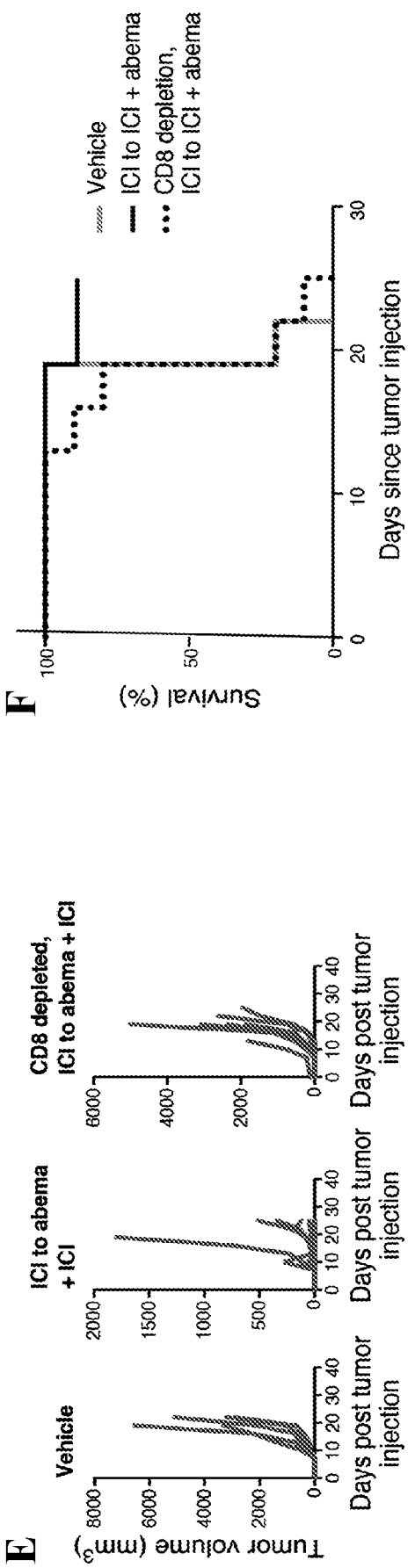

E
Tumor volume (mm3)
Vehicle
ICI to abema + ICI
CD8 depleted, ICI to abema + ICI
Days post tumor injection
F
Survival (%)
Vehicle
ICI to ICI + abema
CD8 depletion, ICI to ICI + abema
Days since tumor injection

FIG. 75E-F

G

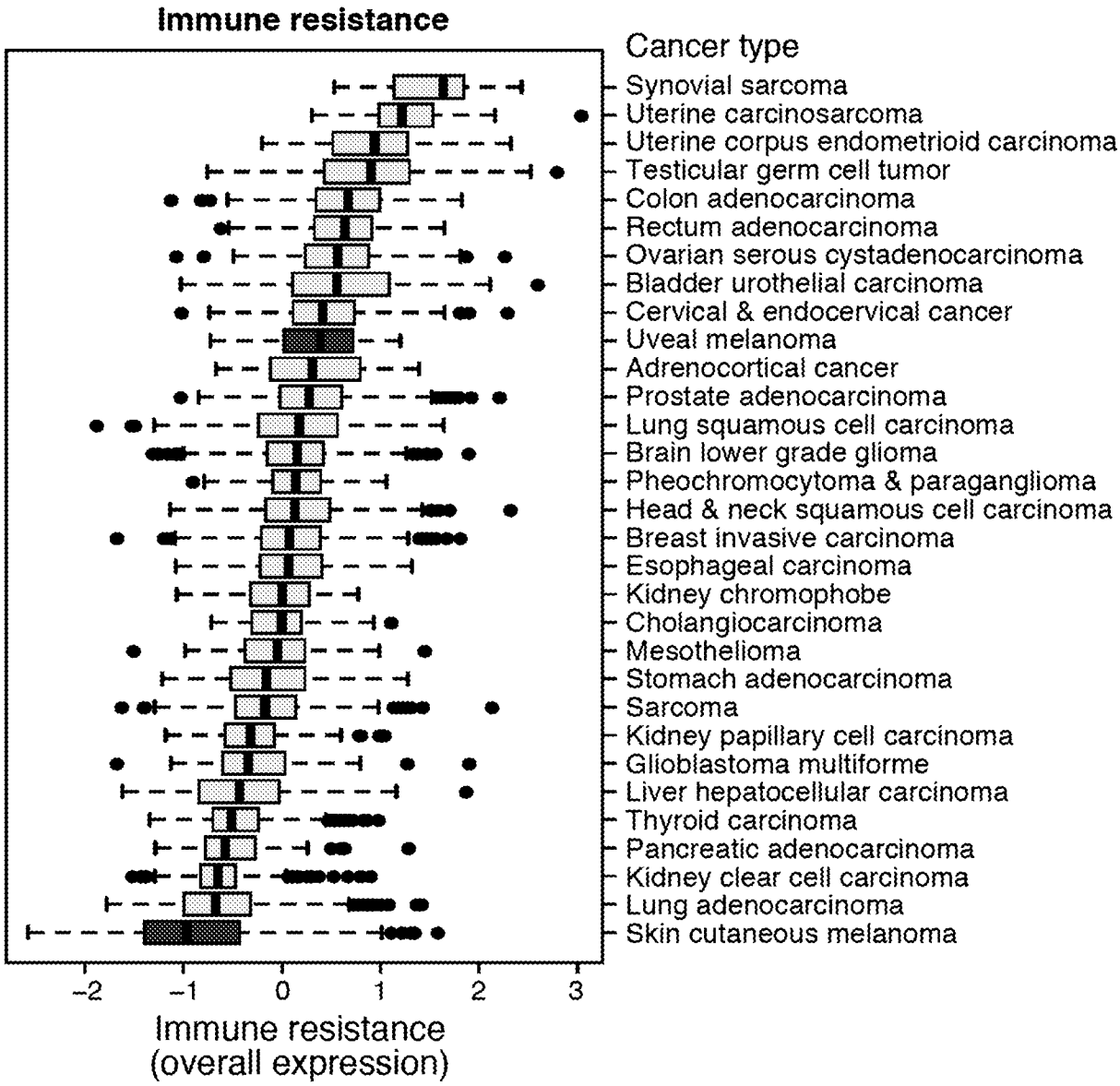

Immune resistance
Cancer type
Synovial sarcoma
Uterine carcinosarcoma
Uterine corpus endometrioid carcinoma
Testicular germ cell tumor
Colon adenocarcinoma
Rectum adenocarcinoma
Ovarian serous cystadenocarcinoma
Bladder urothelial carcinoma
Cervical & endocervical cancer
Uveal melanoma
Adrenocortical cancer
Prostate adenocarcinoma
Lung squamous cell carcinoma
Brain lower grade glioma
Pheochromocytoma & paraganglioma
Head & neck squamous cell carcinoma
Breast invasive carcinoma
Esophageal carcinoma
Kidney chromophobe
Cholangiocarcinoma
Mesothelioma
Stomach adenocarcinoma
Sarcoma
Kidney papillary cell carcinoma
Glioblastoma multiforme
Liver hepatocellular carcinoma
Thyroid carcinoma
Pancreatic adenocarcinoma
Kidney clear cell carcinoma
Lung adenocarcinoma
Skin cutaneous melanoma
−2
−1
0
1
2
3
Immune resistance
(overall expression)

FIG. 75G

H

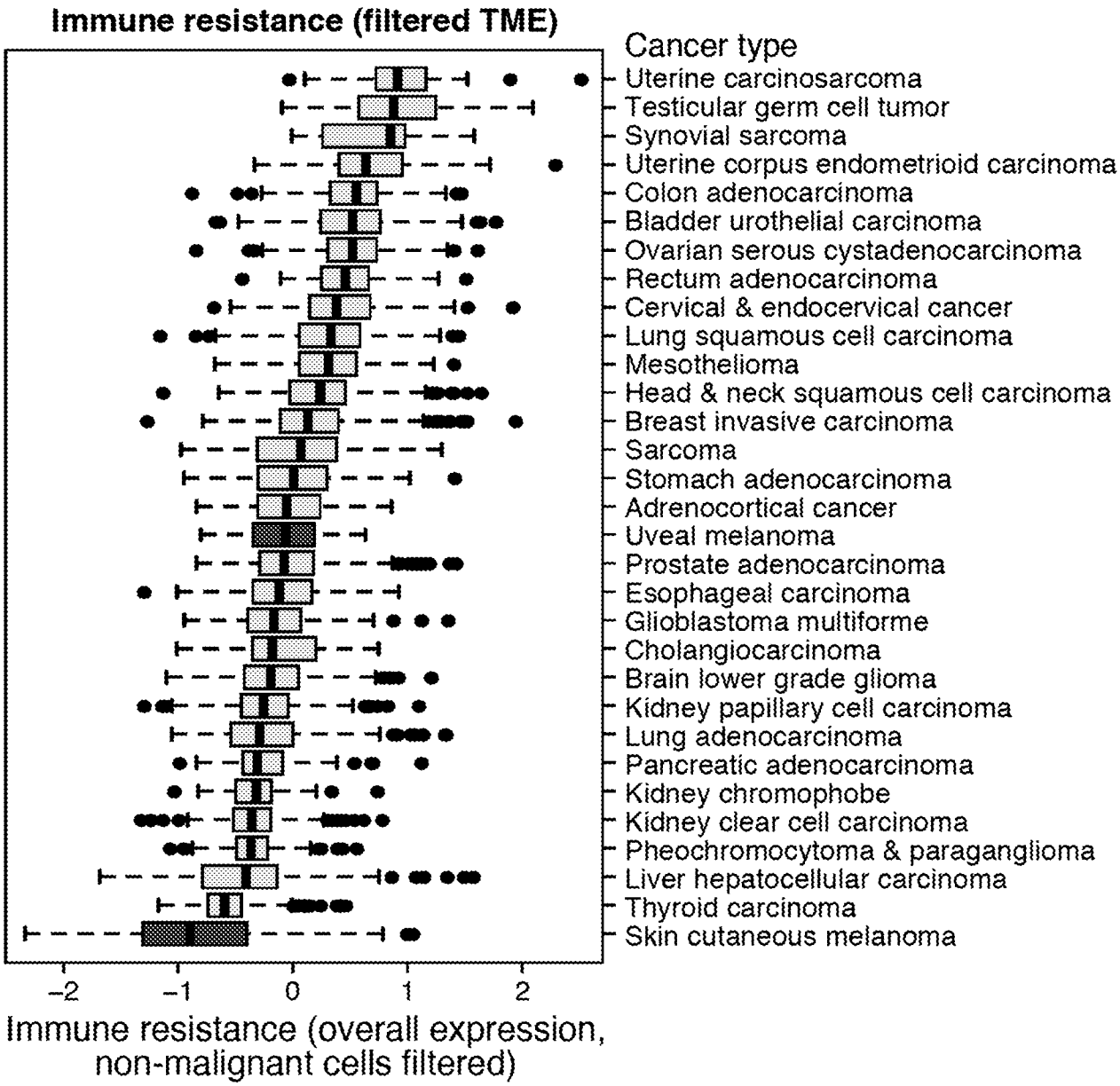

Immune resistance (filtered TME)
Cancer type
Uterine carcinosarcoma
Testicular germ cell tumor
Synovial sarcoma
Uterine corpus endometrioid carcinoma
Colon adenocarcinoma
Bladder urothelial carcinoma
Ovarian serous cystadenocarcinoma
Rectum adenocarcinoma
Cervical & endocervical cancer
Lung squamous cell carcinoma
Mesothelioma
Head & neck squamous cell carcinoma
Breast invasive carcinoma
Sarcoma
Stomach adenocarcinoma
Adrenocortical cancer
Uveal melanoma
Prostate adenocarcinoma
Esophageal carcinoma
Glioblastoma multiforme
Cholangiocarcinoma
Brain lower grade glioma
Kidney papillary cell carcinoma
Lung adenocarcinoma
Pancreatic adenocarcinoma
Kidney chromophobe
Kidney clear cell carcinoma
Pheochromocytoma & paraganglioma
Liver hepatocellular carcinoma
Thyroid carcinoma
Skin cutaneous melanoma
−2
−1
0
1
2
Immune resistance (overall expression, non-malignant cells filtered)

FIG. 75H

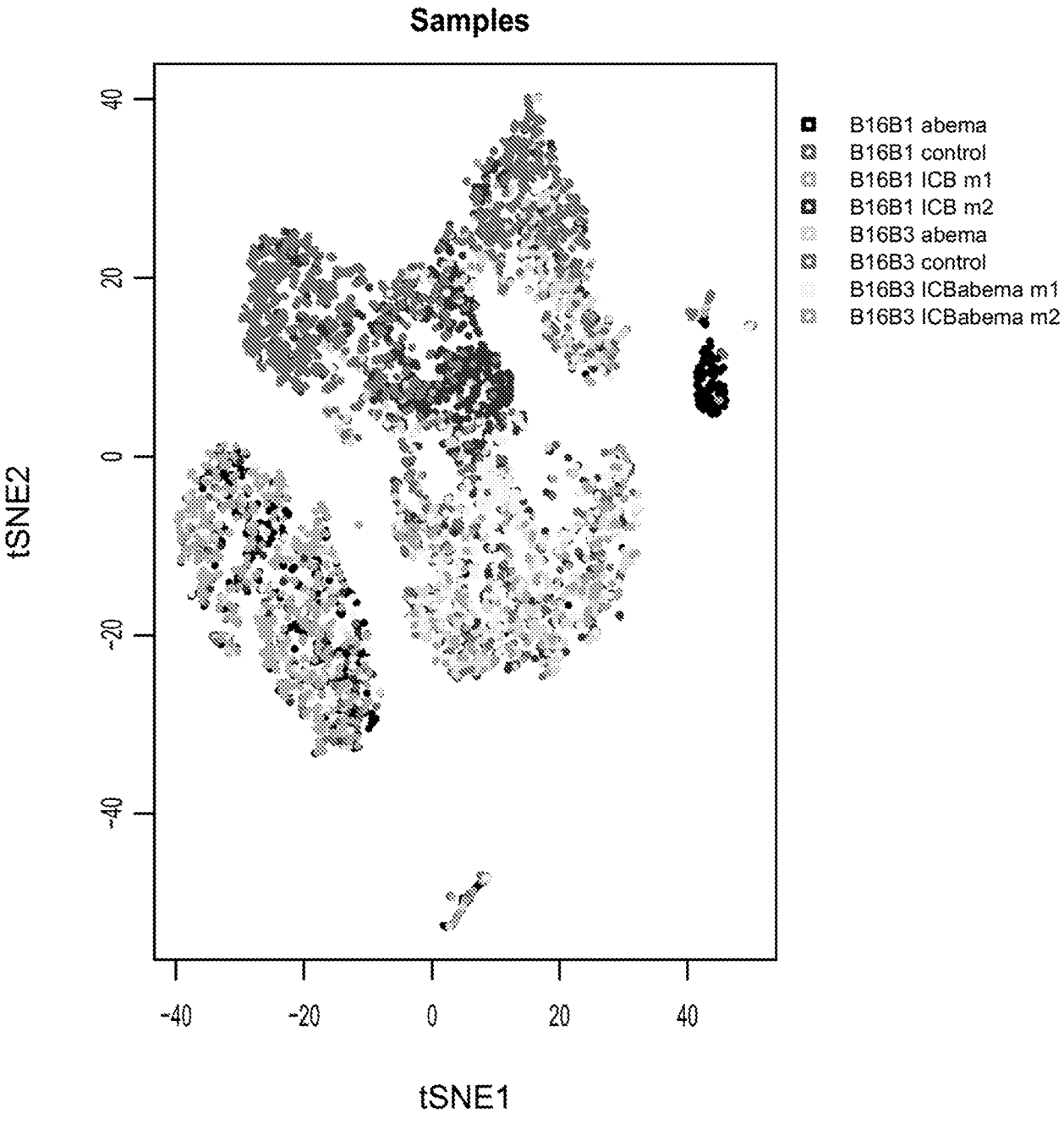

Samples
B16B1 abema
B16B1 control
B16B1 ICB m1
B16B1 ICB m2
B16B3 abema
B16B3 control
B16B3 ICBabema m1
B16B3 ICBabema m2
tSNE2
tSNE1
40
20
0
-20
-40
-40
-20
0
20
40

FIG. 76

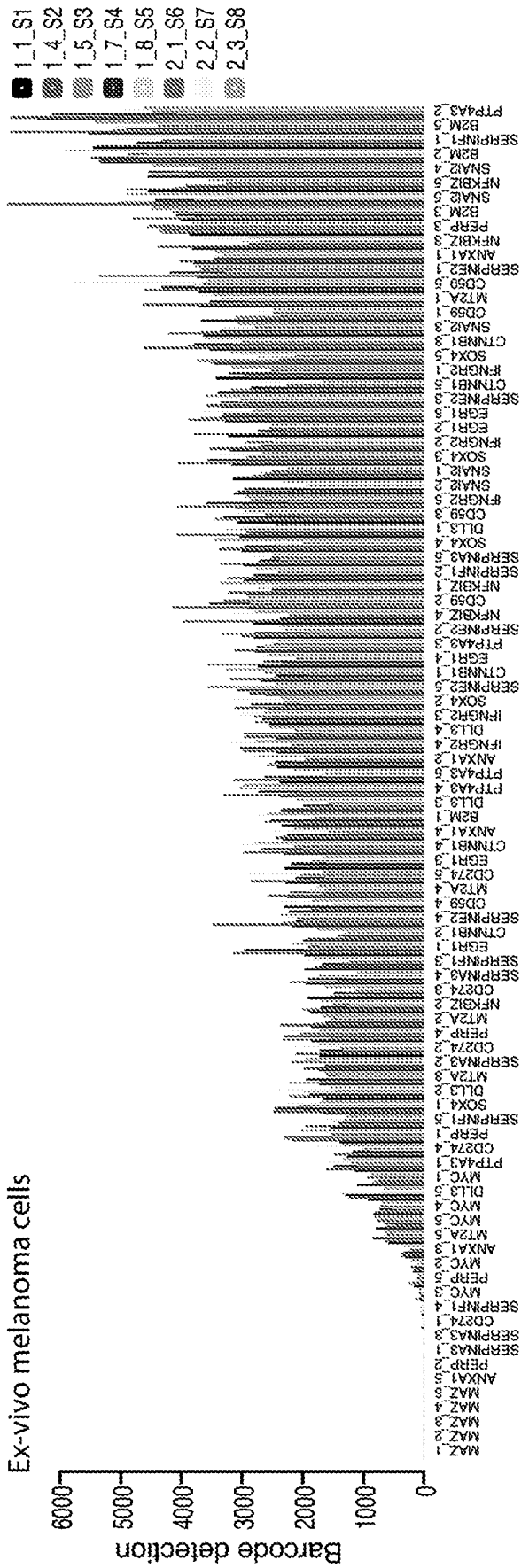

1_1_S1
1_4_S2
1_5_S3
1_7_S4
1_8_S5
2_1_S6
2_2_S7
2_3_S8
Ex-vivo melanoma cells
Barcode detection
0
1000
2000
3000
4000
5000
6000

FIG. 77

INTERNATIONAL SEARCH REPORT

International application No.
PCT/US 18/54020

A. CLASSIFICATION OF SUBJECT MATTER

IPC(8) - G06F 19/22, G16H 50/20, C12Q 1/68 (2018.01)
CPC - G06F 19/22, G16H 50/20, C12Q 1/686, C12Q 1/6869, C12Q 2600/106, C12Q 2600/156, C12Q 1600/158, C12N 2800/52, C12N 2800/60

According to International Patent Classification (IPC) or to both national classification and IPC

B. FIELDS SEARCHED

Minimum documentation searched (classification system followed by classification symbols)

See Search History Document

Documentation searched other than minimum documentation to the extent that such documents are included in the fields searched

See Search History Document

Electronic data base consulted during the international search (name of data base and, where practicable, search terms used)

See Search History Document

C. DOCUMENTS CONSIDERED TO BE RELEVANT

Category*	Citation of document, with indication, where appropriate, of the relevant passages	Relevant to claim No.
Y	US 2017/0107577 A1 (THE COUNCIL OF THE QUEENSLAND INSTITUTE OF MEDICAL RESEARCH) 20 April 2017 (20.04.2017) para [0074]; para [0075]	1, 3, 4, 6, 7/(1,3,4,6)
Y	MESIAS et al. Use of CD200 blockade inhibitor to enhance glioma immunotherapy. Journal for immunotherapy of cancer. December 2015. Vol 3, No 2, P38. Especially page 1, col 1, para 2; page 1, col 1, para 3	1, 3, 4, 6, 7/(1,3,4,6)

☐ Further documents are listed in the continuation of Box C. ☐ See patent family annex.

* Special categories of cited documents:

"A" document defining the general state of the art which is not considered to be of particular relevance

"E" earlier application or patent but published on or after the international filing date

"L" document which may throw doubts on priority claim(s) or which is cited to establish the publication date of another citation or other special reason (as specified)

"O" document referring to an oral disclosure, use, exhibition or other means

"P" document published prior to the international filing date but later than the priority date claimed

"T" later document published after the international filing date or priority date and not in conflict with the application but cited to understand the principle or theory underlying the invention

"X" document of particular relevance; the claimed invention cannot be considered novel or cannot be considered to involve an inventive step when the document is taken alone

"Y" document of particular relevance; the claimed invention cannot be considered to involve an inventive step when the document is combined with one or more other such documents, such combination being obvious to a person skilled in the art

"&" document member of the same patent family

Date of the actual completion of the international search	Date of mailing of the international search report
7 January 2019	24 JAN 2019

Name and mailing address of the ISA/US	Authorized officer:
Mail Stop PCT, Attn: ISA/US, Commissioner for Patents P.O. Box 1450, Alexandria, Virginia 22313-1450 Facsimile No. 571-273-8300	Lee W. Young PCT Helpdesk: 571-272-4300 PCT OSP: 571-272-7774

INTERNATIONAL SEARCH REPORT

International application No.
PCT/US 18/54020

Box No. II Observations where certain claims were found unsearchable (Continuation of item 2 of first sheet)

This international search report has not been established in respect of certain claims under Article 17(2)(a) for the following reasons:

1. ☐ Claims Nos.:
because they relate to subject matter not required to be searched by this Authority, namely:

2. ☐ Claims Nos.:
because they relate to parts of the international application that do not comply with the prescribed requirements to such an extent that no meaningful international search can be carried out, specifically:

3. ☒ Claims Nos.: 11-20, 22-27
because they are dependent claims and are not drafted in accordance with the second and third sentences of Rule 6.4(a).

Box No. III Observations where unity of invention is lacking (Continuation of item 3 of first sheet)

This International Searching Authority found multiple inventions in this international application, as follows:
This application contains the following inventions or groups of inventions which are not so linked as to form a single general inventive concept under PCT Rule 13.1. In order for all inventions to be searched, the appropriate additional search fees must be paid.

--Please see Supplemental Box--

1. ☐ As all required additional search fees were timely paid by the applicant, this international search report covers all searchable claims.

2. ☐ As all searchable claims could be searched without effort justifying additional fees, this Authority did not invite payment of additional fees.

3. ☐ As only some of the required additional search fees were timely paid by the applicant, this international search report covers only those claims for which fees were paid, specifically claims Nos.:

4. ☒ No required additional search fees were timely paid by the applicant. Consequently, this international search report is restricted to the invention first mentioned in the claims; it is covered by claims Nos.:
1, 3, 4, 6, 7(in part) limited to PPIA

Remark on Protest

☐ The additional search fees were accompanied by the applicant's protest and, where applicable, the payment of a protest fee.

☐ The additional search fees were accompanied by the applicant's protest but the applicable protest fee was not paid within the time limit specified in the invitation.

☐ No protest accompanied the payment of additional search fees.

INTERNATIONAL SEARCH REPORT

International application No.
PCT/US 18/54020

Continuation of Box No III - Observations where unity of invention is lacking

Group I+: Claims 1-7, drawn to a method of detecting an immune checkpoint inhibitor resistance (ICR) gene signature in a tumor. The method will be searched to the extent that the ICR gene signature encompasses PPIA. It is believed that claims 1, 3, 4, 6, 7(in part) encompass this first named invention, and thus these claims will be searched without fee to the extent that they encompass PPIA. Additional ICR gene signature(s) will be searched upon the payment of additional fees. Applicants must specify the claims that encompass any additionally elected ICR gene signature(s). Applicants must further indicate, if applicable, the claims which encompass the first named invention, if different than what was indicated above for this group. Failure to clearly identify how any paid additional invention fees are to be applied to the "+" group(s) will result in only the first claimed invention to be searched. An exemplary election would be an ICR gene signature comprising BZW2 (Claims 1, 3, 4, 6, 7(in part)).
Another exemplary election would be an ICR gene signature comprising AHNAK (Claims 1, 2, 4, 5, 7(in part)).

Group II+: Claims 8-10, drawn to a method of detecting an immune cell exclusion gene signature in a tumor. Group II+ will be searched upon payment of additional fees. The method may be searched, for example, to the extent that the immune cell exclusion gene signature encompasses BZW2, for an additional fee and election as such. It is believed that claims 8, 10 read on this exemplary invention. Additional immune cell exclusion gene signature(s) will be searched upon the payment of additional fees. Applicants must specify the claims that encompass any additionally elected immune cell exclusion gene signature(s). Failure to clearly identify how any paid additional invention fees are to be applied to the"+" group(s) will result in only the first claimed invention to be searched. Another exemplary election would be an immune cell exclusion gene signature comprising APOC2 (Claim 8, 9).

Group III: claims 21 and 28, drawn to a method of treating a cancer in a subject in need thereof.

The inventions listed as Groups I+, II+ and III do not relate to a single general inventive concept under PCT Rule 13.1 because, under PCT Rule 13.2, they lack the same or corresponding special technical features for the following reasons:

Special Technical Features

Groups I+ include the special technical feature of a method of detecting an immune checkpoint inhibitor resistance gene signature in a tumor, not required by Groups II+ and III.

Groups II+ include the special technical feature of a method of detecting an immune cell exclusion gene signature in a tumor, not required by Groups I+ and III. [Note, immune cell exclusion gene signature is used to determine immune cell infiltration in a tumor, see para [0171] in instant Specification].

Group III includes the special technical feature of a method of administering a combination treatment regimen comprising an immunotherapy and one or more selected drugs, not required by Groups I+ and II+.

The inventions of Groups I+ each include the special technical feature of a specific immune checkpoint inhibitor resistance gene signature, as recited therein, not required by any of the other inventions of Groups I+.

The inventions of Groups II+ each include the special technical feature of a specific immune cell exclusion gene signature, as recited therein, not required by any of the other Inventions of Groups II+.

Common Technical Features

The inventions of Groups I+, II+ and III share the technical feature of tumor and immune system.
The inventions of Groups I+ and II+ share the technical feature of a method of detecting an immune gene signature.

The inventions of Groups I+ share the technical feature of a method of detecting an immune checkpoint inhibitor resistance (ICR) gene signature in a tumor comprising, detecting in tumor cells obtained from a subject in need thereof the expression or activity of a malignant cell gene signature.

---continued on next sheet---

Continuation from prior sheet

However, these shared technical features do not represent a contribution over prior art in view of US 2017/0107577 A1 to The Council Of The Queensland Institute Of Medical Research (hereinafter 'QIMR').

QIMR discloses (instant claim 1) a method of detecting an immune checkpoint inhibitor resistance (ICR) gene signature in a tumor comprising, detecting in tumor cells obtained from a subject in need thereof the expression or activity of a malignant cell gene signature (para [0074]-"In a seventeenth aspect, the invention provides a method of predicting the responsiveness of a cancer to an immunotherapeutic agent in a mammal, said method including the step of comparing an expression level of one or a plurality of overexpressed genes selected from the group consisting of ADORA2B, CD36, CETN3, CFDP1, KCNG1, LAMA3, NAE1, MAP2K5, PGK1, SF3B3, STAU1 and TXN and/or an expression level of one or a plurality of underexpressed genes selected from the group consisting of APOBEC3A, BTN2A2, BCL2, CAMK4, FBXW4, CAMSAP1, CARHSP1, GSK3B, HCFC1R1, PSEN2, MYB and ZNF593, in one or a plurality of cancer cells, tissues or organs of the mammal, wherein an altered or modulated relative expression level of the one or plurality of overexpressed genes compared to the one or plurality of underexpressed genes indicates or correlates with relatively increased or decreased responsiveness of the cancer to the immunotherapeutic agent"; para [0075]-"Suitably, the immunotherapeutic agent is an immune checkpoint inhibitor. Preferably, the immune checkpoint inhibitor is or comprises an anti-PD1 antibody or an anti-PDL1 antibody").

QIMR discloses (instant claim 2) an ICR signature comprises a ICR-down signature, wherein ICR-down signature is downregulated in a tumor with a high ICR score and upregulated in a tumor with a low ICR score (para [0074]-"In a seventeenth aspect, the invention provides a method of predicting the responsiveness of a cancer to an immunotherapeutic agent in a mammal, said method including the step of comparing an expression level of one or a plurality of overexpressed genes selected from the group consisting of ADORA2B, CD36, CETN3, CFDP1, KCNG1, LAMA3, NAE1, MAP2K5, PGK1, SF3B3, STAU1 and TXN and/or an expression level of one or a plurality of underexpressed genes selected from the group consisting of APOBEC3A, BTN2A2, BCL2, CAMK4, FBXW4, CAMSAP1, CARHSP1, GSK3B, HCFC1R1, PSEN2, MYB and ZNF593, in one or a plurality of cancer cells, tissues or organs of the mammal, wherein an altered or modulated relative expression level of the one or plurality of overexpressed genes compared to the one or plurality of underexpressed genes indicates or correlates with relatively increased or decreased responsiveness of the cancer to the immunotherapeutic agent"; para [0075]-"Suitably, the immunotherapeutic agent is an immune checkpoint inhibitor. Preferably, the immune checkpoint inhibitor is or comprises an anti-PD1 antibody or an anti-PDL1 antibody").

QIMR discloses (instant claim 3) an ICR signature comprises a ICR-up signature, wherein wherein said ICR up signature is upregulated in a tumor with a high ICR score and downregulated in a tumor with a low ICR score (para [0074]-"In a seventeenth aspect, the invention provides a method of predicting the responsiveness of a cancer to an immunotherapeutic agent in a mammal, said method including the step of comparing an expression level of one or a plurality of overexpressed genes selected from the group consisting of ADORA2B, CD36, CETN3, CFDP1, KCNG1, LAMA3, NAE1, MAP2K5, PGK1, SF3B3, STAU1 and TXN and/or an expression level of one or a plurality of underexpressed genes selected from the group consisting of APOBEC3A, BTN2A2, BCL2, CAMK4, FBXW4, CAMSAP1, CARHSP1, GSK3B, HCFC1R1, PSEN2, MYB and ZNF593, in one or a plurality of cancer cells, tissues or organs of the mammal, wherein an altered or modulated relative expression level of the one or plurality of overexpressed genes compared to the one or plurality of underexpressed genes indicates or correlates with relatively increased or decreased responsiveness of the cancer to the immunotherapeutic agent"; para [0075]-"Suitably, the immunotherapeutic agent is an immune checkpoint inhibitor. Preferably, the immune checkpoint inhibitor is or comprises an anti-PD1 antibody or an anti-PDL1 antibody").

The inventions of Groups II+ share the technical feature of a method of detecting an immune cell exclusion gene signature in a tumor comprising, detecting in tumor cells obtained from a subject in need thereof the expression or activity of a malignant cell gene signature.

However, these shared technical features do not represent a contribution over prior art in view of Sweis et al. "Molecular drivers of the non-T-cell-inflamed tumor microenvironment in urothelial bladder cancer" (Cancer Immunology Research. 1 July 2016. Vol 4, No 7, pp 563-568) (hereinafter 'Sweis').

Sweis discloses (instant claim 8) a method of detecting an immune cell exclusion gene signature in a tumor comprising, detecting in tumor cells obtained from a subject in need thereof the expression or activity of a malignant cell gene signature (Abstract-"In this report, we determined tumor-oncogenic pathways correlating with T cell exclusion. We first establish that T-cell-inflamed bladder tumors can be identified by immune gene expression profiling with concordance with CD8+ T cell infiltration. Upregulation of genes encoding immune checkpoint proteins PD-L1, IDO, FOXP3, TIM3, and LAG3 was associated with T-cell-inflamed tumors, suggesting potential for sensitivity to checkpoint blockade. beta-catenin, PPAR-gamma, and FGFR3 pathways were activated in non-T cell-inflamed tumors"; Fig 1).

Sweis discloses (instant claim 9) the exclusion signature comprises an exclusion-down signature, wherein said exclusion-down signature is downregulated in a tumor with T cell exclusion and is upregulated in a tumor with T cell infiltration (page 4, para 2-"Expression of PD-L1 mRNA positively correlated with that of CD8A ($P < 0.0001$, Fig. 2A), and the T-cell-inflamed tumors had higher expression of both genes as compared to the non-T cell-inflamed tumors. A similar positive correlation was observed with other immune-inhibitory markers IDO, FOXP3, TIM3, and LAG3 (Fig. 2B)").

Sweis discloses (instant claim 10) the exclusion signature comprises an exclusion-up signature, wherein said exclusion-up signature is upregulated in a tumor with T cell exclusion and is downregulated in a tumor with T cell infiltration (page 4, para 3-"To identify pathways linked to the non-T cell-inflamed phenotype, we compared gene expression patterns between T-cell-inflamed and non-T cell-inflamed bladder cancers. We found 3,112 genes differentially expressed between the two groups ($Q < 0.01$, Supplementary Table S1), with 730 being preferentially expressed in the non-T cell-inflamed tumors...The top activated upstream regulators identified were beta-catenin and PPAR-gamma (both $P = 0.003$)").

As said technical features were known in the art at the time of the invention, these cannot be considered special technical features that would otherwise unify the groups.

Groups I+, II+ and III therefore lack unity under PCT Rule 13 because they do not share a same or corresponding special technical feature.